Geological Survey of Canada
Commission géologique du Canada

PAPER/ÉTUDE
89-1C

CURRENT RESEARCH, PART C
CANADIAN SHIELD

RECHERCHES EN COURS, PARTIE C
BOUCLIER CANADIEN

Canada

NOTICE TO LIBRARIANS AND INDEXERS

The Geological Survey's Current Research series contains many reports comparable in scope and subject matter to those appearing in scientific journals and other serials. Most contributions to Current Research include an abstract and bibliographic citation. It is hoped that these will assist you in cataloguing and indexing these reports and that this will result in a still wider dissemination of the results of the Geological Survey's research activities.

AVIS AUX BIBLIOTHÉCAIRES ET PRÉPARATEURS D'INDEX

La série Recherches en cours de la Commission géologique paraît une fois par année; elle contient plusieurs rapports dont la portée et la nature sont comparables à ceux qui paraissent dans les revues scientifiques et autres périodiques. La plupart des articles publiés dans Recherches en cours sont accompagnés d'un résumé et d'une bibliographie, ce qui vous permettra, nous l'espérons, de cataloguer et d'indexer ces rapports, d'ou une meilleure diffusion des résultats de recherche de la Commission géologique.

GEOLOGICAL SURVEY OF CANADA
COMMISSION GÉOLOGIQUE DU CANADA
PAPER/ÉTUDE 89-1C

CURRENT RESEARCH, PART C
CANADIAN SHIELD

RECHERCHES EN COURS, PARTIE C
BOUCLIER CANADIEN

1989

Energy, Mines and Resources Canada

Énergie, Mines et Ressources Canada

Available in Canada through

authorized bookstore agents and other bookstores

or by mail from

Canadian Government Publishing Centre
Supply and Services Canada
Ottawa, Canada K1A 0S9

and from

Geological Survey of Canada offices:

601 Booth Street
Ottawa, Canada K1A 0E8

3303-33rd Street N.W
Calgary, Alberta T2L 2A7

100 West Pender Street
Vancouver, British Columbia V6B 1R8

A deposit copy of this publication is also available for reference in public libraries across Canada

Cat. No. M44-89/1C
ISBN 0-660-54776-7

Cover description

Diabase dyke swarm cutting Archean basement that is unconformably overlain by the Ramah Group (background), Torngat Mountains, Labrador. GSC 204806

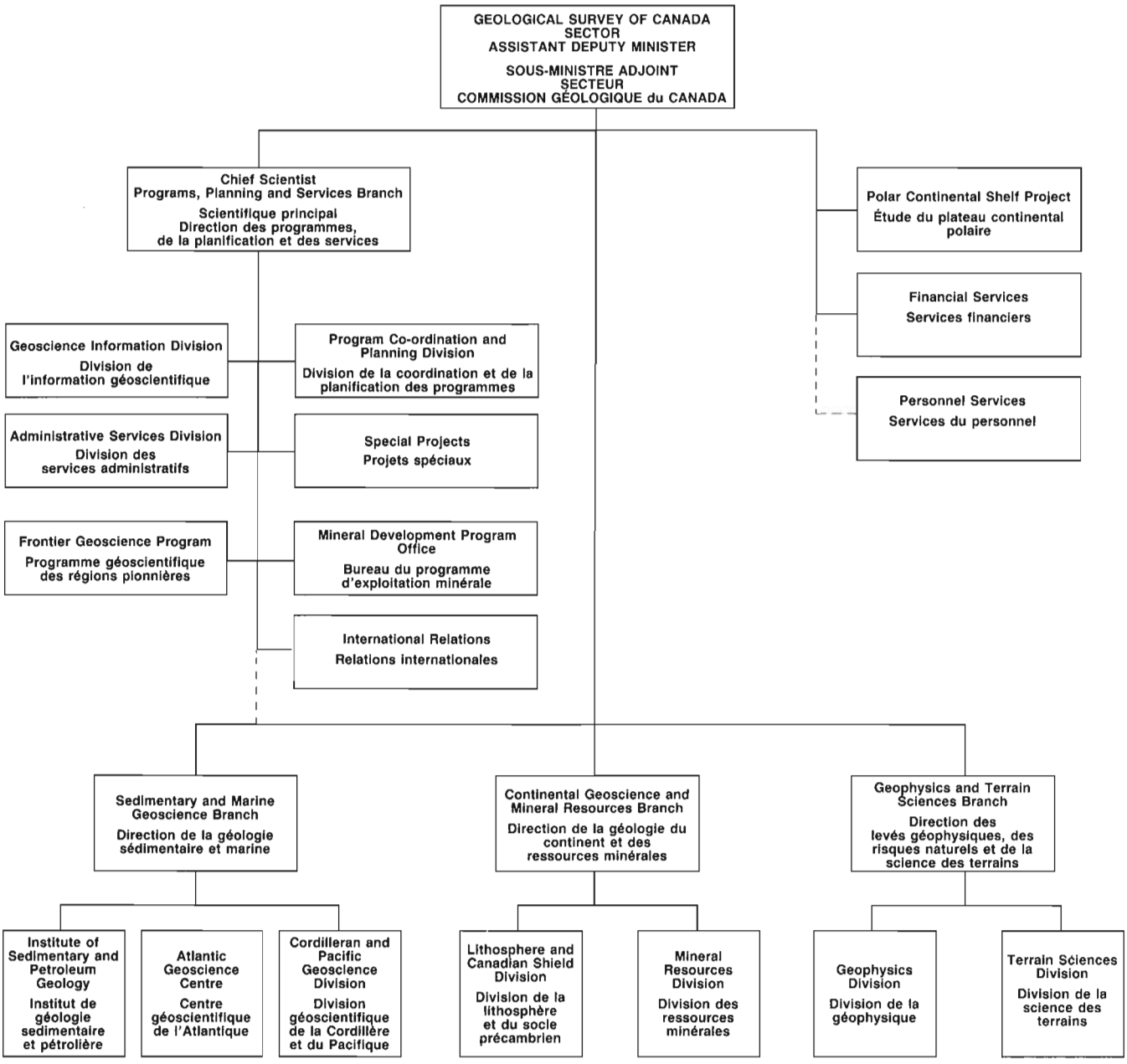
GEOLOGICAL SURVEY OF CANADA
SECTOR
ASSISTANT DEPUTY MINISTER
SOUS-MINISTRE ADJOINT
SECTEUR
COMMISSION GÉOLOGIQUE du CANADA
Chief Scientist
Programs, Planning and Services Branch
Scientifique principal
Direction des programmes,
de la planification et des services
Polar Continental Shelf Project
Étude du plateau continental polaire
Financial Services
Services financiers
Personnel Services
Services du personnel
Geoscience Information Division
Division de
l'information géoscientifique
Program Co-ordination and Planning Division
Division de la coordination et de la planification des programmes
Administrative Services Division
Division des
services administratifs
Special Projects
Projets spéciaux
Frontier Geoscience Program
Programme géoscientifique
des régions pionnières
Mineral Development Program Office
Bureau du programme
d'exploitation minérale
International Relations
Relations internationales
Sedimentary and Marine Geoscience Branch
Direction de la géologie sédimentaire et marine
Continental Geoscience and Mineral Resources Branch
Direction de la géologie du continent et des ressources minérales
Geophysics and Terrain Sciences Branch
Direction des levés géophysiques, des risques naturels et de la science des terrains
Institute of Sedimentary and Petroleum Geology
Institut de géologie sedimentaire et pétrolière
Atlantic Geoscience Centre
Centre géoscientifique de l'Atlantique
Cordilleran and Pacific Geoscience Division
Division géoscientifique de la Cordillère et du Pacifique
Lithosphere and Canadian Shield Division
Division de la lithosphère et du socle précambrien
Mineral Resources Division
Division des ressources minérales
Geophysics Division
Division de la géophysique
Terrain Sciences Division
Division de la science des terrains

Separates

A limited number of separates of the papers that appear in this volume are available by direct request to the individual authors. The addresses of the Geological Survey of Canada offices follow:

601 Booth Street,
OTTAWA, Ontario
K1A 0E8

Institute of Sedimentary and Petroleum Geology,
3303-33rd Street N.W.,
CALGARY, Alberta
T2L 2A7

Cordilleran and Pacific Geoscience Division,
100 West Pender Street,
VANCOUVER, B.C.
V6B 1R8

Pacific Geoscience Centre
P.O. Box 6000,
9860 Saanich Road
SIDNEY, B.C.
V8L 4B2

Atlantic Geoscience Centre
Bedford Institute of Oceanography,
P.O. Box 1006,
DARTMOUTH, N.S.
B2Y 4A2

Geological Survey of Canada
Institut national de la recherche scientifique
Complexe scientifique
2700, rue Einstein
C.P. 7500
Ste-Foy, Quebec
G1V 4C7

When no location accompanies an author's name in the title of a paper, the Ottawa address should be used.

Tirés à part

On peut obtenir un nombre limité de «tirés à part» des articles qui paraissent dans cette publication en s'adressant directement à chaque auteur. Les adresses des différents bureaux de la Commission géologique du Canada sont les suivantes:

601, rue Booth
OTTAWA, Ontario
K1A 0E8

Institut de géologie sédimentaire et pétrolière
3303-33rd St. N.W.,
CALGARY, Alberta
T2L 2A7

Division géoscientifique de la Cordillère et du Pacifique
100 West Pender Street,
VANCOUVER, Colombie-Britannique
V6B 1R8

Centre géoscientifique du Pacifique
B.P. 6000,
9860 Saanich Road
SIDNEY, Colombie-Britannique
V8L 4B2

Centre géoscientifique de l'Atlantique
Institut océanographique de Bedford
B.P. 1006
DARTMOUTH, Nouvelle-Écosse
B2Y 4A2

Commission géologique du Canada
Institut national de la recherche scientifique
Complexe scientifique
2700, rue Einstein
C.P. 7500
Ste-Foy, Québec
G1V 4C7

Lorsque l'adresse de l'auteur ne figure pas sous le titre d'un document, on doit alors utiliser l'adresse d'Ottawa.

CONTENTS

1 | A.F. PARK and S. RALSER
Precambrian stratigraphy and structure of the southwest part of the Tavani map area, District of Keewatin, N.W.T.

11 | R.F. EMSLIE and P.A. HUNT
The Grenvillian event: magmatism and high grade metamorphism

19 | K.M. BETHUNE
Deformation, metamorphism, diabase dykes, and the Grenville Front southwest of Sudbury, Ontario

29 | D.T. JAMES
Basement-cover relations between the Archean Yellowknife Supergroup and the Sleepy Dragon Complex north of Fenton Lake, District of Mackenzie, N.W.T.

37 | N.C. REARDON
The Mystery Island Intrusive Suite and associated alteration haloes, Great Bear Lake, District of Mackenzie, N.W.T.

43 | E. OUELLET
Cartographie détaillée de la région de la rivière du Chef, province de Grenville, Québec

49 | H.H. BOSTOCK
The significance of ultramafic inclusions in gneisses along the eastern margin of the Taltson Magmatic Zone, District of Mackenzie, N.W.T.

57 | S.M. PELECHATY and N.P. JAMES
Progress report on stratigraphy and sedimentology of the Middle Proterozoic Kanuyak Formation and underlying paleokarst, Bathurst Inlet area, northeast Slave Province, N.W.T.

67 | V. RUZICKA
Monometallic and polymetallic deposits associated with the sub-Athabasca unconformity in Saskatchewan

81 | J.E. KING, W.J. DAVIS, T. VAN NOSTRAND, and C. RELF
Archean to Proterozoic deformation and plutonism of the western Contwoyto Lake map area, central Slave Province, District of Mackenzie, N.W.T.

95 | C. RELF
Archean deformation of the Contwoyto Formation metasediments, western Contwoyto Lake area, Northwest Territories

107 | J.P. GROTZINGER, R.D. ADAMS, D.S. McCORMICK, and P. MYROW
Sequence stratigraphy, correlations between Wopmay Orogen and Kilohigok Basin, and further investigations of the Bear Creek Group (Goulburn Supergroup), District of Mackenzie, N.W.T.

121 | K.H. POULSEN, R. BROMMECKER, S.B. GREEN, K.A. BAKER, LIN BAOQIN, SHANG LING, SHEN ERSHU, ZHANG LIDONG, L. DIAMOND, and D. MARSHALL
Contrasts in setting and style of gold deposits in two Archean terranes: Rice Lake District, Canada, and western Liaoning District, China

127 | A.R. MILLER
Highlights of gold studies in the Churchill Structural Province, Kaminak greenstone belt and Hurwitz Group, District of Keewatin, N.W.T.

135 J.A. HANES, D.A. ARCHIBALD, C.J. HODGSON, and F. ROBERT
Preliminary 40Ar/39Ar geochronology and timing of Archean gold mineralization at the Sigma Mine, Val d'Or, Quebec

143 L.B. ASPLER, T.L. BURSEY, and A.R. MILLER
Sedimentology, structure and economic geology of the Poorfish-Windy thrust-fold belt, Ennadai Lake area, District of Keewatin, and the shelf to foredeep transition in the foreland of Trans-Hudson Orogen

157 N.G. CULSHAW, G. CHECK, D. CORRIGAN, J. DRAGE, R. GOWER, M.J. HAGGART, P. WALLACE, and N. WODICKA
Georgian Bay geological synthesis: Dillon to Twelve Mile Bay, Grenville Province of Ontario

165 K.H. WILCOX
Investigation of Missi metasedimentary rocks in the Amisk-Welsh lakes area, Saskatchewan

173 T.D. PETERSON, A.N. LECHEMINANT, and R.H. RAINBIRD
Preliminary report on the geology of northwestern Dubawnt Lake area, District of Keewatin, N.W.T.

185 J.R. HENDERSON, J. GROCOTT, M.N. HENDERSON, and S. PERREAULT
Tectonic history of the Lower Proterozoic Foxe-Rinkian Belt in central Baffin Island, N.W.T.

199 S.M. ROSCOE, M. STUBLEY, and D. ROACH
Archean quartz arenites and pyritic paleoplacers in the Beaulieu River supracrustal belt, Slave Structural Province, N.W.T.

215 D. MOSER
Mid-crustal structures of the Wawa gneiss terrane near Chapleau, Ontario

225 A.D. LECLAIR and G.G. POIRIER
The Kapuskasing uplift in the Kapuskasing area, Ontario

235 O.R. ECKSTRAND, L.N. GRINENKO, H.R. KROUSE, A.D. PAKTUNC, P.L. SCHWANN, and R.F.J. SCOATES
Preliminary data on sulphur isotopes and Se/S ratios, and the source of sulphur in magmatic sulphides from the Fox River Sill, Molson Dykes, and Thompson nickel deposits, northern Manitoba

243 S.S. GANDHI and A.D. PAKTUNC
Au, Pt, and Pd in pitchblende and copper sulphide veins at the Rah, Far, and Jaciar prospects, northern Bear Province, Northwest Territories

255 H.R. SCHMITT
A preliminary report on the distribution of gold in lake sediments and surficial materials at Foster Lake, Manitoba

263 S.S. GANDHI
Rhyodacite ignimbrites and breccias of the Sue-Dianne and Mar Cu-Fe-U deposits, southern Great Bear magmatic zone, Northwest Territories

275 B. DUBÉ, E.R. KOOPMAN, J.M. FRANKLIN, K.H. POULSEN, and M.R. PATTERSON
Preliminary study of the stratigraphic and structural controls of the Lyon Lake massive sulphide deposit, Wabigoon Subprovince, northwestern Ontario

285 C.D. ANGLIN and J.M. FRANKLIN
Preliminary lead isotope studies of base metal and gold mineralization in the eastern Wabigoon Subprovince, northwestern Ontario

293 C.W. JEFFERSON, C.J. BEAUMONT-SMITH, and R.L. LUSTWERK
Stratigraphic and structural settings of iron-formations and gold in the Back River area, District of Mackenzie, N.W.T.

305 C.J. MWENIFUMBO, L.H. THORLEIFSON, P.G. KILLEEN, and B. ELLIOTT
Preliminary results on the use of borehole geophysics in overburden stratigraphic mapping near Geraldton, northern Ontario

313 S.M. ROWINS, A.E. LALONDE, and E.M. CAMERON
Geology of the Archean Murdock Creek intrusion, Kirkland Lake, Ontario

325 R. BROMMECKER, K.H. POULSEN, and C.J. HODGSON
Preliminary report on the structural setting of gold at the Gunnar mine in the Beresford Lake area, Uchi Subprovince, southeastern Manitoba

333 T.D. BRACE and D.H.C. WILTON
Preliminary lithological, petrological, and geochemical investigations of the Archean Florence Lake Group, central Labrador

345 J.M. FINDLAY, T.D. FOWLER, and T.C. BIRKETT
Wakuach Gabbro sills of the Howse Lake area, western Labrador

353 R.J. WETMILLER, M. PLOUFFE, M.G. CAJKA, and H.S. HASEGAWA
Natural and mining-related seismic activity in northern Ontario

363 R.A. BURWASH and R.W. BURWASH
A radioactive heat generation map for the subsurface Precambrian of Alberta

369 F. GOODARZI, S.S. GANDHI, and L.R. SNOWDON
Bitumen in a Lower Proterozoic dolomite hosting Pb-Zn-Cu occurrences, Artillery Lake, Northwest Territories

377 R.A. FRITH, R. GRENIER, R.M. HARRAP, and M. O'DEA
Preliminary geological report of the Snowdrift map area, Slave Structural Province, District of Mackenzie, N.W.T.

385 I.F. ERMANOVICS, M. VAN KRANENDONK, L. CORRIVEAU, F. MENGEL, D. BRIDGWATER, and R. SHERLOCK
The Boundary Zone of the Nain-Churchill provinces in the North River-Nutak map areas, Labrador

395 M. SCHAU and M. DIGEL
Gossans in high grade gneisses from the Blacks Inlet area, west coast of Melville Peninsula, District of Franklin, N.W.T.

405 J.T. BURSNALL
Structural sequence from the southeastern part of the Kapuskasing Structural Zone in the vicinity of Ivanhoe Lake, Ontario

412 AUTHOR INDEX

Precambrian stratigraphy and structure of the southwest part of the Tavani map area District of Keewatin, N.W.T.[1]

Adrian F. Park[2] and Steven Ralser[2]

Park, A.F. and Ralser, S., Precambrian stratigraphy and structure of the southwest part of the Tavani map area, District of Keewatin, N.W.T.; in Current Research, Part C, Geological Survey of Canada, Paper 89-1C, p. 1-10, 1989.

Abstract

The area, southwest of Rankin Inlet, is underlain by the Archean Kaminak Group, a greenstone-metasedimentary sequence, and is overlain by the (?)Lower Proterozoic Hurwitz Group, a quartz-rich sedimentary sequence. Mafic and felsic intrusions occur throughout the area. Archean conglomerates and turbidites contain features indicative of deposition in an extensional terrane. Two phases of Archean deformation are documented. D_1 is characterized by bedding parallel high strain zones and tight, recumbent, westward facing folds. D_2 is characterized by open to tight folds and steeply dipping shear zones; both trending NE/SW. These shear zones show a complex movement history. Deposition of the overlying Hurwitz Group sediments is controlled by syn-sedimentary NE/SW and EW faulting. D_3 constitutes the NE trending folds and fabrics which occur in the Hurwitz Group sediments, and related structures in the Kaminak basement. Metamorphism is up to greenschist facies only in the area of D_1 folding.

Résumé

La région levée, au sud-ouest de l'Inlet Rankin, repose sur le groupe de Kaminak de l'Archéen, séquence de roche verte métasédimentaire, lui-même recouvert par le groupe d'Hurwitz du (?) Protérozoïque inférieur, séquence sédimentaire riche en quartz. Il y a des intrusions mafiques et felsiques dans toute la région. Des conglomérats et des sédiments de courant de turbidité de l'Archéen renferment des entités indiquant que la sédimentation s'est effectuée en zone d'extension. Deux phases de déformation pendant l'Archéen sont bien connues. La phase D_1 est caractérisée par des zones de grande déformation à stratification parallèle et des plis couchés serrés face à l'ouest. La phase D_2 est caractérisée par des plis ouverts à serrés et des zones de cisaillement à fort pendage, tous deux de direction NE-SW. Ces zones de cisaillement présentent une histoire complexe de déplacement. Le dépôt des sédiments du groupe sus-jacent d'Hurwitz est contrôlé par les failles synsédimentaires de direction NE-SW et est-ouest. D_3 représente les plis de direction nord-est et la texture des sédiments du groupe d'Hurwitz et les structures associées du socle que constitue le groupe de Kaminak. Le métamorphisme n'a atteint le stade du faciès des roches vertes que dans la zone de plissement D_1.

[1] Contribution to Canada-Northwest Territories Mineral Development Agreement 1987-91. Project carried by Geological Survey of Canada, Lithosphere and Canadian Shield Division.

[2] Department of Geology, University of New Brunswick, Fredericton, N.B., E3B 5A3.

INTRODUCTION

This report describes bedrock mapping undertaken in the southwest part of Tavani map sheet (NTS 55K/3,4,5,6; universal mercator grid is used to reference localities) at a scale of 1:16 000, during the 1988 field season. The object is to update the lithological mapping, and definition of lithological relationships, stratigraphy, and structure described in the reconnaissance survey of Heywood (1973).

Previous work

The first geological maps of the Tavani area were produced by Lord (1953) and the geology was summarized by Wright (1967). The results of helicopter reconnaissance and a comprehensive review of earlier work were produced by Heywood (1973). Results of recent mapping of the Rankin Inlet area to the northeast and a review of previous work exists in Tella et al. (1986).

ACKNOWLEDGMENTS

We thank S. Tella of the Geological Survey of Canada and P.F. Williams, Department of Geology, University of New Brunswick for organising the project; our field assistants, L. Kennedy and J. McGinn for their contribution. We also wish to thank the following: A.R. Miller, S. Gough, J. Griep for useful discussion; our expeditor, R. Bisset, and our invaluable helicopter crew V. Cobb and B. Eaton. This study was carried out under contract 23233-8-0029/01-52.

PART I — LITHOLOGY, GENERAL STATEMENT

The distribution of lithological units is shown on Figure 1. The area is underlain by the Archean Kaminak Group, a greenstone-metasedimentary sequence, (Davidson, 1970), which is overlain unconformably by the (?) Lower Proterozoic Hurwitz Group, a quartz-rich sedimentary sequence. A variety of mafic to felsic major and minor intrusions occur throughout the area. This report includes revisions to the stratigraphy presented in Heywood (1973).

Kaminak Group

The "Kaminak Group" was defined by Davidson (1970), as an assemblage of mafic to felsic metavolcanic rocks, and associated conglomerates, slate and greywacke. Here, the term is retained for the whole greenstone-metasedimentary assemblage, but the group is subdivided into two discrete formations (Last Lake formation and Mistake Bay formation; informal terms), whose relations to each other are presently unknown.

Last Lake formation

The Last Lake formation occurs on the western side of Gill Lake, extending southwest to Maze Lake, and to the southwest of Last Lake; it also occurs in the east occupying a large area inland from Tavani, north and south of the Ferguson River (Fig. 1).

Lithologies

Mafic metavolcanic rocks dominate this formation, as either pillow lavas with minor interstitial palagonite, or breccias, some of which are pillow breccias. Massive basalt flows occur, but are of minor significance. Basalts (pillowed and massive) are both porphyritic and completely aphanitic, and usually vesicular or amygdaloidal. Vesicles are filled with calcite, quartz or epidote, or occasionally K-feldspar. Minor mafic tuffs occur throughout the sequence.

Intermediate volcanic rocks (andesites) are tentatively identified in two areas (GR813006 and GR684033). They comprise massive flows which may have pillow structures at the top. Both porphyritic and aphanitic types are observed.

Felsic volcanic rocks occur throughout the area (e.g., GR710055, GR801005, GR655879). They are predominantly breccias (pyroclastic and epiclastic) which grade locally into arenites. Flow banded and massive rhyolites are commonly porphyritic.

Conglomerates occur throughout the area, but are particularly well-developed south of East Lake (GR815007) and on the Wilson River (GR816163). They are polymictic, matrix-supported deposits, with maximum clast size ranging from 2 mm to greater than 200 mm, although individual deposits show considerable variation (clasts larger than 800 mm occur on the Wilson River). The largest single conglomerate unit occurs by the Wilson River (GR816163), extending 3 km northeast along strike and reaching at least 1 km in thickness. This conglomerate grades from being granitoid-clast dominated to mafic-clast dominated. The other major conglomerate, south of East Lake, is dominated by granitoid clasts and forms the basal unit of a turbiditic sequence.

Greywackes ranging from pelite through quartz-arenite to conglomerate (maximum clast size 6 cm) show a cyclic development typical of turbidites. They are found south of East Lake and west of Gill Lake.

Quartz-arenites, ranging from quartzite to arkose, occur at GR720065, where they are interlayered with, and grade into, felsic volcaniclastic breccia. Conspicuous arkose bodies also occur south of East Lake (GR820007) and below the conglomerate along the Wilson River (GR822165).

Carbonates are a minor component occurring interstitially in the pillow lavas, and forming impersistent layers in the mafic volcanic breccia and greywacke. A layered dolomite-quartz layer associated with talc schists and pyritiferous black pelites occurs below the conglomerate at the Wilson River (GR828168).

Stratigraphy

The greywackes, with conglomerate units towards their base, always form the uppermost member of the Last Lake formation. In the underlying volcanic part of this formation only local successions can be constructed. A provisional overall stratigraphy is presented in Figure 2.

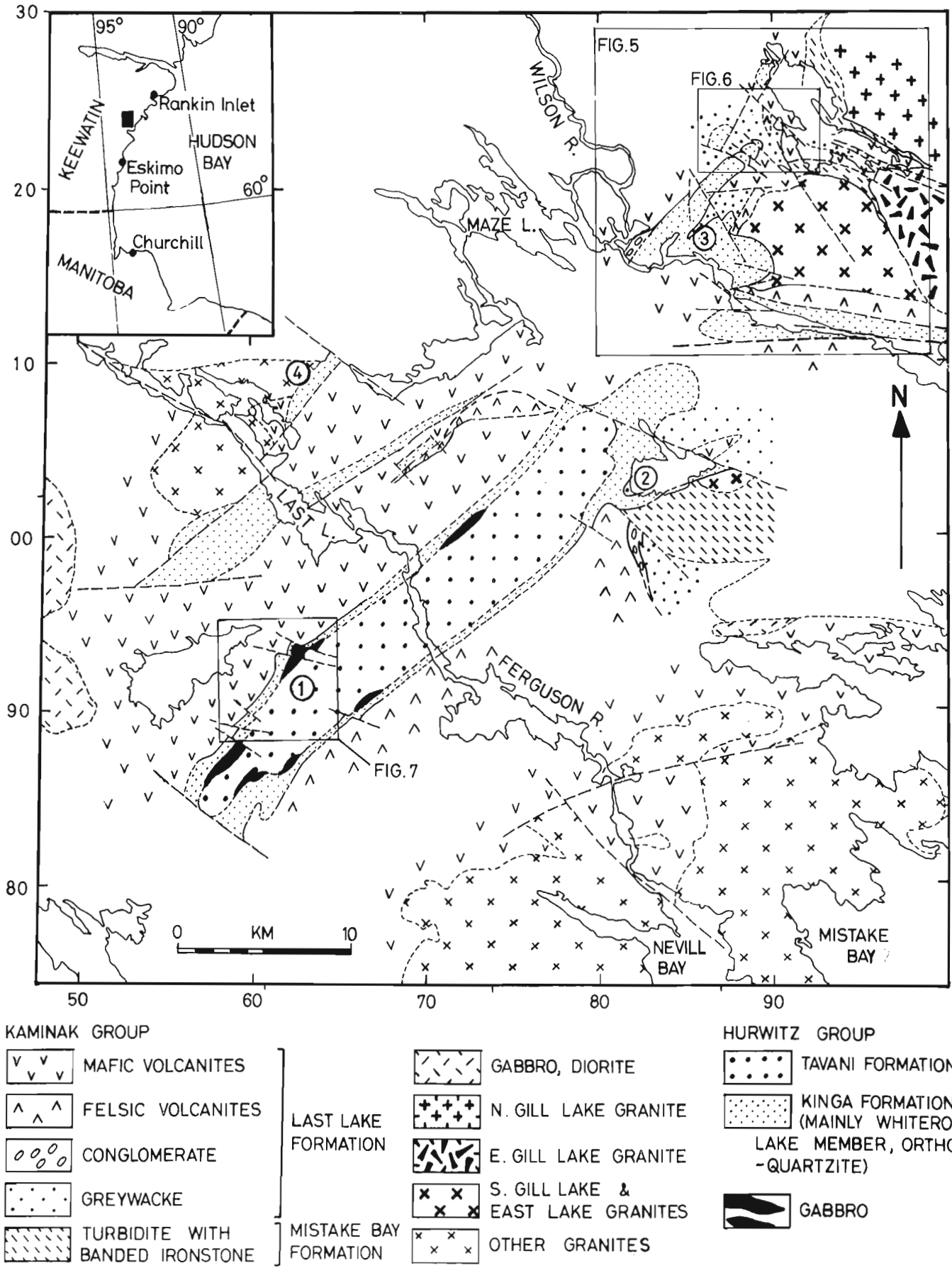

Figure 1. Simplified geology of south western Tavani map area (55K3,4,5,6; modified from Heywood, 1973). Numbers refer to location of sections in Figure 4.

Mistake Bay formation

The Mistake Bay formation occurs in an area southeast to east of East Lake (GR845024), towards Mistake Bay and around the eastern half of Gill Lake.

Lithologies

Greywackes and banded ironstone dominate this formation. Greywackes rangefrom quartzite to coarse lithic wackes and matrix-supported breccia and conglomerate. These are interlayered with fine sandstones, siltstones, shales, and laminated mudstones, showing a cyclic development; typical of turbidites (Fig. 3).

Banded ironstone form an integral part of the turbiditic cycle here (Fig. 3), complete cycles being capped by layers of magnetite and chert (± hematite ± sulphide) interbedded with laminated mudstone. Individual ironstone layers range from less than 1 to 20 millimetres, and the banded ironstone/mudstone units range from less than 10 mm to greater than 2 m.

A variety of sedimentary structures, notably slumped layers, rip-up breccias and channels are present. Volcanic ejecta (shards and bombs) occur throughout the sequence.

Mafic pillow lavas form thin layers (10-20 m) at both Gill Lake and East lake.

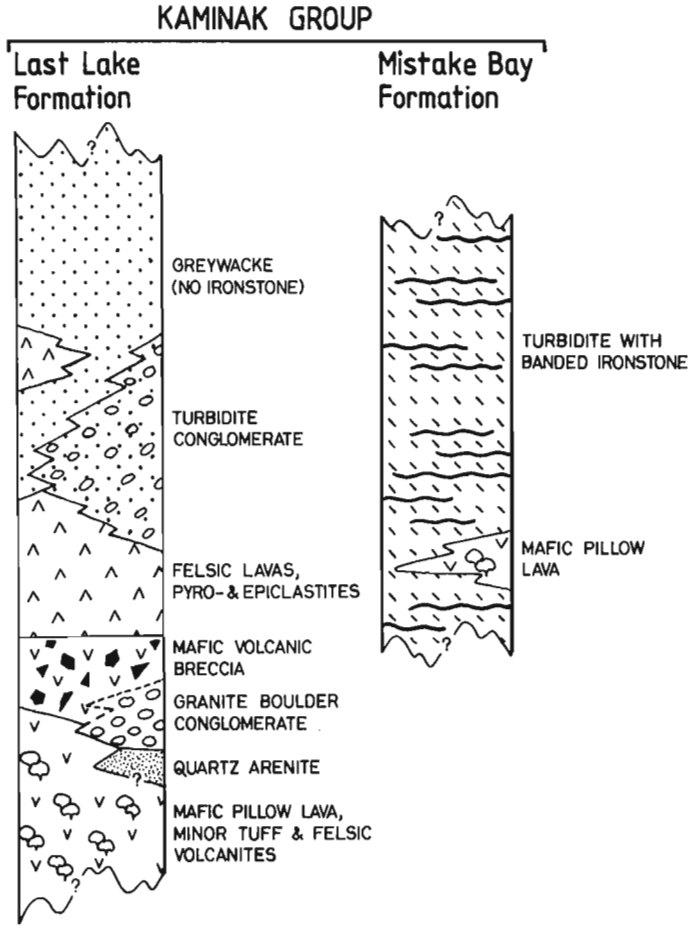

Figure 2. Kaminak Group stratigraphy.

Stratigraphy

No base or top to the Mistake Bay formation is observed. At East Lake it is fault bounded, and at Gill Lake the base is a bedding-parallel high strain zone with granite-bounded contacts. The pillow lavas occur in the exposed lower part of the succession.

The two formations are distinguished on the basis of the following criteria:-

1) Presence of banded ironstones, in the Mistake Bay formation.
2) Presence of the polymictic, granitoid-bearing conglomerate in the Last Lake formation.
3) Lack of deformation and metamorphism in the Mistake Bay formation (see below).
4) Presence of volcanic detritus throughout the Mistake Bay formation.

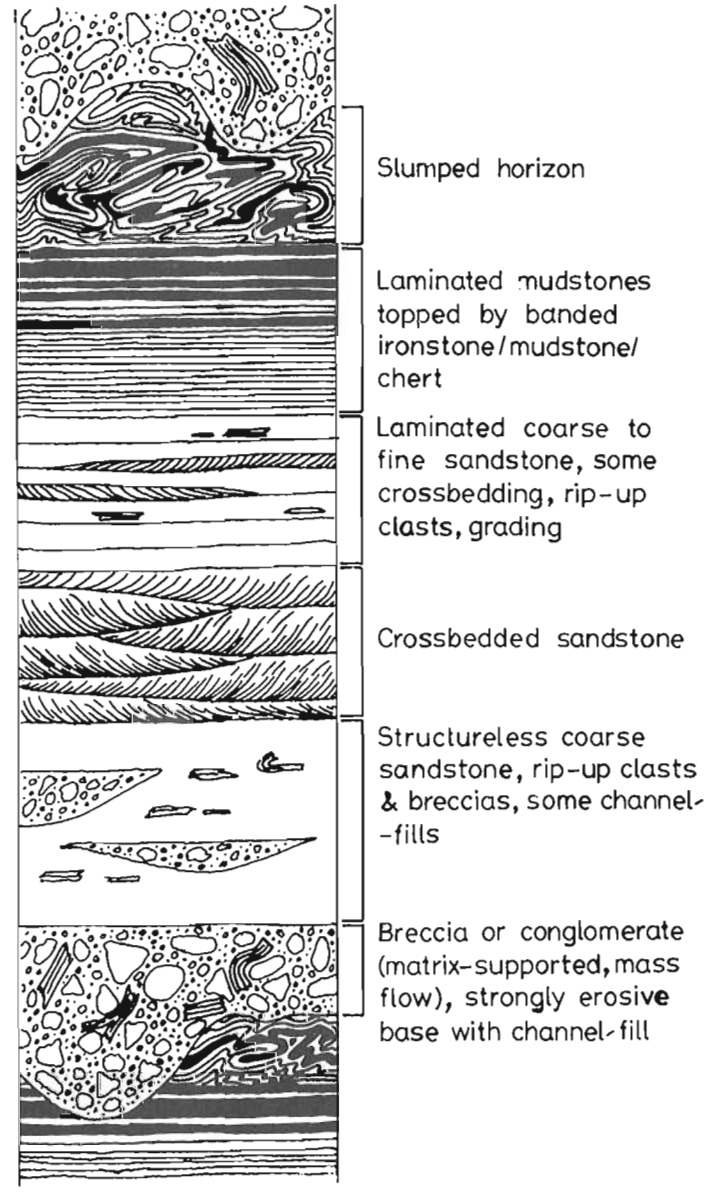

Figure 3. Characteristic depositional cycle in turbidites of the Mistake Bay formation.

Criterion 3 implies that the Mistake Bay formation may be younger than the Last Lake formation. The alternative, that the Mistake Bay formation is the equivalent to the turbiditic upper part of the Last Lake formation would require an explanation for the absence of banded ironstone and the absence of ubiquitous volcanic detritus in the latter. In the course of logging a 270-m section in the Mistake Bay formation, at East Lake, none of the facies variations recorded was found to resemble facies seen in the Last Lake formation.

Hurwitz Group

Lithologies

Outcrop of the Hurwitz Group is dominated by the Whiterock Lake Member of the Kinga Formation (Heywood 1973), which is a white, locally pink, thinly bedded, ripple-marked, orthoquartzite. Locally it is underlain by a grey quartz-arenite (GR806015), or a sequence of shales, siltstones and sandstones, variously reddened (GR8720200) (Fig. 4). The Whiterock Lake Member is overlain by a sequence of feldspathic, lithic or micaceous, white to pink quartz-arenites with minor shales and matrix-supported, polymict conglomerate. The pink lithic quartz-arenite locally contains shale rip-up clasts.

Stratigraphy

The Whiterock Lake Member and the sediments beneath it correspond to the Kinga Formation of Heywood (1973), while the sediments above correspond to the Tavani Formation. No evidence for the existence of the intervening Ameto Formation proposed by Heywood (1973) was found in situ during this field season. There is no field evidence to suggest that the volcanic rocks ascribed to the Happoytiyik Member at Last Lake (Heywood, 1973; Ridler, 1974) belong to the Hurwitz Group; in this report they are considered to be part of the Kaminak Group (Last Lake formation).

Intrusive Rocks

Mafic Intrusions

Gabbros, usually deformed, occur throughout the mafic volcanic rocks of the Last Lake formation (Kaminak Group). Individual bodies vary in size from metres to hundreds of metres. No internal structures, e.g., banding or layering, are observed; instead they are foliated to varying degrees. Grainsize varies from less than 2 mm to more than 5 mm. They are usually sulphide-bearing.

A group of fine-and even-grained gabbros occurs near the contact of theKinga and Tavani formations in the Hurwitz Group. They do not carry a tectonic fabric, but are extensively altered with epidote being abundant. Sulphides occur sporadically throughout.

Intermediate intrusions

Dioritic or quartz-dioritic intrusions occur in the pillow lavas of the Last Lake formation at the northwest end of Gill Lake. One variety is porphyritic with large (up to 10mm) laths of feldspar locally defining flow banding.

Felsic intrusions

Four granitoid plutons are defined, one each south, east and north of Gill Lake, and a body east of East Lake (GR873035).

The North Gill Lake pluton consists of a medium (2-5 mm), even grained granodiorite. The marginal zone along the southern contact is foliated, and its contact with country rock is either agmatite or "schollen migmatite" (Mehnert, 1968).

The East Gill Lake pluton consists of a medium grained, porphyritic granite, with a groundmass grain size around 3 to 4 mm, with pink K-feldspar phenocrysts up to 15 mm long, occasionally rimmed with white plagioclase. Much of this granite is weakly foliated. The contact with the country rock is ill-defined; sheets of granite extend into the country rock, which itself forms extensive rafts in the granite across a zone 50 to 100 m wide. Isolated granite sheets extend further into the country rock.

The South Gill Lake pluton consists of a medium (2-5 mm), even-grained granite that is locally foliated. Feldspars and mafic minerals are extensively altered. The northern and southern contacts are sharp with a few apophyses into the country rock, and a few xenoliths. The eastern and western contacts are poorly exposed, but isolated outcrop

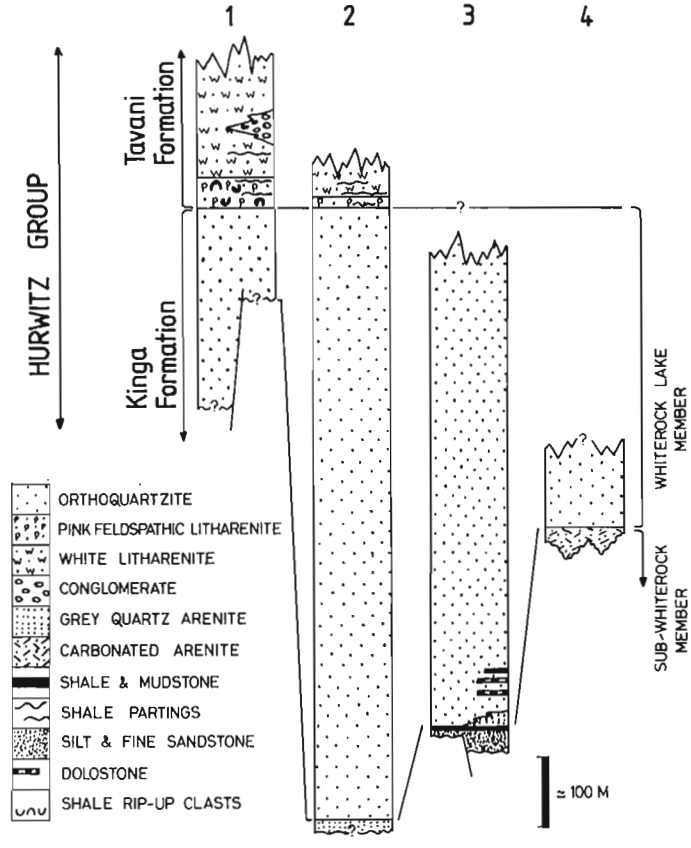

Figure 4. Hurwitz Group stratigraphy; see Figure 1 for location of stratigraphic sections.

suggests that the eastern contact is separated from the East Gill Lake pluton by screens of metasediment. A contact metamorphic aureole is developed and is especially apparent as hornfels in the metagreywackes to the north (see below).

The East Lake pluton, resembles the South Gill Lake pluton but is more extensively altered. Contacts are sharp and a narrow thermal aureole is developed.

Porphyries, both quartz and feldspar bearing are widespread in the mafic volcanic member of Last Lake formation. They form sheets up to 2 to 3 m thick and tens of metres long. They are usually foliated. Field relationships north of Gill Lake suggest a possible affinity with the North Gill Lake pluton.

Plagiogranite (trondhjemite?) occurs as irregular discordant sheets around the northwest end of Gill Lake (GR907275). The sheets are foliated and appear to be related to local intermediate intrusions.

Microgranites, both foliated and non-foliated are common south and northeast of Gill Lake. The foliated microgranites are concordant to the foliation in the country rock and appear to be related to the North Gill Lake pluton. The non-foliated microgranites are discordant to fabrics in the country rocks.

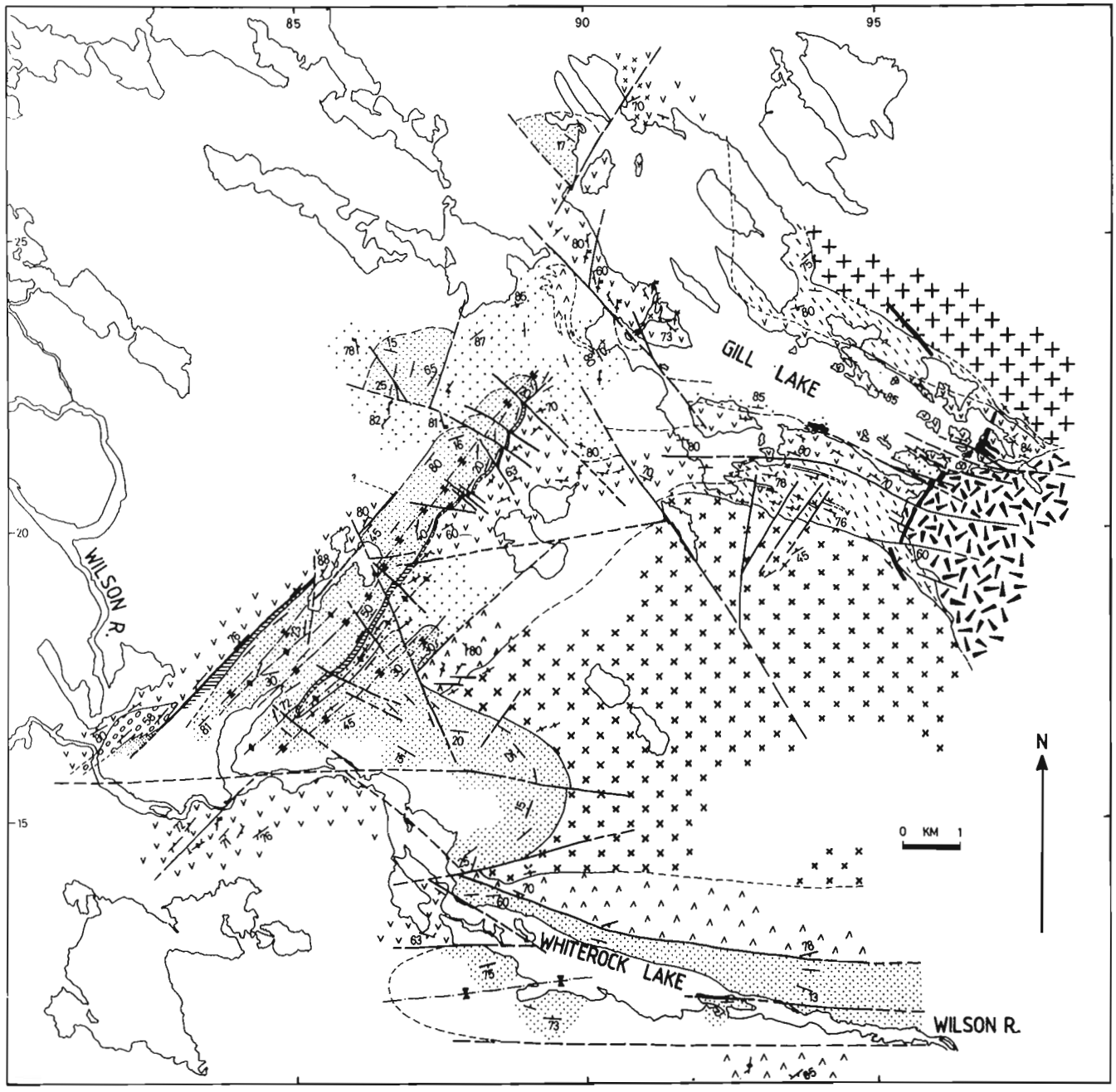

Figure 5. Geological map of Wilson River-Gill Lake area; see Figure 1 for location of map.

Legend (Figure 5)

KAMINAK GROUP (Archean)

MAFIC VOLCANIC ROCKS; MASSIVE & PILLOW BASALT, TUFF & BRECCIA, MINOR MAFIC INTRUSIONS

FELSIC VOLCANIC ROCK; LAVA, PYRO- & EPI-CLASTIC DEPOSITS

GREYWACKE; SLATES, ARKOSE, MINOR CONGLOMERATE & CARBONATE

QUARTZ ARENITE

CONGLOMERATE

TURBIDITE WITH BANDED IRONSTONE

INTRUSIONS (?Archean?)

PRE-(?) & SYNTECTONIC BODIES, FELSIC TO DIORITIC

SYNTECTONIC (D_1, ?D_2) GRANITOIDS (N. GILL LAKE PLUTON)

SYN- & LATE TECTONIC (D_2) GRANITOIDS (E. GILL LAKE PLUTON)

POST-TECTONIC (D_2) GRANITOIDS (S. GILL LAKE PLUTON)

HURWITZ GROUP (Proterozoic)

SHALE, SILTSTONE, SANDSTONE VARIABLY REDDENED

ORTHOQUARTZITE

POST-TECTONIC MAFIC DYKES

BEDDING, OVERTURNED, VERTICAL, YOUNGING

SCHISTOSITY/CLEAVAGE, $S_{1,2,3}$

FOLD AXIAL TRACE, ANTICLINE, SYNCLINE

FAULT, OBSERVED, INFERRED

BOUNDARY, OBSERVED, INFERRED

Mafic Dykes

Two types of mafic dykes are present: narrow (less than one metre), foliated biotite lamprophyres are present around Gill Lake, while larger (up to 20 m wide) basalt-dolerite, locally gabbroic or luecodoleritic dykes, are more extensive. A centre of sorts appears to exist in East Gill Lake (GR968215), from which dykes run west-northwest, north-northeast and south. Zoned plagioclase megacrysts (up to 15 cm), and xenoliths of leucogabbro and anorthosite are common. These dykes locally display sheared, chilled margins, with internal shear zones.

PART 2: STRUCTURE AND METAMORPHISM

The structure of the area is dominated by ductile and brittle shear zones. Polyphase folding is only evident in the northwest (west of Gill Lake; Fig. 5,6). Some shear zone development can be related to this folding, but independent shear zone activity is also evident. Three generations of deformational fabrics (D_1-D_3) are recognized on the basis of refolding and overprinting relationships. The use of D_n should not be taken to represent discrete deformation episodes.

D_1

The products of D_1 take two forms. Layer-parallel high strain zones, especially south and north of Gill Lake, are characterized by the development of a composite ($S_{0\text{-}1}$) schistosity, considered to represent transposed bedding. Phyllonites, mylonites and ultramylonites are developed from gabbro, pillow lavas, mafic volcanic breccia and quartz-feldspar porphyry parallel to $S_{0\text{-}1}$. ?Pseudotachylite is locally developed in mylonitized gabbro. Stretching and mineral lineations are widespread in $S_{0\text{-}1}$ and all are now steep. These high strain zones (shear zones) are commonly developed in the mafic volcanic rocks and gabbros of the Last Lake formation in the Kaminak Group, but along the north shore of Gill Lake such a zone is seen as the interface between the two formations. These high strain zones may represent originally horizontal detachments.

The second form of D_1 is seen where F_1 folds are developed in the greywackes of the Last Lake formation (west of Gill Lake, GR895220). F_1 fold closures are not directly observed, but their presence is deduced from the occurrence of changes of structural facing directions in S_2 (facing here is defined as the younging direction normal to S_0 in a specified cleavage plane (S_n)), and changes in vergence of S_1 and S_0. S_1 is a slaty cleavage (lithons not visible) in pelites, always oblique to S_0, and a fracture cleavage (spacing of 5 to 20 mm) in psammites. Some pelite layers (GR893222) contain an earlier slaty cleavage (S_e), crenulated by S_1. The significance of S_e is presently unknown.

F_1 folds are tight, recumbant, but not isoclinal, and appear to face west (cf. Fig. 6).

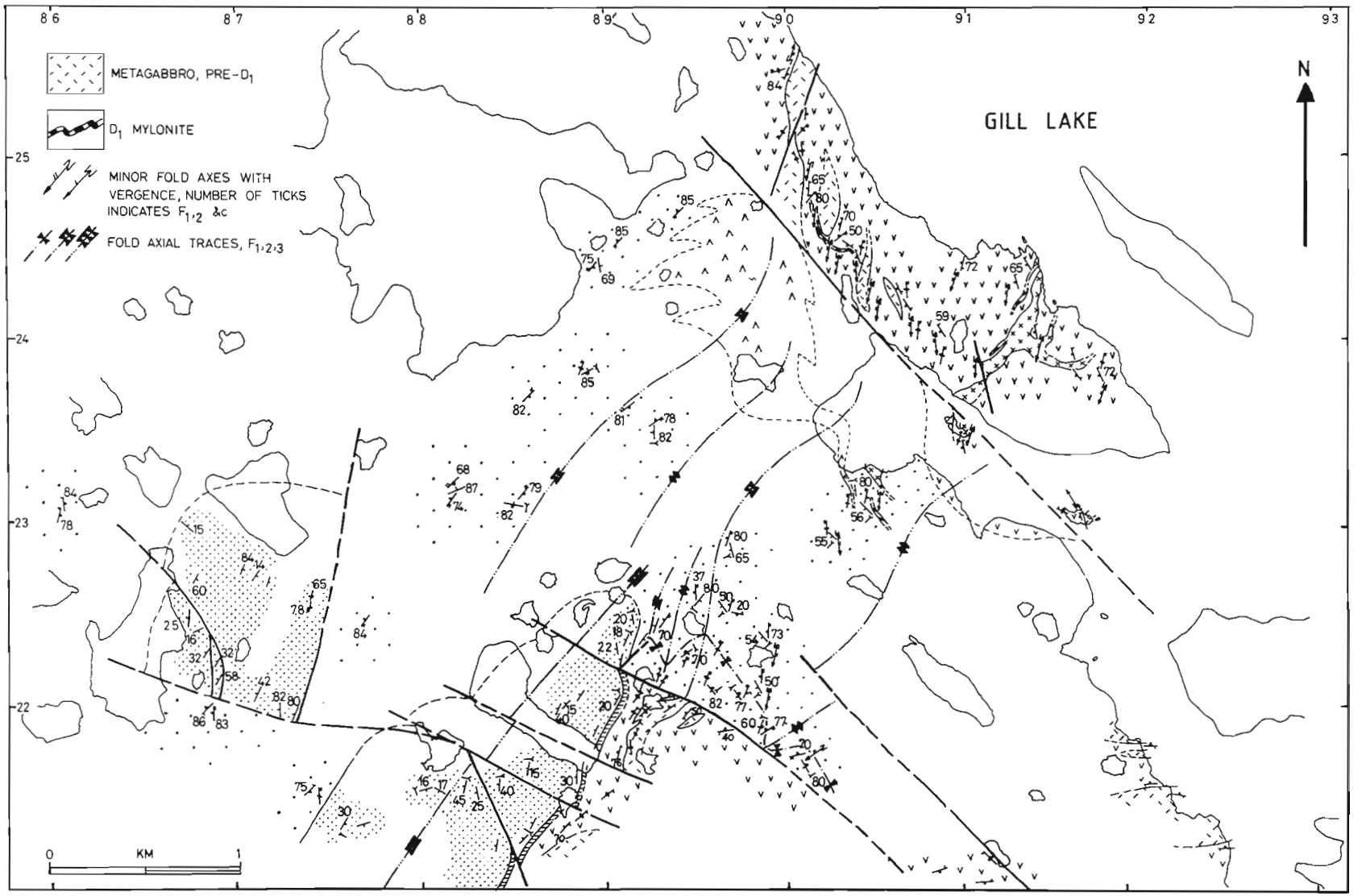

Figure 6. Geological/structural map of an area southwest of Gill Lake; see Figure 1 for location of map; see Figure 5 for legend.

D_2

D_2 is expressed as open to tight folds with an axial planar cleavage (S_2) and steeply dipping shear zones; S2 and the shear zones trend northeast. At GR895220 F_2 folds are present, folding S_1 and refolding S_0 (Fig. 6).

S_2 is a spaced cleavage in both pelites (spacing of 2 to 5 mm) and psammites (spacing of 5 to 20 mm), locally crenulating S_1. Whether S_2 is a fracture or differentiated cleavage is presently unclear.

The northeast-trending shear zones dominate the whole area. A steep stretching lineation is present in the larger of these zones; shear sense has yet to be determined. Minor shear zones with this trend usually contain a horizontal stretching lineation and show a sinistral shear sense. Whether this horizontal movement is strictly D2 is uncertain.

D_3

The sub-Hurwitz unconformity cuts D_2 and earlier structures. D_3 constitutes the folds and fabrics found in sediments of the Hurwitz Group, and reactivated northeast- and east-trending related shear zones in the Kaminak Group basement.

F_3 fold geometry is commonly open, but also showing overturning, with the overturned limbs locally sheared out. All F_3 folds trend northeast and have vertical to subvertical axial planes. S_3 is an irregularly developed axial planar cleavage ranging from a coarse fracture cleavage or intense jointing (spacing of up to 100 mm) to a differentiated cleavage. S_3 is strongest in the sub-Whiterock Member of the Kinga Formation, where it is a fracture cleavage (spacing of 0.5 to 5 mm) in impure, micaceous silts and sandstones, or a slaty cleavage in shale. The slaty cleavage is also developed in the shales and mudclasts of the Tavani Formation.

A conspicuous bedding-parallel stretching lineation is locally developed in the Whiterock orthoquartzite. Other stretching lineations are seen locally onthe S_3 cleavage and in the phyllonitic fabric developed in the sheared out limbs of F3 folds.

Shear zones and faults affect sediments of the Hurwitz Group and its' basement. Some of these carry evidence of reactivation at various times. Growth faulting is apparent during the deposition of both the sub-Whiterock Member and the Whiterock orthoquartzite in the Kinga Formation. This is evidenced by significant changes in thickness across faults at GR615934 (Fig. 7) and GR871195 (Fig. 5). At GR615934 (Fig. 7) more than 300 m of Whiterock Quartzite is present south of the fault, while less than 100 m is found north of the fault. At GR871195 (Fig. 5) there is no evidence for a change in thickness in the Whiterock Quartzite, but thickness of the sub-Whiterock member is reduced by two thirds by the omission of beds north of the fault. In both cases post-depositional reactivation of these faults is evident.

The regionally developed northeast- and east-trending sets of shear zones and faults affect the Hurwitz sediments. Movements on both sets possibly influenced the location of Hurwitz depo-centres. This movement was both syn- and post-depositional. The apparent lack of intragranular deformation in the orthoquartzite suggests this movement began prior to lithification. Many of the F_3 folds in the orthoquartzite appear to be an expression of the reactivation of D_2 shear zones in the sub-Hurwitz basement.

Subsequent movement on both shear zone sets was brittle, with the northeast trending set displaying a sinistral and the east-west set a dextral shear sense.

Post-D_3

Post D_3 movement is evident on both shear zone sets. Movement on these shear zones offsets the axial traces of F_3 folds. Some of these late movements postdate the emplacement of the late mafic dykes.

Relationship of intrusive rocks to structural evolution

The presence or absence of foliations, shear zones and cross-cutting relationships permits the relative timing of

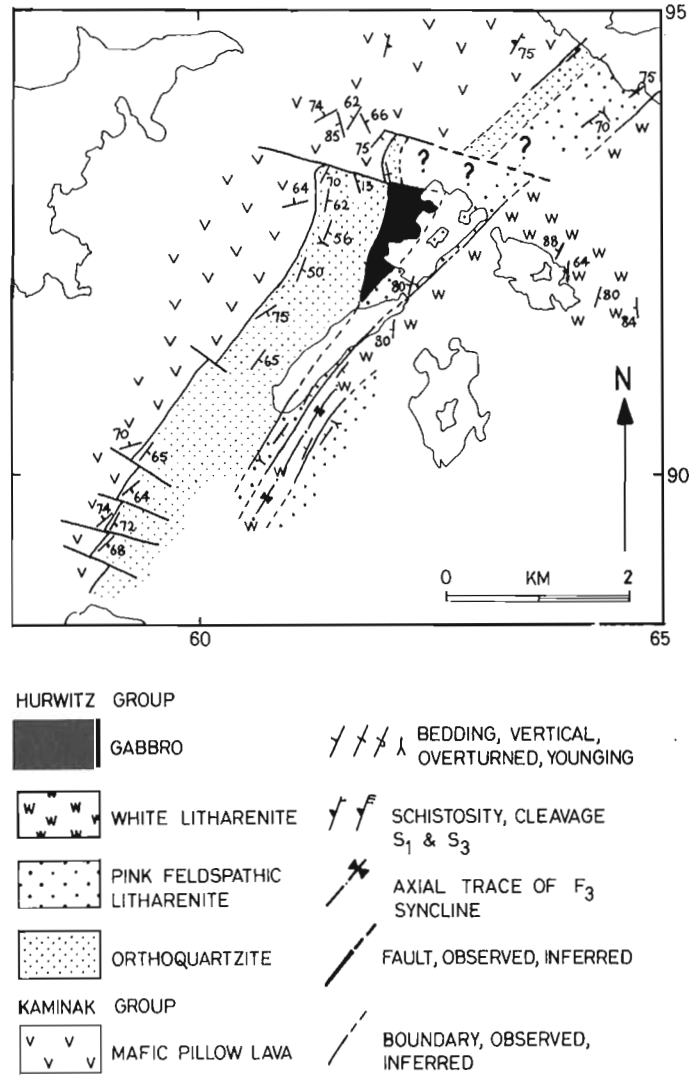

Figure 7. Geological map of an area south of Last Lake, showing growthfaulting affecting the Hurwitz Group on the margin of an F_3 syncline; see Figure 1 for location of map.

Table 1. Structural framework for the geological evolution of the southwest Tavani map area.

Style of Faulting	Deformation Event	Intrusions	Sedimentary Deposition
Faulting Horizontal Lineation			
		Mafic Dykes	
	D_3	Gabbros	
			Hurwitz Group
Faulting Steep Lineation			
		East Lake Granite	
		South Gill Lake Granite	
		East Gill Lake Granite	
Shearing Steep Lineation	D_2		
		North Gill Lake Granite	
Layer Parallel Shearing	D_1		
		Porphyries	
Extension		Gabbros	Kaminak Group

granitoid intrusion to deformation (Table 1). Dating of these intrusions will permit a radiometric calibration of the timescale.

Regional metamorphism

Preliminary observations indicate that most of the area underwent very little or no metamorphic recrystallization. West of Gill Lake greenschist facies metamorphism is evidently pre-D_2 and in strongly deformed pelitic greywacke north of the Wilson River, muscovite and biotite are present. Chlorite is found in most mafic rocks, but its relationship to fabric development is unknown and should not be assumed to represent regional metamorphic mineral growth.

Contact metamorphism

Hornfels is developed in greywackes around the South and the North Gill Lake plutons and the East Lake pluton. This hornfels is characterized by the lack of fissility in the pelitic greywacke and the local appearance of porphyroblasts. A hornfels zone (approximately 10 m wide) is present on the unfaulted southern side of the East Lake pluton. The north and south Gill Lake plutons are also associated with hornfels zones between 10 and 500 m wide, but in both cases these are fault bounded.

Veins

Veins are found in all lithologies and have a variety of mineral fills. The simplest are quartz or quartz+carbonate veins with or without sulphide (commonly pyrite). More complex veins typically display the effects of repeated movement and mineralization. Examples of such complex veins cut the Last Lake formation and the South Gill Lake granitoid. These veins trend both northeast and east-west in shear zones and typically have an early fill of calcite and a green fibrous amphibole. This early fill has undergone cataclasis prior to the injection of quartz-carbonate or quartz with sulphide (pyrite + galena ± chalcopyrite). En echelon quartz-vein arrays are a late stage feature.

CONCLUSIONS

The structural framework for the geological evolution of this area is outlined in Table 1. The conclusions to be drawn at this stage are:

1) Two distinct formations are recognised in the Kaminak Group, though their mutual relationships are at present unknown.

2) The recognition of growth faults in the Mistake Bay formation suggests deposition in some form of extensional regime. The presence of conglomerates throughout both the Mistake Bay formation and the Last Lake formation, and the products of bimodal volcanism are all consistent with such a model.

3) $D_{1\text{-}2}$ deformation and contemporaneous metamorphism are both heterogeneously expressed across the area. A framework encompassing the F_1 folds and the layer-parallel shear zones cannot be constructed at present: these zones may represent extensional or compressional features. D_2 and subsequent deformation occurred within a crustal regime dominated by NE-SW and E-W trending shear zones.

4) D_2 and later movement on NE-SW and E-W trending shear zones influenced, the deposition of the sediments of the Hurwitz Group, and vein mineralisation.

5) Revision of Hurwitz Group stratigraphy suggests that there is no local representative of the Ameto Formation, particularly the mafic volcanic rocks of the Happoytiyik Member, formerly identified NE of Last Lake. These mafic volcanites are now included in the Last Lake formation of the Kaminak Group.

REFERENCES

Davidson, A.
1970: Precambrian geology, Kaminak Lake map area, District of Keewatin; Geological Survey of Canada Paper 69-51.

Heywood, W.W.
1973: Geology of Tavani map-area, District of Keewatin; Geological Survey of Canada Paper 72-47.

Lord, C.S.
1953: Geological Notes on Southern District of Keewatin, Northwest Territories; Geological Survey of Canada, Paper 53-22.

Menhert, K.R.
1968: Migmatites and the Origin of Granitic Rocks, Amsterdam, Elsevier.

Ridler, R.H.
1974: Shallow marine plateau basalts of the Aphebian Hurwitz Group at Last Lake, District of Keewatin; in Report of Activities, Part B, Geological Survey of Canada, Paper 74-1B, p. 195-199.

Tella, S., Annesley, I.R., Borradaile, G.J., and Henderson, J.R.
1986: Precambrian geology of parts of Tavani, Marble Island, and Chesterfield Inlet map areas, District of Keewatin: a progress report; Geological Survey of Canada Paper 86-13.

Wright, G.M.
1967: Geology of the southeastern barren grounds, Parts of the District of Mackenzie and Keewatin; Geological Survey of Canada, Memoir 350.

The Grenvillian event: magmatism and high grade metamorphism

R.F. Emslie and P.A. Hunt
Lithosphere and Canadian Shield Division

Emslie, R.F. and Hunt, P.A., The Grenvillian event: magmatism and high grade metamorphism; in Current Research, Part C, Geological Survey of Canada, Paper 89-1C, p. 11-17, 1989.

Abstract

One hallmark of the Grenvillian event is high grade regional metamorphism that reached peak intensity over a broad region about 1.1 Ga ago. The most widespread, characteristic plutonic igneous activity in the Grenville Province comprises rocks of anorthosite-mangerite-charnockite-granite (AMCG) suites. U-Pb zircon dates from sampling of the major complexes indicate they were intruded during at least three distinct periods at ~1.64, ~1.36, and ~1.16-1.13 Ga. The predominant younger magmatic episode, concentrated in the central part of the province, can be regarded as inaugurating the Grenvillian event which also included one or more subsequent intense thermal pulses, severe crustal deformation, uplift and cooling that affected much of the Grenville Province. High grade metamorphic terranes developed thermal peaks some 50-100 Ma after peak magmatic intensity, denoting a lag in regional heating of the crust that may be explained by existence of a thick, stabilized, subcontinental lithosphere prior to AMCG magmatism.

Résumé

L'un des faits marquants de l'épisode de Grenville a été le métamorphisme régional de forte intensité qui a atteint un maximum dans une région étendue il y a environ 1,1 Ga. L'activité plutonique ignée caractéristique la plus répandue dans la province de Grenville a donné les roches des suites anorthosite-mangérite-charnockite-granite. Les datations U-Pb faites sur le zircon lors d'un échantillonnage de reconnaissance des complexes intrusifs majeurs indiquent qu'ils ont été mis en place pendant au moins trois périodes distinctes il y a environ 1,64, 1,36 et de 1,16 à 1,13 Ga. L'épisode magmatique prédominant le plus ancien, concentré dans la partie centrale de la province, peut être considéré comme ayant amorcé l'épisode de Grenville qui a également englobé une ou plusieurs intenses pulsations thermiques ultérieures, une intense déformation de la croûte et un soulèvement suivi d'un refroidissement qui ont touché une grande partie de la province de Grenville. Environ 50 à 100 Ma après le maximum de l'intensité de l'épisode magmatique, des maximums thermiques se sont manifestés dans les terranes ayant subi un métamorphisme de forte intensité, ce qui indique un retard du réchauffement régional de la croûte qui peut-être expliqué par l'existence d'une épaisse lithosphère subcontinentale stabilisée, antérieure au magmatisme des roches des suites sus-mentionnées.

INTRODUCTION

Rocks that constitute the Grenville Structural Province range in age mainly from Archean to late middle Proterozoic. The wide range of rock ages coupled with attendant polyphase deformation and metamorphism has repeatedly confounded attempts to define precisely what processes the Grenvillian event (or Grenville "orogeny") comprised. A major preoccupation in the Grenville Province has been directed toward sorting out the extended, fragmented history of rocks formed prior to the Grenvillian event (e.g. Wynne-Edwards, 1972; Doig, 1977; Roy et al., 1986; van Breemen et al., 1986). This is an important and necessary pursuit but to some extent it tends to obscure, and deflect attention from, the character of the Grenville event as that term is applied here.

A common view of the Grenvillian "orogeny" has been that of an extended sequence of events beginning perhaps with deposition of the Grenville Supergroup and other sedimentary and volcanic units prior to 1.2 Ga and culminating in uplift, erosion and cooling by about 1.0 Ga (classic orogenic "cycle", e.g. Moore and Thompson, 1980). Stockwell (1982) defined the Grenville Orogeny more narrowly as..."the last period of important widespread folding and closely related regional metamorphism and granitic and pegmatitic intrusions in the Grenville Province". He estimated the start of orogeny at about 1137 ± 17 Ma using the oldest $^{207}Pb/^{206}Pb$ ratio from a cluster of zircon and sphene data then available. Workers in the Adirondacks have tended to equate the Grenville Orogeny with the ~1.1 to 1.0 Ga metamorphic peak regarding the AMCG suites as pre-Grenvillian, e.g. McLelland and Isachsen (1986).

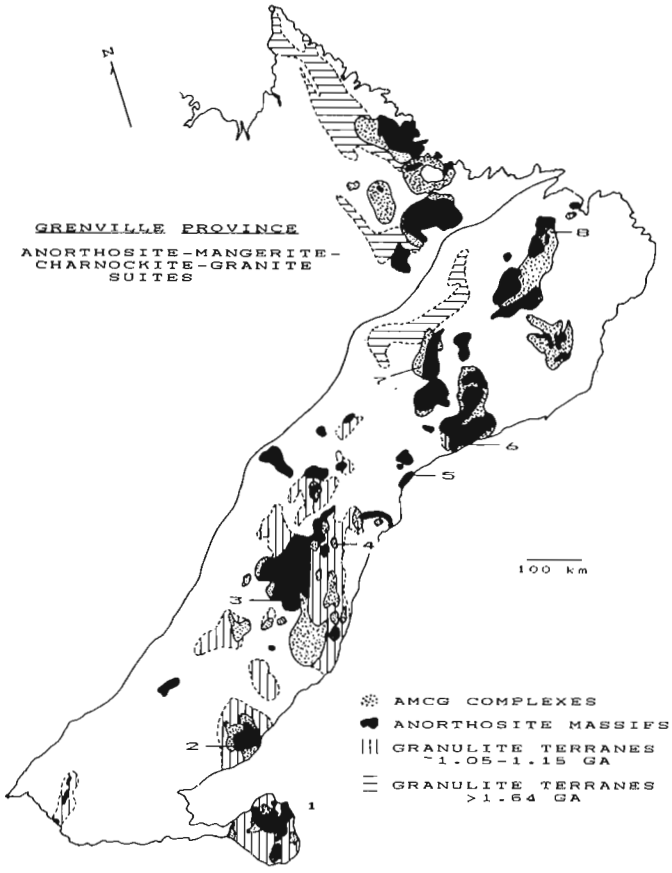

Figure 1. Major mid-Proterozoic anorthosite-mangerite-charnockite-granite (AMCG) suites and major granulite terranes of the Grenville Province and nearby regions. 1) Adirondacks, 2) Morin, 3) Lac St. Jean, 4) Labrieville area, 5) Rivière Pentecote, 6) Lac Allard, 7) Atikonak River, 8) Mealy Mountains.

Historically, the focus of attention with respect to the Grenvillian event has been directed toward deformational effects, regional metamorphism, and late cooling history as reflected mainly by K-Ar mineral ages. Magmatic activity specific to the Grenvillian event has for the most part been only loosely characterized except for local detailed studies. Widespread presence of rocks of igneous anorthosite-mangerite-charnockite-granite (AMCG) suites has been recognized for many years in the Grenville Province (Fig. 1) but their ages are also known to span a time interval of at least 500 Ma (e.g. Emslie et al. 1983). Igneous mangerite and charnockite, as used here, exclude those rocks of igneous origin that achieved charnockitic character only after a granulite grade metamorphic event. Knowledge of the relative abundance of these igneous suites and their distribution with respect to time is needed to establish their relevance to the Grenvillian event. A recent review by Moore (1986) commented, with regard to the Grenville Orogeny ...(p.4), .."Thus it must be viewed primarily as a deformational and metamorphic event in which plutonism has played only a minor role."... and (p.8),... "major plutonic emplacement is, however, *not* a characteristic feature of the Grenvillian Orogeny". These perceptions have been founded largely on evidence from the extreme southwest and extreme northeast of the Grenville Province. The data and viewpoint discussed here relies more heavily on evidence from the central part of the Province and is in direct conflict with that interpretation. Recent geochronological and isotopic studies (Ruiz et al., 1988; Lumbers et al., 1988) suggest that evidence for an important crust-forming event associated with the Grenville Orogeny may yet emerge but it is likely to have been older than 1.2 Ga. A significant crust-forming event is, almost by definition, orogeny and until that aspect is clarified, it may be prudent to designate the post 1.2 Ga magmatic-metamorphic episodes informally as a Grenvillian event.

Estimation of the ages of AMCG suites in the Grenville Province should be a useful first step in distinguishing those that can clearly be related to the Grenvillian event from others that predate it and will permit better understanding of the processes involved. New results directed toward that end are summarized here and preliminary interpretation is offered. A more detailed picture will undoubtedly emerge as further data are accumulated and collated.

GRENVILLIAN MAGMATISM

Voluminous calcalkalic igneous suites that can be related directly to the Grenvillian event are notably absent. Physical evidence for addition of primary calcalkalic igneous arc rocks appears to be limited in amount and is older than 1.2 Ga, i.e. "pre-Grenvillian event". Anorogenic stocks and

small batholiths are known to precede, and can be identified with later stages of, the Grenvillian event. Although the main pulse of Grenvillian AMCG magmatism took place prior to 1100 Ma, magmatism of anorogenic character continued sporadically on a much reduced scale for as much as 150 Ma thereafter.

Critical assessment of Rb-Sr whole rock ages and available U-Pb zircon ages for granitoid rocks of the Central Metasedimentary Belt by Heaman et al.(1986) suggests that magmatism related to the Grenvillian event in that region fell in the range 1125 to 925 Ma. This is on the younger side of the AMCG magmatic activity reported here, occurred on a much smaller scale, and evidently overlapped in time the peak of high grade metamorphism in the central part of the Grenville Province. Granitic and some charnockitic magmatism, also on a reduced scale, occurs in a like time interval in the central part of the Grenville Province and is even rarer in the northeastern part (Gower and Loveridge, 1987; Schärer and Gower, 1988).

AMCG Suites

Igneous mangerite-charnockite-granite suites and related rocks associated with massif anorthosites are alkali-calcic in character (Emslie, 1978; Anderson, 1983). Unlike anatectic magmas formed under relatively wet conditions, parent magmas of these suites had compositions different from wet granite minima and the rocks show mineral evidence of much higher temperatures of generation and crystallization; the magmas do however, evolve toward increasing water contents and may approach fluid-saturated minima at late stages. Because they crystallized, at least in early stages, at high temperatures from relatively alkali-rich magmas, the likelihood of preservation of older relict zircon cores is less likely than in calc-alkalic magmas (Watson and Harrison, 1983). In addition, these igneous charnockitic suites are typically low in U and accordingly crystallized low U zircons which are less susceptible to disturbance by succeeding events. Both these features lead to anticipation that igneous charnockitic zircons may provide superior estimates of the crystallization ages of the rocks.

The sample collection reported upon here is in generally good accord with these expectations. Only one sample from the Atikonak River massif was found clearly to contain a significant, older, inherited component with an upper intercept age near 1.65 Ga, in good agreement with numerous published ages from a broad region adjacent to the north (see Schärer et al., 1986; Schärer and Gower, 1988). That rock is a pyroxene quartz monzonite; a related younger rapakivi granite member of the same suite (presumably crystallized from a more evolved alkali-enriched magma) exhibited no evidence of an older zircon component.

Isotopic ages from most parts of the Grenville Province are faced with the question of what effect high grade metamorphism may have played in partly or totally resetting primary crystallization ages. Although incontrovertible proof is rarely available, the following arguments can be offered in support of igneous crystallization ages for the samples studied:

1. Rock samples were chosen because macroscopically and microscopically they had massive igneous textures with little obvious alteration.
2. Most zircons have prismatic habits, commonly with well-developed faces and terminations.
3. All zircon fractions are characterized by low to very low U contents (most near or below 100 ppm U) thus minimizing radiation damage to crystal structures and potential for lead loss.
4. There is a characteristic lack of evidence for overgrowth as sought by optical methods, HF etching techniques, and SEM examination.
5. Air abrasion treatments (Krogh, 1982) were used to remove any potentially metamict outer rinds and any undetected metamorphic overgrowths.
6. Zircon ages from Grenvillian AMCG suites outside major granulite terranes are not significantly older than those well within them.
7. If zircons are as resistant to resetting as widely believed, it would be remarkable to have reset them by metamorphism to such a tight cluster over so large an area.

Zircon fractions from mangeritic and charnockitic members of major AMCG suites including Morin, Lac St. Jean, Lac Allard, Quebec, and Atikonak River, Labrador have yielded upper intersections with concordia that lie between 1159^{+5}_{-3}, and 1126^{+7}_{-6} (Fig. 2). For reasons already discussed these are believed to be valid estimates of igneous crystallization ages. They are in remarkable agreement with data from the AMCG suite of the Adirondack region by Silver (1969), and Chiarenzelli et al. (1987). Initiation of widespread and abundant AMCG magmatism throughout the central part of the Grenville Province in an interval of about 30 Ma signalled beginning of the Grenvillian event which was marked by arrival of mantle-derived magmas and heating of the subcontinental lithosphere.

Older AMCG suites included in this study were Rivière Pentecote and Mealy Mountains. Mangerite and charnockite samples yielded ages near 1.36 and 1.64 Ga respectively for these suites. Machado and Martignole (1988) reported an age of 1354 $\pm$ 3 Ga for zircon from leuconorite at Rivière Pentecote, interpreted as a crystallization age of the body. A crystallization age of 1350 $\pm$ 50 Ma has been estimated by van Breemen et al. (1986) for the Whitestone anorthosite. These two small bodies are so far the only ones of about that age known in the Grenville Province. Preliminary results of 1.64 Ga for the Mealy Mountains suite reported by Emslie et al. (1983) have been confirmed by analysis of additional zircon fractions. A small intrusion of pyroxene quartz monzonite from the Labrieville area yielded an age of 1.02 Ga; its relationship to the Labrieville anorthosite is not known.

Although many of the chemical and mineralogical characteristics of these mangerite-charnockite-granite suites are shared by A-type granites (Emslie, 1987), the very large volumes of K-rich magma involved are not in harmony with depleted granulitic source materials commonly assigned to A-type granites (e.g. Collins et al., 1982; Whalen et al.,

1987). Large proportions of relatively young, undepleted crust in the source would be a more acceptable solution and indeed seems to have been the case for at least parts of the northeastern Grenville Province (Schärer, 1988). The remainder of the Grenville Province poses a greater dilemma. There is as yet little support for a major crust-forming event during the Grenville Orogeny among the exposed rocks of the Grenville Province. Few, if any, known examples of calc-alkalic magmatism can be unambiguously associated with the Grenvillian event.

Note that high level rapakivi-anorthosite suites of the Baltic Shield formed in crust that was young (1.9-1.7 Ga, e.g. Patchett and Arndt, 1986) relative to their crystallization ages as did the ~1.4 Ga anorogenic granite suites of the midwestern and southwestern United States (Bennett and Depaolo, 1987). This suggests that higher geothermal gradients present in younger crust by virtue of more homogeneous vertical distribution of radioactive heat-producing

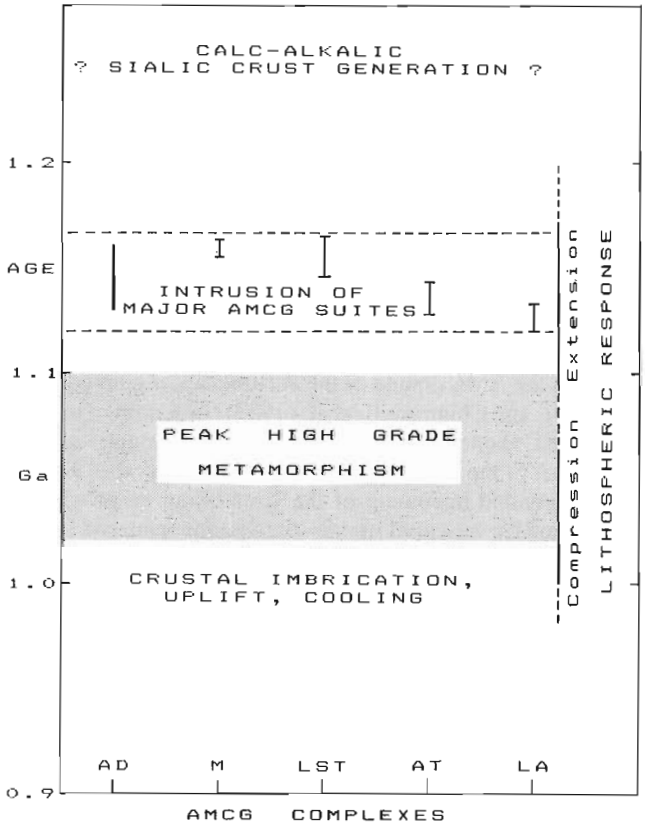

Figure 2. Estimated crystallization ages for major AMCG suites in the central part of the Grenville Province and their relationship to other aspects of the Grenvillian event. AD-Adirondacks, M-Morin, LSJ-Lac St. Jean, AT-Atikonak R., LA-Lac Allard. Data for the Adirondack region from Chiarenzelli et al. (1987) is an indicated range, others are ± 2s uncertainty estimates for individual samples. The wide time interval for peak metamorphism does not imply peak temperatures were maintained that long and may include more than one event in some areas. It reflects uncertainty in generalizing about timing of peak conditions that necessarily were diachronous to some degree over a broad region.

elements may have been a significant factor in determining suitable source materials. Increased heat flow from this source would have been helpful in assisting diapiric magma to rise through the crust.

A recent discussion of the origins of deep-level and high-level Archean granites and charnockites by Condie et al. (1986) includes some observations probably also pertinent to the relationship of A-type and rapakivi granites to igneous charnockites. Deep-level Archean granites of southern India are characterized by notable positive Eu anomalies, are enriched in Ba, Sr, and total REE as well as HFSE (high field strength elements, Zr, Ti, P, etc.). These rocks are believed to be cumulates with variable amounts of trapped liquid and formed by fractional crystallization of granitic liquids. The authors suggest that high-level Archean granites with negative Eu anomalies are the complementary residual liquids from this process. It is likely that a similar relationship existed between high-level, liquid-rich, negative Eu-anomalous classic rapakivis and A-type granites and deeper level, crystal-rich, positive Eu-anomalous mangerite-charnockites.

GRENVILLIAN GRANULITE METAMORPHISM

Timing of high grade regional metamorphism pertaining to the Grenvillian event in the central part of the Grenville Province is not yet precisely defined although it is clear that it postdated intrusion of the major AMCG suites. Rb-Sr whole rock studies in the Morin, Shawinigan and Lac St. Jean areas of Quebec (Barton and Doig, 1972, 1973; Frith and Doig, 1973) suggest that closure of these systems in paragneisses and late granitic intrusions took place between about 1020 and 1071 Ma. These systems would be expected to have closed below metamorphic peak temperatures on the cooling path of a granulite terrane and thus are younger than the peak of Grenvillian metamorphism. That interpretation would accord with U-Pb zircon estimates of a metamorphic peak close to that about 1050 to 1100 Ma recognized in the Adirondacks; Heaman et al. (1986) infer a similar age for peak metamorphism in the Central Metasedimentary Belt. In northeastern Grenville Province, Schärer and Gower (1988) report monazite and sphene ages about 1030 Ma, consistent with a minimum age estimate for metamorphic peak temperatures. It is difficult to escape the conclusion that maximum AMCG magmatism took place some 50 to 100 Ma prior to the widespread metamorphic peak.

Compressive forces recognized as part of the Grenville "orogeny" did not clearly make their presence felt until late in the metamorphic episode, that is the deformational climax probably postdated the metamorphic thermal peak. This interpretation is supported by recognition of juxtaposed slices of contrasting metamorphic grades. Such behaviour is unlike typical orogenic regimes where severe compressional strain begins early and may continue throughout. It is in accord however, with a thick (continental) lithosphere slowly heated mainly by conduction and in that weakened condition, deformed by external forces perhaps acting at a distant plate margin.

DISCUSSION

The Grenvillian metamorphic episode, widely recognized over much of the Grenville Province, was preceded by a major period of anorogenic magmatism largely confined to the central part of the Province. The principal AMCG magmatic activity now exhibited in the Grenville Province is in terranes east, southeast, and northeast of the Central Metasedimentary Belt; high grade though variable regional metamorphism associated with, but succeeding, this magmatism is distributed even more widely in the Province. Development of the Central Metasedimentary Belt, in addition to lack of major AMCG suites, differed in other aspects of its magmatic and metamorphic history (Heaman et al., 1986; Lumbers et al., 1988). Clear evidence for crustal sections composed of imbricate slabs of contrasting metamorphic-structural character thrust toward the northwest exists at the southwestern and northeastern extremities of the Grenville Province (e.g. Davidson, 1986; Gower and Ryan, 1986; Green et al.,1988). Preservation of these relationships implies that major tectonic transport of metamorphic-structural domains took place after peak regional metamorphic intensity (it does not rule out transport prior to or during that peak). Northwest tectonic transport of Parry Sound domain is shown to have begun prior to 1121 $\pm$ 5 Ma ago, and suggested to have been as early as 1159^{+5}_{-4} Ma by van Breemen et al. (1986); northwest-directed transport on ductile shears at the base of the Central Metasedimentary Belt has been interpreted to have occurred about 1060 $\pm$ 6 Ma by van Breemen and Hanmer (1986). The concept that compression-related thrusting was responsible for the ductile shearing has been widely embraced in this region; however, extensional ductile shear is expected to have played a prominent, even dominant, role in many deep crustal sections (e.g. McCarthy and Thompson, 1988) and should not be too hastily discounted as a contributing factor. Several aspects of the Grenvillian event (including reactivation of older terranes, associated anorogenic magmatism, and ductile shears of possible extensional origin) bear closer comparison with Cordilleran metamorphic core complexes. Major AMCG suites are regarded as essentially anorogenic in character (Emslie, 1978; Anderson, 1983; McLelland, 1986); as such, they are expected to have been associated with lithospheric extension.

The interpretation endorsed here is that the Grenvillian event, initiated after 1.2 Ga, combined widespread, separate but closely related, major magmatic and metamorphic episodes imposed upon continental lithosphere and largely pre-existing crust. It was orogenic in the sense that severe tectonism and mountain-building occurred, possibly through continent-continent collision; that aspect, however, was consequent upon immediately preceding, anorogenic processes. Accumulating isotopic evidence suggests that generation of new crust was not an important feature of the Grenvillian event as narrowly defined here, i.e. after about 1.16 Ga, but may have been of significant proportions in an immediately preceding interval (Ruiz et al., 1988; Lumbers et al., 1988; van Breemen et al., 1986). Magmatic activity as treated in the Dewey and Burke (1973) collision model was a consequence of crustal thickening which took place under conditions of a lithosphere thinned to zero. Maintaining that condition for more than a few million years would result in such high degrees of partial melting that the crust would have essentially no strength and could not be mechanically thickened; any realistic model must incorporate a subcrustal lithosphere though it may have been thinned to some degree. Dewey and Burke (1973) specifically regarded the entire AMCG suite as refractory residues remaining after extraction of granitic liquids which rose to higher crustal levels. By contrast, interpretations outlined here emphasize igneous and metamorphic events that for the most part preceded effects that may be ascribed to continental collision. Widespread AMCG magmatic activity and ensuing high grade metamorphism are likely to have been critical factors permitting and controlling subsequent developments during the Grenvillian event. Continent-continent collision acting upon thermally-weakened lithosphere may have been largely responsible for major crustal imbrication and thickening, permitting uplift and erosion to expose once deep crustal levels.

Preliminary assessment suggests that a large part of the central Grenville Province underwent a post-1.2 Ga igneous and metamorphic history broadly similar to that already documented in the Adirondack region. The essential features summarized in Figure 2 are large scale AMCG magmatism which peaked between about 1.16 and 1.13 Ga, followed by widespread granulite grade metamorphism, in part coextensive with the magmatism, but which lagged the magmatic maximum by 0.05-0.10 Ga. Igneous activity, with textural, petrographic, and chemical features described by authors as late, postorogenic, or anorogenic, continued on a much reduced scale (in size and numbers of intrusions) until at least 0.96 Ga.

The notable time correlation between Keweenawan magmatism with AMCG magmatism of the Adirondacks has been commented upon by Silver (1969) and recently by Gordon and Hempton (1986). The latter authors suggest that Keweenawan rifting was induced by continental collision. If the AMCG magmatic suites were fundamentally anorogenic, and as abundant and widespread at 1.16 to 1.13 Ga as indicated by this study, a direct relationship with Keweenawan crustal rifting at 1.12 to 1.10 Ga is more readily accepted as the result of lithospheric extension evolving over a broad region. Moreover, crustal rifting need not necessarily imply lithospheric rifting; it may simply reflect response to lithospheric expansion and extension due to basal heating and to transport of magma batches through it without thinning dramatically. The seismically highly reflective lower crustal section of Manitoulin Terrane (Green et al., 1988) may relate to a zone of ductile extension which linked, via the lower crust, the classic Keweenawan crustal rift zone to the west with more extreme extension that took place in the Grenville Province.

The fact that voluminous AMCG suites appeared over a broad region (more than 3.5×10^5 km^2 in area) of the central Grenville Province over a relatively short time interval suggests that, with care, they may provide a practical and convenient marker for the beginning of the Grenville event. This is in good agreement with Stockwell's (1982) interpretation of timing although he emphasized granitic magmatism rather than the AMCG magmatism more characteristic of the Grenville event.

P-T vectors relating to Grenvillian granulite metamorphism in the Central Granulite Terrane are only traceable for the latter parts of their evolution which indicate near-isobaric cooling (Bohlen et al., 1985; Herd et al., 1986; Martignole, 1986). Evidence for isobaric cooling from a granulite grade peak is not easily reconciled with tectonic doubling of crustal thickness commonly invoked as a requirement to produce granulite terranes (e.g. Bohlen, 1987); the long, slow cooling interval from granulite conditions might be expected to enhance opportunities to record decompression if it occurred. A model for production of granulite terranes in continental extensional regimes by Sandiford and Powell (1986) seems better able to satisfy the requirements of the Grenvillian event. That model postulates normal crustal thickness during heating and cooling and relies upon subsequent unrelated tectonism to raise the granulites to high crustal levels by thrust faults. Imbricate crustal sections known to be present in (and possibly to characterize much of) the Grenville Province are evidence of relatively late severe thrusting and crustal shortening. The attraction of a Sandiford and Powell model for the Grenvillian event is that it is also in accord with the apparent anorogenic character of AMCG suites. The space-time relationship of AMCG magmatism and high grade regional metamorphism is also more easily explained by an anorogenic regime. The conspicuous time lag of about 50 to 100 Ma between peak magmatic activity and metamorphic peak can be explained if onset of AMCG magmatism marked initiation of heating the base of thick subcontinental lithosphere and the metamorphic peak reflected eventual rise of geotherms due to extended conductive heating of the lithosphere. Mafic magma may have tended to pond in the vicinity of the crust-mantle boundary or in the lower crust and could make substantial but not extended contributions to heat flow. Magmatic heating is effective and rapid but is relatively short-lived because of efficient heat transfer by convection. Although periodic spikes of magmatic heat undoubtedly occurred before, during and even after the metamorphic peak, a long-lived conductive heating regime is indicated. This kind of step-heating effect for a lithospheric slab has been modeled for one dimensional heat flow by Bodell and Chapman (1982). The thermal time constant t for a slab is a function of slab thickness l, and thermal diffusivity α which is commonly estimated as 28 to 32 km^2/Ma for the lithosphere (Bodell and Chapman, 1982; Morgan, 1984):

$$t = l^2 / 4\alpha$$

For a slab 80 km thick and $\alpha = 30$, the slab time constant is 53 Ma. For thermal time constants in the range 50 to 100 Ma, slab thicknesses in the range 80 to 120 km are indicated. Stabilized continental lithosphere is commonly considered to lie in the range 100-200 km thick. Although the slab begins to heat rapidly from the base and the mean temperature rise in the slab reaches about 50 % of its maximum value in about 0.2t, it does not approach a maximum steady-state value until about 1.5t which is roughly 80 Ma for an 80 km thick slab. Obviously, estimates for thermal properties of the slab are not closely constrained but even rough approximations can be useful. The model implies that transient thermal pulses probably must be relatively long-lived ($>1.0t$) to produce large granulite terranes by this conductive mechanism.

ACKNOWLEDGMENTS

R. Theriault assisted in sample collection. R. Parrish advised on etching techniques. D. Walker provided expertise on the scanning electron microscope. Advice and assistance of members of the Geochronology Section was generously offered and unsparingly applied. A. Davidson kindly offered acute critical comment.

REFERENCES

Anderson, J.L.
1983: Proterozoic anorogenic granite plutonism of North America; in Proterozoic geology: selected papers from an international symposium, L.G. Medaris Jr., C.W. Byers, D.M. Mickelson, and W.C. Shanks, eds., Geological Society of America, Memoir 161, p. 133-154.

Barton, J.M., Jr. and Doig, R.
1972: Rb-Sr isotopic studies of the Lac Croche complex, Grenville Province, Quebec; Canadian Journal of Earth Sciences, v. 9, p. 1180-1186.
1973: Time-stratigraphic relationships east of the Morin anorthosite pluton, Quebec; American Journal of Science, v. 273, p. 376-384.

Bennett, V.C. and DePaolo, D.J.
1987: Proterozoic crustal history of the western United States as determined by neodymium isotopic mapping; Geological Society of America Bulletin, v. 99, p. 674-685.

Bodell, J.M. and Chapman, D.S.
1982: Heat flow in the north-central Colorado Plateau; Journal of Geophysical Research, v. 87, p. 2869-2884.

Bohlen, S.R.
1987: Pressure-temperature-time paths and a tectonic model for the evolution of granulites; Journal of Geology, v. 95, p. 617-632.

Bohlen, S.R., Valley, J.W., and Essene, E.J.
1985: Metamorphism in the Adirondacks. I. Petrology, Pressure and Temperature; Journal of Petrology, v.26, p. 971-992.

Chiarenzelli, J.R., Bickford, M.E., McLelland, J.M., Isachsen, Y.W., and Whitney, P.R.
1987: Early igneous history of the Adirondack Mountains as revealed by U-Pb zircon analyses; Geological Society of America, Annual Meeting, Program with Abstracts, v.19, No. 7, p. 619.

Collins, W.J., Beams, S.D., White, A.J.R., and Chappell, B.W.
1982: Nature and origin of A-type granites with particular reference to southeastern Australia; Contributions to Mineralogy and Petrology, v. 80, p. 189-200.

Condie, K.C., Bowling, G.P., and Allen, P.
1986: Origin of granites in an Archean high-grade terrane, southern India; Contributions to Mineralogy and Petrology, v. 92, p. 93-103.

Davidson, A.
1986: New interpretations in the southwestern Grenville Province; in The Grenville Province, J.M. Moore, A. Davidson, and A.J. Baer, eds., Geological Association of Canada, Special Paper 31, p. 61-74.

Dewey, J.K. and Burke, K.C.A.
1973: Tibetan, Variscan and Precambrian basement reactivation: products of continental collision; Journal of Geology, v.81, p. 683-692.

Doig, R.
1977: Rb-Sr geochronology and evolution of the Grenville Province in northwestern Quebec, Canada; Geological Society of America Bulletin, v. 88, p. 1843-1856.

Emslie, R.F.
1978: Anorthosite massifs, rapakivi granites, and Late Proterozoic rifting of North America; Precambrian Research, v. 7, p. 61-98.

Emslie, R.F., Loveridge, W.D., Stevens, R.D., and Sullivan, R.W.
1983: Igneous and tectonothermal evolution, Mealy Mountains, Labrador; Geological Association of Canada, Programs with Abstracts, v.8, p. A20.

Emslie, R.F.
1987: Rapakivi suites, igneous charnockites and A-type granite; Geological Society of America, Abstracts with Programs, v.19, p. 655.

Frith, A.R. and Doig, R.
1973: Rb-Sr isotopic ages and petrologic studies of the rocks in the Lac St.Jean area, Quebec; Canadian Journal of Earth Sciences, v. 10, p. 881-899.

Gordon, M.B. and Hempton, M.R.
1986: Collision-induced rifting: the Grenville Orogeny and the Keweenawan rift of North America; Tectonophysics, v. 127, p. 1-25.
Gower, C.F. and Loveridge, W.D.
1987: Grenvillian plutonism in the eastern Grenville Province; in Radiogenic age and isotopic studies: Report 1, Geological Survey of Canada, Paper 87-2, p. 55-58.
Gower, C.F. and Ryan, A.B.
1986: Proterozoic evolution of the Grenville Province and adjacent Makkovik Province in east-central Labrador; in The Grenville Province, J.M. Moore, A. Davidson, and A.J. Baer, eds., Geological Association of Canada, Special Paper 31, p. 281-296.
Green, A.G., Milkereit, B., Davidson, A., Spencer, C., Hutchinson, D.R., Cannon, W.F., Lee, M.W., Agena, W.F., Behrendt, J.C., and Hinze, W.J.
1988: Crustal structure of the Grenville front and adjacent terranes; Geology, v. 16, p. 788-792.
Heaman, L.M., McNutt, R.H., and Krogh, T.E.
1986: Geological significance of U-Pb and Rb-Sr ages for two pretectonic granites from the Central Metasedimentary Belt, Ontario; in The Grenville Province, J.M. Moore, A. Davidson, and A.J. Baer, eds., Geological Association of Canada, Special Paper 31, p. 281-296.
Herd, R.K., Ackermand, D., Windley, B.F., and Rondot, J.
1986: Sapphirine-garnet rocks, St. Maurice area, Quebec: Petrology and implications for tectonics and metamorphism; in The Grenville Province, J.M. Moore, A. Davidson, and A.J. Baer, eds., Geological Association of Canada, Special Paper 31, p. 241-253.
Krogh, T.E.
1982: Improved accuracy of U-Pb zircon ages by the creation of more concordant systems using an air abrasian technique; Geochimica et Cosmochimica Acta, v. 46, p. 637-649.
Lumbers, S.B., Heaman, L.M., and Vertolli, V.M.
1988: Middle Proterozoic history of the CMB, Grenville Province, Ontario; Geological Association of Canada, Program with Abstracts, v. 13, p.A75.
Machado, N. and Martignole, J.
1988: First U-Pb age for magmatic zircon in anorthosites: the case of the Pentecote intrusion in Quebec; Geological Association of Canada, Program with Abstracts, v. 13, p. A76.
Martignole, J.
1986: Some questions about crustal thickening in the central part of the Grenville Province; in The Grenville Province, J.M. Moore, A. Davidson, and A.J. Baer, eds., Geological Association of Canada, Special Paper 31, p. 327-339.
McCarthy, J. and Thompson, G.A.
1988: Seismic imaging of extended crust with emphasis on the western United States; Geological Society of America, v. 100, p. 1361-1374.
McLelland, J.M.
1986: Pre-Grenvillian history of the Adirondacks as an anorogenic, bimodal caldera complex of mid-Proterozoic age; Geology, v. 14, p. 229-233.
McLelland, J.M. and Isachsen, Y.W.
1986: Synthesis of geology of the Adirondack Mountains, New York, and their tectonic setting within the southwestern Grenville Province; in The Grenville Province, J.M. Moore, A. Davidson, and A.J. Baer, eds., Geological Association of Canada, Special Paper 31, pp. 75-94.
Moore, J.M.
1986: Introduction: The 'Grenville Problem' then and now; in The Grenville Province, J.M. Moore, A. Davidson, and A.J. Baer, eds., Geological Association of Canada Special Paper 31, p. 1-11.
Moore, J.M., Jr. and Thompson, P.H.
1980: The Flinton Group: a late Precambrian metasedimentary succession in the Grenville Province, eastern Ontario; Canadian Journal of Earth Sciences, v. 17, p. 1685-1707.
Morgan, P.
1984: Structure and evolution of the continental lithosphere; in Physics and Chemistry of the Earth, v.15, H.N. Pollack and V.R. Murthy, eds., p. 107-193.
Patchett, J.P. and Arndt, N.T.
1986: Nd isotopes and tectonics of 1.9-1.7 Ga crustal genesis; Earth and Planetary Science Letters, v. 78, p. 329-338.
Roy, D.W., Woussen, G., Dimroth, E., and Chown, E.H.
1986: The central Grenville Province: a zone of protracted overlap between crustal and mantle processes; in The Grenville Province, J.M. Moore, A. Davidson, and A.J. Baer, eds., Geological Association of Canada, Special Paper 31, p. 51-60.
Ruiz, J., Patchett, P.J., and Ortega-Gutierrez, F.
1988: Proterozoic and Phanerozoic basement terranes of Mexico from Nd isotopic studies; Geological Society of America Bulletin, v.100, p. 274-281.
Sandiford, M. and Powell, R.
1986: Deep crustal metamorphism during continental extension: modern and ancient examples; Earth and Planetary Science Letters, v. 79, p. 151-158.
Schärer, U.
1988: Origin and evolution of Proterozoic crust in eastern Labrador; Geological Association of Canada, Program with Abstracts, v.13, p. A109.
Schärer, U. and Gower, C.F.
1988: Crustal evolution in eastern Labrador: constraints from precise U-Pb ages; Precambrian Research, v. 38, p. 405-421.
Schärer, U., Krogh, T.E., and Gower, C.F.
1986: Age and evolution of the Greenville Province in eastern Labrador from U-Pb systematics in accessory minerals; Contributions to Mineralogy and Petrology, v. 94, p. 438-451.
Silver, L.T.
1969: A geochronologic investigation of the anorthosite complex, Adirondack Mountains, New York; in Origin of Anorthosite and Related Rocks, Y.W. Isachsen, ed., New York State Museum and Science Service Memoir 18, p. 233-251.
Stockwell, C.H.
1982: Proposals for time classification and correlation of Precambrian rocks and events in Canada and adjacent areas of the Canadian Shield. Part I: A time classification of Precambrian rocks and events; Geological Survey of Canada, Paper 80-19, 135 p.
van Breemen, O., Davidson, A., Loveridge, W.D., and Sullivan, R.W.
1986: U-PB zircon geochronology of Grenville tectonites, granulites and igneous precursors, Parry Sound, Ontario; in The Grenville Province, J.M. Moore, A. Davidson, and A.J. Baer, eds., Geological Association of Canada Special Paper 31, p. 191-207.
van Breemen, O. and Hanmer, S.
1986: Zircon morphology and U-Pb geochronology in active shear zones: studies on syntectonic intrusions along the northwest boundary of the Central Metasedimentary Belt, Grenville Province, Ontario; in Current Research, Part B, Geological Survey of Canada, Paper 86-1B, p. 775-784.
Watson, E.B. and Harrison, T.M.
1983: Zircon saturation revisited; Temperature and composition effects in a variety of crustal magma types; Earth and Planetary Science Letters, v.64, p. 295-304.
Whalen, J.B., Currie, K.L., and Chappell, B.W.
1987: A-type granites: geochemical characteristics, discrimination and petrogenesis; Contributions to Mineralogy and Petrology, v. 95, p. 407-419.
Wynne-Edwards, H.R.
1972: The Grenville Province; in Variations in Tectonic Styles in Canada, R.A. Price and R.J.W. Douglas, eds., Geological Association of Canada, Special Paper 11, p. 263-334.

Deformation, metamorphism, diabase dykes, and the Grenville Front southwest of Sudbury, Ontario

K.M. Bethune[1]
Lithosphere and Canadian Shield Division

Bethune, K.M., Deformation, metamorphism, diabase dykes, and the Grenville Front southwest of Sudbury, Ontario; in Current Research, Part C, Geological Survey of Canada, Paper 89-1C, p. 19-28, 1989.

Abstract

Northwest of the Grenville Front, southwest of Sudbury, Ontario, continuous diabase dykes of the Sudbury swarm (ca. 1240 Ma) crosscut folded Huronian rocks of the Southern Province and mid-Proterozoic granitoid plutons. The dykes lose continuity abruptly at the front, beyond which irregular metadiabase dykes and dyke segments, correlative in age and chemistry, crosscut gneissic fabric in the Grenville Province. Deformation style and metamorphic grade recorded in the dykes change southeastward, parallel with increase in metamorphism in the country rocks. Data presented herein suggest that the dykes' irregular configuration in the Grenville is in part primary, not due to deformation alone. Post-emplacement reorientation was concentrated on discrete mylonite zones near the front but became increasingly penetrative southeastward. Structural telescoping of pre-diabase isograds near the front is suggested by an abrupt change in regional facies and by somewhat lower metamorphic grade in metadiabase than in country rocks.

Résumé

Au nord-ouest du front de Grenville dans la région située au sud-ouest de Sudbury (Ontario), les dykes de diabase continus, verticaux et relativement rectilignes du groupe de dykes de Sudbury (datant d'environ 1240 Ma) recoupent les roches plissées de l'Huronien de la province du Sud et des plutons granitoïdes du Protérozoïque moyen. Les dykes perdent brusquement leur continuité au front, au-delà duquel la métadiabase d'âge et de composition chimique corrélatifs prend la forme de dykes et de segments de dykes de géométrie irrégulière qui recoupent la texture pénétrante des gneiss à l'intérieur de la province de Grenville. Le style de déformation et l'intensité du métamorphisme, tels qu'ils se manifestent dans les dykes, changent en direction du sud-est de manière parallèle à l'accroissement de l'intensité du métamorphisme dans les roches encaissantes. Les données qui sont présentées suggèrent que la configuration irrégulière des dykes dans la province de Grenville est en partie originelle et non exclusivement attribuable à la déformation. La réorientation survenue après la mise en place des dykes a été concentrée dans des zones discontinues de myolite près du front, mais est devenue de plus en plus intrusive en direction du sud-est. Un télescopage structural des isogrades pré-diabases près du front est suggéré par le changement brusque de faciès et par le métamorphisme d'intensité quelque peu moindre dans la métadiabase que dans les roches encaissantes.

[1] Department of Geological Sciences, Queen's University, Kingston, Ontario K7L 3N6

INTRODUCTION

The occurrence of two swarms of diabase dykes in the vicinity of the Grenville Front southwest of Sudbury, reported by Lumbers (1975), Palmer et al. (1977) and Frarey (1985), was corroborated in the Tyson Lake area in 1987 (Bethune and Davidson, 1988). Dykes of the younger of the two swarms, termed the Grenville dykes by Fahrig and West (1986), are composed of tholeiitic diabase, trend east-west and postdate tectonic activity along the front. In contrast, alkaline olivine diabase dykes of the older Sudbury swarm show a change in orientation at the front and clearly have been affected by "Grenvillian" tectonism. Southeast of the front, segments of metadiabase (termed "cataclastic metadiabase" by Lumbers, 1975) show progressively greater strain and increase in metamorphic grade southeastward. Preliminary mapping, petrography and chemistry carried out in 1987 (Bethune and Davidson, 1988) supported Frarey's (1985) contention that contorted lobe- and hook-shaped dyke segments within the Grenville Province in the Tyson Lake area are deformed and metamorphosed equivalents of Sudbury dykes in the Southern Province to the northwest. However, because no single dyke can be traced continuously across the mylonite zone that constitutes the Grenville Front in this region, both an extensive chemical survey and a geochronological study were initiated in the fall of 1987 in order to confirm this correlation across the Grenville Front. In addition, detailed mapping within a 15 by 22 km^2 area (Fig. 1) spanning the front at Tyson Lake, where the highest concentration of Sudbury dykes occurs, was undertaken in 1988 to further document field relationships of the dykes and the rocks they intrude. This paper reports the results of the chemical survey and summarizes further the field relations of the dykes determined to date.

COUNTRY ROCKS

Lithology and structure

In the northwestern part of the map area (Fig. 1; see also Bethune and Davidson, 1988, Fig. 2), sedimentary rocks of the Serpent, Gowganda and Lorrain formations of the Huron Supergroup, and sills of Nipissing diabase within them, are in faulted, intrusive contact with mid-Proterozoic granite (Bell Lake and Annie Lake granites of Frarey, 1985). All of these rocks are severely mylonitized along a northeast-trending zone that passes through the northwestern part of Tyson Lake. Metamorphism in Huronian metasediments immediately northwest of this mylonite zone (which for reasons outlined previously (Bethune and Davidson, 1988, p. 159) is considered the most suitable locus for the Grenville Front) attains lower amphibolite facies, and either predates or is associated with emplacement of the granites.

Southeast of the Grenville Front mylonite zone at Tyson Lake an undivided unit of metasedimentary gneiss consists of quartzite, impure quartzite and fine grained quartz-rich feldspathic gneiss, variably interlayered with biotite-garnet schist, amphibolite and subordinate calc-silicate gneiss. Individual layers rarely exceed 10 m across the strike of tectonic layering, and primary structures are absent except in the hinge areas of a few reclined mesoscopic folds, whose east-trending enveloping surfaces may enclose the traces of bedding. These folds, likely pre-Grenvillian in age, occur in low-strain panels bounded by discrete mylonite or high-strain zones presumed to be Grenvillian in age. They are best preserved in a characteristic unit of rusty quartzite that dominates the metasedimentary assemblage in the central part of Tyson Lake. On approaching the high-strain zones, relict bedding is progressively disrupted and is eventually entirely transposed into parallelism with northeast-striking and southeast-dipping foliation, hereinafter referred to as "Grenville-style".

As discovered by Frarey (1985), the highly strained, transposed character of sedimentary gneisses at Tyson Lake makes correlation with known Huron Supergroup stratigraphy virtually impossible. For example, in most cases it can be demonstrated that, where reasonable lithological comparisons can be made with Huron Supergroup formations, severe tectonic thinning, due perhaps to attenuation on the limbs of folds and/or to out-of-sequence stacking of fault slices, would be required to attain the present configuration of the variously juxtaposed protoliths. Immediately northwest of the front, correlation of metasedimentary units that lie southeast of the Bell Lake and Annie Lake granites with specific Huronian formations may be possible; for example, north of the western part of Tyson Lake a metaconglomerate unit and spatially associated calc-silicate gneiss, minor marble and quartzite, previously mapped and described by Frarey (1985), are most likely correlative with the Bruce, Espanola and Serpent formations. To the southeast, the aforementioned rusty quartzite unit at Tyson Lake could have been derived from the Mississagi Formation, as suggested by Quirke and Collins (1930), but it is much more thinly bedded than is typical of the Mississagi northwest of the front. Correlation with Huronian formations must consider the fact that, southeast of the front, lithologically distinct metasedimentary units are interlayered at scales of tens of metres, whereas the characteristic Huronian lithologies commonly form units many hundreds of metres thick. In addition the succession of distinctive metasedimentary units in the Tyson Lake area does not match the order of Huronian formations. Alternatives to a combination of tectonic thinning and out-of-order stacking of slices suggested above to account for these discrepancies may be that the metasedimentary rocks in the Tyson Lake area represent distal facies equivalents of Huronian formations that have been tectonically transported toward the Southern Province, precluding direct correlation, or that the metasediments are unrelated to the Huron Supergroup (Davidson, 1988).

Metaplutonic rocks southeast of the Grenville Front are represented mainly by foliated or gneissic granite of two types: 1) pink equigranular, relatively leucocratic metagranite that locally grades into greenish-brown rusty-weathering charnockite (C in Fig. 1); and 2) K-feldspar megacrystic or augen granitoid gneiss. The former, tentatively dated at ca. 1.74 Ga (Krogh et al., 1971), could be related to the Killarney granite west of the front (Davidson, 1986), which has been dated at 1742 Ma (van Breemen and Davidson, 1988). The latter appears more like a derivative of the porphyritic Bell Lake granite, which has been dated at 1471 Ma (van Breemen and Davidson, 1988). The

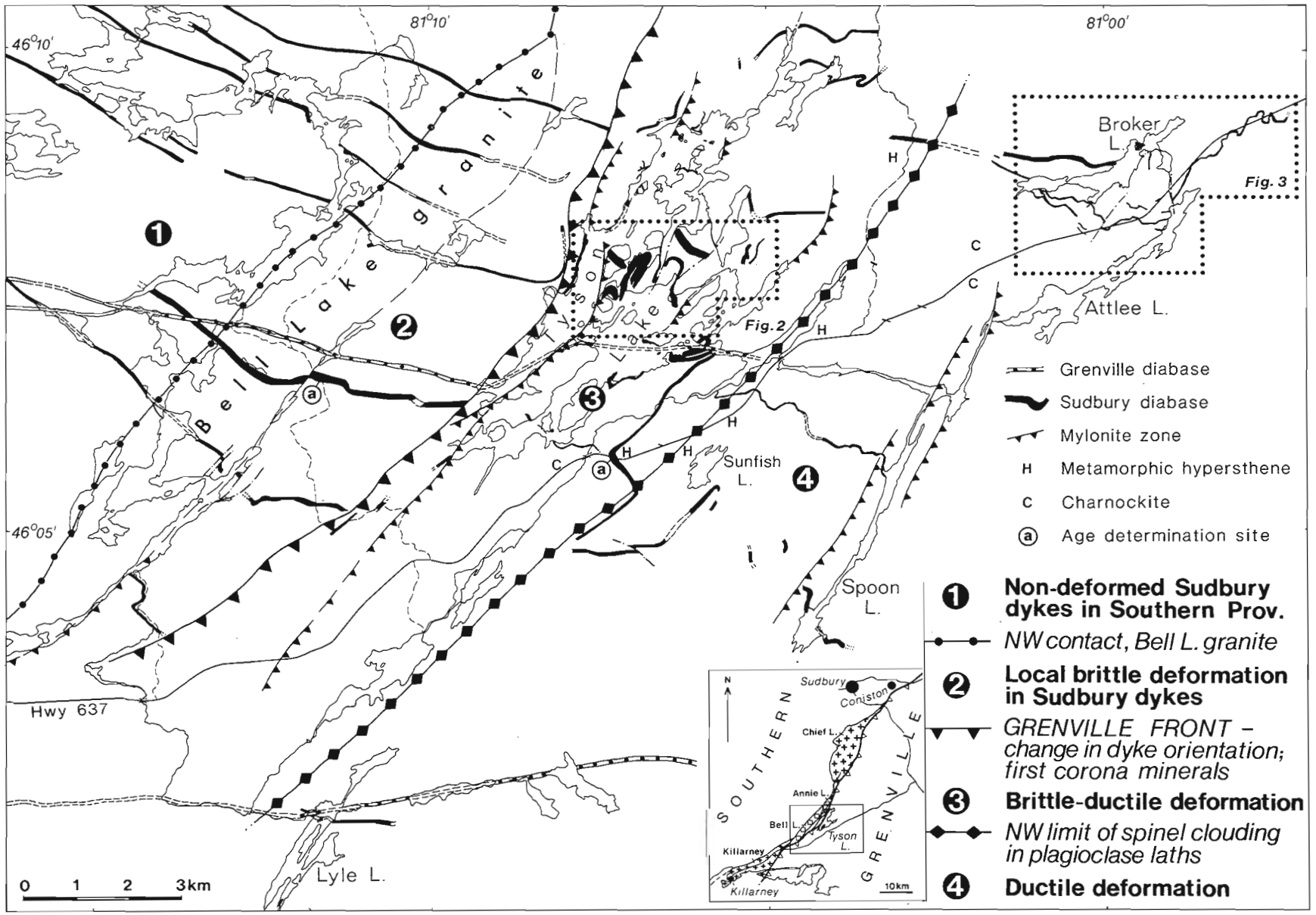

Figure 1. Zonation of deformation and metamorphism of Sudbury diabase dykes in the vicinity of the Grenville Front at Tyson Lake.

metagranite bodies form relatively narrow interdigitations with sedimentary gneiss, either as isolated lenses or as tapering projections from larger masses. They are strongly mylonitized at Tyson Lake and in the vicinity of Spoon Lake (Fig. 1).

Southeast of Tyson Lake, alternating northeast-striking and southeast-dipping units of sedimentary schist and gneiss and plutonic orthogneiss are characterized almost everywhere by a penetrative northeast-oriented planar fabric and strong dip-parallel mineral stretching lineation. Original contacts between metaplutonic and metasedimentary units are rarely preserved. Low-angle discordances between contacts and gneissic fabric in surrounding metasedimentary rocks, however, along with rare inclusions of metasedimentary material within the granitoids, demonstrate former intrusive relationships. Early folds, where discernible, are tightly appressed within the dominant Grenville-style foliation. Almost everywhere, however, transposition of earlier fabrics has resulted in near coaxiality of pre-Grenvillian and Grenvillian structures.

Metamorphism and migmatization

As mentioned previously, Huron Supergroup metasediments attain lower amphibolite facies northwest of the main mylonite which constitutes the Grenville Front at Tyson Lake. Micaceous quartzofeldspathic gneiss and schist, probably derived from the lower Lorrain Formation, contain muscovite stable with quartz; the probable equivalent of Gowganda Formation siltstone is a highly contorted schist containing biotite, muscovite, plagioclase, quartz and rare garnet. The most pronounced increase in metamorphic grade occurs beyond the mylonite to the southeast. Thin sections of granitoid and sedimentary gneisses and schists at Tyson Lake and to the southeast confirm the presence of upper amphibolite to granulite facies assemblages (Frarey, 1985; Bethune and Davidson, 1988). Sedimentary gneisses along highway 637, locally waxy green in colour, contain orthopyroxene together with plagioclase, biotite, quartz and minor garnet. Some mafic gneisses, demonstrably derived from narrow dykes, contain the metamorphic assemblage hypersthene—hornblende—biotite—plagioclase. Thin calc-silicate layers in the same area have the assemblage diopside—wollastonite—scapolite—grossular garnet—plagioclase—quartz. In pelitic units the assemblage quartz—K-feldspar—plagioclase—garnet—biotite—sillimanite is common, and relict kyanite was observed in such an assemblage at one location. Sillimanite is also found in impure quartzite; muscovite occurs with sillimanite in some rocks, but it is not known at present whether the coexistence of these two phases is evidence of prograde or retrograde reaction. The change in grade across the Grenville Front in the Tyson Lake area from lower amphibolite to the first appearance of hypersthene in metasedimentary rocks takes place within 4 km. In the context of the regional structure, this abrupt change is best explained as telescoping due to uplift along the mylonite zones that constitute the Grenville Front. This requires that the highest grade of metamorphism was attained before mylonitization.

Both para- and orthogneisses become increasingly migmatitic southeast of Tyson Lake. The first appearance of migmatitic neosomes in sedimentary gneisses occurs between the main part of Tyson Lake and the western shore of its southeast arm; this "migmatite front" extends along strike to the northwest and southeast and is a gradual transition rather than an abrupt change. Hydrous neosomes containing quartz, feldspar, biotite and hornblende are common where metasedimentary units first become migmatitic. An abrupt increase in metamorphic grade between mid-Tyson Lake and highway 637, however, is attested to by the appearance in neosomes of anhydrous phases such as orthopyroxene in rocks of appropriate bulk composition. Hypersthene is present in both groundmass and neosome in a highly varied succession which includes both mafic and quartzofeldspathic lithologies immediately southeast of Tyson Lake (H in Fig. 1). East-southeastward the proportion of neosome in metasedimentary rocks increases gradually until, near Broker Lake, it locally composes roughly 20 per cent of the rock. As many as three neosome generations may be present; overprinting relationships between more and less deformed neosomes imply a complex structural history. In this area, garnet- and/or magnetite-bearing neosomes in quartzite and quartzofeldspathic gneiss are common, signifying anhydrous conditions and overall higher metamorphic grade.

SUDBURY DIABASE AND METADIABASE

Previous mapping established the paths of six southeast-trending vertical olivine diabase dykes of the Sudbury swarm cutting Southern Province metasedimentary rocks and middle Proterozoic plutonic rocks northwest of Tyson Lake (Fig. 1). Despite minor offsets on northeast-trending faults on approaching the Grenville Province, the dykes have remarkably straight and continuous courses. Coincident with the Grenville Front mylonite zone along the northwestern margin of Tyson Lake, however, the dykes are deflected northeastward. Diabase bodies cutting sedimentary and plutonic gneisses in the Tyson Lake area no longer have typical Sudbury dyke trends, but occur as variably oriented, apparently folded dyke segments which are rarely traceable for more than a kilometre. Macroscopic evidence for increasing degree of deformation and metamorphism of the diabase southeastward into the Grenville Province (Frarey, 1985; Bethune and Davidson, 1988) allows division of the area into four zones (Fig. 1). The different zones encompass dykes or dyke segments with similar metamorphic and structural features. Below is a brief description of dykes in each of these zones, based in part on mapping and follow-up laboratory work in 1987-1988, in part on summer field work in 1988.

Zone 1

This zone includes all non-deformed Sudbury dykes northwest of the Bell Lake granite. Although individual dykes are not perfectly straight and locally may be composed of a series of slightly curved, en echelon segments, the overall trend of all dykes is to the southeast, and dykes are continuous over long distances. For example, one of the widest

dykes of the swarm, referred to as the "Espanola" dyke, can be traced semicontinuously all the way from northwest of Espanola, roughly 50 km west of Sudbury, to the vicinity of the front, a distance of 45 km. A recent U-Pb baddeleyite age of 12384 Ma for this dyke (Krogh et al., 1987) accords well with previous Rb-Sr ages for the Sudbury swarm (ca. 1250 Ma, Palmer et al., 1977). Thin sections of unaltered diabase from this zone typically display an ophitic to subophitic texture with interlocking plagioclase laths surrounded by plentiful olivine, Ti-rich clinopyroxene and subordinate interstitial biotite and iron oxide. Apatite is the dominant accessory mineral.

Zone 2

Immediately southeast of zone 1, straight Sudbury dykes traversing the Bell Lake granite and rocks to the southeast display local brittle deformation. On a macroscopic scale, high densities of brittle-style horse-tail shears and narrow cataclastic zones affect diabase adjacent to northeast-trending faults across which the dykes are laterally offset by a few tens of metres. Thin sections of deformed material show pervasive microfracturing and/or microbrecciation; primary texture and mineralogy are nonetheless preserved. Associated with many brittle shears are low-grade alteration minerals such as chlorite, sericite, epidote and green biotite.

Zone 3

The northwestern margin of Tyson Lake coincides with the northwestern boundary of zone 3. The pronounced change in geometry of dykes, involving a loss of typical southeast continuity and instead the occurrence of variably-oriented dyke segments and irregularly shaped diabase bodies (see Fig. 2), is accompanied by the most significant internal changes within the dykes. Macroscopically the diabase is darker, duller and lacks the well-defined crystallinity of unaltered diabase in zones 1 and 2. Present at all preserved chilled contacts are spongy aggregates of fine grained garnet, the growth of which in some cases appears to be localized along small fractures. In thin section, plagioclase laths are seen to be bent, fractured or kinked, rarely with subgrain development and minor recrystallization. Thin rims of radially-oriented hypersthene surround primary olivine, and garnet occurs in varying amounts about biotite and iron oxide. Besides the general "shattered" appearance imparted to the rock by the deformed feldspars, discrete mesoscopic mylonitic to ultramylonitic shears of no apparent systematic orientation are common. Such shears seem to be restricted to the dykes, i.e. they do not penetrate contacts with adjacent country rocks. In porphyritic diabase (see Bethune and Davidson, 1988, p. 58), primary olivine inclusions in large plagioclase phenocrysts have reacted to produce successive coronas of hypersthene and symplectite composed of amphibole and spinel. The large plagioclase phenocrysts themselves are cut by microfractures which are the sites of variable recrystallization of fine feldspar. In at least one occurrence, deformed and partly retrograded corona assemblages indicate deformation after the peak of metamorphism.

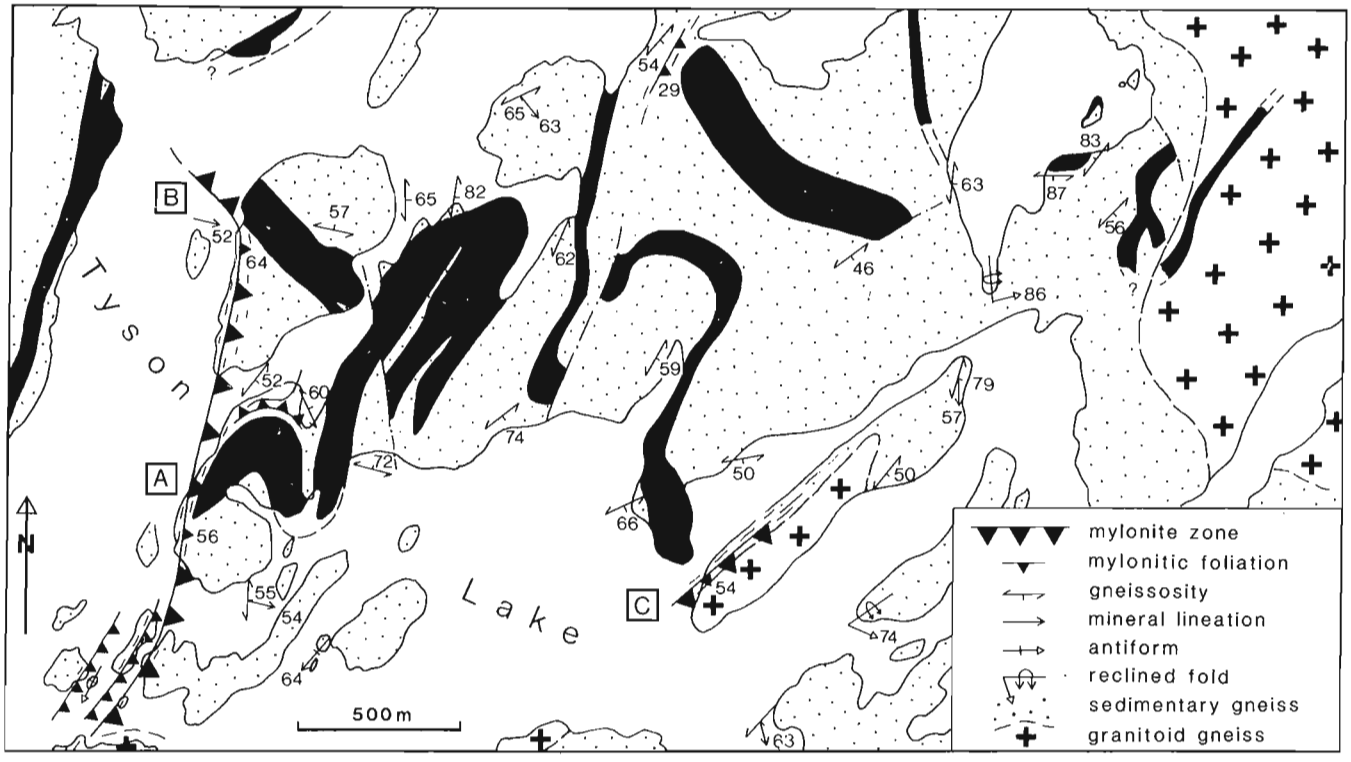

Figure 2. Detail of the form of Sudbury diabase bodies, central Tyson Lake (zone 3). Dash-dot lines are faults; letters in squares are localities mentioned in the text.

Zone 4

The farthest southeast dykes show an even greater degree of deformation and further advances in metamorphic mineral growth and recrystallization. Some dykes in this zone have been traced continuously for as much as 4 km along remarkably sinuous courses (for example, see Fig. 3). Particularly diagnostic, whether the dykes are straight or sinuous, is an obvious penetrative L-S tectonic fabric, invariably with the linear element being much more strongly developed than the planar one. Where least recrystallized, this fabric is defined by crudely aligned, curved plagioclase laths. Original zoning of the plagioclase is enhanced by spinel clouding, the intensity of which increases from northwest to southeast across the zone. Plagioclase in some dykes of zone 3 is very lightly clouded with spinel in comparison; the boundary between zones 3 and 4 is therefore defined by an abrupt increase in spinel clouding of plagioclase just southeast of Tyson Lake, a little southeast of the first appearance of metamorphic hypersthene in the country rocks. The spinel dust is believed to be a metamorphic reaction product due to the migration of Fe and Mg into the plagioclase lattice, where it combines with available Al, at the expense of dispelled Ca (Grant, 1988). Coronas of hypersthene about olivine are normally well developed and garnet is ubiquitous about iron oxide and biotite. In a little-deformed sample collected roughly 1.5 km east of the map area, an outer symplectic corona of garnet about successive shells of hypersthene and clinopyroxene implies significantly higher P-T conditions for reaction (Whitney and McLelland, 1973). Where penetrative fabric is strongly developed, the diabase in this zone is almost entirely recrystallized, consisting of alternating elongate lenses of fine grained garnet, biotite, brown amphibole, plagioclase and both orthopyroxene and clinopyroxene. Pale elongate patches visible on outcrop surfaces of the dyke border zones are aggregates of fine grained, light pink garnet. Mylonitic fabrics are well preserved in discrete shear zones of Ramsay-Graham type which cut the dykes sporadically and, as in zone 3, are both confined to the dykes and of no apparent systematic orientation.

Chemistry

Preliminary whole rock chemistry (Bethune and Davidson, 1988) indicated a strong correlation between metadiabase dykes in the Grenville Province and unaltered Sudbury dykes northwest of the Bell Lake granite. To further test this result, a more extensive chemical survey of dykes from a northwest-southeast transect across the map area was conducted. Table 1 allows comparison of analyses of diabase from the four successive metamorphic and deformational zones described above. Diabase in all zones shows similar enrichment in alkalis, Fe, Ti, P, Ba and Zr. It is evident from these data that metadiabase from zones 3 and 4 in the Grenville Province has virtually the same chemistry as Sudbury diabase northwest of the front. Included in Table 1 for comparison is the average of eleven analyses of Grenville diabase. The alkaline olivine chemistry of Sudbury dykes and their metamorphosed equivalents is in clear contrast to the tholeiitic nature of Grenville dykes.

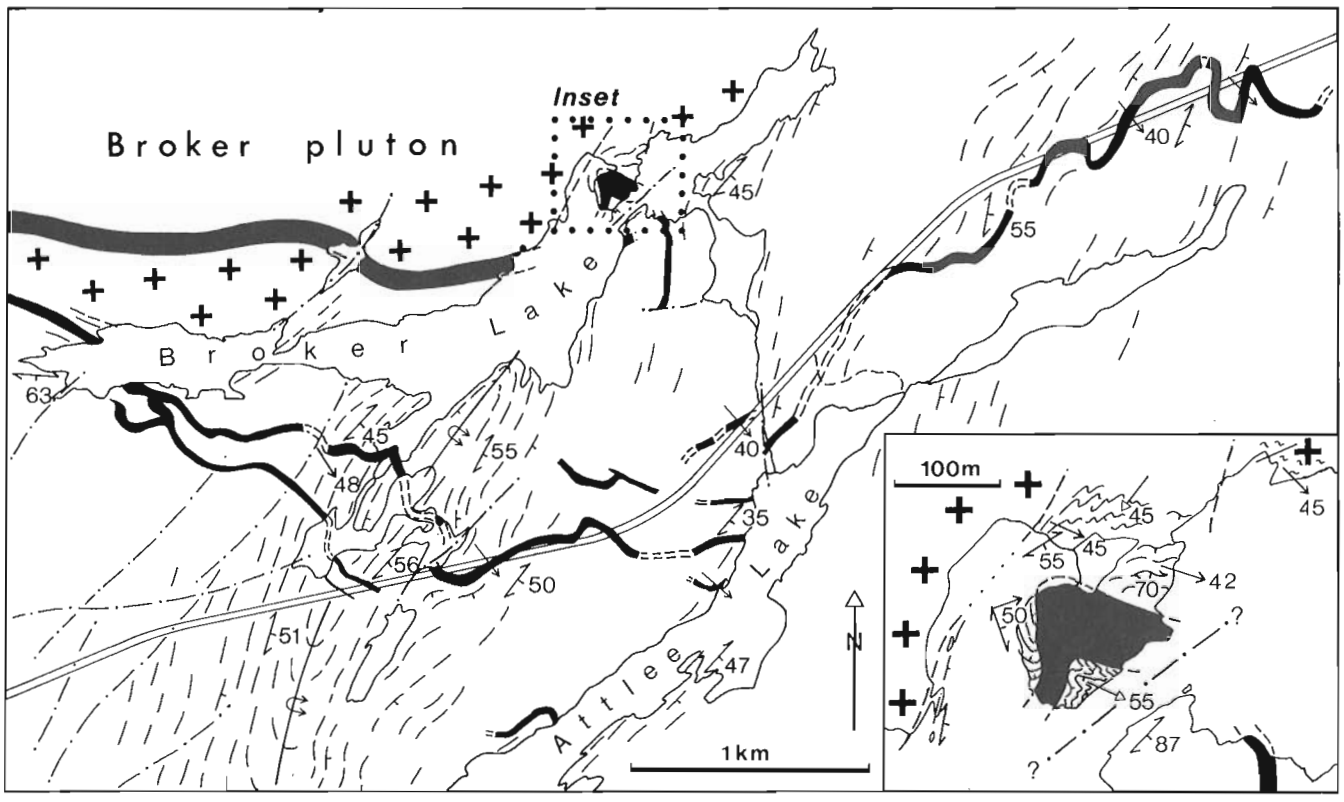

Figure 3. Irregular courses of Sudbury metadiabase dykes in the Broker-Attlee lakes area (zone 4). Symbols are as in Figure 2, except that open-headed arrows in inset indicate minor fold axes. Trends of gneissic layering are shown by short lines. Arrows crossing dykes indicate attitude of lineation within the dykes.

Table 1. Average whole rock chemical analyses and standard deviations of Sudbury diabase from zones 1 to 4 and of Grenville diabase.

	Zone 1 (n=8)		Zone 2 (n=8)		Zone 3 (n=9)		Zone 4 (n=12)		Grenville (n=11)	
SiO_2	47.7	0.7	47.6	0.6	47.4	0.6	48.0	0.5	49.6	0.4
TiO_2	2.90	0.50	2.79	0.32	2.95	0.41	2.89	0.40	1.58	0.31
Al_2O_3	14.6	0.8	14.9	0.8	14.7	0.9	14.6	0.7	14.0	0.5
Fe_2O_3	3.0	0.4	2.8	0.5	3.4	0.8	3.4	0.8	3.5	0.3
FeO	12.5	1.0	12.2	0.7	11.9	1.2	11.8	0.8	9.8	1.0
MnO	0.22	0.02	0.21	0.01	0.21	0.02	0.21	0.01	0.21	0.02
MgO	5.54	0.67	5.50	0.66	5.53	0.70	5.40	0.76	6.97	0.72
CaO	7.68	0.15	7.78	0.21	7.96	0.33	7.74	0.35	11.05	0.65
Na_2O	3.2	0.1	3.3	0.1	3.3	0.1	3.3	0.1	2.1	0.1
K_2O	1.45	0.22	1.32	0.18	1.22	0.26	1.30	0.23	0.34	0.09
P_2O_5	0.60	0.13	0.60	0.13	0.57	0.18	0.62	0.15	0.13	0.03
S	0.10	0.01	0.08	0.02	0.09	0.04	0.09	0.03	0.01	0.01
CO_2	0.1	0.1	0.1	0.1	0.1	0.1	0.1	0.1	0.1	0.1
H_2O	0.6	0.1	0.5	0.1	0.6	0.1	0.5	0.1	1.0	0.1
Total	100.21	0.31	99.68	0.46	99.87	0.53	99.87	0.42	100.25	0.21
ppm										
Ba	686	102	697	88	675	105	707	112	108	19
Sr	310	43	339	49	335	69	324	42	154	23
Zr	221	48	205	43	194	68	212	53	77	18

XRF and rapid chemical analyses were done at the Geological Survey of Canada.

Geochronology

Abnormally high zirconium contents in Sudbury diabases are expressed in the mode by the presence of the igneous mineral baddeleyite (ZrO_2). A U-Pb age of 1238 ± 4 Ma obtained on igneous baddeleyite from the "Espanola" dyke, 45 km northwest of the front (Krogh et al., 1987) is in good agreement with the postulated age of the swarm based on Rb-Sr methods (ca. 1250 Ma, Palmer et al., 1977). Preliminary analyses of baddeleyite separates from Sudbury diabase collected at Lake Panache (15 km northwest of the Grenville Front at Tyson Lake) and at two sites respectively 2.5 km northwest and southeast of the front (**a** in Fig. 1) agree with the "Espanola" dyke age; the seven analyses lie on a discordia whose upper intercept age is 1235 ± 15 Ma (F. Dudás, pers. comm., 1988). Metadiabase in zones 3 and 4 contains baddeleyite rimmed with fine polycrystalline zircon. Davidson and van Breemen (in press) have demonstrated in coronitic metagabbro bodies in the interior of the Grenville Province, an age difference of 120 Ma between polycrystalline zircon overgrowth and the baddeleyite which forms its substrate, suggesting that the overgrowth originated during metamorphism due to an increase in silica activity in the rock. Polycrystalline zircon pseudomorphs of baddeleyite extracted from a metamorphosed Sudbury dyke 5 km southeast of the Grenville Front east of Sudbury have yielded a U-Pb age of ca. 1050 Ma. It is hoped to be able to date primary baddeleyite and metamorphic zircon overgrowth from a single sample of metamorphosed Sudbury diabase in the Tyson Lake area in order to confirm this potential age difference between primary igneous crystallization and metamorphism.

DYKE GEOMETRY IN THE GRENVILLE PROVINCE

Besides showing different styles of internal deformation and metamorphism, dykes of zones 3 and 4 exhibit readily apparent differences in map-scale distribution and geometry. Zone 3 is characterized by more abundant closely spaced dyke segments, a high proportion of which trend northeast. Irregular diabase bodies, in places relatively thick, are common. The discontinuous and seemingly more "telescoped" nature of diabase bodies in zone 3 is in contrast with greater continuity of dykes in zone 4, where sinuous courses are more prevalent, particularly in the narrower dykes. The following observations characterize the dykes in zones 3 and 4.

(1) With almost no exception the dykes cut cleanly across foliation and layering in their country rocks and have relict chilled margins. Northeast-trending dyke segments, although conforming with the strike of gneissic layering on the map, are vertical to steeply southeast-dipping and crosscut less steeply southeast-dipping fabrics.

(2) Dykes or dyke segments, regardless of their width or length, almost everywhere cut up the structural section defined by foliation and gneissic layering in the country rocks; even where curved or apparently folded, the dykes cut a particular straight layer or foliation trace only once. They may, however, cut a particular layer twice if it was repeated by folding before dyke intrusion.

(3) The most discontinuous or sinuous dykes tend to occur within sedimentary gneiss units with varied lithology; dykes within uniform orthogneiss have longer straight segments. At some contacts between sedimentary and granitic gneisses there are perturbations in dyke geometry. Detailed mapping around the hinges of some curved dykes has revealed fabric trajectory patterns in surrounding country rock gneisses indicative of classic "buckle-style" folding of a competent layer in a less competent matrix; the highly sinuous dyke at the far eastern edge of the map area (Fig. 3) is such an example.

(4) Some otherwise continuous dykes end abruptly. These may be natural terminations where the bounding gneisses are not highly strained. In other cases, however, the country rocks are part of regional high strain zones, in which case dykes may have been displaced; lack of adequate outcrop at such terminations generally renders interpretations equivocal.

(5) In neither zone are dykes observed to have intruded across the through-going mylonite zones shown in Figure 1. Mylonitic fabric is observed to be either (a) steeply oriented, subparallel to subvertical dyke contacts, in places with shear fabric penetrating the margin of the dyke itself, or (b) removed from direct contact with diabase such that timing of mylonitization with respect to dyke emplacement is equivocal. The relationship between mylonitization and dyke emplacement is further elaborated below.

(6) At some localities in the map area, two or more relatively closely spaced subparallel dykes exhibit the same sense of deflection at the same structural level adjacent to northeast-trending lineaments. An example of this is at the northwestern side of Tyson Lake, at

the boundary between zones 2 and 3, where several dykes exhibit the same northeastward deflection, and at Spoon Lake where southward deflection is observed close to a mylonite zone.

(7) Adjacent dykes between mylonite zones, for example those traced from the southwestern shore of Tyson Lake to Sunfish Lake and possibly as far as Spoon Lake, crosscut similarly oriented penetrative country rock fabric but usually have mutally independent paths; i.e. the various bends and curves of the dykes are unalike at any given structural level across strike of foliation or gneissic layering.

Most of these observations apply to both zones 3 and 4, but there are clear differences in dyke geometry in the two zones. In zone 3 the dykes occur in relatively short, variously oriented segments, and some have highly convolute map patterns. In zone 4 they are more continuous, and most follow sinuous courses. Examples from each zone are given below.

Examples from zone 3

Diabase bodies on islands and peninsulas in the central part of Tyson Lake (Fig. 2) exhibit a remarkable array of attitudes and shapes. They have the surface form of folds, but although attitudes of layering in the immediately adjacent sedimentary gneisses vary considerably, diabase contacts usually cut steeply across this layering, whatever its attitude. This suggests that, although the dyke orientations may have been modified after emplacement, such modification has only served to enhance originally irregular shapes. The lobe- and hook-shaped diabase bodies are cut off by through-going mylonite zones and late faults; whether they represent a single original intrusion or are tectonically juxtaposed pieces of more than one dyke has yet to be determined. Despite their convolute form, internal deformation, in the form of kinked and bent plagioclase laths, is minimal in many places, and chilled contacts are everywhere well preserved.

Important relationships to post-diabase mylonitization can be evaluated in the western part of Figure 2 map area. Here a major mylonite zone is exposed along the western shores of islands and peninsulas and illustrates the two points outlined in item 5 of the preceding section. At locality A, a hook-shaped diabase body tapers southwestward to a point within sedimentary gneiss. Its western contact is flanked by moderately east-dipping mylonitic rocks that record a sharp westward-increasing strain gradient; kinematic indicators clearly document a westerly thrust sense in this zone. The diabase terminates, however, in gneiss showing no strain related to this mylonite zone; its foliation and layering are truncated at the diabase contact. A branch of the main mylonite wraps the curved north margin of the same diabase but again is not in contact with it. This suggests that during a late stage of deformation the diabase behaved competently while the already-formed mylonitic rocks were warped. Here, then, the relationship between diabase and mylonitization cannot be determined directly, as the diabase neither is mylonitized nor cuts mylonitic fabric.

At locality B, however, the northern extension of the same mylonite zone steepens and swings northwestward adjacent to a thick vertical northwest-striking diabase dyke segment. The southwestern fine grained contact phase of this dyke is strongly sheared to mylonite and ultramylonite in a 3 to 4 m wide zone in which foliation and lineation are oriented identically to those in the mylonite derived from sedimentary gneiss. Strain decreases abruptly toward the interior of the diabase body. Farther east at locality C, the south-trending part of an irregular dyke is apparently truncated by an intense mylonite zone along the contact of a small granite mass.

Examples from zone 4

Figure 3 is a detailed map of dykes and their structural relationships to country rocks in the vicinity of Broker and Attlee lakes. With the exception of the thick east-trending dyke north of Broker Lake, dykes in zone 4 are generally thinner and more continuous than those in zone 3; in addition, all commonly have sinuous courses. The dykes are characterized everywhere, regardless of their width or crosscutting nature, by a fully penetrative, dominantly linear fabric. Most dykes in this region trend east-southeast, essentially perpendicular to regional northeast-oriented, southeast-dipping gneissosity. East of Broker Lake, however, a dyke has been traced for about 3 km along a sinuous course whose overall trend is northeast. This dyke is intersected by the highway in several places, and was originally mapped (Lumbers, 1975) as a number of isolated bodies of "cataclastic metadiabase". The dyke's form has the appearance of ptygmatic folding. It invariably cuts across the layering of its sedimentary gneiss host; its contacts are more steeply inclined to the southeast than gneissic layering along its northeast-trending segments, and at the hinges the contacts pass through vertical and cut sharply across layering. In detail, foliation trajectories in the gneisses close to the pronounced bends show patterns of deflection toward and away from the dyke in a manner analogous to patterns associated with buckle folding of a competent layer in a less competent medium. The same patterns were observed at bends in other places in zone 4, for example along the northwestern shore of Attlee Lake.

A uniformly thick (65 m) dyke follows a gently curving course within the Broker pluton north of Broker Lake. Despite its undeformed appearance, metadiabase in this dyke carries a penetrative mineral stretching lineation (although this is not as pronounced as in the narrower dykes to the south) and exhibits bent plagioclase laths in thin section. However, where it crosses into sedimentary gneiss, as exposed on the peninsula illustrated in the inset of Figure 3, this dyke shows a marked bend and change in thickness. At the outside (northwest) part of its hinge the metadiabase is reduced to well-foliated mylonite in narrow zones subparallel to its contact. Again, foliation trajectories in the generally northeast-trending gneisses are deflected adjacent to the dyke, with tight mesoscopic folds developed in the metasediments on the inside of the dyke arc.

Although it is possible that this dyke is displaced by a fault within Broker Lake (Fig. 3, inset), there is no evidence

along the well-exposed shorelines that this thick dyke is offset and continues to the east. The only possible correlative is the much narrower south-trending dyke exposed at the opposite shore to the southeast. It is suggested that the thickness and continuity of the dyke within the pluton was governed at the time of magma injection by the uniform nature of the orthogneiss, and that magma injected at the same time into the varied sedimentary gneisses formed narrower and less regular dykes. It is clear that the dykes south of Broker Lake were intruded across an already existing fold of Grenville style (Fig. 3). The observed geometries may be due to a simple component of flattening that acted in a direction perpendicular to the trend of dykes which already had irregularities in their courses. What has yet to be determined is the relative proportion between primary sinuosity and subsequent Grenvillian accentuation.

Relationship between metamorphism in country rocks and in metadiabase

Although evaluation of metamorphic mineral assemblages in the Tyson Lake area is as yet far from complete, examination of thin sections made to date suggests a possible mismatch in metamorphic grade in Sudbury metadiabase and its country rocks. Evidence for this comes mainly from the area in zone 3 immediately northwest of the boundary with zone 4. For example, metamorphic hypersthene occurs in gneisses at least 1 km into zone 3. Metadiabase in the same position shows incomplete reaction between primary olivine and plagioclase to give hypersthene coronas surrounded by amphibole—spinel symplectite; hypersthene—clinopyroxene—garnet corona minerals between olivine and plagioclase occur only southeast of this zone boundary. What is more, neosomes associated with the high grade country rock metamorphism do not invade the diabase but are cut by it, and one thin section shows a chilled diabase contact to have cut across a large garnet porphyroblast. It is thus evident that the country rocks underwent high grade metamorphism before emplacement of the Sudbury diabase. Whether or not the gneisses had cooled substantially by the time of dyke intrusion remains conjectural. Resolution of this question bears heavily on the matter of uplift history and on the further question concerning whether metamorphic reactions recorded in metadiabase occurred during initial cooling from magmatic temperature or whether they were the result of altogether later prograde metamorphism. Successful dating of zircon coronas around igneous baddeleyite in metadiabase should help to resolve this question.

It is noted that, in zone 4, hypersthene, clinopyroxene and garnet (the olivine corona assemblage) are recrystallized to very fine polygonal aggregates strung out in the foliation of metadiabase mylonite in the narrow shears within dykes. This is truly indicative of granulite facies conditions during mylonitization. Lack of hydration of such assemblages in metadiabase in general can be explained if the country rocks had already been "dried out" during an earlier metamorphism.

STRUCTURAL HISTORY

Overwhelming evidence that Sudbury dykes in zones 3 and 4 crosscut a penetrative gneissic fabric against which they have preserved chilled contacts, but that the dykes themselves are deformed and metamorphosed, suggests at least a two-stage structural history for the rocks in the vicinity of the Grenville Front in the Tyson Lake area. It should be noted that division of this region into four zones based on southeasterly increase in metamorphism and change in deformation style is primarily a matter of convenience for descriptive purposes. Although there appears to be a marked break at the Grenville Front itself, followed southeastward by a relatively abrupt jump in metamorphic grade between zones 3 and 4, the differences between the zones should be regarded as gradational, at least with respect to post-diabase effects.

Pre-diabase history

If correlation of the rocks in the Grenville Province with those northwest of the front is assumed, it is possible that some evidence of earlier deformation might be preserved in the Grenville Province, at least close to the front. If the metasedimentary rocks around Tyson Lake are indeed correlative with the Huron Supergroup of the Southern Province, they were deformed and metamorphosed during the ca. 1.85 Ga Penokean Orogeny. van Breemen and Davidson (1988) presented evidence for pre-1.40 Ga deformation and metamorphism in the ca. 1.74 Ga Killarney volcanoplutonic complex northwest of the front to the southwest of Tyson Lake. Davidson and Bethune (1988) tentatively correlated felsic and granitoid gneisses in the adjacent Grenville Province with the Killarney complex, a contention supported by U-Pb zircon dating of gneissic granite southwest of Tyson Lake (Krogh et al., 1971). Recognition of either or both of these events in the Grenville Province is hampered by severe reorientation to northeast-striking, southeast-dipping attitudes, except perhaps in low-strain panels in zone 3. It is clear from the evidence already presented, however, that the prevalent Grenville-style structure and high grade metamorphism with accompanying migmatization had already been established before intrusion of Sudbury diabase at ca. 1240 Ma; the age of this major tectonism and its relationship to the development of the Grenville orogen is not yet known.

Post-diabase history

In zone 2, post-diabase deformation is restricted to brittle deformation associated with steep northeast-trending faults. In zone 3 close to the front, diabase intruded as irregular dykes was relatively mildly deformed before and/or perhaps at the same time as development of major mylonite zones, including the one designated as the Grenville Front at the northwestern side of Tyson Lake, which have northwest thrust sense and displace the dykes. Farther southeast, and principally in zone 4, penetrative lineation within the dykes and accompanying buckle folding enhancing former irregularites in the dykes attest to a compressive regime. Accommodation was effected by laterally confined extension directed upward parallel to the lineation that prevails in both the dykes and their country rocks. This implied kinematic sense explains the observed southeastward increase in post-diabase metamorphism and agrees with the kinematics of the mylonite zones in zone 3. The small

mylonitic shears within metadiabase dykes are interpreted as relatively late accommodation structures, but formed while the rocks were still at granulite grade temperature. The latest deformation is manifested by brittle faults that offset deformed Sudbury dykes. All of these structures are transected by the post-orogenic diabase dykes of the Grenville swarm.

ACKNOWLEDGMENTS

The author extends her sincere thanks to Vicki Bowman for her helpful and cheerful assistance in the field. She also gratefully appreciates the help and insightfulness offered by Dugald Carmichael, Herb Helmstaedt, Simon Hanmer and Tony Davidson on their visits during the field season, and thanks the latter for reviewing and improving this manuscript. Special acknowledgment is due to the proprietors of Tyson Lake Marina for their repeated and welcome hospitality.

REFERENCES

Bethune, K.M. and Davidson, A.
1988: Diabase dykes and the Grenville Front southwest of Sudbury, Ontario; in Current Research, Part C, Geological Survey of Canada, Paper 88-1C, p. 151-159.

Davidson, A.
1986: Grenville Front relationships near Killarney, Ontario; in TheGrenville Province, ed. J.M. Moore, A. Davidson and A.J. Baer, Geological Association of Canada, Special Paper 31, p. 107-117.
1988: Two sections across the Grenville Front, Killarney and Tyson Lake areas, Ontario; NATO Advanced Study Institutes Programme, Exposed Cross Sections of the Continental Crust, 59 p.

Davidson, A. and Bethune, K.M.
1988: Geology of the north shore of Georgian Bay, Grenville Province of Ontario; in Current Research, Part C, Geological Survey of Canada, Paper 88-1C, p. 135-144.

Davidson, A. and van Breemen, O.
in press: Zircon and baddeleyite relationships in coronitic metagabbro, Grenville Province, Ontario: implications for geochronology; Contributions to Mineralogy and Petrology.

Fahrig, W.F. and West, T.D.
1986: Diabase dyke swarms of the Canadian Shield; Geological Survey of Canada, Map 1627A.

Frarey, M.J.
1985: Proterozoic geology of the Lake Panache — Collins Inlet area, Ontario; Geological Survey of Canada, Paper 83-22, 61 p.

Grant, S.M.
1988: Diffusion models for corona formation in metagabbros from the western Grenville Province, Canada; Contributions to Mineralogy and Petrology, v. 98, p. 49-63.

Krogh, T.E., Davis, G.L., and Frarey, M.J.
1971: Isotopic ages along the Grenville Front in the Bell Lake area, southwest of Sudbury, Ontario; Carnegie Institution of Washington, Yearbook 69, p. 337-339.

Krogh, T.E., Corfu, F., Davis, D.W., Dunning, G.R., Heaman, L.M., Kamo, S.L., Machado, N., Greenough, J.D., and Nakamura, E.
1987: Precise U-Pb isotopic ages of diabase dykes and mafic to ultramafic rocks using trace amounts of baddeleyite and zircon; in Diabase Dyke Swarms, ed. H.C. Halls and W.F. Fahrig, Geological Association of Canada, Special Paper 34, p. 147-152.

Lumbers, S.B.
1975: Geology of the Burwash area, Districts of Nipissing, Parry Sound, and Sudbury, Ontario; Ontario Division of Mines, Geological Report 116, 158 p.

Palmer, H.C., Merz, B.A., and Hyatsu, A.
1977: The Sudbury dikes of the Grenville Front region: paleomagnetism, petrochemistry and K-Ar age studies; Canadian Journal of Earth Sciences, v. 14, p. 1867-1887.

Quirke, T.T. and Collins, W.H.
1930: The disappearance of the Huronian; Geological Survey of Canada, Memoir 160, 129 p.

van Breemen, O. and Davidson, A.
1988: Northeast extension of Proterozoic terranes of mid-continental North America; Geological Society of America Bulletin, v. 100, p. 630-638.

Whitney, P.R. and McLelland, J.M.
1973: Origin of coronas in metagabbros of the Adirondack Mts., N.Y.; Contributions to Mineralogy and Petrology, v. 39, p. 81-98.

Basement-cover relations between the Archean Yellowknife Supergroup and the Sleepy Dragon Complex north of Fenton Lake, District of Mackenzie, N.W.T.[1]

Donald T. James[2]
Lithosphere and Canadian Shield Division

James, D.T., Basement — cover relations between the Archean Yellowknife Supergroup and the Sleepy Dragon Complex north of Fenton Lake, District of Mackenzie, N.W.T., in Current Research, Part C, Geological Survey of Canada, Paper 89-1C, p. 29-36, 1989.

Abstract

North of Fenton Lake, supracrustal rocks of the Yellowknife Supergroup and rocks from the Sleepy Dragon Complex, which are considered to be possible basement to the Yellowknife Supergroup, can be subdivided into three lithological - structural domains. The domains are composed of: gneisses and metaplutonic rocks of the Sleepy Dragon Complex, unmetamorphosed porphyritic granite, metavolcanic rocks of the Cameron River belt, and metamorphosed greywacke-mudstone turbidites of the Burwash Formation. The contact between the Sleepy Dragon Complex - porphyritic granite domain and the Cameron River metavolcanic domain is everywhere tectonic, marked by moderate to steep, WSW-WNW dipping, ductile shear zones that contain oblique to down-dip mineral elongation lineations. Kinematic indicators from ductile-strained rocks along the contact indicate west-side-down kinematic sense. This suggests that the Sleepy Dragon Complex may have been tectonically unroofed by post-porphyritic granite, ductile, normal faults that followed the lower contact of the Cameron River belt.

Résumé

Au nord du lac Fenton les roches supercrustales du supergroupe de Yellowknife et les roches du complexe de Sleepy Dragon, qui sont considérées comme socle possible du supergroupe de Yellowknife, peuvent être subdivisées en trois domaines lithologiques structuraux. Ces domaines sont les suivants: gneiss et roches métaplutoniques du complexe de Sleepy Dragon et granite porphyrique non métamorphisé, roches métavolcaniques de la zone de Cameron River, grauwacke et pélite métamorphisés mis en place par des courants de turbidité de la formation de Burwash. Le contact entre le domaine de granite porphyrique du complexe de Sleepy Dragon et le domaine métavolcanique de Cameron River est partout tectonique et marqué par des zones de cisaillement ductiles de pendage WSW-WNW modéré à fort qui renferment des linéations minérales obliques. Des indicateurs cinématiques de roches ductiles sous tension le long du contact indiquent que le mouvement s'est fait vers le bas du côté ouest. Cela suggère que le complexe de Sleepy Dragon peut avoir été tectoniquement érodé par des failles normales ductiles postérieures au granité porphyrique qui ont suivi le contact inférieur de la zone de Cameron River.

[1] Contribution to Canada - Northwest Territories Mineral Development Agreement 1987-1991. Project carried by Geological Survey of Canada.
[2] Shield Research Canada, 987 Westminster Place, Kingston, Ontario K7P 1R1

INTRODUCTION

The objectives of this project are to map the part of the Cameron River metavolcanic belt between Fenton Lake and Brown Lake, District of Mackenzie, Northwest Territories and to make a stratigraphic, structural and metamorphic analysis of the metavolcanic belt and adjacent metasedimentary and granitoid terranes. Approximately one-half of this area was mapped in 1988 with the remainder to be covered in 1989. The 1988 field season involved systematic geological mapping at a scale of 1:50 000, with more detailed mapping in the contact zones between the major lithologic — structural domains, which has resulted in a better understanding of the stratigraphic and tectonic evolution of Archean supracrustal sequences in this part of the Slave Province. This project represents a continuation of the 1:50 000 scale mapping of the Cameron River metavolcanic belt by Lambert (1988).

The 1988 map area is entirely within the Carp Lakes 1:250 000 sheet (NTS 85 P) mapped by Moore et al. (1951). Parts of the area mapped in 1988 have also been previously mapped by J.F. Henderson (1941a) (1:63 360 scale mapping of the Gordon Lake area) and Cullen (1988) (1:10 000 scale mapping of the Fenton Lake area). The area mapped in 1988 is contained within NTS map sheets 85 P/2 and P/3.

The mapping has shown that the area can be broadly subdivided into three lithologic - structural domains. The domains are composed of gneisses, meta-plutonic rocks and unmetamorphosed porphyritic granite; metavolcanic rocks; and metamorphosed greywacke-mudstone turbidites. Each domain contains sets of structures that, with few exceptions, do not overprint structures in the other domains. The outstanding structural feature of the area is a zone of high, ductile strain that follows the contact between the domains composed of gneisses, meta-plutonic rocks, and unmetamorphosed porphyritic granite and the metavolcanic rocks (Fig. 1).

LITHOLOGY

Archean pre-Yellowknife supergroup gneissic and plutonic rocks

Sleepy Dragon Complex

Gneisses and meta-plutonic rocks of the Sleepy Dragon Complex (Henderson, 1985) form part of a major block of gneisses and meta-plutonic rocks, and unmetamorphosed granitic plutons that extends for approximately 25 km east and 45 km south and is of unknown extent to the north of the area mapped this year. Henderson (1985) considers the metamorphosed rocks of the Sleepy Dragon Complex to be older than the Yellowknife Supergroup supracrustal rocks. Henderson et al. (1987) report zircon ages of 2819^{+40}_{-3} Ma for granitoid gneisses in the Sleepy Dragon Lake area, and 2663^{+7}_{-5} Ma for a rhyolite (the Turnback Rhyolite) in Yellowknife Supergroup volcanics at the south end of the complex, supporting the hypothesis that the Sleepy Dragon Complex is basement to the Yellowknife Supergroup.

In this area the Sleepy Dragon Complex has been subdivided into two units, one a gneissic unit and the other a meta-plutonic unit herein informally named the Suse Lake granite. Rocks of both units are intruded by unmetamorphosed and massive granitic rocks that are not considered part of the Sleepy Dragon Complex.

The gneisses of the Sleepy Dragon Complex (unit 1, Fig. 1) are a heterogeneous mixture of granitoid gneisses and granitoid migmatite gneisses that are interlayered on all scales and cannot be further subdivided at this scale of mapping. The gneiss unit is composed mainly of biotite tonalite gneiss and tonalitic — granodioritic migmatite gneiss with lesser amounts of hornblende tonalite gneiss and amphibolite agmatite gneiss. Gneissic rocks are commonly intruded on all scales by metamorphosed and deformed dykes and small bodies of foliated, biotite granodiorite-tonalite.

The Suse Lake granite is a metamorphosed and variably foliated alkali feldspar porphyritic granite that is named for exposures at Suse Lake. The Suse Lake granite contains xenoliths of foliated mafic tonalite of uncertain origin and xenoliths of gneiss from the Sleepy Dragon Complex demonstrating that the Suse Lake granite is younger than the gneisses. The Suse Lake granite is typically foliated whereas the porphyritic granite (unit 5, Fig. 1) that also intrudes gneisses in the Sleepy Dragon Complex is massive and unmetamorphosed. This suggests that the Suse Lake granite is older than the porphyritic granite unit. The absence of xenoliths of Yellowknife Supergroup rocks in the Suse Lake granite and the absence of intrusions of Suse Lake granite in Yellowknife Supergroup rocks and the marked discordance between structures in the Suse Lake granite and the adjacent Yellowknife Supergroup metavolcanics suggests that the Suse Lake granite is older than the Yellowknife Supergroup. A sample for radiometric age determination was collected from the Suse Lake granite.

Both the granitoid migmatite gneisses and the Suse Lake granite locally contain deformed amphibolite dykes. The generally northwesterly to north-northwesterly striking dykes are up to several metres wide. They are most common within 1 km of the Sleepy Dragon Complex — Cameron River metavolcanic contact. The dykes are discordant to the structures in the Sleepy Dragon Complex except at the contact between the Sleepy Dragon Complex and the Cameron River metavolcanic belt where dykes, Sleepy Dragon Complex rocks and Cameron River metavolcanics have been deformed by ductile high strain zones. Dykes cannot be traced across the high strain zones from the Sleepy Dragon Complex into the metavolcanics.

In contrast to this area, dense swarms of mafic dykes have been reported from the Sleepy Dragon Complex in the Upper Ross Lake, Webb Lake and Patterson Lake areas, 20 km south-southwest of the map area (J.F. Henderson, 1941b; Davidson 1972; Lambert 1974, 1982, 1988; J.B. Henderson, 1985). These dyke swarms were thought by Baragar (1966) to be related to the (structurally) adjacent mafic flows in the Cameron River metavolcanic belt, and Lambert (1982) and Henderson (1985) have speculated that they represent a subvolcanic conduit system in the basement below the volcanics.

YELLOWKNIFE SUPERGROUP

Cameron River Metavolcanics

The metavolcanics (unit 3, Fig. 1) are part of the Cameron Rivermetavolcanic belt that has been mapped to Upper Ross Lake, 30 km south of Fenton Lake (J.F. Henderson, 1941b; Lambert, 1974, 1977, 1982, 1988; J.B. Henderson, 1985; Cullen, 1988), and to Brown Lake, 40 km north of Fenton Lake (Moore et al., 1951). The Cameron River belt is part of a much larger system of metavolcanic belts that have a combined strike length of greater than 250 km and partially mantle the block of Sleepy Dragon Complex rocks in this part of the Slave Province.

The Cameron River metavolcanics vary in outcrop width from 4 km in the Fenton Lake area to 0.5 km in the central and northern parts of the map area. Structurally the metavolcanics occur in a steeply west-dipping and strongly flattened homoclinal succession. To the west, the metavolcanics are conformably overlain by greywacke-mudstone metasediments of the Burwash Formation. To the east the metavolcanics are in tectonic contact across a ductile shear zone with both the younger plutonic rocks (porphyritic granite unit) and the older rocks of the Sleepy Dragon Complex.

The porphyritic granite east of Fenton Lake (unit 5, Fig. 1) contains xenoliths of Cameron River metavolcanics. This demonstrates that an intrusive contact relationship existed between the Cameron River metavolcanics and the porphyritic granite prior to the ductile strain that overprinted the contact. Metavolcanics east of Fenton Lake, within several hundred metres of the contact with the porphyritic granite, contain small dykes of massive granite and pegmatite that become more abundant towards the contact with the porphyritic granite. Although these dykes cannot be traced across the contact into the porphyritic granite their presence supports the suggestion that the porphyritic granite is younger than the metavolcanics.

In the Fenton Lake area the metavolcanic belt is composed mainly of amphibolite-grade mafic amphibolites. Rocks are black to dark green, variably foliated and commonly steeply lineated. They are non-layered, hornblende - plagioclase rocks that may or may not contain relict pillow and breccia structures. The mafic amphibolite unit also includes minor amounts of intermediate and felsic metavolcanics and rarely, biotite - garnet metasedimentary schist. The mafic amphibolites also contain common occurrences of metre-scale meta-gabbro dykes/sills that make up to 15 per cent of the unit and are most abundant near the structural base of the belt. In the extreme southeast corner of the map area a small, layered meta-gabbro body is present in the mafic amphibolite unit. The metavolcanics in this area also contain a structurally continuous layer of meta-rhyolite that pinches-out southwest of Suse Lake. These rocks are grey, strongly foliated and commonly have a relict porphyritic texture with white or blue quartz phenocrysts, or both quartz and feldspar phenocrysts. Locally, the meta-rhyolite has a brecciated structure. Garnet porphyroblasts in meta-rhyolite are common.

In the Fenton Lake area the contact between the metavolcanics and the Burwash Formation is poorly exposed. The contact is sharp and is marked by steeply west-dipping mafic amphibolites that structurally underlie Burwash Formation metasediments.

North of Fenton Lake, in the Suse Lake, Georic Lake and Lake 355 (unofficial name) areas, the Cameron River belt is composed mainly of massive, pillowed and brecciated mafic amphibolites that make up 75 per cent or more of the total outcrop width. The mafic amphibolites in this area have identical compositions and textures to those in the Fenton Lake area. The mafic amphibolites in this area also contain 1-2 m wide, foliation-parallel, massive meta-gabbro dykes/sills that make up approximately 10 per cent of the mafic amphibolite unit. In general, dykes are equally distributed throughout the section although the base of the unit between Suse Lake and Georic Lake is composed of a dense, 75-m-wide, mafic dyke swarm consisting of 2-3 m-wide, massive amphibolite dykes. Within approximately 10 m of the Cameron River - Sleepy Dragon Complex contact, the dyke swarm contains inclusions of strongly foliated, metagranitoid of the Sleepy Dragon Complex. It is not certain if these inclusions are tectonic or remnants of the country rock into which the dykes were emplaced prior to shearing.

In the Suse Lake and Georic Lake areas the upper part of the Cameron River belt is composed of black, grey and green, finely-layered metavolcanic/volcaniclastic rocks, and mafic and intermediate composition amphibolites. These rocks are interlayered with a minor amount of felsic breccia, semi-pelitic schist and breccias with a carbonate matrix. The felsic breccia, 1 km northwest of Suse Lake, is less than 50 m wide and is composed of a fine-grained, schistose, felsic matrix with clasts (up to 10 cm) of massive felsite and feldspar porphyry. Semi-pelitic schists interlayered with the Cameron River metavolcanics become more abundant towards the top of the section and are similar in composition to the overlying Burwash Formation metasediments.

South of Georic Lake, the contact between the Cameron River metavolcanics and the Burwash Formation is marked by occurrences of a breccia with a carbonate matrix. At its widest exposure the breccia is approximately 50 m wide. The rocks are distinctively black and brown weathering, and composed of rounded to subangular (1-15 cm) metavolcanic clasts and a carbonate matrix. Throughout the map area, occurrences of carbonates along the metavolcanic - Burwash Formation contact are rare.

West of Lake 355, the upper 100 m of the Cameron River belt is composed, from east to west, of intermediate composition metavolcanics, meta-rhyolite and black slate. The intermediate metavolcanics are grey-mauve and black weathering, massive and pillowed, and commonly contain narrow garnetiferous layers, and lenses of carbonate. The meta-rhyolite is grey-weathering, strongly foliated, and porphyritic with blue quartz phenocrysts. Locally, the meta-rhyolite appears to contain relict breccia structures. A 10-m-thick layer of fine-grained black slate overlies the meta-rhyolite and is in turn overlain by greywacke-mudstone turbidites of the Burwash Formation.

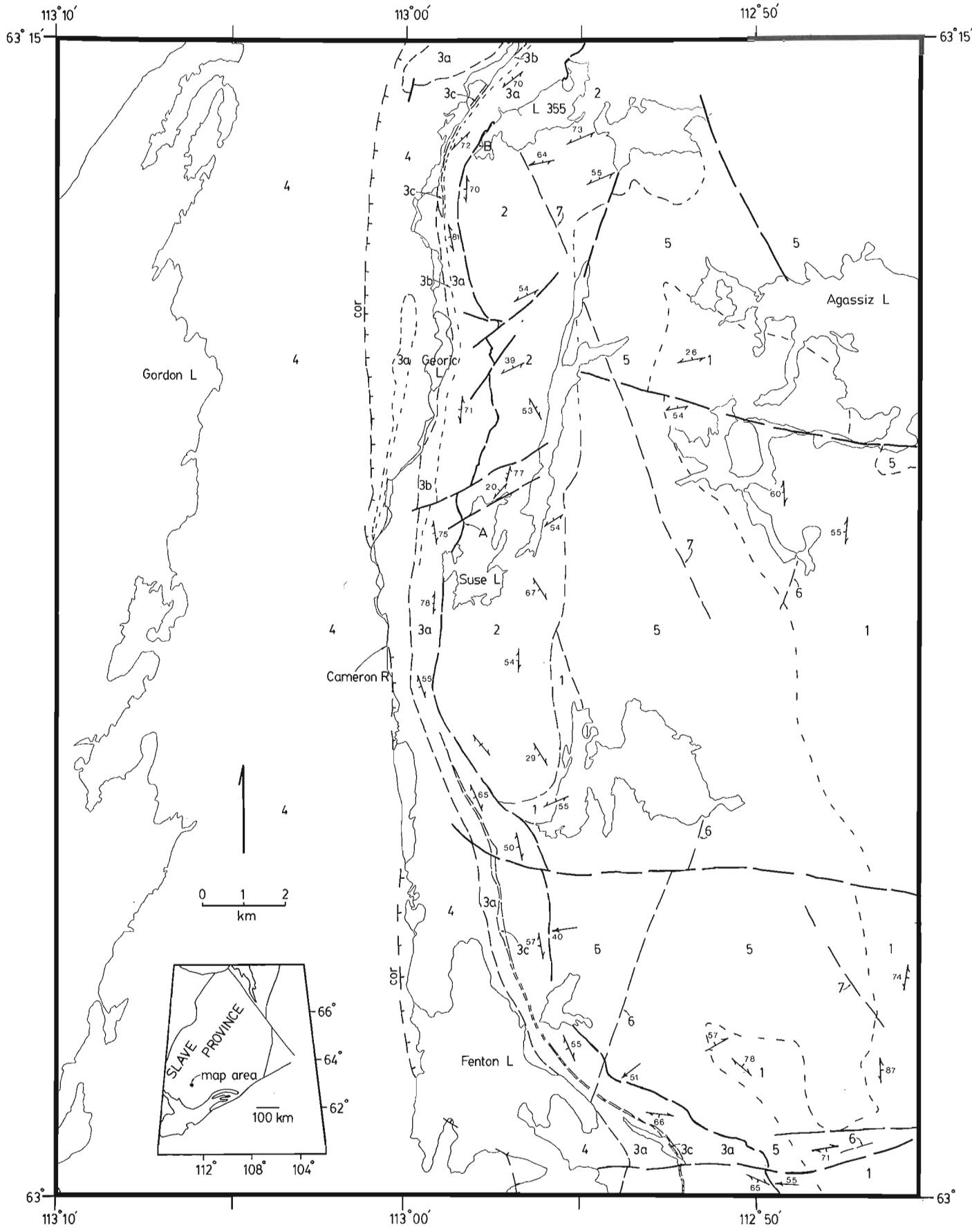
113°10′
113°00′
112°50′
63°15′
63°
Gordon L
Agassiz L
Suse L
Fenton L
Cameron R
L 355
Georic
cor
0 1 2
km
SLAVE PROVINCE
map area
100 km
66°
64°
62°
112°
108°
104°

Rusty-weathering zones of metavolcanics that contain disseminated sulphide minerals are common throughout the Cameron River belt in the map area. The widest and most continuous zones occur east of Fenton Lake along the eastern contact between the meta-rhyolite and the mafic amphibolites, 1 km northwest of Suse Lake along the eastern contact of a felsic breccia, and 1.5 km southwest of Lake 355 along the contacts of a meta-rhyolite.

Burwash Formation

Metamorphosed greywacke and greywacke-mudstone turbidites that occupy approximately 40 per cent of the map area are correlated with the Burwash Formation as defined at Yellowknife by J.B. Henderson (1970) as they may be traced continuously for 90 km to Yellowknife where the formation has been studied in detail by J.B. Henderson (1972, 1975).

Mapping of the metasediments was concentrated mainly along the contact between the formation and the Cameron River metavolcanics as the metasediments west of the Cameron River had been previously mapped by J.F. Henderson (1941a). A relatively small and well-exposed area on the east side of Gordon Lake was mapped in order to supplement J.F. Henderson's map by providing a more detailed structural and metamorphic data base.

The contact between the Cameron River metavolcanics and the Burwash Formation is poorly exposed although the location of the contact is apparent on aerial photographs as it is marked by a distinct topographic break with the metavolcanics forming a steep scarp that rises as much as 80 m above the metasediments. At Fenton Lake the contact is sharp and marked by strongly flattened, and steeply west-dipping and west-facing mafic amphibolites that structurally underlie Burwash Formation metasediments. North of Fenton Lake the contact may be sharp, as in the Fenton Lake area, or somewhat gradational with metavolcanics adjacent to the contact containing layers of metasediment that are similar in composition to Burwash Formation metasediments. In areas where the Cameron River metavolcanics contain interlayered metasediments the contact is placed at the base of the continuous greywacke - mudstone metasedimentary sequence. The contact relationships between the Cameron River metavolcanics and the Burwash Formation suggest that the contact is conformable.

There are no demonstrated occurrences of interbedded metavolcanics and Burwash Formation metasediments in the map area. J.F. Henderson (1941a) has interpreted occurrences of metavolcanics within the Burwash Formation west of Georic Lake to be exposed in an anticlinal core. This structure will be re-mapped in 1989.

The contact between the Cameron River metavolcanics and the Burwash Formation is locally marked by extensive zones of rusty-weathering Burwash Formation. These may contain several percent disseminated sulphides and locally contain arsenopyrite. The best exposed gossan is west of Lake 355 where the contact outcrops along the east shore of Cameron River.

The Burwash Formation consists mainly of metamorphosed, interbedded greywacke and mudstone that are characteristically of uniform thickness and are laterally continuous across the exposed area. Greywacke beds are light-grey or tan weathering and generally less than 2 m thick. Mudstone beds are black weathering and commonly less than 0.2 m thick. Greywacke beds commonly show a colour, grain size and compositional variation from light coloured, sand-sized and relatively quartzo-feldspathic bases to grey-black, finer grained, relatively-pelitic tops, or may be homogeneous.

Greywacke is the dominant lithology in most outcrops. This is especially evident in the area around the central part of Fenton Lake where locally the formation is composed entirely of beds of massive greywacke. In general, the amount of mudstone increases from east-to-west to Gordon Lake.

Metamorphic grade in the Burwash Formation increases from west-to- east, from sub-biotite-grade in the Gordon Lake area to cordierite-grade adjacent to the Cameron River metavolcanics. The cordierite isograd parallels the trace of

Figure 1. Geology of the area immediately north of Fenton Lake. Archean Yellowknife mafic volcanics (unit 3) are separated from Sleepy Dragon gneisses and metamorposed, foliated Suse Lake granite (units 1 and 2) and a younger porphyitic granite (unit 5) that intrudes both the volcanics and the other granitoids, by west side down ductile shear zones.

FIGURE 1 LEGEND

LITHOLOGIC UNITS

Middle Proterozoic
- 7 Mackenzie diabase dykes

Early Proterozoic
- 6 diabase dykes

Archean
- 5 porphyritic granite

Yellowknife Supergroup
- 4 Burwash Formation
- 3 Cameron River metavolcanics
- 3a mafic amphibolite, pillowed mafic amphibolite
- 3b mafic - intermediate metavolcanics
- 3c meta-rhyolite

Sleepy Dragon Complex
- 2 Suse Lake granite
- 1 heterogeneous gneiss

geological contact (approximate, assumed)

foliation (inclined, vertical)

mineral elongation lineation

fault trace

cordierite isograd

the contact between the Sleepy Dragon Complex — porphyritic granite domain and the Cameron River metavolcanic belt. This suggests that the metamorphism of the supracrustal rocks may be related to the intrusion of the porphyritic granite.

POST-YELLOWKNIFE SUPERGROUP INTRUSIVE ROCKS

Porphyritic Granite

Occurrences of unmetamorphosed and massive porphyritic granite are restricted to the eastern part of the map area where it intrudes gneisses of the Sleepy Dragon Complex. Contacts between the gneisses and porphyritic granite units are gradational, marked by zones of a heterogeneous mixture of granite and gneiss that are locally greater than 1 km wide. Approximate contacts on the map are placed where the proportion of granite becomes greater than that of gneiss.

The Cameron River metavolcanic — porphyritic granite contact is everywhere tectonic. Porphyritic granite within approximately 0.5 km of the contact becomes foliated and towards the contact the unit is progressively more highly strained to protomylonite to ultramylonite. A pre-ductile-strain intrusive relationship between the porphyritic granite and the metavolcanics is unequivocally demonstrated by xenoliths of Cameron River mafic amphibolites within the granite.

The granite is white- or pink-weathering and occurs as both an alkali feldspar porphyritic granite and as an equigranular granite. Contacts between the two textural variations are gradational and occur at all scales. This unit contains less than 10 per cent biotite and muscovite. Muscovite is not ubiquitous. This unit also contains a minor amount of pink or white, muscovite-pegmatite and dykes of fine-grained, equigranular leucogranite.

Cullen (1988) has correlated the porphyritic granite unit, based on exposures in Fenton Lake area, with the Morose Granite that has been mapped farther to the south by Davidson (1972) and J.B. Henderson (1985).

Diabase Dykes

All of the lithologic units are intruded by three sets of unmetamorphosed, massive, Proterozoic diabase dykes with strikes approximately 020, 085 and 340 degrees. Ages of the 020 and 085 dykes are uncertain (Indin and Dogrib respectively?). The 340 degree striking dykes belong to the Mackenzie (1220 Ma) set (Fahrig and West, 1986).

Porphyritic granite along the north shore of Agassiz Lake is intruded by a 10-m-thick diabase sill.

STRUCTURAL GEOLOGY

In this section the geometric and kinematic aspects of the structural geology are described and a tentative deformation history is proposed.

Mapping has shown that the area can be subdivided into three lithologic — structural domains that contain sets of structures of distinctly different style and orientation. With a few exceptions, structures from different domains do not overlap in space and their relative timing therefore cannot be unequivocally demonstrated.

GEOMETRIC AND KINEMATIC DESCRIPTIONS OF STRUCTURES

Sleepy Dragon Complex Domain

Gneisses within the Sleepy Dragon Complex exhibit, on the outcrop-scale, complex folds of gneissosity that define fold interference patterns. Most commonly, gneissosity is folded into open domes and basins with fewer occurrences of Type 2 and Type 3 (Ramsay, 1967) fold patterns. More detailed mapping and subdivision of the gneisses will be necessary before map-scale structures can be defined.

In contrast to the structural style in the gneisses, the Suse Lake granite has a variably developed, steeply-dipping foliation that has a northerly- to northeasterly-strike. Commonly, rocks are strongly foliated and contain steeply-plunging mineral elongation lineations.

Cameron River Metavolcanic Domain

The trend of the Cameron River metavolcanic belt and the orientations of structures in the belt truncate the structures in the Sleepy Dragon Complex. This suggests that the structures in the Cameron River metavolcanics are younger than the structures in the Sleepy Dragon Complex.

The few stratigraphic markers that are present in the Cameron River belt and pillow-facing directions suggest that the overall structure of the belt is that of a steep westerly-dipping and west-facing homocline.

The Cameron River belt and the Suse Lake granite are cut by northeasterly-striking faults that, with one exception, do not continue to the upper contact of the metavolcanics. This suggests that these faults may have been active during volcanism and were controlled by pre-existing structures in the basement rocks.

The main foliation throughout the Cameron River belt is variably developed and is approximately parallel to the margins of the belt. This foliation, defined by metamorphic minerals, is observed to be axial planar to minor, isoclinal folds of compositional layering. In rare occurrences these folds are re-folded by the main foliation to produce Type 3 (Ramsay, 1967) interference patterns. Throughout the Cameron River belt, the rocks commonly contain a strongly developed, west-southwesterly- to northwesterly-trending and moderately- to steeply-plunging mineral and/or pillow elongation lineation. Commonly, horizontal outcrop surfaces of pillowed metavolcanics exhibit approximately equant or slightly-elliptical pillows and vertical surfaces that have a streaky appearance defined by highly elongated pillows.

Locally, the main foliation is folded by a steeply-dipping foliation producing north-northwest to north, and south-southeast to south-trending folds that have shallow plunges.

Burwash Formation Domain

Only a cursory examination of structures in the Burwash Formation in the Gordon Lake area was made in 1988. The structure in this area has been previously described by J.F. Henderson (1941a) and Fyson (1975). The structure in this area is dominated by north-northeasterly- to northeasterly-trending, tight to isoclinal and closely spaced folds that are recognized by reversals in stratigraphic facing direction. Folds have vertical to steep easterly-dipping axial surfaces and steeply-plunging fold axes. Traces of bedding visible on aerial photographs suggest that plunges reverse along the strike of the axial surface. The main penetrative cleavage in mudstone in this area is approximately parallel to bedding and axial planar to the folds.

In the northwest corner of the map area, the main penetrative cleavage is overprinted by a northwesterly-striking cleavage. Locally, the main penetrative cleavage and the second cleavage are overprinted by a northeasterly- to north-northeasterly-striking crenulation cleavage in mudstone beds and a fracture cleavage in greywacke beds.

From west to east, towards the contact between the Cameron River belt and the Burwash Formation, the folds in the Burwash Formation become more closely spaced and axial surfaces strike parallel to the contact between the Cameron River belt and the Burwash Formation. Folds in the Burwash Formation adjacent to the contact also involve metavolcanics of the Cameron River belt. West of Lake 355 the metavolcanics are exposed in the core of a steep, southerly-plunging, anticline that has a steep east-dipping axial surface. West of Georic Lake metavolcanics are exposed in the core of a doubly-plunging anticline.

The Burwash Formation adjacent to the metavolcanic belt is at cordierite-grade in contrast to sub-biotite-grade at Gordon Lake. Cordierite is observed to overgrow the main penetrative foliation and since the cordierite isograd is not folded, this demonstrates that metamorphism outlasted the main phases of deformation in the Burwash Formation.

Structure of the Sleepy Dragon Complex — Cameron River Metavolcanic Contact

The structure of the contact between the Sleepy Dragon Complex (Suse Lake granite unit) and the Cameron River metavolcanic belt is described from two locations in the map area. The locations are labelled A and B on Figure 1.

Location A

Along the east and north shores of Suse Lake, massive to foliated Suse Lake granite is cut by 5-30 cm wide, randomly spaced, anastomosing, ductile shear zones that are discordant to the foliation in the Suse Lake granite. The shear zones dip moderately to steeply to the west and have strikes that are approximately parallel to the trace of the contact between the Suse Lake granite and the metavolcanic belt. The shear zones contain protomylonitic to mylonitic fabrics and northwesterly-trending, moderately-plunging (oblique to down-dip) mineral elongation lineations. The attitudes of foliation along the margins of the shear zones and asymmetric feldspar porphyroclasts consistently indicate an oblique to dip-slip, west-side-down kinematic sense.

Within 50 m of the contact the shear zones become more closely spaced (less than 1 m) and the granite becomes strongly foliated with a fabric that is parallel to the orientation of both the shear zones and the contact. The older foliation in the Suse Lake granite is obliterated. Some of the shear zones are marked by high concentrations of epidote and chlorite. Within 40 m of the contact, the porphyritic texture of the Suse Lake granite is destroyed and the rocks are completely recrystallized to produce a 20-m-wide layer of a white, very fine-grained, homogeneous granite. The white granite grades into a 15 m wide, very distinctive, white-weathering, quartz-feldspar-muscovite-biotite granite "schist". The granite "schist" is separated from the metavolcanics by a 5 m wide, rusty-weathering biotite-garnet schist that is in sharp contact with mafic amphibolites of the Cameron River belt. The origin of the rusty-weathering schist is uncertain.

The metavolcanics above the contact are fine-grained, mafic amphibolite schists that have a strongly developed foliation parallel to the contact. The zone of amphibolite schist is of varied width (up to several tens of metres) in this area and grades away from the contact into lesser deformed rocks of the Cameron River belt.

Location B

The Suse Lake granite, within 200 m of the contact with the Cameron River belt, is deformed by a dense network of anastomosing, ductile shear zones. Which are moderate westerly-dipping and contain down-dip mineral elongation lineations. Mesoscopic kinematic indicators were not observed. Locally, sheared granite grades into layers of quartz-feldspar-muscovite-biotite granite "schist", and less commonly contains thin (less than 1 m) layers of rusty-weathering biotite-garnet schist similar to the rusty-weathering rocks at location A. These rocks also contain common occurrences of thin (1-10 cm), deformed and metamorphosed amphibolite dykes. At approximately 50 m from the contact this zone of granite, granite "schist" and sheared granite grades into a layer of completely recrystallized, white, very fine-grained, homogeneous granite. This white granite is in sharp contact with the metavolcanics.

The textural variations in the Suse Lake granite at Location B are similar to the textures reported by Davidson (1972) from the Ross Lake granodiorite in the Sleepy Dragon Lake area, 10 km south of the map area. Near the contact between the Ross Lake granodiorite and the Cameron River belt, Davidson notes that the granodiorite goes through a "progressive reduction to quartz-muscovite schist and even mylonite", and that deformation becomes intense towards the contact where "subsequent recrystallization has produced a dense, white, feldspathic rock with little or nothing to suggest its origin".

Above the contact at Location B, the Cameron River belt is composed of a thin (less than 2 m) layer of strongly foliated, amphibolite schist that grades away from the contact into lesser deformed mafic amphibolites. Clearly recognizable pillows occur within 3 m of the contact.

North of Location B, along the west shore of Lake 355, the contact between the white, recrystallized granite and the metavolcanics can be traced around a series of steep, easterly- plunging, isoclinal Z folds. The metavolcanics that are adjacent to the contact in this area, contain blocks and layers of the granite that are interpreted to be tectonic inclusions.

Structure of the Porphyritic Granite — Cameron River Metavolcanic Contact

East of Fenton Lake, the contact between the porphyritic granite and the Cameron River belt is marked by a ductile shear zone. Towards the contact, the porphyritic granite becomes progressively more highly-strained over a zone of varied width (maximum 500 m). The strain is expressed as a progressive development and strengthening of a westerly-dipping foliation, and ultimately mylonite and ultramylonite within several metres of the contact. Rocks contain west to west-southwest, moderately-plunging mineral elongation lineations. Rare occurrences of kinematic indicators (shear bands and asymmetric feldspar porphyroclasts) suggest a west-side-down sense of shear.

The Cameron River belt adjacent to the contact is composed of fine- grained, strongly foliated, amphibolite schist. The amphibolite schists adjacent to the contact in this area, and at locations A and B, are believed to be the highly strained equivalents of the lesser deformed, massive, pillowed and brecciated mafic amphibolites that are common throughout the Cameron River belt. Rocks in the zone of amphibolite schist do not appear to be retrograded.

DEFORMATION HISTORY

The truncation of structures in the Suse Lake granite by the Cameron River belt suggests that the structures in both the Suse Lake granite, and the gneisses which it intrudes, are older than the structures in the Cameron River metavolcanics.

The relative timing of the development of sets of overprinting structures in the Cameron River metavolcanic and Burwash Formation domains is uncertain. Both domains contain sets of early syn- or syn-metamorphic structures that do not overlap in space with the exception of two folds in the Burwash Formation that expose metavolcanics in anticlinal cores. It is believed that the reason for the differences in structural style and orientation between the two domains is due to the significant contrast in lithology.

The high, ductile strain along the contacts between the Sleepy Dragon Complex (Suse Lake granite) and the Cameron River belt, and the porphyritic granite and the Cameron River belt, post-dates the structures in the Cameron River belt and the intrusion of the porphyritic granite. Kinematic indicators along both contacts indicate that at least the latest movement along the ductile shear zones was west-side-down. This suggests that the Sleepy Dragon Complex may have been tectonically un-roofed by ductile, normal faults that followed the lower contact of the Cameron River belt.

The youngest map-scale structures in the area are easterly-striking dextral faults that displace Archean lithologic and tectonic contacts, and displace the 020 striking Proterozoic diabase dykes.

ACKNOWLEDGMENTS

Chris Drachenberg is thanked for assistance in the field. Maurice Lambert made a visit to the field area. Excellent expediting was provided by Rod Stone and Lynn Parney with the support of the Geology Office, Indian and Northern Affairs Canada in Yellowknife. John B. Henderson reviewed an earlier version of this report.

REFERENCES

Baragar, W.R.A.
1966: Geochemistry of the Yellowknife Volcanic rocks; Canadian Journal of Earth Sciences, v. 3, p. 9-30.

Cullen, R.
1988: Geology and Structure of the Cameron River belt, Fenton Lake area; parts of NTS 85 I/15, P/2; Geology Division, Indian and Northern Affairs Canada, Yellowknife, 2 maps with notes.

Davidson, A.
1972: Granite studies in the Slave Province (Parts of 85 I): in Report of Activities, Part A; Geological Survey of Canada, Paper 72-1A, p. 109-115.

Fahrig, W.F. and West, T.D.
1986: Diabase dyke swarms of the Canadian Shield; Geological Survey of Canada, Map 1627A.

Fyson, W.K.
1975: Fabrics and deformation of Archean metasedimentary rocks, Ross Lake Gordon Lake area, Slave Province, Northwest Territories; Canadian Journal of Earth Sciences, v. 12, p. 765-776.

Henderson, J.B.
1970: Stratigraphy of the Yellowknife Supergroup, Yellowknife Bay Prosperous Lake area, District of Mackenzie; Geological Survey of Canada, Paper 70-26, 12 p.
1972: Sedimentology of Archean turbidites at Yellowknife, Northwest Territories; Canadian Journal of Earth Sciences, v. 9, p. 882-902.
1975: Sedimentology of the Archean Yellowknife Supergroup at Yellowknife, District of Mackenzie; Geological Survey of Canada, Bulletin 246, 62 p.
1985: Geology of the Yellowknife-Hearne Lake area, District of Mackenzie: a segment across an Archean basin; Geological Survey of Canada, Memoir 414, 135 p.

Henderson, J.B., van Breemen, O., and Loveridge, W.D.
1987: Some U-Pb zircon ages from Archean basement, supracrustal and intrusive rocks, Yellowknife - Hearne Lake area, District of Mackenzie, NWT: in Radiogenic Age and Isotopic Studies, Geological Survey of Canada, Paper 87-2, p. 111-121.

Henderson, J.F.
1941a: Gordon Lake, District of Mackenzie, Northwest Territories; Geological Survey of Canada, Map 644A.
1941b: Gordon Lake south, District of Mackenzie, Northwest Territories; Geological Survey of Canada, Map 645A.

Lambert, M.B.
1974: Archean volcanic studies in the Slave-Bear province: in Report of Activities, Part A, Geological Survey of Canada, Paper 74-1A, p. 177-179.
1977: Anatomy of a greenstone belt, Slave Province, Northwest Territories: in Volcanic Regimes in Canada, ed. W.R.A. Baragar, L.C. Coleman and J.M. Hall; Geological Association of Canada, Special Paper 16, p. 331-340.
1982: Synvolcanic intrusions in the Cameron River volcanic belt, District of Mackenzie: in Current Research Part A, Geological Survey of Canada, Paper 82-1A, p. 165-167.
1988: The Cameron River and Beaulieu River volcanic belts, District of Mackenzie, Northwest Territories; Geological Survey of Canada, Bulletin 382.

Moore, J.C.G., Miller, M.L., and Barnes, F.Q.
1951: Carp Lakes, Northwest Territories; Geological Survey of Canada, Paper 51-8, map with descriptive notes.

Ramsay, J.G.
1967: Folding and Fracturing of Rocks; McGraw-Hill, New York, 568 p.

The Mystery Island Intrusive Suite and associated alteration haloes, Great Bear Lake, District of Mackenzie[1], N.W.T.

Nancy C. Reardon[2]

Reardon, N. C., The Mystery Island Intrusive Suite and associated alteration haloes, Great Bear Lake, District of Mackenzie, N.W.T.; in Current Research, Part C, Geological Survey of Canada, Paper 89-1C, p. 37-42, 1989.

Abstract

The Mystery Island Intrusive Suite constitutes a group of sill-like intermediate composition plutons in the Echo Bay area. The plutons consist of seriate, medium grained biotite-hornblende monzodiorite - monzonite - quartz monzodiorite - quartz monzonite (IUGS). The plutons are associated with andesitic stratovolcanoes and were emplaced at two stratigraphic levels: at the base of the andesitic volcanoes; and at higher levels within the complex. Later folding has exposed the plutons and their wall rocks in oblique cross-section. All of the plutons have associated alteration, which is present primarily within the wall rocks above the plutons, but also within and below the plutons. Three alteration types, albitic, magnetite-apatite-actinolite and pyritic were recognized and mapped. The alteration types are crudely zoned, with albitic alteration closest to the plutons followed by the magnetite-apatite-actinolite and pyrite zones. Quartz-carbonate-sulphide veins are spatially associated with the plutons and their alteration haloes.

Résumé

La suite intrusive de Mystery Island constitue un groupe de plutons apparentés à des filons-couches de composition intermédiaire dans la région d'Echo Bay. Les plutons se composent de biotite - monzodiorite à hornblende - monzonite - monzodiorite quartzique - monzonite quartzique sériées à grain moyen. Les plutons sont associés à des stratovolcans andésitiques et étaient situés à deux niveaux stratigraphiques: à la base des volcans andésitiques et à des niveaux plus élevés à l'intérieur du complexe. Un plissement ultérieur a mis à nu les plutons et leurs roches encaissantes en coupes transversales obliques. À chacun des plutons correspond une altération associée, qui est présente principalement dans les roches encaissantes au-dessus des plutons, mais aussi à l'intérieur des plutons et sous ces derniers. Trois types d'altération, albitique, magnétite-apatite-actinolite et pyritique ont été reconnus et cartographiés. Les types d'altération sont grossièrement zonés, l'altération albitique étant la plus rapprochée des plutons et suivie dans l'ordre de la zone de magnétite-apatite-actinolite puis de la zone de pyrite. Des veines de quartz-carbonate-sulfure sont associées dans l'espace aux plutons et à leurs halos d'altération.

[1] Contribution to Canada - Northwest Territories Mineral Development Agreement 1987-1991. Project carried by Geological Survey of Canada, Lithosphere and Canadian Shield Division.

[2] 2552 Windsor Street, Halifax, Nova Scotia B3K 5C3.

INTRODUCTION

The Mystery Island Intrusive Suite (Fig. 1) comprises several plutons of intermediate composition associated with andesitic stratovolcanoes in the western part of the Great Bear magmatic zone, an early Proterozoic continental arc (Hildebrand, 1981; Hildebrand et al., 1987). The plutons have broad alteration haloes and occur in close proximity to formerly rich Ag-U deposits. Although one of the primary exploration targets in the region, the plutons are relatively unstudied. Furthermore, the plutons are exposed in cross-section due to later folding, which provides an excellent opportunity to view and study the plutons and their alteration haloes. The purpose of this study is to investigate the relationships between plutonism, alteration and mineralization, in order to provide a better base for mineral exploration in the Echo Bay area and elsewhere. This paper presents the results of seven weeks of field work during the summer of 1988, when the plutons and their alteration haloes were mapped at a scale of about 1:15 000.

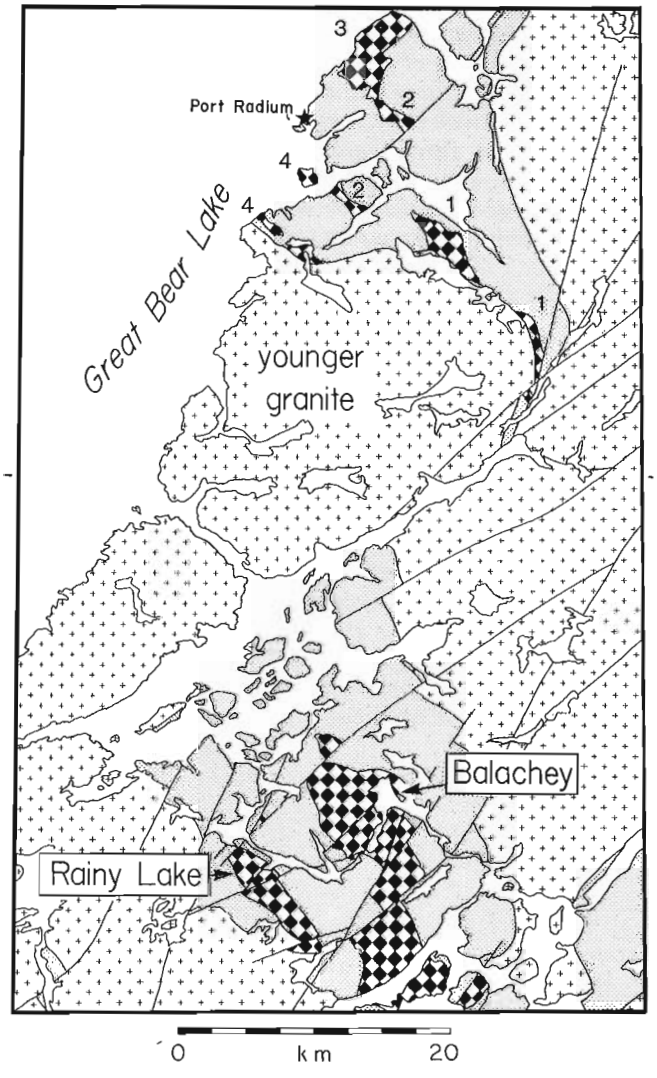

Figure 1. General geology of the Echo Bay area showing the plutons of the Mystery Island Intrusive Suite, modified after Hildebrand (1986). 1 = Contact Lake pluton, 2 = Glacier Lake pluton, 3 = Tut pluton, 4 = Bertrand Lake pluton.

MYSTERY ISLAND INTRUSIVE SUITE

The plutons of the Mystery Island Intrusive Suite are semi-concordant epizonal bodies which are sill-like in cross-section, up to 10 km long and 2 km thick (Fig. 1). They are intermediate in chemical composition and consist of seriate monzodiorite - monzonite - quartz monzodiorite - quartz monzonite (IUGS), although microscopic examination (Cherer, 1988) of samples from two of the plutons indicates the presence of very fine-grained quartz. Accordingly, the rocks may be termed quartz monzodiorite - quartz monzonite - granodiorite granite. Hornblende and biotite are the principal mafic minerals and the relative abundances of the two varies within and among the plutons.

Individual members of the Mystery Island Intrusive Suite (Fig. 1) are informally referred to as the Contact Lake pluton, the Glacier Lake pluton, the Tut pluton and the Bertrand Lake pluton. The Glacier Lake pluton and the Tut pluton are probably the same body, but have been separated by faulting.

Plutons of the suite were emplaced at two distinct stratigraphic levels. TheBertrand Lake pluton intrudes the Port Radium Formation, which consists primarily of laminated to thinly-bedded siltstone, sandstone, ashstone and minor conglomerate, and the lowermost part of the conformably overlying Echo Bay Formation, which consists of andesitic lavas and breccias, intercalated epiclastic rocks, and minor reworked tuff beds (Hildebrand, 1984). The other plutons were intruded high up in the andesites of the Echo Bay Formation. Subsequent folding has exposed the plutons on the southern limb of a north-west trending syncline, except the Tut pluton, which is located in the core of the syncline (Hildebrand, 1984). Younger granitoids have intruded some of the plutons.

Alteration

All of the plutons of the Mystery Island Intrusive Suite are characterized by alteration haloes ranging up to 2 km in thickness. The alteration comprises complex assemblages of albite, magnetite-apatite-actinolite and pyrite. The alteration is found primarily above the plutons, although limited alteration is present both within and below them. Three alteration types were mapped in the field:

1. Albitic alteration characterized by pervasive replacement of original minerals by albite. The resultant rocks are pink-orange to pale pink. In places, however, andesitic lavas are so altered that they weather white. Albitic alteration is generally confined to within 100 m of the pluton, but locally extends up to 1 km from the upper contact of the pluton. Albitic alteration is also found to a limited extent within and below the plutons.

2. Complex magnetite-apatite-actinolite alteration in which disseminations, pods, veins and breccias of actinolite, magnetite and apatite replace original rocks and fill fractures. The three minerals are present in various combinations, concentrations and textures. The width at most can be measured in millimetres or centimetre, but locally exceed 1.5 m. Locally, disseminations of these minerals replace up to 20 per cent of the rock. Actinolite is the most abundant mineral and is

commonly present alone as millimetre to centimetre signal needles, or blades, within the contrt rocks and within the plutons themselves. The next most common assemblage of these minerals is that of actinolite and magnetite octahedra, followed by the addition of apatite as prismatic mauve cristals. In places, veins of atinolite and apatite (without magnetite) were observed. The paragenesis of the minerals from field relations is actinolite, magnetite, apatite. Breccias, which occur as pink (albitized?) fragments in a dark, actinolite-magnetite-rich matrix, are found below the plutons at the lower contact.

3. Pyritic alteration consisting of centimetre-size pyrite pods, rare veins and extensive gossans up to 1 km across. The distribution of pyrite and gossan is irregular and discontinuous. Small amounts of this alteration are found near the upper and lower contacts of the plutons, but commonly it occurs more than 200 m from the plutons.

Pyrite and chalcopyrite are common constituents of quartz-carbonate vein systems in the area, both within the plutons and their country rocks. Veins up to 1 m wide contain brecciated country rocks, and resemble veins in which native silver and pitchblende have been found. These veins are particularly abundant within the Bertrand Lake pluton on Mystery Island.

Contact Lake Pluton

The Contact Lake pluton outcrops along the north side of Contact Lake (Fig. 2). The upper contact is sharp and locally irregular, but in places is obscurred due to extensive alteration of the country rocks and the pluton. The lower contact, more discernable due to less alteration, is sharp and regular but has been largely truncated by the intrusion of a granitic pluton. The Contact Lake pluton is zoned internally, becoming more quartz-rich downward. The pluton is generally a medium-grained seriate biotite-hornblende mon-

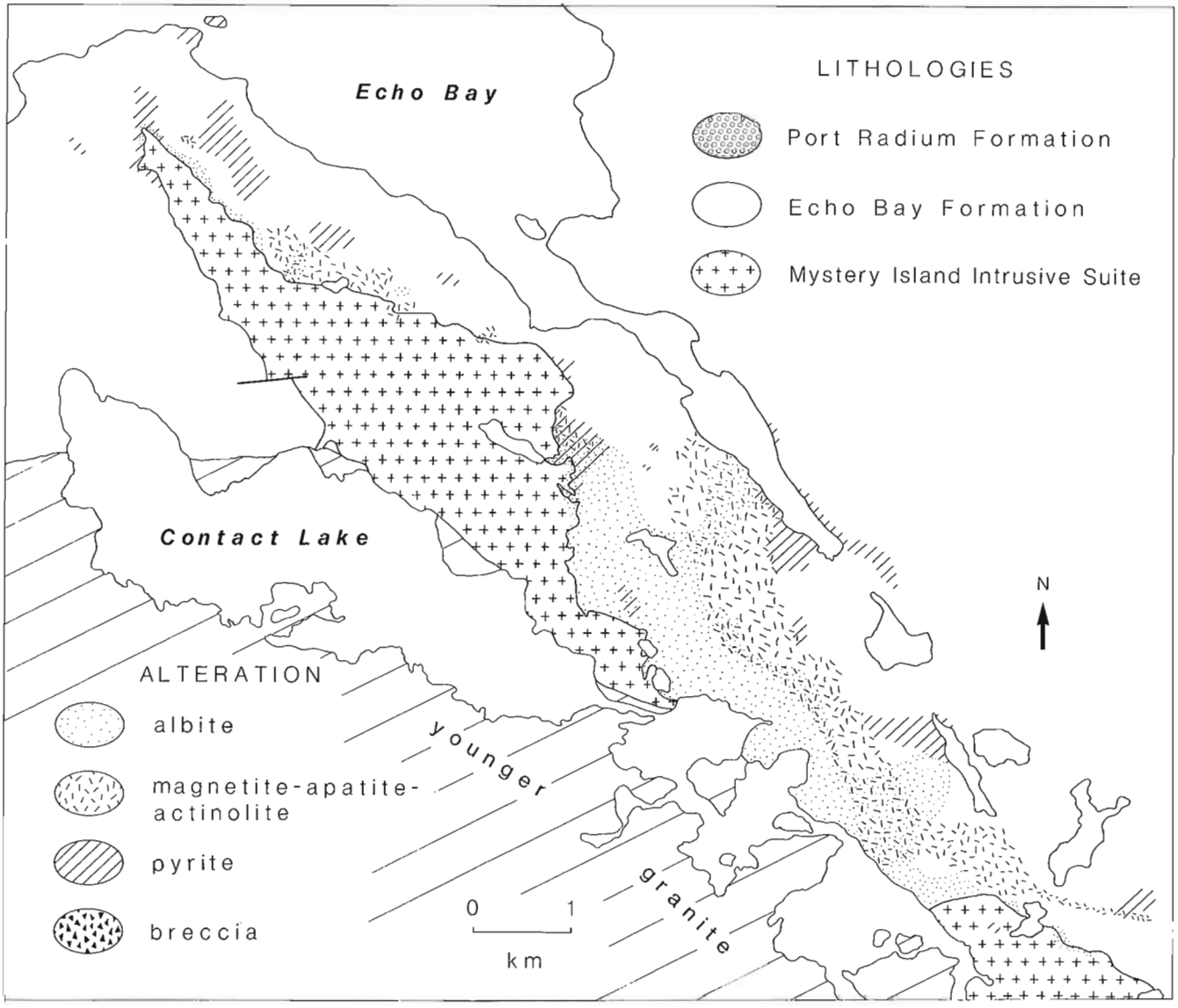

Figure 2. Geological sketch map of the Contact Lake pluton and associated alteration.

zonite to quartz monzonite, but is granitic near the lower contact at Contact Lake (Cherer, 1988). Biotite and hornblende constitute 10 to 15 per cent of the rock.

Rocks above the Contact Lake pluton show the most spectacular example of alteration in the area. Most alteration is concentrated within a long zone that is roughly parallel to the roof of the southeastern half of the pluton, although there is some alteration both below and within the pluton (Fig. 2).Above the pluton, alteration extends upward in a narrow zone which has a core of intensely albitized andesite overlapping a broader area of intense magnetite-apatite-actinolite alteration consisting of disseminations, pods and veins of actinolite-magnetite-apatite generally 1 to 5 cm wide, but ranging up to 15 cm. Locally magnetite-apatite-actinolite constitutes up to 20 per cent of the rocks, giving them a "chicken track" appearance. Apatite is particularly abundant, up to 5 per cent locally. Pyritic alteration is also well pronounced as gossans greater than 50 m in width, which overlap both albitic and magnetite-apatite-actinolite alteration.

Glacier Lake Pluton

The Glacier Lake pluton is cut into two parts by a large right-lateral fault with greater than 2 km separation, and outcrops at Echo Bay and southeast of Glacier Lake (Fig. 3, and 4). Both the upper and lower contacts of the body are sharp, although intense albitization locally obsures their exact position. The pluton has little internal compositional variation and consists of medium-grained, seriate monzodiorite - monzonite - quartz monzodiorite - quartz monzonite. Hornblende and biotite constitute 10 to 15 per cent of the rock and are present in roughly equal amounts.

Alteration near the Glacier Lake pluton is manifested by large, irregular zones of intense pyritization above the body. Other alteration consists of minor disseminations and small veins ($<$ 3 cm wide) of actinolite within the body, the country rocks near the upper contact, and to a limited extent, within country rocks below the pluton. Magnetite-apatite-actinolite alteration is restricted to a narrow U-shaped zone near the southern end of the pluton (Fig. 3) where large veins of actinolite-magnetite-apatite up to 80 cm wide, and containing magnetite crystals to 5 cm, are present. Directly below the pluton, pervasive albitization, magnetite-apatite-actinolite alteration and breccia are present in a narrow zone perpendicular to the lower contact (Fig. 3). Breccia is also present below the pluton at Glacier Lake (Fig. 4).

Tut Pluton

The Tut pluton (Fig. 4) is exposed over 18 km^2 on the shore of Great Bear Lake and occupies the core of a syncline. The upper and lower contacts are, therefore, not extensively exposed. Where seen, however, contacts are abrupt except at the southwest margin of the pluton where areas of intense albitization obscure it. The pluton consists of seriate medium-grained biotite-hornblende monzodiorite - monzonite - quartz monzodiorite - quartz monzonite and contains at least one small area of diorite in sharp contact with the main body of the pluton. Biotite and hornblende constitute 5 to 15 per cent of the rock.

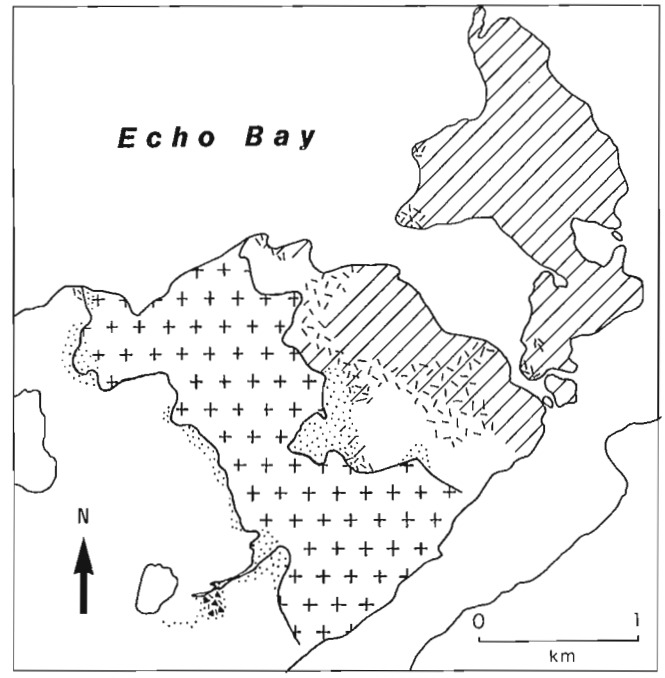

Figure 3. Geological sketch map of the Glacier Lake pluton (southwestern half) and associated alteration. Legend as for Figure 2.

Few altered rocks occur above the upper contact of the Tut pluton since exposure is limited. Near Glacier Lake, actinolite pods and veins up to 1.5 m were observed within the pluton. Pyritized and, locally, hematized andesite are found northeast of the pluton. At the southern contact, small albitized zones are present both within the pluton and the country rocks. In two locations, small zones of breccia with actinolite-magnetite matrix, similar to that seen below the Glacier Lake pluton, were observed. All three types of alteration are found southwest of the pluton, and extend west to the shore of Great Bear Lake and south to Port Radium (Hildebrand, personal communication, 1988). Albitic alteration increases westward toward Great Bear Lake, and magnetite-apatite-actinolite is most prevalent east of the lake within 500 m of the shore. Pyritic alteration dominates east to the magnetite-apatite-actinolite alteration.

Bertrand Lake Pluton

The Bertrand Lake pluton outcrops from the shore of Great Bear Lake eastward beyond Mile Lake, and on a displaced section on Mystery Island (see Fig. 5). The upper and lower contacts of this pluton are abrupt, generally trending parallel to bedding within the Port Radium and Echo Bay formations. Internally, the pluton is homogeneous, consisting of medium-grained, biotite-hornblende monzodiorite. The mafic minerals generally constitute 15 to 20 per cent of the rock, but locally, lower in the body, as much as 40 per cent.

Alteration adjacent to the Bertrand Lake pluton comprises local albitization and common replacement of sedimentary beds within the Port Radium Formation by actinolite. Alteration within the Echo Bay Formation is present as small veinlets and disseminations of actinolite,

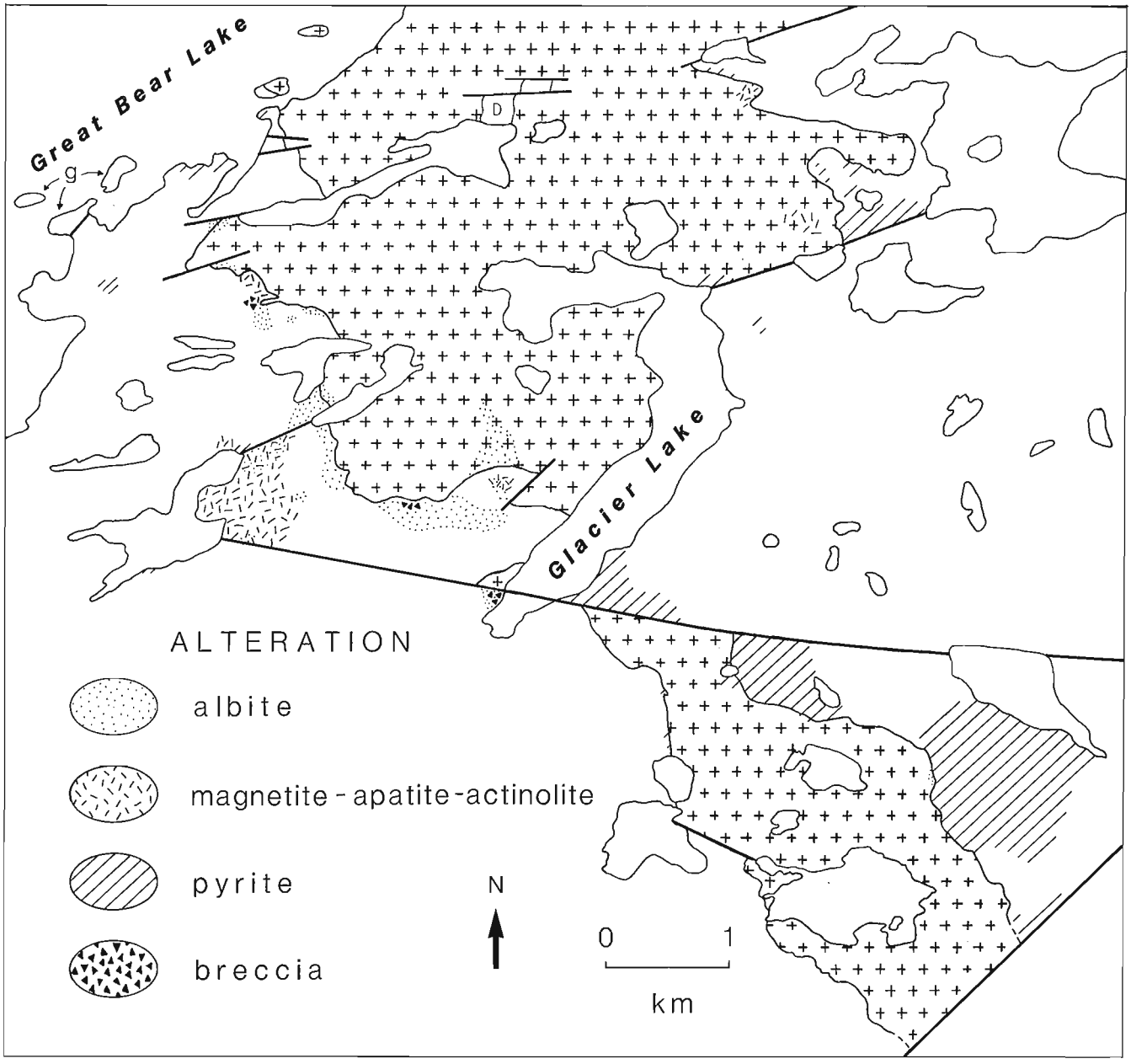

Figure 4. Geological sketch map of the Glacier Lake pluton (northeastern half), Tut pluton (southern half) and associated alteration. D = diorite, g = younger granite. Legend as for Figure 2.

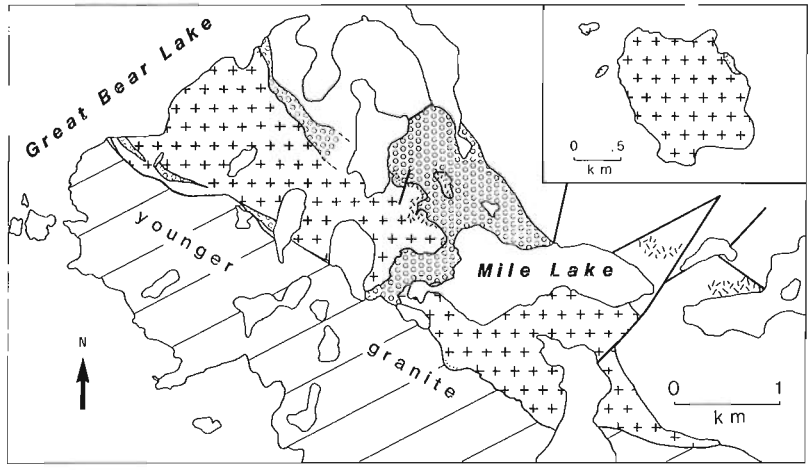

Figure 5. Geological sketch map of the Bertrand Lake pluton and associated alteration halo. Legend as for Figure 2.

and, less commonly, actinolite-magnetite. Apatite was observed but is rare. At the upper contact of the body, intense alteration within the pluton is present as numerous small veins of actinolite, actinolite-magnetite and actinolite-magnetite-apatite, particularly in a small plug just above the pluton northwest of Mile Lake. Minor exposures of the Port Radium Formation occur on Mystery Island and are tightly folded and brecciated, perhaps due to the intrusion of the pluton; replacement of sedimentary beds is extensive and the breccia matrix is primarily actinolite.

SUMMARY AND DISCUSSION

The plutons of the Mystery Island Intrusive Suite have associated alteration found primarily in the country rocks above the roofs of the plutons, but also within the plutons themselves. Albitic, magnetite-apatite-actinolite and pyritic alteration are crudely zoned; the albite zone is present closest to the plutons, followed by the magnetite-apatite-actinolite and pyrite zones. Zoning of similar alteration haloes was observed in and around intermediate plutons in the Conjuror Bay area (Hildebrand, 1986).

A particularly interesting feature of the haloes is that the most intense and widespread alteration occurs above "saddles" or depressions in the upper contacts of the plutons. The best example is located above the Contact Lake pluton (Fig. 2), but this feature is also present above the Glacier Lake pluton (Fig. 3). It may be that meteoric and/or magmatic waters are trapped and circulated longer within the depressions than elsewhere, or possibly that temperatures are higher in such regions due to lateral heat transfer. Additional work will be needed to understand this feature.

The paucity of alteration associated with the Bertrand Lake pluton may reflect differences in temperature, pressure and composition of magma due to the emplacement of this pluton at a lower level in the andesitic complex, or simply to a lack of non-magmatic water within the complex. Another possible explanation of the Bertrand Lake pluton around Mile Lake represent the lateral end of the pluton and that most of the alteration was located above more central portions, much like alteration above the Contact Lake pluton. If so, then alteration southwest of the Tut pluton may be related to an extension of the Bertrand Lake pluton, which is no longer exposed due to emplacement of a younger granite. Consider that zoned alteration southwest of the Tut pluton trends roughly perpendicular to the southwest contact of the pluton, with alteration increasing toward Great Bear Lake. The alteration is concordant with stratigraphy and is within rocks of the Port Radium and lower Echo Bay formations. This is the same stratigraphic level as rocks above the Bertrand Lake pluton. When the effects of younger transcurrent faulting are removed, the Bertrand Lake pluton projects to the area just offshore from the alteration zones, and its upper contact would parallel the zones of alteration. If the Bertrand Lake pluton did continue beneath the Port Radium area and generated the alteration found there, then there is considerable alteration around the Bertrand Lake pluton itself may be a function of exposure rather than any differences related to depth of emplacement or fluid content.

Ag-U mineralization occurs within the plutons of the Mystery Island Intrusive Suite and their alteration haloes. This demonstrates the potential for economic mineralization in the area. Pyritic zones are favorable areas for prospecting because such alteration may act as a chemical trap for mineralization due to: (1) their reducing nature; (2) metal transport as bi-sulphide; or (3) the mixing of metalliferous brines with sources of sulphur.

Quartz-carbonate-sulfide veins in the area have produced native silver and are found both within the plutons and their country rocks; they are particularly abundant within the Bertrand Lake pluton on Mystery Island. Valleys, vegetated areas and subaqueous exposures, where little or no exploration has been carried out to date, are favourable locations for future exploration.

ACKNOWLEDGMENTS

This report is a contribution to the Canada-Northwest Territories Mineral Development Agreement. Robert S. Hildebrand is kindly thanked for his initiation of the project, assistance and suggestions. Marc and Colleen Canulli and CEGB are thanked for the use of their Beaver and freezer, as well as several dinner invitations. Un remerciment special a mon assistant, Stephane Lagace, pour son assistance. Robert Hildebrand and Bruce Taylor critically read the manuscript.

REFERENCES

Cherer, R.M.
1988: Petrology and geochemistry of three plutons of the Mystery Island Intrusive Suite, District of Mackenzie, Northwest Territories; unpublished B. Sc. thesis, University of Toronto.

Hildebrand, R. S.
1981: Early Proterozoic LaBine Group of Wopmay Orogen: Remnant of a continental volcanic are developed during oblique convergence; in Proterozoic Basins of Canada, ed. F. H. A. Campbell; Geological Survey of Canada, Paper 81-10, p. 133-156.
1984: Geology, Echo Bay — MacAlpine Channel area, District of Mackenzie, Northwest Territories; Geological Survey of Canada, Map 1546A, scale 1:50 000.
1986: Kiruna-type Deposits: Their origin and relationship to intermediate subvolcanic plutons in the Great Bear magmatic zone, Northwest Canada; Economic Geology, vol. 81, no. 3, p. 640-659.

Hildebrand, R. S., Hoffman, P. F. and Bowring, S. A.
1987: Tectono-magmatic zone, Wopmay Orogen, northwestern Canada; Journal of Volocanology and Geothermal Research, v. 32, p. 99-118.

Hoffman, P. F. and McGlynn, J. C.
1977: Great Bear Batholith: A Volcano-plutonic Depression; Geological Association of Canada Special Paper 16, p. 170-192.

Cartographie détaillée de la région de la rivière du Chef, province de Grenville, Québec

É. Ouellet[1]
Division de la lithosphère et du bouclier canadien

Ouellet, É., Cartographie détaillée de la région de la rivière du Chef, province de Grenville, Québec; dans Recherches en cours, partie C, Commission géologique du Canada, Étude 89-1C, p. 43-48, 1989.

Résumé

La région étudiée est localisée à la limite sud du parautochtone grenvillien. Cette limite est caractérisée par une grande discontinuité géologique, superposée à de grands contrastes du champ magnétique et à des âges radiométriques, passant du nord au sud de 3000 à 1000 Ma. Le secteur du lac Robereau, représentant la partie ouest de la zone est constitué d'une association de gneiss hétérogène de composition quartzo-feldspathique. La bordure est, correspondant au secteur de la rivière du Chef, est composée de gneiss de composition granitique. La limite est de la région étudiée, correspondant au secteur du lac Desautels, est composée de gneiss quartzo-feldspathiques mésocrates à grenat, des gneiss à sillimanite, grenat et graphite et des orthogneiss de teinte verdâtre. Toutes ces lithologies définissent des bandes, d'orientation linéaire, d'extension latérale variant de quelques centaines de mètres à plus de 8 kilomètres et d'épaisseur décamétrique à kilométrique. L'orientation des foliations concorde avec celles des grandes bandes, d'orientation nord-sud à l'est de la discontinuité géologique et d'orientation nord-est à l'ouest.

Le contact entre les gneiss quartzo-feldspathiques à l'ouest et les gneiss granitiques à l'est représente une discontinuité lithotectonique d'orientation nord-sud, observée sur plus de 6 kilomètres.

Abstract

The region under study is at the southern edge of the Grenville parautochthon. This boundary is characterized by a major geological discontinuity, showing large contrasts in magnetic field, and radiometric ages that decrease from 3000 to 1000 Ma from north to south. The Robereau Lake sector, in the western part of the anomaly zone, comprises an association of heterogeneous quartzofeldspathic gneisses. The eastern edge, in the Du Chef River sector, consists of granitic gneiss. The eastern boundary of the area, in the Desautels Lake sector, consists of mesocratic quartzofeldspathic gneisses with garnet, gneisses with sillimanite, garnet and graphite and greenish orthogneisses. All these lithologies define linear bands that extend laterally from a few hundred metres to more than 8 km, and vary in thickness between a decametre and a kilometre. The orientation of the foliation matches that of the large bands, being north-south in the area east of the geological discontinuity and northeasterly in the area west of the discontinuity.

The contact between the quartzofeldspathic gneisses in the west and the granitic gneisses in the east represents a north-south trending lithotectonic discontinuity that has been observed over a distance of more than six kilometres.

[1] Sciences de la Terre, Université du Québec à Chicoutimi, 555, boul. de l'Université, Chicoutimi, Québec G7H 2B1.

INTRODUCTION

La subdivision tectonique de la ceinture orogénique de Grenville, présentée par Wynne-Edwards (1972), comprend sept grandes divisions. Chacune d'entre elles est caractérisée par des changements lithologiques majeurs, ou par l'apparition de différents styles structural et métamorphique.

Au Québec, un segment de la route 167, reliant Saint-Félicien à Chibougamau traverse du nord au sud: 1) la zone tectonique du front de Grenville, 2) la ceinture centrale des Gneiss et 3) le terrain central des Granulites.

Osborne et Morin (1962) notèrent l'existence d'une ligne de roches vertes, apparaissant au nord du grand massif anorthositique du lac Saint-Jean, à 64 km de la ville de Saint-Félicien. Cette ligne soulignant le contraste lithologique entre des séries de roches ignées à hyperstène, augite et feldspaths de teinte verdâtre au sud-est et des gneiss de composition quartzo-feldspathiques au nord-ouest.

Des études de datation, effectuées par Frith et Doig (1975), provenant de gneiss de composition tonalitique, démontrent une grande discontinuité des âges obtenus. Les échantillons, prélevés sur une distance de 52 km au sud du front de Grenville, présentent des âges archéens d'environ 3000 Ma. Ceux à plus de 52 km au sud du front indiquent des âges grenvilliens de 1100 Ma. Frith et Doig (1975) notèrent que cette grande brisure se superpose à la ligne de discontinuité aéromagnétique d'orientation générale nord-est — sud-ouest (Geological Survey of Canada, 1966).

Rivers et Chown (1986) ont proposés une nouvelle subdivision tectonique de l'est de la province de Grenville, fondée sur des phénomènes structuraux, métamorphiques et lithologiques observés dans les parties ouest du Labrador et est du Québec. Cette subdivision comprend trois grandes composantes, du nord vers le sud: 1) des terrains autochtones, 2) parautochtones, et 3) d'une série de nappes allochtones. En se basant sur des cartes aéromagnétiques, ils proposent que ces subdivisions peuvent être extrapolées le long de la route 167 reliant Chibougamau à Saint-Félicien.

Les travaux de Ciesielski et al. (1985, 1986 et 1988) démontrent que des lithologies et des anciennes structures archéennes se poursuivent à travers le parautochtone.

Par le passé, plusieurs auteurs notèrent la présence d'une discontinuitée lithologique le long de la route de Chibougamau, accentuée par des brisures du relevé aéromagnétique et des âges obtenues par radiodatation. Les hypothèses émises par Rivers et Chown, (1986), voulant que cette discontinuité corresponde à la zone de transition entre le parautochtone et les nappes allochtones ne pouvait, jusqu'à date, être vérifiée dans ce secteur, aucune cartographie détaillée n'étant disponible. C'est dans cet optique qu'une campagne de cartographie fut entreprise dans le but de répondre aux questions soulevée par cette zone anomalique d'orientation nord-sud dans le secteur de la rivière du Chef. Ce projet est greffé au projet Lithoprobe, dans le cadre duquel des transects possibles, longeant la route 167, sont envisagés.

GÉOLOGIE LOCALE

La région cartographiée en 1988, à l'échelle de 1:20 000, d'une superficie de 125 km^2, représente la portion nord-ouest du feuillet 32H6, échelle 1:50 000 (fig. 1).

Cette région fut investiguée par Laurin et Sharma (1975) lors d'une campagne de cartographie de reconnaissance à l'échelle 1:250 000, basée sur des travaux de cartographie détaillés, effectués par Benoit (1960, 1961), Bergeron et Beal (1958), Berrangé (1960) et Laurin (1955 et 1956 a, b). À cette échelle, aucune distinction lithologique ne fut effectuée. Toutes les lithologies furent regroupées dans des complexes gneissiques comprenant des gneiss gris à quartz-plagioclase-biotite et/ou hornblende, homogène à bien rubannés, des gneiss associés riches en hornblende ou biotite et des masses amphibolitiques.

La limite sud-est du secteur cartographié à grande échelle par Ciesielski et al. (1985, 1986 et 1988), couvrant une superficie de 2 500 km^2, correspond à la bordure ouest de la région étudiée. Il y définit le front des granulites, apparaissant comme une discontinuité abrupte du champ magnétique total, causée par la présence de magnétite dans les roches, de corps intrusif de composition intermédiaire à basique et de quelques granulites. Au nord du front des granulites, affleurent les roches du parautochtone. La partie sud, caractérisée par le changement positif du relief, est définie par l'apparition de gneiss de composition granitique, de mangérite, de roches méta-sédimentaires, par des corps intrusifs de composition intermédiaire et basique, ainsi que la présence de clinopyrogène dans les pegmatites.

Les travaux ont permis de subdiviser la région étudiée en trois grands secteurs (fig. 2), regroupés par des associations de gneiss particuliers. Soit, le SECTEUR DU LAC ROBEREAU (ouest), le SECTEUR DE LA RIVIÈRE DU CHEF(centre) et le SECTEUR DU LAC DESAUTELS (est).

SECTEUR DU LAC ROBEREAU

Le secteur du lac Robereau est limité à l'est par la ligne de discontinuité aéromagnétique d'orientation nord-sud.

Il est défini par une succession de gneiss quartzo-feldspathiques regroupés en: 1) des gneiss leucocrates, 2) des gneiss gris leucocrates, 3) des gneiss mésocrates, 4) des gneiss à grenat, 5) des gneiss gris rubanés, 6) des gneiss à hornblende et 7) des gneiss gris avec clinopyroxène. Les gneiss leucocrates ont une granulométrie fine, légèrement rosacés en surface altérée et sont accentués par des mobilisats de composition granitique de 1 à 5 cm d'épaisseur. Ils contiennent une faible concentration de biotite et quartz. Les gneiss gris leucocrates ont une granulométrie fine, et sont caractérisés par la présence de mobilisats de teinte blanchâtre, riches en plagioclase et quartz. Les gneiss mésocrates, à texture lépidoblastique, ont une granulométrie variant de 1 à 2 mm, et sont de teinte gris noirâtre en surface altérée, présentant une très forte concentration de biotite, ou les bandes riches en biotite sont séparées par des mobilisats de composition granitique à granodioritique. Les gneiss à grenat ont une granulométrie fine et sont de teinte gris-rouille

en surface altérée et présentant une forte proportion de biotite et quartz où la gneissosité est définie par des bandes leucocrates de teinte blanchâtre, d'épaisseur centimétrique. Les gneiss gris rubannés sont grisâtre en surface altérée, où le rubannement, d'épaisseur centimétrique à décimétrique, est défini par la variation de concentration de biotite et hornblende. Certaines bandes sont uniquement composées de plagioclase et de biotite. Les gneiss à hornblende, d'aspect grossier et tachetés, à texture nématoblastique sont très pauvres en quartz et peuvent contenir des clinopyroxènes. La granulométrie est généralement supérieure à 1mm. Les gneiss gris à fragments de clinopyroxène et hornblende, ont une matrice à granulométrie grossière principalement composée de plagioclase et de hornblende. Les fragments, souvent elliptiques et de dimension variable, s'orientent généralement selon la foliation. Cet ensemble de gneiss apparaît en bandes linéaires de quelques kilomètres de longueur et présentant des associations lithologiques particulières.

La zone des lacs Mazarin et Nivars correspond à des bandes de gneiss à biotite et grenat de teinte rouille, intercalées à des gneiss leucocrates et mésocrates. Les contacts sont souvent soulignés par la présence de gneiss gris grossiers à fragments de clinopyroxène et hornblende, d'épaisseur décimétrique à décamétrique. La bande de gneiss à biotite et grenat la plus importante, d'une épaisseur de 200 mètres présente une extension latérale de plus de 1 km de longueur. Les gneiss mésocrates ne s'observent que le long de la bordure est du lac Mazarin et sont intercalés aux gneiss leucocrates. Quelques horizons uniquement composés de biotite et hornblende sont également présents.

La bordure ouest de la zone du lac Robereau correspond à des unités de gneiss rubannés, intercalées à des gneiss à biotite et grenat de teinte rouille. Quelques petites bandes ou lambeaux calco-silicatés sont présents, d'aspect tacheté, où la matrice est constituée de cristaux de clinopyroxène, de calcite et d'épidote avec de nombreux fragments de clinopyroxène. Ce groupe d'unités définit une bande linéaire d'une extension latérale minimum de 3,5 km, et d'épaisseur moyenne d'environ 300 m. Cette bande est intercalée à des gneiss leucocrates. La bordure est du lac Robereau correspond à des gneiss leucocrates intercalés à de petites bandes de gneiss à biotite et grenat de teinte rouille, de quelques mètres d'épaisseur.

La zone sud-est, limitée par l'anomalie magnétique, est principalement composée de gneiss grossier à hornblende d'aspect mésocrate.

Une bande de gneiss gris leucocrate, à granulométrie fine et à mobilisats banchâtres affleure entre les gneiss leucocrates de la bordure est du lac Robereau et les gneiss à hornblende affleurant à la zone de bordure sud-est. Elle se distingue par la forte concentration de mobilisats blanchâtres aux orientations variables.

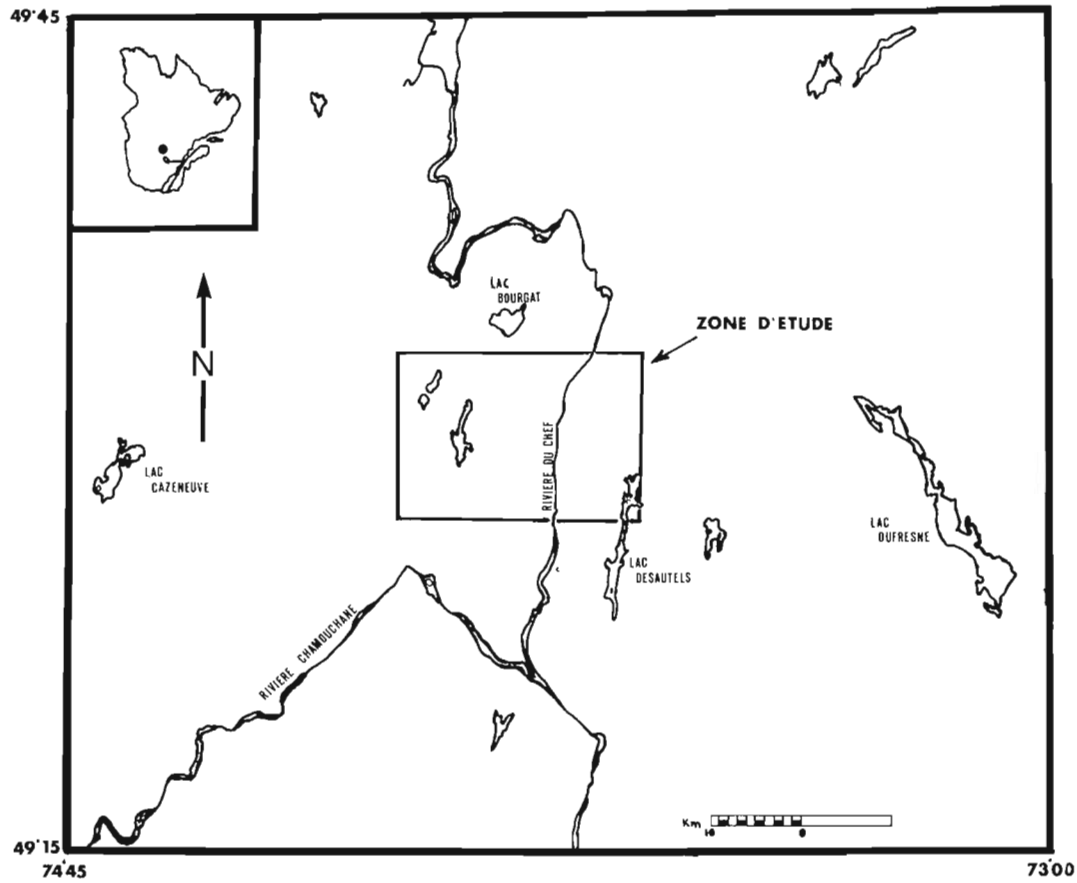

Figure 1. Localisation de la région étudiée.

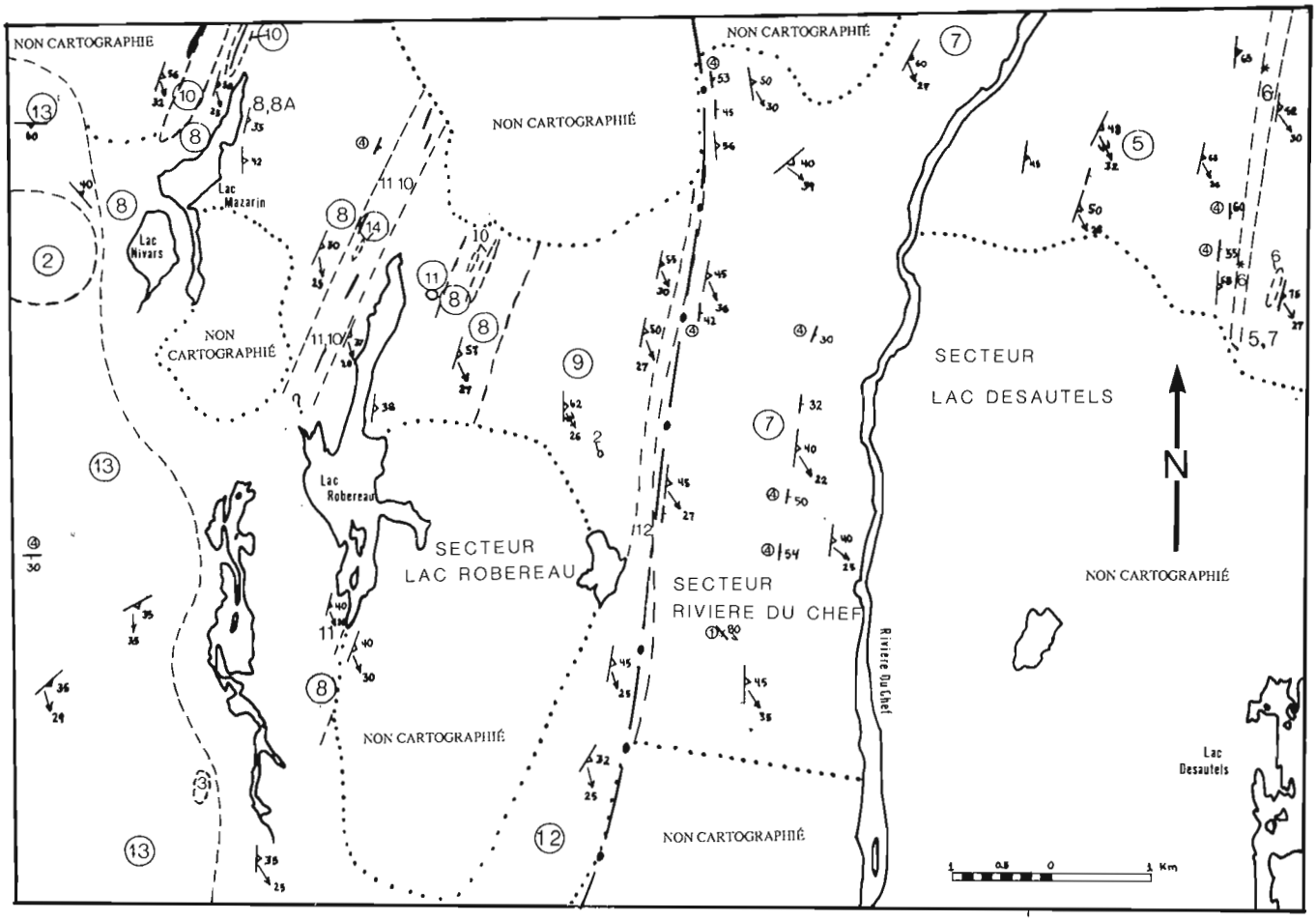

LÉGENDE

1: Dyke de diabase non métamorphisé

2: Pyroxénite transformée en hornblendite

3: Anorthosite

4: Dyke de métabasite

DOMAINE 1 Secteurs de la rivière du Chef et du lac Desautels

5: Gneiss quartzo-feldspathique mésocrate à grenat et épidote

6: Gneiss quartzo-feldspathique à sillimanite, grenat et graphite et orthogneiss de teinte verdâtre.

7: Gneiss de composition granitique

*: Quartzite

DOMAINE 2 Secteur du lac Robereau

Ensemble des gneiss quartzo-feldspathiques

8: Leucocrate à mobilisat de composition granitique avec A: bandes mésocrates

9: Leucocrate, à mobilisat blanchâtre

10: A grenat, de teinte rouille en surface altérée

11: Gris rubanné

12: A hornblende, d'aspect grossier

—: Gris grossier, à fragments de clinopyroxène et hornblende

13: Ensemble de gneiss du type 8, 8A, 9 et 11 (bordure Ouest)

14: Horizon calc-silicatée

SYMBOLES

- Foliation
- Linéation minérale
- Plis parasites
- Dykes
- Contact lithologique
- Discontinuité aéromagnétique
- Secteur non cartographié

Figure 2. Carte géologique détaillée de la région de la rivière du Chef. N.B.: Les secteurs non cartographiés seront couverts en 1989.

La bordure ouest de ce secteur représente un aspect beaucoup plus hétérogène au niveau lithologique, où, une forte proportion des gneiss quartzo-feldspathiques sont fortement injectés par des dykes pegmatitiques. Les bandes linéaires observées plus à l'est ne sont pas continues dans cette zone.

Des lambeaux gneissiques, à texture granoblastique, essentiellement composés de plagioclase avec un faible pourcentage de biotite, hornblende et grenat s'observent dans la bordure ouest. Vers l'est, ils apparaissent sous forme de petits fragments elliptiques généralement inférieurs à 30 cm et se localisent principalement en bordure de ligne de discontinuité aéromagnétique.

SECTEUR DE LA RIVIÈRE DU CHEF

Le secteur de la rivière du Chef est limité à l'ouest par la ligne de discontinuité magnétique et à l'est par la rivière du Chef, d'orientation générale nord-sud. Les principales lithologies rencontrées sont des gneiss de composition granitique à granodioritique. Le premier type correspond à des gneiss granitiques rougeâtres, à granulométrie inférieure à un millimètre, à texture granoblastique, avec faible concentration de biotite, magnétite et petite taches rougeâtres (oxydation). Le second correspond à des gneiss granitiques tachetés, avec une forte proportion de biotite, concentrés sous forme de plage, définissant une excellente foliation. Ces deux types de gneiss s'observent en masse isolée de plusieurs mètres d'épaisseur, ou en alternance commune sous forme de bandes, d'épaisseur centimétrique à métrique, orientées selon la foliation. Ils définissent une bande linéaire d'épaisseur minimale de 1,2 km et présentant une extension latérale minimale de 7,7 km.

SECTEUR DU LAC DESAUTELS

Le secteur du lac Desautels est limité à l'ouest par la rivière du Chef. La principale lithologie rencontrée affleure sur plus de 80 % du secteur étudié. elle correspond à des gneiss quartzo-feldspathiques mésocrates à leucocrates avec biotite, grenat et épidote. La matrice, à granulométrie inférieure au millimètre et à texture lépidoblastique est fortement injectée de mobilisats de composition granitique à granodioritique, contenant de la muscovite et de la magnétite. Son extension latérale s'observe sur plus de 3,3 km. À la limite est du secteur étudié, des bandes de gneiss de composition granitique, à granulométrie fine, sont intercalées aux gneiss quartzo-feldspathiques mésocrates. Les contacts étant orientés selon la foliation.

Un ensemble de gneiss quartzo-feldspathiques de teinte verdâtre en cassure fraîche, de 50 à 250 m d'épaisseur, affleure à la limite est de la région étudiée. Deux composantes définissent ces gneiss verdâtres. La première, de teinte grisâtre en surface altérée, à granulométrie inférieure au millimètre est constituée de biotite, sillimanite, grenat rose et graphite. La seconde de teinte blanchâtre en surface altérée, d'aspect grossier et homogène, à texture ignée fortement étirée selon la déformation est constituée de hornblende, et grenat rose au dimension millimétrique à centimétrique. Une bande de quartzite litée, d'épaisseur métrique, de teinte grisâtre en surface altérée, laiteuse en surface fraîche, à phénocristaux de plagioclase est intercalée aux gneiss verdâtres à granulométrie fine. Ces trois unités définissent une bande planaire d'extension latérale minimale de 3,7 km et furent obserservées au nord, indiquant une extension de plus de 8,8 km.

PYROXÉNITES, MÉTABASITES ET DIKES DE PEGMATITE

Deux masses de pyroxénite, aux cristaux reliques de pyroxène transformés en hornblende, de taille millimétrique à centimétrique, furent cartographiées dans le secteur du lac Robereau. La première, située en bordure ouest, correspond à un corps circulaire de 1 km de diamètre. La seconde, de 20 à 40 m de diamètre apparait à la zone de bordure sud-est, située près de la discontinuité aéromagnétique. Elles représentent des corps boudinés dans les gneiss de composition quartzo-feldspathiques.

De nombreux boudins de métabasites, aux textures gabbroïques souvent conservées affleurent dans la région étudiée. Les assemblages métamorphiques communs sont hornblende — plagioclase — grenat, ou hornblende — plagioclase — grenat — clinopyroxène. Des orthopyroxènes pouvant être observés à certains endroit. Les cristaux de clinopyroxène peuvent être entourés d'une couronne de hornblende. Les masses de métabasite à mobilisats blanchâtre, avec porphyroblastes de clinopyroxène, s'observent presque uniquement du côté des secteurs de la rivière du Chef et du lac Desautels. À quelques endroits, il est possible d'observer les relations ou les dykes de métabasite recoupant les masses gneissiques. Des dykes de métabasites, à grenat et à granulométrie fine, recoupent les masses de pyroxénite.

Les dykes ou veines de pegmatite sont rencontrés dans tous les secteurs, et recoupent généralement l'ensemble des gneiss et des masses de métabasites. Ces dykes d'épaisseur centimétrique à métrique, présentent des orientations varables. Ils sont à granulométrie variant du millimètre au centimètre et peuvent contenir de gros cristeaux de hornblende, biotite, magnétite, ou pyroxène et sont peu touchés par la déformation. Quelques dykes ou veines déformés s'orientent selon la foliation.

STRUCTURE

Trois patrons particuliers de l'orientation des foliations peuvent être déduits dans la région étudiée. Le premier, d'orientation nord-sud, est observé dans les secteurs de la rivière du Chef, du lac Desautels et à la bordure est du lac Robereau. Le second, d'orientation nord-est est localisé dans le centre du secteur du lac Robereau et dans la portion nord du secteur de la rivière du Chef. Ces deux patrons présentant des pendages moyens de 50°. Le troisième correspond à la bordure ouest du secteur du lac Robereau et se caractérise par une hétérogénéité des orientations variant de 320 à 100°, avec pendage de 10 à 60°.

Dans les trois secteurs, les contacts entre les différentes lithologies dépendent tous de l'orientation de la foliation,

développée à cet endroit. Les lentilles de mobilisat développées dans les boudins de métabasites se concentrent en bordure des contacts et s'orientent selon la foliation. Plusieurs de ces métabasites présentent des textures ignées préservées au centre des masses, tandis que les bordures sont fortement touchées par la déformation.

Les linéations présentent une grande constance des attitudes dans les trois secteurs cartographiés. Elles varient de 120 à 180°, où la majorité des linéations présente une orientation de 150°, avec plongée moyenne de 25°. Elle est très développée en bordure de la discontinuité aéromagnétique et du côté du secteur du lac Robereau et son intensité diminue progressivement en s'éloignant vers le nord-ouest. Elles correspondent à 1) des linéations minérales observées essentiellement dans les cristaux de quartz, hornblende et biotite et 2) à des linéations d'étirement, généralement observées dans les fragments d'amphibolite.

Des plis, d'échelle centimétrique à métrique sont observés dans les trois secteurs mais sont peu nombreux et se concentrent surtout dans les gneiss gris leucocrates à mobilisats blanchâtres du secteur du lac Robereau et dans les gneiss quartzo-feldspathiques mésocrates affleurant à l'est de la bande de gneiss à sillimanite, grenat et graphite du secteur du lac Desautels. Ils correspondent à des patrons de plis parasites en S, M et Z, généralement orientés selon la foliation et plongeant selon la linéation.

CONCLUSION

Les grandes variations lithologiques observées de part et d'autre de la ligne de discontinuité aéromagnétique suggère la présence de deux domaines particuliers.

Le premier, situé à l'ouest de l'anomalie, est défini par le secteur du lac Robereau. Il correspond à des associations de gneiss gris de composition quartzo-feldspathique, dans lesquelles sont intercalées quelques corps de métagabbro boudinés et orientés selon la foliation. Ce domaine est caractérisé par un patron de foliations d'orientation nord-est devenant nord-sud près de la bordure ouest de la zone de discontinuité aéromagnétique.

Le second domaine, située à l'est de l'anomalie, correspond aux secteurs de la rivière du Chef et du lac Desautels. Ces secteurs présentent une succession de l'est vers l'ouest, de gneiss de composition granitique, des gneiss quartzo-feldspathiques mésocrates à grenat, des gneiss à sillimanite, grenat et graphite et des orthogneiss de teinte verdâtre. Ce domaine est caractérisé par des foliations moyennes de 005 à 010°, correspondant à l'orientation de l'anomalie magnétique et par une plus grande concentration de petites masses d'amphibolite boudinées. Certains regroupements de boudin s'orientent parrallèlement à la direction du contact entre les deux domaines. Ils peuvent correspondre à des grands dykes boudinés lors de la déformation. Les contacts entre les dykes et l'encaissant s'orientent généralement selon la foliation développée dans les gneiss.

Toute la région étudiée présente un patron régulier de la linéation minérale et d'étirement d'orientation sud-est avec plongée de 25°. Ce patron des linéations est observé jusqu'au front de Grenville et fût développé lors de l'Orogénie grenvillienne. Les études futures axées sur la structure, le métamorphisme, les patrons de pressions et de température et la radiodatation permettront de vérifier l'hypothèse que cette région représente la zone transitionnelle entre le parautochtone et les nappes allochtones prégrenvilliennes, mises en contact lors de l'Orogénie grenvillienne.

REMERCIEMENTS

L'auteur remercie Mme Josée Boudreault, étudiante à l'Université du Québec à Chicoutimi, qui fût d'une aide très précieuse lors de la campagne de cartographie. Il remercie également MM. E. H. Chown de l'Université du Québec à Chicoutimi, T. Rivers de l'Université Memorial de Terre-Neuve, A. Davidson et A. Ciesielski de la Commission géologique du Canada pour leurs précieux conseils et discussions bénifiques à la réalisation de cette première campagne de cartographie.

BIBLIOGRAPHIE

Benoit, F.W.
1960: Géologie de la région Chomedy-Paquet; Ministère des Mines du Québec, Qué., Rapport préliminaire 426, 7 p.
1961: Géologie de la région de Condé; Ministère des Richesses naturelles du Québec, Rapport préliminaire 463, 9 p.

Bergeron, R. et Beall, G.H.
1958: Géologie de la région de Louvigny-Bochart; Ministère des Mines du Québec, Rapport préliminaire 365, 8 p.

Berrangé, J.P.
1960: Géologie de la région d'Antoine; Ministère des Mines du Québec, Rapport préliminaire 429, 14 p.

Ciesielski, A. et Ouellet, E.
1985: Le Front de Grenville dans la région de Chibougamau, Québec; dans Recherches en cours, partie B, Commission géologique du Canada, Étude 85-1B, p. 303-317.

Ciesielski, A., Bellavance, Y. et Joly, M.
1986: Le Front de Grenville à l'est de Chibougamau, Québec; Commission géologique du Canada, Dossier public 1239, 1986.

Ciesielski, A.,
1988: Geological and structural context of the Grenville Front, southeast of Chibougamau, Québec; in Current Research, Part C, Geological Survey of Canada, Paper 88-1C, p. 353-366, 1988.

Frith, R.A., and Doig, R.
1975: Pre-Kenorian tonalitic gneisses in the Grenville Province; Canadian Journal of Earth Sciences, v. 12, p. 844-849.

Geological Survey of Canada
1966: Carte aéromagnétique rivière Mistassini Sud, Québec, n° 7081 G.

Goodwin, A.M. and Ridler, R.H.
1970: The Abitibi orogenic belt; in symposium on basins and geosynclines of the Canadian Shield, ed. A.J. Baer, Geological Survey of Canada, Paper 70-40, p. 1-30.

Laurin, A.F.
1955: Géologie de la région de Ducharme Bouteroue; Ministères des Mines du Québec, Rapport préliminaire 310, 5 p.
1956a: Géologie de la région Migneault-Aigremont. Ministères des Mines du Québec, Rapport préliminaires 317, 5 p.
1956b: Géologie de Lorne-Avaugour; Ministère des Mines du Québec, Rapport préliminaire 329, 5 p.

Laurin, A.F. et Sharma, K.N.M.
1975: Région des rivières Mistassini, Péribonca et Saguenay (Grenville 1965-1967); Ministère des Richesses naturelles du Québec, Rapport géologique 161.

Rivers, T. and Chown, E.H.
1986: The Grenville Orogen in eastern Quebec and western Labrador, definition, identification and tectonometamorphic relationships of autochtonous, parautochtonous and allochtonous terranes; in The Grenville Province, ed. J.M. Moore, A. Davidson, and A.J. Baer; Geological Association of Canada, Special Paper 31, p. 13-29.

The significance of ultramafic inclusions in gneisses along the eastern margin of the Taltson Magmatic Zone District of Mackenzie, N.W.T.

H.H. Bostock,

Bostock, H.H., The significance of ultramafic inclusions in gneisses along the eastern margin of the Taltson Magmatic Zone, District of Mackenzie, N.W.T.; in Current Research, Part C, Geological Survey of Canada, Paper 89-1C, p. 49-56, 1989.

Abstract

Ni-Cr-rich serpentine-talc inclusions within mafic to granitic gneiss at two places 35km apart along the northeast margin of Taltson Magmatic Zone may point to the existence of an Archean or early Aphebian plate margin that extended southward into Alberta.

A complex shear zone lies within a belt of paragneiss that follows the contact between Slave and Deskenatlata granites. Early deformation of the paragneiss involved subhorizontal stretching and preceded or accompanied emplacement of Deskenatlata pluton (1986 Ma.). Dextral strike slip, and likely thrusting from the west and southwest, were accompanied by greenschist facies retrogression. They occurred after emplacement of Slave Granite (1955 Ma), but before sinistral faulting southeast of the dextral Great Slave Lake Shear Zone.

A northeastward directed thrust fault in the northwestern part of the 1936 Ma. Konth granite has associated local pseudotachylite breccia veins spread over several km in the hanging wall. The foot wall contains only south west plunging slickenlines.

Résumé

Des inclusions de serpentine et talc riches en Ni-Cr dans le gneiss mafique à granitique en deux emplacements éloignés de 35 km l'un de l'autre le long de la zone magmatique de Taltson pourraient indiquer l'existence, à l'Archéen ou au début de l'Aphébien, d'une marge de plaque qui se serait prolongée vers le sud en Alberta.

Une zone de cisaillement complexe se trouve dans une zone de paragneiss qui longe le contact entre les granites des Esclaves et de Deskenatlata. Une déformation précoce du paragneiss s'est effectuée par étirement subhorizontal et a précédé ou accompagné la mise en place du pluton Deskenatlata (1986 Ma). Un rejet horizontal dextre, et vraisemblablement un chevauchement depuis l'ouest et le sud-ouest, ont été accompagnés d'une rétromorphose au faciès des roches vertes. Ils se sont produits après la mise en place du granite des Esclaves (1955 Ma), mais avant la formation de failles à déplacement latéral sénestre au sud-est de la zone de cisaillement dextre du Grand lac des Esclaves.

Une faille chevauchante dirigée vers le nord-est dans la partie nord-ouest du granite de Konth mis en place il y a 1936 Ma présente par endroits des veines associées de brèche de pseudotachylite sur plusieurs kilomètres dans la lèvre supérieure. La lèvre inférieure ne renferme que des surfaces de friction plongeant vers le sud-ouest.

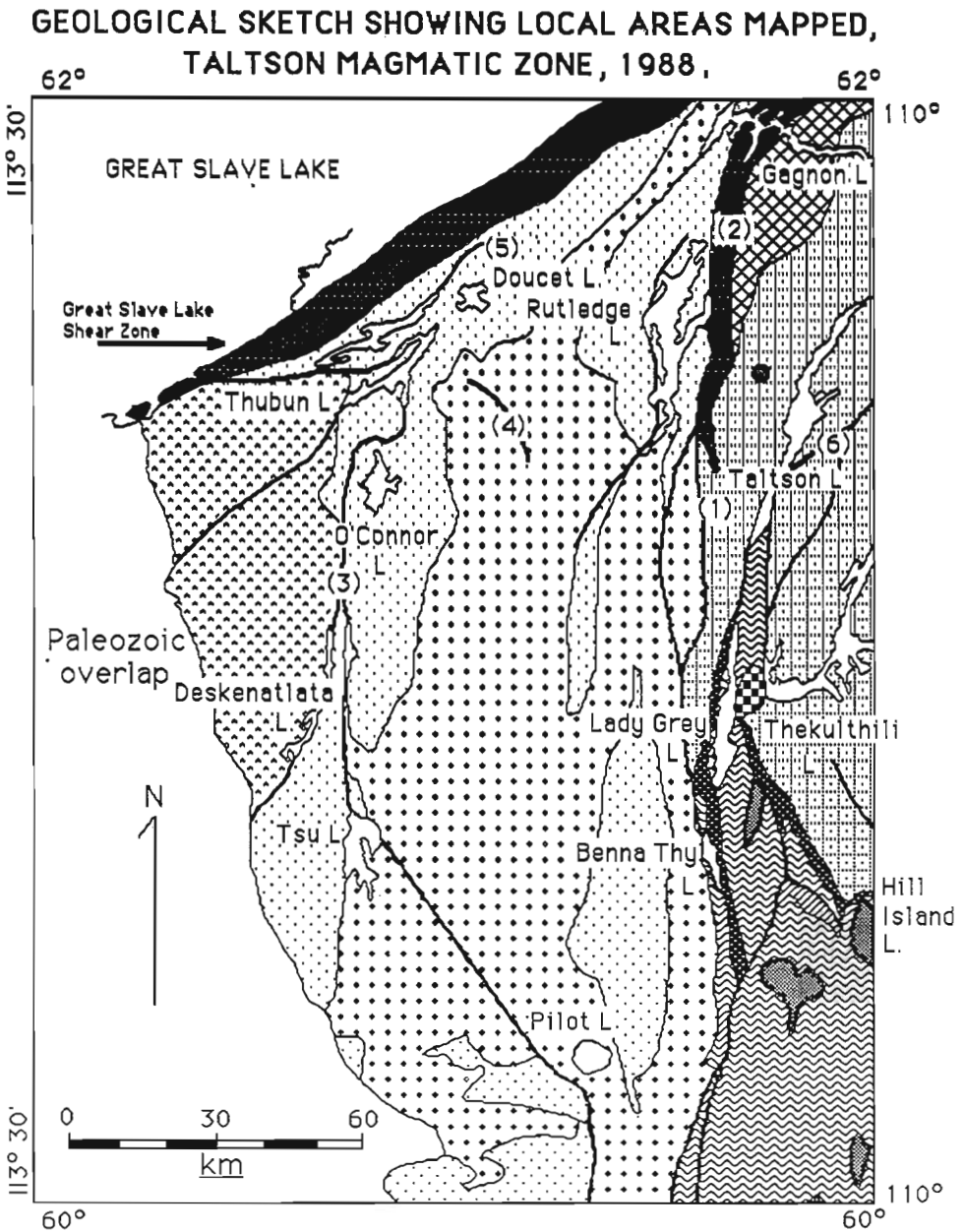

LEGEND

(Supracrustal rocks are not shown on this map)

Mylonite, (some granite, gneiss)

PLUTONS OF TALTSON MAGMATIC ZONE

THEKULTHILI SYENOGRANITE

BENNA THY MONZOGRANITE (1906 Ma.)
(too small to show on map)

NATAEL MONZOGRANITE (1935 Ma.)

KONTH SYENOGRANITE (1936 Ma.)

SLAVE MONZOGRANITE (1955 Ma.)

GAGNON MONZOGRANITE (AGE UNKNOWN)

DESKENATLATA GRANODIORITE (1986 Ma.)

PLUTONIC ROCKS OF THE HINTERLAND

MONZOGRANITE (2436–2334 Ma.)

GNEISSES of the western hinterland including possible equivalents of the eastern gneiss unit supracrustal metasediments and granitic plutons of early to late Aphebian age.

GNEISSES of the eastern hinterland including schlieren gneiss, dioritic rocks; some granite, mafic banded gneiss, BERRIGAN LAKE COMPLEX.

Fault with mylonite

(6) Areas of investigation referred to in the text.

Figure 1. Taltson Magmatic Zone. Numbers refer to local areas mapped in 1988.

INTRODUCTION

This report presents information derived from several dispersed areas examined in 1988 that is significant to interpretation of the Taltson Magmatic Zone. Numbers following headings in the text refer to areas indicated in Figure 1. Earlier reports (Bostock, 1986, 1987, 1988) deal with major parts of the region in a more comprehensive way. A suite of samples was collected across Taltson Magmatic Zone and gneisses to the east in support of a Nd-Sm geochemical study of these rocks to be undertaken at the University of Ottawa.

In this report the term "hinterland" refers to a region of undetermined width which borders the major intrusions of Taltson Magmatic Zone on the east.

THE BERRIGAN LAKE COMPLEX (1)

The Berrigan Lake Complex is best preserved about 25km west of Taltson Lake and within the area immediately to the south. On the west it is bounded by a north-south fault, but along its eastern contact it appears to grade into plutonic breccias and younger granitic rocks. Remnants of similar rocks are recognizable locally within and along the margins of the zone of dextral shear which extends north and south of the complex. The mafic rocks of which it is composed are in large part concealed by heavy forest and lichen cover.

The complex consists of lenticularly banded medium to finegrained, hornblende-plagioclase gneiss with common amphibolite, less common monomineralic hornblende, and fine-grained, plagioclase-rich, lenticular inclusions. Interbanded with these rocks are quartz-rich gneisses and layers to lenses of granitic, locally garnet-bearing, protomylonite. Bands of medium-grained gabbroic anorthosite and hornblende metagabbro were found at two localities near the west marginal fault. Prominent aeromagnetic anomalies follow the west margin of the complex and extend along the shear zone mainly to the north.

At the east margins of the complex the mafic banding is variably intermixed with granitic material within which both angular inclusions and deformed schlieren of a wide variety of lithologies, including those already mentioned, are present. Most significant are local blue-green inclusions (Fig. 3) withraised actinolitic(?) rims and weathered out talc-serpentine cores. In addition there are inclusions with interbanded talc-serpentine and amphibolite, and of amphibolite and fine-grained, white weathering plagioclase-rich rock (Fig. 2). Plagioclase-rich and talc-serpentine inclusions occur either isolated or in trains of three or four inclusions. The heterogeneous matrix varies from hornblende-biotite-rich schist to finegrained hornblende-bearing plagioclase-rich gneiss to hornblende-biotite granite. Gneissosity of the matrix tends to be wavy in contrast to that of the hornblende-plagioclase-rich gneisses in the western part of the complex which, as far as has be seen, tend to be straight though lenticular.

The protolith for the Berrigan Lake Complex may have been a mafic intrusive complex or an isolated remnant of a high grade carbonate quartz-sandstone metasedimentary assemblage. Ultramafic intrusive rocks are known at Rutledge and O'Connor lakes whereas carbonate and calc-silicate gneisses are preserved at a number of places within Taltson Lake sheet but most prominently at Thubun Lakes. ICP (Inductively Coupled Plasma Imission Spectroscopy) analysis (Table 1) of the central zone of an inclusion shows 1900 ppm. Ni and 3500 ppm. Cr suggesting that it is of ultramafic origin.

The most granitic phase of the ultramafic inclusion-bearing gneiss is more closely comparable in composition and texture to some granites of the hinterland to the east (about 1923-25 Ma., Bostock and Loveridge, in press), than to the protomylonitic bands that occur within the complex.

Table 1. Trace elements in an ultramafic inclusion in granite gneiss

Element	Ni	Cr	Co	Ag
ppm	1900	3500	140	1
Absolute error	10	10	5	2
Relative error	+5%	+5%	+5%	

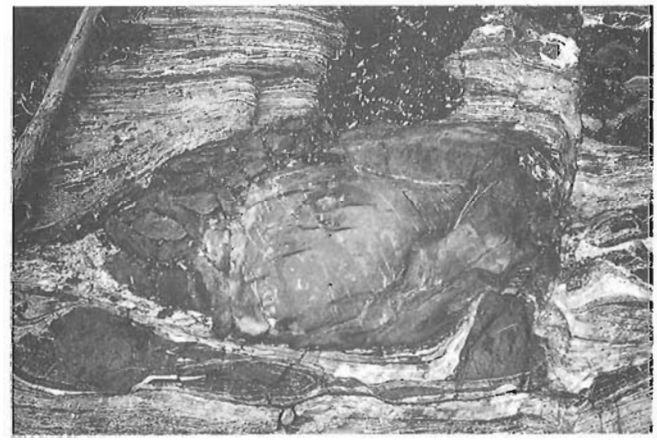

Figure 2. A talc-serpentine inclusion with actinolite-like rim in schistose granodioritic matrix.

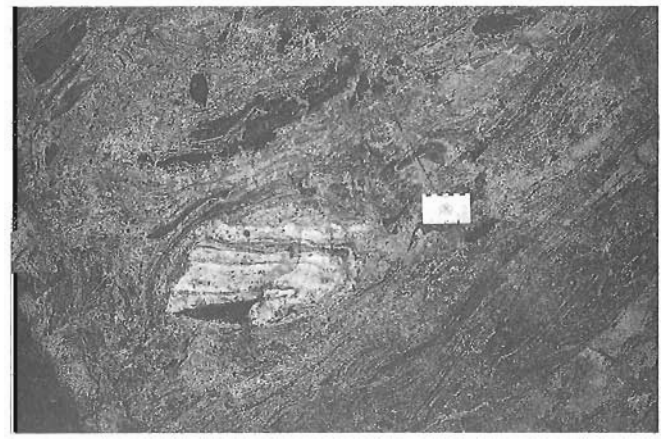

Figure 3. A plagioclase-rich inclusion in schistose granodioritic matrix.

These latter tend to be coarsely K-feldspar porphyroclastic and resemble parts of Konth Granite batholith (1936 Ma., Bostock and Loveridge, in press). Although the point clearly needs confirmation, the most likely age of the granite phase in the inclusion-bearing granitic rocks, based on lithologic correlation, appears to be roughly 1923-25 Ma., and the ultramafics by inference are older than this.

MYLONITE ZONE NORTHEAST OF RUTLEDGE LAKE (2)

A complex zone of mylonites, mostly up to 5km wide, extends south from 62°N near Gagnon Lake to the vicinity of Berrigan Lake. Dextral shear bands and rotated feldspars have been found along this zone and in association with smaller mylonite belts which follow north-south lineaments at least as far south as Benna Thy Lake in the Ft Smith sheet. There, dextral shearing is later than the1906 Ma. (Bostock and Loveridge, in press), age of the Benna Thy granite (at Benna Thy Lake, Fig. 1). At least the northern part of this belt south to Berrigan Lake has had a complex history which predates dextral shear.

The mylonite zone from 10 to 35 km north of Berrigan Lake comprises a mixture of mylonite, amphibolite, granite and gneiss complicated by late zones of cataclasis and metamorphic retrogression. On the easternmost bay of Rutledge Lake metabasites of the Mama Moose Complex (Culshaw,1984) are intruded by a granite that is sufficiently little sheared to demonstrate intrusive relations. Elsewhere gneisses of the Mama Moose metasediments are adjacent to protomylonite or straight gneisses. Within the mylonite zone granitic rocks locally containing zones of diffuse banding, spherical K-feldspar megacrysts 1 to 2 cm in diameter and rodded quartz are interpreted as partially recrystallized mylonite. The granite locally contains amphibolite and monomineralic hornblende inclusions that are angular near the western margin but deformed farther east. Locally they form broad zones of "schlieren inclusion" gneiss. At one place vaguely banded ovoidal megacryst-bearing recrystallized mylonite strikes directly into a zone of granite with abundant angular amphibolite fragments. In contrast, mylonite in the eastern part of thezone appears pristine and varies from coarsely heteroclastic protomylonite (Hanmer, 1987) to ultramylonite. No granites have been found to intrude the eastern mylonite.

A zone of schlieren-inclusion gneiss some hundreds of metres across within the central part of the granite-mylonite belt is characterized by inclusions of amphibolite and metagabbro that have been recrystallized, deformed, and variably contaminated by granite within a fine-grained, gneissic, feldspathic to granitic matrix. The whole has been further deformed so as to impart a wavy irregular banding. Within this zone an isolated outcrop of ultramafic-inclusion gneiss with a coarser more granitic matrix contains a variety of angular inclusions very similar to those seen at Berrigan Lake including trains of both the plagioclase-rich and talc-serpentine-cored varieties.

Possibly two ages of mylonite exist within the mylonite belt. These may be separated by an interval of mafic dyke emplacement followed by granite magmatism, or by granite magmatism which has stoped fragments from a mafic source now not seen at the surface. The similarity of the the two occurrences of ultramafic inclusion gneiss, that at Berrigan Lake some 35 km south of the one northeast of Rutledge Lake, reinforces the view that these breccias are of regional significance.

THE DESKENATLATA-THUBUN LAKES FAULT ZONE (3)

The contact between Deskenatlata Granodiorite and Slave Granite was examined south of O'Connor Lake. Previous mapping to the north and south established that the zone included a belt of metasedimentary gneisses and had suggested that there might be a continuous dextral shear zone along it.

The Deskenatlata Granodiorite at this locality contains remnants and inclusion zones of greenschist facies quartzofeldspathic and calc-silicate metasedimentary gneisses and some amphibolite. The gneisses are conformable to the margin of the granodiorite and display a lineation defined by minor granitic lenses and fold noses that is either subhorizontal or haphazard suggesting that an earlier deformation with subhorizontal stretching directions has been subjected to later deformation. The granodiorite, though foliated, does not show a prominent lineation. Minor granodiorite bodies along the margins of metasedimentary remnants locally cut across the axes of minor horizontal folds.

As the east contact of the granodiorite is approached the proportion of metasedimentary biotite migmatite increases, the granodiorite itself becomes finer grained and more mafic, and small bodies of white foliated to massive leucogranite are locally prominent . East of the granodiorite contact, garnet, largely altered to biotite or chlorite, and fine-grained muscovite patches, possibly pseudomorphous after sillimanite, suggest that the metasediments have been severely retrograded (though no evidence of such early high metamorphic grade was found farther west). Dextral shear bands are present in the metasediments but no horizontal lineation is evident. Rather there is a pervasive subtle lineation defined by fine-grained chlorite biotite that plunges steeply, mostly to the southwest. Local steeply westward dipping shear zones display a strong near down dip lineation of quartz as well as biotite-chlorite. One such zone contains shear bands that indicate west side thrust over rocks to the east.

The subhorizontal lineations expressed within the metasedimentary gneiss engulfed by Deskenatlata Granodiorite represent deformation which occurred either before or during emplacement of the granodiorite (about 1986 Ma., Bostock et al., 1987). It is probably not related to the dextral kinematic indicators because they exist in different domains, and it seems unlikely that most of the relatively delicate dextral shear bands would persist unmodified through recrystallization which accompanied emplacement of Deskenatlata pluton and followed formation of the horizontal lineations. Both steep lineation and dextral shear bands expressed by deformation of biotite-chlorite are likely related and may represent varying stress patterns during the

same period of deformation. Thus the pattern of late deformation is potentially one of intermittent northeastward thrusting and dextral strike slip.

This late deformation affects the Slave Granite and is likely younger than its emplacement. The trend of dextral deformation is cut by sinistral shear atThubun Lakes and the north-south dextral deformation is therefore clearly older than conjugate shearing which took place along the south margin of Great Slave Lake Shear Zone. It may be related to northeastward thrusting evident on Upper Thubun River (see below) which cuts the Konth Granite. Thus thrusting and dextral strike slip may have occurred in the interval between emplacement of Konth Granite (about 1936 Ma., Bostock and Loveridge, in press) and major conjugate movements on the southeast margin of Great Slave Lake Shear Zone.

PSEUDOTACHYLITES NEAR UPPER THUBUN RIVER (4)

Black pseudotachylite veins are erratically distributed over an area of some 10 km^2 or more southwest of a fault that locally follows upper Thubun River.

Other single occurrences were found 3km northeast of Doucet Lake and 2km east of O'Connor Lake. Although these small veins may have been undetected elsewhere, they form a distinct concentration about the locality on Upper Thubun River.

The veins are black to grey and devitrified. They are commonly no more than a millimetre or two thick but they tend to expand locally to form pockets of breccia that may be one metre or more across (Fig. 4). Some veins have a recognizable general trend but most appear to be randomly oriented and irregular in form.

At Upper Thubun River the veins intrude gneisses, Slave Granite, and biotite quartz diorite. They are also present within a 7-m band of grey mylonite which locally follows the river, but there they have a tendency to follow the trend of the mylonite. Shear bands and a steeply southwest plunging lineation suggest that movement was almost entirely dip slip with southwest side upthrown. No pseudotachylite veins were found northeast of the mylonite. Within a hundred metres or so northeast of the fault however, buff white granite is cut by red strained fractures lined with yellow green epidote showing well developed slickensides and steeply plunging grooves parallel to lineation in the mylonite.

The spatial association and asymmetrical distribution of pseudotachylite with respect to the fault along Upper Thubun River, and the subparallel orientation of veins and foliation within the mylonite suggest that veins and mylonite may have formed at about the same time. It is perhaps possible that the fault represented by the grey mylonite is a late listric thrust, and the pseudotachylites developed about an irregularity in the underlying fault plane and were emplaced above it in dilatant zones . In the regional framework the faulting is a late feature which cuts the 1936 Ma. Konth Granite and is therefore post 1936 Ma. It may be related to northeastward thrusting and dextral strike slip along the west margin of Slave Granite that preceded conjugate faulting southeast of Great Slave Lake Shear Zone.

CONJUGATE FAULTING NORTHEAST OF THUBUN LAKES (5)

Two pairs of northeasterly directed conjugate shear zones were mapped at Thubun Lakes in1987 (Bostock, 1988). Sinistral displacement for the southern zone of the more northeasterly pair was assumed to be conjugate to northeasterly directed dextral movements within Great Slave Lake Shear zone.

Exceptionally well developed sinistrally rotated K-feldspars (see Fig. 5) and sinistral shear bands were found within a shear zone roughly 100m wide about 1 km southeast of Great Slave Lake shear zone north of Doucet Lake. The rotated feldspars occur on all three limbs of an "S"-fold some 5m in amplitude (Fig. 6) suggesting that sympathetic minor folding occurred after feldspar rotation. Northeasterly oriented sinistral mylonites at South Thubun Lake related to this deformation cut across the north-south dextral shear zone that follows the contact between Deskenatlata and Slave granites.

Figure 4. A breccia pod along a pseudotachylite vein. Plutonic rock fragments are included in black devitrified glass.

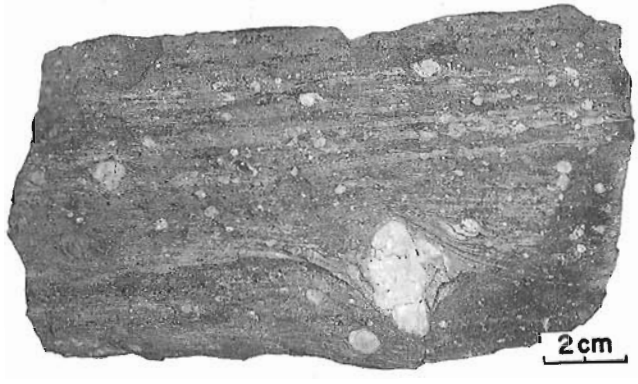

Figure 5. A spalled fragment of protomylonite showing sinistrally rotated feldspar porphyroclasts from the conjugate shear zone northeast of Doucet Lake.

Figure 6. View southwest showing an "S"-fold about 5 m, in amplitude in the conjugate shear zone northeast of Doucet Lake. Sinistrally rotated feldspars (Fig. 2) occur on all three limbs.

This occurrence extends the known length of proposed conjugate shearing to some 15km northeast of Thubun Lakes. It enhances the view that crustal blocks may have been wedged out southwestward along the southeast margin of Great Slave Lake Shear Zone during indentation of Churchill Province by Slave Province as proposed by Gibb and Thomas, (1977); and by Hoffman, (1987).

STRIKE SLIP FAULTS ABOUT MACINNIS LAKE (6)

Basement gneisses beneath Nonacho Group at MacInnis Lake consist of medium grained massive to vaguely foliated monzogranite to quartz diorite with variable proportions of hornblende- to biotite-rich schlieren and larger remnants. The rocks are variably retrograded (chloritized). Scattered remnants of mafic gneiss are present but no paragneiss, recognizable through the presence of alumino-silicates, quartzite or calc-silicate minerals, was found.

Northwest of the lake the basement rocks make up a different assemblage. The oldest are highly contorted grey quartzo-feldspathic gneisses with variable biotite and chlorite content that contain amphibolite inclusions, and are intruded by equigranular monzogranite. Elsewhere massive to megacrystic granite contains variable proportions of gneissic schlieren and pegmatite dykes. Altered glomerophyric basalt forms outcrop-sized bodies that are at least locally dyke-like and intrusive into the country rocks that include pegmatite. Two prominent fault zones were found in the area. One at the southeast corner of MacInnis Lake, trends north-northeast and commonly forms the western contact between basement and the main part of Nonacho Group. No true mylonite was found along the fault zone, but zones of cataclasis are extensive in the adjacent gneisses. Uranium and base metal mineralization have been investigated by diamond drilling in this area. No sense of movement has been determined for this fault zone but it appears to be one of a set of northerly trending faults (most prominent being the fault along Taltson Lake) which elsewhere are known to be sinistral, and to have increasing cataclasis along their northern reaches (Bostock, 1988).

The second fault extends east-northeast from Taltson Lake along the northwest side of MacInnis Lake to 110°W. Dextral shear bands occur both within the basement and within Nonacho Group along either side of the valley leading northeasterly from the northeast end of MacInnis Lake. Small zones of cataclasis are common but no mylonite was found associated with the fault. The basement to the north contains minor dextral shears. The dextral faulting terminates at the north-northeasterly fault along Taltson Lake and is apparently tangent to north-northeasterly faulting immediately east of MacInnis Lake.

It is possible that dextral movement reflects adjustments in the crustal block between two earlier sinistral fault lineaments. These adjustments presumably occurred when the northerly trending lineaments were bent northeastward in response to movement on the Great Slave Lake Shear Zone. The scenario however may not be sufficient to account for the apparent magnitude of movement necessary to produce the differing character of basement gneisses on either side of the fault.

POTENTIAL REGIONAL CORRELATION OF MAFIC ROCKS OF THE HINTERLAND

The data collected suggest that the Berrigan Lake Complex is likely the remnant of a tectonized differentiated mafic intrusion which consisted of ultramafic, gabbroic and anorthositic layers. Significantly, it lies at the western margin of the eastern hinterland. The best current guess as to the age of the granitic material which encloses some of the ultramafic fragments implies that the complex was emplaced during Archean to early Aphebian time. Aeromagnetic anomalies associated with the complex, and outlying ultramafic inclusions, suggest that remnants of it are preserved, perhaps largely at depth, within the enclosing gneisses that extend for at least 35 km along the zone of late dextral shearing to the north. The intrusion is therefore probably large.

A mafic complex bearing some similarity to that at Berrigan Lake has been partly mapped about 10 km northeast of Hill Island Lake (Bostock, 1984). The main body of metagabbro lies on the west margin of the eastern hinterland along a splay from the sinistral Lady Grey-Hill Island-Tazin shear zone and projects southeastward into the eastern hinterland as a poorly known tail of hornblende-plagioclase gneiss, plagioclase-rich metagabbro and granitic rocks. No ultramafic component has been found and high aeromagnetic anomalies do not appear directly related to its surface expression. The minimum dimensions of the complex are about 3 by 15 km.

Age relations between the metagabbro and the surrounding granitic rocks are uncertain because, although the gabbroic rocks form inclusions within and are intruded by the granitic rocks, local exposures show metagabbro apparently intrusive into granitic rocks. On the other hand the granites which widely engulf the metagabbro are unlike the dated younger granites of the region which are muscovite bearing.

They more closely resemble some granites of the25-2300 Ma group dated farther west. Deformation and alteration of the metagabbro, and lithologic correlation of enclosing granites suggest that a best guess for the age of the Hill Island metagabbro is early Aphebian or earlier.

Amphibolite inclusions of varying size are particularly common and widespread through the regional gneiss wedge that forms the western hinterland (Fig. 1). On either side of this wedge major mylonite belts diverge southward. The Allen fault zone (Godfrey and Langenberg, 1978) along the west contact continues south into Alberta. The Lady Grey Lake-Hill Island Lake-Tazin Lake fault zone at the east contact (of which only part is shown on Fig. 1) projects southeastward into Saskatchewan. The amphibolite inclusions are locally known to be enclosed in a foliated granite dated at 2334 Ma. (Bostock and Loveridge, in press) thus it is possible that the western gneiss terrain is one which received a major input of mafic dyke material which predates the 2500-2300 Ma. granites and is thus potentially of the same age as the Berrigan Lake and Hill Island mafic complexes.

SPECULATIVE SUMMARY AND INTERPRETATION

Mapping to date has shown that two large differentiated mafic complexes occur within schlieren gneisses along major faults at the west edge of the eastern hinterland. The western hinterland (Fig. 1) consists in large part of schlieren inclusion gneiss which also contains abundant amphibolite inclusions that may be remnants of a mafic dyke swarm. All of these mafic rocks are thought to predate emplacement of the 23-2500 Ma. granites. The distribution of potentially coeval mafic intrusive rocks points to the hypothesis that they are collectively symptomatic of an Archean or early Aphebian plate margin that developed along the eastern edge of Taltson Magmatic Zone. By this hypothesis the major mafic complexes of the eastern hinterland intruded along the east margin of an incipient spreading axis. Uplift and tensional stress across the axis resulted in fracturing and emplacement of a mafic dyke swarm along it. The current distribution of the eastern and western hinterlands is an artifact of later strike-slip shear which followed much later emplacement of the Taltson batholiths. Clearly this hypothesis requires further substantiation through geochronological and geochemical testing of the lithologic units concerned.

Development of a plate margin along the east side of Taltson Magmatic Zone was likely succeeded by deposition of an assemblage of plate margin sediments. Remnants of these sediments may be preserved in the paragneiss found within the western hinterland and as widespread screens and inclusions within Taltson Magmatic zone. Deposition of local volcanics with base metal (Irwin and Prusti, 1955) and tungsten occurrences (Bostock and Thompson, 1983; Bostock, 1986) was likely related to the evolution of the resulting basin. The age of this assemblage, based on 2500 Ma cross-cutting pegmatite in Alberta, (Baadsgaard and Godfrey, 1972) is consistent with such an interpretation. Early Aphebian plutonism (about 25-2300 Ma) may reflect a change in plate tectonic patterns involving eastward subduction beneath the Churchill Province, from a subduction zone now concealed beneath Paleozoic overlap. Closing of the basin could have provided a setting for emplacement of minor ultramafic bodies such as those reported at O'Connor and Rutledge Lakes (Bostock, 1986; Culshaw, 1984, Bostock,1988). How does this hypothesis fit in with other aspects of geology about Taltson Magmatic Zone?

Two significant observations about Taltson Magmatic Zone find reference within the hypothesis. The presence of chromite in the basal beds of the Nonacho sandstone (Maurice, 1984), which lie unconformably upon gneisses of the eastern hinterland, bear witness to the presence of ultramafic rocks which were more extensively exposed along this boundary during late Aphebian than they now are. The presence within Taltson Magmatic Zone of Archean paragneiss with no confirmed Archean basement except perhaps for locally recognized enclaves (Burwash and Krupicka, 1982) within Slave Granite, can be related to their deposition upon oceanic crust.

A major plutonic phase in Taltson Magmatic Zone began with impingement of Slave Province upon the western Churchill margin (Gibb, and Thomas, 1977; Hoffman,1987). The first recognized event of this phase south of Great Slave Lake Shear Zone was emplacement of the sphene-bearing Deskenatlata Granodiorite (1986 Ma., Bostock et al., 1987), and possibly the undated but mineralogicallysimilar Gagnon Monzogranite. These plutons were succeeded by intrusion of Slave Granite (1955 Ma., Bostock et al., in 1987) and by Konth Granite (1936 Ma., Bostock and Loveridge, in press), which are both cordierite-garnet-bearing granites. Continued eastward oblique collision of Slave Province along Great Slave Lake Shear Zone resulted in a complex sequence of major fault movements extending southward into Alberta and Saskatchewan. Only a partial sequence of some of these events can yet be constructed.

Regional, north-south sinistral shear is expressed along the east margin of Taltson Magmatic Zone both within the hinterland gneisses and within the Konth granite. Discrete sinistral movements were later concentrated along individual shear zones which curve northeastward near their northern limit of mapping. Where both margins of these zones comprise gneisses of the eastern hinterland cataclasis is common. Adjustments between sinistral faults such as that along the northwest shore of MacInnis Lake were likely coeval. Within this interval, or possibly slightly later, northeastward thrusting and dextral strike slip (possibly reflecting subduction related events west of Paleozoic overlap) occurred in the zone between Deskenatlata and Slave plutons and may have extended locally along southwestward dipping faults into Konth Granite. Thrusting was followed by a northeasterly trending system of conjugate faults through Thubun Lakes which follows the southeast margin of Great Slave Lake Shear Zone. This conjugate system may have arisen in response to freezing of sinistral north-south movements along the east margin of Taltson Magmatic Zone which prevented further stress release by major southward movement of the western cratonal margin. Most of this faulting was accompanied by development of lateral zones of variable but commonly intense greenschist facies retrogression.

A late north-south dextral shear zone occurs along the northeast margin of Taltson Magmatic Zone southward from Gagnon Lake. Late shearing postdates emplacement of the minor Benna Thy granite pluton (1906 Ma., Bostock and Loveridge, in press) which shows a dextral C and S fabric related to it. At its northern extremity this dextral shear zone does not cut Great Slave Lake Shear Zone but appears (in unmapped territory north of 62° N) to bend sharply into parallelism with it.

The youngest recognized faulting is predominantly sinistral. It occurs along discrete northwesterly oriented lineaments which commonly contain basalt dykes of the Sparrow Dyke Swarm (Ar/Ar age about 1700 Ma., McGlynn et al., 1974) and later quartz veins both of which locally show the sinistral shear. Less common northeasterly trending lineaments may be the loci of related faults but no dykes or veins have been found along them.

REFERENCES

Baadsgaard, H. and Godfrey, J.D.
1972: Geochronology of the Canadian Shield in northeastern Alberta II. Charles-Andrew-Colin Lake Area; Canadian Journal of Earth Sciences, v. 9, p. 863-888.

Bostock, H.H. and Loveridge, W.D.
1984: Preliminary Geological Reconnaissance of the Hill Island Lake and Taltson Lake Areas, District of Mackenzie; in Current Research, Part A, Geological Survey of Canada, Paper 84-1A, p. 165-170.
1986: Reconnaissance geology of Precambrian rocks of the Fort Resolution, Taltson Lake and Fort Smith areas, District of Mackenzie; in Current Research, Part A, Geological Survey of Canada, Paper 86-1A, p. 35-42.
1987: Geology of the South Half of the Taltson Lake map area, District of Mackenzie; in Current Research, Part A, Geological Survey of Canada, Paper 87-1A, p. 443-450.
1988: Geology of the north half of the Taltson Lake map area, District of Mackenzie; in Current Research, Part C, Geological Survey of Canada, Paper 88-1C, p. 189-198.
—: Geochronology of the Taltson Magmatic Zone and its eastern Cratonic Margin, District of Mackenzie; in Radiogenic Age and Isotopic Studies: Report 2; Geological Survey of Canada, Paper 88-2. (in press).
1983: Fluorescent minerals from the Fort Smith area, District of Mackenzie, N.W.T.; in Current Research, Part B, Geological Survey of Canada, Paper 83-1B, p. 401-402.
1987: Proterozoic geochronology in the Taltson Magmatic Zone, N.W.T.; in Radiogenic Age and Isotopic Studies: Report I, Geological Survey of Canada, Paper 87-2, p. 73-80.

Burwash, R.A. and Krupicka, J.
1982: PreKenoran Basement in Northeastern Alberta; Geological Association of Canada/Mineralogical Association, Abstracts, v. 7.

Culshaw, N.G.
1984: Rutledge Lake, N.W.T.; A Section Across a Shear Belt within the Churchill Province; in Current Research, Part. A, Geological Survey of Canada, Paper 84-1A, p. 331-338.

Gibb, R.A., and Thomas, M.D.
1977: The Thelon Front: A cryptic suture in the Canadian Shield?; Tectonophysics, v. 38, p. 211-222.

Godfrey, J.D. and Langenberg, C.W.
1978: Metamorphism in the Canadian Shield of northeastern Alberta; in Metamorphism in the Canadian Shield, ed J.A. Fraser and W.W. Heywood; Geological Survey of Canada, Paper 78-10, p. 129-138.

Hanmer, S.
1987: Textural map units in quartzo-feldspathic rocks; Canadian Journal of Earth Sciences; v. 24, p 2065-73.

Hoffman P.F.
1987: Continental transform tectonics: Great Slave Lake shear zone (ca. 1.9 Ga.), northwest Canada; Geology, v. 15, p. 785-788.

Irwin, A.B. and Prusti, B.D.
1955: O'Connor Lake (West Half); Geological Survey of Canada; Geological Survey of Canada, Paper 55-9, map with marginal notes.

McGlynn, J.C., Hanson, G.N., Irving, E., and Park, J.K.
1974: Paleomagnetism and age of Nonacho Group sandstones and associated Sparrow Dykes, District of Mackenzie; Canadian Journal of Earth Sciences, v. 11, p. 30-42.

Maurice, Y.T.
1984: Gold, Tin, Uranium and other Elements in the Proterozoic Nonacho Sediments and adjacent Basement Rocks near MacInnis Lake, District of Mackenzie; in Current Research, Part A, Geological Survey of Canada, Paper 84-1A, p. 229-238.

Progress report on stratigraphy and sedimentology of the Middle Proterozoic Kanuyak Formation and underlying paleokarst, Bathurst Inlet area, northeast Slave Province, N.W.T.

Shane M. Pelechaty[1] and Noel P. James[1]
Lithosphere and Canadian Shield Division

Pelechaty, S.M. and James, N.P., Progress report on stratigraphy and sedimentology of the Middle Proterozoic Kanuyak Formation and underlying paleokarst, Bathurst Inlet area, northeast Slave Province, N.W.T.; in Current Research, Part C, Geological Survey of Canada, Paper 89-1C, p. 57-65, 1989.

Abstract

The Kanuyak Formation, a sequence of sandstone, shale and carbonate, unconformably overlies the Parry Bay Formation, a shallow marine dolomite succession, and primarily infills large karst-related depressions along the upper contact of the Parry Bay Formation.

This report outlines the contrasting sedimentology and stratigraphy of the Kanuyak Formation within two depressions at Kanuyak Island. The central depression is filled with lacustrine/playa-lake deposits whereas the northern depression contains predominantly braided fluvial deposits which grade upward into marginal lacustrine or marine mudflat sediments.

The three-dimensional geometry of the enclosing depressions are determined from the paleoenvironmental interpretations of the Kanuyak Formation. Two contrasting morphologies are postulated: an isolated, enclosed depression, such as a true sinkhole (central depression), and an elongate, open-ended karst valley (northern depression). Lacustrine/playa-lake sediments were deposited within the sinkholes whereas fluvial sediments accumulated within the karst valleys. During mature stages of deposition within the karst valleys sediments were deposited within marginal lacustrine or marine mudflat environments.

Résumé

La formation de Kanyuak est une séquence de grès, chiste argileux et de roches carbonatées qui repose en discordance sur la formation de Parry Bay, une succession de dolomies marines déposées en milieu peu profond, et elle remplit principalement de grandes dépressions de type karstique le long du contact supérieur de la formation de Parry Bay.

Ce rapport souligne la sédimentologie et la stratigraphie contrastées de la formation de Kanuyak dans deux dépressions bien mises à nu en coupe à l'île Kanuyak. La dépression centrale est comblée de dépôts lacustres de lac temporaire, alors que la dépression septentrionale renferme principalement des dépôts de cours d'eau anastomosés passant progressivement vers le haut à des sédiments marginaux lacustres ou marins.

La géométrie dans les trois dimensions des dépressions est déterminée d'après les interprétations paléo-environnementales de la formation de Kanuyak. Deux morphologies qui font contraste sont proposées: celle de la dépression fermée isolée, genre véritable doline (dépression centrale) et celle de la vallée karstique allongée à extrémité ouverte (dépression septgentrionale). Des sédiments lacustres de lacs temporaires se sont déposés à l'intérieur des dolines et des sédiments fluviaux se sont accumulés dans les vallées karstiques. Aux stades de maturité du dépôt dans la vallée karstique, les sédiments ont été déposés en milieux lacustre ou marin.

[1] Department of Geological Sciences, Queen's University, Kingston, Ontario K7L 3N6

INTRODUCTION

Initial work during this project, within the Middle Proterozoic Elu Basin of the Bathurst Inlet area, Northwest Territories (Fig. 1, and 2), concentrated on the sedimentology and stratigraphy of the Parry Bay Formation, a sequence of shallow marine carbonates (now dolomite), and a paleokarst profile which defines the upper contact of the Parry Bay Formation (Pelechaty et al., 1988). Major elements of the paleokarst profile, such as U-shaped depressions of varying dimensions, were identified throughout the study area along a well exposed outcrop belt defined by a series of islands within Bathurst Inlet. The outcrop belt trends north-northwest and represents a single vertical section through these sediments. The karst depressions are therefore exposed only as two-dimensional features.

The Kanuyak Formation, consisting of sandstone, shale and minor dolostone, unconformably overlies the Parry Bay dolomite and occurs as sediment fill within karst depressions. During part of the 1988 field season a study of the sedimentology and stratigraphy of the Kanuyak Formation was undertaken to determine various lithofacies within the depressions. This information was in turn utilized to determine the three-dimensional aspect of the depressions. The problem is to determine whether the depressions were isolated, enclosed holes, or sinkholes, or were open-ended valley systems that traversed through the paleokarst terrain.

Below is a description of sediments within two isolated depressions, separated horizontally by approximately 9km, that are exposed in cross-section at Kanuayak Island; the central depression (between sections K3-K4), and the northern depression (between sections K11-K15, Fig. 3). These two examples are chosen to show the end-members of depositional environments represented by the Kanuyak Formation.

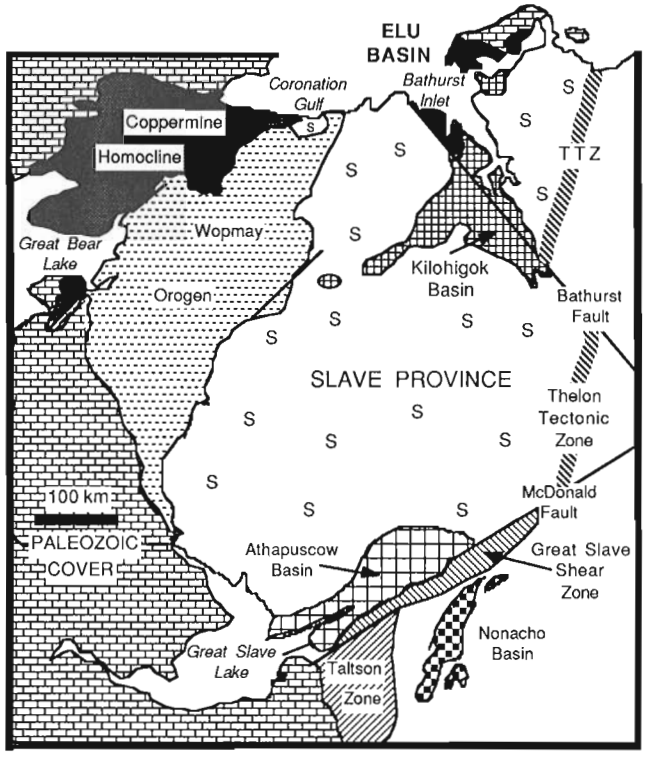

Figure 1. Regional map of Slave Province and location of Elu Basin relative to other tectonic elements (Pelechaty et al.,1988).

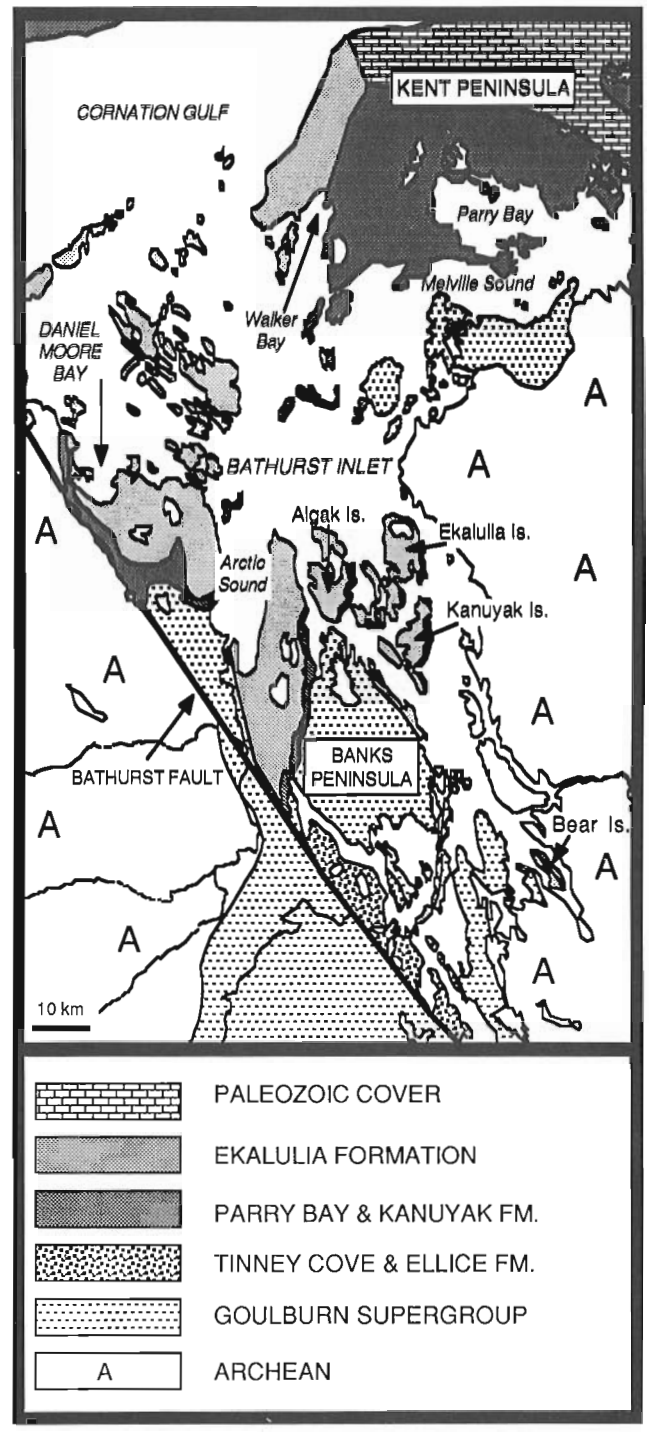

Figure 2. Location map of Middle Proterozoic Parry Bay, Kanuyak, and Ekalulia formations of the Bathurst Inlet area, Northwest Territories. Note location of Kanuyak Island (Pelechaty et al., 1988).

SUB-KANUYAK UNCONFORMITY (PALEOKARST PROFILE)

The sub-Kanuyak unconformity is an irregular paleotopographic surface on top of the Parry Bay Formation. It is exposed largely in two dimensions along the eastern shorelines of a series of north to northwest trending islands within Bathurst Inlet; Bear, Kanuyak, and Ekalulia islands (Fig. 2). Major elements of the sub-Kanuyak unconformity include large depressions up to 3 km wide and 90 m deep and solution-widened joints (grikes) up to 4 m wide. Breccia, composed of locally derived dolomite blocks and chert fragments, generally fills solution-widened joints and occurs as wedge-shaped deposits along margins of depressions. Orientations of depressions and grikes are partially controlled by a conjugate set of paleojoints trending northeast-southwest and northwest-southeast (Pelechaty, 1988; Pelechaty et al., 1988). Rare cavities (caves), now filled with breccia and bedded siliciclastic sediments, are less than a few tens of metres in size and occur within the Parry Bay dolomites 180 m below the unconformity surface. These paleogeomorphic features have been interpreted as part of a complex paleokarst terrain that formed by the dissolution and collapse of Parry Bay carbonates during a period of subaerial exposure (Pelechaty, 1988; Pelechaty et al., 1988).

KANUYAK FORMATION

The Kanuyak Formation on Kanuyak Island is best developed within large depressions along the sub-Kanuyak unconformity. The thickness of the formation is largely controlled by the paleotopography of the underlying paleokarst profile, generally thickest within the central part of depressions and thinest near the margins (Fig. 2). The Kanuyak Formation is covered by Ekalulia Formation flood basalts, which prevents erosion of the soft sediments but also hides the three-dimensional relationships.

Central depression at Kanuyak Island (Section K3-K4)

This depression is nearly symmetrical in cross-section and is approximately 20 m deep and 320 m wide, representing one of the smallest karst-related depressions in this area (Fig. 3,4 and 5a). Thin discontinous beds of breccia along the margins of the depression separate the well-bedded Parry Bay dolomites from the overlying Kanuyak sediments. Parry Bay dolomites are nearly horizontal along the bottom and northern margins of the depression and are tilted at an angle to regional bedding toward the centre of the depression along its southern margin suggesting collapse of dolomite into the depression. Large blocks (up to 5m) of Parry Bay dolomite are present near the southern margin and float within sediments of the Kanuyak Formation (Fig. 5a).

Description of sedimentary fill

Four main lithofacies are present within the depression; massive sandstone, breccia, thinly-bedded sandstone, and interbedded dolomite and mudstone lithofacies.

1. Massive sandstone lithofacies

Massive sandstone occurs between the large dolomite blocks along the southern margin of the depression (Fig. 4). It consists of medium-grained quartz sand and chert clasts up to 3 cm in size and grades laterally into interbedded sandstone, and clast- and matrix-supported breccia toward the center of the depression.

2. Breccia lithofacies

Massive breccia, both clast- and matrix-supported, occur as lenses a few metres in dimension closest to the southern

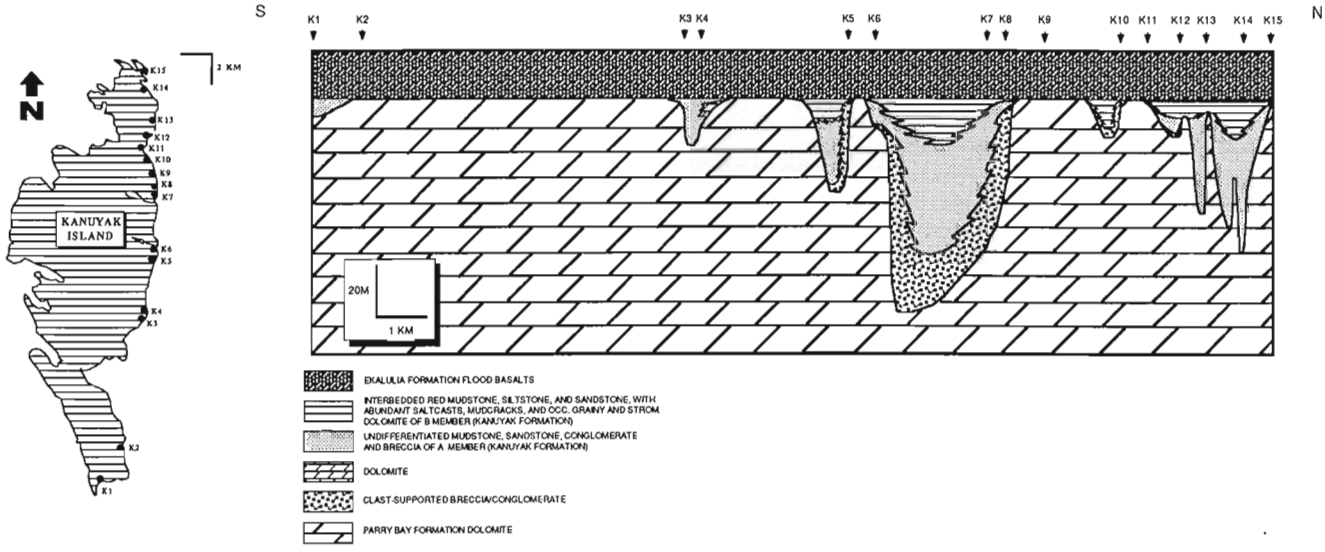

Figure 3. Location map of measured sections along eastern shoreline of Kanuyak Island and corresponding south-north stratigraphic cross-section of the Parry Bay, Kanuyak and Ekalulia formations. Note locations of central depression (sections K3-K4) and northern depression (sections 11-K15, modified after Pelechaty et al., 1988).

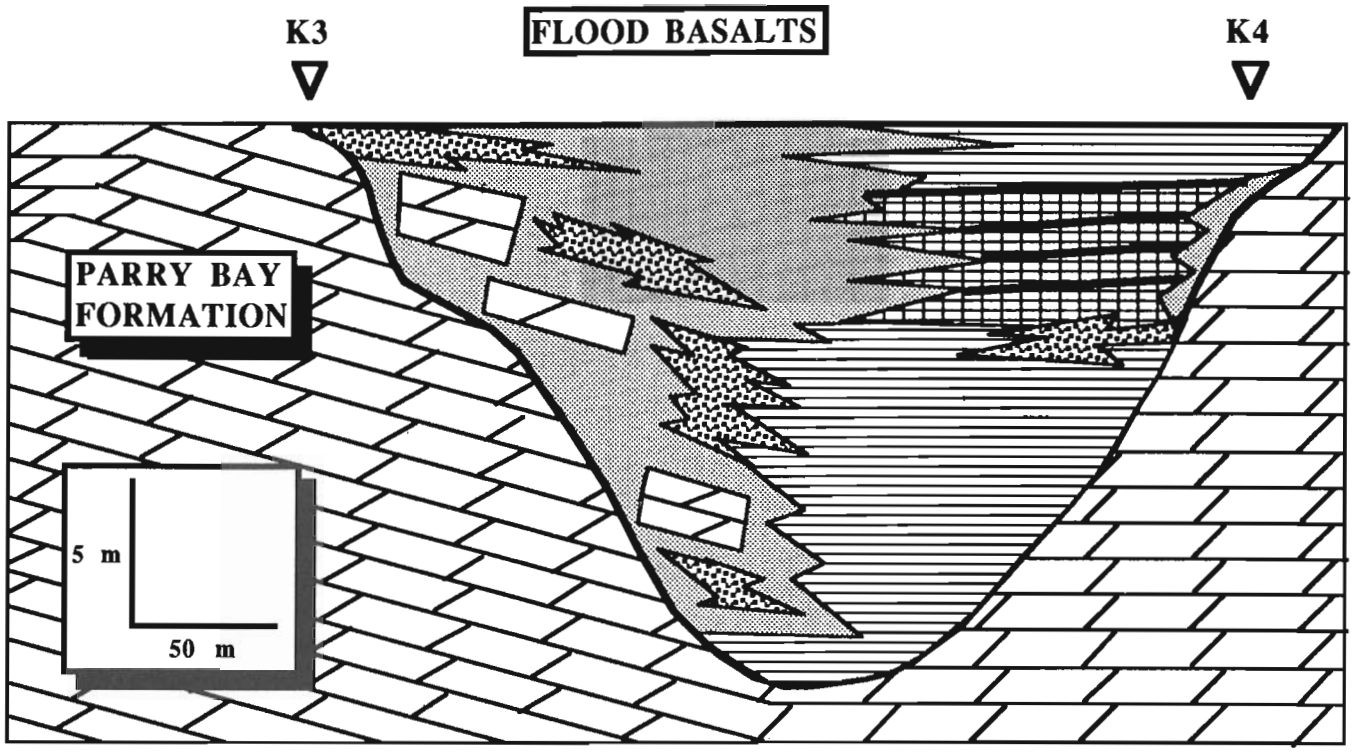

Figure 4. Stratigraphic cross-section of Kanuyak Formation at central depression, Kanuyak Island. Dotted, massive sandstone; stippled, clast and matrix-supported breccia and conglomerate; lined, thinly-bedded sandstone; boxed, dolomite; thick black lines, mudstone.

margin of the depression. Minor occurrences of breccia occur also along its northern margin stratigraphically beneath interbedded dolomite and mudstone (Fig. 4). These sediments in turn pass laterally into thinly-bedded sandstone in the central and northern parts of the depression.

3. Thinly-bedded sandstone lithofacies

It is composed of medium-grained quartz sand, and exhibits low-angle, planar, and minor small-scale trough cross-bedding, symmetrical wave ripples and possible swaley bedding and associated truncation surfaces (Fig. 5b). Paleocurrent measurements within the thinly-bedded sandstone shows a bimodal northeast-southwest paleocurrent distribution.

4. Interbedded dolomite and mudstone lithofacies

This lithofacies fills the remainder of the depression, occurs near the northern margin of the depression and is up to 5.35m thick (Fig. 4). The vertical distribution of lithologies reveals four cyclical stacked dolomite to mudstone sequences (Fig. 4). These sequences pass laterally northward and southward into massive sandstone.

Massive dolostone beds 60-220cm thick, weather white to pink, and are composed of silt to fine-grained dolomite. Horizontal and occassional vertical voids are a few millimetres thick and a few centimetres in length, and are filled with pink to red, medium-grained dolomite spar. Up to 20 % quartz sand and chert fragments occur as "out-sized" clasts within dolomite. Sharp, irregular surfaces with up to 10cm local relief, associated *in situ* breccia, tepees with associated well-developed polygonal plan geometry, anticline structures, fracturing, and rare pisolite characterize the upper contacts of dolomite beds.

Mottled green and red dolomitic mudstone beds drape irregular surfaces of underlying dolomite beds and are generally less than 30cm thick. Horizontal lamination, possible dewatering structures and minor carbonate clasts up to 3cm in size characterize these beds.

Interpretation of sedimentary fill

Sediments within the central depression probably represent lacustrine/playalake deposits. Sedimentary structures within the sandstones suggest deposition within a high-energy, wave-influenced shallow water environment. Clear bimodal paleocurrents from trough cross-beds rule out a fluvial interpretation.

Carbonate and dolomitic mudstone beds were deposited by quiet water during periods of minimal silciclastic input. This environment was relatively restricted to enable precipitation of carbonate and formation of thick beds (now dolomite). The physical characteristics of these dolomite beds are similar to documented lacustrine/playalake deposits (Picard and Lee, 1972). Fracturing, brecciation and other fabrics at the tops of dolomite beds are interpreted to have

formed during subaerial exposure. Fluctuations of the lacustrine/playa lake water level produced oscillations between carbonate production and subaerial exposure (Cheadle, 1986).

The unstratified clast-supported breccia lenses occur close to the depression walls and are interpreted as debris that was shed from from adjacent margins and redeposited within the depression. The deposits were probably reworked within the subaqueous environment (Blatt, et al., 1980; Heward, 1978). The large, isolated dolomite blocks within the depression along the southern margin and the tilted Parry Bay dolomite beds suggest the walls were unstable and periodically blocks fell into the depression.

Figure 5A. Photograph of sediment fill (Kanuyak Formation) within central depression (sections K3-K4) looking northward along eastern shoreline of Kanuyak Island. P, Parry Bay dolomite; m, massive sandstone; t, thinly-bedded sandstone; d, interbedded dolomite (light beds) and mudstone (dark beds); b, large block of Parry Bay dolomite as part of the sediment fill. The black line along the left side of the photograph illustrates the southern margin of the sinkhole. Geologist for scale (arrow).

Figure 5B. Swaley cross-bedding within thinly-bedded sandstone lithofacies (central depression). Ruler is approximately 15cm long.

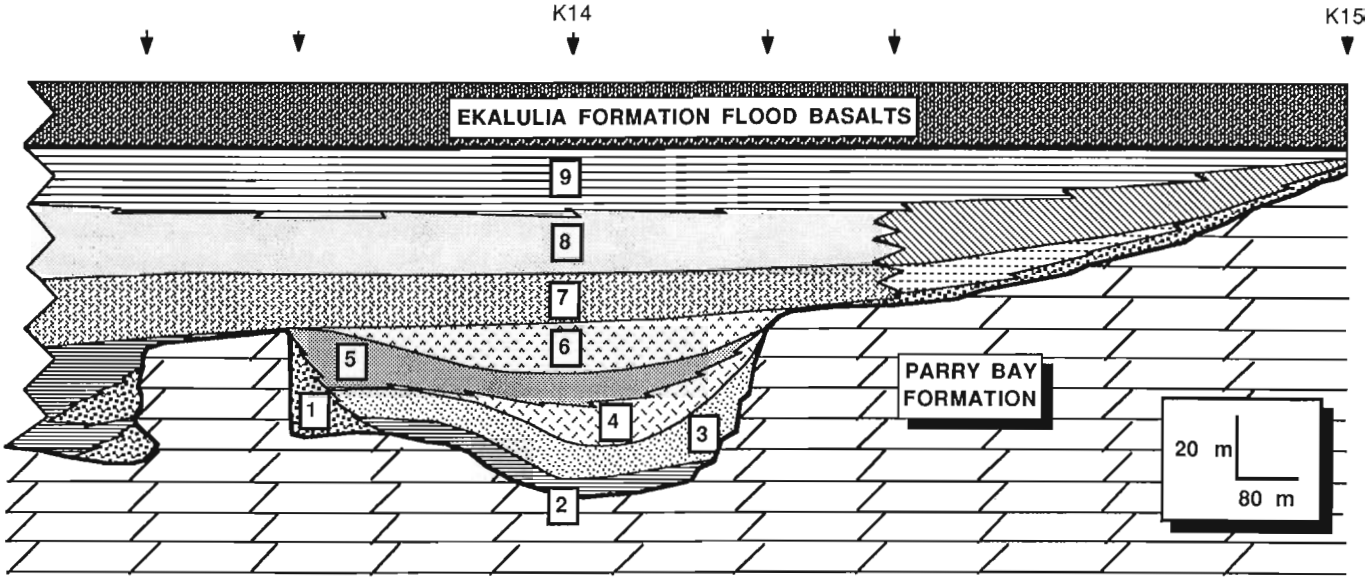

Figure 6. Stratigraphic cross-section of Kanuyak Formation at northernmost part of northern depression. 1, unstratified clast-supported breccia; 2, thinly-bedded red sandstone; 3, interbedded conglomerate and sandstone; 4, stratified clast-supported breccia; 5, coarse- to very coarse-grained sandstone; 6, granule-pebble conglomerate; 7, grey sandstone (horizontal dashed lines = "shaley" part of unit 7); 8, red sandstone (inclined lines = "shaley" part of unit 8); 9, interbedded sandstone, silty mudstone and carbonate.

Northern depression at Kanuyak Island (Section K11-K16)

This depression occurs near the northern end of Kanuyak Island and is paleogeomorphologically more complex than the depression described above (Fig. 3 and 6). This hole is approximately 2.5km wide and 60m at its deepest. The bottom of the depression is stratigraphically variable and consists of three distinct "paleohighs" (Fig. 3). These "paleohighs" effectively subdivide the depression into four smaller sub-depressions and each sub-depression contains an assemblage of lithologies different from adjacent sub-depressions. Below is a description of lithofacies that occur within the northern most sub-depression (sections K14 to K15, Fig. 3, 6 and 7a) and best summarizes the nature of sedimentary-fill within the three remaining sub-depressions.

Figure 7A. Well exposed section of the Kanuyak Formation within the northernmost part of the northern depression or interpreted karst valley at Kanuyak Island. Section is approximately 60m thick. S, interbedded sandstone, silty mudstone (dark beds) and carbonate (light beds) lithofacies; e, Ekalulia Formation flood basalts. The floor of the depression crops out just below water level.

Figure 7B. Northern margin of 10m wide trough cross-beds in horizontally bedded grey sandstone lithofacies (no.7). Vertically oriented hammer for scale.

Description of sedimentary-fill

This sub-depression contains approximately 60m of sedimentary rock (Fig. 7a). In ascending order, the sedimentary fill is subdivided into nine main lithofacies: unstratified clast-supported breccia, thinly-bedded red sandstone, interbedded conglomerate and sandstone, stratified clast-supported breccia, coarse- to very coarse-grained sandstone, granule-pebble conglomerate, grey sandstone, red sandstone, and interbedded sandstone, silty mudstone, and carbonate lithofacies.

1. Unstratified clast-supported breccia lithofacies

The breccia occur as wedge-shaped deposits adjacent to paleotopographic highs of Parry Bay dolomites and as thin (< 1 m) veneers along the Parry Bay Formation at the base of the overlying Kanuyak Formation. Clasts within thedeposits are angular, poorly sorted, composed of dolomite and chert, and up to 1.5m in size. Commonly breccia passes laterally and stratigraphically upward into interbedded conglomerate and sandstone of the Kanuyak Formation. Matrix material is composed variably of medium- to coarse-grained quartz sand, and smaller dolomite and chert fragments.

2. Thinly-bedded red sandstone lithofacies

The thinly-bedded red sandstone lithofacies occurs as a lens-shaped deposit near the bottom of the karst-related depression (Fig. 6). The lithofacies is thickest (3.6m) near the centre of the depression and thins to 0m northward and southward where it laps onto the Parry Bay dolomites and passes laterally into unstratified clast-support breccia respectively. Sandstone is composed predominately of fine- to medium-grained quartz sand. Festoon trough cross-bedding typifies the sedimentary structures at its thickest part and passes laterally into low angle cross-bedding and flat top and sinuous crested wave ripples towards the edges of the lens. Paleocurrent directions from trough cross-bedding within bedsets less than 30cm thick indicate a generally northeast direction (Fig. 8a). Minor red silty-shale beds ($_5$5cm) are intercalated with sandstone throughout and contain minor mudcracks. In addition, mudchips are common along the bases of sandstone beds. Rare large ($_5$25cm), isolated dolomite clasts occur floating within the thinly-bedded sandstone. Bedding within the sandstone drapes around the upper and lower sides of clasts.

Conglomerate lenses less than 10m wide and 1m thick occur near the upper contact of this lithofacies.

3. Interbedded conglomerate and sandstone lithofacies

This lithofacies is up to 6m thick and exhibits variable thickness thining to 0m both northward and southward from the centre of the sub-depression. The lower contact is sharp and erosional when underlain by the Kanuyak Formation and passes northward onto Parry Bay dolomites. Conglomerate is poorly sorted and exhibits common clast-supported and minor matrix-supported fabric. Hints of horizontal stratification and possible trough cross-bedding is present. Clasts

are predominately dolomite and chert and maximum clast size is less than 4cm. Interbedded sandstone beds are 10-20cm thick and composed of coarse- to very coarse-grained quartz sand and minor granule and pebble clasts of dolomite and chert. Trough cross-bedding occur throughout sandstone beds and exhibit similar paleocurrent directions as within the thinly-bedded red sandstone lithofacies (within the northeast quadrant). This lithofacies coarsens-upward with increasing amounts of conglomerate and fines northward and southward passing into interbedded mudstone and trough cross-bedded fine- to medium-grained sandstone. Minor thin ($_{5}$2cm), low angle cross-bedded conglomerate layers occur within the finer grained parts of the lithofacies.

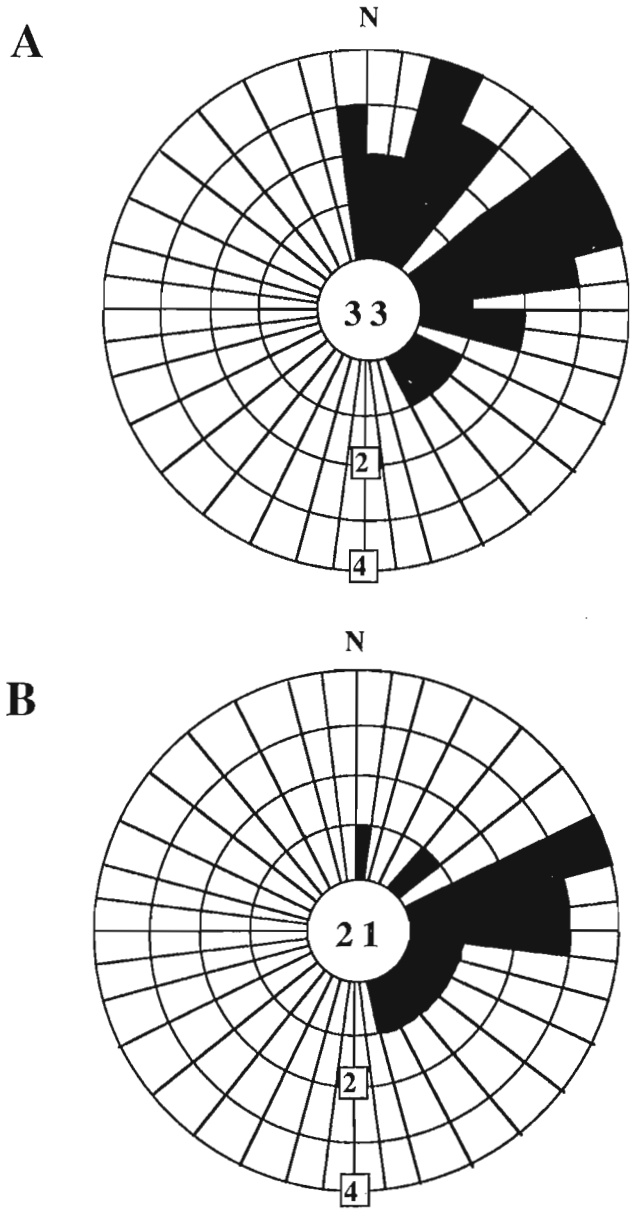

Figure 8. A rose-plot of paleocurrent measurements from trough cross-bedding within the northern depression (sections K14-K14). A) 33 measurements from the thinly-bedded red sandstone lithofacies (no.2), B) 21 measurements from the red sandstone lithofacies (no.8).

4. Stratified clast-supported breccia lithofacies

The stratified clast-supported breccia lithofacies is up to 5.5m thick and exhibits erosional lower and sharp to gradational upper contacts. Stratification within the breccia is defined by horizontal alignment of clasts and appearance of bedding produced by minor interbedded trough cross-bedded sandstone lenses less than 10cm thick with less than 10m of lateral continuity. Inverse grading characterizes this lithofacies with clasts usually 5-40 cm in size near the base and up to 1 m at the top. Matrix material is composed of quartz sand and subrounded to sub-angular clasts of dolomite and chert similar to lithologies of the underlying Parry Bay Formation.

5. Coarse- to very coarse-grained sandstone lithofacies

This lithofacies is up to 6.5m thick and is well-cemented producing blocky weathering when exposed. Bed thickness increases upward from 1-3cm to 6cm thick near the top. Trough cross-bedding, low angle cross-bedding and planar stratification are present. Sandstones are composed predominately of quartz sand, 10-15 % feldspar grains and minor dolomite and chert granules. Rare interbedded green and red mudstone beds less than 4cm thick are present.

6. Granule-pebble conglomerate (grit) lithofacies

Granule-pebble conglomerate or grit is up to 7.2m thick. The lower contact is sharp and irregular with up to 2m local relief. It is massive to horizontally stratified near the base passing upward into large-scale trough cross-bed sets 1m thick. The grit is clast-supported with clasts up to 3cm insize set in coarse- to very coarse-grained sand matrix. Clasts are composed of dolomite, chert, mudstone and sandstone.

7. Grey sandstone lithofacies

The grey sandstone lithofacies is up to 7.9m thick. It is areally more extensive than underlying lithofacies and extends the width of the two northern most sub-depressions (Fig. 6). It is well cemented and composed of moderately well sorted, medium- to occassional coarse-grained quartz sand and minor feldspar (5 %). Beds are up to 1.5m thick but commonly 3-50cm thick. Large-scale trough crossbeds characterize this lithofacies (Fig. 7b). Bed sets are up to 1.5m thick and may be traced tens of meters laterally. Cross-bed sets are largest near the base and decrease in size toward the top passing into festoon trough cross-bedding. Individual foreset beds are up to 10cm thick. Paleocurrents are directed toward the northeast to southeast.

Trough cross-bedded sandstones pass northward to interbedded white sandstone and green siltstone and mudstone and in turn pinch out against the Parry Bay Formation near the northern margin of the depression. Sandstone beds are less than 10cm thick and contain planar, low angle and minor trough cross-bedding. Finer-grained units contain possible mudcracks.

8. Red sandstone lithofacies

This lithofacies is up to 9.5m thick and composed of tabular-bedded, medium to coarse-grained sandstone beds 35-50cm thick. Minor thinly-bedded ($_5$5cm) planar laminated green and red mudstone beds which contain thin lenticular sand units separate sandstone beds. Individual sandstone beds have scoured bases and contain abundant red and green mudchips at the base of beds. Trough cross-beds occur as either "bed-thick" cross-bed sets or smaller scale festoon trough cross-bedding. Trough cross-bed sets are 5-50cm thick and up to 1.5m long. Paleocurrents trend northeast to southeast similar to trends within underlying lithofacies (Fig. 8b). Wave ripple laminations occur at the top of sandstone beds.

The red sandstone lithofacies grades upward into the interbedded sandstone, mudstone and carbonate lithofacies and "shales-out" northward passing into interbedded red sandstone and red mudstone. This unit represents a lateral facies change of the red sandstone lithofacies and thins northward to 0m against the margin of the depression.

9. Interbedded sandstone, silty mudstone and carbonate lithofacies

This lithofacies is the topmost unit of the Kanuyak Formaton (Fig.s 6 and 7a) and is the B Member of Pelechaty et al.(1988). It is less than 10.8m thick and extends across the entire northernmost depression at Kanuyak Island. Sandstone beds are 5-40cm thick and thickest and most abundant near the base. Sandstone is composed of medium- to coarse-grained quartz sand and contains planar and trough cross-beds. Bases of beds are planar, contain abundant mudchips, and exhibit soft sediment deformation and occassional sediment loading structures. Carbonate beds are up to 10cm thick and are thickest and most abundant near the top of the lithofacies. Characteristic buff weathering nicely outlines planar and ripple laminations. Minor tepees and horizontal and vertical fenestrae are present. Thin interbedded ripple sandstones are common. Red silty mudstone beds are typically less than 40cm thick and evenly distributed throughout the lithofacies. Abundant mudcracks and salt casts are present. Minor conglomerate beds are clast-supported, less than 10cm thick and contain rounded to subrounded dolomite clasts up to 1cm in size. Conglomerate may also occur as "clast-thick" layers within silty mudstone beds or commonly as thicker beds that underlie dolomite. The upper 3.8m is dominated by planar and ripple laminated dolomite with minor conglomerate near the base. Brecciation, disrupted bedding and abundant calcite (dedolomite) typifies the upper 10-20cm of this lithofacies when overlain by the Ekalulia Formation flood basalts.

Interpretation of sedimentary fill

The deposits within the northern depression represent a spectum of depositional environments, including: 1) braided fluvial, including two distinct styles of fluvial sedimentation, 2) transitional facies, and 3) marginal lacustrine/marine mudflat environments.

A braided fluvial environment is interpreted for the thinly-bedded red sandstone and upward to the granule-pebble conglomerate lithofacies (Fig. 6). Consistent north to east paleocurrent trends, abundant large-scale and festoon trough cross-bedding, relatively large grain size and the presence of erosional features such as scoured bases of beds suggests deposition within a high energy, unidirectional turbulent flow (Visher, 1972). The fluvial system was confined within the walls of antecendent karst topography.

The grey sandstone lithofacies is interpreted as representing a shift in fluvial style to a lower energy sandy braided fluvial system. Deposition occurred over a broader area as the system aggraded out of the confines of the underlying narrower depression. The red sandstone lithofacies is interpreted as a transitional facies representing deposition of fluvial sandstones later reworked by wave action as evidenced by wave ripples at the top of unidirectional trough cross-bedded sandstone beds. These beds may have been deposited as sand sheets during flood events (Hubert and Hyde, 1982). Mudstone beds were subsequently deposited during periods of quiet water between periods of sandstone deposition.

Many characteristics of the interbedded sandstone, silty mudstone and carbonate lithofacies are well documented within both marginal lacustrine (Fouch and Dean, 1982; Cheadle, 1986; Eugster and Hardie, 1975; Surdam and Wolfbauer, 1975) and marginal marine mudflat environments (Weimer et al., 1982; Klein, 1977) of all ages. Many of the physical sedimentary structures within this lithofacies suggest deposition within shallow water (e.g. horizontal and ripple laminations) punctuated by periods of subaerial exposure and evaporation (e.g. mudcracks and salt casts). Quiescent periods of deposition, as evidenced by abundant mudstone and dolomite, were periodically interupted by sandstone deposition.

DISCUSSION

The Kanuyak Formation represents the first phase of deposition after prolonged subaerial exposure of the Parry Bay dolomites and subsequent development of karst. These sediments record the progressive infill of karst depressions and their depositional history provides a useful tool for interpreting the three-dimensional aspect of the depressions. The sediments are complex within individual depressions and sequences cannot be correlated between depressions.

Sediments within the central depression are interpreted as lacustrine/playalake deposits. This type of depositional environment places constraints on the interpreted three-dimensional aspect of the depression. The restricted nature of the environment suggests that depositon occurred within an isolated, enclosed depression. Such karst-related depressions have been described as sinkholes or dolines within the modern environment (Sweeting, 1973; p.106 of Jennings, 1985) and rock record (Sando, 1974; Desrochers and James, 1988) and may form by a number of different processes, including surface dissolution or collapse of underlying near-surface caves. The orientation of the margins are partially controlled by paleojoints and suggest that the sinkhole may have been slightly elongate verses circular in plan.

Sediments within part of the northern depression are interpreted as braided fluvial through marginal lacustrine or marginal marine mudflat deposits. The braided fluvial sediments within the basal part of the section strongly suggest that the depression was elongate and open-ended in order to allow for free-flowing water to pass through the depression. A karst valley whose floor was traversed by a braided fluvial system can be envisaged for this part of the Kanuayak Formation. Such depositional settings have also been postulated for other paleokarst depressions (e.g. Mississippian karst of Newfoundland, Dix, 1981) and described within the modern environment (Jennings, 1985).

The sandstone, silty mudstone and carbonate lithofacies, which represents the upper most part of the Kanuyak Formation is interpreted as either a marginal lacustrine or marine mudflat environment. A broad plain onto which either lacustrine or marine mudflat sediments were deposited developed after progressive infill of the karst valley and eventual burial of the paleotopographic depression. The areal distribution of these sediments may still have been controlled by buried karst topography because this lithofacies is confined between the outermost margins of the northern depression (Fig. 3).

Karst sinkholes and valleys, in addition to grikes and caves, were sculpted into Middle Proterozoic carbonates during karstification of the Parry Bay Formation. Antecedent joints which dissected the Parry Bay carbonates prior to or coeval with exposure strongly influenced the orientation and geometry of these karst features.

ACKNOWLEDGMENTS

We gratefully acknowledge the Geological Survey of Canada for superb logistical support and the opportunity to work within the Elu Basin. R. Adams, J.P. Grotzinger, S. Hanmer, D.S. McCormick, and P. Myrow are thanked for their enthusiasm and invaluable discussions within the field. I (SMP) would like to thank J.P. Grotzinger for the opportunity of having three summers of "Bathurst" experience and for his continued support, teachings and encouragement during the Beechey and Elu Basin projects. Additional financial support was provided by National Science and Engineering Research Council grant A-9159 (NPJ).

REFERENCES

Blatt, H., Middleton, G., and Murray, R.
1980: Origin of sedimentary rocks; 2nd edition, Prentice-Hall, Inc., Engelwood Cliffs, New Jersey, 782p.

Campbell, F.H.A.
1978: Geology of the Helikian rocks of the Bathurst Inlet area, Northwest Territories; in Current Research, Part A, Geological Survey of Canada, Paper 78-1A. p. 97-106.

Campbell, F.H.A.
1979: Stratigraphy and sedimentation in the Helikian Elu Basin and Hiukitak Platform, Bathurst Inlet-Melville Sound, Northwest Territories: Geological Survey of Canada. Paper 79-8, 18p.

Cheadle, B.A.
1986: Alluvial-playa sedimentation in the lower Keweenanwan Sibley Group, Thunder Bay, Ontario; Canadian Jounal of Earth Science, v.23, p. 527-542.

Desrochers, A. and James, N.P.
1988: Early Paleozoic surface and subsurface paleokarst: Middle Ordovician carbonates, Mingan Islands, Quebec; in N.P. James, and P.W. Choquette, ed., Paleokarst, Springer-Verlag, p. 183-210.

Dix, G.R.
1981: The Codroy Group (Upper Mississippian) on the Port Au Port Peninsula, Western Newfoundland: Stratigraphy, palaeontology, sedimentology and diagenesis; M.Sc. thesis, Memorial University of Newfoundland, St. John's. NFLD, 219 p.

Eugster, H.P. and Hardie, L.A.
1975: Sedimentation in an ancient playa-lake complex: The Wilkins Peak Member of the Green River Formation of Wyoming; Geological Society of America, v.86, p.319-334.

Fielding, C.R.
1984: Upper delta plain lacustrine and fluviolacustrine facies from the Westphalian of the Durham coalfield, NE England; Sedimentology, v.31, p.547-567.

Fouch, T.D. and Dean, W.E.
1982: Lacustrine and associated clastic depositional environments; in P.A. Scholle, and D. Spearing, ed., Sandstone depositional environments, American Association of Petroleum Geologists, Memoir 31, p. 87-114.

Heward, A.P.
1978: Alluvial fan and lacustrine sediments from the Stephanian A and B (La Magdalena, Cinera-Matallana and Sabero) coalfields, northern Spain; Sedimentology v. 25, p. 451-488.

Hubert, J.F., and Hyde, M.G.
1982: Sheet-flow deposits of graded beds and mudstones on an alluvial sandflat-playa system: Upper Triassic Blomidon redbeds, St Mary's Bay, Nova Scotia, Sedimentology, v.29, p. 457-474.

Jennings, J.N.
1985: Karst Geomorphology: Basil Blackwell, 293 p.

Klein, G.D.
1977: Clastic tidal flats; COPCO, Champaign, Illinois, 149p.

Pelechaty, S.M.
1988: Sedimentology and stratigraphy of a Middle Proterozoic paleokarst profile, Elu Basin, Bathurst Inlet area, N.W.T.; Central Canada Geological Conference, Programme and Abstracts, p.80.

Pelechaty, S.M., Grotzinger, J.P., Goodarzi, F., Snowdon, L.R., and Stasiuk, V.
1988: A preliminary analysis of middle Proterozoic karst development and bitumen emplacement, Parry Bay Formation (dolomite), Bathurst Inlet area, District of Mackenzie; in Current Research, Part C, Geological Survey of Canada, Paper 88-1C, p. 299-312.

Picard, M.D., and Lee, R.H.Jr.
1972: Criteria for recognizing lacustrine rocks; in J.K. Rigby, and W.K. Hamblin, ed., Recognition of ancient sedimentary environments, Special Publication no. 16, p.108-145.

Sando, W.J.
1974: Ancient solution phenomena in the Madison Limestone (Mississippian) of north-central Wyoming; Journal of Research, United States Geological Survey, v.2, no.2, p.133-141.

Surdam, R.C., and Wolfbauer, C.A.
1975: Green River Formation, Wyoming: A playa-lake complex; Geological Society of America Bulletin, v. 86, p.335-345.

Sweeting, M.M.
1973: Karst landforms; London, Macmillan Publ. Co., 362 p.

Uisher, G.S.
1972: Physical characteristics of fluvial deposits; in J.K. Rigby, and W.K. Hamblin, ed., Recognition of ancient sedimentary environments, Special Publication no. 16, p.84-97.

Weimer, R.J., Howard, J.D., and Lindsay, D.R.
1982: Tidal flats and associated tidal channels; in P.A. Scholle, and D. Spearing, ed., Sandstone depositional environments, American Association of Petroleum Geologists, Memoir 31, p. 191-245.

Monometallic and polymetallic deposits associated with the sub-Athabasca unconformity in Saskatchewan

V. Ruzicka
Mineral Resources Division

Ruzicka,V., Monometallic and polymetallic deposits associated with the sub-Athabasca unconformity in Saskatchewan; in Current Research, Part C, Geological Survey of Canada,Paper 89-1C, p. 67-79, 1989.

Abstract

Formation of uranium deposits associated with the sub-Athabasca unconformity was controlled by lithostratigraphic and structural features of the basement, such as granitic domes, graphitic/pyritic layers, shear and fracture zones intersecting the unconformity, zones of rock alteration and the distance from the unconformity.

The deposits are either monometallic, containing predominantly uranium minerals, or polymetallic, containing uranium and base metal (particularly Ni,Co and Cu), locally also precious metal, mineral assemblages.

The U-Ni-Co-Cu elemental association provides a diagnostic geochemical signature for the deposits that can be advantageously used in mineral exploration. In addition, the Ni-Co-Cu ratios can be used as a basis for subdivision of the deposits of this type.

Résumé

La formation des gisements d'uranium associés à la discordance sub-Athabaska a été régie par des entités lithostratigraphiques et structurales du socle tel les dômes granitiques, les couches graphiteuses et pyriteuses, les zones de cisaillement et de fracture recoupant la discordance et les zones d'altération des roches ainsi que par la distance à la discordance.

Les gisements sont soit monométalliques, renfermant principalement des minéraux uranifères, soit polymétalliques, renfermant de l'uranium et des métaux de base (en particulier du Ni, du Co et du Cu), avec par endroits des ensembles minéraux renfermant également des métaux précieux.

L'association U-Ni-Co-Cu fournit une signature géochimique permettant d'identifier les gisements dont l'exploration est profitable. De plus, les rapports Ni-Co-Cu peuvent servir de base pour la subdivision des gisements de ce genre.

INTRODUCTION

In 1987 more than one fifth of the western world's Reasonably Assured Resources of uranium, recoverable at up to 130 U.S. dollars/kg U, was attributed to unconformity-associated deposits (OECD Nuclear Energy Agency and the International Atomic Energy Agency, 1988). This proportion is increasing as a result of new discoveries and the diminishing viability of other types of uranium resources characterized by low grades. Individual deposits contain large quantities of uranium resources, overshadowed only by the extremely large uraniferous quartz-pebble conglomerate deposits, and exhibit spectacular ore grades (Fig. 1).

In 1987 the uranium output from unconformity-associated deposits in Canada and Australia represented about one third of the total world production, which amounted to some 36 300 tonnes U. The Canadian Key Lake mine itself contributed about 14 percent of this total output. Production from Canadian unconformity-associated uranium deposits was 8244 tonnes U in 1987, i.e almost two times greater than the output from the deposits associated with quartz-pebble conglomerates at Elliot Lake.

The world's uranium exploration projects are preferentially oriented to areas favourable for this type of mineralization, particularly to the Athabasca and Thelon basins in Canada and the Pine Creek Geosyncline and Kintyre areas in Australia. In Canada the 1987 expenditures in exploring for unconformity-associated uranium deposits amounted to 36.3 million dollars, i.e. 97.6 per cent of the total uranium exploration expenditures. The main exploration projects were carried on in the Athabasca Basin region, Saskatchewan (Fig. 2). Uranium exploration strategies are commonly based on conceptual genetic models that take into account many factors, such as hypothetical source of the metals, lithological and structural controls on the mineralization, geochemical and geophysical signatures of the deposits and the presumed method of metal transport from the source to the site of deposition.

It is commonly assumed that deposits classified as of the same type share the same characteristic features. However, as demonstrated by the comparison between the ores from the Cigar Lake and Key Lake deposits (Ruzicka, 1988), individual deposits may differ substantially from each other. This paper contains some results of comparative studies on deposits associated with the sub-Athabasca unconformity in the Athabasca Basin region, Saskatchewan. Consideration is given, in particular, to factors that controlled their formation, and which can be used for establishing or refining conceptual genetic models for these deposits.

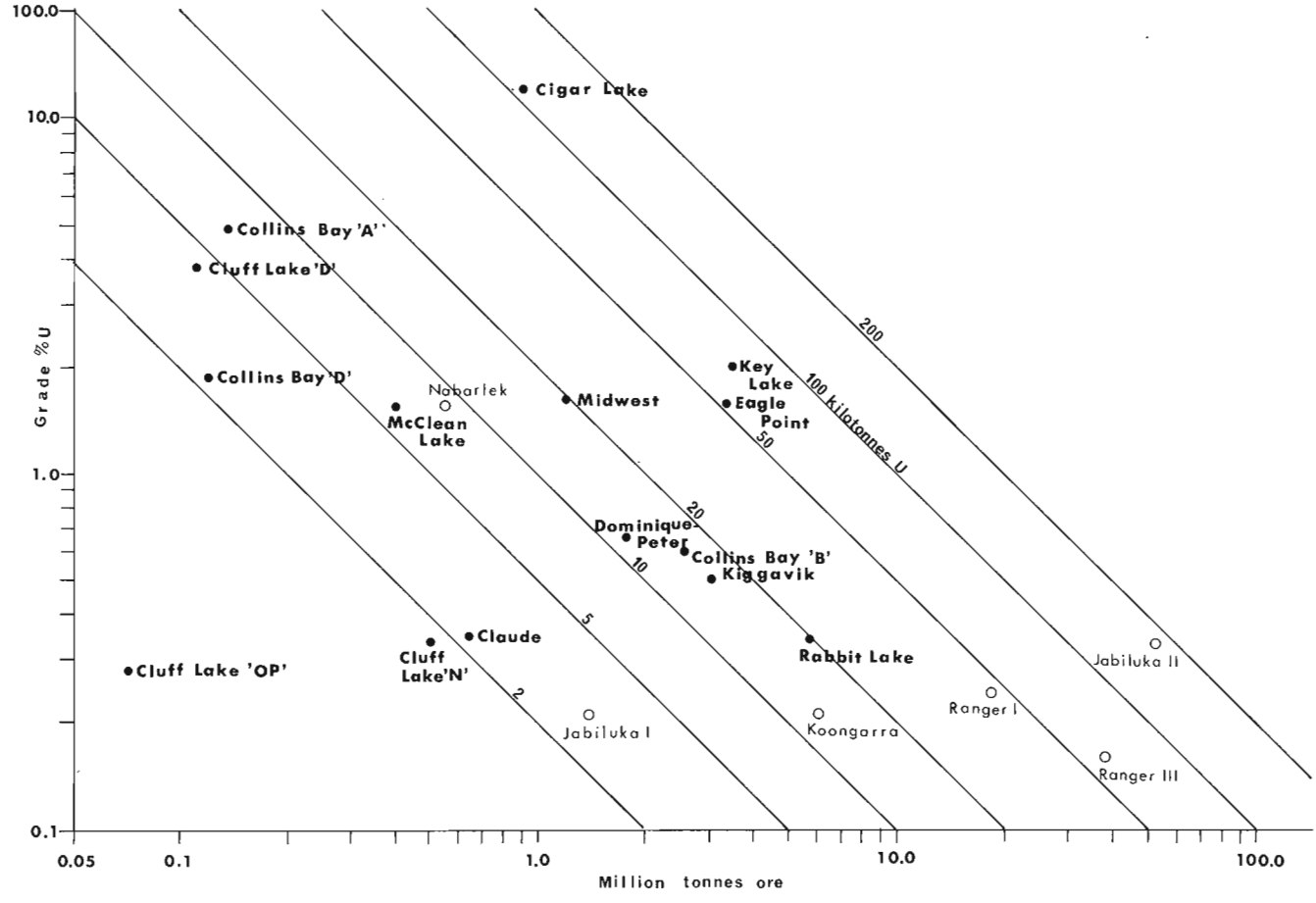

Figure 1. Grade/tonnage diagram for selected unconformity-associated deposits in Canada (dots) and Australia (circles).

LITHOSTRATIGRAPHIC AND STRUCTURAL CONTROLS

The oldest rocks in the Athabasca Basin region are Archean gneisses and granitoid plutons. They commonly form elongated domes flanked commonly by Aphebian metasedimentary rocks, which include graphitic, pyritic, non-graphitic and aluminous pelites and semipelites, calc-silicate rocks, banded iron formation, volcanic rocks and greywackes.

During a post-Aphebian hiatus the crystalline rocks underwent peneplanation with development of a regolith. The Helikian clastic sedimentary rocks were deposited on the regolith or, where the regolith was eroded, on the unaltered basement. The Helikian sedimentation was locally accompanied by volcanism. The crystalline basement rocks and the Helikian cover rocks were intruded by diabase dykes.

The deposits, in terms of the lithostratigraphic controls on localization of the ores and even on the composition of these ores, exhibit many common features, but also show some dissimilarities. The deposits (Fig.3) occur (a) in altered crystalline basement rocks below the unconformity, (b) in both altered basement and sedimentary cover rocks at the unconformity and (c) in the sedimentary rocks at some distance above the unconformity.

Deposits below the unconformity

Deposits in altered crystalline rocks below the unconformity include Rabbit Lake, Eagle Point, Dominique-Peter, Raven and Horseshoe. Their ores are typically monometallic. The deposits occur in various horizons of the Aphebian sequence.

The ores of the **Rabbit Lake** deposit, which consist typically of pitchblende, are confined to altered, brecciated and fractured, meta-arkosic to metapelitic rocks, including graphitic semipelite, plagioclasite and dolomitized limestone. The plagioclasite is a product of sodic metasomatism (Sibbald, 1976). The mineralization is particularly extensive in the proximity of microgranite, which has intruded

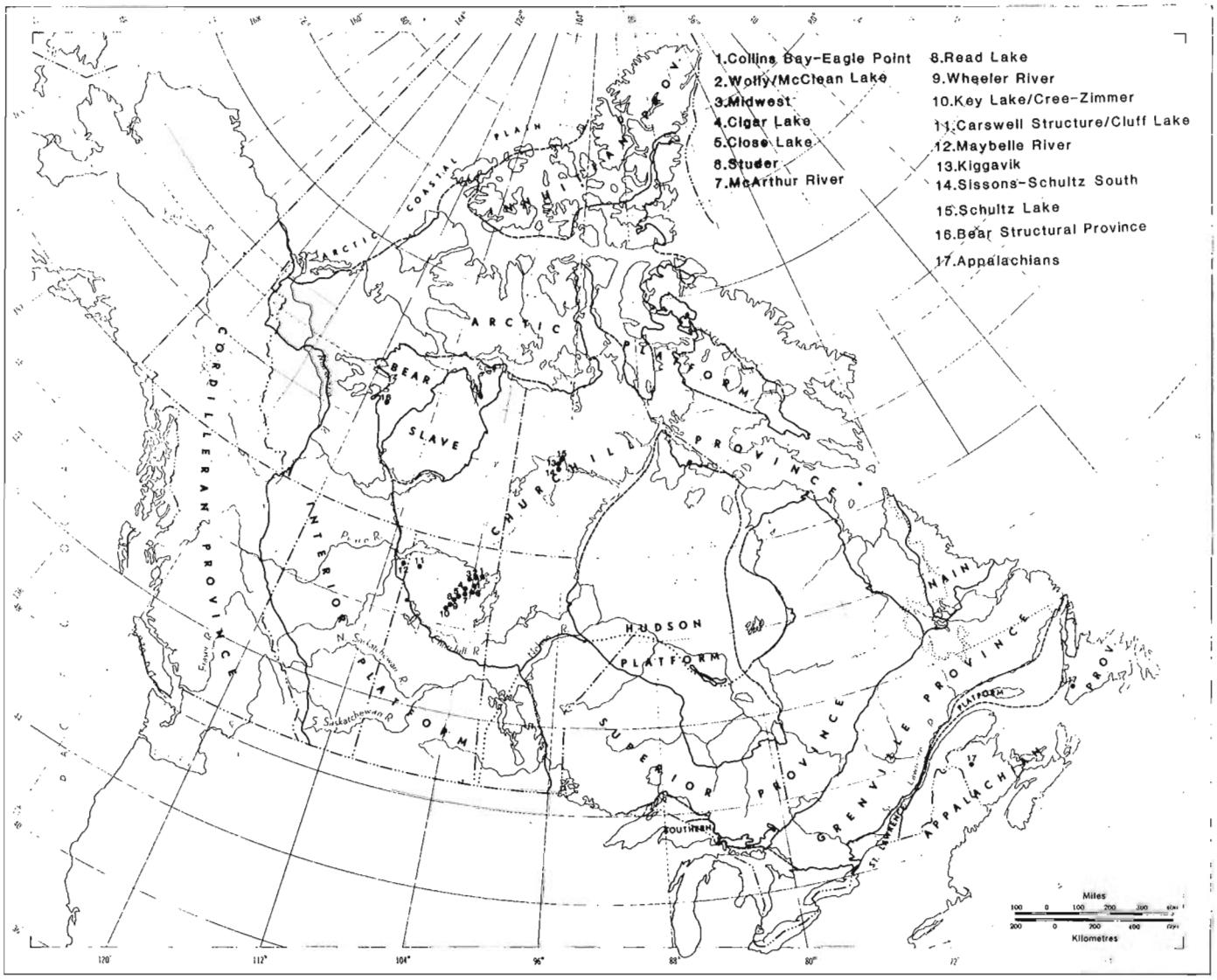

Figure 2. Location of significant uranium exploration projects in Canada in 1987.

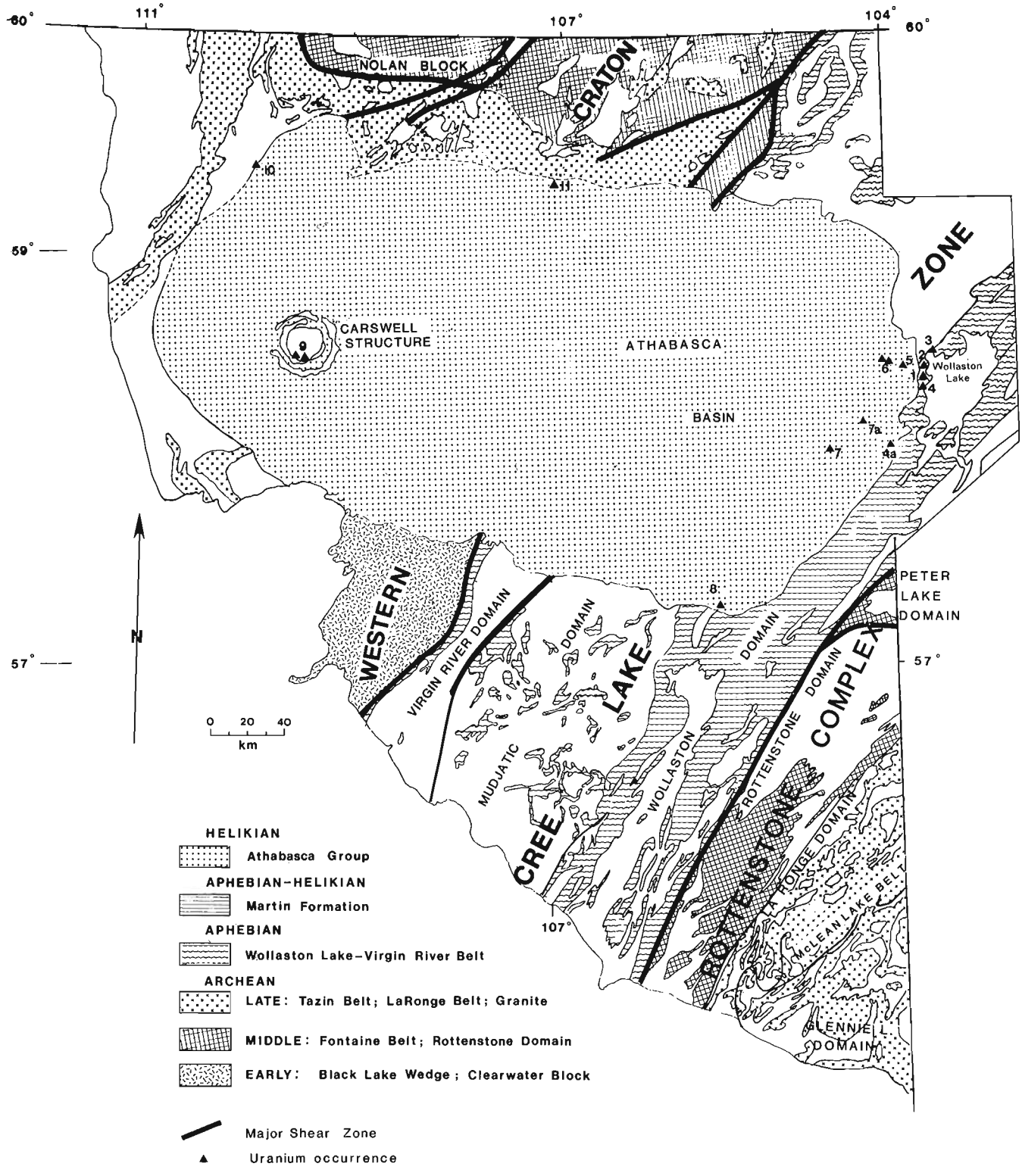

Figure 3. Location of uranium deposits associated with the sub-Athabasca unconformity in the Athabasca Basin region, Saskatchewan. Deposits: 1 = Rabbit Lake; 2 = Collins Bay 'A' and 'B'; 3 = Eagle Point; 4 = Raven and Horseshoe; 4a = West Bear; 5 = McClean; 6 = Midwest and Dawn Lake; 7 = Cigar Lake; 7a = Natona Bay; 8 = Key Lake; 9 = Cluff 'D', Dominique-Peter, OP and Claude; 10 = Maurice Bay; 11 = Fond-du-Lac. Base map after Lewry and Sibbald (1979).

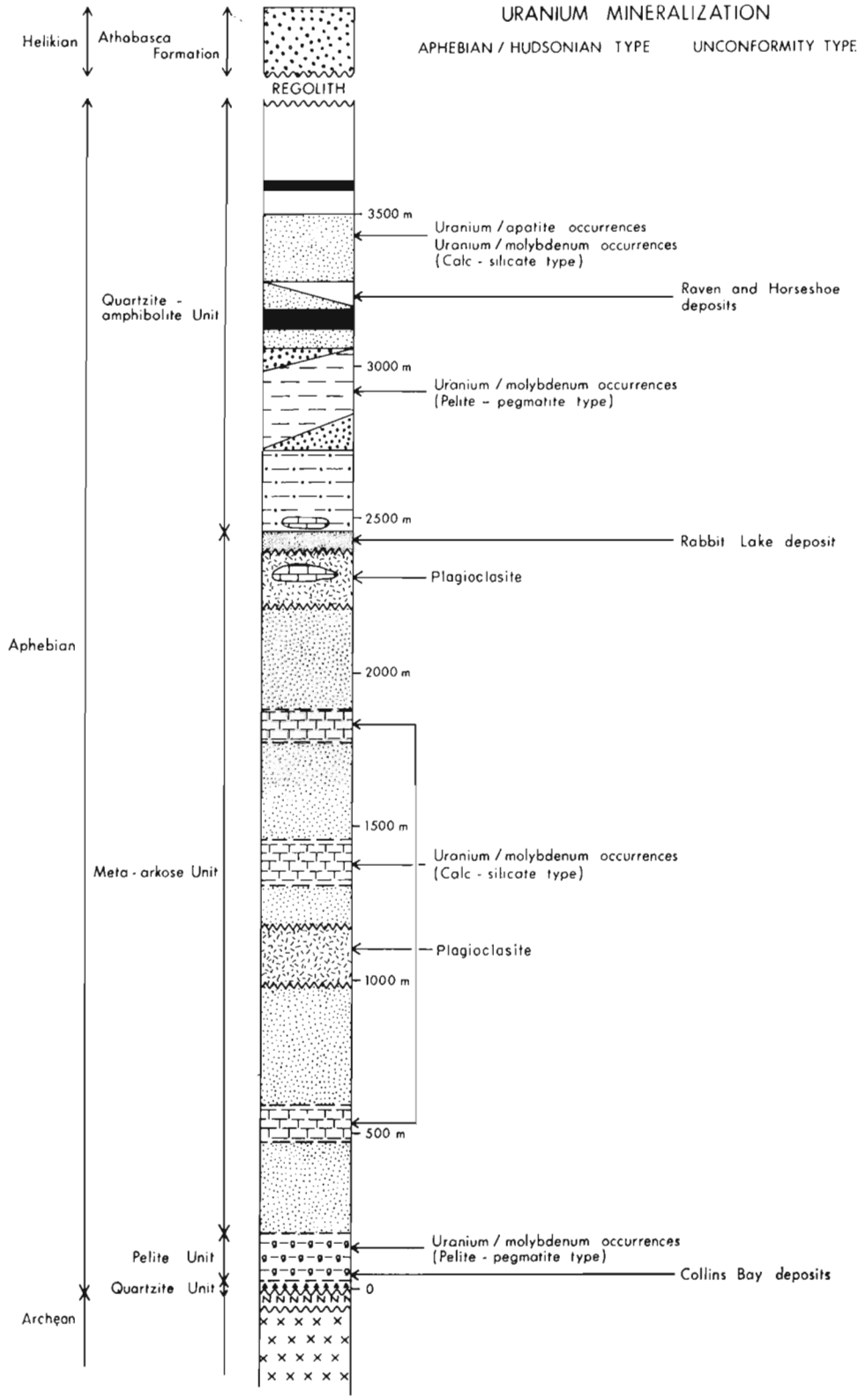

Figure 4. Stratigraphic position of uranium deposits in a part of Athabasca Basin underlain by Wollaston Group rocks. After Hoeve and Sibbald (1978).

the metasedimentary rocks. The deposit occurs in the Quartzite-amphibolite Unit of Hoeve and Sibbald (1978), which is stratigraphically positioned in the upper part of the Wollaston Group sequence (Fig.4).

The ores of the **Eagle Point** deposit, which typically consist of pitchblende and alpha-uranium heptaoxide (Ruzicka and Littlejohn, 1981) occur in a suite of altered Aphebian metamorphic rocks comprising graphitic paragneiss, biotite-, garnet-, cordierite- and sillimanite- quartz-feldspar gneisses, conglomerate, quartzite, calc-silicate, skarn and marble. The suite includes lenses and dykes of pegmatoid and segregations of quartz (Ruzicka, 1988). The deposit is stratigraphically localized in the basal part of the Wollaston sequence, which unconformably overlies Archean granitoid rocks.

The ores of the **Dominique-Peter** deposit, which is located in the Carswell Structure, consist typically of pitchblende in fractures within a zone of blastomylonitized gneisses. The deposit is localized at the base of the Peter River Gneiss at its contact with the underlying Earl River Complex. Both units are Aphebian in age and the contact between them may represent an unconformity. Whole-rock Rb-Sr ages for the Peter River Gneiss reflect an event around 1760 Ma and for the Earl River Complex around 1800 Ma (Bell, 1985). On the basis of Pb-Pb and Sm-Nd whole rock isochrons Juteau *et al.* (1988) concluded that there was a granulite facies metamorphism at about 1900 Ma. Zircon U-Pb data for quartzo-feldspathic gneisses of the Earl River Complex indicate an age of 2120 $\pm$ 10 Ma (Bell, 1985; Juteau *et al.*, 1988). The deposit is localized at the northeastern flank of the Dominique-Peter granitic dome. The recently discovered **Dominique-Janine** deposit is, on the other hand, on the southwestern flank of the same dome.

The pitchblende ores of the **Raven** and **Horseshoe** deposits are confined mainly to the graphitic quartzite horizon, which is fractured and altered by sericitization, chloritization and argillization. The deposits occur in the Quartzite-amphibolite Unit of Hoeve and Sibbald (1978), which consists of sillimanite meta-arkose, amphibolite, graphitic metapelite and quartzite, calc-silicate rocks, phosphates and sillimanite-bearing quartzite. This unit is stratigraphically within the uppermost part of the Wollaston metasedimentary sequence, which has been folded into a syncline and intruded by dykes of granite pegmatite.

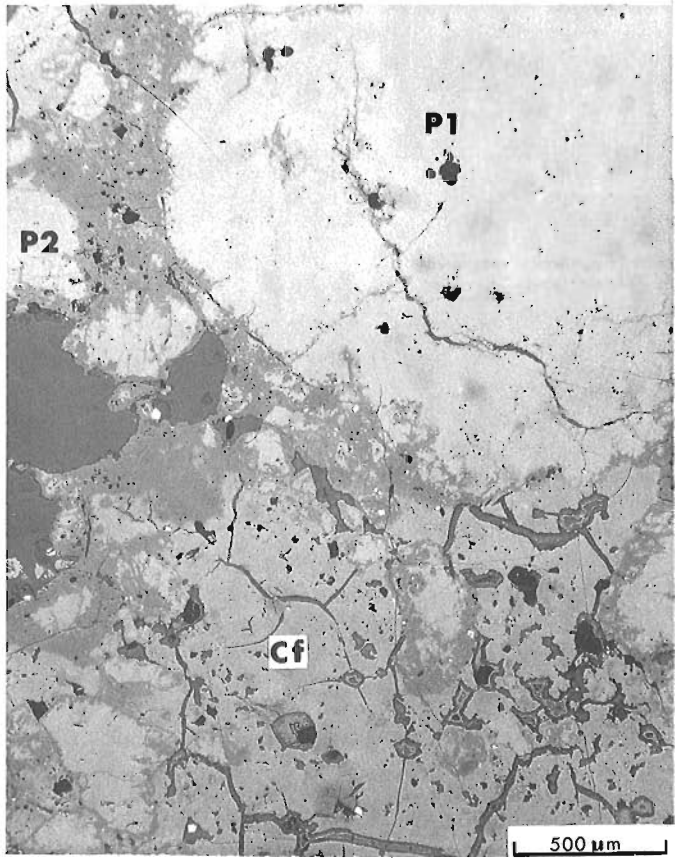

Figure 5. First generation of pitchblende, massive and lustrous (P1), surrounded by second generation of pitchblende (P2) containing inclusions of galena, a Fe mineral and Si, and grading into coffinite (Cf). Cigar Lake deposit. Photomicrograph, reflected light.

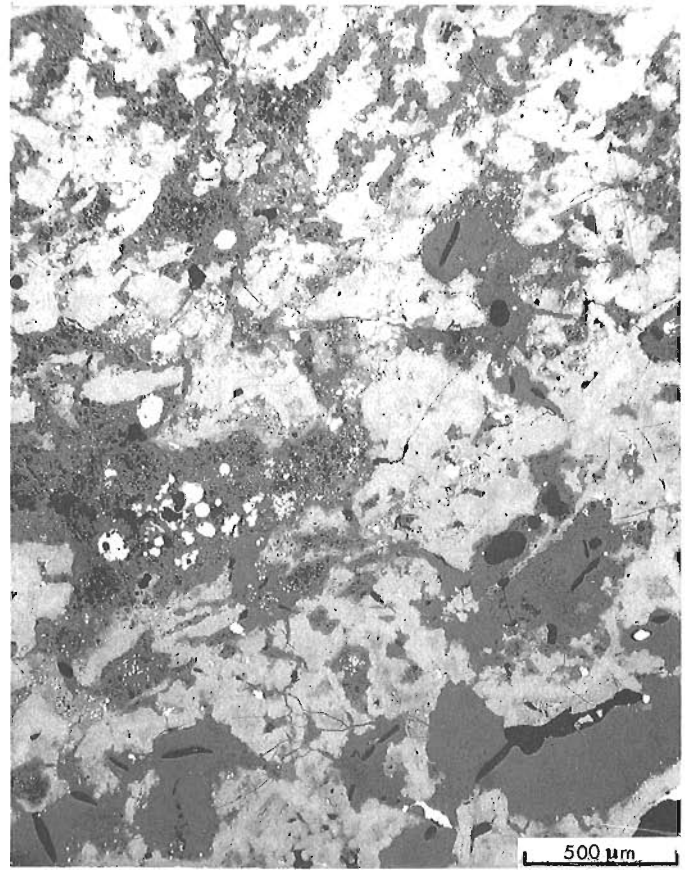

Figure 6. Polymetallic ore from the Cigar Lake deposit: massive pitchblende (light grey) is accompanied by cobaltite, nickeline, chalcopyrite and pyrite (white). Reflected plain light.

Deposits at the unconformity

Deposits which occur immediately at the sub-Helikian unconformity, i.e. within the basal part of the Helikian clastic sedimentary sequence and/or within the uppermost part of the basement rocks, contain polymetallic (U-Ni-Co-As-Cu) mineralization. These include the Key Lake, Cigar Lake, Collins Bay 'A', Collins Bay 'B', McClean, Midwest, and Cluff Lake 'D' orebodies.

The U-Ni-Co-As ores of the **Key Lake** deposit occur in altered rocks of the Athabasca Group and in the basement graphitic gneisses of the Wollaston Group. The polymetallic mineralization formed during at least four main episodes (Ruzicka and Littlejohn, 1981). The Wollaston Group in the area of the deposit comprises biotite-plagioclase-quartz-cordierite gneiss, garnet-quartz-feldspar-cordierite gneiss, amphibolite, calc-silicate rocks, migmatite and granite pegmatite. The Helikian clastic sedimentary rocks of the Athabasca Group rest unconformably on the basement rocks. The host rocks have been subjected to hematitization, kaolinization and chloritization. The deposit is structurally controlled by the northeasterly striking Key Lake fault zone and by the sub-Athabasca unconformity, and lithologically controlled by a graphitic metapelite unit of the Wollaston Group.

The U-Ni-Co-As-Cu ores of the **Cigar Lake** deposit are largely confined to clay-altered clastic sedimentary rocks at the base of the Athabasca Group, i.e. immediately above the unconformity. A small amount of the polymetallic ore extends into the altered basement rocks just beneath the unconformity. Only a minor amount of monometallic mineralization occurs in fractures in the sedimentary cover rocks, as much as two hundred metres above the unconformity. Localization of the deposit is controlled by the basement lithology and by intersections of an east-west shear zone and northeast-southwest lineaments with the sub-Athabasca unconformity. The metamorphic basement rocks are part of the Wollaston Group and consist of two broad units (Fouques *et al.*, 1986): graphitic gneisses with cordierite and calc-magnesian gneisses with amphibole and pyroxene. The graphitic gneisses include two facies: graphitic metapelites with typical augen structure and fine-grained metapelites. The deposit is located on the southern flank of the Swanson granitic dome.

The U-Ni-Co-As-Cu-Mo ores of the **Collins Bay 'A'** and **'B'** zones occur in clay-altered sedimentary rocks of the Athabasca Group. The Collins Bay 'A' zone is localized in the hanging wall of the Collins Bay Fault, whereas the Collins Bay 'B' zone occupies both the hanging wall and footwall of this fault. Localization of the zones is structurally

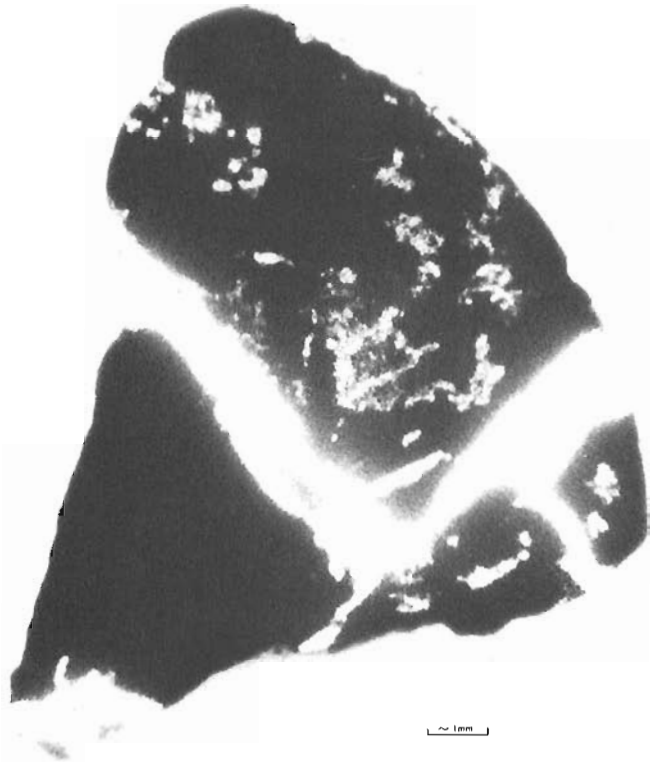

Figure 7. Autoradiograph of a sample from the Eagle Point deposit containing a vein and disseminations of pitchblende (white). The vein is about 1 mm wide.

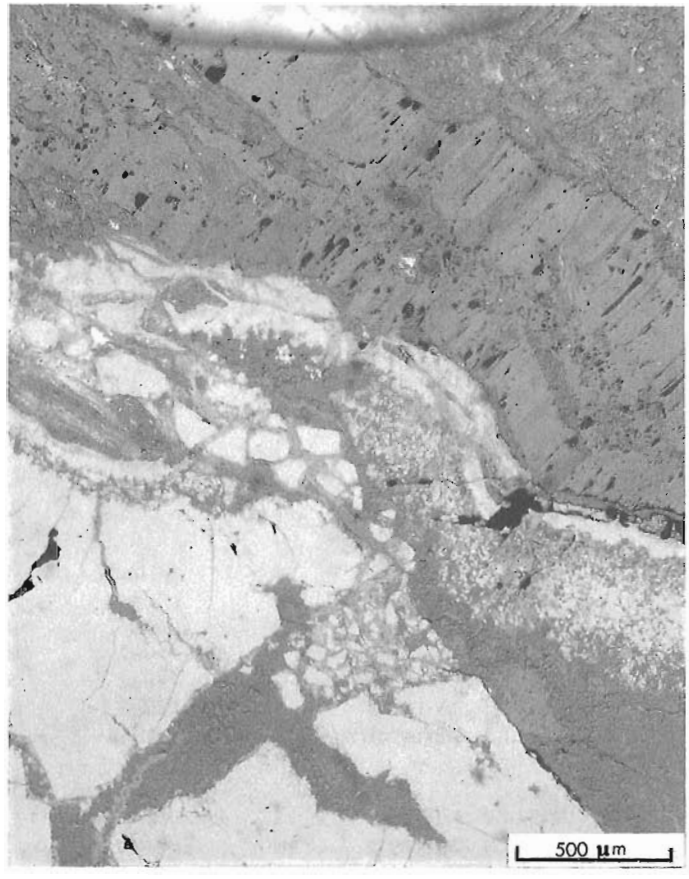

Figure 8. Photomicrograph of a part of the pitchblende vein shown in Fig. 7. The inner part of the vein contains alpha-uranium heptaoxide, which has apparently coalesced outward to massive pitchblende, locally brecciated. Reflected plain light.

Table 1. Ore-forming minerals in deposits associated with the sub-Athabasca unconformity. Deposits: KL = Key Lake; RL = Rabbit Lake; CL = Cigar Lake; CA = Collins Bay 'A'; CB = Collins Bay 'B'; MC = McClean; NB = Natona Bay; MW = Midwest; DC = Cluff 'D'; DP = Dominique-Peter; CE = Claude; OP = OP; MB = Maurice Bay; FL = Fond-du-Lac; EP = Eagle Point. Cd = code of mineral classes. Data compiled from observations by the author; from identification reports by G.M.Lecheminant; and after Fouques *et al.*(1986); Laine (1986); Heine (1986); Wallis *et al.*(1986); Wray *et al.*(1985); Mellinger (1985); Pechmann (1985); Homeniuk and Clark (1986); Blaise and Koning (1985); and Ruhlmann (1985).

	A	B	C	D	E	F	G	H	I	J	K	L	M	N	O	P	Q	R
0				KL	RL	CL	CA	CB	MC	NB	MW	DC	DP	CE	OP	MB	FL	EP
1		Mineral	Formula															
2																		
3		Native Elements																
4	11	Copper (native)	Cu															X
5	11	Gold	Au				X					X	X	X		X		
6	12	Arsenic (native)	As						X									
7	13	Carbon	C	X	X	X		X			X		X	X			X	X
8																		
9		Sulphides																
10	21	Bismuthinite	Bi2S3	X														
11	21	Bornite	Cu5FeS4	X	X	X		X								X		
12	21	Bravoite	(Ni,Fe)S2	X		X		X	X									
13	21	Carrolite	Cu(Co,Ni)2S4		X													
14	21	Chalcocite	Cu2S		X	X										X		X
15	21	Chalcopyrite	CuFeS2	X	X	X		X	X	X	X	X	X	X	X	X		X
16	21	Covellite	CuS	X	X	X		X								X		
17	21	Digenite	Cu9S5			X												
18	21	Djurleite	CuS													X		
19	21	Galena	PbS	X		X	X	X		X	X	X	X	X	X	X		X
20	21	Hauchecornite	Ni9(Bi,Sb,As,Te)2S8	X														
21	21	Jordisite	MoS2			X				X		X						
22	21	Marcasite	FeS2	X		X					X	X	X					
23	21	Millerite	NiS	X				X			X							X
24	21	Molybdenite	MoS2										X	X	X			
25	21	Paraguanajuatite	Bi2(Se,S)3									X	X	X				
26	21	Polydymite	Ni3S4					X										
27	21	Pyrite	FeS2	X	X	X	X	X	X	X	X	X	X	X	X	X	X	X
28	21	Pyrrhotite	FeS															
29	21	Sphalerite	ZnS	X		X			X	X	X				X			X
30	21	Vaesite	NiS2	X														
31	21	Violarite	Ni2FeS4					X										
32																		
33		Sulpharsenides																
34	22	Gersdorffite	NiAsS	X		X		X	X	X	X	X	X		X			X
35	22	Glaucodot	CoFeAsS			X												
36	22	Cobaltite	CoAsS			X												
37	22	Tennantite	(Cu,Fe)12As4S13					X					X	X	X			
38																		
39		Arsenides																
40	23	Maucherite	Ni11As8	X				X			X							
41	23	Modderite	CoAs	X														
42	23	Nickeline	NiAs	X	X	X	X	X	X	X	X	X	X	X		X		
43	23	Pararammelsbergite	NiAs2				X		X	X								
44	23	Rammelsbergite	NiAs2	X		X	X	X		X	X							
45	23	Safflorite	CoAs2					X	X		X							
46	23	Skutterudite	CoNiAs3					X	X			X	X	X				
47																		
48		Tellurides																
49	24	Altaite	PbTe									X	X	X				
50	24	Calaverite	AuTe2									X	X	X				
51																		
52		Selenides																
53	25	Freboldite	CoSe									X	X	X				
54	25	Clausthalite	PbSe	X	X							X	X	X		X		
55	25	Guanajuatite	Bi2Se3										X	X				
56	25	Trogtalite	CoSe2							X		X	X	X				
57																		
58		Stibnites																
59	26	Breithauptite	NiSb	X														

Table 1. (cont.)

	A	B	C	D	E	F	G	H	I	J	K	L	M	N	O	P	Q	R
60																		
61		Oxides																
62	41	Masuyite	UO2.2H2O		X													
63	41	Brannerite	(U,Ca,Ce)(Ti,Fe)2O6										X	X				
64	41	Ilsemannite	MO3O8.nH2O						X							X		
65	41	PbU-Heptaoxide	PbU2O7		X													
66	41	Pitchblende	U3O8	X	X	X	X	X	X	X	X	X	X	X	X	X	X	X
67	41	U-Heptaoxide	U3O7	X	X													X
68	41	Rutile	TiO2	X		X												X
69	41	Annabergite	(NiCo)3(AsO4)2.8H2O	X				X			X							
70	41	Ilmenite	FeTiO3	X														
71	41	Becquerelite	CaU6O19		X													
72	41	Sphene	CaSiTiO5	X														
73	41	Magnetite	(Fe,Mg)Fe2O4	X								X						
74	41	Uraninite	UO2						X			X	X	X	X			X
75	41	Vandendriessheite	PbU7O22		X													
76	41	Woelsendorfite	PbCaU2O7		X													
77																		
78		Hydroxides																
79	42	Goethite	FeO(OH)						X			X				X	X	X
80																		
81		Carbonates																
82	61	Siderite	FeCO3	X		X			X	X						X		
83	61	Liebigite	Ca2(UO2)(CO3)3		X													
84	61	Bayleyite	Mg2UO2(CO3)3		X													
85																		
86		Phosphates etc.																
87	71	Goyazite	SrAl3(PO4)2(OH)5.H2O													X		
88	72	Erythrite	CO3(AsO4)2.8H2O	X							X							
89	73	Tyuyamunite	Ca[(UO2)2VO4]2		X													
90																		
91		Sulphates																
92	81	Retgersite	NiSO4.6H2O	X														
93	81	Ni-Hexahydrite	Ni-MgSO4.6H2O	X														
94	81	Brochantite	Cu4(SO4)(OH)6	X														
95	81	Zippeite	K4(UO2)6(SO4)3(OH)10		X													
96	81	Zircosulphate	Zr(SO4)2													X		
97																		
98		Silicates																
99	91	Uranophane	Ca(UO2)2Si2O7		X													X
100	91	Coffinite	U(SiO)4OH	X	X	X	X	X	X		X	X	X	X	X		X	X
101	91	Kasolite	Pb(UO2)SiO4		X		X											
102	91	Dravite	NaMg3Al6(BO3)3(Si6O18)(OH)4	X												X		
103	91	Boltwoodite	(H3O)K(UO2)SiO4		X													X
104	91	Yttrialite	Y2(Th,U,Pb)Si2O7		X													
105	91	Leonhardtite	Ca2Al4Si8O24.7H2O	X														
106	91	Sklodowskite	Mg(UO2)2Si2O6(OH)2		X													

controlled by the intersection of the Collins Bay fault with the sub-Athabasca unconformity and lithologically controlled by the Pelite unit of Hoeve and Sibbald (1978) at the base of the Wollaston sequence.

The U-Cu-Ni-Co-As-S ores of the **McClean** deposit are associated with the sub-Athabasca unconformity and occur in altered sedimentary rocks of the Athabasca Group and in altered, fractured zones within the basement graphitic metasedimentary units.

The U-Ni ores of the **Midwest** deposit, consisting of the principal ore-forming minerals pitchblende, coffinite, rammelsbergite, gersdorffite and nickeline, are associated with chloritized, fractured Aphebian graphitic metapelites, and particularly (>80 %) with the altered sedimentary rocks of the Athabasca Group.

The U-Ni-Se-Te-Au-Mo ores of the **Cluff Lake 'D'** deposit have been exhausted. The massive polymetallic orebody was confined to a highly mylonitized zone at the unconformity between the Peter River Gneiss and sandstone of the Athabasca Group.

Deposits above the unconformity

The **Fond-du-Lac** deposit occurs in hematitized, carbonatized and silicified sandstone of the Athabasca Group. The uranium mineralization is confined to a network of steeply dipping fractures and to the adjacent porous, coarse-grained facies of the sandstone.

Synopsis

The **lithostratigraphic and structural** features of the Athabasca Basin region are crucial factors that control localization of the uranium and uranium-polymetallic deposits associated with the sub-Athabasca unconformity. As demonstrated above, the most important factors are as follows:

- presence of granitic domal structures in the basement;
- presence of graphitic/pyritic layers in the basement crystalline rocks;
- presence of shears, fracture zones and faults that intersect the sub-Athabasca unconformity;
- presence of clay alteration of the host rocks (chloritization, illitization, kaolinization, sericitization);
- distance from the unconformity: proximal areas are favourable loci for polymetallic mineralization, whereas distal areas (below and above the unconformity) are favourable for monometallic (uranium only) deposits.

MINERAL ASSEMBLAGES

Deposits associated with the sub-Athabasca unconformity contain a large number of ore constituents that accompany the uranium minerals and form specific mineral assemblages.

In the case of the **Cigar Lake** deposit Ruzicka and LeCheminant (1987) concluded that there were three mineralization stages, each of which produced distinct mineral assemblages. The oldest stage is represented by pitchblende and arsenide-sulphide minerals of nickel, cobalt, iron, copper and lead. The second stage produced pitchblende that is accompanied by sulphides of iron, copper and lead, and in the third stage coffinite and pitchblende were deposited in association with abundant gangue minerals.

The **McClean** deposit contains four mineralization facies: (i) an arsenide facies with associated sulphide minerals; (ii) a sulphide facies with some arsenide and sulpharsenide minerals; (iii) a bleached facies in which uranium minerals are accompanied by relicts of minerals from the preceding two facies and by products of clay alteration; and (iv) a hematite facies in which uraninite, pitchblende and coffinite form part of an assemblage of minerals rich in ferric iron. The ores form several pods and each pod exhibits different mixtures and distribution of these facies (Wallis *et al.*,1986).

Observations on ores from deposits associated with the sub-Athabasca unconformity indicate that each deposit contains unique mineral assemblages (Table 1). Although the monometallic deposits (Rabbit Lake, Fond-du-Lac, Dominique-Peter, Claude and OP), contain simple mineral assemblages, their ores are compositionally distinct. Some of these compositional features are:

- the **Dominique-Peter** and **Claude** deposits, which are spatially associated with the Dominique-Peter granitic dome in the Carswell Structure, contain very similar

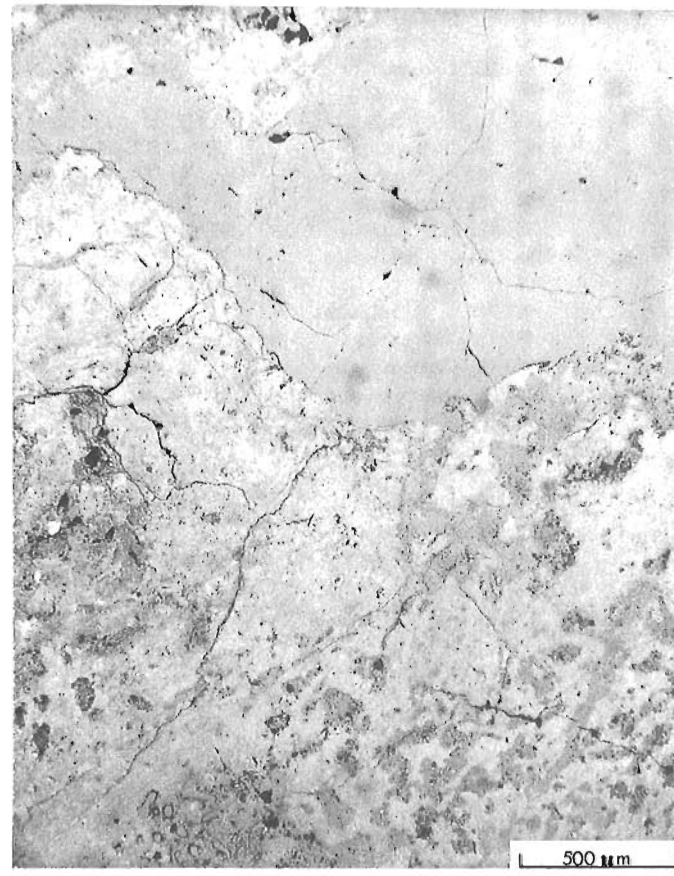

Figure 9. Micaceous alteration products with sooty pitchblende that have invaded a quartz grain in quartzite at the Eagle Point deposit. Reflected plain light.

mineral assemblages that are characterized by a **U + (Bi, Co, Ni, Cu, Mo, Se, Te, Au)** elemental association;
— the **OP** deposit, which is also in the Carswell Structure, is characterized by a **U + (Cu, Mo, Zn)** association and appears to belong to a different geochemical environment;
— in the **Rabbit Lake** deposit a **U + (Cu)** mineral assemblage prevails;
— the **Fond-du-Lac** deposit contains a simple **U + Fe** mineral assemblage.

Ores from polymetallic deposits (Key Lake, Cigar Lake, Collins Bay 'A' and 'B', McClean, Natona Bay, Midwest, Cluff 'D' and Maurice Bay) exhibit unique metallogenic features:
— deposits at the southeastern margin of the Athabasca Basin (Cigar Lake, Collins Bay 'B', McClean, Midwest), with the exception of Collins Bay 'A', contain similar principal mineral assemblages consisting of **U-, Ni-, Co-, Cu-** bearing minerals and relatively minor amounts of **Mo-** and **Zn-** minerals;
— the typical mineral assemblage of the **Cluff 'D'** deposit in the Carswell Structure was pitchblende and gold;
— the principal mineral assemblage of the **Maurice Bay** deposit contains uranium, iron hydroxides and copper sulphides.

At least two generations of uranium minerals commonly occur in the deposits. A typical example is a mineral assemblage from the Cigar Lake deposit (Fig. 5). The sample contains a first generation of pitchblende, which is massive and shiny with a very low content of Si and practically devoid of inclusions of other minerals. The second (younger) generation of pitchblende is less lustrous and contains numerous inclusions of galena, a botryoidal Fe oxide mineral and some Si. The third generation of uranium mineralization is represented by coffinite.

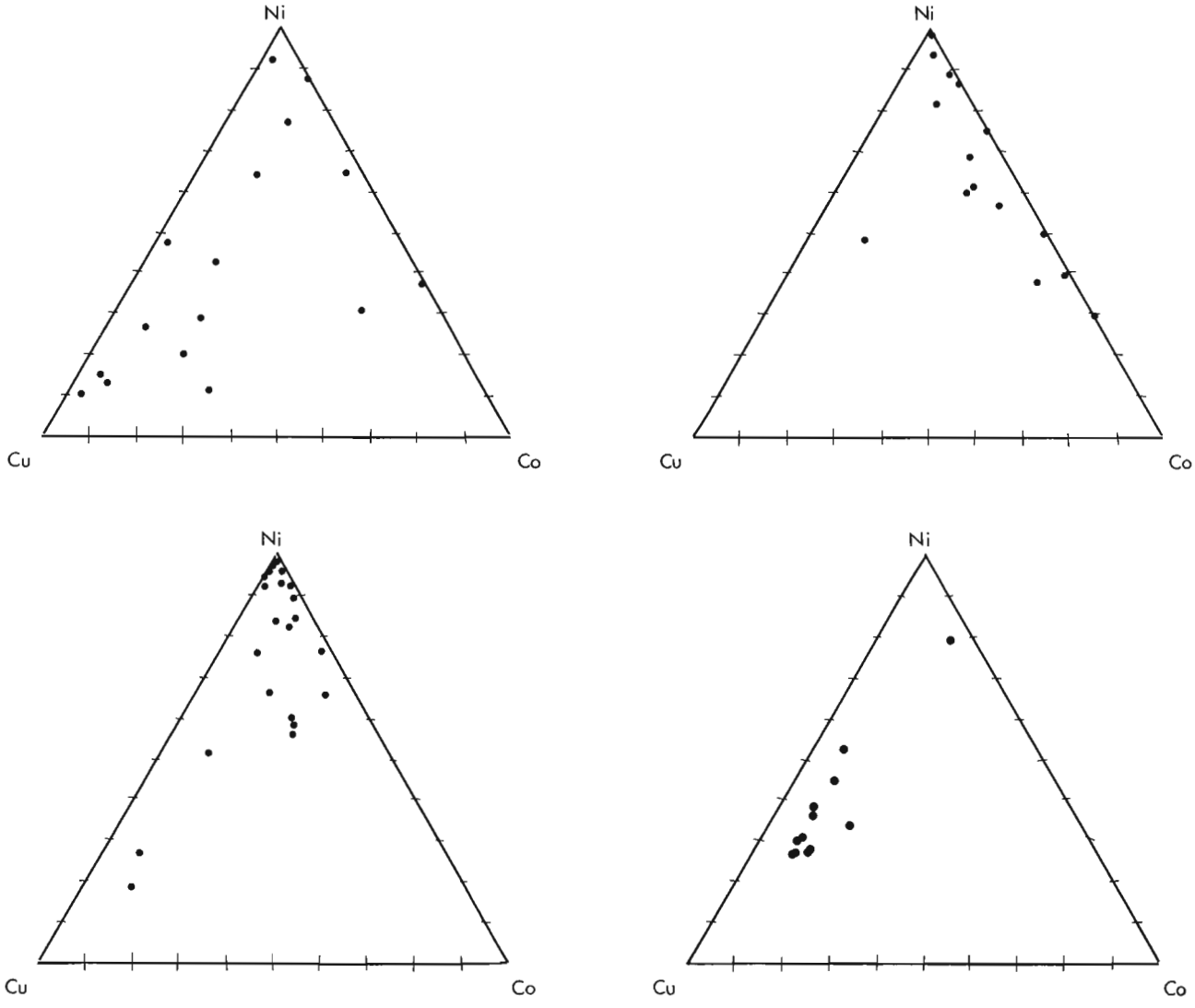

Figure 10. Ternary diagrams for Ni, Co and Cu contents in samples of mineralization from (a) Cigar Lake; (b) Key Lake; (c)Midwest; and (d) Rabbit Lake deposits. (*See* Table 2.)

Table 2. Ni, Co and Cu constituents of mineralized rocks from the Cigar Lake (CL), Key Lake (KL), Midwest (MW) and Rabbit Lake (RL) deposits. Data in weight per cent. The samples, collected by the author, were analyzed by laboratories of the Geological Survey of Canada.

ⓐ Cigar Lake deposit

Sample	Ni	Co	Cu
CL1	0.01	0.005	0.0005
CL2	ND	ND	0.05
CL3	0.03	0.05	0.002
CL4	ND	ND	0.03
CL5	ND	ND	0.05
CL6	0.002	0.005	0.01
CL7	ND	ND	0.015
CL8	0.005	ND	0.003
CL9	0.001	0.001	0.003
CL10	ND	ND	0.007
CL11	ND	ND	0.005
CL12	0.4	0.11	3.2
CL13	0.14	0.091	0.25
CL14	0.1	0.032	0.53
CL15	4.4	0.12	0.25
CL16	0.0024	0.0041	0.0013
CL17	0.18	0.1	1.1
CL18	0.053	0.017	0.13
CL19	0.1282	0.047	0.129
CL20	3.6	0.618	0.446
CL21	4.08	0.242	4.25
CL22	0.6093	0.13	0.218
CL23	11.1	0.31	0.67
CL24	11.27	1.58	0.0236
CL25	0.0099	0.0002	0.0003

ⓑ Key Lake deposit

Sample	Ni	Co	Cu
KL1	0.022	0.01	0.053
KL2	0.0099	0	0.002
KL3	0.32	0.02	0.0022
KL4	1.3	0.01	0.031
KL5	4.8	0.17	0.038
KL6	0.38	0	0.0002
KL7	0.13	0	0.0048
KL8	0.0028	0	ND
KL9	0.7	0.1	0.05
KL10	0.7	0.2	0.02
KL11	0.7	0.07	0.07
KL12	0.7	0.3	0.2
KL13	0.7	0.3	0.07
KL14	0.7	0.1	0.03
KL15	0.15	0.02	0.003
KL16	10	0.5	0.3
KL17	3	0.05	0.2
KL20	0.21	0.0018	0.0008
KL21	20.4	0.049	1.2
KL22	0.033	0.0004	0.0002
KL23	0.55	0.13	0.15
KL24	0.078	0.0005	0.001
KL25	0.047	0.027	0.18
KL26	0.004	0.0008	0.003
KL27	0.019	0.002	0.0014
KL28	0.0022	0.001	0.0007

ⓒ Midwest deposit

Sample	Ni	Co	Cu
MW1	0.015	0.007	0.003
MW2	0.003	0.001	NA
MW3	0.1	0.1	0.002
MW4	1.5	0.5	0.007
MW5	0.35	0.003	0.0014
MW6	0.005	NA	0.02
MW7	10	1.5	0.1
MW8	0.011	0.0052	0.0018
MW9	0.024	0.001	0.0007
MW10	0.022	0.0057	0.018
MW11	0.0095	0.0034	0.001
MW12	0.12	0.29	0.0007
MW13	2	0.22	0.033
MW14	0.02	0.013	0.0024
MW15	0.7	1	0.15
MW16	0.2	0.3	0.007
MW17	1.5	0.2	0.15

ⓓ Rabbit Lake deposit

Sample	Ni	Co	Cu
RL1	0.0046	0.0019	0.0098
RL2	0.0058	0.0025	0.013
RL3	0.019	0.0045	0.029
RL4	0.027	0.0049	0.037
RL5	0.032	0.0043	0.025
RL6	0.048	0.024	0.069
RL7	0.019	0.0064	0.044
RL8	0.069	0.017	0.14
RL9	0.026	0.005	0.027
RL10	0.031	0.0086	0.061
RL11	0.019	0.0062	0.046
RL12	0.016	0.0015	0.0045
RL13	0.024	0.0076	0.058
RL14	0.04	0.012	0.091
RL15	NA	NA	NA
RL16	NA	NA	NA
RL17	NA	NA	NA

The complex nature of the polymetallic ores is exemplified by a sample from the Cigar Lake deposit (Fig. 6). The massive pitchblende is accompanied by cobaltite, nickeline, chalcopyrite, galena and pyrite.

The monometallic deposits exhibit several forms of uranium mineralization. An autoradiograph of a sample from the Eagle Point deposit (Fig. 7) shows a vein of pitchblende that actually represents an aggregate of its euhedral variety (alpha-uranium heptaoxide or tetrauraninite) that retains the original cubic form in the centre of the vein, but which passes gradationally to a solid lustrous mass along the margins of the vein (Fig. 8). The massive pitchblende is locally brecciated (Fig. 8). The autoradiograph also shows irregular patches of pitchblende disseminated in the host rock. The micaceous gangue contains small grains of galena, pyrite, chalcopyrite and, apparently, rutile. The micaceous matrix, which is a product of hydrothermal-diagenetic alteration of the host rock, is intimately associated with sooty pitchblende in the same deposit. Figure 9 shows this assemblage in a specimen in which it has apparently invaded a quartz grain within the host quartzite.

ELEMENTAL ASSEMBLAGES

A comparison of the elemental assemblages of the Cigar Lake and Key Lake deposits indicated that the two deposits exhibit many similarities, although in detail each is unique. Differences in the chemical compositions of ore samples from the deposits were observed in terms of their U, As, Pb, Ni, Cu and Ag contents (Ruzicka, 1988).

It has been pointed out previously in this paper that specific mineral assemblages are associated with distinct geological settings within the Athabasca metallogenic domain. Different compositions of the assemblages may reflect derivation of their constituents from geochemically different sources. For instance, mineral assemblages consisting of U, Ni, Co, Cu, Mo and Zn minerals are typical for the southeastern segment of the Athabasca Basin. Knipping (1974) speculated that uranium in the Rabbit Lake deposit, which is located in this segment, was derived from leaching igneous and metamorphic rocks east of the deposit. Bedrock in this source area include quartzites, metaarkoses, granitic gneisses, mafic intrusives, calc-silicate rocks rich in amphibole, pyroxene and biotite, and metapelites rich in biotite and locally graphite, cordierite and garnet (Hoeve and Sibbald, 1978). On the other hand uranium and gold are typical for polymetallic deposits within the Carswell Structure. Lainé (1985) speculated that granitoid rocks of the Earl River Complex, which are enriched in uranium, may have served as possible source of uranium. The rocks of the Earl River Complex also include mafic gneisses, amphibolitic rocks, and rocks with high magnesium contents suggesting possible komatiitic affinity (Bell *et al.* 1985).

The polymetallic ores contain high proportions of base metals (Tables 2a-c and Ruzicka, 1988), whereas the levels of base metals in the monometallic ores are very low (Table 2d and Ruzicka and LeCheminant, 1987).

It appears that the proportions of certain base metals, particularly Ni, Co and Cu, in ores might be used as a criterion for characterizing certain specific features of an area or deposit. Therefore the Ni, Co and Cu contents of mineralized samples from selected deposits (Tables 2a to 2d) were plotted on ternary diagrams (Figs. 10a to 10d). The plot (Fig. 10a) for the Ni-Co-Cu assemblage of the **Cigar Lake** deposit indicates that these constituents range widely in proportions, although the proportion of cobalt is low in relation to some deposits, such as Midwest. In the case of the **Key Lake** deposit nickel predominates (Fig.10b) over copper and cobalt. The ternary diagram for the Ni-Co-Cu assemblage of the **Midwest** deposit (Fig. 10c) indicates a broad range in Ni to Co ratios and a low proportion, generally less than 1:9 of Cu to Ni + Co. Clustering of the points in the lower left segment of the ternary diagram for the **Rabbit Lake** deposit indicates that Cu generally exceeds Ni, with Cu:Ni in the range 1:1 to 3:1, and that the proportion of Co is low (Fig. 10d) in the predominantly monometallic uranium mineralization. The different proportions of Ni, Co and Cu in the ores from the deposits discussed above are interpreted to reflect derivation of the metals from geochemically different sources.

On the basis of the proportions of Ni, Co and Cu in their ores, the uranium deposits associated with the sub-Athabasca unconformity can be classified into the following groups (the classification is recorded as 'possible' for deposits for which the data base is insufficient):
— Ni+Cu>Co: Cigar Lake, Dominique-Peter;
— Ni+Co>Cu: Midwest;
— Ni>Co+Cu: Key Lake, Collins Bay 'B', West Bear, Maurice Bay, (possibly Collins Bay 'A' and 'D');
— Cu>Ni+Co: Rabbit Lake, (possibly Eagle Point, Dawn Lake, Claude and McClean).

Since the U-Ni-Co-Cu elemental association is a specific diagnostic geochemical signature for this deposit type, it can be also advantageously used in mineral exploration.

ACKNOWLEDGMENT

Critical reading of the paper by R.I. Thorpe and mineral identification by G.M. LeCheminant of the Geological Survey of Canada are sincerely appreciated. The Ni, Co and Cu analyses were done by the chemical laboratories of the Geological Survey of Canada.

REFERENCES

Bell, K.
1985: Geochronology of the Carswell Area, Northern Saskatchewan; in The Carswell Structure Uranium Deposits, Saskatchewan, ed. R.Lainé, D.Alonso and M.Svab, Geological Association of Canada, Special Paper 29, p.33-46.

Bell, K., Cacciotti, A.D. and Schnessl, J.H.
1985: Petrography and geochemistry of the Earl River Complex, Carswell Structure, Saskatchewan — a possible Proterozoic komatiitic succession; in The Carswell Structure Uranium Deposits, Saskatchewan, ed. R.Lainé, D.Alonso and M.Svab, Geological Association of Canada, Special Paper 29, p. 71-80.

Blaise, J.R. and Koning, E.
1985: Mineralogical and structural aspects of the Dominique-Peter uranium deposit; in The Carswell Structure Uranium Deposits, Saskatchewan, ed. R.Lainé, D.Alonso and M.Svab, Geological Association of Canada, Special Paper 29, p.153-164.

Fouques, J.R., Fowler, M., Knipping, H.D. and Schimann, K.
1986: The Cigar Lake uranium deposit: discovery and general characteristics; in Uranium Deposits of Canada, ed. E.L.Evans, The Canadian Institute of Mining and Metallurgy, Special Volume 33, p. 218-229.

Heine, T.
1981: The Rabbit Lake deposit and the Collins Bay deposits; in Canadian Institute of Mining and Metallurgy, Geology Division, Uranium Guidebook, September 8-13, Saskatchewan, p. 87-102.
1986: The geology of the Rabbit Lake uranium deposit, Saskatchewan; in Uranium Deposits of Canada, ed. E.L.Evans, The Canadian Institute of Mining and Metallurgy, Special Volume 33, p. 134-143.

Hoeve, J. and Sibbald, T.I.
1978: On the genesis of the Rabbit Lake and other unconformity-type uranium deposits in northern Saskatchewan, Canada; Economic Geology, v. 73, p. 1450-1473.

Homeniuk, L.A. and Clark, R.J. McH.
1986: North Rim deposits, Athabasca Basin; in Uranium Deposits of Canada, ed. E.L.Evans, The Canadian Institute of Mining and Metallurgy, Special Volume 33, p. 230-240.

Juteau, M., Pagel, M., Michard, A. and Albarede, F.
1988: Assimilation of continbental crust by comatiites in the Precambrian basement of the Carswell structure (Saskatchewan, Canada); Contributions to Mineralogy and Petrology, v. 99, No.2, p. 219-225.

Knipping, H.D.
1974: The concepts of supergene versus hypogene emplacement of uranium at Rabbit Lake, Saskatchewan, Canada; in Formation of Uranium Ore Deposits, International Atomic Energy Agency, Proceeding Series STI/PUB/374, Vienna, p.531-549.

Lainé, R.
1985: Conclusion: The Carswell uranium deposits -an example of not so unique unconformity-related uranium mineralization; in The Carswell Structure Uranium Deposits, Saskatchewan, ed. R.Lainé, D.Alonso and M.Svab, Geological Association of Canada, Special Paper 29, p. 225-230.

Lainé, R.T.
1986: Uranium deposits of the Carswell Structure; in Uranium Deposits of Canada, ed. E.L.Evans, The Canadian Institute of Mining and Metallurgy, Special Volume 33, p. 155-169.

Lewry, J.F. and Sibbald, T.I.I.
1979: A review of pre-Athabasca basement geology in Northern Saskatchewan; in Uranium Exploration Techniques, Proceedings of a Symposium held in Regina, 1978, November 16-17, ed. G.R.Parslow, Saskatchewan Geological Society, Special Publication 4, p. 19-58.

Mellinger, M.
1985: The Maurice Bay uranium deposit (Saskatchewan): geology, host-rock alteration and genesis; in Geology of Uranium Deposits, ed. T.I.I.Sibbald and W.Petruk, The Canadian Institute of Mining and Metallurgy, Special Volume 32, p. 140-150.

OECD Nuclear Energy Agency and the International Atomic Energy Agency
1988: Uranium resources, production and demand; a joint report; Organisation for Economic Co-operation and Development, Paris, 194 pp.

Pechmann, E. von
1985: Mineralogy of the Key Lake U-Ni orebodies, Saskatchewan, Canada: evidence for their formation by hypogene hydrothermal processes; in Geology of Uranium Deposits, ed. T.I.I.Sibbald and W.Petruk, The Canadian Institute of Mining and Metallurgy, Special Volume 32, p. 27-37.

Ruhlmann, F.
1985: Mineralogy and metallogeny of uraniferous occurrences in the Carswell Structure; in The Carswell Structure Uranium Deposits, Saskatchewan, ed. R.Lainé, D.Alonso and M.Svab, Geological Association of Canada, Special Paper 29, p.153-164.

Ruzicka, V.
1988: Uranium resource investigations in Canada, 1987; in Current Research, Part F, Geological Survey of Canada, Paper 88-1F, p. 21-30.

Ruzicka, V. and LeCheminant, G.M.
1987: Uranium and uranium-polymetallic deposits in Canada, 1986; in Current Research, Part A, Geological Survey of Canada, Paper 87-1A, p. 249-262.

Ruzicka, V. and Littlejohn, A.L.
1981: Studies on uranium in Canada, 1980; in Current Research, Part A, Geological Survey of Canada, Paper 81-1A, p. 133-144.

Sibbald, T.I.I.
1976: Uranium metallogenic studies: Rabbit Lake; Summary of Investigations, 1976, Saskatchewan Geological Survey, Saskatchewan Department of Mineral Resources, Miscellaneous Report, p. 115-123.

Wallis, R.H., Saracoglu, N., Brummer, J.J. and Golightly, J.P.
1986: The geology of the McClean uranium deposits, northern Saskatchewan; in Uranium Deposits of Canada, ed. E.L.Evans, The Canadian Institute of Mining and Metallurgy, Special Volume 33, p. 193-217.

Wray, E.M., Ayres, D.E. and Ibrahim, H.J.
1985: Geology of the Midwest uranium deposit, northern Saskatchewan; in Geology of Uranium Deposits, ed. T.I.I.Sibbald and W.Petruk, The Canadian Institute of Mining and Metallurgy, Special Volume 32, p. 54-66.

Archean to Proterozoic deformation and plutonism of the western Contwoyto Lake map area, central Slave Province, District of Mackenzie, N.W.T.

J.E. King, W.J. Davis[1], T. Van Nostrand[2], and C. Relf[3]
Lithosphere and Canadian Shield Division

King, J.E., Davis, W.J., Van Nostrand, T., and Relf, C., Geology of the western Contwoyto Lake map area, District of Mackenzie, N.W.T.: Archean to Proterozoic deformation and plutonism; in Current Research, Part C, Geological Survey of Canada, Paper 89-1C, p. 81-94, 1989.

Abstract

The Contwoyto and Itchen Formation turbidites are migmatitic paragneisses in the northwest and southwest part of the Contwoyto Lake sheet, but remain as sillimanite-muscovite schists east of Contwoyto Lake, to the present limit of mapping. Two belts of dominantly volcaniclastic rocks are intercalated with the Contwoyto Formation. Four generations of Archean structures include two sets of isoclinal folds and cleavages (some faulting) (D_1, D_2), NE-trending cross folding and crenulation cleavage (D_3), and NNW-trending cross folds (D_4). Six episodes of Archean intrusions (C1-C6) are recognized. C1 hornblende-gabbro, C2 porphyritic granodiorite and C3 biotite-tonalite are synvolcanic. C4 biotite-hornblende-diorite and biotite-tonalite are early-syn-D2. C5 biotite-leucotonalite is late-syn-D_2. C6 biotite (±muscorite) granodiorite to syenogranite is pre- to- early-D_3. Isograds resulting from the syn-D_2, low-P/high-T metamorphism outline a cuspate thermal basin. Two gabbro plutons that cut Archean structures may be Early Proterozoic. Both brittle and ductile (mylonitic) fault rocks occur along the Proterozoic fault system.

Résumé

Les dépôts de courants de turbidité des formations de Contwoyto et d'Itchen sont des paragneiss migmatitiques dans les parties nord-ouest et sud-ouest de la feuille Contwoyto Lake, mais restent des schistes à sillimanite et muscovite à l'est du lac Contwoyto jusqu'à la limite de l'étendue actuellement cartographiée. Deux zones de roches principalement volcaniclastiques sont intercalées dans la formation de Contwoyto. Quatre générations de structures de l'Archéen englobent deux ensembles de plis isoclinaux avec schistosité (avec failles) (D_1, D_2), des plis transversaux de direction nord-est avec crénulation (D_3) et des plis transversaux de direction nord-nord-ouest (D_4). Six épisodes d'intrusion (C1 à C6) pendant l'Archéen ont été identifiés: les C1 hbl-gabbro, C2 granodiorite porphyrique et C3 bio-tonalite sont synvolcaniques; les C4 bio-hbl-diorite et bio-tonalite sont hâtives-syn-D_2; le C5 bio-leucotonalite est tardif-syn-D_2; le C6 bio (±musc) granodiorite à syénogranite est pré- à hâtif-D_3. Les isométamorphes résultant du métamorphisme syn-D_2 faible-P/T-élevée délimitent un bassin thermique lobé. Deux plutons de gabbro qui recoupent les structures de l'Archéen peuvent dater du début du Protérozoïque. Il y a des brèches de faille cassantes et ductiles (mylonitiques) le long du réseau de failles du Protérozoïque.

[1] Department of Earth Sciences, Memorial University of Newfoundland, St. John's, Newfoundland, A1B 3X5
[2] 184 University Ave., St. John's, Newfoundland, A1B 1Z7
[3] Department of Geological Sciences, Queen's University, Kingston, Ontario, K7L 3N6

INTRODUCTION

The Contwoyto-Nose Lakes mapping project (Fig. 1) was initiated in 1987 to map at a scale of 1:100 000 the Contwoyto Lake sheet (NTS 76E) and the west half of the Nose Lake sheet (NTS 76F). It is hoped that the results of the mapping will further the understanding of gold and other mineralization in the area. In the course of the project, two topical studies are underway: a study of the petrogenesis, geochemistry and isotopic signature of the igneous units by W.J.D., and a detailed structural, metamorphic and stratigraphic analysis of the low- to medium-grade sedimentary units by C.R. The latter study, supported by the Canada-Northwest Territories Mineral Development Agreement (Project C1.1.1) (Fig. 1), is reported on in greater detail elsewhere by C. Relf. (1989). O. van Breemen and J. Mortensen (G.S.C.) are carrying out geochronological studies in the map area as part of their more regional work (Mortensen et al., 1988). Analytical data and final calculations for ages referenced as 'O. van Breemen, pers. comm.' in this report will be published in Radiogenic Age and Isotopic Studies, Report 3, Geological Survey of Canada Paper 89-2.

Previous work in the area includes 1:500 000 scale mapping during "Operation Bathurst" (Fraser, 1963, 1964), 1:50 000 scale mapping of the northwest corner of the Contwoyto Lake sheet (Tremblay, 1976), and 1:250 000 scale mapping of the west half of the Contwoyto Lake sheet (Bostock, 1980). Numerous geological maps of claim groups are available in the assessment files of Indian and Northern Affairs Canada. Results from the first season of the present project are reported in King et al. (1988).

This report contains: 1) a simplified geological map of the area covered to date, 2) brief descriptions of the high-grade, migmatitic equivalents of the turbiditic Itchen and Contwoyto formations and of two small volcanic belts within the Contwoyto Formation, 3) a summary of the deformation history, 4) a description of the Archean plutonic units and their relative age relations, 5) a discussion of the pattern and origin of metamorphism, 6) a description of two post-Archean plutons, 7) a discussion of fault rocks and kinematics of the Proterozoic fault system, and 8) comments on the tectono-magmatic history of the area. The report concludes with a summary of 1988 field results that may be significant for mineral exploration in the area.

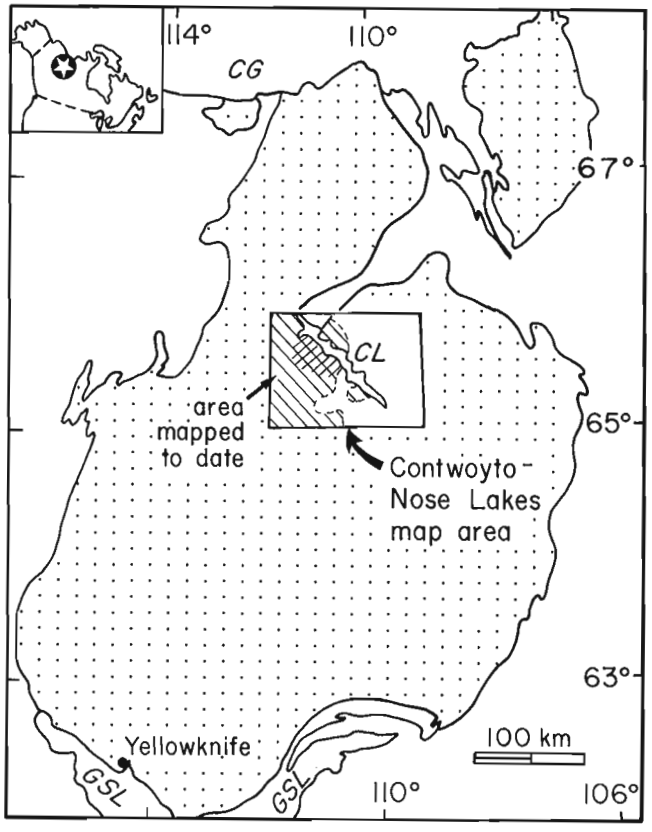

Figure 1. Location of the Contwoyto-Nose Lakes project area. Dot-patterned area is the Slave Structural Province. Inset shows position of the Slave Province in Canada. Diagonal lines show area covered to date; cross-hatch shows area discussed by Relf (1989). CG - Coronation Gulf; CL-Contwoyto Lake; GSL - Great Slave Lake.

YELLOWKNIFE SUPERGROUP

The Archean supracrustal rocks of the map area are part of the Yellowknife Supergroup as defined by Henderson (1970). Bostock (1980) assigned some local formation names as used below.

Contwoyto and Itchen Formations

The turbiditic Contwoyto and Itchen formations are described in Tremblay (1976), Bostock (1980) and King et al. (1988). In brief, the Itchen Formation comprises generally thick bedded turbidites, contains calcareous concretions and is barren of iron formation whereas the Contwoyto Formation comprises generally thin bedded turbidites, and contains iron formation. Localities of iron formation are too numerous to identify on Figure 2.

High-grade equivalents of the Itchen Formation occur as migmatitic paragneisses adjacent to and within the Yamba batholith (Fig. 2). The correlation is based on the lithologic continuum across a metamorphic and structural transition to low-grade Itchen Formation in the Point Lake area west of the present map area (Bostock, 1980; King, 1981, King and Helmstaedt, 1989), and the rare occurrence of calcareous concretions. Primary structures such as bedding and graded beds, are locally preserved and, in many outcrops, it is clear that the first order compositional layering is composed predominantly of recrystallized primary compositional layering (ie. bedding). The migmatitic aspect of the paragneisses is imparted by injected veins of tonalite to monzogranite. The character of the migmatite ranges from lit-par-lit style, where the granitoids occur as veins and sheets within otherwise internally coherent paragneiss (Fig. 4), to a nebulitic style where the paragneisses occur as irregularly shaped, closely packed schlieren and xenoliths in the intruding tonalite (Fig. 5). The lit-par-lit injections range in width from millimetres to kilometres. A characteristic feature of these gneisses is the presence of abundant cordierite in the metamorphic mineral assemblage and in the granitic phase. The cordierite will be discussed further in the section on Archean plutonic units.

High-grade equivalents of the Contwoyto Formation, identified by the presence of iron formation, occur in the

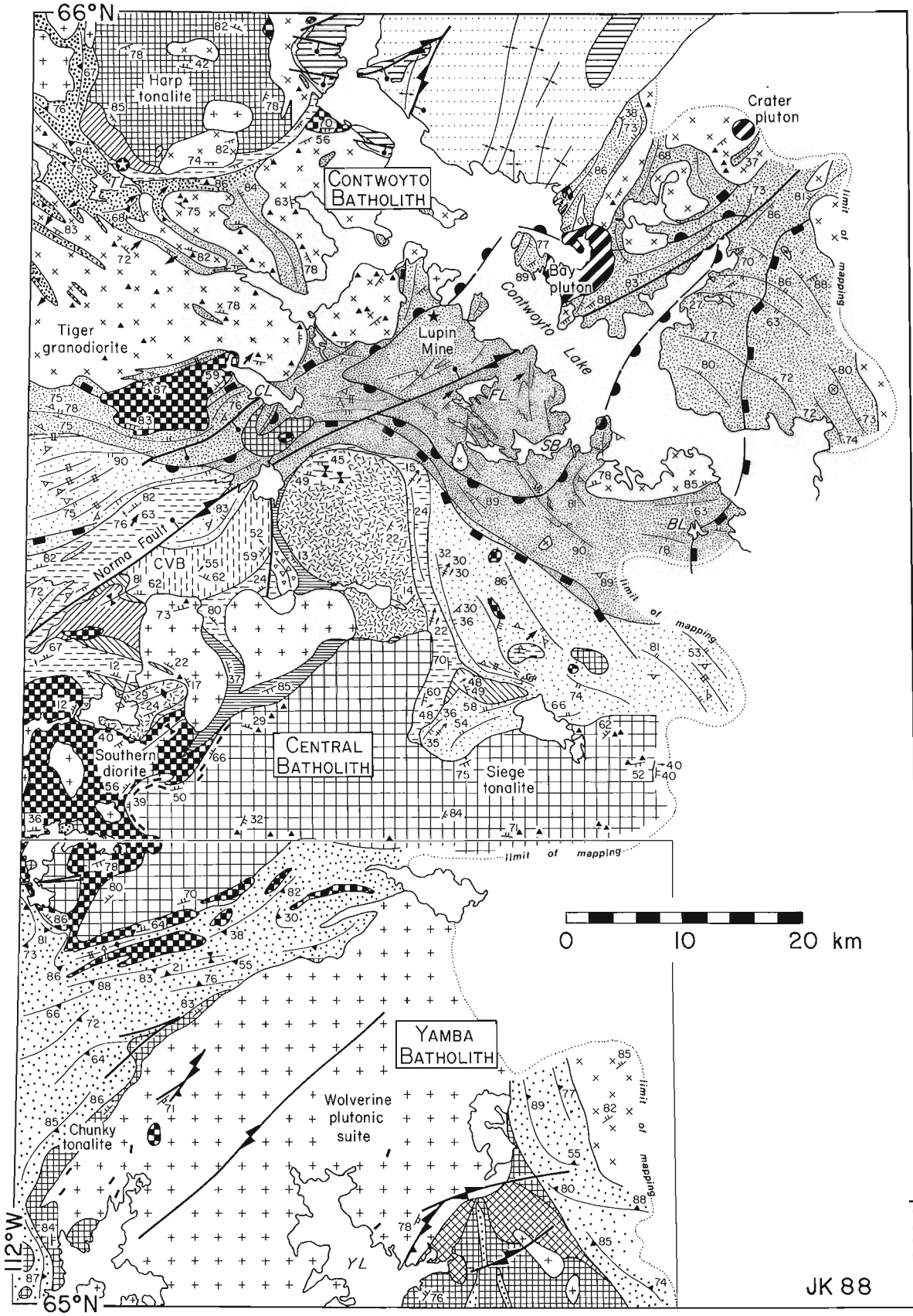

Figure 2. Simplified geological map of the Contwoyto Lake area. Legend is in Figure 3. Cleavages dip steeply (80-90°) when not labelled due to space restrictions. Circled star shows location of Tuk Cu-Mo occurrence. Box shows area covered in Figure 12. Detail in Proterozoic units from Fraser (1963) and Tremblay (1976). Abbreviations: CVB - Central volcanic belt; Bodies of water: BL - Butterfly lake; CL - Concession Lake; FL - Fingers lake; SB - Shallow Bay; TL - Tuk lake; YL - Yamba Lake.

northern part of the map area adjacent to and within the Contwoyto batholith (Fig. 2). In the southern part of the batholith, the Contwoyto Formation occurs as internally coherent, schistose screens and xenoliths, greatly intruded by veins and sheets of granitoids. In the central and northern parts of the batholith, remnants of the Contwoyto Formation occur as densely to moderately packed schlieren and xenoliths in a nebulitic injection migmatite.

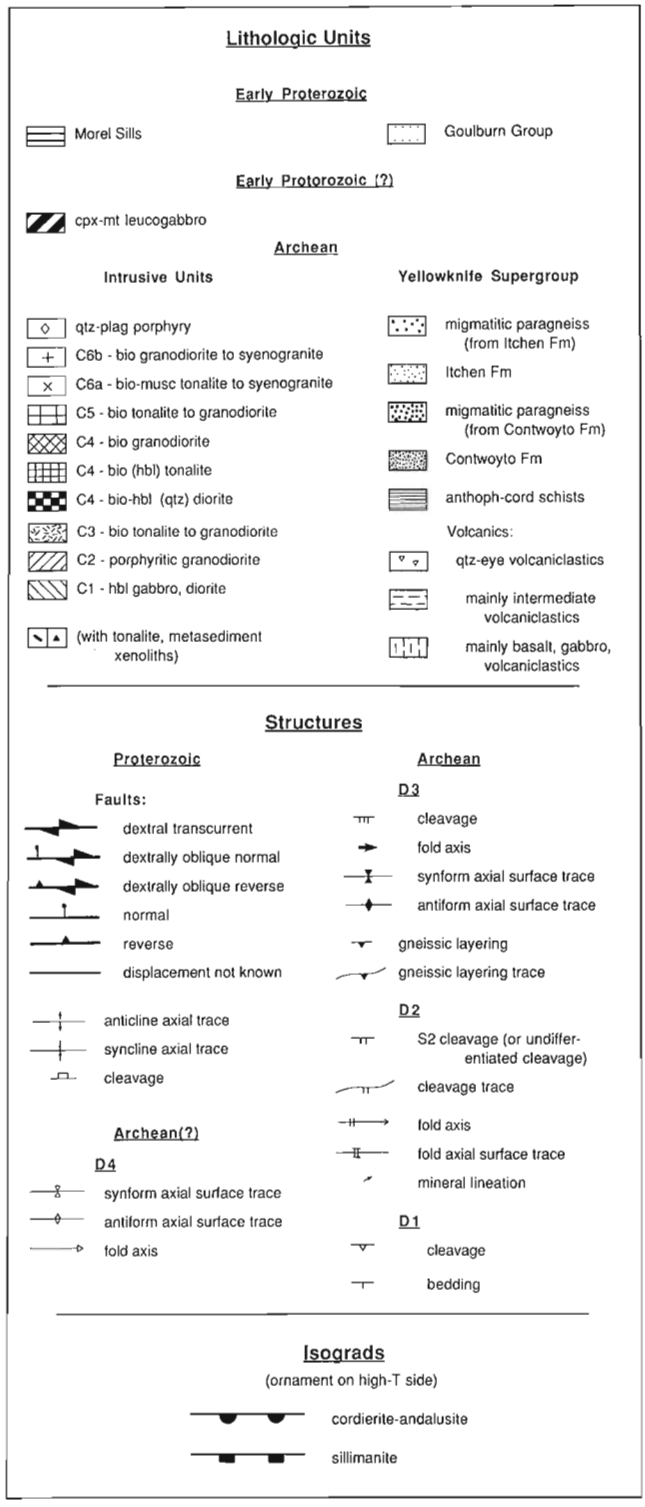

Figure 3. Legend for geological map of Contwoyto Lake area in Figure 2.

Tuk volcanic belt

A narrow belt of volcanogenic rocks, informally referred to here as the 'Tuk volcanic belt', extends from the northwest shore of Contwoyto Lake to northwest of Tuk lake (Fig. 2). These volcanics were not recognized during previous regional mapping although their presence in the immediate area of Tuk lake has been reported by Bain (1978). Many of the units within the belt are fine grained plagioclase-rich, biotite-poor, and characterized by compositional layering, 1 cm to 1 m in thickness. These are interpreted to be volcaniclastic in origin. Conglomerates characterized by intermediate volcanic clasts up to 10 cm in diameter are locally present. Thicker, compositionally homogeneous units are subporphyritic with phenocrysts of plagioclase-hornblende or quartz in fine grained groundmass (Fig. 6). These units are interpreted as flows or hypabyssal intrusions. The volcanogenic units are interlayered with biotite-rich siliciclastic units that are similar to the turbidites of the Contwoyto Formation. Bain (1978) reports locally north-facing top directions in the metasediments,but the belt has been intensely deformed and the regional facing direction is not known. Foliations in the belt dip dominantly southward.

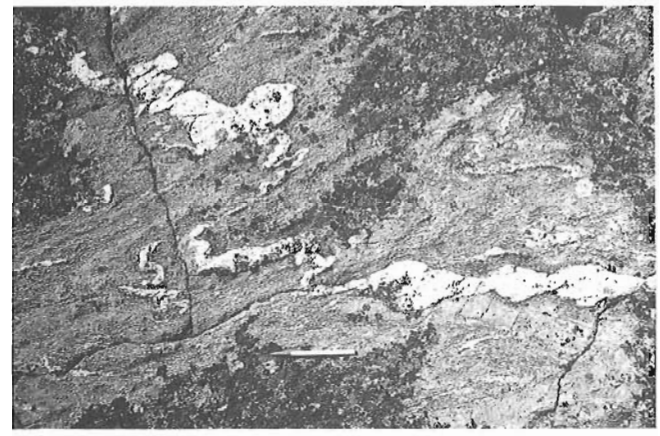

Figure 4. Vein of tonalite in structurally coherent, gneissic Itchen Formation. Vein is isoclinally folded about F_2. Pen is 13.5 cm. (GSC 204699-E)

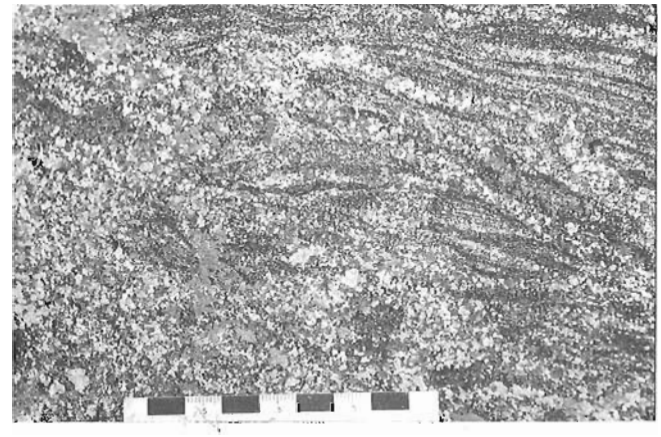

Figure 5. Nebulitic migmatite composed of schlieren of gneissic Itchen Formation in cordierite tonalite. Scale is in centimetres. (GSC 204699-I)

Shallow Bay volcanics

Several thin horizons of volcanogenic rocks are intercalated with the Contwoyto Formation between Fingers Lake and Shallow Bay (Fig. 2). These horizons have been informally named the 'Shallow Bay volcanics' by previous workers in the area (Gardiner, 1986; Kerswill, 1986; Lhotka, 1988). As in the Tuk volcanic belt, the Shallow Bay volcanics are dominantly volcaniclastic in character, although tuffs and pillowed flows are also locally present. C. Relf (1989) describes these units in greater detail.

DEFORMATION HISTORY

Four generations of Archean structures are recognized in the Contwoyto Lake area. These are described prior to the discussion of the plutonic units in this paper in order that the timing of emplacement of the intrusions can be correlated with the deformation events.

The structural nomenclature from King et al. (1988) has been modified to better accommodate the enlarged database. In King et al. (1988), the first set of structures ('D_1') was defined on the basis of one, very small isoclinal fold and variations in 'F_2' plunges. However, further mapping has revealed no more of these folds nor any other requirements (e.g. reversed facing directions) for them. It is more probable that the variations in "F_2" fold plunge are a result of heterogeneous strain during folding resulting in non-cylindrical folds as suggested by King et al. (1988). As a result, 'D_1' of King et al. (ibid) has been dropped and their 'D_2',' D_3' and 'D_4' generations are now termed D_1, D_2 and D_3. A post-D_3 episode of folding was recognized in 1988 and is herein referred to as a D_4 structure.

Structures related to D_1 and D_2 are discussed in detail by Relf (1989). In essence D_1 is manifested by 100 m to km-wavelength isoclinal folds (F_1) with an associated cleavage (S_1) defined by biotite and muscovite. D_2 is manifested by the most obvious folds in the area, isoclines with centimetre- to metre-, to 100 m-scale wavelengths. The associated crenulation or transposition cleavage (S_2) is typically the dominant cleavage in outcrop. A variably developed mineral lineation pitches steeply down S_2. F_1 and F_2 interfere in Type 2 to type 3 interference patterns (Ramsay, 1967) result from F_1-F_2 interference (see Relf, 1989). D_1 and D_2 structures are recognized in low- to medium-grade supracrustal rocks throughout the map area. In the paragneisses, evidence for D_1 is obliterated by coarse recrystallization. Isoclinal folds of gneissic layering are thought to be equivalent to F_2 folds in the medium-grade rocks.

The third deformation (D_3) is expressed as variously developed cleavages (S_3), crenulations and open folds (F_3) whose surfaces and axial planes trend 010°-070° (commonly 050°-060°) and which affect all Archean units (Fig. 2). In metasedimentary rocks the intensity of penetrative strain is domainal, ranging from a weak crenulation to intensely developed crenulation cleavage. Biotite growth occurred during S_3 development. Foliations defined by muscovite and biotite alignment in the C6 plutons (youngest Archean plutons, see below) (Fig. 7) are concordant with adjacent S_3 crenulation cleavage and discordant with the adjacent S_2. (Fig. 2) . They are therefore interpreted to have formed during D_3. Observed D_3 folds are open to chevron folds, with wavelengths of 1 cm to several metres, that plunge down the dip of the pre-existing structures. The trend of S_3 is regionally axial planar to macroscopic, NE-trending folds of S_2 east of Contwoyto Lake (Fig. 2) and it is possible that this map pattern is a function of large-scale D_3 cross folding. In the Itchen gneisses northwest of the Yamba batholith, the F_2 isoclinal folds of gneissic layering are refolded about NE-trending axes resulting in domains of shallow and steep dips of layering (Fig. 8). The dip of the axial plane of these refolds is not known, but the predominance of steep dips over shallow ones implies that the axial planes dip steeply. It is possible, but not proven, that these upright, NE trending folds are correlative with the similarly oriented D_3 folds observed in the lower grade rocks.

The D_2 and D_3(?) folds of the Itchen paragneisses are also refolded about NNE- to NNW-striking, shallow-plunging axes and upright axial surfaces (F_4) (Fig. 8, 9).

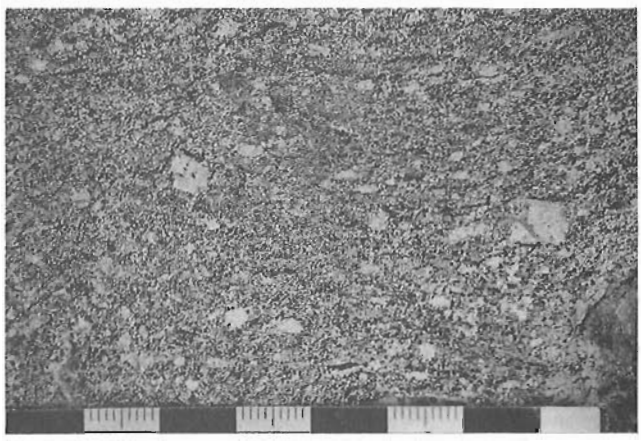

Figure 6. Phenocrysts of plagioclase in one of the thicker, compositionally homogeneous units (flow or sill) of the Tuk volcanic belt. Scale is in centimetres. (GSC 204699-F)

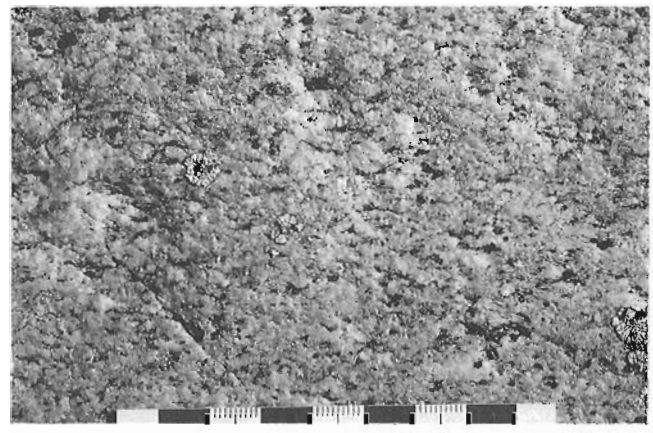

Figure 7. Moderately developed S_3 foliation defined by the alignment of biotite and muscovite in the small C6 tonalite on the east shore of Contwoyto Lake (see Fig. 2). Scale is in centimetres. (GSC 204699-Z)

Observed F_4 folds are very open and have wavelengths of 10 cm to 4 m. Types 1 and 2 fold interference patterns (Ramsay, 1967) are observed where F_4 hinges interfere with NW-trending F_2 or F_3 hinges (Fig. 8, 9). The type of interference patterns is determined by the orientation of the earlier fold. No penetrative fabrics or mineral growth are observed to be associated with the F_4 folds. It is possible that NW-trending cross folding contributed to the curved form of the Central volcanic belt and the configuration of domal structures cored by C3 plutons (Fig. 2) (cf. King et al., 1988).

ARCHEAN PLUTONIC UNITS

We have previously described six episodes of plutonism in the Contwoyto Lake area (King et al., 1988). The episodes are informally designated as 'C1' to 'C6' , referring to their relative time of emplacement in the Contwoyto Lake area. Plutonic phases within each episode are distinguished on the basis of differences in modal composition and textural characteristics. Nomenclature follows that of Streckeisen (1976). In brief, these episodes include: C1 syn-volcanic hornblende gabbros and diorites; C2 - syn-volcanic quartz-porphyritic porphyritic felsic dykes and granodiorite; C3 - late syn-volcanic biotite tonalite to granodiorite; C4 - pre- to syn-D_2 hornblende-biotite gabbro, diorite, quartz diorite, tonalite, and biotite granodiorite and granite; C5 - late syn-D_2 biotite tonalite to granodiorite; C6 post-D_2, early D_3 biotite +/- muscovite granodiorite to syenogranite and associated pegmatites. Observations in 1988 showed that this classification remains valid throughout the plutonic units mapped to date, although, based on more complete examination, the granitoids north of Concession Lake (Fig. 2) are now assigned to the C6 rather than the C5 episode of intrusion. A qualitative summary of time relations between plutonic episodes and sets of structures is presented in Figure 10.

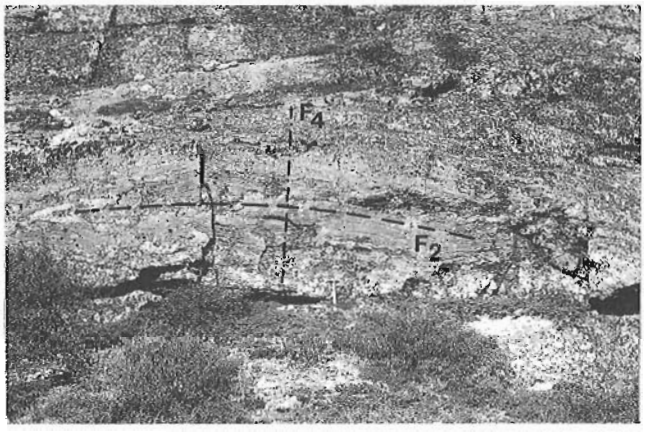

Figure 8. Isoclinal F_2 fold of gneissic layering with shallow dipping axial plane (25°) refolded about an upright, NNW-trending axial plane. The shallow dip of the F_2 axial surface is interpreted to be a result of upright F_3 folding. The superposed, upright fold would therefore be F_4. The F_2-F_3 interference pattern would be type 3; F_3-F_4 interference pattern would be type 2 at this locality. Hammer is 45 cm. (GSC 204699-R)

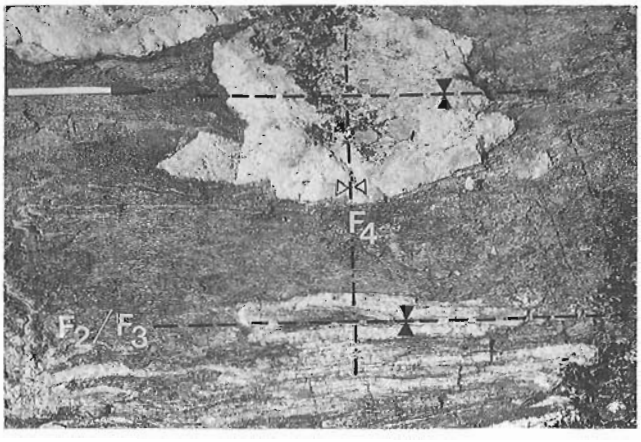

Figure 9. Type 1 interference pattern produced by superposition of upright, NE-trending F_2 or F_3 folds and NW-trending, upright F_4. (GSC204699-T)

The C4-C6 plutons occur within three clusters and as isolated plutons (Fig. 2). The clusters have been named (from north to south) the Contwoyto, Central and Yamba batholiths (Fig. 2). Each contains screens of older sediments, volcanics and, locally, plutons.

Synvolcanic plutonism (C1 to C3)

A pluton and veins of sub-porphyritic biotite granodiorite intrudes the northwest end of the Tuk volcanic belt (Fig. 2). The pluton is characterized by round quartz phenocrysts (2-8 mm) evenly distributed in an equigranular (2-3 mm) groundmass. Rusty weathering characterizes much of the pluton, making compositional classification difficult. Gossans occur along the southern contact. The intrusions are interpreted as syn-volcanic on the basis of similar bulk composition to, and intimate spatial association with, parts of

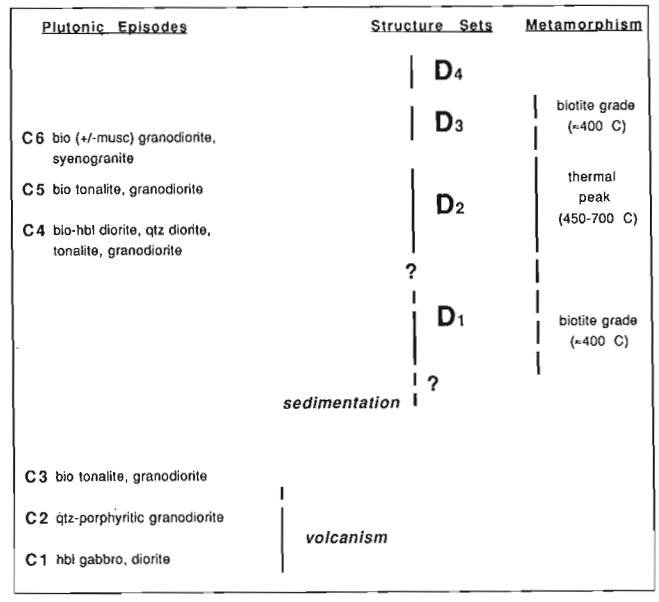

Figure 10. Qualitative summary of temporal relations between plutonic episodes, structure sets and metamorphism.

the Tuk volcanic belt. An occurrence of copper-molybdenum mineralization is located in a gossan zone at the granodiorite-volcanic belt contact (Fig. 2) (Bain, 1978; Bostock, 1980, p. 74). This occurrence has been classified as a porphyry-type deposit by Kirkham et al. (1982).

C4 - Biotite-hornblende diorite, quartz diorite, tonalite and granodiorite

C4 bodies mapped in 1988 include: 1) biotite-hornblende diorite to quartz diorite plutons in the Contwoyto Batholith and tabular bodies south of the Central batholith, 2) biotite (± hornblende) quartz diorite to biotite granodiorite plutons in the Yamba batholith,and 3) biotite-hornblende tonalite in the northern Contwoyto batholith.

The C4 diorites to quartz diorites vary in amounts of hornblende and biotite but are typically medium grained and equigranular. The bodies are usually tabular in exposed section. Even the Southern diorite, whose shape in map view is lobate (Fig. 2), is interpreted to be a thin, shallow dipping sheet whose lobate form is a function of both multiple folding and deformation during intrusion of the C5 Seige tonalite (King et al., 1988).

Two C4 rock types occur within the Yamba batholith. The volumetrically dominant unit is a medium-grained biotite tonalite that has 50% euhedral plagioclase (2-6 mm), 20% sub- to euhedral quartz (2-3 mm), interstitial biotite (1-2 mm) and accessory magnetite and is characterized by a distinctive seriate texture. Granodiorite plutons east of Yamba Lake (Fig. 2) are texturally similar to the tonalites but contain 10-15% K-feldspar. Sharp intrusive contacts have been mapped between the granodiorite and tonalite units but in many places their contact relations are not clear. In some places,the two units may reflect internal pluton variation. As the two are commonly intimately associated, the map units in Figure 2 denote the dominant lithology. The tonalites become locally more potassic where they have been intruded and metasomatized by C6 monzo- to syenogranite.

The tonalite body that outcrops as a thin rim along the west and northwest margin of the Yamba batholith has been informally named the Chunky tonalite (Fig. 2). Remnants of the tonalite are found as a few metre- to kilometre-scale xenoliths within the Wolverine plutonic suite, concentrated mainly near its western margin (Fig. 2). The Chunky tonalite - Itchen paragneiss contact is complex, with numerous sheet-like bodies and veins of tonalite cutting the gneisses, forming an injection migmatite. In many places injection is pervasive and paragneisses occur only as schlieren (Fig. 5). Where intruding the paragneisses, the tonalite remains texturally similar to the Chunky tonalite but is characterized by a more heterogeneous grain size, more abundant, large quartz grains, and abundant biotite-rich clots and schlieren that are clearly derived from the paragneiss. It also contains 1-20% euhedral, hexagonal cordierite crystals (Fig. 11). Where fresh, the cordierite is purple and vitreous in lustre. The cordierite is described by Folinsbee (1941) as being locally of gem quality, although it is fractured. More commonly, the cordierite is replaced or rimmed by a green weathering pinite. The contact between the Chunky tonalite and the cordierite tonalite can apparently occur within one tonalite body, across a transitional zone 2-3 in width. Similar cordierite-rich, migmatitic paragneisses occur as screens between C4 tonalite bodies east of Yamba Lake (Fig. 2) and south of the Wolverine plutonic suite on the Lac de Gras sheet (N.T.S. 76D) (Folinsbee, 1949 and reconnaissance mapping by the authors).

The euhedral form of the cordierite suggests crystallization as a magmatic phase. The spatial association of cordierite with inclusions of sedimentary material suggests that its crystallization may have resulted from a magma enriched in Al due to assimilation of pelitic rocks.

A cordierite-bearing leucotonalite to leucomonzogranite also occurs exclusively within the paragneisses (Fig. 11). It is medium to coarse grained (commonly pegmatitic) and is characterized by the pale grey colour of its K-feldspar and a pale green colour on fresh surfaces. Muscovite and small, euhedral andalusite are accessory phases. Euhedral cordierite is common (Fig. 11),and typically coarse grained (2-50 mm in length). Veins and plugs of this unit cross-cut and therefore post-date intrusion of the Chunky tonalite.

The C4 body north of the Tuk volcanics in the Contwoyto batholith, informally named the Harp tonalite (Fig. 2) varies in composition from the dominant biotite-hornblende tonalite to biotite-hornblende quartz diorite. The Harp pluton is grey-weathering, equigranular and medium grained (2-3 mm) and its mineral assemblage consists of euhedral plagioclase (3-6 mm), euhedral to subhedral hornblende, biotite and accessory magnetite. It is considered to be part of the C4 episode of intrusion on the basis of similar textures, mineral assemblage and state of deformation to parts of other C4 bodies. The Harp tonalite is greatly dismembered by small intrusions of non-foliated C6b bodies and its three-dimensional shape is not known.

All of the C4 bodies are characterized by a weakly to moderately developed foliation that is defined by the alignment of biotite and hornblende and flattened plagioclase and quartz. The foliation is broadly concordant with S_2 in the

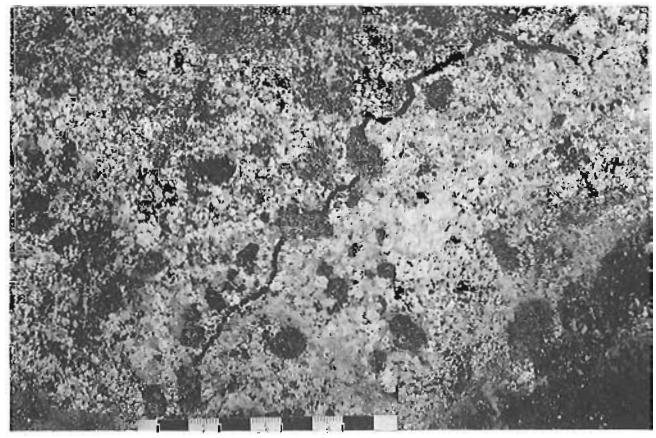

Figure 11. Cordierite-bearing 'chunky-type' tonalite intruded by cordierite-bearing leucotonalite (contact is highlighted). Dark grains are cordierite. Both bodies are veins in the Itchen paragneisses. Scale is in centimetres. (GSC204699-K)

adjacent supracrustal rocks and in places is folded about F_3. The C4 intrusive episode is therefore interpreted to have been emplaced pre- to syn-D_2 (Fig. 10) (cf. King et al., 1988).

C5 - Biotite tonalite to granodiorite

Plutons in the southern Contwoyto batholith, originally classified as C5 intrusives (King et al., 1988) have been redefined as belonging to the C6 episode of plutonism. The Seige tonalite and a similar, small body adjacent to it (Fig. 2) (King et al., 1988) are therefore the only recognized C5 bodies in the area mapped to date. The C5 bodies weather white, are fine grained (1-3 mm), and are characterized by euhedral plagioclase, brownish, subhedral quartz, less than 5 % biotite and accessory magnetite. Much of the main body contains diffuse leucocratic veins and patches of tonalite to granodiorite, millimetres to centimetres in width, that are associated with coarse magnetite . These veins create the appearance of a mixed rock. Xenoliths of country rock, 10 cm to hundreds of metres in size are present throughout most of the Seige tonalite and adjacent C5 pluton.

The contact of the Seige tonalite with the Southern diorite varies in character from sharp at the southwest lobe of the body, to a zone hundreds of metres to kilometres in width that contains intensely veined xenoliths of the host rock. The contact of the small C5 body with the Southern diorite is a 6-10 m wide zone in which the diorite is intensely veined parallel to its D_2 foliation by the tonalite. Approaching the contact zone, the hornblende of the Southern diorite is progressively recrystallized to biotite. The combination of intense veining and alteration produces a rock that is a quartz-biotite-plagioclase gneiss, xenoliths of which are abundant near the contact zone of the pluton. The veining of the tonalite along S_2 surfaces in its host rock substantiates the earlier interpretation (King et al., 1988) that D_2 structures were already present when C5 bodies were emplaced. However, the C5 bodies are locally weakly foliated concordantly with S_2 in the host rocks. The intrusion of this episode of plutons is therefore interpreted to have occurred late in D_2 (Fig. 10).

C6 - Biotite-muscovite granodiorite to syenogranite and associated pegmatites

Two distinct subunits of the C6 intrusive units are recognized. They are: C6a - white weathering, fine to coarse grained, biotite-muscovite tonalite to monzogranite that contains accessory apatite and tourmaline and has abundant associated pegmatitic phases; and C6b - red weathering, medium grained biotite granodiorite to syenogranite that is commonly K-feldspar subporphyritic to porphyritic and has only minor associated pegmatitic phases (C6b).

The C6a bodies constitute the southern part of the Contwoyto batholith and occur as isolated plutons east of Contwoyto and Yamba lakes (to the present extent of mapping) (Fig. 2). The southwestern C6a body in the Contwoyto batholith (Fig. 2) is composite and was informally named the Tiger granodiorite by King et al. (1988). Grain size is heterogeneous and typically ranges from fine grained to pegmatitic in a single outcrop. These intrusions are centimetres to kilometres in width, and are singular or composite tabular bodies (cf. King et al., 1988). They typically parallel the pronounced anisotropy form by the common parallelism of bedding and S_2. Where the bodies appear lobate (Fig. 2) they are in fact composed of numerous sheet-like bodies that parallel arcuate bedding and S_2. The composite plutons are characterized by narrow, relatively coherent screens and abundant xenoliths of metasedimentary rocks at all scales. C6a pegmatites are the areally dominant phase in the easternmost part of the batholith but also occur throughout the batholith and within the adjacent metasedimentary rocks(cf. King et al., 1988). A recent airborne radiometric survey has shown that part of the pegmatite-dominated part of the batholith, immediately northwest of the Lupin Mine (Fig, 2), has anomalously high uranium (Geological Survey of Canada, 1988).

C6b plutons constitute the central part of the Yamba batholith and occur as small isolated bodies throughout the map area (Fig. 2). The large area of C6b bodies in the Yamba batholith is informally named the 'Wolverine plutonic suite'. It is composed of numerous, texturally distinct, units of biotite granodiorite to syenogranite; biotite monzogranite is the dominant composition. Sharp contacts between internal units of the pluton can be locally recognized, but, for the most part, differences between units are too subtle and lichen cover too extensive to map them at the present scale. All units are pink to rusty red in colour. The various phases of the Wolverine plutonic suite are medium- to coarse-grained and are commonly K-feldspar subporphyritic to porphyritic. The K-feldspar phenocrysts are subhedral to euhedral, range in size from 25 cm and characteristically contain inclusions of euhedral plagioclase crystals. Biotite forms 10-15 % of the rock and muscovite 0-3 %. In three localities garnet forms up to 1 % of the rock. In a number of localities throughout the plutonic suite, the K-feldspar phenocrysts are aligned in planar or linear preferred orientations. It is not known whether the alignment is a product of magmatic flow or due to syn-magmatic deformation. The alignment of K-feldspars, and the local foliations related to Proterozoic faulting (see below), are the only penetrative fabrics observed in the Wolverine plutonic suite. The contact of the Wolverine suite with the adjacent tonalites and paragneiss is typically a diffuse zone, 2-20 m in width, in which the wallrocks are intensely veined by the monzogranite and are affected by potassic metasomatism. The plutonic suite contains a small number of tonalite and diorite enclaves, 3 m to 2 km in scale that are similar in composition and texture to those of the C4 units outside of the Wolverine pluton. Only a few smaller enclaves were observed.

The isolated C6b plutons range in composition from biotite monzogranite to biotite syenogranite and, like the Wolverine plutonic suite, are characteristically K-feldspar subporphyritic to porphyritic. Around Olga Lake these bodies were recognized to be at least in part coalesced sheet complexes (King et al., 1988). Elsewhere the three-dimensional shapes of the bodies are not known.

Some C6a plutons are moderately foliated parallel to S_3 in adjacent supracrustal rocks (Figs. 2, 6). and narrow C6b veins are locally folded by F_3 (King et al., 1988). Both C6a and C6b bodies cross cut S_2. Such observations confirm the interpretation (King et al., 1988) that the C6 plutons were emplaced post-D_2 and pre- to early in D_3 (Fig. 10).

Quartz-plagioclase porphyry

A small body and numerous veins of quartz-plagioclase porphyry occur in the Contwoyto Formation east of Contwoyto Lake (Fig. 2). The bodies contain a well developed cleavage that is concordant with S_2 in the adjacent metasediments. They must therefore have been emplaced pre-to syn-S_2, but their relationship to other pre- to syn-D_2 intrusive units is not known.

Magnetic signatures of the plutonic units

The magnetic signatures of the plutonic rocks, as represented on the contoured 1:250 000 aeromagnetic survey map of the Contwoyto Lake area (G.S.C. map 7206G), are locally distinctive. In the southern part of the map area the C4 tonalites have a high magnetic susceptibility which contrasts with the low signature of the adjacent Itchen paragneisses and C6 plutons (Fig. 12). The sharp gradients between areas of contrasting susceptibility correspond well with geological contacts, including screens of paragneisses in the Yamba batholith and domains of tonalite and diorite inclusions in the Wolverine plutonic suite (compare Fig. 2 and 12) and were successfully used as a predictive mapping tool. However, in the north part of the map area, similar C4 tonalites as well as other units such as magnetite-bearing C3 tonalites, C4 diorites, and intermediate to mafic vol-

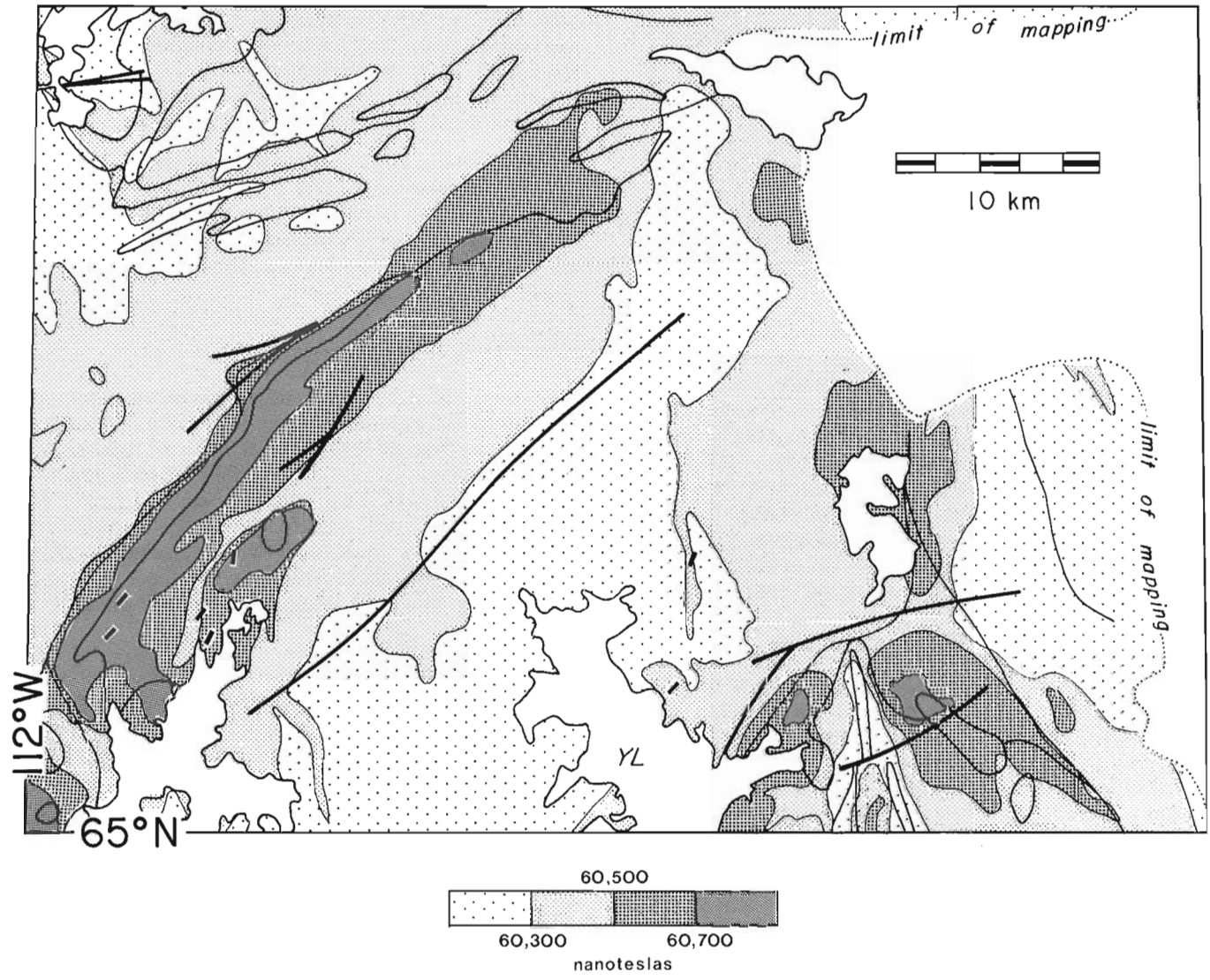

Figure 12. Magnetic pattern of the southwest part of the Contwoyto Lake map area (modified from GSC aeromagnetic survey map 7206G) superposed on geologic contacts of Fig. 2. Location is outlined by box in Figure 2. Heavy lines are Proterozoic faults; thinner lines are geologic contacts.

canics, which would normally be considered to have high magnetic susceptibilities, show little or no contrast with the adjacent, low-susceptibility metapelites and C6 granitoids. Magnetic susceptibilities of each of the rock types will be measured in order to document their expected signatures.

METAMORPHISM

The biotite, cordierite-andalusite and sillimanite-muscovite metamorphic mineral zones defined in 1987 have been extended to the east side of Contwoyto Lake (Fig. 2). The cordierite-andalusite isograd closes in a continuous,four-cornered loop that outlines a 'thermal basin' cored by the biotite zone. The sillimanite isograd is approximately concordant with the cordierite-andalusite isograd except that, within the limits of the completed mapping, it remains open at the corners of the loop. Staurolite occurs sporadically within the cordierite-andalusite zone as independent grains or mantled by cordierite or andalusite. The occurrence of staurolite appears to be strongly dependent on bulk composition and a staurolite isograd could not be mapped. A second biotite zone occurs at Concession Lake (Fig. 2), bounded to the southeast by the cordierite isograd and to the northwest by a fault that has a component of S-side-down displacement. Further west, current and previous mapping have shown that, from its neck at Concession Lake, the sillimanite zone widens westward. North of Point Lake, it is again cored by cordierite-andalusite and biotite zones (King, 1981; King et al., 1988; King and Helmstaedt, 1989) (Fig.2).

The maximum-phase assemblage in the Itchen Formation south of the Central batholith and within the Yamba batholith (Fig. 2) is cordierite-plagioclase-sillimanite-biotite-K-feldspar, indicative of transitional amphibolite-granulite facies metamorphism (Turner, 1981). Small, diffuse zones of igneous-textured quartzo-feldspathic material may represent partial melts. The transition from sillimanite-muscovite schists to the cordierite-K-feldspar-sillimanite gneisses has not yet been mapped in the Contwoyto Lake area, although it has been documented immediately west of the present map area (King, 1981; King and Helmstaedt, 1989).

At the northwest and northeast margins of the isograd loop, the Contwoyto Formation remains as structurally coherent, sillimanite-muscovite schists although it is intruded by numerous sheets of monzogranite (Fig. 2). The metasediments lose their coherency as xenoliths and screens of sillimanite-muscovite schists and become schlieric migmatites at the northern margin of the cluster of C6 monzogranite bodies in the Contwoyto batholith (Fig. 2). Mineral assemblages diagnostic of higher-T conditions (e.g. cordierite-K-feldspar) were not recognized in these migmatites.

The S_1 biotite-muscovite cleavage, present throughout the map area, is evidence of pre-thermal peak, regional metamorphism during D_1. The syn-thermal peak isograds transect F_2 axial surface traces (Fig. 2), and thermal-peak minerals are aligned along S_2 and deformed by S_3. S_3 is defined by biotite-muscovite growth in all mineral zones. The thermal culmination is therefore interpreted to have reached a maximum synchronous with S_2 development, with equilibration of the present metamorphic assemblages occurring after D_2 folding, Cooling to biotite grade occurred by D_3 time. A qualitative summary of the temporal relationship of metamorphism with the plutonic episodes and structure sets is presented in Figure 10.

Because of an apparent increase in grade toward the C5 Seige tonalite, we have previously suggested that the metamorphic map pattern was related to the thermal regime during C5 emplacement. However, mapping during 1988 has shown that 1) the plutons of the Contwoyto batholith, toward which grade apparently increases, are of the C6, not C5, intrusive episode, and 2) the C5 Seige pluton occurs between the medium-grade (sillimanite-muscovite) and high-grade (cordierite-K-feldspar) rather than coring the thermal culmination (Fig. 2). With the information available from the present mapping, it does not seem that the metamorphic zonation is spatially related to any one pluton or suite of plutons (Fig. 2). The low-P, high-T conditions of metamorphism preclude elevation of the geotherm at the exposed structural level exclusively by tectonic thickening (Lux et al., 1986). We believe that it is more likely that the thermal-peak metamorphic zonation is caused by increased heat flow during magmatism.

The origin and P-T conditions of the pre-thermal peak regional metamorphism, of which the syn-D_1 biotite-muscovite growth is evidence, is not known. It may have been related to the early phases of magmatism and/or to crustal thickening during D_1 (e.g. Thompson and England, 1984).

POST-ARCHEAN PLUTONS

Two compositionally and texturally distinct plutons were recognized on the east side of Contwoyto Lake, immediately south of the Peacock Hills (Fig. 2). Both are expressed as pronounced highs on contoured 1:250 000 scale magnetic anomaly maps (GSC Map 7206G, Contwoyto Lake). The 'Bay pluton' (informal name) is composed of coarse-grained leucogabbro which comprises 3-10 cm, sometimes swallow-tailed plagioclase with interstitial clinopyroxene and magnetite (Fig. 13). The mafic minerals are typically subhedral to

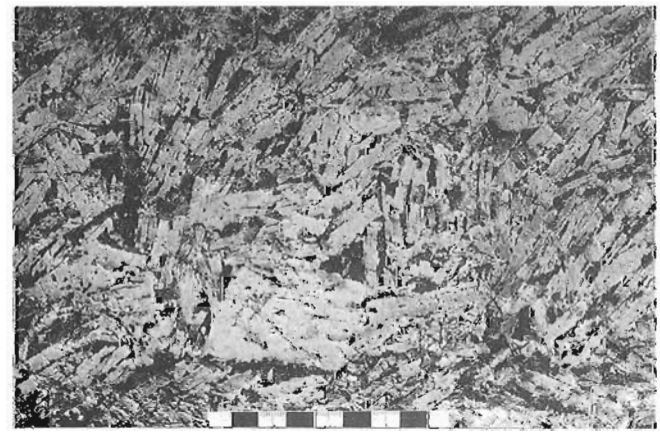

Figure 13. Coarse euhedral plagioclase with interstitial clinopyroxene and magnetite in a leucogabbro phase of the Bay gabbro. Scale is in centimetres. (GSC204699-U)

anhedral and occur interstitially to the plagioclase. Biotite occurs as a deuteric alteration product but the unit is not metamorphosed (A. Lalonde, pers. comm.). Variations in grain size and abundance of plagioclase occur in the pluton but were not mapped in sufficient detail to determine their significance. Near-horizontal compositional layering was locally observed. A body of fluorite-bearing granodiorite occurs in the core of the pluton. The gabbro is cut by at least two generations of fine grained, gabbro dykes that contain phenocrysts of plagioclase, hornblende or magnetite. The dykes are in turn intruded by small veinlets of tonalite that do not appear in the host coarse gabbro. Disseminated sulphides (pyrite, pyrrhotite) occur throughout the gabbros and sulphide-rich gossans occur locally.

The 'Crater pluton', (Fig. 2), is crater-like in its topographic relief. Its high, 0.5 km wide rim is clinopyroxene-magnetite gabbro similar in texture to the Bay pluton. The low-weathering core unit is cumulate-textured, medium-grained (2-5 mm) magnetite gabbro that contains small amounts of orthopyroxene. Biotite occurs as a late, very minor alteration; the unit is unmetamorphosed (A. Lalonde, pers. comm.).

The contacts of the Bay and the Crater plutons were not observed but, at the map scale, the bodies appear to truncate the F_3 refolds of the area and cut the C6 Archean intrusions (ca. 2585 Ma, O. van Breemen, pers. comm.) (Fig. 2). Mackenzie dykes (1267+/-2 Ma, LeCheminant and Heaman, in prep.) transect the Bay pluton. An intrusive suite with a compositional range and magnetic expression similar to that of the Bay and Crater plutons, the Booth River Intrusive Suite (BRIS), is exposed 100 km northeast of the Bay and Crater plutons (Roscoe, 1985). The suite intrudes Archean granitic and supracrustal rocks and is nonconformably overlain by the Early Proterozoic Goulburn Group (Roscoe, ibid.). An alkali-feldspar granite in the BRIS has yielded a U-Pb zircon age of 2023+/-2 Ma (Roscoe et al., 1987). The isolated Gumbo Lake leuconorite, correlated with the BRIS by Roscoe (1985) is located at the north end of a continuous, high magnetic anomaly that extends southward, beneath the Goulburn Group, to the vicinity of the Bay pluton. This magnetic high may represent a second, relatively extensive complex of Early Proterozoic plutons like the BRIS of which the Bay and Crater plutons are part.

A swarm of small, tabular gabbroic bodies that outcrop on the east shore of Contwoyto Lake, adjacent to the Goulburn Group (Fig. 2) have a texture distinct from that of the C4 diorites in the area but similar to one of the phases of the Bay pluton. The gabbros are characteristically seriate, with 1-10 mm subto euhedral plagioclase in a fine- grained groundmass of hornblende and biotite. The swarm lies within the magnetic anomaly that extends between the Gumbo Lake and Bay plutons. It is possible that these bodies are also correlative with the BRIS.

PROTEROZOIC FAULTING

King et al. (1988) have argued that the Norma fault and two other faults in the Concession Lake area (Fig. 2) are part of the Proterozoic NE-NW conjugate fault system that affects the northwestern Canadian Shield (Hoffman, 1984; Tirrul, 1984). This summer the trace of the Norma fault was extended to the east side of Contwoyto Lake and a set of faults of similar orientation and interpreted age were identified in the southwest corner of the Contwoyto Lake map area (Fig. 2). For the most part, the faults are expressed as linear topographic depressions filled with glacial detritus. However, sufficient fault rocks are exposed along the margins of the depressions to examine the kinematic framework and physical conditions of the faulting event.

Fault rocks along the depressions include microbreccia, gouge and pseudotachylyte (derived from brittle deformation mechanisms) as well as protomylonite, mylonite, and ultramylonite (derived through brittle-ductile and ductile deformation mechanisms. The ductile strained zones are not continuous along any one fault trace but occur as either (1) discontinuous and anastomosing strands, millimetres to metres in scale, often enveloped by, or adjacent to, zones of intense brittle faulting or cataclasis or (2) discontinuous envelopes of ductile strain adjacent to the fault traces. The ductile fault rocks observed in the Contwoyto Lake area contrast with the dominantly brittle fault rocks documented along the fault system elsewhere in the Slave Province and in Wopmay Orogen (Lord and Parsons, 1947; King, unpublished data).

Observed kinematic indicators include stepped striae on slickensides in the brittle fault rocks, and , in ductile strain zones, C-S fabrics (Berthé et al., 1979) (Fig. 14) and shear bands (extensional crenulation cleavage) (Platt and Vissers, 1980). The number of kinematic indicators observed was not numerous, due to poor exposure, but the inferred senses of displacement on faults of the same orientation were consistent. Displacements appear to be dominantly dextral transcurrent with minor normal displacement on ENE-trending (040°-070°) faults (displacement vector ± 5° pitch), oblique reverse on NE-trending faults (displacement vector pitching 50°-65° on ca. 50°-70° inclined planes), reverse on NS-trending faults and normal on WNW -trending faults (095°-100°). A summary of the predicted kinematic framework derived from these observations is presented in Figure 15. Individual faults may branch or curve, with

Figure 14. Dextrally asymmetric C-S fabrics adjacent to the NE-trending fault in the centre of the Wolverine pluton. View is normal to the foliations and parallel to the lineation. Scale is in centimetres. (GSC204699-M)

resulting changes in their kinematics. The pattern of displacement on the fault system is consistent with approximately EW shortening and and both NS and vertical extension. This kinematic framework is similar to that determined for the fault system in parts of the foreland of Wopmay Orogen (Hoffman et al., 1984) except that there is more abundant, albeit qualitative, evidence for dip slip displacement on the fault system in the Contwoyto Lake area.

In acute triangle zones where two faults branch, a distinct but weakly developed foliation defined by flattened quartz grains and the preferred alignment of biotite, muscovite and/or chlorite, is locally developed. This occurs whether the zones are millimetres or kilometres in dimension. The foliation, strikes NNE and dips steeply. The spatial restriction of this foliation to the branch zones of the Proterozoic faults suggests that it is Proterozoic.

Several narrow, schistose to mylonitic shear zones identified in the Contwoyto area during the 1987 field season were previously interpreted to be Archean in age (D_4^b of King et al., 1988) on the basis of their relatively high temperatures of deformation. In light of our new understanding of the Proterozoic faulting, it is now thought that these shear zones are also Proterozoic in age.

This faulting event postdates the 1.88 to 1.84 Ga Great Bear magmatic zone of western Wopmay Orogen (Hoffman and Bowring, 1984). The event is known to predate the 1663 Ma Narakay Volcanic Complex of the Coppermine Homocline (Bowring and Ross, 1985) but is probably older than 1.81 Ga (Hoffman, 1980, Hoffman and Bowring, 1984).

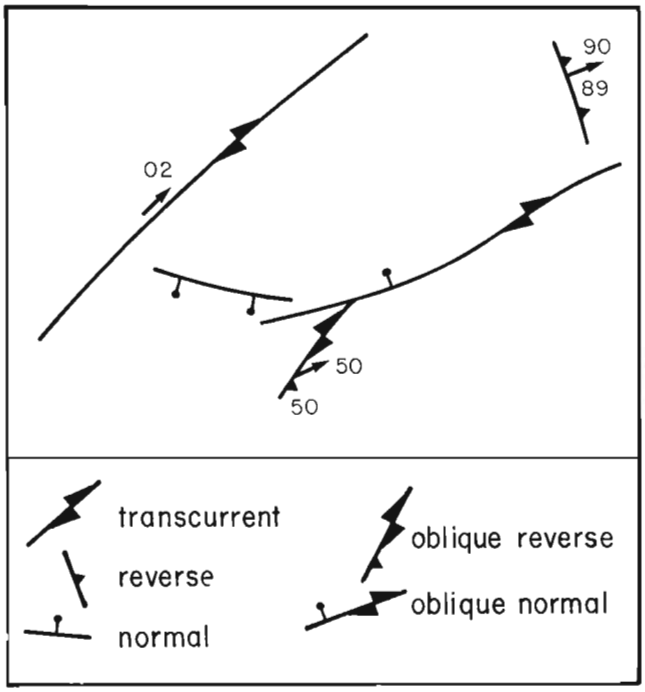

Figure 15. Sketch of the generalized geometric and kinematic framework of the Proterozoic fault system in the Contwoyto Lake area. Arrows represent the pitch of mineral stretching lineations or striae on slickensides on the fault surfaces.

SUMMARY OF TECTONOMAGMATIC HISTORY

In the Contwoyto Lake area, the earliest episode of magmatism is represented by the Central Volcanic Belt and C1 to C3 intrusions. U/Pb ages for zircons in these bodies are in the range of 2670-2650 Ma (Mortensen et al., 1988; O. van Breemen, pers. comm.). This magmatism is part of the second (2671-2663 Ma) episode of Slave volcanism as defined by the regional geochronological studies of Mortensen et al. (1988). No deformation associated with this magmatic episode has been recognized. The onset of the second major episode of magmatism, as represented by C4 and C5 intrusions occurred at ca. 2616-2608 Ma (O. van Breemen, pers. comm.). This coincided with D_2 and the thermal peak of metamorphism. At some time, either overlapping with the first magmatic episode, or in the 40 Ma interval between dated episodes, the Itchen and Contwoyto Formation turbidites were deposited and the first deformation occurred (although see also Mortensen et al., 1988 for a discussion of the possible significance of a 2604 Ma porphyritic unit in the Contwoyto Formation). Late in, or after, the final C6 episode of intrusion at ca. 2585 Ma (O. van Breemen pers. comm.), during cooling of the thermal culmination, the area was affected by regional NW-SE directed compression (D_3), and subsequently by approximately E-W directed compression(D_4).

The dominance of intermediate volcanic rocks, the physical character of the volcanics (cf. King et al., 1988), and preliminary geochemical studies by W.J.D. (Davis and King, 1988; Davis, unpub. data), suggest that at least the C1 to C4 episodes may have affinities to modern continental arc magmatism. The C5 and C6 episodes have fertile crustal sources (Davis and King, 1988). The reason for the apparently episodic nature of the arc magmatism is not known.

Subsequent to the Archean tectonism, the area was uplifted and eroded. The northern part of the area was the locus of 'anorogenic' mafic magmatism, possibly ca. 2023 Ma, and acted as a cratonic platform for deposition of the Early Proterozoic Goulburn Group. The through-going conjugate fault system, developed between 1840 Ma and 1810 Ma, records east-west shortening of the northwest Canadian Shield.

IMPLICATIONS FOR EXPLORATION

Results of the 1988 field season that are of particular interest to exploration geologists include:

1. Areas designated as hybrid rocks west of Contwoyto Lake (Bostock, 1980) and as biotite gneiss and migmatite east of Contwoyto Lake (Fraser, 1963, 1964) have been subdivided into intrusive and metasedimentary (Contwoyto Fm) components (Fig. 2). Except in the northwest part of the Contwoyto batholith, the metasedimentary screens and xenoliths in these areas are schistose and internally relatively coherent. Some of the larger xenoliths and screens of Contwoyto Formation may be potential exploration targets for Lupin-type gold mineralization.

2. The protolith of the paragneisses within and adjacent to the Yamba batholith was the Itchen Formation. Therefore there is little exploration potential in these gneisses for Lupin-type gold mineralization.

3. Two belts of volcanogenic rocks, dominantly intermediate in composition, were mapped within the Contwoyto Formation Fig. 2) and proved useful as stratigraphic and structural markers. Their presence confirms that some volcanism was contemporaneous with the deposition of the Contwoyto Formation.

4. The C6 plutons are interpreted to have been emplaced post-D_2 whereas the 'late' quartz veins that cut the Lupin ore unit are interpreted to have developed syn- to late D_2 (King et al., 1988, Relf, 1989). This suggests that the veins were not generated by processes directly related to the C6 plutons or pegmatites.

5. A porphyritic granodiorite and a mappable volcanic belt were recognized to be spatially associated with the Tuk copper-molybdenum occurrence (Fig. 2). Although detailed mapping would be required to ascertain the genetic relationship between the mineralization and the pluton, the results of our mapping are entirely consistent with the deposit being of porphyry type as recognized by Kirkham et al. (1982).

ACKNOWLEDGMENTS

Anne Seguin and Mike Wingate were very enthusiastic and able assistants and contributed considerable independent mapping. Mike is specifically thanked for providing us with his mineralogical expertise. Janien Schwarz outdid her culinary reputation. We are grateful to Otto van Breemen for his interest and for providing us with radiometric ages, to Dugald Carmichael (Queen's University) for discussions during his visit and to Rod Stone and Lynn Parney for their efficient expediting services. André Lalonde (University of Ottawa) is thanked for his remarkably prompt petrographic report of the Bay and Crater gabbros. Critical reading by Robert Hildebrand, John Henderson and John Kerswill greatly improved the text. We also gratefully acknowledge the excellent 1:250 000 scale map of Hewitt Bostock which has continued to provide the base for our mapping west of Contwoyto Lake.

REFERENCES

Bain, D.J.
1978: An Archean volcanogenic Cu-Mo showing west of Contwoyto Lake, Northwest Territories; BSc thesis, University of Western Ontario, London, Ontario, 47 p.

Berthé, D., Choukroune, P., and Jegouzo, P.
1979: Orthogneiss, mylonite and non-coaxial deformation of granites: The example of the South Armorican Shear Zone; Journal of Structural Geology, v. 1, p. 32-42.

Bostock, H.H.
1980: Geology of the Itchen Lake area, District of Mackenzie; Geological Survey of Canada, Memoir 391.

Bowring, S.A. and Ross, G.M.
1985: Geochronology of the Narakay Volcanic Complex: implications for the age of the Coppermine Homocline and Mackenzie igneous events; Canadian Journal of Earth Sciences, v. 22, p. 774-781.

Davis, W.J. and King, J.E.
1988: Geochemical evolution of plutonism in the central Slave Province; Geological Association of Canada, Mineralogical Association of Canada, Program with Abstracts, v. 13, p. A30.

Folinsbee, R.W.
1941: Optic properties of cordierite in relation to alkalies in the cordierite-beryl structure; American Mineralogist, v. 26, p. 485-500.
1949: Lac de Gras, District of Mackenzie, Northwest Territories; Geological Survey of Canada, Map 977A, scale 1:250 000.

Fraser, J.A.
1963: Geology, Northeastern District of Mackenzie, Northwest Territories; Geological Survey of Canada, Map 45-1963, scale 1:506 880.
1964: Geological notes on northeastern District of Mackenzie, Northwest Territories; Geological Survey of Canada, Paper 63-40.

Gardiner, J.J.
1986: Structural geology of the Lupin gold mine, Northwest Territories; MSc thesis, Acadia University, Wolfville, Nova Scotia, 206 p.

Geological Survey of Canada
1988: Preliminary release of airborne gamma ray spectrometric colour maps at 1:100 000 scale, Lupin Mine area, Northwest Territories; Geological Survey of Canada, Open File 1921.

Henderson, J.B.
1970: Stratigraphy of the Archean Yellowknife Supergroup, Yellowknife Bay Prosperous Lake area, District of Mackenzie; Geological Survey of Canada, Paper 70-26.

Hoffman, P.F.
1980: Wopmay Orogen: A Wilson cycle of early Proterozoic age in the northwest of the Canadian Shield; in The Continental Crust and Its Mineral Deposits, ed. D.W. Strangway; Geological Association of Canada Special Paper 20, p. 523-549.
1984: Geology, northern internides of Wopmay Orogen, District of Mackenzie, Northwest Territories; Geological Survey of Canada, Map 1576A, scale 1:250 000.

Hoffman, P.F. and Bowring, S.A.
1984: Short-lived 1.9 Ga continental margin and its destruction, Wopmay Orogen, northwest Canada; Geology, v. 15, p. 785-788.

Hoffman, P.F., Tirrul, R., Grotzinger, J.P., Lucas, S.B., and Eriksson, K.A.
1984: The externides of Wopmay Orogen, Takujuq Lake and Kikerk Lake map area, District of Mackenzie; in Current Research, Part A, Geological Survey of Canada, Paper 84-1A, p. 383-395.

Kerswill, J.A.
1986: Gold deposits hosted by iron formation in the Contwoyto Lake area, Northwest Territories; in An International Symposium on Geology of Gold Deposits, Gold '86, ed. A.M. Chatter; Poster volume, Toronto, Ontario, p. 82-85.

King, J.E.
1981: Low-pressure regional metamorphism and progressive deformation in the eastern Point Lake area, Slave Province, N.W.T.; unpublished MSc thesis, Queen's University, Kingston, Ontario, 187 p.

King, J.E. and Helmstaedt, H.
1989: Deformational history of an Archean fold belt, eastern Point Lake area, Slave Structural Province, N.W.T.; Canadian Journal of Earth Sciences, (in press).

King, J.E., Davis, W.J., Relf, C., and Avery, R.W.
1988: Deformation and plutonism in the western Contwoyto Lake map area, central Slave Province, District of Mackenzie, N.W.T.; in Current Research, Part C, Geological Survey of Canada, Paper 88-1C, p. 161-176.

Kirkham, R.V., McCann, C., Prasad, N., Soregaroli, A.E., Vokes, F.M. and Wine, G.
1982: MOLYFILE - An index-level computer file of Molybdenum deposits and occurrences in Canada; in Molybdenum in Canada Part 2: Geological Survey of Canada, Economic Geology Report 33, p. 116.

Lhotka, P.G.
1988: Geology and geochemistry of gold-bearing iron formation in the Contwoyto Lake region, Northwest Territories, Canada; University of Alberta, Edmonton, Atta. PhD thesis, 223 p.

Lord, C.A. and Parsons, W.H.
1947: The Camsell River map area; Geological Survey of Canada, Map 1014A.

Lux, D.R., DeYoreo, J.J., Guidotti, C.V., and Decker, E.R.
1986: Role of plutonism in low-pressure metamorphic belt formation; Nature, v. 323, p. 794-797.

Mortensen, J.K., Thorpe, R.I., Padgham, W.A., King, J.E., and Davis, W.J.
1988: U-Pb zircon ages for felsic volcanism in Slave Province, N.W.T.; in Radiogenic Age and Isotopic Studies: Report 2, Geological Survey of Canada, Paper 88-2, in press.

Platt, J.P. and Vissers, R.I.M.
1980: Extensional structures in anisotropic rocks; Journal of Structural Geology, v. 2, p. 397-410.

Ramsay, J.G.
1967: Folding and Fracturing of Rocks; McGraw-Hill, New York, 568 p.

Relf, C.
1989: Archean deformation of the Contwoyto Formation metasediments, western Contwoyto Lake area, N.W.T.; in Current Research, Part C, Geological Survey of Canada, Paper 89-1C.

Roscoe, S.M.
1985: The Booth River Intrusive Suite, District of Mackenzie; in Current Research, Part A, Geological Survey of Canada, Paper 85-1A, p. 141-144.

Roscoe, S.M., Henderson, M.S., Hunt, P.A., and van Breemen, O.
1987: U-Pb zircon age of an alkaline granite body in the Booth River Intrusive Suite, N.W.T.; in Radiogenic Age and Isotopic Studies: Report 1; Geological Survey of Canada, Paper 87-2, p. 95-100.

Streckeisen, A.
1976: To each plutonic rock its proper name; Earth Science Reviews, v. 12, p. 1-33.

Thompson, A.B. and England, P.C.
1984: Pressure-temperature-time of regional metamorphism II. Their inference and interpretation using mineral assemblages in metamorphic rocks; Journal of Petrology, v. 25, p. 929-955.

Tirrul, R.
1984: Regional pure shear deformation by conjugate transcurrent faulting, externides of Wopmay Orogen, N.W.T.; Geological Association of Canada, Mineralogical Association of Canada, Program with Abstracts, v. 9, p. 111.

Tremblay, L.P.
1976: Geology of northern Contwoyto Lake area, District of Mackenzie; Geological Survey of Canada, Memoir 381.

Turner, F.J.
1981: Metamorphic Petrology, 2nd ed.; McGraw-Hill, New York, 524 p.

Archean deformation of the Contwoyto Formation metasediments, western Contwoyto Lake area, Northwest Territories[1]

C. Relf[2]
Lithosphere and Canadian Shield Division

Relf, C., Archean deformation of the Contwoyto Formation metasediments, western Contwoyto Lake area, Northwest Territories; in Current Research, Part C, Geological Survey of Canada, Paper 89-1C, p. 95-105, 1989.

Abstract

Detailed mapping in the western Contwoyto Lake area has delineated the Shallow Bay volcanics within the metasediments of the Contwoyto Formation, confirming that volcanism accompanied the deposition of the turbidites and iron-formation. Two phases of isoclinal folding and cleavage have affected the supracrustal rocks, resulting in fold interference patterns between types 2 and 3 of Ramsay. High T/low P metamorphism peaked during the second folding. A third deformation produced domainal crenulations and minor folds, and may be responsible for macroscopic folds of S2. Quartz veins in the turbidites and iron-formation have been subdivided into 5 types, based on their interpreted chronology of emplacement. The majority of quartz veins formed during the thermal peak.

Résumé

La cartographie détaillée de la région à l'ouest du lac Contwoyto a permis de délimiter les roches volcaniques de Shallow Bay à l'intérieur des métasédiments de la formation de Contwoyto, ce qui confirme que le volcanisme a accompagné les dépôts de courants de turbidité et la formation ferrifère. Deux phases de plissement isoclinal et formation de schistosité ont touché les roches supercrustales produisant des interférences entre les types 2 et 3 de Ramsay. Le métamorphisme T élevée/faible P a atteint un maximum pendant le deuxième épisode de plissement. Une troisième déformation a produit des crénulations domaniales et des plis mineurs et pourrait avoir produit les plis macroscopiques de la surface de schistosité S2. Les veines de quartz dans les dépôts de courants de turbidité et la formation ferrifère ont été subdivisées en 5 types d'après l'intepprétation de la chronologie de leur mise en place. Ces veines de quartz se sont en majorité formées pendant le maximum thermique.

[1] Contribution to Canada — Northwest Territories Mineral Development Agreement 1987-1991. Project carried by Geological Survey of Canada

[2] Department of Geological Sciences, Queen's University, Kingston, Ontario, K7L 3N6

INTRODUCTION

This study was undertaken in 1987 in conjunction with the Contwoyto — Nose lakes regional geological mapping project (King et al., 1988; King et al., 1989) (Fig. 1) to examine the structural, metamorphic and stratigraphic history of the metasedimentary rocks in the area, which host the gold-bearing iron formation. This report summarizes the results of independent mapping by the author during the 1988 field season.

The geology of the Contwoyto Lake area was previously summarized by Fraser et al. (1964) at 1:500 000 reconnaissance scale, by Tremblay (1976) at 1:50 000 scale (northwest part of the Contwoyto Lake map sheet), by Bostock (1980) at 1:250 000 (west half of the Contwoyto Lake sheet), and most recently by King et al. (1988, 1989). As well, assessment reports containing detailed geological and geophysical maps of claim groups are available through the Archives Office of Indian and Northern Affairs Canada.

The present study focusses on: 1) the Archean deformation history and fold interference patterns in the Contwoyto Formation metaturbidites west of Contwoyto Lake, 2) the relationship between metamorphism and deformation, and 3) the timing of quartz vein emplacement relative to the various phases of deformation.

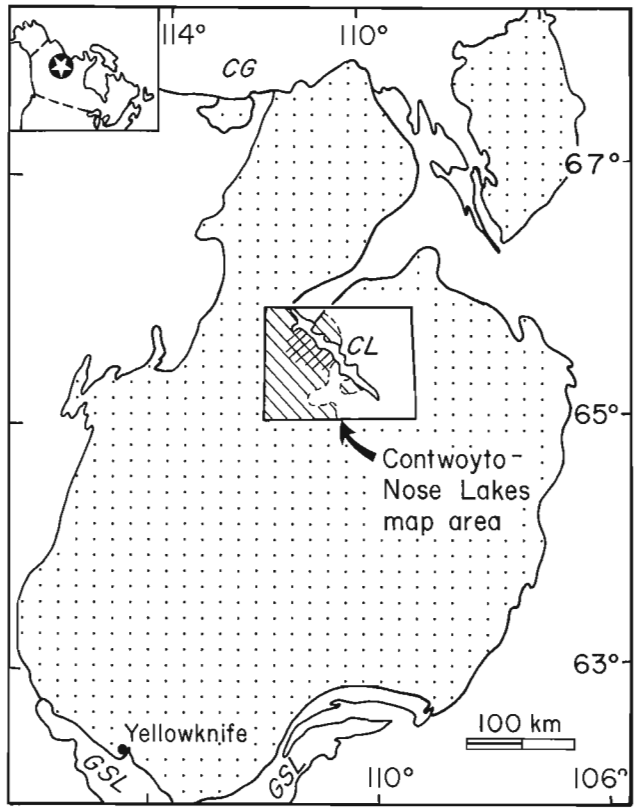

Figure 1. Location of the Slave Structural Province. Cross-hatched area shows area covered by this report; diagonal lines show area covered by King et al. (1989).

YELLOWKNIFE SUPERGROUP

In the western part of the Contwoyto Lake map area, the supracrustal rocks of the Yellowknife Supergroup (Henderson, 1970) have been subdivided into four formations (Bostock, 1980), three of which are exposed in the present map area. They are the Contwoyto Formation, the Itchen Formation, and the Point Lake Formation. Bostock (ibid.) concluded that the Itchen Formation overlies the Contwoyto Formation, which overlies and interfingers with the Point Lake Formation. Rocks of the Yellowknife Supergroup have been regionally metamorphosed in the area (see below).

The Contwoyto Formation is dominated by thinly-bedded metaturbidites (Bostock, 1980; King et al., 1988). Bedding thickness is generally less than 10 cm, although in places it is known to exceed 1 metre. In contrast, the Itchen Formation is characterized by thicker, more massive beds, ranging from 2 cm to 2 m, with an average between 10 and 25 cm. The Contwoyto and Itchen formations are further distinguished by the presence of iron formation and volcanogenic rocks in the Contwoyto Formation (Bostock, 1980; King et al., 1988), and by the occurence of calcareous concretions in the Itchen Formation (Bostock, 1980).

The Point Lake Formation is a general grouping of all felsic to mafic volcanogenic rocks (Bostock, 1980). Volcanic rocks of the Central Volcanic Belt (described by Bostock 1980 and by King et al., 1988), are therefore considered to be part of the Point Lake Formation by Bostock (1980). However, King et al. (1988) suggested that they may be a part of a different volcanic sequence, based on the occurrence of the Itchen Formation between the Contwoyto Formation and the Central Volcanic Belt.

North of Shallow Bay (Fig. 2), several horizons of mainly intermediate volcaniclastic rocks, informally named the Shallow Bay volcanics (Gardiner, 1986; Lhotka, 1988), are present within the Contwoyto Formation. They are intercalated with the sediments, and are continuous over a strike length of 5 km between Fingers Lake and Shallow Bay. Similar volcanogenic rocks were observed intermittently along strike over another 4 km, south of Shallow Bay (Fig. 2).

The dominant unit of the Shallow Bay "volcanics" is a felsic to intermediate epiclastic sediment. Where bedding is recognizable, single beds vary in thickness from 2 mm to 10 cm, with an average thickness of 2 to 3 cm. Elsewhere, beds in this unit are massive and are up to 5 m thick. Due to heavy lichen cover, it is difficult to trace the thinner beds for more than a few metres along strike but some of the more massive beds have been mapped along strike for tens of metres.

Volcaniclastics with lapilli- to block-sized clasts supported in a very fine-grained chloritic matrix make up a significant portion of the Shallow Bay "volcanics" (Fig. 3). The clasts are angular to subrounded, commonly poorly sorted, and include fragments of fine-grained diorite to quartz diorite, aphanitic clasts of intermediate composition, and plagioclase phenocrysts up to 1 cm (Fig. 4). Individual layers can be traced along strike for up to about 25 m. Some of the layers may represent debris flows.

In a number of places along the belt of Shallow Bay "volcanics", well developed cross laminations are present in finely layered felsic material (Fig. 5), which suggests deposition in shallow water. On the north shore of Shallow Bay, a poorly exposed mafic to intermediate unit with possible pillow structures is exposed (Fig. 6). The unit is about 1 m thick and can be traced for 20 m along strike.

Where contacts between the Shallow Bay "volcanics" and the Contwoyto Formation metasediments were observed, they appear to be conformable, and no evidence of dislocation between the two units was found. Thus although folding (see below) has undoubtedly caused structural repetitions of the stratigraphy, the interlayered nature of the sedimentary and volcanogenic rocks is believed to be primarily depositional.

Lhotka (1988) considered the Shallow Bay "volcanics" to be part of the Point Lake Formation (cf. Bostock, 1980). If this correlation is correct, the deposition of the Contwoyto and Point Lake formations must have overlapped in time, and the Shallow Bay "volcanics" may represent the last stages of Point Lake volcanism, as suggested by Bostock (1980).

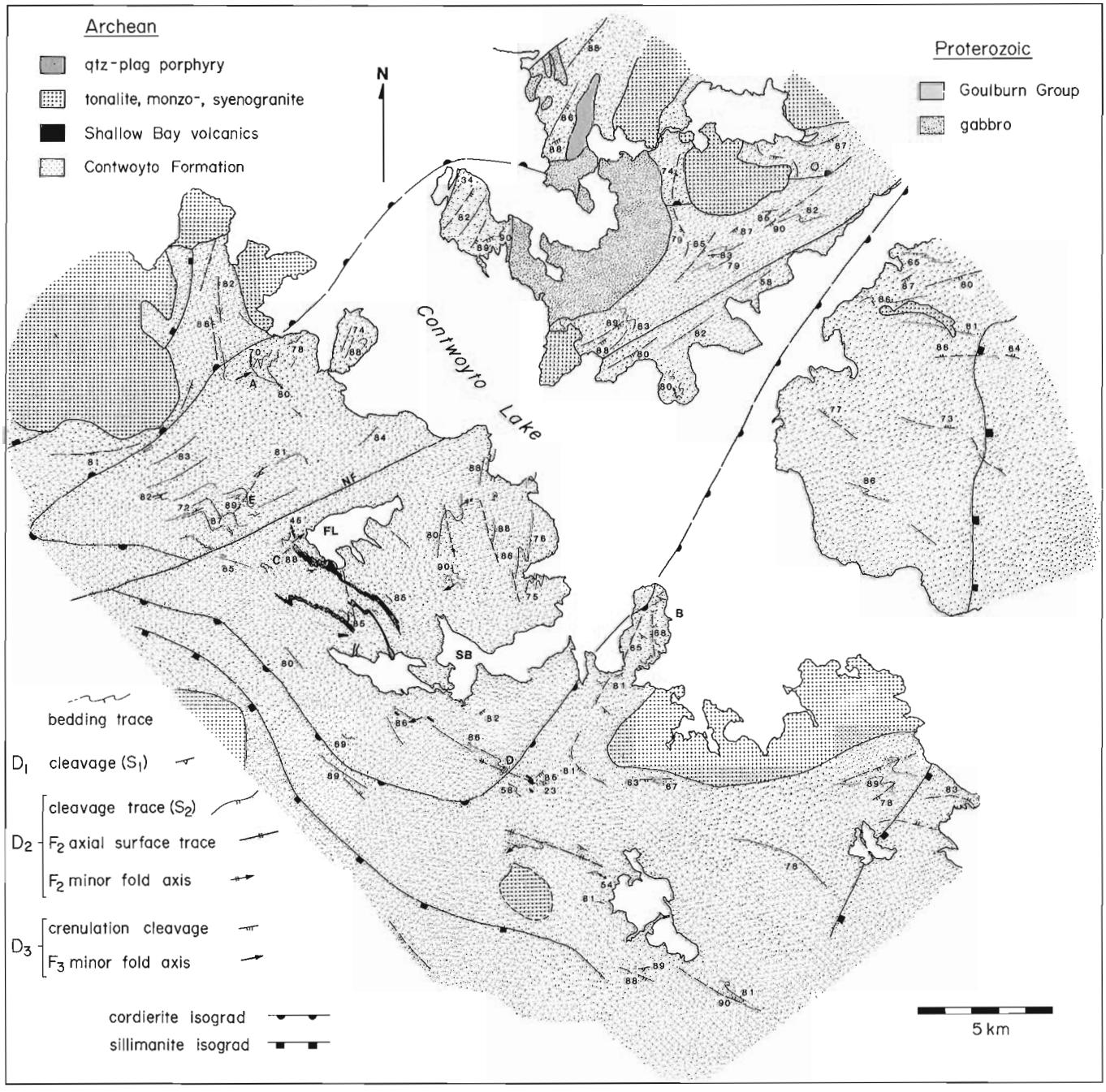

Figure 2. Simplified geology and structure of the western Contwoyto Lake area. SB = Shallow Bay, FL = Fingers Lake, NF = Norma Fault (Proterozoic).

The presence of the Shallow Bay "volcanics" within the Contwoyto Formation indicates that there was on-going volcanism during the deposition of the iron formation-bearing turbidites. Although the origin of the iron formation is not well understood, a genetic link with volcanic activity, as envisaged by Bostock (1980), Kerswill (1986) and others, appears likely. With only a few exceptions (e.g. the Lupin ore unit), volcanogenic or hypabyssal units were found stratigraphically within a few metres of iron formation horizons in the map area. Most are not traceable over strike lengths of more than 10 m, and commonly are less than 1 m thick. In a regional review of the Slave Province, McGlynn and Henderson (1970) noted that occurrences of iron formation are spatially associated with the interfaces between sedimentary and volcanic packages.

Locally there is a change in the character of the turbidites from greywacke (psammite) to shale (pelite) across horizons of iron formation (e.g. across the Lupin ore unit) (Bullis, 1988). Where observed, this facies change is confined to several metres on either side of the iron formation. However, this difference was not observed across every iron formation, and similar facies changes not spatially associated with iron formation were commonly observed. It is uncertain whether local changes in sedimentation were a factor in the deposition of the iron formation.

In the Contwoyto Lake area, supracrustal rocks are intruded by at least six phases of Archean plutons (Tremblay, 1976; Bostock 1980; King et al. 1988, 1989), and by two Proterozoic mafic intrusions (King et al., 1989).

DEFORMATION

Detailed structural analysis has resulted in modifications of the regional deformational history presented by King et al. (1988). King et al. (1989) described four generations of structures in the Yellowknife Supergroup metasediments (D1 to D4), the first of which involved early tilting or folding of the beds to account for the variable plunges of the early (D2) folds. D1 has now been excluded from the nomenclature, since the geometry of the deformed rocks does not require an early folding to produce the observed fold interference patterns. Variation in early fold plunges are interpreted to be the result of non-cylindrical folding due to heterogeneous strain. The revised structural nomenclature is therefore:

Figure 3. Intermediate volcaniclastic layers bearing lapilli-sized clasts in a chloritic matrix (Shallow Bay volcanics).

Figure 4. Volcaniclastic rock with clasts of diorite to quartz diorite, plagioclase phenocrysts, and aphanitic fragments of intermediate composition. This unit may be a debris flow (Shallow Bay volcanics).

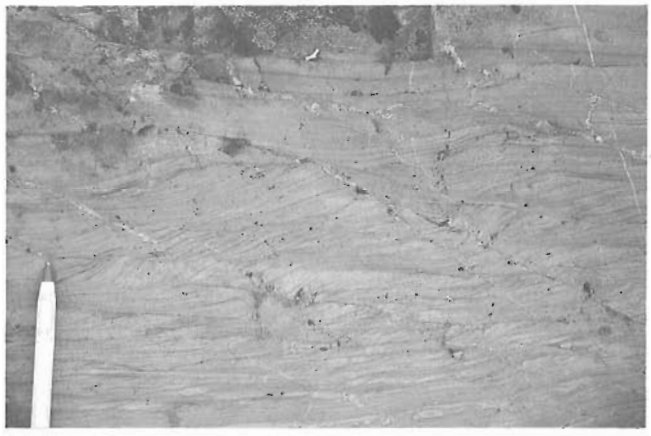

Figure 5. Cross laminations in a finely bedded felsic epiclastic unit (Shallow Bay volcanics).

Figure 6. Possible pillows in a fine-grained unit of mafic to intermediate composition (Shallow Bay volcanics).

D1 — pre-thermal-peak isoclinal folding and cleavage development; D2 — syn-thermal-peak isoclinal folding, associated faulting, and cleavage development; and D3 — post-thermal-peak, NE-trending, open folding and crenulation cleavage formation.

The iron formations are useful marker horizons in mapping the local stratigraphy and structure. However, their discontinuity along strike and the absence of penetrative tectonic fabrics within them limits their use in detailed structural analysis.

D1

F1 folds in the map area are tight to isoclinal, have steep axial planes and plunge moderately to steeply. F1 closures are rarely observed, but can be inferred from changes in facing direction or from bedding-cleavage relationships. The largest recognized F1 folds have wavelengths on the order of 100 m, and appear to dominate the F1 folding event. Higher order F1 closures with wavelengths from a few centimetres to several metres were observed locally.

Variations in plunge of about 30 to 40° were noted in F1 fold axes. Careful examination of the folds has revealed no fold closures or reversals of facing directions which require an earlier folding event to account for them. The variations in F1 fold plunges are therefore interpreted to be the result of non-cylindrical F1 folding.

F1 folding was accompanied by the formation of a penetrative cleavage (S1) defined by an alignment of biotite and muscovite. The S1 cleavage is commonly preserved in microlithons between S2 surfaces, or as inclusion trails in porphyroblasts of cordierite. S1 was not recognized in many localities. This may be due to: 1) domainal development of S1 (as previously noted by Fyson and Helmstaedt, 1988, in the southern Slave Province); or 2) transposition of S1 onto S2 such that S1 is indistinguishable from S2.

D2

F2 folds are the most obvious mesoscopic folds in the map area. They are tight to isoclinal, with steeply to moderately dipping axial planes and axes that plunge steeply down the dip of F1 fold limbs. The largest recognized F2 folds have wavelengths on the order of hundreds of metres. Smaller scale folds vary continuously from a few centimetres to 50 m in wavelength. The dominant F2 folds are a few metres in wavelength.

F2 folds were observed more commonly than F1 folds due to: 1) F2 folds having a smaller dominant wavelengths than F1 folds, and 2) F1 axial planes and S1 cleavage being folded into parallelism with the F2 axial plane in large domains, making their distinction difficult. An example of the latter occurs east of Fingers Lake (Fig. 2). This region is characterized by a sub-vertical, north-south striking cleavage (interpreted to be S2), and steeply dipping beds whose dominant strike is slightly clockwise from the cleavage, but which is locally counterclockwise. The interpreted fold pattern is one of steeply plunging Z-shaped F2 folds. No F1 closures or evidence of S1 cleavage were observed, but stratigraphic facing reversals from east to west on the long limbs of the folds suggest an earlier isoclinal folding event with an axial trace parallel to that of F2.

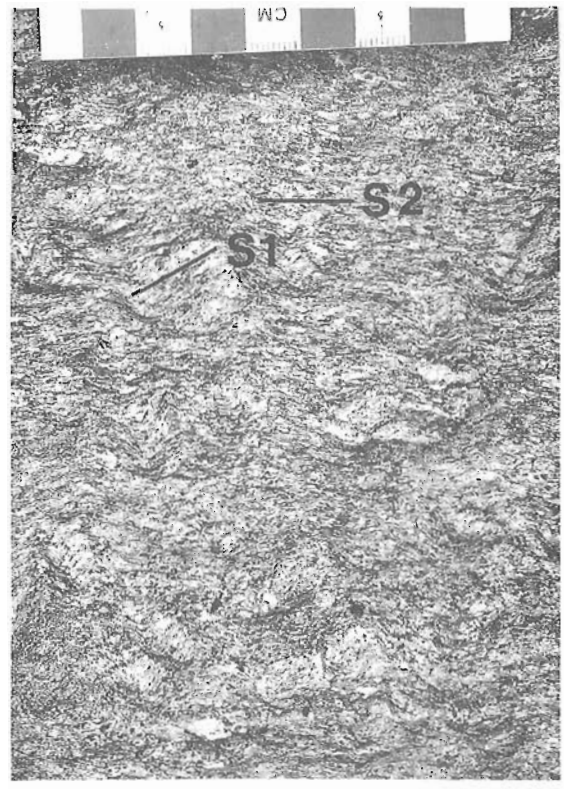

Figure 7. Metapelite from the cordierite zone with S2 cleavage in the matrix, and S1 preserved in cordierite porphyroblasts (counterclockwise from S2).

The axial planar cleavage to F2 folds (S2) is the dominant tectonic fabric in all metamorphic grades in the map area. In the biotite zone, S2 is morphologically identical to S1 and the two cleavages can only be distinguished where both are preserved and superposed. In the cordierite — andalusite zone, S2 is preserved in the matrix as a well developed, penetrative, biotite — muscovite crenulation or transposition cleavage along which cordierite is locally elongate down dip. S2 wraps around porphyroblasts, and locally is preserved within them as a very weakly developed crenulation of S1 inclusion trails (Fig. 7).

D3

The third episode of deformation was domainal, and produced crenulations of S2, open folds with wavelengths commonly less than one metre, but in places on the order of 10 m, and possibly macroscopic folds with kilometre scale wavelengths (King et al., 1989). F3 folds have steep to vertical axial planes with variable strikes between 010 and 080, with an average between 040 and 060. Their axes plunge down the limbs of pre-existing folds. In the biotite zone, F3 folds are generally recognized as open chevron folds of bedding and S2 cleavage, whereas above the cordierite isograd, F3 folds gently fold the S2 surface, and the hinge zones are rounded.

At the map scale, S2 surfaces define broad open folds. The curvature of S2 is particularly evident in Figure 2 around large plutons, where S2 is grossly parallel to the contact and curves around it. Macroscopic folds are also present in the area east of Contwoyto Lake (King et al., 1989), where no plutons have been mapped to date. It is possible that these large scale folds are related to D3, and their shape and distribution was locally controlled by the plutons.

Fold interference patterns

In the map area, there are extensive domains where the axial trace of F2 folds is parallel to the axial trace of F1 folds. Only in the vicinity of F1 hinge zones, where the axial traces of F1 and F2 are at high angles, do fold interference patterns between F1 and F2 become obvious. The interference patterns vary between Types 2 (mushroom-like) and 3 (coaxial) of Ramsay (1967).

Macroscopic superposed fold patterns are rare, the most notable being the "Lupin Structure" (R. Bullis, personal communication) (locality A, Fig. 2), which resembles a steep-sided dome that is open to the northeast. The interference pattern here is interpreted to be a Type 2 pattern (Fig. 8). The trace of the F1 axial plane is oriented east-northeast, while that of F2 is approximately north-south.

On the peninsula at locality B (Fig. 2), tight to isoclinal folds of bedding (interpreted as F1 since no folded cleavage was observed) with near-vertical, approximately east-west striking axial planes and steep to moderate east-plunging axes were observed. Farther south on the same peninsula, a steep, west-dipping north-south striking cleavage is axial planar to tight, steeply south-plunging folds of bedding and, locally, of S1 cleavage. Since both bedding and cleavage are folded, they are interpreted as F2 folds. Although no mesoscopic interference patterns of F2 on F1 were found

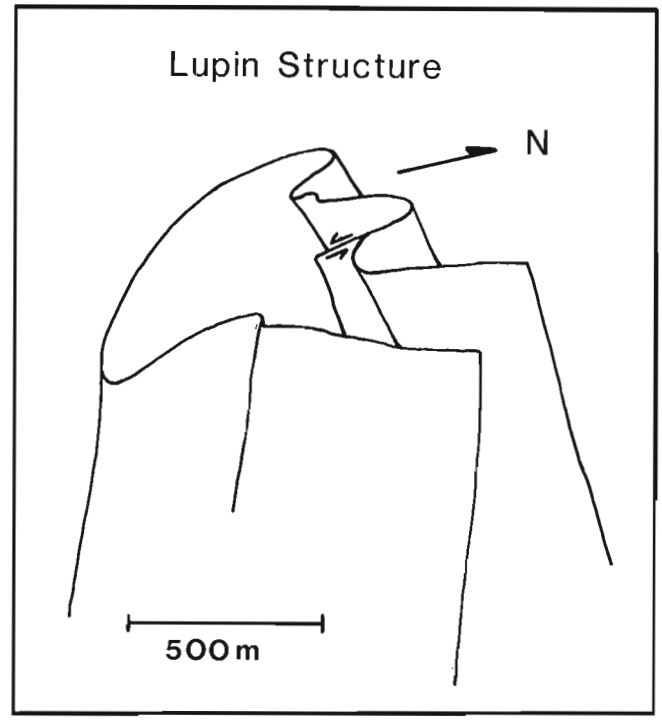

Figure 8. Sketch of the 3 dimensional shape of the Lupin Structure. Data from R. Bullis (pers. comm., 1988).

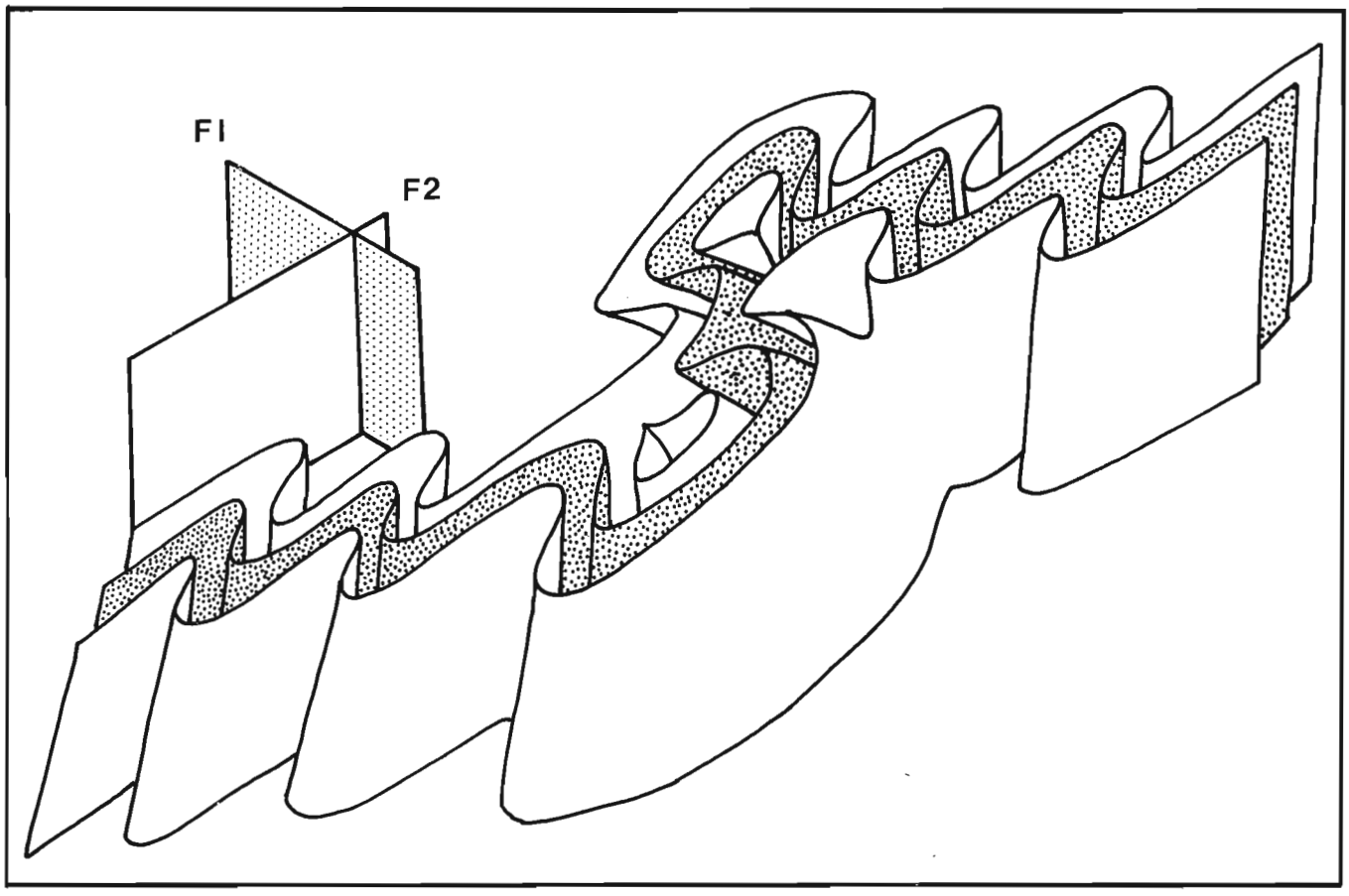

Figure 9. Schematic 3 dimensional diagram showing the geometry of a type 2 fold interference pattern, based in part on data from locality B, Figure 1. Note the similarity of parts of this geometry with that of the Lupin Structure (Fig. 8).

on the peninsula, the superposition of these two fold orientations yields a Type 2 interference pattern as illustrated in Figure 9. Perhaps the main part of the peninsula, where F2 folds are present, lies on a long limb of an F1 fold, in which case no small scale interference fold patterns would be observed due to the absence of F1 closures.

At localities C and D (Fig. 2), 10 m-scale type 3 interference patterns were mapped (Fig. 10). F1 and F2 fold axes are subparallel here, and their axial planes are at a high angle (Fig. 11). Small scale type 3 interference patterns were observed as well, in a number of localities (Fig. 12).

F3 folds do not significantly change the mesoscopic F1-F2 interference patterns.

METAMORPHISM

The cordierite and sillimanite isograds mapped in the area separate three metamorphic zones: the biotite zone, the cordierite zone, and the sillimanite zone (Fig. 2). Andalusite occurs in the cordierite zone, and its first appearance coincides closely with that of cordierite. Staurolite occurs locally within the cordierite zone, but its presence is greatly dependent on the bulk composition of the protolith, and thus a staurolite isograd could not be mapped.

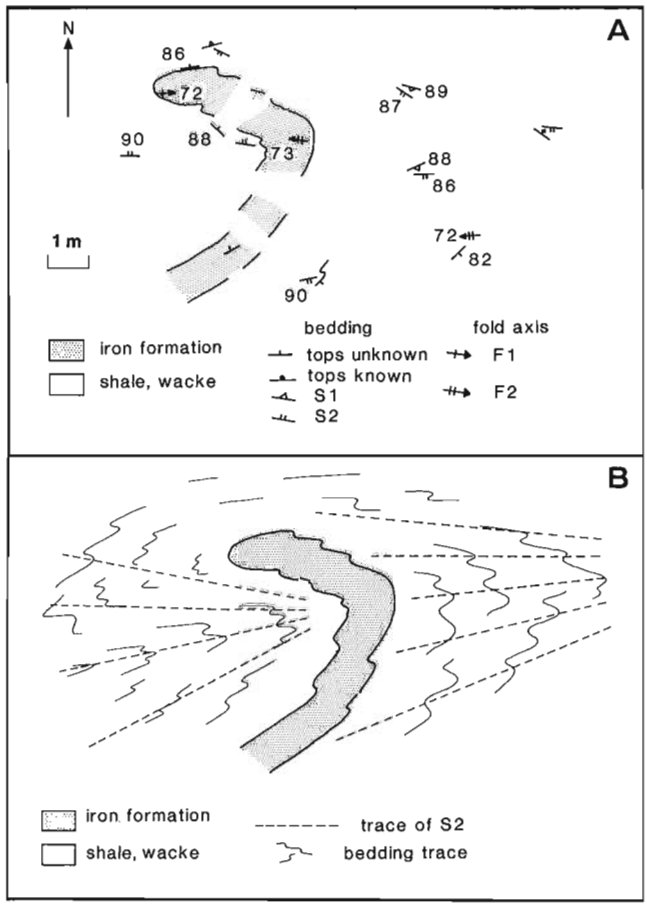

Figure 10. Type 3 fold interference pattern from locality D on Figure 2: A) field data, B) interpretation of the shape of the fold and pattern of axial planar cleavage.

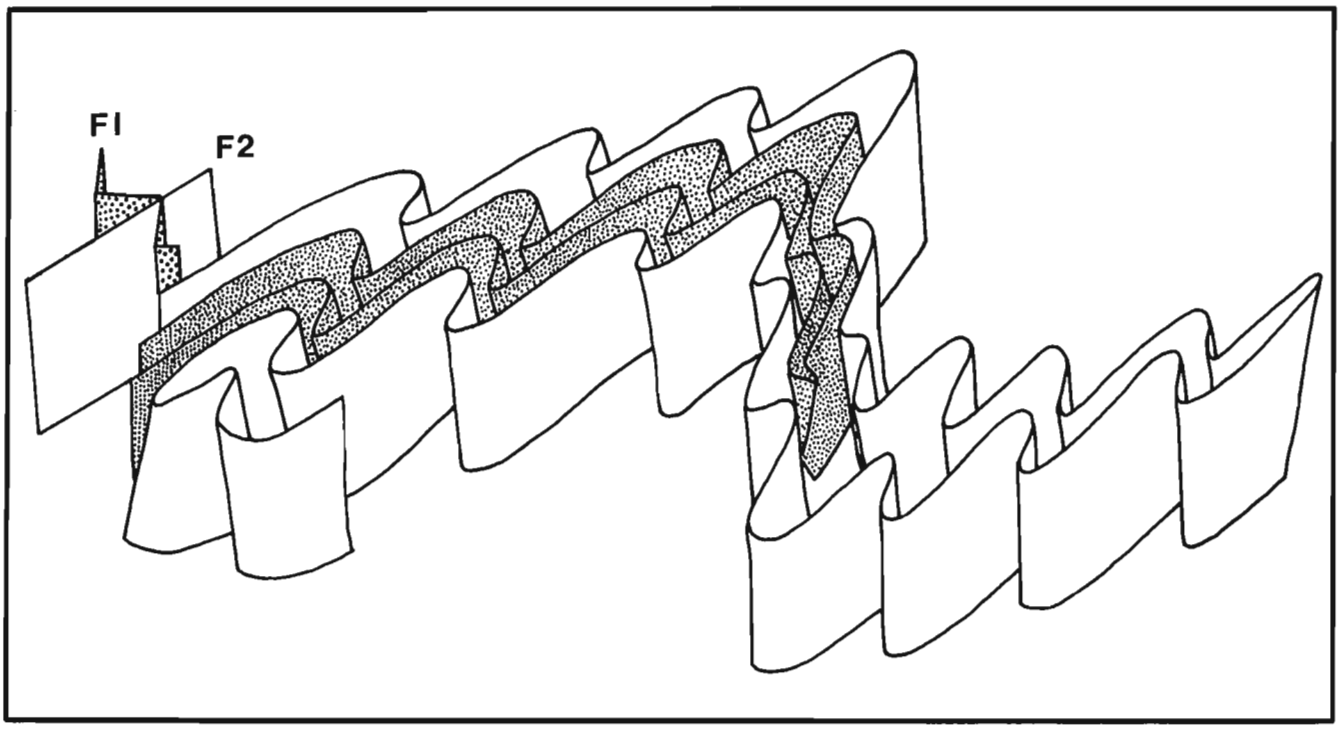

Figure 11. Schematic 3 dimensional diagram showing the geometry of a type 3 fold interference pattern, based in part on data from locality E, Figure 1.

The isograds define a closed loop (Fig. 2), outlining a thermal low centred on Contwoyto Lake southeast of Lupin. On a more regional scale (see King et al., 1989) the isograds define a series of irregular domes and basins, suggesting that they are regionally undulating surfaces. Since D3 and Proterozoic deformation (King et al., 1989) postdate metamorphism, the topology of the isograd surfaces has undoubtedly been influenced by these events.

Within the biotite zone, biotite porphyroblasts overgrow the S1 cleavage, and are themselves slightly crenulated by S2, implying growth during D2. Above the cordierite isograd, S1 cleavage is most commonly preserved as inclusion trails of mica within the cordierite porphyroblasts. S2 wraps around the cordierite grains, and is commonly expressed as a weak crenulation of inclusion trails within the porphyroblasts. Cordierite and sillimanite lie in the S2 cleavage planes, and commonly show a preferred linear alignment roughly down dip. These textures indicate that the thermal peak coincided with D2 deformation, with final mineral equilibration occuring after the start of S2 cleavage formation. D1 and D3 accompanied a regional low (biotite) grade metamorphism (Fig. 13).

Mineral assemblages and reaction textures documented in the field indicate that metamorphism was high T/low P. The assemblage andalusite — cordierite — staurolite — biotite — muscovite — quartz (at B in Fig. 2) lies within the cordierite zone, and is stable within bathozone 2 of Carmichael (1978), implying P between 2.2 and 3.3 kbar. Staurolite is preserved in the cores of andalusite crystals, suggesting that andalusite grew at the expense of staurolite by the following reaction:

$$\text{staur} + \text{musc} + \text{cord} \rightleftharpoons \text{bio} + \text{and} + \text{water}.$$

In bathozone 2 this reaction takes place at about 500 to 520°C, and 2.5 to 3.0 kbar (Carmichael et al., 1987).

Cordierite — garnet — biotite — muscovite were also found to coexist in the cordierite zone. This assemblage occurs sporadically in the cordierite zone south of Fingers Lake, and on the east side of Contwoyto Lake north of the Norma Fault. It is also stable in bathozone 2 (Carmichael, 1978). Temperatures in biotite grade rocks probably did not exceed about 450°C (Carmichael et al., 1987), and the first appearance of sillimanite probably occurred at approximately 525°C, based on the Holdaway aluminosilicate triple point (Holdaway, 1971).

QUARTZ VEINS

Four generations of Archean quartz veins and one generation of Proterozoic veins have been distinguished in the metasediments. They have been classified on the basis of relative timing of emplacement: Type 1) pre- to syn - D1, Type 2) syn - D2, Type 3) late -syn to post - D2, Type 4) syn - D3 veins, and Type 5) Proterozoic veins. The second and third groups are further subdivided based on orientation, style and extent of deformation.

The bulk of the quartz veins range in thickness from less than 1 mm to about 4 cm, with an average between 2 and 3 mm. Types 2a and 3b veins up to 60 cm in width were observed locally. Quartz veins cut the sediments at all metamorphic grades, with no apparent spatial relationship to any plutons. Thus the quartz is interpreted to have been derived

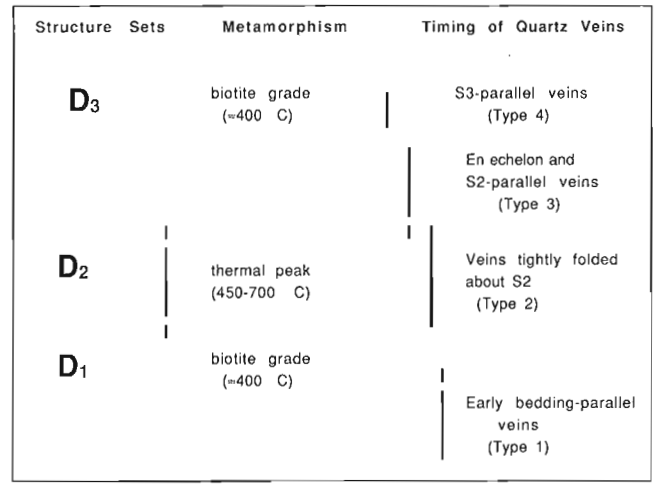

Figure 13. Qualitative summary of relative timing between structure sets, metamorphism and quartz veins types.

Figure 12. Small scale type 3 fold interference pattern in graded metaturbidites from locality E on Figure 1.

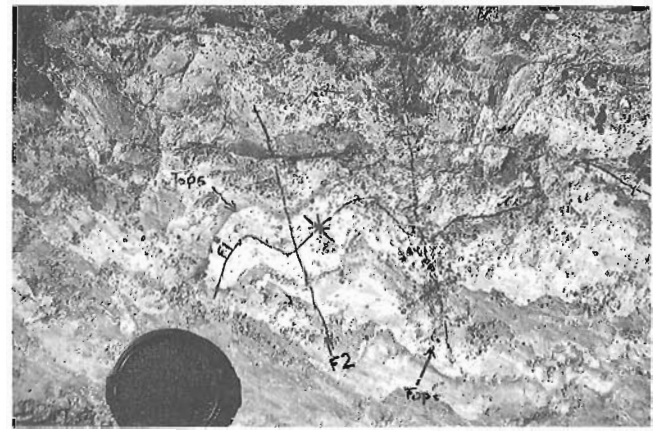

Figure 14. Type 1 quartz vein hosted in metapelite, folded by F1 and F2.

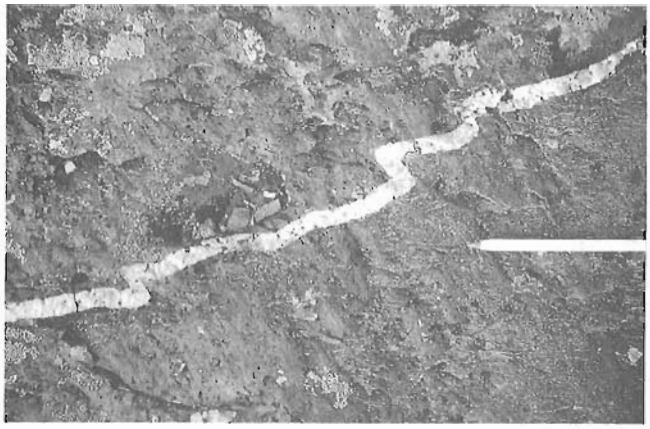

Figure 15. Type 2b quartz vein hosted in metapelite, folded about S2 with an "S" asymmetry.

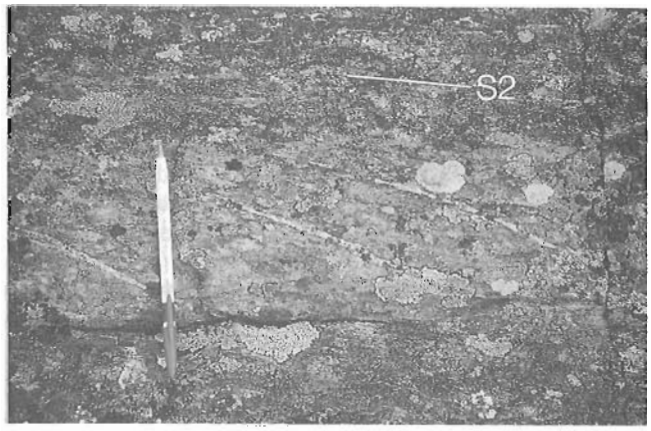

Figure 16. Type 3b en echelon quartz veins confined to a sandy layer within mixed sandy and shaly beds.

in large part from fluids associated with regional metamorphism (cf. Yardley, 1986), rather than locally from magmatic fluids generated by cooling plutons.

Type 1

In a few localities, bedding-parallel quartz veins have been involved in F1 (and F2) folds (Fig. 14). These veins are therefore interpreted to have intruded pre- to syn - D1. Their emplacement was likely controlled by the anisotropy associated with compositional layering. As discussed previously,there are domains where bedding, S1 and S2 are subparallel, and in these areas, early (Type 1) bedding parallel veins cannot be distinguished from later veins whose emplacement was controlled by the cleavage.

Type 2

Type 2 veins have been variably deformed by F2 folding, as well as F3. The majority of quartz veins are classified as Type 2, and their emplacement accompanied peak thermal conditions in the area. Type 2 veins have been subdivided further:

Type 2a

Type 2a veins parallel the S2 cleavage, and have been pinched and swelled along S2, with local boudinage. Their emplacement was controlled by the S2 cleavage, and subsequent shortening across this plane during D2 resulted in their extension. It is possible, however, that some of these veins are earlier (Type 1) veins which have subsequently been transposed onto the S2 plane and extended.

Type 2b

Type 2b veins are tightly to isoclinally folded about S2. Veins whose enveloping surfaces are clockwise to S2 define "Z" folds about S2, while counterclockwise veins define "S" folds (Fig. 15). Type 2b veins oriented orthogonally to S2 form tight "M" folds (Fig. 16). The symmetric distribution of these veins about S2 suggest that their intrusion coincided with D2. Several examples of isoclinally folded veins with boudinaged limbs were observed. These veins would be classified as a combination of Types 2a and 2b.

Type 3

Type 3 veins, interpreted to be late syn- to post-D2, have undergone little or no D2 strain, but all of the D3 strain. They have been subdivided into two groups:

Type 3a

Type 3a veins lie in the S2 cleavage plane and are not apparently deformed. Their coincidence with S2 suggests that their emplacement was controlled by this cleavage, but the lack of visible D2 strain within them restricts their formation to latest-syn- to slightly post-D2.

Type 3b

Type 3b veins define en echelon arrays oriented at a high angle to S2, which have seen little or no D2 deformation, and thus are believed to be late syn- to post-D2. They are generally confined to more competent layers such as iron formation and sandy beds within the turbidite sequence (Fig. 16). The large (0.5 m) quartz veins with arsenopyrite haloes cutting the Lupin Structure are interpreted to belong to Type 3b, because they have a constant orientation relative to F2 folds, and in places are slightly buckled about F2.

Type 4

Veins classified as Type 4 intrude parallel to the axial planes of F3 folds, and locally along S3 cleavage planes, and therefore are interpreted to be syn - D3 in age. These veins are generally very thin (less than 5 mm), and are sparsely and sporadically distributed.

Type 5

A fifth set of quartz veins are associated with Proterozoic faulting in the area (King et al., 1988; 1989). These veins are distinguished from Archean veins by their unrecrytallized texture.

Stokes et al. (1988) classified turbidite-hosted quartz veins near Gordon Lake, N.W.T., and Fyson (1987) has worked extensively with quartz veins in metasediments near Yellowknife. In both studies, veins were classified according to orientation, morphology, and/or interpreted chronology of emplacement. A comparison of vein types from the present study to those of Stokes et al. (ibid.) and Fyson (ibid.) reveals a number of similarities in the histories of vein emplacement and deformation in different parts of the Slave Province.

SUMMARY

In summary, the presence of the Shallow Bay "volcanics" within the Contwoyto Formation demonstrates that volcanic activity accompanied deposition of the turbidites and the iron formation in the Contwoyto Formation.

Two sets of tight to isoclinal folds were recognized which, in their present orientation, define types 2 and 3 fold interference patterns (Ramsay, 1967). A third folding event has locally "crinkled" the layers at the mesoscopic scale, and may have altered the map pattern on a regional scale.

Quartz veins can be subdivided into five groups based on the timing of their emplacement: Type 1 veins are pre- to syn-D1, Type 2 are syn-D2, Type 3 are late syn- to post-D2, Type 4 are syn-D3, and Type 5 are Proterozoic. The most important veins volumetrically have been classified as Type 2. The quartz veins which cut the Lupin ore unit and are spatially associated with arsenopyrite and gold are classified as Type 3b.

Implications for gold exploration

Results of this study which may be of specific interest to gold exploration in the area include the following:

1. The delineation of a volcanogenic package within the Contwoyto Formation lends additional support to the concept of a genetic link between volcanic activity and the presence of iron formation, as postulated by Bostock (1980), Kerswill (1986), and others. Locally, a change in sedimentary facies may have controlled the deposition of the iron formation as well.
2. The role that quartz veins play in gold mineralization is currently under debate (Kerswill, 1986; Lhotka and Nesbitt, 1987; Lhotka, 1988), although the spatial association of gold with "late" (Type 3b) quartz veins is undisputed. The criteria used to classify these quartz veins may be useful in identifying similar veins which may be associated with gold mineralization elsewhere.
3. The distribution of all vein types appears to be unrelated to the distribution of plutons. Hence gold associated with quartz veins is not interpreted to be related to any of the plutons exposed in the area.
4. Systematic structural mapping has shown that the geometry of the fold interference pattern is predictable, and therefore individual iron formation horizons may be followed by careful examination of the fabrics preserved in the adjacent sediments.

ACKNOWLEDGMENTS

The author wishes to express thanks to Anne Seguin for her cheerful assistance in mapping the sediments. Janet King provided outcrop consultations and acted as a sounding board for evolving ideas. Numerous discussions with exploration geologists, in particular Ralph Bullis of Echo Bay Mines, helped to locate key outcrops and provided structural data in the third dimension. B. Davis is thanked for discussions on volcanic rocks, and Janien Schwarz for her cooking. D. M. Carmichael is thanked for helpful discussion on the metamorphic assemblages. J. King, H. Helmstaedt, S. Tella, J. Percival and J. Kerswill critically reviewed and improved the manuscript. Rod Stone and Lynn Parney provided efficient and friendly expediting services from Yellowknife.

REFERENCES

Bostock, H.H.
1980: Geology of the Itchen Lake area, District of Mackenzie; Geological survey of Canada, Memoir 391.

Bullis, H.R.
1988: The geology of Lupin; The Northern Miner Magazine, August, 1988, p. 20-21.

Carmichael, D.M.
1978: Metamorphic Bathozones and Bathograds: a measure of the depth of post-metamorphic uplift and erosion on the regional scale; American Journal of Science,v. 278, p. 769-797.

Carmichael, D.M., Helmstaedt, H.H. and Thomas, N.
1987: A field trip in the Frontenac Arch with emphasis on stratigraphy, structure and metamorphism; meeting of Friends of the Grenville, Ganaoque, Onario, 1987, 24p.

Fraser, J.A.
1964: Geological notes on northeastern District of Mackenzie, Northwest Territories; Geological Survey of Canada, Paper 63-40.

Fyson, W.K.
1987: A succession of quartz veins in Archean metaturbidites, Yellowknife Bay, Slave Province; Canadian Journal of Earth Sciences, v. 24, p. 698-710.

Fyson, W.K. and Helmstaedt, H.
1988: Structural patterns and tectonic evolution of supracrustal domains in the Archean Slave Province, Canada; Canadian Journal of Earth Sciences, 25, p.301-315.

Gardiner, J.G.
1986: Structural geology of the Lupin gold mine, Northwest Territories. M.Sc. thesis, Acadia University, Nova Scotia, 206 p.

Henderson, J.B.
1970: Stratigraphy of the Archean Yellowknife Supergroup, Yellowknife Bay-Prosperous Lake area, District of Mackenzie; Geological Survey of Canada, Paper 70-26.

Holdaway, M.J.
1971: Stability of andalusite and the aluminosilicate phase diagram; American Journal of Science, v. 271, p. 97-131.

Kerswill, J.A.
1986: Gold deposits hosted by iron formation in the Contwoyto Lake area, Northwest Territoies; in Poster Volume, An International Symposium on Geology of Gold Deposits, Gold '86, ed. by A.M. Chatter, Toronto, Ontario, p. 82-85.

King, J.E., Davis, W.J., Relf, C., and Avery, R.W.
1988: Deformation and plutonism in the wetern Contwoyto Lake area, Central Slave Province, District of Mackenzie, N.W.T.; in Current Research Part C, Geological Survey of Canada Paper 88-1C, p. 161-176.

King, J.E., Davis, W.J., Van Nostrand, T., and Relf, C.
1989: Archean to Proterozoic deformation and plutonism of the western Contwoyto Lake map area, central Slave Province, District of Mackenzie, N.W.T.; in Current Research, Part C, Geological Survey of Canada, Paper 89-1C.

Lhotka, P.G.
1988: Geology and geochemistry of gold-bearing iron formation in the Contwoyto Lake region, Northwest Territories, Canada; Ph.D. thesis, University of Alberta, Edmonton, 223 p.

Lhotka, P.G. and Nesbitt, B.E.
1987: Epigenetic gold hosted by iron formation at the Lupin mine, Contwoyto Lake, N.W.T.; Geological Association of Canada, Program with Abstracts, Yellowknife '87.

McGlynn, J.C. and Henderson, J.B.
1970: Archean volcanism and sedimentation in the Slave Structural Province; in Symposium on Basins and Geosynclines of the Canadian Shield, ed. by A.J. Baer, Geological Survey of Canada, Paper 70-40, p. 31-44.

Ramsay, J.G.
1967: Folding and Fracturing of Rocks; McGraw-Hill Inc., New York, 568 p.

Stokes, T., Culshaw, N., and Zentilli, M.
1988: Structural mapping of the Gordon Lake "refold", N.W.T.: a model for the focussing of late-stage, gold-bearing quartz breccia-vein systems; Part of Canada-N.W.T. Mineral Development Agreement, Open File Report, I.N.A.C. Geology Division, Yellowknife, E.G.S. 1988-4, 23 p.

Tremblay, L.P.
1976: Geology of northern Contwoyto Lake area, District of Mackenzie; Geological Survey of Canada, Memoir 381.

Yardley, B.W.D.
1986: Fluid migration and veining in the Connemara Schists, Ireland; in Fluid-Rock Interactions During Metamorphism; ed. by J.V. Walther and B.J. Wood; Advances in Physical Geochemistry v. 5, Springer-Verlag, New York, p. 109-131.

Sequence stratigraphy, correlations between Wopmay Orogen and Kilohigok Basin, and further investigations of the Bear Creek Group (Goulburn Supergroup), District of Mackenzie, N.W.T.

J.P. Grotzinger[1], R.D. Adams[1], D.S. McCormick[2], and P. Myrow[3]
Lithosphere and Canadian Shield Division

Grotzinger, J.P., Adams, R.D., McCormick, D.S., and Myrow, P., Sequence stratigraphy, correlations between Wopmay Orogen and Kilohigok Basin, and further investigations of the Bear Creek Group (Goulburn Supergroup), District of Mackenzie, N.W.T.; in Current Research, Part C, Geological Survey of Canada, Paper 89-1C, p. 107-119, 1989.

Abstract

Results indicate that the Rifle, Beechey, Link, and basal Burnside Formations are correlative with the lower member of the Odjick Formation (Coronation Supergroup). The lower Burnside Formation is also correlative with the middle member of the Odjick Formation. Correlatives of the Hackett Formation and Kimerot Group are not present in the Coronation Supergroup. In the Tinney Hills area the Rifle Formation is divided into four sequences.

The marine to alluvial transition in the north Tinney Hills is characterized by three main associations of facies which represent storm-influenced marine shelf, lower delta slope, and upper delta slope. Additionally, studies of areally extensive conglomerate intervals indicate transport of gravel across the entire Slave craton, in excess of 200 km. This requires a fundamental change in the distribution of subsidence across the basin. Areally-extensive conglomerates indicate reduced subsidence rates in the proximal part of the basin. The transition from lower Burnside Formation deltaic and distal alluvial facies to gravelly proximal alluvial facies probably records a shift from subsidence-dominated foreland sedimentation to erosion- and uplift-dominated sediment redistribution.

Résumé

Les résultats indiquent que les formations de Rifle, de Beechey et de Link ainsi que la formation de base de Burnside sont en corrélation avec le membre inférieur de la formation d'Odlick (supergroupe de Coronation). La partie inférieure de la formation de Burnside est également en corrélation avec le membre central de la formation d'Odjick. Des indications de corrélation entre la formation de Hackett et le groupe de Kimerot ne sont pas présentes dans le supergroupe de Coronation.

La transition des dépôts marins aux dépôts alluviaux dans la partie septentrionale des collines Tinney est caractérisée par trois grandes associations de faciès représentant la plate-forme marine influencée par les tempêtes, le talus inférieur du delta et le talus supérieur du delta. De plus, des études d'intervalles étendus de conglomérat indiquent qu'il y a eu transport de gravier en travers de tout le craton des Esclaves, soit sur plus de 200 km. Cela exige une modification fondamentale de la répartition de la subsidence dans l'ensemble du bassin. Les conglomérats occupant une grande superficie indiquent des taux de subsidence réduits dans la partie proximale du bassin. La transition des faciès deltaïques et alluviaux distaux de la partie inférieure de la formation de Burnside aux faciès alluviaux proximaux graveleux marque probablement une évolution de la sédimentation d'avant-pays dominée par la subsidence en une redistribution des sédiments dominée par l'érosion et le soulèvement.

[1] Department of Earth, Atmospheric, and Planetary Sciences, Massachusetts Institute of Technology, Cambridge, Mass. 02139
[2] Lamont-Doherty Geological Observatory of Columbia University, Palisades, N.Y. 10964
[3] Department of Geology, Colorado College, Colorado Springs, Co. 80903

INTRODUCTION

Several projects were finished during the field season of 1988. These are discussed on a topical basis and include: 1) correlation of stratigraphic units in the Bear Creek Group, as determined on both a formational and sequence stratigraphic basis, from Kilohigok Basin to the autochthon of Wopmay Orogen (JPG); 2) identification and correlation of sequence stratigraphic units in the Rifle Formation(JPG, RDA, PM); and 3) description and interpretation of the marine-alluvial facies transition in the Burnside Formation, and stratigraphic relations within its lower part (DSM).

STRATIGRAPHIC CORRELATIONS BETWEEN KILOHIGOK BASIN AND WOPMAY OROGEN

A complete transect of the Bear Creek Group has been mapped from the Bear Creek Hills to the northern Tinney Hills along the east side of Bathurst Inlet, and from the Western River to Contwoyto Lake. These two outcrop belts are separated by the Bathurst Fault which has approximately 135 km of sinistral slip (Fig. 1). In addition to the mapping, sections were measured along the two transects, as well as at Rockinghorse outlier and in the autochthon of Wopmay Orogen. Figure 2 shows the correlations (palinspastic) between the Bear Creek Group and the lower Odjick Formation in the autochthon of Wopmay Orogen at the north end of Takijuq Lake. The 15 sections that form the basis for this figure were measured on a bed-by-bed basis, and then condensed to generate summary sections that illustrate first-order stratigraphic features.

All stratigraphic units thicken toward the southeast (palinspastic) corner of the basin (Fig. 2). Section 15 is located at the north end of the Tinney Hills and it should be noted that equivalent sections at the southern Tinney Hills and Bear Creek Hills are approximately twice as thick, and therefore not plottable at the scale chosen for this paper. For the most part, formation boundaries are equivalent to sequence boundaries, and therefore closely approximate time slices (sensu Van Wagoner et al., 1987)

Across the Slave craton, all units thin over the Gordon Bay Arch, culminating in major downcutting of the Burnside Formation fluvial units, and thicken again into the Wolverine Canyon area (Fig. 2). This indicates that the Gordon Bay arch was a continually active feature throughout all of Bear Creek Group time. Continuing to the west, the lowermost units (e.g. Hackett Formation) thicken toward the Rockinghorse area, intermediate units (e.g. Beechey and Link formations) show no significant changes in thickness, and uppermost units (e.g. Burnside Formation) thin significantly and cut down into older units. This suggests that this area evolved from intial low subsidence, to no net subsidence, to a positive arch area later on. Toward the Takijuq area, older units (e.g. correlatives of Hackett Formation) were initially not deposited or have been removed by arching of this area during deposition of the equivalents of the lower Rifle Formation. Uppermost units (e.g. probable upper Rifle through Burnside equivalents) thicken markedly relative to the Rockinghorse area. This suggests that the Takijuq area initially was a positive arch area (Hackett and lowermost Rifle time) evolving to a rapidly subsiding area with time (upper Rifle through Burnside time).

Several statements can be made concerning the correlations between Wopmay Orogen and Kilohigok Basin. First, equivalents of the Hackett Formation are missing in the Takijuq Lake area (Fig. 2). Second, the base of the Coronation Supergroup in the Takijuq Lake area is almost coincident with the condensed interval of the lower Rifle Formation. This is probably the best time line between basins and allows a high degree of confidence to be assigned to these correlations. Third, the middle Odjick Formation is almost certainly correlative with the lower Burnside Formation.

Given the correlations presented in Figure 2 and the several ash beds which have been found at critical stratigraphic levels (Fig. 2), it should be possible to erect a calibrated chronostratigraphy between the lower Coronation Supergroup and Bear Creek Group. Inital results of U-Pb zircon dating on ash beds suggest that the age of the lower Hackett Formation (section 15; Fig. 2) may be 1.95-1.97 Ga (S.A. Bowring, pers. comm., 1988), and that the Link Formation (section 6; Fig. 2) is on the order of 1.93 Ga (Bowring and Grotzinger, in press). An ash bed collected at section 12 (Fig. 2) lies on the contact between the upper Rifle and Beechey formations, and although not yet dated, it should be on the order of 1.94-1.95 Ga. If correct, then this would potentially date the timing of onset of passive margin subsidence in Wopmay Orogen. Note that this boundary continues into Wopmay Orogen (section 1), where it most likely correlates with the top of a coarsening-

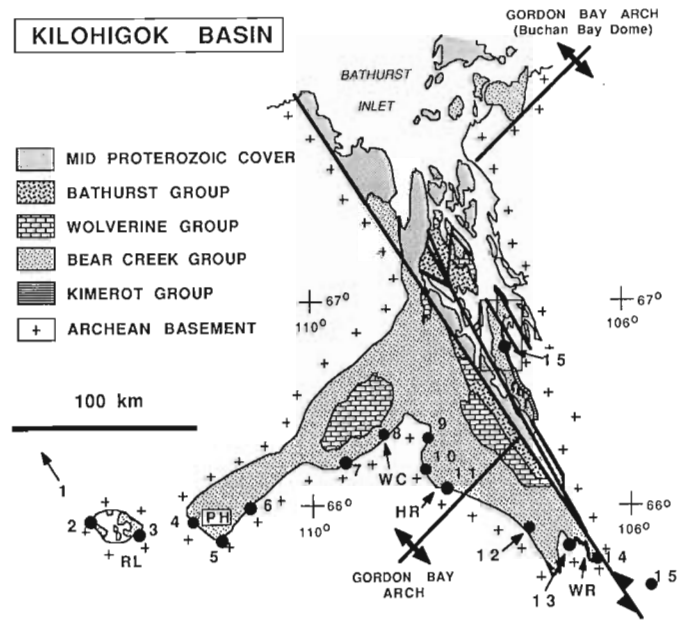

Figure 1. Location map of measured sections shown in Figure 2. Kilohigok Basin is shown without palinspastic restoration for movement along the Bathurst Fault. 15* marks the palinspastic location of section 15 which is palinspastically positioned in Figure 2. Section 1 is located at the north end of Takijug Lake, approximately 95 km due northwest of sections 2 and 3. The box marks the location of the map shown in Figure 3. RL, Rockinghorse Lake; PH, Peacock Hills; WC, Wolverine Canyon; HR, Hackett River; WR, Western River.

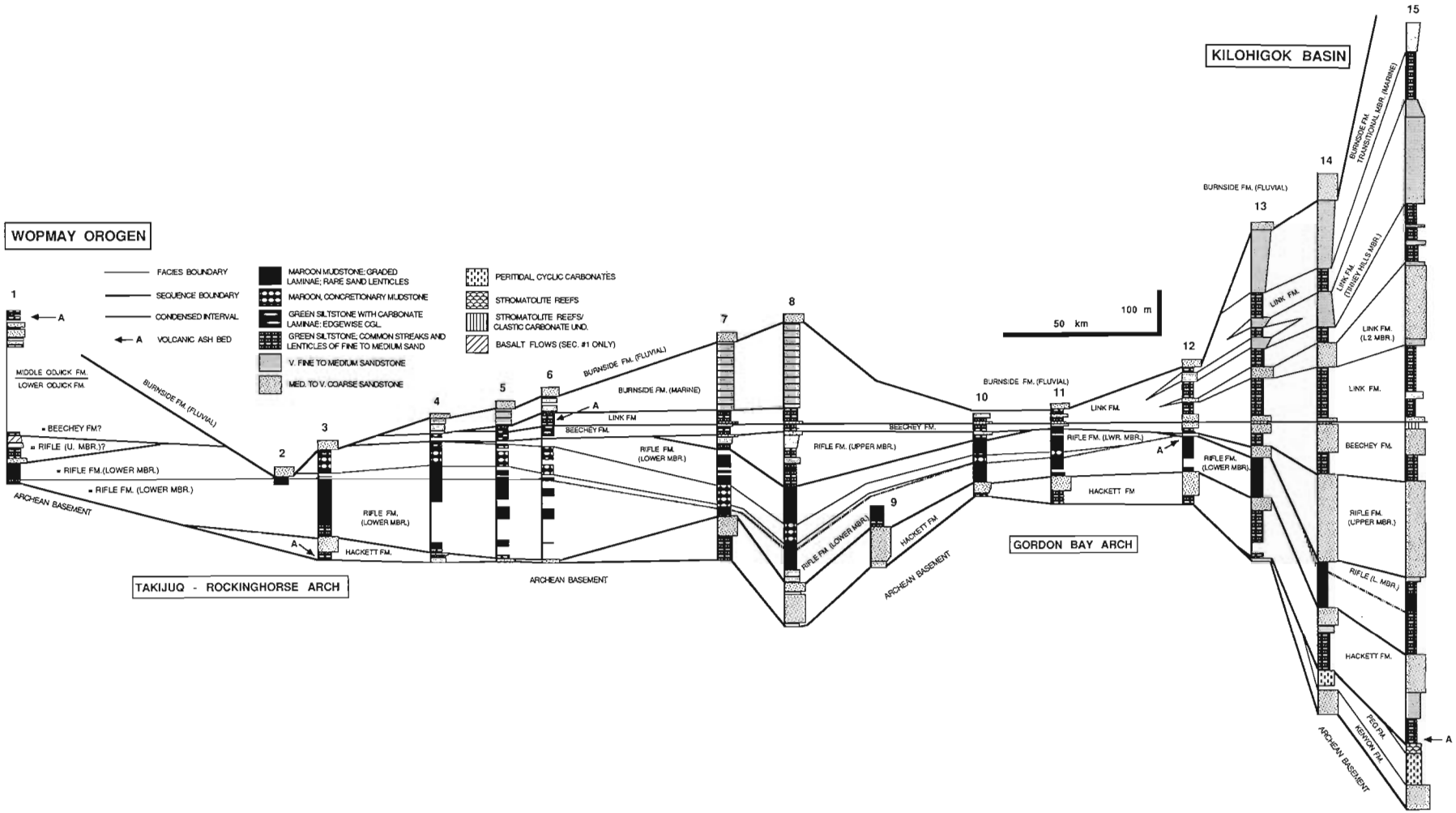

Figure 2. Stratigraphic correlations between Bear Creek Group (Kilohigok Basin; sections 4-15); Rockinghorse Outlier; sections 2,3) and lower Coronation Supergroup (Odjick Formation; Wopmay Orogen; section 1). Section 1 is located at the north end of Takijug Lake, approximately 95 km due northwest of sections 2 and 3.

upward sequence that culminates in a 20-m-thick section of basalt flows. Rapid subsidence is demonstrated by units above this level, consistent with the initiation of thermal (passive) subsidence.

The ramifications of the correlations combined with U-Pb zircon dating are manifold. These involve the interpretation and temporal calibration of major events in both Wopmay Orogen and Thelon Tectonic Zone, the establishment of geodynamic and temporal links between the two, and the quantitative assessment of early Proterozoic lithospheric rheology. Manuscripts are in preparation by J.P. Grotzinger and S.A. Bowring concerning these issues.

SEQUENCE STRATIGRAPHY OF RIFLE FORMATION IN THE TINNEY HILLS AREA

Sequence stratigraphy overview

The concepts of sequence stratigraphy (Vail, 1987) provide a new way of organizing and analyzing stratigraphic and facies data from sedimentary rocks in a chronostratigraphic framework that can be used in strata where no biostratigraphic control is present. Much of the terminology used in this section is defined in Van Wagoner, et al. (1987) and Vail (1987). The following discussion is to be read in conjunction with Figures 3 and 4.

In the Tinney Hills area the Rifle Formation is divided into four sequences with sequence boundary I, the oldest boundary in the Rifle, essentially at the Rifle/Hackett formation boundary and the associated sequence I, encompassing the lower Rifle siltstones and the lower Rifle sandstones (Fig. 3,4). Sequence I has the greatest preserved thickness of sediments in the Rifle Formation and is essentially a complete sequence with lowstand, transgressive and highstand systems tracts represented, though lowstand sands are missing from this area. This relative completeness may reflect an influence on sedimentation controlled primarily by eustatic sea level with any tectonic influence simply augmenting the eustatic signature. In this case the combined signature of eustasy and tectonics is to create accommodation through a relative rise in sea level.

Sequences II and III are wholly within the upper Rifle sandstones and are much thinner than sequence I. Sequence II is made up mostly of highstand deposits with very thin lowstand and transgressive deposits. The bulk of the sandstones in these two systems tracts was probably deposited away from the area of the Tinney Hills outcrops, with the lowstand sediments farther to the south (basinward) and the transgressive sediments farther to the north (toward Gordon Bay Arch). The thin total thickness and the large lateral distances between deposits are probably the result of a stronger tectonic influence on sedimentation interfering with a pure eustatic signature coupled with sedimentation in an area of very low topographic gradient. The effect of the combined tectonic and eustastic signal was to create very little accommodation resulting in thin preserved deposits.

In sequence III the only lowstand sandstones preserved in this area are fluvial sediments filling an incised valley. The incised valley is at least 40 m deep and less than 6 km wide and was cut by sequence boundary III into the highstand units of sequence II during the fall in sea level that created the sequence boundary. Lowstand nearshore marine sandstones are probably located to the south (basinward). The transgressive systems tract has several parasequences but is cut into by sequence boundary IV which has also eroded away all of the sequence III highstand deposits. In this sequence eustasy alone can explain the distribution of lowstand and transgressive deposits and tectonics may have only contributed to the large fall of sea level that created sequence boundary IV.

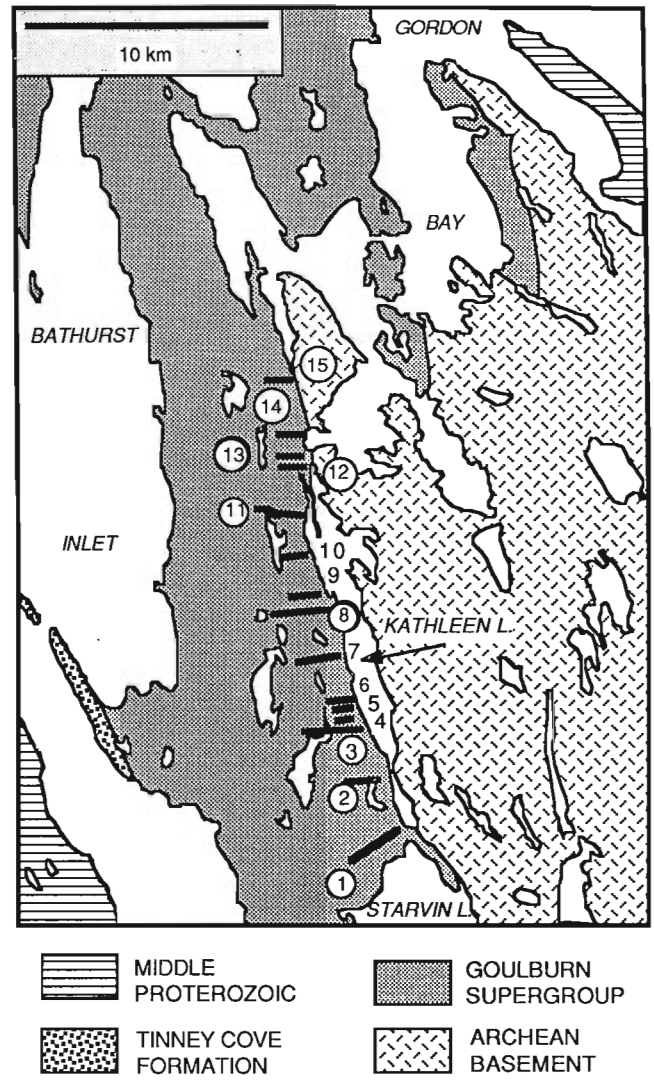

Figure 3. Location map of measured sections illustrated in Figure 4. See Figure 1 for location of this map in Kilohigok Basin.

Most of sequence IV is in the basal part of the Beechey Formation except for thin lowstand and transgressive systems tract deposits within the Rifle in the southern Tinney Hills area. Over most of the Tinney Hills there are no preserved lowstand and transgressive deposits, and the condensed secton rests directly on the sequence boundary. This is the result of a rapid rate of tectonic uplift amplifying a eustatic fall and dominating a eustatic sea level rise with no accommodation being created over much of the Tinney Hills area until the earliest highstand. The highstand siltstones and carbonates of the lower Beechey Formation were not studied for this part of the project and are not discussed.

Sequence descriptions

Each of the four sequences is bounded above and below by sequence boundaries that are Vail unconformities. Each unconformity was formed in response to an abrupt lowering of relative sea level caused by a combination of eustatic sea level change and tectonic uplift. Unconformities in the Rifle Formation can be recognized by a combination of several criteria: a regional surface of exposure with nondeposition and/or erosion; one or more wide spread and well-developed paleosols; an abrupt basinward shift in depositional environments. In the Tinney Hills, erosion is recognized along at least part of each sequence boundary.

Sequence I

The lowest sequence boundary, sequence boundary I, is located at the formation boundary between the Rifle Formation and the underlying Hackett Formation. In several areas there are debris flow deposits directly on top of lower shoreface sandstones of the Hackett Formation and these debris flows are interpreted as forming in response to a rapid fall in sea level. The change in sea level resulted in erosion of more landward sediments that were transported in debris flows to their present position directly on top of the sequence boundary.

Shelf siltstones and mudstones are found on top of these debris flows and also directly on top of the Hackett Formation where debris flows are absent. The fine-grained sediments are distal equivalents of nearshore sandstones of the lowstand systems tract. It is important to note here that there is a general upwards increase in the amount of carbonate concretions in the shales that culminates in a laterally continuous one-to-two metre thick dolomite bed near the middle of the lower Rifle siltstone. The dolomite bed is unusual because of its thickness, lateral continuity, and the presence of small, deep-water stromatolites that colonized areas of hardgrounds that formed during this period of starved deposition. An increase in percent of concretions is also seen in the far southern part of the Tinney Hills in a more distal position from the source of clastic sediments, but there the dolomite bed is found in the lower part of the siltstone (compare section 1 with section 5). The increase in numbers of concretions is most likely due to a decrease in the rate of siliciclastic sedimentation. This trend culminates in the formation of the dolomite bed under conditions of almost no influx of clastic sediments resulting in a starved basin. The dolomite bed is interpreted to be a condensed section on top of lowstand siltstones. During this time clastic sedimentation occured far landward of the Tinney Hills during coastal onlap, resulting in greatly diminished transport of siliciclastic sediment into this part of the basin.

The siltstones above the condensed section generally have few concretions and exhibit an overall coarsening-up trend consisting of increasing numbers and thicknesses of thin (less than 50 cm), wave-influenced, sandstone beds. These siltstones are the distal equivalents of early highstand nearshore marine sandstones. A rapid vertical facies change records the arrival of later highstand nearshore marine sandstones deposited as the shoreline prograded into the area of the Tinney Hills. This sandstone is a major Gilbert-type delta complex and is the final preserved unit in the first sequence.

Sequence II

Sequence boundary II is formed on top of the Gilbert-type delta complex in the highstand of sequence I. North of section 5 it is characterized by an exposed surface with incipient paleosol development. In some areas small-scale (less than one metre of relief) karst developed at the sequence boundary, formed by erosion of carbonate-cemented (micrite) fluvial sandstones. Maximum progradation of the underlying delta complex stopped just south of section 5 as shown by the preservation of depositional relief along the delta-front beds just below the boundary and by knickpoint erosion that removed some delta-front sands and deposited them farther downslope as debris flows. These debris flows can be correlated several kilometres to the south into a part of the section that is dominantly siltstone with only minor amounts of sandstone. The initiation of erosion of delta front beds and resultant debris flows records a fall in sea level and a basinward shift in deposition. The surface formed by this can be correlated landward as a surface of little to no deposition with long exposure and paleosol development. Thin fluvial deposits and paleosols are preserved on top of the sequence boundary.

Little of the lowstand systems tract for sequence II is found in the Tinney Hills. Apparently, most of the lowstand deposition bypassed this area and occurred in a more basinal location. This was probably due to the fall in sea level moving the shoreline basinward of the Tinney Hills area. However, the sequence boundary in the vicinity of sections 5, 4 and 3 does parallel the dipping depositional surface of the underlying delta front and this dip may have prevented building up of any substantial accumulation of sand if the shoreline did remain in the vicinity of the southern Tinney Hills. If this is the case, then the sands may have repeatedly flowed farther downslope as gravity-slide deposits and are probably, in part, equivalent to turbiditic sands present in the Bear Creek Hills area.

The first nearshore sandstone of the transgressive systems tract to be preserved in this area can be seen in sections 4 and 5 and is a small deltaic parasequence. This parasequence onlaps the sequence boundary near the top of the preserved delta front of the underlying highstand deposits and deltaic facies grade into fluvial sediments and associated paleosols. Any succeeding nearshore marine parasequences

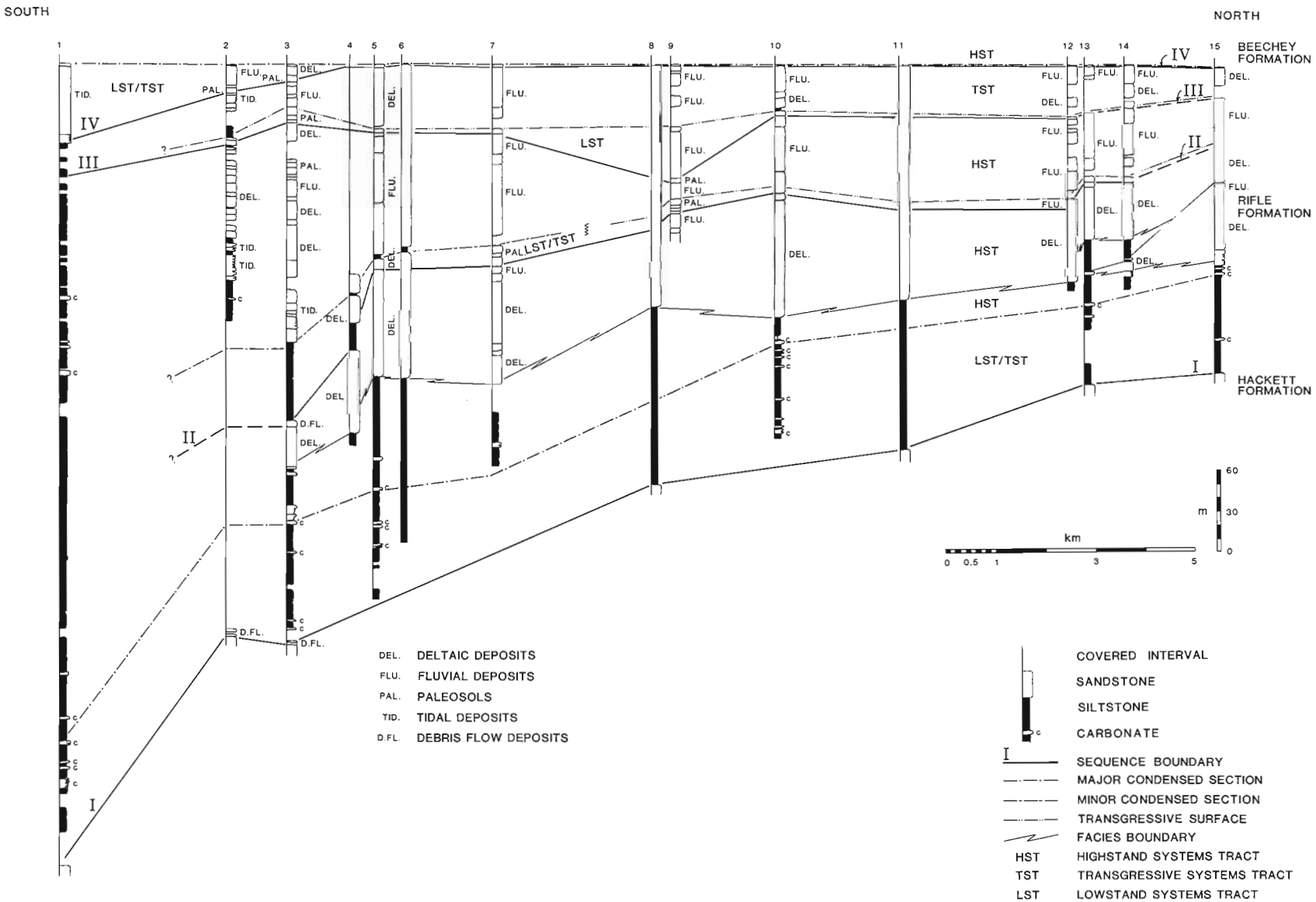

Figure 4. Sequence stratigraphy of Rifle Formation in Tinney Hills area. See text for discussion.

stepped shoreward a great enough distance to be north of the Tinney Hills outcrop. Such a significant backstep indicates that the coastal plain at this time probably was at a very gently inclined angle. This low gradient for the coastal plain is consistent with the apparent very rapid regression of the shoreline as the highstand prograded back over the area. A minor condensed section is preserved in sections 3 through 7 and is interpreted to be the result of starved sedimentation in shallow shelf waters while nearshore sedimentation was occurring farther landward. This supports the interpretation that additional nearshore lowstand parasequences were deposited north of the Tinney Hills. This surface can be correlated across the Tinney Hills north of section 7, shows decreasing influence of submergence to the north, and has less than 1 m of recognizable marine sandstone on top of it.

North of section 5 the only preserved sediments between sequence boundary II and the transgressive surface are fluvial sediments and associated paleosols that were deposited during the transgressive systems tract. It is also likely that some of this thin non-marine section was deposited during part of the lowstand systems tract. Accommodation for non-marine sediments can be low-to-nonexistent during lowstand as it can also be for non-marine sediments associated with initial parasequences of the transgressive systems tract. This explains why there is only a few metres of sandstones assigned to the lowstand and transgressive systems tracts of sequence II.

The highstand systems tract is composed of fluvial sandstones and paleosols from section 6 to the north end of the Tinney Hills; to the south there is an interfingering with nearshore marine units. Both tidal deposits and Gilbert-type delta deposits occur that are dominantly sandstone and which in turn interfinger and grade laterally to the south with deeper-water siltstones. This trend continues until in section 1 only siltstones are preserved for this interval.

Sequence III

The third sequence boundary is very much like the second boundary in that it is a marked surface of exposure and paleosol development. However, erosion into the underlying nearshore marine highstand deposits is not shown in the Tinney Hills outcrops. Instead there is an incised valley formed at the sequence boundary that cuts down at least 40 m (see section 9) into the highstand fluvial deposits of sequence II. The sequence boundary is also a marked surface of exposure and paleosol development at the base of this incised valley implying that there was a period of non-deposition, exposure and weathering before infilling with subsequent fluvial deposits. The incised valley is recorded in section 9, but is not recognized in either section 7 to the south or 10 to the north. This constrains the exposed width of the valley to some value less than the approximately 6 km between sections 10 and 7. The incised valley is a part of the lowstand systems tract of sequence III and will connect downdip with nearshore lowstand deposits: however these are not preserved in the Tinney Hills outcrops and are probably present as part of the basinal turbidite sequence in the Bear Creek Hills area. Between sections 2 and 1 there is a facies change from thin fluvial/paleosol deposits to marine siltstones. The lack of well-developed nearshore marine sandstones in this transition may be due to either a silty and muddy low-energy shoreline at this time or to a facies change from nonmarine to lagoonal or distributary bay facies.

A transgressive surface is recognized on top of the thin fluvial/paleosol deposits and on top of the fluvial deposits in the incised valley. This transgressive surface has also left an overprint on the paleosols beneath it, but to a lesser degree than is found along the transgressive surface in sequence II. The deposits of the transgressive systems tract include a mix of small Gilbert-type deltaic sediments and fluvial units forming at least two parasequences with the line of the outcrop oblique to depositional strike. Tidal deposits of this systems tract are also found in section 2 and these are in a probable third parasequence on top of the deltaic units. There is also a lateral facies change between the tidal sandstones of section 2 and the marine siltstones of 1.

No highstand deposits of sequence III were preserved in the Tinney Hills. All deposits were stripped off by the formation of sequence boundary IV. It is not uncommon to have part or all of the highstand systems tract removed by thesucceeding sequence boundary although this is the first occurrence of this in the Rifle Formation.

Sequence IV

From a little south of section 5 to the north end of the Tinney Hill, sequence boundary IV is immediately overlain by a 1- to 2- m thick mixed siliciclastic and carbonate bed that is the condensed section for sequence IV. No lowstand or transgressive systems tract sediments are preserved between the sequence boundary and the transgressive surface. The formation boundary between the Rifle Formation and the overlying Beechey Formation is placed at the base of the mixed siliciclastic and carbonate bed that forms the condensed section and this places the sequence boundary and the formation boundary at the same surface. Immediately overlying the mixed bed are the Beechey siltstones and carbonates that are a part of the highstand of sequence IV. It is important to note here that the formation boundary between the Rifle and the Beechey formations coincides with the sequence boundary only when the sequence boundary coincides with the base of the condensed section. This contrasts with the first sequence boundary that is essentially equivalent to the Rifle/Hackett formation boundary.

The sequence boundary is an eroded surface with evidence for exposure and weathering and a very strong overprinting by the condensed section. Microdigitate stromatolites are often found within carbonate-filled dissolution vugs in this interval. Just south of section 5 the sequence boundary and the condensed interval start to diverge from each other and lowstand or transgressive systems tract sediments are preserved. It is not possible to resolve which systems tract these sediments belong to due to a lack of sufficient outcrop to determine fully the lateral relationship of these sediments to the sequence boundary. The sandstones at the top of sections 3 and 2 are fluvial whereas the poorly exposed sandstones at the top of section 1 are probably tidal in origin. The thin, mixed siliciclastic

and carbonate bed of the condensed section is at the top of the sandstones in all three sections and is in turn overlain by the highstand Beechey siltstones and carbonates. There is about 12 m of fluvial sandstone between sequence boundary and condensed section in section 3, about 22 m of fluvial deposits in section 2, and about 55 m of tidal deposits in section 1. Note again that in this southern part of the area there is a large separation between sequence boundary and formation boundary.

In section 2 the sequence boundary localy scours down more than 8 m into the underlying transgressive systems tract of sequence III. There is evidence of exposure and paleosol development with some fluvial deposition along the southern part of the sequence boundary, especially where the scour and channel-formation occurs. The channel is about 150 m wide across the face of the outcrop.

Depositional environments

Nearshore marine depositional environments in the upper Rifle Formation are interpreted to include tidal and Gilbert-type deltaic environments. Deltaic deposits occur more frequently than do the tidal deposits and also make up the thickest individual units. Additionally, deltaic deposits are found in the northern and central part of the area studied whereas tidal deposits occur in the southern part (more basinward). Two varieties of sandy, braided to low-sinuosity fluvial systems are recognized; one is thought to be more distal to source whereas the other is more proximal. A spectrum of paleosols can also be recognized which are critical to identifying exposure surfaces along sequence boundaries.

Deltaic units

The deposits interpreted to be formed in a type of Gilbert delta are characterized by pronounced sloping foreset surfaces (clinoforms) that dip to the south-southwest at 5 to 25 degrees (after correction for structural dip) and are overlain by horizontal topset beds. The dominant sedimentary structure in these foresets is $2^1/_2$D crossbedding formed from straight-crested dunes with scour in front of the dune. Preserved height of the crossbedding ranges from 5 to 120 cm with most in the range of 15 to 50 cm. Trough (3D) and planar (2D) cross-bedding occur but are secondary and tend to be smaller; seldom with a preserved height greater than 60 cm and most in the range of 5 to 40cm. Crossbeds are arranged in tabular to wedge-shaped bedsets with gently undulatory to planar erosional bedset surfaces. Broad, shallow channels from 1 to 5 m deep and 20 to 60 m wide are common in the foreset portion of the deltaic units, especially in the more proximal foresets. These channels are filled with 21/2D, trough, and planar crossbedding organized in bedsets that are oriented as lateral accretion deposits. Foreset sandstone is subarkosic with medium to coarse, subround to subangular grains with quartz and carbonate cements. Carbonate cementation promotes pitted weathering surfaces.

The topset part of the Gilbert-type deltaic deposits is also comprised of crossbedding, with the occurrence of trough and $2^1/_2$D crossbeds about equal in frequency. Preserved height ranges from 10 cm to 40 cm with occasional 50- to 60- cm beds; bedset geometry is similar to that in the foresets but channels tend to be uncommon. Topset sandstone is also subarkosic, and generally medium to coarse, but coarse to very coarse sand and micrite-cemented sandstone clasts 1 to 10 cm are also common. Subangular to subround grains are both quartz and carbonate cemented and intervals with carbonate cements and pitted weathering occur frequently.

The most distal sandstone deposits are referred to as 'toeset' units. The transition from prodelta siltstones and shales to toeset sandstones is very rapid, occurring over a vertical interval of a few tens of centimeters. Toeset sedimentary structures include: horizontal, planar-laminated beds of sandstone, siltsone and shale from 1 to 10 cm thick; current-rippled beds of sandstone and siltstone from 1 to 10 cm thick; and $2^1/_2$D crossbeds of sandstone from 5 to 35 cm thick. Bedsets are tabular with little, if any, erosion at the base. Planar-laminated sandstones are very fine to fine; current ripples are medium to fine; and $2^1/_2$D crossbeds are medium to coarse depending on the height of the crossbed, smaller beds having finer grains. Composition is subarkosic to arenitic with quartz cement.

Within the toesets there are vertical trends of coarsening up, of an increase in bed thickness, and a change from mostly planar-laminated beds to current ripples to crossbeds. Most of the grain-size segregation in the delta occurs in the toeset beds with little segregation in the foresets, even though they make up the bulk of the delta, and only some segregation in the topset beds. There is very little silt- and clay-sized material in the toeset, foreset, or topset parts of the delta deposits and this is interpreted to be due to efficient bypassing of these sub-environments with deposition of fines in the prodelta/open shelf area.

Overall trends of the Gilbert-type deltas include coarsening up, thickening up of beds, a progressive change to higher energy sedimentary structures, and the gross change in bedset geometry from toeset to foreset to topset.

Tidal deposits

Tidal deposits, found in the southern part of the field area, are characterized by relatively thin, 1- to 5- m, intervals that have pronounced vertical trends of either thickening and coarsening upwards or thinning and fining upwards . A higher percentage of shale and siltstone is found in these deposits than is found in either the Gilbert-type deltaic units or the fluvial deposits described below. Average sizes of bedsets, beds and sedimentary structures are smaller in the tidal deposits than in the deltaic rocks. Tabular bedsets are generally less than 70 cm thick and average 10 to 40 cm thick. Trough, $2^1/_2$D, and planar crossbeds range up to 80 cm in preserved height and average 20 to 30 cm; current and wave ripples are 1 to 3 cm high; beds of horizontal, planar laminated sandstones, siltstones, and shales are less than 20 cm thick with most less than 10 cm; flaser, wavy, and lenticular bedding are all 5 to 10 cm thick. Subarkosic to arkosic sandstones with very fine to coarse, subround to subangular grains are characteristic of these rocks. The tidal deposits include intervals interpreted as tidal channels, pos-

sible tidal deltas, and tidal flats based on the vertical association of sedimentary structures and the vertical trends in bed thickness and grain size.

One 2-m-thick interval with several tidal channel deposits was identified. Each channel is comprised of $2^1/_2$D crossbeds arranged in lenticular bedsets nested within a lenticular scour cut into lower tidal flat deposits. Coarse to medium sand is found within the channels and in the surrounding tidal flat beds. These deposits are characterized by their lenticular geometry.

Possible tidal delta deposits are 2 to 5 m thick and are marked by coarsening up and thickening up trends. Sedimentary structures at the base include mostly current ripples with some wave ripples and horizontal planar laminated beds comprised of very fine to medium sand, silt, and clay. The top is made up of $2^1/_2$D and planar crossbeds 10 to 30 cm in preserved height arranged in tabular bedsets and is comprised of medium and coarse sand. There is also a gradual transition between upper and lower parts of these deposits with respect to sedimentary structures and grain size.

Intervals 1.5 to 4.5 m thick and interpreted as possible tidal flat deposits have marked fining up and thinning up vertical trends with mostly medium to coarse sand at the base, and fine to medium sand with interbedded and interlaminated silt and clay at the top. Trough and $2^1/_2$D crossbeds are found in the base, often with reactivation surfaces that form sigmoidal bedsets (bundles). Current ripples, flaser bedding, wavy bedding, lenticular bedding, and horizontal planar laminated beds are all found the upper portion. There is a gradual transition between upper and lower parts both in dominant grain size and in types of sedimentary structures.

Fluvial deposits

Two distinct styles of sand-rich fluvial deposition are recognized in the Rifle Formation. One style is interpreted to be somewhat proximal, sand-rich, braided river deposits whereas the second is interpreted to be either more distal braided river deposits or low-sinuosity fluvial deposits. The proximal braided river sandstones are thought to have been deposited in a braid plain environment and the distal fluvial sandstones are thought to have been deposited in a coastal plain environment close to the shoreline. Proximal fluvial sandstones are characterized by a lack of tabular bedsets, trough crossbedding with a subordinate amount of $2^1/_2$D crossbedding, a reddish-brown weathering color, and a large number of intervals with carbonate (micrite) cement and very pitted weathering surfaces. Distal fluvial sandstones are characterized by tabular bedsets, roughly equal proportions of trough and $2^1/_2$D crossbedding, common broad and shallow channels, and interbedded micrite-cemented intervals with most of the micrite cement concentrated in the tops of beds and bedsets. There is little vertical change in grain size, bed or bedset thickness, or types of sedimentary structures in either the proximal or distal fluvial deposits.

Proximal fluvial sandstones

Trough crossbedding predominates in these sandstones with some $2^1/_2$D crossbedding also occurring. Preserved height of the crossbedding ranges from 5 to 80 cm, with an average of 15 to 35 cm. There are also some contorted crossbeds scattered throughout the deposits, often at the base of an interval. Grain size varies from medium to very coarse, many of the deposits are coarse to very coarse and overall the proximal deposits are coarser than are the distal deposits. The sandstone is subarkosic in composition and grains are subround to subangular.

Distal fluvial sandstones

Trough and $2^1/_2$D crossbedding occur with approximately equal frequency in these sandstones and range in preserved height from 5 to 50 cm with an average of 15 to 40 cm. A few current ripples 2 to 5 cm high occur with small trough crossbeds 5 to 20 cm in height in one section and may represent rarely preserved deposition at or near the top of a bar. Contorted crossbeds are about as common in the distal fluvial sandstones as in the proximal sandstones. Tabular bedsets range from 20 to 150 cm in thickness with most ranging from 50 to 100 cm. Some broad, shallow channels occur and are filled with trough and $2^1/_2$D crossbedding. These channels are similar to those described in the foreset and topset beds of the Gilbert-type deltas. Grain size averages medium to coarse but some very coarse sand also occurs. Some sandstone clasts 7 to 15 cm also occur. Composition is subarkosic and grains are subround to subangular.

Topset sandstones of the Gilbert-type deltas are very similar to the distal fluvial sandstones with respect to sedimentary structures, bedset geometry, channels, grain size and composition, and general overall appearance. It is often difficult to decide where topset deposits end and distal fluvial deposits begin and both vertical and lateral position of a unit must be taken into account. It is this strong similarity to topset deposits that has guided the interpretation of these fluvial deposits as being formed in a coastal plain environment distal to a sediment source and close to the shoreline.

Alternating proximal and distal fluvial sandstones

Two intervals in Section 7 (50 m and 20 m in thickness) have alternating proximal and distal fluvial sandstones where the proximal sandstones are less than or equal to 1 m in thickness and the distal sandstones are less than or equal to 2 m in thickness. This thin and repeated alteration may be due to the section being located in an area of interfingering facies or it may record parasequences in a subaerial setting with little accommodation. Each pair or couplet of distal overlain by proximal is capped by carbonate micrite cement in the upper 10 to 30 cm, interpreted to likely represent a period of exposure and nondeposition.

MARINE-ALLUVIAL TRANSITION AND STRATIGRAPHIC RELATIONSHIPS WITH THE LOWER BURNSIDE FORMATION

The 1988 season of sedimentological and stratigraphic field studies of the Burnside Formation concentrated on the transition from the marine shelf facies in the upper Link Formation to the braided alluvial facies which characterize the majority of the Burnside Formation. The details of alluvial facies and overall evolution of the Burnside Formation were discussed in previous reports (Grotzinger et al. 1987; McCormick and Grotzinger 1988). This section outlines two aspects of the marine-alluvial transition. First, the sedimentology of the transition at one superbly-exposed section (north Tinney Hills) is detailed. Second, the stratigraphy of the upper Link and the lower Burnside formations from the Tinney Hills to the crest of the Gordon Bay Arch are shown and the implications are discussed for the transition within the Kilohigok foreland basin from southeast-facing marine shelf ramp to northwest-flowing alluvial system.

Marine-alluvial transition

The marine to alluvial transition in the north Tinney Hills is characterized by three main associations of facies which represent storm-influenced marine shelf, lower delta slope, and upper delta slope.

The marine shelf association comprises six grayish-green siltstone facies which are commonly arranged in the following vertical succession: laminated mudstone, mm-scale graded mudstone-siltstone couplets; millimetre-to centimetre-scale siltstone in mudstone commonly containing starved wave ripples (Fig. 5a); 5-30 cm beds of hummocky or swaley cross-stratified coarse siltstone and very fine-grain sandstone (Fig. 5b); parallel- to wavy-laminated silt and sand with common siltstone- and sandstone-filled gutters 5-20 cm deep (Fig. 5c); and massive to parallel-laminated siltstone beds 5-200 cm thick. This progression of facies suggests deposition on a storm-influenced muddy shelf (Johnson and Baldwin 1986). The upward sequence of textures and sedimentary structures suggest passage from conditions of suspension fall-out and weak density flows below storm wave-base (laminated mudstone, graded couplets) through storm-wave influenced structures of progressively higher energy and sediment supply (wave rippled siltstone, hummocky/swaley beds, gutter siltstones; Fig. 5a-b). This succession is seen particularly well in one section just below the lower contact of the Burnside Formation (Fig. 6: 0-30 metres) and suggests progressive shallowing and progradation of a storm-influenced muddy shelf. Gutters are very uniformly aligned ($111°/291° \pm 13°$, $n=12$). Thick massive to laminated beds of siltstone are interpreted as prodelta deposits of density currents under conditions of high sediment supply (Elliot 1986). This facies commonly passes up to red delta front siltstones.

The transition from hummocky/swaley cross-stratified facies to gutter facies does not match the sequence of Dott and Bourgeois (1982) of storm-dominated progradational shelves in which the thickest bedded swaley cross-stratified facies represent the shallowest shoreface environment. In this study, the predominance of gutters which locally are isolated in siltstone and their occurrence with thin discontinuous silt or sand beds (Fig. 5c) suggest that storm conditions promoted erosion and bypassing along the nearshore sea floor,rather than deposition of amalgamated hummocky or swaley beds. Myrow et al. (1988) describe a similar succession from the late Precambrian-early Cambrian of Newfoundland which they suggest may be more representative of fine-grained storm-influenced shelves.

The lower contact of the Burnside Formation is marked by the transition from shelf to lower delta slope association. The coarsening-upward delta slope association comprises several facies (Fig. 5d-e). The occurrence of this association is restricted to the lower few metres of the Transitional Member of the Burnside Formation (Fig. 6: 40-51 metres). This association is marked by the first occurrence of red siltstone/mudstone beds which are interbedded with wave rippled, very fine-grained sandstone. Upward, siltstone beds (1-5 cm) appear with single-grain horizontal to wavy-parallel laminae composed of fine to medium sand at the base of beds. There is an upward increase in bed thickness. Current, wave, and interference ripples are common. Locally, hummocky cross-stratified sandstone beds occur. The most distinctive feature of this association, other than the red colour, is the presence of abundant soft sediment deformation structures, such as flame, load, and ball-and-pillow structures, convolute laminae, and entire beds which have slumped (Fig. 5d-e; 6: 43-46 m). No desiccation cracks are found, but irregular, disconnected three-armed cracks are locally present which are interpreted as subaqueous shrinkage (synaeresis) cracks.

The abundance of wave-formed structures, such as wave and interference ripples, the presence of synaeresis cracks, and lack of desiccation cracks, suggest deposition in a very shallow subaqueous environment which was not subaerially exposed. Soft-sediment deformation and red colour support high rate of terrigenous input which caused slope oversteepening and promoted slumping. This association is most consistent with the lower slope of a prograding fluvial-dominated delta (Elliot 1986). This interpretation is supported by vertical stratigraphic trends which put this association between prodelta shelf and upper delta front-delta plain associations (Fig. 6).

The lower delta front association passes upward into upper delta front-delta plain associations which have been described by McCormick and Grotzinger (1988). The upper delta slope comprises mostly tabular-bedded, horizontally-laminated, very fine- to fine-grain sandstone with wave ripples, mud clasts, and internal scouring (Fig. 6: 52-95 m). Passage from delta slope to delta plain is characterized by a change from isolated to laterally and vertically-persistent trough crossbedded fine- to medium-grain sandstone (Figure 6: 95-113 metres). As reported previously, the horizontally-laminated sandstone is interpreted as wave-reworked braid delta distributary mouth shoals and swash bars. The isolated trough crossbeds are interpreted as braid delta distributary channels which occasionally cut across the

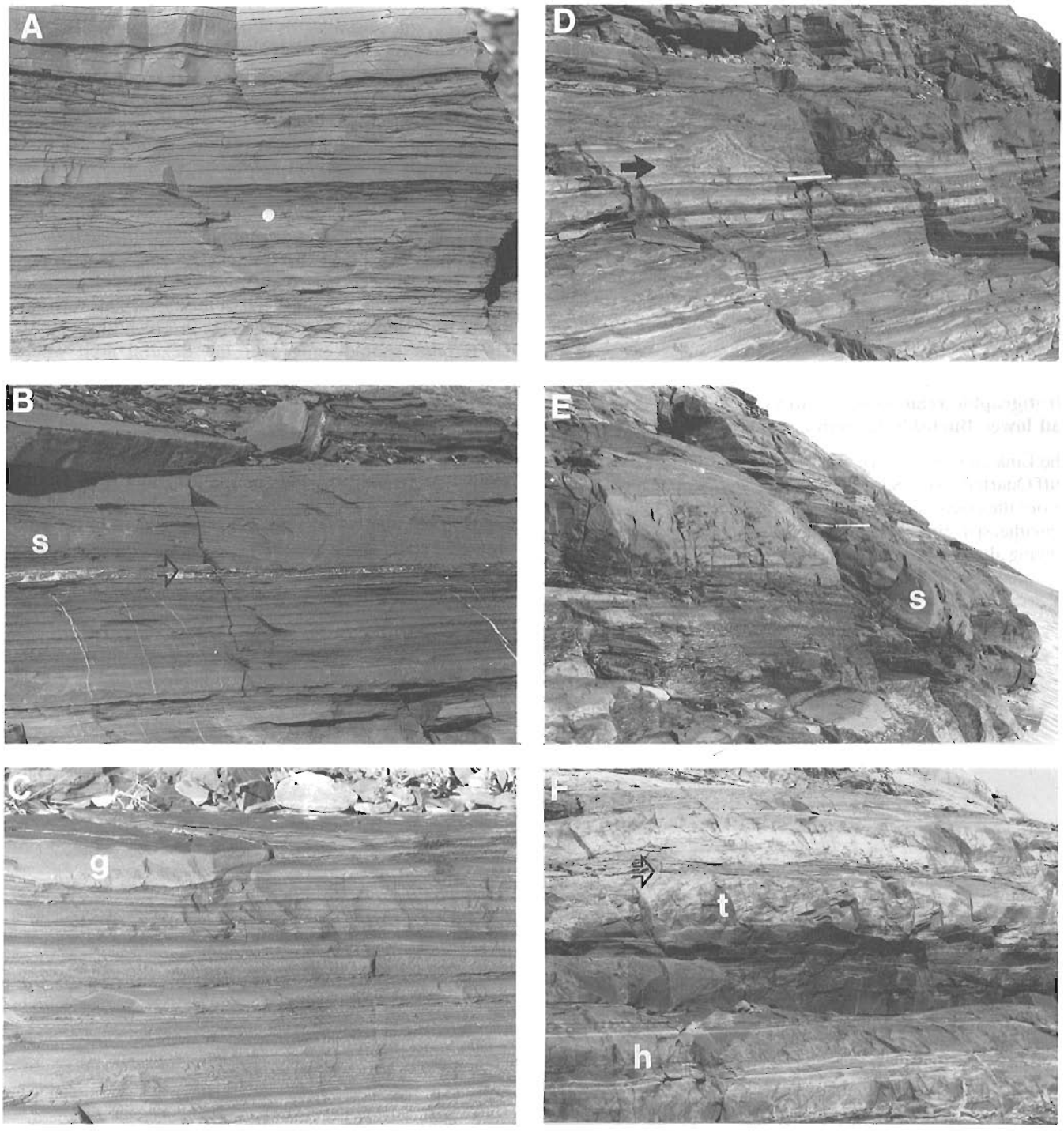

Figure 5. Transitional marine shelf to deltaic associations. A) wave rippled siltstone-mudstone facies. Coin for scale. B) Hummocky-swaley cross-stratified facies. Truncated swaley bed (s) interbedded with wave rippled and horizontally laminated siltstone. Arrow points to pocketknife for scale. C) Gutter facies. Note how gutter (g) passes laterally into thin wavy to parallel laminated siltstone bed. Coin for scale (lower right of gutter). D) Wave rippled red sandstone-siltstone facies. Arrow points to highly deformed horizon which is injected into overlying bed. The overlying bed is highly contorted and passes laterally into a slumped horizon (see next photo). Hammer for scale. E) Slumped bed (s) cuts out about 2.5 m of section. Bed dips at about 30 to regional bedding but has remained internally parallel laminated and coherent. Laterally this bed passes into contorted, fluidized sandstone. Hammer for scale above slumped bed. F) Delta front/delta plain sandstones. Trough cross-bedded sandstone (t) with common mud chips are sharply interbedded tabular horizontally laminated sandstones (h). Arrow points to pocket knife for scale.

delta platform during strong floods. Interestingly, at the section at north Tinney Hills, a strong correspondence between gutter orientations and trough cross bedding in overlying facies at this location suggests that gutters may have been formed by erosive storm-surge ebb currents that were aided by flood currents from distributary channels of the prograding braid delta.

The criteria to distinguish between marine and alluvial facies for the Burnside Formation may be useful for other Precambrian sandstone successions. By distinguishing between the two, it may help to identify unconformity-bounded depositional sequences which are time-stratigraphic units essential for intra-basinal correlation (Christie-Blick et al. 1988; Grotzinger et al. 1988). The identification of such disconformities within the Burnside Formation is discussed below.

Stratigraphic relationships within the Link and lower Burnside formations

The Link and lower Burnside Formations (Transitional and Buff Quartzite members; McCormick and Grotzinger 1988) record the conversion of the Bear Creek foreland basin from a southeast-facing shallow marine ramp to a northwest-flowing alluvial system (Grotzinger et al. 1988). Two major proximal-to-distal trends are evident. First, the lower interval from the base of the Link Formation to the base of the main conglomeratic unit in the Burnside Formation define a northwest-tapering wedge which thins over the Gordon Bay Arch, thickens towards Wolverine Canyon, then thins towards Rockinghorse Lake (Fig. 2). This geometry mimics the underlying lower BearCreek Group (Fig. 2) (Grotzinger and McCormick, 1988). Towards the crest of the Gordon Bay Arch, within the Link Formation, coarsening-upward sequences which culminate in medium-grain, well-sorted, white trough crossbedded sandstone with glauconite are more common. These sequences closely resemble shallow marine sand bars (Johnson and Baldwin, 1986). The increasing abundance of wave-influenced sandy shelf facies in the Link Formation to the northwest suggests that the cratonic foreland experienced shallow water conditions more frequently than the proximal end of the basin. This relationship is predicted for a foreland basin in which lower subsidence rates should exist over the flexural arch where sediment supply rate would be more likely to keep pace with subsidence and thus maintain shallow water conditions.

Within the Transitional Member of the Burnside Formation, delta plain facies pinch out to the northwest and this member is entirely composed of upper delta front facies. The Buff Quartzite Member, which is composed of the medial braid plain facies, pinches out southeast of the arch crest so that the upper delta slope facies is abruptly overlain by proximal braid plain facies (Fig. 2). This suggests that the contact between the Link and Burnside formations is an

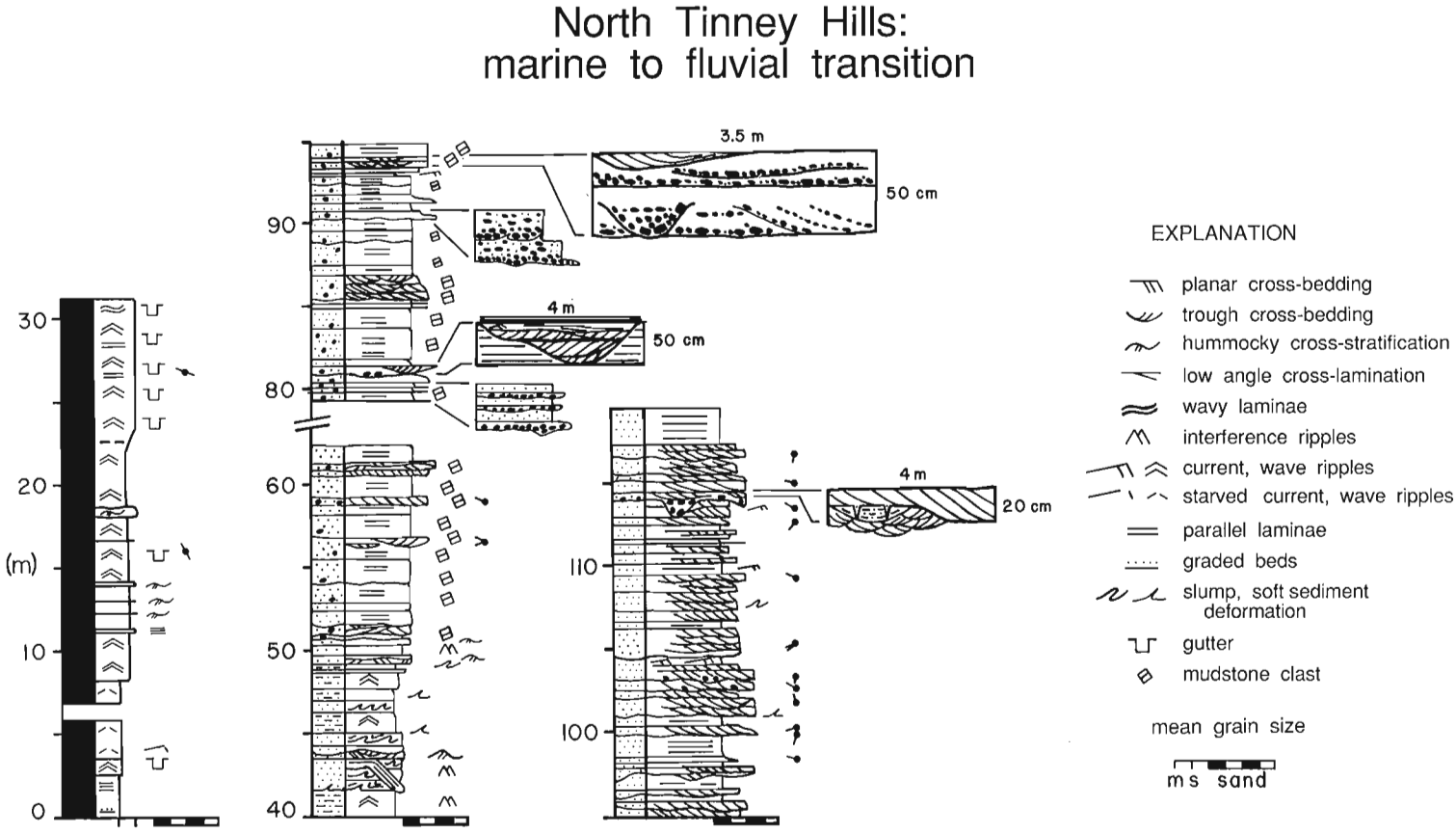

Figure 6. Measured section of the upper Link and Transitional Member of the Burnside Formation at north Tinney Hills. Omitted intervals are covered. Small black circles with tails indicate paleocurrent directions: double tails are gutter trends which are ambiguous with respect to flow direction, and single tails are trough cross-bed azimuths. The northwest to southwest mode of troughs strongly suggest that flow through gutters was to the northwest down a prodelta slope.

erosional unconformity. Northwest of the Gordon Bay Arch, towards Wolverine Canyon this transition is increasingly gradational. At Rockinghorse Lake, the basal Burnside pebbly sandstone rests abruptly on sub-wave-base red mudstones, again suggesting erosional unconformity at the base of the Burnside Formation (Fig. 2).

The transport of gravel across the entire Slave craton, in excess of 200 km, requires a fundamental change in the distribution of subsidence across the basin. Modelling of gravel transport by Paola (1988) suggests that areally-extensive conglomerates, especially in foreland basins, indicate reduced subsidence rates in the proximal part of the basin. Heller et al. (1988) suggest that coarsening-upward profiles in the distal parts of foreland basins indicate when convergence and thrust loading have ceased and erosion predominates which causes unloading and flexural rebound of the hinterland. This uplift causes erosion of previously-deposited foreland basin strata and progradation of the alluvial system over the foreland. This interpretation is supported by uniformly northwest-directed paleocurrents in the foreland indicating long-term overfilling of the depocentre. If this interpretation is correct, then the transition from lower Burnside Formation deltaic and distal alluvial facies to gravelly proximal alluvial facies record this shift from subsidence-dominated foreland sedimentation to erosion- and uplift-dominated sediment redistribution.

REFERENCES

Bowring, S.A. and Grotzinger, J.P.
—: New U-Pb zircon and stratigraphic constraints on the evolution of Wopmay Orogen, NWT, Canada; EOS (abstract). in press.

Christie-Blick, N., Grotzinger, J.P., and von der Borch, C.C.
1988: Sequence stratigraphy in Proterozoic successions; Geology, v. 16, p. 100-104.

Dott, R., Jr., and Bourgeois, J.
1982: Hummocky stratification: significance of its variable bedding sequences; Geological Society of America Bulletin, v. 93, p. 663-680.

Elliot, T.
1986: Deltas, in, H.G. Reading (ed.); Sedimentary Environments and Facies (2nd. ed.); Blackwell Scientific Publications (Boston, MA), p. 113-154.

Grotzinger, J.P., and Gall, Q.
1986: Preliminary investigations of Early Proterozoic Western River and Burnside River Formations: evidence for foredeep origin of Kilohigok Basin, N.W.T., Canada; in Current Research, Part A; Geological Survey of Canada, Paper 86-A, p. 95-106.

Grotzinger, J.P., and McCormick, D.S.
1988: Flexure of the Early Proterozoic lithosphere and the evolution of the Kilohigok Basin (1.9 Ga), northwest Canadian Shield; in K. Kleinspehn and C. Paola (ed.), New Perspectives in Basin Analysis. Springer-Verlag (New York), p. 405-430.

Grotzinger, J.P., McCormick, D.S., and Pelechaty, S.M.
1987: Progress report on the stratigraphy, sedimentology, and significanceof the Kimerot and Bear Creek groups, Kilohigok Basin, District of Mackenzie; in Current Research, Part A; Geological Survey of Canada, Paper 87-1A, p. 219-238.

Grotzinger, J.P., Gamba, C., Pelechaty, S.M., and McCormick, D.S.
1988: Stratigraphy of a 1.9 Ga foreland basin shelf-to-slope transition: Bear Creek Group, Tinney Hills area of Kilohigok Basin, District of Mackenzie; in Current Research, Part A; Geological Survey of Canada, Paper 88 1-C, p. 313-320.

Heller, P.L., Angevine, C.L., Winslow, N.S., and Paola, C.
1988: Two-phase stratigraphic model of foreland basin sequences; Geology, v. 16, p. 501-504.

Johnson, H.D., and Baldwin, C.T.
1986: Shallow siliciclastic seas; in H.G. Reading (ed.), Sedimentary Environments and Facies (2nd. ed.); Blackwell Scientific Publications (Boston, MA), p. 229-282.

McCormick, D.S. and Grotzinger, J.B.
1988: Aspects of the Burnside Formation, Bear Creek Group, Kilohizok Basin, District. Mackenzie, N.W.T.; in Current Research Part C, Geological Survey Canada, Paper 88-1C, p. 321-334.

Myrow, P.M., Narbonne, G.M., and Hiscott, R.N.
1988: Storm-shelf and tidal deposits of the Chapel Island and Random Formations, Burin Peninsula: facies and trace fossils; Geological Association of Canada, Annual Meeting, Guidebook B6, 108 p.

Paola, C.
1988: Subsidence and gravel transport in alluvial basins; in K. Kleinspehn and C. Paola (ed.), New Perspectives in Basin Analysis; Springer-Verlag (New York), p. 231-244.

Vail, P.R.
1987: Seismic stratigraphy interpretation using sequence stratigraphy:Part 1: Seismic stratigraphy interpretation procedure; in A.W. Bally (ed.), Atlas of seismic stratigraphy; v. 1, p. 1-10.

Van Wagoner, J.C., Mitchum, R.M., Posamentier, H.W., and Vail, P.R.
1987: Key definitions of sequence stratigraphy; in A.W. Bally (ed.), Atlas of seismic stratigraphy, v. 1, p. 11-14.

Contrasts in setting and style of gold deposits in two Archean terranes: Rice Lake District, Canada, and Western Liaoning District, China

K.H. Poulsen, R. Brommecker, S.B. Green, K.A. Baker[1], Lin Baoqin[2], Shang Ling[3], Shen Ershu[2], Zhang Lidong[2], L. Diamond[4] and D. Marshall[4]

Poulsen, K.H., Brommecker, R., Green, S.B., Baker, K.A., Lin Baoqin, Shang Ling, Shen Ershu, Zhang Lidong, Diamond, L., and Marshall, D., Contrasts in setting and style of gold deposits in two Archean terranes: Rice Lake District, Canada, and Western Liaoning District, China; in Current Research, Part C, Geological Survey of Canada, Paper 89-1C, p. 121-125, 1989.

Abstract

The objective of this joint Sino-Canadian gold study is the comparison of the setting and styles of mineralization in the Archean terranes of both countries. In Canada, gold deposits of Archean age, as exemplified by the Rice Lake District in southeastern Manitoba, are hosted by Archean granite-greenstone terranes of low metamorphic grade. In China, gold deposits of Mesozoic age, as exemplified by the Western Liaoning District, are typically hosted by Archean gneisses of medium to high metamorphic grade. These fundamental differences are further reflected in the composition, structure, alteration and nature of ore fluids in the two districts.

Résumé

L'objectif de cette étude conjointe sino-canadienne sur l'or est la comparaison des cadres et des types de minéralisation dans les terranes de l'Archéen des deux pays. Au Canada, les gisements aurifères de l'Archéen, comme ceux du district de Rice Lake au sud-Est du Manitoba, se trouvent de manière caractéristique dans les terranes de granite-roche verte faiblement métamorphisé de l'Archéen. En Chine, les gisements aurifères du Mésozoïque, comme ceux de la partie occidentale du district de Liaoning, se trouvent de manière caractéristique dans les gneiss moyennement à fortement métamorphisés de l'Archéen. Ces différences fondamentales se reflètent d'avantage dans la composition, la structure, l'altération et la nature des fluides minéralisés dans les deux districts.

[1] Mineral Resources Division.
[2] Shenyang Institute of Geology and Mineral Resources, PRC.
[3] Liaoning Institute of Geology and Mineral Resources, PRC.
[4] Ottawa-Carleton Geoscience Centre.

INTRODUCTION

In 1985, the Geological Survey of Canada entered into a Memorandum of Understanding with the Ministry of Geology and Mineral Resources of the People's Republic of China for the purpose of developing the exchange of ideas and joint research projects concerning fossil fuel and mineral resources. Consequently, the senior author and D.C. Findlay of the Mineral Resources Division visited China in 1987 to establish the terms of reference for a Sino-Canadian study of gold in Archean terranes. They also visited the western Liaoning gold district located in the North China Platform, 360 km northeast of Beijing. The next phase of the project involved a five-week visit to Canada by a team of Chinese scientists in the summer of 1988. The team first visited gold deposits in southern British Columbia with B. E. Taylor and then toured the Archean greenstone belts of northwestern Ontario with J.M. Franklin and F. Robert. They subsequently spent three weeks mapping the geology of gold deposits with Canadian colleagues in the Rice Lake gold district, southeastern Manitoba. This report contains a preliminary account of points of contrast and comparison between Rice Lake and western Liaoning Districts and their gold deposits.

REGIONAL SETTING

The Rice Lake District is located in the western part of the Uchi Subprovince of Superior Craton (Fig. 1). Rice Lake District shares many of the attributes of Superior Province greenstone belts. Well preserved volcanic lithologies predominate principally as basaltic flows and porphyritic dacitic volcaniclastic rocks. Metasedimentary rocks fall into two categories: turbiditic metagreywackes that are conformable with volcanic rocks in the southeastern part of the district, and crossbedded arenites which unconformably overlie the volcanic rocks near the town of Bissett, in the western part of the district. Layered synvolcanic sills containing fine- to medium- grained gabbroic rocks are a common feature in all parts of the volcanic succession and a large tonalitic intrusion, the Ross River Pluton, is also thought to be synvolcanic (Turek et al., 1987). All major rock units within the district are of Archean age and have been affected by late Archean (2700 Ma) low grade metamorphism, although, medium grade metamorphic rocks are encountered northward and southward in the Wanipigow and Manigotagan gneissic belts respectively. Upright to reclined folds and several generations of low grade cleavage developed in conjunction with metamorphism.

The Western Liaoning District is in the eastern part of the Yanshan uplift of the North China Platform (Fig. 2). Like many of the uplifts of the North China Platform, it contains a wide variety of medium to high grade gneissic lithologies. Most common are plagioclase-hornblende-biotite gneisses and orthogneisses composed of tonalite, trondjhemite and granodiorite (TTG). Remnants of possible greenstone belt rocks are locally preserved as amphibolites, layered metapyroxenite enclaves and oxide iron formation. All of the mafic and felsic gneisses in Western Liaoning District are of Archean age and have been affected by late Archean medium to high grade metamorphism (Anshan Movement) and locally by early Proterozoic medium grade metamorphism (Zhong tiao Movement). Successive generations of complex folds and foliations accompanied the two metamorphic events. Paleozoic and Mesozoic magmatic activity has been imprinted on much of the Archean terrane in Western Liaoning District. Porphyritic granitoid bodies

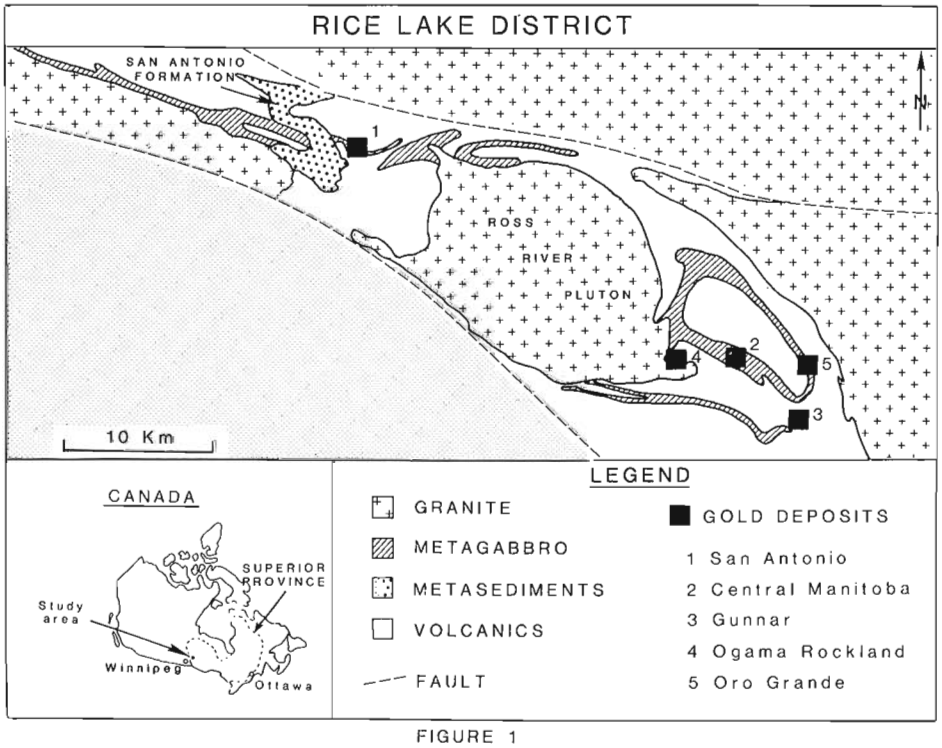

FIGURE 1

Figure 1. Geology and Gold Deposits of the Rice Lake Greenstone Belt, southeastern Manitoba, Canada.

of Permian age intrude the Archean rocks and both are overlain unconformably by a gently to moderately dipping sequence of unmetamorphosed volcanic flows (principally flow banded rhylolite), tuffs and epiclastic rocks of Jurassic to Cretaceous age. These rocks, as well as their basement, are intruded by late Jurassic to early Cretaceous dioritic to granodioritic stocks and plugs.

DISTRIBUTIONS OF GOLD DEPOSITS

The major gold deposits of Rice Lake District are distributed around the margins of the Ross River Pluton within the mafic parts of the volcanic succession (Fig. 1). In particular, three of the deposits considered (Table 1) occur within or near the top of differentiated gabbroic sills, the fractionated portions of which are characterized by modal quartz, granophyric texture and pegmatoid segregations. One deposit, the Gunnar, occurs at the intersection between pillowed basaltic flows and a quartz feldspar porphyry dyke; another, the Ogama-Rockland occurs entirely within the Ross River Pluton.

The major gold deposits of the Western Liaoning District are distributed in two clusters (Fig. 2). In the northern part of the area, Jinchanggouliang, Erdougou and Changagao deposits occur around the periphery of the Jurassic/Cretaceous Xiduimiangou granodiorite and are hosted by Archean gneisses, Mesozoic volcanic rocks and Permian granite, respectively (Table 1). Xiatazigou and Dongwujia deposits occur in the southern part of the area and are hosted principally by plagioclase-hornblende-biotite gneisses and iron formation.

DYKES

Although hypabyssal dykes are a common feature of both districts, they have a different tectonic significance.

In the Rice Lake District, dykes are ubiquitous (Stockwell, 1945) and cut all lithologies except the crossbedded arenites of the San Antonio Formation. As such, they are common features in the vicinity of gold deposits and tend to be cut by ore-bearing structures. Most varieties are of felsic composition and commonly are quartz- and/or feldspar-phyric. Lamprophyre dykes locally cut and are cut by quartz veins at the Gunnar deposit.

In Western Liaoning District, dykes are principally of Mesozoic age and cut Archean gneisses, Paleozoic granites

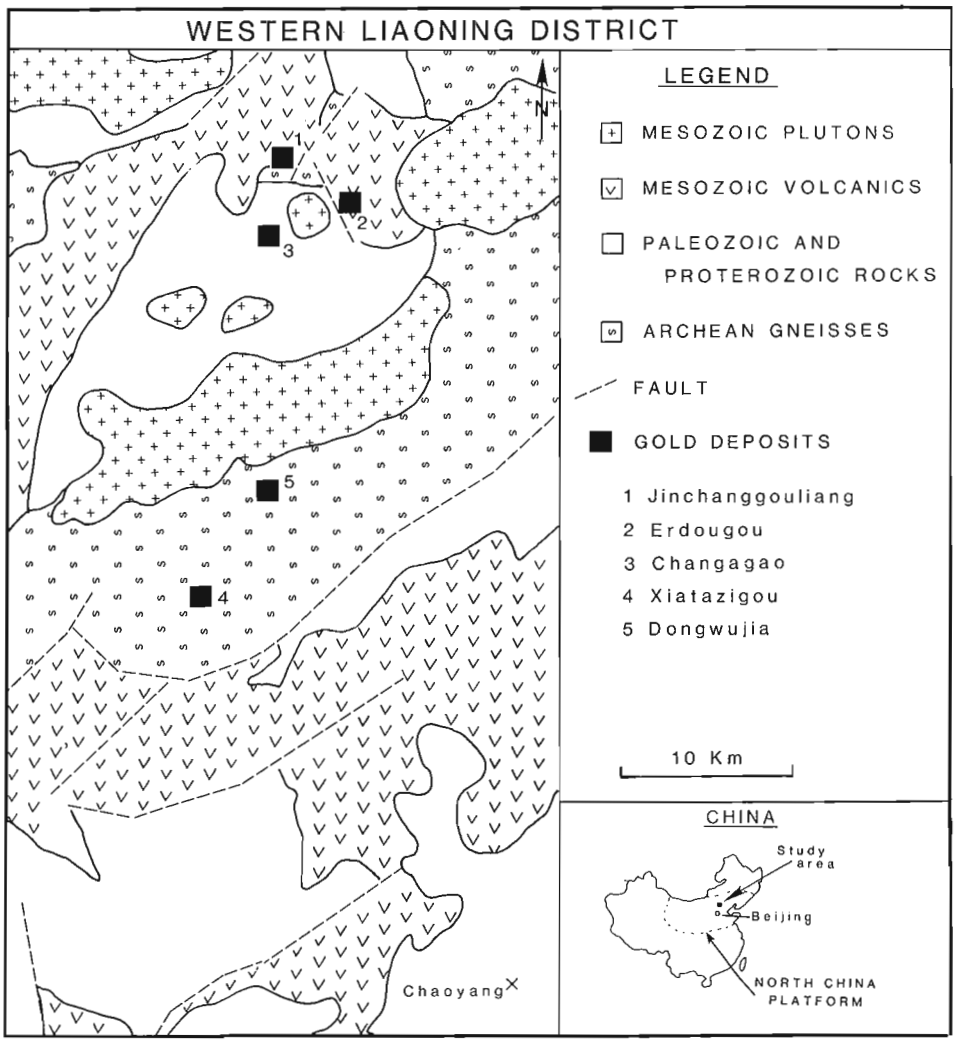

Figure 2. Geology and Gold Deposits of the Western Liaoning area, northeast China.

FIGURE 2

and Mesozoic volcanic rocks. Diorite, granodiorite and lamprophyre compositions are common and among the felsic varieties, some are quartz- and feldspar-phyric. Ore structures commonly cut or follow Mesozoic dykes.

ORE STRUCTURES

Structural controls on the specific location of ore veins are important in both districts, but the structures are of different styles.

In Rice Lake District, gold-quartz veins are typically hosted by shear zones comprising phyllonitic schists which cut all lithologies, including dyke rocks. Brittle fracturing and veining within and adjacent to competent rocks is commonly observed, and combined with the ductile nature of the host shear zones, suggests formation at moderate crustal depths. Shear zones are arranged into northwest- and northeast- striking sets and typically have dextral reverse and sinistral reverse movements, suggesting development in a compressive tectonic environment.

In Western Liaoning District, the structures which control the location of ore veins are faults and fractures that cut all rock types including some Mesozoic dykes. Ore-bearing faults commonly contain fault gouge and breccia, suggesting a shallow level of development. Normal faults are the rule and indicate development in an extensional tectonic environment.

VEIN COMPOSITION

In both districts, veins are the principal source of ore, although considerable differences exist in their composition.

In the Rice Lake District, veins contain gold in excess of silver in a ratio of approximately 7:1. Vein mineralogy of deposits is dominated by quartz with lesser and variable amounts of ankerite and albite. Principal sulphide minerals,

Table 1. Comparison of size, setting and composition of veins in Rice Lake and Western Liaoning gold districts.

RICE LAKE DISTRICT

deposit	approximate size (Tonnes Au)	host rocks	vein composition
San Antonio	> 40 T	fine grained leucogabbro	quartz-ankerite-pyrite-albite
Central Manitoba	> 5 T	quartz gabbro and cherty siltstones	quartz-chalcopyrite-pyrrhotite-pyrite-albite
Gunnar	> 3 T	metabasalt and quartz-feldspar porphyry dyke	quartz-ankerite-pyrite-chlorite
Ogama-Rockland	2 T	tonalite	quartz-pyrite-chalcopyrite-ankerite
Oro Grande	< 1 T	quartz gabbro	quartz-pyrite-pyrrhotite-chlorite

WESTERN LIAONING DISTRICT

deposit	approximate size (Tonnes Au)	host rocks	vein composition
Jinchanggouliang	> 20 T	plagioclase-hornblende-biotite gneiss and Mesozoic dykes	pyrite-chalcopyrite-sphalerite-galena-tetrahedrite-quartz-calcite
Erdougou	> 10 T	Mesozoic rhyolite and diorite dykes	pyrite-chalcopyrite-galena-tetrahedrite-quartz
Changagao	> 2 T	porphyritic Paleozoic granite	pyrite-chalcopyrite-galena-tetrahedrite-quartz
Xiatazigou	2 T	plagioclase-hornblende-biotite gneiss	pyrite-arsenopyrite-pyrrhotite-chalcopyrite-quartz
Dongwujia	2 T	meta-iron formation and lamprophyre dykes	pyrite-arsenopyrite-chalcopyrite-quartz-ankerite

in decreasing order of abundance, are pyrite, pyrrhotite, chalcopyrite and sphalerite, with rare galena and tellurides. Tourmaline, chlorite and sericite are common accessory minerals. Native gold commonly occurs within pyrite or chalcopyrite and a second generation occupies fractures in quartz or chloritic slickensides (Stephenson, 1971).

In Western Liaoning District, veins contain silver in excess of gold in a ratio of approximately 4:1 and are rich in sulphides by comparison with quartz. The vein mineralogy at different deposits shows a temporal progression through four assemblages:

1) pyrite - quartz - biotite - K-feldspar
2) pyrite - Sb sulphides - quartz - electrum - sericite and minor K-feldspar - minor gold
3) galena - sphalerite - tetrahedrite - chalcopyrite - electrum
4) marcasite - chalcopyrite - bornite - chalcocite - quartz - calcite - sericite - clay minerals and rare native silver.

ALTERATION AND ORE FLUIDS

Effects of hydrothermal alteration adjacent to veins are well recorded in both districts, but these are of substantially different types.

In the Rice Lake District, hydrothermal alteration is dominated by deposition of carbonate minerals. Near quartz veins, hydrous metamorphic assemblages are progressively replaced by calcite and chlorite, ankerite and sericite, and locally albite and pyrite. Such alteration typically extends 1 to 10 m from ore veins and is dominantly controlled by faults and fractures. The importance of CO_2 as a constituent of ore- forming fluids is further reflected by fluid inclusion compositions in vein quartz. Inclusion fluids were trapped in the temperature range of 250°-350°C, are of low salinity (5 Wt% NaCl equivalent) and contain approximately ten mole percent of CO_2. (Diamond, unpublished data).

In Western Liaoning District, wall rock minerals are progressively replaced by high temperature biotite - K-feldspar and pyrite, by medium temperature sericite - chlorite - pyrite and minor K-feldspar and by low temperature calcite - sericite - adularia and clay minerals. The superimposed alteration envelopes extend laterally up to 25 to 30 m on either side of individual veins and fractures. Fluid inclusion analyses (Zhang, unpublished data) support the observed variations in veins and alteration mineralogy. As at Rice Lake, salinities are low (5 Wt% NaCl equivalent) but inclusion trapping temperatures range from 450°C down to less than 200°C and inclusion fluids contain low mole fractions of CO_2, typically one percent.

DISCUSSION

It is evident from the foregoing descriptions that, although there are some points of comparison, there are many points of contrast in setting and style of gold deposits in these two Archean terranes.

The contrasting points can be attributed to two main factors: the inherent differences in metamorphic grade of the Archean rocks between the two areas and the superposition of Mesozoic magmatic activity on the Archean rocks in Western Liaoning District. There is little doubt from the weight of the evidence presented that the formation of the gold deposits in Western Liaoning District is largely related to upper crustal Mesozoic magmatic activity, but there remains the important question as to the role of the Archean basement terrane. In Western Liaoning District, as in other parts of the North China Platform, there is as strong a spatial correlation of gold deposits with Archean gneisses as there is with centres of Mesozoic magmatism. One explanation put forward by Chinese geologists for this dual correlation, is that in the North China Platform, as in other parts of the world, preferential concentration of gold took place in Archean greenstone belts and their metamorphosed remnants, and that they provide a source for reconcentration of gold by Mesozoic magmas and their fluids. In many respects, such a "source bed" or "lateral secretion" concept is not unlike many current models proposed for gold deposits of strictly Archean age requiring preconcentration of gold in exhalative or felsic magmatic deposits for subsequent remobilization into quartz veins by metamorphic fluids. The essential unresolved question in all of these cases is which of the ore forming constituents are derived from host rocks and which are inherent to the primary fluid. This topic will be addressed by further study of the deposits of Western Liaoning District by a Sino-Canadian team in 1989. It is hoped that the results will provide some new insights into genetic and exploration models for gold deposits in the Archean terranes of both Canada and China.

ACKNOWLEDGMENTS

F. Robert, R. Thorpe and J. Franklin made numerous useful suggestions to improve the manuscript.

REFERENCES

Stockwell, C.H.
1945: Beresford Lake, Rice Lake and Gem Lake; Geological Survey of Canada, Maps 809A, 810A and 811A.

Stephenson, J.
1971: Gold Deposits of the Rice Lake - Beresford Lake Greenstone Belt, Southeastern Manitoba; Manitoba Mines Branch Publication 71-1, p. 337-385.

Turek, A., Keller, R., Weber, W., and VanSchmus, W. R.
1987: U-Pb Zircon Geochronology of the Rice Lake Greenstone Belt; in Report of Field Activities 1987, Manitoba Energy and Mines, Minerals Division, p. 119-121.

Highlights of gold studies in the Churchill Structural Province, Kaminak greenstone belt and Hurwitz Group, District of Keewatin, N.W.T.[1]

A.R. Miller
Mineral Resources Division

Miller, A.R., Highlights of gold studies in the Churchill Structural Province, Kaminak greenstone belt and Hurwitz Group, District of Keewatin, N.W.T.; in Current Research, Part C, Geological Survey of Canada, Paper 89-1C, p. 127-134, 1989.

Abstract

Field and petrographic studies indicate two contrasting styles of gold mineralization in the District of Keewatin. In the "Fat Lake" area, mineralization is hosted by quartz diorite that intruded pillowed basaltic flows of the Kaminak Group. This mesothermal type of mineralization is in deformed quartz veins related to steeply dipping Archean ductile shear zones. In the Shear Lake deposit, gold is contained in late, near-vertical, east-west-trending brittle fault and breccia zones that cut the folded Proterozoic Hurwitz orthoquartzite and penetrate the Archean Henik Group metagreywackes. Gold-bearing pyritic fractures, faults and breccias are vertically zoned: an upper kaolinite grades into a chlorite then into a lower biotite zone. The Shear Lake gold deposit is interpreted as being Proterozoic and epithermal. Hence both Archean and Proterozoic volcano-sedimentary sequences need to be evaluated for gold mineralization in the District of Keewatin.

Résumé

Des études pétrographiques et des études sur le terrain indiquent deux types de minéralisation aurifère contrastés dans le district de Keewatin. Dans la région du lac Fat, la minéralisation se trouve dans la diorite quartzique qui a été pénétrée par des coulées basaltiques de lave en coussins du groupe de Kaminak. Cette minéralisation de type mésothermal prend la forme de veines de quarts déformées associées à des zones de cisaillement ductiles de fort pendage de l'Archéen. Au gisement de Shear Lake, l'or se trouve dans les tardives zones faillées de rupture fragile et dans les zones bréchiformes presque verticales de direction est-ouest qui recoupent l'orthoquartzite plissée de la formation d'Hurwitz du Protérozoïque et pénètrent les métagrauwackes du groupe d'Henik de l'Archéen. Les fractures, failles et brèches avec or et pyrite sont verticalement zonées; une zone supérieure de kaolinite, une zone de chlorite et une zone inférieure de biotite. Le gisement aurifère de Shear Lake est interprété comme étant épithermal et d'âge protérozoïque. Ainsi, dans le district de Keewatin, il est nécessaire d'évaluer à la recherche de minéralisations aurifères les séquences volcano-sédimentaires de l'Archéen et du Protérozoïque.

[1] Contribution to Canada-Northwest Territories Mineral Development Agreement 1987-1991. Project carried by Geological Survey of Canada.

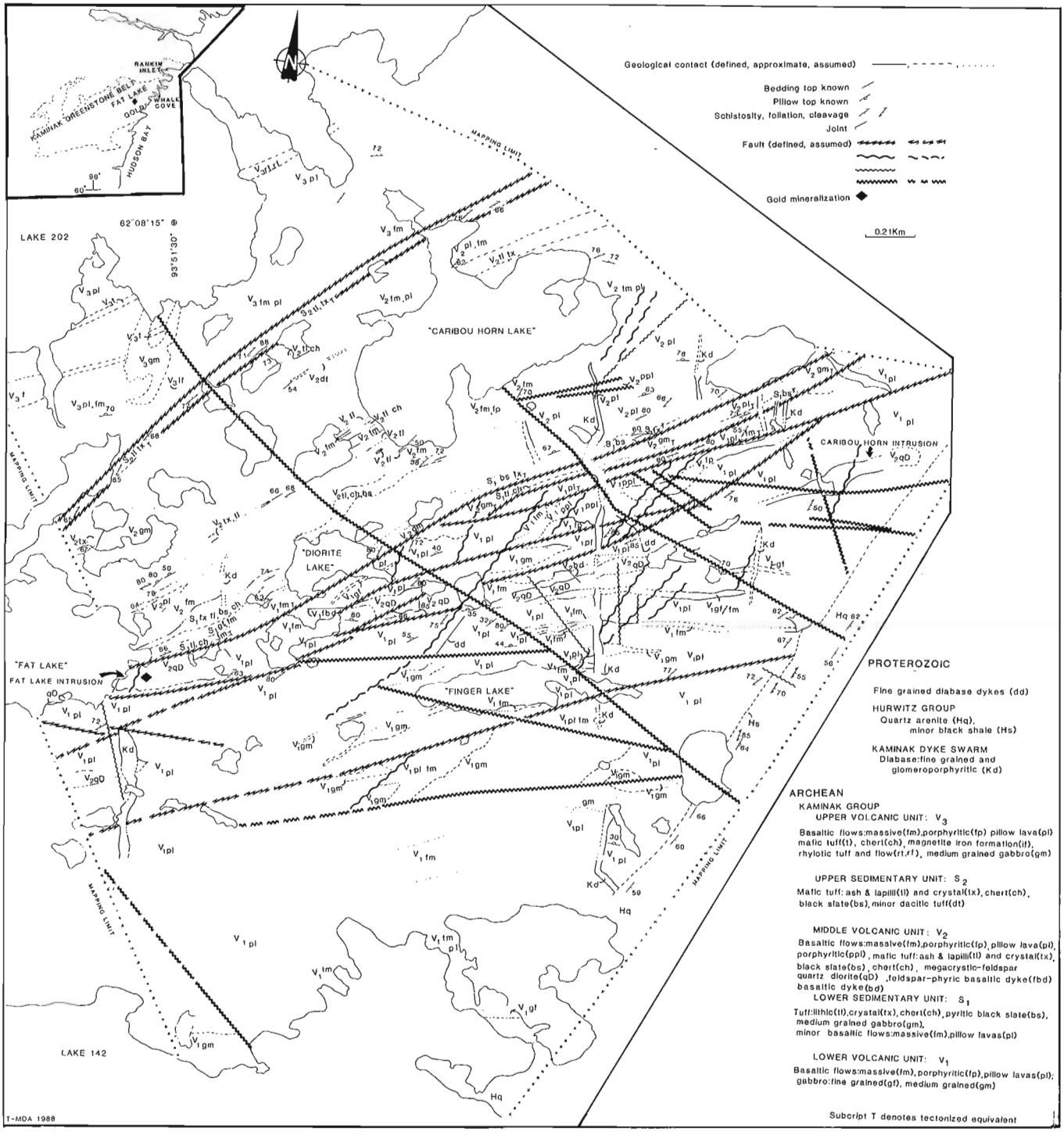

Figure 1. Geology of part of the Tavani Map-area, 55K/4, and the Fat Lake gold deposit.

INTRODUCTION

This is a progress report under the project entitled " GOLD METALLOGENY, CHURCHILL STRUCTURAL PROVINCE" part of the Canada-Northwest Territories Mineral Development Agreement. The project is designed to document the types of gold occurrences, prospects and deposits by regional mapping in order to identify their lithological and structural settings. This includes detailed examination of altered and mineralized zones.

Field studies during 1988 were focused in the northeastern and southwestern portions of the Kaminak Greenstone belt: a) the Fat Lake prospect, Tavani map-area, NTS 55K/4 and b) the past producer, Shear Lake deposit, Kognak River map-area, NTS 65G/8, c) the past producer, Cullaton Lake B-Zone deposit, Kognak River map-area, NTS 65G/8, d) a gold occurrence in NTS 65G/8, Kognak River map-area, 5 km east of lake 860 e) gold prospects in the "Happy Lake" area, NTS 55L/10 and f) Turquetil Lake gold discovery, NTS 55E/13. This progress report deals only with the geology of the Fat Lake prospect, Shear Lake deposit and only minor remarks on the Cullaton Lake B-Zone. The latter remarks pertain only to comparisons between the Shear Lake and B-Zone deposit types.

GEOLOGY OF PART OF THE TAVANI MAP-AREA, (55K/4) AND THE FAT LAKE GOLD MINERALIZATION

Introduction

The Fat Lake prospect is in the northeastern portion of the Archean Kaminak greenstone belt (Davidson, 1970). The Kaminak belt in a portion of the Tavani map-area 55K/4 consists predominantly of low metamorphic grade mafic volcanic rocks: massive and pillowed flows, tuff and breccia with related gabbroic intrusions (Wright,1967; Heywood,1973). Park and Ralser(1989) are revising the stratigraphy and structure of the Kaminak Group in part of the Tavani map-area (55K/3,4,5,6).

Mapping in 1988 extended from "Fat Lake" northeastward to just east of "Caribou Horn Lake"(Fig. 1) and refined: i)the volcanic stratigraphy in the predominantly mafic volcanic pile, ii)the size, form and composition of mafic intrusions, iii) types, relative age and geometry of fault groups and iv) the relationship of gold to lithology, structure and alteration.

Stratigraphy of the"Fat Lake" map-area

The Kaminak Group volcanic-intrusive stratigraphy in the map-area (Fig. 1) has been subdivided into three metavolcanic units with intervening metasedimentary units. The volcanic pile is interpreted to be an upright homocline stiking on average 220-230 degrees and dipping to the northwest at 40-60 degrees.

Lower volcanic unit (V1)

The lower volcanic unit (Fig. 1), comprises a variety of metabasaltic volcanic rocks, predominantly aphyric pillowed and massive flows, subordinate feldspar-phyric pillowed and massive flows and related fine- to medium-grained gabbroic equivalents.

Unit V1 is distinguished from the overlying S1 unit by an absence of metasedimentary rocks. Pillow tops throughout this unit as determined from "lava-shelves" indicate a uniformly northwest-younging sequence (Tella et al., 1986). The contact between unit V1 and the overlying S1 is a northeast-trending shear zone. However, the boundary between V1 and S1 is interpreted to have been conformable, representing the transition from voluminous basaltic volcanism to deposition of fine-grained tuffaceous, clastic and chemical sediments.

Lower sedimentary unit (S1)

Unit S1, the lower of two major metasedimentary facies in the map-area, is an intercalated thinly bedded sequence of white, grey to bluish black pyritic chert, pyritic and non-pyritic black slate, and ash- to lapilli-sized tuffacous sediments. The lack of coarse detritus, the abundance of disseminated sulphide and the fine-grained black carbonaceous sediments indicate an euxinic basin that received a proportion of its clastic debris from distal volcanism. The thickest section of this unit is preserved between "Fat Lake" and "Diorite Lake". Here the section includes fine-grained massive and pillowed basaltic flows and gabbroic units, the latter possibly representing coarser parts of flows. Northeastward from "Diorite Lake" this stratigraphic unit is thinner and less well exposed. This eastern segment of S1 was intruded by concordant and discordant medium grained gabbroic bodies. Sedimentary, volcanic and intrusive rocks exhibit varying development of a penetrative foliation related to northeast faulting.

Middle volcanic unit (V2)

The middle volcanic unit, V2, conformably overlies the lower sedimentary unit and is distinguished from it on the basis of an increasing proportion of massive and pillowed basaltic flows. The character of volcanism is similiar to the V1 unit with phyric and aphyric lavas and coeval gabbroic intrusions. The principal lithological difference between unit V1 and V2 is the distribution of tuffaceous sediments, crystal and lapilli tuff, accompanied by sulphidic chert and pyritic black argillite and slate. Minor dacitic lithic tuff record the onset of felsic pyroclastic volcanism (Heywood,1973).

Two separate intrusions of quartz diorite composition, V2qD, were recognized, one on the southeast shore of "Fat Lake"(termed the Fat Lake intrusion) and the second extending from the southeast end of "Diorite Lake" northeastwards for approximately 2 km(termed the Caribou Horn intrusion). It is uncertain if the intrusions are syn-volcanic or younger than the V1/S1 package and this will be tested by a variety of geochronological techniques. They appear to be sills or slightly discordant tabular bodies that conform to the regional northwest dip. Contacts of the Fat Lake intrusion are deformed by the northeast-trending shear zone that is centred in S1 and the adjacent units of V1 and V2. However, contacts of the Caribou Horn intrusion south of the

V1/S1 shear zone are well preserved. The contact undulates with slight variations in topography suggesting a moderate northwesterly dip to the intrusion.

These intrusions are characterized by 5- mm to 10- cm megacrysts of subhedral to anhedral feldspar, set in a medium-grained, equigranular, interlocking feldspar + hornblende ± pyroxene assemblage. Accessory phases throughout these intrusions include fine-grained disseminated pyrite, chalcopyrite and subhedral titanite grains up to 3.0 mm containing exsolution lamallae of ilmenite. The Fat Lake intrusion is the most altered of the two intrusions because of deformation by the northeast-trending shear zone. (see mineralization below).

Upper sedimentary unit (S2)

The second major sedimentary unit, S2, conformably overlies the volcanic and sedimentary rocks of unit V2 and consists of mafic lithic and crystal tuff with minor chert. This unit is thinner than the S1 sedimentary units and lacks intrusions of gabbroic and quartz diorite composition. Unit S2 like S1, contains a well defined penetrative foliation related to a second northeast-trending shear zone.

Upper volcanic unit (V3)

The uppermost unit in the map-area, V3, is an intercalated sequence of massive and pillowed basaltic flows, mafic tuff, minor quartz-eye rhyolite flows and rhyolitic lapilli tuff. These felsic rocks are along strike from felsic volcanic rocks to the northeast (Heywood, 1973).

Kaminak dykes

Early Proterozoic igneous activity predating sedimentation of the Hurwitz Group is represented by a swarm of north-trending feldspar-phyric diabase dykes (Kaminak dykes of Davidson, 1970). Rapid textural variation occurs locally along strike within single dykes from fine-grained diabasic to coarse glomeroporphyritic. Regionally, the Kaminak dykes in the Fat Lake area lie within a zone of little deformation and metamorphism (Davidson, 1970). Locally these dykes can exhibit a weak foliation where they are intersected by northeast shear zones. This foliation was developed presumably during Proterozoic reactivation of Archean northeast-trending shear zones.

The southeastern margin of the Kaminak Group is overlain by deformed Hurwitz Group rocks consisting of pink to red, thinly bedded and ripple-marked orthoquartzite (Hq) and underlying minor black shale (Hs). Small rubble crops of cleaved black shale were observed near outcrops of Kaminak volcanic rocks. Cliff-forming outcrops of Kaminak Group mafic volcanic rocks adjacent to the inferred Hurwitz contact are extensively epidotized. This contact is inferred to be tectonic, possibly related to thrusting or flexural slip associated with Hurwitz deformation.

The uppermost unit in the map-area comprises narrow northeast- and northwest-trending fine-grained diabase dykes, dd. No field criteria were observed to determine whether these dykes pre-date or post-date Kaminak dykes.

Structure of the "Fat Lake" map-area

Lava shelf top determinations in the three volcanic units, as well as grading in tuffaceous and chemical sedimentary rocks indicate a homocline with a northwest younging direction. Local reversals in the dip of chert beds near the southwest end of "Caribou Horn Lake" suggest a minor syncline whose axial trace trends northeasterly along the southeastern edge of that lake.

The abundance of outcrop in the study area has permitted the definition of numerous fault trends and types including their relative age relationships. The most important structures with respect to mineralization are the 050 and related 030 shear zones. The best exposed relationships were mapped along the S1 unit and adjacent units V1 and V2. These shears are characterized by zones where the original volcanic and/or gabbroic rocks have been converted to carbonate+epidote+chlorite schist. The clockwise rotations of foliation planes within the composite northeast-trending structures and lineations imply a dextral sense of movement. Park and Ralser (1989) state that these Archean faults have had a protracted movement history and were important in influencing sedimentation of the overlying Hurwitz Group metasediments.

In the map area, pre-Hurwitz north-trending Kaminak dykes (Kd), and northeast- and northwest-trending, narrow, fine-grained diabase dykes (dd) are weakly foliated where intersected by these structures. The northeast-striking schist zones are composite in form. Lithons which display less deformation are seperated by bands of chlorite-carbonate schist. These fault directions are interpreted as originating in a ductile regime in contrast to the remaining sets. The remaining sets in order of chronology, ($\sim$010° followed by 270° and 310-320°), are characterized by very thin schist zones and bands of closely spaced fracture cleavage respectively. These faults are interpreted as having been developed in a brittle regime.

Alteration and mineralization

Proven gold reserves to depths of 67 m on four veins in the Fat Lake quartz diorite are 52 500 tons grading 0.325 oz gold per ton (Northern Miner, Aug. 15/88). Gold-bearing veins are preferentially developed in the quartz diorite and extend into the foliated pillow lavas of unit V1. However, veins that extend into the wall rocks thin rapidly and terminate a few metres beyond the quartz diorite contact. Gold-bearing quartz veins are highly irregular in plan and exhibit features that suggest development in a host rock that was undergoing progressive deformation. Some veins are folded, some boudinaged, others folded and transposed and some exhibit a layered structure from repeated opening and filling. Vein-filling assemblages are quartz + Mg-Ca-bearing carbonate ± chlorite accompanied by weakly disseminated pyrite + chalcopyrite + sphalerite + galena + gold.

The Fat Lake quartz diorite comprises two alteration assemblages: i) foliated black chloritic-rich zones that bound quartz veins and ii) lithons between quartz veins where the idiomorphic texure is preserved but where alteration is indicated by epidote-like discoloration. In thin sec-

tion, few primary textures are preserved in the chlorite-rich zones except for relict 1 mm anhedral quartz grains. The primary feldspar and mafic minerals have been replaced by streaky and finely felted Fe-chlorite with Mg-Ca carbonate, fine grained quartz, and traces of sulphide and titanite. Lithons between the chloritic zones have an assemblage of epidote, chlorite, quartz, relict plagioclase and hornblende, trace actinolite, Mg-Ca carbonate and titanite with ilmenite exsolution lamallae and magnetite.

Gold mineralization in the Fat Lake quartz diorite is associated with steeply dipping Archean ductile shear zones. Geology contrasts between the host intrusion and country rocks account for the localization of quartz veins with gold in the intrusion. The intrusion responded in a brittle manner compared to more ductile deformation in the adjacent volcanic and sedimentary units (Roberts, 1987). Alteration assemblages including the replacement of magnetite and titanite appear similar to the Victory Gold Mine, W. Australia (Clark et al., 1986). In addition magnetite-ilmenite-bearing intrusions cut by Archean shear zones have high exploration potential for mesothermal gold mineralization. The source of the gold remains speculative: i) gold may have been associated with fluids migrating through the shear zone system and subsequently deposited in a chemically reactive and structurally prepared rock unit, or ii) gold and associated base metals were remobilized from the S1 tuffaceous and chemical sedimentary unit into the structurally prepared quartz diorite.

KOGNAK RIVER MAP AREA, 65G/8

Introduction

The Shear Lake deposit was discovered in 1947 or 1948 and additional exploration was carried out in the early 1960s and 1980s. Cullaton Lake Gold Mines Ltd. proceeded with underground development and mining between 1983 to 1985. Mining ceased in 1985. As the mineralized outcrops in the mine area are extensively oxidized, field studies focused on logging core preserved in the storage area at the Cullaton B-Zone mine. Three cross sections (Fig. 2) were selected across the east-west trending ore body.

Regional geology from Cullaton Lake to Shear Lake area

The following aspects of Hurwitz Group regional geology are only highlighted and the reader is referred to Eade (1974) and Eade and Chandler (1975) for additional data. The oldest Archean supracrustal rocks in the Cullaton Lake area are the intercalated metasedimentary and metavolcanic rocks of the Henik Group (Eade, 1974). Southwest of Cullaton Lake, the Henik Group consists predominantly of fine-grained metagreywacke and argillite with intercalated magnetite-chert iron-formation that have been metamorphosed to biotite-grade greenschist facies. One of these magnetite-chert iron formations, containing significant pyrrhotite with gold, hosts the Cullaton B-Zone gold deposit. Minor mafic tuff, flows and felsic flows are present in this distal turbidite sequence (Eade, 1974).

The lower three formations of the Hurwitz Group metasediments have been metamorphosed to lower greenschist facies. Orthoquartzite (Kinga Formation), shale and siltstone (Ameto Formation) and dolostone, argillite, siltstone (Watterson Formation) overlie Archean metagreywackes and are preserved as a series of domes and basins in the Cullaton Lake area. Two structural aspects of the Hurwitz fold belt may be significant in terms of the structural and mineralization history of the Shear Lake gold deposit: i) fold geometry and associated steep faults and ii) thrust faults.

In Figure 5 of Eade (1974), the geometry of the basal orthoquartztite and overlying fine-grained clastic sediments in the Cullaton-Shear lakes area indicates initial folding about north-plunging upright folds with associated reverse faulting parallel to axial traces. Eade (1974) interpreted a second deformation to have involved east-west cross faulting and block rotation to account for stratigraphic repetition. The east-west trending faults are parallel to the second phase regional folds whose axial traces trend westerly to northwesterly. Additional structural studies are necessary in the Cullaton to Shear lakes area to assess the relation between folding and faulting. Thrusts involving basement have been locally documented in parts of the Hurwitz fold belt (Eade, 1974; Tella et al., 1986; Aspler et al., 1989). East-trending, south-dipping thrust faults in the greater Cullaton area are along orthoquartzite-basement contacts, suggesting a basement-cover detachment surface.

Geology and mineralization of the Shear Lake deposit

Raman et al., (1986) described the Shear Lake gold deposit as being vein-type, in the basal Hurwitz orthoquartztite, and in a series of parallel to subparallel fracture systems that trend east-west. Logging of the Shear Lake core has extended the information presented by Raman et al. (1986).

Two major directions of faults are recognized in the Shear Lake deposit (Fig. 2). These are i) an early subhorizontal band of intensely crushed and altered orthoquartzite that is at or near the Proterozoic-Archean boundry and is transected by ii) narrow, vertical fracture and fault zones. The three cross sections of Figure 2 display gold-bearing, fracture-fault zones through a portion of the Shear Lake deposit. These geological cross sections were redrafted from cross sections supplied by Cullaton Lake Gold Mines Ltd., (presently Corona Corporation). The data and interpretation was derived from several drill holes on each section and these are identified on Figure 2. Geological data from the other drill holes, contacts and lithologies, were incorporated onto these sections in light of ideas evolved during this study. The nomenclature for the identification of the various mineralized fracture-fault zone, E17 to E27, was taken from company sections.

The two fault types exhibit different alteration assemblages and styles of deformation. Megascopically, the flat fault zone is easily identified in the host orthoquartzite by a gradational colour change from snow white to orange tan and a well defined quartz grain elongation. Petrographically, this unit is composed of a very fine grained quartz mosaic which can contain relict lithic fragments of orthoquartzite. Textural and petrofabric characteristics of quartz

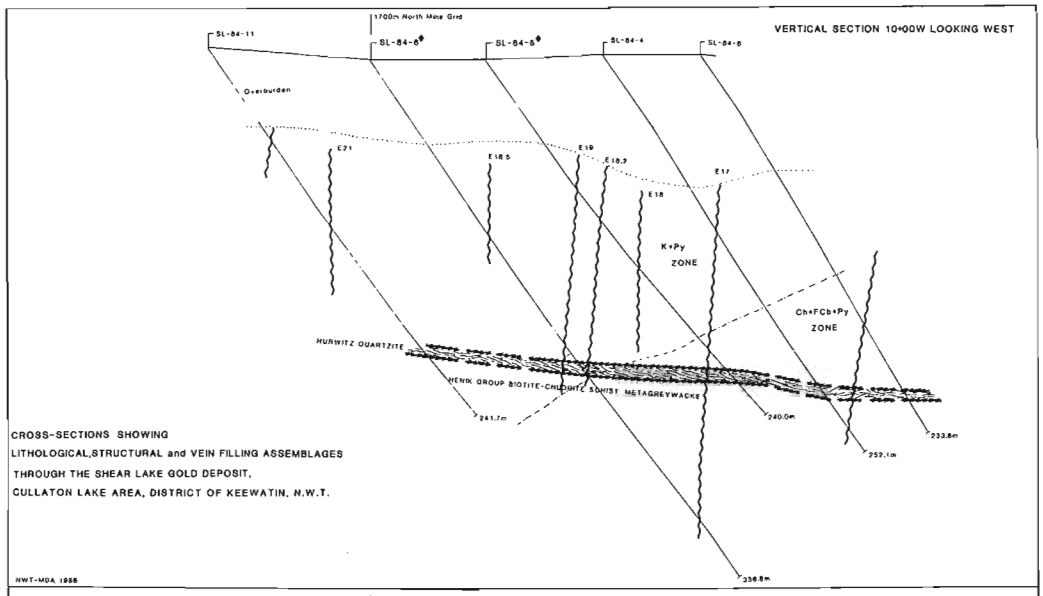
1700m North Mine Grid
VERTICAL SECTION 10+00W LOOKING WEST
SL-84-11
SL-84-6
SL-84-5
SL-84-4
SL-84-8
Overburden
E21
E18.5
E19
E18.3
E17
E18
K+Py ZONE
Ch+FCb+Py ZONE
HURWITZ QUARTZITE
HENIK GROUP BIOTITE-CHLORITE SCHIST METAGREYWACKE
241.7m
240.0m
233.8m
257.1m
338.8m
CROSS-SECTIONS SHOWING
LITHOLOGICAL,STRUCTURAL and VEIN FILLING ASSEMBLAGES
THROUGH THE SHEAR LAKE GOLD DEPOSIT,
CULLATON LAKE AREA, DISTRICT OF KEEWATIN, N.W.T.
NWT-MDA 1988

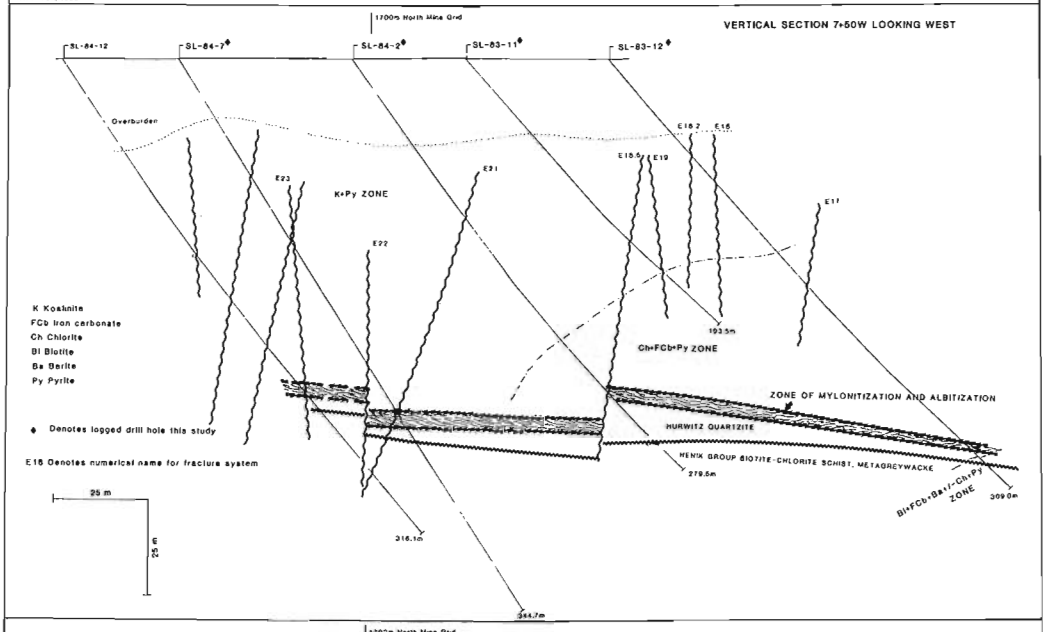
1700m North Mine Grid
VERTICAL SECTION 7+50W LOOKING WEST
SL-84-12
SL-84-7
SL-84-2
SL-83-11
SL-83-12
Overburden
E18.2
E16
E18.5
E19
E23
E31
E17
K+Py ZONE
E22
K Kaolinite
FCb Iron carbonate
Ch Chlorite
Bi Biotite
Ba Barite
Py Pyrite
Denotes logged drill hole this study
E16 Denotes numerical name for fracture system
193.5m
Ch+FCb+Py ZONE
ZONE OF MYLONITIZATION AND ALBITIZATION
HURWITZ QUARTZITE
HENIK GROUP BIOTITE-CHLORITE SCHIST, METAGREYWACKE
279.5m
Bi+FCb+Ba+/-Ch+Py ZONE
309.0m
25 m
E
25
316.1m
344.7m

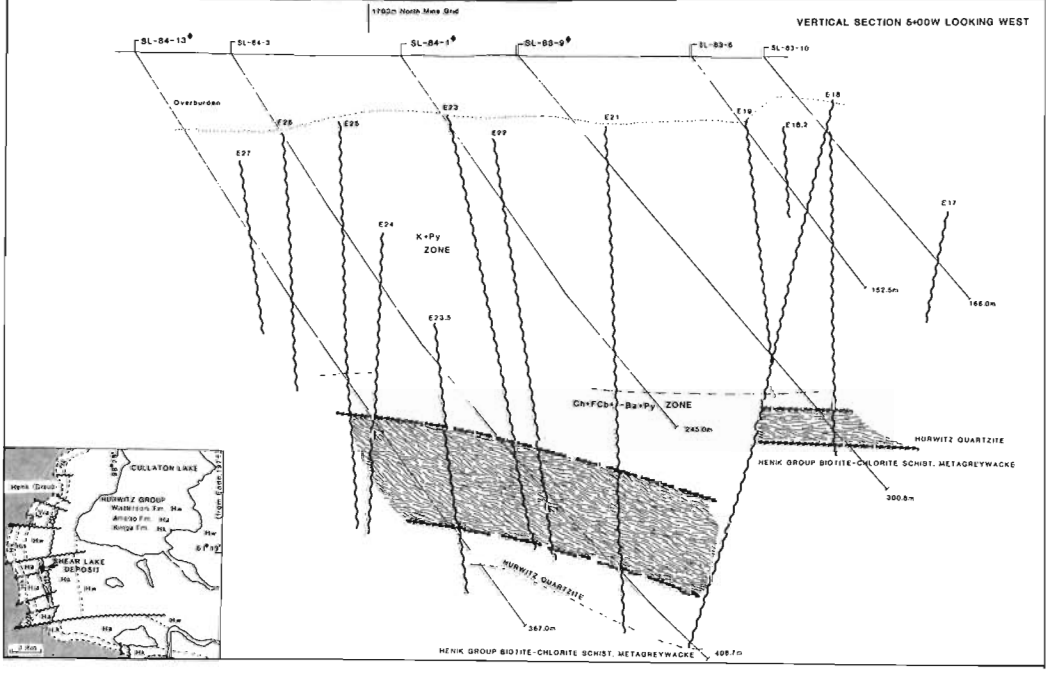
1700m North Mine Grid
VERTICAL SECTION 5+00W LOOKING WEST
SL-84-13
SL-84-3
SL-84-1
SL-83-9
SL-83-6
SL-83-10
Overburden
E25
E23
E21
E19
E18
E18.3
E27
E99
E17
E24
K+Py ZONE
E23.5
152.5m
166.0m
Ch+FCb+-Ba+Py ZONE
245.0m
HURWITZ QUARTZITE
HENIK GROUP BIOTITE-CHLORITE SCHIST, METAGREYWACKE
300.0m
HURWITZ QUARTZITE
367.0m
HENIK GROUP BIOTITE-CHLORITE SCHIST, METAGREYWACKE
408.7m
CULLATON LAKE
HURWITZ GROUP
SHEAR LAKE DEPOSIT

suggest that this subhorizontal band of crushed orthoquartzite is a cataclasite and that the Hurwitz Group may be allochthonous in the Cullaton Lake area.

A second important feature of this zone of grain size reduction is the partial to locally complete replacement of the granulated orthoquartzite by fine-grained to locally medium-grained albite. Subhedral interlocking albite grains lack strain lamallae and certainly implies that the sodium metasomatism postdates tectonism.

In thin section, albite grains have a dusty appearance due to ultrafine inclusions of an opaque mineral, assumed to be hematite. This albite + hematite assemblage correlates well with the gradational orange-tan discoloration of the white orthoquartzite.

In these sections mineralization is restricted to thirteen steeply dipping zones of closely spaced fractures and breccia. The orthoquartzite between fracture zones is foliated, weakly to unfractured and lacking in sulphide veins. Fracture-fault zones are 3-4 m in width, have been followed along strike for 500 m (section 5+00W to section 10+00W) and penetrate the Hurwitz-Henik contact at an average vertical depth of 200 m below surface.

Mining was confined to the gold-bearing, sulphide filled fractures and breccias in the orthoquartzite. However, sulphide mineralization with associated vein filling assemblages extends into the Archean Henik Group schists and transposed metagreywacke. In drill core, fracture planes with their respective vein filling assemblages range from 30 to 55 degrees to the core axis and in many of the mineralized zones fractures occur as a conjugate set having an acute interangle of 20-30 degrees.

As shown in Figure 2, the pyrite + gold-bearing veins are vertically zoned through the orthoquartzite into Archean schists and metagreywacke. The zonation is defined by the combination of minerals filling veins and breccias in the orthoquartzite and basement metagreywacke and derived schists. Mineralogical contacts are defined on the first appearance of a diagnostic phase as determined during logging and confirmed through limited follow up petrography and X-ray identification. Refining of this zonation will continue together with microprobe analyses of silicate, carbonate, sulphate and opaque phases. Gold is presumed to be distributed throughout this vertical zonation because it was mined from veins in the upper oxidized clay-rich portion of the vein system (W.S. Hamilton, pers. comm. 1988) and gold is present as inclusions in pyrite in the lowest parts of this system. Wall rock alteration is non-existent to minimal throughout the greater part of the vein system because of the inertness of the host orthoquartzite. These vein assemblages can be viewed as products derived from the hydrothermal fluid and thus the vein assemblages may track the compositional evolution of the fluid.

Figure 2. Cross sections showing lithological, structural and vein filling assemblages through the Shear Lake gold deposit, Cullaton Lake area, District of Keewatin, N.W.T.

The following assemblages contain quartz and pyrite (from top to bottom): i) KAOLINITE ZONE: kaolinite ii) CHLORITE ZONE: iron chlorite + iron carbonate ± kaolinite ± white mica ± barite and iii) BIOTITE ZONE: biotite + iron carbonate + barite ± iron chlorite ± white mica. The kaolinite zone can be subdivided into a heavily oxidized upper subunit and a lower sulphide bearing subunit. Vein assemblages in the upper kaolinite subunit are: hematite + limonite + kaolinite + free gold. This mineral assemblage is interpreted as a post-glacial weathering cap superimposed on a sulphide + clay vein network. Weathering effects, hematite and limonite are most common in the upper kaolinite zone near the overburden contact and decrease rapidly downward through the lower kaolinite zone and are rare in the chlorite zone. Minor amounts of albite have been observed in the chlorite and biotite zones. This presence of albite suggest a link between extensive cataclastic zones, albitization and the vertical mineralogical zonation noted above.

In summary, the vertically zoned vein networks that constitute the Shear Lake deposit are hosted primarily in the Proterozoic Hurwitz orthoquartzite. The low metamorphic grade of the Hurwitz Group rocks, coupled with the brittle character of the mineralized faults, the variation in vein assemblages principally clay and sulfate minerals and the gold/silver ratio in gold grains support an epithermal setting for this gold mineralization.

Comparison of Shear Lake and B-Zone deposits

The B-Zone deposit is interpreted as a structurally controlled Archean mesothermal gold deposit hosted in chert+magnetite iron formation. The mineralized portion of the iron formation is restricted to a major flexure in the B-Zone iron formation. The mineralized iron formation within this flexure, probably a fold closure, is characterized by variable concentrations of pyrrhotite+gold with magnetite. Sulphide zones are restricted to this zone of closure in the iron formation and this same segment of the iron formation has been the locus of hydrothermal alteration. This alteration is characterized by an extensive zone of chloritization which is centred on and immediately peripheral to the zone of closure. Chlorite with carbonate prevasively replace the chert-magnetite iron formation and the adjacent chlorite schists which were derived from the Henik Group metagreywackes and metaargillites. This zone of chloritization is accompanied by flooding of the altered iron formation by quartz and quartz+iron carbonate veins. The distribution of arsenopyrite is erratic in the pyrrhotite-bearing segment of the iron formation and arsenopyrite does occur in and peripheral to vein networks. Based upon preliminary microprobe analyses, the composition of gold grains from the B-Zone is: Au: 91 wt%, Ag: 9 wt%. The above features contrast markedly with those of the Shear Lake deposit: 1) age (B-Zone: Archean; Shear Lake: Proterozoic) 2) geometry of mineralization (B-Zone: sulphide lenses in a chert+magnetite iron formation that are distributed in and near a fold closure; Shear Lake: narrow vertical fracture and fault zones crossctting the Proterozoic and Archean stratigraphy) 3) metallic phases associated with gold (B-Zone: pyrrhotite, arsenopyrite; Shear Lake: pyrite) 4) gangue assemblages (B-Zone: chlorite, iron carbonates,

quartz; Shear Lake: kaolinite, chlorite, iron carbonate, barite, biotite, quartz, white mica and 5) the composition of gold grains. Consequently the Hurwitz fold belt merits exploration for epithermal deposits in conjunction with the search for more traditional mesothermal deposits present in Archean greenstone belts such as the Kaminak belt.

ACKNOWLEDGMENTS

The author is greatly indebted to: Corona Corporation for field logistical support, access to and permission to publish data on the Shear Lake deposit and especially to William Hamilton of Corona for his continuing support throughout all aspects of this project and valuable discussions on Shear Lake geology; Borealis Exploration for discussions on and access to drill core from the Fat Lake property, Tavani map-area and L.R. Vrenier for field assistance. Rotary winged aircraft for the Tavani project was supported through Polar Continental Shelf Project #138-86. V. Cobb, pilot and B. Eaton, engineer are thanked for their superb logistical support throughout the project. J.A. Kerswill, C.W. Jefferson and L.B. Aspler critically read the manuscript and added greatly to its clarity. M. Bonardi is thanked for the electron microprobe analyses of gold grains

REFERENCES

Aspler, L.B., Bursey, T.L. and Miller, A.R.
1989: Sedimentology, structure, and economic geology of the Poorfish-Windy thrust-fold belt, Ennadai Lake area, District of Keewatin, and the shelf to foredeep transition in the foreland of Trans-Hudson Orogen; in Current Research, Part C, Geological Survey of Canada, Paper 89-1C.

Clark, M.E., Archibald, N.J. and Hodgson, C.J.
1986: The structural and metamorphic setting of the Victory Gold Mine, Kambalda, Western Australia; in Macdonald, A.J., ed., Proceedings of Gold '86, an International Symposium on the Geology of Gold: Toronto, 1986, p. 243-254.

Davidson, A.
1970: Precambrian geology, Kaminak Lake map-area, District of Keewatin; Geological Survey of Canada, Paper 69-51.

Eade, K.E.
1974: Geology of Kognak River Area, District of Keewatin, Northwest Territories. Geological Survey of Canada, Memoir 377.

Eade, K.E. and Chandler, F.W.
1975: Geology of Watterson Lake (west half) map-area, District of Keewatin, Geological Survey of Canada, Paper 74-64.

Heywood, W.W.
1973: Geology of the Tavani map-area, District of Keewatin; Geological Survey of Canada, Paper 72-47.

Northern Miner
1988: Boralis borrows $25 million to finance Fat Lake project. Vol. 74, No. 23, p. 2.

Park, A.F. and Ralser S.
1989: Precambrian stratigraphy and structure of the southwest part of the Tavani map area, District of Keewatin, N.W.T.; in Current Research, Part C, Geological Survey of Canada, Paper 89-1C, Report 1.

Raman, S., Kruse, J. and Tenney, D.
1986: Geology, geophysics and geochemistry of the Cullaton B-Zone gold deposit, N.W.T., Canada; in Gold in the Western Shield edited by L.A. Clark, C.I.M.M. Special Volume 38, p. 307-321.

Roberts, R.G.
1987: Ore deposit Models #11. Archean Lode Gold Deposits. Geoscience Canada, v. 14, no. 1, p. 37-52.

Tella, S., Annesley, I.R., Borradaile, G.J. and Henderson, J.R.
1986: Precambrian geology of parts of Tavani, Marble Island and Chesterfield Inlet map-area, District of Keewatin: a progress report. Geological Survey of Canada, Paper 86-13.

Wright, G.M.
1967: Geology of the southeastern barren grounds, Northwest Territories. Geological Survey of Canada, Memoir 350.

Preliminary $^{40}Ar/^{39}Ar$ geochronology and timing of Archean gold mineralization at the Sigma Mine, Val d'Or, Quebec

J.A. Hanes[1], D.A. Archibald[1], C.J. Hodgson[1], and F. Robert[2]
Mineral Resources Division

Hanes, J.A., Archibald, D.A., Hodgson, C.J., and Robert, F., Preliminary $^{40}Ar/^{39}Ar$ geochronology and timing of Archean gold mineralization at the Sigma Mine, Val d'Or, Quebec; in Current Research, Part C, Geological Survey of Canada, Paper 89-1C, p. 135-142, 1989.

Abstract

The Sigma Mine at Val d'Or, in the Abitibi Belt, is a typical vein-type gold deposit. Although the relative timing of gold mineralization with respect to magmatism, metamorphism and deformation in the mine is well documented, precise isotopic age constraints are lacking. Results of this $^{40}Ar/^{39}Ar$ study on metamorphic amphibole indicate that the regional metamorphism occurred at ca. 2.67-2.69 Ga. Muscovite from the gold-bearing veins yields a precise plateau age of 2579 $\pm$ 3 Ma (2 σ), whereas biotite from the veins shows disturbed age spectra. The mild disturbance of the biotite is attributed to later diabase dyke emplacement, and the $^{40}Ar/^{39}Ar$ dyke age suggests that this event is younger than 2.3 Ga. Although the amphibole and mica ages bracket the vein formation between 2690 and 2580 Ma, it is concluded, based on all evidence, that the muscovite plateau age is the time of vein and gold formation, which thus occurred ~ 100 Ma after regional metamorphism.

Résumé

Le gîte de la mine Sigma à Val d'Or, Québec, dans la zone de l'Abitibi, est un gisement d'or filonien typique. Si l'âge relatif de la minéralisation aurifère par rapport au magmatisme, au métamorphisme et à la déformation est bien documenté à la mine, des contraintes précises provenant d'âges isotopiques sont absentes. Les résultats de la présente étude $^{40}Ar/^{39}Ar$ sur des amphiboles métamorphiques indiquent que le métamorphisme régional a eu lieu autour de 2,67 à 2,69 Ga. De la muscovite provenant de veines aurifères donne un âge de plateau précis de 2579 $\pm$ 3 Ma (2 σ), alors que la biotite provenant de ces veines présente une spectre d'âge perturbé. Cette légère perturbation de la biotite peut être attribuée à l'emplacement subséquent d'un dyke de diabase, et l'âge $^{40}Ar/^{39}Ar$ du dyke indique que cet événement est plus jeune que 2,3 Ga. Même si les âges de l'amphibole et de la msucovite confinent l'âge de la minéralisation aurifère entre 2690 et 2580 Ma, on conclu, en se basant sur l'ensemble de l'évidence disponible, que l'âge du plateau de la muscovite correspond à l'âge de formation des veines aurifères, qui a donc eu lieu environ à 100 Ma après le métamorphisme régional.

[1] Department of Geological Sciences, Queen's University, Kingston, Ontario K7L 3N6
[2] Geological Survey of Canada, 601 Booth Street, Ottawa, Ontario K1A 0E8

INTRODUCTION

The characteristic geological features of Archean lode gold deposits, and their relative time of formation, are well known from mapping distributions and superposition relationships observed on scales ranging from the regional to the microscopic (Colvine et al., 1988; Robert and Brown, 1986a, b). The genetic significance of the spatial and temporal relationships among features, however, remains uncertain in the absence of an absolute time framework. Thus, absolute dates are vitally important in gold exploration, because our understanding of the genetic significance of a feature associated with mineralization inevitably influences our perception of its relevance as a criterion for exploration area selection.

Much progress towards the development of an absolute time framework for the events encompassing gold oreformation in the Archean has been made recently by high-precision U/Pb dating of zircons to determine the ages of felsic igneous rocks in greenstone belts (e.g. Corfu and Andrews, 1987; Marmont and Corfu, 1988). However, because of the paucity of U-bearing hydrothermal and metamorphic minerals, the method is generally not suited to dating mineralization, alteration and metamorphism. The $^{40}Ar/^{39}Ar$ method is capable of yielding high-precision ages in the Archean on a variety of mineral and rock types (e.g. Hanes et al., 1985; Layer et al., 1987), and the mineral ages can be combined with the closure temperatures to yield information on the thermal history of a region. The $^{40}Ar/^{39}Ar$ step-heating approach has been applied in recent studies of Archean gold deposits (e.g. Masliwec et al., 1986, 1985; Layer et al., 1987).

We chose the Sigma gold deposit, located near Val d'Or in the southeastern part of the Abitibi greenstone belt, for a detailed $^{40}Ar/^{39}Ar$ study because it is typical of the large and economically important class of Archean, shear-related, vein-type lode gold deposits. In addition, the geology of the deposit has been well documented in a recent series of papers (Robert and Kelly, 1987; Robert and Brown, 1986a, b; Robert et al., 1983).

A concurrent U-Pb study of the Sigma Mine and environs is being done at the Geochronology Laboratory, Royal Ontario Museum, Toronto (Ling Wong; Queen's M.Sc. student).

GEOLOGICAL SETTING

The Sigma gold deposit, located at Val d'Or, Quebec in the southeastern part of the Abitibi greenstone belt (Fig. 1), comprises a series of auriferous quartz-tourmaline veins controlled by a kinematically-related system of subvertical ductile shear zones and subhorizontal extension fractures (Robert and Brown, 1986a, b; and Robert et al., 1983). The vein-bearing fractures cut steeply-dipping, weakly- to moderately-foliated mafic to intermediate volcanic flows and volcaniclastic rocks, and irregular diorite porphyry intrusion and a series of steeply-dipping, unfoliated feldspar porphyry dykes. The volcanic rocks and diorite porphyry are part of the Upper Malartic Group, considered to be approximately correlative with other volcanic rocks of the Abitibi Belt with U/Pb zirconi ages in the range 2700-2730 (Mortensen, 1987; Nunes and Jensen, 1980; Nunes and Pyke, 1980). The feldspar porphyry dykes have not been dated yet, but are petrologically similar to late- to post-tectonic intrusions found in many similar gold deposits throughout the Abitibi Belt, dated in the range 2675-2690 Ma (Frarey and Krogh, 1986; Marmont and Corfu, 1988).

The volcanic rocks, diorite porphyry and feldspar porphyry dykes have been metamorphosed from lower to upper greenschist facies assemblages. Enveloping the veins is a zoned wall-rock alteration sequence, consisting of a cryptic outer zone and visible inner zone. Textures indicate that vein-filling and wall-rock alteration were approximately contemporaneous, but clearly post-date metamorphism. Within the veins, most of the gold occurs in late fractures and in zones of recrystallized quartz; significant amounts of gold are also associated with pyrite in wall-rock alteration zones. Fluid inclusion studies indicate that the gold mineralization took place at a minimum depth of ca. 5-7 km and in the temperature range 300-400°C (Robert and Kelly, 1987; see also Sibson et al., 1988). The temperature estimate is corroborated by temperatures estimated from isotopic fractionation between hydrothermal minerals (Kerrich, 1983). The last significant geological event in the mine was the emplacement of two thin northerly-trending diabase dykes which cut the veins.

SAMPLING AND ANALYTICAL METHODS

Nine mineral separates and one whole-rock dyke sample from Sigma Mine were analysed by the incremental $^{40}Ar/^{39}Ar$ step-heating method. Two analyses were on

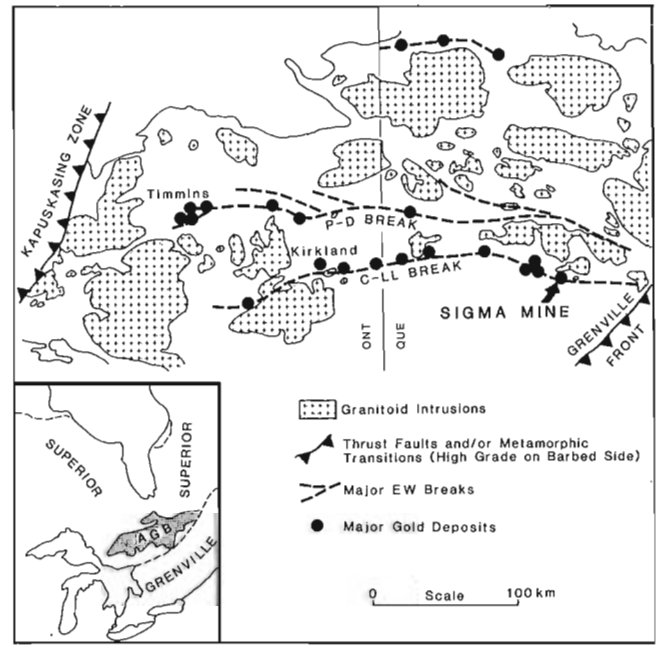

Figure 1. Simplified location map for Sigma Mine. In inset map, AGB stands for Abitibi Greenstone Belt, P-D is the Porcupine-Destor Break, and C-LL is the Cadillac-Larder Lake Break.

metamorphic amphibole that occurs as large (up tp 5 cm diameter) porphyroblasts in the porphyritic diorite at the deep levels of the mine. Three muscovite and three biotite samples from vertical and flat veins in the 14th to the 38th levels of the mine were step-heated. These micas crystallized at the time of vein formation and gold deposition (Robert and Brown, 1986b). The late diabase dykes were too fine-grained to permit mineral separation, and whole-rock chips from one of the dyke margins were analyzed.

A muscovite sample from a gold-bearing quartz vein on the Davidson-Tisdale property (Piroschco, 1985) in Tisdale Township east of Timmins, Ontario was also step-heated.

The samples and irradiation standards were irradiated for 200 MWH in site 5C in the water-moderated, enriched-uranium research reactor at McMaster University, Four standards were used in this study: hb3gr hornblende (1072 Ma); MMHB hornblende (519.5 Ma); Obedjiwan biotite (962 Ma); and hornblende G-14-4 (1007 Ma). Standards were evenly spaced along the length of each irradiation canister. J-values for the unknowns were estimated by interpolation.

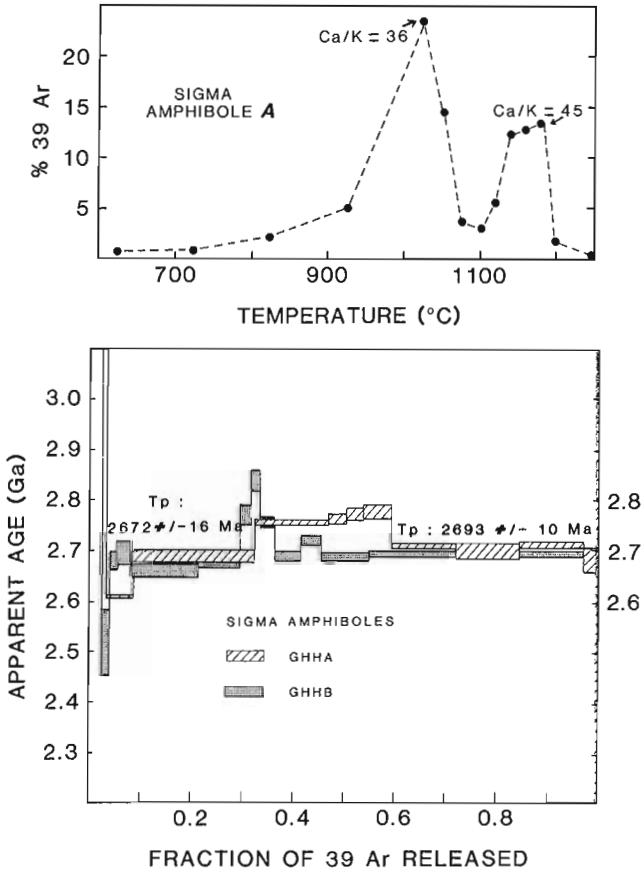

Figure 2. Age spectra (lower) for Sigma amphiboles GHHA and GHHB, and ^{39}Ar release spectrum for amphibole GHHA (upper). In this, and all succeeding age spectrum diagrams, the vertical heights of the bars represent $\pm$ 2 σ SE. In the ^{39}Ar release spectrum, the Ca/K ratios for the two release pulses were determined from the $^{37}Ar/^{39}Ar$ ratios obtained during the experiment.

The irradiated samples were analyzed using an ultra-high vacuum, stainless-steel, argon extraction system, online to a substantially modified MS-10 mass spectrometer run in the static mode. Details of the step-heating procedures are reported in Hanes et al. (in press).

PRESENTATION AND DISCUSSION OF THE RESULTS

The isotope data for the ten $^{40}Ar/^{39}Ar$ step-heating analyses are presented in the form of step-heating age spectra in Figures 2 to 6 (data tables are available from the authors). In the age spectra, the vertical heights of the bars for each fraction represent $\pm$ 2 σ SE, suitable for comparing within-spectra ages (i.e., error in J=O). A conservative 0.5% error in J estimates can be used for between spectra age comparisons of samples irradiated together; this corresponds to an additional ca. $\pm$ 7 Ma error in step ages.

The blank-corrected ^{36}Ar contents of the gas fractions of the muscovite and biotite are too low to provide meaningful results on an isotope correlation plot ($^{39}Ar/^{40}Ar$ versus $^{36}Ar/^{40}Ar$). Such results for the amphibole separate and diabase dyke whole-rock are discussed below.

Amphibole

Metamorphic amphibole grains from the porphyritic diorite on the 38th level of Sigma Mine are composed of two amphiboles. The cores are predominantly magnesio-hornblende with a probe-determined Mg/Mg+Fe ratio of 0.76, Ca/K ratio of 58 and K_2O content of 0.17%. Ferro-hornblende (Mg/Mg+Fe = 0.48; Ca/K = 33; K_2O = 0.30%) occurs as rims on, and as patches and blebs along fracture and cleavage planes in, the magnesio-hornblende.

Two step-heating analyses were conducted: 1) a fifteen-step run on an 88 mg sample comprising five small amphibole chunks (AMPHIBOLE GHHB), and 2) a fourteen-step run on a single 190 mg amphibole crystal (AMPHIBOLE GHHA). The integrated ages of 2727 and 2755 Ma, respectively, for the two samples are anomalously high in comparison to the 2700-2730 Ma U/Pb zircon ages for the Abitibi greenstone belt volcanics (Mortensen, 1987), and are attributed to the presence of excess argon. However, the step-heating method has permitted the extraction of a meaningful age.

The two amphibole age-spectra (Fig. 2) are similar in character. In the first three percent of ^{39}Ar release, the ages are in excess of 3.1 Ga. Anomalously high ages are also obtained from the intermediate steps (from 30% to 35% gas release for AMPH GHHB, and 35% to 60% for AMPH GHHA). With the exception of the two steps from 3% to 9% gas release (which have dates less than 2620 Ma), the remainder of the gas fractions fall in a narrow range of ages from ca. 2.67 to 2.70 Ga. For AMPH GHHB, this represents 85% of the gas released, and for AMPH GHHA, 65%.

The ^{39}Ar is released in two major pulses (1000°C and 1150°C) that correspond with those gas fractions having this

narrow range of ages (Fig. 2). These pulses clearly correspond to gas release from the two different amphibole phases. Based on the apparent Ca/K ratios calculated from the $^{37}Ar/^{39}Ar$ ratio for each gas fraction (e.g. Hanes et al., 1985) in comparison with the microprobe-determined values, the ferro-hornblende is responsible for the first pulse, while the magnesio-hornblende is responsible for the higher temperature pulse (Fig. 2). This is inaccord with observations of a direct relationship between closure temperature and (Mg/Fe+Mg) ratio for amphiboles (Onstott and Peacock, 1987). The Ca/K value of 58 for the probe-derived Ca/K ratio of the magnesio-hornblende is somewhat higher than the experimentally-derived value of 45. This discrepancy is attributed to the difficulty in measuring such low values of K_2O (0.17 %) with the electron microprobe, rather than from simultaneous release of gas from the two amphiboles, as the two release pulses do not significantly overlap (Fig. 2).

The five gas fractions for both samples derived from the ferro-hornblende give an intergrated age of 2672 ± 16 Ma (2 σ), while the eight steps for gas from the magnesio-hornblende provide an integrated age of 2693 ± 10 Ma (2 σ). The slightly younger integrated age for the ferro-hornblende fractions might reflect the effect of slow cooling acting on a difference in closure temperature between the two amphiboles Onstott and Peacock, 1987), or else the age of retrograde alteration of the magnesio-hornblende to produce the ferro-hornblende rims. Alternatively, the age difference may be due to minor argon loss from the ferro-hornblende, as suggested by the young ages in the low temperature part of the age spectra (Fig. 2).

The 2693 ± 10 Ma integrated age for the magnesio-hornblende is taken as the best estimate of the time that this amphibole was formed, or that the region cooled through the magnesio-hornblende closure temperature following metamorphism. A 2698 ± 22 Ma age is derived from a correlation plot for steps 5 to 12 of GHHA, which is in good agreement with the 2693 Ma age.

Muscovite

Four step-heating analyses were done for muscovite from quartz veins: three from veins on the 14th, 19th and 33rd levels of Sigma Mine, and one from a gold-bearing quartz vein from the Davidson-Tisdale Property near Timmins, Ontario. The age spectra for the Sigma muscovite samples are shown in Figure 3, and the Davidson-Tisdale muscovite in Figure 4.

M-1427 is a single muscovite booklet (8 mm diameter), M-3302 is a number of flakes (average 4 mm diameter) and M-1901 is a sample of fine-grained (less than 2 mm diameter) muscovite. The Davidson-Tisdale sample is a number of flakes, each ca. 4 mm in diameter.

All three Sigma muscovites display young ages in the first few, low-temperature, steps that climb rapidly from a low of ca. 2.1 Ga to a well-defined plateau at ca. 2580 Ma. For the 21-step run on muscovite M-1427, over 95 % of the spectrum (17 steps) yields a plateau age of 2579 ± 03 Ma (2 σ), which is mimiced by a twenty-step run on muscovite M-3302 with a plateau age of 2574 ± 04 Ma (2 σ) over 90 % of the gas. The spectrum for muscovite M-1901 shows

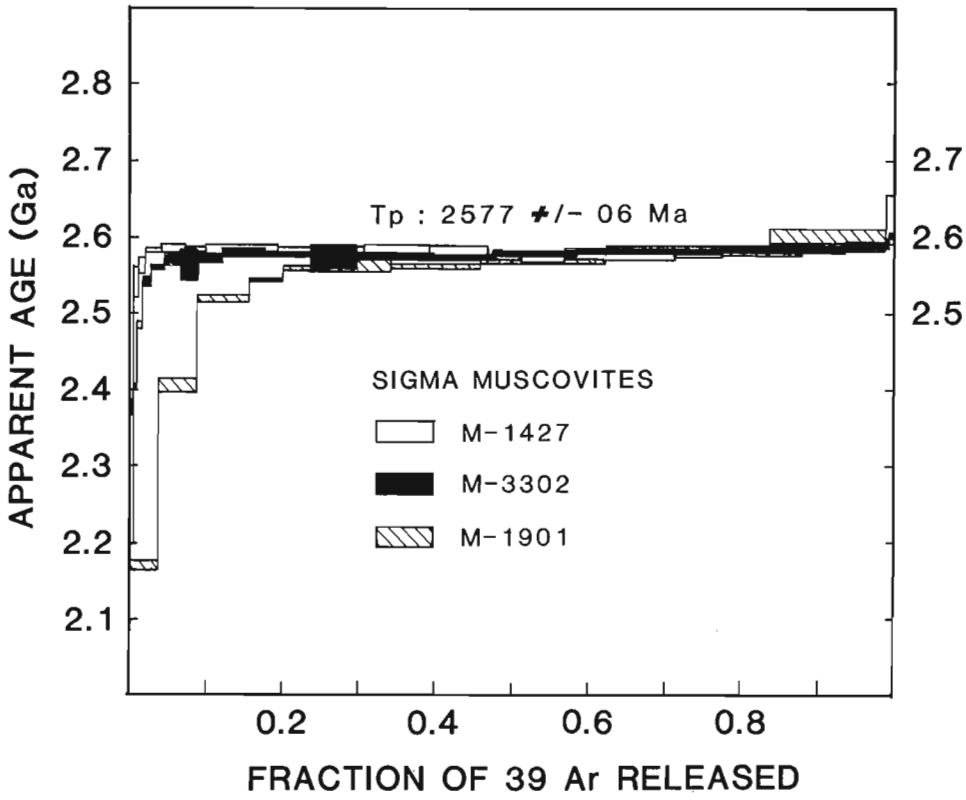

Figure 3. Age spectra for Sigma muscovites 1427, 3302 and 1901. Tp is the plateau age calculated from all three samples.

significantly more argon loss than the other two, but also climbs to the 2580 Ma plateau. The extent of argon loss is inversely proportional to the grain-size of the separates. This suggests that the actual grain size may be the effective radius of diffusion for these muscovites.

As muscovite 1427 shows virtually no argon loss, the precise 2579 ± 03 Ma plateau age is taken as the best estimate of the time of last closure through the muscovite closure temperature (350 ± 50°C; Purdy and Jager, 1976), with the micas not having been significantly reheated since.

The Davidson-Tisdale muscovite has an age spectrum similar in form to the Sigma muscovites (Fig. 4), but climbs to a significantly older plateau age (2615 ± 04 Ma (2 σ) over 80% of the gs release). Again, this date is accepted as the time of last closure of the muscovite.

Biotite

Three biotite concentrates from gold-quartz veins in Sigma Mine have been step-heated. Their age spectra are plotted with the muscovite 1427-08 and amphibole spectra for reference (Fig. 5). Biotites 3316-01 and 3816-07 are from two flat veins attached to the same subvertical vein in which biotite 3216-02 was collected. Thus, all three biotite samples are from the same vein system. Sample 3816 consisted of one booklet of biotite (diameter ca. 6 mm), while the other two samples were finer-grained separates (diameter ca. 1 mm).

The integrated ages for the three biotite samples range from 2431 to 2533 Ma. All three age spectra are disturbed, and show similar patterns (Fig. 5). The first step in each spectrum has an age of ca. 1.0 Ga. There is then an increase in ages to a local maximum between 3% and 25% gas release, followed by a monotonic drop-off in ages to a trough at around 50% gas release. Finally, all spectra climb again monotonically to a maximum age in the last step. This type of pattern is very common for biotites which have suffered partial argon loss (Berger, 1975; York and Lopez-Martinez, 1986). The degree of the disturbance of the Sigma biotites appears to be grain-size related, as the least disturbed biotite is the coarsest-grained. This aspect of the $^{40}Ar/^{39}Ar$ systematics of the biotites will be discussed in more detail elsewhere (Hanes et al., in preparation).

Sample 3816-07 shows the least argon loss and the maxima of the spectrum at low and high temperatures closely approach the muscovite plateau ages of 2580 Ma (Fig. 5). It is therefore tentatively concluded that the biotite samples passed through their closure temperature (280 ± 40°C; Harrison et al., 1985) at nearly the same time as the muscovite, and have since suffered variable degrees of argon loss. This loss may have resulted from diabase dyke emplacement, or activity associated with Grenvillian orogeny (1.2-1.0 Ga).

Diabase dyke

A whole-rock chunk from the chilled margin of one of the dykes in Sigma Mine was analyzed in a nineteen-step run (Fig. 6). The integrated age of 3372 Ma is anomalously high due to the presence of excess argon. This is revealed by the U-shape of the age spectrum (Fig. 6), a common form for diabase dykes with excess argon (Hanes, 1987). In such

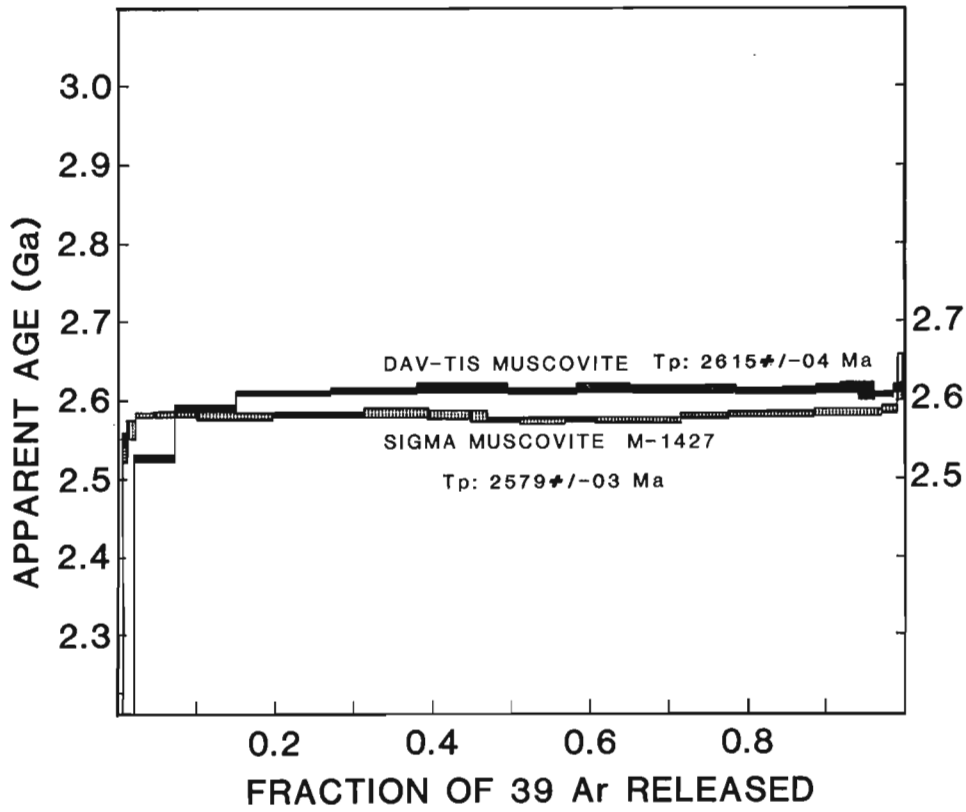

Figure 4. Age spectra plot for Davidson-Tisdale muscovite (black) with Sigma muscovite 1427 (dotted) for comparison. Tp is the plateau age.

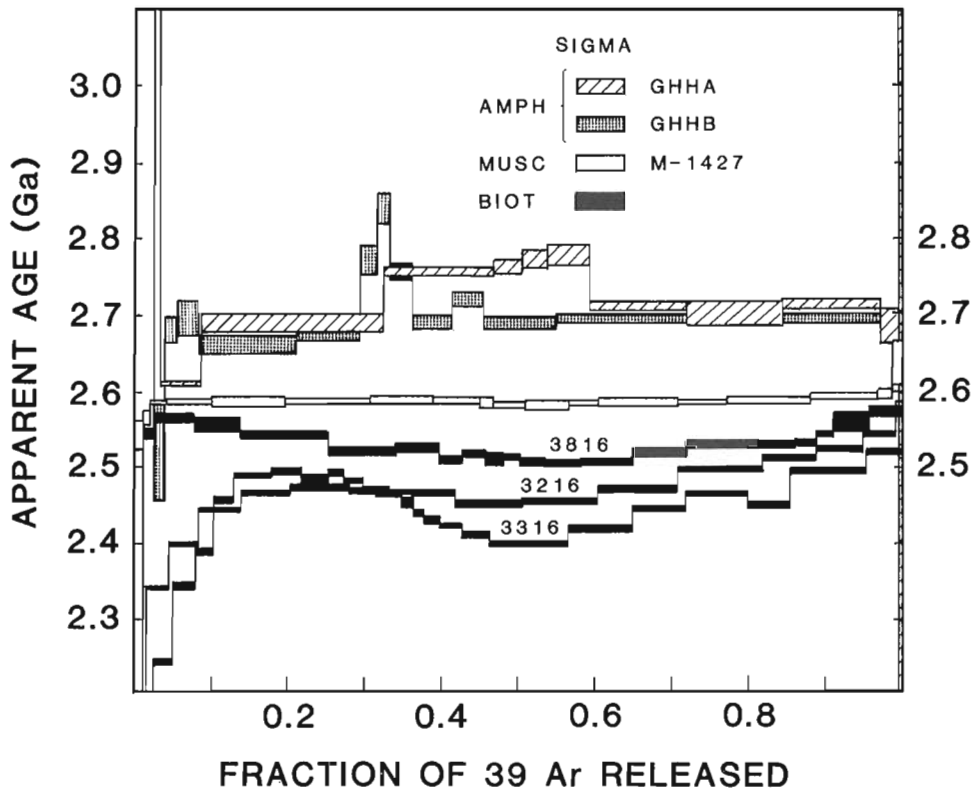

Figure 5. Age spectra for Sigma biotites 3816, 3216 and 2216 (black) with Sigma muscovite 1427 (clear) and Sigma amphibole GHHA (slashed) and GHHB (dotted) for comparison.

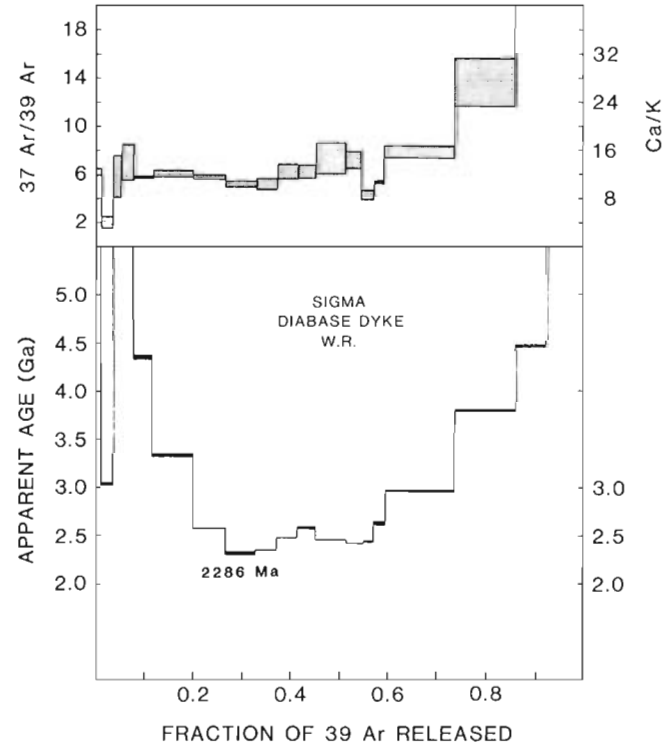

Figure 6. Age spectrum plot (lower) and $^{37}Ar/^{39}Ar$ (Ca/K) spectrum (upper) for Sigma diabase dyke whole-rock.

cases, the trough of the U has been used as a maximum estimate of the time of dyke emplacement, which would imply an age of less than 2300 Ma for the Sigma diabase. This strongly supports the earlier assumption (Robert and Brown, 1986a) that the diabase dykes in Sigma Mine are part of the Preissac swarm (2150 ± 20 Ma; Hanes and York, 1979).

SYNTHESIS AND CONCLUSIONS

The sequence and timing of events, from oldest to youngest, in the Val d'Or region of the Abitibi greenstone belt, based on geological studies (Robert and Brown, 1986a), regional geochronology (Marmont and Corfu, 1988; Mortensen, 1987; Frarey and Krogh, 1986; Nunes and Pyke, 1980; Nunes and Jensen, 1980) and our $^{40}Ar/^{39}Ar$ study in the Sigma Mine is summarized in Table 1.

From the $^{40}Ar/^{39}Ar$ data, gold mineralization is bracketed between the age of regional metamorphism (ca. 2675-2690 Ma) and the vein-muscovite age of ca. 2580 Ma. Many workers view Archean gold deposits as magmatic-hydrothermal in origin, analogous to Phanerozoic porphyry Cu-Mo deposits (Wood et al., 1986; Mason and Melnik, 1986), with gold deposition being related to the ca. 2675-2690 Ma porphyries. This would require that he 2580 Ma muscovite age of Sigma Mine is the result of slow cooling or an episodic reheating event, rather than the time of mineralization.

Slow cooling is considered unlikely, as the vein systems are thought to have formed at shallow to moderate crustal depths (Robert and Kelly, 1987; Sibson et al., 1988). The maintenance of high temperatures in the narrow range of 350-450°C (based on the muscovite and amphibole closure temperatures) at such levels would require highly unusual conditions of heat input from depth, for which there is no other evidence (Hanes et al., in preparation). Furthermore, a discrete post-vein thermal event is deemed unlikely, as such an event would need to be at the same temperature as the original vein-forming event (300-400°C; Robert and Kelly, 1987), and might also be expected to lead to decrepitation of fluid inclusions.

Thus, the 2580 Ma age on the muscovite gives the age of the vein- and gold-forming hydrothermal event at Sigma Mine, and the gold mineralization is ca. 100 Ma later than regional metamorphism. Vein emplacement and gold mineralization on the Davidson-Tisdale property was also young (2615 Ma), but slightly earlier than at Sigma. Based on U-Pb studies on high-grade regions of the Superior Province, Corfu (1988, 1987) argued that magmatic and fluid activity continued until after 2600 Ma in the deep Archean crust, reflecting a process of downward, vertical accretion of the Archean crust. It is possible that the near-surface, gold-forming hydrothermal event is related to these deep-crustal process (e.g. Colvine et al., 1988).

ACKNOWLEDGMENTS

This research was supported by a contract from Energy, Mines and Resources (DSS Contract No. 20ST.23233-5-0734), and grants from the Natural Science and Engineering Research Council of Canada and the Queen's University Advisory Research Committee. The authors wish to thank Les Mines Sigma (Quebec) Ltee. for providing access to the mine and to mine samples. We acknowledge also the help of the staff of McMaster Reactor. The Geochronology Laboratory at Queen's University is supported by an NSERC Operating Grant to Dr. E. Farrar. Randy Parrish is thanked for his critical review of the manuscript.

REFERENCES

Berger, G.W.
1975: $^{40}Ar/^{39}Ar$ step heating of thermally overprinted biotite, hornblende and potassium feldspar from Eldora, Colorado; Earth and Planetary Science Letters, v. 26, p. 387-408.

Colvine, A.C., Fyon, J.A., Heather, K.B., Marmont, S., Smith, P.M., and Troop, D.G.
1988: Archean Lode Gold Deposits In Ontario; Ontario Geological Survey, Miscellaneous Paper 139, 136 p.

Corfu, F.
1988: Differential response of U-Pb systems in coexisting accessory minerals, Winnipeg River; Contributions to Mineralogy and Petrology, v. 98, p. 312-325.

Corfu, F.
1987: Inverse age stratification in the Archean crust of the Superior Province: evidence for infra- and subcrustal accretion from high resolution U-Pb zircon and monazite ages; Precambrian Research, v. 36, p. 259-275.

Corfu, F. and Andrews, A.J.
1987: Gechronological constraints on the timing of magmatism, deformation, and gold mineralization in the Red Lake greenstone belt, northwestern Ontario; Canadian Journal of Earth Sciences, v. 24, p. 1302-1320.

Frarey, M.J., and Krogh, T.E.
1986: U-Pb zircon ages of late internal plutons of the Abitibi and eastern Wawa subprovinces, Ontario and Quebec; in Current Research, Part A, Geological Survey of Canada, Paper 86-1A, p. 43-48.

Hanes, J.A.
1987: Dating of Precambrian mafic dyke swarms by the Rb-Sr, K-Ar and Sm-Jd methods; in Mafic Dyke Swarms, ed. H.C. Halls and W.F. Fahrig; Geological Association of Canada, Special Paper 34, p. 137-146.

Hanes, J.A. and York, D.
1979: A detailed $^{40}Ar/^{39}Ar$ age study of an Abitibi dyke from the Canadian Superior Povince; Canadian Journal of Earth Sciences, v. 16, p. 1060-1070.

Hanes, J.A., Clark, S.J., and Archibald, D.A.
—: A $^{40}Ar/^{39}Ar$ geochronological study of the Elzevir batholith and its bearing on the tectonothermal history of the southwestern Greenville Province, Canada; Canadian Journal of Earth Sciences. (in press.)

Hanes, J.A., York, D., and Hall, C.M.
1985: An $^{40}Ar/^{39}Ar$ geochronological and electron microprobe investigation of an Archean pyroxenite and its bearaing on ancient atmospheric compositions; Canadian Journal of Earth Sciences, v. 22, p. 947-958.

Harrison, T.M., Duncan, I., and McDougall, I.
1985: Diffusion of ^{40}Ar in biotite: temperature, pressure and compositional effects; Geochimica et Cosmochimica Acta, v. 49, p. 2461-2468.

Kerrich, R.
1983: Geochemistry of gold deposits in the Abitibi Greenstone belt; Canadian Institute of Mining and Metallurgy, special volume 27, 75 p.

Layer, P.W., McMaster, N.D., and York, D.
1987: The dating of Ontario's gold deposits; Ontario Geological Survey, Miscellaneous. Paper 136, p. 27-34.

Masliwec, A., McMaster, D., and York, D.
1986: The dating of Ontario's gold deposits; Ontario Geological Survey, Miscellaneous. Paper 130, p. 107-114.

Masliwec, A., York, D., Kuyibida, P., and Hall, C.M.
1985: The dating of Ontario's gold deposits; Ontario Geological Survey, Miscellaneous. Paper 127, p. 223-228.

Marmont, S. and Corfu, F.
1988: Timing of gold introduction in the Late Archean tectonic framework of the Canadian Shield: evidence from U-Pb zircon geochronology of the Abitibi sub-province; Bicentennial Gold 88, Melbourne, Australia.

Mason, R. and Melnik, N.
1986: The anatomy of an Archean gold system — the McIntyre-Hollinger complex at Timmins, Ontario, Canada; p. 40-55 in Proceedings of Gold '86, an International Symposium on the Geology of Gold, ed. A.J. MacDonald, Konsult International Inc., Toronto, 517 pages.

Mortensen, J.K.
1987: U-Pb chronostratigraphy of the Abitibi greenstone belt; Geological Association of Canada, Program with Abstracts, v. 12, p. 75.

Nunes, P.D. and Jensen, L.S.
1980: Geochronology of the Abitibi metavolcanic belt, Kirkland Lake area-progress report; in Summary of Geochronology Studies 1977-79, ed. E.G. Pye, Ontario Geological Survey, Miscellaneous. Paper 92, p. 40-45.

Nunes, P.D. and Pyke, D.R.
1980: Geochronology of the Abitibi meatvolcanic belt, Timmins-Matachewan area- Progress report; in Summary of Geochronology Studies 1977-79, ed. E.G. Pye, Ontario Geological Survey, Miscellaneous. Paper 92, 45 p.

Onstott, T.C. and Peacock, M.W.
1987: Argon retentivity of hornblendes: a field experiment in a slowly cooled metamorphic terrane; Geochimica et Cosmochimica Acta, v. 51, p. 2891-2903.

Piroshco, D.W.
1985: Relationship of hydrothermal alteration to structure and stratigraphy at the Coniarum and Davidson-Tisdale gold deposits, Tisdale Township, Northeastern Ontario; M.Sc. thesis, Queen's University, 102 p.

Purdy, J.W. and Jager, E.
1976: K-Ar ages of rock-forming minerals from the Central Alps; The Institute of Geology and Mineralogy, University olf Padua, Padua, Italy, Memoir 30, 31 p.

Robert, F. and Brown, A.C.
1986a: Archean gold-bearing quartz veins at the Sigma Mine, Abitibi greenstone belt, Quebec: Part I. Geologic relations and formation of the vein system; Economic Geology, v. 81, p. 578-592.
1986b: Archean gold-bearing quartz vein formation at the Sigma mine, Abitibi greenstone belt, Quebec: Part II. Vein paragenesis and hydrothermal alteration; Economic Geology, v. 81, p. 593-616.

Robert, F. and Kelly, W.C.
1987: Ore-forming fluids in Archean gold-bearing quartz veins at the Sigma Mine, Abitibi greenstone belt, Quebec, Canada; Economic Geology, v. 82, p. 1464-1482.

Robert, F., Brown, A.C., and Audet, A.J.
1983: Structural control of gold mineralization at the Sigma Mine, Val d'Or, Quebec; Canadian Institute of Mining and Metallurgy Bulletin, v. 76, p. 72-80.

Sibsòn, R.H., Robert, F., and Poulsen, K.H.
1988: High-angle reverse faults, fluid pressure cycling and mesothermal gold-quartz deposits; Geology, v. 16, p. 551-555.

Wood, P.C., Burrows, D.R., Thomas, A.V., and Spooner, E.T.C.
1986: The hollinger-McIntyre Au-quartz vein system, Timmins, Ontario, Canada; Geological characteristics, fluid properties and light stable isotope geochemistry; p. 56-80 in Proceedings of Gold '86, an International Symposium of the Geology of Gold, ed. A.J. Macdoald, Konsult International Inc., Toronto, 517 pages.

York, D. and Lopez-Martinez, M.
1986: The two-faces mica; Geophysics Research Letters, v. 9, p. 973-975.

Sedimentology, structure, and economic geology of the Poorfish-Windy thrust-fold belt, Ennadai Lake area, District of Keewatin, and the shelf to foredeep transition in the foreland of Trans-Hudson Orogen[1]

Lawrence B. Aspler[2], Terry L. Bursey[3] and A.R. Miller

Aspler, L.B., Bursey, T.L. and Miller, A.R., Sedimentology, structure, and economic geology of the Poorfish-Windy thrust-fold belt, Ennadai Lake area, District of Keewatin, and the shelf to foredeep transition in the foreland of Trans-Hudson Orogen; in Current Research, Part C, Geological Survey of Canada, Paper 89-1C, p. 143-155, 1989.

Abstract

The principal structural elements in the Poorfish-Windy belt are: northwest-propagating piggyback thrusts (including a NW-vergent duplex cut by in sequence, breaching thrusts); northwest-vergent macrofolds; and NNW-and NNE-trending normal faults. The thrusts are responsible for a minimum horizontal shortening of 75 km. The sedimentary record of the Hurwitz Group and Kiyuk Group (new name, replaces Ennadai Group) is compatible with a simple model in which the Kinga shelf was drowned by a north- and northwest-migrating foredeep; cycles of sedimentation may be related to rates of thrust front migration/ loading. Conglomerate, arkose and arkose-clast breccia of the Kiyuk Group are inferred to be alluvial fan, stream and talus deposits formed ahead of a thrust front that carried Hurwitz Group and basement to erosional levels. Numerous gossans are inferred to be structurally controlled. Gold and arsenic anomalies in Hurwitz and Kiyuk Group rocks suggest that structural traps in these units may be favourable exploration targets.

Résumé

Les principaux éléments structuraux de la zone de Poorfish-Windy sont les suivants: chevauchements redressés se propageant vers le nord-ouest (incluant un chevauchement avec rupture double en succession de recoupement de vergence nord-ouest); des macroplis de vergence nord-ouest; et des failles normales de direction nord-nord-ouest et nord-nord-est. Les chevauchements sont responsables d'un raccourcissement horizontal minimum de 75 km. Le profil sédimentaire des groupes d'Hurwitz et de Kiyuk (nouveau nom, remplace le groupe d'Ennadai) est compatible avec un modèle simple dans lequel la plate-forme de Kinga a été submergée par une avant-fosse en migration vers le nord et le nord-ouest; les cycles sédimentaires peuvent être associés aux taux de migration/chargement du front de chevauchement. Le conglomérat, l'arkose et la brèche à clastes d'arkose du groupe de Kiyuk seraient des dépôts de cône de déjection, fluviaux et de talus formés à l'avant d'un front de chevauchement qui aurait porté le groupe d'Hurwitz et le socle aux niveaux d'érosion. Les nombreux chapeaux de fer cartographiés seraient contrôlés par la structure. Les anomalies en or et en arsenic des roches des groupes d'Hurwitz et de Kiyuk suggèrent que les pièges structuraux dans ces unités pourraient constituer des cibles favorables pour l'exploration.

[1] Contribution to the Canada-Northwest Territories Mineral Development Agreement 1987-1991. Project carried jointly by the Geological Survey of Canada (Mineral Resources Division), Government of the Northwest Territories (Energy Mines and Resources Secretariat) and Geology Division, Department of Indian Affairs and Northern Development, Yellowknife.

[2] 215 Fifth Avenue, Ottawa, Ontario K1S 5B6

[3] Department of Geology, Carleton University, Ottawa, Ontario K1S 5B6

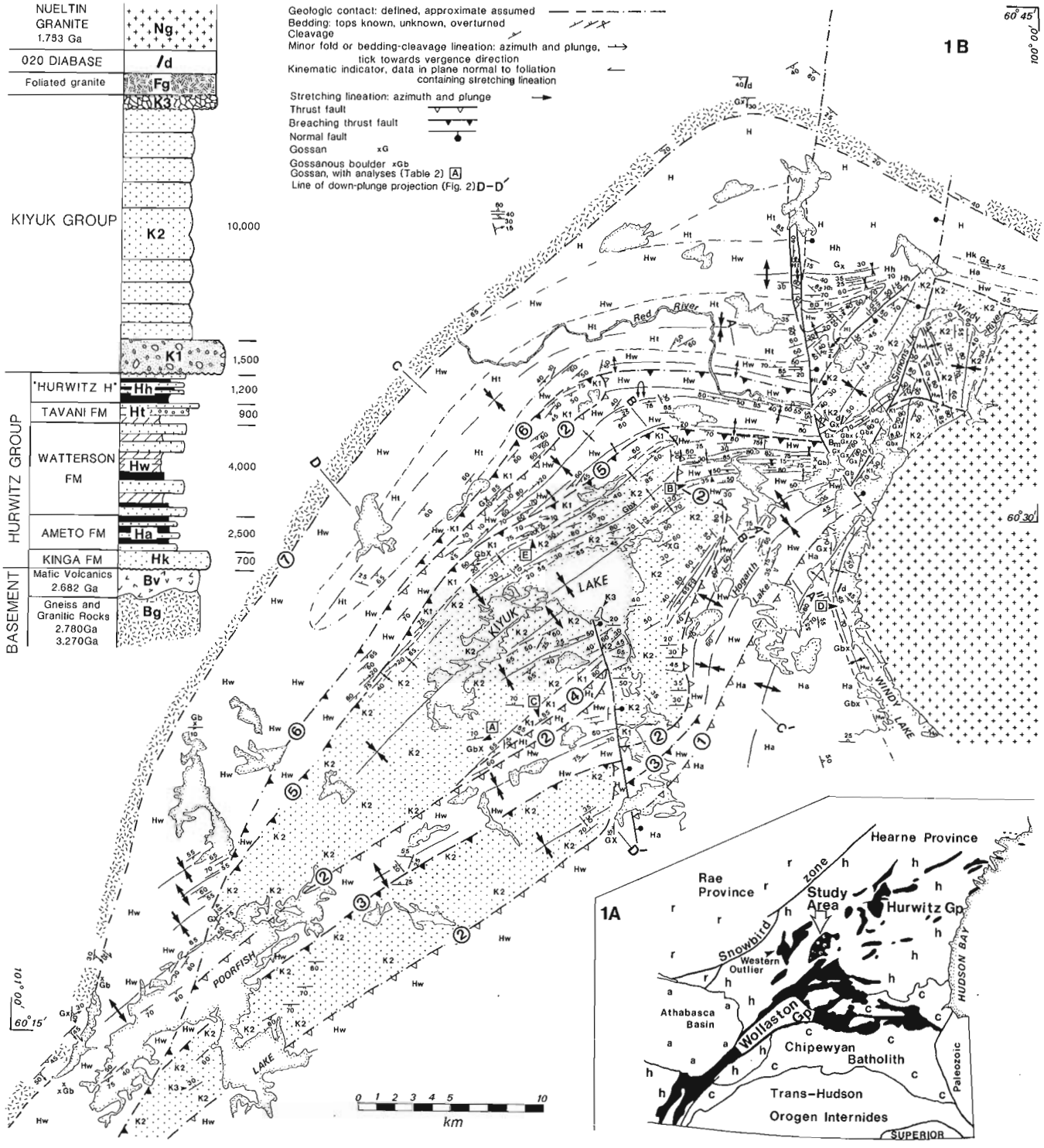

Figure 1. A) Location of study area with respect to Hurwitz Group and Wollaston Group exposures, Trans-Hudson Orogen and the Snowbird tectonic zone (generalized after Hoffman, 1988). B) Generalized geology, Poorfish-Windy Lake area. Thicknesses (in metres) are best estimates based on map data. Stratigraphic position of K3 breccia with respect to K2 sandstone is uncertain. Nueltin age is U-Pb zircon from Nueltin-like granite west of Tulemalu Lake (Loveridge et al., 1988) and is similar to Rb-Sr ages from the Nueltin type-area by Wanless and Eade (1975). Mafic volcanic age is U-Pb zircon from northeastern Saskatchewan (Chiarenzelli and Macdonald, 1986). Age of basement gneiss is U-Pb zircon south and west of Poorfish Lake (Loveridge et al., 1988).

INTRODUCTION

Hurwitz Group and Kiyuk Group (new name, see below) rocks in the Ennadai Lake area (65C) form low metamorphic grade outliers strategically located south of the Snowbird tectonic zone, the site of postulated ca. 1.92-1.85 Ga suturing of the Hearne and Rae provinces (Hoffman, 1988) and north of the ca. 1.87 Ga collisional zone in Trans-Hudson Orogen (Fig. 1A, Lewry et al., 1985; Hoffman, 1988). Reconnaissance work (Eade, 1971) suggested that coarse clastic sediments of the Kiyuk Group represent a molassoid sequence which could provide an indirect record of processes and events in the Snowbird zone or in Trans-Hudson Orogen.

This report presents preliminary structural data (Fig. 1, 2) and sedimentological and stratigraphic data (summarized in Table 1) derived from 1:50 000-scale mapping in the Poorfish-Windy Lakes area. These data indicate continental sedimentation of the Kiyuk group in a northwestward migrating foredeep, and deformation of the Group as a northwest-vergent thrust-fold complex due to progressive foredeep advance. We propose a tentative regional model in which shelf quartz arenites of the Kinga Formation were drowned during migration of the same foredeep, dynamically linked to Trans-Hudson Orogen.

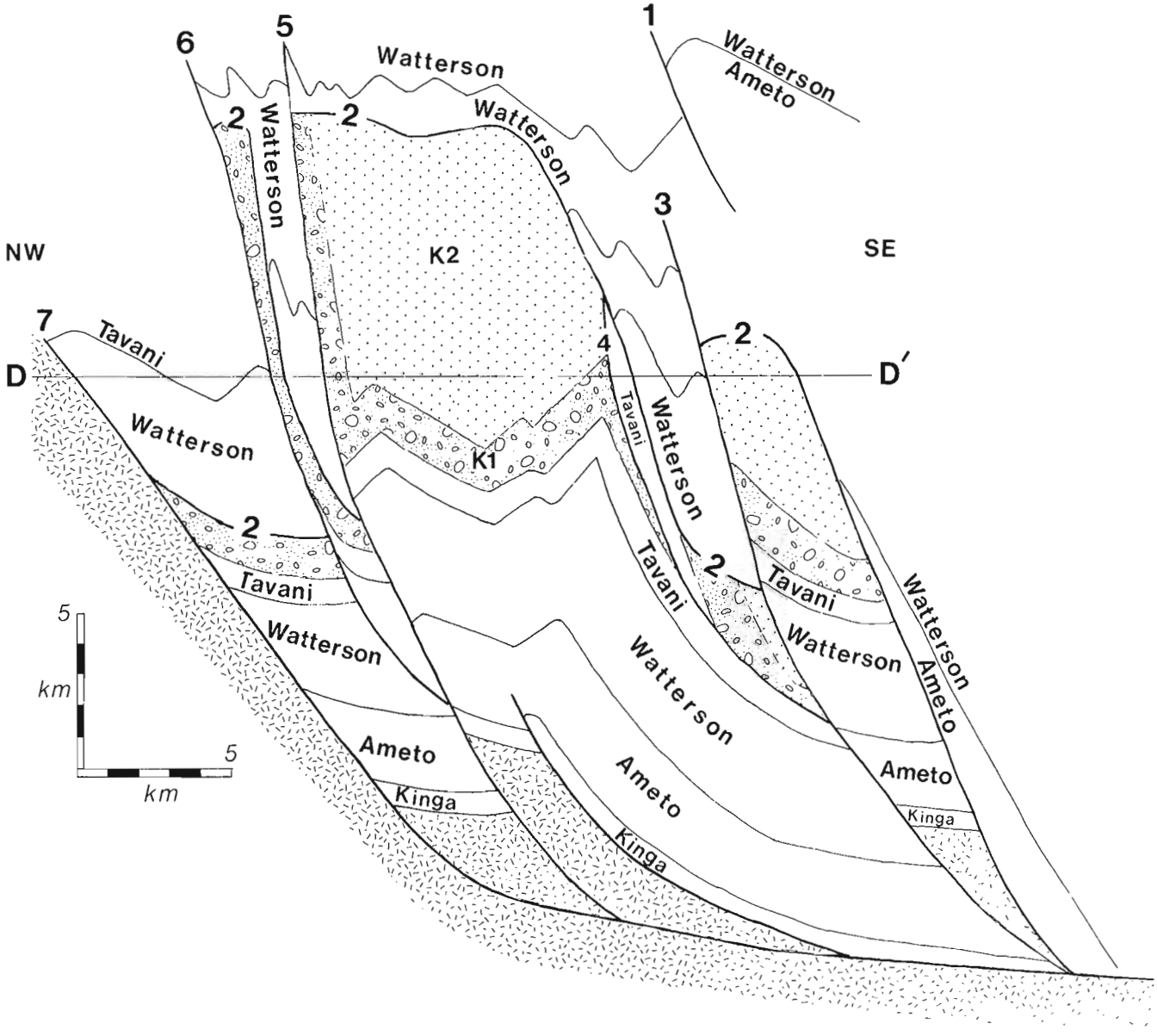

Figure 2. Downplunge projection, Poorfish-Windy thrust-fold belt. Using a generalized regional plunge of 20° to the northeast and east, sections drawn through A-A'-A'', B-B', and C-C' were projected up-plunge onto D-D' (see Stockwell, 1950). It should be noted that over the domain of the projection, the structure is not strictly cylindrical; minor folds and bedding/cleavage lineations deviate from 20° plunge (see Fig. 1B).

Table 1. Description, environmental interpretation and significance of map units, Poorfish-Windy belt.

UNIT		DESCRIPTION	INTERPRETATION	COMMENTS
Nueltin Granite		Granite, granodiorite and quartz monzonite, locally fluorite-bearing; non-foliated		U-Pb zircon 1753 + 3/-2 Ma (Loveridge et al., 1988) (cf Rb/Sr Wanless and Eade, 1975)
020 Diabase		Narrow (<5 m) 020°-trending, near vertical diabase cuts basement, Hurwitz Gp. and Kiyuk Group. Cuts thrust-fold fabrics; cut by NNE-trending fault.	Post thrust-fold deformation but pre late cross faults	Baddeleyite geochronology will be attempted
Foliated granite sill		Intrudes K2 sandstone; foliation is concordant with cleavage in adjacent sandstone	Post Kiyuk but pre-thrust-fold deformation	Zircon geochronology will be attempted
KIYUK GROUP	K3	Framework-inact breccia with 2-80 cm angular clasts exclusively of arkose, probably derived from K2 (Fig. 6D). Cemented by hematitic botryoidal quartz and tremolite-actinolite (the latter probably from a dolomitic precursor). Tabular clasts define a crude bedding	Talus, indicates cannibalization of K2, possibly due to syn-sedimentary faulting	Because of poor outcrop and structural complications it is uncertain if K3 is a separate unit above K2 or a local member within K2.
	K2	Arkose with parallel stratification, low angle cross-stratification and, less commonly, wedge-planar and trough cross sets (Fig. 6A, B, C). Rare pebbly beds with granitic and carbonate fragments; mudstone layers and mudchip breccias	Fluvial deposits adjacent to K1 alluvial fans. Flash floods dispersed as areally extensive, unchanneled high energy sheets with flood deceleration generally too rapid to permit the development and migration of lower flow regime bedforms	Limited paleocurrent data (Fig. 7) display high variance, which may represent unchanneled flash floods spreading laterally across piedmonts. Sense of flow is opposite (westward in Kiyuk Lake, eastward north of Windy Lake) and may indicate basin segmentation during sedimentation
	K1	Massive to thickly-bedded conglomerate with local (to 3m) arkose interbeds (Fig. 5). Subrounded to angular clasts up to 80 cm; clast/matrix ratios 4/6 to 9/1; framework intact and framework disrupted but generally coarse-sand matrix. 90% foliated and massive granitic clasts; also with mafic volcanic, quartz arenite, carbonate, arkose, quartz-magnetite iron formation, banded sandstone-siltstone clasts.	Alluvial fans with low-viscosity flash-flood processes predominant. Clast compositions imply basement and Hurwitz Group uplifted to erosional levels; thick conglomerate section implies significant topographic relief	Sub-K1 unconformity is not exposed in map area; all lower contacts are faults. In the western outlier supracrustal clasts are predominant (60%) and we speculate that these may form the lower part of the section and indicate cover to basement stripping. Some outcrops mapped by Eade (1971) as part of the K1 have been reassigned to the Tavani Fm. or K3.
HURWITZ GROUP	Hurwitz "H"	Siltstone, arkose and slate; siltstone to sandstone ratio varies from 7/3 to 5/5; commonly arranged in cm-dcm fining-upward cycles in the sequence erosional base to massive or graded medium-grained arkose to fine-grained arkose (locally parallel-stratified) to siltstone (and locally mudstone) (Fig. 4C, D). Rare cryptalgal laminate lenses at base.	Small-scale fining-upward cycles, absence of subareal indicators suggest turbidity current-like sedimentation at below wave-base depths.	New unit that overlies Tavani Fm in Simons Lake Sheet (65/C/9). The name "Hurwitz H" is used informally, following Bell's (1968) alphabetical format
	Tavani Formation	Quartz arenite, conglomerate with quartz arenite and carbonate clasts, local cryptalgal laminate. In contrast to Kiyuk conglomerate Tavani conglomerate consists of quartz arenite and carbonate clasts exclusively, has a quartz arenite to calc-arenite matrix, are commonly well-stratified, and are not interbedded with arkose. Clasts are angular to well-rounded; granule-pebble sizes are predominant; quartz arenite to carbonate clast ratios vary from 8/2 to 2/8. Conglomerates are both framework intact and framework disrupted; matrix remains coarse sand. Cycles between components are not evident, upper contacts of cryptalgal laminates are erosional.	Preliminary model of cryptalgal laminates as shallow subtidal deposits, quartz arenite as shallow water to subareal deposits and conglomerates being intraformational, from reworking (fluvial or tidal channel migration/collapse, syn-sedimentary faulting, sea-level fluctuation?) of early cemented (e.g. Dickson, 1985, Thiry et al., 1988) carbonates and quartz-arenites	In type area Tavani Fm is compositionally immature (Bell, 1968, Heywood, 1973), but in Kognak River (Eade, 1974) and Tulemalu-Yathkyed (Eade, 1986) areas "impure quartzites" are prominent. Transition from Watterson in map area is conformable, although to the east is a basin-margin sub-Tavani unconformity that cuts into progressively deeper stratigraphic levels (Bell, 1970a).
	Ducker Formation	Not developed in map area (cf. Eade, 1971) greywacke and siltstone		A direct Watterson to Tavani transition is common (Eade, 1974, 1986, Eade and Chandler, 1975)
	Watterson Formation	Dcm to m-scale interlayers of cryptalgal laminate and dcm-scale arkose to siltstone fining-upward cycles (Fig. 3C, D, E, F). Carbonate/siliciclastic ratios range from 4/6 to 9/1; carbonate rocks are generally predominant.	Siliciclastic component may represent more proximal (relative to Ameto) turbidite sedimentation; carbonate rocks shallow subtidal.	Interlayering may represent shoaling-upward aggradational cycles, the significance of which (autocyclic vs allocyclic) needs to be evaluated
	Ameto Formation	Siltstone, slate, arkose. Fining-upward cycles of arkose (locally graded or with parallel-stratification or small-scale cross stratification) to siltstone to mudstone (Fig. 3B). Siltstone to sandstone ratio 3/7 to 1/9.	Below wave-base sedimentation interrupted by turbidity-like currents	Transition from supermature quartz arenites of Kinga to texturally and compositionally immature Ameto appears to be abrupt. Possibility of mafic volcanic rocks in map area being Ameto Fm. cannot be precluded
	Kinga Formation	Snow white to pale-grey weathering fine-grained quartz arenite with parallel stratification (Fig. 3A).	Platform deposits, possibly multi-cyclic and/or derived from zones of intense tropical weathering (eg. Bell 1968, 1970a)	Intraformational breccia at the top of Kinga led Bell (1970a) to infer a sub-Ameto unconformity
	Padlei Formation	Not exposed in map area; slate, siltstone, conglomerate, sandstone (Bell, 1970a, b, Eade, 1974)		
BASEMENT		Mafic volcanic rocks with local silicification pods and possible remnant pillow selvages		2.682 ± .0059 Ga (U-Pb zircon, Chiarenzelli and Macdonald, 1986), from northern Saskatchewan
		Thickly stratified gneiss (Kasba Lake gneiss of Loveridge et al., 1988) cut by granitic rocks; granitic protomylonite.		Gneiss yields to U-Pb zircon age populations of ca 3 270 and 2.780 Ga (Loveridge et al., 1988).

Numerous gossans were found during mapping (Fig. 1). Anomalous gold and arsenic values in Hurwitz Group and Kiyuk Group rocks cut by thrusts and late cross-faults suggest that structural traps within the Proterozoic sequence may be favourable exploration targets.

Stratigraphic nomenclature: abandonment of "Ennadai Group" and introduction of "Kiyuk Group"

Use of the term "Ennadai" in the literature has been ambiguous. Historically, the domain of metavolcanic and metasedimentary rocks that extends from northeastern Saskatchewan to Rankin Inlet has been called the Ennadai-Rankin (or Rankin-Ennadai) greenstone belt (e.g. Wright, 1967, p. 76). Parts of this belt have yielded Archean U-Pb zircon ages (Chiarenzelli and Macdonald, 1986; Mortensen and Thorpe, 1987). However, Eade and Chandler (1975 p. 8) and Wanless and Eade (1975) casually introduced the term "Ennadai Group" for a unit of Proterozoic conglomerate and arkose that unconformably overlies the Hurwitz Group in the Ennadai Lake area. Subsequently, Macdonald (1984) used "Ennadai Group" for Archean metavolcanic rocks southwest of Ennadai Lake, but again, without rigorous definition. Hence the term "Ennadai Group" has never been formally defined, and has been applied to rocks both below and above the Hurwitz Group, in the same region.

The term "Ennadai Group" should be abandoned to eliminate confusion resulting from its application to different rock sequences. A new name, the Kiyuk Group, is proposed here for conglomerates, arkoses, and arkose-clast breccias that unconformably overlie the Hurwitz Group. The group outcrops in two northeast-trending outliers, one comprising the present study area, and the "western outlier", southeast of Ennadai Lake (Fig. 1A). It is uncertain if the two outliers represent the remnants of a once-continuous basin or if they represent depocentres that were isolated during sedimentation. The type-area is at Kiyuk Lake where rocks of the unit are exposed in a gently northeast-plunging, northwest-vergent syncline and in related thrust sheets (Fig. 1,2). Three sub-units are designated: the K1 conglomerate; K2 arkose; and K3 arkose-clast breccia (Table 1).

STRUCTURAL ANALYSIS

Poorfish-Windy thrust-fold belt

Northwest-propagating "piggy-back" thrusts, northwest-verging folds, and late NNW- and NNE-trending normal faults are the principal structural elements in the Poorfish-Windy lakes area (Figs. 1 and 2).

Kinematic indicators in Hurwitz and Kiyuk cover rocks are rare, hence the inferred direction of thrust transport is based on vergence of macrofolds and map-scale geometric relationships. The thrust faults were recognized on the basis of older-over-younger contractional contacts, repetition of stratigraphy, and footwall cutoffs against fault 2 which juxtaposes rocks of the Watterson Formation over the Kiyuk Group, and forms the roof of a duplex. Folding in the footwall ahead of thrust propagation is considered responsible for this thrust cutting down section as well as upsection, ie. the thrust cuts through a pre-folded sequence (break-back thrusting of Butler, 1987, see also Price, 1965, p. 85-88). Unambiguous evidence that the thrusts developed in the classical piggyback or in sequence array (eg. Boyer and Elliott, 1982, Butler, 1987) comes from the observation that fault 2 is cut by successively lower and westward thrusts 3, 5, and 6 (breaching thrusts of Butler and Coward, 1984).

The breaching has resulted in repetition of the previously thrusted Watterson-over-Kiyuk package and an apparently extensional younger-over-older structural stacking. Hence Kiyuk Group rocks (footwall of fault 2) in the hanging wall of faults 3, 5, and 6, are juxtaposed against Watterson Formation rocks (hanging wall of fault 2) in the footwall of faults 3, 5, and 6 (Fig. 2). The possibilty that the younger-over-older geometry of faults 3, 5, and 6 represents true extensional, southeast-side down movement is rejected because if this were the case, what should be observed in the footwall of (eg.) fault 5 is the sequence (east to west): Kiyuk conglomerate over Tavani Formation over Watterson Formation, ie. the original stratigraphic sequence beneath fault 2. The alternative that faults 5 and 6 are depositional contacts representing the basal unconformity of the K1 conglomerate cut into the Watterson Formation, is also rejected because of the paucity (less than a few percent) of clasts derived from the Watterson and the highly strained nature of the rocks close to the contact.

Folds in the Kiyuk Group are open with a kink geometry. In contrast, folds in the Watterson Formation generally are tight and non-parallel. The high concentration of folds in the Watterson Formation in the hanging wall of fault 2 is considered to represent a train that developed ahead of fault detachment, unrelated to ramping in the underlying thrust (fault detachment folds of Jamison, 1987). The folds are markedly disharmonic with respect to folds in the Kiyuk Group immediately beneath the thrust (Fig. 2).

Locally, within the core of the syncline along Kiyuk Lake, K2 sandstones are apparently strain-free. A spaced cleavage defined by micaceous segregations, probably from pressure solution (eg. Borradaile et al., 1982) is generally developed. Spacing of cleavage domains decreases from decimetre-scale to centimetre-and millimetre-scale toward the faults. Clasts in K1 conglomerate are commonly aligned, and define a penetrative fabric. Clast pull-aparts, indented clast boundaries, and squeeezing of soft clasts between hard clasts suggest brittle, pressure solution and ductile flow processes respectively, controlled by clast rheology. Hurwitz Group rocks generally bear a penetrative cleavage: argillaceous rocks commonly display a slaty cleavage; spacing in arenaceous and carbonate rocks is commonly on a centimetre-scale. In the Watterson Formation, cleavage refraction (low angle with respect to bedding in carbonate members, high angle in sandstone members) is common.

NNE- and NNW-trending normal faults crosscut thrust-fold related structures. Closely spaced joint sets and fault gouge west of Simons Lake and on the Red River, suggest brittle processes.

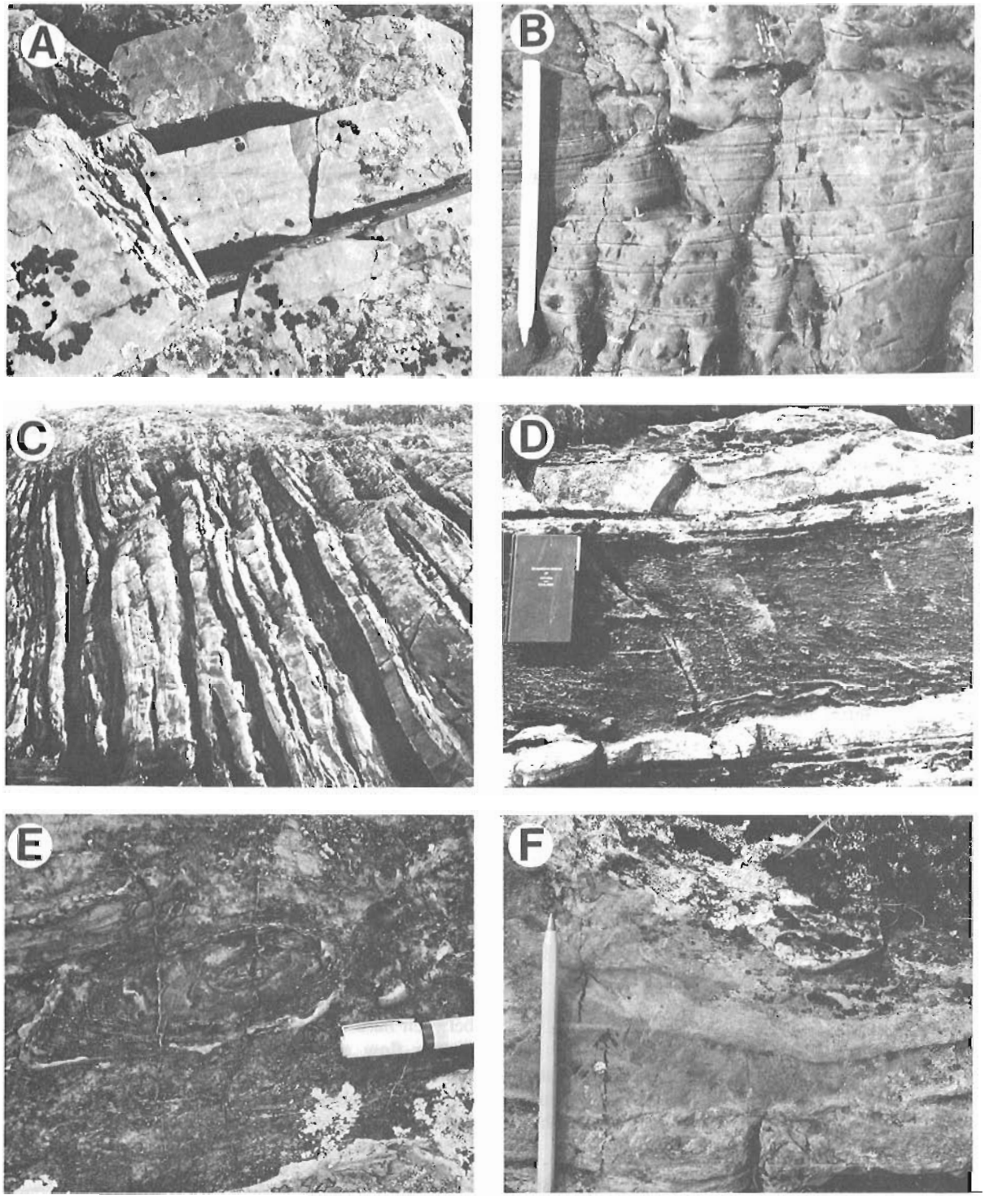

Figure 3. Hurwitz Group map units. A) Parallel stratified quartz arenites, Kinga Formation, GSC 204692-K. B) Small-scale sandstone to siltstone fining-upward cycles, Ameto Formation. Note load casts and flame structures (upper right) and small-scale cross stratification (lower right), GSC 204692-X. C) Interbedded cryptalgal laminates (recessive-weathering) and arkose to siltstone fining-upward cycles, Watterson Formation. Note lense-like character of some of the interlayers, GSC 204692-Y. D)Cryptalgal laminates, Watterson Formation, GSC 204692-U. E) Oncolites, Watterson Formation, GSC 204714-A. F) Arkose to siltstone fining-upward cycles, Watterson Formation, GSC 204714-B.

Estimate of shortening

The degree of basement involvement and the manner in which the faults merge at depth on the down-plunge projection (Fig. 2) are not rigorously controlled. The assumption of significant basement involvement is based on the predominance of basement-derived clasts in the K1 conglomerate. Direct evidence of basement involvement may be the fault that emplaces mafic volcanic rocks over K1 conglomerates on northern Windy Lake (Fig. 1B), but assignment of the volcanics to the basement complex (vs. Happotyik member, Ameto Formation) is uncertain.

Depth to basement on Figure 2 was determined by stacking down the Hurwitz Group stratigraphy below surface geology. Uncertainties include accuracy of thicknesses used and precise level of detachment. Ongoing analysis of locally developed lower to middle greenschist facies metamorphic assemblages may help provide depth constraints.

A crude estimate for the amount of shortening across the belt of 75 %, or 75 km, was determined using a simplistic un-faulting procedure. This is a minimum value; shortening accomodated by folding and cleavage are not considered. More importantly, by un-faulting along the fault dips portrayed in Figure 2, lower to middle greenschist-grade Hurwitz Group rocks are brought to unrealistic depths (60 km). Hence the faults either flatten at shallower levels than shown in Figure 2, or have been steepened by back-rotation due to movement along lower, westerly thrusts. In either case, flatter fault dips imply larger horizontal translation.

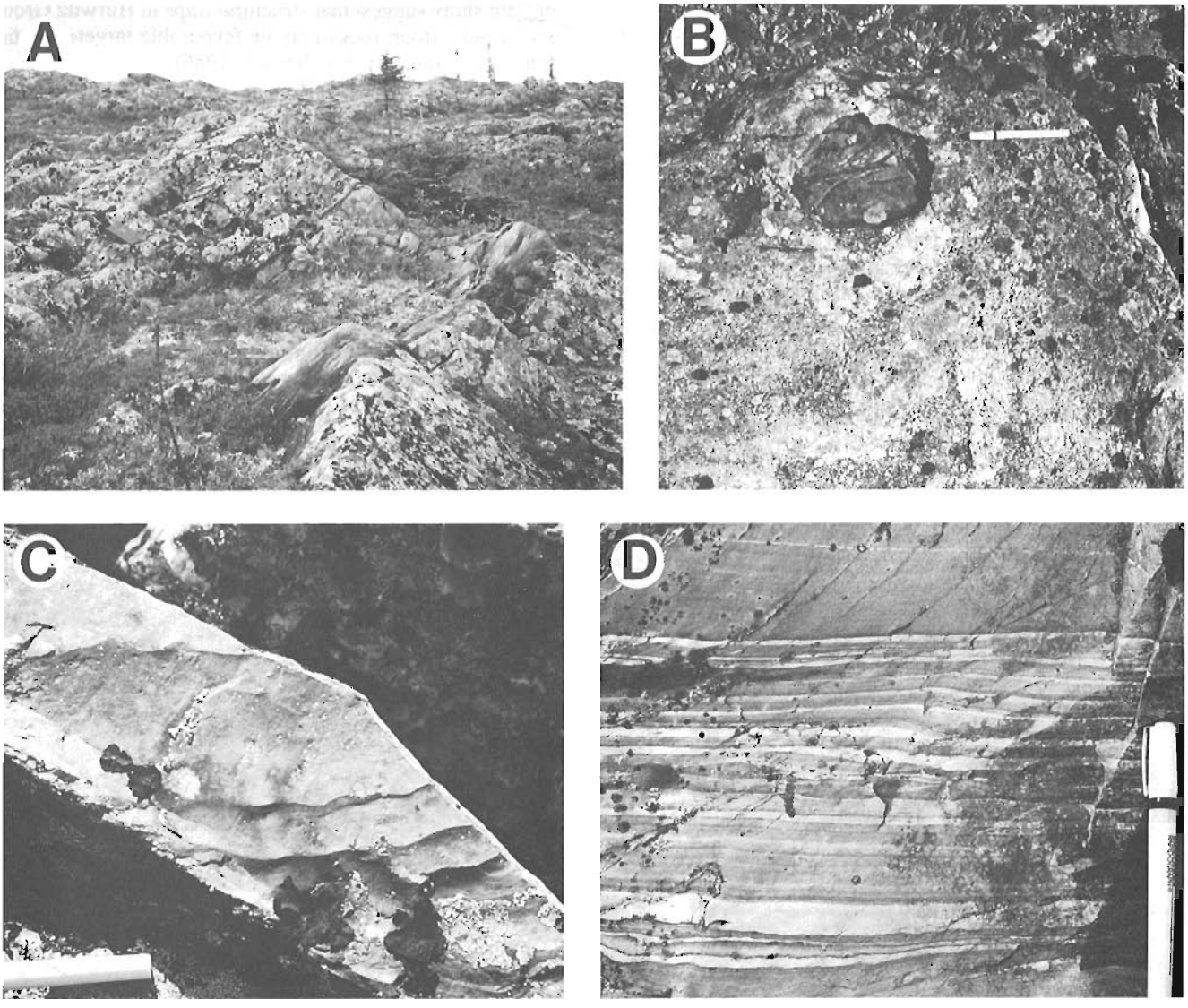

Figure 4. A) Interbed of cryptalgal laminate within quartz arenite, carbonate-clast conglomerate, Tavani Formation, GSC 204692-V. B) Cryptalgal laminate and quartz arenite clast conglomerate, Tavani Formation, GSC 204692-F. C) Sandstone to mudstone fining-upward cycles, "Hurwitz H" , GSC 204692-T. D) Interlaminated sandstone and siltstone, "Hurwitz H", GSC 204692-S.

Relationship to adjacent areas

Relationships east of the map area are obscured by poor outcrop and the Nueltin granite, but basement exposures about 20 km southeast of Poorfish Lake and in the Nueltin Lake area (Eade, 1971, 1973), may represent deeper crustal levels of the same thrust complex that were driven westward and to erosional levels during sedimentation of the Kiyuk Group. This is consistent with an apparent increase in metamorphic grade expressed in Hurwitz and Wollaston Group rocks to the southeast (Fraser, 1962; Eade, 1971; Weber et al., 1975).

The sense of movement along the westernmost fault (fault 7), and the nature of the link from the map area to the western outlier, are uncertain. Kinematic data from two outcrops of granitic protomylonite west of Poorfish Lake (Fig. 1B), including rotated porphyroclasts (δ and ς types of Passchier and Simpson, 1986), grain pull-aparts and shear bands, indicate that fault 7 may have an east side-down sense. If this is valid, fault 7 could be analogous to normal faults in thrust belts such as the Flathead fault in the southern Canadian Cordillera (Price, 1965). If the fault is a thrust and the limited kinematic data record only later, normal-sense reactivation, the younger-over-older relationship may represent: 1) a basement-cover décollement over a basement ramp, with Hurwitz Group and Kiyuk Group rocks in the western outlier being exposed in the footwall of a lower thrust; 2)the eastern margin of a basement-cored antiformal stack (Boyer and Elliott, 1982) with the western outlier in the hanging wall of the foreland-dipping segment of the duplex; or 3) basement-cover infolding, with fault 7 representing large-scale flexural-slip of cover rocks out of a synclinal core and the western outlier a separate synformal cusp (see Harris et al., 1987; Hoffman, in press).

ECONOMIC GEOLOGY

Numerous gossans were mapped during the present study, both in outcrop and in float (Fig. 1B). Mineralization appears to be epigenetic, occurring as fracture-fillings and irregular pods that transect primary structures. Gossans were found in each map unit except the Nueltin granite. Although some are related to thrust-deformation, a high concentration in the northern Windy Lake area, close to the NNW and NNE cross-faults, suggests remobilization along these late structures.

Preliminary analytical results on gossan samples (Table 2) indicate that anomalous gold and arsenic are localized in fractured Hurwitz Group and Kiyuk Group rocks. In the District of Keewatin, recent attention has been focussed on the gold potential of Archean greenstones. Gold has been recognized in Hurwitz Group rocks since the early 1940s, and was mined from pyritic gold veins at the Shear Lake deposit (Raman et al., 1986, Miller, 1989). Results from the present study suggest that structural traps in Hurwitz Group and Kiyuk Group rocks may be favourable targets for disseminated gold (see Romberger, 1986).

DISCUSSION

Lewry et al., (1985) proposed a model for Trans-Hudson Orogen that entails deposition of a shelf sequence (Hurwitz and Wollaston groups) and deformation of this sequence in the development of a north or northwest-vergent fold and thrust terrane during ca. 1.87 Ga collision from the south or southeast (see also Hoffman, 1988). Data from the present study indicate large-scale (at least 75 km), in sequence, northwest-directed thrusting of basement, Hurwitz Group and Kiyuk Group rocks. However, it is critical to emphasize

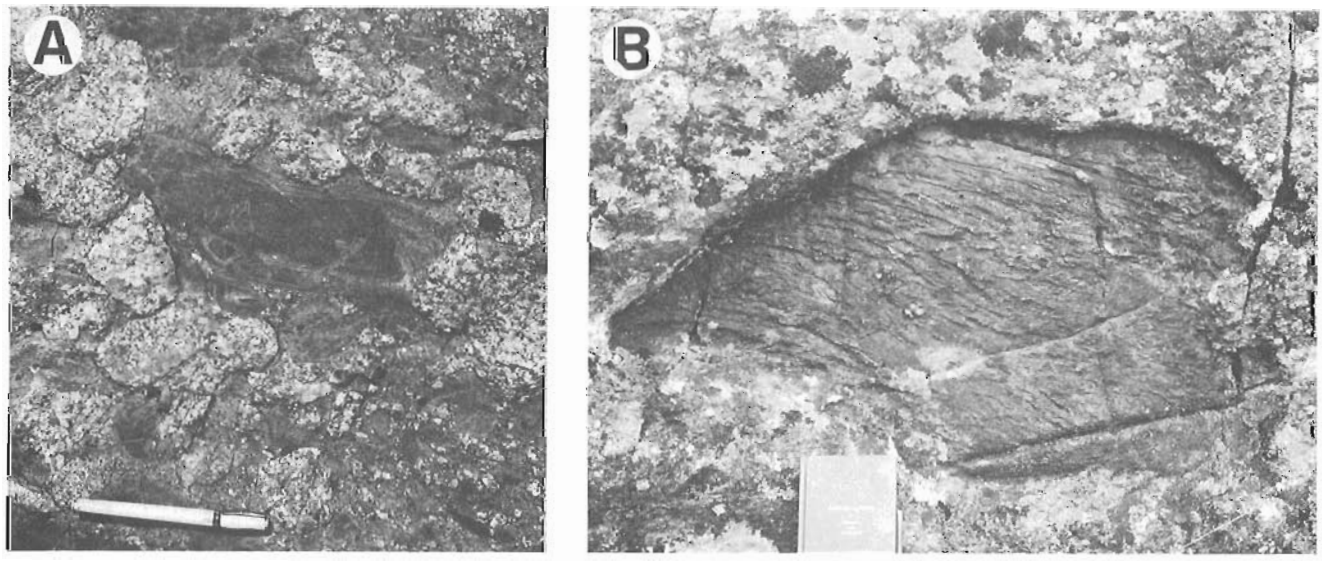

Figure 5. K1 conglomerate. A) subangular to well rounded granitic clasts (light weathering) and dark mafic volcanic clast, GSC 204692-Z. B) Boulder of Watterson Formation-derived cryptalgal laminate in K1 conglomerate, GSC 204692-L.

Table 2. Preliminary analytical results. See Figure 1B for sample locations. All analyses are by neutron activation with detection limits of: Au, 2 ppb; As, 0.5 ppm; W, 1 ppm; Ni, 20 ppm; Cr, 20 ppm.

Field Sample #	Letter on Fig. 1B	Location (UTM)	Host Rock	Formation	Opaque Mineralogy	Gangue Mineralogy	Remarks	Geochemical Assays				
								Au (ppb)	As (ppm)	W (ppm)	Ni (ppm)	Cr (ppm)
17-3	A	65C/7 149 963	Quartz arenite	Tavani	Pyrite	Minor chlorite	Oxidized float; disseminated fine grained pyrite; clusters of pyrite aggregates to 7 mm. Interpretation: Diagenetic sulfides modified by metamorphism	110	320	37	32	56
18-5A	B	65C/9 266098	Quartz vein cutting meta-carbonate with tremolite-actinolite	Watterson	Pyrite	--	<1% fine grained pyrite disseminated in rusty quartz vein; depending on orientation, veins rotated/folded concordant with thrust/fold-related fabrics in host	6	212	1	<20	<20
20-8-B	C	65C/8 216967	5 cm-wide quartz vein cutting conglomerate	Kiyuk (K_1)	Hematite	--	Hematite after sulfides filling fractures in gray white quartz vein. Vein cuts across thrust/fold-related fabric in host	1660	7.7	1	<20	<20
26-6C	D	65C/8 345032	Quartz arenite	Tavani	Pyrite	--	Disseminated pyrite through biotitic quartz arenite; minor quartz veins; highly oxidized	<2	782	1	87	49
L-2-2	E	65C/9 181069	Metacarbonate	Watterson	Pyrite, arsenopyrite	Quartz, albite(?), chlorite	Oxidized float; microfractured and veined with very fine grained quartz (chert-like) + albite(?). Fine grained pyrite and arsenopyrite confined to veins	<150	>9000	49	<20	<20

that, as summarized by Hoffman (in press), apparent vergence is not regionally consistent in the District of Keewatin. Structures verge southeast between Yathkyed and Imkula lakes (Eade, 1986), north in the Henik Lakes area (Eade, 1974), south (Davidson, 1970) and north (Bell, 1968) in the Kaminak Lake area, both north and south in the Whiterock belt (Bell, 1968) and south in the Marble Island area (Tella et al., 1986).

It is not known what the predominant sense of vergence is, or if there is one. Furthermore, it is not clear what the pattern represents: 1) crustal shortening by regional-scale basement-cover infolding, with local thrust-fold belts of opposing vergence being a consequence of large-scale flexural-slip of supracrustal rocks out of cuspate synforms and over lobate basement antiforms (see Ramsay, 1967; Harris et al., 1987; Hoffman, in press); 2) basement-involved backthrusting antithetic to the predominant sense and the development of (in this case basement-cored) "pop-ups" (see Tirrul, 1983; Price, 1986; Butler, 1987); 3) Laramide-style basement uplifting along low-angle thrusts with a vergence that is inconsistent from uplift to uplift (Berg, 1981, Gries, 1983) or 4) the superposition of two unrelated structures, an older southeast and south vergent set related to postulated collision in the Snowbird tectonic zone, and a younger, north-vergent set related to collision in Trans-Hudson Orogen (Hoffman, in press).

Despite these questions, the sedimentary record of the Hurwitz and Kiyuk groups is compatible with a simple model in which the Kinga shelf was drowned by a north and northwesterly migrating foredeep causally linked to Trans-Hudson Orogen. Some of the fundamental elements in the model that follows were expressed in classical "geosynclinal" language by Bell (1970a; see also Young, 1984, 1988). The treatment below is qualitative, drawing on early studies of foreland sedimentation by Price (1973) and Eisbacher (1974) and recent analysis of Proterozoic foredeeps by Hoffman (1987). An attempt at developing a more sophisticated geodynamic model (eg. Beaumont, 1981; Quinlan and Beaumont, 1984; and Stockmal et al., 1986) is in progress.

We suggest that: 1) the shelf to foredeep transition is marked by the sub-Ameto unconformity in which the pre-Ameto period of emergence noted by Bell (1970a) records the northwestward passage of the peripheral bulge (Young, 1988);

2) the change in provenance implied by the non-quartzose composition of arenites in the Ameto (relative to the Kinga) and the abrupt change from shelf to basinal depositional setting indicates rapid loading of thrust sheets and a rapid deepening that inhibited the development of an outer ramp facies (see Fig. 1 in Hoffman, 1987);

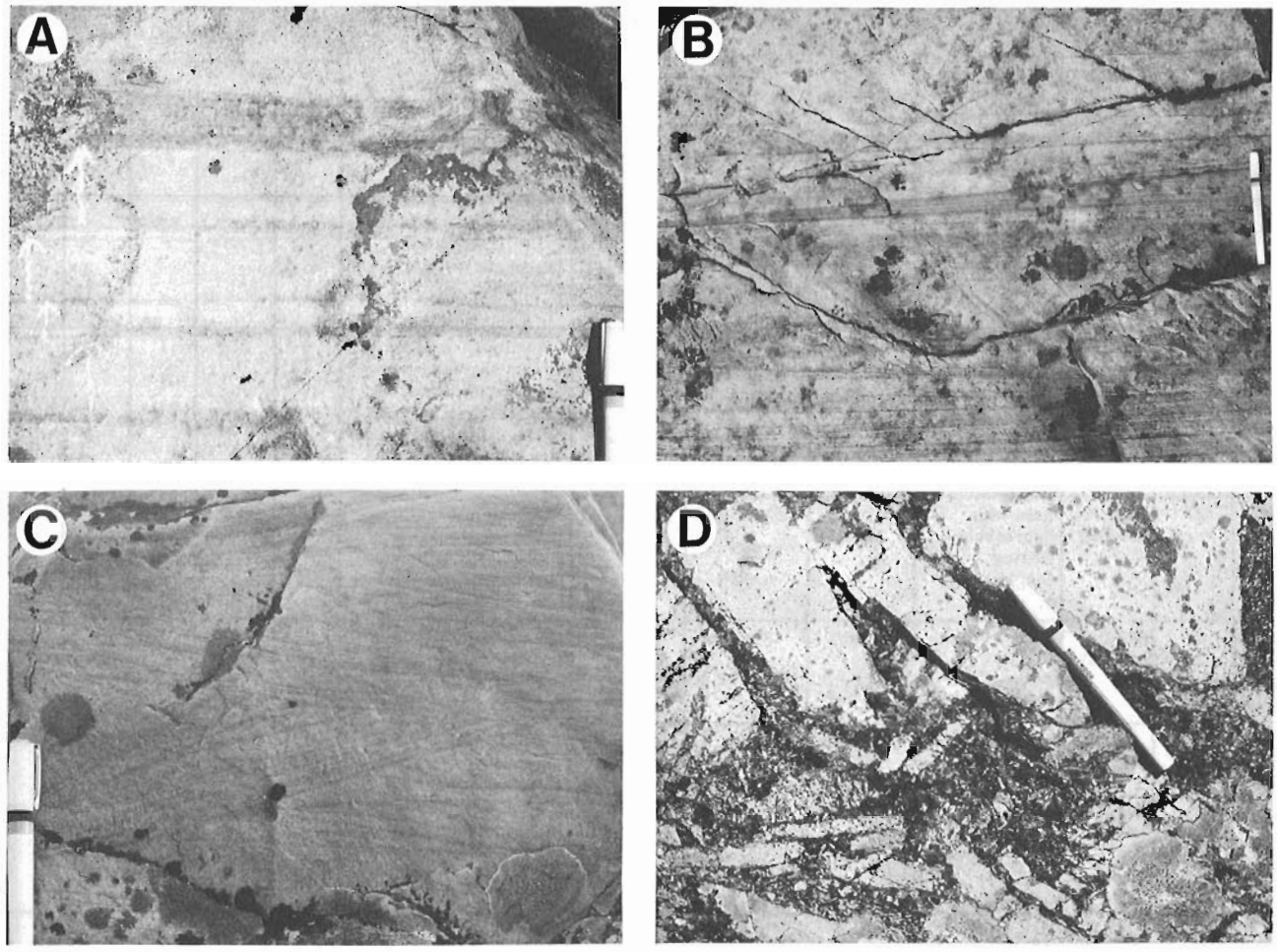

Figure 6. A) Parallel stratified arkose with heavy mineral- rich to heavy mineral- poor fining-upward cycles, K1 unit, GSC 204692-D. B) Parallel stratified and low angle cross stratified arkose, K2 unit, GSC 204692-M. C) Trough cross stratified arkose, K2 unit, GSC 204692-R. D) Framework intact breccia of tabular arkose fragments, K3 breccia, GSC 204692-E.

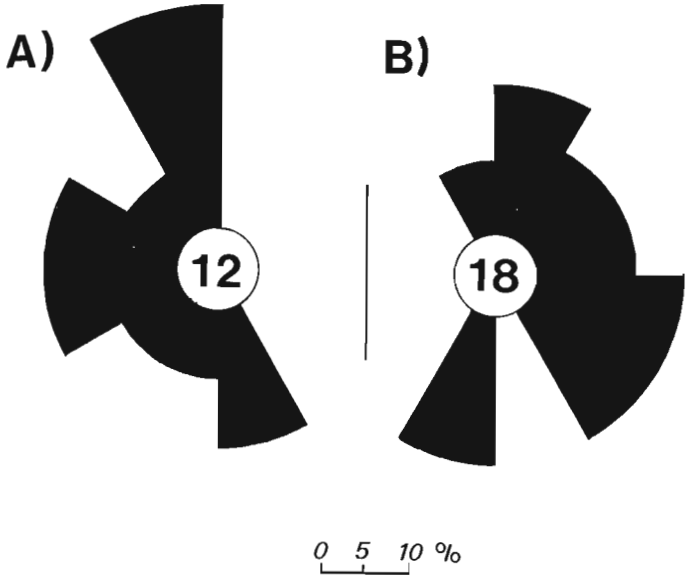

Figure 7. Paleocurrent roses, K2 arkose, A) Kiyuk Lake, B) north of Windy Lake. Data are from low and high angle planar cross strata and trough cross strata and have been rotated to correct for dip of bedding. Because of low values, a plunge correction was not made.

3) mafic volcanic flows, tuffaceous greywackes and gabbroic sills within the Ameto Formation may be examples of axial zone foredeep magmatism emphasized by Hoffman (1987);

4) the shoaling-upward sequence from the Ameto to the Watterson Formation represents relatively slow rates of thrust loading that permitted the development of a shelf on the hinterland side of the axial zone;

5) fine grained rocks of the Ducker Formation represent the onset of a second coarsening-upward sequence in which rapid thrust loading caused sudden deepening and drowning of the Watterson shelf;

6) the sub-Tavani unconformity and the Tavani conglomerate on Pork Peninsula, whose sequence of clasts supports progressive stripping from sub-Tavani Hurwitz to basement (Bell, 1970a), provide the first direct evidence of uplift to erosional levels of Hurwitz Group rocks, and mark the rapid progradation of subareal facies directly ahead of the thrust-fold belt (Bell's "harbinger of the Hudsonian orogeny"; see also Young, 1988);

7) uplift and erosional stripping of sub-Tavani units on the east, due to the arrival of the thrust front, was concurrent with uninterrupted sedimentation in the west, as indicated by the lateral transition from angular unconformity on the east to conformable sub-Tavani relations on the west and in the present map area (see also Bell, 1970a, Fig. 4; Miall, 1978; DeCelles et al., 1987);

8) the lateral change in composition of the Tavani Formation, from predominantly arkose in the east to quartz-rich on the west and in the present study area, reflects increasing distance away from the thrust front (sediment transport distance greater than thrust front migration) and possibly, a contribution from recycling of Kinga Formation quartz arenites that was less diluted by basement-derived debris;

9) sedimentation of the Hurwitz "H" in the present map area represents sudden deepening (renewed rapid thrusting?) immediately prior to the arrival of basement-cored thrust sheets, an erosional front and deposition of coarse grained alluvium of the Kiyuk Group (see also DeCelles et al., 1987); and

10) the Kiyuk Group was subsequently thrust-fold deformed (in part cannibalized?) by continued westward migration of the thrust complex.

Implicit in the model is a dynamic link to processes in the hinterland of Trans-Hudson Orogen; the Hurwitz-Kiyuk sedimentary record is interpreted in terms of rates of thrusting and loading which is in turn related to rates of convergence in the hinterland, and possibly to subducted slab geometry (see Dickinson and Snyder, 1978; Royden et al., 1987). Hence the model is testable; geochronology on axial zone magmatic rocks (Happotyik member and related sills) currently being undertaken by J. Patterson (pers. comm., 1988), on dacite and andesite flows mapped by Taylor (1963) in the Kasba Lake area (sampled by S. Roscoe, pers. comm., 1988), on the pre-thrust foliated granite and the post-thrust diabase dykes in the present map area, are critical first tests. Also implicit in the model is an assumption of a predominantly northwestward structural vergence. Clearly, an understanding of the cause of the opposing vergence pattern, quantitative estimates of relative shortening, and palinspastic restorations are required.

ACKOWLEDGMENTS

This project was funded through the Canada-Northwest Territories Mineral Development Agreement as a co-operative effort by: Geology Division, Department of Indian Affairs and Northern Development, Yellowknife; Mineral Resource Division, Geological Survey of Canada; and the Government of the Northwest Territories, Energy Mines and Resources Secretariat. We are indebted to C.W. Jefferson and W.A. Padgham for having faith in the project and for last minute negotiations that enabled us to get into the field. Martin Irving smoothed out some logistical problems. John Broome is thanked for his advice on the interpretation of geophysical data and for providing reformatted aeromagnetic maps. Sample preparation by Richard Lancaster during the field season enabled speedy preliminary petrography. B.W. Charbonneau is thanked for the loan of scintillometers and for discussions regarding potential skarn mineralization.

We benefitted from discussions with P.F. Hoffman and A. N. LeCheminant during development of the project proposal; P.F. Hoffman is thanked for giving us pre-prints of works in progress, particularly the DNAG map; A.N. LeCheminant helped us in our quest for baddeleyite. Jack Henderson's insights helped to clarify our ideas during preparation of the manuscript. B. Hodgins provided field assistance. Jim Snobble's enthusiasm was an inspiration. Critical comments by R.T. Bell, C.W. Jefferson and S. Tella helped to improve the manuscript.

REFERENCES

Beaumont, C.
1981: Foreland basins; Geophysical Journal of the Royal Astronomical Society, v. 65, p. 291-329.

Bell, R.T.
1970a: The Hurwitz Group-a prototype for deposition on metastable cratons; in Symposium on basin and geosynclines of the Canadian Shield, edited by A.J. Baer, Geological Survey of Canada Paper 70-40, p. 159-169.
1970b: Preliminary notes on the Hurwitz Group, Padlei map area, Northwest Territories; Geological Survey of Canada, Paper 69-52, 13p.
1968: Preliminary notes on the Proterozoic Hurwitz Group, Tavani (55K) and Kaminak Lake (55L) areas, District of Keewatin; Geological Survey of Canada, Paper 68-36, 17p.

Berg, R.R.
1981: Review of thrusting in the Wyoming foreland; Contributions to Geology of the University of Wyoming, v. 19, p. 93-104.

Borradaile, G.J., Bayly, M.B., and Powell, C.McA.
1982: Atlas of Deformational and metamorphic rock fabrics; Springer-Verlag, New York, 551p.

Boyer, S.E. and Elliott, D.
1982: Thrust systems; American Association of Petroleum Geologists Bulletin, v. 66, p. 1196-1230.

Butler, R.W.H.
1987: Thrust sequences; Journal of the Geological Society of London, v. 144, p. 619-634.

Butler, R.W.H. and Coward, M.P.
1984: Geological constraints, structural evolution, and deep geology of the northwest Scottish Caledonides; Tectonics, v. 3, p. 347-365.

Chiarenzelli, J.R., and Macdonald, R.
1986: A U-Pb zircon date for the Ennadai Group; in Summary of Investigations 1986, Saskatchewan Geological Survey, Saskatchewan Energy and Mines Miscellaneous Report 86-4, p. 112-113.

Davidson, A.
1970: Precambrian Geology, Kaminak Lake map-area, District of Keewatin; Geological Survey of Canada, Paper, 69-51, 27p.

DeCelles, P.G., Tolson,R.B., Graham, S.A., Smith, G.A., Ingersoll, R.V., White, J., Schmidt, C.J., Rice, R., Moxon, I., Lemke, L., Handschy, J.W., Follo, M.F., Edwards, D.P., Cavazza, W., Caldwell, M., and Bargar, E.
1987: Laramide thrust-generated alluvial-fan sedimentation, Sphinx Conglomerate, southwestern Montana; American Association of Petroleum Geologists Bulletin, v. 71, p. 135-155.

Dickinson W.R. and Snyder, W.S.
1978: Plate tectonics of the Laramide Orogeny; in Laramide Folding Associated With Basement Block Faulting in the Western United States, edited by V. Matthews Geological Society of America, Memoir 151, p. 355-366.

Dickson, J.A.D.
1985: Diagenesis of shallow-marine carbonates; in Sedimentology, Recent Developments and Applied Aspects, edited by P.J. Brenchley and B.P.J. Williams Special Publication of the Geological Society, Blackwell Scientific, Oxford, p.173-188.

Eade, K.E.
1986: Precambrian geology of the Tulemalu Lake-Yathkyed Lake area, Districtof Keewatin; Geological Survey of Canada, Paper 84-11, 31p.
1974: Geology of Kognak River area, District of Keewatin, Northwest Territories; Geological Survey of Canada, Memoir 377, 66p.
1973: Geology of Nueltin Lake and Edehon Lake (west half) map-areas, District of Keewatin; Geological Survey of Canada, Paper 72-21, 29p.
1971: Geology of Ennadai Lake map-area, District of Keewatin; Geological Survey of Canada, Paper 70-45, 19p.

Eade, K.E. and Chandler, F.
1975: Geology of Watterson Lake (west half) map area, District of Keewatin; Geological Survey of Canada, Paper 74-64, 10p.

Eisbacher, G.H.
1974: Molasse — Alpine and Columbian; Geoscience Canada, v. 1, p. 47-50.

Fraser, J.A.
1962: Geology, Kasmere Lake, Manitoba, Geological Survey of Canada, Map 31-1962.

Gries, R.
1983: Oil and gas prospecting beneath Precambrian of foreland thrust plates in Rocky Mountains, American Association of Petroleum Geologists Bulletin, v. 67, p. 1-28.

Harris, C.W., Gibson, R.G., Simpson, C., and Eriksson, K.A.
1987: Proterozoic cuspate basement-cover structure, Needle Mountains, Colorado, Geology, v. 15, p. 950-953.

Heywood, W.W.
1973: Geology of Tavani map-area, District of Keewatin; Geological Survey of Canada, Paper 72-47, 14p.

Hoffman, P.F.
—: Subdivision of the Churchill Province and Extent of the Trans-Hudson Orogen; in The Early Proterozoic Trans-Hudson Orogen of North America, edited by J.F. Lewry and M.R. Stauffer. Geological Association of Canada, Special Paper. (in press).

Hoffman, P.F.
1988: United plates of America, the birth of a craton: Early Proterozoic assembly and growth of Laurentia; Annual Review of Earth and Planetary Sciences, v. 16, p. 543-603.

Hoffman, P.F.
1987: Early Proterozoic foredeeps, foredeep magmatism, and Superior-type iron formations of the Canadian Shield; in Proterozoic lithospheric evolution, edited by A. Kroner. American Geophysical Union Geodynamic Series 17, p. 85-98.

Jamison, W.R.
1987: Geometric analysis of fold development in overthrust terranes; Journal of Structural Geology, v. 9, p. 207-219.

Lewry, J.F., Sibbald, T.I.I., and Schledewitz, D.C.P.
1985: Variation in character of Archean rocks in the western Churchill Province and its significance; in Evolution of Archean Supracrustal Sequences, edited by L.D. Ayres, et al., Geological Association of Canada, Special Paper 28, p. 239-261.

Loveridge, W.D., Eade, K.E., and Sullivan, R.W.
1988: Geochronological studies from Precambrian rocks from the southern District of Keewatin; Geological Survey of Canada, Paper 88-18, 36p.

Macdonald, R.
1984: Notes on the Ennadai Group; in Summary of Investigations 1984, Saskatchewan Geological Survey, Saskatchewan Energy and Mines, Miscellaneous Report 84-4, p. 76-77.

Miall, A.D.
1978: Tectonic setting and syndepositional deformation of molasse and other nonmarine-paralic sedimentary basins; Canadian Journal of Earth Sciences, v. 15, p. 1613-1632.

Miller, A.R.
1989: Highlights of gold studies in the Churchill Structural Province, Kaminak greenstone belt and Hurwitz Group, District of Keewatin, NWT; in Current Research, Part C, Geological Survey of Canada, Paper 89-1C.

Mortensen, J.K., and Thorpe, R.I.
1987: U-Pb zircon ages of felsic volcanic rocks in the Kaminak Lake area, District of Keewatin; in Radiogenic Age and Isotopic Studies: Report 1, Geological Survey of Canada, Paper 87-2, p. 123-128.

Passchier, C.W., and Simpson, C.
1986: Porphyroclast systems as kinematic indicators; Journal of Structural Geology, v. 8, p. 831-843.

Price, R.A.
1986: The southeastern Canadian Cordillera: thrust faulting, tectonic wedging, and delamination of the lithosphere; Journal of Structural Geology, v. 8, p. 239-254.
1973: Large scale gravitational flow of supracrustal rocks, southern Canadian Rockies; in Gravity and Tectonics, edited by K.A. DeJong and R.A. Sholten, Wiley, New York, p. 491-502.
1965: Flathead map-area, British Columbia and Alberta; Geological Survey of Canada, Memoir 336, 221p.

Quinlan, G.M. and Beaumont, C.
1984: Appalachian thrusting, lithospheric flexure, and Paleozoic stratigraphy of the Eastern Interior of North America; Canadian Journal of Earth Sciences, v. 21, p. 973-996.

Raman, S., Kruse, J., and Tenney, D.
1986: Geology, geophsics and geochemistry of the Cullaton B-zone gold deposit, N.W.T., Canada; in Gold in the Western Shield, edited by L.A. Clark, Canadian Institute of Mining and Metallurgy, Special Volume 38, p. 307-321.

Ramsay, J.G.
1967: Folding and fracturing of rocks; McGraw-Hill, New York, 568p.

Romberger, S.B.
1986: Ore Deposits #9. Disseminated gold deposits; Geoscience Canada, v. 13, p. 23-31.

Royden, L., Patacca, E., and Scandone, P.
1987: Segmentation and configuration of subducted lithosphere in Italy: an important control on thrust-belt and foredeep-basin evolution; Geology, v. 15, p. 714-717.

Stockmal, G.S., Beaumont, C., and Boutilier, R.
1986: Geodynamic moels of convergent margin tectonics: transition from rifted margin to overthrust belt and consequences for foreland-basin development; American Association of Petroleum Geologists Bulletin, v. 70, p. 181-190.

Stockwell, C.H.
1950: The use of plunge in the construction of cross-sections of folds; Proceedings of the Geological Association of Canada, v. 3, p. 97-121.

Taylor, F.C.
1963: Snowbird Lake map-area, District of Mackenzie; Geological Survey of Canada, Memoir 333, 23p.

Tella, S., Annesley, I.R., Borradaile, G.J., and Henderson, J.R.
1986: Precambrian geology of parts of Tavani, Marble Island and Chesterfield Inlet map areas, District of Keewatin: a progress report; Geological Survey of Canada, Paper 86-13, 20p.

Thiry, M., Ayrault, M.B., and Grisoni, J.-C.
1988: Ground-water silicifiication and leaching in sands: Example of the Fontainebleau Sand (Oligocene) in the Paris Basin; Geological Society of America Bulletin, v. 100, p. 1283-1290.

Tirrul, R.
1983: Structure cross-sections across Asiak Foreland thrust and fold belt, Wopmay Orogen, District of Mackenzie; in Current Research, Part B, Geological Survey of Canada, Paper 83-1B, p. 253-260.

Wanless, R.K. and Eade, K.E.
1975: Geochronology of Archean and Proterozoic rocks in the southern District of Keewatin; Canadian Journal of Earth Sciences, v. 12, p. 95-114.

Weber, W., Schledewitz, D.C.P., Lamb, C.F., and Thomas, K.A.
1975: Geology of the Kasmere Lake-Whiskey Jack Lake (north half) area (Kasmere Project); Manitoba Mineral Resources Division, Geological Services Branch Publication 74-2, 163p.

Wright, G.M.
1967: Geology of the southeastern barren grounds, parts of the Districts of Mackenzie and Keewatin; Geological Survey of Canada, Memoir 350, 91p.

Young, G.M.
1988: Proterozoic plate tectonics, glaciation and iron formations; Sedimentary Geology, 58, p. 127-144.

Young, G.M.
1984: Proterozoic plate tectonics in Canada, with special emphasis on evidence for a late Proterozic rifting event; Precambrian Research, v. 25, p. 233-256.

Georgian Bay geological synthesis: Dillon to Twelve Mile Bay, Grenville Province of Ontario

N.G. Culshaw[1], G. Check[1], D. Corrigan[1], J. Drage[1], R. Gower[2], M.J. Haggart[1], P. Wallace[1], and N. Wodicka[1]
Lithosphere and Canadian Shield Division[3]

Culshaw, N.G., Check, G., Corrigan, D., Drage, J., Gower, R., Haggart, M.J., Wallace, P., and Wodicka, N., Georgian Bay geological synthesis: Dillon to Twelve Mile Bay, Grenville Province of Ontario; in Current Research, Part C, Geological Survey of Canada, Paper 89-1C, p. 157-163, 1988.

Abstract

Subdivisions of southern Britt and southwest Parry Sound domain contain relatively large amounts of high grade metasupracrustal rocks. These are interlayered with intrusive granitoid sheets in parts of Parry Sound domain, resulting in bimodal layered gneiss, now in granulite facies. Equally important in southeastern Parry Sound domain is quartz diorite orthogneiss. A thin, characteristic quartzite—meta-anorthosite association floors Parry Sound domain against underlying Go Home subdomain and has been traced into Moon River subdomain where it is overturned. Possibly an attenuated equivalent of similar associations in the Parry Sound shear zone to the northwest, it may mark the base of the Parry Sound allochthon; the tectonic position of the structurally lower part of Moon River subdomain requires further evaluation. Northwest-trending folds in Britt domain may postdate emplacement of the Parry Sound allochthon; they are associated with extensional tectonics along the west side of the synclinorium in southern Britt domain.

Résumé

Des subdivisions de la partie sud du domaine de Britt et de la partie sud-ouest du domaine de Parry Sound renferment des volumes relativement importants de roches d'origine supracrustale ayant subi un métamorphisme intense. Dans le domaine de Parry Sound ces roches sont interstratifiées par endroits avec des filons-couches granitoïdes, ce qui a entraîné la formation de gneiss stratifié, maintenant dans le faciès des granulites. L'orthogneiss à diorite et quartz présente tout autant d'intérêt dans la partie sud-est du domaine de Parry Sound. Une mince association caractéristique de quartzite et méta-anorthosite sépare la partie inférieure du domaine de Parry Sound du domaine sous-jacent de Go Home et a été suivie dans le subdomaine de Moon River où elle est renversée. Il peut s'agir d'un équivalent atténué d'associations analogues dans la zone de cisaillement de Parry Sound située au nord-ouest et pourrait correspondre à la base de l'allochtone de Parry Sound; le cadre tectonique de la partie du subdomaine de Moon River qui lui est structuralement inférieure reste à évaluer de manière plus approfondie. Les plis de direction nord-ouest dans le domaine de Britt peuvent être postérieurs à la mise en place de l'allochtone de Parry Sound; ils sont associés aux mouvements tectoniques de distension le long du côté ouest du synclinorium de la partie sud du domaine de Britt.

[1] Department of Geology, Dalhousie University, Halifax, Nova Scotia B3H 3J5.
[2] Department of Geology, The Johns Hopkins University, Baltimore, Maryland.
[3] Contribution to Canada - Ontario Mineral Development Agreement 1985-1990. Project carried by Geological Survey of Canada.

INTRODUCTION

This report outlines the preliminary results of the second of three season's mapping of a corridor across tectonic strike in the Central Gneiss Belt of the Grenville Province, Ontario. This work was funded by the Canada-Ontario Mineral Development Agreement 1984-1989 under Project C.2.3, "Georgian Bay Geological Synthesis". The corridor extends from Key Harbour, situated close to the southeast boundary of the Grenville Front Tectonic Zone, southeast to Port Severn, beyond which Paleozoic sedimentary rocks cover the Shield. An important aim of the traverse is to explore further the tectonic history of this part of the Grenville Province, building on the reconnaissance mapping of Davidson et al. (1982). Following work in 1987 to the northwest (Culshaw et al., 1988), mapping was undertaken in 1988 in the central part of the corridor, an area 55 km in length and increasing in width southeastward from 15 to 28 km. The northwest part of this area is within southern Britt domain (see inset in Fig. 1); the remainder is mainly within the Parry Sound shear zone and the interior of Parry Sound domain, but extends into Moon River and Go Home subdomains to the southeast (Davidson et al., 1982; Culshaw et al., 1983). This area has already received considerable attention, especially from workers in structural geology (Waddington, 1973; Schwerdtner and Mawer, 1982; Nadeau, 1984; Davidson, 1984; Hanmer, 1984; van Berkel and Schwerdtner, 1987), but despite this, many details of the geology are not well known.

SUMMARY OF FINDINGS

In the northeast part, mapping was completed in Britt domain and resulted in lithological subdivision of the previously described Sand Bay and Nadeau Island gneiss associations (Culshaw et al., 1988) and recognition of southeastward extension of the structurally lower Pointe-au-Baril granitoid complex. Map units within the Sand Bay association outline subhorizontal, northwest-trending second folds which are coaxial with folds of larger amplitude in the lower part of the overlying Parry Sound shear zone. The lowest levels of the attenuated western limb of the synclinorium in Britt domain contain kinematic indication of extensional tectonics, namely dextral displacement with top side obliquely downward to the southeast.

The northernmost part of Parry Sound domain (P1, inset in Fig. 1) contains a widespread, southward-dipping supracrustal assemblage of mafic and metasedimentary gneisses that is lithologically distinct from the adjacent Sand Bay gneiss association in Britt domain. Its lowermost unit includes quartzite and is cut by mafic dykes that were not observed in overlying units. The interior part of Parry Sound domain (P2) is a composite granulite facies gneiss terrane formed of interlayered granitoid, mafic and metasedimentary units which in places are individually mappable. These rocks may include a continuation of the supracrustal rocks to the north (P1), modified by later plutonism. To the south and east the Parry Sound domain is dominated by metaplutonic rocks of intermediate composition in which supracrustal intercalations are subordinate and differ from those to the north. Reworked Parry Sound domain granulites retrograded to amphibolite facies abut rocks of Go Home and Moon River subdomains to the southeast.

Within Moon River subdomain a prominent anorthosite layer associated with a thin but continuous supracrustal unit (quartzite, amphibolite and minor paragneiss) can be traced across the map area and separates different gneiss and migmatite packages (M1 and M2, inset in Fig. 1). This assemblage lies structurally above Go Home subdomain to the south but reverses dip within Moon River subdomain around the hinge of an overturned antiform. Although much thinner, the similarity of this assemblage to the northern supracrustal assemblage in the Parry Sound shear zone, together with similarities in the rocks below it in Go Home subdomain and Britt domain, tempt correlation.

Britt domain

In southeast Britt domain (Fig. 1) the structurally highest two gneiss associations (Sand Bay and Nadeau Island; Culshaw et al., 1988) dominate the geology, but elements of the lower two (Key Harbour and Bayfield) are present in the western limb of the synclinorium that lies parallel to the coast of Georgian Bay. The Sand Bay association is distinctly bimodal; it is composed predominantly of migmatitic quartzofeldspathic gneiss (fS in Fig. 1) accompanied by minor amounts of amphibolite, marble, calc-silicate rock and quartzite; the less voluminous but very characteristic member is grey, plagioclase-quartz-biotite schist (Dillon schist, dS in Fig. 1) that may contain epidote, scapolite and apatite and commonly encloses quartz pods. Mafic dykes were not observed.

The Sand Bay association overlies and is infolded with the Nadeau Island association. Although migmatitic, Nadeau Island rocks are recognizable in the north as orthogneisses of granitic, granodioritic and tonalitic composition (gN). Southward, toward the base of Parry Sound domain these rocks are replaced by metatexite and diatexite with abundant leucosomes containing hornblende neoblasts, commonly intergrown with epoidote. Northwest of Parry Sound the migmatites are closely associated with pink, leucocratic alaskitic gneiss; similar rocks west of Parry Sound may be within the Sand Bay association (pS?). Alaskitic gneiss is a common Central Gneiss Belt lithology, large units of it occurring in the Bayfield gneiss association (Culshaw et al., 1988) as well as southeast of Parry Sound domain (see below). The Nadeau Island association contains scattered pods and bodies (up to 1 km in longest dimension) of metagabbro (g in Fig. 1), some of which contain eclogite-like rocks (e), and of coronitic olivine metagabbro (c) (Needham, 1987). Pseudo-eclogite is associated with a string of small anorthosite bodies among offshore islands a few kilometres northwest of the Parry Sound shear zone. These types of mafic plutonite are not present in either the Sand Bay association or the interior of Parry Sound domain.

Three units of 'single cycle' granitoid orthogneiss (Culshaw et al., 1988) have been outlined in Britt domain. A large body of hornblende granite and granodiorite (g2) outcrops in the westernmost chain of offshore islands. It lies structurally below the Nadeau Island and Sand Bay associations to the east, and can be linked northward to similar rocks in the Pointe-au-Baril complex (Culshaw et al., 1988, Fig. 1). Among these islands are occurrences of country rock that have the characteristics of the Key Harbour association to the north, including the presence of metamafic dykes with large relict plagioclase phenocrysts. About 10 km northwest of Dillon (Fig. 1), a lens of granodiorite orthogneiss is assigned to the Bayfield gneiss association. In the northern part of the map area a large body of hornblende granodiorite orthogneiss with K-feldspar augen and metamorphic garnet (Shawanaga pluton, g3) is similar in many respects to the Britt pluton (Culshaw et al., 1988); it encloses a mass of older granitoid gneiss of the Nadeau Island association within which earlier folds are refolded, along with the Shawanaga pluton, about a major, gently southeast-plunging antiform. A few kilometres north and west of Parry Sound a narrow sheet of granite orthogneiss (g4) conforms with the trend of layering in southeasternmost Britt domain. On the west side of the northeast peninsula of Parry Island this unit thins and is repeated about a reclined fold. Referred to as the 'marginal orthogneiss', it has been dated (U-Pb on zircon) at 1346 Ma (van Breemen et al., 1986).

Parry Sound domain

Parry Sound domain (Fig. 2) is formed of several assemblages of supracrustal gneiss, orthogneiss and composite gneiss. These are arranged such that the domain is compositionally zoned subparallel to the strike of the Parry Sound shear zone along the northwest margin. In the northwest, the structurally lowest level is occupied by the Lighthouse gneiss association (LP1), formed of interlayered metasedimentary gneiss and amphibolite. In places the metasediments have decametric layering of alternating quartzofeldspathic and pelitic compositions, perhaps suggesting an original wacke-shale succession. They are interlayered at all scales with garnet-bearing amphibolite, possibly once sills or mafic volcanic rocks, although no evidence for either of these origins is preserved. Rusty-weathering feldspathic paragneiss occurs in the structurally higher parts of this unit. A quartzite layer (LqP1) can be traced across most of Parry Island and islands to the west and lies close to a thin but continuous mylonitized marble unit. In low strain areas west of Parry Island crosscutting relationships between metamorphosed mafic dykes and quartzite are preserved. Such dykes are apparently absent in the overlying paragneiss and amphibolite of the Lighthouse association.

Another quartzite unit (Three Mile Island quartzite, tqP1) lies up-section from the Lighthouse association quartzite, and like it is interlayered with amphibolite which, however, cannot be shown to have been dykes, although mafic dykes are locally preserved in an underlying unit of tonalitic to granodiorite orthogneiss (tP1). The overlying Armer Bay association (aaP1) is dominated by garnet amphibolite lacking relict igneous texture, and also contains interlayered, migmatitic, feldspathic paragneiss and rare pelitic gneiss. This assemblage has comparable lithologies to the Lighthouse assemblage, but in different proportions.

Anorthosite and related rocks and their gneissic equivalents (a6, ag6) occur within the Parry Sound shear zone in bodies ranging in size and shape from the 10x5 km pluton on western Parry Island to elongate sheets and slivers and to isolated boudins within straight gneisses. The Parry Island body contains orthopyroxene megacrysts up to 1 m long at several locations and encloses a mass of mafic granulite (gr) that includes pseudo-eclogite. From Parry Sound to the southwest, gabbroic anorthosite of the south-extending tail of the Whitestone pluton (Nadeau, 1984) is in places barely recognizable due to extreme mylonitization; it is closely associated with granodiorite to monzonite orthogneiss (mn6), itself commonly deformed in comparable fashion.

In the interior part of Parry Sound domain southeast of Parry Island, the McLaren Island gneiss assemblage (mcP2) contains two main rock types interlayered at outcrop and at map scales. It is a straight-layered, granulite facies gneiss unit composed of granitoid and mafic types, both of which form small mappable units. The mafic granulite component commonly displays a structure of lenses or pods rich in garnet, clinopyroxene, plagioclase and/or scapolite. Locally preserved crosscutting relationships indicate the intrusive nature of the granitoid component. This bimodal unit may represent dismemberment of a former mafic volcanic succession by voluminous intrusion of granitic material. Elongate units in the cores of northeast-trending antiforms are more uniformly granitoid; one of these is surrounded by a unit of semipelitic to pelitic granulite (Spider Bay metasedimentary granulite, sP2). Characterized by abundant garnet, interlayered amphibolite and local rusty zones, this unit is the host to two small copper prospects. In addition to small-scale mafic components that may have formed through disruption of mafic dykes, and nondescript mafic granulite (bP2), possibly supracrustal in origin, McLaren Island granulite encloses kilometre-scale units of plutonic-textured mafic granulite (gP2) derived from gabbro.

A granulite or retrograded granulite facies orthogneiss of intermediate composition, termed the Moon Island gneiss (mgP2), underlies much of southeastern Parry Sound domain. Ranging from diorite to quartz diorite in composition, it contains only a small proportion of amphibolite or mafic granulite and even less material of metasedimentary origin. Plagioclase-phyric mafic dykes, however, occur thoughout this unit and are restricted to it. Compositionally similar rocks, although usually much retrograded to amphibolite facies (rpP2), can be traced to both the contact with the underlying Go Home subdomain to the south and to the overlying, structurally lower part of Moon River subdomain (G and M1, inset in Fig. 1). They are recognized by the presence, in low strain areas, of mesoscopic textures characteristic of granulite, the presence of sporadic feldspar-phyric mafic dykes, and the occurrence of altered or partly altered orthopyroxene, especially in feldspathic

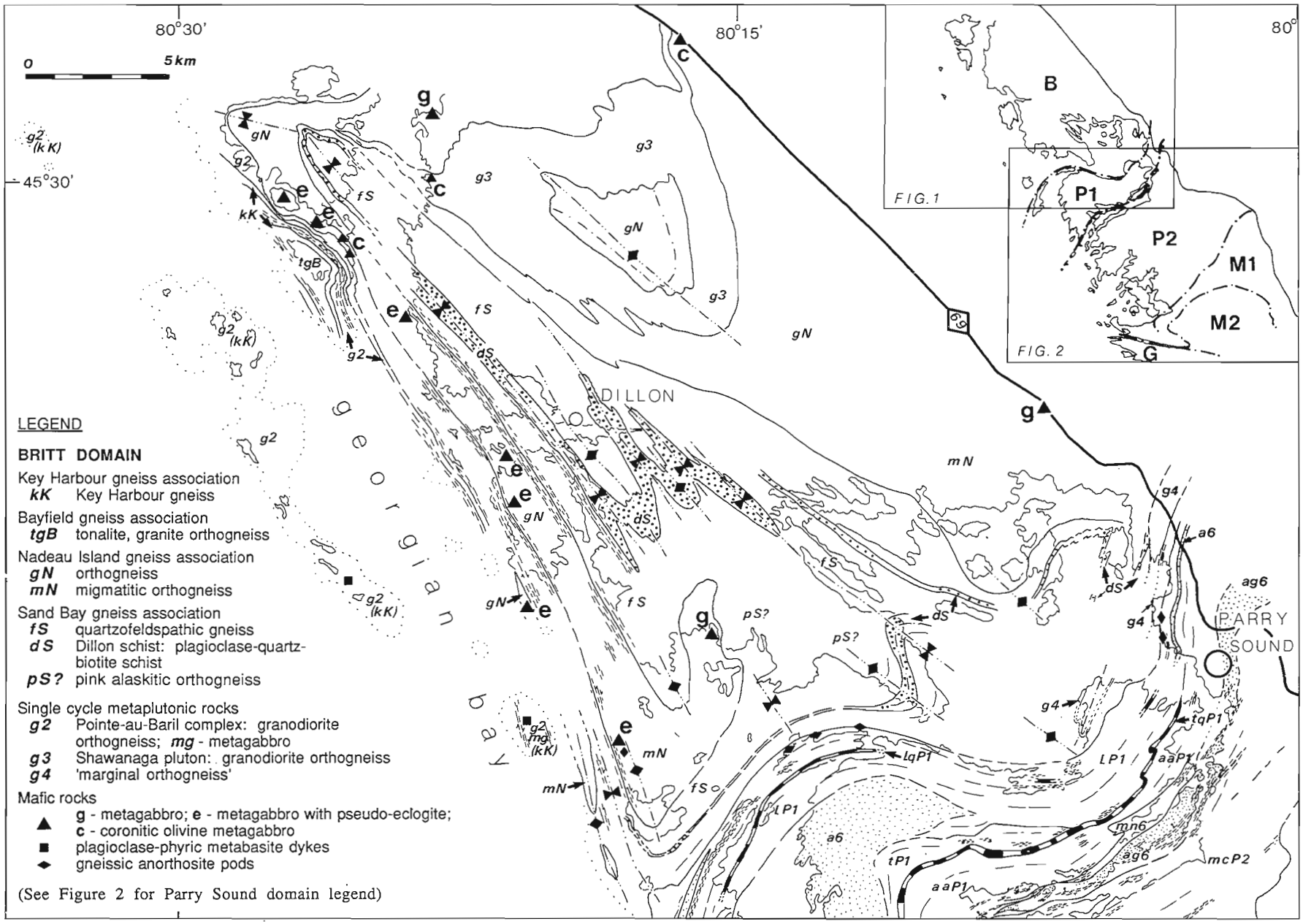

Figure 1. Geological sketch map of parts of Britt and Parry Sound domains. Long dashes indicate straight gneiss; multiple short dashes, mylonite and protomylonite. Shear sense for strike slip displacement is shown by arrow pairs, and for dip slip by ball on the down side. Limit of small-island outcrop is indicated by fine dotted line.

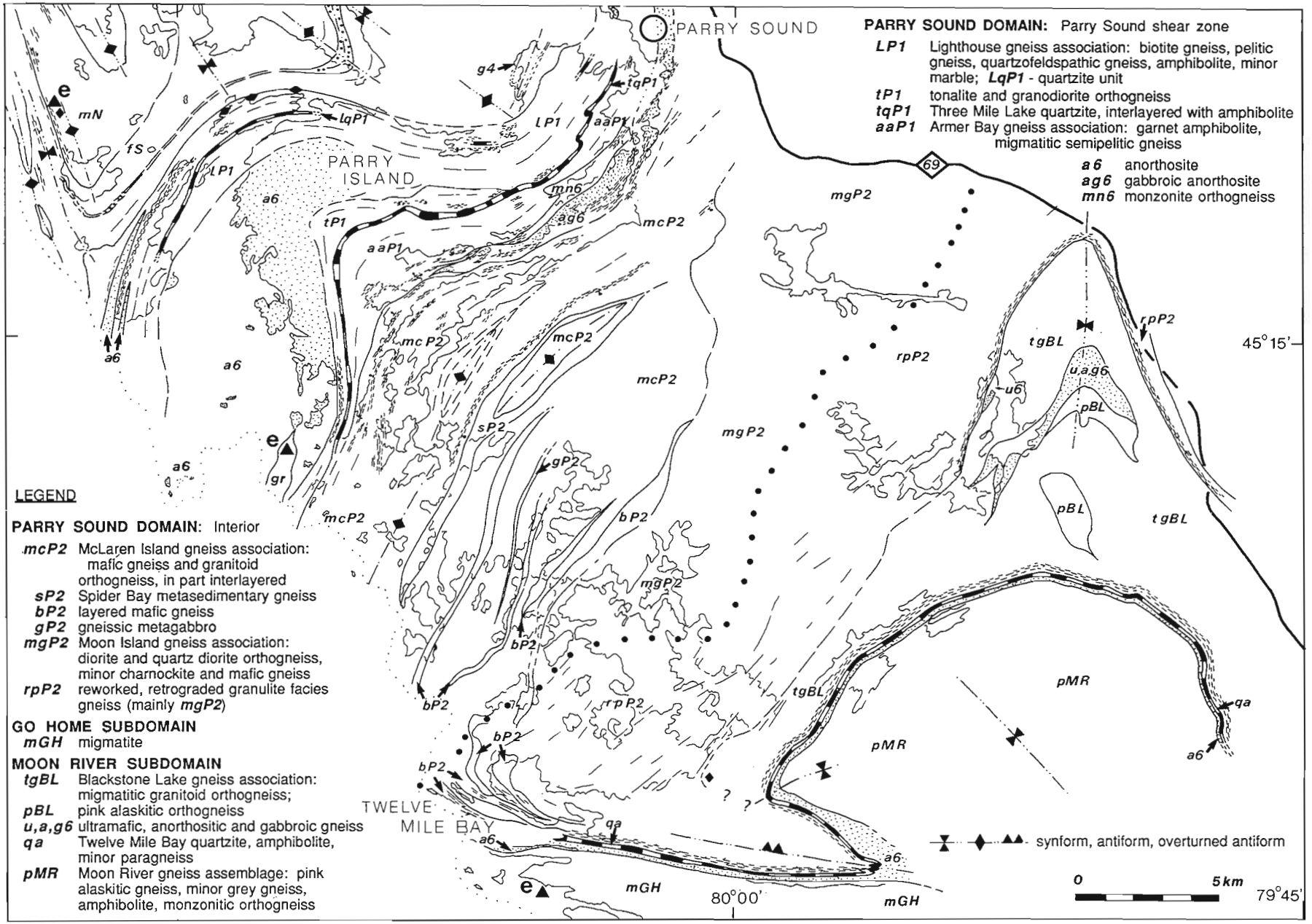

Figure 2. Geological sketch map of parts of Parry Sound domain and Go Home and Moon River subdomains. Symbols as for Figure 1.

'sweats' where it may form the cores of hornblende metacrysts. The reworking is progressive, beginning in the northwest by static retrogression of granulite facies minerals, localized shear zone development and larger scale refolding, e.g. north of Twelve Mile Bay. Southeastward, semi-continuous belts of southeast-dipping straight gneiss and blocky, tectonically disrupted gneiss appear, leading ultimately to tight refolding or transposition. Some details of the structure in the area north of Twelve Mile Bay have been outlined by Hanmer (1984), who described a tectonic mesh structure along this boundary. The retrograded gneiss is everywhere accompanied by pegmatite; a composite of straight gneiss and strongly deformed pegmatite make up the typical gneiss assemblage in the southeast part of this area.

Go Home subdomain

In the Twelve Mile Bay area, the southern boundary of Parry Sound domain is marked by a north-dipping belt of well layered gneiss that includes a thin but important marker assemblage of gneissic anorthosite (a6) and quartzite with amphibolite and minor paragneiss (qa), discussed more fully in the section on Moon River subdomain. South of this marker unit lies a terrane of migmatite with lesser amounts of alaskite. This assemblage (mGH) closely resembles the Nadeau Island gneiss association in southern Britt domain (mN, top left in Fig. 2), being dominantly granodioritic in composition, and having similar mesoscopic texture and voluminous leucosomes with hornblende neoblasts associated with epidote, and containing small pseudo-eclogitic metabasite bodies.

Moon River subdomain

The anorthositic gneiss (a6) that lies along Twelve Mile Bay has been traced semi-continuously for tens of kilometres farther east and southeast (Davidson et al., 1982, Fig. 30.3), where it is taken as the boundary between Go Home and Moon River subdomains. In association with the quartzite-amphibolite unit (qa), it also forms a connected marker unit within Moon River subdomain, where it is overturned with respect to its disposition along Twelve Mile Bay; it outlines the closure of what has been referred to as the Moon River synform (Waddington, 1973). Whereas north of Twelve Mile Bay this assemblage underlies what appear to be reworked Parry Sound domain rocks (rpP2), in the northern lobe of Moon River subdomain it overlies an assemblage of layered gneiss, migmatitic toward the southeast, of predominantly granitic, granodioritic and tonalitic composition (Blackstone Lake gneiss association, tgBL), disposed about a large, south-plunging synform. These rocks lack any hint of a former granulite facies history and do not resemble most Parry Sound lithologies, although small amounts of folded, reworked Parry Sound rock (rpP2) occur along the sheared northwest margin. The gneisses are intruded in the cores of folds by generally concordant alaskite bodies (pBL). Also within this assemblage is an elongate body of gabbro, ultramafic rock and minor anorthosite, and their deformed and amphibolitized equivalents (u, a, g6). This body, in places enclosed within alaskite, is concordant with the surrounding rocks and folded with them.

Southeast of and structurally above the quartzite-anorthosite unit is an assemblage of layered to uniform, weakly to strongly foliated, pink alaskite (pMR) similar to that associated with migmatites elsewhere in the map area. This is interlayered with a minor amount of amphibolite and, along the northern edge, an elongate monzonitic orthogneiss body (van Berkel and Schwerdtner, 1986). Migmatite becomes more prevalent to the southeast.

STRUCTURAL INTERPRETATION

Nature of the Parry Sound shear zone

The Parry Sound shear zone as outlined by Davidson (1984, Fig. 3; 1986, Fig. 4) extends from the northern boundary of marked tectonic attenuation, coinciding closely with the northern boundary of the Lighthouse association on Parry Island, to the belt of mylonites developed in the anorthositic gabbro to the south, bordering and in places including what here has been named the McLaren Island association. Within the north part of the shear zone, straight gneisses within the Lighthouse association show considerable extension (e.g., boudinage) in the foliation perpendicular to the lineation, and structures indicative of non-coaxial strain are rare. True mylonite (i.e., demonstrably reduced in grain size) with kinematic indicators forms only thin layers at this lower level. Mylonite with marked grain refinement and abundant kinematic indicators (CS fabric, rotated augen, foliation fish, etc.) becomes increasingly abundant toward the south side of the shear zone, culminating in parallel belts south of Parry Island (Fig. 2). This upper level contains some of the classic localities depicted by Davidson (1984, Fig. 5 and 6) and presents plentiful confirmation of the well known thrust shear sense. These mylonites appear to have formed under amphibolite facies conditions, though not necessarily throughout their history. A few kilometres southeast of the Parry Sound shear zone, and separated from it by a belt of less deformed rock, there is a mylonite zone adjacent to the Spider Bay metasedimentary unit (sP2). CS fabrics in this mylonite indicate top-side-down displacement (extension); host rock granulite facies assemblages are retrograded.

In summary, there appear to be two, perhaps three types of tectonite associated with the Parry Sound shear zone, each with a different strain history: 'straight gneisses' formed during early coaxial strain, mylonite formed in a simple shear thrust regime, and later extensional mylonite. It is noted that many of the granulite gneisses in Parry Sound domain have remarkably straight layering and display blunt-ended mafic boudins and intrafolial folds. Deformation occurred under granulite facies conditions, as shown by the presence of hypersthene in sweats formed at boudin necks. The form of boudinage of mafic layers indicates the low competence of the enclosing granitoids at that grade. Strain geometry in these rocks is similar to that shown by the straight gneisses in the lower part of the Parry Sound shear zone, and it is tempting to correlate these fabrics.

Tectonics in the Go Home and Moon River subdomains and relationship to the Parry Sound shear zone

The quartzite-amphibolite (qa) and anorthosite gneiss (a6) association in Twelve Mile Bay diverges to the northeast from the Go Home-Parry Sound boundary to an interior position within Moon River subdomain, along with a dip reversal about a major reclined antiform between these two segments. It is tempting to draw parallels between this association, although an order of magnitude thinner, and the Lighthouse and Armer Bay associations in the Parry Sound shear zone. If this correlation is made, then there may be two, perhaps more, repetitions of this unit in the Parry Sound shear zone, suggesting the possibility of duplexing. If the Twelve Mile Bay association marks the locus of a thrust sole at the base of Parry Sound domain (nappe), a problem is raised concerning the origin and significance of the amphibolite-grade unit (tgBL) and associated rocks that lie between the granulites and retrograded granulites of Parry Sound domain and the alaskitic core of Moon River subdomain. It is possible that they may be a more voluminous equivalent of the sheets of granodiorite that lie within the reworked Parry Sound domain to the west, but they could also constitute a separate allochthonous unit. Layering in these gneisses describes a moderately south-plunging fold which is disharmonic with respect to the Twelve Mile Bay association and the overlying alaskitic rocks in the core of the Moon River structure, and must therefore be 'unglued' from them (Schwerdtner, 1987). A suitable place for décollement would be in the high strain zone beneath the Twelve Mile Bay association, in which lineations are down-dip to the southeast. Northwestward displacement of the Moon River core is suggested by the form of the reclined fold to the southwest, but there are conflicting indications of kinematic sense along the Go Home-Parry Sound boundary (Hanmer, 1984). Further work is needed to unravel the complicated geometry and timing of deformation events in this region.

Northwest-trending folds in Britt domain

The synclinorium in southeastern Britt domain (Fig. 1) is a subhorizontal structure. At its southeast end, several fold axial traces seem to be truncated by the straight gneisses at the base of the Parry Sound shear zone. Axes of these folds, however, plunge increasingly more steeply southeastward and are coaxial with the major fold pair apparent in the Parry Sound shear zone. It is thus possible that the two are related, which would mean that the northwest-trending folds in Britt domain are younger than the development of Parry Sound straight gneisses.

The synclinorium is flanked on its west side by a wide, gently east-dipping high strain zone, expressed by zones of mylonite formed from mafic and felsic gneisses, extreme disruption of large pegmatites within the Dillon schist, development of disrupted migmatite and straight gneiss and the occurrence of sheath folds. This high strain zone displays an element of simple shear. Sigma and delta forms in small augen (Passchier and Simpson, 1986) in the mylonites and disrupted migmatites, and shear bands in the outer islands extension of the Pointe-au-Baril complex give a dextral sense of shear with an oblique top-side-down component parallel to the stretching lineation. This deformation took place at amphibolite grade and was accompanied by copious emplacement of pegmatite. At the southern end of this zone, west of Parry Island, these high strain rocks terminate in a zone of folding; this is interpreted to be the propogating tip of the shear zone. The synclinorium is flanked to the east by a doughnut-shaped structure resembling a fold interference pattern, outlined by rocks of the Shawanaga pluton.

In summary, the evidence at present suggests that the northwest-trending folds in southeast Britt domain are relatively late structures and are extensional in nature.

REFERENCES

Culshaw, N.G., Corrigan, D., Drage, J., and Wallace, P.
1988: Georgian Bay geological synthesis: Key Harbour to Dillon, Grenville Province of Ontario; in Current Research, Part C, Geological Survey of Canada, Paper 88-1C, p. 129-133.

Culshaw, N.G., Davidson, A., and Nadeau, L.
1983: Structural subdivisions of the Grenville Province in the Parry Sound — Algonquin region, Ontario; in Current Research, Part B, Geological Survey of Canada, Paper 83-1B, p. 243-252.

Davidson, A.
1984: Identification of ductile shear zones in the southwestern Grenville Province of the Canadian Shield; in Precambrian Tectonics Illustrated, edited by A. Kröner and R. Greiling, Schweizerbart'sche Verlagsbuchhandlung, Stuttgart, p. 263-279.
1986: New interpretations in the southwestern Grenville Province; in The Grenville Province, edited by J.M. Moore, A. Davidson and A.J. Baer, Geological Association of Canada, Special Paper 31, p. 61-74.

Davidson, A., Culshaw, N.G., and Nadeau, L.
1982: A tectono-metamorphic framework for part of the Grenville Province, Ontario; in Current Research, Part A, Geological Survey of Canada, Paper 82-1A, p. 175-190.

Hanmer, S.K.
1984: Structure of the junction of three crustal slices; Ontario Gneiss Segment, Grenville Province; in Current Research, Part B, Geological Survey of Canada, Paper 84-1B, p. 109-120.

Nadeau, L.
1984: Deformation of Leucogabbro at Parry Sound, Ontario; M.Sc. thesis, Carleton University, Ottawa, Canada, 191 p.

Needham, T.W.
1987: Geological setting of two metagabbroic bodies, central Britt domain, southwestern Grenville Province, Ontario; in Current Research, Part A, Geological Survey of Canada, Paper 87-1A, p. 507-603.

Passchier, C.W., and Simpson, C.
1986: Porphyroclast systems as kinematic indicators; Journal of Structural Geology, v. 8, p. 831-843.

Schwerdtner, W.M.
1987: Interplay between folding and ductile shearing in the Proterozoic crust of the Muskoka - Parry Sound region, central Ontario; Canadian Journal of Earth Sciences, v. 24, p. 1507-1525.

Schwerdtner, W.M., and Mawer, C.K.
1982: Geology of the Gravenhurst region, Grenville Structural Province, Ontario; in Current Research, Part B, Geological Survey of Canada, Paper 82-1B, p. 195-207.

van Berkel, J.T., and Schwerdtner, W.M.
1986: Precambrian geology of the Moon River area, Muskoka and Parry Sound Districts; Ontario Geological Survey, Geological Series Map P2954.

van Breemen, O., Davidson, A., Loveridge, W.D., and Sullivan, R.W.
1986: U-Pb zircon geochronology of Grenville tectonites, granulites and igneous precursors, Parry Sound, Ontario; in The Grenville Province, edited by J.M. Moore, A. Davidson and A.J. Baer, Geological Association of Canada, Special Paper 31, p. 191-207.

Waddington, D.H.
1973: Foliation and Mineral Lineation in the Moon River Synform, Grenville Structural Province, Ontario; M.Sc. thesis, University of Toronto, Toronto, Canada.

Investigation of Missi metasedimentary rocks in the Amisk-Welsh lakes area, Saskatchewan

K.H. Wilcox[1]
Lithosphere and Canadian Shield Division

Wilcox, K.H., Investigation of Missi metasedimentary rocks in the Amisk-Welsh lakes area, Saskatchewan; in Current Research, Part C, Geological Survey of Canada, Paper 89-1C, p. 165-171, 1989.

Abstract

Five phases of superimposed deformation have been recognized in Missi metasedimentary rocks in the Amisk-Welsh lakes area, Saskatchewan. A structural basin resulting from phase 1 and phase 2 interference dominates the area and has been subsequently affected by phase 3 flattening and sinistral shear. Phase 4 deformation resulted in large-scale, open, northeast-trending folds. Late, brittle north-striking faults are attributed to phase 5 deformation. Two periods of metamorphism were recognized, low grade syn-phase 2 and higher grade post-phase 2.

Résumé

Cinq phases surimposées de déformation des roches métasédimentaires de Missi ont été reconnues dans la région des lacs Amisk et Welsh (Saskatchewan). Un bassin structural résultant de l'interférence de la phase 1 et de la phase 2 domine la région et a été par la suite influencé par la phase 3 d'aplatissement et de cisaillement sénestre. La quatrième phase de déformation a produit des plis ouverts de grande échelle de direction nord-est. Les tardives zones faillées de rupture fragile et de direction nord sont attribuées à la cinquième phase de déformation. Deux périodes de métamorphisme ont été identifiées, l'une de faible intensité correspondant à la phase 2 et une deuxième, d'intensité plus forte, postérieure à la phase 2.

[1] Department of Geology and Geophysics, University of Calgary, Calgary, Alberta, T2N 1N4

INTRODUCTION

Geological mapping was continued in the summer of 1988 as part of a four-year project initiated in 1985 to delineate structure, stratigraphy and metamorphism within the Kisseynew gneiss belt of the Trans-Hudson Orogen (Ashton and Wheatley, 1986). Mapping was extended into the lower metamorphic grade Flin Flon belt in 1988 to obtain an understanding of the chronology of structural and metamorphic events.

Field work, at a scale of 1:20 000, was concentrated on a study of the Missi Group and adjacent Amisk Group rocks in an area in Saskatchewan, 20 km west of Flin Flon, Manitoba. The study area extends from Amisk Lake to west of Welsh Lake and includes adjacent parts of two 1:50 000 NTS map sheets, 63L/9 and 63L/16. Bush roads and grid lines provide access to the area.

The regional geology has been summarized by Byers and Dahlstrom (1954), Stauffer and Mukherjee (1971) and Bailes and Syme (1987). A lower volcano-sedimentary package, the Amisk Group, is unconformably overlain by a clastic sequence, the Missi Group (Byers and Dahlstom, 1954). One phase of deformation preceded and four phases postdated the deposition of the Missi Group (Bailes and Syme 1987). It is hypothesized that the Flin Flon belt and the Kisseynew gneiss belt were contiguous, with sediment being shed off the Flin Flon volcanic arc into an adjacent (Kisseynew) basin (Bailes 1980). The Kisseynew gneiss belt consists primarily of grey-wacke sediments in the amphibolite facies, laterally associated with the Amisk Group. The change from volcanic to basinal clastic rocks is generally coincident with the prograde staurolite "out" isograd within meta-sediments in the Snow Lake area (Froese and Moore, 1980). In the Flin Flon area, Byers and Dahlstrom (1954) separate the Kisseynew gneiss belt the based of on higher metamorphie grade.

The Amisk-Welsh Lakes area has been mapped previously on a scale of 1:63 360 by Byers and Dahlstrom (1954). Parts of the area were remapped by Ahuja (1970), Longiaru (1980), Hattie (1986), and Ashton et al. (1987). A gold prospect in the Robinson Creek area has been mapped in detail by Pearson (1982).

STRATIGRAPHY

The Amisk Group consists of variably deformed mafic volcanic and pyroclastic rocks and subvolcanic intrusions in the Comeback Bay-Martin Lake area and argillaceous units in the Grassy-Welsh Lakes area. Plagioclase-chlorite-actinolite assemblages are found in the Amisk Lake area and plagioclase-hornblende in the Martin Lake area. Metasediment assemblages include biotite-staurolite-garnet-aluminosilicate (de Tombe, 1987).

The Missi Group is divided into the following informal units: basal conglomerate, pebbly sandstone and grit, and arenite (lithic arenite to lithic wacke). The basal conglomerate and arenite are laterally persistent whereas the others are not. Polyphase deformation and laterally discontinuous units make detailed stratigraphy of the Missi Group difficult. It has been postulated that the Missi Group was deposited in an alluvial fan/fluvial environment (Stauffer and Mukherjee 1971). Post-depositional intrusions include a feldspar porphyry and a mafic porphyritic gabbro.

Conglomerate

The basal conglomerate is approximately 600 m thick and consists of pebbles, cobbles and boulders which are moderately well sorted within bedding horizons and set in a sandy matrix. Clasts are derived from the underlying Amisk Group and mainly consist of mafic to felsic volcanic and granitoid rocks. Clast shape is difficult to ascertain because of strain but, in relatively undeformed regions, spherical granitoid and elliptical volcanic clasts were observed. Centimetre- to metre-thick sandstone beds are widespread but subordinate to conglomerate. The amount of sand in the conglomerate unit increases upward and the stratigraphic top is marked either by an abrupt contact with the overlying sandstone or by a 100 m transitional zone of interlayered conglomerate and sandstone. Mineral assemblages are dependent upon metamorphic grade: quartz, feldspar, carbonate and chlorite occur at lower grade and biotite, hornblende and garnet at higher grade.

Pebbly sandstone and grits

This unit is restricted to an area inland from the North Channel and Comeback Bay of Amisk Lake. It is characterized by two interlayered units, a matrix-supported pebbly sandstone to conglomerate with well sorted pebbles and a quartzofeldspathic granule-sized unit that weathers white. Clast lithology is similar to that of the basal conglomerate and decimetre-scale fining upward sequences were locally observed in both rock types. Pebbly sandstones and grits occur directly above the basal conglomerate and mark the transition between conglomerate and sandstone. They may be laterally continuous but deformation has locally reduced the grain size, making a distinction difficult. This unit has a maximum thickness (uncorrected for deformation) of 300 m.

Pebbly sandstone is characterized by <3 m wide interlayered sand and conglomerate beds with an average clast size of approximately 4 cm. Some beds are well cleaved due to the fine-grained micaceous matrix and contain structures described below.

Quartz and feldspar constitute from 65 to 90% of the grits with subordinate lithic fragments. Biotite or chlorite are present depending upon metamorphic grade. Pebbles and cobbles occur in conglomeratic beds 20 cm to 4 m wide and as isolated clasts within the granule matrix. Pebble lags locally mark scour surfaces, and isolated pebbles of white vein quartz are common. Five to fifty cm sets of planar to trough crossbeds are defined by 1 to 3 cm magnetite-defined foreset laminae. Top directions are defined by arcuate scour surfaces, bedding truncations, arcuate laminae (where weakly deformed), pebble lag and rare fining-upward sequences.

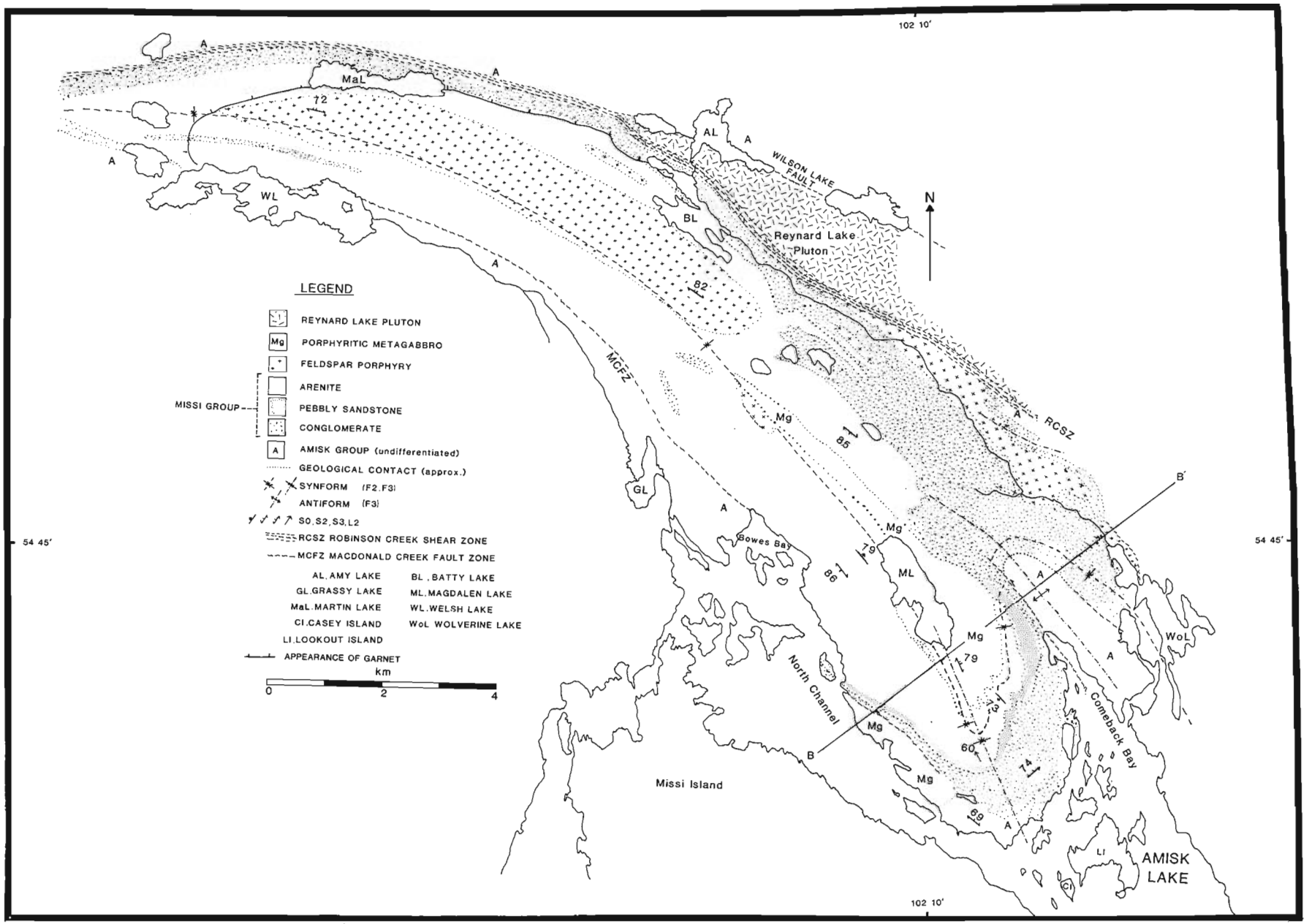

Figure 1. Geological map of the Amisk-Welsh Lakes area.

Arenite (lithic arenite to lithic wacke)

In the study area, the bulk of the Missi Group consists of arenite and minor wacke. Recrystallized quartz, feldspar, and lithic clasts(?) range from fine to medium sand sized. Crossbedding is preserved in weakly deformed areas and is similar to that described above. Isolated pebbles of variable mineralogy are also common but conglomerate beds are rare. Mineral assemblages are similar to those in the conglomerate; however, white mica is locally an important component. This unit has an estimated stratigraphic thickness of 1200 m.

Feldspar porphyry and porphyritic metagabbro intrude the Missi rocks. The genetic relationship is not fully understood at this time but units appear to be pre- to syn-phase 2 deformation.

Feldspar porphyry

Feldspar porphyry is found in pinkish weathering, metre wide dykes as well as elliptical bodies up to 1 km wide totally enclosed within Missi sediments or in fault contact with Amisk rocks. Where weakly deformed, plagioclase phenocrysts vary from 3 to 10 mm and are set in a fine-grained matrix that is variably schistose. The groundmass is composed of chlorite, biotite, white mica, feldspar and minor quartz. Crosscutting relationships were not observed and, where exposed, contacts are parallel to the S2 foliation. Rare cm-scale xenoliths(?) identical to clasts in the conglomerate were observed in areas adjacent to contacts. The porphyritic rocks lack any igneous layering and are remarkably homogeneous. They are apparently separated from the Reynard Lake Pluton described by Byers and Dahlstrom (1954). Some workers consider the feldspar porphyry to be a reworked tuff, but an intrusive origin is favoured because (1) of the homogeneity and lack of internal layering, (2) no flow features were recognized, and (3) apparent "clasts" probably are xenoliths incorporated during intrusion.

Porphyritic metagabbro

This rock type occurs in one large body in the Magdalen Lake area and in centimetre-to metre-wide dykes and sills throughout the entire map area. Local dyke swarms are also common. The rock consists of a medium-grained equigranular feldspar-biotite groundmass with coarse-grained stubby amphibole phenocrysts. Relict pyroxene may also be present. Crosscutting contacts were observed east of Magdalen Lake. Most of the unit outcrops as a chlorite schist due to intense deformation and metamorphism and may be confused with chlorite schists of the Amisk Group.

STRUCTURE

A pre-Missi folding event, which created opposing facing directions and a high angle unconformity between the Missi and Amisk groups was demonstrated by Bailes and Syme (1987). No additional evidence for this was observed in the study area. Superimposed structures thought to be associated with five distinct phases of deformation were recognized in the Missi Group. These phases are termed phase one to phase five (P_1 to P_5) and do not include the pre-Missi folding event. The first two phases involve ductile folding; the third involves folding and brittle-ductile faulting; the fourth is a regional folding phase that has caused a warping of units; and the fifth involves brittle faulting.

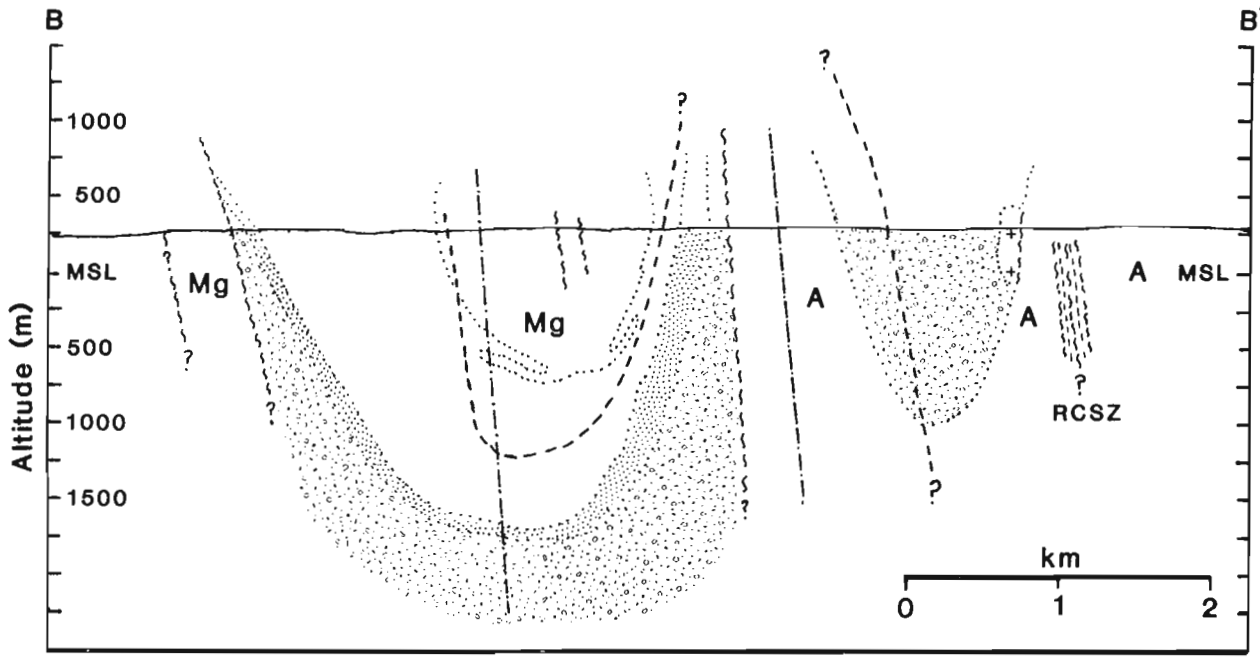

Figure 2. Schematic cross section B-B/. Lithologic contacts and hinge surface (F_2) projected using L_2 plunge of 45° and local S_2 measurements.

Phase 1 deformation (P_1) formed a synclinal structure cored by the Missi arenite. There is no fabric associated with this phase. The most convincing evidence is the overall basin structure which is a result of P_2 deformation. There is very little mesoscopic evidence other than in an outcrop south of Magdalen Lake, where P_2 cleavage transects a tightly folded sand bed within the conglomerate with 10 m wavelength and 14-m amplitude.

Phase 2 (P_2) is a major compressional event with well-developed axial planar cleavage. It is responsible for the elongate type 1 (Ramsay, 1967) basin interference pattern observed on the map. This basin has been informally termed the Magdalen Basin. Previously unmapped basal conglomerate was observed in the Welsh Lake area and helps define the interference pattern.

P_2 is contemporaneous with low grade metamorphism so that syn-kinematic chlorite and biotite define an axial planar foliation (S_2). Micas are generally sub-parallel to bedding except in hinge zones where bedding is at a high angle to S_2. It is suspected that there is a sequence of mesoscopic isoclinal folds in the hinge zone rather than one large arcuate closure. P_2 hinge zones are locally difficult to distinguish because of intense P_3 deformation.

P_2 is also responsible for the flattening and extension of clasts. Aspect ratios in areas of relatively weak P_3 deformation (Casey and Lookout islands) were measured. X-Z ratios in mafic to intermediate volcanic clasts commonly exceed 20:1 whereas granitoid clasts range from 5:1 to 1:1. Lineated boulders are prevalent within the conglomerate in the North Channel area. Stretching of pebbles has been accommodated by both brittle and ductile means, depending upon clast rheology. Long axes of lineated clasts (L_2) define the X axis. A mineral lineation and abundant quartz-filled extension veins (in the Y-Z plane) occur within clasts. Y-Z quartz veins contain fibres (stretching direction) parallel to the X axis. Outcrops southwest of Magdalen Lake (just northeast of a small unnamed lake) are L-tectonites. One measured granitoid clast has a Y-Z cross section that is 15 x 10 cm and an X axis of 1.7 m. Bedding/S_2 intersections appear colinear to L_2 in this area. L_2 plunges average 45° to the north-northwest in the North Channel area and are quite shallow inland from the Bowes Bay area. Intense P_3 deformation has eradicated most L_2 lineations in the Comeback Bay area and north of the North Channel area.

P_3 folds and faults are heterogeneously developed and locally refold S_2 and F_2. P_3 hinge surfaces (F_3) dip steeply to the northeast or southwest. Hinge lines (L_{3h}) plunge from 45 to 90° to the northwest in the Comeback Bay area. North of Comeback Bay, L_{3h} lineations locally define neutral to reclined folds. L_{3h} lineations gradually become shallow to the northwest so that plunge averages 35° in the Batty Lake area. The distribution of minor folds defines a number of mesoscopic antiforms and synforms otherwise not apparent from bedding contacts. This arises because some bedding contacts are aligned parallel to P_3 hinge surfaces (F_3) and appear undeformed, whereas S_2 is intensely folded.

P_3 minor folds have a relatively consistent shape and are most evident in the conglomerate where they are outlined by previously flattened clasts.

'Z' folds are characterized by tight closures and strongly attenuated 345° limbs with short, stubby 300° trending limbs. Limb:length ratios commonly exceed 25:1. Attenuated limbs can be considered minor sinistral shear zones. 'Z' folds can be isolated or occur in centimetre- to metre-wide 'Z' zones.

'S' folds are tight similar folds without appreciable limb thinning. The asymmetry is not as pronounced as in 'Z' folds. Sinistrally rotated granitoid boulders are common in outcrops or domains where 'S' asymmetry is dominant. It is thought that during P_3 deformation elliptical boulders, which were at a high angle to F_3 planes, were deflected into the flattening plane. Adjacent intermediate to mafic volcanic clasts, which were already oblate from P_2 deformation, behaved viscously and were deflected creating asymmetric folds around the clasts. Early in the rotation the trace of F_3 in a straight line. With continued sinistral rotation, the trace of the hinge surface became curved. This sequence of formation is directly analogous with porphyroblast rotation and microfold development (Vernon, 1988).

'M' folds are commonly high-amplitude, low-wavelength similar folds. Closures are tight to isoclinal.

A discontinuous, spaced cleavage (S_3) is defined by micaceous laminae with spacing of 3 to 10 cm. Some planes have an apparent sinistral offset of less than 5 cm. Cleavage planes commonly diverge 10 to 15° to the west from F_3 and are locally coplanar with S_2.

Minor folds are absent in the sandstone unit in the North Channel area. Two fabrics were observed in this area. S_2 is defined by elliptical quartz grains and S_3 is defined by white mica partings usually subparallel and only locally distinguishable from S_2.

P_3 minor folds become isoclinal and eventually rootless as the Amisk Group contact is approached in the Robinson Creek area. Lithologic contacts define an overall 'Z' asymmetry in this region. Isoclinal folds also gradually become rootless during P_3 transposition associated with increased metamorphic grade.

The Reynard Lake Pluton between Batty and Amy lakes is a granodioritic body with apparent S-C fabric (Berthe et al., 1979) indicating a sinistral shear sense. S planes are defined by steeply dipping 315° trending elliptical quartz grains. C planes are defined by an abrupt sinistral deflection of quartz as well as by biotitic partings. C planes strike at 280°.

In the Martin Lake area, P_3 isoclinal folds are refolded by a northwest-trending crenulation with consistent 'S' asymmetry. This crenulation is also evident in white mica-rich Missi wackes between Martin and Welsh Lakes. Mica fish (Lister and Snoke, 1984) were also observed. Both features indicate a sinistral shear sense. Although these features appear to locally postdate P_3 isoclinal folding, it is thought that they are formed in a sinistral shear zone continuous with P_3 deformation. The change from tight to isoclinal folding,

overall 'Z' fold asymmetry of S_2, late 'S' crenulations, mica fish and S-C fabric indicates the existence of a major P_3 sinistral shear zone, the Robinson Creek Shear Zone (RCSZ). The RCSZ defines the eastern boundary to the Magdalen Basin. In the Amy Lake area it may be a related to the Wilson Lake Fault (Byers and Dahlstrom, 1954). It separates the Missi Group from the Amisk sequence in the Wolverine Lake and Martin Lake areas and from the Reynard Lake Pluton in the Batty Lake area.

The Magdalen Basin is bounded on the west side by a late P_3 fault system, the MacDonald Creek Fault Zone (MCFZ) (Byers and Dahlstrom, 1954), which separates Missi and Amisk groups. Amisk Group units are truncated and basal Missi conglomerate is missing adjacent to this fault. The MCFZ differs from the RCSZ in that P_3 folding is absent. A heterogeneously developed mineral lineation that plunges gently to the northwest was observed in the Amisk Group. Rare, post-metamorphic, layer-parallel breccias were also observed. The sense of displacement is unresolved at this time.

Phase 4 (P_4) deformation resulted in the Embury Lake fold (Mukherjee, 1968), a megascopic folding of all preexisting structures about a northeast-trending axial plane. There are no associated fabrics but P_2 and P_3 fabrics change strike from WNW to N over 10 km.

Phase 5 (P_5) deformation was a heterogeneously developed brittle faulting event. North-south trending faults with minor (metre) sinistral displacements are abundant northwest of Welsh Lake. These are probably coeval with late north-south faults recognized along the Sturgeon-Weir River (Pyke, 1966), Granite Lake (Ashton et al., 1987), and Ross Lake (Byers and Dahlstrom, 1954). These features are part of a larger array possibly associated with the Tabbenor Fault Zone (Ashton et al., 1987).

METAMORPHISM

Metamorphic grade generally increases northward. Chlorite appears stable in Missi metasediments in the Amisk Lake area. The first appearance of biotite is difficult to map because of patchy, discontinuous development; however, biotite and chlorite partially define folded S_2 fabric. The first appearance of garnet is more obvious. Garnet was first observed in arenaceous metasediments on Batty Lake. It appears to overprint S_2 and occurs adjacent to the Reynard Lake Pluton. The garnet isograd parallels the conglomerate-arenite contact from Batty Lake to just southwest of Martin Lake (Fig. 1). This may indicate bulk compositional constraints. The isograd trends southwest then southerly from Martin to Welsh Lake. The relationship of the garnet isograd to P_3 folds is uncertain at this time.

De Tombe (1988) outlined andalusite-sillimanite, kyanite-sillimanite and staurolite + muscovite + quartz = sillimanite + garnet + biotite + H_2O isograds in the Welsh Lake area. Garnet, staurolite, and andalusite occur in Amisk metasediments in the Grassy Lake area; however, garnet first occurs in the Welsh-Martin Lakes area within Missi metasediments. Aluminosilicates are rare within Missi metasediments making comparison with de Tombe's data difficult. The apparent misalignment of Amisk and Missi garnet isograds can possibly be explained in three ways (K. Ashton, personal communication). The first is that they are a result of contact metamorphism by the Reynard Lake and Neagle Lake plutons (plus other intrusions) (Byers and Dahlstrom, 1954; Longiaru, 1980; de Tombe, 1988). Longiaru (1980) delineated a greenschist/amphibolite transition (albite-oligoclase and actinolite-hornblende) attributed to contact metamorphism adjacent to the Reynard Lake Pluton. The second is that the Magdalen Basin is a tectonic slice in which low grade assemblages are surrounded by higher-grade assemblages. It could also be that isograds are folded during P_3 or offset along P_3 shear zones, however de Tombe (1988) reported very little deformation of porphyroblasts. A third explanation is that the composition of Missi metasediments was not appropriate for uniform development of minerals. These topics will be investigated in detail as part of the author's master's thesis.

SUMMARY

Detailed mapping has outlined a band of basal conglomerate which helps to define a type 1 (Ramsay, 1967) basin interference pattern in the Amisk-Welsh lakes area. Subsequent sinistral shear during P_3 deformation occurred along the appressed boundaries of this basin. Garnet growth appears to postdate P_2 deformation but its relationship to P_3 is uncertain.

ACKNOWLEDGMENTS

The author wishes to thank Ken Ashton and Edgar Froese for guidance and support and critically reviewing the manuscript. Lisa Kotowski provided able field assistance. Thanks also to Kelly Dies, Saskatchewan Mineral Development Corporation, for providing grid line maps and helpful discussion. Philip Simony critically reviewed the manuscript and provided advice during a visit to the area.

REFERENCES

Ahuja, S. P.
1970: Structural analysis of the Amisk and Missi rocks north of Amisk Lake Saskatchewan; M.Sc. thesis, University of Saskatchewan, 89p.

Ashton, K.E., and Wheatley, K.
1986: Preliminary report on the Kisseynew gneisses in the Kisseynew-Wildnest lakes area, Saskatchewan; in Current Research, Part B, Geological Survey of Canada Paper, 86-1B, p. 305-317.

Ashton, K.E., Wilcox, K.H., Wheatley, K.J., Paul, D. and de Tombe, J.
1987: The boundary zone between the Flin Flon domain, Kisseynew gneisses and Hanson Lake Block, northern Saskatchewan; in Summary of Investigations 1987, Saskatchewan Geological Survey, p. 131-134.

Bailes, A.H.
1980: Origin of Early Proterozoic volcaniclastic turbidites, south margin of the Kisseynew sedimentary gneiss belt, File Lake, Manitoba; Precambrian Research, v. 12, p. 197-225.

Bailes, A.H. and Syme, E.C.
1987: Geology of the Flin Flon-White Lake area; Manitoba Energy and Mines, Geological Services Branch, Map GR87-1-1.

Berthe, D., Choukroune, P., and Jegouzo, P.
1979: Orthogneiss, mylonite and non-coaxial deformation of granites; the example of the South Armorican shear zone; Journal of Structural Geology, v. 1, p. 31- 42.

Byers, A.R. and Dahlstrom, C.D.A.
1954: Geology and mineral deposits of the Amisk-Wildnest lakes area, Saskatchewan; Saskatchewan Department of Mineral Resources, Report 14, 177p.

de Tombe, J.
1988: The metamorphic stability fields of the Welsh Lake area in east-central Saskatchewan; B.Sc. thesis, Queen's University, 46p.

Froese, E. and Moore, J.M.
1980: Metamorphism in the Snow Lake area, Manitoba; Geological Survey of Canada, Paper 78-27.

Hattie, I.E.
1986: The geology and geochemistry of a Robinson Creek gold occurrence, north of Amisk Lake, Saskatchewan; M.Sc. thesis, University of Saskatchewan, 170p.

Lister, G.S. and Snoke, A.W.
1984: S-C mylonites; Journal of Structural Geology, v. 6, p. 617-638.

Mukherjee, A.C.
1968: Structural analysis of the Missi metasedimentary rocks near Flin Flon,Manitoba; M.Sc. thesis, University of Saskatchewan, 64p.

Longiaru, S.J.
1980: Structure and metamorphism of the northeast Amisk Lake area, Saskatchewan; M.Sc. thesis, University of Saskatchewan, 119p.

Pearson, J.G.
1982: Gold metallogenic studies: Amisk Lake eastern area; in Summary of Investigations 1982, Saskatchewan Geological Survey, Miscellaneous Report 82-4, p. 64-70.

Pyke, M.W.
1966: The geology of the Pelican Narrows and Birch Portage area, Saskatchewan; Saskatchewan Department of Mineral Resources, Report 93, 68p.

Ramsay, J.G.
1967: Folding and fracturing of rocks (First edition); McGraw-Hill Book Company,New York, , 568p.

Stauffer, M.R. and Mukherjee, A.
1971: Superimposed deformations in the Missi metasedimentary rocks near Flin Flon, Manitoba; Canadian Journal of Earth Sciences, v. 8, p. 217-242.

Vernon, R.H.
1988: Microstructural evidence of rotation and non-rotation of mica porphyroblasts; Journal of Metamorphic Geology, v. 6., p. 595-601.

Preliminary report on the geology of northwestern Dubawnt Lake area, District of Keewatin, N.W.T.

T.D. Peterson[1], A.N. LeCheminant[1], and R.H. Rainbird[2]

Peterson, T.D., LeCheminant, A.N. and Rainbird, R.H., Preliminary report on the geology of northwestern Dubawnt Lake area, District of Keewatin, N.W.T.; in Current Research, Part C, Geological Survey of Canada, Paper 89-1C, p. 173-183, 1989.

Abstract

Archean basement rocks underlie Early Proterozoic Dubawnt Group sedimentary and volcanic rocks in the Dubawnt Lake area. Megacrystic granite and biotite leucogranite with associated mafic rocks intruded a supracrustal-granitoid gneiss domain. Contact zones are strongly lineated and older gneiss septa are sheared and migmatized.

Lower Dubawnt Group rocks (Christopher Island and Kunwak formations) are exposed in an extensional basin centred on Dubawnt Lake. Syndepositionally faulted sequences tilted towards the basin centre are interpreted as alluvial fan, braided stream, and lake deposits. Flat-lying upper Dubawnt Group Pitz Formation rhyolites and Thelon Formation conglomerates and sandstones unconformably overlie lower Dubawnt Group sequences and granitoid basement rocks. Saprolitic regoliths are preserved beneath the Thelon Formation. Potassic volcanic rocks and minette dykes of the Christopher Island Formation resemble shoshonites and other K-rich mafic rocks typically found in arc environments, but lack plagioclase. Minette dykes are prominent on the Colorado Plateau, and lower Dubawnt Group basins may have developed upon an intracratonic uplift of similar dimensions.

Résumé

Des roches du socle archéen reposent sous les roches sédimentaires et volcaniques non déformées du groupe de Dubawnt datant du Protérozoïque inférieur dans la région située au nord-ouest du lac Dubawnt. Du granite mégacristallin associé à des roches mafiques en partie hybrides et des massifs syntectoniques de leucogranite à biotite ont pénétré un domaine supracrustal de gneiss granitoïde. Les noyaux des massifs de granite sont peu déformés, mais les zones de contact présentent des linéaments très marqués et les séparations de gneiss plus anciennes sont bréchifiées, cisaillées et migmatisées.

D'épaisses séquences de roches de la partie inférieure du groupe de Dubawnt (formations de Christopher Island et de Kunwak) sont mises à nu dans un bassin de distension centré sur le lac Dubawnt. Les couches faillées pendant leur mise en place plongent vers le centre du bassin et sont interprétées comme ayant été déposées dans des cônes de déjection et des vallées de cours d'eau anastomosés avec lacs temporaires. Les coulées de rhyolite horizontales de la formation de Pitz de la partie supérieure du groupe de Dubawnt et les conglomérats et grès de la formation de Thelon recouvrent en discordance les séquences de la partie inférieure du groupe de Dubawnt et les roches du socle granitoïdes. Des régolithes saprolitiques sont conservés sous la formation de Thelon. Les roches volcaniques potassiques et les dykes de minette de la formation de Christopher Island ressemblent aux shoshonites et à d'autres roches mafiques riches en potassium présentes de manière caractéristique en milieu d'arc mais ne renferment pas de plagioclase. Les dykes de minette sont proéminents sur le plateau du Colorado, et les bassins de la partie inférieure du groupe de Dubawnt ont pu être mis en place sur un soulèvement intracratonique de dimensions analogues.

[1] Lithosphere and Canadian Shield Division.
[2] Department of Geology, University of Western Ontario, London, Ontario N6A 5B7.

INTRODUCTION

The Dubawnt Lake map area (Fig. 1) is underlain by a basement of variably deformed, mostly granitic intrusions emplaced into strongly deformed granitoid gneisses with minor supracrustal remnants. These units are unconformably overlain by Early Proterozoic continental volcanic and sedimentary rocks of the Dubawnt Group. Mapping at 1:50 000 initiated in the 1988 field season is the first in the area since the reconnaissance mapping of Wright (1967) and Donaldson (1969) and the canoe epic of Tyrrell (1898). The mapping will contribute to ongoing petrogenetic studies of Dubawnt Group magmatism, which ranges from potassic alkaline (minette) dyke swarms and flows (Christopher Island Formation) to epizonal high-silica fluorite granite and contemporaneous silicic lavas and pyroclastic flows (Pitz Formation). The northwestern shoreline of Dubawnt Lake, numerous islands, and some inland areas have been mapped (Fig. 2) and preliminary results are presented in this paper.

The 1:500 000 geological compilation by Eade (1981) shows that the geology northwest of Dubawnt Lake is dominated by flat-lying upper Dubawnt Group (Thelon Formation) quartz arenites and pebbly conglomerates (Donaldson, 1969). Lower Dubawnt Group rocks in the study area occur mainly in one fault-bounded basin 30 km long, one of several east- to north-easterly trending basins containing lower Dubawnt Group rocks in the central District of Keewatin (Fig. 1). The largest of these is the 250 km long Baker Lake Basin. The basin considered here is largely covered by Dubawnt Lake itself, but excellent exposures of its periphery and of adjacent basement rocks are found on shoreline outcrops. Inland exposures of all lithologies are generally poor and lichen cover is intense.

PRE-DUBAWNT GROUP BASEMENT COMPLEX

More than 90 percent of the basement consists of presumed Archean granites associated with dioritic intrusions and apparent hybrids between them. Thin septa (≤ 100 m) of older gneisses between these intrusions are variably deformed and migmatitic near the contact. All basement units are cut by biotite lamprophyre dykes. Diabase dykes of the 1.27 Ga Mackenzie swarm represent the youngest igneous activity in the area.

The older gneisses are grey granodioritic and tonalitic orthogneisses with quartz-feldspar-biotite paragneiss and minor amphibolite and iron-formation (sulphide and oxide facies). Pelitic schists are notably absent and metamorphic grade is uncertain. The older gneisses are strongly deformed, having undergone metamorphism and several phases of tight folding before intrusion of the younger granites. Structures in gneisses at granite contacts are overprinted by strong shear. Exposures of the older gneisses away from these contact zones have not been mapped in detail and little is known of earlier structures in them.

The older gneisses are intruded by two suites of intrusive rocks with contrasting lithologies but similar structural

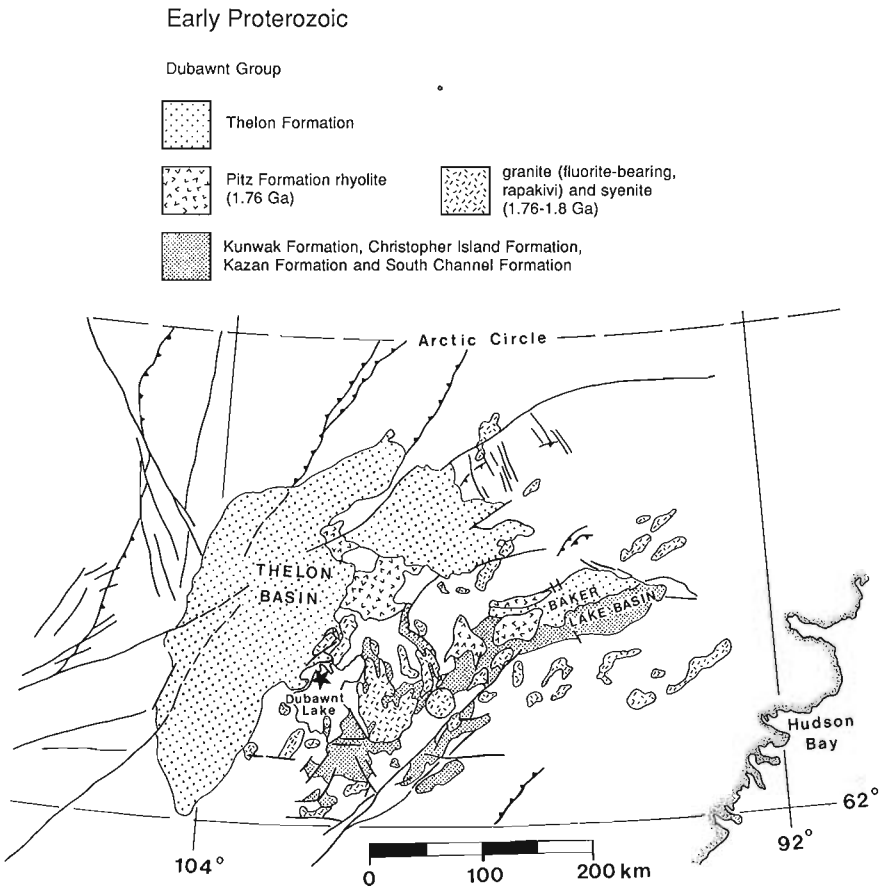

Figure 1. Simplified geological map showing the regional distribution of Dubawnt Group rocks; the star indicates the location of the study area.

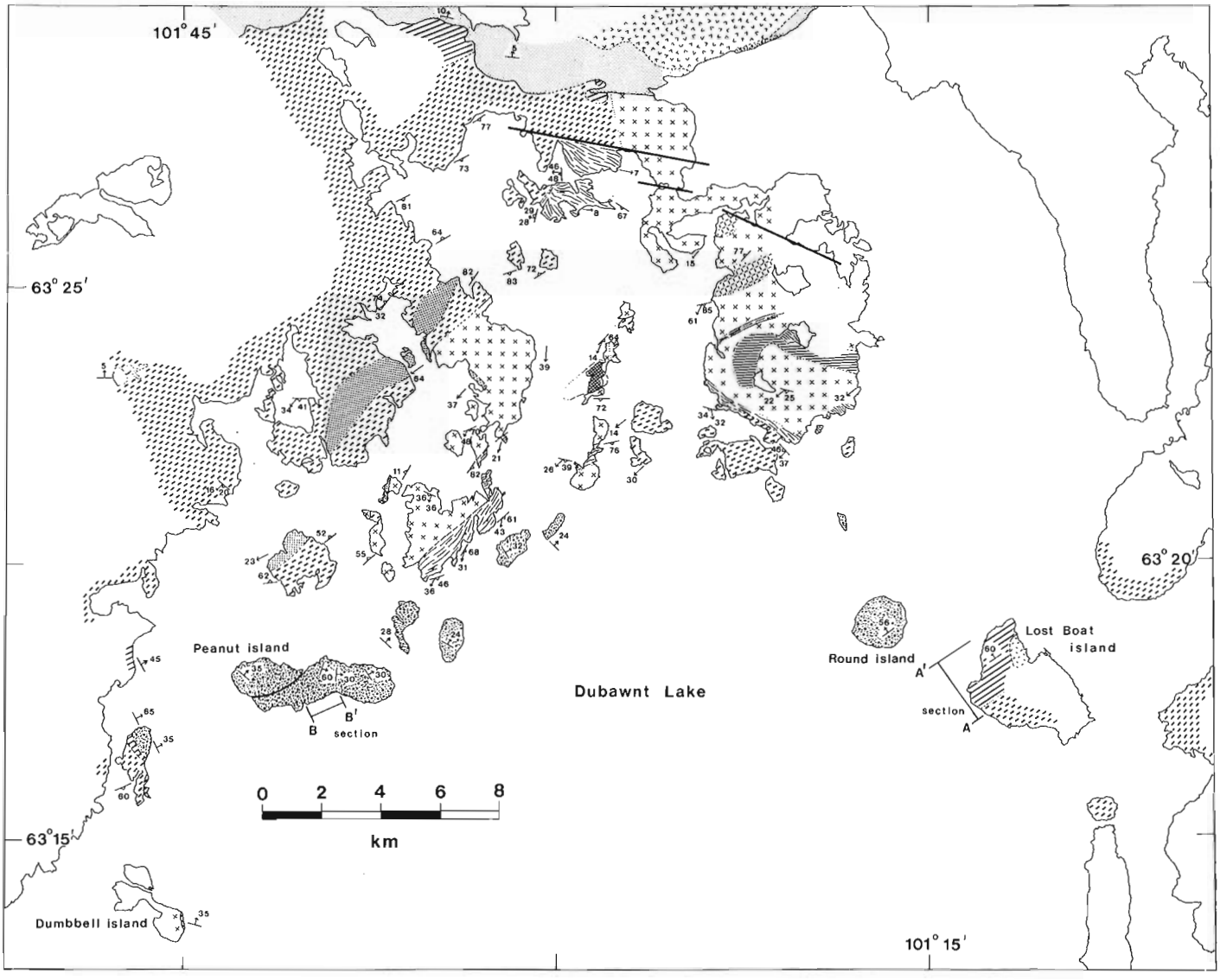

Early Proterozoic

Dubawnt Group

- Thelon Formation: conglomerate, sandstone
- Pitz Formation: quartz- and K-feldspar -phyric rhyolite flows
- Fluorite granite; quartz- and K-feldspar-phyric
- Kunwak Formation: red conglomerate, sandstone and siltstone
- Christopher Island Formation: potassic volcanic flows and volcaniclastic sediments

Archean

- Leucogranite: medium-grained, biotite-bearing
- Monzonite: fine-grained, hornblende-bearing.
- Granodiorite
- Megacrystic granite; K-feldspar megacrysts
- Diorite, gabbro
- Peridotite
- Mixed ortho- and paragneisses, locally migmatitic

Figure 2. Geology of northwestern Dubawnt Lake. Informal names are used to identify islands described in the text.

style. The megacrystic granite suite is made up of large plutons of K-feldspar megacrystic granite with enclaves of diorite in the form of diffuse, hybridized bodies to sharp, cuspate pillow-like forms and angular inclusions. The megacrystic granite is cut by diorite, leucogranite, aplite, and pegmatite dykes. Syn-kinematic leucocratic biotite granite is structurally beneath megacrystic granite and was probably the source of many of the dykes in it. The mafic member of the leucogranite suite is a hornblende monzonite which formed separate intrusive bodies and hybrids with the leucogranite. Some of the leucogranite bodies are sills 20 or more metres thick; deformation was concentrated near contact zones and produced weak foliation and strong southerly-plunging lineation. Narrow, variably dipping, mostly east-west trending mylonitic shear zones crosscut the intrusive bodies. Younger, selectively hematized and clay-altered, east-west brittle faults occur in basement rocks of the northern part of the map area.

Megacrystic granite, diorite, and peridotite

Megacrystic granite is the most extensive and characteristic rock type in a diverse but largely bimodal plutonic suite which ranges in composition from peridotite to granite. These rocks have been variably deformed and metamorphosed, but igneous textures and mineralogy are locally well preserved. The intrusive suite includes large homogeneous plutons of coarse grained porphyritic to megacrystic granite, discrete mafic and ultramafic bodies, and hybrid rocks that retain textural evidence for mixing and mingling of mafic and felsic magmas.

The megacrystic granite contains abundant 1-6 cm crystals of perthitic microcline in a coarse grained matrix of quartz, plagioclase, biotite and hornblende. Accessory minerals are magnetite, apatite, sphene and zircon. Small dykes and veins of fine- to medium-grained pink biotite granite and aplite cut the megacrystic granite. Most of these dykes are broken and transposed subparallel to the foliation. Narrow high strain zones occur, and contacts with the older gneisses are strongly deformed. Similar large bodies of deformed megacrystic granite have been mapped south of Dubawnt Lake and between Wharton Lake and Aberdeen Lake (Tella et al., 1981; LeCheminant et al., 1983). The megacrystic granite exposed northwest of Wharton Lake was emplaced as part of a major episode of Archean magmatism with an age range of 2.58-2.61 Ga (LeCheminant et al., 1987b).

The mafic intrusions range in composition from peridotite to diorite and occur mainly in the southwest part of the map area. The most homogeneous rock is a medium grained biotite diorite to gabbro that contains 60-70% normally zoned plagioclase. Early crystallized orthopyroxene is partly enclosed by clinopyroxene, biotite and strongly zoned amphibole. Myrmekite occurs along plagioclase grain boundaries adjacent to interstitial quartz. Accessory minerals are K-feldspar, apatite, zircon and opaques. The mafic intrusions occur as irregular crosscutting dykes and sheets subparallel to the foliation in the enclosing granite.

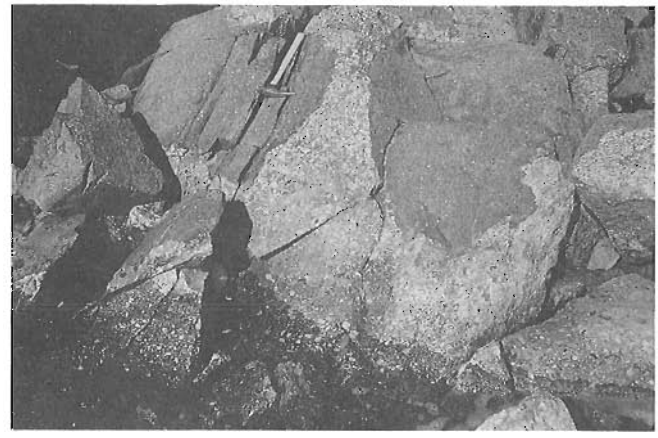

Figure 3. Net-viened complex in megacrystic granite. The diorite pillows have dark, fine-grained margins and are interpreted as resulting from injections of mafic magma into still-fluid granite. GSC #204724.

Contact zones are extremely heterogeneous and display a wide range of pillowed and net-veined mafic rocks enclosed in granite (Fig. 3) or in hybrid rocks of intermediate composition. The best preserved mafic pillows have sharp cuspate boundaries with a dark finer grained outer margin. Dispersed mafic inclusions may be of several generations, some of which contain rimmed K-feldspar megacrysts and rounded, partly resorbed quartz xenocrysts. The mafic inclusions range up to several metres in length and most are moderately to strongly elongate. Elongation may be a primary feature resulting from magmatic flow, but in most cases later deformation has overprinted and accentuated any primary elongations. There is a strong tendency for high strain zones to occur along contacts between megacrystic granite and diorite. Nevertheless, preserved primary textures associated with the dispersal of mafic inclusions in more felsic rocks strongly indicates contemporaneous mafic and granitic magmatism (Blake, 1981; Vernon, 1983, 1984).

An ultramafic intrusion approximately 2 km by 0.8 km is exposed on several small islands northeast of the main intrusions of the diorite-gabbro suite. The ultramafic body is responsible for a discrete positive magnetic anomaly which extends about 1 km southwest of the islands. The intrusion is a homogeneous medium grained black peridotite with cumulate olivine, orthopyroxene and chromite enclosed in clinopyroxene (?), amphibole and phlogopite. Traces of Ni-bearing pyrrhotite were identified by microprobe analysis. Olivine is largely altered to serpentine and magnetite and fine grained talc forms a rim around altered pyroxenes and partly altered amphibole. The intrusion is in tectonic contact along its southeastern side with mylonitic biotite granite (see below). The body is interpreted as an olivine-rich cumulate, perhaps the basal part of a layered intrusion, derived from the same source of mafic magma as the diorite-gabbro bodies.

Leucogranite suite

Granitic rocks of the leucogranite suite range from biotite granodiorite to granite with colour index from 1-10. White-weathering biotite granites in the west part of the map area contain minor muscovite. Little deformed, pink weathering, medium grained biotite granites in the north-central part of the map area consist of subhedral sodic plagioclase and anhedral quartz and perthitic K-feldspar. Euhedral magnetite is less than 1 %. Both euhedral and anhedral zircons are abundant in clots of biotite, and anhedral zircons are also surrounded by quartz. Deformed leucogranites have an easily visible lineation due to transposed clots of hematized biotite.

A fine grained monzonite, associated only with pink leucogranite, is grey to dark green weathering and commonly contains xenoliths of the older gneisses. Heterogeneous monzonite and leucogranite hybrid rocks occur in the contact zones and are abundantly intruded by leucogranite and pegmatite dykes, some of which are tightly folded. Hybrid rocks are spotty pink and green weathering and can be fine grained and homogeneous on a scale of several metres, but heterogeneous rocks are more common. Amphibole-alkali feldspar pegmatite occurs in one hybridized zone.

A pluton of white-weathering leucocratic biotite granite is poorly exposed in low-lying rubbly outcrops in the west-central part of the map area. The fine- to medium-grained granite is weakly foliated and strongly lineated, and contains 1-3 % biotite and trace amounts of muscovite. Rafts of biotite-hornblende granitoid gneiss occur within the leucogranite adjacent to contacts with the older gneiss unit. Contacts with megacrystic granite typically are sheared, although in one case, the two rocks are in sharp but non-chilled contact. Both the megacrystic granite and the leucocratic biotite granite are cut by dykes and sheets of pink aplite, and by irregular dyke-like mafic intrusions of the diorite-gabbro suite.

A large ($\approx$50 km^2) composite body of pink leucogranite, monzonite, and granodiorite underlies the central part of the map area. The intrusion is well exposed on its western margin, where a leucogranite sill overlying a migmatitic gneiss breccia outcrops along the shoreline. Although the contacts (both with the older gneisses and earlier monzonite) are frequently migmatitic, no evidence of in situ partial melting is present (eg., melanosomes) and the migmatites grade continuously into nondeformed intrusive breccias. Leucogranite and pegmatite dykes are both nondeformed and folded/transposed in the same outcrop, suggesting that dyke intrusion was both syn- and post-kinematic. This is consistent with the observation that only the margins of the granite bodies are lineated, perhaps due to a hot, fluid central portion being present during deformation. Leucogranites are consistently finer grained near their contacts with older gneisses. A suite of samples from a transect beginning in nondeformed granite and ending at a migmatitic contact shows that deformation in the leucogranite began with suturing of quartz boundaries, followed by production of strain shadows in quartz and finally by bending and microfaulting of plagioclase feldspar and transposition of biotite clots as grain size was gradually reduced.

The origin of the synintrusive stress regime is uncertain, but it is related locally to emplacement of the megacrystic granite. The southern margin of the composite leucogranite body is structurally beneath megacrystic granite and separated from it by strongly sheared gneiss injected by megacrystic granite. Stretching lineations across the contact trend southwest with a plunge of about 40°; hence the leucogranite may be in the footwall of a northerly-directed thrust fault. Contacts between megacrystic granite and leucogranite with no intervening older gneisses are rare, and all observed were tectonized except one. This and the presence of sheared pegmatitic to aplitic leucogranitic dykes in megacrystic granite suggests near simultaneous emplacement of both granite types. However, the ambient stress field was almost certainly not neutral, since consistent south-plunging stretching lineations are developed across nearly the entire map area.

Lamprophyre and diabase dykes

All pre-Dubawnt Group basement rocks are cut by recessive-weathering mica-rich lamprophyres, mainly minettes. The 30 mapped dykes range up to 3 m wide and have an average orientation of 113°. East to east-southeasterly trends predominate although 10 dykes define a southeasterly-trending cluster. No intersecting dykes were observed. The dykes are not deformed; mica phenocrysts and calcite-filled amygdules tend to be aligned subparallel to chilled margins, and granitoid xenoliths and partly resorbed quartz xenocrysts occur in some dykes. The lamprophyres are part of a large regional swarm of K-rich alkaline dykes that were, in part, feeders for overlying Christopher Island Formation lavas and pyroclastic flows (LeCheminant et al., 1987a). Their average east-southeast trend is similar to lamprophyre orientations in the Baker Lake area and provides further indication that dyke emplacement was associated with predominantly north-south extension. Most dykes are not vertical, but have southerly dips of between 60° and 75°. These dips may reflect northerly to northeasterly rotations produced during extensional subsidence associated with the deposition of the Kunwak Formation.

Diabase dykes of the Mackenzie swarm trend approximately 315° in the map area, with thicknesses of about 20-30 m. All have well chilled margins and some contain abundant granophyre and biotite. Some outcrops show indistinct, wispy, contact-parallel layering of unknown origin.

DUBAWNT GROUP

Christopher Island Formation

Christopher Island Formation flows and volcaniclastic sediments are separated from the basement unconformity by interbedded conglomerate and conglomeratic sandstone containing locally-derived basement clasts. Sedimentary facies in overlying volcaniclastic successions reflect intermittent uplift associated with the formation of extensional basins and changes in drainage patterns resulting from volcanic activity. The Christopher Island Formation volcanic

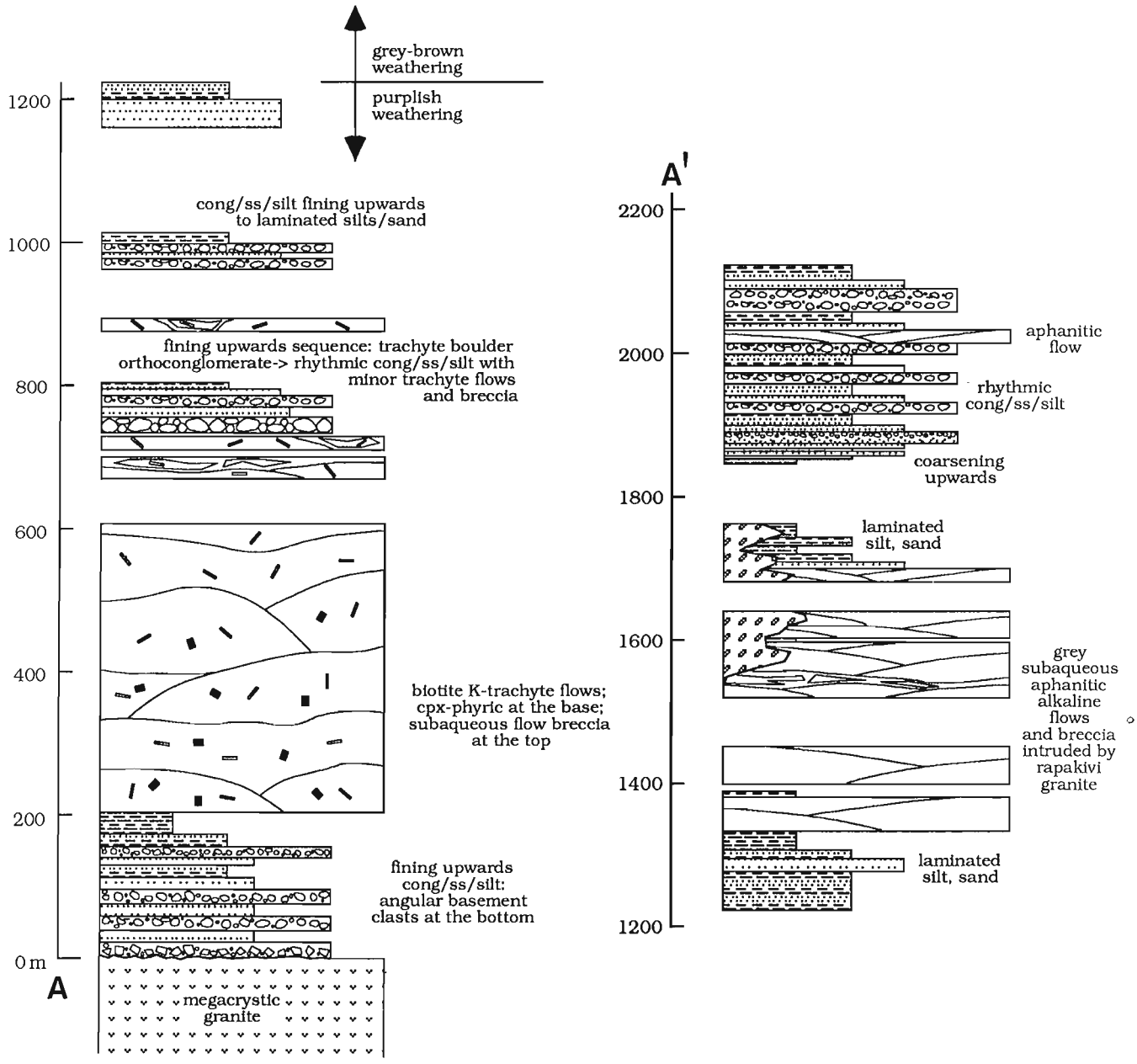

Figure 4. Stratigraphic section for the Christopher Island Formation on Lost Boat island. The bottom 500 m are poorly exposed and are inferred largely from ice push. Note the fining upward sequence in fluvial sediments overlying the porphyritic mafic trachyte flows and the association of aphanitic flows with lacustrine sediments.

Figure 5. Trachyte boulder orthoconglomerate at Lost Boat Island. Well-rounded clasts of mafic biotite trachyte and felsic trachyte are in a poorly-sorted matrix of trachyte sand and pebbles. GSC #204724-B.

rocks are mainly K-rich trachyandesites (latites) and trachytes (LeCheminant et al., 1987a). In the absence of chemical analyses the volcanics are described as mafic or felsic trachytes, primarily on the basis of their macroscopic phenocryst content.

A measured section through the Christopher Island Formation on the west side of Lost Boat Island[1] (Fig. 4) contains 2 km of volcanic and sedimentary rocks. A poorly exposed 200 m thick basal unit overlying an unexposed basement unconformity consists of planar-bedded, angular to subangular, granite-clast paraconglomerate (maximum clast size 4 cm) interbedded with pebbly crossbedded lithic arenite, fining upwards to interbedded lithic arenite and siltstone. Sandstones and siltstones are brick-red, similar to fine-grained Kunwak Formation sediments. At Dumbbell Island, Christopher Island Formation beds onlap basement at a high angle to bedding, but at Lost Boat Island the contact is sub-horizontal.

The basal sediments at Lost Boat Island are overlain by 450 m of thin (1-10 m) flows of mafic trachyte which are rich in clinopyroxene and phlogopite near the base; the uppermost flows, which are well exposed, contain no clinopyroxene. Flow tops are marked by angular flow breccia in a matrix of unsorted, fine grained sediment derived from flows. No true pillows were observed, but a subaqueous environment is suggested by hyaloclastite and chilled margins in breccia fragments. On Dumbbell Island, radial pipe vesicles and bulbous flow tops are prominent at the top of the youngest flow.

The lower flow unit is overlain by a boulder orthoconglomerate with well-rounded clasts of trachyte up to 75 cm; basement clasts are extremely rare and the matrix is composed of trachyte pebbles, sand, and silt (Fig. 5). This grades up through crudely-bedded sandy cobble paraconglomerate to rhythmicly-bedded conglomerate, sandstone and siltstone interbedded with minor trachyte flows. The sediments fine upward over about 150 m to parallel-laminated siltstone and fine sandstone. Sorting and the incidence of normally graded beds increase up section. Conglomeratic layers in the rhythmic units have sharp bases which commonly are irregular due to loading. They form the bases of graded beds, 30-100 cm thick, and indicate rapid deposition, perhaps by turbidity currents. The Lost Boat Island flows may have been erupted on a valley floor occupied by lakes and braided streams.

Siltstones and sandstones overlying the mafic trachyte flows and coarse sediments are distinctly purple-weathering, but a gradational change in sediment composition occurs and over a short interval the purplish-weathering siltstones are overlain by 100 m of grey to yellow-brown siltstones. The grey-brown siltstones are overlain by 350 m of grey, aphyric lavas interbedded with both laminated siltstone and massive grey siltstone beds about 3 m thick. Tops of flows ($\leq$ 10 m thick) are marked by hyaloclastite and a concentration of geopetal amygdules filled with quartz and epidote (Fig. 6), and by fractures filled with laminated silt. Flow bottoms are weakly amygdaloidal. The laminated and massive siltstones are interpreted as lacustrine, presumably deposited as volcanic ash into relatively still water. Some beds in laminated siltstone are replaced by epidote, reinforcing the impression that they are ash equivalents of the lavas. It is noteworthy that desiccation features such as mud curls and chips, which are abundant in the Kunwak Formation and present in other Christopher Island Formation sections (LeCheminant et al, 1981), are absent from the Lost Boat Island section. Aphyric, oxidized and highly vesicular lavas, poorly exposed along a beach on the north boundary of the map area, may be the subaerial equivalent of the grey lavas. Eruption of the mafic trachyte flows was evidently accompaniedby faulting, which resulted in the deposition of coarse clastic rocks, but the aphyric lavas were erupted during a period of relative stability. Lacustrine basins may have been formed by intermittent damming of valleys by volcanic flows.

The grey flows are overlain by syndepositionally faulted, current rippled siltstone and weakly crossbedded fine sandstone, which coarsen upward over a partly covered interval of 100 m to purplish rhythmicly-bedded conglomerate, sandstone and siltstone, similar to the rhythmic units below the grey flows. Mafic trachyte clasts predominate, but clasts of both basement granitoids and aphanitic lava also occur. One thin aphanitic flow is present near the top of the section.

X-ray diffractometry of the aphyric lavas indicates they contain mostly alkali feldspars with minor amphibole, chlorite, and quartz. They are thus mineralogically distinct from the mafic trachytes which make up most Christopher Island Formation flows, although alkali feldspar-phyric flows were described by Blake (1980), and clasts of feldspar-phyric felsic trachyte occur in the coarse clastic rocks on Lost Boat Island. Petrographic study shows no microphenocrysts or trachytic textures, hence, the lavas were probably erupted crystal-free.

Evidence of pyroclastic volcanic activity in the Christopher Island Formation in the study area is restricted

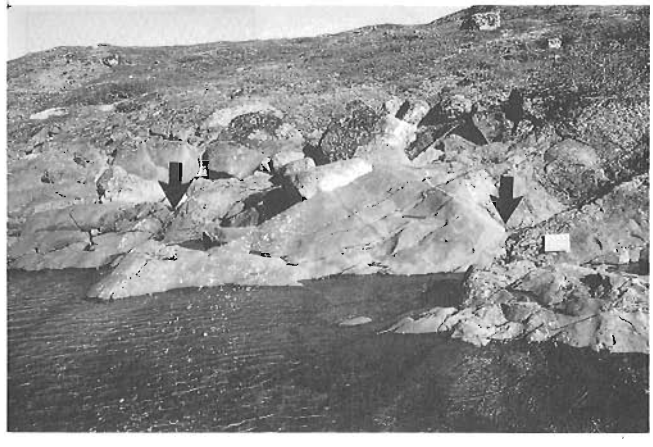

Figure 6. Aphyric grey lavas at Lost Boat island. The arrows indicate the top and bottom of one flow (top to the left), which has a concentration of amygdules filled with quartz in the upper one third. The smooth weathering surface is a result of very small grain size, due to the lavas being erupted crystal-free. GSC #204724-J.

[1] Lost Boat Island, Dumbbell Island, Round Island and Peanut Island are informal names.

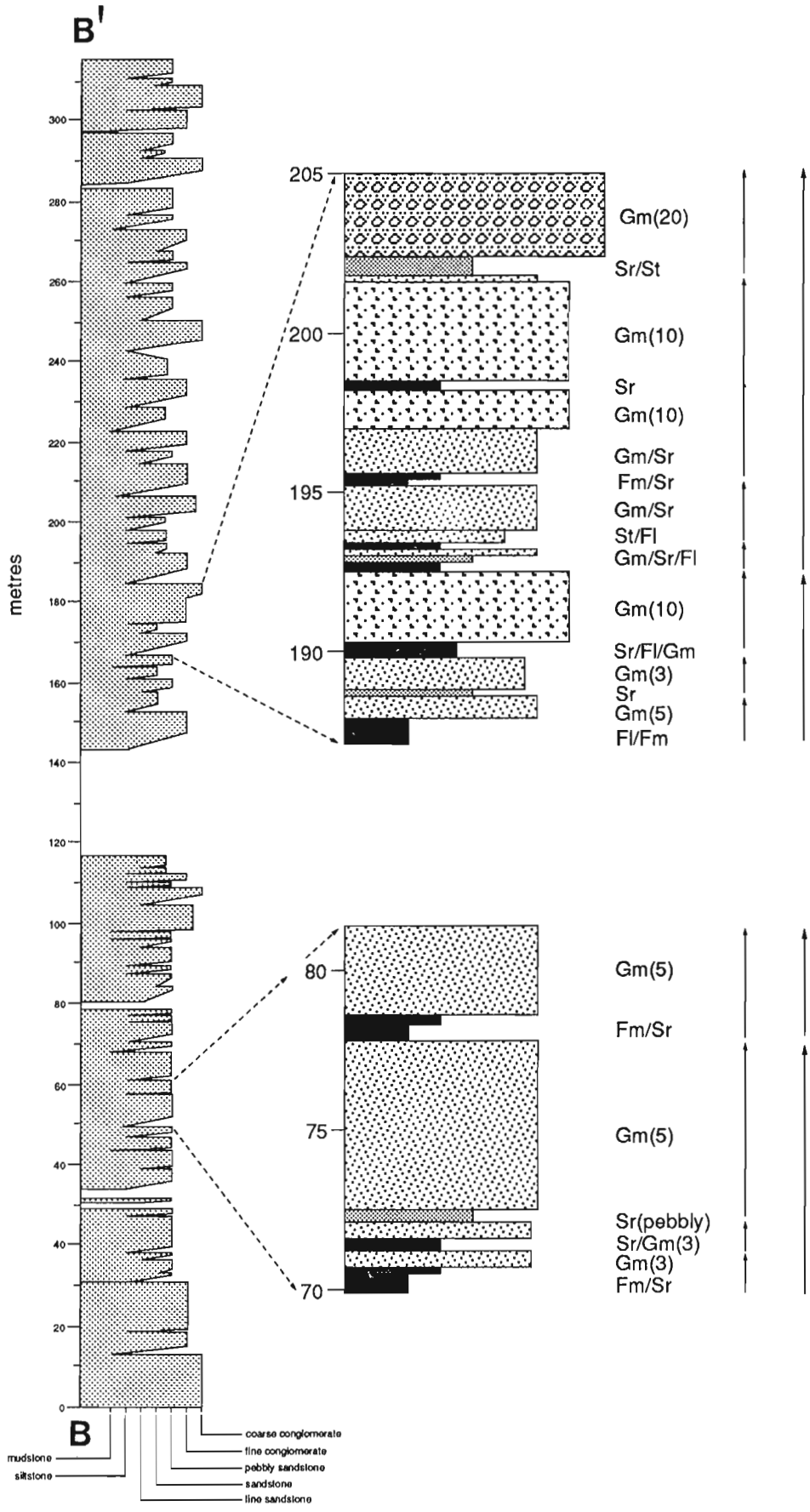

Figure 7. Stratigraphic section for the Kunwak Formation on the south shore of Peanut island showing details of typical coarsening-upward cycles. Note that some of the megacycles are composed of a series of smaller coarsening-upward cycles. Fl = parallel-laminated mudstone and siltstone; Fm = Fl with desiccation features; Sr = ripple cross-laminated fine sandstone; St = trough cross-bedded sandstone; Gm(10) = massive to crudely stratified orthoconglomerate (with maximum clast size of 10 cm). Facies identifiers adapted from Miall (1977).

to the possible lacustrine tuffs described above, and to accretionary lapilli tuffs filling fractures in mafic trachyte flows on Dumbbell Island. No volcanic vents were identified.

Kunwak Formation

The Kunwak Formation is a thick sequence of coarse clastic rocks which conformably overlies the Christopher Island Formation. On the northwest side of Dubawnt Lake it is exposed on islands forming a north-easterly trending belt, with crystalline basement to the north and with Christopher Island Formation to the southwest and southeast. Strata on the east side of this belt (Round Island) dip north-westerly into the basin at 50°-60°; on the west side (Peanut Island) strata dip northeasterly from 30° to 60° (Fig. 2). Inferred thickness of the formation is more than 10 km if no fault repetitions occur.

A summary of a detailed section measured along the south shore of Peanut Island is given in Figure 7. The most abundant lithofacies is a poorly sorted orthoconglomerate composed mainly of cobble- to boulder-size clasts of local basement granitoids. The conglomerate is also composed of about 20 percent Christopher Island Formation trachyte clasts and rare banded gneiss and vein quartz clasts. The relative proportion of locally derived clasts increases upsection, indicating progressive unroofing of the adjacent basement rocks. Clasts are angular to subrounded and average 25-30 cm in the coarsest units (maximum 1.5 m). The matrix is composed of red silty to coarse sand and comprises less than 10 percent of the rock. Bedding is difficult to recognize in the coarsest units, although some bed tops are marked by a calcite-cemented horizon, possibly a calcrete. Finer units display well defined parallel stratification with subtle normal and reverse grading. A positive correlation between bed thickness and maximum clast size was observed.

On the south side of Peanut Island, conglomerate occurs at the top of coarsening upward cycles which have abrupt contacts with overlying finer grained sediment. Complete cycles, which are 1-10 m thick, begin with parallel-laminated mudstone with desiccation cracks passing up through ripple crosslaminated siltstone and fine sandstone to parallel- and cross-stratified pebbly sandstone, and finally crudely- stratified orthoconglomerate with sandy interbeds. Incomplete cycles lack mudstone and begin with fine sandstone. The fine sediments display graded and convolute lamination, climbing current ripples and wave ripples with crest orientations from northeast to east. Limited paleocurrent data from crossbedded pebbly sandstones on Peanut Island give transport directions to the south and southeast. A small island of unsorted talus breccia separates the basement from Round Island, where sediments similar to those on the south side of Peanut Island are exposed.

It is notable that the island outcrops are distributed in an east-west trending belt which is truncated to the north by basement granitoids (Fig. 2). In at least three areas the contact appears to be quite abrupt; at the westernmost locality it is an exposed fault. Although the contact is obscured by water everywhere else, there is a strong suggestion that the

Figure 8. Kunwak Formation, Round island. Planar and trough-cross bedded sandstones and minor siltstones are interbedded with crudely bedded orthoconglomerate containing white clasts of basement granitoids. GSC #204724-A.

northern boundary is a basin margin fault zone from which coarse, locally-derived sediments were shed to the south and southeast. This interpretation is corroborated by the overall southerly fining of facies on Peanut Island.

Coarse, poorly sorted and weakly stratified orthoconglomerates are interpreted as subaerial debris flow deposits. Debris flow deposits are interbedded and likely intertongue with finer-grained, parallel-stratified and rare crossbedded orthoconglomerates and poorly sorted pebbly sandstones. These are interpreted as being waterlain, perhaps stream channel and sheetflood deposits. Possible calcrete horizons on debris flow tops, the ubiquitous red colour and the abundance of desiccation cracks and mud chips in fine sediments are all suggestive of arid conditions.

These deposits display many of the features of alluvial fans as summarized in Rust and Koster (1984). Stacked coarsening-upward cycles (Fig. 7), are inferred to result from repeated uplift along the basin margin fault zone. Larger scale (50-200 m) coarsening or fining upward megacycles were not observed. Such a setting would account for the coarse grain size, great thickness and rapid down-dip facies changes observed in these deposits. Similar interpretations have been made for the Kunwak Formation in the Baker Lake Basin and in the Wharton Basin by LeCheminant et al. (1981).

Pitz Formation and fluorite granite

Rhyolitic volcanic flows of the Pitz Formation overlie the Kunwak and Christopher Island formations. Exact contact relations are indeterminate; exposures are limited to rubbly ridges along the northern edge of the map area (Fig. 2).The flows are homogeneous K-feldspar- and quartz-rich porphyritic rhyolite similar to Pitz Formation lithologies exposed in the Baker Lake Basin (Donaldson, 1965; LeCheminant et al., 1981, 1983). A regolith zone, approximately 2 m thick, occurs on Pitz Formation flows beneath the Thelon Formation; weathering has caused kaolinization

of feldspar and bleaching of the maroon-coloured groundmass. In some instances, weathering is localized along joints in the rhyolite.

A fluorite-bearing quartz-phyric leucocratic granite intrudes the grey aphyric lavas and associated siltstones of the Christopher Island Formation on the east side of Lost Boat island. A similar suite of shallowly emplaced granites is regionally associated with Pitz Formation extrusive rocks (LeCheminant et al., 1981, 1987b).

Thelon Formation

The Thelon Formation conglomerates and sandstones unconformably overlie basement granitoids and all other Dubawnt Group strata. Several small mesas in the northern part of the map area define part of the southern margin of the Thelon Basin which extends north and west of Dubawnt Lake. Island outcrops on Dubawnt Lake originally mapped as Thelon Formation (Donaldson, 1969) are here assigned to the Kunwak Formation. Thelon rocks are readily distinguished by relatively low dips ($<15°$) and by the presence of Pitz Formation rhyolite clasts in basal conglomerates.

Only thin (10-15 m) basal successions of the Thelon Formation are preserved in the present map area. Immediately above the unconformity is poorly indurated massive to faintly parallel-stratified cobble to boulder orthoconglomerate. Framework clasts are rounded to very well rounded and include varying proportions of Pitz Formation rhyolite, Christopher Island Formation trachyte, white and pink quartz arenite (Amer Group?), feldspathic arenite, and several types of basement granitoids. The matrix content is high, up to 50 % in some outcrops. The matrix is composed of weathered and poorly sorted granitoid detritus cemented by white kaolinite. The clay may have been derived from a thick saprolite which is exposed in several areas below the unconformity. The saprolite is unusual in that it displays little or no effects of burial metamorphism. Sericitization of clay-altered feldspars is a very common feature of most Precambrian regoliths (Holland, 1984; Grandstaff et al., 1986). The absence of sericitization indicates that the sub-Thelon saprolite was not deeply buried at any time.

The basal conglomerate is overlain and interbedded with parallel-stratified pebble orthoconglomerate, pebbly sandstone and planar crossbedded sandstone. These rocks are better sorted and indurated than the basal conglomerate. The framework contains fewer locally-derived clasts and a higher percentage of well-rounded more resistant lithologies, particularly white quartz arenite. The matrix is a salmon-coloured, poorly- to moderately well-sorted feldspathic arenite with blotchy hematitic alteration. A few paleocurrent measurements suggest transport north, toward the centre of the Thelon basin and away from the older basin in Dubawnt Lake to the south. Local relief on the underlying unconformity is indicated by the fact that the basal unit is more discontinuous than the upper unit.

Basal Thelon strata at Dubawnt Lake are tentatively interpreted as braided fluvial deposits (see Donaldson, 1969; Cecile, 1973). The basal conglomerates were formed by mechanical abrasion of chemically weathered basement lithologies. The gradual upsection increase in textural and compositional maturity reflects higher energy conditions and increasing distance of sediment transport.

DISCUSSION

The Pitz and Thelon formations have previously been assigned with underlying Kunwak and Christopher Island Formation rocks to a single stratigraphic group on the basis of spatial association and some similarity in sedimentary style (Donaldson 1965, 1967). However, in the Dubawnt Lake area there are profound differences in the style and location of basin development. Faulting was contemporaneous with deposition of the Kunwak Formation and occured prior to the beginning of Pitz Formation volcanism. The faulting rotated crustal blocks containing lower Dubawnt Group rocks in toward the centre of Dubawnt Lake. The great thickness of Kunwak alluvial sediments on the west side of the basin, and dips shallowing upsection there, indicate that faulting and rotation of crustal blocks was concurrent with sedimentation. Dips of Christopher Island Formation and Kunwak Formation beds indicate basinward rotation was greater on the east side where combined lower Dubawnt Group deposits are a minimum of 2.7 km thick. The area between is completely covered by Dubawnt Lake.

Upper Dubawnt Group rocks are nearly flat-lying, and paleocurrent directions for the Thelon Formation (Donaldson, 1965, 1967) indicate directions of transport opposite to those in the Kunwak Formation (north and westerly versus south and easterly). These are arguments for redefining the Dubawnt Group by separating lower and upper Dubawnt Group rocks into two new groups. New assignments are required to emphasize the differences in tectonic style which the lower and upper Dubawnt Group rocks suggest.

The mafic potassic flows of the Christopher Island Formation are the extrusive equivalents of minette dykes (LeCheminant et al., 1987a). Minette dykes are common in certain intracratonic uplifts, such as the Colorado Plateau (Roden et al., 1979) and the igneous associations and style of sedimentation there are very similar to those of the lower Dubawnt Group (Rowley et al., 1978; Roden et al., 1979). Basins containing lower Dubawnt Group rocks may have developed upon an intracratonic uplift of similar dimensions as the Colorado Plateau. Extrusive equivalents of minettes are rarely identified, a situation which has led to some confusion regarding their terminology and complicates assigning them to a tectonic environment. Their potassic nature, and the presence of fault-bounded basins containing braided fluvial deposits led Blake (1980) to suggest that the Christopher Island Formation volcanics are equivalent to potassic igneous rocks (high-K calc-alkaline rocks and shoshonites and related types) of southeast Papua. This would imply that they are the result of subduction zone processes, and related to post-orogenic extension. However, the equation with shoshonites is misleading, since true shoshonites are plagioclase-bearing lavas (Nicholls and Carmichael, 1969) which have no equivalents in the Christopher Island Formation. Although braid plain deposition is prominent in Papua, topographic relief there is

primarily the result of volcanism and tectonic uplift associated with subduction (Davies and Smith, 1971). Christopher Island Formation lavas are associated with the formation of extensional basins, and no intermediate igneous rocks occur, hence, there appears to be no direct relationship between subduction tectonics and the Christopher Island Formation.

ACKNOWLEDGMENTS

We thank Natalie Morisset, Jacqueline Murray and Bob Spark for their enthusiastic field assistance and mapping contributions. Al Donaldson and his assistants Hendrik Falck and Klaus Vogel enlivened the first two weeks of work. Al Donaldson in particular contributed extensively to our work on the Dubawnt Group and read a preliminary draft of this report. Forrest Hutchinson and John Schrock of Duluth, Minnesota provided friendly air transportation that allowed us to examine the Dubawnt Group section west of Grant Lake and the impact structure at Nicholson Lake.

REFERENCES

Blake, D.H.
1980: Volcanic rocks of the Paleohelikian Dubawnt Group in the Baker Lake-Angikuni Lake area, District of Keewatin, N.W.T.; Geological Survey of Canada, Bulletin 309, 39 p.
1981: Intrusive felsic-mafic net-viened complexes in north Queensland; BMR Journal of Australian Geology and Geophysics, v. 6, p. 95-99.

Cecile, M.P.
1973: Lithofacies analysis of the Proterozoic Thelon Formation, NWT (including computer analysis of field data); Unpublished M.Sc. thesis, Carleton University, Ottawa, 119 p.

Davies, H.L., and Smith, I.E.
1971: Geology of eastern Papua; Geological Society America, Bulletin, v. 82, p. 3299-3312.

Donaldson, J.A.
1965: The Dubawnt Group, Districts of Keewatin and Mackenzie; Geological Survey of Canada Paper 64-20, 11 p.
1967: Two Proterozoic clastic sequences: a sedimentological comparison; Proceedings of the Geological Association of Canada, v. 18, p. 33-54.
1969: Descriptive notes (with particular reference to the late Proterozoic Dubawnt Group) to accompany a geological map of central Thelon Plain, Districts of Keewatin and Mackenzie (65M, NW1/2; 66B, C, D, 75P E1/2, 76 A E1/2); Geological Survey of Canada Paper 68-49.

Eade, K.E.
1981: Geology of Dubawnt Lake (NTS 65NW, NE) map area, District of Keewatin, N.W.T.; geological map, scale 1:500 000 with legend, Geological Survey of Canada, Open File 771.

Holland, H.D.
1984: The Chemical Evolution of the Atmosphere and Oceans; Princeton University Press, 582 p.

Grandstaff, D.E., Adelman, M.J., Foster, R.W., Zbinden, E., and Kimberley, M.M.
1986: Chemistry and mineralogy of Precambrian paleosols at the base of the Dominion and Pongola Groups (Transvaal, South Africa); Precambrian Research v. 32, p. 97-131.

LeCheminant, A.N., Ianelli, T.R., Zaitlin, B., and Miller, A.R.
1981: Geology of Tebesjuak Lake map area, District of Keewatin: A progress report; in Current Research, Part B, Geological Survey of Canada, Paper 81-1B, p. 113-128.

LeCheminant, A.N., Ashton, K.E., Chiarenzelli, J., Donaldson, J.A., Best, M.A., Tella, S., and Thompson, D.L.
1983: Geology of Aberdeen Lake area, District of Keewatin: preliminary report; in Current Research, Part A, Geological Survey of Canada, Paper 83-1A, p. 437-448.

LeCheminant, A.N., Miller, A.R., and LeCheminant, G.M.
1987a: Early Proterozoic alkaline igneous rocks, District of Keewatin, Canada: petrogenesis and mineralization; in Pharaoh, T.C., Beckinsale, R.D., and Rickard, D. (eds), Geochemistry and Mineralization of Proterozoic Volcanic Suites, Geological Society of London Special Publication 33, p. 219-240.

Miall, A.D.
1977: A review of the braided-river depositional environment; Earth Science Reviews, v. 13, p. 1-62.

Nicholls, J., and Carmichael, I.S.E.
1969: A commentary on the absarokite-shoshonite-banakite series of Wyoming,U.S.A; Schweiz. Mineral. Petrog. Mitt. 49, p. 47-64.

Roden, M.F., Smith, D., and McDowell, F.W.
1979: Age and extent of potassic volcanism on the Colorado Plateau; Earth and Planetary Science Letters v. 43, p. 279-284.

Rowley, P.D., Anderson, J.J., Williams, P.L., and Fleck, R.J.
1978: Age of structural differentiation between the Colorado Plateaus and Basin and Range provinces in southwestern Utah; Geology v. 6, p. 51-55.

Rust, B.R., and Koster, E.H.
1984: Coarse alluvial deposits; in Walker, R.G. (ed), Facies Models, Geological Society of Canada Geoscience Canada Reprint Series 1.

Tella, S., Eade, K.E., Miller, A.R., and Lamontagne, C.G.
1981: Geology of the west half of the Kamilukuak Lake map area, District of Keewatin; a part of the Churchill structural province; in Current Research, Part A, Geological Survey of Canada, Paper 81-1A, p. 231-240.

Tella, S., Heywood, W.W., and Loveridge, W.D.
1985: A U-Pb age on zircon from a quartz syenite intrusion, Amer Lake area, District of Keewatin, NWT; in Current Research, Part B, Geological Survey of Canada, Paper 85-1B, p. 367-370.

Tyrrell, J.B.
1898: Report on the Dubawnt, Kazan, and Ferguson rivers and the north-west coast of Hudson Bay and on two overland routes from Hudson Bay to Lake Winnipeg; Geological Survey of Canada, Annual Report 1896 v. 9, Part F, p. 1-218.

Vernon, R.H.
1983: Restite, xenoliths and microgranitoid enclaves in granites; Journal and Proceedings, Royal Society of New South Wales, v. 116, p. 77-103.
1984: Microgranitoid enclaves in granites-globules of hybrid magma quenched in a plutonic environment; Nature, v. 309, p. 438-439.

Wright, G.M.
1967: Geology of the southeastern barren grounds, parts of the Districts of Mackenzie and Keewatin; Geological Survey of Canada Memoir 350, 91 p.

Tectonic history of the Lower Proterozoic Foxe-Rinkian Belt in central Baffin Island, N.W.T.

J.R. Henderson, J. Grocott[1], M.N. Henderson[2], S. Perreault[3]
Lithosphere and Canadian Shield Division

Henderson, J.R., Grocott, J., Henderson, M.N. and Perreault, S., Tectonic history of the Lower Proterozoic Foxe-Rinkian Belt in central Baffin Island, N.W.T.; in Current Research, Part C, Geological Survey of Canada, Paper 89-1C, p. 186-197, 1989.

Abstract

The stratigraphy throughout the belt comprises a lower platformal facies (carbonate, quartzite, pelite) overlain by a basinal turbiditic flysch facies. An assemblage of mafic-ultramafic flows, sills, epiclastic and chemical rocks is locally abundant at the bottom of the basinal facies in Baffin Island and West Greenland. Rocks of biotite grade are exposed in the Dewar Lakes area of central Baffin Island, where two episodes of low P-high T metamorphism, and three periods of regional deformation are defined. The first metamorphism (M_1), uniformly sillimanite-grade and recognized only in the lower metapelite-quartzite assemblage, occurs over hundreds of square kilometres. The second metamorphism (M_2) affects the entire supracrustal sequence, and increases progressively southward from biotite to migmatite grade. The first deformation and metamorphism were contemporaneous; D_1 recumbent-fold axes trend E-W, but the kinematics are unclear. D_2 north-directed transport accompanied M_2. Elliptical Archean-basement-cored domes characterizing D_3 are compressional features.

Résumé

La stratigraphie de la zone comprend un faciès de plate-forme à la base (carbonate, quartzite, pélite) recouvert par un faciès de bassin de flysch turbiditique. Un assemblage de roches mafiques et ultramafiques comprenant coulées, sills, roches épiclastiques et chimiques est localement abondant à la base du faciès de bassin dans l'île Baffin et au Groenland occidental. Des roches du faciès métamorphique à biotite affleurent dans la région de Dewar Lakes au centre de l'île Baffin où deux épisodes de métamorphisme de faible P-haute T° et trois épisodes de déformation régionale ont été reconnus. Le premier métamorphisme (M_1), partout de la zone à sillimanite et présent seulement dans l'assemblage inférieur métapélite-quartzite est observé sur des centaines de km^2. Le deuxième métamorphisme (M_2) affecte toute la suite de couverture et augmente progressivement vers le sud de la zone à biotite à celle de migmatite. La première déformation et le premier métamorphisme sont contemporains; les axes de plis couchés D_1 sont d'orientation est-ouest, mais leur cinématique n'est pas claire. Transport de direction nord pendant D_2 accompagne M_2. Les dômes elliptiques à centre de socle archéen caractérisant D_3 résultent d'une compression.

[1] School of Geological Sciences, Kingston Polytechnic, Kingston upon Thames, England, KT1 2EE, U.K.
[2] Mineral Resources Division.
[3] Department of Geological Sciences, McGill University, Montréal, P.Q., H3A 2A7.

INTRODUCTION

The 1988 field season followed up on the work of 1987 which concentrated on the area of the Dewar River and along the Boas River to the east. The main objectives of the project were to carry-out detailed mapping in order to clarify the stratigraphy, structure and metamorphisn of the area. Special emphasis was placed on defining the extent and number of mafic and ultramafic units within the supracrustal succession, as well as their possible economic potential.

This report concentrates on new data gathered during 1988 and how they affect the 1987 interpretations, and only briefly repeats some of the previous results. In Baffin Island, the Foxe Belt is composed of Archean granitic gneiss overlain by a Proterozoic cover. A thin quartzite-metapelite unit at the base is overlain by an assemblage of mafic-ultramafic flows and sills with associated epiclastic beds and iron-formation, which passes upward into a thick succession of psammitic-to-pelitic metagreywacke. Towards the south, in the supracrustal belt, metamorphism increases to migmatite grade, and basement and cover are progressively assimilated by 1.9-1.7 Ga granite batholiths.

Because structural styles vary, especially in proximity to the Archean basement and the migmatite zone, our observations are presented in three sections: 1) Structure of the Dewar River area, 2) Structure of the Western River and 3) Regional metamorphism (Fig.1).

STRUCTURE OF THE DEWAR RIVER AREA

Mapping of basement-cored antiforms continued with the aim of establishing the kinematics of early Proterozoic displacements. Structural analysis concentrated on the South Jackson Lake and Harris Lake antiforms (Fig.2). In this account, attention is focused on the eastern part of the Harris Lake antiform.

Our earlier work in the north of the area did not determine whether the large ductile strains recorded in the rocks were due to crustal shortening or crustal extension (Henderson et al., 1988). In the Harris Lake area however, cross sections drawn by Tippett (1984) show stratigraphic duplication by folding in the Harris Lake antiform (HLA). Our reinvestigation confirms basement-cover repetition in the antiform and additionally relates this to low-angle ductile overthrusting, most probably towards the north during D_2. This study also addresses a major problem outstanding from our previous work which concerns the kinematic significance of the occurrence of two sets of stretching lineations in the Foxe Belt along the Dewar River (Henderson et al. 1988, p.103)

STRUCTURAL INTERPRETATION OF HARRIS LAKE ANTIFORM

The structural interpretation shown in the geological sketch map (Fig.2) of the Harris Lake antiform (HLA) and of the

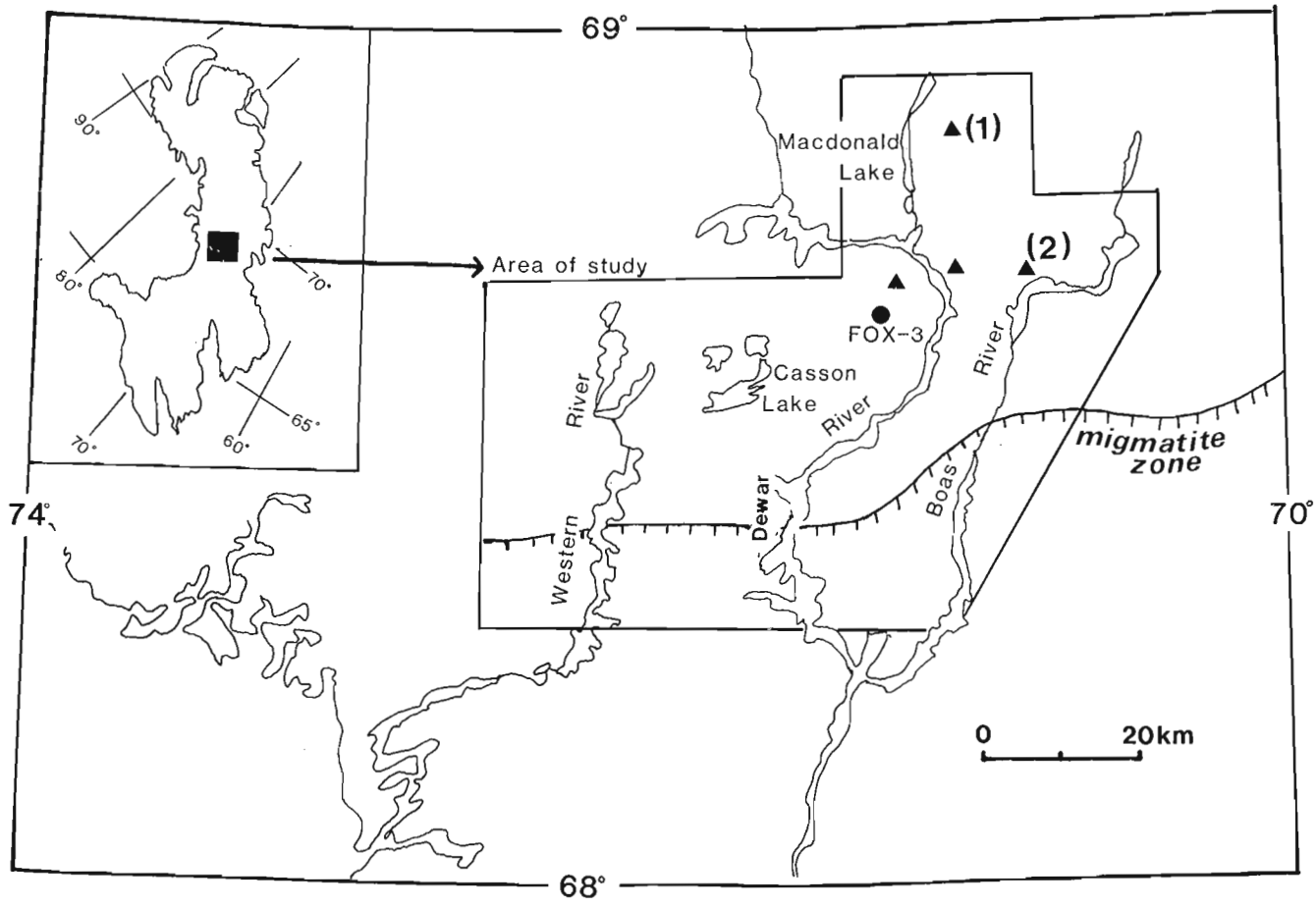

Figure 1. Location map showing principal geographical features mentioned in the text. Solid triangles mark locations of critical M_1 assemblages, and the hachured line marks the northern limit of the M_2 migmatite zone.

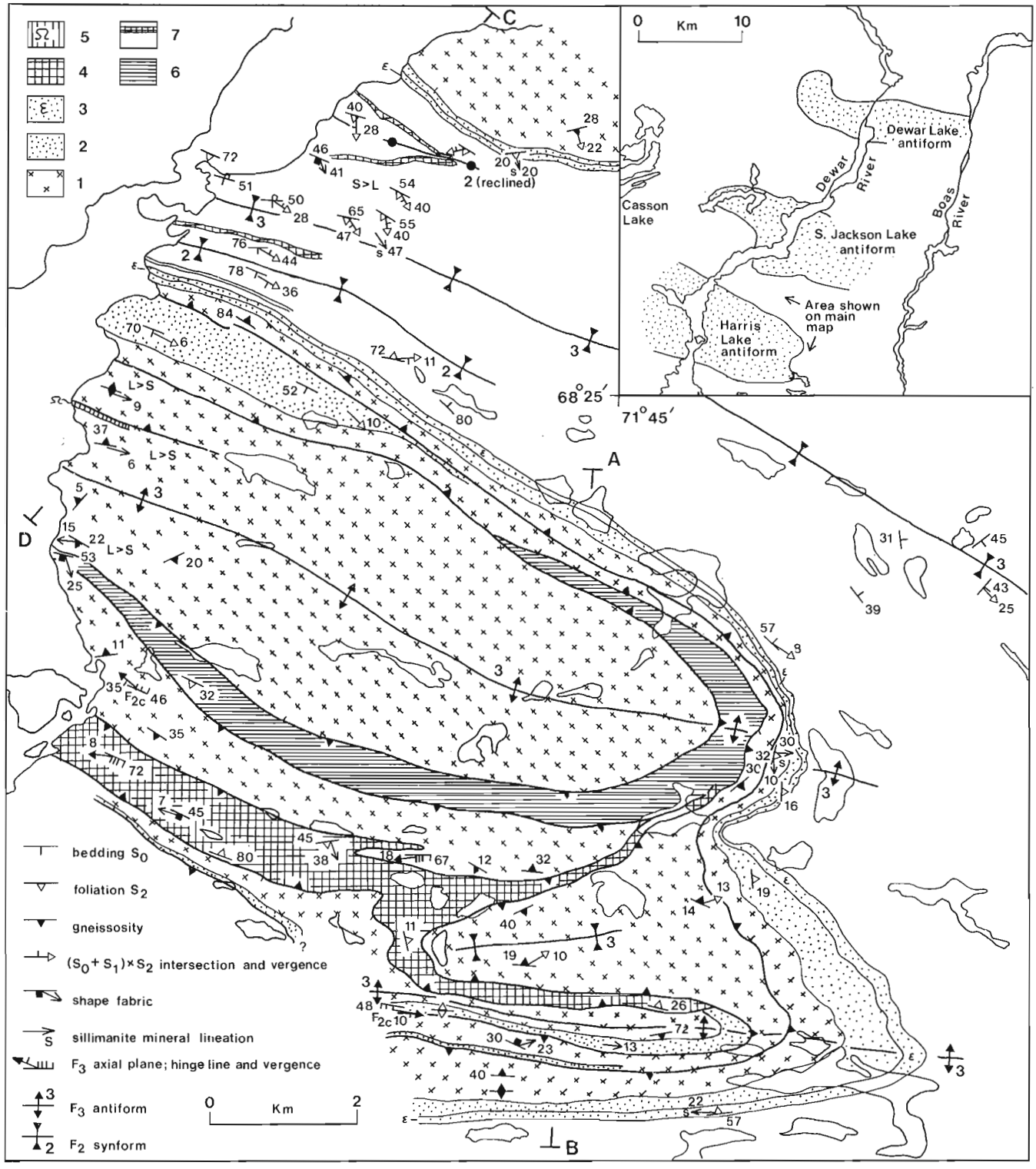

Figure 2. Geological sketch map of eastern Harris Lake antiform. Key to ornaments: 1 (biotite granodiorite gneiss), 2.(quartzite), 3 (quartzite + metapelite), 4 (quartzitic paragneiss with amphibolite layers to 100m thick), 5.(marble + calcsilicate gneiss), 6 (ultramafic + amphibolitic sheets & lenses interleaved with granodiorite gneiss), 7 (psammitic-pelitic metagreywacke + amphibolite layers), unpatterned area is underlain by metagreywacke. D_1, D_2, and D_3 are recognized throughout the Dewar Lakes area (Fig.1). Folds designated F_{2c} formed between D_2 and D_3, and are not recognized outside of the area of Figure 2. Lines of cross-sections A-B and C-D (Fig.3) are shown.

synformal domain to the north which separates it from the South Jackson Lake antiform (SJLA) is amplified by two cross-sections (Fig.3). These figures reveal a pile of thin basement-cover thrust sheets folded by rather upright folds responsible for the basement-cored dome which is the major element of the map pattern. The thrust sheets are dominated by thin basement slabs, while thrust zones are decorated by slices of strongly ductilely deformed cover (c.f. Pulvertaft,1986). Where these slices consist of mafic-ultramafic rocks, derived from a sequence of flows and sills, believed to occur stratigraphically at the base of the turbidite flysch, omission of the underlying quartzite-metapelite formation indicates that out-of-sequence thrusting (Morley,1988) was involved. Assuming that Figure 3 was drawn in the transport direction (see below), absence of mafic-ultramafic rocks in the footwall of thrust T_2 demonstrates a minimum displacement of 5km on this surface alone.

Timing of thrusting

Most of the rocks depicted in Figure 2 contain a penetrative foliation. At several localities in micaceous quartzite and at one locality in metagreywacke, it could be demonstrated in the field that this foliation is a crenulation cleavage, S_2. Increase in the intensity of this fabric towards lithological contacts, inferred to be tectonic because of the omission or duplication of stratigraphy, suggests that thrust interleaving was D_2. This does not rule out that thrust interleaving also occurred during D_1.

Direction of thrusting

Most lineations at deeper structural levels in the eastern part of Harris Lake antiform trend E-W with a shallow plunge (Fig.2). Northwards, within the area underlain by metagreywacke, lineations of all types become progressively more steeply pitching on S_2 and the resultant change into a N-S trend persists into the upper part of the basement of the South Jackson Lake antiform (Fig.2).

The linear element of shape fabrics tends to dominate in basement gneiss (Fig.2, L>S domains). In contrast, the metagreywackes exhibit more steeply pitching linear fabrics which become N-S trending as dip decreases to the north. They contain L_2 intersection lineations, sillimanite-quartz-aggregate shape fabrics with an oblate shape and sillimanite lineations. Lineation domains such as these can be identified throughout the Dewar River area.

It is tempting to relate the E-W linear elements at deeper structural levels of the Harris Lake antiform to formation of D_2 basement-cover thrust sheets. However a number of observations argue against this interpretation.

1) In the zones of highest D_2 strain, where strongest E-W lineations would be expected, lineations are weak or absent.

2) Prominent E-W lineations and L>S tectonite fabrics occur in lower strain domains between thrust zones (Fig.2).

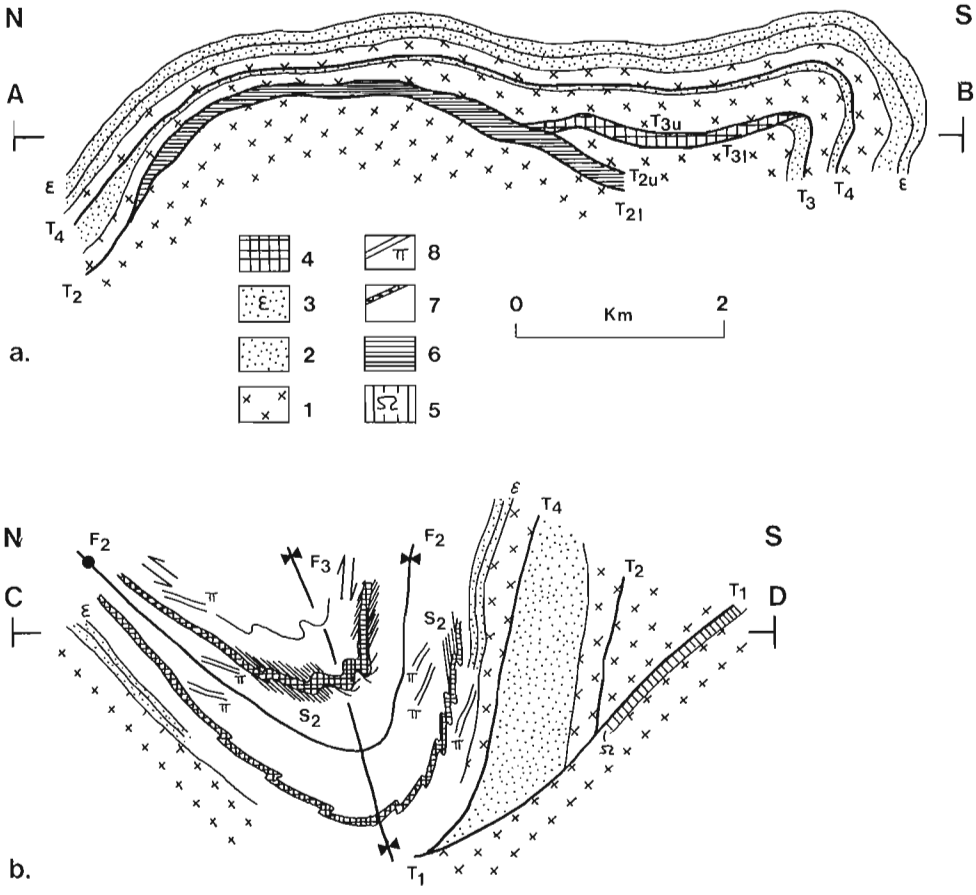

Figure 3. Cross-sections drawn through the area of the Harris Lake antiform (Fig.2). Ornamentation of rock units is the same as Figure 2. See text for discussion.

3) Some N-S trending sillimanite mineral lineations and stepped slickenfibre lineations indicating transport of the hangingwall to the north occur in the quartzite-metapelite formation which mantles the Harris Lake antiform. These lineations are present in domains generally dominated by E-W lineations. On the other hand, E-W gently plunging mineral lineations have not been observed in the domain of steeply pitching or N-S trending lineations between Harris Lake antiform and South Jackson Lake antiform. However Henderson et al. (1988), described N-S sillimanite lineations folded by F_2 in the Boas River area which they attributed to D_1.

4) Branch lines in the Harris Lake antiform thrust pile trend E-W, implying N-S transport. For example an E-W branch line between thrusts T_1 and T_2 (Fig.3b) exists because T_1 is parallel to a strongly ductily deformed screen of marble and dips moderately N (Fig.2), whereas T_2 dips steeply N in the hangingwall of T_1, parallel to foliation in the hangingwall which becomes intense in a zone of ultrabasic lenses which decorate T_2 near Harris Lake.

These observations are consistent with formation of the basement-cover thrust sheets of the Harris Lake antiform during D_2 overthrusting to the north. Steeper pitch of L_2 in the greywacke, their progressive reorientation to a N-S trend and development of oblate shape fabrics in sillimanite-quartz aggregates are all consistent with higher progressive D_2 strain to the N between Harris Lake antiform and South Jackson Lake antiform.

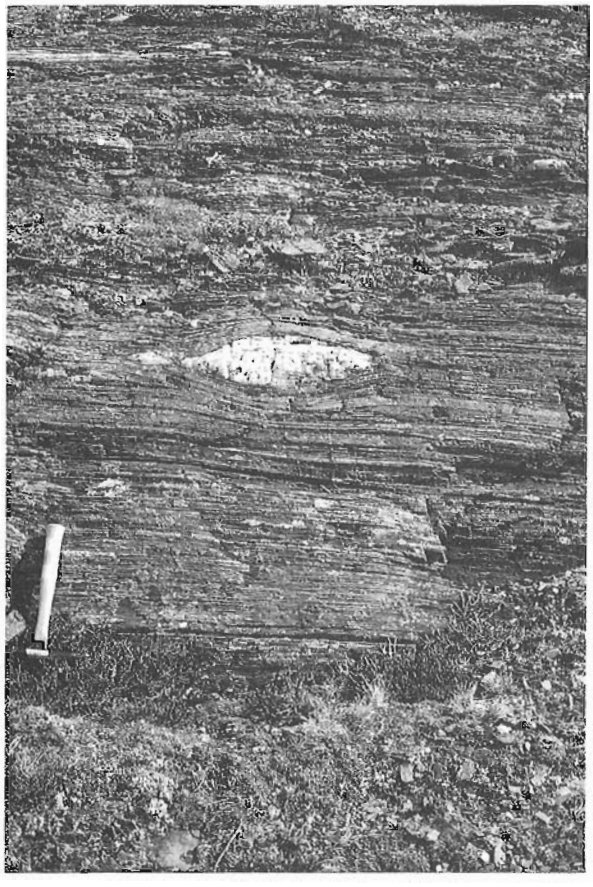

Figure 4. Mylonitic metagreywacke on the steeply dipping south limb of the Dewar Lake antiform (Fig.1, Inset) containing a quartz lens slightly asymmetric to the trace of the mylonitic foliation. The asymmetry is interpreted to signify a dextral shear-sense during D_1. GSC 204726-Q.

Relative age of Harris Lake antiform

Crenulations and close to tight mesoscopic folds deform S_1 and S_2 throughout the eastern Harris Lake antiform area. The D_1 and D_2 structures are folded by upright to steeply inclined periclinal F_3 (Fig. 2, 3). The Harris Lake antiform can be interpreted as a major F_3. However the D_2 thrust geometry described suggests that a D_2 antiformal stack may contribute to the geometry of Harris Lake antiform. To the north, a major F_2 in metagreywacke is refolded by an F_3 synform. Flexural slip on the limbs of this F_3 synform apparently has permitted emplacement of D_3 pegmatites in tension gash orientations (Fig.3b).

CORRELATIONS

The structural evolution outlined above can be integrated with that of Henderson et al. (1988), although some interpretations must be modified. In the Dewar Lake antiform (DLA), gneissic basement with a cover of quartzite, pelite and amphibolite is mantled by a major mylonite zone at the base of the metagreywacke formation. Asymmetric back-rotated quartz lenses derived from veins suggest that displacement of the hanging wall was to the west (Fig.4).

S_2 in the quartzite verges off the Dewar Lake antiform crest both N and S (Henderson et al.1988, Fig.4). It was thought that S_2 intensified structurally upwards into the mylonitic shear zone but subsequent thin section study shows that a distinct angle between S_2 biotite foliation and mylonitic layering persists throughout the shear zone. The intersection between S_2 and mylonitic layering yields a subhorizontal, faint, E-W lineation in the mylonitic rocks. This overprinting raises the possibility that formation of the mylonitic layering was a D_1 event. Since quartz lens asymmetry (Fig.4) seen on surfaces perpendicular to the dip of the mylonitic layering seems related to the mylonitic deformation, cover-to-the-west transport may be associated with D_1 rather than D_2 as stated in our previous report. However it should be noted that there is no evidence of E-W transport in the Western River area where D_1 structures can be recognized.

Mylonitic rocks at the base of the metagreywacke also mantle the South Jackson Lake antiform and, like those of the Dewar Lake antiform, they are interpreted as accomodating hanging wall-to-the-west displacement during D_1. Strongly deformed rocks also occur at the base of the greywacke in the Harris Lake antiform, but asymmetric quartz lenses do not provide a systematic kinematic indicator.

The gently east plunging North Jackson Lake synform (NJLS) lies between the Dewar Lake antiform and the South Jackson Lake antiform (Fig.2). Traced to the W, the axial trace of this fold can be seen to post-date a large F_1 isoclinal recumbent fold (Fig. 5, 7). The axial plane cleavage of the North Jackson Lake synform is therefore probably S_2. In the Dewar River area, below this synform, but above the mylonitic shear zone of the Dewar Lake antiform, S_o/S_2 intersection lineations rotate towards a steeply pitching

stretching lineation defined by sillimanite-quartz aggregates and quartz shape fabrics. S_2 associated with the North Jackson Lake Synform can also be traced continuously down the structural section into the mylonitic rocks where it overprints the mylonitic foliation. This allows correlation of S_2 throughout the supracrustal sequence on the S side of the Dewar Lake antiform.

In the Harris Lake antiform, D_1 appears to have been a large strain, possibly having an E-W extension lineation, now reflected as a component in shape fabrics strongly modified by D_2. These remarks also apply to D_1 of the Dewar Lake antiform where in addition D_1 mylonites accomodated transport of the hangingwall to the west. Finally, D_3 upright folding comprised a component of the Harris Lake antiform and may be responsible for other upright E-W trending folds in the Dewar River area.

AREA OF THE WESTERN RIVER

The area along the Western River (Fig.5) was propitious to mapping for several reasons. Logistically, because raised terraces provide good landing strips, and navigable water exists across strike for 30km, and geologically, because macroscopic folds of three generations have a common, gentle eastward plunge (Fig.6) which permits easier down-plunge viewing than in the Dewar River area. Also the mafic-ultramafic rock assemblage provides a very good marker horizon for mapping macroscopic folds. Metamorphism in the northern part of the Western River was moderate and permitted a few bedding-facing determinations; in the south, widespread migmatization occurred which totally obliterated primary-facing indicators. The main points made clear in the mapping of this area are summarized below.

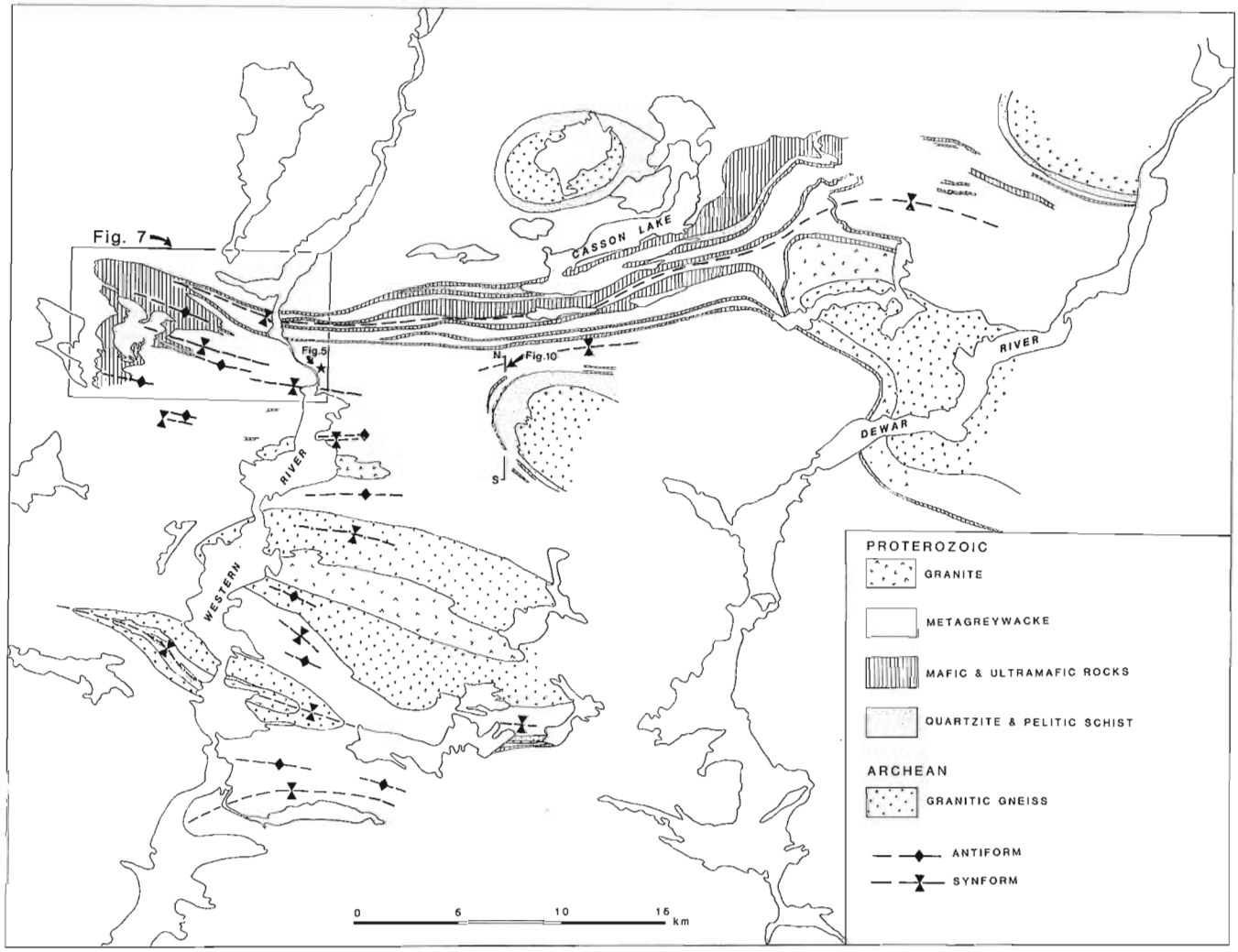

Figure 5. Geological sketch map of Western River area. Axial traces of D_2 folds are shown. The area of Figure 7 is outlined, and the line N-S shows the location of the diagrammatic cross-section in Figure 10. The star marks the location of Figure 8.

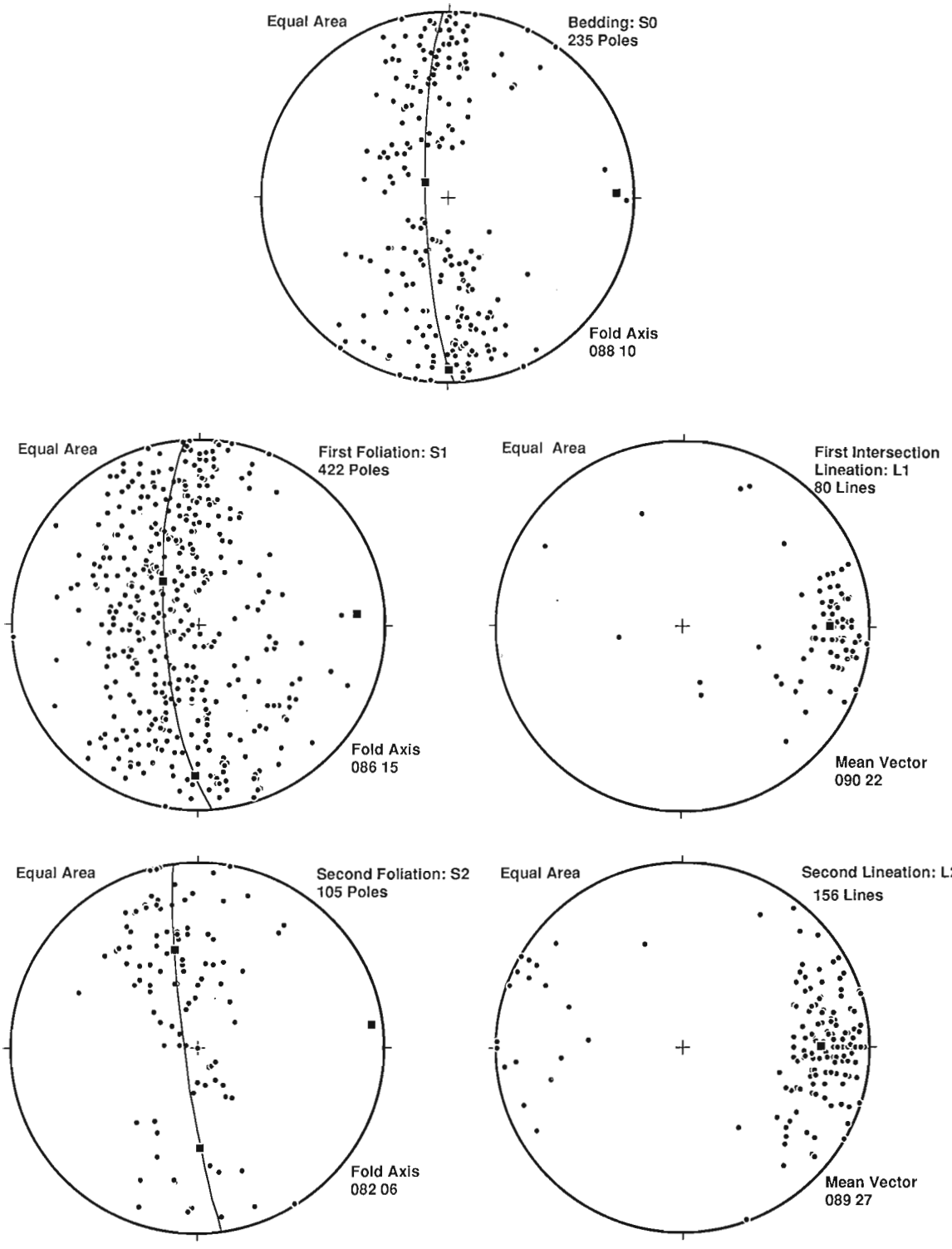

Figure 6. Lower-hemisphere equal-area projections of structural fabric elements from Western River area (Fig.5). The solid squares on plots of poles to planar elements are the three eigenvectors defining best-fit great-circle girdles and fold axes. Solid square on plots of linear elements is the cone axis defining the best-fit fold axis. (Compiled on Stereonet program courtesy of R. Allmendinger).

1) The extreme western limit of the mafic-ultramafic assemblage within the Western River area is characterized by a uniformly south-directed S_1 vergence, an inverted stratigraphy, and a N-S regional strike with a gentle E dip. These data are interpreted to define the lower limb of a large east-plunging, reclined D_1 fold (Fig.7). The sequence youngs away from the vergence boundary along its reclined western portion. The U-shaped trace of the D_1 fold is due to coaxial D_2 (? and D_3) refolding. Mapping in the area is incomplete, and it is not definitely known whether the fold closes to the south or the north. If it closes north, it is a downward-facing anticline, and may be a parasitic fold on the overturned limb of a larger north-closing D_1 fold-nappe. Tippett (1984) postulated a similar structure on the basis of regional stratigraphic relationships in the Casson Lake area (Fig.5).

2) D_1 has an associated penetrative cleavage which commonly appears parallel to or makes a very small angle with bedding. Where bedding-parallel shear during D_2 is the reverse of D_1 cleavage vergence, an S_2 crenulation cleavage is developed. S_2 crenulations are most noticeable in pelitic units, where their progressive increase in amplitude and refraction can be used as an indication of graded bedding and stratigraphic facing (Fig.8). On D_2 fold limbs where bedding-parallel shear and S_1 vergence are in the same orientation during D_2 and D_1, the early cleavage is reinforced and is parallel to bedding and no crenulation cleavage occurs (Fig.9).

3) D_3 does not have an associated cleavage, but D_3 folds rotate the previous cleavages and minor folds, commonly causing "off the dome" vergence. This is illustrated in Figure 10, which is a diagrammatic N-S section through the western termination of the Harris Lake antiform along the line shown in Fig.5. The D_3 olds are periclinal, and appear to be restricted to a NNE-SSW trending belt between Western and Dewar rivers (Fig. 2, 5).

4) To the southwest of the mapped area shown in Figure 5, D_1 is not distinguishable, most probably because of an obliteration of D_1 minor folds resulting from the combined increase in the intensity of D_2-related deformation and metamorphism (M_2). There is no doubt that D_1 affected the area however as S_2 is commonly a crenulation cleavage and D_2 folds deform a bedding-parallel differentiated layering.

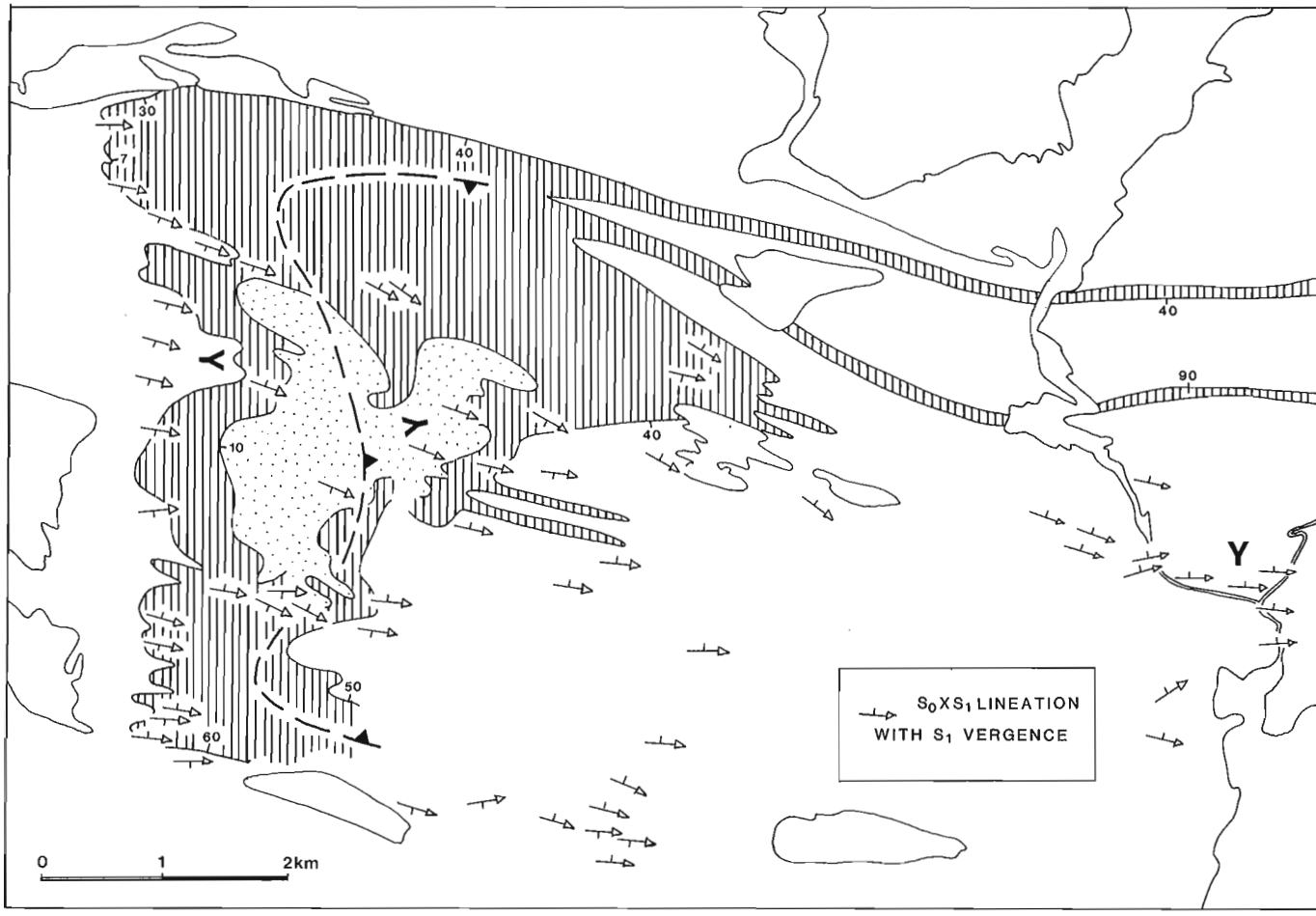

Figure 7. Geological sketch map of northwest part of Western River area showing a portion of the axial trace of a D_1 fold reclined gently eastward. The F_1 vergence boundary is indicated by the thick dash line. The rocks young away from the vergence boundary. S_0XS_1 intersection lineations plunge 5-20° E. See text for further explanation.

5) Both D_2 and D_3 mesoscopic folds increase in abundance southward into the migmatite terrane. The vergence of the D_2 fold-thrust system appears to be northward. The D_3 fold system does not reveal a systematic vergence, but the southward increase in abundance of F_3 structures suggests northward vergence.

METAMORPHISM

Jackson and Morgan (1978) recognized that the Foxe Belt in central Baffin Island is affected by high T-low P metamorphism. Subsequently, Tippett (1984) showed that the area around Dewar Lakes is characterized by a syn-kinematic metamorphism (high T-low P) increasing from NW to SE, reaching conditions of T=720°C at 4 kbars (400MPa) in the migmatite zone. He also showed that the grade of metamorphism varies from upper greenschist to granulite facies and that the isograds are folded. Henderson et al. (1988) showed that a metamorphic hiatus or very steep isotherms exist between the quartzite-metapelite sequence and the overlying turbiditic metagreywacke facies. They suggested that a metamorphic hiatus, if present, may be due to extensional shearing post-dating an early metamorphism.

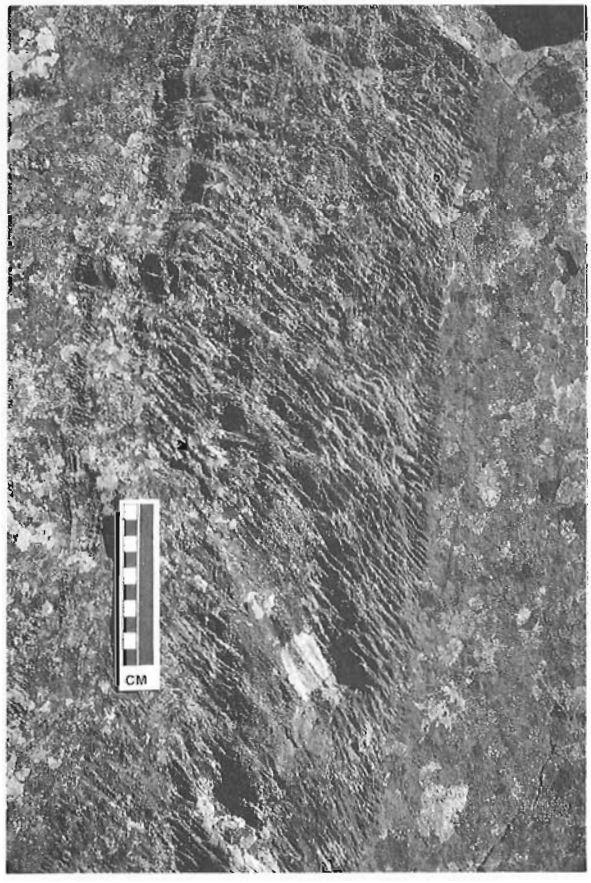

Figure 8. Steeply north-dipping metaturbidite beds with south-dipping S_2 crenulation cleavage developed only in the pelitic part of the beds. The slight steepening of S_2 toward the south suggests cleavage refraction toward the top of a graded bed. Outcrop on Western River at the star on Figure 5. GSC 204726-J.

Two metamorphic events around Dewar Lakes area

Field work in 1988 showed that the Dewar Lakes area (Fig.1) is characterized by two metamorphic events (M_1 and M_2) of medium-to-high temperature and low pressure. Both belong to the andalusite- sillimanite facies series. The first metamorphism (M_1) is syn-D_1 and is recognized over several hundred kilometres. M_1 reaches the staurolite-sillimanite zone (staurolite-out reaction) and has been recognized only in the lowest part of the supracrustal sequence (quartzite-metapelite, rarely amphibole-iron formation). M_1 is apparently truncated by a high strain or mylonite zone at the base of the metagreywacke sequence.

The second metamorphic event (M_2), was syn-D_2 and shows an increase in grade from upper greenschist north of Dewar Lake antiform to migmatite at the southwest limit of mapping (Fig.1). M_2 affects the entire supracrustal sequence and probably also the granitic basement. A post-D_2 retrograde metamorphism locally affects rocks in the area.

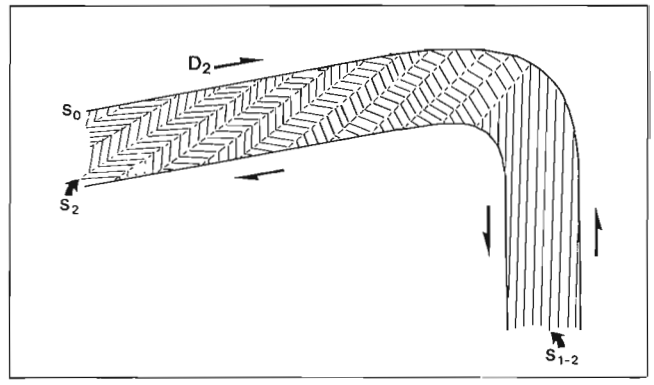

Figure 9. Diagrammatic illustration of S_2 crenulations preferentially developed on D_2 fold limbs where S_1 vergence is in the opposite sense to D_2 bedding-parallel shear.

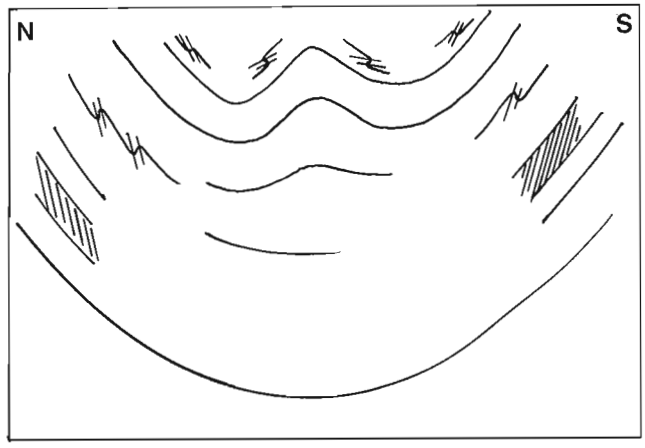

Figure 10. Diagrammatic cross section showing off-the-dome vergence ("cascading folds") resulting from the D_3 Harris Lake antiform uplifted within a larger D_2 synform. See Fig 5 for location of line N-S.

First metamorphism (M1)

Coarse muscovite-biotite +/- garnet is widespread in compositionally layered quartzite-metapelite. Crenulated fibrous sillimanite and deformed coarse sillimanite crystals are common in most metapelitic layers. Kink bands and folded muscovite-biotite porphyroblasts and a strong metamorphic layering (S_1) suggest that M_1 was syn-D_1. However, kinked muscovite after sillimanite, and similar structural features can be related to D_2 and possibly D_3. The effect of M_2 overprinting M_1 becomes stronger from N to S and southward from Dewar Lake antiform it becomes difficult to distinguish between the two metamorphic events.

In the most northern part of the region studied, east of MacDonald Lake (Fig.1 locality 1), M_2 is low grade (biotite zone) and does not affect M_1 assemblages except for some M_2 muscovite and chlorite and late growth of garnet. In a single exposure, a 10m thick pelitic unit overlying the basal quartzite shows strong compositional layering with quartz-rich and mica-rich centimetre scale layers. M_1 assemblages from the metapelite are:

1) garnet-staurolite-muscovite-quartz-plagioclase,
2) garnet-staurolite-quartz-plagioclase +/- muscovite,
3) garnet-staurolite-sillimanite-biotite-muscovite-quartz-plagioclase,
4) garnet-sillimanite-biotie-muscovite-quartz-plagioclase.

In assemblages 1 to 3, prograde chlorite is observed as inclusions in garnet, and staurolite is observed as inclusions in garnet in assemblage 4. Two possible reactions to produce these mineral assemblages are:

chlorite + garnet + muscovite =
staurolite + biotite + H_2O (M_1A)

staurolite + muscovite =
garnet + sillimanite + biotite + H_2O (M_1B)

The pelitic schists consist of layers rich in garnet porphyroblasts (>70% garnet) alternating with garnet-staurolite-quartz rich layers (Q domains) and mica-sillimanite layers (M domains). The Q domains are composed of garnet porphyroblasts (5 to 30mm) in a matrix of coarse staurolite, muscovite, fibrous sillimanite and biotite. Garnet porphyroblasts show a history of complex growth; an inclusion-free core is surrounded by a star-like pattern of opaque inclusions and finally by an inclusion-free rim which is commonly corroded at contacts with M domains.

Some garnets show minor rotation, but most of them appear to have simply overgrown the matrix during D_1. Apparently, quartz was removed by solution in M domains, concentrating garnet and fibrous sillimanite-wrapped garnet porphyroblasts. Complex crenulations in fibrous sillimanite layers suggest sillimanite is syn-D_1 and subsequently was folded during D_2. Coarse prismatic sillimanite is locally found in some lenses wrapped by fibrous sillimanite; it is also found as inclusions in garnet suggesting a two-stage

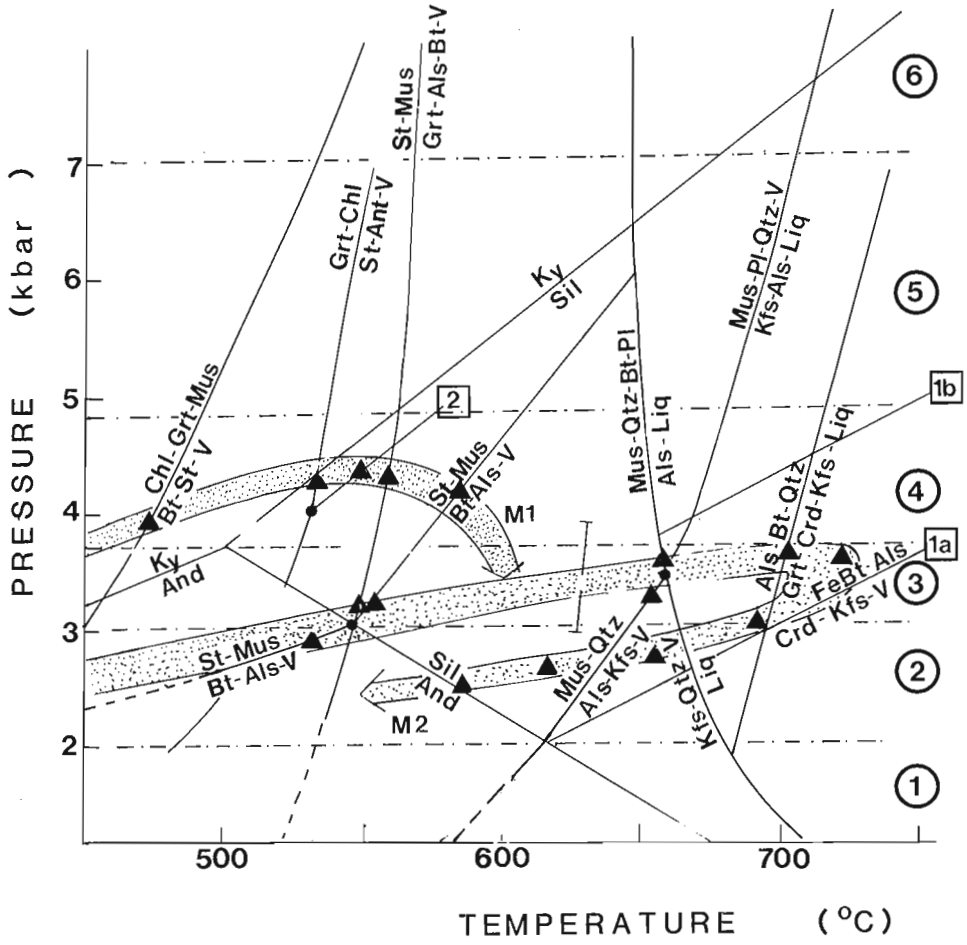

Figure 11. P-T diagram (M. St-Onge, pers. comm.) for Dewar Lakes area. M_1 and M_2 paths are based on assemblages observed in thin section (solid triangles). Line 1a is Fe biotite + aluminosilicate = cordierite + - microcline + vapour, and line 1b is the same reaction, but with 30 mole% Fe (from Jamieson, 1984). Line 2 is the reaction staurolite + anthophyllite = garnet + cordierite + vapour. Bathozones 1-6 are from Carmichael (1978).

growth of sillimanite. Locally, staurolite porphyroblasts show syn-D_1 growth and deformation and probable recrystallization during M_2-D_2. Some garnets show an inclusion trail (S_i) in the core with inclusion-free rims possibly representing an M_2 overgrowth. From this outcrop and from other nearby localities, it is clear that the centimetre scale compositional layering is metamorphic.

In the Boas River area (Fig.1, locality 2), the assemblage garnet-ferrogedrite-cordierite-staurolite-biotite-quartz-ilmenite was found in a metapelitic bed associated with iron-formation overlying the quartzite-metapelite sequence. Chlorite inclusions in garnet suggest the following reaction occurred:

chlorite + garnet = ferrogedrite + staurolite (M_1C).

However, staurolite is only found in quartz-rich layers with ferrogedrite, and the occurrence of cordierite coexisting with garnet is probably produced by the reaction:

staurolite + ferrogedrite = garnet + cordierite + H_2O (M_1D).

The conditions for M_1 (Fig.11) were from T = 500-600°C in bathozone 4 (Carmichael, 1978). The M_1 peak was probably reached during D_1

Second metamorphism (M_2) in pelitic rocks

M_2 was coeval with D_2 and charnockite-granite emplacement in the south. M_2 affected the entire supracrustal sequence and increases from upper greenschist (biotite zone) to granulite facies (in migmatite zone). Evidence of M_2 overprinting M_1 is observed in the basal sequence (quartzite-metapelite) but it becomes difficult to distinguish between M_1 and M_2 in the staurolite-sillimanite zone. However, andalusite is a diagnostic mineral for M_2; where it is present in quartzite-metapelite, it overgrows M_1 assemblages.

M_2 can be divided into 5 zones in the mapped area.

1) biotite zone
2) staurolite-andalusite zone
3) sillimanite zone
4) sillimanite-microcline zone
5) cordierite-garnet zone

Zones 4 and 5 can also be grouped together to form the migmatite zone.

Field mapping of these zones showed that the pattern of isograds is very complex. Except for the migmatite (melting) isograd, which is clearly defined, all other isograds show a distribution reflecting the effect of folding during D_2 and D_3.

Timing of M_2 with phases of deformation and retrogression

Textural evidence, such as garnet porphyroblasts including S_1 as S_i and deflecting S_2, suggests that M_2 porphyroblasts grew from early to late D_2 and were deformed and probably recrystallized in some cases during D_3. It is clear that M_2 index minerals show a sequential growth during D_2 in pelitic parts of the metagreywacke sequence. Where M_1 is overprinted by M_2, the growth of porphyroblasts resulted in a complex history. Figure 12 shows the apparent growth history of metamorphic minerals of M_1 and M_2 from D_1 to D_2. Evidence of M_1 and D_1 in the migmatite terrane has been completely obliterated by M_2. Porphyroblasts grew during D_2 in the migmatite and the main foliation is S_2. The migmatitic layering is folded, indicating that F_3 mesoscale folds appear ubiquitously in the migmatite terrane; whereas mesoscale F_3 are rare features in the lower-grade rocks. Syn-D_2 growth of index minerals produced rotation and

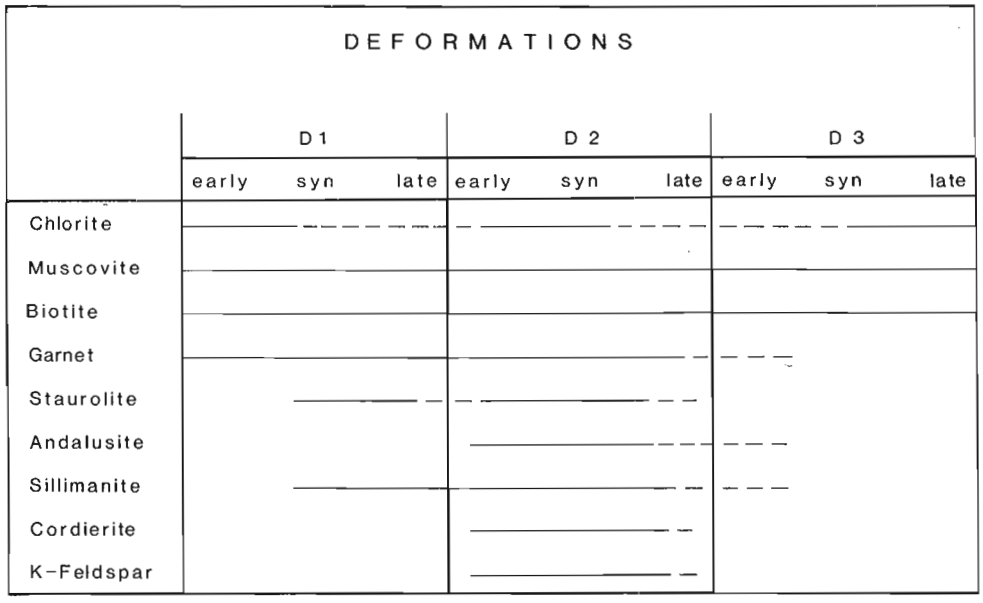

Figure 12. Chart showing the growth of certain minerals with phases of deformation.

syn-kinematic growth of garnet, elongated growth of cordierite parallel to S_2 and a N-S lineated sillimanite fabric. Leucosome indicates that it was folded as it formed during D_2, but it is also seen to crosscut S_2, suggesting that M_2 outlasted D_2 folding in the migmatite zone. Polygonization of D_2 fabrics and recrystallization at medium-to-low temperature accompanied D_3.

Retrograde andalusite, muscovite, chlorite, green biotite and pinitization of cordierite are the result of an influx of water during or after D_3, at temperatures between 300 and 450°C. In zones 1 to 3, this retrogression is patchy. Muscovite, chlorite and green biotite formed at the expense of M_2 minerals. Kinked, retrograde muscovite suggests that some retrogressive minerals grew during D_3 or were deformed later.

DISTRIBUTION AND DEFORMATION OF PEGMATITES

Many pegmatite dykes cut up-section, from the Archean basement into the basal quartzite-metapelite sequence. These granitic pegmatites were injected and deformed during late stages of D_1 and during D_2. North of the Dewar Lake antiform, pegmatites are mainly affected by D_1 and D_2 shearing. However relatively few of the pegmatites cross the quartzite-metagreywacke contact and most are limited to the Archean basement and the lower few hundred metres of cover rocks. As the migmatite zone is approached, pegmatites become ubiquitous and show strong D_2 and D_3 folding. Most appear to be late D_2-early D_3 and cut older granites which appear to be related to the batholiths south of the mapped area (Fig.1).

Spatially, the migmatite zone is closely related to the distribution of early tectonic granites. From Tippett's(1984) map and our preliminary compilation, it seems that the cordierite-garnet isograd follows the northern contact of the south Baffin batholith zone. Two questions can be asked. Is M_2 produced by the emplacement of these batholiths, or is a high geothermal gradient responsible for producing both M_2 and the batholiths?

It is clear that these two events are related and it implies that M_2 developed under a high geothermal gradient typical of the andalusite-sillimanite facies series. An integrated model must consider tectonic regimes involving both high temperature and compressional deformation without major crustal thickening.

ECONOMIC MINERAL POTENTIAL

The mafic-ultramafic unit and associated iron formation have been mapped continuously along strike for over 40km. They are repeated by folding and thrusting during D_1 and D_2 and retrograded by the contemporaneous metamorphisms. Analyses of selected samples collected in 1987 have not revealed any highly anomalous base or precious metal values. Ni content of ultramafic rocks is average, and apparently does not bode well for PGE potential (L. Hulbert, pers. comm.). The iron formation is composed primarily of pyrrhotite and graphite and the maximum Au value in samples analyzed so far is 40 ppb.

Analyses of metagreywacke bedrock samples selected from eight localities close to lakes with sediment As anomalies in excess of 250ppm reported by Cameron (1986) have given As values of 16 to 56ppm, but with no associated Au values. These localities are northwest of the areas easily accessible by walking from the Western and Dewar rivers, and more detailed helicopter-supported follow-up work in future is necessary to determine the bedrock source of the arsenic.

CONCLUSIONS

Preliminary results from this past field season demand some revision of the 1987 interpretations. The Piling Group sequence of basal quartzite-pelite, chemical sediments plus mafic rocks and psammitic-pelitic turbidites argues for an extended passive margin environment of deposition. It was previously thought (Henderson et al., 1988) that D_1 may have been a ductile extensional event because of the absence of D_1 compressional features in the northern Dewar River area. Mapping in the Western River area has revealed the existence of large D_1 recumbent folds. Farther south, an increase in M_2 and D_2 has obliterated evidence of D_1, and we have too little evidence to speculate on the polarity of D_1 compression.

N-S sillimanite lineations may indicate north-directed D_1 and D_2 transport. Recumbent D_2 folding is also observed in the Western River area. So far our work indicates that D_2 produced north-verging folds, with thrust detachments and basement-cover imbrications most obvious on the flanks of basement-cored D_3 antiforms along Dewar River.

D_3 produced relatively upright folds that are very periclinal. Fold interference caused by D_3 is responsible for at least some of the basement-cored "domes" between Western and Dewar rivers. For example, the west-plunging, west end of the Harris Lake antiform occurs in the middle of a larger east-plunging D_2 synform, but the east end of the Harris Lake antiform may be due partly to D_2 imbrication of basement-cover thrust slices.

Along Dewar River, an E-W lineation represented by sillimanite and quartz-shape fabrics is interpreted as extensional, but its age is ambiguous at this stage: F_1, F_2 and F_3 axes being also generally E-W trending. In the Dewar River area a top-to-the-west sense of shear may be correlated with D_1, however lack of evidence for E-W extension during D_1 in the Western River area may argue for a shear localized in the vicinity of the basement-cover contact that does not persist into the Western River region.

Metamorphic analysis is in agreement with the structural sequence presented above. Progressive metamorphism during D_1 brought the basal sequence to sillimanite zone, but the overlying metagreywacke remained in biotite zone. It is obvious now that M_1 lower-grade rocks overlie significantly higher-grade rocks, and that they are separated by a D_1 shear zone. Beyond this, the D_1/M_1 event is not clear. During M_2 a general increase of metamorphism southward at relatively low pressure accompanied D_2 north directed thrusting and folding. The relationship between the D_2/M_2 event and the south Baffin batholith emplacement is not clear at this point.

ACKNOWLEDGMENTS

Isabelle Derome, Peter Heijke, and Suzanne Nacha contributed significantly to the mapping. We thank Bill Morgan for providing us with unpublished geological maps of the Western River area. Cees Van Staal kindly reviewed the manuscript, and offered many helpful criticisms. Helicopter support in mid-August was provided and partially subsidized by Polar Continental Shelf Project. We are very grateful for the many favours extended to us by the personnel at Dewar Lakes North Warning System site. Grocott gratefully acknowledges the Anglo-Canadian Scientific Exchange Scheme for funding his study visit to Canada. Heijke gratefully acknowledges the Dr. Schürmannfonds for trans-Atlantic travel expenses.

The study of ultramafic rocks within this project is supported by the Canada — N.W.T. Mineral Development Agreement, Project C1-2-4 carried by the Mineral Resources Division of GSC.

REFERENCES

Cameron, E.M.
1986: Regional geochemical reconnaissance: an introduction to the interpretation of data from Central Baffin Island, District of Franklin; Geological Survey of Canada, Paper 86-10, 22 p.

Carmichael, D.M.
1978: Metamorphic bathozones and bathograds: a measure of the depth of post-metamorphic uplift and erosion on the regional scale; American Journal of Science, v. 278, p. 769-797.

Henderson, J.R., Grocott, J., Henderson, M.N., Falardeau, F., and Heijke, P.
1988: Results of fieldwork in Foxe Fold Belt near Dewar Lakes, Baffin Island, N.W.T.; in Current Research, Part C, Geological Survey of Canada, Paper 88-1C, p. 101-108.

Jackson, G.D. and Morgan, W.C.
1978: Precambrian metamorphism on Baffin and Bylot Islands; Geological Survey of Canada, Paper 78-10, p. 249-267.

Jamieson, R.A.
1984: Low pressure cordierite-bearing migmatites from Kelly's Mountain, Nova Scotia; Contributions to Mineralogy and Petrology, v. 86, p. 309-320.

Morley, C.K.
1988: Out-of-sequence thrusts; Tectonics, v. 7, p. 539-561.

Pulvertaft, T.C.R.
1986: The development of thin thrust sheets and basement-cover sandwiches inthe southern part of the Rinkian Belt, Umanak District, West Greenland; Gronlands Geologiske Undersogelse Rapport 128, p.75-87.

Spear, F.S.
1986: Yet another petrogenetic grid for pelitic schists; Geological Society of America, Abstracts with Programs, v. 18, p. 758.

St-Onge, M.R.
1984: The muscovite melt bathograd and low-P isograd suites in north-central Wopmay Orogen, N.W.T., Canada; Journal of Metamorphic Geology, v. 2, p. 315-326.

Tippett, C.R.
1984: Geology of a transect through the southern margin of the Foxe Fold Belt (mainly NTS 27B), Central Baffin Island, District of Franklin; Geological Survey of Canada, Open File 1110.

Archean quartz arenites and pyritic paleoplacers in the Beaulieu River supracrustal belt, Slave Structural Province, N.W.T.[1]

S.M. Roscoe, M. Stubley[2] and D. Roach[3]

Roscoe, S.M., Stubley, M. and Roach, D., Archean quartz arenites and pyritic paleoplacers in the Beaulieu River supracrustal belt, Slave Structural Province, N.W.T.; in Current Research, Part C, Geological Survey of Canada, Paper 89-1C, p. 199-214, 1989.

Abstract

Quartz arenite recently recognized at Beniah Lake, 140 km northeast of Yellowknife, has been found to be part of a much more extensive formation, the Beniah formation, deposited at the base of the northern part of the Beaulieu River supracrustal belt. Another clastic sedimentary unit, divisible into conglomerate and quartzose arenite members, has been found as a synclinal remnant unconformably overlying volcanic rocks. Folds and cleavage in these strata reflect a complex history of deformation in the belt. Slightly uraniferous, slightly auriferous, pyritic quartz pebble beds are present in both formations. These reveal the existence in the Slave structural province of a potential exploration target - pyritic gold paleoplacers.

Résumé

On a constaté qu'une arénite quartzique, récemment identifiée au lac Beniah à 140 km au nord-est de Yellowknife, faisait partie d'une formation beaucoup plus étendue mise en place à la base de la partie nord de la zone supracustale de Beaulieu River. Une autre unité sédimentaire clastique, qui se laisse subdiviser en un membre conglomératique et un membre principalement composé d'arénite quartzique, constitue un vestige de synclinal recouvrant en discordance des roches volcaniques. Dans ces strates, les plis et la schistosité témoignent d'une histoire complexe d'épisodes de déformation survenus dans la zone. Il existe dans les deux formations des couches de galets quartzeux légèrement uranifères et légèrement aurifères. Ces dernières révèlent l'existence, dans la province structurale des Esclaves, de paléoplacers d'or pyriteux jusque-là non identifiés, qui pourraient représenter une cible d'exploration digne d'intérêt.

[1] Contribution to Canada-Northwest Territories Mineral Development Agreement 1987-1991
[2] Mineral Development Agreement, Government of the Northwest Territories, Yellowknife, N.W.T.
[3] Ottawa-Carleton Geoscience Centre, Ottawa, Canada

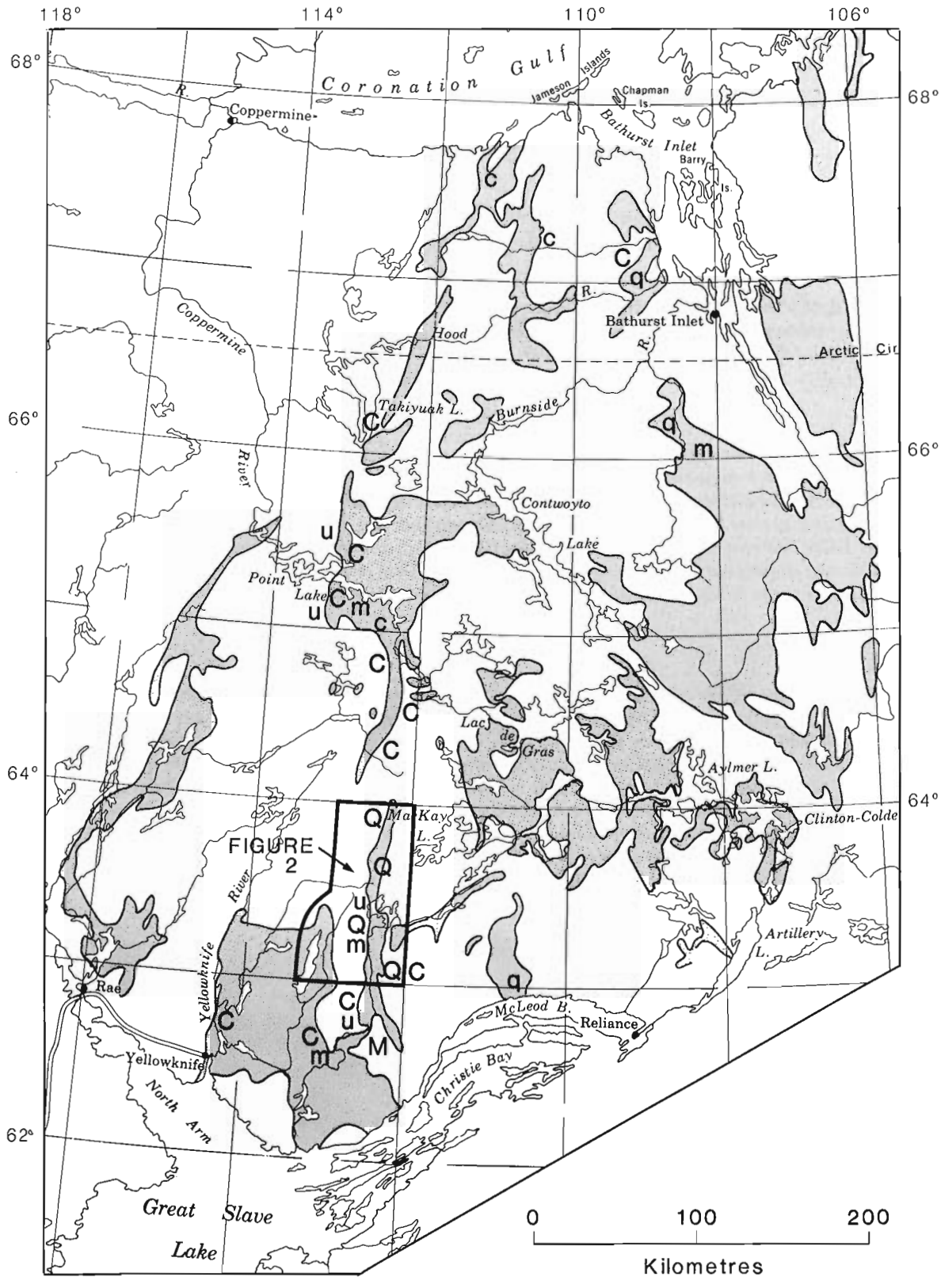

Figure 1. Beaulieu River and other Archean supracrustal belts, Slave structural province, N.W.T. Index to study area (Fig. 2), northern part of Beaulieu River supracrustal belt is indicated; C - conglomerate formation, M - marble or calc-silcate rock, Q quartz arenite, U - ultramafite, lower case letters indicate minor occurrences.

INTRODUCTION

Quartz arenite and associated ultramafitic rock at Beniah Lake (85P/8) 145 km northeast of Yellowknife, NWT, (Fig. 1, 2) in the northern section of the Beaulieu River supracrustal belt (Miller, et al., 1951) was reported by Covello et al. (1988). This was the first report of such quartz-rich Archean clastic sedimentary rocks within the Slave structural province. Mapping by D. Roach in 1988 revealed important extensions of the orthoquartzite-bearing formation which is herein referred to as the Beniah formation.

Additional occurrences of chemically mature and supermature clastic metasedimentary rocks were found in several places as much as 70 km north of Beniah Lake (85P/9 and 16) along the belt of dominantly volcanic rocks of the Beaulieu supracrustal belt (Fig. 2). Another previously unreported quartz-rich arenite unit was mapped in 1988 by M. Stubley 30 km south of Beniah Lake in the Spencer Lake map sheet (85P/1). It differs from the Beniah formation and other occurrences of quartzite to the north in its lithologies, lithostratigraphic associations, chemical maturity and state of deformation. We refer to it herein as the Beaulieu Rapids formation.

Both the Beniah formation and the Beaulieu Rapids formation contain thin lenses of slightly uraniferous and auriferous pyritic quartz-pebble conglomerate. The formations require evaluation not only for new clues to the early tectonic history of the Slave structural province but also as possible hosts for paleoplacer gold deposits.

BENIAH FORMATION

The Beniah formation is nowhere well exposed and, in areas of most extensive exposures, it is so intensely deformed and riddled with intrusions of gabbro that interpretations of its local structural configurations and stratigraphic relationships are uncertain. For descriptive purposes it is useful to refer to two areas where outcrops of quartz arenite are abundant: a southern area (S in Fig. 3), centred 3 km west of the south end of Beniah Lake and a northern one 3 km north of this (N in Fig. 3).

Quartzite beds in the southern area strike 120°, dip steeply south, and top southward as indicated by cross stratification and other primary structures (Covello et al., 1988). The quartzites are bordered to the south by south-facing pillowed basalt flows and truncated to the northwest by a breccia zone that separates them from basalt. The area of quartzite beds changes towards the northeast into a broad zone of highly foliated rocks lacking recognizable primary structures. Quartzite, siliceous siltstone, felsic crystal tuff and serpentinite, all with steeply-dipping northeasterly-striking mylonitic foliation, are exposed in sparse outcrops along a 3-km-length of this sheared zone. Dextral movement along the zone is indicated by shear bands in the foliation and by broad clockwise curvatures of stratigraphic trends and foliations north of the zone. Little-deformed ultramafic rock including serpentinized dunite with layers of cumulate chromite grains outcrops south of the shear zone as reported by Covello et al. (1988). This body is apparently within the same structural block as the pillowed basalt that overlies quartzite to the southwest. Steeply-dipping stratification is discernable through a 1300-m cross-strike width in the southeastern part of the area, but this does not provide a satisfactory measure of minimum thickness of the formation. On the one hand, beds have been thinned tectonically as indicated by steeply plunging long axes of highly stretched, slightly flattened pebbles. On the other hand, the section has been expanded by abundant intrusions of gabbro, mainly northerly-striking dykes. Siliceous siltstone and minor dark grey siltstone are present in upper and lower parts of the section and beds of polymict paraconglomerate and quartz-pebble conglomerate are present near the top.

In the broadest part of the northern area (N), beds of quartz arenite, siliceous siltstone, minor conglomerate, ultramafite, iron formation and basalt strike 060 and dip steeply south across a width of 1300 m. The clastic metasedimentary rocks contain a central lens or tongue up to 300 m thick that includes, in stratigraphically ascending order, ultramafite, banded magnetite-chert iron formation, and basalt with south-facing pillows. The area is bordered to the south by pillowed basalt that faces south and extends 2 km south to the faulted margin of the southern area (S) of quartzite exposures. The most extensive exposures of quartzite are on a peninsula at the narrows of a lake at the north margin of the north area (Fig. 4). The northernmost, stratigraphically lowest, beds include several lenses of slightly radioactive pyritic quartz-pebble conglomerate (Fig. 8a). Radioactive conglomerate beds (Fig. 8d) are also present south of the central band of basalt. It is possible that the basalt band represents a faulted strip of the same major basalt unit that overlies the formation and that the quartz arenite is also duplicated in this area.

Along strike to the west, where outcrops are sparse, the formation appears to thin abruptly and interfinger with siliceous siltstone, rhyolite, rhyolite clast conglomerate (Fig. 8c), calc-silicate rock (Fig. 8b), and silicate iron formation. Some or most of the intercalations may be fault slices. The extension of the Beniah formation west of area N (Fig. 3), as indicated by a few outcrops of quartzite and siliceous siltstone, is truncated south of the southwest arm of Beniah Lake by a north-striking fault that separates the strata from a block of gneiss and granite about 1 km wide. This block is flanked to the west by a major north-striking shear zone. Highly deformed quartz arenite and some beds of pyritic, weakly radioactive, quartz-pebble conglomerates have been traced 9 km northward along the west side of Beniah Lake in this shear zone (Fig. 3). A thin body of ultramafite flanks the east side of the northernmost of these quartzite outcrops. A granite intrusion a few hundred metres thick separates the quartz arenite band (and locally the ultramafite lens) from migmatitic gneiss to the east along the shore of the lake.

QUARTZ ARENITE NORTH OF BENIAH LAKE

Outcrops of quartz arenite were found and examined during reconnaisance trips along the Beaulieu River supracrustal belt which extends 65 km north of Beniah Lake. These newly recognized occurrences are at latitudes 63°29′N

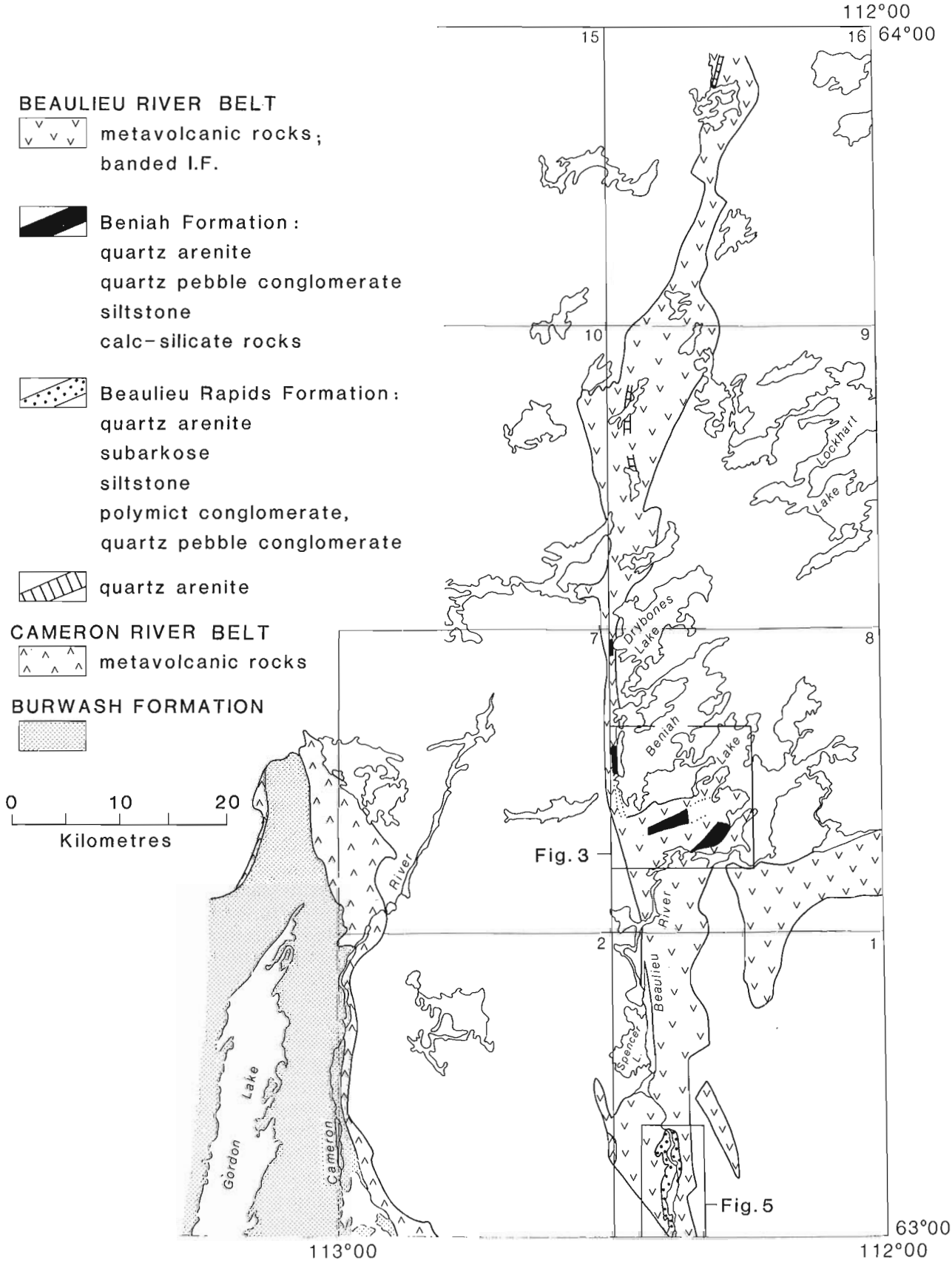

Figure 2. Beaulieu River supracrustal belt in east half of Carp Lakes map-area (85P/1,2,7,8,9,10,16) Areas of Figure 3, and 5, are indicated.

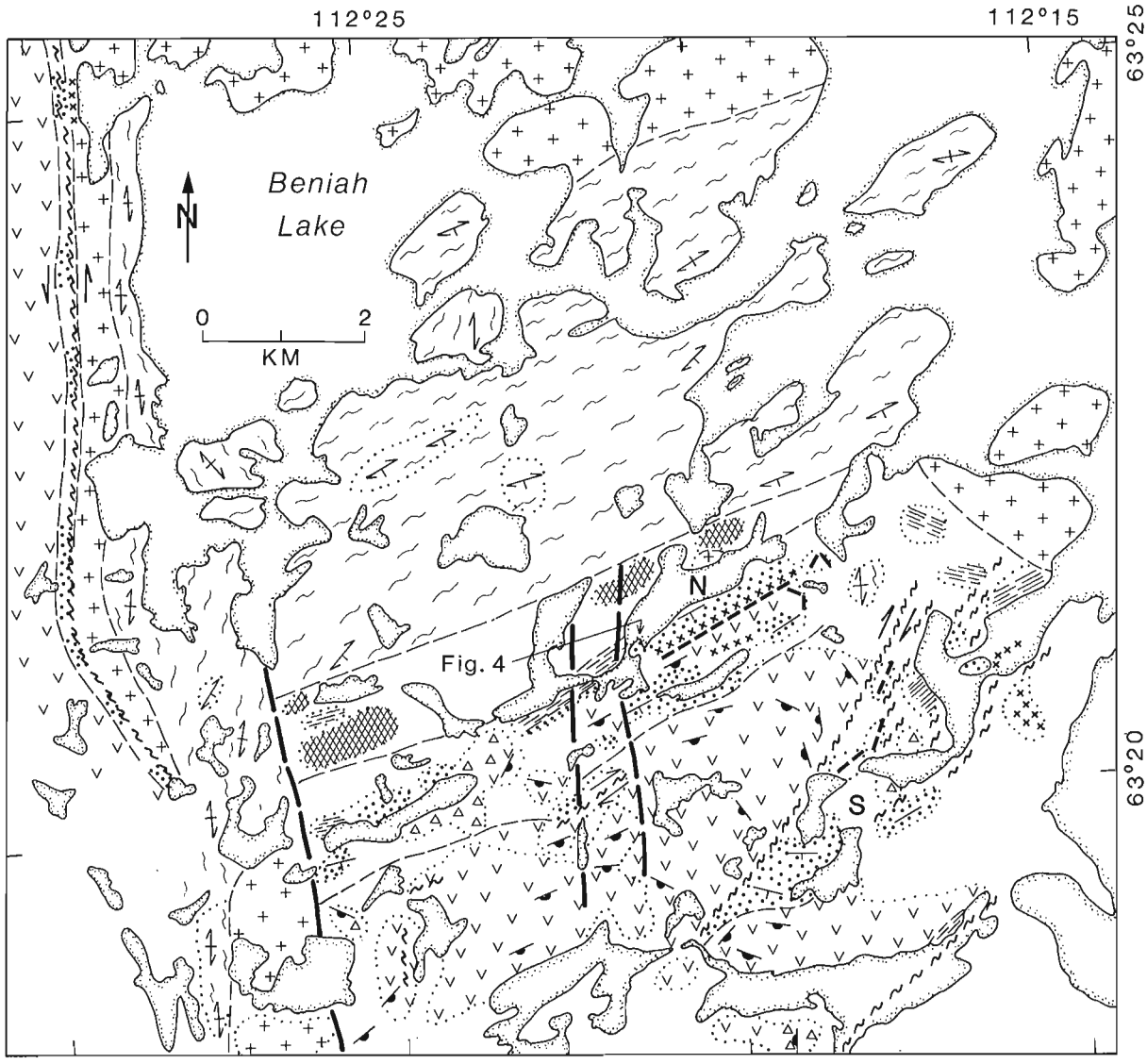

LEGEND

granite

mafite

mafic volcanics

metadunite, metapyroxenite

Iron Formation

Beniah Formation: quartzite, siltstone, conglomerate

N –northern area
S –southern area

rhyolite

quartz–muscovite, chlorite, biotite schist

quartzo–feldspathic migmatitic gneiss

foliation

pillow facing

bedding (tops known, unknown)

shear zone

fault

Figure 3. Distribution of quartz arenite and associated rocks at Beniah Lake (85P/8) Location of Fig. 4 is indicated.

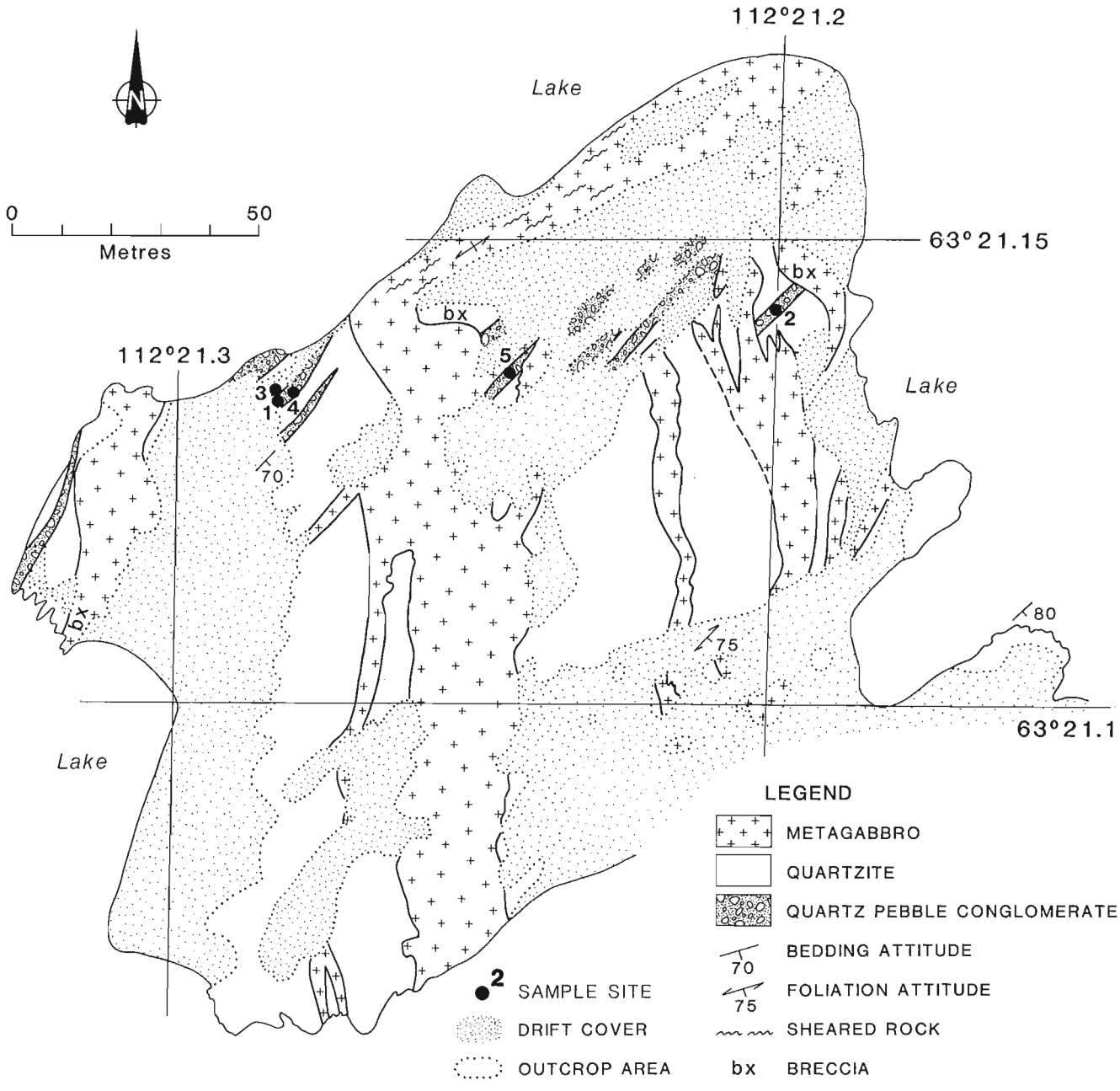

Figure 4. Quartz arenite with pyritic quartz pebble beds, BeniahLake area (85P/8)

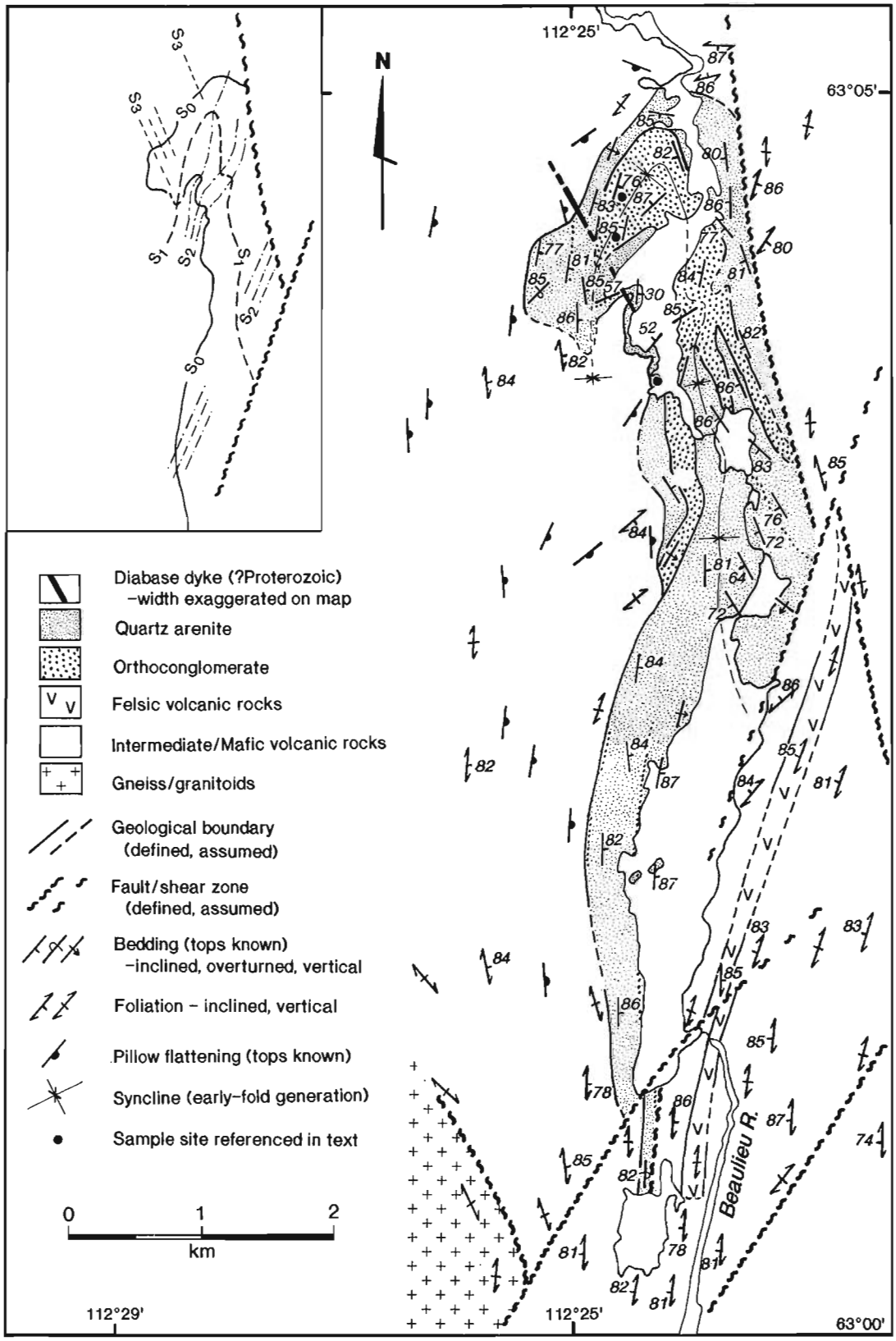

Figure 5. Metasedimentary rocks along Beaulieu River system (NTS 85P/1) Inset summarizes main structural features and fold overprint relationships within the metasediments. Lakes outside Beaulieu River system not shown.

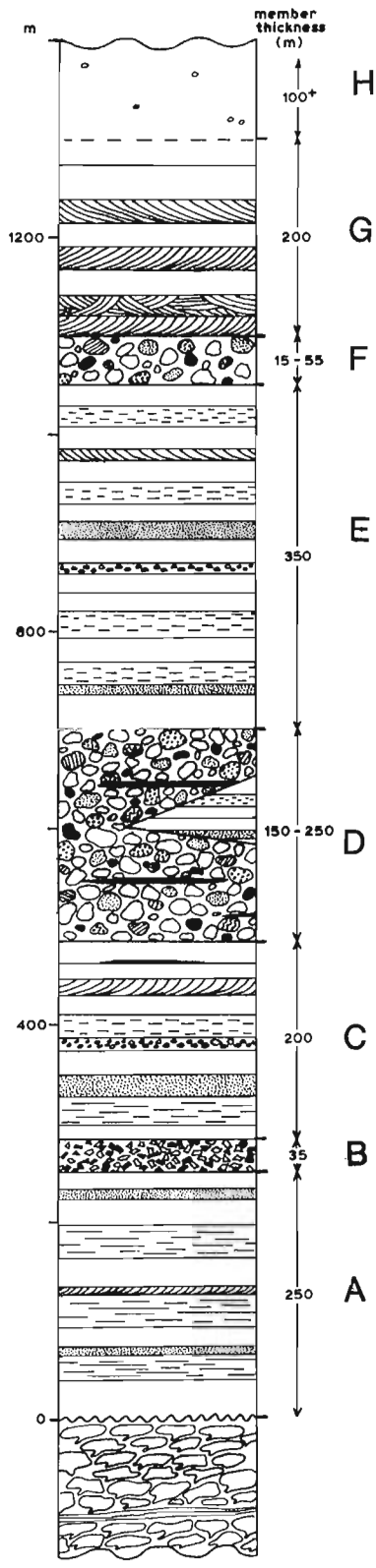

eroded top

fine grained quartz arenite, massive thick beds, rare quartz clasts

gradational contact

fine to medium grained quartz arenite with quartz grit and quartz pebble lenses, trough crossbeds
(best exposures on island at 63°01.9'N,112°24.3'W)

polymictic conglomerate, pebbles, cobbles and boulders mainly clast supported, no green clasts and pyritic layers as present in lower (D member) conglomerate
(observe on smaller island and west shoreline of south lake)

interbedded quartzose to feldspathic arenite and siltstone; rare grit and pebble beds, some rusty coloured siltstone beds; elevated radioactivity in some pebbly beds with diseminated pyrite; strong F_2 and S_2 development in silty layers, constitutes much of the southwest limb of the F_1 syncline

polymictic conglomerate; mainly clast supported;. mainly cobbles to boulders in quartz grit with interstitial muscovite and chlorite; clasts of vein quartz, rhyolite, chert, mafite, diorite, quartz diorite, granodiorite, gneiss, gabbro, amphibolite, felsic tuff, banded iron formation and possible mylonite; slightly radioactive pyritic layers; bright green (fuchsitic) felsic clasts present and locally abundant;
(well exposed at north lake)

interbedded quartz arenite, subarkose to arkose, siltstone, quartz grit with quartz pebbles and thin quartz pebble conglomerate lenses; pyrite concentrations, mainly in slightly radioactive gritty and pebbly but also along fractures and in'non-radioactive' beds.

'sharpstone conglomerate' small pebble-sized, angular clasts of probable volcanic rock, closely spaced but largely matrix supported in quartz grit. ('non-radioactive')

interbedded quartz arenite, siltstone, subarkose to arkose, quartz grit with quartz and volcanic pebbles scattered and also sorted in layers; parallel laminated; less commonly, massive or trough crossbedded; pyritic radioactive gritty and pebbly beds

unconformity, angular?
altered top of basalt sequence locally exposed, paleosol?

thick succession of metavolcanic rocks, mainly pillowed basalt with pillow breccia, volcaniclastic rocks

Figure 6. Composite stratigraphic section, Beaulieu Rapids formation in area of Figure 5.

(Drybones Lake), 63°38′N, 63°40′N, 63°41′N, and at 63°57′N near the north end of the belt. The quartzite band at the latter locality (Fig. 8k) is exposed across 50 m and cannot be more than 75 m wide. The quartz arenite at 63°38′N outcrops across a width of several hundred metres. These outcrops are likely along extensive bands of quartz arenite correlative with the Beniah formation which may have been deposited, therefore, over a large area.

BEAULIEU RAPIDS FORMATION

A thick sequence of previously unreported quartz-rich arenites and rudites is well exposed 30 km south of Beniah Lake along an 8-km section of the Beaulieu River system in NTS 85P/1. These strata, herein referred to as the Beaulieu Rapids formation[1], are preserved within a fault-truncated, southerly-plunging syncline (Fig. 5). The formation overlies mafic volcanic rocks at the east boundary of a fault-bounded block. The subjacent steeply-dipping, east-facing volcanic rocks extend up to 6 km west of the synclinal axis, where they have faulted contacts with gneissic rocks. The contact between volcanic and stratigraphically overlying sedimentary rocks can be mapped precisely in many areas of abundant outcrop. It is completely exposed in some places. Discordance between pillow elongations, the contact, and bedding in the overlying strata is the rule, rather than the exception. In many cases, a high angular discordance between bedding in the upper sequence and the contact is clearly due to faulting. In places, however, alteration of the basalt tentatively interpreted as paleosol suggests that the contact is unfaulted. It seems most likely that the contact is an erosional surface. It is also possible that the rocks were folded prior to their erosion and deposition of the sedimentary strata. Refold patterns of a well-developed foliation in the volcanic rocks are consistent with this possibility but a complex deformational history outlined below has obscured relevant evidence.

The quartz-rich character of Beaulieu Rapids arenites invites speculation that the formation might be correlative with the Beniah formation, the only other extensive occurrence of chemically submature to supermature clastic sediments known in the Slave structural province. The two formations, however, differ in a number of respects in addition to the possibly irrelevant fact that the Beaulieu Rapids formation, which is comparatively less deformed, lacks extensive sections of nearly pure quartz arenite that characterize the Beniah formation. It contains thick polymictic conglomerate members and, unlike the Beniah formation, it is not associated with ultramafic rocks or iron formation. It overlies a thick pile of mafic volcanic rocks that may in part be equivalent to basalt flows that overlie the Beniah formation.

[1] The Beaulieu Rapids formation outcrops along lakes and intervening rapids on the Beaulieu River system. Apart from Beaulieu River, there are no named geographic features in the area 'Rapids Formation' might be considered a more appropriate name in view of Henderson's (1985) usage of the term Beaulieu Group for all Archean volcanic units in the Hearne lake area. In this report the cumbersome designation 'volcanic rocks of the Beaulieu River supracrustal belt' is used instead of Beaulieu Group to avoid an implication that these rocks are known to be correlative with volcanic rocks in the Yellowknife supracrustal belt.

Three folding episodes have deformed the Beaulieu Rapids formation. A single, large-scale, tight syncline, F1, with an axial plane that dips steeply west was formed during the first episode. Where it is unaffected by subsequent deformation, it plunges gently south. Minor folds and foliation associated with F1 are rare. Tight folds (F2) up to several hundreds of metres in wave length were formed during a second event. Most spectacularly, refolding of the north end of the F1 syncline has produced a tight bend in the trace of its axial plane. The F2 folds have variable north-northeasterly plunges in subvertical axial surfaces and are associated with S2, the most prominent foliations. Subvertical lineations and elongations were produced in both the Beaulieu Rapids formation and the underlying volcanic rocks. A final deformation event produced outcrop-scale open buckle folds about locally developed, north northwest-striking, subvertical S3 crenulation cleavage in both the sedimentary and volcanic sequences.

A composite stratigraphic column constructed from the broadly symmetric succession of lithologies found within the F1 syncline is shown in Figure 6. The individual members (Fig. 8d, e, f, g, h) are extensive but vary in thickness and composition along strike. The total preserved thickness of the formation, as the sum of thicknesses of individual members, is estimated as 1200 to 1500 m. Way-up indicators, including crossbeds, channels, and rare graded beds, are abundant in the arenaceous rocks. Foreset attitudes, reconstructed as most probable prior to the complex deformation, suggest generally southerly directions of paleocurrents during deposition of the formation.

The Beaulieu Rapids formation resembles the Jackson Lake Formation (Jolliffe, 1942; Henderson, 1985) at Yellowknife in some respects but it appears to be chemically more mature. It may be more similar to some metasedimentary rocks in the Winter Lake map area (NTS 86A) at the north side of the Carp Lakes map area (85P). Extensive bands of conglomeratic rocks in this area (Fraser, 1968) and in the Keskarrah Formation (Bostock, 1980) in the Point Lake area are indicated in Figure 1. Fraser (1968) describes conglomerates with abundant quartz clasts and with "a quartzose arenaceous matrix". He also reports arenites that "consist chiefly of quartz with up to 20% biotite and 15% feldspar". Two small specimens of metasedimentary rocks from his collection were available for examination. They are quartzose and pyritic.

RADIOACTIVE STRATA

Pronounced lithostratigraphic variations in radioactivity are found in both the Beniah and Beaulieu Rapids formations. Least radioactive, scarcely higher than over-water background, are quartz arenite beds in the Beniah formation. Thin, impure, micaceous interlayers and siltstone beds are slightly more radioactive and gritty, poorly sorted beds yield counts more than twice background. Rusty conglomeratic beds with disseminated pyrite are more than 3 times and local pyrite-rich spots more than 10 times background. The radioactive conglomerates include a polymictic variety containing a preponderance of quartz pebbles, but oligomictic conglomerate beds (Fig. 8d) are generally more pyritic and radioactive. Highly stretched beds of quartz pebble/cobble

Table 1. Analyses of radioactive specimens

	SiO2	Al2O3	K2O	Na2O	CaO	MgO	FeO	TiO2	Pyrite	Au	Hg	U	Th	Ce	Y	P	Zr	Cr	As	Co	Ni	Cu	Zn	Pb
	%	%	%	%	%	%	%	%	%	ppb	ppb	ppm	ppm	ppm	ppm	ppm	ppm	ppm	ppm	ppm	ppm	ppm	ppm	ppm
SAMPLE																								
88RF40	76.5	6.5	1.6	0.5	0.1	1.4	1.5	0.7	8.1	76	43	324	435	219	58	340	1160	470	13	134	190	460	61	250
88RF40A	86.9	5.7	1.5	0.2	0.1	0.6	0.7	0.3	1.8	2	7				<10	100	149	90	5		77	81	60	52
88RF41	65.1	12.2	1.3	2.5	1.6	2.1	6.8	0.52	3.6	12	9	64	82	165	41	290	507	2450	14	160	1600	640	260	36
88RF42	81.1	6.8	1.9	0.2	.0.0	0.7	1.5	0.4	4.9	17	14				46	130	402	200	53		71	80	38	40
88RF43	84.1	6.8	1.1	0.8	0.5	1.2	1.2	0.33	1.4	4	11	21	38	100	14	170	203	120	4	36	69	150	31	24
88RF43B	85.3	6.4	0.7	1.3	0.8	1.1	0.9	0.3	1.6	1	11				14	120	186	110	5		77	190	35	36
88RF44	61.2	16.2	1.9	3.1	1.9	2.8	4.9	0.67	4.4	3	5	109	126	294	58	530	537	270	5	194	340	420	53	48
88RF45A	77.3	8.6	1.6	0.5	0.2	2.3	2.8	0.5	2.1	<1	7				44	180	484	260	7		78	270	50	40
88RF47	70.2	13.5	2.3	0.2	0.4	1.9	5.5	0.62	0.9	630	19	287	155	116	23	240	618	130	4	22	44	79	86	32
88RF48	73.9	9.2	1.5	0.1	0.2	1.4	5.3	0.57	3.4	44	8	254	162	113	33	480	1280	130	36	55	88	140	66	36
88RF48B	69.5	12.4	2.1	0.2	0.4	1.7	6.2	0.7	2.4	410	11				53	250	977	150	10		70	100	77	36
88RF49	73.7	10.8	2.3	0.2	0.1	1.3	4.5	0.62	2.1	180	11	57	87	128	21	340	608	110	69	37	30	29	53	28
88RF50	56.7	9.6	1.5	0.2	0.1	1.8	9.6	0.67	14.1	250	34	83	47	89	13	580	262	100	180	100	120	130	85	32
88RF52	62.5	14.1	2.8	0.2	0.1	1.9	9.7	1.15	0.7	48	19	13	19	105	13	655	312	190	69	11	19	51	87	32
88RF53A	64.7	10.3	1.1	0.2	0.8	2.1	8.8	1.1	5.8	80	20	190	287	238	38	830	2620	170	75	104	140	120	89	48
88RF53B	66.4	7.6	1.1	0.1	0.3	1.3	8.7	0.72	8.2	200	30	104	101	94	21	568	1220	350	110	114	1400	240	310	28
88RF53C	61.8	9.5	1.7	0.2	0.2	1.5	8.2	0.7	11.2	58	18				18	420	604	100	120		140	230	68	16
88RF54	72.1	10.1	1.1	0.3	0.7	1.4	4.1	0.51	6.1	6	26	137	285	226	33	524	1400	96	34	106	90	150	40	72

Analyses by X-Ray Assay Laboratories Limited, multi-method, multi-element package.
S reported as FeS_2; Fe, as FeS_2 and FeO.

Locations samples 88RF40 - 45 see Fig. 4.

88RF40 and 40A - drillcore sample site 1,
41 - cuttings from site 1 drillhole;
42 - drillcore sample site 2 beneath site 1.
43 - drillcore site 4 50 cm NE of site 1.
44 - drillcore site 5. 45A broken rocks at 4.

Locations samples 88RF47-54 see Fig. 5.

Site 1:
88RF47 - core specimen vertical drillhole at 63°04.55'N, 112°24.65'W
48 and 48B - specimen from inclined drillhole at same location.
49 - outcrop sample 7 m NE of drillholes.

Site 2:
87RF50 and 52 - core specimens from vertical drillhole at 63°04.45'N, 112°24.6W
53A, B, C - specimens from inclined drillhole at same locality.

Site 3:
54 - core specimen from inclined drillhole at 63°03.7'N, 112°24.3'W.

conglomerate are present along the west side of Beniah Lake and less deformed occurrences are well-exposed on a peninsula (63°21.1′N, 112°21.2′W) on a lake south of the west arm of Beniah Lake (Fig. 4). A light drill was used to obtain short core samples from several pyritic conglomerate beds (Fig. 8a) at this locality. Analyses of selected specimens (88RF40-47) are given in Table 1.

Outcrops of quartz arenite and conglomerate members of the Beaulieu Rapids formation are more radioactive than those of metavolcanic rocks. This prompted us to examine radiometric profiles obtained in an 1971 airborne gamma spectrometer survey in the area (Geological Survey of Canada, 1973). Several flight lines that crossed the formation showed little change in radioactivity patterns, but one at the south end of the southern lake in Figure 5 (latitude 63°01′N) shows an anomaly marked by a sharp peak in total count, uranium count and ratio of uranium to thorium.

In the Beaulieu Rapids formation, as in the Beniah formation, higher radioactivity on outcrops is coincident with coarser grained beds — quartz grit, pebbly grit, and quartz

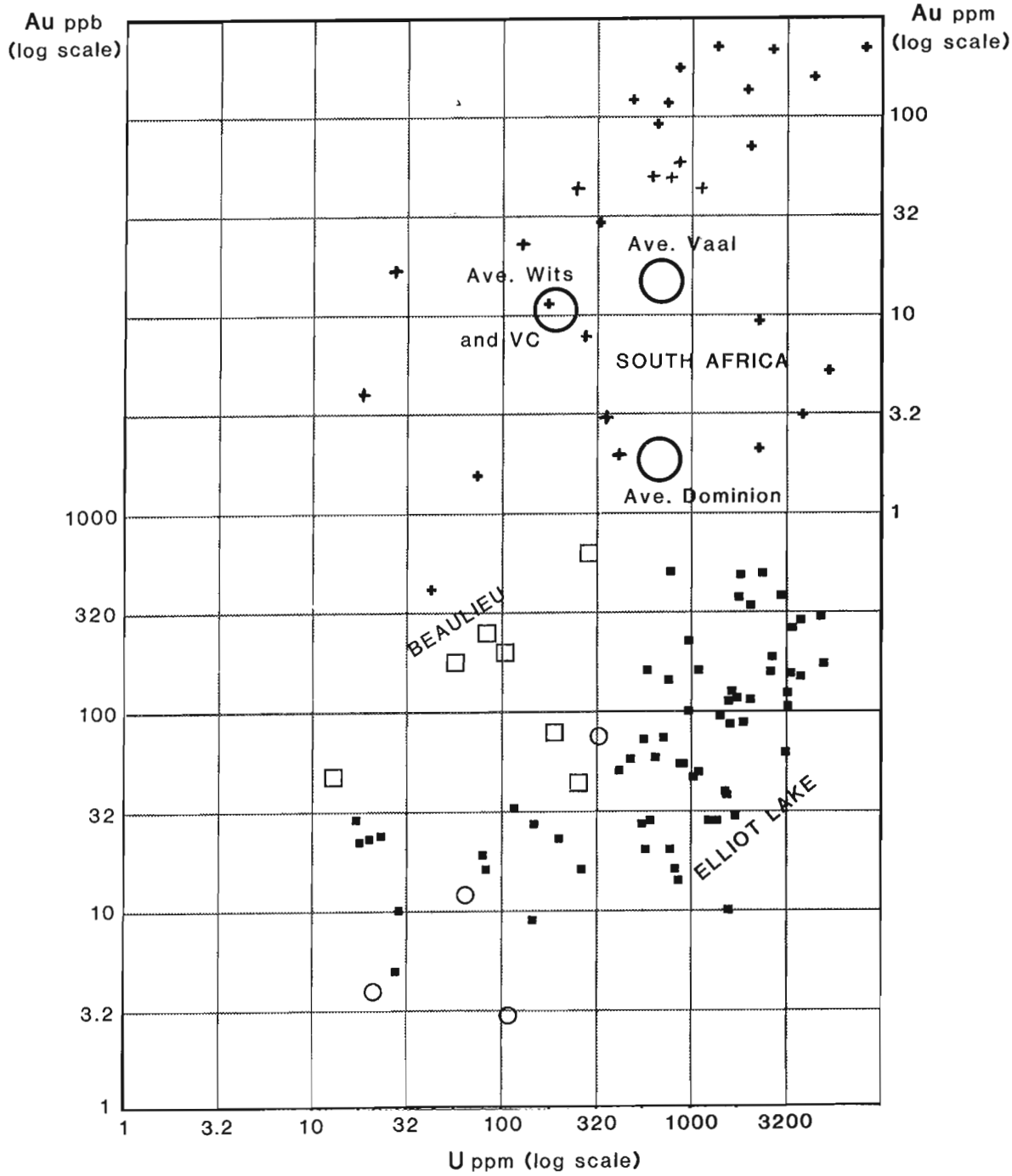

Figure 7. Gold and uranium in quartz pebble conglomerate, Beniah and Beaulieu Rapids formations (Table 1) and Elliot Lake, Canada, and South African conglomeratic ores ○ Beniah formation; □ Beaulieu Rapids formation; ■ samples from ore sections in mines at Quirke Lake in the Elliot Lake area (data from Ross, 1981). Au and U contents of ores mined in Witwatersrand and Dominion ore zones, R.S.A. (from various sources) are indicated.

pebble conglomerate — and with rusty-weathered zones marking concentrations of disseminated pyrite. The D member of the Beaulieu Rapids formation(Fig. 6, 8i, 8j) contains the most abundant and the most radioactive pyritic grit and quartz pebble lenses (Fig. 8e). Pyrite is more abundant in the most highly radioactive beds than in less radioactive beds. Many iron sulphide concentrations, however, are related to fracturing or pelitic character of beds and are not especially radioactive. The most radioactive beds, locally up to 170 times and 60 times background, were found at 63°04.55′ N, 112°24.65′ W and 63°04.45′ N, 112°24.6′W respectively (Fig. 5). Partial analyses of selected specimens from a rock sample (88RF49) and drill cores (88RF47-53) obtained at these localites are listed in Table 1. Another specimen (54) was obtained at 63°03.7′N, 112°24.3′W.

Initial examinations of specimens of radioactive clastic rocks from both of the arenaceous formations, indicate that more than one species of radioactive mineral is present and that these occur as minute grains associated with grains of pyrite, titanium and rare earth-bearing minerals, and zircon. These suites of concentrated detrital heavy minerals are distinguished from normal (black sand) suites by their content of abundant pyrite in lieu of magnetite and hematite. Layers containing the greatest concentrations of heavy minerals were deposited, together with quartz pebbles and granules, by especially vigourous currents. In these and in other repects, such as relatively high ratios of uranium to thorium, they resemble the least radioactive of pyritic quartz pebble beds in subarkose formations in the lower part of the Huronian Supergroup (Roscoe, 1969). Like the Huronian, Witwatersrand and other similar ancient heavy mineral concentrations, the radioactive conglomerate beds in the Beaulieu River belt can be classified as pyritic paleoplacers without regard to post-depositional modifications and redistributions or possible additions of constituents.

Figure 8a. Pyritic quartz pebble conglomerate in quartz arenite, Beniah formation near Beniah Lake. Sample locality 1 in Figure 4. Conglomerate is distinctly radioactive. Photo D. Roach.

It is noteworthy that most of the small, highly selected samples from the Beaulieu belt, despite low uranium contents, contain as much gold as Ross (1981) found in samples from ore zones at Elliot Lake. The available data suggests Au/U ratios up to 0.005 in Beaulieu Rapids conglomerates, intermediate between ratios of about 0.0001 in Elliot Lake ores and ratios up to 0.14 in Witwatersrand gold ores (Fig. 7).

DISCUSSION

The non-turbiditic metasedimentary rocks and ultramafite near Beniah Lake show an interesting colinearity with most of the few occurrences of orthoconglomerates, ultramafic rocks, and carbonate rocks that have been recognized in the Slave province (Stockwell, 1933; Fraser, 1964, 1968; Henderson, 1985; Henderson and Easton, 1977; Easton et al, 1982; Lambert and van Staal 1987; Padgham, 1985) as shown in Figure 1. They are arrayed along a 300 km north-south zone that may lie along the boundary between two major divisions of the Slave structural province that have been postulated by Kusky (1988).

The consistent spatial associations between quartz

Figure 8b. Calc-silicate rock near Beniah. Lake Photo S. Roscoe

Figure 8c. Rhyolite clast conglomerate associated with quartzose arenite, Beniah, Lake Photo S. Roscoe

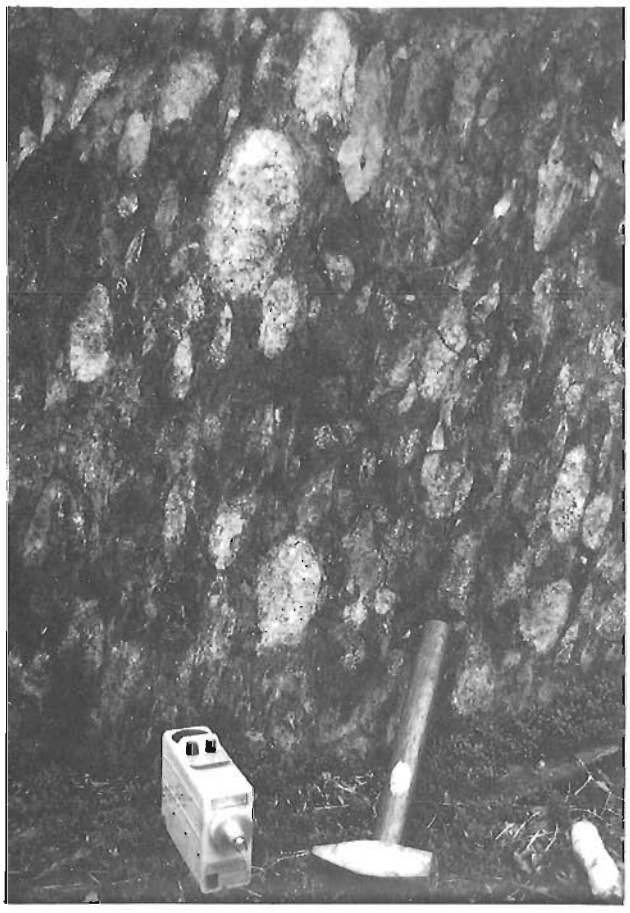

Figure 8d. Polymictic conglomerate rich in quartz clasts Matrix, containing disseminated pyrite, is rusty weathering and slightly radioactive. Photo S. Roscoe

Figure 8e. Radioactive pyritic conglomerate bed in C member, Beaulieu Rapids formation, 63°04.47′N, 112°24.6′W. Lens cap providing scale is atop vertical drill-hole site of specimen 88RF52. Another hole 20 cm west with an inclination of 60°E (right) drilled through the conglomerate bed provided core specimens 53A, B, and C. Photo M. Stubley

Figure 8f. Quartz arenite and quartz grit in C Member, Beaulieu Rapids formation 63°04.2′N, 112°24.5′W. Hammer handle points north, scintillometer is atop gritty rusty-weathering, slightly radioacitve layer. Photo S. Roscoe

Figure 8g. Contact of E arenite member and overlying F conglomerate member, Beaulieu Rapids formation 63°01.8′N, 112°24.4′W. Photo S. Roscoe

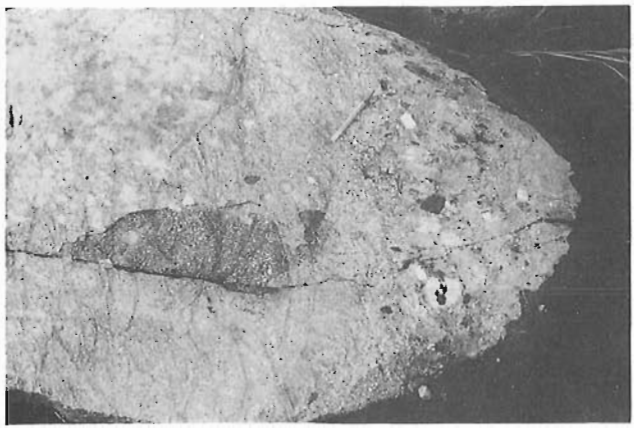

Figure 8h. Trough crossbedding in arenite, Beaulieu Rapids formation, uppermost C Member 63°04.5′N, 112°23.7′W. Photo M. Stubley

Figure 8i. Stratification in conglomerate, including an arenite lens, D member, Beaulieu Rapids formation 63°03.5′N, 112°24′W. Photo M. Stubley

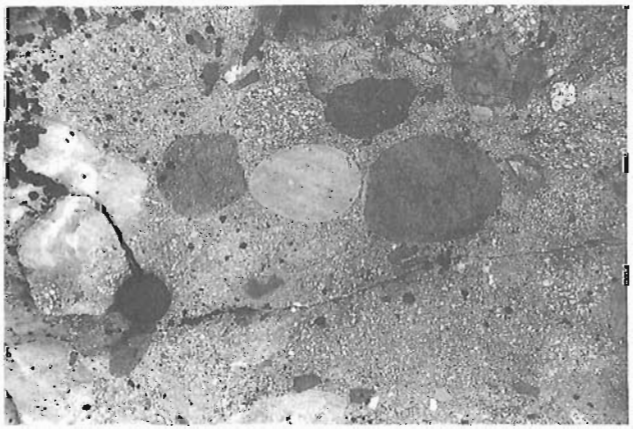

Figure 8j. Rounded cobbles in poymictic conglomerate, D member, Beaulieu Rapids formation 63°04.5′N, 112°24.6′W. Lens cap for scale, Photo M. Stubley

Figure 8k. Outcrop of quartz arenite at 63°57′ N, 112°18′W. Photo S. Roscoe

arenite of the Beniah formation, ultramafic rock, and migmatitic gneiss are noteworthy. Nowhere is there evidence that the formation or ultramafic rock is separated from the gneiss by an appreciable thickness of underlying supracrustal rocks within a given structural block. The gneiss is similar to the gneisses of the Sleepy Dragon Complex which pre-date deposition of the Beaulieu supracrustal rocks (Henderson, 1985; Lambert and van Staal, 1987). The relationships are in accord with a supposition that the assemblage of quartz arenite, associated siltstones, minor rhyolites, conglomerates, carbonates (calc-silicate rocks), silicate iron formation, banded magnetite-chert iron formation, ultramafic intrusions and perhaps ultramafic flows were deposited upon a metastable gneissic basement prior to eruption of the dominantly mafic volcanic rocks of the Beaulieu supracrustal belt. Remarkably, precisely the same assemblage is present at Lac Sakami in Quebec (Roscoe and Donaldson, 1988) and it also includes uraniferous pyritic quartz pebble conglomerate beds.

Ultramafic rocks, clast-supported polymictic conglomerate, and banded chert-magnetite iron formation have been mapped at the base of the Sunset Lake basalt sequence at Amacher Lake 50 km south of Beniah Lake (Lambert and van Staal, 1987). This assemblage, flanked to the west by the Sleepy Dragon granitoid gneiss terrane and overlain to the east by pillowed basalt, is similar to the assemblage of strata associated with quartz arenite at Beniah Lake and it occupies a similar stratigraphic position[1]. The intensely deformed Amacher Lake assemblage is only 11 km south of the synclinal remnant of relatively little deformed Beaulieu Rapids arenites and orthoconglomerates (Fig. 5). The latter overlie several kilometres of mafic metavolcanic rocks that are apparently contiguous with Sunset Lake basalts as mapped previously by Lambert (1988, Fig. 3) to within 1 km of the south end of the outcrop area of Beaulieu Rapids formation. Thus it appears that the Beaulieu River supracrustal belt contains not only one, but two formations distinguished by chemically mature to supermature arenites. One of these, the Beniah formation, was deposited, evi-

[1] The Raquette Formation (Henderson, 1985) at Upper Ross Lake (63°43′N, 113°07′W) is also analogous to the Beniah Lake formation in stratigraphic position and, moreover, it contains quartz-rich arenites.

dently over an extensive area, prior to major volcanic eruptions in the Beaulieu River supracrustal belt . The other, the Beaulieu Rapids formation, was deposited subsequent to an important part of the volcanism in the belt. It may have postdated all volcanism but this is not known as the formation has been found capping volcanics only in one fault-bounded domain. Conglomerates in the Beaulieu Rapids formation contain clasts of most of the rock types found in the belt and of gneiss and were probably deposited subsequent to important deformation and erosion of the volcanic pile. Arenites were derived from a moderately to intensely weathered granitoid provenance similar to source rocks of the Beniah formation.

It is remarkable that two such distinctive formations, obviously important in interpretations of the history of development of the Slave province and possibly significant as prospecting targets, could have escaped discovery through more than 50 years of prospecting and geological investigations, as they are located along a major waterway and are less than 150 km from Yellowknife. This highlights the need for detailed mapping in Slave supracrustal belts.

It is noteworthy also that both formations contain slightly uraniferous, slightly auriferous, pyritic quartz pebble conglomerate beds. This distinctive type of rock has been documented in no more than 15 distinct localities and stratigraphic units. The best known are the rich uranium paleoplacer ores in the lower part of the Huronian Supergroup, rich paleoplacer gold and gold-uranium ores in South Africa and Brazil, sub-ore grade auriferous pyritic paleoplacers in India and Australia and sub-ore grade uraniferous pyritic paleoplacers at Sakami Lake in Quebec, near Padlei in NWT., near Laramie, Wyoming and in the Black Hills, South Dakota. These new Archean examples of heavy detrital mineral concentrations containing pyrite in lieu of magnetite or hematite are consistent with the proposition that such heavy mineral suites are time bounded and record the existance of an extremely oxygen deficient (and possibly H_2S-bearing) atmosphere prior to mid-Huronian time or about 2.4-2.3 Ga (e.g. see Frarey and Roscoe, 1970; Roscoe, 1973, 1981).

The newly identified mature clastic sedimentary formations in the Beaulieu River supracrustal belt are among the few identified situations in the world where one might reasonably seek pyritic paleoplacer gold ores. The exploration strategy would be to seek up-current areas in the formations, where more abundant, thicker, better sorted, larger pebble gravels and richer concentrations of heavy minerals might have been deposited. In the case of the Beniah formation, only a linear belt extending north from the weakly radioactive pebble beds is available for exploration so one would have to hope that this also happens to be the upstream direction. In the case of the Beaulieu Rapids formation, exploration possibilities would depend upon discoveries of other, more proximal, areas of preserved strata north of the recently recognized synclinal remnant. Gold concentrations four orders of magnitude greater than in common rocks are required to produce ores like those in the Witwatersrand (Fig. 7). Maximum concentrations found to date in the Beaulieu belt are only two orders greater. Some of these are associated with pebbles as large as those in Elliot Lake ores so there might be little hope that ore grade concentrations were formed even in the most proximal fluvial environments. Adequate metal sources might not have existed. Ratios of Au/U in weakly radioactive conglomerates provide some indication of the richest concentrations that might conceivably be found in a given district or stratigraphic unit. The ratios in conglomerates in the Beaulieu Rapids formations suggest that rich heavy mineral concentrations, if found therein, would likely contain much more gold than than Elliot Lake ores but less than Witwatersrand ores. It is unlikely that they would be of interest primarly for uranium for many decades in view of currently available extremely high grade uranium resources.

About half the world's recorded production of gold as well as a large proportion of uranium production has been obtained from pyritic paleoplacers. Despite caveats cited above, possibilities of discovering gold paleoplacers in the Beaulieu River belt and in other Slave province supracrustal belts are intriguing and worth pursuing in concert with exploration for other types of deposits. In the latter context, it should be noted that the relatively radioactive Beaulieu Rapids formation may contain more gold than other supracrustal rocks in the Slave province, thus rendering it a favourable source and host for epigenetic gold deposits.

ACKNOWLEDGMENTS

The three authors collaborating in this study have worked separately with individual reponsibilities under the Canada-Northwest Territories Mineral Development Agreement. Stubley and Roach report to the Government of the Northwest Territories (GNWT) and the Geology Division of Indian and Northern Affairs Canada (INAC) in Yellowknife, Roscoe to the Geological Survey of Canada (GSC). These organizations provided equipment and logistical support for the three field operations. Rod Stone, under contract to the Geological Survey, provided superb expediting services from Yellowknife. INAC provided additional assistance to Roach through the Northern Research Group, University of Ottawa. Roscoe based his field investigations and was boarded at Roach's and Stubley's field camps. Hendrik Falck assisted him in obtaining drillcore specimens. Stubley was ably assisted in the field by Jay Pan and Christine Bovaird; Roach, by Julie Lamirande.

This study benefited from discussions in the field with W.K Fyson, J.B. Henderson, D.T. James, J.K. Morteson, and W.A. Padgham. Reviews by J.B. Henderon, C.W. Jefferson and R.F.I Scoates and comments by W.A. Padgham improved the manuscript.

REFERENCES

Bostock, H.H.
1980: Geology of the Itchen Lake area, District of Mackenzie; Geological Survey of Canada, Memoir 391, 101 p.

Covello, L., Roscoe, S.M., Donaldson, J.A., Roach, D. and Fyson,W.K.
1988: Archean quartz arenite and ultramafic rocks at Beniah Lake, Slave structural province, NWT.; in Current Research, Part C, Geological Survey of Canada, Paper 88-1C, p. 223-232.

Easton, R.M., Boodle, R.L., and Zalusky, L.
1982: Evidence for gneissic basement to the Archean Yellowknife Supergroup in the Point Lake area, Slave Structural Province; in Current Research, Part B, Geological Survey of Canada, Paper 82-1B, p.33-41.

Frarey, M.J. and Roscoe, S.M.
1970: The Huronian Supergroup north of Lake Huron; in Symposium on basins and geosynclines of the Canadian Shield, ed. A.J. Baer, Geological Survey of Canada, Paper 70-40.

Fraser, J.A.
1964: Geological notes on northeastern District of Mackenzie, Northwest Territories; Geological Survey of Canada, Paper 63-40. 20 p.
1968: Geology Winter Lake, District of Mackenzie; Geological Survey of Canada, Map 1219A with marginal notes.

Geological Survey of Canada
1973: Airborne gamma spectrometric survey, Yellowknife, NWT; Geological Survey of Canada, Open File 124

Henderson, J.B.
1985: Geology of the Yellowknife-Hearne Lake area, District of Mackenzie: a segment across an Archean Basin; Geological Survey of Canada, Memoir 414, 135 p., Map 1601A.

Henderson, J.B. and Easton, R.M.
1977: Archean supracrustal-basement rock relationships in the Keskarrah Bay map-area, Slave Structural Province, District of Mackenzie; in Current Research, Part A, Geological Survey of Canada, Paper 77-1A, p. 217-221

Jolliffe, A.W.
1942: Yellowknife Bay, Northwest Territories, Geological Survey of Canada Map 709A.

Kusky, Timothy
1988: Accretion of the Archean Slave Province; in Crust of South India, Journal of the Geological Society of India, v. 31, no. 1, p. 63-65.

Lambert, M.B.
1988: Geology of the Sunset Lake subarea of the Cameron River and Beaulieu River volcanic belts, District of Mackenzie, Northwest Territories; B. Lambert Geological Survey of Canada, Bulletin 382, Figure 3.

Lambert, M.B. and van Staal, C.R.
1987: Archean granite-greenstone boundary relationships in the Beaulieu River volcanic belt, Slave Province, NWT; in Current Research, Part A, Geological Survey of Canada, Paper 87-1A, p. 605-618.

Miller, M.L., Barnes, F.Q., and Moore, J.G.C.
1951: Carp Lakes; Geological Survey of Canada, Paper 51-8, map marginal notes by J.G.C. Moore

Padgham, W.A.
1985: Observations and speculations on supracrustal successions in the Save structural province, in Evolution of Archean Supracrustal Sequences, Eds. L.D. Ayres, P.C. Thurston, K.D. Card, and W. Weber, Geological Association of Canada, Special Paper 28, p. 133-151.

Roscoe, S.M.
1969: Huronian rocks and uraniferous conglomerates in the Canadian Shield; Geological Survey of Canada, Paper 68-40, 205 p.
1973: The Huronian Supergroup, a Paleoaphebian succession showing evidence of atmospheric evolution; in Huronian stratigraphy and sedimentation, Ed. G.M. Young, The Geological Association of Canada, Special Paper No. 10, p. 31-47.
1981: Temporal and other factors affecting deposition of uraniferous conglomerates; in Genesis of uranium and gold-bearing Precambrian quartz-pebble conglomerate, Ed. F.C.Armstrong, United States Geological Survey, Professional Paper 1161-A-BB, p. W1-W17.

Roscoe, S.M. and Donaldson, J.A.
1988: Uraniferous pyritic quartz pebble conglomerate and layered ultramafic intrusions in a sequence of quartzite, carbonate, iron formation and basalt of probable Archean age at Lac Sakami, Quebec; in Current Research, Part C, Geological Survey of Canada, Paper 88-1C, p. 117-121.

Ross, D.I.
1981: The distribution of gold and other elements in the uranium conglomerates of Elliot Lake, Canada; MSc. Thesis, McMaster University, Hamilton, Ontario.

Stockwell, C.H.
1933: Great Slave Lake-Coppermine River area, Northwest Territories; Geological Survey of Canada, Summary Report 1932, Part C, p. 37-63.

Mid-crustal structures of the Wawa gneiss terrane near Chapleau, Ontario

Desmond Moser[1]
Lithosphere and Canadian Shield Division

Moser, D., Mid-crustal structures of the Wawa gneiss terrane near Chapleau, Ontario; in Current Research, Part C, Geological Survey of Canada, Paper 89-1C, p. 215-224, 1989.

Abstract

Regional deformation in the Wawa gneiss terrane involves three phases: early production of gneissic layering, development of F_2 folds, and movement along extensional high-strain zones that produced regional variations in the continuity of gneissic textures and attenuation of deformed mafic xenoliths. Two areas show additional structural complexity, probably resulting from preservation of early structures in the Borden Lake belt and from later, superposed structures in the Robson-Floranna lakes area.

Résumé

La déformation régionale du terrain gneissique de Wawa comprendrait trois phases: la formation initiale d'une stratification gneissique, le développement de plis F_2, et un mouvement le long de zones de distension fortement déformées qui ont produit des variations régionales dans la continuité des textures gneissiques, et l'atténuation des xénolites mafiques déformés. Deux régions montrent une complexité structurale supplémentaire, qui résulte probablement de la conservation des structures initiales dans la zone de Borden Lake, et de l'apparition de structures ultérieures surimposées, dans la région des lacs Robson et Floranna.

[1] Department of Geological Sciences, Queen's University, Kingston, Ontario, K7L 3N6

INTRODUCTION

Wawa gneiss terrane constitutes the mid-crustal part of the oblique crustal cross section recognized by Percival and Card (1985) in the Wawa-Chapleau region. Bounded to the west by low-grade rocks of the Michipicoten greenstone belt and to the east by high-grade gneisses of the Kapuskasing structural zone, tonalitic rocks of the Wawa gneiss terrane crystallized at pressures of about 5 - 6 kbar (Percival, 1986) and were deformed under conditions of amphibolite-facies metamorphism. This study focuses on part of the Wawa gneiss terrane (WGT) near Chapleau, Ontario, first mapped at reconnaissance scale by Thurston et al., (1977). Further work at 1:100 000 scale documented gradational lithological, structural and metamorphic changes from amphibolite to granulite facies in the Chapleau area (Percival, 1981). Recent work on the structure of the WGT (Moser, 1988) defined a tentative chronology of structural and magmatic events in the immediate Chapleau area. This paper presents additional results based on 1:50 000 mapping of a larger area (Fig. 1, inset), conducted during the summer of 1988. The objectives of the study were as follows:

1) To investigate the regional extent and character of previously identified deformation phases (particularly those indicating extensional strain);
2) To study the nature of the amphibolite to granulite transition between the WGT and the southern Chapleau Block of the Kapuskasing structural zone; and
3) To provide surface structural information to aid in interpretation of LITHOPROBE seismic reflection profiles.

GENERAL GEOLOGY

Wawa gneiss terrane is located in the eastern Wawa subprovince of the Superior Province. It is composed predominantly of massive and gneissic tonalitic units with subordinate components of supracrustal rocks and late granitoid bodies. Two major mafic dyke swarms, the Matatchewan/Hearst and Kapuskasing, crosscut the region. Most of the intrusive and high temperature deformation events were complete by the time of emplacement of the older Hearst/Matatchewan swarm at 2454±2 Ma (Heaman et al., 1988).

Figure 1 is a generalized lithological map of the study area. Exposure is good to fair with the exception of two sand plains in the central and southeastern parts. The mappabale units are described below in approximate chronological order.

LITHOLOGY

Mafic gneiss

This unit occurs at both amphibolite and granulite grade. The amphibolites are fine grained, equigranular, hornblende-rich gneisses containing 10 - 35 % plagioclase, 5 % biotite and up to 5 % quartz. Retrograde epidote (up to 5 %) is associated with hornblende. Gneissic layering, on the 5-mm to 3-cm scale, is defined by either tonalitic leucosome, deformed pegmatite veinlets or variations in the proportion of mafic to felsic minerals. Mafic gneiss occurs as thin linear belts in the Highbrush Lake area, where rare, relict garnet and clinopyroxene are present.

Mafic rocks with the assemblage garnet - clinopyroxene - hornblende - biotite - plagioclase - quartz occur in the Robson and Borden Lake structures at the eastern edge of the study area. The proportion of mafic to felsic minerals is the same as for the amphibolites; however, as much as 10 % of the mafic component consists of garnet and clinopyroxene. The Robson Lake rocks have 5 cm-scale layering defined by hydrous/anhydrous mineral assemblages, a structure similar to that of mafic gneisses of the Kapuskasing structural zone further east. Cummingtonite (after orthopyroxene) was identified in leucosome from these rocks (J. Percival, pers. comm., 1988).

Paragneiss

A metasedimentary origin is inferred for this unit based on its aluminous composition. It is a fine-grained, equigranular, garnet-biotite-quartz-plagioclase gneiss with up to 20 % mafic minerals. Orthopyroxene was reported from paragneiss north of Como Lake (Percival, 1983). Gneissic layering is defined by a discontinuous, medium-grained, plagioclase -quartz leucosome which is 1 - 2 cm thick and spaced 5 to 10 cm apart. This unit occurs as rafts, up to several kilometres in size, within tonalitic gneisses in the central, northwestern and northeastern parts of the map area.

Quartzofeldspathic gneiss, diatexite

Commonly associated with paragneiss is a biotite (10 %) - plagioclase-quartz gneiss. Generally it is a fine-grained, quartz-rich gneiss with medium-grained, plagioclase-quartz segregations, characterized by variable thickness (0.5-3 cm) and "clotty" textures. The leucosome has similar appearance to that in paragneiss. Interspersed with this predominant rock type is a medium-grained, compositionally similar diatexite with 30-cm-scale, oblong xenoliths of paragneiss.

Borden Lake belt

A coherent lithological package with locally preserved supracrustal features is recognized in the Borden Lake area. It consists of both mafic and felsic components including: a) heterogeneous mafic gneiss with well defined compositional layering. Structures interpreted as deformed pillows (Fig. 4f) were recognized locally, suggesting a metavolcanic origin for the unit. Metamorphic grade increases toward the east based on the appearance of garnet and garnet-clinopyroxene assemblages; b) metasedimentary rocks including quartzofeldspathic gneiss, sandstone and metaconglomerate. Clast compositions in metaconglomerate are predominantly felsic (Percival, 1981); c) a felsic, muscovite-bearing schist featuring 1 - 5 cm quartz lenticles. Components a) and b) generally occur as mappable units but are also interlayered at the 10-m scale at two localities. Component c) was observed at only one location northwest of Borden Lake.

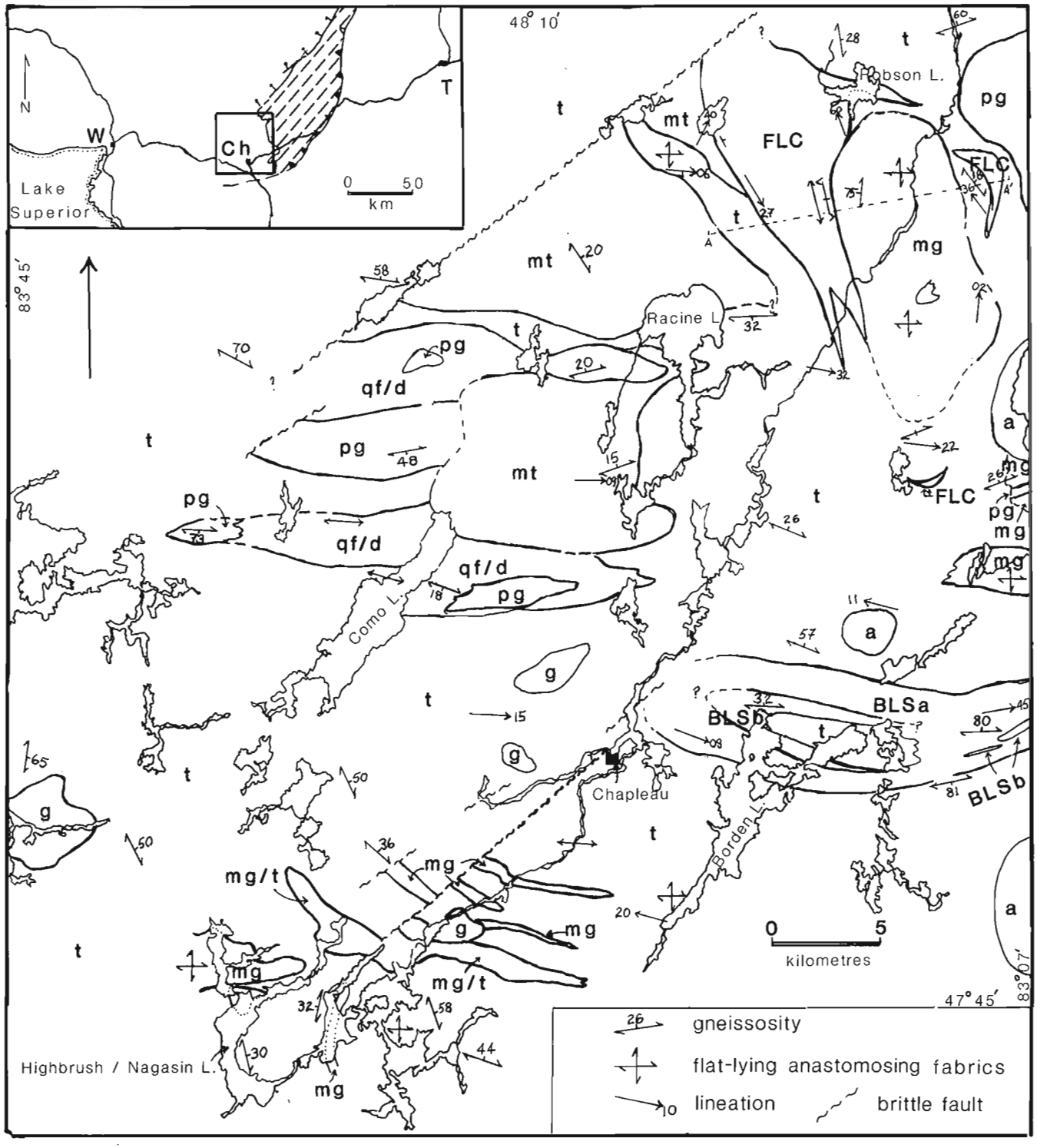

Figure 1. Generalized geological map of the southeastern Wawa gneiss terrane. Inset shows study area relative to the Kapuskasing structural zone (patterned) and the towns of Wawa (W) Chapleau (Ch) and Timmins (T). The following map units are described in the text: mg: mafic gneiss; pg: paragneiss; qf/d: quartzofeldspathic gneiss/diatexite; BLSa, b: Borden Lake sequence metavolcanic, metasediment; t: tonalite, tonalite gneiss; mt: mafic tonalite; FLC: Floranna Lake complex; g: granite, granodiorite; a: alkalic rock - carbonatite complex.

Tonalitic suite

These rocks are fine- to medium-grained, biotite-hornblende ± epidote tonalites with mafic contents generally less than 15 %; mafic tonalites with 15 - 25 % mafic constituents form a separate mappable unit. Tonalites vary texturally from massive, through foliated, to gneissic. Gneissic fabric is generally defined by 1 - 3 cm leucocratic layering spaced at a 2 - 5 cm scale. Leucosome is richer in quartz and poorer in plagioclase with respect to the host rock; borders are discrete and locally accentuated by a melanosome of biotite. Generally there is no change in grain size across such contacts although hornblende and biotite may be coarser within the leucosome. Several phases of leucosome are present in some rocks.

Mafic xenoliths are common throughout the tonalites, making up 2 - 30 % of individual outcrops, with an average of approximately 5 %. They range from 5 cm to several metres in maximum dimension with an average of 30 cm. Map-scale xenoliths several kilometres in length occur in the Highbrush/Nagasin Lake area.

Most xenoliths are mafic gneisses similar in composition and texture to the mafic gneiss unit. Although hornblende-plagioclase assemblages are prevalent, both epidote and garnet-clinopyroxene assemblages are present in xenoliths in the western and eastern parts of the map area respectively. In both examples, the xenoliths display amphibolitic rims 1 - 2 cm wide. A second, less common type of mafic xenolith is more prevalent in the eastern half of the map area. These round, 5 - 15 cm inclusions are medium-grained, massive, equigranular hornblende (60 %) - clinopyroxene (30 %) - palgioclase (10 %) rocks.

Floranna Lake complex

This coherent, crescentic plutonic complex is made up predominantly of massive to strongly foliated and lineated monzonite and diorite; tonalite, gabbro and pyroxenite are rare. Phenocrysts of clinopyroxene, rimmed by amphibole, and coarse feldspar, surrounded by granular feldspar, are common in monzonite and diorite.

Foliated to massive granite, granodiorite

Several hornblende (5 %) and biotite (< 5 %) - bearing granite to granodiorite bodies, 1 - 3 km across, crosscut tonalites in the central and southwestern parts of the field area. Small bodies in the Highbrush/Nagasin Lakes area are lineated whereas foliated and massive fabrics prevail elsewhere.

Proterozoic alkalic rock - carbonatite complexes

Three ovoid carbonatite complexes occur near the eastern border of the field area. In order of age they are: the Borden Township intrusion (1872 ± 13 Ma Pb/Pb; Bell et al., 1987); the Lackner Lake complex (1092 ± 21 Ma Rb/Sr; Bell and Blenkinsop, 1980); and the Nemegosenda Lake intrusion (~ 1100 Ma K-Ar; Gittins et al., 1967).

STRUCTURE

Regional trends

In general, planar fabric elements in the area strike west-northwest and dip predominantly to the north. Gentle dips (0-30°) of gneissosity become progressively more common in a west-to-east transect. Notable exceptions include the Borden Lake belt, characterized by subvertical dips, and the Robson / Floranna Lake area with north-south striking gneissosity and foliation. Several wide areas have sporadic zones of subhorizontal planar fabrics, referred to as domes by Percival (1981): the Highbrush Lake area; the area west of Racine Lake; and the area east and southeast of Robson Lake.

Linear fabric elements such as mineral lineations and minor fold axes generally have east-west trends and gentle plunges. However, an additional set of north-south lineations occurs in the Robson Lake structure (Fig. 1).

Deformation sequence

A preliminary structural sequence for the orthogneisses of the Chapleau area (Moser, 1988) included three regionally significant phases of Archean deformation: 1) formation of gneissic layering (S_1); 2) folding (F_2) of this gneissosity; and 3) subsequent normal offset of this fabric within zones of subhorizontal ductile deformation (D_3). Further mapping has revealed additional regional complexity in the deformation history: local structural sequences not corresponding to the three regional phases are recognized in the Robson/Floranna Lakes and Borden Lake areas. A detailed account of each local and regional phase is presented in relative chronologic order below.

Borden Lake belt

The Borden Lake belt is a 5 - km wide, ENE-striking metavolcanic-metasedimentary package that extends eastward into the Kapuskasing structural zone (Percival, 1981; Burnsall, 1989). Mafic rocks develop garnet-clinopyroxene assemblages at the expense of hornblende and plagioclase and metasedimentary rocks become orthopyroxene-bearing paragneisses from west to east, suggesting that metamorphic grade increases easterly along strike.

Most of the contacts between rocks of the Borden Lake belt and surrounding tonalite are transposed and provide no information on relative ages. However, tonalitic gneiss on the southeastern border of the belt contains metre-scale blocks of mafic gneiss with an inherited foliation. Therefore, the early deformation in the belt predates tonalite emplacement and subsequent regional deformation.

The belt has the overall structural form of a large isocline with a steep axial surface and shallow to moderate easterly plunge. The core of the structure is a thin body of tonalitic gneiss. A well exposed section on the southern limb of the isocline shows an interlayered sequence of paragneiss, metaconglomerate and metavolcanic rocks with possible relict pillows, tightly folded with a wavelength of 100 to 200 cm. In contrast, the poorly exposed northern limb consists entirely of mafic gneiss with a straight, continuous

gneissosity and local high-strain zones of sub-millimetre-scale hornblende-plagioclase assemblages. Whereas the regional dip of gneissosity in this area is shallow to moderate, fabrics in both the Borden Lake belt and contact gneisses dip sub-vertically. South of the Borden Lake belt, tonalitic gneisses have steeply oriented extensional structures, in contrast to the regional association between extensional structures and subhorizontal orientations. Lineations within the belt have the regional east-west, gently plunging orientation.

Because of poor exposure, the western end of the structure was not observed. Although it is tentatively interpreted as a fold closure, there appear to be significant differences in both lithological and structural character between the mafic gneisses of the northern and southern limbs. The abrupt western termination could alternatively be an intrusive contact with tonalite or a brittle normal fault.

A three-phase, Archean deformation sequence was postulated by Bursnall (1989) for high-grade mafic gneiss and paragneiss, 30 km eastward along strike from Borden Lake. Briefly, it consists of: 1) generation of gneissic fabrics (S_1); 2) development of northeast-trending, tight to isoclinal folds (F_2); and 3) further folding (F_3), followed by development of ductile shear zones. Evidence for the first two phases of this sequence are observed in the Borden Lake area, in the form of tight to isoclinal folds of gneissic layering.

Regional phase one: development of gneissic structures

Gneissic layering is generally the earliest structure present in tonalites and may have formed during or subsequent to tonalite emplacement. The pre-F_2 distribution and intensity of gneissic layering is not known, owing to subsequent overprinting and/or enhancement by later deformation. The regional distribution and continuity of gneissic fabrics and the effect of subsequent deformation is discussed in greater detail below.

Regional phase two: folding of gneissic fabric

The most common structures developed in this phase are isolated, tight to isoclinal, intrafolial folds which occur sporadically throughout the field area, except in the northwest quadrant. The wavelength of folds corresponds to the scale of gneissic layering, about 6 - 10 cm on average. Where preserved, anticline - syncline pairs display amplitudes at the 1 metre scale. Commonly only one limb and the fold nose are preserved, the missing limb having presumably been sheared off. Fold axes are generally shallow, east-west structures, although axial planes vary from upright to recumbent. Other, open to moderate, metre-scale folds are observed locally in the tonalites but their relative chronological position is not yet determined. It is possible that this regional second phase can be further subdivided.

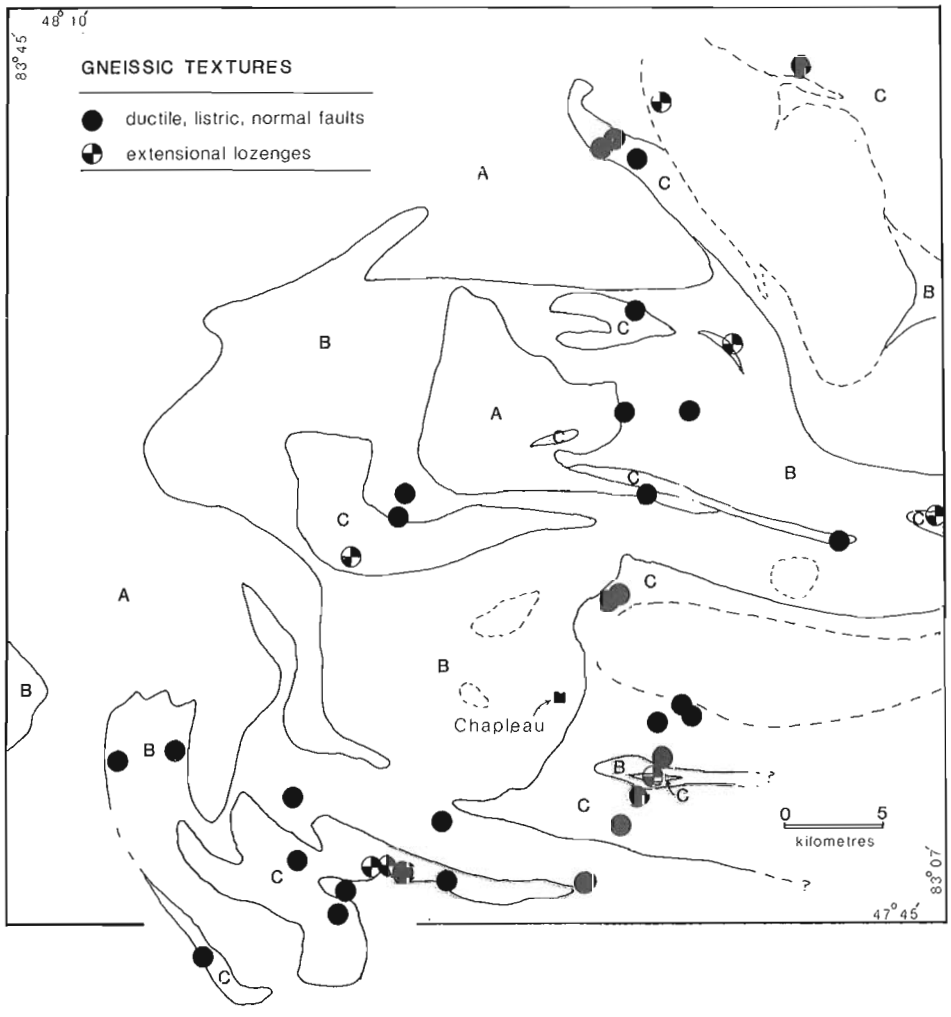

Figure 2. Regional distribution of gneissic fabric grades within quartzofeldspathic gneisses. Grade reflects continuity of gneissic textures as determined at outcrop scale, with 'A' and 'C' gneissosity being the least and most continuous respectively (see text for further definition). Areas within dashed lines indicate units unsuitable for classification scheme. Filled circles represent small-scale, ductile, listric, normal faults. Segmented circles represent anastomosing, ductile deformation zones (lozenges).

Regional phase three: development of ductile displacement zones

This is the final and most pervasive phase of regional ductile deformation. It is almost invariably associated with well lineated, sub-horizontal gneissic fabrics, consistently offset in a normal sense along high-strain zones. There are two distinct expressions of this extensional deformation: ductile, listric, normal faults; and anastomosing, ductile, deformation zones (lozenges).

The ductile, listric, normal faults (Fig. 2), the most common form of extensional strain, are restricted to gneissic tonalite lithologies. Individual faults are an average of 50 cm in length before they sole out parallel to gneissosity (Fig. 4e). The angle between this sole and the displacement zone ranges between 135 and 120°. Where markers are available, the average offset is about 10 cm. The faults generally occur as north-south trending sets indicating a predominant kinematic sense of either top to the east or west; conjugate sets are less common. The displacement surface is a narrow discontinuity in which gneissic fabric is deflected and thinned. It is generally less than 1 cm wide and shows no major grain size reduction with respect to the host gneiss. The displacement zone is commonly a locus for later generations of tonalitic leucosome.

The second style of phase-three deformation involves anastomosing, ductile shear fabrics which enclose lozenge-shaped domains of less-deformed rock (Fig. 4d). The lozenges have long axes measuring 1 - 2.5 m and short axes of 0.8 - 1.5 m, in a cross-sectional view perpendicular to the median plane of the structure. Deflection of gneissic layering along enclosing shear zones indicates normal offset sense, consistent with extensional deformation.

These structures are most common where mafic and tonalitic gneisses are interlayered at a scale of several metres. An exception occurs on the western border of the Floranna Lake complex, where anastomosing ductile shears, 5 - 10 cm in width, have formed in a locally massive hornblende diorite. Structures similar in scale and kinematics to those outlined here have been described in nappe or thrust tectonic regimes (Ramsay and Allison, 1979; Choukroune and Gapais, 1983).

Robson Lake/Floranna Lake structures

The Robson Lake "dome" (Percival, 1981) is an ovoid body roughly 10 by 12 km, located in the northeastern quadrant of the field area. The core of the structure consists mainly of migmatitic mafic gneiss with some paragneiss and

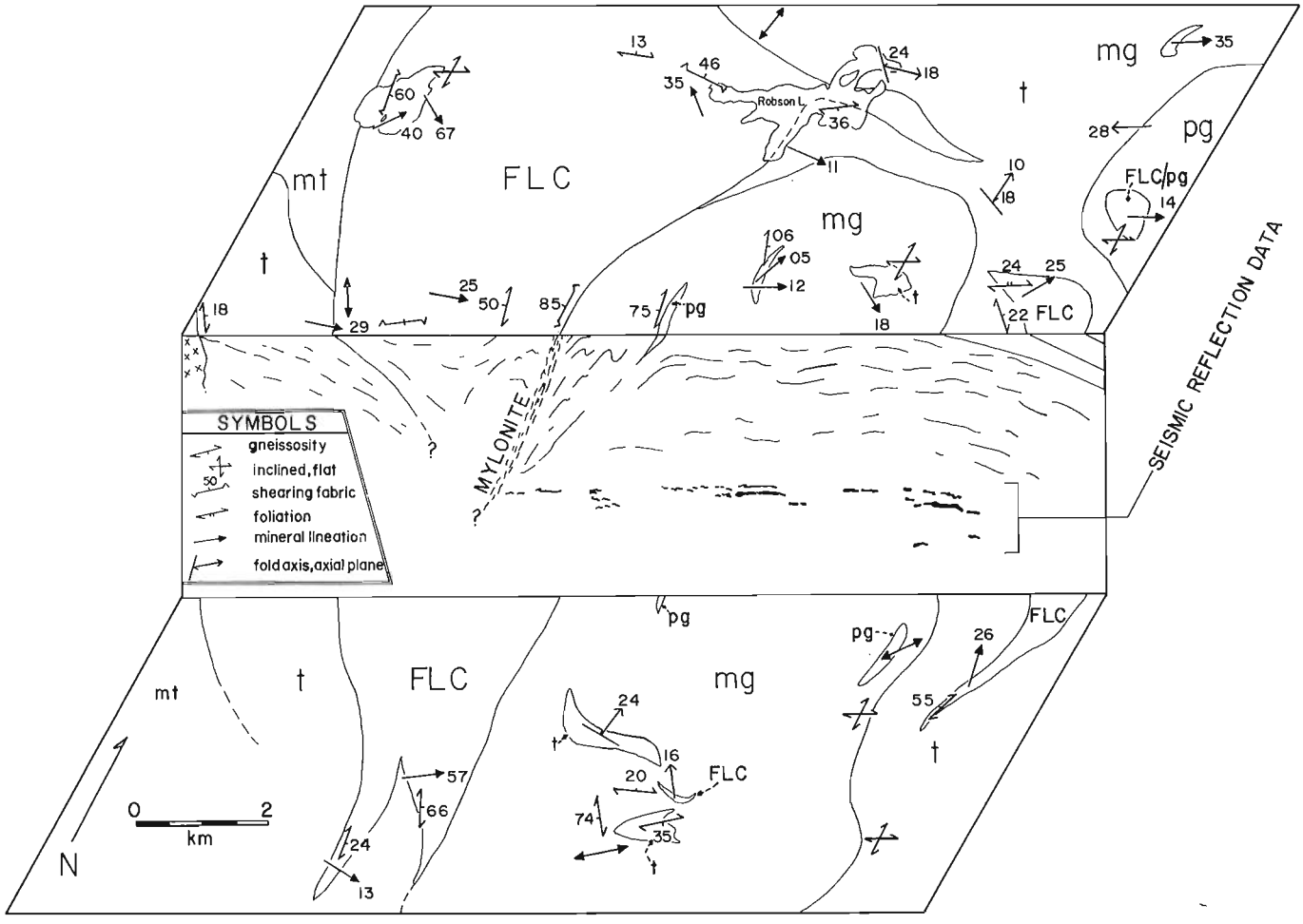

Figure 3. Cross section through the Robson-Floranna Lakes structure, based on surface structural information and seismic reflection data from LITHOPROBE line 4. Symbols as in Figure 2. Structural data illustrates the complexity of this area.

tonalitic gneiss. Assemblages of garnet-clinopyroxene-hornblende-plagioclase-quartz in mafic gneiss are similar to those in the Kapuskasing zone to the east. The structure is bordered on the west by the Floranna Lake complex (FLC) and on other sides by tonalitic gneiss interlayered with mafic gneisses, paragneisses and dioritic gneisses associated with the FLC.

With respect to the regional structural trends, this area is anomalous in terms of both linear and planar fabric elements. As shown in Figure 3, planar fabrics vary widely in orientation across the area. Those within the FLC strike north-south, with moderate to steep dips. Some of these are the result of sporadic shear zones which vary in width from 10 cm to 2 m. A steep, 100-m-wide zone of complex ductile deformation and refolded, high-strain fabrics marks the central eastern contact of the FLC with mafic gneiss. Fabrics in mafic gneiss steepen as they approach this zone and metamorphic minerals such as clinopyroxene become flattened and deformed. Mineral lineations associated with these shear zones plunge moderately to subhorizontaly. No consistent kinematic sense was determined.

In contrast, planar fabrics within the central Robson Lake structure have chaotic, moderate to subhorizontal orientations. Broad domal folds observed near Chapleau River have wavelengths and amplitudes of 8 m and 2 m respectively. Due to poor exposure, regional patterns are difficult to discern, however a broadly undulatory regional fabric would be consistent with the above-mentioned character of planar fabric orientations.

Two sets of linear fabric elements are recognized: a regionally consistent, shallow, east-west set; and a set of local, north-south mineral and fold-axis lineations. Both are present throughout the area and do not exhibit a strong relation to lithology as do the planar fabrics. Figure 3 presents an east-west cross section across the centre of the Robson-Floranna Lakes structure, parallel to part of Line 4 of the LITHOPROBE seismic reflection survey. It includes detailed structural data to illustrate the complex fabric relationships described above.

Brittle faults

Northeast-trending brittle faults occur throughout the study area. Where offsets are not observed directly, faults are inferred by the presence of centimetre-scale, epidote-filled fracture sets in rocks proximal to topographic lineaments; tonalites weather a distinctive dull orange. The faults post-date all other structural and intrusive events with the exception of the Proterozoic carbonatites. They are likely related to major Proterozoic brittle faults of the same trend to the northeast (Percival and McGrath, 1986) and east (J.T. Bursnall, 1989).

Gneissic fabric map

The field area is dominated by tonalitic rock types with minor compositional range but wide diversity of fabric. As a result, a fabric classification scheme was developed to better describe regional variations in rock character. Because most of the rocks are gneissic, the field grading system was based on objective criteria such as the continuity of gneissic layering at the outcrop scale. This approach to subdividing gneisses is similar to that used by Davidson et al. (1982) and Hanmer and Ciesielski (1984).

All quartzofeldspathic rocks with compositional layering were assigned a grade, A, B, or C, depending on the character of their gneissic fabric. In the 'A' gneisses, fabric is defined by leucocratic segregations (commonly 1 to 3 cm wide and spaced at 2 to 5 cm). In addition to this leucocratic layering, 'B' and 'C' gneissosity is defined by deformed, inherited heterogeneities such as pegmatite dykelets of mafic xenoliths. The characteristics of each gneissic grade are listed below and illustrated in Figure 4.

A: This grade applies to rocks in which the gneissosity varies widely at the outcrop scale. Individual gneissic layers are generally continuous for less than 0.5 m (Fig. 4a).

B: These gneisses contain a planar fabric which, unlike 'A' gneisses, is consistent in orientation but is of limited continuity (less than 1 m (Fig. 4b)).

C: This grade pertains to rocks in which gneissic layering is more consistent in orientation than 'B' and is continuous for greater than 1 m (Fig. 4c).

A generalized map of regional gneissic textures (Fig. 2) shows an overall trend of increasing gneissic continuity from west to east, toward the amphibolite-granulite transition. The broad transition zone between domains of predominantly 'A' and 'C' grade gneisses is generally parallel to the ragged, approximately north-south, amphibolite-granulite boundary zone to the east. Domains of 'C' grade gneiss within this zone are irregular amoeboid patches, 4 - 10 km in maximum dimension, with a high proportion of subhorizontal fabric orientations.

Mafic gneiss xenoliths generally become increasingly attenuated with increasing gneissic continuity. Similarly, the regional east-west mineral lineation is generally stronger in 'C' than in 'B' grade tonalitic gneisses and is absent in gneisses of grade 'A'. Gneissic grade in quartzofeldsaphic gneisses (Fig. 2) therefore serves as a crude approximation of relative strain intensity throughout the region. It is important to emphasize that the patterns in this diagram represent cumulative strain of all events, thermal and/or tectonic, which have contributed to the creation or enhancement of gneissic fabrics.

Seismic reflectors

Seismic profiles recorded recently during a LITHOPROBE reflection survey show a highly reflective crust below part of the study area (A. Green, pers. comm., 1988). Most of the reflectors are subhorizontal, although a few events project toward the surface in the Highbrush Lake area. This area is within one of the domains of 'C' grade gneissic fabrics in mafic and tonalitic gneisses interlayered at a scale of about 20 - 30 m. Further data processing is necessary to determine the precise location of the intersection of these reflectors with the surface for purposes of identification.

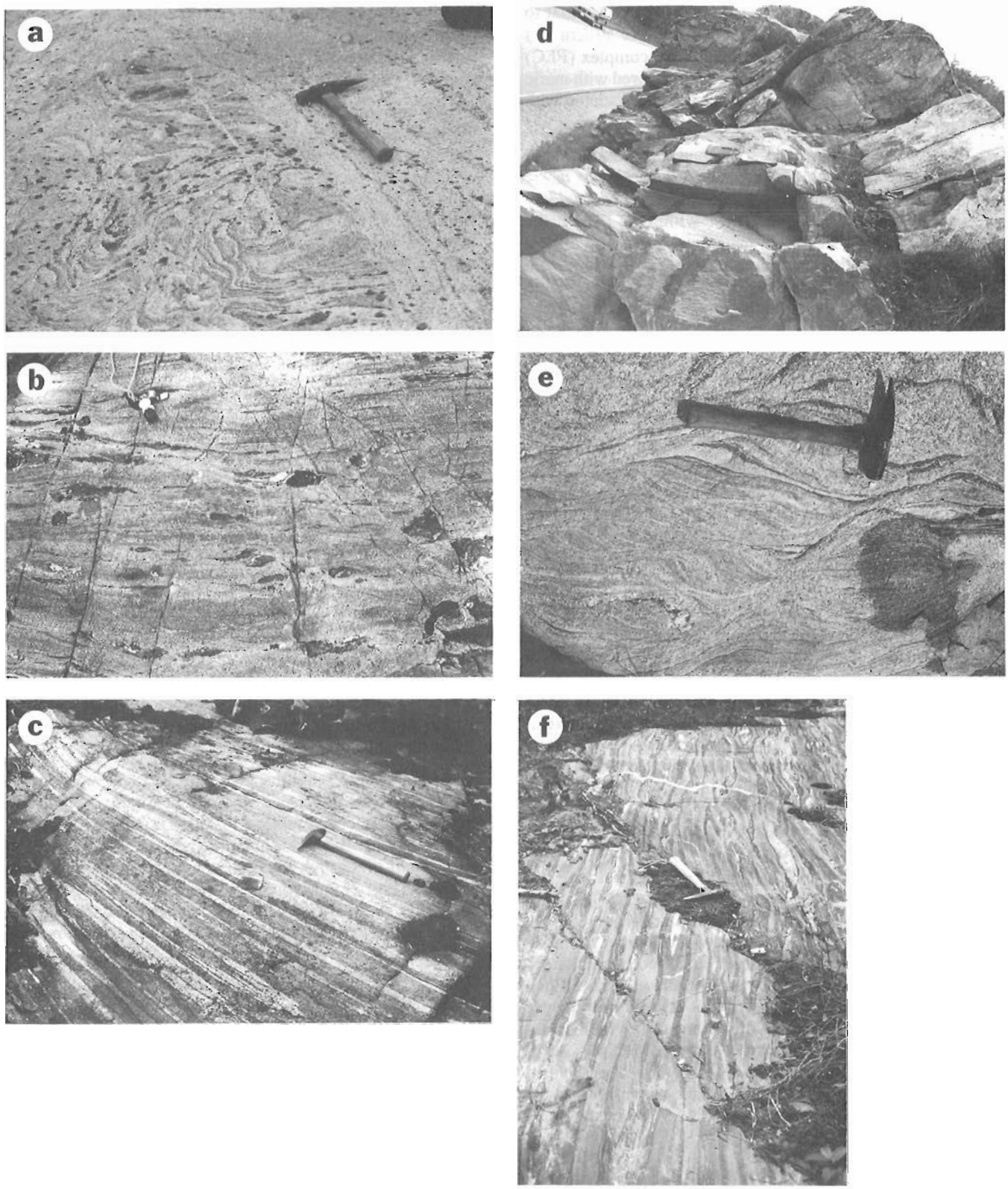

Figure 4. Field photographs of structures described. a), b), c) examples of type 'A', 'B', and 'C' gneissic textures respectively. d) extensional lozenges in interlayered mafic and tonalitic gneiss in the Sideburned-Highbrush Lakes area (notebook is 24 cm long). e) ductile, listric, normal faults in tonalitic gneiss near Racine Lake. f) relict, deformed and metamorphosed pillows in mafic rocks of the Borden Lake belt, 2 km from eastern map boundary.

DISCUSSION

Borden Lake belt

The Borden Lake belt preserves evidence for deformation that is older than both tonalite intrusion and high-grade metamorphism. Zircon from tonalite clasts in metaconglomerate near Borden Lake yielded an age of 2664 ± 12 Ma (Percival et al., 1981), younger than the minimum age of tonalite in the WGT of 2707 Ma (Percival and Krogh, 1983). Accepting the age of the tonalite clast would require that deposition, burial and deformation of the conglomerate took place after the completion of tonalite magmatism. The recent field evidence presented here supports the view that the clast age represents a reset date due to later deformation and metamorphism (Percival, 1988). Further geochronological work on this belt is planned in order to better constrain the age of the supracrustal package (T. Krogh, pers. comm., 1988).

The Borden Lake area is at the western end of a belt of supracrustal rocks that crosses the WGT-KSZ boundary. A prograde metamorphic transition from amphibolite to granulite facies may be recorded within the belt; its nature will be examined during further petrographic study.

Distribution of extensional structures and gneissic textures

Most of the 'B' and 'C' grade gneissic fabrics are considered to be the product of regional third-phase deformation and therefore, the distribution of grades shown in Figure 2 broadly reflects the character of regional strain during this phase. In the central north-south corridor of the area, strain is laterally heterogeneous, becoming more pervasive as subhorizontal orientations become more prominent to the east in deeper structural levels.

In light of the numerous outcrop-scale extensional fabrics noted by Moser (1988), one of the aims of the recent field work was to test for larger-scale structures of similar geometry, related to the same deformation. These were expected to be expressed as kilometre-scale, curvilinear, high-strain zones, enclosing lenses of less- deformed rock. Based on the regional strain distribution indicated by the gneissic textures map, it is apparent that such large domains are not present, aside from the regional, 'A' to 'C' strain gradient. Rather, amoeboid patches of high-strain ('C') gneiss are associated with small-scale, localized, pervasive ductile fabrics. The conditions of deformation were apparently such that, on a regional scale, strain was equally distributed as opposed to being localized along finite zones of major movement.

Robson/Floranna Lake structure

The relative age of variably oriented fabric elements in the Floranna/Robson Lake area is not yet clear. The orientation of the FLC perpendicular to the regional strike indicates relatively late emplacement, possibly associated with development of minor shear zones. The deformed metamorphic minerals in the eastern FLC contact also indicate late movement along this zone. However, minor amounts of typical FLC rock types occur within tonalite and mafic gneiss around the Robson Lake structure. It remains to be determined whether this post-metamorphic strain is associated with regional Archean deformation or with some later event. Possible models to be tested include: 1) late (Proterozoic) doming due to brittle uplift on the Ivanhoe Lake fault; possible scenarios include an underlying duplex structure or ramp in the gently-dipping fault; 2) doming due to intrusion of a pluton (considered unlikely in view of the lack of crosscutting plutonic phases in the area and the presence of subhorizontal reflectors at shallow levels beneath the structure (Fig. 3)); and 3) doming related to extension; the dome may represent a structure analogous to an extensional core complex; however, the minor structures do not appear to resemble those related to regional extension in the southern part of the area. Further structural analysis of this area and dating of the FLC will attempt to discount some of these possibilities.

SUMMARY

Regional deformation in the southern WGT involved early generation of gneissic layering, production of locally preserved F_2 folds and development of widespread, extensional, D_3 high-strain zones. Variations in the continuity and regularity of gneissic layering (Fig. 2) relate to the regional strain distribution resulting from the D_3 event, characterized by widespread, distributed strain rather than localized intense deformation along discrete zones. It is possible that one such zone of pervasive local deformation in the Highbrush Lake area corresponds to a zone of shallow, subhorizontal seismic reflections.

Two areas of complex local deformation are recognized. In the Borden Lake belt, supracrustal rocks have an older set of structures than the surrounding tonalitic gneisses. In the Robson / Floranna Lakes area, both regional east-west and local north-south structures are present; the age and generation mechanisms of these fabrics are as yet undetermined and may be the result of doming which postdates regional deformation in the tonalites.

Further work will concentrate on analysis of the metamorphic transition in the Borden Lake belt, detailed fabric analysis of extensional structures and fabrics from the Robson/Floranna Lakes area, and placing geochronological constraints on plutonism and tectonism during construction of the Wawa gneiss terrane.

ACKNOWLEDGMENTS

Katrina Moser is thanked for high quality field assistance. J.A. Percival provided valuable direction in mapping and substantial beneficial revision to the report. The writer is grateful to J.T. Bursnall, A. Leclair and J. Hanes for illuminating discussions in the field. Partial funding of this project through a NSERC LITHOPROBE grant (Contribution No. 81) to J. Hanes is gratefully acknowledged.

REFERENCES

Bell, K., and Blenkinsop, J.
1980: Ages and initial $^{87}Sr/^{86}Sr$ ratios from alkalic complexes in Ontario; Ontario Geological Survey, Miscellaneous Paper 93, p. 16-23.

Bell, K., Blenkinsop, J., Kwon, S.T., Tilton, G.R., and Sage, R.P.
1987: Age and radiogenic isotopic systematics of the Borden carbonatite complex, Ontario, Canada; Canadian Journal of Earth Sciences, v. 24, p. 24-30.

Bursnall, J.T.
1989: Structural sequence from the southeastern part of the Kapuskasing Structural Zone in the vicinity of Ivanhoe Lake, Ontario; in Current Research, Part C, Geological Survey of Canada, Paper 89-1C.

Choukroune, P. and Gapais, D.
1983: Strain patterns in the Aar granite (central Alps): orthogneiss developed by bulk inhomogeneous shortening; Journal of Structural Geology, v. 5, p. 411-418.

Davidson, A., Culshaw, N.G., and Nadeau, L.
1982: A tectono-metamorphic framework for part of the Grenville, Parry Sound region, Ontario; in Current Research, Part A, Geological Survey of Canada, Paper 82-1A, p. 175-190.

Gittins, J., McIntyre, R.M., and York, D.
1967: The ages of carbonatite complexes in eastern Canada; Canadian Journal of Earth Sciences, v. 4, p. 651-655.

Hanmer, S.K. and Ciesielski, A.
1984: A structural reconnaissance of the northwest boundary of the Central Metasedimentary Belt, Grenville Province, Ontario and Quebec; in Current Research, Part B, Geological Survey of Canada, Paper 84-1B, p. 121-131.

Heaman, L.M.
1988: A precise U-Pb zircon age for a Hearst dyke; Geological Association of Canada, Program with Abstracts, v. 13, p. A53.

Moser, D.
1988: Structure of the Wawa gneiss terrane near Chapleau, Ont; in Current Research, Part C, Geological Survey of Canada, Paper 88-1C, p. 93-99.

Percival, J.A.
1981: Geological evolution of part of the central Superior Province based on relationships among the Abitibi and Wawa subprovinces and the Kapuskasing structural zone; Ph.D. thesis, Queen's University, Kingston, Ontario, 300 p.
1983: High grade metamorphism in the Chapleau-Foleyet area, Ontario; American Mineralogist, v. 68, p. 667-686.
1986: The Kapuskasing uplift: Archean greenstones and granulites; Geological Association of Canada, Field Trip Guide 16.
1988: The Kapuskasing uplift: cross section through the Archean Superior Province; in Exposed Cross Sections of the Continental Crust, NATO Advanced Study Institute Field Guide, p. 1-49.

Percival, J.A. and Card, K.D.
1985: Structure and evolution of Archean crust in central Superior Province, Canada; in Evolution of Archean Supracrustal Sequences, ed. L.D. Ayres, P.C. Thurston, K.D. Card, and W. Weber, Geological Association of Canada, Special Paper 28, p. 179-192.

Percival, J.A. and Krogh, T.E.
1983: U-Pb zircon geochronology of the Kapuskasing structural zone and vicinity in the Chapleau-Foleyet area, Ontario; Canadian Journal of Earth Sciences, v. 20, p. 830-843.

Percival, J.A. and McGrath, P.H.
1986: Deep crustal structure and tectonic history of the northern Kapuskasing Uplift of Ontario: an integrated petrological-geophysical study; Tectonics, v. 5, p. 553-572.

Percival, J.A., Loveridge, W.D., and Sullivan, R.W.
1981: U-Pb zircon ages of tonalitic metaconglomerate cobbles and quartz monzonite from the Kapuskasing structural zone in the Chapleau area, Ontario; in Rb-Sr and U-Pb Isotopic age studies, report 4, in Current Research, Part C, Geological Survey of Canada, Paper 81-1C, p. 107-113.

Ramsay, J.G. and Allison, I.
1979: Structural analysis of shear zones in a deformed granite from the Pennine zone, Swiss Alps; Schweizerische Mineralogische und Petrographische Mitteilung, v. 59, p. 251-279.

Thurston, P.C., Siragusa, G.M., and Sage, R.P.
1977: Geology of the Chapleau area, Districts of Algoma, Sudbury, and Cochrane; Ontario Division of Mines, Geological Report 157, 293 p.

The Kapuskasing uplift in the Kapuskasing area, Ontario[1]

A.D. Leclair[2] and G.G. Poirier[3]
Lithosphere and Canadian Shield Division

Leclair, A.D. and Poirier, G.G., The Kapuskasing uplift in the Kapuskasing area, Ontario; in Current Research, Part C, Geological Survey of Canada, Paper 89-1C, p. 225-234, 1989.

Abstract

In the Kapuskasing area of the central Superior Province, the Kapuskasing uplift includes migmatitic mafic gneiss and paragneiss of the Groundhog River and northern Chapleau blocks, and tonalite gneiss, granodiorite and metavolcanic rocks of the Val Rita block. A voluminous suite of massive granodiorite, quartz monzonite and granite, and younger syenite to diorite plutons are emplaced in foliated to gneissic granitoids and metavolcanic rocks of the Wawa subprovince, and metagreywacke of the Quetico subprovince. Emplacement of dykes related to the Proterozoic Cargill complex is temporally associated with movement on the Lepage Fault.

The prominent regional foliation (S1) is deformed by small-scale, tight to open F2 folds and by map-scale, northeast-trending, upright F3 folds. Extensional shear-bounded "lozenge" structures developed in the tonalite gneiss after folding. Vertical displacement on the major northeast-trending faults that bound the tectonic blocks gave the Kapuskasing uplift its characteristic structural architecture.

Résumé

Dans la région de Kapuskasing, dans le centre de la province du lac Supérieur, le soulèvement de Kapuskasing comprend le gneiss mafique de caractère migmatitique, et le paragneiss des blocs de la partie nord de la rivière Groundhog et de Chapleau, ainsi que le gneiss tonalitique, la granodiorite et les roches métavolcaniques du bloc de Val Rita. Une série volumineuse de granodiorite massive, de monzonite quartzique et de granite, et de plutons plus récents dont la composition variée de syénitique à dioritique, a été mise en place dans les roches granitoïdes et métavolcaniques dont la nature varie de feuilletée à gneissique de la sous-province de Wawa, et dans les métagrauwackes de la sous-province de Quetico. La mise en place des dykes associés au complexe protérozoïque de Cargill est reliée dans le temps à un mouvement survenu le long de la faille de Lepage.

La schistosité régionale dominante (S_1) est déformée par des plis F_2 de petite envergure serrés à ouverts, et par des plis F_3 redressés d'importantes dimensions à l'échelle de la carte et de direction nord-est. Des structures de distension, limitées par des cisaillements et disposées en "losanges", se sont formées dans le gneiss tonalitique après la phase de plissement. Le rejet vertical caractérisant les grandes failles de direction nord-est qui limitent les blocs tectoniques, a donné au soulèvement de Kapuskasing son architecture caractéristique.

[1] Contribution to Canada-Ontario Mineral Development Agreement 1985-1990. Project carried by Geological Survey of Canada.

[2] 510-200 Lafontaine Ave., Vanier, Ontario K1L 8K8.
[3] Department of Geological Sciences, McGill University Montreal, Quebec H3A 2K6.

INTRODUCTION

The Kapuskasing uplift, a well exposed cross section of the continental crust, has stimulated national and international interest among workers studying three-dimensional aspects of the crust. It presents a unique opportunity to examine the deep crustal root of the mineral-rich Abitibi and Wawa belts and their possible links with higher-level mineralization processes. Geological and geophysical LITHOPROBE investigations have been focused mainly on the southern part of the uplift with limited information for the north. This mapping project, funded by the Canada-Ontario Mineral Development Agreement (Project C.7.3), is one of a number of studies underway in the Kapuskasing area aimed at improving the geological and geophysical database. An understanding of crustal-scale structures, magmatism and metamorphism at deep structural levels is essential for assessment of economic potential in the area. Results of integrated studies in the Kapuskasing area will provide a more complete picture of the nature of the uplift in its entirety.

In the Kapuskasing area, the Kapuskasing uplift transects the east-west trending Abitibi and Wawa volcanoplutonic and Quetico-Opatica metasedimentary subprovinces (Card and Ciesielski, 1986). It includes parts of the Groundhog River, Val Rita and northern Chapleau blocks which are bounded by major northeast-trending faults (Percival, 1985; Percival and McGrath, 1986) (Fig. 1) and characterized by distinct lithology, internal structure and metamorphic conditions (Leclair and Nagerl, 1988). The marked geological and geophysical disparities among these tectonic blocks are an indication of different origin. Field work in the Kapuskasing area during 1988 continued to improve the existing reconnaissance-scale mapping in the Val Rita block region and west of the Lepage fault. It covered the area of the Val Rita block characterized by an enigmatic, arcuate gravity high (Fig. 1). The recent Kapuskasing LITHOPROBE seismic reflection survey showed a highly reflective upper crust beneath the Val Rita block with shallow-dipping reflectors (A. Green pers. comm., 1988), and a significantly different structural architecture than that to the south.

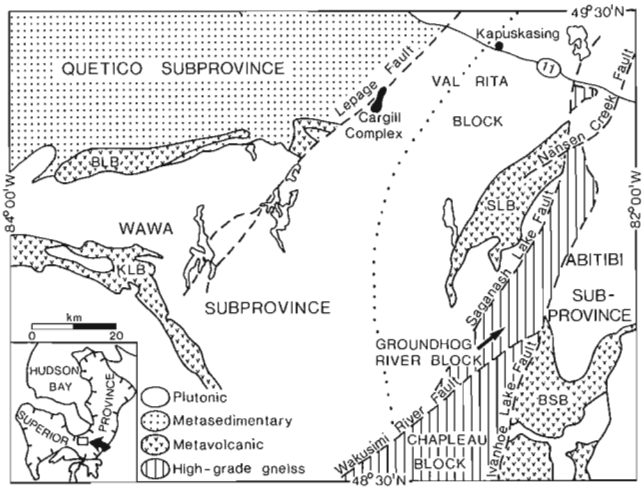

Figure 1. Location of major geological features in the Kapuskasing area showing subprovinces of the central Superior Province and regional structural elements of the Kapuskasing uplift (after Card and Ciesielski, 1986; Percival and McGrath, 1986). Inset shows the position of the Kapuskasing area in the Superior Province. Dotted line represents approximate axis of arcuate gravity and aeromagnetic anomalies of the Val Rita block. Metavolcanic belts are: BSB, Belford-Strachan belt; SLB, Saganash Lake belt; KLB, Kabinakagami Lake belt; BLB, Buchanan Lake Belt.

LITHOLOGY

Lithological designations are slightly modified from previous definitions in Leclair and Nagerl (1988). The units of migmatitic, felsic intrusive and hybrid rocks of Bennett et al. (1967) and Thurston et al. (1977) have been subdivided and refined, owing to more detailed mapping. The metatexites and diatexites of Berger et al. (1986) are redefined as tonalitic gneisses. Classification and nomenclature of plutonic rocks follow Streckeisen (1976). The following descriptions include mentions of geological relationships and interpreted relative chronology (Fig. 2).

Mafic gneiss

Migmatitic mafic gneiss of the Groundhog River and northern Chapleau blocks is described in Leclair and Nagerl (1988). It also occurs as discrete narrow units within paragneiss near the Lepage fault (see below).

Paragneiss

Migmatitic paragneiss in the Kapuskasing area is restricted to the Kapuskasing zone and the western edge of the Val Rita block (Fig. 2). In general, it is compositionally layered at the scale of 1 to 10 cm and has an overall quartz-rich composition, with 10-40 % orthopyroxene-bearing leucosome. Paragneiss units of the Groundhog River and northern Chapleau blocks are further described in Leclair and Nagerl (1988). Those in the Val Rita block are part of a thin wedge of metasedimentary granulites that trends northeasterly east of the Lepage fault (Percival and McGrath, 1986). They consist predominantly of fine- to medium-grained granoblastic melanosome (60-80 %) and coarse-grained leucosome (20-40 %), both composed of assemblages of garnet-orthopyroxene-biotite-plagioclase-quartz. Orthopyroxene is difficult to identify in places due to extensive yellowish brown weathering. At a few localities, migmatitic mafic gneiss occurs as thin discrete units interdigitated with the paragneiss. It is composed of garnet, clinopyroxene, hornblende, plagioclase and quartz, producing layers up to ~20 cm thick with internal layering caused by differences in modal proportions. Decimetre- to metre-scale inclusions of mafic gneiss within paragneiss are also present in one outcrop north of Kapuskasing. Some contain garnet-clinopyroxene-rich pods with hydration rims of hornblende. The origin of these inclusions is uncertain, but it is possible that they represent boundinaged early mafic dykes or calc-silicate-rich rocks.

Metavolcanic rocks

Four widely separated metavolcanic belts occur in the Kapuskasing area (Fig. 1). They comprise mainly mafic to intermediate metavolcanic rocks, with some units of felsic metavolcanic and minor intercalated metasedimentary rocks, all of which contain amphibolite-facies mineral assemblages.

Belford-Strachan belt

The Belford-Strachan belt of the Abitibi subprovince is dominated by fine-grained, massive and foliated, mafic to intermediate metavolcanic rocks, and a few discrete felsic units (mainly dacite), with thin interbeds of metatuff and minor volcanogenic metasediments (Bennett, 1969). These rocks are regionally metamorphosed to greenschist and

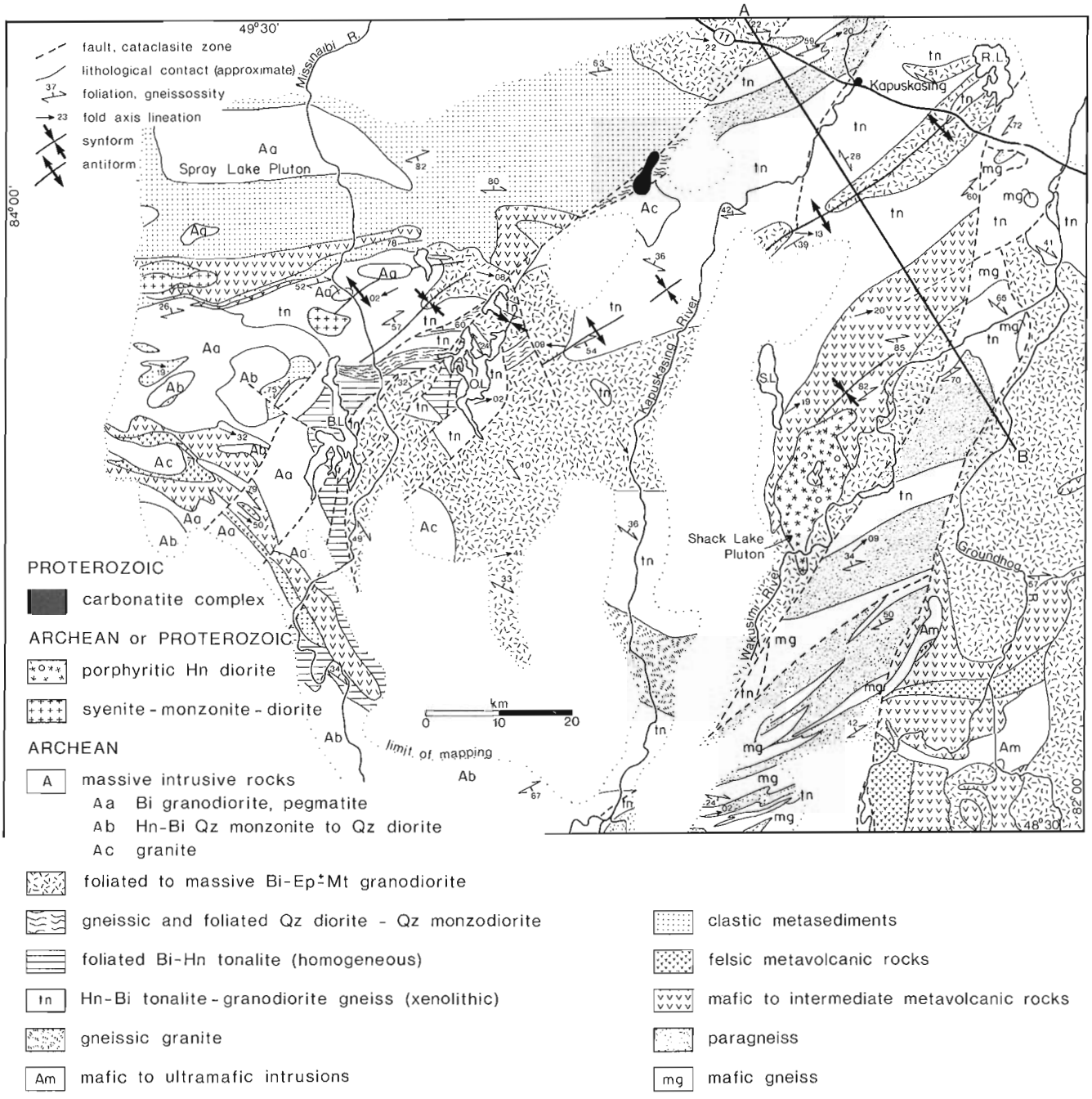

Figure 2. Simplified geological map of work to date in the Kapuskasing area, comprising the south half of Kapuskasing (NTS 42G) and the north half of Foleyet (NTS 42B) map areas. It includes areas originally mapped by McMurchy (1960), Bennett et al (1967), Bennett (1969), Thurston et al. (1977) and Berger et al. (1986). R.L. — Remi Lake; S.L. — Saganash Lake; O.L. — Opasatika Lake; B.L. — Brunswick Lake.

amphibolite facies. They are intruded by an elongate unit of magnetite-rich gabbro with minor serpentinite and diorite (unit Am, Fig. 2), which in turn is truncated by felsic intrusive rocks.

Saganash Lake belt

The Saganash Lake belt in the eastern Val Rita block consists almost entirely of fine- to medium-grained, foliated amphibolite, regarded as the metamorphic equivalent of mafic to intermediate massive and pillowed lava flows (cf. McMurchy, 1960; Thurston et al. 1977). It also includes subordinate garnet amphibolite, metatuff, oxide-facies iron formation and intermediate to felsic pyroclastic breccias, with minor intercalated beds of greywacke, quartzite and arkose. This arcuate northeast-trending belt of supracrustal rocks is intruded by diorite of the Shack Lake pluton and tonalitic gneiss, and terminates against the Saganash Lake fault (Leclair and Nagerl, 1988). Granitoid dykes, probably related to a pluton of foliated to massive granodiorite, cut the belt along its eastern margin.

Kabinakagami Lake belt

The easternmost extremity of the Kabinakagami Lake belt occurs in the study area south of Brunswick Lake. It consists mostly of fine- to medium-grained, layered and foliated (homogeneous) rocks that range from mafic to felsic, but the dominant composition is probably andesitic. These rocks commonly interfinger with intermediate, mafic and felsic compositions on the outcrop scale. Garnet porphyroblasts are present in many exposures. Thurston et al. (1977) noted significant occurrences of felsic metavolcanic rocks which form a mappable unit (Fig. 2) that includes thinly layered metatuff, foliated feldspar porphyry and minor pyroclastic breccia, and ranges from rhyolite to dacite. Well developed millimetre to centimetre-scale layering is widespread in the Kabinakagami Lake belt. It is likely inherited primary compositional layering (bedding), making some layered rocks identifiable as volcaniclastics, mostly tuffs. A thin fringe of siliceous metasedimentary rocks, similar to those in the Quetico subprovince, borders the belt on the south near the Missinaibi River. These rocks also occur as rare intercalations in the volcanic pile. Metavolcanic rocks are intruded by massive and gneissic granitoids which are locally sheared near the contact. The belt roughly coincides with strong positive aeromagnetic anomalies (Geological Survey of Canada, 1984).

Buchanan Lake belt

This east-trending belt of metavolcanic rocks is referred to here as the Buchanan Lake belt. It comprises mainly massive and pillowed flows of mafic to intermediate composition, with associated tuffs and pillow breccias, and felsic units made up of rhyolite to dacite tuffs and pyroclastic breccias (Berger et al., 1986). These rocks are intercalated with minor oxide-sulphide facies iron formation and clastic metasedimentary rocks. North of Opasatika Lake, a separate belt of mafic metavolcanic rocks consists of ash tuffs, and pyroclastic breccias with minor flows (Berger, 1985).

Quetico metasedimentary subprovince

Over its entire 1200-km-length, the Quetico subprovince is characterized by monotonous clastic metasedimentary rocks at greenschist to granulite facies, as well as derived migmatite and peraluminous granitic plutons (Card and Ciesielski, 1986). The easternmost segment of this belt is exposed in the northwestern part of the Kapuskasing area, where it terminates against the Lepage fault to the east and is intruded by granitoid rocks to the south (Fig. 1). It represents the most extensive occurrence of supracrustal rocks in the map area. These clastic metasediments consist predominantly of fine- to medium-grained turbiditic greywackes, with minor interbedded pelite, chert, amphibolitic and tuffaceous metasediments, and sulphide-oxide facies iron formation (Bennett et al., 1967; Berger et al., 1986). The metagreywacke is composed essentially of quartz, plagioclase and biotite, with or without garnet. Berger et al. (1986) reported pelitic assemblages of garnet-sillimanite-biotite-muscovite-quartz-plagioclase$\pm$K-feldspar near the southern contact of the belt. Primary sedimentary structures are difficult to recognize owing to recrystallization associated with amphibolite facies regional metamorphism. Bedding is poorly to well developed, ranging from centimetre to metre scale in thickness. Further lithological subdivision of the Quetico clastic rocks proved to be impracticable because of their overall similarity and poor exposure density.

South of the Quetico subprovince, steeply dipping clastic metasediments occur as metre- to kilometre-scale inclusions in massive intrusive rocks. These are interpreted as roof pendants of Quetico greywackes in a relatively high-level plutonic suite (see below) of white leucogranodiorite and pegmatite, which commonly contain garnet, muscovite and biotite, characteristic minerals of S-type granitoids generated, at least in part, by anatexis of the Quetico greywackes (cf. Card and Ciesielski, 1986; Percival, in press; and references therein).

Quetico-Wawa subprovince boundary

The southern boundary of the Quetico subprovince varies significantly in character along its length (Percival, in press; and references therein). In the Kapuskasing area, Berger (1985) considered metavolcanic rocks of the Buchanan Lake belt to be part of the Quetico subprovince, implying that the southern Quetico boundary is at the contact between metasedimentary rocks and plutons to the south. However, these plutons contain roof pendants of metagreywacke, suggesting that Quetico rocks extended further south prior to intrusion of biotite granodiorite. These relationships suggest that the Quetico-Wawa subprovince boundary is transitional over a wide zone, and will require further mapping and interpretation.

Gneissic granite

This rock-type is restricted to a few outcrops along the Kapuskasing River, and its regional extent is not yet known. It is a medium-grained, biotite-magnetite granite to locally granodiorite gneiss, with rare epidote and/or hornblende. The presence of magnetite is reflected by the relatively

stronger aeromagnetic expression for this unit. K-feldspar-rich layers and pods are common. The gneissic granite is injected by numerous undeformed pegmatite dykes and veins of granitic composition.

Hornblende-biotite tonalite-granodiorite gneiss

This unit is volumetrically the most abundant, constituting about half of the Wawa subprovince in the Kapuskasing area. It corresponds roughly to what Bennett et al. (1967) referred to as the migmatite-metasedimentary-metavolcanic complex. Berger et al. (1986) applied the migmatite terminology proposed by Brown (1973) (i.e. metatexite and diatexite), according to the percentage of mobilizate, to rocks of this unit. Although the term metatexite may be applicable in certain cases this usage was not adopted in favour of more descriptive rock names.

Tonalite to granodiorite gneiss is characterized by a highly variable field appearance caused by differences in composition, texture, structural complexity and amount of xenoliths and pegmatite veins. However, this dominantly orthogneissic unit could not be subdivided because of the small scale of these variations and the low outcrop density. The rock is grey to white, fine- to coarse-grained and contains variable proportions of ubiquitous biotite, hornblende, minor epidote and rare magnetite. This unit also includes mafic tonalite gneiss, as well as minor pyroxenite and melagabbro. Heterogeneous, xenolithic and migmatitic tonalite gneisses were recognized, but are not at mappable scale. Gneissic layering in heterogeneous tonalite is generally discontinuous, irregular and contorted, ranging in thickness from 1 to 30 cm (Fig. 3). It is comparatively much more regular in orientation around and west of Opasatika Lake. Xenolithic tonalite gneiss contains between about 1 and 30 per cent subangular to highly stretched mafic xenoliths composed of hornblende, plagioclase and quartz with or without clinopyroxene. These xenoliths are centimetre- to metre-scale, some with an internal fabric that is at an angle to the gneissosity. Tonalite gneiss contains up to ~35 per cent concordant, leucocratic, pink to white, generally coarser grained layers of granite to tonalite. This leucosome phase commonly contains hornblende, and may have formed as a result of segregation and/or lit-par-lit injection. Tonalite is also injected by up to ~20 per cent late, crosscutting, coarse-grained to pegmatitic veins and pods of granite to granodiorite composition. A study by Ann Doyle on the geochemistry of tonalite gneisses near Kapuskasing will form the basis of a B.Sc. thesis at Carleton University.

Figure 3. Heterogeneous tonalite gneiss containing layered and foliated mafic xenoliths and late, crosscutting granitic pegmatites. (GSC 204709-D).

Foliated biotite-hornblende tonalite

This unit is restricted mainly to a few areas around Opasatika and Brunswick Lakes (Fig. 2). It contains less than 5 per cent elongated mafic xenoliths composed of hornblende, plagioclase and rare biotite. This tonalite is easily distinguished from the gneissic tonalite because of its homogeneity and foliation. It is intruded by massive biotite tonalite and late pegmatite dykes.

Gneissic and foliated quartz diorite - quartz monzodiorite

This unit varies texturally from gneissic to foliated on the regional scale and is distinctly more mafic than surrounding tonalite and granodiorite units. It is dominated by quartz diorite, with less common monzodiorite; both are light grey to green, medium grained and contain hornblende and biotite with accessory epidote and sphene. Mafic minerals constitute between about 10 and 30 per cent of the rock. Homogeneous to gneissic mafic and ultramafic xenoliths make up less than 1 per cent of individual outcrops. At several localities along the Lepage fault, rocks of this unit are extremely brecciated and hardly recognizable.

Foliated to massive biotite-epidotemagnetite granodiorite

The units of granodiorite in the Abitibi belt and eastern Val Rita block, which are mapped and described separately in Leclair and Nagerl (1988), are now recognized as parts of the same unit that extends as far west as Brunswick Lake (Fig. 2). This unit is almost exclusively composed of medium- to coarse-grained, biotite-epidote ± magnetite granodiorite, but includes minor tonalite. Foliated biotite ± epidote tonalite prevails northwest of Opasatika Lake. The rocks are generally leucocratic, white to grey, equigranular, foliated to massive, and locally gneissic. At outcrop scale, they display only subtle variation in texture and mineralogy, having a homogeneous appearance with usually less than 2 per cent mafic xenoliths and pegmatite dykes. Pink K-feldspar phenocrysts, up to 2 cm long, occur at many localities. Magnetite is a common phase in areas near Opasatika Lake, Remi Lake and west of Kapuskasing. Mafic xenoliths are subangular to subrounded and mainly hornblende-plagioclase-quartz amphibolite with local clinopyroxene. Some have an internal fabric, although the enclosing granodiorite is relatively massive. Crosscutting relationships with the surrounding tonalitic gneisses are rarely exposed, and those observed are highly deformed and difficult to interpret. Nonetheless, the granodiorite is inferred to be younger, pending additional evidence.

Massive to weakly foliated intrusive rocks

Plutons and associated pegmatite of this suite are common in the western and southern parts of the map area (Fig. 2). They are subdivided into three main phases (granite, quartz monzonite - quartz diorite and granodiorite) on the basis of modal composition and textural characteristics. They were emplaced into the metavolcanic and metasedimentary belts and adjacent foliated and gneissic tonalite. Regional amphibolite-facies metamorphism indicates emplacement roughly at mid-crustal levels. A tentative chronology of emplacement places the granodiorite and associated pegmatite as the latest phases in the suite, and the quartz monzonite to quartz diorite possibly synchronous with the granite.

Granite

Three isolated bodies dominated by granite (monzogranite), but including minor quartz monzonite and granodiorite, have been partly mapped to date. The two east of Missinaibi River have textural and mineralogical affinities, consisting of white to light pink, homogeneous, medium-grained biotite leucogranite with or without hornblende, epidote and magnetite. Pegmatite pods and dykes, and subrounded mafic xenoliths (hornblende-plagioclase-quartz ± clinopyroxene), together constitute less than 5 per cent of individual outcrops. The third body, which cuts metavolcanic rocks of the Kabinakagami Lake belt, is a porphyritic biotite granite with distinctive euhedral K-feldspar megacrysts 2 to 3 cm long. This rock type is pink, homogeneous and massive to locally foliated, and contains rare autoliths of biotite-rich granite. Equant to locally augen-shaped K-feldspar megacrysts form approximately 30-50 per cent of the rock.

Hornblende-biotite quartz monzonite to quartz diorite

These rock-types occur as small round bodies within granodiorite and as large bodies in the southern part of the area, where their full size is not yet known. They are generally homogeneous, equigranular, medium to coarse grained, and contain accessory epidote and sphene. They are more mafic than granitoid rocks of the same suite (i.e. units Aa and Ac), with mafic minerals constituting approximately 10-30 per cent of the rock. The most common composition is quartz monzonite to quartz monzodiorite, but the unit includes quartz diorite and subordinate granite. The southern exposures contain centimetre- to metre-scale inclusions (up to 10 per cent) of mafic and tonalitic gneisses. They form an extensive unit that is probably equivalent to Percival's (1981) unit 10c to the south.

Biotite granodiorite and associated pegmatite

Granitoid and pegmatitic rocks of this unit form a large batholith west of Brunswick Lake and satellite intrusions to the north. They are generally leucocratic, white to light grey, locally pink, and contain less than 10 per cent biotite with or without magnetite. The granodiorite is homogeneous, equigranular, fine- to medium-grained and may also contain epidote. Locally, it contains distinctive grey quartz phenocrysts up to ~2 cm set in a creamy white groundmass of feldspars. Associated pegmatites occur north of the Kabinakagami Lake belt where they exist as dykes and irregular crosscutting bodies of metres to tens of metres in scale. They are generally distinguished from other pegmatites by large, white K-feldspar grains and well developed graphic textures. Although this unit is dominated by granodiorite and pegmatite, it sometimes includes tonalite and monzogranite compositions and some thin aplite dykes. Mafic xenoliths (<1 per cent) composed of hornblende-plagioclase-quartz ± biotite constitute less than 1 per cent of the plutons. The northern exposures of the batholith are characterized by numerous xenoliths of metagreywacke, presumably derived from the Quetico subprovince, and the presence of garnet, muscovite and biotite. There is a direct spatial relation between aluminous mineralogy in intrusive rocks and metasedimentary xenoliths. Further north, the Spray Lake pluton of the Quetico subprovince (Berger et al., 1986) consists of white to light grey, fine- to medium-grained, foliated biotite ± epidote tonalite to granodiorite.

Syenite - monzonite - diorite

These rocks occur as kilometre-scale plutons and plugs and centimetre- to metre-scale dykes that intrude other plutonic units. They are massive, coarse grained to pegmatitic and usually pink weathering. The only two mappable bodies occur west of Missinaibi River; the westernmost is hornblende monzonite (Berger et al., 1986) and the other, which corresponds to a zone of high magnetic relief, consists of pyroxene-biotite-magnetite syenite and subordinate clinopyroxene-hornblende diorite. It commonly contains K-feldspar phenocrysts up to 1 cm long and angular xenoliths of tonalite to granodiorite gneiss. These plutons and associated intrusions might be members of the suite of Proterozoic alkalic rock - carbonatite complexes associated with the Kapuskasing zone.

Figure 4. Lamprophyre dykes of the Cargill complex emplaced in quartz diorite gneiss near the Lepage fault. Crosscutting relationships show that early lamprophyre dykes and the small brittle faults that offset them are cut by late intermediate and thin felsic dykes. (GSC 204709-I).

Cargill complex

Emplaced in quartz diorite gneiss and granite, the Cargill complex pins the Lepage fault. It consists of ultramafic rocks ranging from olivine clinopyroxenite to amphibolite, and a younger carbonatite suite (Sage, 1983; Twyman, 1983). Sovite dykes less than 50 cm wide intrude ultramafic rocks (Butler, 1988). Fenitization is common along fractures and faults in the country rocks. Sandvik and Erdosh (1977) suggested that the Cargill complex is transected by a northeast-trending dextral fault, producing two subcomplexes and the characteristic peanut-shaped magnetic signature. At one locality near the Lepage fault, field relationships show that at least three generations of dykes related to the Cargill complex were emplaced at different times with respect to the faulting. In general, centimetre-scale lamprophyre dykes and the small brittle faults that offset them are cut by thin intermediate and felsic dykes (Fig. 4). The difference in age between these dykes is unknown, but is probably very small. In this context, apparently conflicting U-Pb dates of1907 ± 30 Ma (Kwon, 1986) and 1888 ± 3 Ma (L. Heaman, pers. comm. 1988) reported for the Cargill complex may indicate temporal closeness of magmatic pulses. Isotopic determinations on the dykes could potentially place tight constraints on the age of the Lepage fault. The crosscutting relationships of these dykes with respect to faults as well as the petrography and composition of each set in relation to the Cargill complex will be documented in detail by Matthew Pyne as part of a B.Sc. thesis project at Carleton University.

Diabase dykes

At least two sets of late, black- to brown-weathering diabase dykes were mapped west of Kapuskasing River. The most common are north- to north-northwest-trending, decimetres to 50 metres wide, and contain greenish plagioclase phenocrysts up to 2 cm diameter. These dykes locally form relatively high ridges, and some were traced for at least 7 km. They belong to the Hearst/Matachewan swarm of Ernst and Halls (1984) which also cut granulites of the Groundhog River block (Leclair and Nagerl, 1988). The second set consists of roughly northeast-trending dykes which cut the Hearst/Matachewan dykes. These dykes are less well exposed and range generally from 2 to 30 metres in thickness. They are fine- to medium-grained, and sparsely plagioclase porphyritic. This set probably includes members of the Kapuskasing swarm of Percival (1981), and possibly of the Preissac swarm. Northeast-trending olivine-bearing dykes are tentatively correlated with the Abitibi swarm. Further work is required to properly differentiate the northeast-trending dykes in the Kapuskasing area.

STRUCTURE

Stuctural elements

Primary structures (S_0) in the Kapuskasing area are limited to bedding in metavolcanic and metasedimentary rocks and a few pillow structures in the Saganash Lake and Buchanan Lake belts. In most units layering is inferred to be primary bedding, although strain-induced layering is also a possible interpretation. Top indicators in supracrustal rocks show a predominantly southward younging direction in the southern Quetico subprovince (Berger et al., 1986). Elsewhere, they are largely obliterated by deformation and amphibolite-facies regional metamorphism.

The most prominent planar structural element is a generally well developed, pervasive foliation (S1), defined by the alignment of biotite and less common hornblende. Compositional layering in gneisses, primary layering in metavolcanic and metasedimentary rocks and lithological contacts of deformed rocks are part of this foliation. A summary map (Fig. 5) shows the distribution of orientations of S1 structures. The Kapuskasing zone is dominated by a northeasterly structural grain with generally northwesterly dip.

Folds

Two, and possibly three, systematic fold sets that predate faulting have been recognized. The earliest, F_2, are small-scale, roughly east-west-trending, tight to open folds of the S_1 surface, with rare axial-surface fabrics. The plunge of

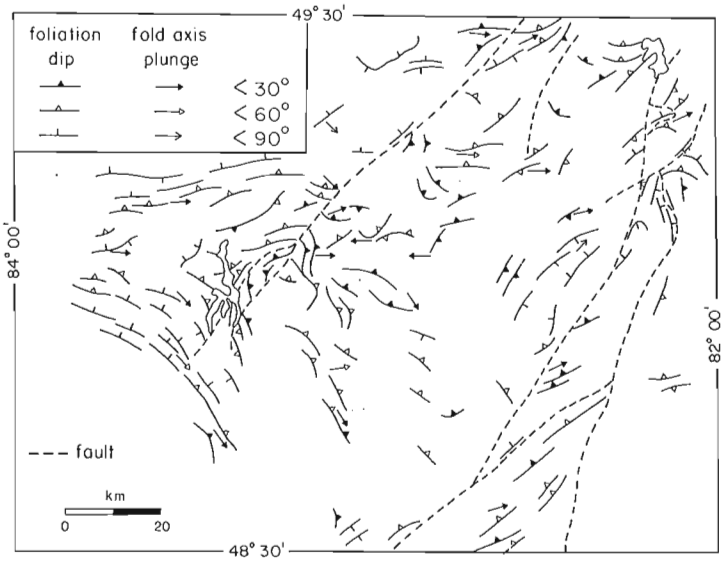

Figure 5. Summary map showing the orientation of planar and linear structural elements across the Kapuskasing area.

F_2 axes is subhorizontal (0-300), predominantly in an easterly direction, with azimuths of approximately 070 to 120 degrees. F_2 folds are especially common around Opasatika Lake. South of Opasatika and Brunswick lakes, F_2 axes plunge to the south-southeast. Folds in the Buchanan Lake belt reported by Berger et al. (1986) could be of this generation. Rare intrafolial folds of variable trend are possibly pre-F_2.

A younger fold set, F_3, is inferred to postdate minor F_2 folds. It is characterized by northeast-trending, upright, map-scale folds of the S_1 surface, without an associated axial-planar fabric. Folds of this generation are shown in Figure 2. Variations and reversals in plunge direction of F_2 folds may be attributed to this late fold set. F_3 folds vary in style from tight to broad, open warps. They are most commonly developed in tonalite-granodiorite gneiss, but one tight synform of this generation forms the axis of the Saganash Lake belt.

Lozenges and associated structures

Extensional shears bounding less-deformed lozenges, such as described by Moser (1988, 1989) in the Chapleau area, are developed locally in heterogeneous tonalite gneiss of the Kapuskasing area. Outcrops containing "lozenge" structures display a gentle, wavy pattern of the gneissic layering,characterized by a series of three dimensional waveforms, metres in wavelength and less in amplitude, bounded by ductile shear zones along which layering is attenuated and truncated (Fig. 6). The third dimension of these waveforms is rarely exposed because of the low profile of outcrops. In plane view, they appear as concentric structures with inward- or outward-dipping gneissosity (Fig. 7). Rare cross sections show that boundaries are ductile shear zones with a consistent, normal sense of displacement. Locally, a roughly east-trending subhorizontal stretching lineation is associated with these lozenges.

Late, northwest-trending shear bands have been observed at a few localities in tonalite gneiss and foliated granodiorite. They indicate a predominantly dextral sense of displacement, forming an apparent conjugate set with less well developed sinistral ones; such structures may be related to the lozenge style of deformation.

Shear-bounded lozenges are interpreted as manifestations of a subhorizontal extensional event that occurred at mid-crustal level prior to uplift (Moser, 1988). A seismic reflection profile across tonalite gneiss of the Val Rita block displays shallow-dipping, dome-shaped reflectors in the upper crust. It is possible that these domal culminations could be an expression of large-scale lozenge-like structures.

Major faults

The major northeast-trending faults that bound the Groundhog River, Val Rita and northern Chapleau blocks (Fig. 1) coincide with prominent aeromagnetic lineaments and extensive zones of cataclasis and brittle faulting. These zones, less than 1 km wide, are characterized by impressive networks of randomly oriented brittle offsets, fractures and discontinuous pseudotachylite veinlets that mutually crosscut and coalesce (Leclair and Nagerl, 1988) (Fig. 8). Fault-related structures such as fractures, cataclasite, tectonic breccia, fault gouge and thin mylonitic seams are common near these faults. Rocks near the fault trace are cataclasites with unrecognizable protoliths. Hematitic alteration and/or development of epidote and chlorite occur along fractures and faults. In general, these major faults affected diabase dykes of the Preissac (Leclair and Nagerl, 1988) and Kapuskasing swarms (Percival and Card, 1985), dated respectively at 2140 $\pm$ 40 Ma (Hanes and York, 1979) and 2040 Ma (Hanes et al., 1986), and are plugged by carbonatites as old as the Cargill complex (1888 $\pm$ 3 Ma; L. Heaman, pers. comm., 1988). However, the faults are not all the same age, as is discussed below.

The Lepage fault separates the Val Rita block from the Quetico subprovince, and extends southwestward into the Wawa subprovince, terminating near the Kabinakagami Lake belt (Fig. 1). In the northern part of the Kapuskasing area, it juxtaposes amphibolite-facies metasedimentary and granitoid rocks against tonalitic orthogneiss and metasedimentary granulite to the east. It joins the Rufus Lake fault of Berger et al. (1986) (the name "Lepage fault" is retained in this report). The Lepage fault loses its aeromagnetic expression southward, where metavolcanic rocks of the Kabinakagami Lake belt extend essentially uninter-

Figure 6. Oblique view through "lozenge" structures. Note the two waveforms separated by a zone of discontinuity and deflection of the layering. (GSC 204709-A).

Figure 7. Plane view of subhorizontal lozenge. Note the inward dip of the layering. (GSC 204709-C).

rupted across the southern projection of the fault trace. Percival and McGrath (1986) calculated a 60-70 degrees northwest dip and 7-10 km west-side-down normal displacement for the Lepage fault. The apparently large vertical displacement in the north progressively decreases southward and is distributed over a series of splays in the Opasatika-Brunswick Lake area (Fig. 2).

The Nansen Creek fault truncates the Groundhog River block and crosses the Saganash Lake fault into metavolcanic rocks of the Saganash Lake belt. East of the Saganash Lake fault, the dip of the foliation in mafic gneiss and massive to gneissic granitoids steepens close to the Nansen Creek fault. The southwest extension of the Nansen Creek fault cannot be traced because of limited bedrock exposure and weak aeromagnetic expression. However, mylonite and sheared iron formation in drill cores, more or less along strike of the fault trace (see Fig. 3 and Table 1 in Leclair and Nagerl, 1988), are possibly related to this fault. A north-south seismic reflection line crossing the Saganash Lake belt and Nansen Creek fault showed that gently-dipping reflectors are offset, north-side-down, at the fault by about 6 km. This component of movement is consistent with the disappearance of granulite to the north as generally higher crustal levels are exposed.

The Saganash Lake fault juxtaposes granulite gneisses of the Groundhog River and northern Chapleau blocks against amphibolite-facies metavolcanic rocks and massive to gneissic granitoids of the Val Rita block. It has been interpreted as a west-dipping, spoon-shaped listric normal fault, with about 10 km of maximum vertical displacement near the Saganash Lake belt, diminishing to the north and south (Percival and McGrath, 1986; Leclair and Nagerl, 1988). This sort of geometry and sense of movement is consistent with the preservation of supracrustal rocks in the Saganash Lake belt, implying relatively high crustal levels. It may also explain the arcuate, convex-west shape of the gravity and aeromagnetic anomalies of the Val Rita block (cf. Percival and McGrath, 1986).

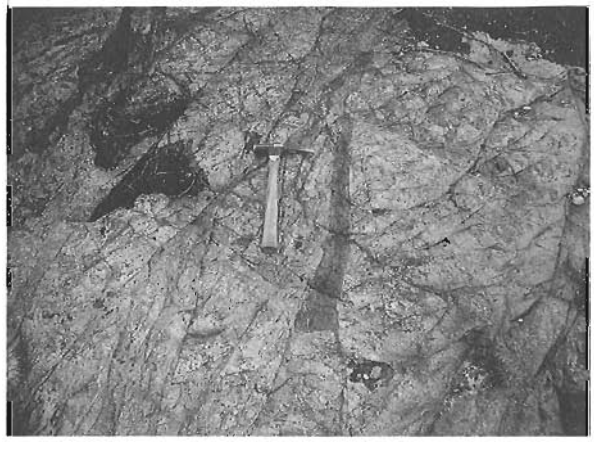

Figure 8. Highly fractured granite near the Lepage fault showing a complex network of brittle offsets, fractures and pseudotachylite veins (black vein in the centre of the picture). (GSC 204709-G).

Geological relationships described above are portrayed in a schematic northwest-southeast vertical cross section across the Val Rita and Groundhog River blocks (Fig. 9). The exposed crustal section of the Val Rita block displays a transition from granulite gneiss near the Lepage fault to amphibolite-facies metavolcanic rocks of the Saganash Lake belt to the east. It is reversed and apparently shorter than the transition between supracrustal and granulite-facies rocks to the south (cf. Percival and Card, 1985), probably because of large displacement on bounding listric normal faults. A 3 kbar paleopressure gradient between the Lepage and Saganash Lake faults was predicted from gravity modelling (Percival and McGrath, 1986). This will be tested by applying the hornblende barometer (Hammarstrom and Zen, 1986) to a suite of tonalites in the Val Rita block.

ECONOMIC POTENTIAL

Several workers have inferred linkages between lode gold deposits in supracrustal domains and geochemical depletion in the lower crust. Colvine et al. (1988; and references therein) proposed a genetic model whereby gold and incompatible elements (e.g. K, Li, Rb, B, Cs, U, Th) are partitioned into CO_2-rich fluids during granulitization of the lower crust and transported via crustal-scale structures to the upper crust, where they accumulate in structurally-controlled sites such as adjacent to the Kirkland-Larder Lake fault. If this model is valid for the Superior Province, the deep crustal rocks of the Kapuskasing structural zone should contain evidence of CO_2-rich fluids and geochemical depletion, including gold. However, metamorphic fluids in Kapuskasing granulites were aqueous, based on migmatitic textures which imply hydrous melts at 700-800°C (Percival, 1983). Furthermore, Truscott and Shaw (1988) reported only minor depletion of lithophile elements from Kapuskasing rocks and anomalous gold values were

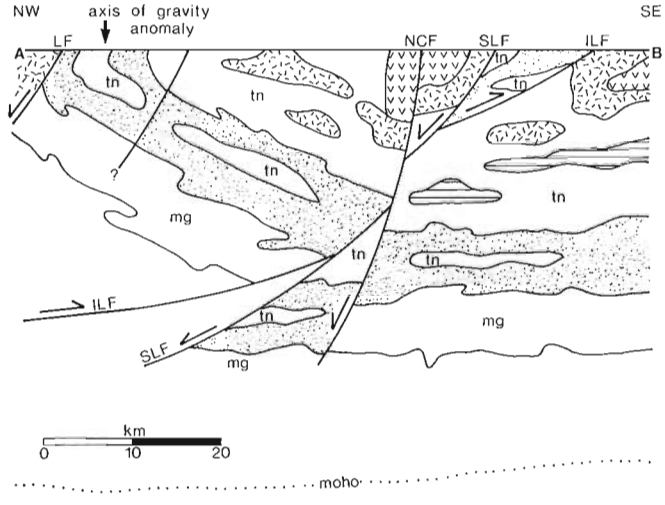

Figure 9. Schematic NW-SE cross section showing geological relationships between the Grounhog River and Val Rita blocks and inferred displacement along major bounding faults. Depth of Moho is taken from refraction studies of Boland and Ellis (in press). The location and legend for the section are shown in Fig. 2. Abbreviations: LF-Lepage fault, NCF-Nansen Creek fault, SLF-Saganash Lake fault, ILF-Ivanhoe Lake fault.

reported by Noranda Exploration Co. Ltd. from the northern Chapleau block. Although more information is needed to assess gold potential in granulites, these observations would appear to indicate that granulites of the Kapuskasing uplift may not be significantly depleted in lithophile elements or gold. Granulites of the Ashuanipi complex contain some elevated gold levels (Thomas and Butler, 1987) and prospective gold showings. Plans are underway to obtain geochemical data on granulites from the Kapuskasing area.

ACKNOWLEDGMENTS

The enduring and cheerful assistance of Ann Doyle and Matthew Pyne made the summer's work an enjoyable experience. Discussions with John Percival helped to identify problems of regional significance and to put the geology into proper perspective. Separate field trips with Desmond Moser, John Hanes and John Percival through the Kapuskasing area tested some of our ideas and are greatly appreciated. Estella Nkwate shared her observations on the peculiar gravity signature of the Kapuskasing area. Brigitte Leclair helped with the drafting of figures. Spruce Falls Power and Paper Co. Ltd. kindly provided lodging facilities at Camp 15 on the Kapuskasing River. The manuscript benefited from thorough reviews by John Percival. Lithoprobe contribution No. 82.

REFERENCES

Bennett, G.
1969: Geology of the Belford-Strachan area, District of Cochrane; Ontario Department of Mines, Geological Report 78, 30 p.

Bennett, G., Brown, D.D., George, P.T., and Leahey, E.J.
1967: Operation Kapuskasing; Ontario Department of Mines, Miscellaneous Paper 10, 98 p.

Berger, B.R.
1985: Hearst-Kapuskasing area, District of Cochrane; Ontario Geological Survey, Miscellaneous Paper 126, p. 95-98.

Berger, B.R., MacMillan, D.W., and Roy, P.L.
1986: Precambrian geology of Rykert, Fergus and parts of Abbott and Opasatika Townships, Hearst-Kapuskasing area, Algoma and Cochrane Districts; Ontario Geological Survey, Preliminary Map P. 2962, scale 1:31 680.

Boland, A.V., and Ellis, R.M.
—: Velocity structure of the Kapuskasing uplift from seismic refraction studies, northern Ontario; Journal of Geophysical Research. In press.

Brown, M.
1973: The definition of metatexis, diatexis and migmatite; Proceedings of the Geological Association, v. 84, p. 371-382.

Butler, S.H.
1988: Petrography and mineral chemistry of sovite dykes of the Cargill carbonatite complex, Kapuskasing, Ontario; B.Sc. thesis, Queen's University, Kingston, Ontario, 47 p.

Card, K.D., and Ciesielski, A.
1986: Subdivisions of the Superior Province of the Canadian Shield; Geoscience Canada, v. 13, p. 5-13.

Colvine, A.C., Fyon, J.A., Heather, K.B., Marmont, S., Smith, P.M., and Troop, D.G.
1988: Archean lode gold deposits in Ontario; Ontario Geological Survey, Miscellaneous Paper 139, 136 p.

Ernst, R.E., and Halls, H.C.
1984: Paleomagnetism of the Hearst dyke swarm and implications for the tectonic history of the Kapuskasing structural zone, northern Ontario; Canadian Journal of Earth Sciences, v. 21, p. 1499-1506.

Geological Survey of Canada
1984: Magnetic anomaly map, Timmins (NM-17); Map NM-17-M; scale 1:1 000 000.

Hammarstrom, J.M., and Zen, E-An
1986: Al in hornblende: an imperical igneous geobarometer; American Mineralogist, v. 71, p. 1297-1313.

Hanes, J.A., and York, D.
1979: A detailed $^{40}Ar/^{39}Ar$ age study of an Abitibi dyke from the Canadian Superior Province; Canadian Journal of Earth Sciences, v. 16, p. 1060-1070.

Hanes, J.A., Archibald, D.A., and Lee, J.K.W.
1986: Reconnaissance $^{40}Ar/^{39}Ar$ geochronology of Kapuskasing, Matachewan, and Hearst dykes in the Kapuskasing structural zone and adjacent Abitibi and Wawa greenstone belts, Ontario; Geological Association of Canada, Program with Abstracts, v. 11, p. 77.

Kwon, S.T.
1986: Lead-strontium-neodymium isotope study of the 100 to 2700 Ma old alkalic rock — carbonatite complexes in the Canadian Shield: inferences on the geochemical and structural evolution of the mantle; Ph.D. thesis, University of California at Santa Barbara, 226 p.

Leclair, A.D., and Nagerl, P.
1988: Geology of the Chapleau, Groundhog River and Val Rita blocks, Kapuskasing area, Ontario; in Current Research, Part C, Geological Survey of Canada, Paper 88-1C, p. 83-91.

McMurchy, R.C.
1960: Geology of the Saganash-Wakusimi Lake area; Ontario Department of Mines, v. 69, Part 3, 19 p.

Moser, D.,
1988: Structure of the Wawa gneiss terrane near Chapleau, Ontario; in Current Research, Part C, Geological Survey of Canada, Paper 88-1C, p. 93-99.
1989: Mid-crustal structures of the Wawa gneiss terrane near Chapleau, Ontario; in Current Research, Part C, Geological Survey of Canada, Paper 89-1C.

Percival, J.A.
1981: Geology of the Kapuskasing structural zone in the Chapleau-Foleyet area; Geological Survey of Canada, Open File 763.
1983: High-grade metamorphism in the Chapleau-Foleyet area, Ontario; American Mineralogist, v. 68, p. 667-686.
1985: The Kapuskasing structure in the Kapuskasing-Fraserdale area, Ontario; in Current Research, Part A, Geological Survey of Canada, Paper 85-1A, p. 1-5.
—: A regional perspective of the Quetico metasedimentary belt, Superior Province, Canada; Canadian Journal of Earth Sciences. In press.

Percival, J.A., and Card, K.D.
1985: Structure and evolution of Archean crust in central Superior Province, Canada; in Evolution of Archean Supracrustal Sequences, ed. L.D. Ayres et al., Geological Association of Canada, Special Paper 28, p. 179-192.

Percival, J.A., and McGrath, P.H.
1986: Deep crustal structure and tectonic history of the northern Kapuskasing uplift of Ontario: an integrated petrological-geophysical study; Tectonics, v. 5, p. 553-572.

Sage, R.P.
1983: Geology of the Cargill Township carbonatite complex; Ontario Geological Survey Open File Report 5400, 46 p.

Sandvik, P.O., and Erdosh, G.
1977: Geology of the Cargill phosphate deposit, northern Ontario; Canadian Institute of Mining and Metallurgy Bulletin, v. 70, p. 90-96.

Streckeisen, A.
1976: To each plutonic rock its proper name; Earth Science Reviews, v. 12, p. 1-33.

Thomas, A., and Butler, J.
1987: Gold reconnaissance in the Archean Ashuanipi complex of western Labrador; in Current Research, Newfoundland Department of Mines and Energy, Report 87-1, p. 237-255.

Thurston, P.C., Siragusa, G.M., and Sage, R.P.
1977: Geology of the Chapleau area, Districts of Algoma, Sudbury, and Cochrane; Ontario Division of Mines, Geoscience Report 157, 293 p.

Truscott, M.G., and Shaw, D.M.
1988: Average composition of lower and intermediate continental crust, Kapuskasing structural zone and Wawa domal gneiss terrane, Ontario (abstract); NATO Advanced Study Institute, "Exposed Cross Sections of the Continental Crust", p. 32.

Twyman, J.D.
1983: The generation, crystallization and differentiation of carbonatite magmas; evidence from the Argor and Cargill complexes, Ontario; unpublished Ph.D. thesis, University of Toronto, Toronto, Ontario.

Preliminary data on sulphur isotopes and Se/S ratios, and the source of sulphur in magmatic sulphides from the Fox River Sill, Molson Dykes and Thompson nickel deposits, northern Manitoba[1]

O.R. Eckstrand, L.N. Grinenko[2], H.R. Krouse[3], A.D. Paktunc, P.L. Schwann[4] and R.F.J. Scoates

Eckstrand, O.R., Grinenko, L.N., Krouse, H.R., Paktunc, A.D., Schwann, P.L. and Scoates, R.F.J., Preliminary data on sulphur isotopes and Se/S ratios, and the source of sulphur in magmatic sulphides from the Fox River Sill, Molson Dykes, and Thompson nickel deposits, northern Manitoba; in Current Research, Part C, Geological Survey of Canada, Paper 89-1C, p. 235-242, 1989.

Abstract

Sulphides from three mafic-ultramafic suites of the Circum-Superior Belt in northern Manitoba contrast markedly in their sulphur isotope and Se/S ratios, and thus indicate different sources of sulphur. Sulphur isotope values of the Fox River Sill disseminated sulphides average about +9 per mil, clearly indicating a crustal source, but that source is not sulphide iron-formation (-0.3 per mil) stratigraphically lower in the sequence. The wide range of $\delta^{34}S$ values (0.7 to 17.4 per mil) and Se/S ratios suggests mixing of sulphur from more than one source.

Sulphur isotope ratios of sparsely disseminated sulphides in the Molson Dykes lie near mantle values, and may point to a mantle source. Se/S ratios show much scatter, greatly exceeding the mantle range.

Nickel sulphide ores of the Thompson Nickel Belt have tightly clustered $\delta^{34}S$ ratios (+4 per mil), the same as barren wallrock sulphides. Se/S ratios of the ores overlap those of barren sulphides, but extend about halfway toward mantle values, suggesting that mantle sulphur in the original magma was massively contaminated by wallrock sulphides to form the nickel sulphide ores.

Résumé

Dans le nord du Manitoba, les sulfures de trois séries mafiques et ultramafiques de la zone périphérique du lac Supérieur (Circum-Superior Belt), diffèrent nettement les uns des autres du point de vue des rapports isotopiques du soufre et des taux Se/S; ces variations établissent que le soufre aurait donc des sources différentes. Les valeurs isotopiques du soufre dans les sulfures disséminés du filon-couche de Fox River sont en moyenne de +9 pour mille environ, signe que le soufre provient clairement de la croûte, mais que cette source n'est pas une formation ferrifère sulfurée (-0,3 pour mille) située à un niveau stratigraphique plus bas de la séquence. La vaste gamme des valeurs $\delta^{34}S$ (0,7 à 17,4 pour mille) et les taux Se/S semblent indiquer qu'il y a eu mélange de soufre en provenance de plusieurs sources.

Les rapports isotopiques du soufre dans les sulfures faiblement disséminés des dykes de Molson se rapprochent des valeurs caractéristiques du manteau, ce qui pourrait indiquer qu'ils proviennent d'une source située dans le manteau. Les taux Se/S font preuve d'une dispersion sur une surface beaucoup plus importante dans tout l'intervalle du manteau.

Les minerais sulfurés du nickel de la zone nickélifère de Thompson sont caractérisés par des $\delta^{34}S$ étroitement groupés (+4 pour mille), comme les sulfures de la roche encaissante stérile. Les taux Se/S des minerais recouvrent ceux des sulfures stériles, mais se rapprochent approximativement à mi-chemin des valeurs caractérisant le manteau; on en déduit que le soufre issu du manteau dans le magma originel aurait pu être massivement contaminé par les sulfures de la roche encaissante, avant de former les minerais sulfurés nickélifères.

[1] Contribution to the Canada-Manitoba Mineral Development Agreement, 1984-1989. Project carried by the Geological Survey of Canada.

[2] Department of Geochemistry, Moscow State University, USSR
[3] Department of Physics, University of Calgary, Calgary, Alta. T2N 1N4
[4] Department of Geology, Carleton University, Ottawa, Ont. K1S 5B6

INTRODUCTION

Nickeliferous magmatic sulphides of different character are associated with three different ultramafic-mafic intrusive suites in the northwestern part of the Circum-Superior Belt and adjoining Superior Province, northern Manitoba (Fig.1). The Aphebian ultramafic-associated, sulphide-rich nickel deposits of the Thompson Nickel Belt lie in the Circum-Superior Belt, and currently represent the third largest nickel-producing district in the world. Some 200 km to the east, also in the Circum-Superior Belt, the 250-km long Aphebian Fox River Sill contains extensive sparsely disseminated nickel sulphide mineralization, which is presently being explored for its platinum potential. The Molson Dyke swarm intrudes the adjoining Archean, and is known to contain sporadic sparsely disseminated sulphides.

The Fox River Sill and related mafic volcanic and mafic/ultramafic intrusive rocks and the Molson Dykes have been shown to have identical chemical characteristics, which prompted the suggestion that these suites are comagmatic (Scoates and Macek, 1978; Scoates, 1981; Baragar and Scoates, 1981; Baragar and Scoates, 1987). Heaman et al. (1986) have demonstrated that the two suites are coeval (1883 Ma, U-Pb zircon studies), thus strongly supporting the hypothesis of a comagmatic relationship.

Preliminary sulphur isotope determinations on Fox River Sill disseminated sulphides indicated substantial contamination by crustal sulphur. As a consequence, it became of interest to establish the isotopic character of sulphur in the coeval Molson Dyke sulphides. Such data might indicate whether similar contamination and similar sources of sulphur were involved in formation of the Molson Dyke sulphides. It could also contribute to better appreciation of genesis of different styles of sulphide mineralization within an extensive and diverse comagmatic suite.

The nickel ore-related serpentinites of the Thompson Nickel Belt were at first thought to be related to the Molson Dykes (Bell, 1971; Scoates and Macek, 1978; Peredery et al., 1982). However whole rock Pb-Pb model ages based on the sulphide ores (2320 ±20 Ma; Cumming et al., 1982) together with structural observations (Bleeker and Macek, in press) indicate that the Thompson Belt serpentinites are

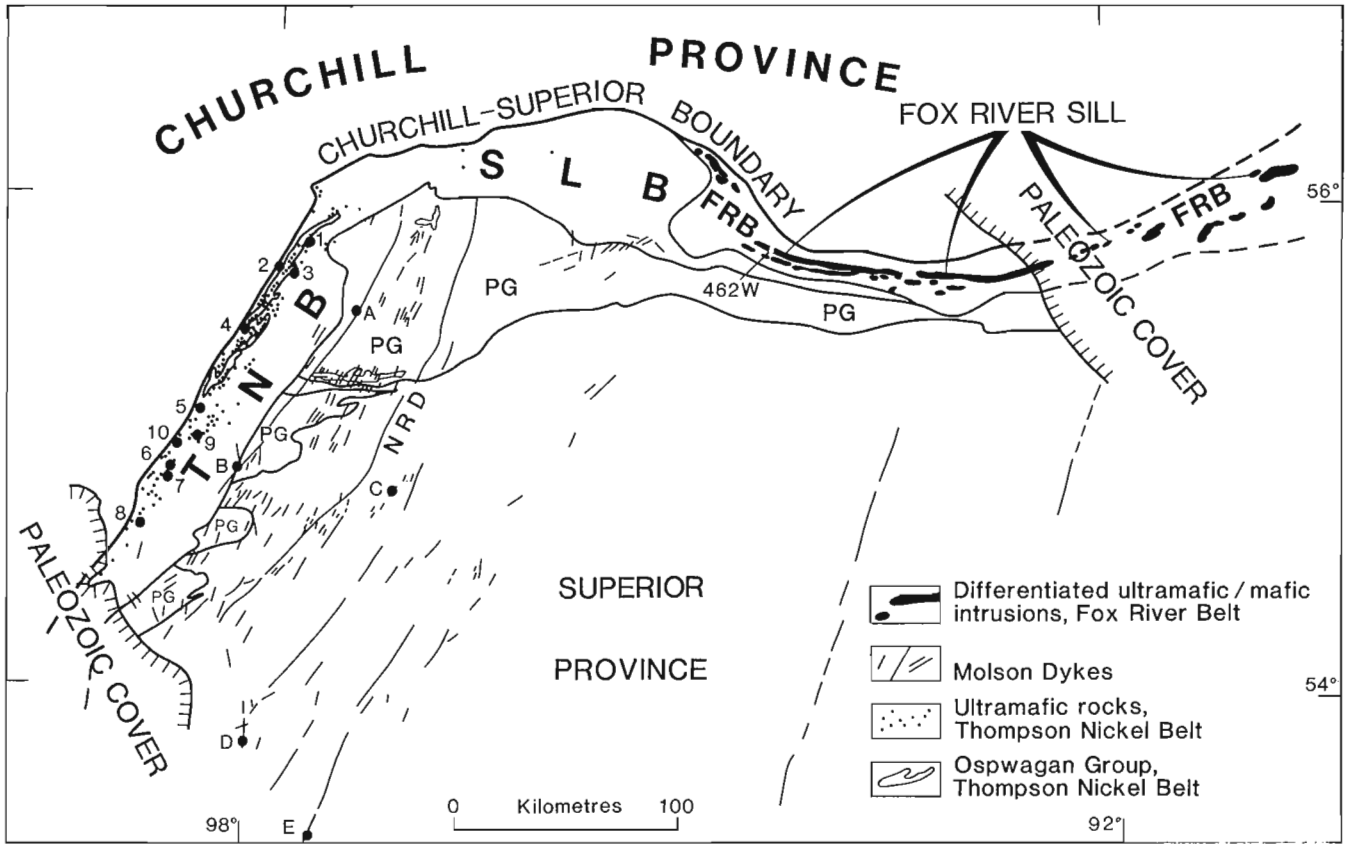

Figure 1. Location map of northwestern Superior Province (Archean) and adjoining Churchill Province (Proterozoic). The Pikwitonei Granulite (PG) terrane is the northeastern-most part of the Superior Province. The Circum-Superior Belt in this area includes the Thompson Nickel Belt (TNB), the Split Lake Block (SLB) and the Fox River Belt (FRB). The Nelson River Dyke(NRD) is the largest of the Molson Dykes. Sample localities (circled): 1) Fox River Sill: "462W" indicates the diamond drill section where all samples from the Fox River Sill were obtained. 2) Molson Dykes: A = Cuthbert Lake, B = Sipiwesk Lake, C = Cross Lake, D = Playgreen Lake, E = Belanger River. 3) Thompson Belt nickel deposits: 1 = Mystery Lake, 2 = South Manasan, 3 = Thompson mine, 4 = Pipe No. 2 mine, 5 = Soab South mine, 6 = Bowden, 7 = Bucko, 8 = Manibridge mine. In addition, barren sulphide localities: 9 = Halfway Lake and 10 = Setting Lake.

older. The sulphur isotopic and Se/S data for Thompson nickel sulphide ores present clear evidence for contamination by wallrock sulphides (O.R. Eckstrand, unpublished data). Thus they constitute a major occurrence of magmatic sulphides from a contrasting ultramafic suite in the same region as the Fox River Sill and Molson Dykes.

The origin of sulphur in these three magmatic suites is of interest because it could provide 1) better understanding of the genesis of the sulphides, 2) additional constraints on the evolution of the hosting intrusions, and 3) possible guidelines to exploration. Towards this objective, some preliminary data on sulphur isotope and Se/S ratios in the three magmatic suites are presented here.

Most of the analyses of sulphur isotopes in samples from the Fox River Belt and all of those from the Molson Dykes were carried out at the University of Calgary (L.N.G. and H.R.K.) using extraction by oxidation to SO_2. The remainder were done at the OCCGS/GSC Stable Isotope Facility at the University of Ottawa (as noted in Table 1) using extraction by reduction to H_2S. Analysis of sulphur and selenium was performed at Geological Survey of Canada laboratories. Determination of sulphur contents at low concentrations was done by Hall and Vaive (1989), and selenium was done by G.Hall and W.H.Nelson using a hydride extraction/atomic absorption technique.

FOX RIVER SILL

The Fox River Sill is a layered mafic-ultramafic intrusion in the Fox River Belt which is part of the Circum-Superior Belt in northeastern Manitoba (Fig. 1). The sill has an age of 1882.9 +1.5/-1.4 Ma (U-Pb zircon; Heaman et al., 1986). Geology of the Belt has been described by Scoates (1981) and Baragar and Scoates (1981). The Fox River Belt is a 15-20 km wide, steeply north-facing homoclinal sequence composed of sedimentary and volcanic rocks and ultramafic to mafic differentiated sills which have been metamorphosed to sub-greenschist to greenschist facies. Sedimentary rocks comprise the Lower (5 km), Middle (1 km) and Upper (1 km) Sedimentary formations. They consist mainly of fine grained, finely laminated quartz-rich siltstone, argillite and shale with interlayered sandstone, quartzite and dolomite. Iron formation and carbonaceous shales occur in the Lower Sedimentary formation. Small differentiated sills intruded the upper part of the Lower Sedimentary formation, whereas the Fox River Sill intruded the siltstone-sandstone sequence of the Middle Sedimentary formation. Ultramafic to mafic volcanic rocks are intercalated with the sediments and constitute the Lower (3 km) and Upper (2 km) Volcanic formations. They are thought to be related to the small differentiated intrusions and the Fox River Sill, respectively.

The Fox River Sill is over 2 km thick, has an east-west strike length of 250 km and dips steeply to the north. It is subdivided into the three series shown in Figure 2. The Main Layered Series is further subdivided into the Lower Central Layered Zone (LCLZ), comprising cycles of thick dunite layers alternating with thinner peridotite and pyroxenite layers, and the Upper Central Layered Zone (UCLZ), a succession of numerous thin cyclic units composed of dunite, peridotite, pyroxenite and gabbro. Cumulus mineral assemblages of these units are listed in Figure 2. The transition from LCLZ to UCLZ is characterized by the appearance of plagioclase as a major cumulus mineral. The LCLZ and UCLZ differ markedly in sulphide content. Disseminated sulphides are virtually absent in LCLZ rocks except near the top of the zone, but are common in UCLZ rocks.

Sulphide minerals within the Fox River Sill are minor but ubiquitous, seldom exceeding 3 volume per cent (Scoates and Eckstrand, 1986). The overall sulphide mineralogy is relatively simple, principally consisting of iron-nickel-copper-sulphur assemblages. Pyrrhotite, pentlandite, chalcopyrite, cubanite and mackinawite are the main sulphide minerals (Schwann and Scoates, 1988). They commonly

Table 1. Sulphur isotope and Se/S ratios, Fox River Belt.

	Sample No.	S (ppm)	Se (ppm)	Se/S × 10⁶	δ³⁴S‰*
	C-21				-0.50
	C-3				-0.72
	C-4				2.0
CUTHBERT LAKE	C-46				0.02
	C-5				0.23
	C-6.2				-1.18
	C-9				0.13
	C1	926	0.21	227	0.22
	C12	199	0.20	1005	-0.37
	C15	331	0.13	393	-3.86
	C35	241	0.09	373	-0.72
	C53	3321	0.53	160	0.11
	103	962	0.18	187	-0.36
SIPIWESK LAKE	105	599	0.25	417	-0.99
	106	728	0.35	481	-1.26
	109	1243	0.48	385	-1.19
	110	594	0.27	455	-1.01
CROSS LAKE	219-1	449	0.16	356	-2.55
	219-3	958	0.33	344	-0.67
PLAYGREEN LAKE	1196B				-0.60
BÉLANGER RIVER	390				1.49

*Grinenko and Krouse, University of Calgary

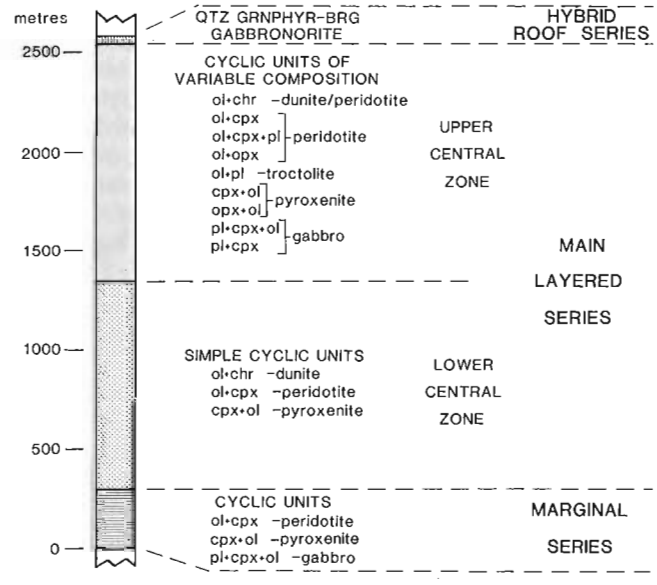

Figure 2. Composite stratigraphic section of the Fox River Sill, showing its main subdivisions and the sampled interval.

form polymineralic grains with pyrrhotite or pentlandite cores and chalcopyrite borders. Galena, sphalerite and bornite occur in minor amounts. Sulphides are commonly cuspate and bleb-like, occupying intercumulus areas. They are partially replaced by second generation sulphide, magnetite or silicate, and remobilized into secondary sulphide veinlets. Anomalous PGE concentrations (Pt+Pd > 100 ppb, up to 900 ppb) are present in three distinct horizons associated with intervals of disseminated sulphides (Schwann, in preparation).

MOLSON DYKES

A suite of mafic dykes known as the Molson Dyke swarm (Fahrig et al., 1965; Scoates and Macek, 1978) intrudes the Superior Province rocks in north-central Manitoba. The westerly and northerly extent of the dykes is limited by the Churchill-Superior boundary. Although some of the dykes occur as far as 300 km to the east of the Thompson Nickel Belt, they are mainly concentrated in the area between the Nelson River and the Thompson Nickel Belt (Fig. 1). The dykes occur both in the greenstone terrane (Gods Lake subprovince) of the Superior Province and in their higher grade equivalents in the Pikwitonei granulite domain to the west. The latter is believed to represent a thickened and tilted oblique section of the Archean crust (Paktunc and Baer, 1986).

The average strike of the swarm is about 030°, and dips are vertical to subvertical (Scoates and Macek, 1978). The dykes range in composition from gabbro to olivine-hornblende pyroxenite and hornblende peridotite (Paktunc, 1987; Scoates and Macek, 1978). The ultramafic dykes are thicker than the mafic varieties and have greater continuity along strike. The dykes are commonly undeformed and fresh. Zircons obtained from pegmatitic portions of the dykes yielded ages of 1883.7 +1.7/-1.5 and 1883 ±2 Ma (Heaman et al., 1986), the same as that of the Fox River Sill.

The dykes are apparently composite in nature. Composition appears to be a function of the dyke thickness, the thicker dykes being ultramafic (Scoates and Macek, 1978). Within-dyke variations are interpreted to have resulted from flow differentiation of multiple injections of magma carrying suspended olivine and minor chromite crystals (Paktunc, 1987). Orthopyroxene and clinopyroxene crystallized following magma emplacement in the vertical dyke conduits. Plagioclase and hornblende were the latest phases to crystallize from the intercumulus melt. Within-swarm variations are believed to have resulted from withdrawal of magmas from different parts of a zoned magma chamber or chambers.

THOMPSON NICKEL SULPHIDE DEPOSITS

The Thompson Nickel Belt is a northeasterly-trending part of the Circum-Superior Belt (Fig. 1) that has been intensely deformed by the Hudsonian tectonic event. It includes Archean gneisses that represent retrograded granulites, and infolded Aphebian metasedimentary and metavolcanic rocks that have been termed the Ospwagan Group (Scoates et al.,1977; Weber and Scoates, 1978). The following descriptions are taken from Zurbrigg (1963), Coats et al. (1972), Peredery et al. (1982) and Paktunc (1984).

The ultramafic rocks with which the nickel sulphide ores are associated commonly occur within the Ospwagan Group. They include serpentinized peridotite and dunite and minor orthopyroxenite. Some bodies display compositional layering attributable to fractional crystallization. Ultramafic rocks have been moderately to tightly folded and some have been totally dismembered by deformation (as at Thompson where the ultramafic consists of clusters of blocks strung out along the ore horizon). However, well preserved relict cumulus olivine textures are commonly present in the interiors of ultramafic bodies. Of significance to the present study is the spatial association of the ore-bearing ultramafics at the Thompson and Pipe 2 mines with sulphide iron formation of the Ospwagan Group (Bleeker and Macek, in press).

The nickel ores comprise interstitial, massive, breccia and vein sulphides. Pyrrhotite and pentlandite are the principal ore minerals, together with minor chalcopyrite and cubanite. Ni/Cu ratios of the ores range from 11 to 16.

The nickel deposits that were sampled are indicated in Figure 1 and include all types of sulphide. Barren sulphides of several types were sampled. These include sulphide iron formation from Thompson and Pipe 2 mines, and massive and breccia sulphides in schists and pegmatites from South Manasan, Soab South mine, Halfway Lake and Setting Lake.

Table 2. Sulphur isotope and Se/S ratios, Molson Dykes.

		Sample No.	S (ppm)	Se (ppm)	Se/S×10⁶	$\delta^{34}S_{CD}$ ‰
	UCLZ	1-7005	566	0.17	300	4.8 (1)*
	UCLZ	1-7025	8187	2.33	285	9.2 (2)
	UCLZ	1-7037	125	0.05	400	8.3 (1)
	UCLZ	1-7049	93	0.005		0.7 (1)
	UCLZ	1-7134	2339	0.36	154	10.7 (1)
	UCLZ	1-7164	5994	0.71	118	10.9 (1)
	UCLZ	1-7185	6375	2.37	372	12.1 (1)
	UCLZ	1-7200	12422	2.61	210	12.3 (2)
	UCLZ	1-7215	1881	1.12	595	11.7 (1)
	UCLZ	1-7218	2034	0.92	452	11.8 (2)
	UCLZ	1-7232	853	0.17	199	7.9 (1)
	UCLZ	1-7247	1037	0.34	328	9.5 (1)
FOX RIVER	UCLZ	2-7285	1351	0.08	59	4.1 (1)
INTRUSION	UCLZ	2-7290				4.9 (1)
	UCLZ	2-7320				7.1 (1)
	UCLZ	2-7369				6.0 (1)
	UCLZ	2-7491	3381	0.51	151	10.1 (2)
	UCLZ	2-7500	819	0.14	171	8.4 (1)
	UCLZ	2-7533	7618	1.49	196	10.1 (2)
	UCLZ	2-7545	18042	2.67	148	10.5 (2)
	UCLZ	2-7554	595	0.20	336	9.2 (1)
	UCLZ	5-7829				7.2 (1)
	UCLZ	5-7830				4.3 (1)
	UCLZ	5-7835	4545	0.67	147	9.2 (1)
	UCLZ	5-7850	4095	0.46	112	10.1 (1)
	UCLZ	5-7906	76	0.02		6.1 (1)
	UCLZ	5-7913	523	0.35	669	10.9 (1)
	UCLZ	5-7971	95	0.02		3.9 (1)
	UCLZ	5-7972	25	0.02		3.6 (1)
	UCLZ	5-9012	108	0.005		6.0 (1)
	UCLZ	5-9027	194	0.31	1598	6.5 (1)
	UCLZ	5-9028	144	0.12	833	8.2 (1)
	LCLZ	1-7267	2647	0.29	110	17.4 (2)
	LCLZ	1-7268	2744	0.60	219	16.6 (2)
	LCLZ	2-7281	2368	0.55	232	17.3 (1)
		FR 27	13400			-2.4 (1)
		FR 28	12500			-0.8 (1)
		FR 29	5300			-0.9 (1)
LOWER		FR 30	17400			0.75 (1)
SEDIMENTARY		FR 31	15400			0.4 (1)
FORMATION		FR 33	17600			-1.05 (1)
		FR 34	3500			0.1 (1)
		FR 35	6200			0.27 (1)
		FR 36	15500			0.6 (1)
		FR 38	8800			-0.89 (1)
		FR 39	10400			-1.42 (1)
		FR 44	900			2.16 (1)
		FR 46	600			-0.26 (1)

*(1) Grinenko and Krouse, University of Calgary; (2) OCCGS/GSC Stable Isotope Facility, University of Ottawa

DISCUSSION OF RESULTS

Analytical data for $\delta^{34}S$, S and Se for the Fox River Sill and Molson Dykes are listed in Tables 1 and 2, and plotted in Figures 3 and 4. Se/S ratios are considered suspect where Se values are at or near the detection limit and therefore have not been utilized in those instances.

Fox River Sill

Sulphur isotope data for sulphides of the Fox River Sill (Fig. 3) range from near zero to +17 per mil, but are mostly greater than +6 per mil. As mantle values of $\delta^{34}S$ are known to be near zero, the Fox River Sill data clearly indicate an important crustal contamination component. Furthermore the large range of values suggests the possibility of mixing of sulphur from two or more sources having different $\delta^{34}S$ values.

An additional interesting characteristic of the data is the grouping into two or possibly three distinct populations. The three values averaging about +17 per mil are the only LCLZ data, and they appear to form a separate population distinct from the UCLZ data (Schwann, in prep.). A possible interpretation is that the magma from which the LCLZ

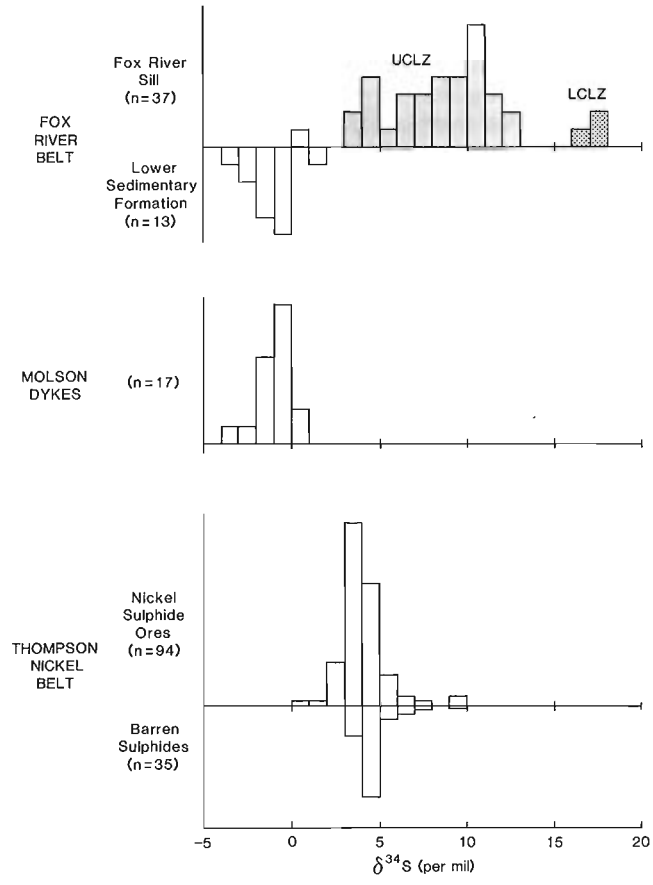

Figure 3. Sulphur isotope data for magmatic sulphides of the Fox River Sill, Molson Dykes and Thompson Belt nickel sulphide deposits, and for barren sulphides of the Lower Volcanic Formation in the Fox River Belt and of the Thompson Nickel Belt.

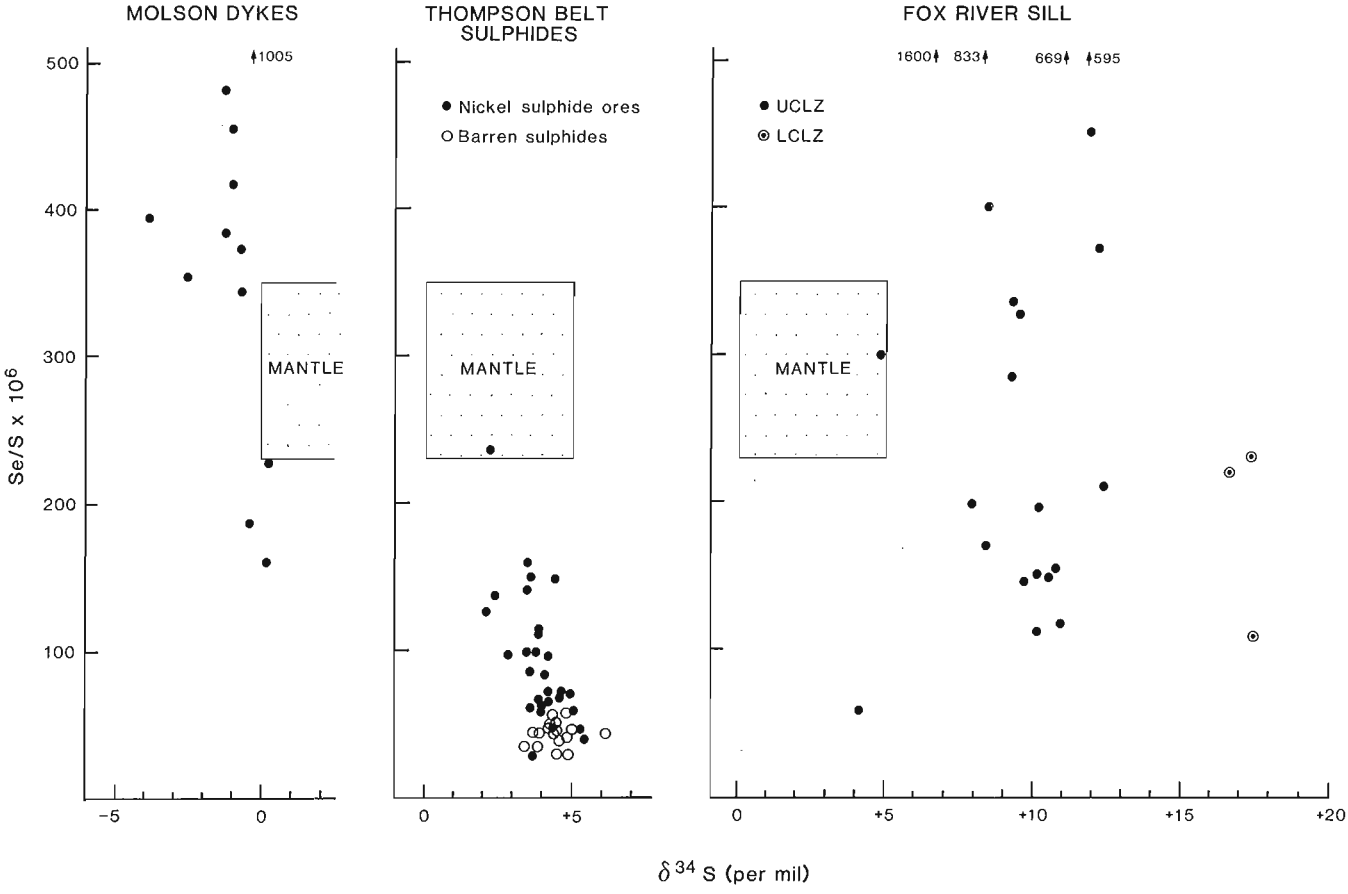

Figure 4. Sulphur isotope ratios ($\delta^{34}S$) versus selenium-sulphur ratios (Se/S x 106) for sulphides of the Fox River Sill, Molson Dykes and the Thompson Nickel Belt.

was formed was strongly contaminated with isotopically heavy sulphur from some crustal source. Subsequent magmas produced the UCLZ with its wide range of lighter $\delta^{34}S$ values. This may have resulted from differing admixtures of sulphur from several crustal sources that had lighter $\delta^{34}S$ values.

When combined with Se/S ratios (Fig.4), the data for the Fox River Sill show an even greater scatter. Se/S ratios range from strongly depleted to strongly enriched relative to mantle values. This degree of scatter is difficult to explain simply by mixing of sulphur from different sources.

The source of the contaminating sulphur must be sought somewhere in the crustal rocks through which the parental magmas of the Fox River Sill have risen. These would include the Proterozoic supracrustal rocks of the Fox River Belt that underlie the Sill, and Archean basement rocks. To date the only representatives of these candidates that have been analyzed are sulphidic iron formation from the Lower Sedimentary formation. The resulting $\delta^{34}S$ values (Fig. 3) clearly demonstrate that these rocks could not have been the source of the contaminating sulphur in the Fox River Sill.

Molson Dykes

The sulphur isotope ratios determined for the Molson Dykes (Fig. 3) have slightly negative values, near those of the mantle. They contrast sharply with those of the Fox River Sill, and clearly indicate a different sulphur source, possibly the mantle. Se/S ratios in the Molson Dykes (Fig. 4), like those of the Fox River Sill, show a large range that includes mantle values.

Thompson Nickel Belt

Sulphur isotopic data for the nickel sulphide ores of the Thompson Nickel Belt (Fig. 3) are quite similar to those of the barren wall rock sulphides, and both resemble mantle values. Consequently these data do not discriminate between barren wall rock sulphides and mantle as the source of sulphur in the nickel sulphides. However if the Se/S ratios are also taken into consideration (Fig. 4), it becomes clear that the nickel ores resemble the barren wall rock sulphides much more closely than they do the mantle. The nickel ores overlap the barren sulphides, and extend about halfway toward mantle values (Fig. 4). It appears likely, therefore, that the original magma with a certain content of mantle sulphur was massively contaminated by barren wall rock sulphides. This process was essential to the genesis of the nickel sulphide ores. Similar interpretations based on sulphur isotope and Se/S ratios were proposed for nickel sulphides of the Moxie and Katahdin intrusions in Maine (Thompson and Naldrett, 1984), and the Crystal Lake intrusion, Ontario (Eckstrand and Cogulu, 1986).

General

The Fox River, Molson Dyke and Thompson magmatic sulphides have mutually distinct sulphur isotope and Se/S ratios. Furthermore the amount of dispersion of the data differs significantly among the three suites (Fig. 4, 5). In the case of sulphur isotope ratios this has been attributed to mixing of sulphur from different sources. However in the case of Se/S ratios there may be an additional factor, as the amount of scatter appears to be related to the abundance of

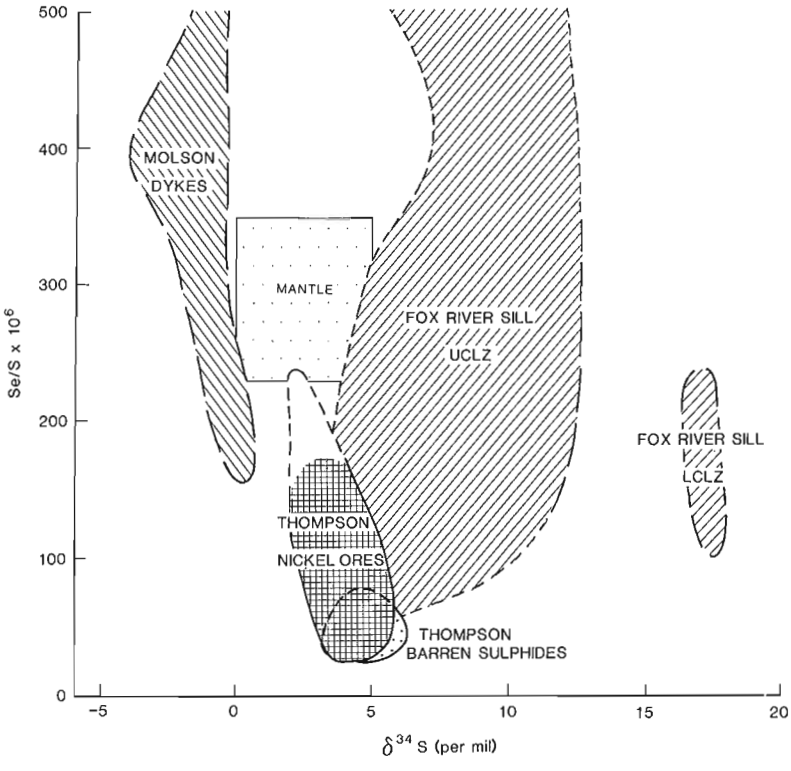

Figure 5. Comparison of $\delta^{34}S$ and Se/S x 106 ratios of sulphides of the Fox River Sill, Molson Dykes and the Thompson Nickel Belt.

sulphides in the rocks. In the Fox River Sill and the Molson Dykes, where sulphides constitute less than 3 per cent of the rocks, Se/S ratios have extreme ranges. In contrast the Thompson nickel ores which contain 10 to 75 per cent sulphides show much smaller ranges of values. The process that produces wide-ranging Se/S ratios in low sulphur sulphide ores is not well understood, but may be related to 1) sulphur mobility at late stages of sulphide crystallization or 2) redistribution of sulphur associated with serpentinization.

CONCLUSIONS

1. Sulphur isotope and Se/S ratios of magmatic sulphides of the Fox River Sill, Molson Dykes and Thompson Nickel Belt show well defined mutual differences that are considered to reflect different sources of sulphur.
2. Sulphur isotope ratios in the Fox River Sill indicate that the sulphur is mainly of crustal origin, and that the amount and/or type of sulphur contamination was different in the magmas of the LCLZ and the UCLZ. Both $\delta^{34}S$ and Se/S show wide scatter.
3. Sulphur isotope ratios of Molson Dyke sulphides lie near mantle values, whereas Se/S ratios show considerable scatter.
4. Thompson nickel sulphide ores have $\delta^{34}S$ and Se/S values that overlap those of barren wall rock sulphides, and extend about halfway toward mantle values. The nickel ores are considered to have formed when ultramafic magmas containing some mantle sulphur became extensively contaminated with barren wall rock sulphides.
5. Sulphur isotopic data together with Se/S ratios shed important light on the genesis of these magmatic sulphide deposits.

ACKNOWLEDGMENTS

We gratefully acknowledge A.P. Pryslak of BP Resources, W.V. Peredery and other staff members of INCO Limited, C.J.A. Coats of Falconbridge Limited, and I.F. Ermanovics of the Geological Survey of Canada for their assistance or permission in obtaining samples. Work on the Fox River Sill was supported in part by the Canada-Manitoba Mineral Development Agreement.

REFERENCES

Baragar, W.R.A. and Scoates, R.F.J.
1981: The Circum-Superior Belt: A Proterozoic Plate Margin? in Precambrian Plate Tectonics, ed. A. Kroner, Elsevier Scientific Publishing Company, Amsterdam, p. 297-330.

Baragar, W.R.A. and Scoates, R.F.J.
1987: Volcanic geochemistry of the northern segments of the Circum-Superior Belt of the Canadian Shield; in Geochemistry and Mineralization of Proterozoic Volcanic Suites, ed. T.C. Pharaoh, R.D. Beckinsale and D. Rickard, Geological Society, London, Special Publication No. 33, p. 113-131.

Bell, C.K.
1971: Boundary geology, upper Nelson River area, Manitoba and northwestern Ontario; Geological Association of Canada, Special Paper No. 9, p. 11-39.

Bleeker, W. and Macek, J.J.
1988: Thompson Nickel Belt Project: Pipe Pit Mine; in Report of Field Activities, 1988, Manitoba Energy and Mines, p. 111-115.

Coats, C.J.A., Quirke, T.T., Bell, C.K., Cranstone, D.A., and Campbell, F.H.A.
1972: Geology and mineral deposits of the Flin Flon, Lynn Lake and Thompson areas, Manitoba, and the Churchill-Superior Front of the Western Precambrian Shield; 24th International Geological Congress, Guidebook A31.

Cumming, G.L., Eckstrand, O.R., and Peredery, W.V.
1982: Geochronologic interpretations of Pb isotope ratios in nickel sulfides of the Thompson Belt, Manitoba; Canadian Journal of Earth Sciences, v. 19, p. 2306-2324.

Eckstrand, O.R. and Cogulu, E.
1986: Se/S evidence relating to genesis of sulphides in the Crystal Lake Gabbro, Thunder Bay, Ontario; Geological Association of Canada / Mineralogical Association of Canada / Canadian Geophysical Union Joint Annual Meeting, Program with Abstracts, v. 11, p. 66.

Fahrig, W.F., Gaucher, E.H. and Larochelle, A.
1965: Paleomagnetism of diabase dykes of the Canadian Shield; Canadian Journal of Earth Sciences, v. 2, p. 278-279.

Hall, G.E.M. and Vaive, J.E.
1989: The determination of sulphur in geological materials by pyrohydrolysis and ion chromatography: comparison with other production-oriented methods; in Current Research, Part F, Geological Survey of Canada Paper 89-1F.

Heaman, L.M., Machado, N., Krogh, T.E., and Weber, W.
1986: Precise U-Pb zircon ages for the Molson dyke swarm and the Fox River sill: Constraints for Early Proterozoic crustal evolution in northeastern Manitoba, Canada; Contributions to Mineralogy and Petrology, v. 94, p. 82-89.

Paktunc, A.D.
1984: Petrogenesis of ultramafic and mafic rocks of the Thompson Nickel Belt, Manitoba; Contributions to Mineralogy and Petrology, v. 88, p. 348-353.
1987: Differentiation of the Cuthbert Lake ultramafic dikes and related mafic dikes; Contributions to Mineralogy and Petrology, v. 97, p. 405-416.

Paktunc, A.D. and Baer, A.J.
1986: Geothermobarometry of the northwestern margin of the Superior Province; implications for its tectonic evolution; Journal of Geology, v. 94, p. 381-394.

Peredery, W.V. and Geological Staff
1982: Geology and nickel sulphide deposits of the Thompson belt, Manitoba: in Precambrian Sulphide Deposits, ed. R.W. Hutchinson, C.D. Spence and J.M. Franklin, Geological Association of Canada, Special Paper 25, p. 165-209.

Schwann, P.L.
—: Petrology, Geochemistry and PGE Distribution of part of the Layered Series (UCLZ), Fox River Sill, western lobe, 462 W Section, northeastern Manitoba; M.Sc. thesis, Carleton University. (in prep.)

Schwann, P.L. and Scoates, R.F.J.
1988: Petrology of platinum-group element mineralized units, Upper Central Layered Zone, Fox River Sill, northeastern Manitoba; in Program with Abstracts, Geological Association of Canada/Mineralogical Association of Canada, Joint Annual Meeting, v. 13, p. 110.

Scoates, R.F.J.
1981: Volcanic rocks of the Fox River Belt; Manitoba Department Energy and Mines, Geological Report 81-1, 109 p.

Scoates, R.F.J. and Eckstrand, O.R.
1986: Platinum-group elements in the upper central layered zone of the Fox River sill, northeastern Manitoba; Economic Geology, v. 81, p. 1137-1146.

Scoates, R.F.J. and Macek, J.J.
1978: Molson dyke swarm; Manitoba Mineral Resources Publication 78-1, 53 p.

Scoates, R.F.J., Macek, J.J., and Russell, J.K.
1977: Thompson Nickel Belt Project; in Report of Field Activities, 1977, Manitoba Mineral Resources Division, p. 47-53.

Thompson, J.F.H. and Naldrett, A.J.
1984: Sulphide-silicate reactions as a guide to Ni-Cu-Co mineralization in central Maine, U.S.A.; in Sulphide Deposits in Mafic and Ultramafic Rocks, ed. D.L. Buchanan and M.L. Jones, Proceedings IGCP Projects 161 and 91, Third Nickel Sulphide Field Conference, Perth, Western Australia, 23-25 May, 1982, Institution of Mining and Metallurgy, London, p. 103-113.

Weber, W. and Scoates, R.F.J.
1978: Archean and Proterozoic metamorphism in the northwestern Superior Province and along the Churchill-Superior boundary, Manitoba: in Metamorphism in the Canadian Shield, ed. J.A. Fraser and W.W. Heywood, Geological Survey of Canada, Paper 78-10, p. 5-16.

Zurbrigg, H.F.
1963: Thompson Mine geology; Canadian Institute of Mining and Metallurgy Bulletin, v. 56, p. 451-460.

Au, Pt, and Pd in pitchblende and copper sulphide veins at the Rah, Far, and Jaciar prospects, northern Bear Province, Northwest Territories[1]

S.S. Gandhi and A.D. Paktunc
Mineral Resources Division

Gandhi, S.S. and Paktunc, A.D., Au, Pt, and Pd in pitchblende and copper sulphide veins at the Rah, Far, and Jaciar prospects, northern Bear Province, Northwest Territories; in Current Research, Part C, Geological Survey of Canada, Paper 89-1C, p. 243-253, 1989.

Abstract

Concentrations of Au, Pt and Pd, up to 55, 40 and 55 ppm respectively, are found in pitchblende-rich veins of the Rah prospect, and up to 1 ppm of each of these metals in uraniferous, copper sulphide-rich quartz veins of the Far and Jaciar prospects. The veins contain varying proportions of uraninite, pitchblende, coffinite, chalcopyrite, bornite, digenite, covellite, Cu-Bi sulphides and Co-Ni sulpharsenides. Precious metals occur as electrum, Au-Pd alloy, tellurides of Au, Ag and Pd, and hollingworthite. Platinum minerals have not been identified. The veins are at, or near, the unconformity between late Aphebian volcano-plutonic basement and a Helikian continental siliciclastic sequence, marked by hematitic regolith. Vein formation is interpreted as related to reactivation of northeast-trending basement faults and circulation of meteoric waters at the faulted unconformity. A number of similar uraniferous veins occur in the Bear Structural Province and remain to be tested for precious metals.

Résumé

Dans les veines riches en pechblende de la zone productive possible de Rah, on rencontre des concentrations de Au, Pt et Pd atteignant parfois 55, 40 et 55 ppm respectivement, et dans les filons quartziques uranifères, riches en sulfures de cuivre, des zones productives possibles de Far et de Jaciar, les concentrations de chacun de ces métaux atteignent jusqu'à 1 ppm. Les filons contiennent des proportions variables d'uraninite, de pechblende, de coffinite, de chalcopyrite, de bornite, de digénite, de covellite, de sulfures de Cu et Bi et de sulfarséniures de Co et Ni. Les métaux précieux se présentent sous forme d'électrum d'alliages de Au et Pd, de tellurures de Au, Ag et Pd et de hollingworthite. On n'a pas identifié de minéral platinifère. Les filons sont situés à l'emplacement, ou à proximité, de la discordance située entre le socle volcano-plutonique datant de l'Aphébien supérieur et la séquence silicoclastique continentale d'âge hélikien, et marquée par la présence d'un régolite hématitique. On interprète la formation des filons comme le résultat de la réactivation de failles de direction nord-est dans le socle, et de la circulation des eaux météoriques au niveau de la discordance créée par les failles. Un certain nombre de filons uranifères du même type existent dans la province structurale de l'Ours, et feront l'objet de dosages des métaux précieux.

[1] Contribution to Canada-Northwest Territories Mineral Development Agreement 1987-1991. Project carried by the Geological Survey of Canada.

INTRODUCTION

The polymetallic veins of the Eldorado and Terra mines region at Great Bear Lake have been well known since the the 1930s for their uranium-silver association (Lang et al., 1962). Other precious metals, however, have not been reported in them. The uranium exploration boom in the 1970s led to the discovery of many other uranium occurrences north and northeast of Great Bear Lake (Fig. 1). At one of these, namely the Rah prospect, discovered and explored by Cominco Limited, the presence of gold and platinum in pitchblende veins was detected. Further exploration on the prospect, however, was curtailed due to the decline in uranium market that followed, and the claims were allowed to lapse. Interest in the property was revived when Aber Resources Limited restaked the claims in 1987, and launched a precious metals exploration program under their 'Corhill' project. The project also incorporated exploration of the surrounding region, including the Far and Wet prospects (Fig. 2). The company also submitted two samples from the Rah property, containing notable amounts of U, Au, Pt and Pd, for a detailed mineralogical study to the Geological Survey of Canada. This study was combined with investigation of other samples from the property, and samples from the copper sulphide-rich veins of the Far and Jaciar prospects, which were collected by the first author during 1977 and 1978. Results of this preliminary study reveal interesting polymetallic associations that have important implications to the regional metallogeny and resource potential, as discussed below.

GENERAL GEOLOGY

The Rah, Far and Jaciar prospects are in the northern part of the Great Bear magmatic zone (Fig. 1). It is an area of gently folded, felsic volcanic rocks and associated sediments of the McTavish Supergroup, which have been intruded by plagioclase-hornblende porphyry and younger granites. This suite of rocks is in turn unconformably overlain by the Hornby Bay Group (Fig. 1 and 2; Hoffman, 1984). The volcanic and intrusive rocks were emplaced during the Great Bear magmatic activity 1890-1840 Ma ago (Hoffman, 1980). The overlying strata of the Hornby Bay Group are continental and siliciclastic (Fraser et al., 1970; Kerans et al., 1981). The age of this little deformed sequence is indicated by a U-Pb zircon date of 1663 $\pm$ 8 Ma on intermediate to felsic interbedded volcanic rocks of the Narakay Islands in the Great Bear Lake (Bowring and Ross, 1985). The basal unconformity is marked by red hematitic paleoweathering of the basement rocks which extends to a depth of a few tens of metres and has produced an unevenly distributed hematite-rich regolith. The thickest exposures of the regolith are near Fault River (Fig. 1 and 2).

A set of northeast-trending, nearly vertical faults affect the whole Great Bear region (Hoffman, 1984). They are prominent features of the Rah prospect area (Fig. 2). They are accompanied by related major and minor faults, and commonly have right-lateral displacement, in places reaching up to several tens of kilometres. The faults predate the deposition of Hornby Bay Group, but some have been reactivated and have affected the strata of this group (Fig. 2). Quartz veins, up to 20 m thick and commonly trending northeast, are developed along parts of these faults throughout the Bear province. Their age relationship with the Hornby Bay Group is not certain. More than one generation of quartz veins occurs, and some quartz veins cut the group, but the development of the larger quartz veins may be concurrent with the deposition of the siliciclastic sequence or may even pre-date it. Concurrence is suggested by a strongly silicified sandstone dyke in the basement granite at the Rah prospect.

RAH PROSPECT

The Rah prospect was discovered in 1976 by Cominco Limited, through a follow-up of the company's regional lake water geochemical survey. It was explored by extensive trenching and limited drilling during the period 1976-1978 (Herring and Delpierre, 1976, 1978; Herring, 1978). It remained dormant until 1987 when Aber Resources Limited restaked it in search for uranium-precious metals association.

The prospect is at the south margin of a northeast-trending graben-like structure in which basal beds of the Hornby Bay Group are preserved (Fig. 2). The basement rocks are felsic porphyry and granite. Hematite-rich regolith is preserved at the unconformity.

Veins containing uraninite, pitchblende, coffinite, chlorite, quartz, calcite, hematite, and traces of other minerals, are sparsely distributed in massive granite within an area approximately 400 by 100 m (Fig. 2). A number of trenches have been excavated in this area. The veins are up to one centimetre thick, and have an easterly trend and steep dips, but variations in attitude are common. Discontinuities and bifurcations are also observed. The total strike length of the major veins exposed is approximately 370 m. Uranium minerals are distributed unevenly along them, in aggregates up to 5 mm thick and up to a few metres long. They also occur as disseminations within the wall rock, over a few centimetres from the veins. Chip samples across the veins exposed in trenches returned some high grade values up to 2.1 wt % U over a width of 1 m. For the most part, however, the assays are between 0.08 and 0.2 wt % U over widths of 0.5 m. A drill hole under the trenched zone intersected five mineralized zones (Appendix A, footnote). The best drill intersection was 1.78 per cent U over a true width of 2.39 m at a depth of approximately 43 m below a trench exposing a high grade vein (Herring and Delpierre, 1978).

The host granite is coarse, hypidiomorphic granular, with biotite as the main mafic mineral. Near the surface, the rock is rather fragile and has a pervasive red coloration. The alteration decreases in intensity with depth as observed in drill core. Chemical analyses of a drill core sample from 80 m depth shows that it is a highly potassic granite (Appendix A). In thin section this rock shows an abundance of altered potash feldspar and quartz, some chloritized biotite, traces of iron oxides, sphene and zircon, and fine grained alteration patches of chlorite, sericite, calcite and iron oxide.

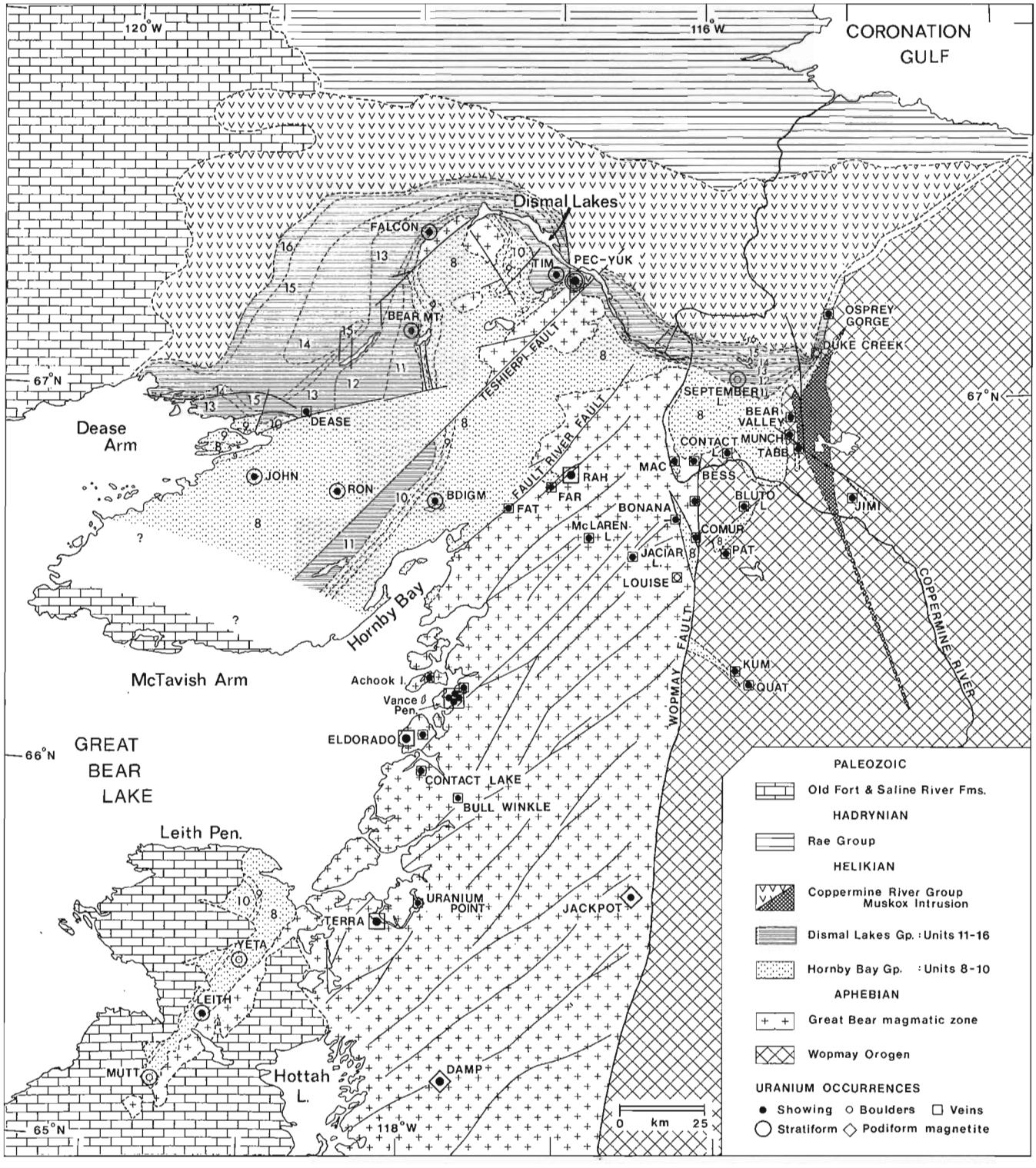

Figure 1. Simplified geology and main uranium occurrences of the northern Bear structural province, showing location of the Rah, Far and Jaciar prospects.

The pitchblende veins are close to a major northeast-trending fault. A few small, barren quartz veins are encountered in the trenched zone, but these are insignificant compared to the giant quartz veins found 5 km to the northeast along the fault (Fig. 2), and in the drill hole at the trenched zone (Appendix A, footnote). Some of these quartz veins are older than the pitchblende veins, some are younger. A strongly silicified sandstone dyke occurs in the granite about 150 m southwest of the showing area. It is up to 5 m wide, vertical, trends northeast and pinches out in that direction (Herring and Delpierre, 1976). Quartz veins occur along its margins. Pitchblende fracture-filling occurs on its southern wall.

FAR PROSPECT

The Far prospect, 7 km southwest of the Rah prospect, was discovered at the same time as the latter by Cominco Limited. A radioactive locality on Far 54 claim was trenched (Herring and Delpierre, 1978). The trench exposed quartz veins up to 5 cm wide. Copper sulphides occur as massive aggregates in the veins. The veins are steep and occur in sub-Hornby Bay Group hematitic paleoregolith and highly altered felsic porphyry. Weakly anomalous radioactivity is associated with the veins and is also encountered locally in the regolith.

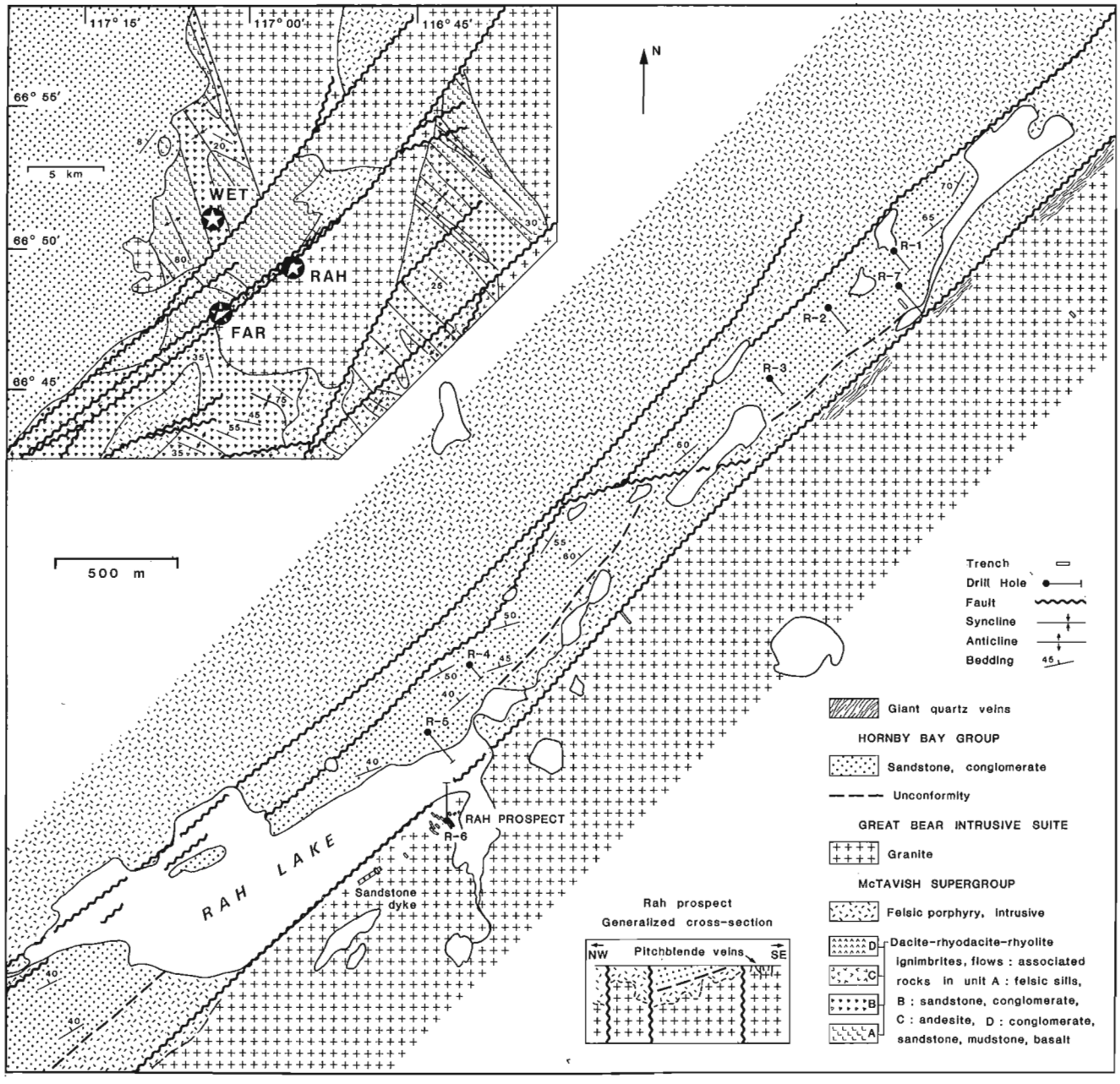

Figure 2. Geology of the area around Rah prospect, Northwest Territories. After Herring and Delpierre, 1978, and Hoffman, 1984.

JACIAR PROSPECT

The Jaciar prospect, 32 km southeast of the Rah prospect, was discovered in 1977 by Hudson's Bay Oil and Gas Company Limited during an airborne gamma-ray spectrometer survey (King and Penanka, 1977). Further exploration by the company in 1978, included excavation of several trenches across a set of quartz veins where anomalous radioactivity was detected (King et al., 1978). The veins trend east-northeast, and occur along a fault zone cutting the felsic volcanic and argillitic units of the McTavish Group (Fig. 3). The veins are up to 0.5 m metre thick, dip steeply, and form a zone over 300 m long and up to 10 m wide. Copper sulphides and pyrite occur as coarse aggregates in the quartz veins, and some of these contain pitchblende, secondary uranium minerals, hematite, and up to 28 g/t Ag and traces of Au. The massive quartz veins are cut by thin clear quartz veins, and these in turn are cut by vuggy quartz veins with thin hematite coating on the quartz crystals.

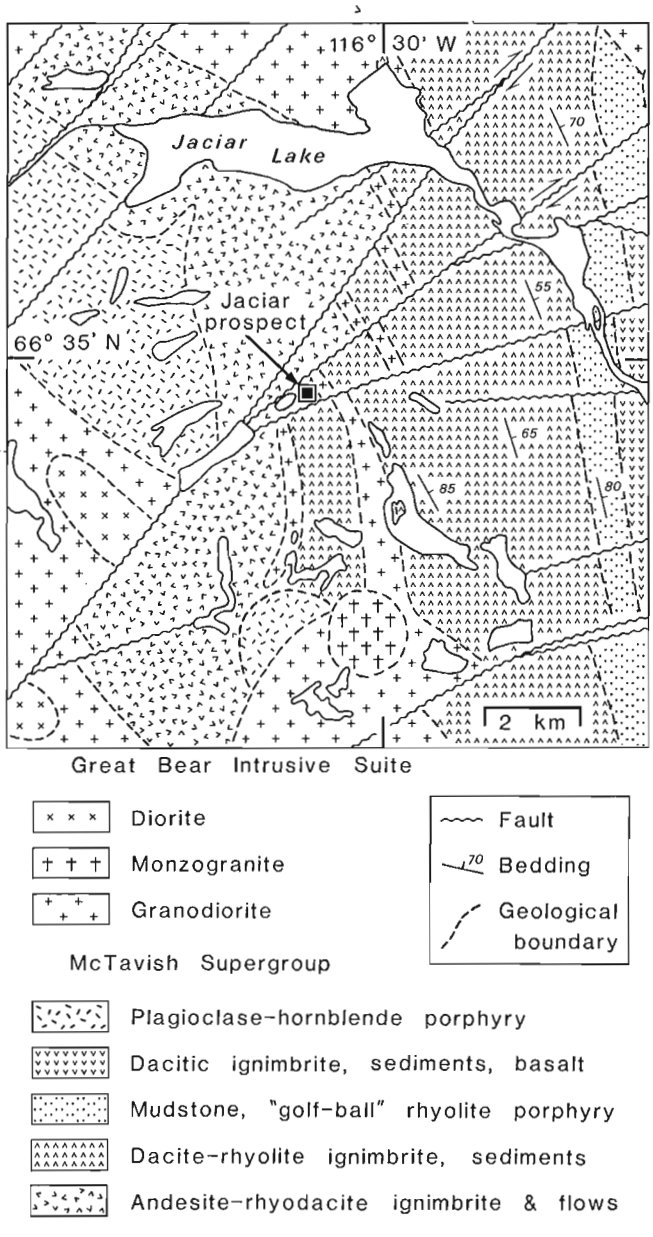

Figure 3. Geology of the Jaciar prospect, Northwest Territories. After Hoffman, 1984.

WHOLE-ROCK ANALYSES

Selected samples of pitchblende-rich and copper sulphide-rich material were analyzed for precious metals and several other related elements (Table 1). Some of the precious metal contents are extremely high. One sample from the Rah prospect, for example, contains 56 ppm Au, 47 ppm Ag, 48 ppm Pd and 39 ppm Pt. The reliability of the analyses was checked by submitting the same sample powders to another laboratory using a different analytical technique. The two sets of results are comparable (Table 1).

Other elements that show notable concentrations in the Rah samples are Pb, Zn, Cu, Co, Ni, Fe and Mo. Contents of these elements, except for Cu and Fe, are relatively lower in Far and Jaciar samples.

MINERALOGY AND PETROGRAPHY

Detailed mineralogical and petrographical studies using optical microscope, electron microprobe and scanning electron microscope were carried out on seventeen polished sections; thirteen from the Rah prospect, and two each from the Far and Jaciar prospects. Characterization of some of the phases was made by utilizing automated SEM-IA techniques (Paktunc and Walker, 1988).

A wide variety of minerals including silicates, oxides, sulphides, arsenides, sulpharsenides, tellurides, sulphates, native metals and alloys, is present in the samples, and proportions of these minerals vary greatly from sample to sample. In the present study, attention was focused on minerals containing precious metals.

Apart from the presence of common accessory phases such as apatite and zircon, Ce- and Ce-La monazites and xeontime containing Dy, are abundant in granite adjacent to some of the veinlets of the Rah prospect. They are generally less than 25 microns in length and have subhedral to euhedral crystal outlines.

URANIUM MINERALS

The samples from the Rah prospect contain pitchblende, uraninite and coffinite. These minerals occur as veins, in colloform/botryoidal aggregates, in ring-like forms (Fig. 4) and as discrete grains that are usually less than 25 microns in diameter.

Uraninite appears to be an earlier phase because pitchblende veins are found to cut across both uraninite veins and discrete grains of uraninite.

COPPER SULPHIDES AND ASSOCIATED MINERALS

Sulphide minerals are abundant in the samples of Far and Jaciar prospects, and are relatively less abundant than uranium minerals in the samples of the Rah prospect. They include chalcopyrite, bornite, pyrite, covellite, digenite, Cu-Bi sulphides, Ni-Fe sulphides, galena and sphalerite. Bornite and chalcopyrite are the most abundant sulphide phases. Chalcopyrite usually occurs in the form of disseminated grains. It is also found as irregular blades or crystallographically oriented intergrowths in bornite (Fig. 5).

Table 1. Analyses of vein samples from the Rah, Far and Jaciar prospects, Northwest Territories

Sample Number	GFA-77-TR-7-RAH	GFA-TR-77-5-RAH	GFA-TR-76-3-RAH	R108076-TR-3-RAH	R108077--TR-3-RAH	GFA-77-TR-A-FAR	GFA-78-TR-3-JAC
Au ppb	56000	1300	1100			38	970
" "	(65449)	(1445)	(1114)	(25992)	(4903)	(38)	(1111)
Ag "	47000	5000	4000			15000	<500
Os "	<10	<3	<5			<4	<5
Ir "	<4	<5	<2			<1	<2
Ru "	<4	<5	<2			<1	<2
Rh "	<4	<5	<2			<1	<2
" "	(2)	(2)	(6)			(2)	(2)
Pt "	39000	5200	5900			40	850
" "	(41772)	(5559)	(6216)	(35010)	(9704)	(30)	(883)
Pd "	48000	5600	4000			21	1100
" "	(56960)	(5929)	(4252)	(26506)	(4115)	(16)	(1160)
Re "	<4	<5	<2			<1	<2
U ppm	5240	7490	6290			1380	2120
Pb "	4700	1900	1200			280	110
Zn "	44	330	100			81	55
Cd "	2	1	1			<1	<1
Cu "	2000	290	1100			98000	8900
Co "	220	130	300			39	14
Ni "	140	68	110			13	17
Fe "	35000	18000	55000			49000	25000
S "	2300	1200	4900			69900	11300
Ti "	1800	790	1100			930	680
Mn "	310	170	290			68	380
Cr "	76	30	40			46	16
Mo "	46	18	35			2	3
Ca "	1400	2200	1400			600	600
Mg "	4100	2500	3600			2600	11000
K "	8900	27000	14000			3900	4700
P "	600	410	2900			1100	280

Notes: **i)** Analyses, except those in brackets and excluding S, are by X-ray Assay laboratories Limited, Toronto, using the following methods: U-Delayed Neutron Activation; Platinum Group Elements-Fire Assay/Plasma Mass Spectrometry; Other elements-Direct Current Plasma Mass spectrometry.
ii) Analyses in brackets by Acme Analytical laboratories Limited, Vancouver, using Inductively Coupled Plasma Mass Spectrometry.
iii) Analyses of S using rapid chemical method by the Analytical Geochemistry Secion, Geological Survey of Canada, Ottawa.
iv) Samples R108076 & R108077 are adjacent chip samples over 15.3 cm each, across a vein in Trench 3 of the Rah prospect. Other samples are grab samples. The Rah prospect samples are of pitchblende-rich veins. The Far prospect sample is from a quartz-copper sulphide vein cutting the sub-Hornby Bay Group paleoregolith. The Jaciar prospect sample is from copper sulphide-rich part of a quartz vein near the west end of a giant quartz vein zone.

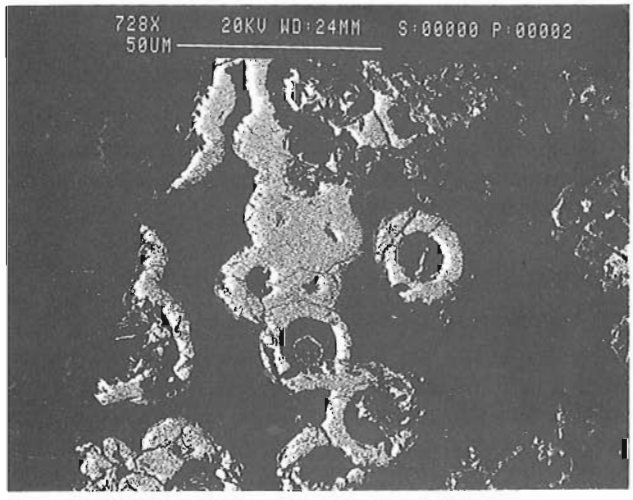

Figure 4. Backscattered electron image of pitchblende occurring in ring- like form, Rah prospect.

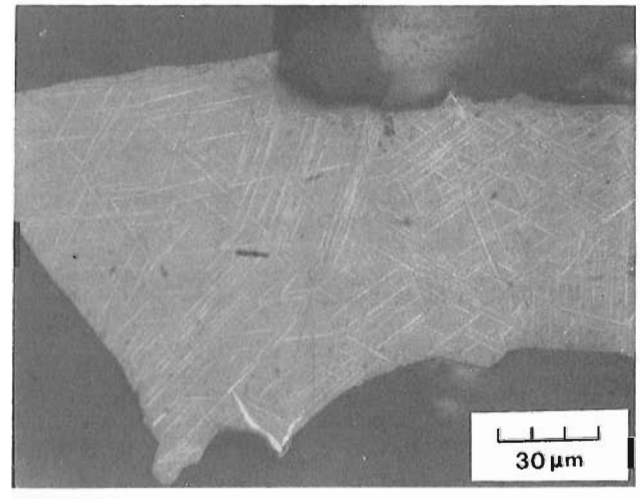

Figure 5. Photomicrograph showing chalcopyrite exsolution in bornite. Far prospect. Reflected light, partially crossed nicols.

Subhedral to euhedral pyrite grains, ranging in size from 50 to 400 μm, occur as inclusions in chalcopyrite and bornite (Fig. 6). Covellite is a replacement product of bornite, and is developed along irregular veins and patches. Greyish blue digenite is found as discrete anhedral grains occurring along the grain boundaries of bornite and chalcopyrite. Sphalerite and Ni-Fe sulphides are minor sulphide phases.

Cu-Bi sulphides are widely distributed in samples from all the three prospects, but they are not abundant. They range in size from several microns to 50 microns, and are anhedral to euhedral in outline (Fig. 7). They are commonly associated with the Cu- and Cu-Fe sulphides, and less commonly with quartz. Most of the Cu-Bi sulphides appear to be an emplectite ($BiCuS_2$).

Cobalt sulpharsenides are observed in the Rah and Far samples. They are usually less than 20 microns in length, and often form skeletal crystals. Native bismuth is found in the samples from the Far prospect, and occurs as small (up to 20 μm in diameter) anhedral to subhedral grains, scattered in Cu-Bi sulphides, Cu-Fe sulphides and in coffinite (Fig. 8). Several very small (i.e. 2 μm) grains of barite were encountered in samples from the Jaciar prospect.

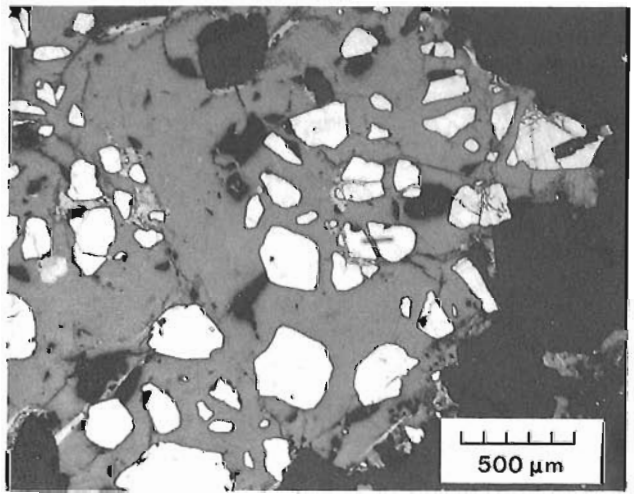

Figure 6. Photomicrograph of subhedral pyrite grains enclosed in bornite. Far prospect. Reflected light.

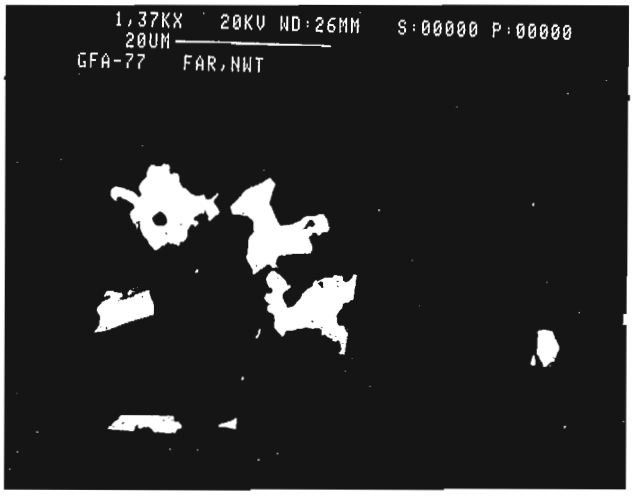

Figure 7. Backscattered electron image of anhedral bismuth-copper sulphide grains (white) in bornite (black), Far prospect.

PLATINUM GROUP AND PRECIOUS METAL MINERALS

Five platinum-group minerals including a palladium telluride, a palladium-bismuth telluride, two rhodium sulpharsenides, and one gold-palladium alloy, have been identified in the samples from the Rah and Far prospects, but none were found in the samples of Jaciar prospect. Furthermore, no platinum mineral or platinum-bearing phase has been identified as yet in any of the samples. An earlier mineralogical study on two polished thin sections of the Rah samples, carried out by Cominco Laboratory in Vancouver, also did not identify any platinum-bearing mineral (J.D. Blackwell, personal communication, 1987). This situation is somewhat puzzling in view of significantly high platinum abundances

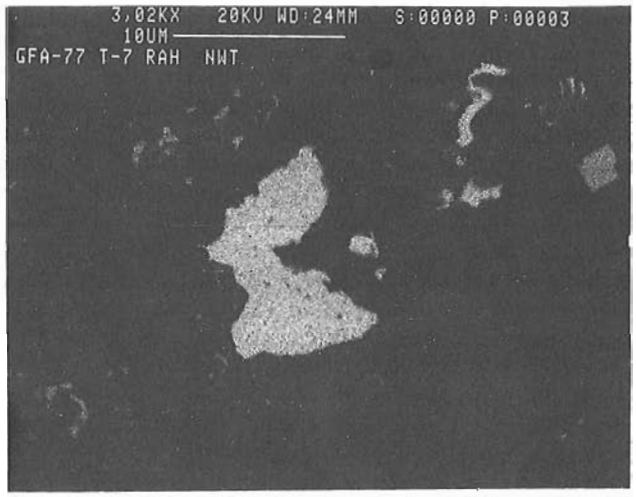

Figure 8. Backscattered electron image of native bismuth grains (grey) enclosed in coffinite and Co-arsenide (black), Rah prospect.

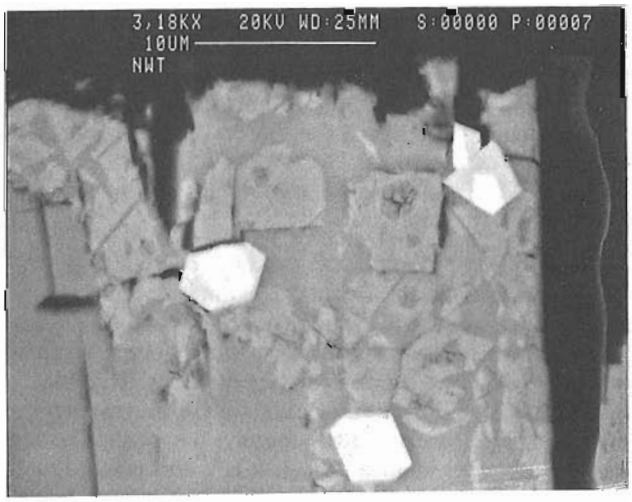

Figure 9. Backscattered electron image of several hollingworthite grains enclosed in chalcopyrite. Slightly darker phase in the hollingworthite grains is (Co, Fe, Rh)AsS. Far prospect.

in some of the samples analyzed (Table 1). A similar problem is encountered in the mineralogy of the Nicholson Cu-U-Au-Pt-Pd deposit in northern Saskatchewan. A spectrographic study by Hawley et al. (1953) suggested that platinum may be present in native gold as solid solution (Robinson, 1955), but more recent attempts in identification of platinum-bearing phases in the deposit have failed so far (L.J. Cabri, Canada Centre for Mineral and Energy Technology, Personal Communication 1988, and A.D. Paktunc, Unpublished data). Further work is required to resolve the problem.

In the Rah and Far prospects, platinum-group minerals are associated with base metal sulphides. Hollingworthite (RhAsS) is identified in the samples of the Far prospect. It occurs as euhedral grains enclosed within the Cu-Fe sulphides (Fig. 9). Average grain size is about 5 microns. Most of the grains contain intergrowths of (Co,Fe,Rh)AsS. Palladium tellurides form complex intergrowths with Ag-Pb tellurides and Ag-Pb-Bi tellurides at the Rah and Far prospects. Palladium-bismuth tellurides, probably a michenerite or moncheite (PdBiTe), are anhedral and usually less than 5 μm in size (Fig. 10). Palladium-gold alloy is found in association with an electrum (AuAg) grain (Fig. 11). Associated with the Pd minerals are some Au and Ag minerals. Sylvanite (AuAgTe) is found in the Far samples. It forms subhedral grains that are usually less than 3 microns in diameter. Submicron size particles of Ag-tellurides (Fig. 11) are usually associated with the Ni-Fe sulphides in these samples. Clausthalite was identified in the Rah samples by Cominco Laboratory.

ISOTOPIC AGE DETERMINATION

A pitchblende separate from a high grade sample from Trench 5 of the Rah prospect, collected by the first author, was analyzed for isotopic age determination. Analyses by the Geospec Consultants Limited, Edmonton, Alberta, done in 1981, are as follows:

U: 7.988 per cent, Pb: 0.1954 per cent, $^{204}Pb/^{206}Pb$: 0.0012441, $^{207}Pb/^{206}Pb$: 0.0919491, $^{208}Pb/^{206}Pb$: 0.0600076

These data yield a point that is highly discordant on the concordia plot, indicating lead loss or uranium gain. The calculated ratio of $^{206}Pb/^{204}Pb$ is 803.8 and of $^{207}Pb/^{204}Pb$ is 73.908. The $^{207}Pb/^{206}Pb$ age (minimum age) from these, with a common lead correction based on galena samples from the Terra mine near Great Bear Lake ($^{206}Pb/^{204}Pb$: 15.70, $^{207}Pb/^{204}Pb$: 15.35 and $^{208}Pb/^{204}Pb$: 35.35; Thorpe, 1974) is approximately 1050 Ma.

The above pitchblende date must be regarded with caution because a single discordant data point is inadequate, and in this particular case the sample analyzed is likely to contain some uraninite which is paragenetically older, as noted earlier. On the other hand, formation of pitchblende may be due to local remobilization of uranium from uraninite and may be fairly close in age to uraninite deposition. In that case, the date may be meaningful. It is worth noting in this regard that pitchblendes from other occurrences in the northern Bear province also yield discordant data points on the concordia plot. Calculated ages for most of them range between 1420 and 1000 Ma, whereas others are younger (Thorpe, 1974; Miller, 1982).

DISCUSSION

The pitchblende-rich veins of the Rah prospect and the copper sulphide-bearing quartz veins of the Far and Jaciar prospects represent a large number of mineralogically similar veins in the northern Bear province. The quartz-rich veins resemble the giant quartz veins along major northeast-trending faults, except for the local concentrations of copper sulphides. The giant quartz veins are commonly barren, with only minor chlorite and hematite along the walls, but pitchblende and hematite do occur in some, usually in a younger generation of smaller quartz veins. It appears that all the veins could be parts of a wide spectrum, marked by extreme variation in abundance of gangue minerals. The

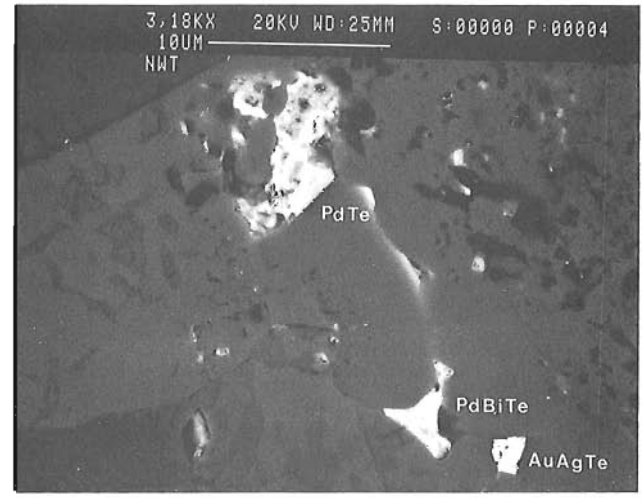

Figure 10. Backscattered electron image showing palladium-bismuth telluride (PdBiTe), palladium telluride (PdTe) and sylvanite (AuAgTe) grains enclosed in chalcopyrite, Rah prospect.

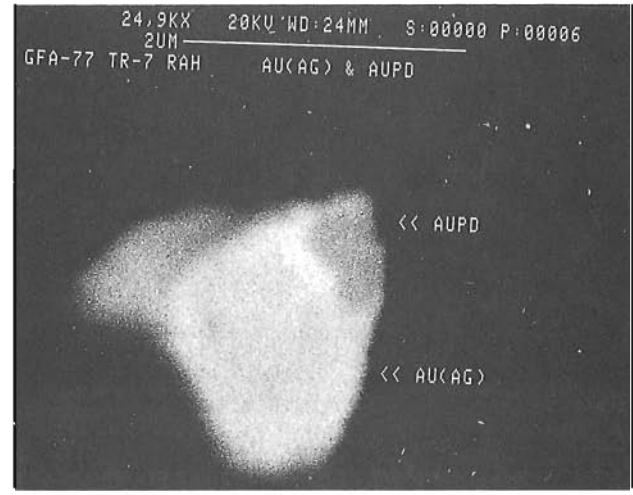

Figure 11. Backscattered electron image of a grain consisting of electrum (AuAg) and PdAu alloy, Rah prospect.

mineralogical and geochemical characters of the Rah, Far and Jaciar veins show their common, inherent polymetallic character. In this respect they also resemble the polymetallic veins of the Eldorado and Terra mines. Most of the other uraniferous and sulphide-rich veins in the Bear province remain to be studied in detail, and it is possible that many may turn out to be polymetallic. This has important implications for the resource potential, particularly in terms of precious metals.

Pitchblende veins at the Rah and Far prospects formed after the deposition of the basal beds of the Hornby Bay Group, judging from the paleoweathered host felsic porphyry at the Far prospect, and fracture-fillings occurrence of pitchblende in a sandstone dyke within the granite basement at the Rah prospect, and by the isotopic data discussed above. The tensional fractures along which the veins are localized, are subsidiary to the northeast-trending faults that form in the graben-like structure containing remnants of the Hornby Bay Group. The timing of this faulting or reactivation of pre-Hornby Bay Group faults in the basement, is not known well, but it is likely to be close to the time of formation of the pitchblende veins.

In the case of the Rah and Far prospects, a noteworthy feature is the proximity to the sub-Hornby Bay Group unconformity. This is considered here as a relevant factor in the genesis of the veins. The general geological setting of the veins is similar to that of the unconformity-related deposits at the base of the Athabasca Group, although there are notable differences in host-rock, morphology and alteration: the unconformity-related deposits occur along metasediments in the basement of the Athabasca Group, form very elongate lensoid ore bodies parallel to the sub-Athabasca unconformity, and have a strong illitic alteration halo. Such differences may, however, be explained if the veins are regarded as deep roots of unconformity-related deposits or as formed by remobilization of metals from such deposits consequential to their modification or destruction during uplift caused by faulting or epeirogeny.

The metal association of uranium, base and precious metals in the prospects is intriguing in that the ultimate geochemical sources of the metals have to be lithologically very different. In the near surface environment, however, all these metals are known to have similar behaviour in terms of solution, transportation and deposition. The pitchblende-gold association, in particular, is noted at several other places in the northwestern Canadian Shield, and is attributed to supergene or low temperature hydrothermal processes. Examples are at Twin Lakes in the Bathurst Inlet region (Roscoe, et al., 1986), at Boomerang Lake and Deep Rose Lake in the Thelon basin (Gandhi, 1988), at MacInnis Lake in the Nonacho basin (Gandhi and Prasad, 1980) and at Nicholson mine in northern Saskatchewan (Hawley et al., 1953; Robinson, 1955). Search for the platinum-group elements in association with pitchblende-gold has started only recently, and much remains to be learned.

A key factor in bringing these lithogeochemically diverse elements together is, in the writers' opinion, a pre-concentration at the low latitude lateritic paleoweathering during middle Proterozoic time. This medium provides a variety of local conditions where metals could be trapped to a varying degree of concentration and stability. An example of an unusual local condition at the sub-Hornby Bay Group unconformity is seen at the WET claims 6 km northwest of the Rah prospect (Fig. 2). Here oval structures, with hematite-specularite shell and core of thin quartz network enclosing voids left after dissolution of pyrite crystals, are found at quartz-pyrite veins in the basement of felsic volcanic rocks (Fig. 13). These so called 'watermelon' structures are up to 40 cm long. Precious metals and uranium occur at the margin of the shell and in surrounding regolithic material. The final concentration of the metals in veins could occur in passive or tensional environments through the agency of circulating meteoric waters over a long period of time. Repeated mobilization and redeposition could occur periodically during epierogenic uplift. This could explain paragenetically different stages of uranium mineralization, and consequent isotopic disequilibrium and resetting.

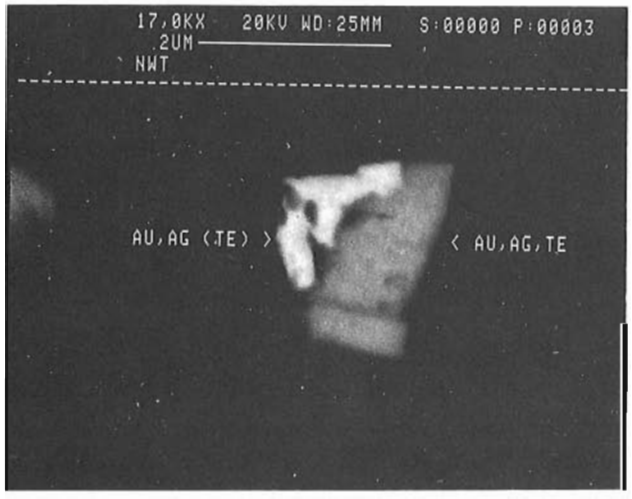

Figure 12. Backscattered electron image of a sylvanite grain attached to an electrum grain. Far prospect.

Figure 13. Photograph of a hematite-shelled oval structure ('watermelon' structure) at the sub-Hornby Bay Group unconformity, WET claims (Fig. 2). Scintillometer length is 20 cm.

CONCLUSION

Uranium- and copper-bearing veins at the Rah, Far and Jaciar prospects are polymetallic, contain significant amounts of precious metals, and have a complex mineralogy. They differ considerably in the relative proportions of the metallic and gangue minerals, but have common features in their proximity to the Aphebian-Helikian unconformity, structural control by reactivation of northeast-trending basement faults, and Helikian or younger age. It is postulated that the veins formed through the agency of circulating meteoric waters which transported the metals concentrated earlier at the unconformity and redeposited them at favourable structural sites. The process is regional in scope, and numerous other veins in the Bear structural province are likely to have formed in the same manner. Little is known about the precious metal contents of most of these veins; therefore, they merit further investigation towards a better understanding of the regional metallogeny and resource potential of the province.

ACKNOWLEDGMENTS

The authors are grateful to Aber Resources Limited, in particular to V.A. Tanaka and J.D. Blackwell, for providing information on the presence of precious metals at the Rah prospect and prompting this study, and permitting incorporation of unpublished data in this paper. Thanks are also due to M.E.R. Delpierre, who as a project geologist for Cominco Limited familiarized the first author in the geology and exploration of the Rah and Far prospect area during visits in 1977 and 1978. The Jaciar prospect was examined by the first author in 1978 with geologists of Hudson's Bay Oil and Gas Company Limited. G. Mosher of Aber Resources Limited provided field guidance to him in the WET claims area in 1988. R.T. Bell and S.M. Roscoe of the Geological Survey of Canada, who have visited the Rah prospect area, generated stimulating discussions, and also critically reviewed the manuscript. The opinions expressed here, however, are the responsibility of the authors. A partial financial support for the study was obtained from the Canada-Northwest Territories Mineral Development Agreement through project C.1.2.5.

REFERENCES

Bowring, S.A. and Ross, G.M.
1985: Geochronology of the Narakay Volcanic Complex: implications for the age of the Coppermine homocline and Mackenzie igneous events; Canadian Journal of Earth Sciences, v. 22, no. 5, p. 774-780.

Fraser, J.A., Donaldson, J.A., Fahrig, W.F., and Tremblay, L.P.
1970: Helikian basins and geosynclines of the northwestern Canadian Shield; Symposium on Basins and Geosynclines of the Canadian Shield, editor A.J. Baer, Geological Survey of Canada, Paper 70-40, p. 213-238.

Gandhi, S.S.
1988: Geology and uranium potential of the Thelon basin and adjacent basement in comparison with the Athabasca basin region; Proceedings of the meeting in Saskatoon, 1978; International Atomic Energy Agency, Vienna (in press).

Gandhi, S.S. and Prasad, N.
1980: Geology and uranium occurrences of the MacInnis Lake area, District of Mackenzie; in Current Research, Part B, Geological Survey of Canada, Paper 80-1B, p. 107-127.

Hawley, J.E., Rimsaite, Y., and Lord, T.V.
1953: Lead bead method of spectographic analyses of platinum metals, gold, silver and bismuth in sulphide and uranium ores; Transactions Canadian Institute of Mining and Metallury, v. 56, p. 19-26.

Herring, B.G.
1978: Evaluation work conducted in the RAH Lake area, N.W.T., in 1977: Claims RAH 1-103; FAR 1-110; Cominco Limited, Vancouver; Department of Indian and Northern Affairs, Document 080815, 11 p.

Herring, B.G. and Delpierre, M.E.R.
1976: Evaluation work carried out on the RAH 1-103 and FAR 1-110 claims in the Great Bear Lake area; Cominco Limited, Vancouver; Department of Indian and Northern Affairs Document 061594, 7 p.
1978: Report on evaluation work carried out on the RAH claim property, N.W.T.; Work performed during 1978; Cominco Limited, Vancouver; Department of Indian and Northern Affairs, Document 061950, 10 p.

Hoffman, P.F.
1980: Wopmay Orogen: a Wilson cycle of early Proterozoic age in the northwest of the Canadian Shield; in The Continental Crust and its Mineral Deposits, ed. D.W. Strangway; Geological Association of Canada, Special Paper 20, p. 133- 156.
1984: Geology, Northern Internides of Wopmay Orogen, District of Mackenzie, Northwest Territories; Geological Survey of Canada, Map 1576A, scale 1:250 000.

Kerans, C., Ross, G.M., Donaldson, J.A., and Geldsetzer, H.J.
1981: Tectonism and depositional history of the Helikian Hornby Bay and Dismal Lakes groups, District of Mackenzie; in Proterozoic Basins of Canada, ed. F.H.A. Campbell, Geological Survey of Canada, Paper 81-10, p. 157-182.

King, A. and Panenka, J.
1977: Report on exploration of the Jaciar Lake area, District of Mackenzie; Hudson's Bay Oil and Gas Limited; Department of Indian and Northern Affairs, Document No. 061680, 19 p.

King, A., Wittstock, J. and Slack, D.J.
1978: Geological, ground and airborne geophysical, and lake sediment and water geochemical report on Permit 463, NTS 86K10; Hudson's Bay Oil and Gas Company Limited; Department of Indian and Northern Affairs Document 061834, 30 p.

Lang, A.M., Griffith, J.W. and Stacey, H.R.
1962: Canadian deposits of uranium and thorium, Geological Survey of Canada; Economic Geology, Series No. 16, 324 p.

Miller, R.G.
1982: Geochronology of uranium deposits in the Great Bear batholith, Northwest Territories; Canadian Journal of Earth Sciences, v. 19, no. 7, p. 1428-1448.

Paktunc, A.D. and Walker, D.A.
1988: Automated image analysis techniques on the study of platinum-group minerals; Geological Association of Canada, Mineralogical Association of Canada, Canadian Society of Petroleum Geologists. Joint Annual Meeting, Program with Abstracts, v. 13, p. A94.

Robinson, S.C.
1955: Mineralogy of uranium deposits, Goldfields, Saskatchewan; Geological Survey of Canada, Bulletin 31, p. 16-18.

Roscoe, S.M., Green, S.B., and Gandhi, S.S.
1986: Uranium, gold and selenide minerals locally concentrated in drift at 'Twin Lakes' near Bathurst Inlet, N.W.T.; in Current Research, Part B, Geological Survey of Canada, Paper 86-1B, p. 47-56.

Thorpe, R.I.
1974: Lead isotope evidence for the genesis of silver-arsenide vein deposits of the Cobalt and Great Bear lake areas, Canada; Economic Geology, v. 69, p. 777-791.

APPENDIX A

Chemical analyses of a drill core sample of granite, Rah prospect, Northwest Territories.*

Sample No.		DDH-'78-R-6 113.7 m **
SiO_2	wt %	77.80
TiO_2	....	0.07
Al_2O_3	....	11.20
Cr_2O_3	....	nd
Fe_2O_3	....	0.60
FeO	....	0.60
MnO	....	0.03
MgO	....	0.71
CaO	....	0.24
Na_2O	....	0.10
K_2O	....	7.26
H_2O T	....	1.20
CO_2 T	....	0.20
P_2O_5	....	nd
S	....	nd
Total	.....	100.01
Ba	ppm	173
Nb	....	41
Rb	....	368
Sr	....	83
Y	....	35
Zr	....	92

*All analyses by XRF, except FeO, H_2OT (I) CO_2 T (I), C and S by rapid chemical methods. Fe_2O_3 = Fe_2O_3 (XRF) − 1.11034 × FeO (volumetric). nd: not detected. Analyses by the Analytical Geochemistry Section, Geological Survey of Canada, Ottawa.

**Drill log summary, Hole '78-R-6:-45° (Fig. 2); Granite: 0-134.19 m; Quartz vein zone-134.19-197.13 m; Fault zone: 197.13-201.47 m; Porphyry: 201.47-223.11 m; Mineralized zones - 4.78-5.03 m; 7.67-7.82 m; 7.98-8.13 m; 21.09-21.56 m; and 41.73-44.48 m.

A preliminary report on the distribution of gold in lake sediments and surficial materials at Foster Lake, Manitoba[1]

H.R. Schmitt
Mineral Resources Division

Schmitt, H.R., A preliminary report on the distribution of gold in lake sediments and surficial materials at Foster Lake, Manitoba; in Current Research, Part C, Geological Survey of Canada, Paper 89-1C, p. 255-262, 1989.

Abstract

Lake sediment investigations along the Johnson Shear Zone in the Lynn Lake greenstone belt identified concentrations of up to 30 ppb Au in profundal lake sediments from Foster Lake. Sampling of till, peat, humus, black spruce (Picea mariana) *and surface waters overlying a mineralized shear zone north of Foster Lake encountered elevated concentrations of Au, As, Sb, Mo and W adjacent to exposed mineralization and dispersed down-ice toward Foster Lake. Gold concentrations up to 4.9 ng L^{-1} in surface waters suggest mobilization of Au by organic or anionic complexes in weakly acid surface waters. The aim of this study is to document some of the complex natural processes that lead to accumulation of Au in lake sediments. While lake sediments are now widely used in exploration for Au, there is relatively little information on the controls on transportation and precipitation of Au.*

Résumé

L'exploration des sédiments lacustres bordant la zone de cisaillement de Johnson dans la zone des roches vertes de Lynn Lake a permis d'identifier des concentrations d'or (Au) atteignant parfois 30 ppb dans les sédiments lacustres profonds prélevés dans le lac Foster. Dans des échantillons de till, de tourbe, d'humus, d'épinette noire (Picea mariana) *et des eaux de surface recouvrant une zone de cisaillement minéralisée située au nord du lac Foster, on a rencontré des concentrations élevées de Au, As, Sb, Mo et W à proximité de minéralisations exposées, et des concentrations plus dispersées en aval de l'écoulement glaciaire, en direction du lac Foster. Des concentrations de Au pouvant atteindre 4,9 ng L^{-1} dans les eaux de surface semblent indiquer une mobilisation de Au par des complexes organiques ou anioniques dans les eaux de surface faiblement acides. La présente étude a pour but de décrire quelques-uns des processus naturels complexes responsables de l'accumulation de Au dans les sédiments lacustres. On utilise maintenant très communément des sédiments lacustres pour la prospection de Au, mais on dispose de relativement peu d'information sur les facteurs qui régissent le transport et la précipitation de Au.*

[1] Contribution to the Canada – Manitoba Mineral Development Agreement 1984-1989. Project carried by Geological Survey of Canada.

INTRODUCTION

The geochemistry of Au in supergene environments has received much attention over the last decade. Webster and Mann (1984), Mann (1984), Webster (1986), Hall *et al.* (1986), and Stoffregen (1986) have demonstrated that Au occurring in bedrock, once exposed to supergene weathering processes, may become complexed, transported and reprecipitated under low-temperature oxidizing acid to alkaline conditions. The mobility of Au is influenced by the interaction of host rock, groundwater and surficial deposit chemistry, geomorphology, and climate.

This paper reports preliminary results for a study of gold mobilization into lake-bottom sediments at Foster Lake located 15 km south of Lynn lake, Manitoba. Foster Lake is adjacent to the Johnson Shear Zone, a 40-km-long and up to 0.5 km wide zone of variable shearing and deformation in Wasekwan Group metavolcanic and metasedimentary rocks of Aphebian age. Significant, but as yet uneconomic, gold-bearing veins occur along the shear zone (Fedikow *et al.*, 1986).

Regional lake sediment and water geochemical surveys carried out in Granville Lake map area (64C) during 1983 (Geological Survey of Canada, 1984, 1986) and an in-fill lake sediment and water geochemical survey carried out in 1987 (Schmitt, manuscript in preparation) identified elevated concentrations of gold in profundal lake sediments adjacent to the Johnson Shear Zone. Consequently, Foster Lake area was chosen for detailed multi-media geochemical sampling in order to characterize surficial and chemical dispersion phenomena that mobilize gold into lakes. This work is primarily intended to aid the interpretation of regional geochemical data for mineral exploration, and to aid the design of future lake sediment geochemical surveys.

Sampling at Foster Lake in 1985, 1987 and 1988 entailed the collection of: lake bottom and stream sediments; surface waters from lakes, streams, bogs, trenches and seeps; peat; humus; black spruce *(Picea mariana)* twigs and needles; till; and mineralized and unmineralized bedrock. Apart from drainage sediments, sampling was carried out on two 150-m-wide by 300-m-long grids encompassing mineralized segments of the shear zone.

Although a wide variety of elements have been analyzed, this report will focus on the distribution of gold.

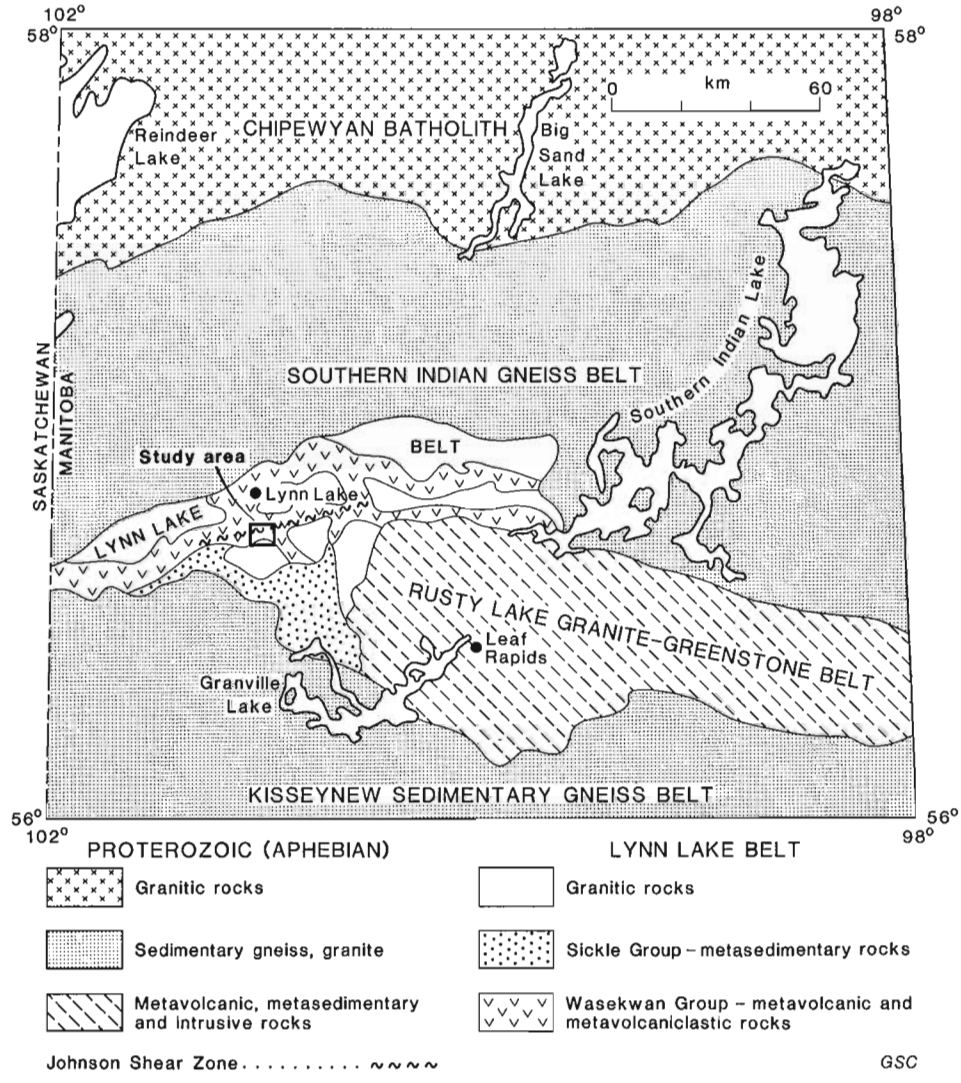

Figure 1. Location and regional geology of the study area (after Zwanzig *et al.*, 1985).

BEDROCK GEOLOGY

The study area lies within the southern part of the Lynn Lake greenstone belt (Fig. 1), and contains a complex sequence of metamorphosed tholeiitic, aphyric and porphyrytic basalts overlain by turbidite units and mafic to felsic volcanic rocks belonging to the Wasekwan Group, which are intruded by mafic to felsic plutons and dykes (Gilbert *et al.*, 1980; Fedikow *et al.*, 1986).

Recent mapping by geologists of Sherritt Gordon Mines (1983) (now Lynn Gold Resources) and by Ferreira (1986), describes the north side of Foster Lake as underlain by up to 275 m of intercalated mafic to felsic fine-grained metasedimentary rocks, flanked to the south by a foliated alkali granite sill, and to the north by at least 200 m thick massive plagioclase-bearing mafic metavolcanic flows, tuffs and minor gabbro. Undivided intermediate to mafic volcanic rocks occur east and southeast of Foster Lake, with tonalite and diorite of the Pool Lake intrusive suite present to the south and west (Fig. 2).

The Johnson Shear Zone trends subparallel to the strike of Wasekwan Group rocks and is represented by a low ridge of positive relief characterized by a well developed foliation oriented 240°/60°N; shear and fracture cleavage, variable to intense chloritization, silicification, carbonate-clay alteration, localized brecciation, and sulphide mineralization occur (Ferreira, 1986).

SURFICIAL GEOLOGY

Surficial sediments in the Lynn Lake area were deposited by southerly flow and deglaciation of Keewatin lobe ice (Kaszycki and Dilabio, 1986). Surficial sediments at Foster Lake include glacial till, ice-contact eskers and kames, organic bogs, and minor alluvial sediments. Ice-contact deposits and bedrock striae record ice movement directions of 170° to 210°, essentially normal to the strike of bedrock units. Bedrock represents less than 5 per cent of surface units, yet its structure is clearly visible on airphotos owing to the thin surficial veneer.

Till is generally <1.5 m thick to discontinuous, but accumulations >2 m thick occur in local depressions and on the lee side of prominent bedrock forms. Till exhibits poor stratification, has a predominant sandy matrix and contains abundant locally-derived bedrock fragments, cobbles and boulders. Pervasive oxidation of the till matrix extends to depths of 0.3 to 1.5 m. The variability in till composition and fabric observed over a limited areal extent suggests that more than one till unit may be present.

Esker and kame complexes trend 180 to 200° and are represented by up to 1-km-long sinuous ridges 5 m high by 50 m wide, and ridges 10 m high by 200 m wide respectively.

Peaty organic deposits mantle well-indurated clay-rich till in most depressions. Discontinuous permafrost was found at 30 cm depth along bog fringes and may completely underlie smaller bogs as indicated by summer surface bog water temperatures as low as 4°C.

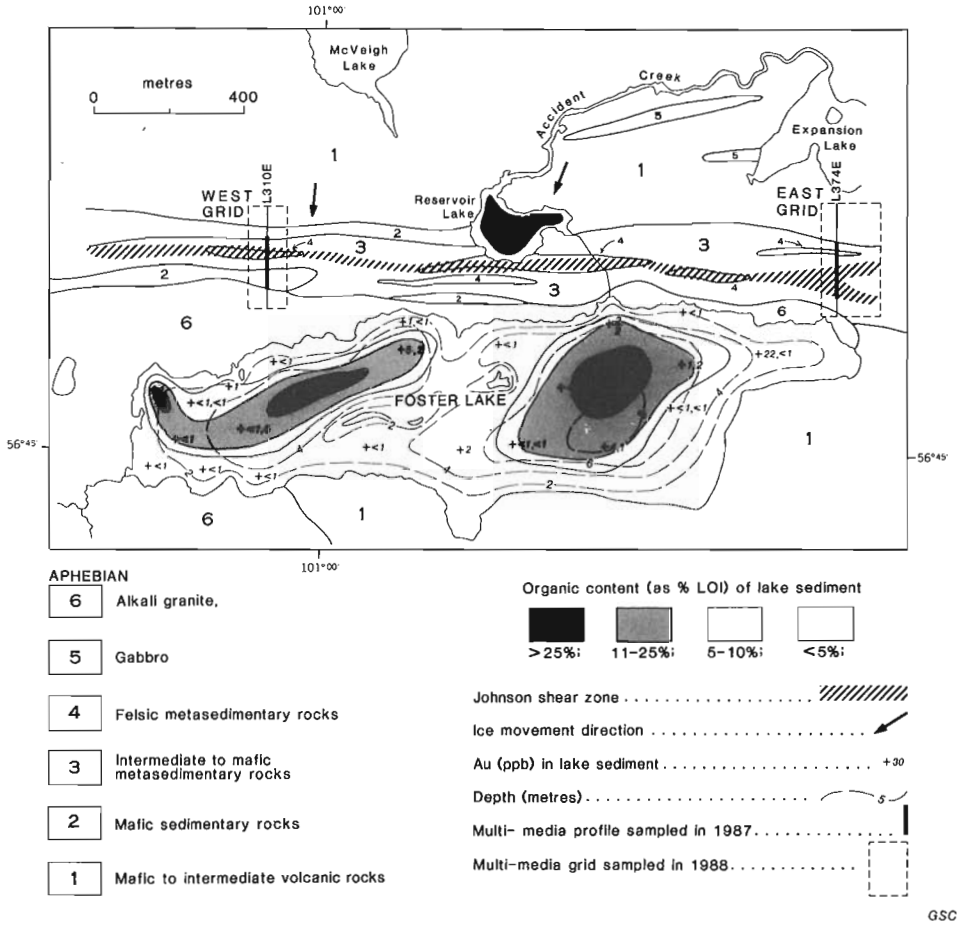

Figure 2. Geology, distribution of Au (ppb) in lake sediments, and location of multi-media geochemical sampling grids at Foster Lake.

MINERALIZATION

North of Foster Lake a zone up to 20 m wide and traceable over 1.5 km along strike contains locally abundant sulphide-bearing quartz veins associated with well-developed fracture cleavage, localized carbonate and sericite alteration, and fibrous amphibole.

Sulphides in quartz veins consists of 1-20% pyrrhotite, <1-10% pyrite, arsenopyrite, and trace galena, chalcopyrite, and sphalerite as disseminated grains, streaks, and aggregates along cleavage planes, and less commonly as massive clots and blebs in 5-20 cm wide veins (Ferreira, 1986; Baldwin *et al.*, 1985). Disseminated magnetite occurs in felsic metasedimentary and tuffaceous rocks within and adjacent to the zone.

Gold values locally exceed 20 000 ppb in pyritic quartz veins, compared to values typically <100 ppb for volcanic and sedimentary rocks within and adjacent to the shear zone, and values up to 30 ppb for the alkali granite near its contact with metasedimentary rocks (Sherritt Gordon Mines, 1983).

FIELD AND ANALYTICAL METHODS

Lake sediments were collected from an inflatable boat using a modified model of the GSC 1976 lake sediment sampler (Coker *et al.*, 1979). Where field duplicates were collected, or more than one sampling attempt was necessary for adequate material, drift from the site was minimized to less than 5 m or sampling was repeated. During sample retrieval, care was taken to wash out and discard the top several cm of sediments material.

Dried samples were ball-milled and sieved to — 177 microns by Golder Associates Ltd., and analyzed by Bondar — Clegg and Company Ltd. for some or all of Zn, Cu, Pb, Ni, Co, Ag, Mn, As, Mo, Fe, Hg, loss-on-ignition, U, V, Cd, Sb, S, Cl, Ba, Sr, and Au. Gold analyses were performed on a 10 g sample by Chemex Laboratories Ltd. by fire assay preconcentration followed by instrumental neutron activation to achieve a detection level of 1 ppb. Analytical methods for other elements are summarized in Geological Survey of Canada regional geochemical Open File 1641 (1988).

Lake waters were collected at most sediment sites in 250 mL Nalgene bottles from at least 30 cm below the water surface; other waters (*i.e.*, bogs, streams) were collected as deep as possible taking care not to agitate bottom sediments. Chemex Laboratories Ltd. analyzed waters for some or all of pH, F, U, Ca, Mg, and alkalinity; in addition a direct current plasma (DCP) multielement analysis provided useful information for Ca, Mg, Na and Sr. In addition to laboratory analyses of waters, *in-situ* determinations of temperature, pH, conductivity and salinity were carried out using a Corning pH Tempmeter 4 and YSI Model 33 Salinity-Conductivity-Temperature meter.

Several 1 L water samples were collected and analyzed for Au at the Geological Survey of Canada. Br_2-HCl/MIBK extraction was followed by graphite furnace-atomic absorption spectrophotometric analysis (GFAAS) as described by Hall *et al.* (1986) to attain a detection level of .001 ppb (1 ng L^{-1}).

Till samples weighing 5 to 10 kg were collected from pits hand-dug by shovel to depths of 1.5 m or until bedrock was encountered, whichever was the shallower. Several size fraction splits have been generated. To date a −63 micron (−250 mesh) and heavy mineral concentrate (s.g. >3.32) have been analyzed at Bondar—Clegg and Company by instrumental neutron activation for Au, Na, Sc, Cr, Fe, Co, Ni, Zn, As, Se, Br, Rb, Zr, Mo, Ag, Cd, Sn, Sb, Te, Cs, Ba, La, Ce, Sm, Eu, Tb, Yb, Lu, Hf, Ta, W, Ir, Th and U.

Peat samples weighing from 1 to 4 kg were collected from pits hand-dug to depths of 0.3 to 1.0 m over the eastern grid (Fig. 2). Air dried samples were cleaned of woody parts, and a 50-100 g subsample ashed overnight at 470°C. Approximately 1 g of encapsulated ash was analyzed at Activation Laboratories Ltd. by instrumental neutron activation analysis for Au plus a suite of elements similar to till samples above, but excluding Cd, Sn, Te and Zr, and including Ca, K, Hg, Nd and Sr.

Picea mariana (black spruce) twigs and needles representing 5-8 years growth were collected within 3 m of each till, peat and humus site. A 30-50 g sample of twigs only was ashed, encapsulated and analyzed using procedures similar to that for peat, and those described by Dunn (1988).

Bedrock and humus samples are presently being processed.

RESULTS

Table 1 is a preliminary summary of Au concentration in surficial materials. The table illustrates pronounced secondary dispersion of Au in the Foster Lake area at concentrations well above detection levels for all media types. The wide range of Au concentrations, especially between media types, stresses the importance of identifying controls on Au accumulation so that geochemical analyses of these media can be applied to mineral exploration. The following discussion provides a more detailed description of Au distribution.

Figure 2 shows the distribution of Au in lake-bottom sediments from Foster and Reservoir lakes.

Foster Lake, sampled from 24 sites, contains two basins up to 9 m deep separated by a partially eroded northeast trending esker (Fig. 2). Lake sediment material was olive-grey to green with a silty to thixotropic gel consistency. Gold concentrations range up to 18 ppb in the western basin and 30 ppb in the eastern basin. Highest Au concentrations occur in the organic-rich (26% LOI) profundal sediments compared to silty (5% LOI) near shore sediments.

Reservoir Lake sediments are considerably more organic-rich (30-50% LOI) and returned values up to 17 ppb Au.

Preliminary results are available from two 200 m profiles sampled along L310E and L374E over and down-ice of mineralized zones (Fig. 2, 3 and 4). Samples were collected at stations 10 to 30 m apart.

The western grid (Fig. 2 and 3) represents an area of positive relief mantled by a thin veneer of locally-derived

Table 1. Preliminary summary of gold concentrations in surficial materials at Foster Lake.

[1]Media	N	X (ppb)	Range (ppb)	Detection Level (ppb)	[2]Analytical Method
Lake-bottom sediment			<1 to 30		FANA
– Foster	37	3.4		1	
– Reservoir	6	7.3		1	
– Regional	1293	1.0		1	
Till			5 to 160		INA
– (<63 μ)	15	54	30 to 6660	2	
– HMC (>3.3)	13	1054		2	
Peat	7	29	14 to 47	5	ASH/INA
Picea mariana (Black spruce twigs)	19	9	<5 to 39	5	ASH/INA
Surface water	8	.0013	<.001 to .005	.001	GFAAS

[1] Media sampled but for which results are not yet available include; humus, bedrock, groundwater, filtered lake waters, stream sediments and water.
[2] FANA – fire assay preconcentration – neutron activation
ASH/INA – instrumental neutron activation of ashed sample
GFAAS – Br2 – HCl – MIBK extraction followed by graphite furnace – atomic absorption

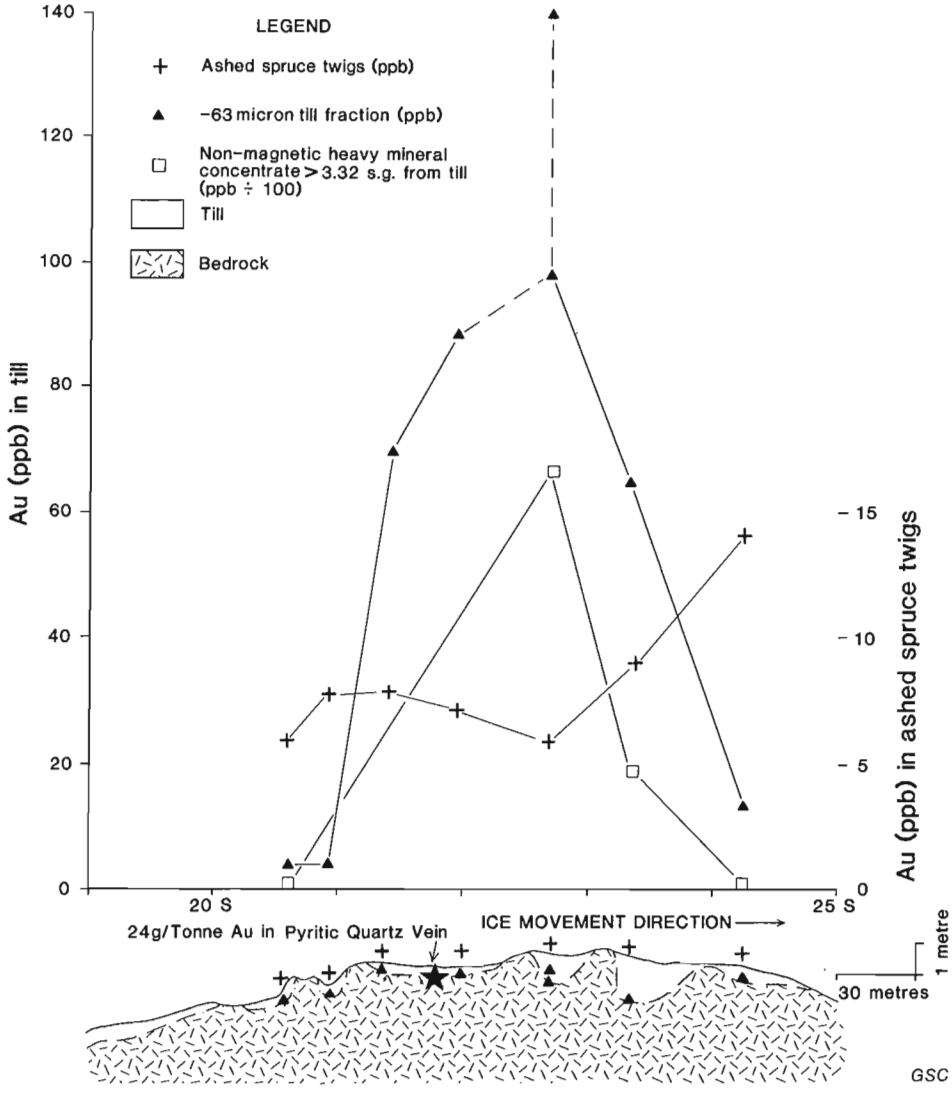

Figure 3. Distribution of Au (ppb) in till and black spruce on L310E. Note that Au concentrations in heavy mineral concentrates are divided by 100.

till and patchy melt-out (?) sand deposits. The area is heavily vegetated by black spruce. On L310E, the −63 micron-size fraction of tills contained up to 140 ppb Au, 28 ppm As, and 262 ppm Cr up to 75 m down-ice of oxidized gold-bearing pyritic quartz veins exposed in shallow trenches. Analyses of the non-magnetic fraction of heavy mineral concentrates from these till samples revealed similar trends with up to 6660 ppb Au, 14 ppm As, 1000 ppm Cr as well as 1.4 ppm Sb, and 224 ppm W.

Gold concentrations in ashed black spruce twigs from corresponding sites reveal a gradual increase in values from 5-7 ppb overlying mineralization to 14 ppb 75 m down-ice. The highest values for As (6.6 ppm) and Co (17 ppm) occur near mineralization, the opposite is true for Sb which ranges from 0.4 ppm over mineralization to 1.0 ppm 50 m down-ice. Since vegetation will tend to integrate the geochemical signature of bedrock and surficial material (Dunn, 1988), lithogeochemical data will be required to fully assess the biogeochemical response.

The eastern grid (Fig. 2 and 4) encompasses an area of subdued relief with numerous peat bogs and fens interspersed with higher areas of till-mantled bedrock. The northwestern and southeastern parts of the grid contain prominent ice contact deposits. The 200-m profile sampled on L374E (Fig. 4) crossed two boggy areas which resulted in the collection of peat samples instead of till. At the north and south ends of the profile a thin veneer of till mantles deformed silicified metasedimentary rocks containing disseminated pyrite, magnetite and trace galena.

Till samples contained up to 160 ppb Au, 160 ppm Cr, 15 ppm As, and 30 ppm W in the -63 micron size fraction. Element concentrations in the corresponding non-magnetic heavy mineral separates range up to 904 ppb Au, 1000 ppm Cr, 37 ppm As, 1350 ppm W, 19 ppm Mo, and 4 ppm Sb.

Peat samples were collected at sites overlying till at either end of the profile, and from below groundwater level in bogs. Peat with a noticeable silty composition (69.4 % ash) overlying till at the south end of the profile, yielded

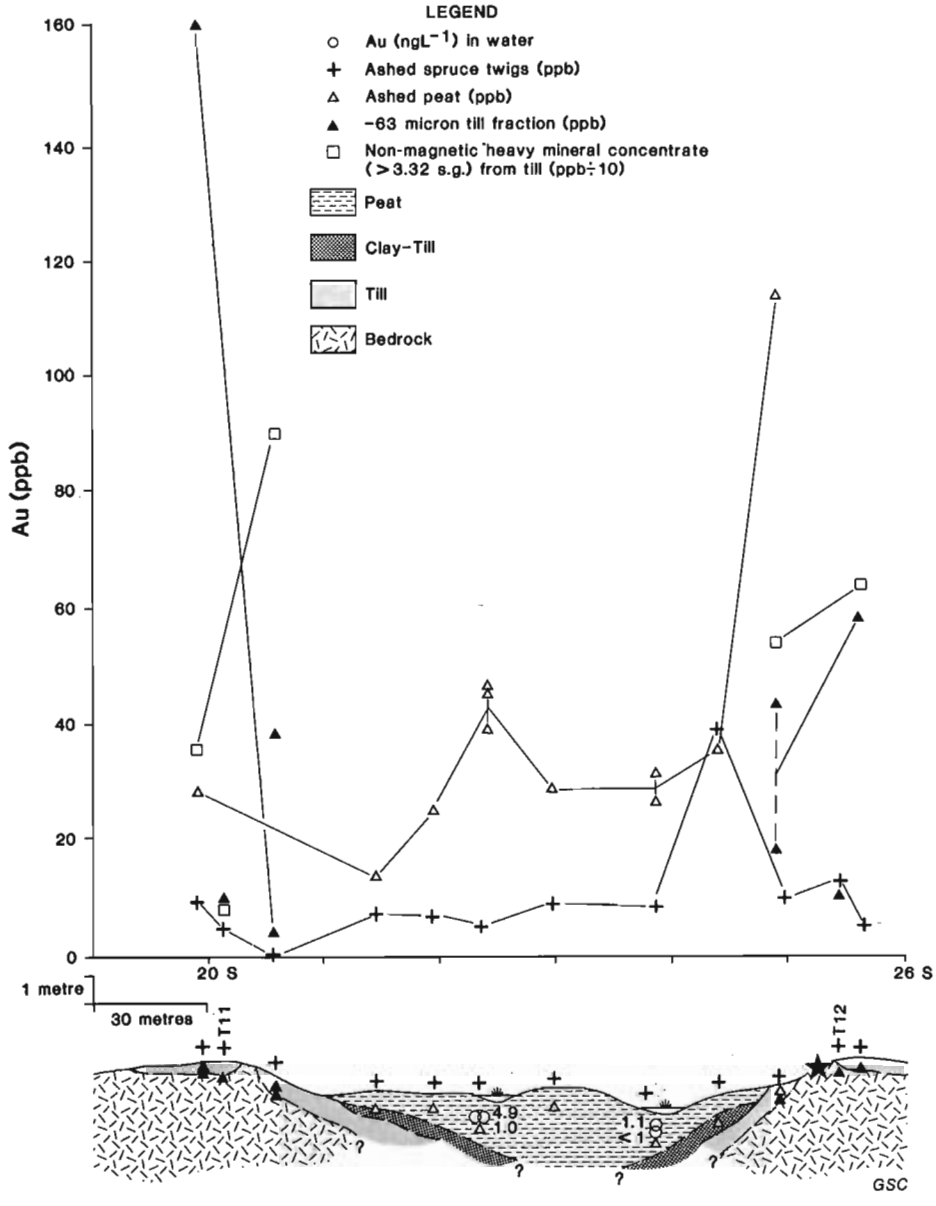

Figure 4. Distribution of Au (ppb) in till, peat, ashed black spruce twigs, and waters on L374E. Note that Au concentrations in heavy mineral concentrates are divided by 10. Samples T11 and T12 were collected 30 m east of L374E.

114 ppb Au, 1200 ppm As, and 3.8 ppm Sb. The Au value for this peat sample was not used in calculating the mean Au content of peat in Table 1 owing to the chemical and physical difference to other peat samples. Bog peat values range up to 35 ppb Au, 14 ppm As, 26 ppm Mo, 2.3 ppm Sb, and 5 ppm W.

Gold concentration in ashed spruce twigs range from 5 to 9 ppb over bogs, and <5 to 39 ppb over and adjacent to till mantled bedrock. Arsenic and Sb concentrations fluctuate over a narrow range of values; As 3.1 to 7.8 ppm, Sb 0.5 to 1.0 ppm.

Four 1 L water samples collected from surface bog waters (pH 5.4-6.2) on L374E contained up to .0049 ppb Au. Water (pH 6.4) collected from trenches adjacent to an arsenopyrite-bearing quartz vein approximately 200 m west of L310E contained up to .0023 ppb Au. The analytical results combine the analysis of Au desorbed from sample container walls with bromine-hydrochloric acid and analyses of 1 L of water filtered through 0.45 micron millipore-filter; the values are thus thought to represent total Au occurring as dissolved organic or anionic complexes (Hall *et al.*, 1986; Hamilton *et al.*, 1983).

DISCUSISON

Preliminary review of geochemical data for surficial materials collected at Foster Lake indicate significant secondary dispersion of Au. Mean Au concentrations of lake sediment from Foster and Reservoir Lakes of 3.4 ppb and 7.3 ppb noticeably exceed mean Au concentrations of 1.0 ppb from an earlier regional lake sediment survey (Geological Survey of Canada, 1986). The auriferous nature of the Johnson Shear Zone is thus reflected in the chemical composition of some of the adjacent lake bottom sediments.

In addition to Au, elevated concentrations of As, W, and Cr, and to a lesser extent, Sb and Mo were encountered in some or all of till, peat, and black spruce twigs collected over and down-ice of the Johnson Shear Zone. Metallic sulphides or oxides of Sb, Mo, and W have not been reported from Au occurrences along the Johnson Shear Zone by recent workers (Baldwin *et al.*, 1985), although the association of these elements with Au mineralization is well documented for many Precambrian deposits (Boyle, 1979). Future geochemical exploration along the Johnson Shear Zone should therefore include analyses of these elements on a routine basis.

Although much analytical and interpretive work is required to complete this study, some preliminary observations can be made on the environment of Au dispersion:

(1) The principal source of Au at Foster Lake is in pyritic quartz veins contained in intensely foliated, fractured and altered intermediate to felsic metasedimentary rocks belonging to the Wasekwan Group. Pyrrhotite and accessory arsenopyrite, galena, and chalcopyrite may accompany Au mineralization; the presence of molybdenum, tetrahedrite, or other antimony-sulphides, and scheelite is suggested by surficial geochemistry. Contribution of Au to the surficial environment by unmineralized rock with high background Au contents must also be considered.

(2) The Shear Zone's positive relief has exposed mineralization to glacial erosion and transport south toward Foster Lake. The Shear Zone is presently covered by a discontinuous veneer of till in a moist, vegetated environment, thus permitting mineralized bedrock and till to be exposed to oxidizing conditions. Oxidation of mineralized bedrock, till, and decaying vegetation contributes to formation of acid solutions containing humic, polysaccharide, sulphate and hydroxide constituents which are able to complex positively charged metal ions (Baker, 1973; Boyle *et al.*, 1975; Cameron, 1977; and Rose *et al.*, 1979). The movement of these solutions through surficial sediments and in surface waters, their reduction and precipitation in bogs, and uptake by vegetation may result in the observed secondary dispersion patterns.

(3) The accumulation of Au in lake bottom sediments is the natural consequence of the above dynamic process involving many chemical and physical pathways.

ACKNOWLEDGMENTS

This study forms part of a MSc research program in progress at University of Ottawa under the direction of Eion Cameron. I would like to gratefully acknowledge the very capable field assistance by Danny Scholtz and Danny Wright, and express my thanks to Steven Amor, Chief Geochemist, and Lynn Kelly, former Exploration Geologist of Lynn Gold Resources who kindly provided company geological data and with whom I have had several stimulating discussions regarding geochemical exploration at Foster Lake. Judy Vaive carried out the Au determinations on bulk waters, and Colin Dunn introduced me to aspects of biogeochemical sample collection and processing. Don Hornbrook and Eion Cameron are thanked for their constructive review of the manuscript.

The study was substantially funded through the Canada — Manitoba Mineral Development Agreement (1984-1989).

REFERENCES

Baker, W.E.
1973: The role of humic acids from Tasmanian podzolic soils in mineral degradation and metal mobilization; Geochimica et Cosmochimica Acta, v. 37, p. 269-281.

Baldwin, D.A., Parbery, D., Boden, S., and Michielsen, A.
1985: Mineral deposit studies in the Lynn Lake and Barrington lake areas; in Report of Field Activities, 1985, Manitoba Energy and Mines, p. 20-28.

Boyle, R.W.
1979: The geochemistry of gold and its deposits; Geological Survey of Canada, Bulletin 280.

Boyle, R.W., Alexander, W.M., and Aslin, G.E.M.
1975: Some observations on the solubility of gold; Geological Survey of Canada, Paper 75-246 p.

Cameron, E.M.
1977: Geochemical dispersion in lake waters and sediments from massive sulphide mineralization, Agricola Lake area, Northwest Territories; Journal of Geochemical Exploration, v. 7(3), p. 327-348.

Coker, W.B., Hornbrook, E.H.W., and Cameron, E.M.
1979: Lake sediment geochemistry applied to mineral exploration; in Geophysics and Geochemistry in the Search for Metallic Ores, ed. P.J. Hood, Geological Survey of Canada, Economic Geology Report 31, p. 434-477.

Dunn, C.E.
1984: Biogeochemical method and surveys, southern La Ronge belt; in Summary of Investigations, 1984, Saskatchewan Geological Survey, Miscellaneous Report 84-4, p. 95-103.
1988: Reconnaissance level biogeochemical surveys for gold in Canada; in Prospecting in Areas of Glaciated Terrain — 1988, ed. D.R. MacDonald, Canadian Institute of Mining and Metallurgy, p. 433-448.

Fedikow, M.A.F., Baldwin, D.A., and Taylor, C.
1986: Gold mineralization associated with the Agassiz Metallotect and the Johnson Shear Zone, Lynn Lake greenstone belt, Manitoba; in Gold in the Western Shield, ed. L.A. Clark, Canadian Institute of Mining and Metallurgy, Special Volume 38, p. 361-378.

Ferreira, K.
1986: Geological investigations in the Foster Lake — Wasekwan Lake area; in Report of Field Activities, 1986, Manitoba Energy and Mines, p. 13-17.

Gilbert, H.P., Syme, E.C., and Zwanzig, H.V.
1980: Geology of the metavolcanic and volcaniclastic rocks in the Lynn Lake area; Manitoba Department of Energy and Mines, Geological Paper GP80 — 1, 118 p.

Geological Survey of Canada
1984: Regional lake sediment and water geochemical reconnaissance data, Manitoba, 1983; Open File 999, NTS 64C.
1986: Regional lake sediment and water geochemical resonnaissance data, Manitoba, 1985; Open File 1288, NTS 64C.
1988: Regional lake sediment and water geochemical reconnaissance data, Manitoba, 1987; Open File 1641, NTS 63H (NE), 631, 63P (SE).

Hall, G.E.M., Vaive, J.E., and Ballantyne, S.B.
1986: Field and laboratory procedures for determining gold in natural waters: relative merits of preconcentration with activated charcoal; Journal of Geochemical Exploration, v. 26, no. 3, p. 191-202.

Hamilton, T.W., Ellis, J., Florence, T.M., and Fardy, J.J.
1983: Analysis of gold in surface waters from Australian gold fields: an investigation into direct hydrogeochemical prospecting for gold; Economic Geology, v. 78, p. 1335-1341.

Kaszycki, C.A. and DiLabio, R.N.W.
1986: Surficial geology and till geochemistry, Lynn Lake — Leaf Rapids region, Manitoba; Geological Survey of Canada, Paper 86-1B, p. 245-256.

Mann, A.N.
1984: Mobility of gold and silver in lateritic weathering profiles — some observations from western Australia; Economic Geology, v. 39, p. 38-49.

Rose, A.W., Hawkes, H., and Webb, J.S.
1979: Geochemistry in Mineral Exploration; Academic Press, Second Edition, p. 13-35.

Sherritt Gordon Mines
1983: Geological map of the Foster Lake area; internal company map, scale 1:4,800.

Stoffregen, R.
1986: Observations on the behaviour of gold during supergene oxidation at Summitville, Colorado, U.S.A., and implications for electrum stability in the weathering environment; Applied Geochemistry, v. 1, p. 549-558.

Webster, J.G.
1986: The solubility of gold and silver in the system Au-Ag-S-O_2-H_2O at 25°C and 1 atm.; Geochimica et Cosmochimica Acta, v. 50, p. 1837-1845.

Webster, J.G., and Mann, A.N.
1984: The influence of climate, geomorphology and primary geology on the supergene migration of gold and silver; Journal of Geochemical Exploration, v. 22, p. 21-42.

Zwanzig, H.V., Parker, J.S.D., Schwedewitz, D.C.P, and Van Schmus, W.R.
1985: Lynn Lake regional compilation and geochronology; in Report of Field Activities, 1985; Manitoba Energy and Mines, p. 6-8.

Rhyodacite ignimbrites and breccias of the Sue-Dianne and Mar Cu-Fe-U deposits, southern Great Bear magmatic zone, Northwest Territories†

S.S. Gandhi
Mineral Resources Division

Gandhi, S.S., Rhyodacite ignimbrites and breccias of the Sue-Dianne and Mar Cu-Fe-U deposits, southern Great Bear magmatic zone, Northwest Territories; in Current Research, Part C, Geological Survey of Canada, Paper 89-1C, p. 263-273, 1989.

Abstract

A sequence of potassic rhyodacite ignimbrites and associated volcaniclastic rocks occur near Mazenod Lake in the Aphebian Faber Lake volcanic belt. The sequence is more than 3 km thick, moderately deformed, and is intruded by dacite porphyry and quartz monzonite-granodiorite. Breccia zones in the sequence at the Sue-Dianne and Mar deposits are irregular and pipe-like, and are characterized by abundant magnetite-specularite in the matrix with epidote, chlorite, small amounts of chalcopyrite, and up to 150 ppm uranium. The larger Sue-Dianne deposit contains drill indicated resources of 8.16 million tonnes averaging 0.8% Cu. Younger high grade pitchblende veins exposed at its surface have a limited depth extent.

The brecciation and mineralization are interpreted as hydrothermal, related to late magmatic processes in a calc-alkaline volcano-plutonic complex. The deposits are variants of the magnetite-apatite-actinolite veins, pods and breccia-fillings that are widely distributed in the Great Bear magmatic zone. The pitchblende veins represent later supergene uranium concentrations.

Résumé

On rencontre près du lac Mazenod dans la zone volcanique aphébienne de Faber Lake, une séquence d'ignimbrites à rhyodacite potassique, et de roches volcanoclastiques associées. La séquence a plus de 3 km d'épaisseur, est modérément déformée, et est traversée par des intrusions de porphyre dacitique et de granodiorite à monzonite quartzifère. Les zones bréchiques de la séquence, à l'emplacement des gisements de Sue-Dianne et de Mar qui sont irrégulières et en forme de cheminée, et caractérisées par une matrice qui contient des quantités abondantes de magnétite et spécularite, accompagnées d'épidote, de chlorite, d'un peu de chalcopyrite et de concentrations d'uranium pouvant atteindre 150 ppm. Le gisement plus grand de Sue-Dianne contient des ressources indiquées par forage, qui s'élèvent à 8,16 millions de tonnes métriques de minerai contenant en moyenne 0,8 % de Cu. Les filons plus récents qui contiennent de la pechblende de forte teneur et y affleurent en surface ont une épaisseur limitée.

On a interprété la bréchification et la minéralisation comme étant d'origine hydrothermale, et liées à des processus magmatiques tardifs qui se sont déroulés dans un complexe volcano-plutonique de nature calco-alcaline. Les gisements sont des variantes des filons, masses minéralisées allongées et remplissages de brèches contenant de la magnétite, de l'apatite et de l'actinolite, lesquelles structures sont très répandues dans la zone magmatique de Great Bear. Les filons de pechblende représentent un enrichissement tardif supergène en uranium.

† Contribution to Canada - Northwest Territories Mineral Development Agreement 1987-1991. Project carried by the Geological Survey of Canada.

INTRODUCTION

The Sue-Dianne deposit is the largest copper-uranium deposit in the southern Great Bear magmatic zone (Fig. 1). It was initially a uranium prospect when discovered in 1974. Further exploration during 1970s by Noranda Exploration Company Limited revealed only limited uranium potential, but copper content was significant enough for it to be regarded as a subeconomic copper deposit. The exploration also revealed a similar but smaller deposit, namely the Mar deposit, 2.5 km to the north-northeast (Fig. 1). The present study was undertaken to better define their geological setting, petrochemistry of the host volcanic sequence and intrusions, and the metallogenic features. It is a part of a broader regional metallogenic study started in 1987 under the Canada- Northwest Territories Mineral Development Agreement (Gandhi, 1988).

PREVIOUS WORK

Regional geological mapping in the southern part of the Great Bear magmatic zone by Kidd (1936), Lord (1942), Wilson and Lord (1942), Fraser (1967) and McGlynn (1968, 1979), outlined a belt of rhyodacite volcanics and dacitic feldspar porphyry in a granite terrain (Fig. 1). This belt has a distinctly high regional magnetic response (Geological Survey of Canada, 1963, 1969 a, b; Gandhi, 1988; Charbonneau, 1988).

Mineral Exploration of the belt proceeded intermittently from 1934 to the late 1970s, mainly for uranium and copper. The main discoveries are the Rayrock uranium mine and Sue-Dianne deposit, and in addition there are a number of small occurrences including the magnetite-rich Fab U-Cu showings (Gandhi, 1988) and pitchblende veins in the vicinity of Rayrock mine (Lang et al., 1962). The Rayrock mine exploited pitchblende in a giant quartz vein system and produced 150 tonnes of uranium during 1957.

The Sue-Dianne deposit was discovered through follow-up exploration of a strong radiometric anomaly detected by an airborne gamma-ray spectrometer survey conducted in 1973 by the Geological Survey of Canada (Charbonneau, 1988). The SUE and DIANNE claims staked by prospector Dave Smith of Yellowknife, were optioned by Noranda Exploration Company Limited in 1974. Exploration conducted by the company through 1975-1977, including drilling of 2333 m in 14 holes, outlined drill indicated resources of 8.16 million tonnes averaging 0.8 per copper (Climie, 1975, 1976; J.L. Biczok, Noranda Exploration Company Limited, personal communication, 1988). The smaller Mar zone was explored by one drill hole 137 m long (Prest, 1977a; Bryan, 1979). Additional surface exploration was conducted by the company in the present study area (Prest, 1977b; Bryan, 1978, 1980). A mineralogical and geochronological study of pitchblende veins at the Sue-Dianne deposit was conducted by Miller (1981, 1982) as a part of a broader study.

REGIONAL GEOLOGY

The Great Bear magmatic zone is characterized by abundant volcanic and volcaniclastic rocks of intermediate to felsic composition and related intrusions emplaced approximately 1850 Ma ago in a continental arc setting (Hoffman, 1980; Hildebrand, 1986). The rocks are weakly to moderately deformed, and are metamorphosed to subgreenschist or greenschist facies. The Faber Lake volcanic belt in the southern part of the magmatic zone is dominated by rhyodacitic ignimbrite and associated flows, tuffs and volcaniclastic sediments, and extensive massive porphyritic dacite, which is regarded as largely subvolcanic intrusive, but parts of it may be extrusive (McGlynn, 1979; Gandhi, 1988). Andesitic flows and quartz monzonite intrusions related to the volcanism were recognized in the area of Fab U-Cu showings by Gandhi (1988). The younger granites of the Great Bear batholith surround the volcanic belt.

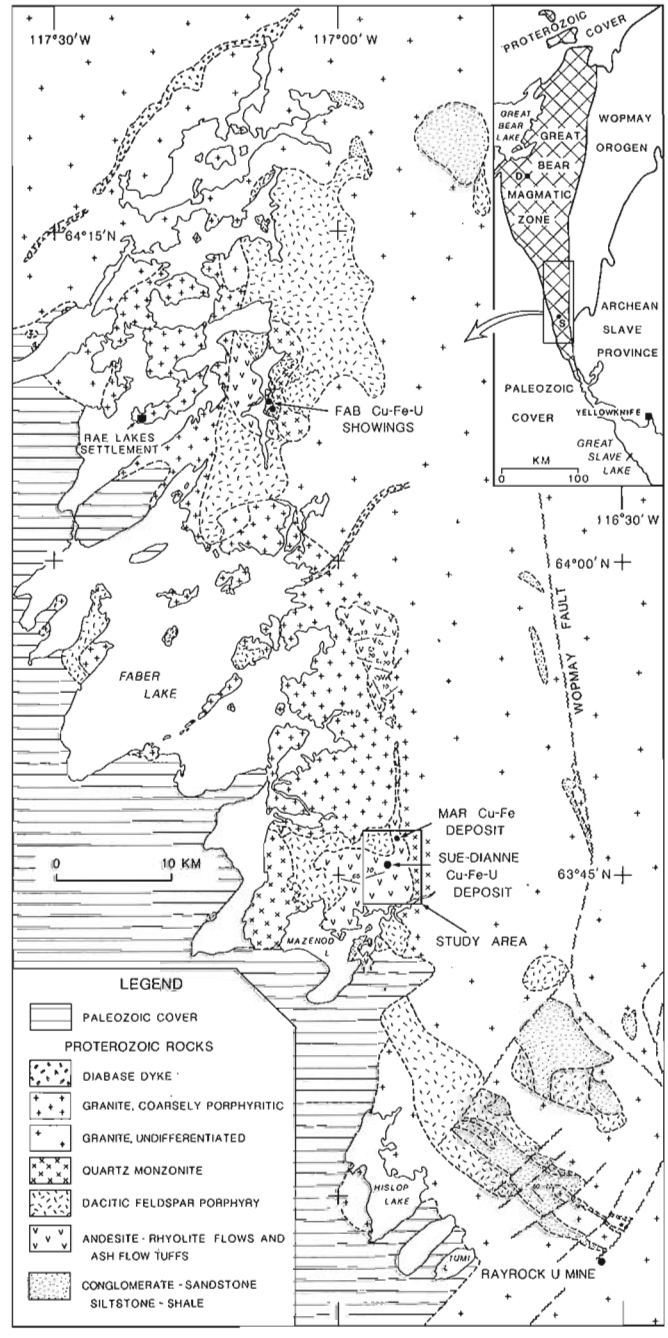

Figure 1. General geology of the Faber Lake volcanic belt and location of the study area. Inset map: S - Sue-Dianne deposit, D - Damp deposit.

GEOLOGICAL SETTING OF THE SUE-DIANNE AND MAR DEPOSITS

The Sue-Dianne and Mar deposits are hosted by an extensive rhyodacite ignimbritic sequence which is more than 3 km thick in the study area (Fig. 2). It is folded, faulted and intruded by dacite porphyry and quartz monzonite-granodiorite. Seven units are distinguished in the sequence (Fig. 2). Units 1 to 4 west of Dianne Lake dip steeply to the north-northwest, and units 5, 6 and 7 east of the lake dip moderately to steeply eastwards. The volcanic units include more than one extrusive member and in addition lenses of volcaniclastic sediments. They display eutaxitic structures. Minor open folds and faults are common in the area. The rocks are altered to a varying degree, most intensely near the deposits. Veinlets containing quartz, epidote, chlorite, magnetite, specularite and calcite, in varying proportions, are common throughout the area, and giant quartz veins occur close to a northeast-trending fault that is located along the northeast arm of the Dianne Lake.

Volcanic and volcaniclastic rocks

The felsic volcanic rocks are characterized by porphyritic texture. Phenocrysts of sodic plagioclase and less abundant potash feldspar, quartz and minor altered mafic silicate, are set in fine grained quartzo-feldspathic matrix that contains abundant, finely disseminated magnetite crystals. These crystals impart grey colour to the matrix and a weakly to

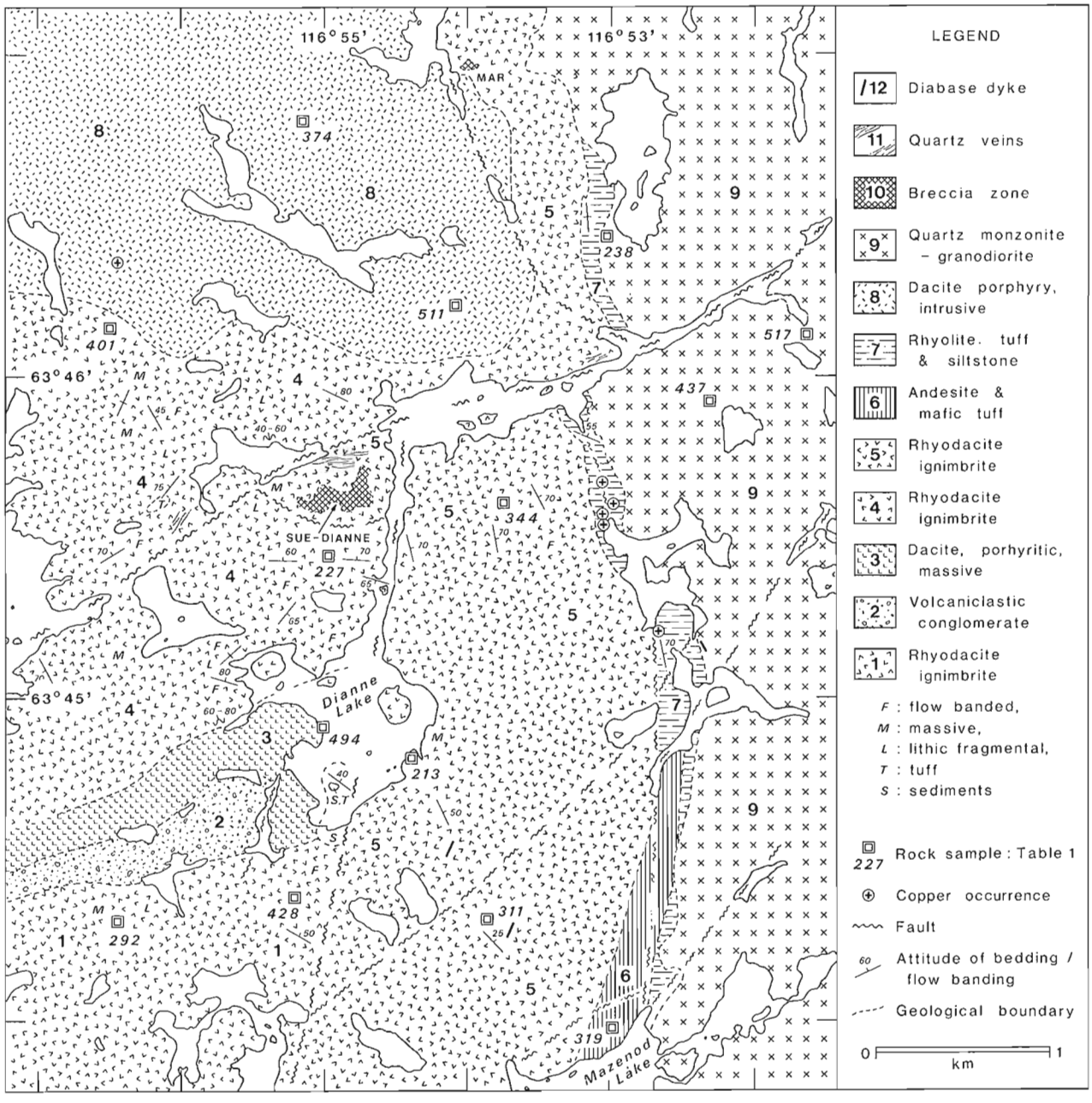

Figure 2. Geology of the area around Sue-Dianne Cu-Fe-U deposit, Northwest Territories.

moderately magnetic character to the rock. Feldspar microlites occur in some rocks. Zircon and apatite occur as accessories. Feldspars are cloudy in thin sections due to alteration, and the mafic silicates are altered to chlorite and oxide aggregates. Epidote occurs as an alteration product and as veinlets. Quartz and chlorite veinlets are also common.

The proportion of phenocrysts varies considerably and the rocks range from massive to flow banded or foliated to fragment-rich in character. Units 1 and 4 are relatively more variable in these respects than other units. Some of the extrusive members in unit 4 show well defined flow banding or compaction foliation in the lower part of the flow (Fig. 3, 4 and 5), grading upwards into massive rocks with a few lithic fragments (Fig. 4 and 6), and with a fragment-rich top. Small lenses of fine to coarse volcaniclastic sediments are intercalated with the volcanics, but these are not extensive enough to serve as marker beds. Rocks of units 1 and 4 contain well developed laths of plagioclase that are 4 to 8 mm long, and make up 15 to 30 per cent of the rock, and smaller phenocrysts of potash feldspar, quartz and altered mafic minerals, each of which makes up less than 5 per cent of the rock. The matrix in many of these rocks displays flowage lines that curve around the randomly oriented phenocrysts. In some rocks, however, the plagioclase laths are oriented subparallel to the flowage direction. Flow banding or compaction foliation is best defined by thin quartzo-feldspathic layers or elongate streaks (Fig. 3, 4 and 5). The thickness, length and spacing between these streaks vary considerably in different parts of an individual extrusive member, and from one member to an other. In thin section, the quartzo-feldspathic streaks show slightly coarser grain size than the grey matrix, and relatively less abundant magnetite crystals. Most of the streaks have cores of quartz grains coarser than those in the matrix.

Unit 3 is distinctive in several respects; it is massive, contains only plagioclase as phenocrysts (Fig. 7), and rare inclusions of lithic fragments. It grades into a border phase containing smaller feldspar phenocrysts, and flow banding is seen in a few places at its south margin. Unit 5 is also generally uniform, and is characterized by an abundance of phenocrysts, which make up 40 to 60 per cent of the rock. It is buff, white or pale pink in contrast to units 1, 3 and 4 which are grey. Phenocrysts of quartz, sodic plagioclase, potash feldspar (perthite and microcline) and altered mafic

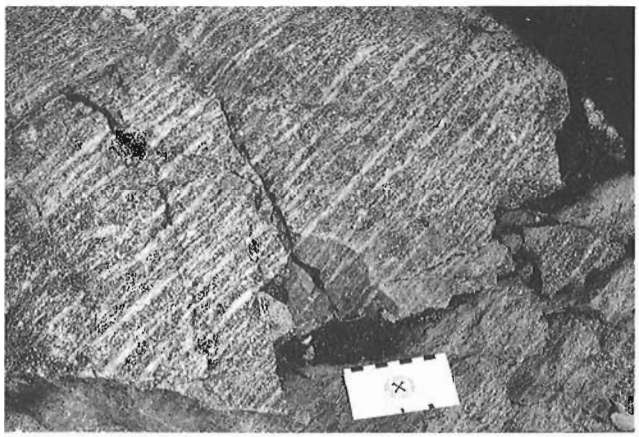

Figure 3. Flow banded dacitic ignimbrite, unit 4; 2 km west-southwest of the Sue-Dianne breccia zone (Fig. 2). GSC Photo 204718-T.

Figure 5. Flow banded dacitic ignimbrite, unit 4; sample 227 (Fig. 2). Note dark cross-cutting veins of hematite, and associated wallrock alteration that obscures the banding. GSC Photo 204718-H.

Figure 4. Dacitic ignimbrite showing some flow bands and inclusions of volcanic fragments, 150 m northeast of the exposure in Figure 3. GSC Photo 204718-S.

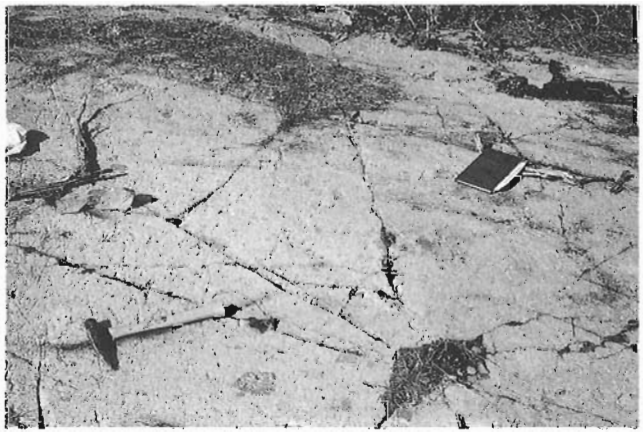

Figure 6. Massive part of a dacitic ignimbrite, unit 4; 100 m north of sample 227 (Fig. 2). GSC Photo 204718-G. Note lithic fragments.

mineral commonly make up approximately 15, 30, 10 and 3 per cent respectively of the rock. They are euhedral to subhedral and 3 to 5 mm long, but many are smaller and impart a seriate texture to the rock. Some phenocrysts are broken, and a few of the quartz phenocrysts have distinctly embayed margins indicating resorption. Chlorite and iron oxide commonly form whispy aggregates or streaks. Lenticular inclusions of pumice or lapilli are common and emphasize flowage foliation (Fig. 8). Some parts of the unit, however, are rather massive, for example, near the south shore of Dianne Lake, and the finer grained eastern margin. The rhyolitic rocks of unit 7 resemble the marginal phase of unit 5 and their inclusion in a separate unit is based on their association with thinly bedded siltstone, massive grey siltstone and felsic tuffs.

Unit 2 is the thickest and most extensive volcaniclastic part of the sequence in the area. The eastern part of the unit contains cobbles up to 50 cm in diameter on the south side (Fig. 9) and progressively smaller clasts to the north (Fig. 10), indicating top to the north. Most of the clasts are of porphyritic volcanic rocks and siltstones. A few pebbles of magnetite crystal aggregates are sparsely distributed in the unit (Fig. 10). Proportion of clasts decreases towards the southwest. Matrix is a highly altered mixture of pumice, lithic fragments, and porphyritic material similar to rhyodacite volcanic rocks. The unit may be a lahar.

The feldspar porphyritic andesitic and mafic tuffaceous rocks of unit 6, the only relatively mafic volcanic rocks in the area, form a very minor part of the sequence. The rocks are highly epidotized, and their contacts are poorly exposed. The andesitic rocks contain phenocrysts of an altered mafic silicate and a few smaller grains of quartz. The rocks are cut by numerous veinlets of quartz, epidote and chlorite. Tuffaceous rocks are more abundant in the north, and their equivalents occur as lenses in unit 7, which also includes lenses of grey siltstone, thinly bedded light-coloured siltstones, and rhyolitic rocks that resemble marginal phase of unit 5 (Fig. 11).

Intrusive Rocks

Dacite porphyry (unit 8) and quartz monzonite-granodiorite (unit 9) are major intrusions in the area. The dacite porphyry probably connects with a body of intrusive dacite porphyry to the southwest (Fig. 1), mapped by McGlynn (1979). He regarded it as a synvolcanic, intrusive equivalent of the dacitic volcanic rocks.

Figure 7. Feldspar-porphyritic dacite of unit 3; location 500 m west-southwest of sample 494 (Fig. 2). GSC Photo 204718-K.

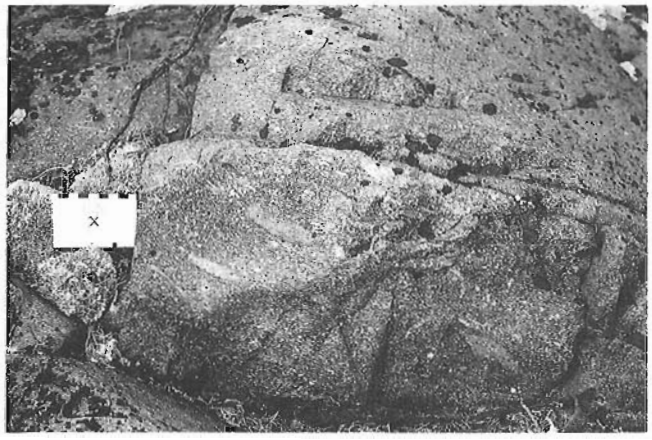

Figure 8. Volcaniclastic conglomerate of unit 2; location 1 km southwest of Dianne Lake (Fig. 2). GSC Photo 204718-M.

Figure 9. Volcaniclastic conglomerate of unit 2 (Fig. 2). Note magnetite pebble left of centre; 100 m north of outcrop in Figure 3. GSC Photo 204718-P.

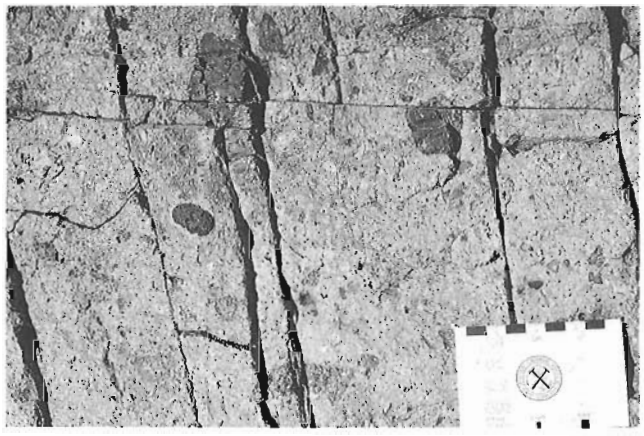

Figure 10. Rhyodacite of unit 5; location 300 m east of sample 344 (Fig. 2). Note lenticular lapillae or pumice fragments and flowage foliation. GSC Photo 204718-R.

The dacite porphyry contains phenocrysts of oligoclase or andesine, up to 5 mm long, that comprise up to 25 per cent of the rock. A few phenocrysts of potash feldspar and quartz are also present in many places. Scattered clusters of mafic silicates, up to 5 mm long, are now mostly aggregates of chlorite, iron oxides and sphene. Felty aggregates of chloritized biotite, and accessory zircon and apatite are present. The matrix is fine grained, equigranular, containing nearly equal proportions of quartz and sericitized feldspar. Weathered outcrops of the porphyry are buff white to red. Alteration is pronounced in the southeastern part of the unit.

The quartz monzonite-granodiorite pluton is well exposed in the east, and contains numerous xenoliths of units 3, 4 and 5 along its north-trending boundary. Its texture is characterized by abundant phenocrysts of plagioclase, and fewer but larger phenocrysts of potash feldspar up to 3 cm long (Fig. 11). The phenocrysts are commonly euhedral, make up to 70 per cent of the rock and are randomly oriented. The matrix is medium grained and contains quartz, feldspar, chloritized biotite and hornblende, magnetite, sphene and traces of apatite and zircon. Quartz content ranges from 10 to 20 per cent, but at some places near the margin it is somewhat greater and the rock appears granitic.

The breccia zones of the Sue-Dianne and Mar deposits (unit 10), which are described below in greater detail, are tentatively regarded here as either coeval or somewhat younger than the quartz monzonite-granodiorite intrusion, but the age relation is not certain. Some massive milky quartz veins (unit 11), up to 1 m thick, are found along and in the vicinity of a northeast-trending fault that passes through the intrusion. The fault appears younger than the north-south trending fault along Dianne Lake that is marked by hematization and epidotization. A few small fresh-looking diabase dykes (unit 12), up to 2 m thick, occur in the study area.

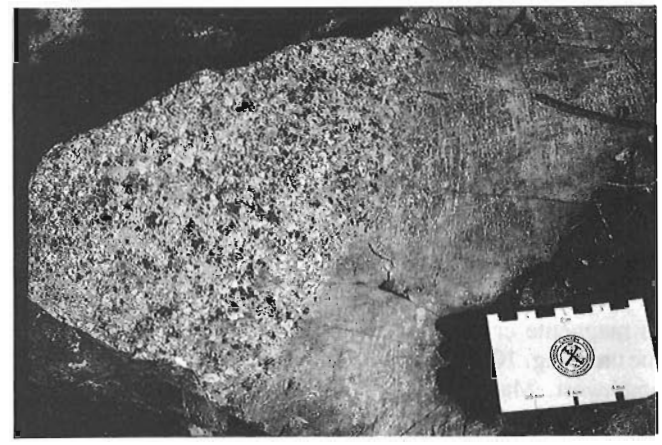

Figure 11. Contact of rhyolitic volcanic and quartz monzonite-granodiorite intrusion, sample site 267 (Fig. 2). GSC Photo 204718-A.

Table 1. Chemical analyses of selected volcanic and intrusive rocks, and samples from breccia zone of the Sue-Dianne Cu-U-Fe deposit, Mazenod Lake area, Northwest Territories.

Analysis #		1	2	3	4	5	6	7	8	9	10	11	12	13	14	15	16	17	18	19
Sample #		292	428	494	227	401	213	311	344	319	374	511	517	437	267	S-1-A	S-1-B	S-2-A	238	S-1-C
Map Unit		1	1	3	4	4	5	5	5	6	8	8	9	9	9	10	10	10	10	10
SiO_2	%	63.60	70.70	67.30	68.70	67.10	66.70	70.50	68.80	54.30	68.90	68.80	68.40	68.20	67.30	70.50	68.80	61.20	41.20	34.60
Al_2O_3		15.80	15.50	15.90	16.00	15.60	15.50	14.80	14.10	16.90	14.80	15.40	14.90	15.00	15.00	14.60	16.00	18.50	13.40	10.50
TiO_2	"	0.60	0.34	0.67	0.28	0.42	0.58	0.33	0.31	0.70	0.42	0.38	0.54	0.44	0.56	0.25	0.38	0.45	0.39	0.37
FeO	"	2.10	1.20	2.50	1.23	3.10	1.60	1.50	2.30	5.20	1.90	1.10	2.30	2.20	2.70	0.80	1.50	2.50	2.40	9.20
Fe_2O_3	"	2.60	1.80	2.80	2.80	0.60	3.80	1.30	2.20	2.40	0.60	1.30	1.30	0.70	1.40	1.30	1.50	1.70	24.60	30.60
MnO	"	0.09	0.04	0.11	0.02	0.14	0.05	0.06	0.05	0.28	0.04	0.03	0.05	0.05	0.07	0.01	0.06	0.11	0.08	0.06
MgO	"	1.09	0.45	1.60	0.29	0.99	1.39	0.79	0.73	5.14	1.03	0.37	1.42	1.18	1.70	0.31	0.71	1.55	1.18	0.49
CaO	"	4.36	1.19	0.25	0.54	2.32	0.74	0.93	1.36	6.01	2.56	0.22	1.86	1.88	1.99	0.36	1.25	0.15	0.29	0.32
Na_2O	"	3.10	3.70	3.40	4.60	2.70	3.30	3.50	2.60	3.30	3.40	3.60	2.50	2.40	2.60	1.70	6.00	3.40	0.19	0.10
K_2O	"	4.25	5.39	4.14	5.01	5.30	5.41	5.90	5.98	2.37	5.22	7.97	6.12	6.61	4.96	9.97	3.49	9.70	9.01	8.15
P_2O_5	"	0.17	0.07	0.14	0.07	0.10	0.14	0.07	0.06	0.15	0.09	0.06	0.15	0.13	0.16	0.06	0.09	0.10	0.11	0.14
H_2O_T	"	1.10	0.90	1.90	0.70	1.10	1.30	0.80	0.70	2.80	1.00	0.40	1.10	1.00	1.60	0.30	0.70	1.10	2.30	0.70
CO_{2T}	"	1.60	0.30	0.00	0.20	0.20	0.10	0.10	0.10	0.30	0.00	0.00	0.00	0.00	0.10	0.10	0.00	0.00	0.10	0.00
S	"	0.00	0.00	0.00	0.00	0.00	0.00	0.00	0.01	0.00	0.00	0.00	0.01	0.02	0.00	0.00	0.00	0.00	0.07	0.92
Total		100.46	101.58	100.71	100.44	99.67	100.61	100.58	99.30	99.85	99.96	99.63	100.65	99.81	100.14	100.26	100.48	100.46	95.32	96.15
Ba	ppm	792	858	663	815	1072	857	1054	916	444	917	1475	899	1086	1140	2586	743	1853	2803	2258
Be	"	2.6	2.4	2.1	3.1	2.6	2.2	2.5	3.2	2.2	2.6	1.2	2.6	2.5	3.0	0.8	2.0	0.8	6.5	2.3
Co	"	14	6	10	2	10	9	6	8	39	7	3	10	9	11	3	7	11	85	74
Cr	"	49	20	11	9	21	43	16	20	120	20	13	17	15	24	7	13	17	69	9
Cu	"	20	4	8	9	26	11	10	12	19	14	7	14	20	24	14	3	0	4300	8900
La	"	44	52	41	53	56	41	47	67	28	44	12	100	81	110	36	29	28	350	58
Nb	"	51	42	50	59	51	34	60	32	27	42	48	27	56	63	51	52	67	0	3
Ni	"	19	8	6	1	6	15	5	10	46	9	0	5	6	8	0	4	4	34	27
Rb	"	149	217	200	261	220	214	213	238	156	154	345	225	202	165	280	117	297	631	203
Sr	"	262	126	65	92	199	79	110	164	237	167	60	284	328	277	66	87	37	0	7
V	"	62	25	32	9	35	85	25	34	150	32	18	44	35	49	7	27	34	270	87
Y	"	30	71	37	29	67	62	65	74	61	33	28	48	34	31	66	75	65	0	37
Yb	"	2.3	2.2	3.1	2.7	2.4	2.1	2.0	2.2	1.7	2.7	1.9	4.0	3.2	2.5	1.8	2.1	2.6	8.0	2.3
Zn	"	100	23	140	18	65	52	45	42	75	37	19	34	63	61	13	44	90	110	72
Zr	"	257	234	259	313	320	233	236	228	167	325	325	316	271	362	291	265	349	289	154

Notes: 1) Analyses by the Analytical Chemistry Section, Mineral Resources Division, Geological Survey of Canada, Ottawa.
2) All analyses by x-ray fluorescence method except FeO, H_2OT, CO_2T and S by rapid chemical method and Fe_2O_3T in Analysis 18 by ICP-MS method.
3) Fe_2O_3 is calculated using the formula: $Fe_2O_3 = Fe_2O_3$ (XRF) - 1.11134 X FeO (Volumetric).
4) Sample locations in Figure 2 (Analyses 1 to 14) and in Figure 3 (Analyses 15 to 19); S-1-A, B & C are from drill hole S-1 at 29.5 m, 123.2 m and 90.2 m respectively and S-2-A is from drill hole S-2 at 84.3 m; other samples are from outcrops, and belong to the GFA-88 series.

PETROCHEMISTRY

Chemical analyses of 19 samples of the volcanic and intrusive rocks of the study area, and including some altered and mineralized rocks of the Sue-Dianne deposit, are presented in Table 1. The felsic volcanic rocks (analyses 1 to 8) are calc-alkaline dacite to rhyolite, with potash predominant over soda. Their silica content ranges between 66.7-70.5 per cent, except for one sample (analysis 1) that contains lower silica and higher CaO and CO_2, reflecting the abundance of secondary calcite observed in thin section. The andesite sample represents the volumetrically subordinate intermediate part of the volcanic sequence. It is distinctive chemically in having a higher soda content than its potash content. The intrusive dacite and quartz monzonite-granodiorite (analyses 10 to 14) show chemical affinity to the felsic volcanic sequence. The assemblage is similar, in terms of the major, minor and trace elements, to the volcano-plutonic complex 40 km to the north at Fab Lake (Gandhi, 1988). The intrusive rocks are slightly more siliceous than their textural equivalents in the Fab Lake area. The difference is more pronounced in case of the quartz monzonite-granodiorite with 67.3 to 68.4 per cent silica as compared with 62.0 per cent silica in the Fab Lake quartz monzonite (Gandhi, ibid). There are, however, quartz-feldspar porphyritic dykes in the Fab Lake area that are very similar in composition to the quartz monzonite-granodiorite, and represent more siliceous differentiates of the quartz monzonite. The quartz monzonitic intrusions are older than, and chemically distinct from, the more extensive granites of the Great Bear magmatic zone (Gandhi, ibid).

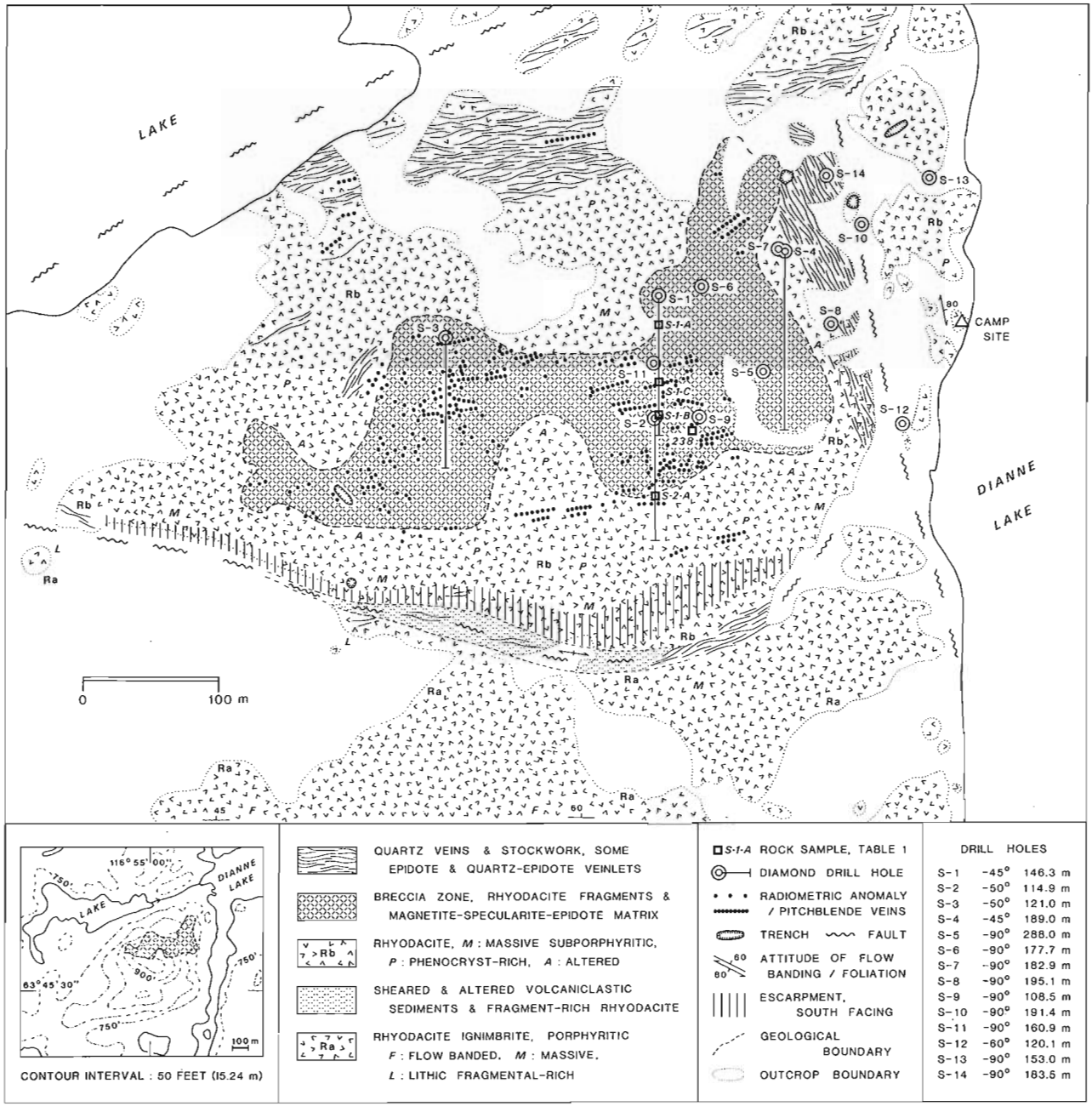

Figure 12. Surface geology and diamond drill holes of the Sue-Dianne Cu-Fe-U deposit, Northwest Territories.

The overall chemical character of the belt is consistent with a continental arc setting of the Great Bear magmatic zone as proposed by Hoffman (1980) and Hildebrand (1986). The samples from the Sue-Dianne breccia zone and adjacent altered rocks (analyses 15 to 19) show enrichment in potash and barium in comparison with unaltered or little altered rocks, except in case of one sample (analysis 16) which shows soda enrichment. The data indicate considerable alkali metasomatism accompanying mineralization.

SUE-DIANNE Cu-Fe-U DEPOSIT

The deposit is in a magnetite-cemented breccia zone, approaching a pipelike form and plunging steeply to the east as seen from excellent surface exposure and 14 drill holes, including one to a depth of 300 m (Fig. 12 and 13). The fragments of rhyodacitic volcanic rocks range in size from a fraction of a centimetre to a few tens of centimetres, but most are 2 to 10 cm long. They tend to have rounded outlines (Fig. 14). Some fragments are clearly of lithic fragmental volcanic rock. In the core of the zone, where magnetite is abundant in the matrix, fragments have intense red alteration colour due to hematization. Lithological distinction among the altered fragments is difficult as original textures are obscured. The fragments contain abundant fine grained granoblastic material, in places seen as replacement products of feldspar phenocrysts. This feature is attributed to alkali metasomatism. Chlorite and epidote are also abundant in the altered rock, and occur as disseminated grains, aggregates and veinlets. Disseminated iron oxide crystals are coarser, and tend to form aggregates, in the altered rocks in contrast to those in the unaltered volcanic rocks. On the margins of the core zone, brecciation is commonly restricted to narrow dyke-like zones, and alteration of fragments is not as intense as in the core zone. Some of these narrow breccia zones show alignment of fragments. The wall rocks of these zones have larger blocks of differing lithologies, including flow banded and streaky blocks that show differing orientations. Epidote veins are common along margins of these blocks. Numerous epidote and quartz-epidote veins also occur in and near the breccia zone. Larger quartz veins up to 1 m thick, form an outer, stockwork-like zone that nearly completely envelopes the deposit (Fig. 10).

The matrix in the core part of the breccia zone consists predominantly of magnetite, with varying proportions of maghemite and specularite, and some fine dark aggregates of quartzo-felspathic material speckled with the oxides and mafic silicate minerals. Magnetite forms fine- to medium-grained aggregates. Its abundance is highly variable, ranging up to 50 per cent of the rock. In addition, pods and veins composed essentially of magnetite, and up to 25 cm wide, are encountered at many places. Specularite is not readily distinguishable from magnetite megascopically, and its proportion is thus difficult to estimate. Some large clusters of specularite are, however, noted in outcrops and in polished slabs. Oxide-rich samples that are weakly magnetic contain abundant specularite, and some magnetite partially altered to specularite.

Copper sulphides are distributed as veinlets, stringers and disseminations mostly within the matrix of the breccia, and to a lesser extent in the fragments. Chalcopyrite is the dominant phase, but bornite and chalcocite are widely distributed and predominate over chalcopyrite in some sections of drill core. Disseminations and small aggregates of copper sulphides within magnetite indicates a very close paragenetic relationship between them.

Pitchblende occurs in the deposit as veinlets and fracture-fillings at the surface, and they caused a strong uranium anomaly which in an airborne radiometric survey conducted by the Geological Survey of Canada led to the discovery of the deposit (Charbonneau, 1988). None of the drill holes, however, intersected any significant radioactivity, although many of the drill core samples in and adjacent to the copper-rich sections assayed 75 to 150 ppm U, whereas most other samples contained less than 30 ppm U (Climie, 1976). The trend of the pitchblende veins at the surface is easterly and their dips are steep or vertical (Fig. 10). The veins are transgressive with respect to the magnetite cemented breccia. They contain varying amounts of quartz, calcite, and hematite, and locally copper sulphides. Miller (1981, 1982) identified other mineral phases containing Bi, Se and Te, including the rare mineral kawazulite.

Figure 13. View of the western past of the hill on which the Sue-Dianne breccia zone is exposed. Looking southeast (Figs. 2 and 12). GSC Photo 204718-J.

Figure 14. Breccia zone with magnetite-rich matrix, Sue-Dianne deposit, 150 m south of drill hole S-3 (Fig. 12). Horseshoe magnet, on magnetite vein to the left, is 2.5 cm long. Looking east-northeast. GSC Photo204718-I.

The drill core samples were analyzed for Cu, Au, Ag and U by Noranda Exploration Company Limited. Some of the 1.52 m (5 ft) length samples yielded assays as high as 2.50% for Cu, 1.75 oz/t Ag, and 150 ppm U, but the gold content was low, ranging from traces to 0.010 oz/t (J.L. Biczok, Noranda Exploration Company Limited, personal communication, 1988). High copper values, which commonly occur in iron rich samples, are accompanied by high Ag and U contents. Limited data indicate some enrichment in Co, Cr, La, Rb, V, Yb and Zn (Table 1).

MAR Cu-Fe DEPOSIT

This deposit is in a breccia-pipe very similar to that of the Sue-Dianne deposit, as reported by Prest (1977b) from surface geology and by Bryan (1979) from drill core of a vertical hole. The present study included a brief examination of this core, along with some of the core from the Sue-Dianne deposit, and it showed their striking similarities. The intensely brecciated, magnetite-rich Mar breccia zone is 115 m long, up to 55 m wide and extends to a vertical depth of more than 135 m. The country rock is mostly rhyodacite, commonly massive and porphyritic with quartz and feldspar phenocrysts, and it shows flow banding in places (Prest, 1977b). Intrusive dacitic porphyry is also present in the vicinity of the breccia zone. Some of the fragments in the breccia resemble the porphyry. The matrix of the breccia is massive, medium grained magnetite, which has chalcopyrite veinlets, fracture fillings and disseminations. Veinlets of chlorite, epidote and quartz are common in and around the breccia. Radioactivity is two to three times background over the breccia zone, but radioactive minerals are not reported (Prest, 1977b). The drill hole intersected some copper values comparable to those encountered at the Sue-Dianne deposit (Bryan, 1979).

OTHER MINERAL OCCURRENCES

A few other occurrences of magnetite as veins and localized enrichments in volcanic rocks, and as pebbles in volcaniclastic rocks (unit 2) are found in the study area. Traces of copper sulphides in stringers were encountered in a trenched showing northwest of Sue-Dianne deposit (Fig. 2). East of the deposit a few copper occurrences near the quartz monzonite contact have fractures showing malachite and azurite stains. The northern occurrences were reported by the Noranda Exploration Company Limited, and the southernmost one was discovered during the present mapping. Specularite veins are widely distributed throughout the area. They are up to 2 cm thick, contain varying amounts of quartz and a dark fine-grained mineral, probably chlorite. They occur in all the major units and are also associated with giant quartz veins.

ORIGIN OF MINERALIZATION

The breccia at the Sue-Dianne and Mar deposits are in an intermediate to felsic volcano-plutonic environment. Hence the breccia development, and deposition of magnetite and associated minerals as matrix, are regarded here as processes related to late magmatic activity in a subjacent reservoir. It is apparent that the host ignimbritic sequence was deformed prior to the brecciation. The deformation may be due, in part at least, to the caldera collapse. The dacite porphyry intrusion shows little indication of deformation, but it does have, in some places, chlorite-epidote alteration similar to that in the breccia zone. Its emplacement, which was probably immediately after the deformation, predated the breccia formation. Dacite porphyry in the Fab Lake area is cut by magnetite-apatite-actinolite veins (Gandhi, 1988).

It is postulated here that a volatile-rich, late magmatic fraction was generated at the time of, or soon after, the intrusion of quartz monzonite-granodiorite, which is part of the volcano-plutonic complex. These fluids caused the brecciation, which released the volatile pressure, and this stage was followed by the transport of magmatic fluids, from which magnetite and copper sulphides were deposited in open spaces created by the brecciation. It may be noted that in terms of abundances of iron and copper, and of the general geological setting, the Sue-Dianne deposit bears resembles to that of the porphyry copper deposits as discussed by Climie (1976). On the other hand, the scarcity of hydrous phyllosilicates and pyrite, indicates significant differences in the character of magmatic/hydrothermal fluids and physico-chemical conditions of deposition. Climie (ibid) noted the mineralogical differences, and hence the distinction from typical porphyry copper deposits. He also considered quartz and epidote veins at the deposit as an outer alteration halo, thus suggesting a zonation resembling that in porphyry copper deposits. During the present study, however, quartz veins up to 1 m thick, were encountered away from the deposit along a northeast trending fault (Fig. 2). Such giant quartz veins and stockworks, many of which contain minor amounts of epidote, chlorite and hematite or specularite, are common along other northeast-trending, right-lateral faults, and along related subsidiary fractures, that transect the Great Bear magmatic zone and post-date the younger granites of the magmatic zone. The quartz veins around the Sue-Dianne deposit are here interpreted as part of such a giant quartz vein zone along the northeast-trending fault, connected through a system of subsidiary faults and splays. This is supported by the fact that many of these veins cut across the alteration zone and magnetite-rich matrix of the breccia. Furthermore, the lack of a comparable large quartz vein zone around the Mar breccia and the Fab Lake occurrences, indicates that such abundant quartz veining is not a necessary part of the magnetite-copper sulphide mineralization. Some of the smaller quartz-epidote veins and silicification of the country rock are, however, considered here as related to the mineralization, particularly in view of the fact that silica may be released during strong alkali metasomatism and be deposited in veins nearby.

As seen in a few polished sections, specularite apparently is developed as a replacement of magnetite. This may represent a later lower temperature phenomenon. Further mineralogical studies, however, are required to understand the formation and significance of specularite in the deposit.

The pitchblende veins are clearly younger than the magnetite - copper sulphide mineralization. They are controlled by steep, easterly trending fractures and extend to a depth of only a few tens of metres. They have been

interpreted as supergene concentrations by Climie (1976). Observations during the present study, and the isotopic data presented by Miller (1982), support this hypothesis. Miller's data on six samples from two hand specimens containing pitchblende define a chord on concordia plot with lower and upper intercepts at 184 ± 10 Ma and 1201 ± 62 Ma, which according to the model favoured by Miller (ibid) results from the presence of common and radiogenic lead components that may have come from a 1201 + 62 Ma old uranium source or an uninterpretable mixed contaminant.

The isotopic age is significantly younger than the Aphebian volcano- plutonic complex and the breccia-hosted mineralization related to the complex. The presence of magnetite, bornite and chalcocite provide a reducing environment in which the circulating oxidized ground waters carrying dissolved uranium could precipitate the metal. Concomittent oxidation of magnetite to maghemite, and to hematite or specularite, would thus represent a complimentary reaction. In addition to the supergene uranium concentration, a primary uranium enrichment in the deposit is indicated by the drill core samples containing up to 150 ppm U over aggregate lengths of several metres. The high grade pitchblende veins may represent a reconcentration of this uranium, rather than of uranium from external sources.

REGIONAL METALLOGENIC IMPLICATIONS

The Sue-Dianne and Mar deposits are considered here as belonging to a group of magnetite-rich veins, pods and breccia-fillings that are widely distributed in, and genetically related to, the Great Bear magmatic zone and its extension in the east arm of Great Slave Lake. They contain varying amounts of actinolite, apatite, chalcopyrite, pyrite and pitchblende, and rarely cobalt-nickel arsenides and fluorite. Hematite, calcite, quartz, chlorite and epidote may occur with the above minerals or as veins in and around the occurrences. The magnetite concentrations in the Great Bear Lake and Great Slave Lake regions are commonly rich in actinolite and apatite (Badham, 1978; Badham and Morton, 1978; Gandhi and Prasad, 1982; Hildebrand, 1986). Those in the central and southern Great Bear magmatic zone are relatively poor in these two minerals, but contain significant amounts of chalcopyrite and host pitchblende veins; for example, the Fab occurrences (Gandhi, 1988), the Sue-Dianne and Mar deposits and the recently discovered Damp U-Cu-Fe deposit near south of Great Bear Lake (Fig. 1, inset). The Sue-Dianne deposit is at present the largest known among the group in terms of tonnage. The Damp deposit has a surface area comparable to that of the Sue-Dianne deposit, but drilling on it to date is to a relatively shallower depth (Climie, J.A., Central Electricity Generating Board of Canada, personal communication, 1988). The variations in mineralogy and morphology of the deposits may be a function of depth of formation, regional metallogenic zoning and local geological conditions.

The occurrences in this group are similar to the much larger magnetite-apatite-actinolite deposits of the Kiruna area in northern Sweden (Parak, 1975; Hildebrand, 1986), and to the Pilot Knob magnetite deposit in the St. Francois Mountains in Missouri, U.S.A. (Wracher, 1976; Panno and Hood, 1983), in terms of their mineralogy, and general geological setting. The Kiruna and Pilot Knob deposits are stratabound, and occur in intermediate to felsic volcanic sequences near coeval felsic intrusions of Early and Middle Proterozoic age respectively. A wider spectrum of magnetite deposits in Yangtze valley in China has been grouped as the 'porphyrite' iron deposits by the Research Group of Porphyrite Iron Ore (1977). They include a variety of veins, pods, breccia-fillings, stratiform and replacement deposits, and encompass a considerable mineralogical variation. They are regarded as genetically related to Mesozoic continental volcanism and associated plutonic activity. The volcanic rocks are dominantly porphyritic andesite, but include mafic and felsic varieties.

CONCLUSIONS

The Sue-Dianne and Mar deposits are in hydrothermal breccia zones, which are related to late stage magmatic activity of the felsic calc-alkaline volcanoplutonic complex in which they occur. Magnetite and copper sulphides were deposited in the zones by hydrothermal solutions. The deposits represent a variety of the magnetite-apatite-actinolite concentrations that occur as veins, pods and breccia-fillings which are widely distributed in the Great Bear magmatic zone.

ACKNOWLEDGMENTS

Noranda Exploration Company Limited kindly provided unpublished exploration data to the author and permission to incorporate them in this paper. Discussions with R.T. Bell of the Geological Survey of Canada, in the field and during preparation of manuscript were very helpful. The regional metallogenic perspective benefited from the writer's visit to the Kiruna deposits in 1988, and thanks are due to Karl-Enar Hansson of LKAB Prospektering AB for his guidance during the visit. The opinions expressed here, however, are the responsibility of the author.

Archie Arrowmaker of Rae Lakes settlement provided able assistance to the author during two and a half weeks of fieldwork carried out in 1988. The work was supported financially by the Northwest Territories Mineral Development Agreement under sub-project C.1.2.5 of project 711-7771. This paper benefitted from the critical reviews by R.T. Bell and S.M. Roscoe of the Geological Survey of Canada.

REFERENCES

Badham, J.P.N.
1978: Magnetite-apatite-amphibole uranium and silver-arsenide mineralizations in the lower Proterozoic igenous rocks, east arm, Great Slave Lake, Canada; Economic Geology, v. 73, p. 1474-1491.

Badham, J.P.N. and Morton, R.D.
1976: Magnetite-apatite intrusions and calc-alkali magmatism, Camsell River, N.W.T.; Canadian Journal of Earth Sciences, v. 13, p. 348-354.

Bryan, D.
1978: Geological and magnetometer surveys performed on the Noranda owned Maz-6 claim group, Mazenod Lake area, District of Mackenzie (85-N-10, 15); Department of Indian and Northern Affairs Document 081127, 4 p.
1979: Geological Report on a diamond drilling program performed on the Noranda owned Mar-1 claim group, Mazenod Lake area, District of Mackenzie (85-N-15); Department of Indian and Northern Affairs Document 081030, 2 p.
1980: Report on geological and magnetometer surveys performed on the Noranda owned Maz-5 and Dan 1-6 claim groups, Mazenod Lake area, District of Mackenzie (85-N-10, 11); Department of Indian and Northern Affairs Document 081128, 8p.

Charbonneau, B.W.
1988: Gamma spectrometric and magnetic anomalies associated with Cu-U mineralization, Faber Lake volcanic belt, District of Mackenzie, N.W.T.; in Current Research, Part C, Geological Survey of Canada, Paper 88-1C, p. 255-258.

Climie, J.A.
1975: Geological reconnaissance and airborne radiometric survey of the Dianne/Sue groups, District of Mackenzie (85-N-10, 15); Noranda Exploration Company Limited; Department of Indian and Northern Affairs Document 088230, 7 p.
1976: Geological, geophysical and drill investigations of the Dianne/Sue Groups, District of Mackenzie (85-N-10, 15); Noranda Exploration Company Limited; Department of Indian and Northern Affairs Document 080524, 9 p.

Fraser, J.A.
1967: Geological map, Hardisty Lake (West Half); District of Mackenzie, Northwest Territories; Geological Survey of Canada, Map 1224A, scale 1 inch to 4 miles.

Gandhi, S.S.
1988: Volcano-plutonic setting of U-Cu bearing magnetic veins of FAB claims, southern Great Bear magmatic zone, Northwest Territories; in Current Research, Part C, Geological Survey of Canada, Paper 88- 1C, p. 177-187.

Gandhi, S.S. and Prasad, N.
1982: Comparative petrochemistry of two cogenetic monzonitic laccoliths and genesis of associated uraniferous actinolite-apatite-magnetite veins, east arm of Great Slave Lake, District of Mackenzie; in Uranium in Granites, ed. Y.T. Maurice; Geological Survey of Canada, Paper 81-23, p. 81-90.

Geological Survey of Canada
1963: Aeromagnetic Map 2939G, Rae Lake, District of Mackenzie, Northwest Territories.
1969a: Aeromagnetic Map 7203G, Hardisty Lake, NTS 86C, District of Mackenzie, Northwest Territories.
1969b: Aeromagnetic Map 7197G, Marian River, NTS 85N, District of Mackenzie, Northwest Territories.

Hildebrand, R.S.
1986: Kiruna-type Deposits: Their Origin and Relationship to Intermediate Subvolcanic Plutons in the Great Bear Magmatic Zone, Northwest Canada; Economic Geology, v. 81, no. 3, p. 640-659.

Hoffman, P.F.
1980: Wopmay Orogen: a Wilson cycle of Early Proterozoic age in the northwest of the Canadian Shield; in Continental Crust and its Mineral Deposits, ed. D.W. Strangway; Geological Association of Canada, Special Paper 20, p. 523-549.

Kidd, D.F.
1936: Rae to Great Bear Lake, Mackenzie District, N.W.T.; Geological Survey of Canada, Memoir 187, 44 p.

Lang, A.H., Griffith, J.W., and Steacy, H.R.
1962: Canadian Deposits of Uranium and Thorium; Geological Survey of Canada, Economic Geology Report 16, 324 p.

Lord, C.S.
1942: Geological Map, Snare River, District of Mackenzie, Northwest Territories; Geological Survey of Canada Map 690, scale 1:253 440.

McGlynn, J.C.
1968: Tumi Lake, District of Mackenzie, Geological Survey of Canada Map 1230A, scale 1:63 360.
1979: Geology of the Precambrian rocks of the Riviere Grandin and in part of the Marian River map areas, District of Mackenzie; in Current Research, Part A, Geological Survey of Canada, Paper 79-1A, p. 127- 131.

Miller, R.G.
1981: Kawazulite Bi_2Te_2Se, related bismuth minerals and selenian covellite from the Northwest Territories; Canadian Mineralogist, v. 19, p. 341- 348.
1982: The geochronology of uranium deposits in the Great Bear batholith, Northwest Territories; Canadian Journal of Earth Sciences, v. 19, no. 7, p.1428-1448.

Panno, S.V. and Hood, W.C.
1983: Volcanic stratigraphy of the Pilot Knob iron deposits, Iron Country, Missouri, Economic Geology, v. 78, no. 5, p. 972-982.

Parak, T.
1975: The origin of Kiruna iron ores; Sveriges Geologiska Undersokning, Series CNR 709, v. 69, no. 1, 209 p.

Prest, S.E.
1977a: Geological and geophysical investigations of the Dianne extension (12-19, 21-49), Mag (1-25), and Sue (8) claims, District of Mackenzie, N.W.T. (85-N-10, 15); Noranda Exploration Company Limited; Department of Indian and Northern Affairs Document 080635; 11 p.
1977b: Geological and geophysical investigations of the Mar claim group, District of Mackenzie, N.W.T. (85 N 15); Noranda Exploration Company Limited; Department of Indian and Northern Affairs Document 080646, 10 p.

Research Group of Porphyrite Iron Ore of the Middle-Lower Yangtze Valley
1977: Porphyrite iron ore - A genetic model of a group of iron ore deposits in andesitic volcanic area; Acta Geological Sinica, v. 51, no. 1, p. 1- 18.

Wilson, J.T., and Lord, C.S.
1942: Geological Map, Ingray Lake, District of Mackenzie, Northwest Territories; Geological Survey of Canada, map 697A, scale 1: 253 440.

Wracher, D.A.
1976: Geology of the Pilot Knob magnetite deposit, southeast Missouri; in Studies in Precambrian Geology of Missouri, ed. Eva B. Kisvarsanyi; Missouri Department of Natural Resources, Report of Investigations No. 61, p. 155-163.

Preliminary study of the stratigraphic and structural controls of the Lyon Lake massive sulphide deposit, Wabigoon Subprovince, northwestern Ontario[1]

B. Dubé[2] and E.R. Koopman[3], J.M. Franklin[3], K.H. Poulsen[3], and M.R. Patterson[4]

Dubé, B., Koopman, E.R., Franklin, J.M., Poulsen, K.H. and Patterson, M.R., Preliminary study of the stratigraphic and structural controls of the Lyon Lake massive sulphide deposit, Wabigoon Subprovince, northwestern Ontario; in Current Research, Part C, Geological Survey of Canada, Paper 89-1C, p. 275-284, 1989.

Abstract

The Lyon Lake stratiform massive sulphide deposit, in the Sturgeon Lake area is hosted by a quartz crystal-rich rhyolite. The basal mafic member of the overlying volcanic cycle forms the hanging wall to the ore. The footwall to the ore consists of an upper interbedded ash and lapilli fragmental tuff, of rhyolitic composition. Underlying the rhyolite is a sequence of sedimentary rocks containing an extensive Banded Iron Formation(BIF), indicative that a low temperature hydrothermal event occurred prior to sulphide deposition. All strata, dykes and ore are folded. The dominant structure controlling the ore distribution is a major flexure characterized by a hinge line shallowly plunging to the east-southeast. Striations measured on bedding, foliation, and fault planes are subparallel to the hinge line and result from stretching along the fold axis. The hanging wall-footwall contact is characterized by a high strain zone which is possibly related to the folding event.

Résumé

Le gisement stratiforme de sulfures massifs de Lyon Lake localisé dans la région du lac Sturgeon, est contenu dans une rhyolite riche en cristaux de quartz. Le membre mafique basal du cycle volcanique sus-jacent forme le toit de la zone minéralisée. Le mur du minerai est constitué d'une couche supérieure composée de cendres et de conglomérat volcanique à lapilli interstratifié de nature rhyolitique. Au-dessous de la rhyolite se trouve une séquence de roches sédimentaires contenant une formation ferrifère rubanée de grande étendue, preuve de la manifestation d'un épisode hydrothermal de basse température avant la mise en place des sulfures. Toutes les couches, tous les dykes et tout le minerai sont plissés. La structure qui a principalement déterminé la répartition du minerai est une grande flexure caractérisée par une charnière à faible plongement en direction est sud-est. Les stries mesurées sur les plans de litage, de schistosité et de faille sont subparallèles à la charnière, et résultent d'un étirement s'étant manifesté selon l'axe des plis. Le contact entre le toit et le mur est caractérisé par la présence d'une zone fortement déformée, peut-être associée à l'épisode de plissement.

[1] Contribution to the Canada-Ontario Mineral Development Agreement 1985-1990. Project carried by the Geological Survey of Canada, Mineral Resources Division.

[2] Sciences de la terre, Université du Québec à Chicoutimi, Chicoutimi, Québec, G7H 2B1.

[3] Geological Survey of Canada, 601 Booth St., Ottawa, Ontario, K1A 0E8

[4] Noranda Mines, Lyon Lake Division, Ignace, Ontario, P0T 1T0.

INTRODUCTION

The Lyon Lake mine in the Sturgeon Lake mining camp, is a typical volcanogenic massive sulphide deposit (Franklin et al., 1981). It occurs within the Wabigoon volcano-sedimentary Subprovince of the Archean Superior Province of the Canadian Shield (Goodwin et al., 1972). The Lyon Lake mine has produced more than 2 600 000 tons of ore at a grade of 8.54 % Zn, 1.28 % Cu, 4.47 % Ag, and 0.95 % Pb, since it began operation in 1980. The area has been previously studied on a regional scale by Franklin et al., (1977) and by Trowell (1974, 1983) and on a local scale by Hinzer (1977), Harvey and Hinzer (1981), Roberts (1981), Friske (1983), and Mumin (1988). Geologists from University of Minnesota-Duluth are at present undertaking a regional stratigraphic and volcanologic study for the Geological Survey of Canada as part of the Sturgeon Lake Project under the Canada-Ontario Mineral Development Agreement. Structural complexities within the ore zones became more evident as mining progressed, necessitating detailed structural mapping as an aid to projecting the stratigraphic control of the orebodies to greater depth within the mine area. Two months of underground mapping, together with core logging, provided an opportunity to establish a broad structural framework for the deposit. The main purpose of this paper is to describe the stratigraphy and the style of deformation in and around the Lyon Lake deposit and to demonstrate the importance of local structural features as controls for the localization of the orebody.

REGIONAL GEOLOGY

The South Sturgeon Lake volcanic group is a part of the Wabigoon Subprovince, a 2.7 - 2.9 Ga metavolcanic and metasedimentary sequence (Franklin et al., 1975).

The strata strikes west-northwest, dip steeply (65°-75°) to the north, face north and occupy the south limb of a syncline centered through Sturgeon Lake (Trowell, 1983; Groves et al., 1988). The volcanic pile exceeds a total apparent thickness of 9 000 metres (Franklin, 1977; Trowell, 1974, 1983) and is in contact with granitic rocks to the south. Volcanic rocks are divided into three major mafic to felsic cycles (Fig. 1); local sedimentary rocks are more abundant near the top of each cycle (Franklin et al., 1977). In the western part of the South Sturgeon Lake area, the lowermost cycle contains the subvolcanic Beidelman Bay trondhjemite body near its base (Poulsen and Franklin, 1981).

Six Cu-Zn volcanogenic massive sulphide deposits occur in the middle and upper felsic units of the lowermost cycle. The Mattabi and F-Zone sulphide bodies are near the middle and the Lyon Lake, Creek Zone, Sub Creek Zone, and Sturgeon Lake Mine orebodies are at the top of this cycle (Trowell, 1983, Fig. 1).

Regionally, the rocks contain middle to upper greenschist assemblages, with lower almandine - amphibolite assemblage towards both the eastern and southern extents of the South Sturgeon Lake area (Trowell, 1974,1983; Groves, 1984).

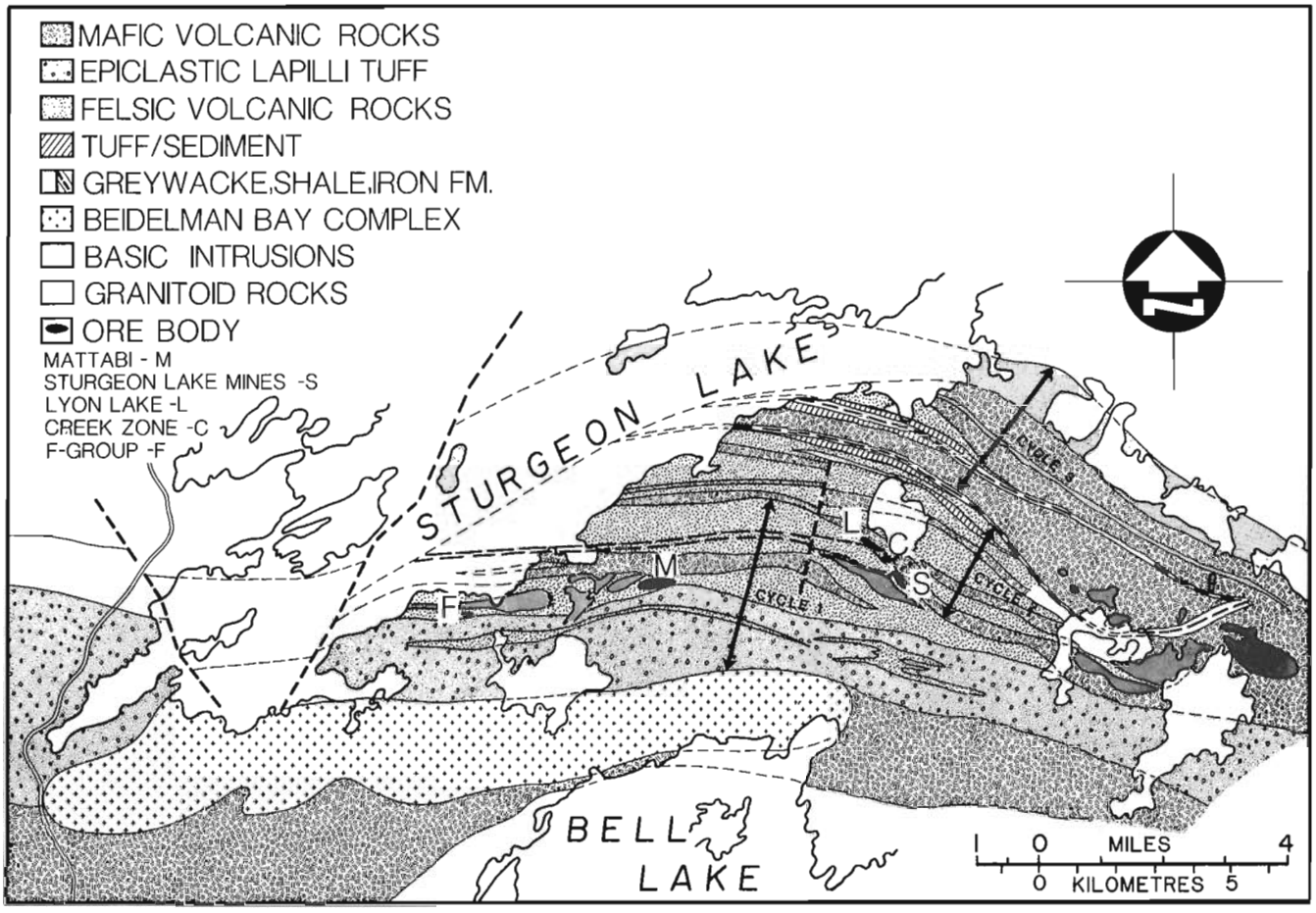

Figure 1. Geological map of the southern Sturgeon Lake area with the locations of the massive sulphide deposits. (Modified from Franklin et al., 1977).

LITHOLOGY AND STRATIGRAPHY OF THE LYON LAKE MINE

The Lyon Lake deposit occurs at the top of Cycle 1 (Franklin, 1977), the lowermost cycle (Fig. 1). The basal mafic unit of the overlying cycle forms the hanging wall to the ore zone. The lithologic units described below represent a compilation of detailed underground mapping and diamond drill hole data of the upper 100 m of cycle 1 and lower 100 m of cycle 2 (Fig. 2). A 700 m thick unit of massive to amygdaloidal pillowed andesitic flows, overlain by 1200 m of feldspar-phyric dacitic flows immediately underlie the host rocks to the ore deposits. Rock names are based on megascopic observations and are intended as general field terms.

Sedimentary strata

A sequence of sedimentary rocks including quartz-rich pelite, graphitic shale, greywacke, massive pyrrhotite - pyrite lenses and banded iron formation (BIF) occur at an average of 30 m below the ore lens (Fig. 2). Depending on thickness and degree of folding of the BIF component, this sedimentary unit ranges in apparent thickness from 20 to 60 m. It may possibly be thicker since the lower contact was rarely intersected in drill core or underground workings. Further mapping is required to determine its true extent, and thus its usefulness as an effective marker horizon.

The sedimentary rocks consist of medium-grained felsic quartzose pelite with up to 10 % feldspathic pelite interbedded with greywacke, graphitic shale, and graphitic pelite.

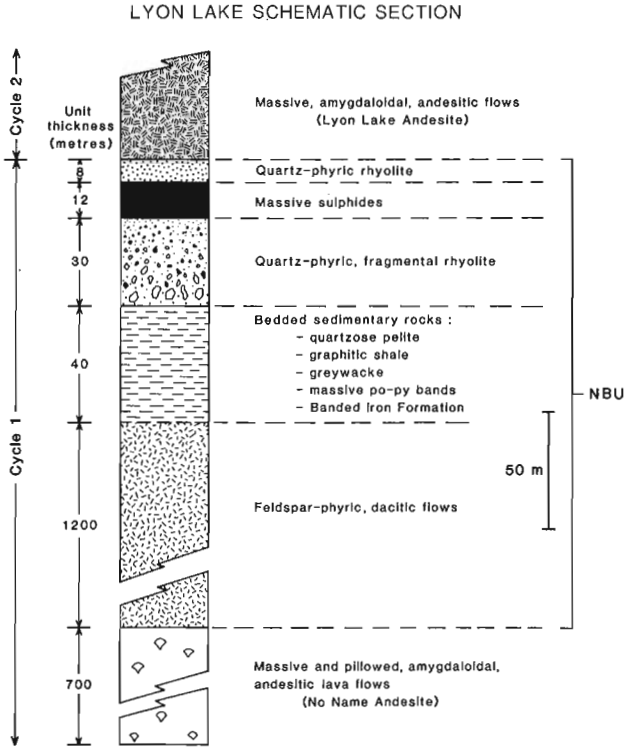

Figure 2. Idealized stratigraphic column of the Lyon Lake mine area. The portions of the lower NBU Rhyolite and No Name Lake Andesite are modified from Hinzer (1977) and Mumin (1988).

The sequence commonly fines upwards from greywacke at the base to graphitic shale at the top, and it is capped by an Fe-oxide or Fe-carbonate banded iron formation. Sedimentary strata associated with the iron formation have an average thickness of 15 to 45 cm, and consist of ovoid blebs of pyrite and chlorite (up to 15 %), typically 1 to 5 mm in width, oriented parallel to bedding. Several quartz - feldspar rich beds are banded; pink bands, 10 to 25 mm thick alternate with whitish-grey bands of the same thickness.

Banded Iron Formation

The lateral extent of the BIF encompasses the area of the mine workings and was intersected in drill core approximately 2 km along strike on either side of the mine. It is more laterally extensive than described by previous workers.

At the 600-foot (200 m) level (upper part of the mine), non-magnetic iron-carbonate and cherty beds, each 2.5 to 10 cm thick, are interlayered with 5 to 15 cm thick chloritic beds. The cherty beds contain 1 to 2 cm thick stringers and veinlets of pyrrhotite and pyrite; pyrrhotite is slightly magnetic. Schistosity is developed in the chloritic beds parallel to bedding. Locally, deformation has caused boudinage and fracturing of iron-carbonate and cherty beds. The cherty beds commonly contain millimetre-thick laminations of iron-carbonate and chert. At this depth in the mine, the BIF is intercalated with greywacke and felsic volcanic flows.

At the 1000-foot (335 m) level, the iron formation is distinctly different, and composed of strongly magnetic Fe-oxide, associated with quartz-phyric volcanic flows, stratigraphically above and below. Magnetite occurs as fine laminations in cherty beds, or as individual beds 2.5 cm thick, interlayered with 2.5 to 15 cm thick chloritic beds and 7 to 24 cm thick cherty and iron-carbonate beds.

At the 1580-foot (525 m) level ramp, the BIF is composed of 1 to 2 cm thick magnetite beds interbedded with 1 to 2 cm thick grey and black chert and iron-carbonate beds. The grey chert and iron-carbonate beds commonly contain fine laminations of magnetite and iron-carbonate. Cherty beds up to 30 cm thick contain thin beds and laminations of magnetite, 3 to 10 mm thick. Between these cherty beds, 2.5 to 15 cm thick argillite and chlorite beds occur. Commonly, cherty beds are fractured perpendicular to bedding. On this level, BIF is interbedded with graphite and quartzose pelite and beds of massive pyrrhotite and pyrite. Bedding in the sediments is defined by chlorite beds, graphitic shale and massive pyrrhotite - pyrite beds. Also, some beds contain massive chlorite; disseminated and vein-type pyrrhotite appear to have replaced ovoid ooliths and flakes oriented parallel to bedding.

At the 1800-foot (600 m) level iron-carbonate BIF, similar to that observed at the 600-foot (200 m) level (upper mine), is associated with graphitic pelite.

Thin bands and laminations of chert and magnetite, associated with volcanic rocks and greywacke, indicate that this BIF is a typical Algoman Type iron formation (Gross, 1965).

The variable composition, thickness of beds, and variable relationships of iron formation to sedimentary and volcanic strata may be the result of lateral facies changes, recurring beds of iron formation, or structural repetition.

Rhyolite

The quartz-phyric rhyolite unit overlying the sedimentary sequence forms the immediate host and footwall rocks to the massive sulphide body, and is composed of 1 to 15 % of 1 to 3 mm blue, and less commonly grey, quartz eyes (Fig. 2). This fine-grained, light-grey unit is up to 30 m thick and consists predominantly of a felsic lithic fragmental rock with interbedded felsic ash towards the top. A unit of coarse volcanic breccia occurs at the base. Up to 15 % blue quartz and rare feldspar phenocrysts are concentrated in the upper 10 to 16 m of the unit. This upper quartz-crystal rich member hosts the massive sulphide deposits.

The felsic fragmental rock that is the dominant member of this unit is composed of cherty and felsic lithic clasts ranging from ash to block in size, and more commonly lapilli-sized fragments in an altered, quartz-phyric, chlorite-, carbonate-, and sericite-bearing matrix.

Andesite

The Lyon Lake Andesite (Trowell, 1983) forms the hanging wall to the massive sulphide horizon (Fig. 2), and varies from massive to strongly schistose at its base. A zone of high strain is common, although not ubiquitous, at the contact with the underlying felsic rocks. The andesite consists of interlayered massive to amygdaloidal sheet-flows and fragmental rocks. Some units contain abundant feldspar phenocrysts. Rounded to elongate amygdules (5 %) ranging in size from 2 to 20 mm (locally up to 30 mm) are filled predominantly with quartz, and commonly rimmed with carbonate. Also, abundant 1 to 10 mm thick, irregularly distributed quartz and iron-carbonate stringers and fractures in massive units and parallel to the foliation characterize the unit. Pillows were not observed, however, very fine grained, 1 cm thick chlorite layers, which may represent sheet-flow contacts, occur in undeformed areas.

Intrusive rocks

Three types of dykes observed are medium-grained lamprophyric, medium-grained feldspathic intermediate, and fine grained mafic types. Their attitudes relative to the strata are variable, from subparallel to a high angle. Lamprophyric dykes are the most abundant, and locally occupy the contacts between volcanic and sedimentary strata. They consist of 20 to 30 %, linearly oriented mafic (amphibole?) phenocrysts (2 to 5 mm), altered to chlorite, in a leucocratic medium-grained matrix.

Sulphide lenses

The Lyon Lake volcanogenic massive sulphide deposit consists of at least three ore zones, the Lyon Lake Zone, Creek Zone, and Sub Creek Zone (Fig. 3). Total tonnage mined as of May 1988 was 2 600 000 tons with an average grade

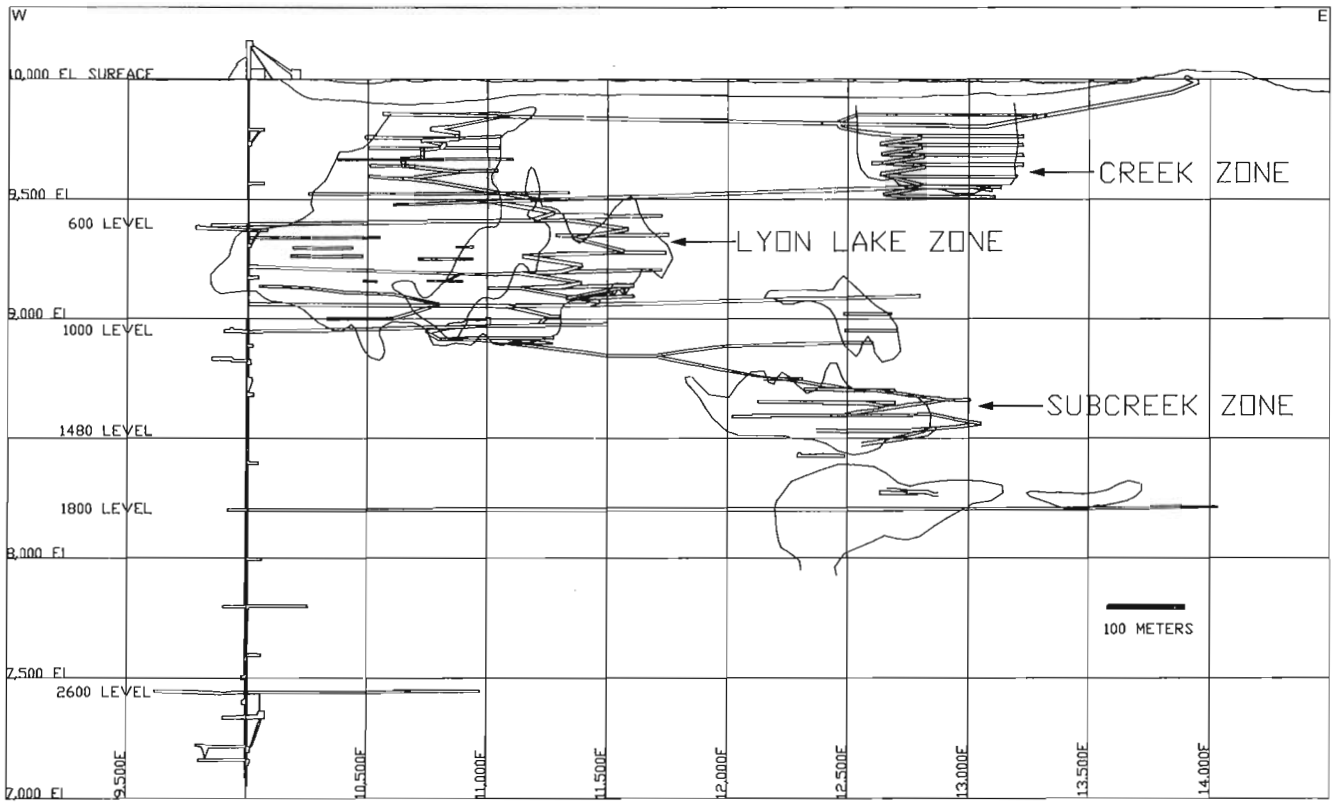

Figure 3. Longitudinal section looking north showing the location of the three ore zones, including the Lyon Lake mine. (After Noranda Mines, Lyon Lake Division).

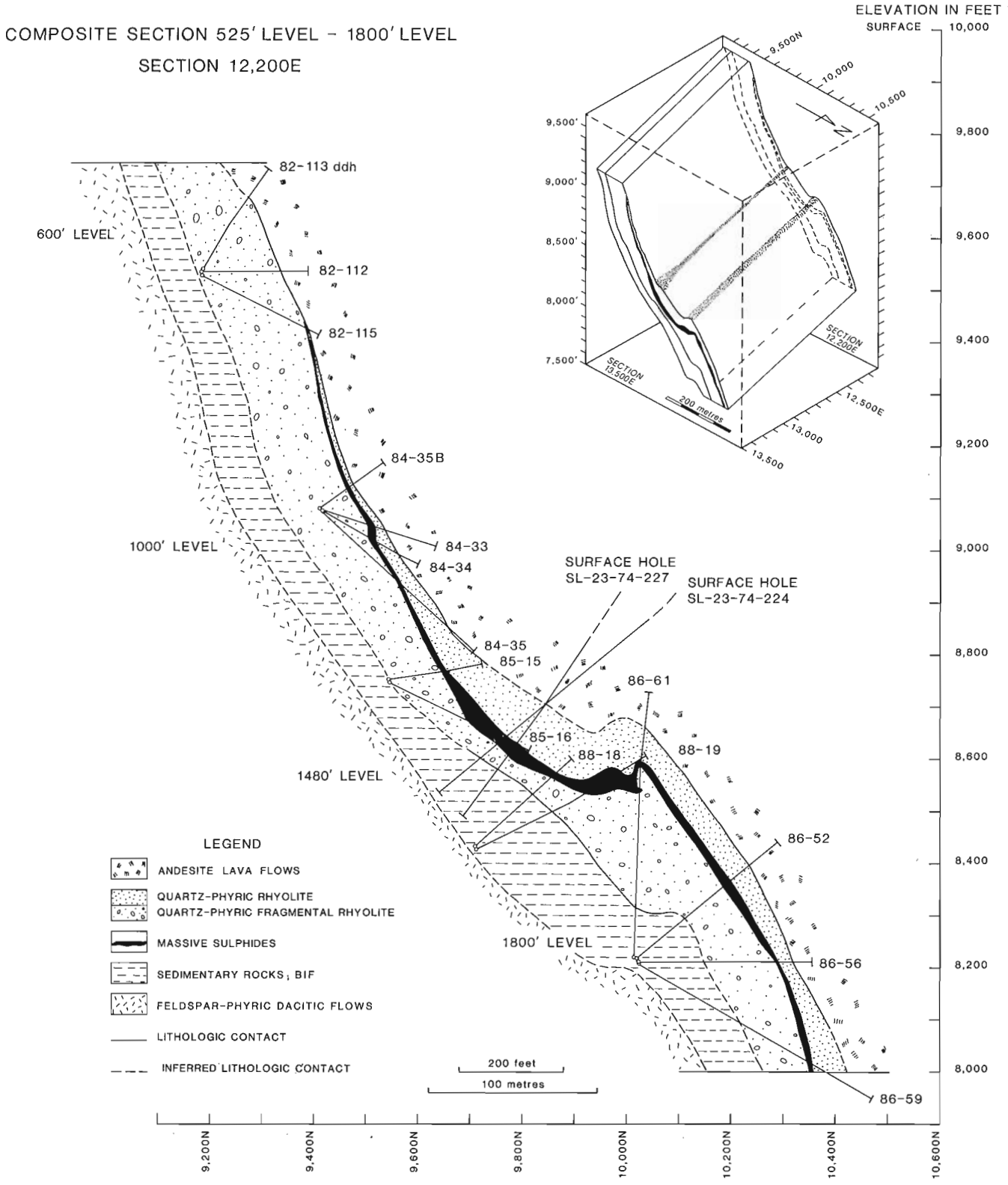

Figure 4. Composite cross section (12,200E) of the Sub Creek Zone. Inset: isometric projection of the deposit showing the plunge of the major flexure. North arrow indicates Mine North which is 40° east of true north. (Note: Section 13,500E is a projection of Section 12,200E).

of 8.54 % Zn, 1.28 % Cu, 4.47 % Ag, and 0.95 % Pb. All three zones occur in the same horizon, the blue quartz-phyric rhyolite at the top of cycle 1 (Franklin et al., 1977). Locally, the Lyon Lake Andesite is in contact with the ore.

The sulphides form several stacked or en echelon concordant, massive sulphide lenses (Harvey and Hinzer, 1981). The sulphide lenses comprise discontinuous and contorted bands of coarse grained sphalerite and pyrite, varying from fine laminations to massive bands up to 3 m thick. Pyrrhotite and chalcopyrite are present locally as thin beds or stringers. Locally, gross zonation of sulphides occurs where bands of sphalerite are predominant at the margins and pyrite bands are most abundant in the core of the lens. Banding is generally subparallel to bedding.

STRUCTURE

Folding

In the mine area, the rocks generally face and dip north (65°-75°), but detailed mapping in the mine (1:240 or 1 inch=20 feet) indicated that all of the stratigraphic units, dykes and massive sulphide lenses are folded. The dominant structural feature affecting the ore distribution is a major flexure (Fig. 4), located between the 1000-level and the 1480-level, with a hinge line plunging shallowly east-southeast. Smaller folds with wavelengths of up to 10 m are abundant on all levels and these have a southward vergence (Bell, 1981) on north dipping limbs and a northward vergence on south dipping limbs of the larger fold. Figure 5A illustrates the distribution of poles to bedding and the hinge lines measured on small folds in individual lithologic units. This pole distribution defines a near-cylindrical fold characterized by a calculated hinge line trending 102° and plunging 35° east. This orientation is very close to the average measured hinge lines trending 094° and plunging 38° east. The axial surface related to this folding is oriented at 295°/72° (Fig. 5A). In the iron formation and sedimentary strata, the mechanism of folding is flexural and the folds belong to classes 1b and 1c (Ramsay, 1967). This type of folding may reflect the influence of layering and the high ductility contrast between the layers, particularly in the iron formation where chert and/or carbonate layers alternate with chlorite- and/or magnetite-rich layers.

The major flexure of the ore is particularly obvious on the 1480-level. In contrast to the upper and lower levels, the "flat ore" and the other lithologic units within the flexure are thicker and subhorizontal and/or shallowly south or north dipping. Here, the ore is in the nose of the main flexure. Figure 5B illustrates the pole distribution of the ore contact with the surrounding rocks. This pole distribution defines a great circle oriented at 210°/74° and with a calculated hinge oriented at 120°/16°. The plunge of this hinge line is shallower than that of the mesoscopic folding (35°-40°) as defined in Figure 5A. The plunge difference between the flexure and the mesoscopic folds may reflect a primary orientation of the ore lenses, or the more irregular orientation and thickness of the ore lenses in contrast to the volcanic and sedimentary strata, or a non-coaxial deformation history. The recognition of the "flat ore" zones resulting from folding is important in determining an appropriate mining method, and the plunge of folds is critical to provide direction in locating the extension of "flat ore" at depth.

A fracture cleavage axial planar to the large and small folds was observed in the felsic rocks whereas a schistosity is present in the chloritic, sericitic and more ductile rocks. These foliations strike parallel to, but dip more steeply than the envelope of bedding (Fig. 5C). This angular relationship confirms that the area is on the south limb of a major syncline. En echelon subhorizontal quartz veins are common throughout the mine. The average orientation of the veins is 200°/20°, which is statistically subperpendicular to the axial plane cleavage (Fig. 5C). Therefore, the veins are probably related to the folding and indicate a direction of stretching in the mine sequence. Striations on bedding and schistosity-cleavage planes have been observed locally. The striations generally have a shallow plunge to the east (Fig. 5E and 5F) and are approximately subparallel to the measured fold hinge. The striations may have resulted from oblique stretching of the fold.

Underground mapping indicates that all types of dykes have been folded. Like the bedding planes, the dykes show southward vergence of folds in north-dipping dykes and northward vergence of folds in south-dipping dykes. Figure 6A illustrates pole distribution of dykes and shows that they are statistically parallel to schistosity and cleavage (Fig. 5C). Locally, nonfolded dykes cut highly deformed iron formation and have a slip surface at the contact with the folded rocks. Compositionally similar dykes may be strongly folded in other areas. The folds responsible for the deformation of those dykes are probably disharmonic (De Sitter, 1956). The contrast in rheological properties between the iron formation and the dykes possibly affected the wavelength and/or the amplitude of the folds resulting in different folding patterns. The original orientation of these dykes is also a major constraint; any dyke having a primary orientation parallel to the axial surface will not be folded, but will have a discontinuity at its contact, whereas dykes contained within the fold axis and perpendicular to the axial surface will show maximum folding. Consequently, the various primary orientations of the dykes and the disharmonic type of folding could explain the apparent local nonfolded character of some dykes.

In the iron formation, local evidence of earlier folds has been observed. Early isoclinal and refolded folds are superposed by the small folds of the main deformation. In the 1580 ramp, some folds have a subhorizontal axial plane and may belong to this earlier fold generation. The fold axes of earlier and main stage folds are probably coaxial, as shown by the distribution of poles of the beds in early folds (Fig. 6B). This pole distribution is compatible with the poles of the beds in the entire mine (Fig. 5A). Our data do not allow us to clearly establish the relationship between these two generations of folds. Because the iron formation is easily deformed, it is quite possible that some early folds may have been produced by the same folding event as that responsible for the overall fold pattern observed at the mine scale, or that the early folds have a primary "soft sedimentary origin".

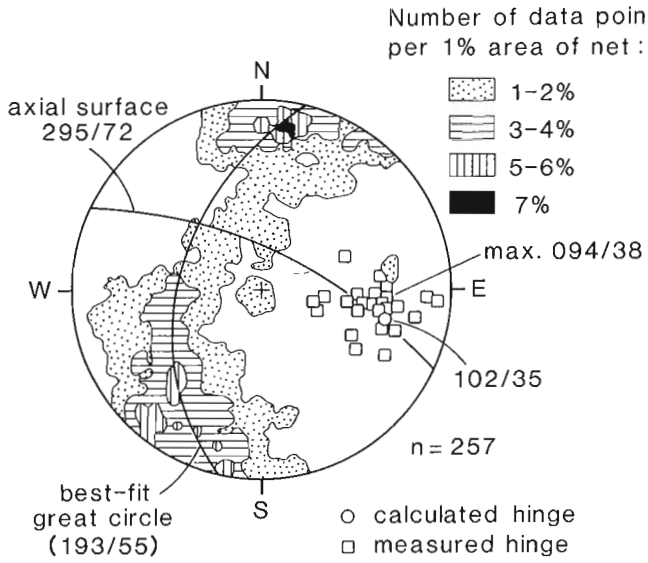

A. Contoured poles to bedding and hinge line.

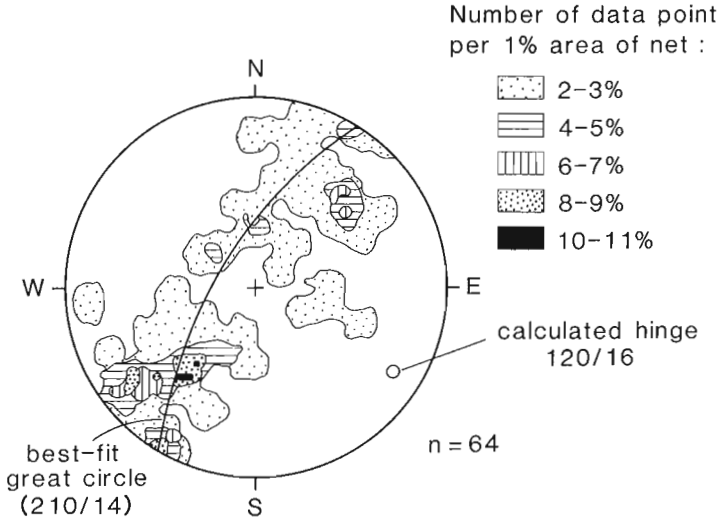

B. Contoured poles to ore contact with enclosing rocks.

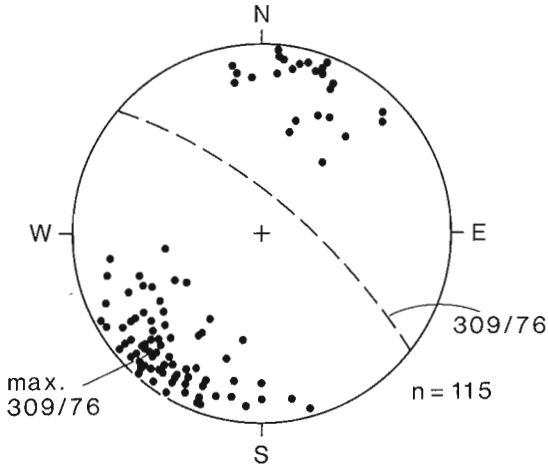

C. Poles to schistosity and cleavage.

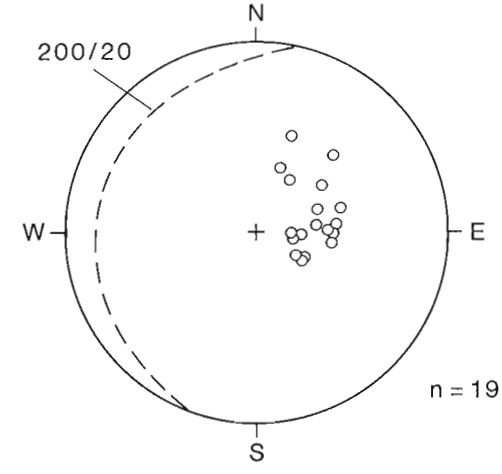

D. Poles to sub-horizontal quartz veins.

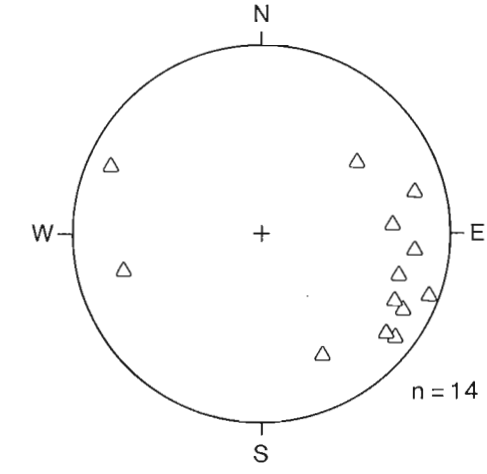

E. Striations on bedding plane.

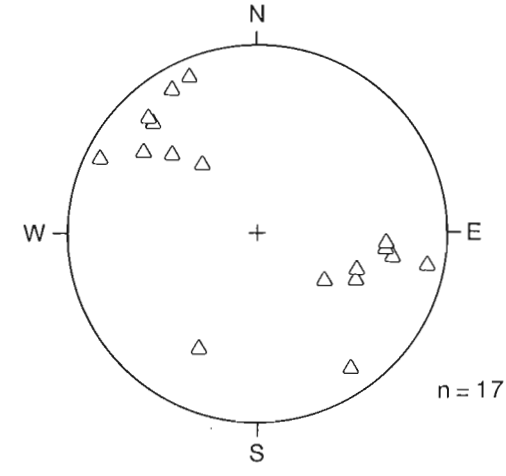

F. Striations on schistosity and cleavage.

Figure 5. Equal projections (lower hemisphere) of folds and their related structural elements: A- Contoured poles to bedding. Crosses represent measured hinge lines and the open circles represent the location of the hinge line according to the best fit great circle; B- Contoured poles of the ore contact with enclosing rocks. The open circle shows the location of the hinge line according to the best fit great circle; C- Poles to foliation. The average orientation of foliation is shown; D- Poles to subhorizontal quartz veins. Average orientation is shown; E- Striations on bedding planes; and, F- Striations on foliation planes.

FAULTS

Faults are typically brittle and characterized by a sharp planar discontinuity, commonly without any deformation in enclosing wall rocks. The faults dip steeply to the north (306°/78°) and strike subparallel to the overall strike of the strata (Fig. 7a). These late faults are not affected by folding and are discordant to the bedding. These fault planes are filled by quartz and carbonate where they intersect competent rock, such as dykes. Slickenlines on different faults plunge east and, according to the steps, the latest movement was mostly oblique and dextral (Fig. 7B). The oblique displacement seems very small, in the order of 1 to 5 m (based on offset of the BIF in the 1580 ramp). The faults may represent shear surfaces contemporaneous with folding and may be related to stretching parallel to the fold axis. The oblique movement may also be related to reactivation of earlier faults.

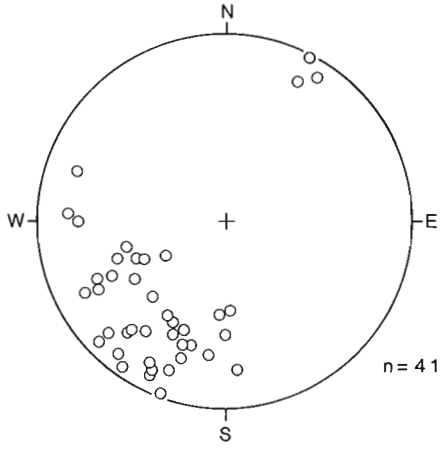

A. Poles to dyke.

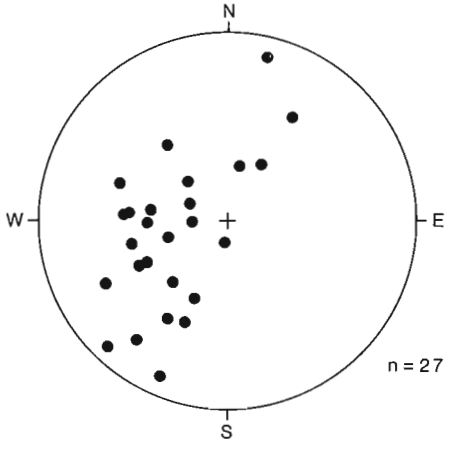

B. Poles to bedding associated with early folds.

Figure 6. Equal area projections (lower hemisphere) showing: A- Poles of dykes; and, B- Poles to bedding associated with early folds (1580 ramp).

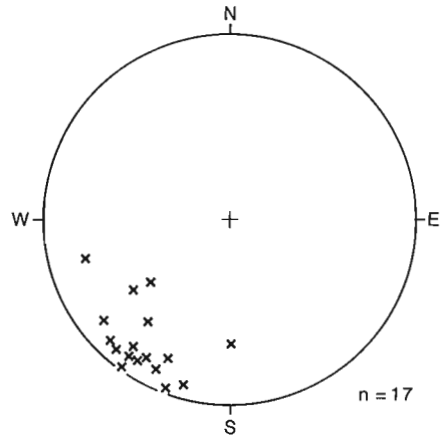

A. Poles to fault.

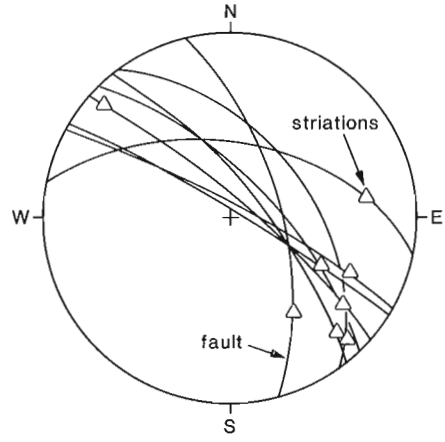

B. Striations measured on fault.

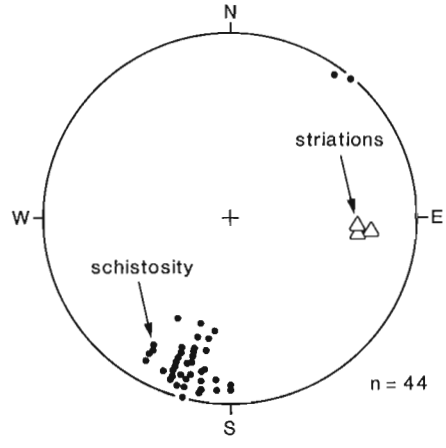

C. Poles to schistosity and striations related to sheared hanging wall

Figure 7. Equal area projections (lower hemisphere) showing: A- Poles of faults; B- Fault planes and related striations; and, C- Poles to schistosity and striations related to the hanging wall shear (600 level, station area).

Lenticular zones of quartz breccia, containing iron carbonate and sulphide, are located at or near the contact between the ore and its footwall or hanging wall. These quartz breccias are discontinuous and subparallel to the stratigraphy. The breccias probably originated in dilatant zones formed during folding. These dilatant zones may represent small discontinuities or fault zones. The fractures in quartz are filled with up to 40% sulphides consisting of pyrite, sphalerite, chalcopyrite, and galena. Slickenlines oriented 127°/15° have been observed on one of these quartz breccias, suggesting that the latest movement was slightly oblique, and compatible with movement on the brittle faults. These "quartz breccias faults" have not produced a significant displacement of the ore. They are probably related to folding and are particularly abundant in the 1480-level area, where the ore is located in the nose of a fold. On the 1260-level, in the hanging wall to the ore, this breccia is associated with a ductile shear zone that contains steeply dipping en echelon tension gashes.

NATURE OF THE HANGINGWALL-FOOTWALL CONTACT

The orientation of the contact between the Lyon Lake Andesite (hanging wall) and the quartz-eye rhyolite (footwall) varies from northwest in the Lyon Lake and Sturgeon Lake mines areas, to easterly, north of the Mattabi mine area (Fig. 1). This contact truncates several graphitic argillite units in the footwall, and is close to the ore horizon. Franklin et al. (1977, 1981) suggested that the deposits may have formed on a local intravolcanic unconformity surface.

Underground exposures reveal that the contact is generally a high strain zone. Detailed mapping on the 600- and 1000-levels and core logging, revealed that the andesite-rhyolite contact is characterized by a strong schistosity in the andesite and a well-defined schistosity or fracture cleavage in the rhyolite footwall. On the 600-level, the high strain zone is more than 100 m wide in the andesite hanging wall, and is 10 to 15 m wide in the rhyolite footwall. This high strain zone is marked by a well-defined schistosity oriented at 286°/75° (Fig. 7C). The dip of the schistosity is variable from subvertical furthest into the hanging wall, to 50° to 70° near the contact with the footwall. Mineral lineations or striations are not present on the schistosity planes in the andesite, but a few striations have been observed on cleavage planes in the rhyolite footwall, and at a dyke contact (Fig. 7C). These striations are subparallel to the hinge line of the mesoscopic folds (Fig. 5A). Subhorizontal quartz veins (15-20 cm thick and up to 5 to 10 m long) may indicate that this high strain zone is related to vertical extension. Locally, brittle faults and fracture planes are oriented subparallel to the schistosity but dip more steeply, and a horizontal intersection lineation between the fracture plane and the schistosity is present. Many quartz-carbonate veinlets were observed along the schistosity plane or filling brittle fault planes.

DISCUSSION

Prior to initiation of this project, the staff at Lyon Lake had recognized an eastward plunging linear orientation of orebodies in the mine as illustrated by Figure 3. The purpose of this study has been to assess the degree to which this is a result of the primary disposition of the ore as opposed to subsequent deformation. The Lyon Lake ore lenses occur at the top of a sequence of felsic pyroclastic flows and volcaniclastic sediments. The BIF is laterally extensive, and is a useful stratigraphic marker horizon. As the thickest portion of the iron formation and its associated sedimentary strata seems to correspond to the thickest ore section, it is possible that the hydrothermal vents for both the iron formation and the sulphides were coincident structures. Alternatively, both ore and iron formation could have been "thickened" by subsequent folding. The presence and thickness of Fe-oxide BIF beneath the ore reflects an extensive low temperature hydrothermal event sustained over a period of time prior to the hydrothermal event related to sulphide deposition.

The present study has also shown that axes of minor folds throughout the mine have a relatively consistent orientation subparallel to the long axes of orebodies and therefore folding offers a likely explanation for the linear nature of the ore lenses and for the occurrence of "flat zones". Other minor structures such as extensional veins, schistosity and striated planar surfaces are also consistent with tectonic shortening and extension of the orebodies and their enclosing rocks. En echelon distribution of ore lenses within the productive horizon, may reflect the deformation of several primary sites of ore deposition but could also be attributable to an en echelon folding pattern (Campbell, 1955). Further study is required to test the viability of the second hypothesis.

Faults, though common throughout the mine, appear to have limited control on ore distribution. No significant lithological or ore displacement related to faults was observed, but faulting is compatible with the observed style of folding.

The high strain zone located at the contact between the footwall and hanging wall was also observed to the east, in the Sturgeon Lake Mine area. According to Franklin et al. (1977), "thrustlike movement of the hanging wall basaltic andesite unit caused intense deformation and possible folding of the upper part of the orebody". The striations observed in the high strain zone are subparallel to the hinge of the folds and suggest that the high strain zone may have formed during folding. But, because the entire stratigraphic succession in the eastern part of the area (Fig. 1) is transected by the Lyon Lake Andesite (hanging wall), it is probable that this high strain zone corresponds to a major fault zone.

ACKNOWLEDGMENTS

The authors wish to thank C. Imrie Supervisor of Engineering/Geology of Noranda Mines, Lyon Lake Division and their geology staff for their generous assistance, helpful comments, and permission to publish. We wish to acknowledge the constructive advice and critical discussions provided by F. Robert and A.G. Plant of the Geological Survey of Canada, and F. Robert for critical review and comments on the manuscript. Thanks are also due to R. Morton, P. Jongewaard, and G. Hudak of the University of Minnesota-Duluth for stimulating discussions in the field. Kim Nguyen is thanked for drafting the diagrams.

This project was conducted as part of the Sturgeon Lake Sulphide Project of the Canada-Ontario Mineral Development Agreement (COMDA).

REFERENCES

Bell, A.M.
1981: Vergence: an evaluation; Journal of Structural Geology, v. 3, p. 197-202.

Campbell, J.D.
1955: En echelon folding; Economic Geology, v. 53, p. 448-472.

De Sitter, L.U.
1956: Structural geology; McGraw-Hill, London, 552 p.

Franklin, J.M., Sangster, D.F., and Lydon, J.W.
1981: Volcanic associated massive sulphide deposits; Economic Geology, 75th anniversary volume, p. 485-627.

Franklin, J.M., Gibb, W., Poulsen, K.H., and Severin, P.
1977: Archean metallogeny and stratigraphy of the South Sturgeon Lake area; Mattabi field trip: 23rd annual meeting of the Institute of Lake Superior Geology, 75 p.

Franklin, J.M., Kasarda, J., and Poulsen, K.H.
1975: Petrology and chemistry of the alteration zone of the Mattabi massive sulfide deposit; Economic Geology, v. 70, p. 63-79.

Friske, P.W.B.
1983: Wall-rock alteration and ore genesis at the Lyon Lake deposits, Northwestern Ontario; University of New Brunswick, Ph.D. thesis.

Goodwin, A.M., Ambrose, J.W., Ayres, L.D., Clifford, P.M., Currie, K.L., Ermanovics, I.M., Fahrig, W.F., Gibb, R.A., Hall, D.H., Innes, M.J.S., Irvine, T.N., McLaren, A.S., Norris, A.W., Pettijohn, J.F., and Ridler, R.H.
1972: The Superior province; Geological Association of Canada, Special Paper 11, p. 527-624.

Gross, G.A.
1965: Geology of iron deposits in Canada. General geology and evaluation of iron deposits; Geological Survey of Canada, Economic Geology Report 22, Volume 1, 181 p.

Groves, D.A.
1984: Stratigraphy and alteration of the footwall volcanic rocks beneath the Archean Mattabi massive solfide deposit, Sturgeon Lake, Ontatio. M.Sc. thesis, University of Minnesota, Duluth, MN.

Groves, D.A., Morton, R.L., and Franklin, J.M.
1988: Physical volcanology of the footwall rocks near the Mattabi massive sulfide deposit, Sturgeon Lake, Ontario; Canadian Journal of Earth Sciences, v. 25, p. 280-291.

Harvey, J.D., and Hinzer, J.B.
1981: Geology of the Lyon Lake ore deposits, Noranda Mines Limited, Sturgeon Lake area, Ontario; Canadian Institute of Mining and Metallurgy Bulletin, v. 74, no. 833, p. 77-84.

Hinzer, J.B.
1977: Geology, geochemistry, Lake and Creek ore zones, Sturgeon Lake; Unpublished M.Sc. thesis, University of Western Ontario, London, Ontario.

Mumin, A.H.
1988: Tectonic and structural controls on massive sulfide deposition in the south Sturgeon Lake volcanic pile, Northwestern Ontario and Hydrothermally altered rocks associated with the Lyon Lake Archean, volcanogenic massive sulfide ore deposits, Sturgeon Lake, Northwestern Ontario; M.Sc. thesis, University of Toronto, 138 p.

Poulsen, K.H., and Franklin, J.M.
1981: Copper and gold mineralization in an Archean trondhjemitic intrusion, Sturgeon Lake, Ontario; in Current Research, Part A, Geological Survey of Canada Paper 81-1A, p. 9-14.

Ramsay, J.G.
1967: Folding and fracturing of rocks; McGraw-Hill, New York, 568 p.

Roberts, G.W.
1981: An examination of structural and stratigraphic ore controls, Lyon Lake mine, Ontario; Noranda Mines, Internal company report, 13 p.

Trowell, N.F.
1983: Geology of the Sturgeon Lake area, districts of Thunder Bay and Kenora; Ontario Geological Survey Report 221, 97 p.
1974: Geology of the Bell Lake-Sturgeon Lake area, districts of Thunder Bay and Kenora; Ontario Geological Survey Report 114, 67 p.

Preliminary lead isotope studies of base metal and gold mineralization in the eastern Wabigoon Subprovince, northwestern Ontario

C.D. Anglin and J.M. Franklin
Mineral Resources Division

Anglin, C.D. and Franklin, J.M., Preliminary lead isotope studies of base metal and gold mineralization in the eastern Wabigoon Subprovince, northwestern Ontario; in Current Research, Part C, Geological Survey of Canada, Paper 89-1C, p. 285-292, 1989.

Abstract

Zinc-lead-silver occurrences in the Onaman and Tashota areas of the eastern Wabigoon belt, Ontario, consist of disseminated and vein sulphides in Archean volcanic rocks. Their galena has lead isotope compositions with unusually high $^{207}Pb/^{204}Pb$ ratios, relative to most massive sulphide deposits in Superior Province. Model ages for the Onaman samples are very close to the U-Pb - zircon ages of the host felsic volcanic rocks. Both textural and isotopic data are consistent with an epithermal origin for these occurrences. The Tashota occurrences have exceptionally old (ca. 2900 Ma) model ages, indicating the possible presence of old crust.

Galena specimens from gold-bearing mesothermal vein deposits near Geraldton are isotopically rather inhomogeneous. Although no age significance can be attached to their compositions, these indicate a complex source for the lead, possibly dominated by their local wall rocks.

Résumé

Les venues de zinc, plomb et argent que l'on rencontre dans les régions d'Onaman et de Tashota dans l'est de la zone de Wabigoon, en Ontario, se composent de sulfures disséminés et disposés en filons dans les roches volcaniques d'âge archéen. La galène qu'elles contiennent présente une composition en isotopes du plomb caractérisée par des rapports inhabituellement élevés de $^{207}Pb/^{204}Pb$, si l'on compare avec la plupart des gisements de sulfures massifs de la province du lac Supérieur. Les âges modèles des échantillons d'Onaman sont très proches de ceux des roches volcaniques encaissantes de nature felsique, déterminés à l'aide de la méthode U/Pb appliquée aux zircons. Les données texturales et isotopiques confirment toutes deux l'origine épithermale de ces venues. Le fait que les venues minéralisées de Tashota ont des âges types exceptionnellement élevés (environ 2900 Ma) témoigne de la présence possible d'une croûte ancienne à cet endroit.

Les échantillons de galène prélevés dans des gisements filoniens mésothermaux aurifères, près de Geraldton, sont de caractère isotopique plutôt hétérogène. Même si l'on ne peut établir aucun lien significatif entre leur âge et leur composition, ces échantillons indiquent que le plomb provient d'une source complexe, peut-être déterminée par la nature des roches encaissantes locales.

INTRODUCTION

Lead isotopic analyses of galenas from base metal and gold deposits are potentially useful for determining ages of emplacement, and as tracers of the components of the fluids that were responsible for the deposit. Lead isotope model ages are potentially inaccurate, but they can be useful if the applied lead evolution model is well constrained by independently determined ages for deposits containing lead minerals, and where the analyzed galena samples probably formed under source and depositional conditions appropriate for the model. Pb isotopes provide a very effective tracer of geological processes, as they can indicate the amount of homogenization of a mineralizing fluid, and the possible source rocks from which the lead was derived.

The eastern Wabigoon Subprovince contains numerous gold and base metal deposits and occurrences (Fig. 1). In the Beardmore and Geraldton areas (BG), along the southeastern margin of the subprovince, 10 mines produced approximately 3 million ounces of gold from 1934 to 1968 (Mason et al., 1985). The Onaman-Tashota metavolcanic belt, to the north of the BG, hosts numerous base-metal massive sulphide deposits and occurrences, porphyry copper-molybdenum, and vein-gold deposits. As part of a continuing study of the metallogeny of the Wabigoon belt, intensive investigations of stratigraphic, structural and geochemical aspects of mineralization were undertaken in both the Geraldton and Onaman areas (Anglin, 1987; Osterberg, 1985). Placing absolute age constraints on these various types of mineralization is important in determining stratigraphic and genetic relationships between districts and deposit types.

In the Onaman Lake area a sequence of subaerial felsic volcanic rocks hosts unusual Pb-Zn-Ag sulphide mineralization, which is known as the Headway-Coulee prospect. The alteration and rock types are similar to those of the volcanogenic massive sulphide deposits at Sturgeon Lake (Franklin et al., 1975), but most of the sulphides at Onaman Lake are in veins. The alteration associated with these veins has been metamorphosed along with the host rocks, but it is not clear whether this mineralization represents a syngenetic massive sulphide type deposit or is epigenetic. About 30km north, near Tashota, Ontario, several occurrences of Zn-Pb-Ag mineralization were discovered by Canamax Ltd. (D. Waddington, pers. com.). Although poorly documented, these are at least superficially similar to the Onaman occurrences. Comparison of model lead ages from the Onaman sulphides with the age of the host rocks (Anglin et al., 1988) and comparing the lead isotopic composition of sulphides in both the Onaman and Tashota areas with those from established syngenetic sulphide deposits may elucidate this problem.

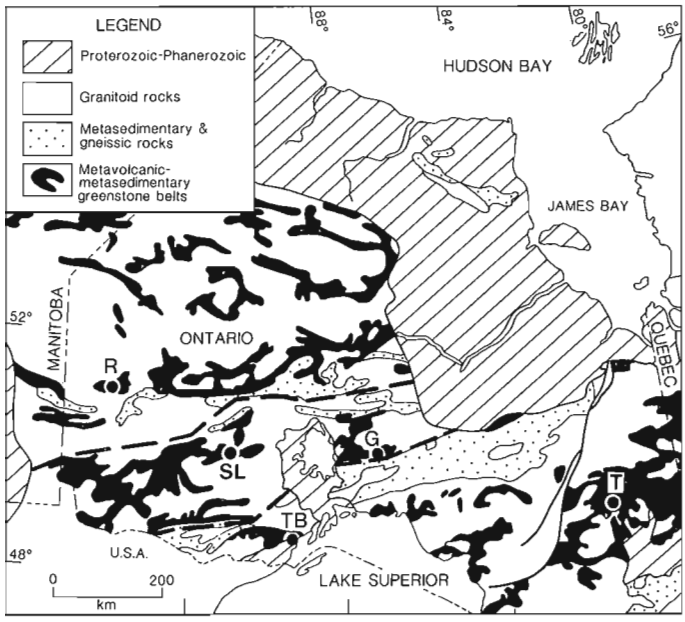

Figure 1. Northern Ontario location map. Greenstone belts are represented by the solid pattern. The Wabigoon Subprovince is outlined by a heavy dashed line. T = Timmins, G = Geraldton, TB = Thunder Bay, SL = Sturgeon Lake, R = Red Lake.

In the Geraldton area, gold mineralization occurs in quartz veins and fracture zones that crosscut all Archean lithologies, including quartz-feldspar porphyritic intrusions. These intrusions are the youngest lithologies in the area to be crosscut by the gold mineralization; their crystallization age therefore is the maximum age of gold emplacement. The close spatial relationship between felsic intrusions and gold mineralization here (Anglin, 1987), and recognized also at many of the largest gold camps in the Superior and Churchill Provinces (Hodgson and MacGeehan, 1982), has been interpreted to indicate a possible genetic relationship. Again, the lead isotopic composition of galena samples from gold deposits and occurrences, and comparison of their model lead ages with the ages of the host rocks may help clarify this relationship.

The objectives of this lead isotope study are therefore, 1) to obtain model lead ages for galena from the base metal mineralization, for comparison with the U/Pb ages of the host rocks and, to gain insights into the origin of the mineralizing fluids, and 2) to obtain reconnaissance lead isotope analyses of galenas from the gold mineralization, for comparison with the base metal galena compositions, and for information on the source of the gold-bearing fluids. The results of a U-Pb zircon study of the host rocks to the base metal mineralization in the Onaman area, and to the gold mineralization at Geraldton are discussed in detail in Anglin et al. (1988) and only the ages are presented here.

REGIONAL GEOLOGY

The Wabigoon Subprovince (WS) of the Canadian Shield is in northwestern Ontario and is bounded to the north by the English River and Winnipeg River subprovinces, and to the south by the Quetico Subprovince (Fig. 1). It is a typical granite-greenstone terrain of Archean age consisting of a supracrustal assemblage of predominantly volcanic rocks with lesser amounts of sedimentary rocks. The supracrustal rocks have been intruded by granite, syenite and gabbro plutons (Card, 1983; Blackburn et al., 1985). The WS extends easterly for approximately 900 km and is as much as 150 km wide. Thurston (1980), and Mason and White (1986) divided the eastern Wabigoon Subprovince (east of Lake Nipigon) into two belts; 1) the Beardmore-Geraldton belt, to the south of the Paint Lake Fault, and 2) the Onaman-Tashota metavolcanic belt north of this fault (Fig. 2).

GEOLOGY OF THE ONAMAN AREA

The Onaman Lake greenstone area, in the central part of the Onaman-Tashota belt, is an elongate zone of volcanic and minor sedimentary rocks,approximately 4 km wide, situated between two very large plutons of biotite-hornblende trondhjemite and granodiorite (Fig. 2). The volcanic area is a north-facing homocline of pillowed basalt, with 200 to 300 m of felsic volcanic and sedimentary rock near the centre of the volcanic pile (Thurston, 1980). Discontinuous iron formations are intercalated with the basalt and the felsic tuff. The volcanic sequence is much thicker to the southeast in the Con Creek area (Amukun, 1980).

Felsic volcanic rocks and associated quartz-feldspar porphyry intrusive bodies, along with sedimentary strata, occur near the stratigraphic top of many of the sequences (Thurston, 1980). The felsic rocks consist of ash tuff and porphyritic flows, and are interlayered with polymictic diamictite (Osterberg, 1985). The tuff beds formed as hydrovolcanic eruption products, in shallow subaqueous conditions (Osterberg, 1985).

Sulphide mineralization was discovered in the Onaman River area in 1949 by Headvue Mines Ltd. The largest of the Pb-Zn-Ag occurrences which are collectively known as the Headvue or Headway-Coulee prospect (Shklanka, 1969), itself consists of a series of 13 lenses of disseminated and vein-type sulphides, predominantly in the felsic strata, near their contact with the underlying mafic flows. Several other occurrences, including the Con Creek (Amukun, 1980) and Cane Resources occurrences, are in the same sequence as the Headway-Coulee occurrences, but may be at a slightly lower stratigraphic position.

The Headway-Coulee occurrence contains more than 600 000 tonnes of zinc-lead-silver mineralization (Shklanka, 1969) in chloritoid- and sericite-bearing felsic and mafic volcanic rocks. Copper vein mineralization occurs in the underlying mafic volcanic flows, approximately 200m (stratigraphically) below the Pb-Zn-Ag zones. A few kilometres to the east, gold was mined from the Tashota-Nipigon Mine.

Pyrite, sphalerite, galena, and minor chalcopyrite occur in quartz and carbonate veins and as disseminated zones. A typical grade for the occurrence is 4% Zn, 2% Pb, 145 g/tonne Ag and 2.8 g/tonne Au. The Con Creek occurrences are similar, with 4.7% Zn, 3,6% Pb, 0.41% Cu, 185 g/tonne Ag, and 1 g/tonne Au (data from Amukun, 1980, table 17).

The footwall rocks of the Headway Coulee deposit are highly altered (Osterberg, 1985). Carbonate alteration is pervasive, and zones of quartz-sericite, iron chlorite and chloritoid alteration occur near the deposits. A conformable zone of quartz-kyanite rock stratigraphically overlies the Headway-Coulee deposit.

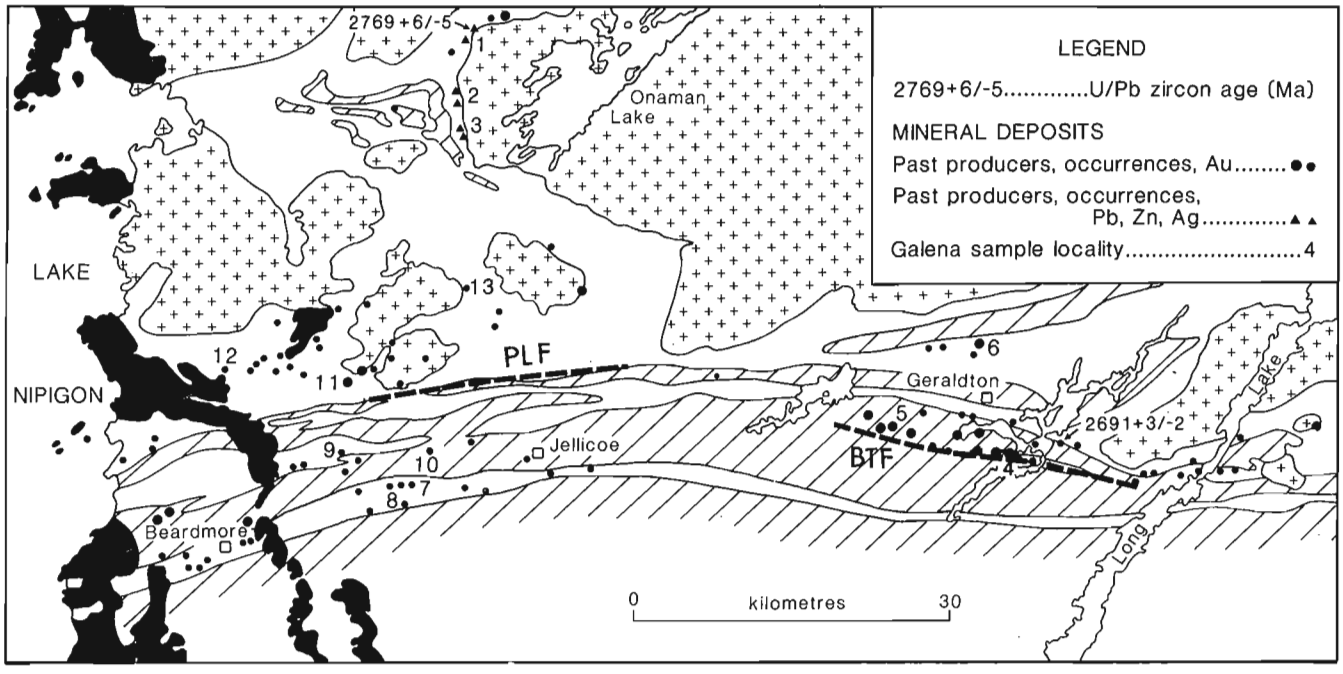

Figure 2. Geological map of the southeastern Wabigoon Subprovince (after Pye et al., 1965) showing the Beardmore-Geraldton and Onaman-Tashota belts. Gold past-producers and occurrences are shown in large and small solid circles respectively, Pb-Zn past-producers and occurrences are shown in solid triangles. The locations of the U-Pb zircon samples are indicated by an arrow from the age obtained on the sample. The numbers refer to galena samples listed in Table 1. Note, samples numbered 14 to 16 are located near Tashota, located off the map sheet approximately 20 km to the north of sample location 1 (see Pye et al., 1965), and samples numbered 17 to 22 are from the Fort Frances area, located approximately 400 km west of Thunder Bay (see Poulsen (1986) for detailed sample locations). Heavy dashed lines represent the Paint Lake Fault (PLF) and the Bankfield-Tombill Fault (BTF). Rock types: solid pattern = Proterozoic diabase dykes and sills; crosses = granitic and gneissic rocks; diagonals = metasedimentary rocks; white = metavolcanic rocks.

The genesis of the deposits is obscure. The most intense alteration is largely stratigraphically below the deposits, and has been metamorphosed. Based on Osterberg's (1985) interpretation of the origin of the alteration, the sulphides were precipitated immediately below the sea floor. The quartz-kyanite rock overlying the deposits is probably a metamorphosed siliceous sinter. In many aspects the deposits are similar to those of epithermal origin.

Anglin et al. (1988) report a U-Pb zircon crystallization age of 2769 +6/-5 Ma for a porphyritic rhyolite flow unit from the Onaman Lake area which establishes the age of the host rock sequence to the base metal mineralization. This sequence is clearly significantly older than the similar-looking volcanic sequence at Sturgeon Lake (lower cycle = 2735 Ma, uppermost cycle = 2718 Ma, Davis et al., 1985; Blackburn et al., 1985), and is relatively old for extrusive volcanic activity in the Wabigoon Subprovince (see compilation of western Wabigoon Subprovince age dating by Blackburn et al., 1985, p.107, Fig. 16). The Wabigoon greenstone belts probably formed over a longer interval than most of those in the Abitibi Subprovince (Mortensen, 1987).

Galena samples for lead isotope analysis were also obtained from three base metal sulphide occurrences in the Onaman area (Headvue, Con Creek, and Cane Resources), all within the stratigraphic assemblage that contains the felsic volcanic unit sampled for zircon age determination.

The Tashota area has not been examined in detail for this study. Amukun (1977) reported that it consists of a belt of volcanic strata that may be the northern extension of the Onaman volcanic sequence. The volcanic rocks are bounded to the west by an Archean granitic pluton, the Robinson Lake stock, and an older complex of metamorphic rocks, the Elbow Lake stock. The sulphides examined in this study occur as veins and disseminations in silicified volcanic rocks. The alteration assemblage associated with this mineralization has probably been metamorphosed, and the occurrences thus may be similar in origin to the Tashota sulphides. Galena samples were supplied by D. Waddington of Canamax Ltd., from three separate occurrences.

GEOLOGY OF THE GERALDTON AREA

In the Geraldton area, gold mineralization is in veins and fracture zones in sedimentary rocks, including iron formation, mafic and felsic intrusions, and mafic volcanic rocks. The felsic intrusive rocks cut all other lithologies except for diabase dykes and rare lamprophyre dykes, both of which cut gold-bearing structures (Horwood and Pye, 1955).

Gold was first discovered in the Geraldton area in the early 1930's. The camp was active intermittently from then until 1968, producing almost 3 million ounces (93.3 tonnes) of gold from 10 mines (Mason et al., 1985). The gold mineralization is probably mesothermal in origin (Anglin, 1987), and is primarily in quartz veins, with significant additional gold in disseminated pyrite-arsenopyrite zones in felsic intrusions. Veins and disseminations are superimposed on all Archean rock types in the area, including the youngest Archean lithologies, feldspar and quartz-feldspar porphyries. Unmetamorphosed Proterozoic diabase dykes, mineralogically similar to Keweenawan dykes and sills near Lake Nipigon, crosscut gold mineralization; the latter dykes place a minimum absolute age constraint on the time of gold emplacement of 1109.7 $\pm$ 2 Ma (Davis and Sutcliffe, 1984).

Sedimentary rocks, which dominate the supracrustal rocks of the Geraldton area, consist of greywacke-siltstone turbidites, conglomerate and iron formation. This assemblage is bounded to the north by mafic volcanic rocks and to the south, across the Bankfield-Tombill Fault (BTF), by a sequence of homogeneous greywacke-siltstone turbidite beds. The BTF is the most prominent fault in the camp. To the north of the BTF the sedimentary and volcanic rocks have been intruded by hornblende-bearing mafic dioritic and gabbroic bodies. A suite of feldspar and quartz-feldspar porphyries also intruded the rocks north of the BTF, including the mafic intrusions. They are preferentially localized within the northern sedimentary assemblage, but also crosscut the volcanic rocks at several locations east of Geraldton.

The majority of gold occurrences, and all the major mines in the Geraldton area are within the heterogeneous assemblage of sedimentary rocks surrounding and north of the BTF. The deposits are spatially closely associated with the BTF and the felsic porphyritic intrusions. At several of the mines, including the Hard Rock, MacLeod-Cockshutt, and Bankfield Mines, the quartz-feldspar porphyries were an important host rock for quartz and quartz-carbonate veins and disseminated pyrite-bearing gold ore.

The felsic porphyritic intrusive dykes and sills are the youngest lithologies in the area to be crosscut by gold mineralization; thus, they represent the maximum age for emplacement of the mineralization. The relationship between felsic intrusions and gold have been explained by the following hypotheses; 1) felsic intrusions are the source of the gold and fluids for metal transport, as in the classic magmatic hypothesis; 2) felsic intrusions represent a preferential site for deposition of gold; 3) felsic intrusions indicate the presence of a structure that localized both their emplacement and the flow of gold-bearing fluids; or, 4) the relationship is coincidental.

To establish the absolute timing of intrusion, and therefore the maximum age for the gold emplacement, Anglin et al. (1988) sampled a relatively unaltered feldspar porphyry for zircon U-Pb isotopic analysis. This yielded a crystallization age of 2691^{+3}_{-2} Ma., which clearly indicates that these rocks are not contemporaneous with volcanism in the Onaman Lake area. Although no other ages have been obtained on volcanic rocks in the Beardmore-Geraldton or Onaman-Tashota belts, none of the ages of extrusive rocks that have been dated in the western Wabigoon Subprovince (Blackburn et al., 1985) are similar, but the 2691 Ma age does correlate very well with other post-volcanic felsic intrusive events.

Gold veins and zones of disseminated pyrite mineralization clearly cut the porphyry bodies at Geraldton, and must have been emplaced later than the time of intrusion. The gold mineralizing event is clearly not contemporaneous with volcanism in the eastern WS. Determination of the absolute age of gold emplacement is more difficult, as the veins do

not contain minerals useful for conventional radiometric isotopic age determinations. However, analysis of the lead isotopic composition of galenas from these veins will enable a comparison with galenas from volcanic-associated sulphide deposits, and through use of a suitable lead evolution model may permit some estimate of the age of vein formation.

Galena samples for lead isotopic analyses were collected from three gold deposits in the Geraldton area (Hard Rock, Bankfield, and Gulch mines) and several vein gold occurrences in the Beardmore-Geraldton belt (Bema, Maki, Metalore, and Walters Township), and the Tashota-Nipigon belt (Wilkinson Lake, Meader Township and Brenbar Gold Mine) (Fig. 2).

Lead isotope analytical procedures are outlined in the Appendix.

DISCUSSION OF RESULTS

A) Onaman and Tashota sulphide deposits

The galena samples from the Onaman Lake area Pb-Zn-Ag mineralization (Table 1) have an average model age of 2757 $\pm$ 16 Ma (using the Thorpe model for Abitibi belt, and 2 sigma error). These ages are within error of the U-Pb zircon age determination of their host rocks, supporting the interpretation that these are volcanogenic massive sulphide deposits. The calculated μ and w values (average of 9.24, average w of 37.81) are atypically higher than ratios for most Superior Province massive sulphide deposits (average μ of 8.53, average w of 34.78), but are almost as high as many of the deposits in the Slave Province (Franklin and Thorpe, 1982).

The data form a linear array on both the $^{207}Pb/^{204}Pb$ vs. $^{206}Pb/^{204}Pb$ and $^{208}Pb/^{204}Pb$ vs. $^{206}Pb/^{204}Pb$ plots (Fig. 3). Although these lines could be considered statistically valid secondary isochrons, they are too steep to be interpreted as such. The linear variation over a small compositional range (c.f. classical secondary isochrons, e.g. Faure, 1986) may have resulted from mixing of lead from two or more sources within the reservoir zone. This inhomogeneity is not typical of most individual massive sulphide deposits or districts (Franklin et al., 1983). As the lead isotope composition of syngenetic galena in massive sulphide deposits is believed to represent the isotopic composition of the hydrothermal reservoir zone (the volume of substrata from which the metals were obtained for the hydrothermal fluid), the variations in composition of the Onaman galena may indicate that the source region is quite inhomogeneous, and that the hydrothermal fluids were poorly mixed, or tapped different regions of the source area during the period of sulphide deposition. Alternatively, the deposit may not be syngenetic; however, the similarity between the model age and the age of the host rocks, and the clearly pre-metamorphic age of the alteration indicate that the deposit probably formed penecontemporaneously with the enclosing felsic volcanic strata.

Only a few massive sulphide deposits in the Superior Province exhibit similarly radiogenic lead isotopic compositions. The best examples are the Wind Bay and Gagne Lake occurrences in the Western Wabigoon Subprovince (Poulsen, 1984). These deposits have a much more homogeneous lead isotopic composition than the galena samples from Onaman. Poulsen (1984) described these deposits as having many characteristics typical of massive sulphide deposits,

Table 1. Eastern Wabigoon Lead Isotope Data.

NO.[1]	SAMPLE LOCATION	SAMPLE NO.	206/204	207/204	208/204	MODEL AGE[2] (Ma)
Onaman Lake area Pb-Zn-Ag deposits:						
1	Headvue Mine	FR76-52	13.464	14.705	33.292	2764
1	Headvue Mine	FR76-54	13.497	14.743	33.338	2768
2	Cane Resources	TQ82-150	13.484	14.727	33.317	2765
2	Cane Resources	TQ82-151	13.452	14.682	33.302	2755
3	Con Creek	FR81-802	13.454	14.676	33.301	2748
3	Con Creek	FR81-802	13.447	14.674	33.282	2752
Beardmore-Geraldton Belt gold deposits:						
4	Hard Rock Mine	TQ88-24	13.381	14.490	33.182	2648
5	Bankfield	TQ82-130	13.910	14.793	33.755	2474
6	Gulch Mine	FR66-508	17.086	15.368	35.686	635
7	Maki occurrence	FR81-801	13.366	14.515	33.222	2685
8	Metalore Resources	FR81-803	13.376	14.545	33.233	2703
9	Watson Lake (Bema)	FRA83-245	16.122	15.383	35.364	1360
10	Walters Twp.	TQ84-156	14.698	15.054	34.431	2092
Tashota-Nipigon belt gold deposits						
11	Brenbar Gold Mine	FR81-100	13.412	14.544	33.266	2671
11	Brenbar Gold Mine	FR81-100	13.412	14.547	33.270	2674
12	Meader Twp.	TQ87-7	13.444	14.560	33.357	2657
13	Wilkinson Lake	TQ86-56	13.376	14.537	33.205	2696
Tashota area base metal occurrences						
14	Tashota A	TQ84-46	13.228	14.655	33.047	2921
15	Tashota B	TQ84-47	13.114	14.605	32.953	2978
16	Tashota C	TQ84-48	13.613	14.744	33.328	2673
Fort Frances area (Western Wabigoon) base metal occurrences						
17	Wind Bay	TQ80-67	13.410	14.559	33.274	2730[3]
18	Gagne Lake	TQ80-68	13.410	14.564	33.291	2735
19	Gagne Lake	TQ84-160	13.408	14.556	33.279	2730
20	Gagne Lake	TQ84-160	13.410	14.564	33.285	2735
21	Gagne Lake	TQ84-161	13.415	14.562	33.281	2729
22	Gagne Lake	TQ84-161	13.418	14.567	33.289	2730

Footnotes
1. refers to sample numbers on Figures 2 and 3.
2. model ages are calculated using Thorpe's (pers. comm. 1986) Abitibi model (parameters of this model are given in the text).
3. Model ages for the galenas from the Fort Frances region are calculated using Thorpe's Western Superior model (pers. comm., 1986; A_o=9.34, B_o=10.496, C_o=29.636, t_o=4420).

and thus the hydrothermal system in which the mineralizing fluids formed was probably well mixed (Sage et al. 1987).

Galena samples from the Geneva Lake and Stralak deposits, which are in a small, isolated, greenstone belt (age unknown) north of Sudbury, form a secondary isochron (Franklin et al., 1983). These galenas also have relatively high $^{207}Pb/^{204}Pb$ compositions compared to the compositions for Superior Province massive sulphide deposits (Franklin and Thorpe, 1982) which form the Superior Province paleoisochron , indicated as the "VMS line" on Figure 3. The Geneva Lake and Stralak deposits possibly were derived from very radiogenic source rocks, but the geological relationships of the deposits are complex, involving possible lead redistribution during atleast three events that followed massive sulphide deposition (Franklin et al., 1983). Thus the Onaman samples and those from Western Wabigoon are likely the only unmodified galenas with unusually high μ and w ratios from Superior Province massive sulphide deposits.

The source rocks for the Onaman deposits, as well as for the deposits in Western Wabigoon Subprovince, must have contained more lead enriched in $^{207}Pb/^{204}Pb$ relative to most other massive sulphide districts in Superior Province. Several possible explanations for this include the following. Such radiogenic lead could have been derived from basalt that may have been derived from undepleted mantle, and had a higher ratio than that typical of the mantle from which most Archean basalts were derived. Alternatively, the source rocks may in part be much older than the felsic rocks which host the mineralization. With a sufficient difference between age of source rocks and age of sulphide deposition, a significant radiogenic component of the lead could have formed. As a third alternative, the magmas which formed the entire sequence of volcanic rocks in the Onaman area may have passed through much older crust, and thus may have been contaminated by radiogenic lead. The second and third hypotheses could be tested further by additional age determinations; analysis of rock-lead isotopic compositions in the area are required to test the first. An old crustal source for lead has also been suggested by Thorpe et al. (1987) and Sage et al. (1987) for base-metal and gold occurrences in the Wawa and Atikokan areas.

Two of the samples from base metal-silver occurrences in the Tashota area (Fig. 2) have very low $^{206}Pb/^{204}Pb$ ratios relative to all other gold and massive sulphide deposits in this study, and consequently have very old model ages (ca 2.9 Ga). Their μ ratio is about 9.6, higher than that for all massive sulphide deposits and the Onaman sulphides. The third sample has a much higher $^{206}Pb/^{204}Pb$ composition, and consequently a younger model age. It has a similarly high μ ratio to the other two samples, indicative of a

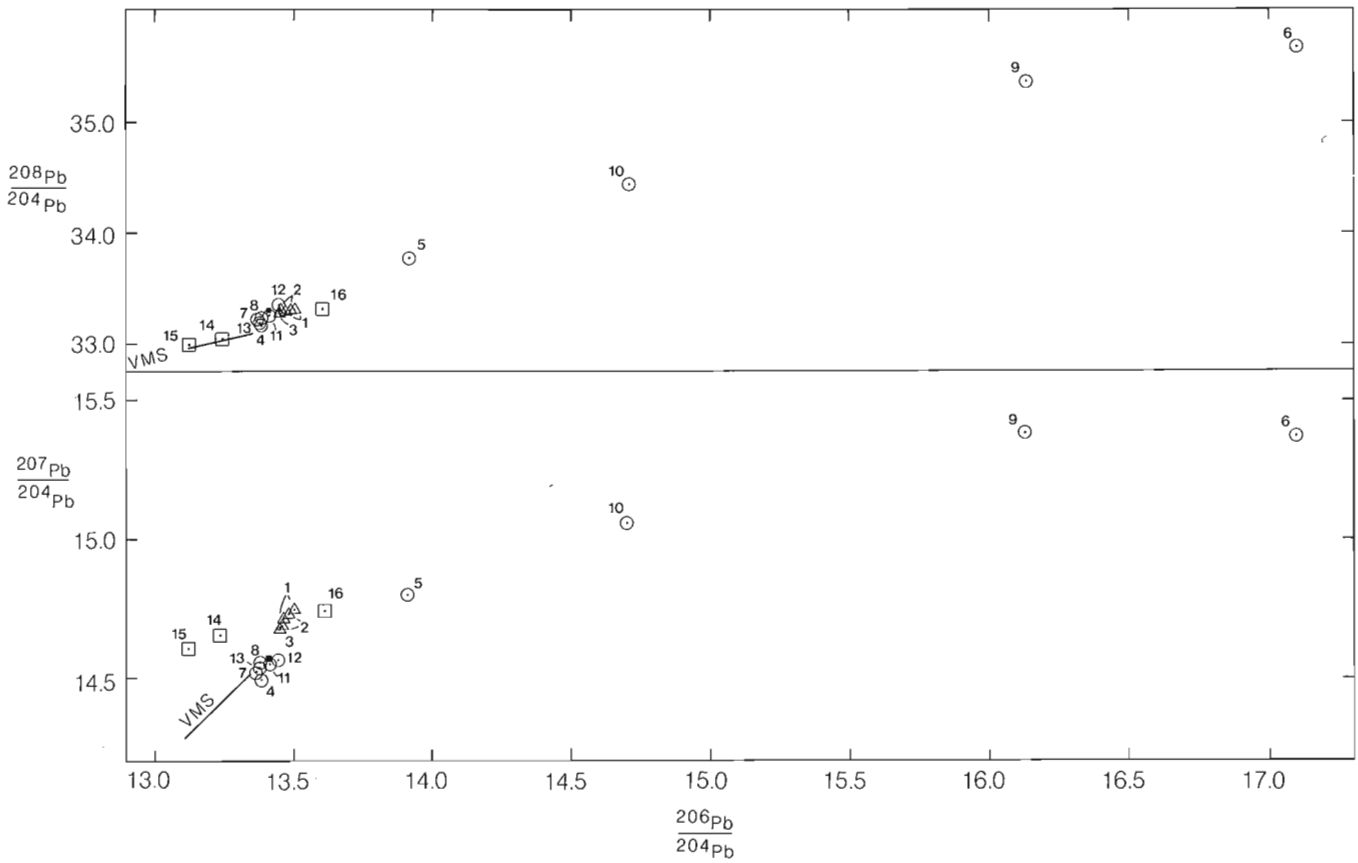

Figure 3. Lead isotope plots of galena data listed in Table 1. Numbers refer to those listed in Table 1. Open circles = gold mineralization; open triangles = Onaman Lake Pb-Zn mineralization; open squares = Tashota area base metal mineralization; small solid square = Fort Frances base metal mineralization (sample numbers 17 to 22). The solid line labelled VMS represents the volcanogenic massive sulphide line of Thorpe (1986).

possible common parent lead for all three samples. This sample may indicate that the lead for the Tashota occurrences may have been remobilized from older rocks at a considerably later time, either during later Archean volcanism or through contact metamorphism with the adjacent granite. It also may represent a younger mineralizing event.

The Tashota area may contain very old rocks compared with most of the Superior Province greenstone belts. These older rocks may include the volcanic strata which host the sulphides. Alternatively, the host strata may be underlain by older crust, in which a large portion of the mineralizing fluid was generated. Some of this fluid may have interacted with the host strata to yield the more highly radiogenic sample. Tonalite with a 3.0 Ma age has been described by Davis et al. (1988), from the Caribou Lake area, which is about 50 km west of Tashota.

B) Beardmore - Geraldton gold deposits

Galena is very rare in the largest gold deposits in the Beardmore-Geraldton belt, but slightly more common in the smaller deposits, particularly those within the Onaman-Tashota volcanic rocks (Fig. 2). Use of these data to establish a genetic model for these deposits must be done cautiously, as the precise paragenetic relationship between the galena and gold is not known. The galena data are broadly distributed (Fig. 3), and with the possible exception of the sample from the Hard Rock Mine, are all radiogenic with respect to most Archean massive sulphide deposits. Application of any lead evolution model to obtain model ages for galena specimens from veins must be used with caution, as the great variability in their isotopic compositions indicate a very complex history.

The galena samples from the Beardmore-Geraldton gold deposits may be divided into two groups. All but four of the samples (5, 10, 9 and 6) form a cluster mid-way between the top end of the massive sulphide line and the Onaman data (Fig. 3). The inhomogeneity and the lack of linear distribution of these data indicate that the galenas, and perhaps the gold-bearing fluids, cannot solely be attributed to a single source rock or well-mixed fluid, magmatic or otherwise. All but one of the deposits occurs in volcanic strata. Both magmatic-hydrothermal and seafloor-hydrothermal fluids are homogeneous and would not likely have produced lead of such variable composition, relative to isotopic compositions of galena from individual massive sulphide districts (Franklin and Thorpe, 1982). A variety of crustal sources, including the local wall rocks, probably supplied at least some of the lead. The isotopic compositions may have resulted from mixing of a homogeneous lead from the mineralizing fluid with lead from various wall rocks. Given the very small amount of galena in these deposits, its composition was probably very easily affected by lead derived from the adjacent wall-rocks. As basalt is relatively depleted in radioelements, the relatively low $^{206}Pb/^{204}Pb$ values may reflect the dominance of this rock as a source.

The remaining four samples form a moderately good linear array. Two-stage calculations on various combinations of these samples, either with or without those in the aforementioned cluster, do not yield a geologically reasonable interpretation. The large variation in composition precludes their origin from a well mixed source. All of these deposits are in sedimentary strata, which may represent a better source of radiogenic lead than the volcanic strata.

CONCLUSIONS

1) The coincidence of the model ages of the Onaman samples with the U/Pb -zircon ages of the host rocks indicates the probability that these deposits formed penecontemporaneously with the volcanic strata. The morphology of the deposits is more consistent with their origin as epithermal veins rather than volcanic-associated massive sulphide deposits.

2) The high μ ratios for the Onaman galena samples indicate that these deposits obtained their lead from a source rock with much more radiogenic lead than is typical of other Superior Province greenstone belts. The linear distribution of these data suggest some inhomogeneity in the source area. The Onaman area may be underlain by much older crust, which interacted either directly with the fluids or with the melts which formed the immediate volcanic sequence.

3) The Tashota occurrences are probably in very old Archean strata; alternatively the fluids originated in older underlying crust.

4) The great inhomogeneity of the lead isotope compositions of the galenas from the gold veins of the Geraldton area precludes their derivation from a well-mixed magmatic-hydrothermal source. The lead may have been derived from a great variety of crustal sources, including local wall rocks. The isotopic compositions probably represent mixing of lead from both the local rocks and the mineralizing fluid, and thus yield results which are difficult to interpret regarding the origin of the gold-bearing fluids.

ACKNOWLEDGMENTS

S. Osterberg of the University of Minnesota-Duluth provided much new data on the Onaman area. J. Mason, J. Scott and C. McConnel of the Ontario Department of Mines and Northern Affairs introduced JMF to the Onaman area, and assisted us with the study. D. Waddington of Canamax Resources Ltd. provided the samples and geological information for the Tashota area. K.H. Poulsen provided unpublished lead isotope data for deposits in the Fort Frances area. R.I. Thorpe generously provided his data for model age calculation, organized the analyses, and reviewed the manuscript.

REFERENCES

Amukum, S.E.
1977: Geology of the Tashota Area, District of Thunder Bay; Ontario Geological Survey Report 167, 90 p.

Amukun, S.E.
1980: Geology of the Conglomerate Lake area, District of Thunder Bay; Ontario Geological Survey Report 197, 101 p. Accompanied by map 2429, scale 1:31 680.

Anglin, C.D.
1987: Geology, Structure and Geochemistry of Gold Mineralization in the Geraldton area, Northwestern Ontario, MSc thesis, Memorial University of Newfoundland, 283 p.

Anglin, C.D., Franklin, J.M., Loveridge, W.D., Hunt P.A., and Osterberg, S.A.
1988: Use of zircon U-Pb ages of felsic intrusive and extrusive rocks in eastern Wabigoon Subprovince, Ontario, to place constraints on base metal and gold mineralization; in Radiogenic Age and Isotopic Studies Report 2, Geological Survey of Canada, Paper 88-2.

Blackburn, C.E., Bond, W.D., Breaks, F.W., Davis, D.W., Edwards, G.R., Poulsen K.H., Trowell, N.F., and Wood, J.
1985: Evolution of Archean volcanic-sedimentary sequences of the Western Wabigoon Subprovince and its margins: a review; in Evolution of Archean Supracrustal Sequences; L.D. Ayres et al., (ed.). Geological Association of Canada, Special Paper 28.

Card, K.D.
1983: Regional geological synthesis, central Superior Province: reconnaissance investigations in the Nakina area, Ontario; in Current Research, Part A, Geological Survey of Canada, Paper 83-1A, p. 25-27.

Davis, D.W., Krogh, T.E., Hinzer, J., and Nakamura, E.
1985: Zircon dating of polycyclic volcanism at Sturgeon Lake and implications for base metal mineralization; Economic Geology, v. 80, p. 1942-1952.

Davis, D.W., Sutcliffe, R.H., and Trowell, N.F.
1988: Geochronological constraints on the tectonic evolution of a late Archean greenstone belt, Wabigoon subprovince, northwestern Ontario, Canada; Precambrian Research, v. 39, p. 171-191.

Davis, D.W. and Sutcliffe, R.H.
1984: U-Pb ages from the Nipigon Plate, abstract in GAC-MAC Program with Abstracts, v. 9, p. 57; Geological Association of Canada/Mineralogical Association of Canada Joint Annual Meeting, London, May 14-16, 1984.

Faure, G.
1986: Principles of Isotope Geology; second edition; Smith-Wiley Intermediate Geology Series.

Franklin, J.M., Roscoe, S.M., Loveridge, W.D., and Sangster, D.F.
1983: Lead isotope studies in Superior and Southern Provinces; Geological Survey of Canada Bulletin 351.

Franklin, J.M., and Thorpe, R.I.
1982: Comparative metallogeny of the Superior, Slave and Churchill provinces; in H.S. Robinson Memorial Volume, Precambrian Sulphide Deposits, R.W. Hutchinson, C.D. Spence, and J.M. Franklin, editors; Geological Association of Canada Special Paper 25, p. 3-90.

Franklin, J.M., Kasarda, J., and Poulsen, K.H.
1975: Petrology and alteration chemistry of the alteration zone of the Mattabi massive sulphide deposit; Economic Geology, vol. 70, p. 63-79.

Hodgson, C.J. and MacGeehan, P.J.
1982: Geological characteristics of gold deposits in the Superior Province of the Canadian Shield; in Hodder, R.W. and Petruk, W. editors, Geology of Canadian Gold Deposits, CIM Special Volume 24.

Horwood, H.C. and Pye, E.C.
1955: Geology of Ashmore Township; Ontario Department of Mines Annual Report, vol 60, part 5, 105 pp.

Mason, J., and White, G.
1986: Gold occurrences, prospects and deposits of the Beardmore-Geraldton area, Districts of Thunder Bay and Cochrane; Ontario Geological Survey, Open File Report 5630, 680 p.

Mason, J., White, G., and McConnell, C.
1985: Field guide to the Beardmore-Geraldton metasedimentary-metavolcanic belt; Ontario Geological Survey Open File Report 5538, 73 p.

Mortensen, J.K.
1987: Preliminary U-Pb zircon ages for volcanic and plutonic rocks of the Noranda-Lac Abitibi area, Abitibi Subprovince, Quebec; in Current Research, Part A, Geological Survey of Canada, Paper 87-1A, p. 581-590.

Osterberg, S.A.
1985: Stratigraphy and Hydrothermal Alteration of Archean Volcanic Rocks at the Headway-Coulee Massive Sulphide Prospect, Northern Onaman Lake area, Northwestern Ontario, unpublished MSc thesis, University of Minnesota at Duluth, 114 p.

Poulsen, K.H.
1984: Archean tectonics and mineralization, Rainy Lake, northwestern Ontario; unpublished PhD thesis, Queen's University, Kingston, 342 p.

Pye, E.G., Harris, F.R., Fenwick, K.G., and Baillie, J.
1965: Tashota-Geraldton Sheet, Thunder Bay and Cochrane Districts, Ontario Department of Mines, Geological Compilation Series Map 2102, scale 1 inch to 4 miles or 1:253 440.

Sage, R.P., Thorpe, R., and Berdusco, E.
1987: Field trip guidebook, geology of the Michipicoten Iron Formation, lead isotope data; Institute on Lake Superior Geology, thirty-third annual meeting, part 3.

Shklanka, R.
1969: Copper, Nickel. Lead and Zinc Deposits of Ontario, Ontario Department of Mines, Mineral Resources Circular No. 12.

Thorpe, R.I., Sage, R.P., and Franklin, J.M.
1987: Lead isotope evidence for an old crustal source for many ore leads in the Wawa region; Institute on Lake Superior Geology, Proceedings and abstracts, v. 33, part 1, p. 76-77 (Wawa Ontario, May 12-13).

Thurston, P.C.
1980: Geology of the Northern Onaman Lake area, District of Thunder Bay; Ontario Geological Survey Report 208, 81 p. Accompanied by Map 2411, scale 1:31 680, and Chart A.

York, D.
1969: least squares fitting of a straight line with correlated errors; Earth and Planetary Science Letters, v. 5, p. 320-324.

Appendix

Lead isotope procedures

The samples of galena were mechanically separated from the silicate portions of the rock by a combination of magnetic and super-panner methods. The samples were analyzed by Geospec Consultants Ltd., Edmonton, Alberta. They were prepared by dissolving a small amount of sample in 10 ml of high purity 2N HCl, and evaporating the solution slowly until PbCl2 crystallized. The crystals were extracted from the solution, washed in 4n HCl, dried and dissolved in water. An aliquot of 1 to 2 grams was loaded onto a rhenium filament in a silica gel-phosphoric acid mixture and analyzed on a Micromass MM-30 mass spectrometer. The isotopic ratios presented in Table 1 are accurate to 0.1 % of the stated values, based on replicate analyses, and periodic measurements of the SRM-981 standard.

Data sets which form distinctive linear arrays are subject to linear regression using the method of York (1969). Model ages were calculated using a model prepared by Thorpe (pers. comm., 1986) which has been developed using aset of galena analyses from massive sulphide deposits from the Abitibi belt for which the ages are well constrained by U-Pb (zircon) age determinations. The parameters for this model, using the nomenclature of Faure (1986) are A_o=9.304, B_o=10.512, C_o=29.60, To= 4420 Ma. The data, with model ages where appropriate, are presented in Table 1 and Figure 3.

Stratigraphic and structural settings of iron-formations and gold in the Back River area, District of Mackenzie, N.W.T.[1]

C.W. Jefferson, C.J. Beaumont-Smith[2], and R.L. Lustwerk

Jefferson, C.W., Beaumont-Smith, C.J. and Lustwerk, R.L., Stratigraphic and structural settings of iron-formations and gold in the Back River area, District of Mackenzie, N.W.T.; in Current Research, Part C, Geological Survey of Canada, Paper 89-1C, p. 293-304, 1989.

Abstract

The volcanic Back Group and the overlying sedimentary Beechy Lake Group are interfingered and punctuated by three ferruginous chemical sedimentary sequences (CSS). The lowest CSS is sulphide-dominated and volcanic-hosted; the highest is oxide-dominated and sediment-hosted. The middle, most auriferous CSS comprises iron-carbonate-cemented volcanic breccias and grits, overlain by oxide facies iron-formation, in turn overlain by sulphide facies iron-formation and slates which are intercalated with discontinuous volcanic and shallow intrusive rocks.

The main folds (F2) are large and open in volcanic units; parasitic folds of various sizes in sedimentary units are tight, moderate to sleepy plunging and transected by axial planar crenulation cleavages (S2). Shallowly and steeply plunging kink folds (F3, F4?) and associated fracture cleavage trend northerly and northwesterly. The most auriferous units are grey, sulphidic, crack-seal quartz veins that are stratabound within the middle CSS and were deformed by F2 folds.

Résumé

Le groupe volcanique de Back et le groupe sédimentaire sus-jacent de Beechy Lake sont interdigités, et caractérisés par trois séquences de sédiments chimiques ferrugineux. La séquence de sédiments ferrugineux la plus profonde est dominée par des sulfures et contenue dans des roches volcaniques; la plus élevée est dominée par des oxydes et contenue dans des sédiments. La séquence intermédiaire, la plus riche en or, contient des brèches volcaniques et des grès grossiers qui sont cimentés par des carbonates de fer et recouverts par une formation ferrifère à faciès oxydé, laquelle est à son tour recouverte par une formation ferrifère à faciès sulfuré et par des ardoises intercalées avec des roches volcaniques discontinues et des roches intrusives peu profondes.

Les plis principaux (F2) sont vastes et ouverts dans les unités volcaniques; des plis secondaires semblables de dimensions diverses, présents dans les unités sédimentaires, sont serrés, moyennement à fortement plongeants et recoupés par un clivage de crénulation axial (S2). Des flexures répétées (F3, F4?), les unes plongeant faiblement, les autres fortement et le clivage de fracture associé ont une direction nord et nord-ouest. Les unités à la plus haute teneur en or sont des filons de quartz gris sulfurés, de type « crack-seal » et formant des interstratifications à l'intérieur de la séquence intermédiaire de sédiments chimiques; ces filons ont été déformés par des plis F2.

[1] Contribution to Canada-Northwest Territories Mineral Development Agreement 1987-1991, Project carried by Geological Survey of Canada, Mineral Resources Division.

[2] Department of Geology, University of New Brunswick, Fredericton, N.B. E3B 5A3

INTRODUCTION

Iron-formations in the volcanic Back Group and sedimentary Beechy Lake Group (Tremblay, 1971; Frith, 1987) have been mapped by Lambert (1976, 1981, 1982), Moore (1977), and others cited by these authors. All rocks are remarkably well preserved despite four probable phases of deformation and lower greenschist to lower amphibolite facies of metamorphism. Virtually all chemical sedimentary units shown on Figure 1 have been explored for base and precious metals.

This is the initial report of a multifaceted collaborative study including comparison of barren and auriferous iron-formation (C.W.Jefferson, R.L.Lustwerk), and detailed structural-stratigraphic mapping of the Back River volcanic and sedimentary complex (C.Beaumont-Smith, M.B.Lambert and C.W.Jefferson). Stratigraphic geochemistry and petrography (R.L.Lustwerk) will help to document the setting of gold occurrences, many of which are associated with iron-formation. In 1987, one month of 1:10 000-scale mapping, detailed core logging and sampling was focussed mainly on chemical sedimentary rocks in the eastern part of the volcanic complex along the Back River (Fig. 2, 3).

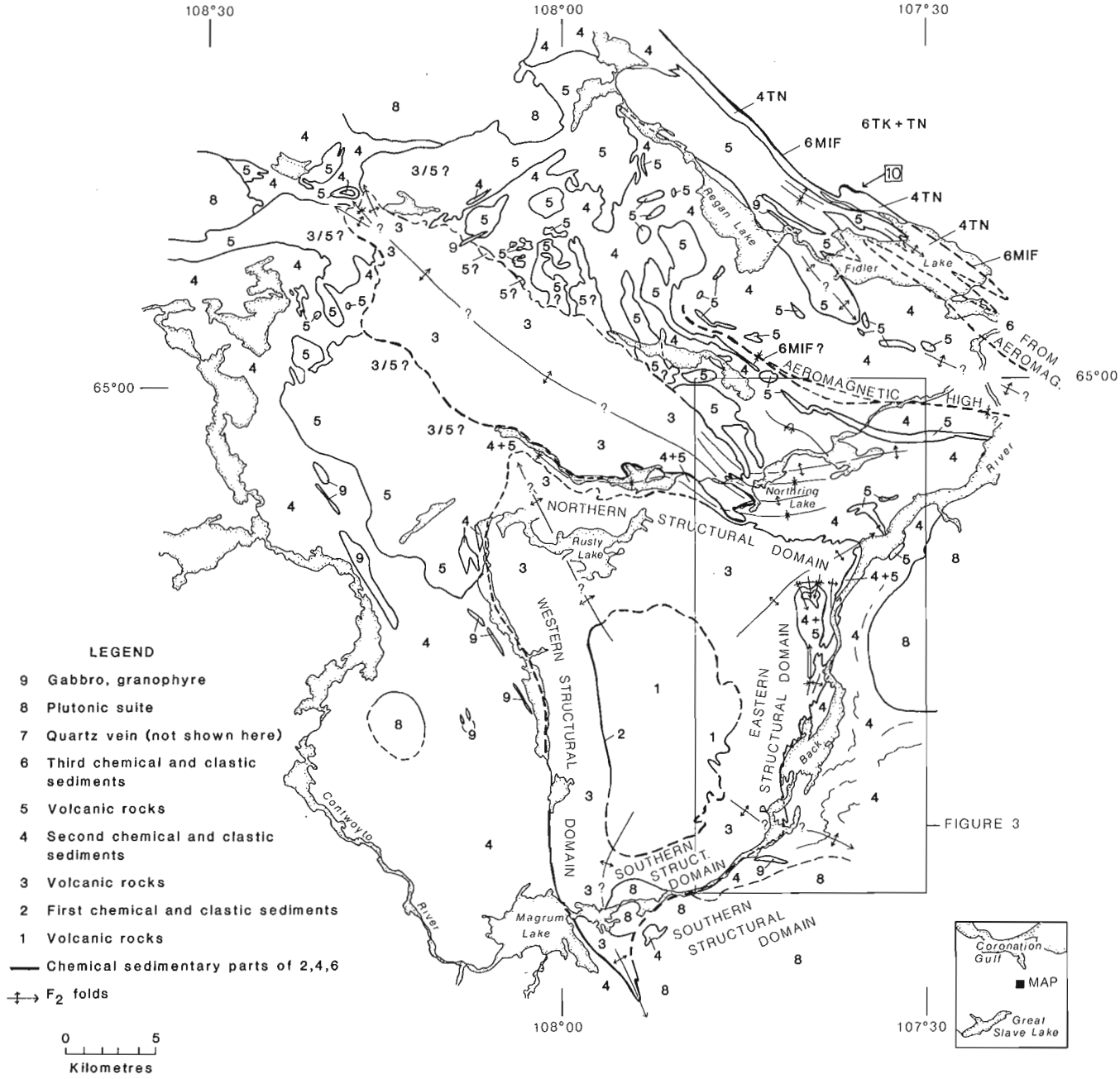

Figure 1. Back River greenstone belt, based on Lambert (1978, Fig. 32.1; 1981) and detailed mapping of this study (Fig. 3). Numeral 10 in box shows location of Figure 11.

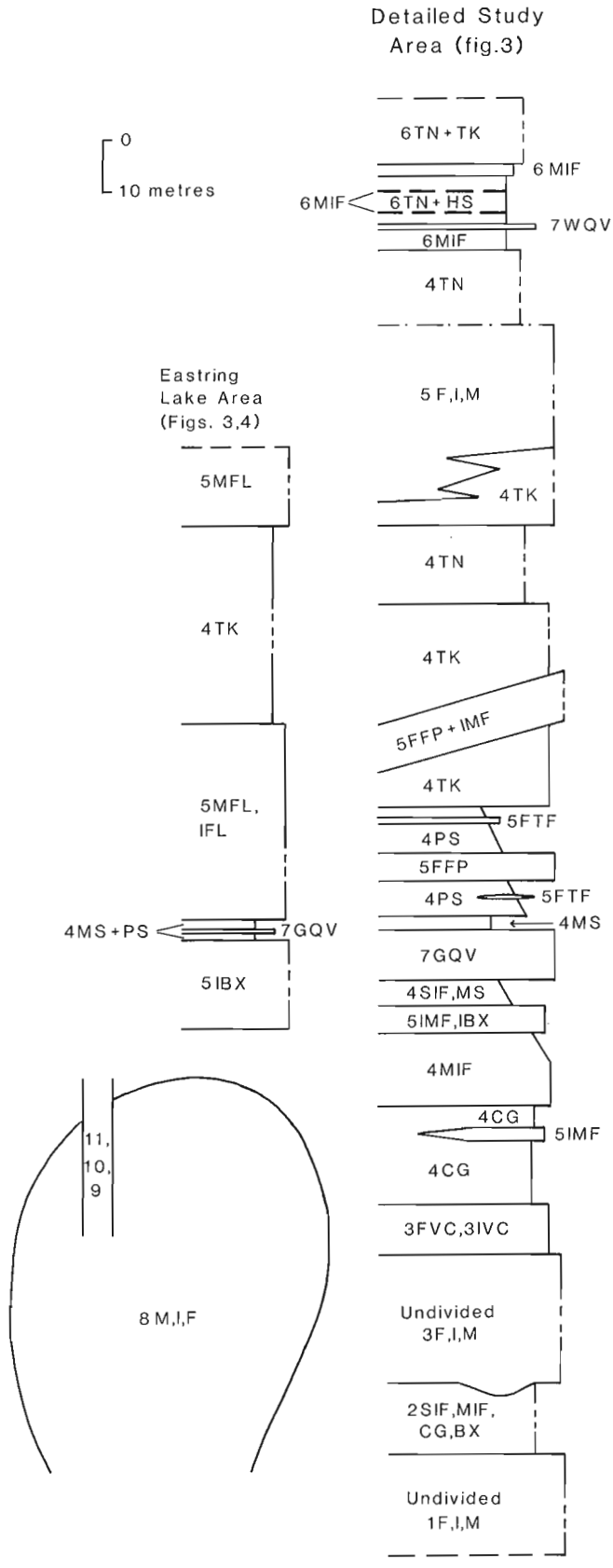

Figure 2. Stratigraphic relationships in the eastern part of the Back River complex (Fig. 3). Relative chronology is based on structural, sedimentological and volcanological criteria. Abbreviations are explained in Table 1 and text. Broken vertical lines indicate units thicker than shown at this scale.

MAP UNITS

Map units (Table 1, Fig. 2) are labelled in chronological order, from oldest to youngest. This paper deals mainly with chemical sedimentary units and immediately adjacent volcanic rocks in the area of Figure 3. Lambert (1978, 1981, 1982) has detailed the stratigraphy of the volcanic rocks and generally described the region.

Units 1, 2 and 3, lower volcanic and chemical sedimentary rocks

Chemical and clastic sedimentary rocks of unit 2 dip gently outward in an irregular circular pattern (Moore, 1977) around a central assemblage of mainly felsic volcanic rocks (unit 1, Fig. 1). Unit 2 comprises chemical sedimentary rocks (SIF, MIF, PT) (Fig. 5) and breccias (2BX) which contain volcanic, clastic-sedimentary, and massive pyrite blocks (Fig. 6). A ring of massive felsic lenses (?3FM) and carbonate impregnated breccias (2CG) were mapped by Lambert (1981) at approximately the same stratigraphic horizon as 2SIF; at locality 5 (Fig. 5), a massive felsic flow cuts downward into unit 2.

Unit 3 is a heterogenous, laterally interfingered contiguous sequence of mafic, intermediate and felsic flows, pyroclastics and crudely to well bedded volcaniclastic rocks similar to those of unit 1. The uppermost parts of unit 3 (FVC, IVC) are massive to indistinctly bedded, coarse to fine breccias and conglomerates comprising only volcanic clasts (not subdivided in Fig. 3). Preferential development of garnets in 3FVC and 3IVC suggests a more aluminous composition possibly resulting from syn-volcanic alteration. Clasts in 3IVC/FVC resemble the underlying, mainly andesitic to felsic, flows and breccias.

Unit 4, middle chemical and clastic sedimentary rocks

The basal, chemical sedimentary sequence of unit 4 is 50 to 80 m thick and continuously overlies volcanic rocks of unit 3 (Fig. 3). Contacts between subunits are gradational. The base of unit 4 is marked by iron-carbonate-cemented clastic rocks (4CG) overlain by oxide facies iron-formation (4MIF). The overlying sulphide facies iron-formation (4SIF), carbonaceous pyritic slates (4PS) and about 1.5 km of remarkably thick-bedded turbidites (4TK) are intercalated with laterally varied volcanic and shallow intrusive rocks of unit 5. Grey quartz veins (unit 7) are stratabound within 4SIF. Subunits 4CG through 4PS are inferred to further delimit the top of unit 3 in other parts of the Back River complex (Fig. 1).

Carbonate grit (subunit 4CG), overlies subunit 3IVC and is a distinctive, deep brown to tan weathering volcanic conglomerate fining upward to trough crossbedded sandstone cemented by ferroan dolomite, siderite and calcite (Moore, 1977). It ranges from 1 to 200 m thick and is locally intercalated with subunits 3IVC/FVC. Clasts in subunit 4CG are similar in composition to the immediately underlying subunits 3IVC/FVC. Finer grained portions contain oolites (Lambert, 1978).

Thin-bedded magnetite-chert ± siderite facies iron-formation (subunit 4MIF; Fig. 8), 1 to 20 m thick, overlies

Table 1. Tentative comparison of map units used in this paper with previous units.

Informal Units Used In This Paper (younging from 1 to 11)	Lambert 1981	Lambert 1978	Moore, 1977 Pl.1,2 1:50K	Moore, 1977	Frith, 1987
9-11:gabbro, diabase, lamprophyre dykes and sills	13-15	10	1	N/A	P_M
8: intermediate to felsic rocks of Regan Intrusive Suite	10-12	9	N/A	N/A	AR
7: GQV: grey quartz veins in 4SIF	N/A	N/A	5b	N/A	N/A
WQV: white quartz veins in 6HS	N/A	N/A	N/A	N/A	N/A
6: TB: turbiditic greywackes	1	1	4a	6	A_{BL}
Third chemical sed. sequence:				black	
HS: hematitic graphitic slate	N/A	N/A	N/A		N/A
MIF: magnetite iron-formation	1a	N/A	N/A		-*-
TN: thin bedded turbidites	N/A	N/A	N/A		A_{BL}
5: volcanic and shallow intrusive rocks intercalated with unit 4	2-8	3-8		11-15 9-10	A_B(part) AI
F: undivided felsic	4,6	4-7	5		
FFP: feldspar porphyry	4		2		
FQF: quartz-feldspar rhyolite	6,?11		2		
FCG: flanking conglomerate	o°O°o		N/A		
FTF: tuff	4				
I: undivided intermediate	3	4	7,8		
IMF: massive foliated intrus.	3		N/A	N/A	
IBX: breccia, debris flows	3				
M: undivided mafic	2,8	3	7		
MFL: jointed amygdal. flows	2				
MBX: breccia with carb.+sulph.	2				
4: TK: mainly thick bedded greywackes	1	1	4a	6?	A_T
TN: mainly thin bedded greywackes	1	1	4a	6?	A_T
Second chemical sed. sequence:			4,5,6	6	A_T
PS: pyritic slates	1	N/A	5b	4	
MS: massive sulphide breccia	1a	N/A	5b	1	
SIF:sulphide iron-formation	1a	N/A	5b	1	
MIF:magnetite iron-formation	1a	N/A	5a	1	
CG: carbonate-impregnated grit	6,9,▲	2,7	6	3	
3: contiguous volcanic rocks					A_B(part);
F: undivided felsic	4,6,7	5,6	8,9	9	correlate
FM: massive dome/lense/dyke	6				with A_H ?
FTF: tuff	4				
FBX+CG: breccia+conglomerate	7b				
I: undivided intermediate	3	4	7,8	9-15	
IP: pillowed	P				
IBX: breccia	3,4				
IVC: volcaniclastic	4,5,3e	7	3	2	
M: undivided mafic	2,3b	3	7		
MFL: amygdaloidal flow	2				
2: First chemical sed. sequence: sulphidic (SIF) and magnetitic (MIF) cherts, py. turbidites (PT) carbonate-rich (CG) breccia (BX)	gossan (\\\\\\) ▲▲	approx contact of 4/5; 6(part)	N/A	1,3,4	A_B(part); correlate with A_H ?
1: contiguous volcanic and shallow intrusive rocks:	4-7a	4,5,6	N/A	2,10, 11,14	A_B(part); correlate
F: felsic; FM: massive	6				with A_H ?
FBX: breccia	7a				
FTF: tuff	4,5				

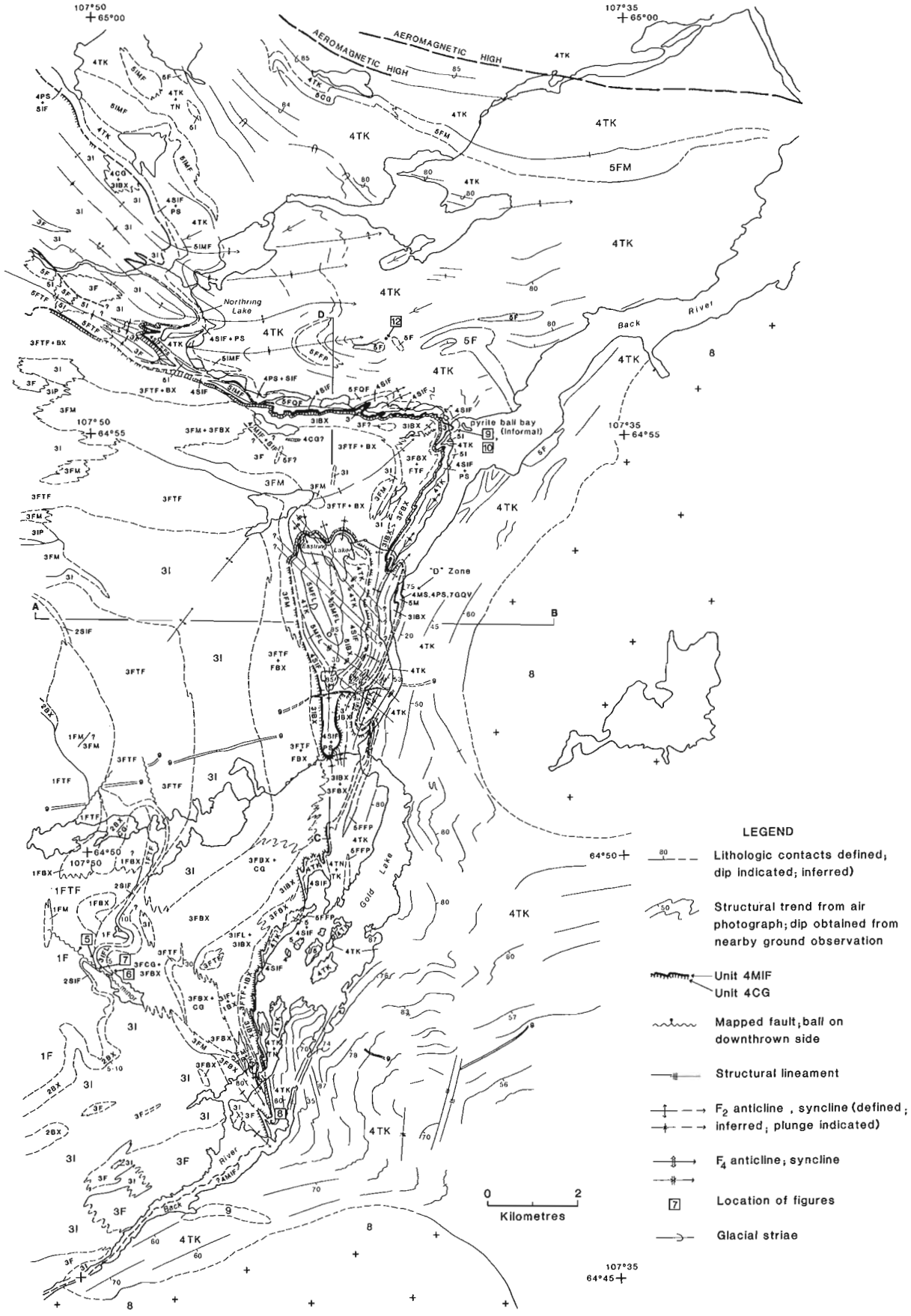

Figure 3. Southeastern side of the Back River complex (Fig. 1), compiled at 1:50 000 including data from Lambert (1981), Moore (1977) and 1:10 000 scale mapping of this study. Map units are listed in Figure 2 and Table 1. Numerals in boxes show locations of figures in this paper. Eastring Lake Syncline is the guitar-shaped structure west of the D-Zone with Eastring Lake at its north end.

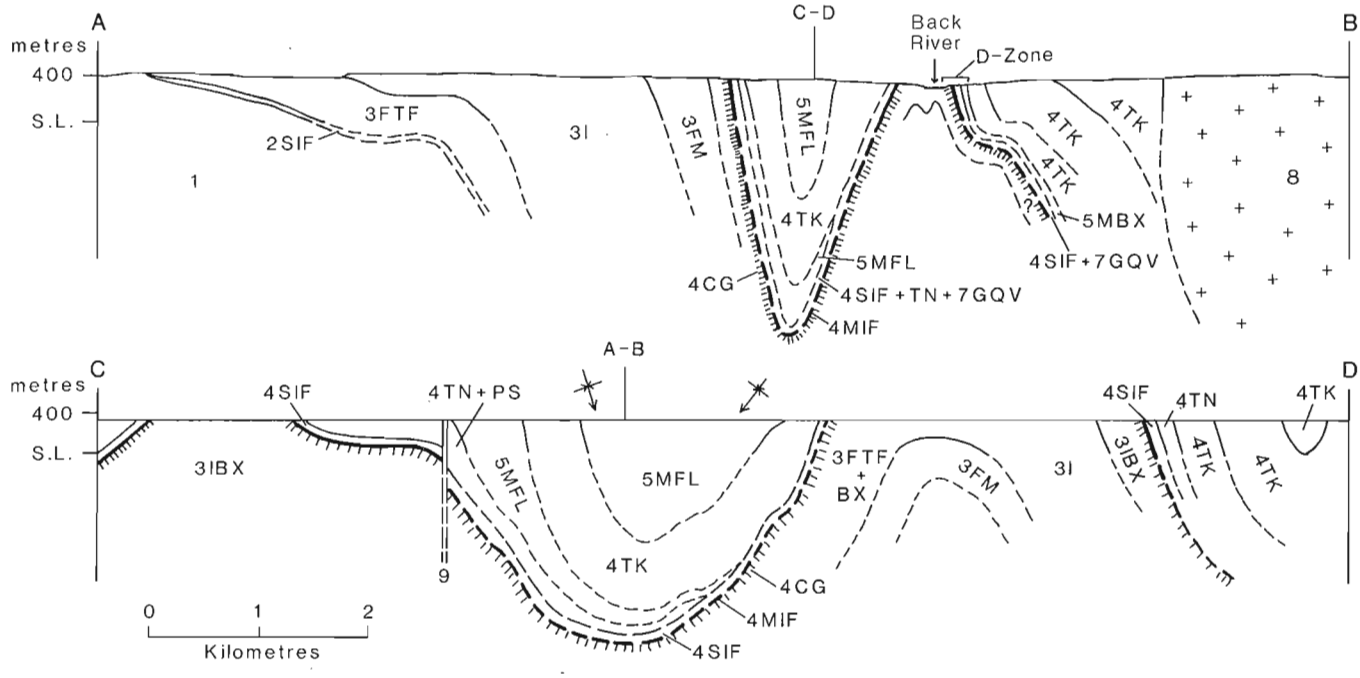

Figure 4. Tentative cross sections of the Eastring Lake Syncline located in Figure 3. A-B: east-west projection. C-D: projection along approximate axis, depth inferred from projection of axial plunges.

Figure 5. Bedded cherty sulphidic tuffs of unit 2 overlain and downcut by massive felsic flow of unit 3 (location in Fig. 3). GSC 204686-D.

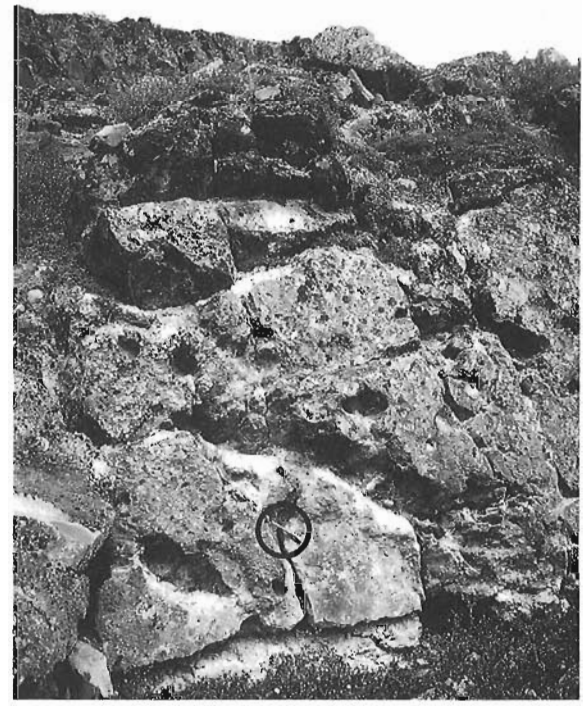

Figure 6. Breccia at the top of unit 2 (location in Fig. 3); holes are rimmed by relict massive pyrite. Hammer is circled. GSC 204686-A.

4CG and contains ash-tuff interlaminae near its base. Iron-bearing silicate minerals range from chlorite in lower metamorphic facies through grunerite and hornblende in higher metamorphic facies. The ratio of chert to the sum of magnetite and siderite ranges from about 2:3 to 3:2 over lateral distances of kilometres. Pyrite is locally disseminated as small cubes and also forms thin veins that crosscut and invade the laminae.

Sulphidic rocks overlie 4MIF, range in thickness up to 30 m and include three extensively drilled subunits (4SIF, 4MS and 4PS) whose weathering products form a continuous zone of orange frost boils with blocks of grey sulphidic vein quartz (7GQV, Fig. 11), volcanic breccia (5IBX) and powdery bleached chert. Subunit 4SIF comprises greyish bedded chert with discrete laminae of fine-grained pyrite, as well as bands of abundant disseminated pyrite.

Subunit 4MS is breccia with a texturally massive matrix of pyrite near its base, grading upward to pyrrhotite with minor chalcopyrite. The breccia is interpreted as tectonic because the angular, centimetre-sized fragments are composed of immediately adjacent rock types (e.g. 5IBX, 7GQV, 4PS and 4TN) and the walls of some fragments are matched. In contrast, the volcanic breccia (subunit 5IBX) has an intact, somewhat rounded framework and contains mainly disseminated sulphide minerals.

Black pyritic slate (subunit 4PS) is the uppermost of the sulphide-bearing rocks, but is locally intercalated with the lower sulphidic subunits. The slate is 10 to 15 m thick and comprises two rock types interbedded on a scale of 1 to 10 cm: massive to laminated black graphitic slate to porcellanite, and massive to subtly graded very fine grey sand to silt (less than 15 % by volume). In drill core and at 'pyrite ball bay' (Fig. 3, 9) the pyrite and pyrrhotite are sparsely to densely disseminated in millimetre to centimetre laminae, form botryoidal clusters, and are injected into brecciated slate.

The overlying thick-bedded turbidites (subunit 4TK) form decimetre-thick packages which are rhythmically alternated with thin-bedded graphitic turbidites (subunit 4TN) and intercalated with volcanic rocks of unit 5. The turbidites are 100 m thick in the Eastring Lake Syncline (Fig. 3); at least 1.5 km thick east of Back River and between Northring and Fidler lakes. The beds in subunit 4TK are massive to trough cross-laminated, one to several metres thick, and contain abundant clear quartz grains. These are among the most coarse-grained and thick-bedded turbidites in the Slave Province (Henderson, 1975).

Figure 7. Gently north-plunging, east-verging fold (F2?) deforms sulphidic turbidites of unit 2 and a weak bedding-parallel foliation. View toward north (location in Fig. 3), GSC 204684-A.

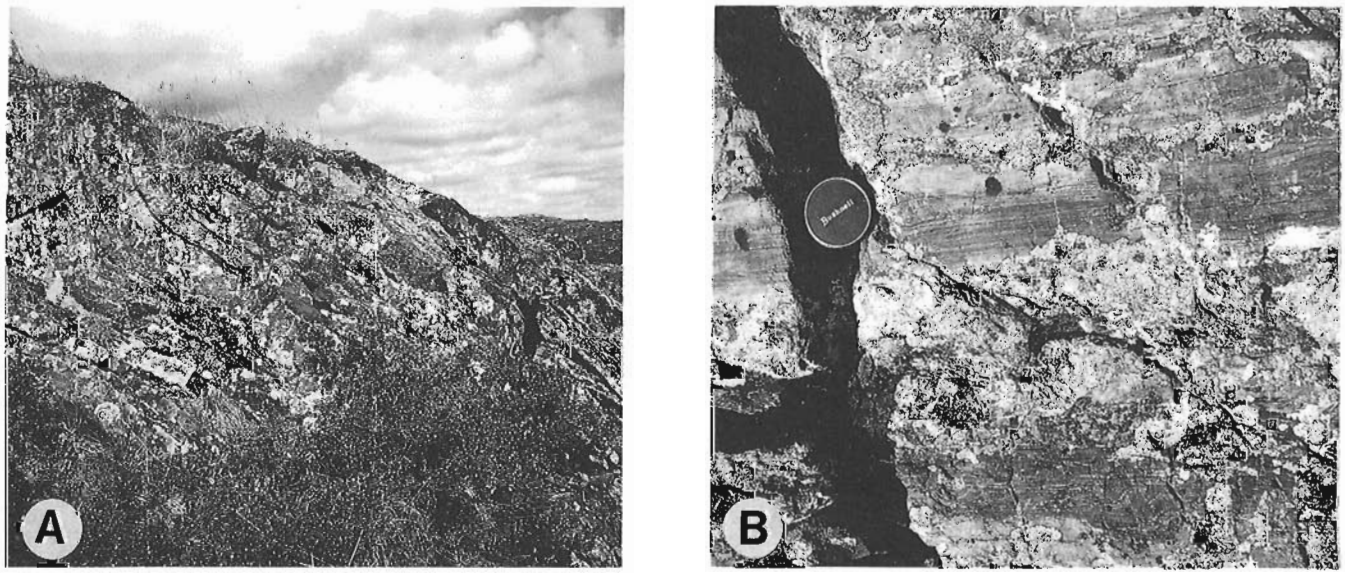

Figure 8. Typical magnetite-chert iron-formation (4MIF). A: open fold (F3) with spaced fracture cleavage, south of Gold Lake (location in Fig. 3), width of view about 5 m, GSC 204686-K. B: detail of laminae, lens-cap 5.5 cm, GSC 204686-I.

Unit 5

Unit 5 comprises volcanic and shallow intrusive rocks that overlie subunit 4MIF, are intercalated with and form lenses within the remainder of unit 4, and underlie subunit 6MIF (Table 1). Unit 5 includes many rock types which are similar to those of units 1 and 3, and which have been described in the series of reports cited by Lambert (1982). Near Back River, fragmental rocks of unit 5 generally fine upward, are less than 10 m thick and are intercalated between 4MIF and 4PS. Carbonate and sulphide minerals are disseminated in both fragments and matrix. Where unit 5 is absent 4MIF grades upward to 4SIF over about 10 cm.

In the Eastring Lake Syncline (Fig. 4) the sequence above subunit 4MIF comprises 100 m of thick-bedded volcanic debris flows, 1 m of pyritic slate (4PS) with stratabound quartz vein (7GQV), 50 m of amygdaloidal mafic flows (5MFL), 100 m of thick-bedded turbidites (4TK), and 100 m of jointed amygdaloidal mafic flows (5MFL).

Most of the large feldspar porphyries (5FFP), quartz-feldspar rhyolite lenses (5FQF), and massive biotite-foliated intermediate intrusions (5IMF) mapped in Figure 3 are located in pyritic slates (4PS) and thick-bedded turbidites (4TK) between 50 and 300 m above 4MIF.

Numerous disconnected intrusive and extrusive assemblages up to several kilometres wide in the northern part of Figure 1 are tentatively assigned to unit 5. Many of these assemblages are flanked laterally by breccias and conglomerates, and overlie turbidites (Lambert, 1982). The second chemical-sedimentary sequence is inferred to separate contiguous volcanic rocks of unit 3 from overlying units 4 and 5 in this area. Volcanic rocks mapped by Lambert (1981) in the Fidler Lake area are also tentatively assigned to unit 5.

Unit 6, upper chemical and clastic strata

Unit 6 includes the third chemical sedimentary sequence and overlying greywackes which have been examined for this study only at locality 10 in the Fidler-Regan lakes area (Fig. 1). Some turbidites of unit 4 intervene between units 5 and 6, and volcanic rocks of unit 5 appear to lense out beneath unit 6 toward the southeast. Recessive hematitic slates (6HS) and thin bedded turbidites (6TN) contain the third iron-formation (6MIF). Differences between these rocks and their unit 4 counterparts (4PS, 4TN and 4MIF) are as follows:

(1) Thin-bedded turbidites and slates, at least 100 m thick, separate 6MIF from underlying volcanic rocks and host the magnetite iron-formation. In contrast, volcanic and shallow water carbonate rocks are proximal to, and intercalated with, iron-formation 4MIF.

(2) The iron-formation 6MIF, although banded, commonly has less than 10% chert compared to 40-60% in 4MIF. It is composed mainly of magnetite with a significant proportion of argillaceous clastic sediment and variable amounts of hematite. Bedding is less distinct and S2 cleavage much better developed (Fig. 10) than in 4MIF (Fig. 8).

(3) Pyrite and pyrrhotite the third chemical sedimentary sequence are located mainly in small pods associated with white quartz veins and in cross-cutting shear zones (Cunningham and Glatiotis, 1988).

(4) The black slates (6HS) contain hematite but little pyrite, in contrast to the pyritic subunit 4PS.

(5) The associated quartz veins are smaller, less abundant and white (7WQV) compared to the grey quartz veins (7GQV) in subunit 4SIF.

(6) Subunit 6MIF has a very strong aeromagnetic anomaly whereas 4MIF cannot be distinguished aeromagnetically.

Units 7 to 11, quartz veins and igneous intrusions

Grey resistant quartz veins (7GQV) are best developed in the area of the Eastring Lake Syncline, especially in the D

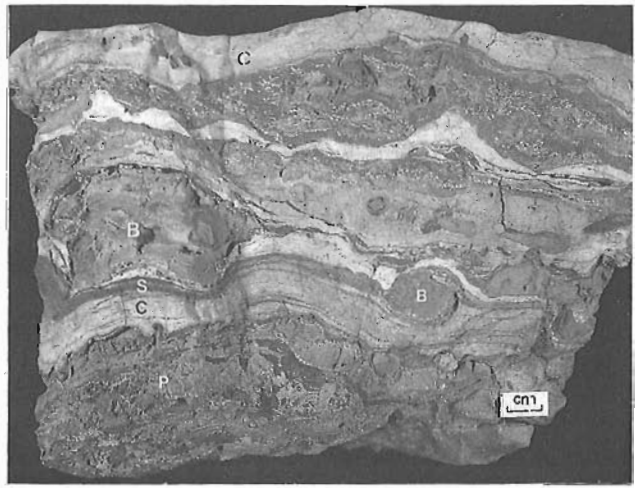

Figure 9. Finely laminated densely disseminated pyrite (P) and botryoidal pyrite (B) and chert (C)of subunit 4PS from 'pyrite ball bay' (Fig. 3).

Figure 10. Well cleaved (steep S2) indistinctly banded oxide facies of iron-formation (6MIF), north of Regan Lake (Fig. 1). GSC 204686-L.

zone (Fig. 3) of Moore (1977) who termed them "Toby quartz". The veins are oriented sub-parallel to bedding but are locally crosscutting at low angles. They are stratabound in that they are restricted to the sulphidic (4SIF, MS, PS) subunits. The veins range from 1 cm to 20 m in apparent thickness and consist of black to light grey quartz with crack-seal inclusions of graphitic slate (Fig. 11). Minor pyrite, arsenopyrite and ankerite are irregularly concentrated on their margins. The veins are auriferous (see "Distribution of Gold").

Igneous intrusions include diorite to quartz monzonite plutons of the Regan Intrusive Suite (8) and gabbro-diabase dykes of several orientations and ages (units 9, 10, 11) which have been described by Lambert (1981, 1982) and Hill and Frith (1982).

STRUCTURE

Four possible generations of folds have been observed based on overprinting relationships and style. The first generation of structures is expressed as small, isoclinal, intrafolial folds (F1) (Fig. 12) and axial-planar bedding-parallel foliation (S1). F1 was rarely observed, and conclusive overprinting relationships with younger folds are lacking, however S1 is crenulated by S2 (Fig. 13). In massive units S1 is expressed as a poorly developed differential layering which has been folded by younger structural elements.

The main deformation (F2) is recorded by very large open folds of the volcanic rocks and tight, moderate to steeply plunging, cylindrical folds which verge toward closures of the very large folds. The abrupt changes in the contact between units 3 and 4, previously interpreted as faults, were traced as steeply plunging F2 folds (Fig. 3). Gently north-plunging, east-verging folds observed in unit 2 (Fig. 7) differ in orientation but are tentatively assigned to F2 as they are of similar style and also deform a bedding-parallel foliation.

The distinct foliation throughout the region is S2, axial planar to the main folds. S2 is a very finely spaced crenulation cleavage (Fig. 13) with slaty aspect in the turbidites, and a more widely spaced crenulation cleavage in volcanic rocks. A moderately plunging to subhorizontal stretching lineation (L2) is located in the plane of S2. In the southern portion of the study area where the metamorphic grade increases towards amphibolite facies, L2 is expressed by the alignment of elongate metamorphic porphyroblasts in the plane of S2. S2 is typically refracted at interfaces between argillaceous and arenaceous beds in the turbidites. Small pull-aparts involving blocks of arenaceous beds within more argillaceous material are interpreted as products of stretching along F2 fold limbs.

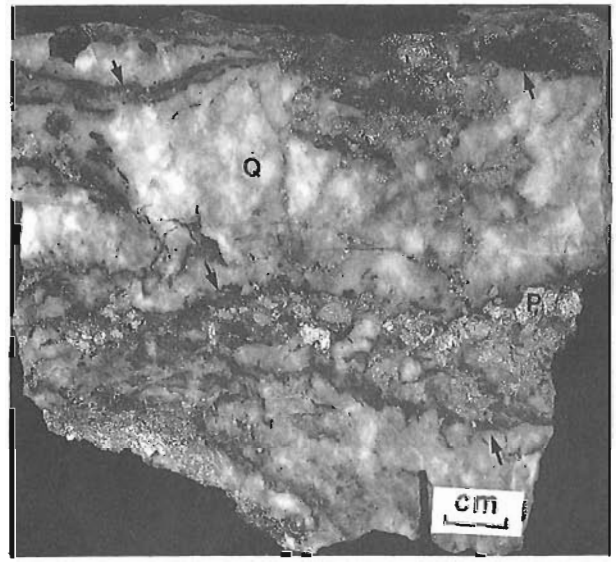

Figure 11. Pyrite (P) and crack-seal inclusions of slate (arrows) in grey quartz (Q) vein (7GQV) from 'pyrite ball bay' (Fig. 3).

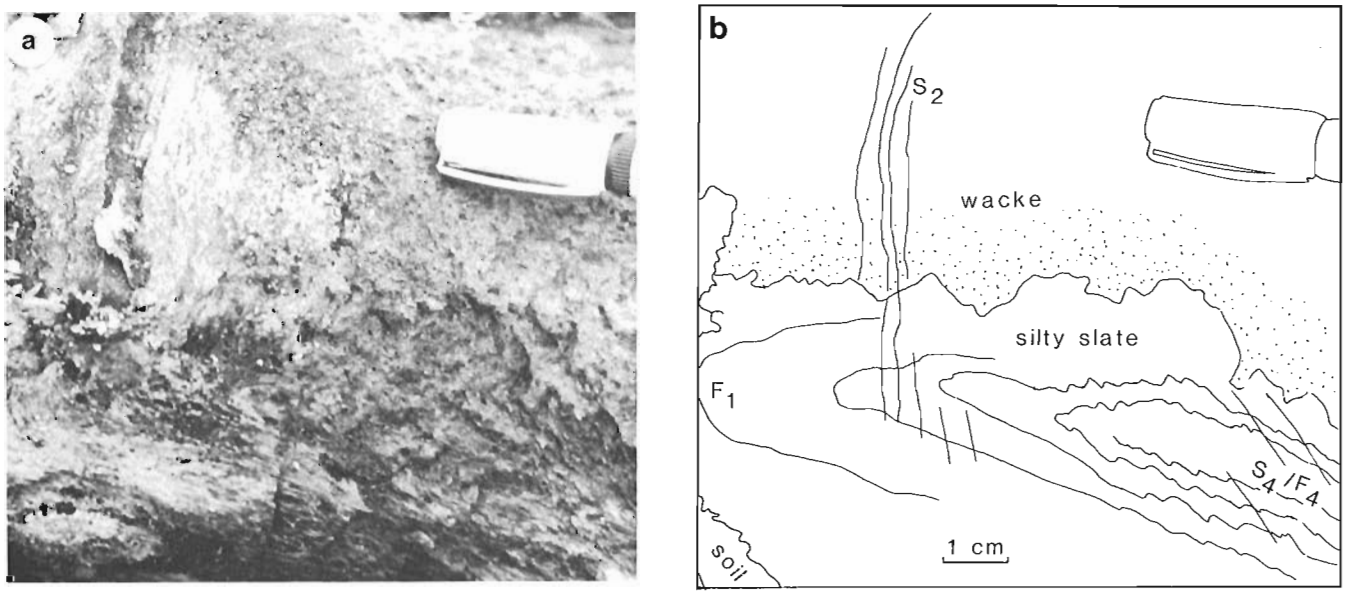

Figure 12. Example of intrafolial folds (F1) located in eastern and northern domain (Fig. 3). a: photograph; b: sketch from photograph.

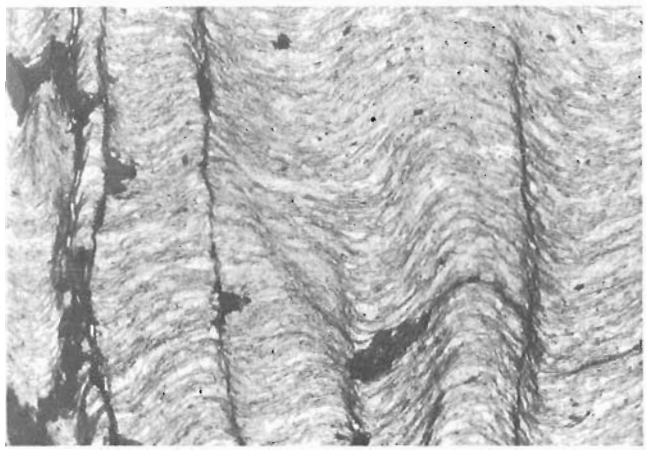

Figure 13. Typical S2 cleavage crenulations of S1 fabric in argillaceous turbidite, plane polarized light, width of view 900 μm.

The best documented very large folds of the volcanic complex are the south-plunging anticline which was recognized by Lambert (1981) east of Magrum Lake (Fig. 1) and the northeast-plunging anticline west of 'pyrite ball bay' (Fig. 3). A facies change between locally bedded felsic (3FBX) and andesitic (3IBX) pyroclastic rocks occurs along the axis of the northeast-plunging fold. Two other very large anticlines are inferred at the northwest and southeast corners of the large dome which is centred on unit 1. The extensions of the axes of these four very large folds are the boundaries of four structural domains (Fig. 1): northern, eastern, southern, and western. Within each domain the trends of large to small main folds and related cleavages are relatively uniform and differ from those of adjacent domains. The different main cleavage trends in the northern and eastern domains (Fig. 14) are interpreted as being of the same generation for the following reasons:

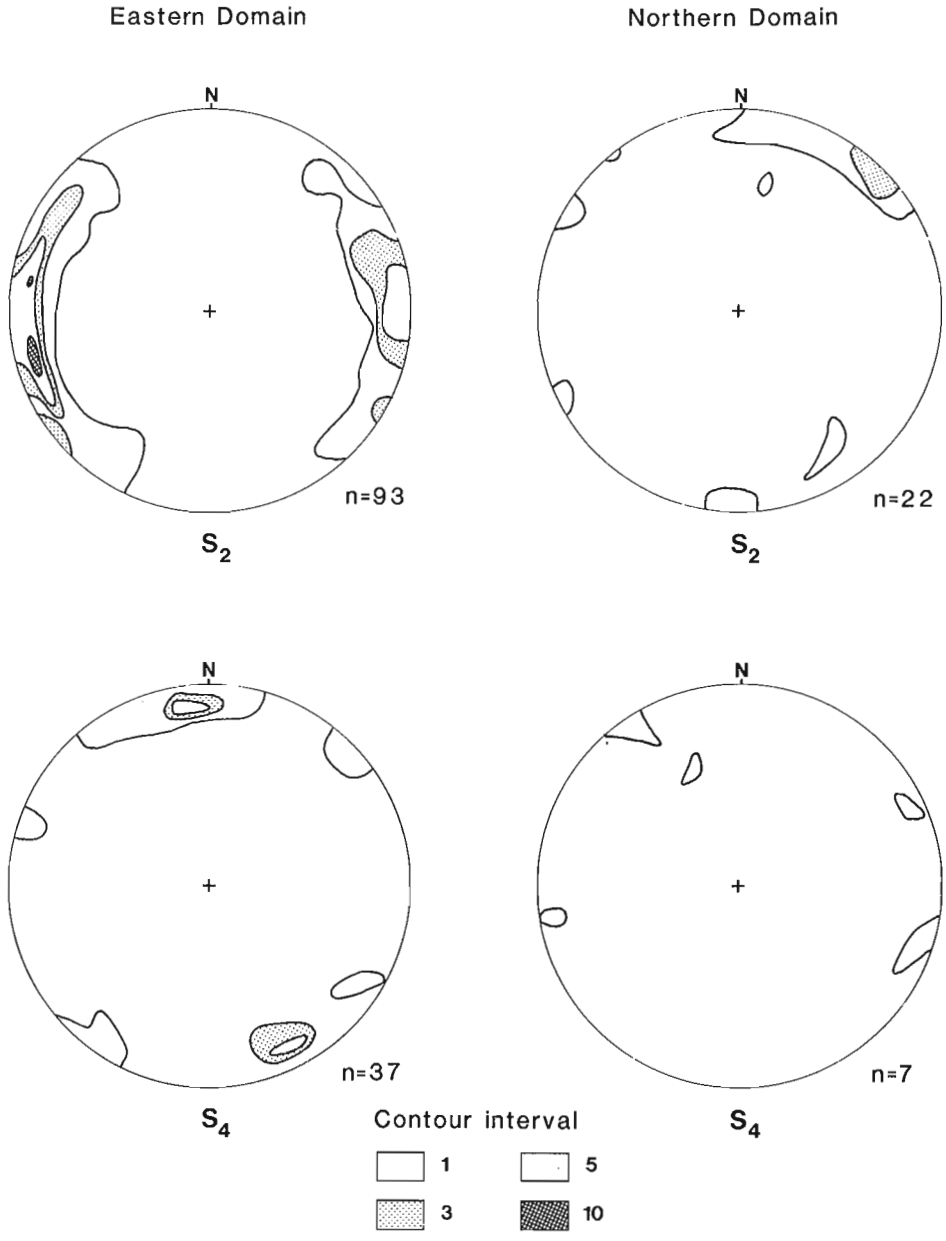

Figure 14. Contoured (% area) lower hemisphere equal-area projections of major structural elements in eastern and northern structural domains.

(i) they and their associated folds are of the same style;

(ii) overprinting relationships are consistent in each domain;

(iii) the main parasitte folds related to S2 in each domain verge toward the very large fold, closure at 'pyrite ball bay'.

The northern domain is characterized by overall east-west-trending folds whose axes plunge easterly and curve gently in a southward-convex arc within the area of Figure 3. In detail, S2 strikes northeasterly at the transition from unit 3 to 4 (northern Fig. 3), east-west within the turbidite sequence (units 4, 5) and east-southeasterly in the area of Regan and Fidler lakes (Fig. 1).

The eastern structural domain is characterized by generally north-south-trending S2. Most F2 folds affecting the contact between units 3 and 4 are strongly asymmetric. North of 61°51'N the folds plunge northeasterly and south of this latitude the folds plunge southeasterly. Limbs of F2 folds are strongly attenuated and sheared parallel to S2, with sedimentary stratigraphy being locally truncated against the volcanic rocks.

The large, guitar-shaped, Eastring Lake Syncline (Fig. 3, 4) is named after the lake at its north end. This syncline may be either a disharmonic second generation sheath fold, an interference basin caused by refolding of a large F1 structure by F2, or a combination of the two. Within the eastern structural domain, it is anomalous in several ways:

(a) It is a doubly plunging syncline, with very steep southerly plunges at the north end that oppose others of the eastern domain near it.

(b) The infolding of unit 4 sedimentary rocks into unit 3 has not been observed elsewhere in the area of Figure 3.

(c) The 50 m and 100 m sequences of basalt flows (5MFL) which brackett thick-bedded turbidites (4TK) are not present elsewhere in Figure 3.

(d) Numerous gold occurrences have been determined by prospecting and drilling (Moore, 1977) around this structure.

Very large folds of the volcanic rocks (F2?), other than the four noted above, are inferred from air photographs and from structural-stratigraphic data presented by Lambert (1981). One such inferred fold is the doubly plunging anticline cored by unit 3 which extends northwest from Northring Lake (Fig. 1). The southeast end of this structure comprises a number of smaller folds whose axes curve easterly within sedimentary rocks of unit 4 (Fig. 3).

The third generation of structures comprises shallowly plunging, open kink folds (F3), associated weak axial planar crenulation cleavage (S3) and weak, shallowly plunging crenulation lineation on S2 surfaces. In relatively competent rocks S3 forms rare fracture cleavages which transect S2. These structures were observed in the southern area of Fig. 3 and their relationship to the steeply plunging kink folds (F4) are not yet defined.

The youngest structures are open, commonly steeply plunging kink folds (F4) which locally form conjugate box folds. The orientation of the associated foliation (S4) is generally at a high angle to S2 and cleavage morphology varies depending on the competency of the host rocks. S4 in units 4 and 6 (turbidites) is a distinct, spaced, crenulation cleavage, locally differentiated in argillaceous beds. In relatively competent units, S4 is commonly a spaced fracture cleavage. The northwest-trending folds that refold the Eastring Lake Syncline and the irregular folds in unit 4 between the two plutons to the southeast (Fig. 3) are possibly F4.

Minor vertical faults post-date most folds and significantly affect outcrop patterns mainly in units 1 and 2 where dips are very shallow. A northeast-side-down offset of about ten metres is suggested for the northwest-trending fault at localities 5, 6, 7 on Figure 3.

METAMORPHISM

A northeast-to-southwest metamorphic facies gradient within the southern part of Figure 1 comprises chlorite-grade lower greenschist (between Northring Lake and the Back River) through biotite-almandine garnet (Moore, 1977) upper greenschist (east side of volcanic complex) to lower amphibolite facies defined by staurolite-corderite-andalusite (Magrum Lake area). The metamorphic gradient appears to have been developed during or shortly after S2, because the above porphyroblasts are elongate and concentrated along S2.

Possible early alteration of subunits 3IVC/FVC which immediately underlie the carbonate grit (4CG) is suggested by restricted development of garnets in them at greenschist metamorphic facies. In upper greenschist to amphibolite facies rocks, garnets are widespread.

DISTRIBUTION OF GOLD

Moore (1977) noted three key aspects of gold distribution:

1. Significant gold in iron-formation and associated rocks has been found mainly in the vicinity of the Eastring Lake Syncline (Fig. 3, 4).
2. Sulphide (4SIF) and oxide (4MIF) facies of iron-formation average about 60 ppb Au, grey quartz veins (7GQV) about 700 ppb Au, and the chert and chert-sulphide breccia (4MS?) about 1300 ppb Au.
3. The grey crack-seal quartz veins (7GQV) contain up to 85 000 ppb Au.

Moore (1977) concluded that the gold was concentrated first in the iron-formation by exhalative processes, then remobilized during metamorphism into the quartz veins along with arsenic and bismuth. Moore's conclusions are compatible with our preliminary data. The grey quartz veins are similar to auriferous crack-seal quartz veins in the Meguma Group of Nova Scotia, which are interpreted to have developed early during a main deformation event (Henderson and Henderson, 1986). Fluid overpressures (ie. fluid pressures larger than confining pressure) during the early stage of folding caused separation along planes of weakness, i.e. bedding, which were at that time oriented approximately parallel to the maximum principle stress. Fluids moving at this time might have been capable of carrying gold (Henderson and Henderson, 1986).

In the detailed study area the grey quartz veins and the disseminated pyrite and pyrrhotite are deformed by F2. Disseminated coarse-grained arsenopyrite associated with the veins is relatively undeformed, suggesting that arsenic was mobilized after D2. The timing and mechanism of gold emplacement are not yet determined.

SUMMARY AND DISCUSSION

The upper part of the Back Group volcanic complex and the sedimentary Beechy Lake Group are interfingered. Three ferruginous chemical sedimentary sequences (units 2, base of 4, base of 6), each less than 100 m thick, provide marker units that may be useful in formal subdivisions and regional correlations of the two groups. Unit 2 is sulphide-dominated and volcanic-hosted; the base of unit 6 is oxide-dominated and sediment-hosted. The most auriferous chemical sedimentary sequence begins at the base of unit 4 with iron-carbonate-cemented volcanic breccias and grits, overlain by oxide-facies iron-formation, in turn overlain by sulphide-facies iron-formation and sulphidic slates intercalated with discontinuous volcanic and shallow intrusive rocks.

Because the entire chemical sedimentry sequence of 4CG through 4PS is ferruginous, the paleo-environment apparently remained enriched in iron throughout the time represented by deposition of this sequence. The development of iron-formation as a distinct and laterally continuous facies was therefore dependent on the reduction of fragmental input into the depositional basin. During times of higher fragmental input (volcanic and clastic) the concentration of ferruginous minerals was diluted, but iron-rich rocks such as the siderite-rich and pyrrhotitic carbonate grit, sulphidic volcaniclastic rocks and shales continued to be deposited. The carbonate, oxide and sulphide ferruginous units appear to be the products of original depositional and diagenetic conditions, with limited replacement reactions. The pronounced vertical variation and lateral continuity of ferruginous subunits at the base of 4 and 6 therefore suggest basin-wide changes in f_{S_2}, f_{CO_2}, f_{O_2} and pH during their deposition. The apparent lack of carbonate and sulphide facies of iron-formation at the base of unit 6 may be related to the general lack of volcanic activity during its deposition.

Very large folds of the volcanic rocks and tight, cylindrical, parasitic folds on their limbs (all F2) are responsible for the main deformation of units. Steeply plunging parasitic folds offset the volcanic-sedimentary (3-4) contact, as shown in Figure 3. Easterly and northerly trends of distinct axial planar crenulation cleavages (S2) respectively characterize the northern and eastern structural domains in the area of Figure 3. Steeply and shallowly plunging open kink folds (F3, F4?) trend northerly and northwesterly in the same area.

Significant concentrations of gold have been found in grey, sulphide-bearing quartz veins (Moore, 1977) that are bedding-parallel, were formed during early stages of second-generation deformation and were later deformed by these folds. These veins are best documented in the vicinity of the Eastring Lake Syncline.

ACKNOWLEDGMENTS

Helicopter support by Polar Continental Shelf Project was shared with W.A. Padgham (Indian and Northern Affairs Canada). Fixed wing support was shared with R. Johnstone (Government of Northwest Territories). Access to core was provided by Silver Hart Mines Ltd., Cominco Ltd., and Pamorex Minerals Inc. (G.G. Goucher). Discussions with J.R. Henderson, M.N. Henderson, K. Mann, and F. Robert provided insight into map problems. Constructive reviews and discussions with G. Gross, J. King, M.B. Lambert, D. Moore, C.R. Van Staal and P.F. Williams improved the paper. Technical assistance by N. Kim, R.D. Lancaster and W.A. Spirito is much appreciated.

REFERENCES

Cunningham, M. and Glatiotis, M.
1988: Geology and structure of Algood Claims, Regan Lake area (abstract); in Exploration Overview 1988, Northwest Territories Geology Division, Indian and Northern Affairs Canada, p. 31-32.

Frith, R.A.
1987: Precambrian geology of the Hackett River area, District of Mackenzie, N.W.T.; Geological Survey of Canada, Memoir 417, 61 p.

Henderson, J.B.
1975: Sedimentological studies in the Yellowknife Supergroup in the Slave Structural Province; in Report of Activities, Part A, Geological Survey of Canada, Paper 75-1A, p. 325-330.

Henderson, M.N. and Henderson, J.R.
1986: Constraints on the origin of gold in the Meguma Zone, Ecum Secum area, Nova Scotia; Maritime Sediments and Atlantic Geology, v. 22, p. 1-13.

Hill, J. and Frith, A.A.
1982: Petrology of the Regan Lake Intrusive Suite in the Nose Lake - Beechy Lake map area of District of Mackenzie, N.W.T.; Geological Survey of Canada, Paper 82-8. 26p.

Lambert, M.B.
1976: The Back River Volcanic Complex, District of Mackenzie; in Report of Activities, Part A, Geological Survey of Canada, Paper 76-1A, p. 363-367.
1978: The Back River Volcanic Complex - a cauldron subsidence structure of Archean age; in Current Research, Part A, Geological Survey of Canada, Paper 78-1A, p. 153-158.
1981: The Back River Volcanic Complex, District of Mackenzie, N.W.T.; Geological Survey of Canada, Open File 848 (1:50 000-scale map).
1982: Felsic domes and flank deposits of the Back River Volcanic Complex, District of Mackenzie; in Current Research, Part A, Geological Survey of Canada, Paper 82-1A, p. 159-164.

Moore, D.W.
1977: Geology and geochemistry of a gold-bearing iron-formation and associated rocks, Back River, Northwest Territories; M.Sc. thesis, University of Toronto, 186 p.

Tremblay, L.P.
1971: Geology of Beechy Lake map-area, District of Mackenzie; Geological Survey of Canada, Memoir 365, 56 p.

Preliminary results on the use of Borehole geophysics in overburden stratigraphic mapping near Geraldton, northern Ontario

C.J. Mwenifumbo, L.H. Thorleifson[1], P.G. Killeen, and B. Elliott
Mineral Resources Division

Mwenifumbo, C.J., Thorleifson, L.H., Killeen, P.G. and Elliott, B., Preliminary results on the use of borehole geophysics in overburden stratigraphic mapping near Geraldton, northern Ontario; in Current Research, Part C, Geological Survey of Canada, Paper 89-1C, p. 305-311, 1989.

Abstract

Geophysical data from four boreholes near Geraldton indicate that two tills in this area are distinguishable by their different signatures in natural gamma ray, density and magnetic susceptibility logs. The thick massive upper till consisting of compact silty diamicton can be divided into three units from the geophysical logs. The upper unit is fairly heterogeneous and has lower radioactivity, lower density and lower magnetic susceptibility than the middle unit which is homogeneous in terms of clay content. The lower unit consists of sand and silty sand diamicton and is characterized by low radioactivity. The lower till, which contains anomalous values of gold and sulphides, is very heterogeneous with large amplitude variations in all the geophysical parameters. Magnetic susceptibility highs within the lower till appear to be related to the presence of locally-derived mineralized debris. Magnetic susceptibility logging, may provide valuable supplementary data for stratigraphic mapping and for identifying sections containing mineralized debris.

Résumé

Des données géophysiques recueillies dans quatre trous de sondage réalisés près de Géraldton, indique que deux tills dans cette région ne peuvent être distingués l'un de l'autre par leurs signatures gamma naturelles, densimétriques et de susceptibilité magnétique. On peut subdiviser l'unité supérieure, massive et épaisse, de till composé d'un diamicton limoneux compact, en trois unités, d'après les diagraphies géophysiques. L'unité supérieure est assez hétérogène et se caractérise par une radioactivité, une densité et une susceptibilité magnétique plus faibles que celles de l'unité intermédiaire, cette dernière homogène du point de vue de sa teneur en argile. L'unité inférieure se compose d'un diamicton sableux et limon sableux, et se caractérise par une faible radioactivité. L'unité de till inférieure, qui contient des teneurs anomales en or et sulfures, est très hétérogène et se caractérise par de grandes variations d'amplitude de tous les paramètres géophysiques. Les pointes de susceptibilité magnétique que l'on observe dans l'unité de till inférieure semblent liées à la présence de débris minéralisés de provenance locale. Le recours à la diagraphie de la susceptibilité magnétique peut se traduire par un apport important de données supplémentaires précieuses pour l'établissement de coupes stratigraphiques et l'identification des coupes contenant des débris minéralisés.

[1] Terrain sciences division.

INTRODUCTION

Studies of the stratigraphy and composition of drift in the Beardmore-Geraldton area have been initiated under the Canada-Ontario Mineral Development Agreement 1985-1990 to test the usefulness of these sediments in exploration geochemistry. Glacially eroded gold and associated sulphides have been detected in the till and studies are underway to determine strategies for tracing this gold to its bedrock source.

Overburden drilling in the Wildgoose Lake area (Thorleifson and Kristjansson, 1988) has indicated the presence of two till units. The upper till is a Paleozoic carbonate-rich till which has been transported southward from the James Bay Lowland with little incorporation of local debris. In contrast, the lower till is locally derived and has yielded gold and sulphide anomalies. Borehole logging measurements were carried out with the following objectives: a) to determine whether till units can be distinguished by borehole geophysics, b) to test for heterogeneity in what appears to be thick massive till, and c) to determine whether sulphide-rich till can be detected. Four holes drilled approximately 14 km west of Geraldton (Fig. 1) were cased with 10 cm thin-walled PVC pipe to ensure that they remained open for borehole geophysical measurements to be made at a later date. Hole R was perforated with vertical slots to facilitate electrical resistivity and induced polarization measurements. All the holes were logged with natural gamma ray, gamma gamma density, magnetic susceptibility and temperature tools. The measurements were carried out in a continuous logging mode. Holes O and R were drilled 50 m apart to depths of 43 and 50 m, respectively. Holes P and Q are 109 m apart with depths of 30 and 32 m, respectively. Although natural gamma spectral logging measurements were recorded, only the total count gamma ray logs which monitor the overall natural gamma radiation from the surrounding media are presented. Low count rates observed in these sediments, in addition to the attenuation of gamma rays by the casing and fluids in these large diameter holes, produced gamma counts in the K, U and Th windows with extremely poor counting statistics. No attempt, therefore, was made to convert these data into concentrations of the three radioelements. Preliminary interpretations of the geophysical logs obtained in these four holes are presented in this paper.

LOG DESCRIPTION AND DATA ACQUISITION

Natural gamma ray

Gamma ray measurements are used to detect variations in natural radioactivity due to changes in the concentrations of the trace elements uranium and thorium, as well as changes in concentration of the major element potassium. The principal source of the natural gamma radiation in sedimentary environments is potassium-40 in clay minerals such as illite and montmorillonite. Also in immature sands, abnormal concentrations of K-feldspar minerals may contribute significantly to the natural gamma radioactivity. Full gamma ray energy spectra were recorded in 256 channels covering an energy range from approximately 0.1 MeV to 3.0 MeV. Four standard windows provide information on total count (0.1 to 3.0 MeV), potassium, uranium and thorium. The scintillation detector used was a 32 mm X 127 mm sodium iodide (NaI(Tl)) detector and the logging speed was 1 m / minute. The gamma ray data were accumulated every 3 seconds giving a sample every 5 cm.

Gamma gamma density

The gamma gamma density probe consists of a Cobalt 60 gamma ray source in addition to a gamma ray detector. The density-probe response is primarily a function of the rock bulk density. Gamma rays emitted by the source are scattered by the enclosing sediments or rocks. Density information is determined from the backscattered gamma rays in the energy window from about 100 keV to 500 keV. The number of backscattered gamma rays is inversely proportional to the electron density of the rock. The electron density of the rocks is also related to secondary physical properties which include porosity, water content and chemical composition of the rock.

The acquisition system for the density data is the same as that used for the natural gamma ray spectral logging. The radioactive source in the probe was a 10 mCi cobalt 60 source and the detector was a 25 mm x 76 mm NaI(Tl) detector. The source-detector spacing for the logging data presented in this paper was 17 cm. All data were acquired with a logging speed of 3 m/minute with sample time of 1 second giving a measurement every 5 cm.

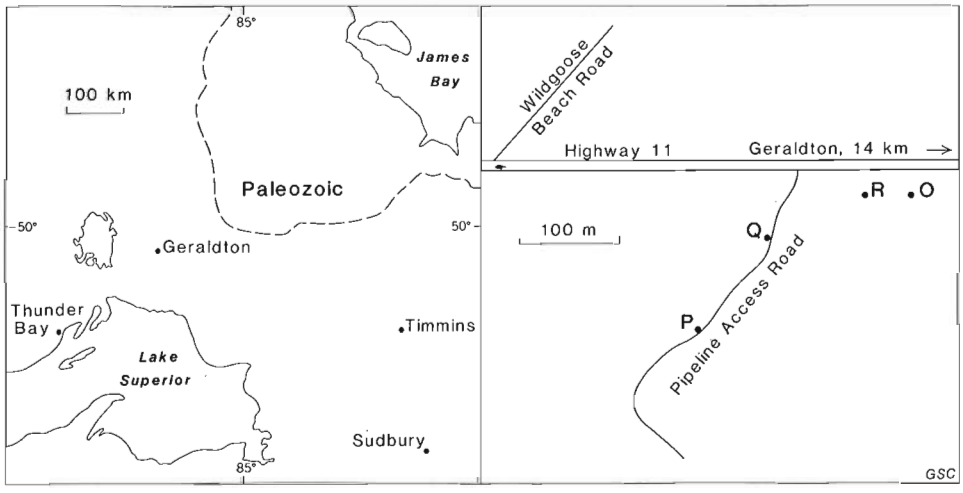

Figure 1. Location map of the boreholes.

Magnetic susceptibility

The magnetic susceptibility of a volume of rock is a function of the amount of ferromagnetic minerals (magnetite, ilmenite and pyrrhotite) contained within the rock. Magnetic susceptibility measurements can therefore provide a rapid estimate of the magnetic minerals in the rock. These measurements may be interpreted to reflect lithological changes, degree of homogeneity and the presence of alteration zones within the rock mass. Susceptibility measurements were acquired with a Geo Instruments probe interfaced to the GSC digital signal processing unit developed by Bristow (1985). There is a choice of four sensitivity ranges on this system (20, 80, 320 and 1280 x 10^{-3} SI units) with the highest setting giving a measurement resolution of approximately 0.005 x 10^{-3} SI units. Susceptibility data are acquired continuously at a sample rate of approximately 5 samples per second. All the holes were logged at 3 m/minute providing a measurement every 1 cm along the hole length.

Temperature

The normal geothermal gradients are perturbed to varying degrees by a number of factors: a) changes in lithology with different thermal properties (thermal conductivity and thermal capacity); b) ground water flow; c) presence of minerals or fluids undergoing endothermic or exothermic processes such as the expansion of gas, the oxidation of sulphide minerals and radioactive decay; and d) seasonal and climatic temperature variations. The most prominent temperature anomalies are those caused by ground water flow, water having a heat capacity 3 to 5 times that of the rock. The objectives of temperature logging in overburden studies are two-fold: a) location of the water table and ground water flow in and out of the borehole, b) lithostratigraphic mapping, assuming a quiet geothermal environment and a reasonable thermal conductivity contrast between the different sediments intersected by the drill hole.

The temperature probe consists of a 10 cm long tip of thermistor beads with a sensitivity of 0.0001 degrees Celsius. Changes in temperature are recorded as changes in the thermistor resistance and then converted into true temperatures with the use of an inverse operator and appropriate probe time constant. The temperature gradients are derived from the temperature data by a combined gradient and smoothing operator. All the temperature logs were run down the hole and the data were acquired continuously. The logging speed was 3 m/minute with data sampled every 1 cm. This high spatial resolution of data is necessary for the determination of accurate temperature gradients with the use of gradient operators.

Stratigraphy

Boreholes O and R encountered two different till sequences: the upper till consists primarily of compact silty diamicton, rich in Paleozoic carbonate granules and pebbles, and the lower till consists of silty and sandy diamicton interlayered with sand. The lower till has a high concentration of locally derived debris including sulphide minerals with few Paleozoics. Hole O was continuously cored to bedrock at 42.9 m and hole R was cored from 25 m to bedrock at 50.3 m. Core was not recovered in the upper section of hole R to reduce costs. It is likely that the lithology intersected in this part of the hole is similar to that of hole O. An additional 1.5 m into bedrock in each hole, was also cased. The bedrock at both sites consists of Precambrian greywacke. Abundant sulphides were encountered at about 41.5 m in hole R. This hole was then cased with perforated casing in order that induced polarization measurements could be carried out to precisely locate the sulphide occurrences.

Boreholes P and Q were drilled 109 m apart intersecting the basement rock at 29.8 and 32.0 m, respectively. Hole P which was continuously cored, encountered only the upper till sequence consisting of compact carbonate rich silty diamicton. Although hole Q was only cored from 25 m to bedrock, it is likely that the upper part of this hole is similar to the neighboring hole P. Bedrock at P is Precambrian greywacke and that at Q is diabase. Some sand layers were found at the base of the till at site Q.

FIELD RESULTS AND DISCUSSIONS

Borehole O

Figure 2 shows the total count gamma ray, gamma gamma density (in arbitrary units), magnetic susceptibility, temperature and temperature gradient logs for hole O. The temperature and temperature gradient logs are plotted on the same track with the temperature identified as T and the gradient log as TG. Based on the gamma ray, density and susceptibility logs, the upper till unit may be divided into 3 units; A, B and C. The upper unit A from 0 to 14.5 m corresponds to the compact silty diamicton, the middle unit B from 14.5 to 30.1 m corresponds to the very compact silty diamicton and the lower unit C from 30.1 to 35 m corresponds to sand and sandy diamicton. Unit A is fairly heterogeneous (see gamma ray and density log) and is characterized by a lower,more variable, gamma radioactivity, density and susceptibility than unit B. Variations in the gamma ray signature are probably due to variations in clay content. A higher clay content (more silty layers) usually correlates with increases in radioactivity. Some of the higher susceptibility values between 3.5-5 m and around 7.5 m correlate with higher density. These zones may contain heavy minerals plus magnetite and/or pyrrhotite. Unit B is characterized by fairly uniform gamma radioactivity. The density and susceptibility logs show an increase in both parameters from 15 to 19 m followed by a fairly constant response towards the base of the unit with the exception of a prominent low density, low susceptibility section around 27-28 m. This zone is similar in character to unit A. Hardness measurements done on the core using a hand held penetrometer indicate that unit B is harder than unit A and probably explains the higher density measurements observed in this unit. An increase in density or hardness is more likely due to compositional and porosity changes. Unit A is probably sandier and more porous. The sand layers in unit C are characterized by lower radioactivity than the silty layers which have higher levels of gamma ray activity similar to those observed in unit B (e.g. 31-32 m). There is a general increase in susceptibility towards the base of unit C with two fairly prominent narrow high susceptibility anomalies.

These anomalies may be due to concentrations of magnetic minerals such as magnetite and/or pyrrhotite (recovered core is being analyzed for magnetic mineral content).

The lower till is divided into two units: D, from 35 to 40.0 m, and E, from 40.0 m to bedrock. Both units contain sand and sandy diamicton layers, however, unit D is very heterogeneous with several zones of anomalously high radioactivity. The average density and susceptibility are lower than unit C above and unit E below, but are highly variable. Sulphides were observed between 37 and 38 m which may explain the higher susceptibilities and densities at this location. Since the lower till consists of locally derived material, some of the variations in the geophysical responses may be due to variations in concentration of bedrock materials.

The upper 15 m of the hole corresponding to unit A shows very large negative temperature gradients which decrease in amplitude with depth. These may be due to several factors; seasonal variations in temperature which propagate downward, low velocity water flow (the upper section is more affected by drainage) and lithological variations. Correlation of the temperature gradients with the other geophysical parameters is therefore difficult. A step change in temperature at about 3.5 m indicates the water level in the borehole. Ambient temperatures at the time of logging were cooler than the borehole fluids and thus we see a cooling effect of the upper metre of borehole water. In general the temperature data show the effects of a warming trend on the ground surface. Because of the shallow depths these effects are more likely a result of annual temperature variations. The decrease in temperature with depth in the till is a result of the colder glaciation temperatures from the time of its deposition which have not yet recovered to reflect the present geothermal gradients (increasing temperatures with depth).

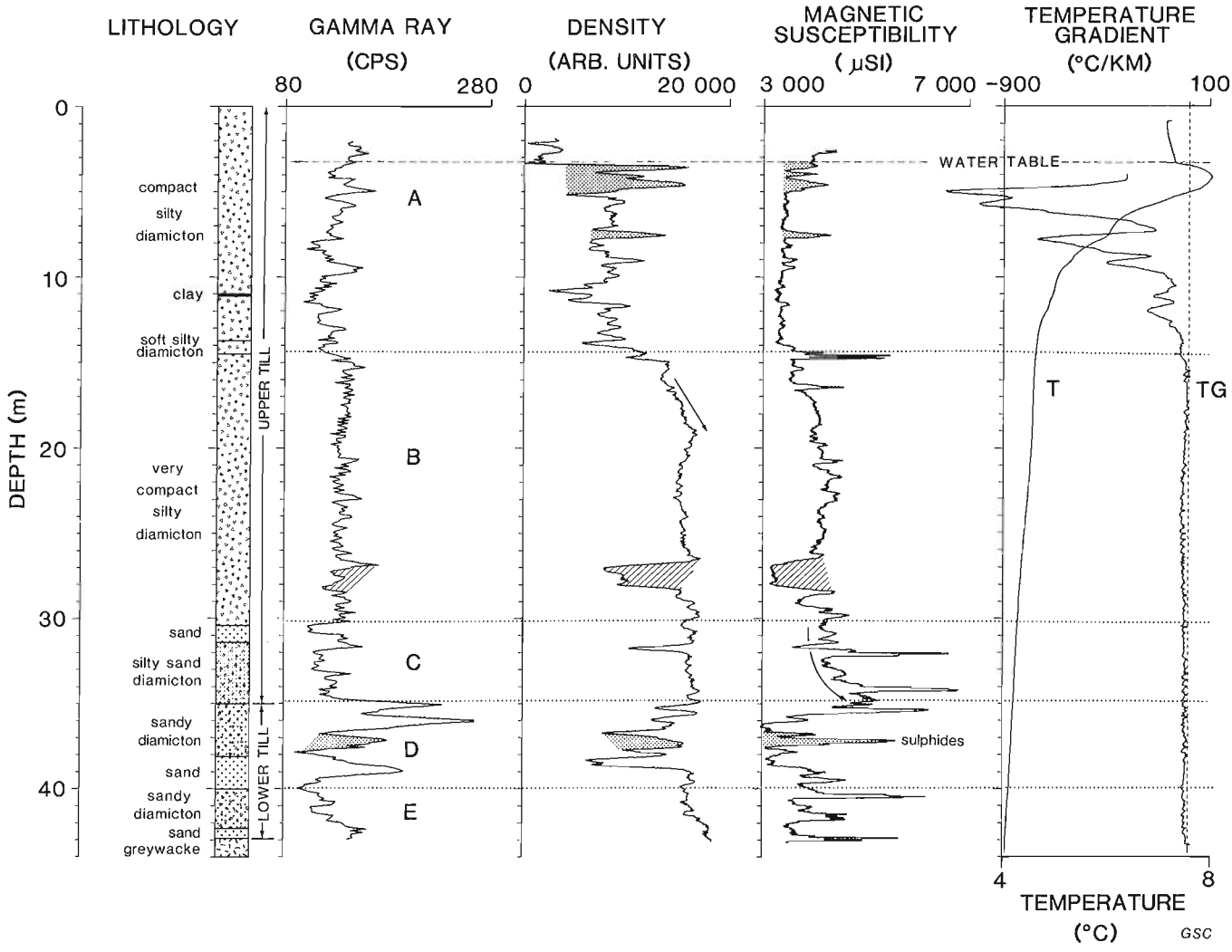

Figure 2. Lithology, total count gamma ray, density (in arbitrary units), magnetic susceptibility, temperature (T) and temperature gradient (TG) logs for borehole O. The letters A, B, C, D and E indicate units derived from the geophysical measurements. Sections showing distinctive correlation between density and magnetic susceptibility are shaded.

Borehole R

Figure 3 shows the natural gamma ray, density, magnetic susceptibility, temperature and temperature gradient logs for hole R. Hole R was cased with perforated casing into bedrock at 50.3 m. However, logs were acquired only to 40 m because the hole filled with sediments. This logged interval mainly consists of the upper till sequence. The susceptibility log shows fairly low and uniform values except for numerous narrow anomalously high zones which may be related to local concentrations of magnetic minerals. The boulder between 32.0 and 33.2 m is an example of local occurrences of material within this till sequence with high susceptibility and density. The till may be divided into three units primarily based on the gamma ray log: unit A, from 0 to approximately 15 m, shows relatively lower gamma ray activity than unit B, between from 15 and 32 m. These two units correspond to units A and B in hole O. Unit C consists of sand and sand-silt-diamicton which is characterized by lower gamma ray activity. Although the changes in radioactivity are relatively small, they are clearly identifiable. The density variation within the entire till sequence are not very characteristic of the lithologic changes as observed in hole R. The top 5 m, however, shows higher density and susceptibility values. This may be a less porous, more dense section of the till reflecting compositional changes.

The temperature data shows almost the same information as was observed in hole O: high negative gradients within the upper unit A. The water level is clearly discernable from the log at approximately 2.0 m. The ambient surface temperatures are cooler than the water temperatures within the first metre below the water table.

Resistivity and induced polarization measurements were discouraging because the noise level resulting from the slotted pipe was quite high relative to the signal level. The resistivity log, however, showed relatively higher resistivities from approximately 32 m to the bottom of the logged interval. This corresponds to the sand-silt diamicton unit C.

Borehole P

Figure 4 shows the lithology, natural gamma ray, density, magnetic susceptibility, temperature and temperature gradient logs for hole P. The lithologic log shows a uniform massive compact silty diamicton of the upper till sequence, but the density and magnetic susceptibility indicate that the upper section of the hole is different from that observed in the lower portion of the hole. The till sequence may be divided into two units: unit A, between 2 and 11 m with a lower density and lower susceptibility and unit B, between

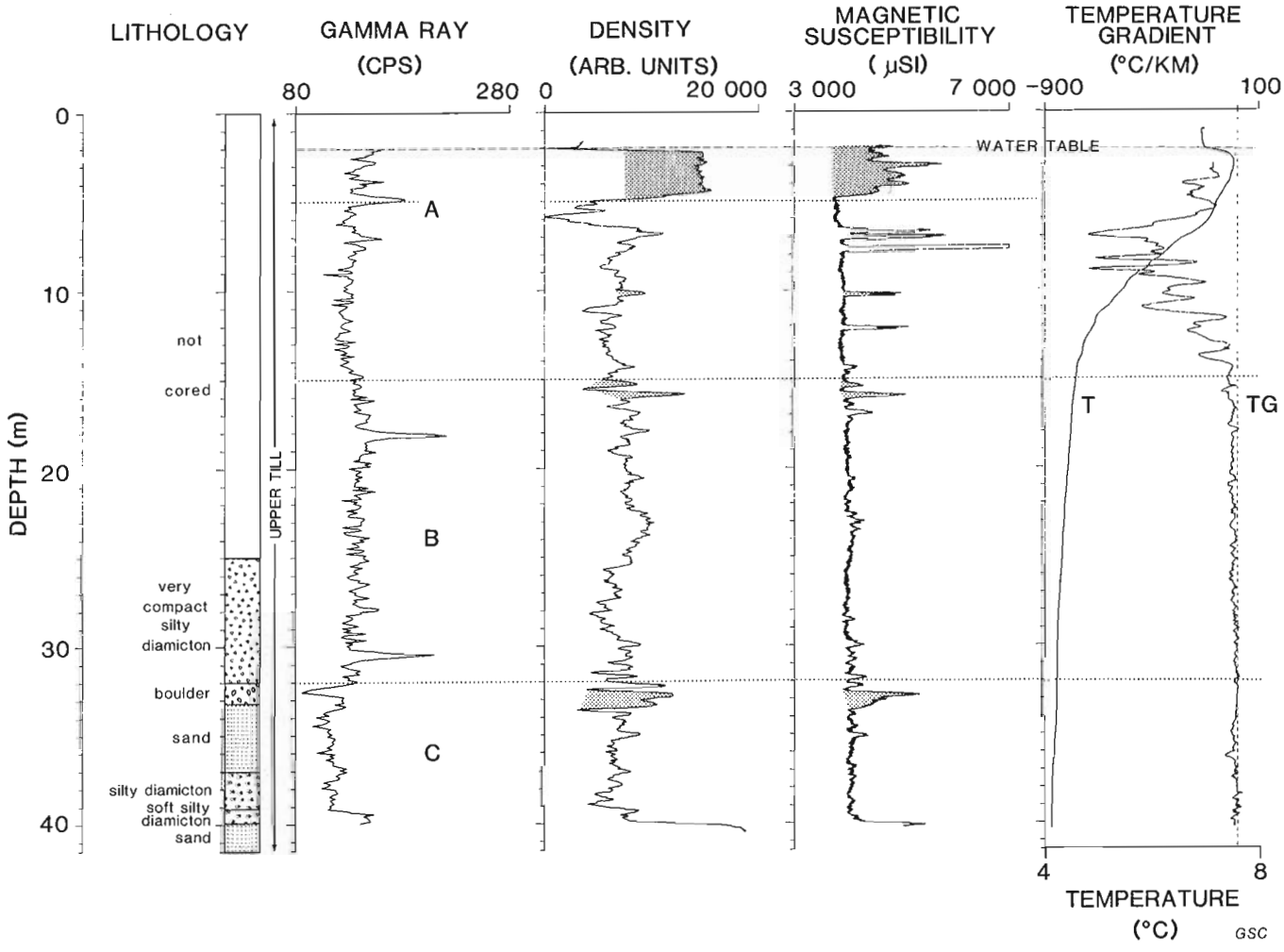

Figure 3. Lithology, total count gamma ray, density (in arbitrary units), magnetic susceptibility, temperature (T) and temperature gradient (TG) logs for borehole R. The hole was cased with perforated casing to bedrock at 50.3 m but was logged only through the Upper Till to 40 m where a blockage occurred. It was cored from 25 m to bedrock. The division of the upper till into units A, B and C is primarily based on the gamma ray log.

11 m and bedrock which is higher. Correlation between density and susceptibility in this upper portion is very good. A higher density in unit B implies that this unit is more compact and different in composition. This is also indicated by the susceptibility data. The gamma ray log shows relatively lower radioactivity in unit A than in unit B which may be due to differences in the clay content between these two units. From 11 m to approximately 18 m within unit B there is a general increase in radioactivity which levels off towards the bottom of the hole. The temperature data again show that the upper sections of these holes behave fairly similarly with respect to surface temperature variations and groundwater movements. The upper sections of these holes are sandier than the bottom sections. The lower susceptibility and density zones between 12 and 14 m correlate with low penetrometer measurements indicating that they are softer and less dense.

Borehole Q

Figure 5 shows the lithology, gamma ray, density, magnetic susceptibility, temperature and temperature gradient logs for hole Q. The gamma ray data show a fairly constant radioactivity with slightly lower values in the top half of the hole between 1 and 15 m. Magnetic susceptibility shows low values down to 22 m; below this depth the susceptibility values begin to increase gradually towards the bottom of the hole, perhaps because there is an increase in locally-derived debris within the till sequence. Between 28 m and the bottom of the hole, the geophysical logs show a decrease in radioactivity and an increase density and magnetic susceptibility. The lithological log indicates layers of sand and silty sand in this part of the hole. This portion of the hole is similar to unit C in the upper till sequence observed in hole O. The density data show more variability all along this till sequence and there are numerous density increases which correlate with increases in the susceptibility and natural gamma ray data (e.g. 16-18 m, 21-23 m). The temperature data indicate that the water level in this hole is at approximately 2.5 m.

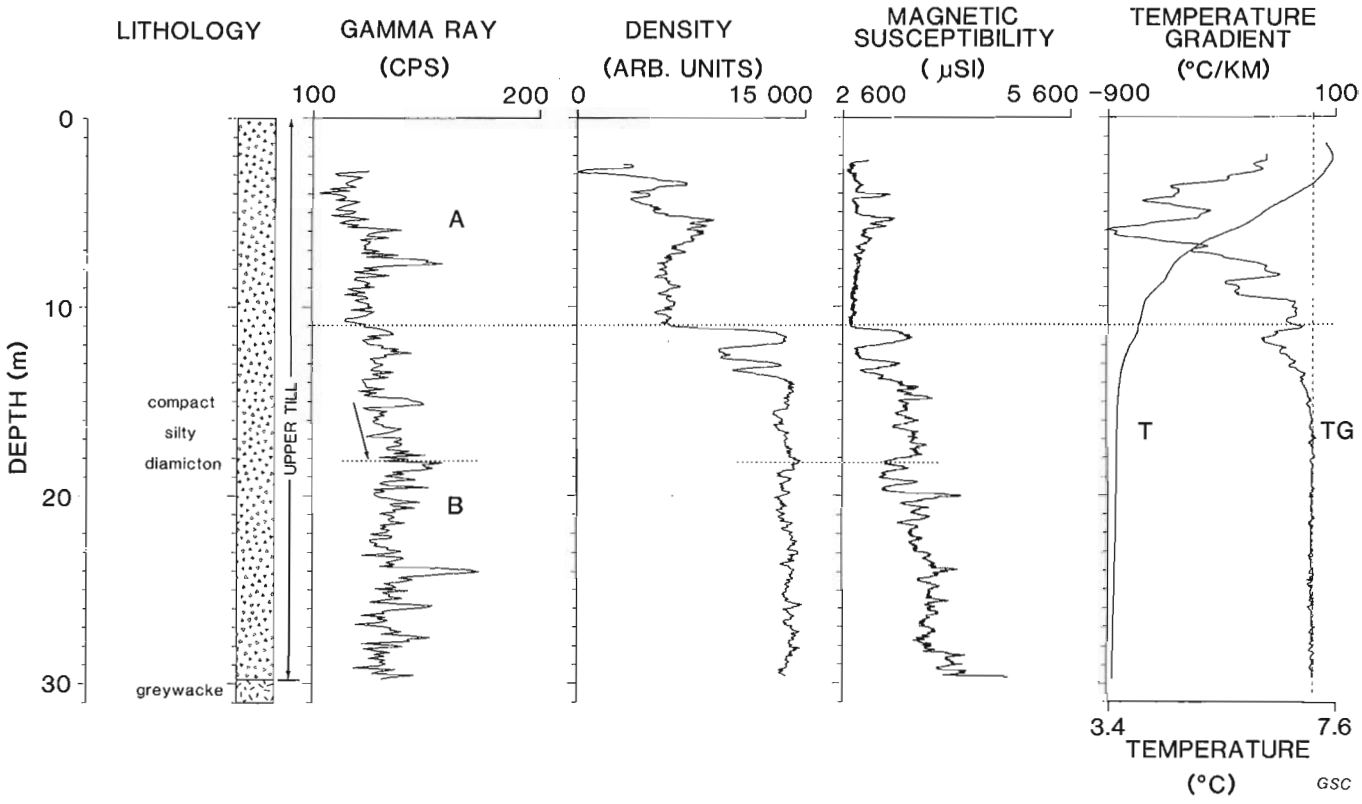

Figure 4. Lithology, total count gamma ray, density (in arbitrary units), magnetic susceptibility, temperature (T) and temperature gradient (TG) logs for borehole P. This hole only encountered the upper till sequence which is divided into units A and B equivalent to those observed in borehole O.

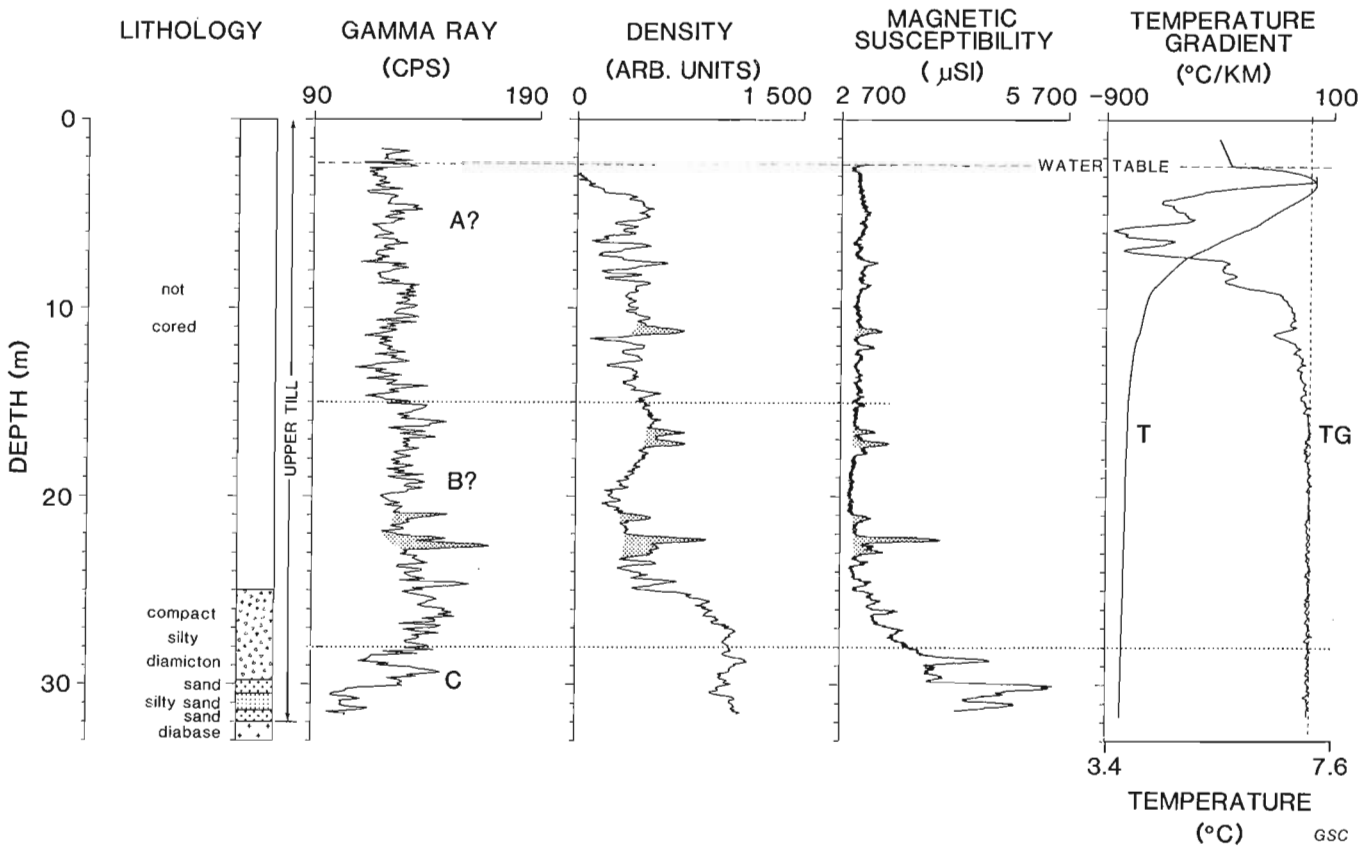

Figure 5. Lithology, total count gamma ray, density (in arbitrary units), magnetic susceptibility, temperature (T) and temperature gradient (TG) logs for borehole Q. Hole Q was cored from 25 m to bedrock at 32 m and intersected only the upper till unit.

CONCLUSIONS

The geophysical data indicate that the upper till sequence of compact silty diamicton may be subdivided into 3 additional units, the upper unit probably being less silty and lower in density than the middle unit. Increases in susceptibility probably correlate with increases in silt content of the diamicton. Variations in natural gamma radioactivity may be interpreted as variations in the composition of the till; the more silty sections showing relatively higher radioactivity due to increased clay content. The bottom part of the upper till is sandier and is characterized by lower levels of radioactivity. The lower till is missing in holes P and Q and even though it was encountered in hole R, geophysical logs were not obtained below the upper till. The lower till observed in hole O is very heterogeneous which is probably due to the variations in the concentration of the locally derived bedrock debris. The underlying bedrock, consisting of greywacke-bearing sulphides, is the likely source for glacially eroded debris which may cause radioactivity and magnetic susceptibility anomalies in the overlying till.

Borehole geophysics does (in this area at least) provide valuable supplementary data and apparently homogeneous sediments are shown to be divisible. The distribution of magnetic susceptibility highs probably relate to the presence of locally-derived mineralized debris. The data also provide a check on core depth measurements as well as the presence and thickness of lithological units inferred from visual inspection of sediment recovered by drilling. Inferences were also made regarding intervals which were not cored. More detailed interpretations on these data will be possible as more information on core laboratory analyses become available.

ACKNOWLEDGMENTS

The overburden drilling program was funded by the Canada-Ontario Mineral Development Agreement Program 1985-1989.

REFERENCES

Bristow, Q.
1985: A digital signal processing unit for the Geo Instruments magnetic susceptibility sensors, with analogue and RS-232C outputs; in Current Research, Part B, Geological Survey of Canada, Paper 85-1B, p.463-466.

Thorleifson, L.H and Kristjansson, F.J.
1988: Stratigraphy and visible gold content of till in the Beardmore-Geraldton area, northern Ontario; in Current Research, Part C, Geological Survey of Canada, Paper 88-1C, p. 217-221.

Geology of the Archean Murdock Creek intrusion, Kirkland Lake, Ontario

Stephen M. Rowins[1], André E. Lalonde[1] and Eion M. Cameron
Mineral Resources Division

Rowins, S.M., Lalonde, A.E. and Cameron, E.M., Geology of the Archean Murdock Creek intrusion, Kirkland Lake, Ontario; in Current Research, Part C, Geological Survey of Canada, Paper 89-1C, p. 313-323, 1989.

Abstract

The Murdock Creek intrusion, immediately southwest of Kirkland Lake, Ontario, in the Abitibi belt, is a composite syenitic pluton, of presumed late Archean age, consisting of six distinct units. It is a member of a suite of late-tectonic syenitic intrusions located within and adjacent to the Kirkland Lake-Larder Lake fault zone, which host virtually all of the gold mineralization in the Kirkland Lake camp. Field relationships between the various rock types and preliminary petrographic evidence indicate that the Murdock Creek intrusion evolved from a single pulse of relatively anhydrous and oxidized syenitic magma which crystallized and differentiated in situ. Recent studies have shown that the gold deposits in the Kirkland Lake mining camp were derived from oxidized hydrothermal fluids; one possibility is that such fluids evolved from oxidized felsic magmas. The oxidized nature of the Murdock Creek magma suggests that a genetic connection between magma and ore fluids should be further examined. The absence of either a distinct metamorphic contact aureole or a peripheral cataclastic zone produced during plutonic emplacement, suggest that intrusion occurred at mesozonal depths.

Résumé

L'intrusion Murdock Creek, sise immédiatement au sud-ouest de Kirkland Lake dans la zone d'Abitibi, est composée de six unités plutoniques distinctes, toutes présumées d'âge archéenne. Elle est membre d'une suite d'intrusions syn- à tardi-tectoniques que l'on retrouve à l'intérieur ou en bordure de la zone faillée de Kirkland Lake-Larder Lake. Ces intrusions encaissent pratiquement tous les gîtes d'or du camp minier de Kirkland Lake. Les relations temporelles ainsi que la pétrographie indiquent que l'intrusion provient de la solidification et de la différenciation in situ d'une unique impulsion de magma anhydre et oxidé. Des études récentes démontrent que les gîtes d'or de la région de Kirkland Lake sont dérivés de fluides hydrothermaux oxidés; il est possible que ces fluides aient eux-mêmes évolués à partir de magmas felsiques oxidés. La nature oxidée du magma de Murdock Creek encourage une étude plus approfondie du lien génétique possible entre magma et fluides minéralisants. L'absence d'une auréole thermique distincte ou encore d'une zone cataclastique périphérique au pluton indiquent un emplacement dans la mésozone.

[1] Department of Geology, University of Ottawa, Ottawa, Ontario K1N 6N5.

INTRODUCTION

The Murdock Creek intrusion is a composite syenitic pluton, of presumed late Archean age, immediately southwest of Kirkland Lake, Ontario, in the southern part of the ~2.7 Ga Abitibi belt in the Superior Structural Province (Fig. 1). The pluton is one of a suite of late-tectonic (Colvine et al., 1988) syenitic intrusions within and adjacent to the Kirkland Lake-Larder Lake fault zone. The intrusions host about 97% of the gold mineralization in the camp (Hodgson, 1986). A close spatial association between felsic intrusions and lode gold deposits in Archean greenstone terranes has long been recognized; possible temporal and genetic links between the two are the topics of considerable study (Hodgson, 1983; Cameron and Carrigan, 1987; Cameron and Hattori, 1987; Colvine et al., 1988). The acceptance of any genetic model has, however, been hampered by a lack of evidence documenting the evolution of the felsic magmas from which the intrusions were derived. This is, in part, due to the extensive alteration around major gold deposits, which destroys the primary igneous minerals of the intrusion used to document magmatic evolution (e.g. Czamanske and Wones, 1973). An investigation of the Murdock Creek intrusion commencing in 1987 showed that the western portion of the pluton is unaffected by the shearing, quartz-veining and carbonatization which have extensively modified the rest of the pluton. This provides an opportunity to estimate the intensive parameters (P, T, $P(H_2O)$, $P(O_2)$) and to evaluate the relative oxidation state of the magma(s). Cameron and Hattori (1987) found that sulphides from the Kirkland Lake gold ores were depleted in ^{34}S, indicating isotopic fractionation in the ore fluids between sulphate and sulphide phases. This evidence for relatively oxidized fluids is supported by the occurrence of sulphate minerals and hematite with the gold mineralization. Cameron and Hattori (1987) suggested that such fluids could have been derived from an oxidized felsic magma. Documenting the oxidation state of the Murdock Creek magma is an initial step in testing this hypothesis. This paper describes the results of field work and preliminary petrographic studies carried out in 1987-88.

GEOLOGICAL SETTING

The volcanic, sedimentary and related intrusive rocks of the Kirkland Lake district form the southern limb of an elongate, east-plunging synclinorium (Fig. 2). All rocks in the region have been metamorphosed, but the prefix "meta" is omitted in the text. The supracrustal rocks have been divided into two successions, representing two cycles of volcanism, referred to by Jensen (1980) as the Lower and Upper supergroups. Each cycle was initiated by komatiitic volcanism, followed by tholeiitic, calc-alkaline, and finally alkalic cycles. The two cycles are separated by sedimentary units comprising argillite, conglomerate, greywacke, chert and iron-formation. The dominant structural feature of the area is the major east-west trending Kirkland Lake-Larder Lake fault zone, a narrow sinuous belt approximately 60 km long and up to 5 km wide, that extends from Matachewan in the west through Noranda towards Val d'Or in the east. Displacements along this fault and the Porcupine-Destor fault, major faults in the Abitibi belt, have been interpreted to be dominantly strike-slip (Hubert et al., 1984) or normal-slip (Dimroth et al., 1983). Subsequent reactivation of the existing structures, predominantly as reverse faults (Sibson et al., 1988), has resulted in a complicated structural zone in which gold mineralization and late felsic plutonism have been focused.

The Murdock Creek intrusion is emplaced within the mafic and ultramafic lava flows of the Larder Lake Group (Jensen, 1980). To the north, the pluton is in fault-contact with the greywacke and tuffaceous conglomeratic sediments of the Timiskaming Group (Thomson, 1950).

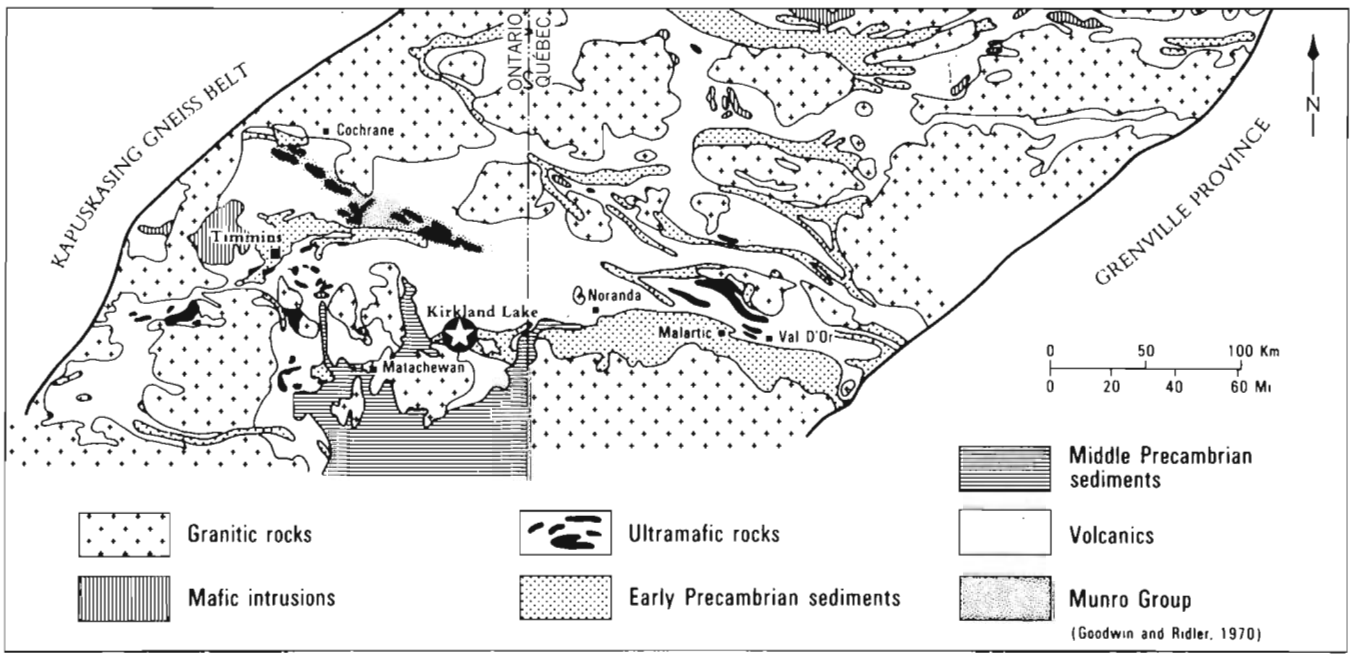

Figure 1. Geology of the Abitibi belt (after Goodwin and Ridler, 1970).

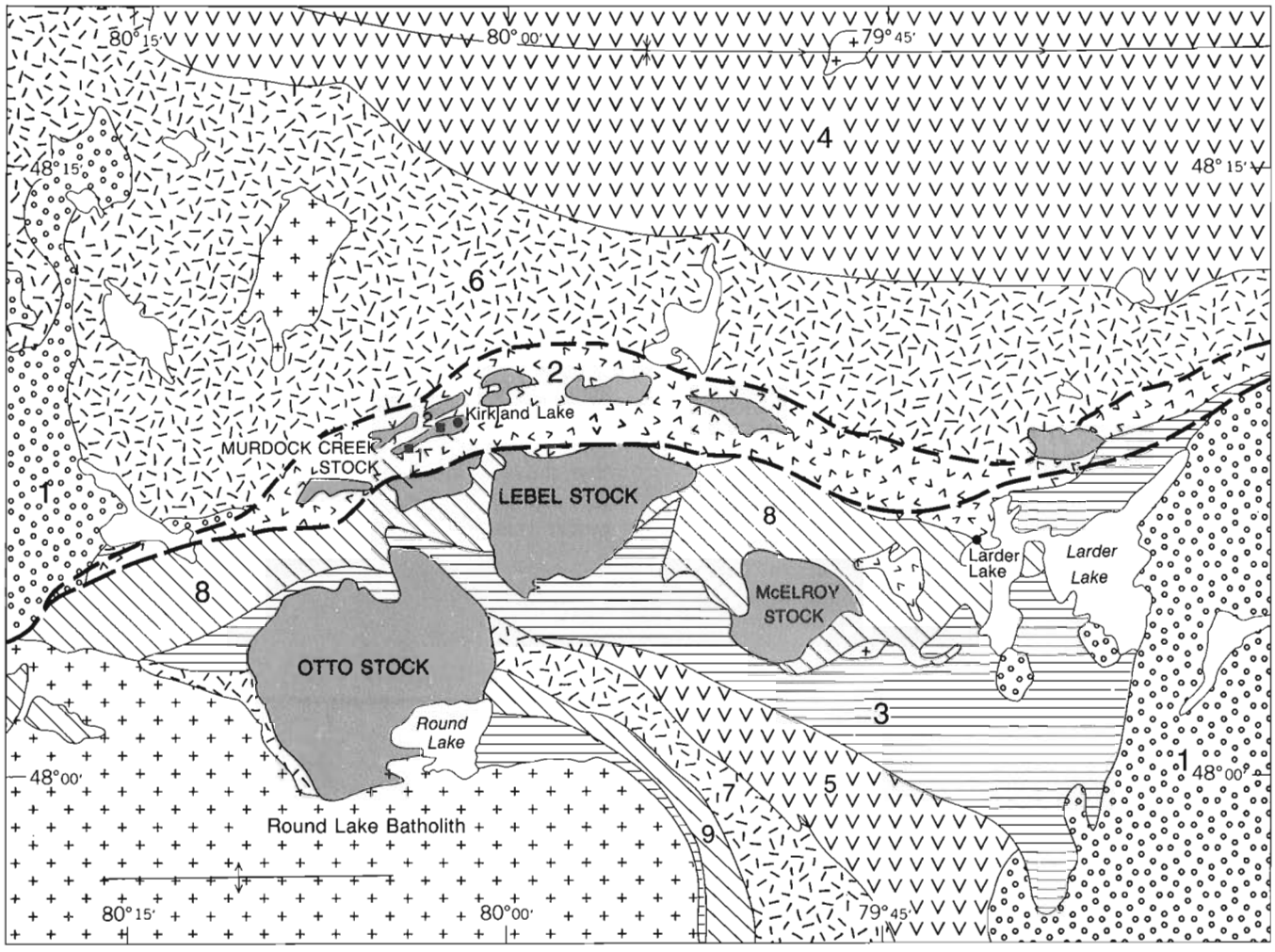

1. *COBALT GROUP*

Syenitic rocks

Trondhjemitic rocks

2. *TIMISKAMING GROUP*
Alkalic volcanic rocks and associated sedimentary rocks

3. *LARDER LAKE GROUP*
Intercycle sedimentary rocks, calc-alkalic tuffs, komatiitic volcanic flows, and ultramafic intrusive rocks

4. *BLAKE RIVER GROUP*
5. *SKEAD GROUP*
Calc-alkalic volcanic rocks

6. *KINOJEVIS GROUP*
7. *CATHARINE GROUP*
Tholeiitic volcanic rocks

8. *LARDER LAKE GROUP*
9. *WABEWAWA GROUP*
Komatiitic volcanic rocks

Kirkland Lake-Larder Lake Fault Zone
Anticline
Syncline
Macassa Mine 1
Lake Shore Mine 2

km
0 10

GSC

Figure 2. Geology of the Kirkland Lake area (modified from Jensen, 1978).

DESCRIPTION OF THE FIELD UNITS

All plutonic rocks described in this paper are classified according to the IUGS nomenclature (Streckeisen, 1976). The following study is based primarily on rock units forming the western part of the intrusion where the primary mineralogy and igneous textures largely escaped deformation and alteration.

At the present level of erosion, the Murdock Creek intrusion outcrops as a crudely elliptical body, elongated in an east-west direction parallel to the Larder Lake-Kirkland Lake fault zone. A thin, heterogeneous mafic margin encloses an extensive alkali-feldspar syenite core. The intrusion is a composite body consisting of six mappable units: 1) clinopyroxenite, 2) meladiorite, 3) hornblendite, 4) melamonzonite, 5) melasyenite, and 6) alkali-feldspar syenite (Fig. 3) . With the possible exception of hornblendite, these units exhibit regular and gradational contacts in the field. Textural and mineralogical evidence given below suggest that the units are from a single pulse of syenitic magma which crystallized and differentiated in situ. The following is a description of the six units, beginning with the oldest.

1) Clinopyroxenite

Clinopyroxenite is massive, homogeneous and medium-grained. It is dark greenish black but may weather brownish grey. It outcrops as a thin (10-300 m thick), discontinuous marginal unit at the western periphery of the intrusion, where it comes in contact with basalts of the Larder Lake Group and fluvial sediments of the Timiskaming Group. The clinopyroxenite is typically fresh, except near contacts with the country rock or where intruded by pink alkali-feldspar syenite dykes. In the field, a fine grained textural variant of clinopyroxenite may be difficult to distinguish from basalt; however, close examination reveals that the basalts possess a metamorphic fabric defined by the segregation of felsic (plagioclase and quartz) and mafic (amphibole) minerals into discrete bands, 0.05 to 1.0 mm wide. This imparts a "streaked" appearance to the rock. In addition, the older intruded basalts are usually more altered than the clinopyroxenite, with abundant epidote, calcite and quartz veins.

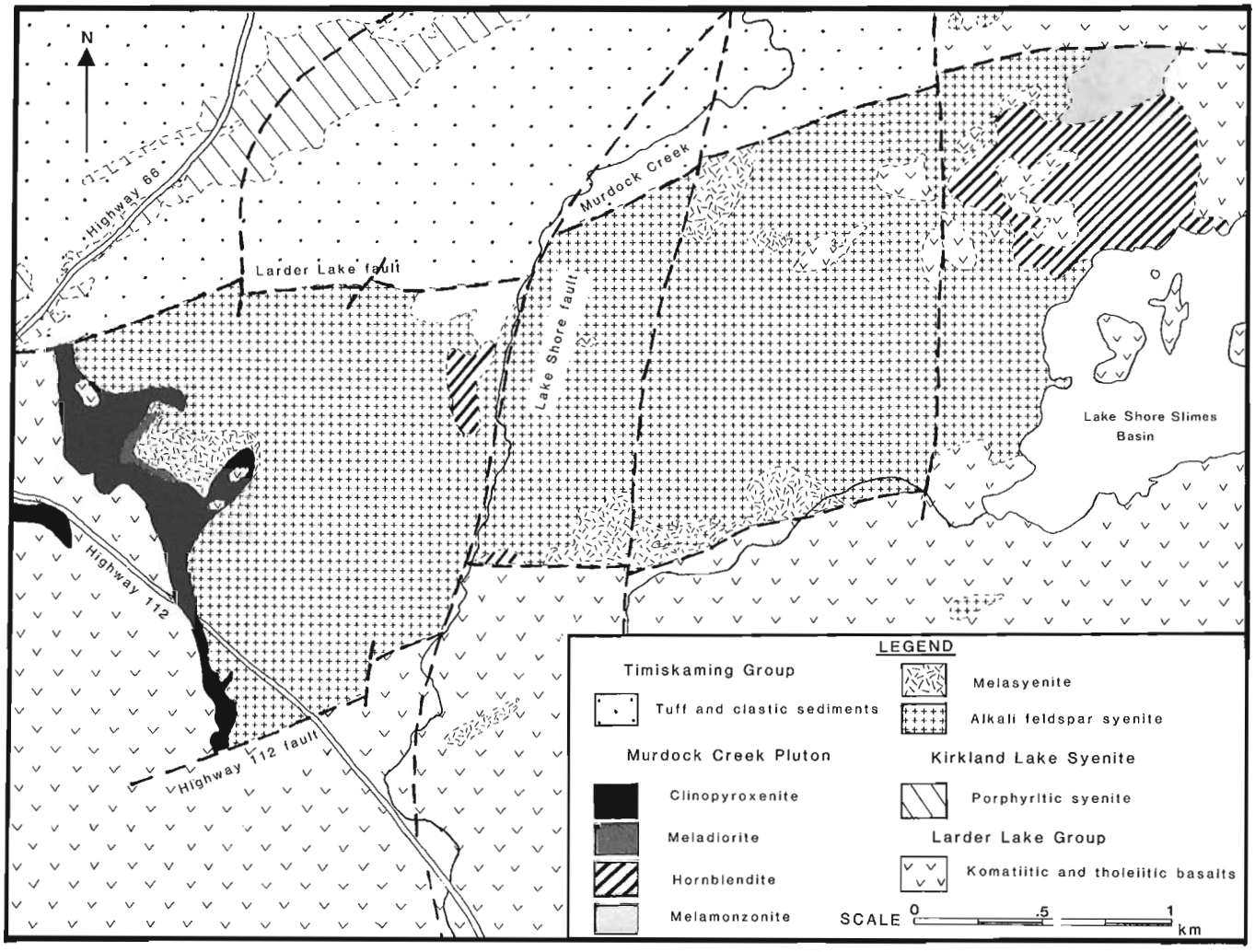

Figure 3. Geology of the Murdock Creek intrusion (Thomson, 1950 and this paper).

2) Meladiorite

Meladiorite is a dark green, medium grained rock that may be either massive or foliated. It is a minor unit that occurs as a thin (0-50 m thick), discontinuous unit in the northwest mafic margin of the intrusion. The rock has a distinctive spotted appearance in the field produced by greenish-white plagioclase laths set in a dark green matrix of clinopyroxene, amphibole and biotite. Meladiorite may be slightly porphyritic with plagioclase phenocrysts up to 1 cm in length. The preferential alignment of these plagioclase laths may yield a weak to moderate primary foliation, however the rock's texture is usually massive.

3) Hornblendite

Hornblendite is a texturally heterogeneous rock recognized by its greenish black colour, coarse euhedral hornblende crystals (0.5-10.0 mm across) and rough, knobby-weathered surface (Fig. 4). Considerable variation in grain size occurs, with medium- and coarse-grained variants in the same outcrop. Hornblendite outcrops sporadically throughout the mafic margin, except in the northeastern extremity of the intrusion where it forms an extensive (500-700 m) peripheral body. Pink alkali-feldspar syenite dykes and xenoliths of basalt are common.

4) Melamonzonite

Melamonzonite is a minor unit, transitional between meladiorite and melasyenite. This unit is quite heterogeneous varying from fine to medium grained, and from syenitic- to clinopyroxene-rich, over tens of centimetres. Melamonzonite is massive and greyish green when fresh, but becomes light brownish grey upon weathering. Subequal proportions of pale yellowish green perthite and plagioclase irregularly distributed throughout a dark greenish black matrix of clinopyroxene, biotite and amphibole, results in a mottled appearance. Pink alkali-feldspar syenite dykes intrude the melamonzonite in the northwestern part of the intrusion.

5) Melasyenite

Melasyenite is a transitional unit which becomes increasingly leucocratic towards the core of the intrusion, away from the mafic margin. The rock is medium grained, massive to trachytic, with pale orange-pink perthite crystals set in a slightly finer-grained matrix of dark green clinopyroxene, biotite and amphibole. Mafic varieties can appear slightly porphyritic with coarse subhedral perthite laths set against a medium grained mafic groundmass, imparting a spotted appearance similar to that exhibited by the meladiorite. The coarse grained perthite crystals (10-15 mm across) commonly exhibit colour zoning in which a pink core is enclosed by a greyish white rim. Plagioclase crystals are smaller (1-4 mm across) and possess a milky-white luster. As the rock becomes more leucocratic its textures and mineral distributions become increasingly homogeneous, the spotted appearance giving way to a more evenly coloured pink syenite. Based on the highly mafic composition of this unit (40-50 % mafic minerals) with respect to the alkali-feldspar syenite ($\approx$ 10-20 %), the melasyenite is interpreted to be the last mafic unit to crystallize. This is consistent with its location along the interior contact of the mafic margin with the extensive alkali-feldspar syenite core.

6) Alkali-feldspar syenite

Reddish pink alkali-feldspar syenite is the most extensive rock unit of the pluton. It occupies the central core of the intrusion. The unit is heterogeneous, medium to coarse grained, massive or well-foliated, in which case the foliation is defined by the parallel alignment of reddish perthite laths and dark green, columnar mafic minerals (predominantly clinopyroxene). This trachytic alignment is generally concordant with the internal contacts between the various plutonic units, however, it is locally discordant. The most intense red colouration of the feldspars coincides with the most strongly altered mafic silicates, both adjacent to faults and small shear zones within the intrusion. A coarse grained variant with pinkish grey, subhedral perthite crystals ranging up to 3 cm in length outcrops in the west-central part of the intrusion as small irregular bodies, tens of metres across. This coarse textural variant grades subtly over several metres into the much more common, medium grained alkali-feldspar syenite.

FIELD RELATIONSHIPS

The Murdock Creek intrusion may be subdivided into two separate domains on the basis of degree of alteration and deformation. West of the north-trending Lake Shore fault (Thomson, 1950), syenitic units are fresh with only minor shearing and attendant alteration. East of this fault, the rock is intensely sheared and altered (Fig. 3). Features distinctive of deformation and the attendant flow of hydrothermal fluids are areas of low relief, such as along stream beds (i.e., Lake Shore fault, Highway 112 fault); sheared and carbonated rock; silicification and resultant quartz-veining; chloritization and pyritization of mafic minerals; intense reddening of the feldspars; and the development of mylonitic or cataclastic rock textures.

Figure 4. Rough, knobby-weathering surface of hornblendite.

Dykes and cognate inclusions are distributed throughout the intrusion, with an anomalous concentration of basaltic xenoliths in the northeastern corner of the pluton. These large (20-200 m diameter) basaltic xenoliths are possibly roof pendants. Late, fine- to medium-grained alkali-feldspar syenite dykes frequently cut both the crystallized mafic margin and its enclosed basaltic xenoliths without any preferred orientation. Basaltic xenoliths not contained in the mafic margin but in the younger alkali-feldspar syenite core, are also intruded by pink alkali-feldspar syenite dykes which have been derived directly from the enclosing syenitic melt. Small angular xenoliths of the intruded rock frequently occur within these dykes.

Dykes of bright red, pegmatitic alkali-feldspar syenite (1-30 cm wide) occurring either singly or together in small swarms intrude medium-grained, alkali-feldspar syenite. These coarse pegmatites are leucocratic and weather-out as resistant ridges against the finer-grained, less resistant, alkali-feldspar syenite (Fig. 5). These late pegmatite dykes are also frequently associated with small shear zones in the intrusion. One small, irregular, lamprophyre dyke (10-20 cm wide) was observed cross cutting alkali-feldspar syenite in the southwestern corner of the intrusion. The lamprophyre consists almost exclusively of brown biotite (>90%) with subordinate apatite, magnetite and titanite.

Along the western edge of the intrusion, the contact between the clinopyroxenite and the Larder Lake basalts consists of a heterogeneous 200 m wide zone of intermingled altered clinopyroxenite and basalt. Numerous lime-green epidote veins and pale pink calcite veins with euhedral green amphibole needles (2-15 mm long) occur throughout this zone. Dark lime-green epidote pods with anastomosing alteration selvages, found within this zone, may give the appearance of pillow basalts, however, this feature is not primary but results from alteration. Late, quartz-bearing, whitish-grey felsic dykes intrude this heterogeneous contact zone. These dykes are not related to the syenitic magma of the Murdock Creek intrusion, since primary quartz is virtually absent in units forming the intrusion. However, small salmon-pink coloured alkali-feldspar syenite dykes, distinctly different from the quartz-bearing variety do appear directly equivalent to the Murdock Creek plutonic unit. Since these two dyke varieties are not exposed together, their relative ages are not known.

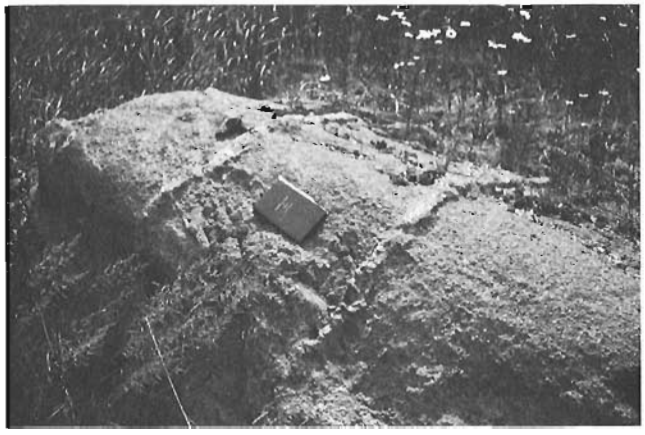

Figure 5. Resistant late dykes of pegmatitic, alkali-feldspar syenite in alkali-feldspar syenite.

PETROGRAPHY OF THE UNITS

Clinopyroxenite

This fine- to medium-grained ultramafic unit consists almost entirely of pale green pleochroic diopsidic pyroxene (as determined by preliminary microprobe analysis), with subordinate amounts of secondary biotite and amphibole. Pyroxene crystals range from 0.3 mm to 3.0 mm in length, are typically subhedral, and are often in mutual contact with neighbouring grains. The texture is not cumulate as there is no evidence of gravitational settling. Ovoid inclusions of apatite, zircon and opaque oxides and sulphides are numerous. Tiny acicular inclusions often encircle the core of some pyroxenecrystals (Fig. 6). These "rods" or "needles" are about 0.1 mm long and are dark brown at high magnification. Similar acicular inclusions have been noted in amphibole by Gorbatschev (1960) and have been interpreted as possible "exsolution" needles of titanite.

Uralitization of pyroxene is widespread and pleochroic greenish brown hastingsitic amphibole occurs as irregular patches throughout primary pyroxene. Fibrous, pale blue and faintly pleochroic actinolite replaces both primary pyroxene and secondary amphibole, beginning along crystal margins and proceeding inwards along fractures and cleavage planes. Both varieties of amphibole are deuteric. Subhedral, brown biotite flakes are commonly interstitial between the larger pyroxene crystals and also in irregular aggregate clusters with magnetite, apatite and titanite. The titanite may occur as discrete subhedral wedges or as an exsolution corona around magnetite, the latter being the product of sphenitization, commonly attributed to subsolidus oxidation (Carmichael and Nicholls, 1967).

Plagioclase, along with biotite, is interstitial to the pyroxene. Usually it is intensely saussuritized and sericitized, though faint albite twinning may still be discernable. Minor accessory phases include epidote, calcite, quartz, zircon, pyrite, and chalcopyrite. Pyroxene crystallized first followed by plagioclase and the primary accessory phases. In general, the clinopyroxenite unit is a hypidiomorphic-granular rock.

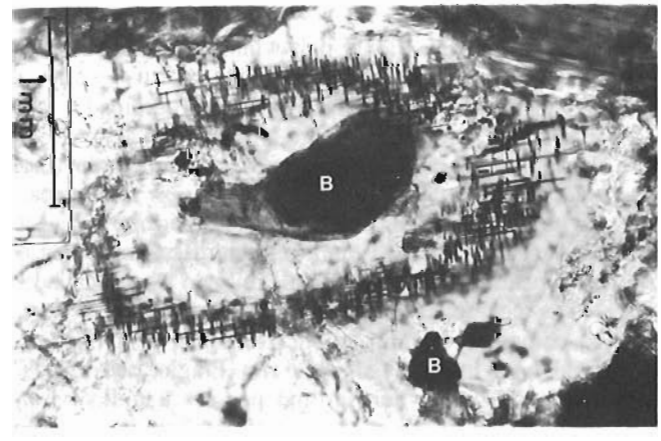

Figure 6. Acicular needles of titanite (?) encircling the core of clinopyroxene crystal, which also contains biotite inclusions (B).

Meladiorite

Mineralogically and texturally, meladiorite is very similar to the marginal clinopyroxenite unit, except that plagioclase is a significant phase (colour index(CI) = 55 ± 15). Pale green, unzoned pyroxene, ranging from diopside to salite in composition, is the dominant mafic silicate; brown biotite and uralitic amphibole are minor constituents. Pyroxene grains are equant, subhedral and range in size from 0.5 to 5.0 mm; actinolitic alteration along crystal faces is common. Tiny exsolution needles of titanite(?) similar to those in the clinopyroxenite also occur in this unit. Unzoned plagioclase (An_{30-34}) laths, 0.7 to 8.0 mm in length, are typically altered to sericite, calcite and epidote. In the foliated variants, these aligned laths are weaved, along with subhedral biotite, into foliation bands which wrap around and partially replace pyroxene, indicating a period of post-crystalline flattening.

Opaque minerals (predominantly magnetite) may account for up to 2 % of the rock. Magnetite and apatite occur together in the foliated biotite bands. Minor sulphide phases are present and include chalcopyrite, bornite and covellite. These occur together in small, rounded composite grains. Under reflected light, brass-yellow chalcopyrite forms sharp, straight criss-crossing exsolution lamellae in a purple bornite host, producing a distinctive basketweave exsolution texture (Ramdohr, 1969). Along grain boundaries and fractures, both chalcopyrite and bornite are altered to blue covellite. Other minor phases in the meladiorite include potassium feldspar, quartz, calcite, epidote, and rutile. In the meladiorite unit, pyroxene and plagioclase crystallized simultaneously. The meladiorite is a hypidiomorphic-granular rock.

Hornblendite

Hornblendite shows wide diversity in textures and mineral proportions. Hornblende constitutes 50-70 % of the rock with subordinate diopsidic pyroxene and green biotite. Equant, twinned, pleochroic crystals of greenish brown hornblende (3.0-15.0 mm diameter) become porphyritic in the coarser variants and possess mutually interfering grain boundaries (Fig. 7). Colourless secondary tremolite replaces the hornblende. Pale green, diopsidic pyroxene may constitute up to 30 % of the rock. These grains are small (0.4-1.0 mm), subrounded and occur with saussuritized plagioclase, perthite, quartz and biotite in a hypidiomorphic groundmass. Late alteration of the mafic silicates to chlorite and calcite is minor; calcite veinlets and patches are found preferentially along cleavage planes in the hornblende. Accessory phases include titanite, zircon, rutile, pyrite, chalcopyrite and magnetite. In this rock, hornblende was the first liquidus phase followed by pyroxene and late feldspar. The rock texture varies from hiatal-porphyritic to hypidiomorphic-inequigranular.

Melamonzonite

Melamonzonite (CI = 50 ± 10) is distinctive by variable proportions of feldspar minerals and a wide diversity of mineral textures. Coarse to medium-grained plagioclase and perthite laths (0.4-6.0 mm long) are extensively saussuritized and sericitized. Ragged and sutured crystal margins are indicative of minor recrystallization, though foliation is absent. Mafic minerals tend to occur in 0.5 to 6.0 mm lenticular clots of near-equal proportions of pyroxene, amphibole and biotite. Larger, pale green diopsidic pyroxene (1.0-3.0 mm diameter) crystals are frequently uralitized and altered to greenish brown biotite to various degrees. Uralite pseudomorphs after pyroxene may subsequently undergo patchy alteration to pale blue, fibrous actinolite. Apatite is abundant as inclusions in biotite.

Titanite is a prominent accessory occurring as minute grains clustered around biotite and as late exsolution coronas mantling magnetite. The spatial association between ferromagnesian minerals, magnetite, apatite and titanite is strong and may result from immiscibility between coexisting Fe-rich and silica-rich liquids during the later stages of solidification of the syenitic melt (Philpotts, 1967; 1981). Feldspars crystallized simultaneously and in apparent equilibrium. They were closely followed by pyroxene which underwent later alteration to amphibole and biotite. Distribution of the accessory phases, magnetite and apatite, seem to indicate broadly coeval crystallization with the ferromagnesian minerals. Melamonzonite is a hypidiomorphic-granular rock.

Melasyenite

The predominance of perthitic alkali-feldspar over plagioclase is the main distinguishing feature of the melasyenite (CI = 40 ± 10). In most other respects, the melasyenite resembles the melamonzonite unit. Perthite crystals are typically twinned, subrounded laths ranging from 0.5 to 8.0 mm in length; perthitic intergrowths are of the vein and bleb varieties. This wide range in perthite crystal size is believed to have resulted from the movement of primary perthite laths in a viscous, partially crystallized syenitic magma or crystal-mush, producing substantial granulation of phenocryst edges. Sericitic alteration of perthite to white mica, epidote and calcite is widespread and strongest along fractures and zones of weakness. Plagioclase (An_{18}) is rare and usually saussuritized.

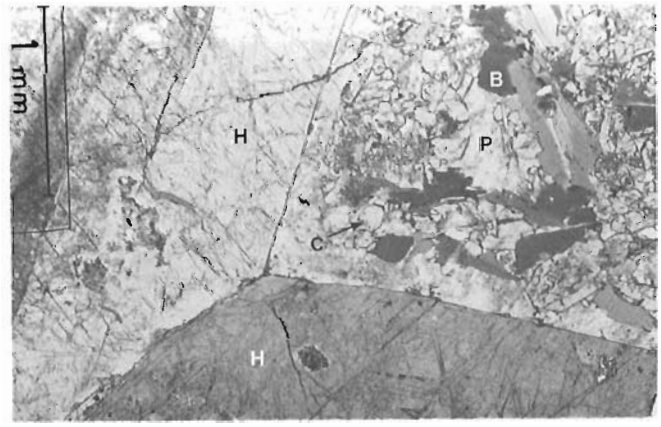

Figure 7. Crystals of hornblende (H) with mutually interfering grain boundaries. Hypidiomorphic groundmass of saussuritized plagioclase (P), clinopyroxene (C), and biotite (B).

Diopsidic pyroxene, brown biotite, uralitic amphibole, magnetite and apatite tend to occur in mafic clots (1.0-8.0 mm in diameter) interstitial to the larger perthite laths; this possibly resulting from liquid immiscibility as previously described (Fig. 8). Pyroxene is similar to that found in other units of the intrusion and may occasionally have inclusions of the tiny dark brown exsolution rods. Accessory phases include titanite and zircon. The paragenesis of this unit is comparable to the melamonzonite, with feldspar crystallizing first, followed by pyroxene and alteration products.

Alkali-feldspar syenite

Alkali-feldspar syenite (CI = 20 ± 15) consists principally of subhedral, perthitic feldspar crystals (75-90 %) which vary from fine to coarse grained. Exsolution intergrowths include vein, bleb, patch and interlocking varieties. Turbidity is heterogeneously distributed, being most intense along thin fractures. In some instances, sodic domains are sufficiently coarse to permit identification of albite twinning, and are more turbid than the potassic domains which display the characteristic grid-twinning of microcline. In the trachytic varieties of alkali-feldspar syenite, perthite grains have ragged crystal margins rimmed by a fine grained mosaic of polygonal albite and quartz. Where granulation of perthite crystal margins is minimal, only recrystallized films of clear albite are formed along the crystal margins. Plagioclase is rare but when present occurs as small sericitized masses, interstitial to the larger perthitic feldspar.

Equant, subhedral to euhedral, pyroxene crystals (0.3-10.0 mm in diameter) are slightly pleochroic and compositionally zoned, with bright green aegirine-augite rims and pale green diopside or salite cores (Fig. 9). Alteration of pyroxene is variable, with uralitic replacement most common. In more altered alkali-feldspar syenites, pale blue actinolite may completely pseudomorph pre-existing pyroxene. Less commonly, there is complete pseudomorphous replacement of pyroxene by very pale green tremolite. Amphibole is frequently retrograded to brown biotite containing minute rutile crystals(after titanite); biotite may also display incipient alteration to chlorite.

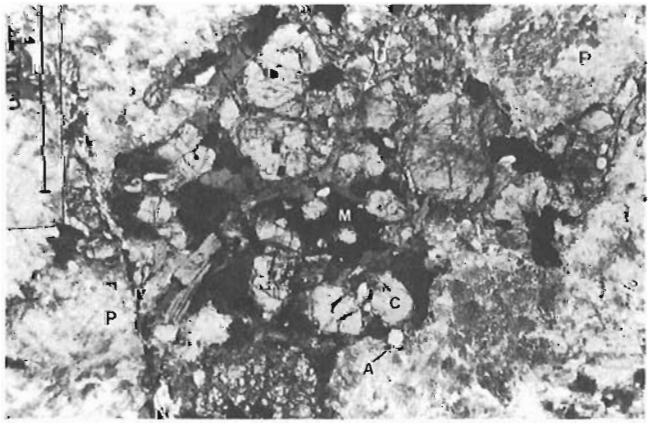

Figure 8. Clinopyroxene (C), uralitic amphibole (U), magnetite (M), and apatite (A) in mafic clots interstitial to perthitic feldspar (P).

Titanite is a prominent accessory in alkali-feldspar syenite and is of two distinct generations: 1) large (1.0-6.0 mm) euhedral, wedge-shaped crystals are an early primary phase, randomly distributed throughout the unit (Fig. 10), and 2) a much later generation forms coronas or partial coronas around anhedral magnetite grains, the result of subsolidus oxidation (sphenitization) of titaniferous magnetite. Other late alteration features include quartz-calcite and biotite-chlorite veinlets which preferentially replace feldspar and pyroxene along fractures and cleavages. Small anhedral sulphide masses composed of pyrite, chalcopyrite, bornite and covellite are present in trace amounts. Chalcopyrite, bornite and covellite occur together and display the same "basketweave" texture which was observed in the meladiorite unit. Perthitic feldspar crystallized first followed by pyroxene and its subsequent alteration products. The overall rock texture is hypidiomorphic-granular.

STRUCTURE

The northern periphery of the Murdock Creek intrusion is truncated by the east- trending Larder Lake fault. This dips to the south at about 60° (Thomson, 1950) and delineates

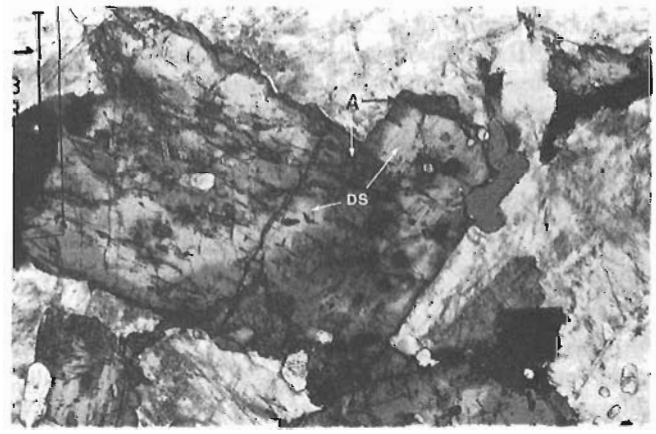

Figure 9. Zoned clinopyroxene with aegirine-augite rims (A) and diopside-salite cores (DS), surrounded by turbid perthitic feldspar.

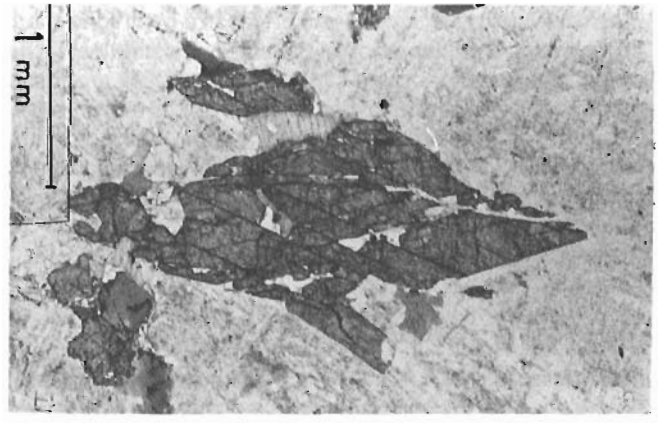

Figure 10. Euhedral crystals of primary titanite in turbid perthitic feldspar.

the southern boundary of the Kirkland Lake-Larder Lake fault zone. Along the fault and extending approximately 100-200 m out on either side is a zone of intense carbonatization overprinting both the syenitic rock and sedimentary units of the Timiskaming Group. Calcite and dolomite are the principal carbonate minerals. Shearing and mylonitization may be so intense that recognition of the protolith is impossible. Later periods of brittle deformation lead to the development of quartz veins throughout the carbonated rock (Fig. 11).

A previously unrecognized fault has been identified trending in an easterly direction along the southern edge of the pluton at the intrusive contact with basalts of the Larder Lake Group. This is a zone of weakness due the difference in mechanical competency between the two lithologies and would thus localize any faulting due to changes in the regional stress regime. The east-trending southern fault, informally referred to as the "Highway 112 fault", is a complex mylonitic and cataclastic brecciated zone outlined by green carbonatized (fuchsite-bearing) rocks. Several north-trending post-ore faults, later than the east-west shear zones, may record significant lateral and vertical displacement (Thomson, 1950).

Figure 11. Quartz veins cutting intensely sheared and carbonated rock.

Figure 12. Fragmented feldspar (F) and fibrous reibeckitic amphibole (A) define a protoclastic texture, produced during minor shearing and alteration of alkali-feldspar syenite.

Within the alkali-feldspar syenite core of the intrusion there are numerous small shear zones, several metres wide, associated with alkali-feldspar syenite pegmatite dykes. Shearing produced a protoclastic texture, where intensely reddened feldspars are fragmented and blue reibeckitic amphibole replace the earlier mafic silicates (Fig. 12). The occurrence of the shears exclusively within the alkali-feldspar syenite, in association with alkali amphibole and pegmatite, suggests that they acted as pressure-release conduits along which late-magmatic, volatile-rich fluids were forcefully expelled during the final stages of magma solidification. In the alteration zones adjacent to the major faults, alkali-feldspar syenite commonly contains numerous thin and parallel (0.5-2.0 mm wide) cleavage surfaces or slip shears coated with dark green chlorite. These are interpreted as pressure-solution surfaces related to local stresses during faulting (Fig. 13).

METAMORPHISM

Volcanic rocks in the Kirkland Lake area underwent regional burial metamorphism to prehnite-pumpellyite grade at pressures of about 1 kb according to Jolly (1974). Subsequent overprinting of the regional metamorphism is common where plutonic bodies have intruded into the supracrustal rocks generating contact aureoles of variable size and grade. However, unlike several other syenitic intrusions in the area (Otto stock, Lebel stock), the Murdock Creek intrusion has not generated a significant metamorphic aureole or fine grained chill-margin.

EVIDENCE OF MAGMATIC OXIDATION IN THE MURDOCK CREEK INTRUSION

In the introduction it was briefly noted that Cameron and Hattori (1987) identified the ore fluids at Kirkland Lake as being relatively oxidized, since they contained a significant proportion of their total S content as sulphate. A number of smaller deposits in the Timmins-Kirkland Lake area were also shown to have been derived from oxidized fluids, as well as major deposits, such as Hemlo, Ontario, and

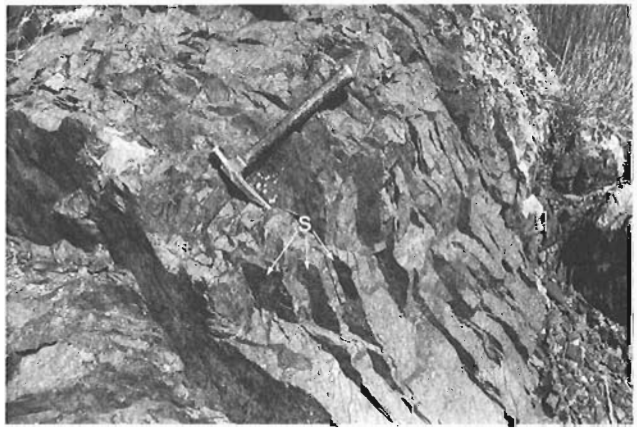

Figure 13. Alkali-feldspar syenite with thin, parallel cleavage surfaces or slip shears (S) marked by dark green chlorite.

Kalgoorlie, Australia. There are only two realistic sources for these fluids: oxidized felsic magmas (Cameron and Hattori, 1987) and fluids derived during oxidative metamorphism of the lower crust (Cameron, 1988). For the Kirkland Lake camp the close spatial relationship between syenitic intrusions and gold suggests that this association be tested. There are presently no data to precisely identify the temporal relationship between the intrusions and the gold. Since the veins cut the syenites, they clearly post-date the exposed portions of these intrusions. However, whether there was a sufficiently long interval to exclude the syenite magma as a source for the gold is unknown. To obtain more precise geochronological information is one of the objectives of this project.

Oxidized fluids of magmatic origin must have equilibrated with a similarly oxidized magma. Petrographic evidence from the Murdock Creek intrusion suggests that oxidizing conditions prevailed during the crystallization of some of the rock units. Evidence of this includes, Mg-rich clinopyroxene, abundant primary titanite, and the predominance of magnetite over ilmenite. Alkali-feldspar, which is intensely reddened by hematite, reflects postmagmatic oxidation, possibly inherited from the late magmatic stage. Mg-enrichment in pyroxene indicates oxidizing conditions during crystallization, when Fe, as Fe^{2+} and Fe^{3+} partitioned into magnetite. Under these conditions, Mg^{2+} substitutes for Fe^{2+} in pyroxene (Czamanske and Wones, 1973). Verhoogen (1962) showed that primary titanite required relatively oxidizing conditions for its formation and Carmichael and Nicholls (1967) calculated limits in f_{O_2}-temperature space. Cameron and Carrigan (1987) noted the abundance of primary titanite in various felsic intrusions spatially associated with gold mineralization in the Abitibi belt. The dominance of magnetite over ilmenite has been used by Chappell and White (1974) and Ishihara (1977) to separate the more "oxidized" I-type (magnetite series) granitoids from the "reduced" S-type (ilmenite series). All rock types from Murdock Creek contain magnetite but lack ilmenite, and thus broadly correspond to the oxidized I-type granitoids. Finally, the presence of turbid red feldspar in most of the units may indicate that oxidizing conditions were maintained throughout the crystallization of the intrusion and continued into the postmagmatic stage, when late, oxidizing fluids produced the turbidity in the feldspars. The red colouration is due to the presence of finely divided hematite flakes lining the walls of fluid inclusions in the alkali-feldspar. This hematite results from the dissolution of nearby ferromagnesian minerals (Boone, 1969).

These preliminary observations of magmatic oxidation will be followed by estimation of the oxygen fugacity during the different stages of magmatic crystallization.

SUMMARY

The continuous compositional spectrum shown by the units forming the Murdock Creek intrusion, along with the gradational nature of thus contacts, indicate that the platon formed from a single pulse of relatively anhydrous and oxidized syenitic magma which crystallized and differentiated in situ. Internal dykes related to the specific plutonic units and observed flow foliations suggest that movement of magma continued after the earlier units had solidified. The lack of miarolitic cavities and porphyritic textures suggest that early and rapid vesiculation of the melt did not occur. Furthermore, the absence of either a distinct contact aureole or a peripheral cataclastic zone produced during plutonic emplacement indicates that intrusion occurred at mesozonal depths. Late reactivations of the Larder Lake and Highway 112 faults has resulted in post-emplacement shearing and alteration along the northern and southern margins of the intrusion. The near total absence of modal quartz or feldpathoid minerals indicates that the magma(s) were silica saturated. The minor exposure of the mafic margin of the intrusion indicates that the bulk of the magma was relatively felsic.

The crystallization sequence in the melanocratic Murdock Creek rocks is clinopyroxene (salite or diopside), apatite, titanite, plagioclase (andesine to oligoclase) and alkali-feldspar. An exception to this sequence is the hornblendite where igneous hornblende precedes clinopyroxene. However, in the felsic rocks, the sequence is reversed with alkali-feldspar being the first liquidus phase followed by plagioclase, clinopyroxene, apatite and titanite. Magnetite is both a late and an early crystallizing mineral. It is preferentially associated with apatite and the ferromagnesian minerals, suggesting that an immiscible Fe-oxide-phosphate liquid may have separated during crystallization of the magma. Zircon is an accessory in the more felsic rock types. Amphibole (except in hornblendite), some titanite, and biotite are secondary reaction products around clinopyroxene and magnetite, related to deuteric effects rather than to later prograde metamorphism.

Petrographic evidence and preliminary electron microprobe analyses of the ferromagnesian silicates indicate that some of the plutonic units from the Murdock Creek intrusion crystallized under relatively oxidizing conditions. Turbid red feldspars reflect postmagmatic oxidation which may be inherited from the late-magmatic stage.

Ongoing research includes a detailed study of the mineral chemistry and the whole rock geochemistry which characterizes the individual rock types. In addition, U-Pb zircon, titanite and rutile radiometric age determinations of the extensive alkali-feldspar syenite and an adjacent carbonated and sheared melasyenite hosting hydrothermal gold mineralization is underway to establish the relationship between emplacement of the Murdock Creek intrusion and gold mineralization in the Kirkland Lake camp.

ACKNOWLEDGMENTS

We are grateful to Mike Dyment and Jocelyn Kidston for pointing out several interesting field exposures in the Kirkland Lake area. Bob Garrett and Keiko Hattori kindly reviewed the manuscript.

REFERENCES

Boone, G.M.
1969: Origin of clouded red feldspars: petrologic contrasts in a granitic porphyry intrusion; American Journal of Science, v. 267, p. 633-668.

Cameron, E.M.
1988: Archean gold: relation to granulite formation and redox zoning in the crust; Geology, v. 16, 109-112.

Cameron, E.M., and Carrigan, W.J.
1987: Oxygen fugacity of Archean felsic magmas: relationship to gold mineralization; in Current Research, Part A, Geological Survey of Canada, Paper 87-1A, p. 281-298.

Cameron, E.M., and Hattori, K.
1987: Archean gold mineralization and oxidized hydrothermal fluids; Economic Geology, v. 82, p. 1177-1191.

Carmichael, I.S.E., and Nicholls, J.
1967: Iron-titanium oxides and oxygen fugacities in volcanic rocks; Journal of Geophysical Research, v. 72, p. 4665-4687.

Chappell, B.W., and White, A.J.R.
1974: Two contrasting granite types; Pacific Geology, v. 8, p. 173-174.

Colvine, A.C., Fyon, J.A., Heather, K.B., Marmont, S., Smith, P.M., and Troop, D.G.
1988: Archean lode gold deposits in Ontario; Ontario Geological Survey, Misc. Paper 139, 136 p.

Czamanske, G.K., and Wones, D.R.
1973: Oxidation during magmatic differentiation, Finnmarka complex, Oslo area, Norway; 2, The mafic silicates; Journal of Petrology, v. 14, p. 349-380.

Dimroth, E., Imreh, L., Goulet, N., and Rocheleau, M.
1983: Evolution of the south-central segment of the Archean Abitibi belt, Quebec. Part II: Tectonic evolution and geomechanical model; Canadian Journal of Earth Sciences, v. 20, p. 1355-1373.

Goodwin, A.M., and Ridler, R.H.
1970: The Abitibi orogenic belt; Geological Survey of Canada, Paper 70-40, p. 1-30.

Gorbatschev, R.
1960: On the alkali rocks of Almunge. A preliminary report on a new survey; Geological Institute, University of Uppsala Bulletin, v. 39, p. 1-69.

Hodgson, C.J.
1983: Preliminary report on the Timmins-Kirkland Lake area gold deposits file; Ontario Geological Survey, Open File Report 5467, 160p.
1986: Place of gold ore formation in the geological development of the Abitibi greenstone belt, Ontario, Canada; Transactions of the Institution of Mining and Metallurgy (Section B: Applied Earth Science), v. 95, p. B183-B194.

Hubert, C., Trudel, P., and Gelinas, L.
1984: Archean wrench fault tectonics and structural evolution of the Blake River Group, Abitibi belt, Quebec; Canadian Journal of Earth Sciences, v. 21, p. 1024-1032.

Ishihara, S.
1977: The magnetite-series and ilmenite-series granitic rocks; Mining Geology, v. 267, p. 633-668.

Jensen, L.S.
1978: Archean komatiitic, tholeiitic, calc-alkalic and alkalic volcanic sequences in the Kirkland Lake area; p. 327-359 in Toronto '78 Field Trips Guidebook, edited by A.L. Currie, and W.O. Mackasey, Geological Association of Canada, 361 p.
1980: Kirkland Lake-Larder Lake synoptic mapping projects, Districts of Cochrane and Timiskaming; in Summary of Field Work, 1980, by the Ontario Geological Survey, edited by V.G. Milne, et al., Ontario Geological Survey, Miscellaneous, Paper 96, p. 55-60.

Jolly, W.T.
1974: Regional metamorphic zonation as an aid in the study of Archean terrains: Abitibi regions, Ontario; Canadian Mineralogist, v. 12, p. 499-508.

Philpotts, A.R.
1967: Origin of certain iron-titanium oxide and apatite rocks; Economic Geology, v. 62, p. 303-315.
1981: A model for the generation of Massif-type anorthosites; Canadian Mineralogist, v. 19, p. 233-253.

Ramdohr, P.
1969: The ore minerals and their intergrowths. Vols. 1 and 2; Oxford, Pergamon, 1207 p.

Sibson, R.H., Robert, F., and Poulson, K.H.
1988: High-angle reverse faults, fluid pressure cycling, and mesothermal gold-quartz deposits; Geology, v. 16, p. 551-555.

Streckeisen, A.
1976: To each plutonic rock its proper name; Earth Science Reviews, v. 12, p. 1-33.

Thomson, J.E.
1950: Geology of Teck Township and the Kenogami Lake area, Kirkland Lake gold belt; Ontario Department of Mines Annual Report for 1948, Part 5, v. 57, p. 1-53.

Verhoogen, J.
1962: Distribution of titanium between silicates and oxides in igneous rocks; American Journal of Science, v. 260, p. 211-220.

Preliminary report on the structural setting of gold at the Gunnar mine in the Beresford Lake area, Uchi Subprovince, southeastern Manitoba[1]

R. Brommecker[2], K.H. Poulsen and C.J. Hodgson[2]
Mineral Resources Division

Brommecker, R., Poulsen, K.H. and Hodgson, C.J., Preliminary report on the structural setting of gold at the Gunnar mine in the Beresford Lake area, Uchi Subprovince, southeastern Manitoba; in Current Research, Part C, Geological Survey of Canada, Paper 89-1C, p. 325-332, 1989.

Abstract

Three phases of ductile deformation and one early phase of brittle deformation have affected the rocks in the Gunnar mine area. The earliest structures are brittle faults and fractures which controlled emplacement of felsic dykes and breccia dykes. Gold occurs in shear zones initiated in the first ductile deformation (D1). Movement on the D1 shears likely continued throughout a second deformation (D2). Lamprophyre dykes and gold mineralization were approximately coeval and occurred during the culmination of D1 or the beginning of D2, well after any felsic magmatism. The Beresford Lake Deformation Zone (a high strain zone to the east of the mine site) may have been important in localizing the mineralization.

Résumé

Trois phases de déformation ductile et une phase de déformation fragile ont agi sur les roches de la région minière du Gunnar. Les structures les plus anciennes sont des failles fragiles et des fractures qui ont déterminé la mise en place des dykes felsiques et des dykes bréchiques. L'or se manifeste dans des zones de cisaillement apparues durant la première phase de déformation ductile (D1). Le mouvement survenu sur les cisaillements D1 s'est probablement poursuivi pendant toute la durée d'une seconde déformation (D2). La mise en place des dykes lamprophyriques et la minéralisation aurifère ont été approximativement contemporaines et ont eu lieu après la culmination de D1 ou le début de D2, bien après tout épisode de magmatisme felsique. La zone de déformation de Beresford Lake (zone fortement déformée à l'est de l'emplacement de la mine) a peut être joué un rôle important en ce qui a trait à l'emplacement de la minéralisation.

[1] Contribution to the Canada Manitoba Mineral Development Agreement 1984-1989. Project carried by the Geological Survey of Canada.

[2] Department of Geological Sciences, Queen's University, Kingston, Ontario, K7L 3N6.

INTRODUCTION

This report summarizes the results of three months of mapping at a scale of 1:2500 by the senior author in the vicinity of the Gunnar mine (Fig. 1). The Gunnar mine was a significant gold producer (approximately 100 000 oz. production; Stephenson, 1971) in the southeastern part of the Rice Lake greenstone belt. Excellent exposure, the result of many past forest fires, makes the area attractive for a detailed mapping project. The objective of the project is to determine the structural history of the area, with particular emphasis on the controls on gold mineralization. The outline of the study area is shown in Figure 1.

Previous work

The area has been mapped previously several times (Stockwell and Lord, 1939; Weber, 1971; Seneshen and Owens, 1985); these maps are less detailed than that of the present study.

STRATIGRAPHY

All the rocks in the study area have been metamorphosed to greenschist facies. However, the prefix "meta" has been omitted from rock names for simplicity, and rocks are classified principally by their primary textures. Three formations can be distinguished within the map area (Campbell, 1971; Fig. 2). From oldest to youngest they are: the Gunnar Formation, the Stormy Lake Formation and the Narrows Formation.

Gunnar Formation

The Gunnar Formation consists mainly of pillowed and massive basalts. Single flows can have both massive and pillowed sections. The massive basalts are commonly fine to medium grained. Contacts between flows are typically marked by 1 to 10 m wide pillow breccia units or narrow 1 to 10 cm wide laminated, cherty interflow sedimentary rocks. Flows are commonly amygdaloidal and/or variolitic, with quartz or calcite filling the amygdules. Pillows display concentric cooling cracks, have more felsic cores than rims, and typically have epidotized selvages. Interpillow spaces are filled variably with hyaloclastite, quartz±(calcite-epidote) and locally pyrite. Selvages are commonly 1 to 3 cm wide.

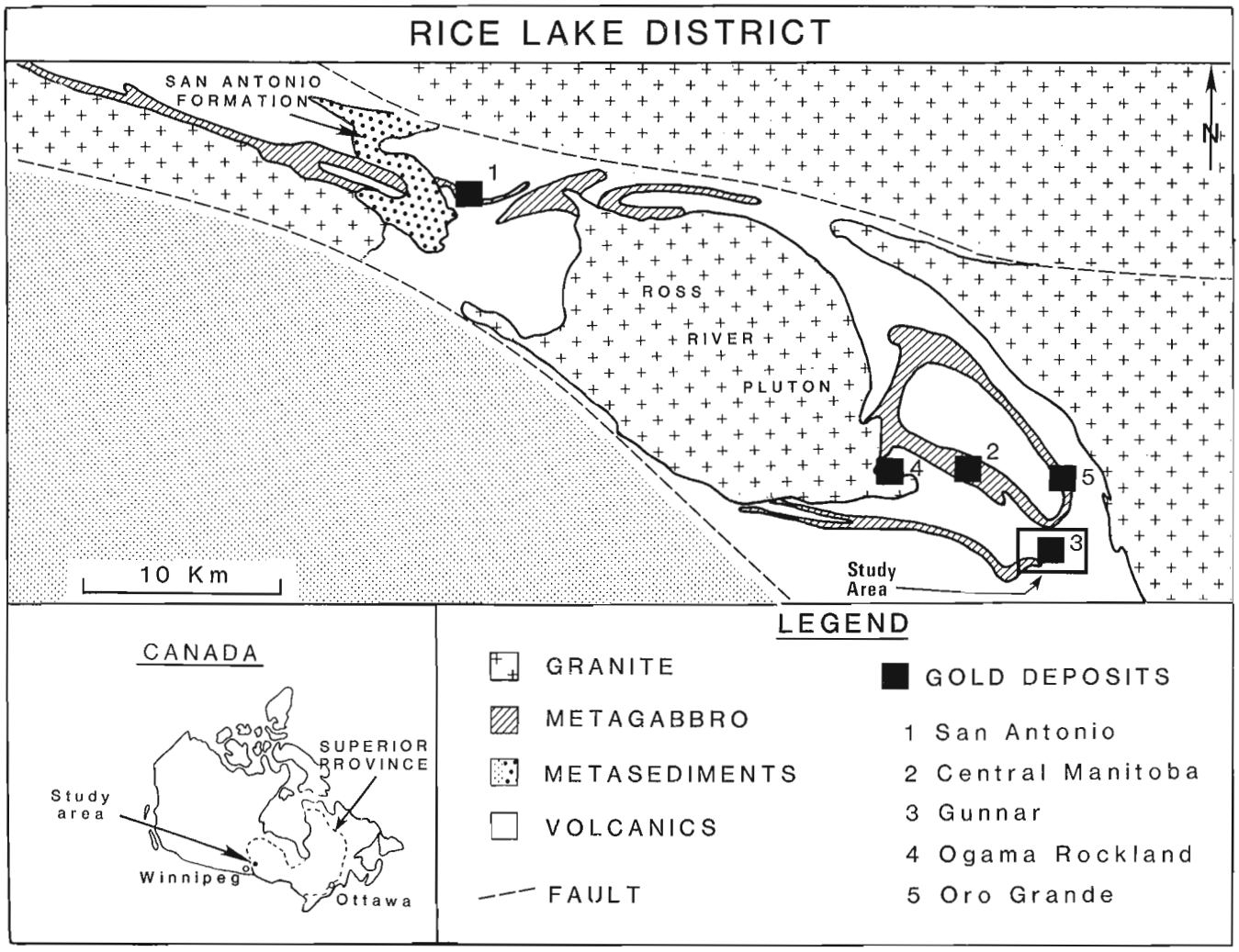

Figure 1. Study area location map.

Stormy Lake Formation

The Stormy Lake Formation is dominated by sedimentary rocks of various compositions including tuffaceous sandstone, pisolithic sandstone and siltstone, greywacke, arkose, chert, argillite, and iron formation. Beds are 1 to 10 cm thick. Tuff and tuff breccia are found in minor, 1 to 10 m thick bands within the formation. Also present are debris flows with mainly intermediate composition feldspar porphyritic clasts (50 %), fewer mafic to intermediate fine grained clasts (30 %), and rare tonalitic to granitic clasts. The clasts range from 10 to 30 cm long and commonly fine upwards in individual flow units. A fining upwards debris flow is present at the base of the Stormy Lake Formation at its contact with the Gunnar Formation, except on the eastern limb of the Eastern Anticline where the contact is at least locally faulted (Fig. 2). The rocks at and near the lower contact of the Stormy Lake Formation are strongly foliated, indicating the possibility that the Stormy LakeGunnar contact is a major fault. Gabbroic sills are abundant in the Stormy Lake Formation and constitute up to 50 % of its stratigraphic thickness.

Narrows Formation

In the study area, the Narrows Formation consists mainly of intermediate heterolithic volcanic breccia and tuff breccia. Fragments typically comprise over 70 % of the rock and vary from 10 cm to 1 m in diameter. Although mappable sections with andesitic or rhyodacitic clasts are common, the dominant fragment type is plagioclase ± (quartz) porphyritic dacite. Bands of lapilli tuff, greywacke, and mafic flows also occur. The nature of the contact between the Narrows Formation and underlying Stormy Lake Formation is obscured by high strain and intrusions.

INTRUSIONS

Mafic intrusions

Mafic dykes and sills intrude all formations in the map area. Semiconcordant sills (20 to 200 m thick) are especially abundant in the Stormy Lake Formation. The thick sills contain medium- to coarse-grained gabbroic rocks and commonly are layered. The top third of a sill is commonly a

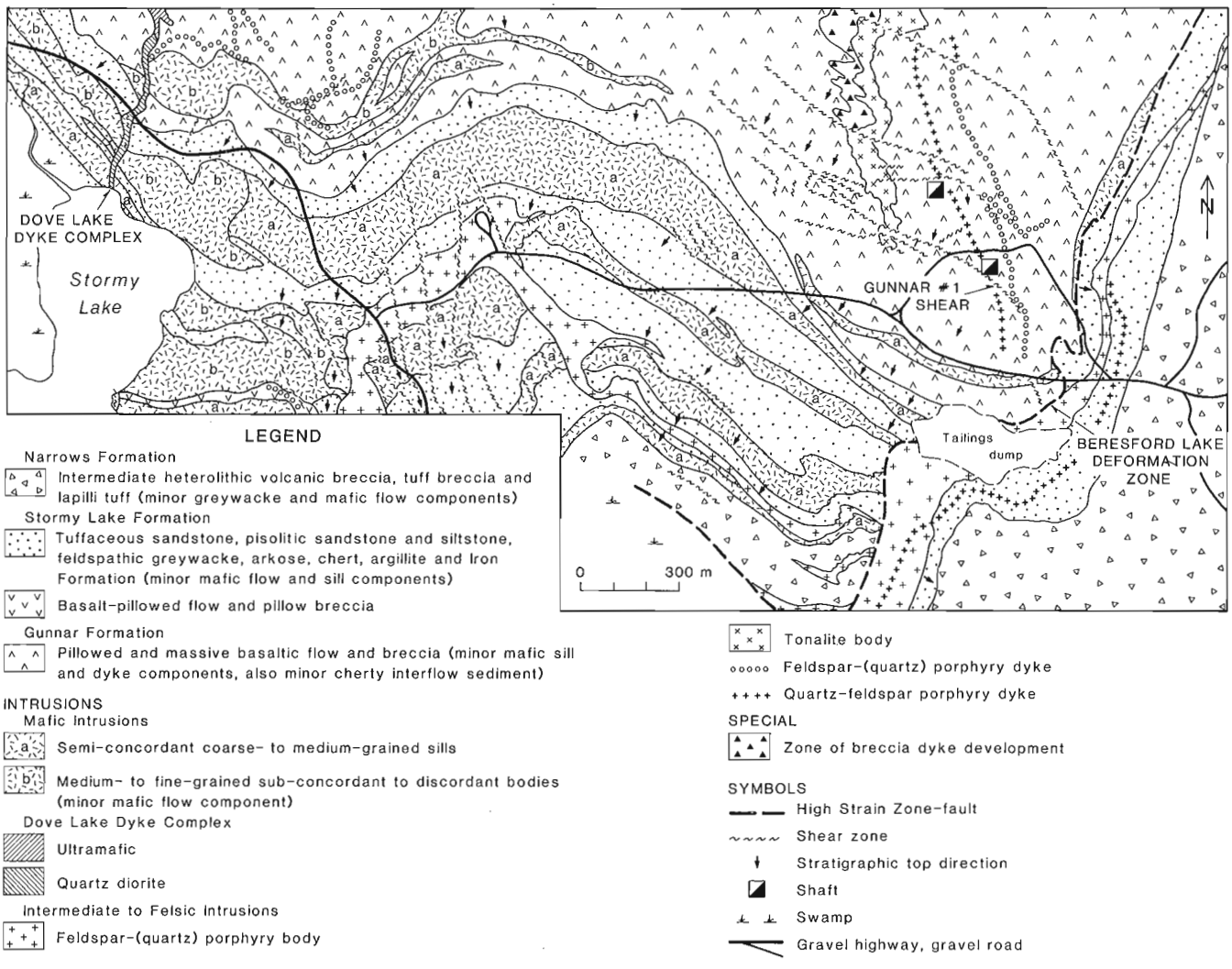

Figure 2. Simplified geological map of the study area.

leucogabbro, characterized by modal quartz, granophyric textures, pegmatoid patches, and abundant magnetite, whereas the lower two-thirds is typically an equigranular melagabbro. In addition, subconcordant to discordant mafic bodies containing medium- to fine-grained gabbro appear to intrude the large sills but may be broadly synchronous, disruptive phases of the sills. The mafic dykes and sills represent the earliest intrusive event.

Dove Lake Dyke Complex

A series of dykes intrude an important regional shear zone known as the Dove Lake Shear (Campbell 1971; Fig. 2). One of these is an ultramafic dyke, described by Scoates (1971), extending from Dove Lake (approximately 4 km NW of the northwest corner of the study area) to a point about 1 km north of Stormy Lake. This ultramafic body and the spatially associated zone of highly schistose and carbonatized rocks of the Dove Lake Shear have been traced to the northwest part of the study area. Southward along strike from the ultramafic unit is a medium grained quartz diorite dyke which is also foliated and carbonated. These dykes obviously cut the gabbroic sills and all threeformations. The presence of both sheared and unsheared intrusions occupying the Dove Lake Shear indicates that intrusion and shearing were probably synchronous.

Intermediate to felsic intrusions

Irregularly shaped feldspar ± (quartz) porphyry intrusions occur within the Stormy Lake Formation. They typically comprise 40 to 70 % tabular plagioclase phenocrysts (1 to 2 mm long) and 1 to 5 % quartz phenocrysts (1 to 2 mm in diameter) in a fine grey-green matrix. Narrow (1 to 15 m wide) feldspar ± (quartz) porphyry dykes are common in all three formations. Feldspar ± (quartz) porphyry bodies and dykes cut the mafic sills and dykes.

An irregular elongate body of tonalitic composition, which ranges from medium-grained and equigranular to quartzfeldspar porphyritic, intrudes the Gunnar Formation near the mine (Fig 2).

Quartz-feldspar porphyry dykes, 3 to 8 m thick with 10 to 40 % quartz phenocrysts (3 to 10 mm diameter) and 10 to 30 % feldspar phenocrysts (5 to 10 mm) in a grey aphanitic matrix occur within the Stormy Lake Formation and Gunnar Formation. In the Stormy Lake Formation the quartz-feldspar porphyry dykes intrude both the mafic sills and dykes as well as the feldspar ± (quartz) porphyry bodies.

Other intrusions

A set of narrow (10 cm to 1 m wide) lamprophyre dykes with mafic phenocrysts (chlorite after hornblende?), minor biotite and rare felsic fragments occur sporadically near the mine and crosscut the tonalite body. A set of narrow (10 cm to 1 m wide) mafic dykes with well developed chilled margins and large mafic phenocrysts in the dyke centres are uncommon but widely distributed, and intrude mafic sills and dykes as well as the feldspar ± (quartz) porphyry bodies.

A series of breccia dykes that form tabular to irregular bodies, 10 cm to 1 m wide, which truncate features such as pillow selvages and bedding, occurs on the northwest margin of the tonalite body. These dykes consist of angular fragments of host rock (Gunnar Formation) commonly 1 to 10 cm in length in a fine grained mafic matrix. The fragment to matrix ratio is about 50:1. About 2 % of the fragments resemble fine grained phases of the tonalite. These dykes both are cut by, and cut, quartz-albite veins which are spatially associated with the tonalite body.

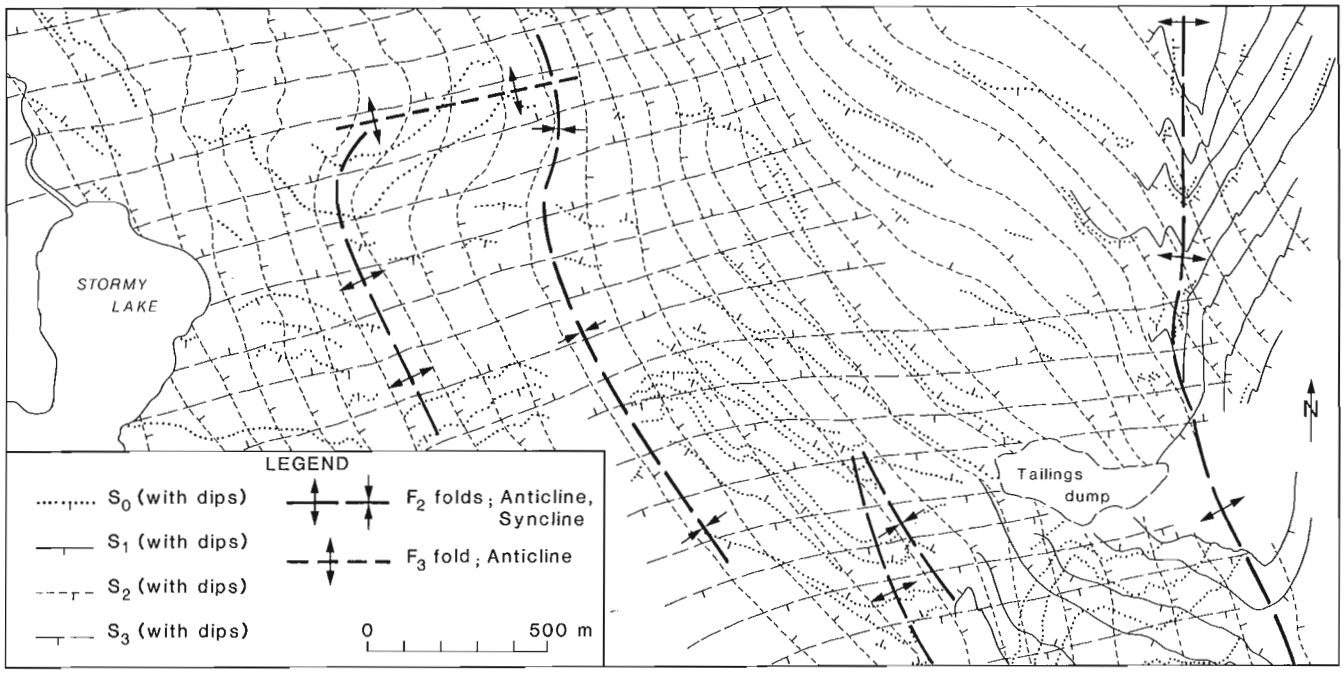

Figure 3. Simplified structural trend map of the study area.

STRUCTURE

Good facing data were obtained from graded beds, pillows, crossbedding, ripup clasts, scour and fill structures, sediment draping as well as modal layering in the gabbro sills. The facing directions, combined with lithological trends, define a series of NNW- to N-trending anticlines and synclines as the major structural features in the map area (Fig. 2). The anticline on the eastern side of the area, here termed the Eastern anticline, is a major regional feature as mapped by Stockwell and Lord (1939). In addition, a major structural discontinuity, across which certain lithological units are truncated, was identified between the eastern and western limbs of the Eastern Anticline and is here termed the Beresford Lake Deformation Zone.

At mesoscopic scale, conventional overprinting relationships indicated that at least three distinct generations of minor folds and cleavage were developed during the formation of the large structures (Fig. 3, Table 1). A major deflection in the strike of the earliest cleavages was noted in the northwest part of the study area (Fig. 3) further assisting in the definition of large scale folds. Furthermore, shear zones and faults are ubiquitous mesoscopic scale structures and these appear to have developed throughout the deformation history. Table 1 summarizes the observed temporal relationships between deformation, intrusion and mineralization in the map area.

Folds and cleavage

Three cleavages with associated folds were recognized in the study area. These are assigned to three deformational generations termed D1, D2, and D3. The earliest cleavage (S1) is a penetrative foliation and flattening fabric which was strongly developed during D1 east of the Beresford Lake Deformation Zone. The foliation is generally bedding-parallel, but is locally oblique to bedding at a high angle. Folds with axial planar S1 cleavage are rare and generally are intrafolial or isoclinal. The most readily recognized D1 folds are found within the zone of transposition and faulting which constitutes the Beresford Lake Deformation Zone. In an outcrop about 200 m east of the southern Gunnar shaft

Table 1. Summary of the geological development of the study area.

Time	Oldest ----------				Youngest
Deformation Event	D*	D1	D2	D3a	D3b
Foliation Type	None	S1 Penetrative flattening	S2 Penetrative crenulation pressure sol.	S3 Crenulation	None
Average Strike and Dip of foliation		Variable Mostly layer parallel	340/80	260/85	Kink bands Z 265/85 S 055/90
Mesoscopic Fold Profile	None known	Intrafolial Rare isoclines Fig. 4a	Chevron to isoclinal Fig. 4b, 4c	Chevron Fig. 4c	Kinks, box Fig. 4d
Average Plunge of Fold Axes		Variable	130/80 to 160/60	070/70	Z 080/70 S 055/60
Effect on Distribution of Lithologies	Unknown	Beresford Deformation Zone	Major syncline and anticlines	ENE trending fold in S2?	
Faulting and Shearing	Brittle faults Gouge	Shear zones of all scales	Shear zones mostly narrow	Uncommon	
Orientations of Faulting and Shearing	Bedding ‖	Bedding ‖ now trend from 300-20, folded	Mostly 355/80, 320/80 conjugates?		
Dominant Veining and Mineralization in Shears		VA ---- VC VB Gold			
Intrusion: Mafic sills and dykes		Lamprophyre Dove Lake Dykes			
Intrusion: Tonalite feldspar-(quartz) porphyry	----				
Intrusion: Quartz-feldspar porphyry	----				
Metamorphism	----	Greenschist			

Figure 4. Outcrop scale illustrations of the overprinting relationships of successive generations of deformation.

a) S1,F1 overprinted by S2,F2

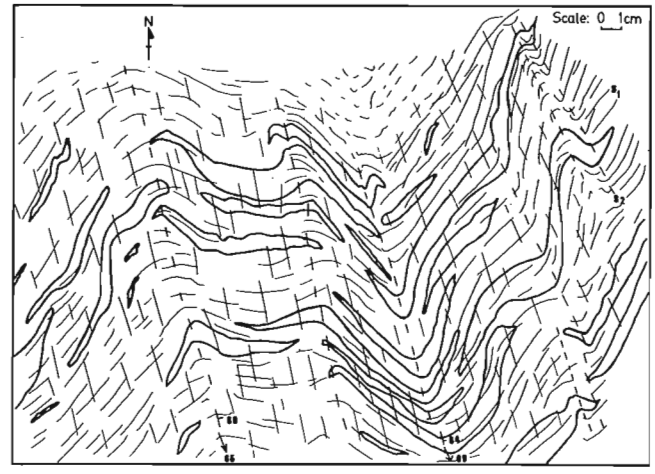

b) S1 overprinted by S2,F2

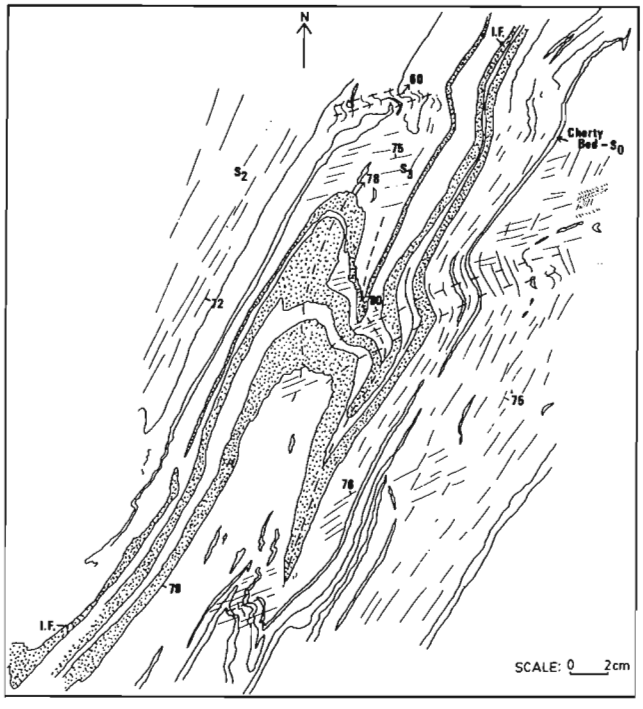

c) F2,S2 overprinted by S3,F3

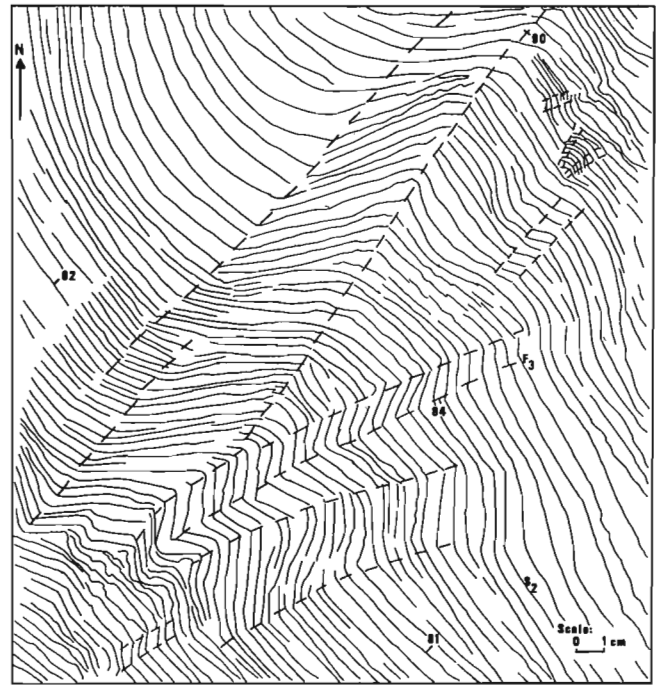

d) Conjugate kinks of D3 generation

within this highly strained zone, an intrafolially folded S1 cleavage and parallel chlorite band is refolded about S2 (Fig. 4a). This is provisionally interpreted as a D1 intrafolial fold, later refolded by D2. It is unclear how D1 affects rock distribution in the study area, although east of Beresford Lake, D1 resulted in major isoclinal folds.

A second cleavage (S2), which cuts and crenulates S1 and which is commonly axial planar to the major anticlines and synclines, was variably developed during D2 throughout the map area. S2 generally trends NNW and dips steeply ENE. In areas where S1 is not developed, S2 is simply a penetrative cleavage and flattening fabric. The majority of mesoscopic folds with S2 axial planar cleavages are chevron shaped (Fig. 4b) to isoclinal (Fig. 4c), with steep plunges to the southeast. Mesoscopic F2 folds commonly maintain constant S-asymmetries on the west limbs and Z-asymmetries on the east limbs of anticlines. D2 resulted in the major mappable NNW trending synclines and anticlines in the area.

A final single deformation (D3) is divided into D3a and D3b according to the style of deformation. D3a is characterized by the formation of a crenulation cleavage (S3) axial planar to chevron folds, and D3b is characterized by the formation of conjugate kink bands. S3 cleavage crenulates all fabrics in the study area, and generally trends just N of E and dips steeply north. It is strongly developed in the NW portion of the study area. S3 is axial planar to small chevron shaped to open parallel mesoscopic folds (Fig. 4c) of S1 or S2. The F3 folds commonly plunge steeply to the east-northeast. Kink bands were preferentially developed in the highly schistose rocks during D3b. Conjugate kink bands of D3b formed at approximately the same time as S3 cleavages, with orientations consistent with development in the same stress field, as kink bands and S3 cleavages were never seen cutting one another, and kink bands locally become S3 crenulation cleavages along their axial surface. Z-shaped kink bands trend EW and dip steeply south whereas S-shaped kink bands trend NE and are subvertical on average. Where both Z and S kink bands occur together, they form box folds (Fig. 4d). The mean orientation of S3 lies between orientations of the two sets of kink bands. It is therefore believed that D3a and D3b are different manifestations of the same deformation, and are dependant on the intensity of D3 and the nature of the rock being deformed.

A large change in strike of the penetrative cleavage (S2) occurs in the NW part of the study area (Fig. 3). This might be explained by folding of S2 during D3, because S2 is symmetrical about the mean orientation of S3 in this area. S0 would be folded along with S2 during D3, and restoring S2 to its original orientation in this area would result in S0 trending NS before D3, this orientation being perpendicular to the bedding trend south of the area. Therefore, either the angular relationship between S2 and S0 must have changed radically during D3, or the NNE trend of the S2 cleavage is the result of it being refracted into a strong NE trending zone of S1 cleavage. These possibilites require further study.

Shear zones and faults

Three generations of faults and shear zones are recognized and are assigned to D*, D1, and D2. D1 shears appear to have been reactivated during D2 making it difficult to distinguish them from D2 shears.

A brittle deformation event (termed D*) prior to greenschist metamorphism is implied by field relationships between dykes, brittle faults, and metamorphism. In the Gunnar mine area (Fig. 2), a set of ESE trending, steeply dipping (D*) brittle faults, characterized by gouge, appear to be healed and overprinted by greenschist metamorphism. Such faults do not offset ductile shear zones and were observed to be folded by F2 and overprinted by S2. Felsic dykes were probably emplaced into parallel fractures (now trending NS in the mine area) during D*, since an apophysis of a quartz-feldspar porphyry dyke intrudes a D* brittle fault and is also cut by the D* fault.

Ductile shearing was initiated during D1 and continued to develop throughout D2. D1 shear zones are variable in width (1 cm to 10 m), have many orientations and shear senses, and contain lineations with highly variable trends and plunges. Lineation plunges, within D1 ductile shear zones of the same orientation, are commonly highly variable. In many cases D1 shear zones display more than one generation of lineation. Some D1 shear zones are distinctly folded by D2 and cut by S2. Because shear zones are not commonly observed offsetting or even intersecting each other, distinct generations cannot be determined easily, and many shears assigned to D1 may have been reactivated during D2.

D2 shear zones mostly developed late in D2. They are generally narrow (a few centimetres) and are characterized by consistent orientations. Many D2 shears belong to a set of conjugate shears. D2 shear zones are recognized by their relatively consistant orientations. Two dominant orientations of D2 shear zones, 355°/80° and 320°/80°, appear to be conjugates.

All shear zones may have formed and progressively rotated during the D1 and D2 deformations with only the final set (D2 shears) showing constant attitude and shear sense.

All shear zones are affected by D3 kink bands and some, such as the Dove Lake Shear, are cut by S3. Limited shear zone development or movement is therefore attributed to D3.

There are three major high strain zones in the area:

1. The Beresford Lake Deformation Zone: As already discussed, this is a D1 structure and is characterized by strong S1 development and transposition of S0. It is a major structural continuity, since map units are truncated across it. This zone has mineral lineations plunging moderately southeast.
2. At the southern edge of the map area a NW-trending D1 or D2 structure is characterized by a strong foliation, 100:1 stretching lineations plunging steeply southeast, and local carbonatization. This may be a continuation of, or a splay from, the Beresford Lake Deformation Zones

3. In the western part of the study area, the Dove Lake Shear is a high strain zone characterized by dykes, local carbonatization and shearing. It has steeply east-plunging lineations. There is a 100 m offset of lithological contacts across the Dove Lake Shear.

GOLD MINERALIZATION

Three dominant types of quartz veins in shear zones are recognized in the area. These are provisionally termed VA, VB, and VC veins. VA veins are low in gold content (<200ppb), and consist of quartz and pyrite±calcite. VB veins consist of quartz-ankerite-sulphides-gold and have associated carbonate alteration. VC is characterized by quartz-chlorite-calcite.

The majority of gold from the Gunnar mine was extracted from a zone of VB veins localized at the intersection of the quartz-feldspar porphyry dyke and the Gunnar #1 shear, near the southern shaft (Fig. 2; Stockwell and Lord, 1939). The #1 shear is an ESE trending subvertical D1 shear with mineral lineations plunging moderately to the west-northwest. The steeply east-dipping, north-trending dykes in the mine area are offset sinistrally in plan and early fractures curve sinistrally into the shear. The oblique-slip movement indicated by the lineations requires north side down movement, given the indicated sinistral horizontal component. To the west, the Gunnar #1 shear becomes narrow, and north-trending conjugate shears become more prevalent. To the east, the #1 shear curves to a southeasterly orientation and is lost in a parallel zone of strong S1 foliation which has been folded by D2. Parallel shear zones to the north of the Gunnar #1 shear have various lineation plunges and movement senses, but also curve into more southeasterly orientations to the east.

The timing of the gold mineralization can be constrained with respect to intrusion, deformation, and mineralization by the following relationships:

1. Shears with VA veins are folded about F2 folds and cut by S2 cleavage.
2. VA and VB veins are typically found only in D1 shears.
3. VA and VB veins are both locally found in different parts of the same D1 shear zone
4. VC veins are common in both D1 and D2 shears, indicating that VC probably represents a late phase of mineralization.
5. Lamprophyre dykes cut some VA veins and are offset by the shear zones containing other VA veins, indicating that those D1 shears which host VA veins and which ceased movement early in D1, predate lamprophyre intrusion.
6. Lamprophyre dykes are either offset by VB bearing shears or have intruded them with only slight fracture development in the dykes (Stockwell and Lord, 1939). This indicates the VB veins in the D1 shears must have formed coincidentally with the lamprophyre dykes.

Since lamprophyre dykes cut some VA veins and some VA veins are folded, the lamprophyres must have intruded near the end of D1 or later. Since VB mineralization is not in the D2 shears, VB veining and accompanying gold mineralization must have occurred very late in D1 or early in D2.

DISCUSSION

Although most of the gold in the Gunnar mine was obtained from veins near the intersection of the quartz-feldspar porphyry dykes and shears, the porphyry dykes are clearly earlier than the gold mineralization. Therefore, the dykes must have structurally affected the ore-bearing environment in some way so as to produce higher grade gold mineralization near their contacts. Perhaps the dykes behaved more brittlely in the ductile shear zones than the surrounding basalts and this resulted in a zone of greater or more persistant dilatancy being developed within or adjacent to them.

Proximity to the Beresford Lake Deformation Zone is another feature that may be important in the localization of gold in the Gunnar mine area. The Beresford Lake Deformation Zone has many features in common with major Archean tectonic zones such as the Cadillac Break or the Porcupine-Destor Break including transposition, strong development of cleavages, lithological truncations, and intrafolial fold development. Gold deposits are commonly spatially associated with such tectonic zones. It may, therefore, be profitable to concentrate exploration near and along the Beresford Lake Deformation Zone and its presumed extensions northward and southward from the study area.

ACKNOWLEDGMENTS

The authors wish to express their gratitude to Dave Busch of Homestead Resources who provided access to the property and much helpful information. Kathryn Baker is thanked for assistance in the field and in preparing this document. Critical review by François Robert resulted in an improved manuscript.

REFERENCES

Campbell, F.H.A.
1971: Stratigraphy and sedimentation of part of the Rice Lake Group, Manitoba; in Geology and Geophysics of the Rice Lake region, Southeastern Manitoba (Project Pioneer); edited by W.D. McRitchie and W. Weber, Manitoba Mines Branch, Publication 711, p.135-188.

Scoates, R.F.J.
1971: Ultramafic rocks of the Rice Lake Greenstone Belt; in Geology and Geophysics of the Rice Lake Region, Southeastern Manitoba (Project Pioneer); edited by W.D. McRitchie and W. Weber, Manitoba Mines Branch, Publication 711, p.135188.

Seneshen, D.M. and Owens, D.J.
1985: GS23 Geological Investigations in the Stormy Lake Area; in Manitoba Energy and Mines, Geological Services, Report of Field Activities, 1985, p. 112-119 and map 1985R1, 1:10 000 scale.

Stephenson, J.F.
1971: Gold deposits of the Rice Lake-Beresford Lake Greenstone Belt, Southeastern Manitoba; in Geology and Geophysics of the Rice Lake Region, Southeastern Manitoba (Project Pioneer); edited by W.D. McRitchie and W. Weber; Manitoba Mines Branch, Publication 711, p.135-188.

Stockwell, C.H. and Lord, C.S.
1939: Halfway Lake-Beresford Lake Area, Manitoba; Geological Survey of Canada, Memoir 219.

Weber, W.
1971: Geology of the Long Lake-Gem Lake area; in Geology and Geophysics of the Rice Lake region, southeastern Manitoba (Project Pioneer); edited by W.D. McRitchie and W. Weber, Manitoba Mines Branch, Publication 711, p.135-188.

Preliminary lithological, petrological, and geochemical investigations of the Archean Florence Lake Group, central Labrador[1]

Terry D. Brace[2] and Derek H.C. Wilton[2]

Brace, T.D. and Wilton, D.H.C., Preliminary lithological, petrological, and geochemical investigations of the Archean Florence Lake Group, central Labrador; in Current Research, Part C, Geological Survey of Canada, Paper 89-1C, p. 333-344, 1989.

Abstract

The Florence Lake belt occurs in the most southerly portion of the Archean Nain Province, immediately north of the Proterozoic supracrustals of the Labrador Central Mineral Belt. The Florence Lake Group consists dominantly of mafic metavolcanic rocks with minor metasedimentary and metafelsic volcanic rocks. Ultramafic rocks, variably serpentinized and altered to talc-carbonate, occur as concordant intrusions within the group. The group was later intruded by the Archean tonalitic-trondhjemitic Kanairiktok Intrusive Suite. Geochemically, the mafic volcanics resemble tholeiitic ocean floor basalts, whereas the felsic volcanics are calc-alkaline. Proterozoic diabase and gabbroic dykes cut all other lithologies. Carbonatized ultramafics at the Baikie showing contain nickeliferous pyrrhotite with elevated PGE contents.

Résumé

La zone de Florence Lake se trouve dans l'extrême sud de la province archéenne de Nain, immédiatement au nord des roches supracrustales protérozoïques de la zone minérale Centrale du Labrador. Le groupe de Florence Lake se compose principalement de roches métavolcaniques mafiques, accompagnées de quelques roches métasédimentaires et roches volcaniques métafelsiques. Les roches ultramafiques, diversement serpentinisées et altérées en carbonate et talc, se présentent sous forme d'intrusions concordantes à l'intérieur de ce groupe. Ce dernier a plus tard été traversé par la suite intrusive archéenne de Kanairiktok, de caractère tonalitique et trondhjemitique. Géochimiquement, les roches volcaniques mafiques ressemblent aux basaltes tholéïtiques des fonds marins, tandis que les roches volcaniques felsiques sont calco-alcalines. Des dykes protérozoïques de diabase et de gabbro recoupent tous les autres types de roches. Les roches ultramafiques carbonatisées de la venue de Baikie contiennent de la pyrrhotine nickélifère caractérisée par une teneur élevée en éléments du groupe du platine (EGP).

[1] Contribution to the Canada-Newfoundland Mineral Development Agreement 1984-1989. Project carried by the Geological Survey of Canada, Mineral Resources Division.

[2] Department of Earth Sciences/Centre for Earth Resources Research, Memorial University of Newfoundland, St. John's, Newfoundland, A1B 3X5.

INTRODUCTION

Regional geological mapping on a scale of 1:50,000 was carried out during the summer of 1987 in the Florence Lake Greenstone Belt, an Archean supracrustal sequence located approximately 200 km northwest of Goose Bay and 55 km southwest of the coastal village of Hopedale, Labrador (Fig. 1).

The project was undertaken (i) to re-examine known mineral occurrences in the Florence Lake area, in particular the Baikie showings, which have reported anomalous Ni and PGE concentrations; and (ii) to determine the petrography and establish the chemical affinities of lithologies within the Florence Lake Greenstone Belt.

Work to date has involved petrographic studies, electron-microprobe analyses, and major and trace element analyses of approximately forty-five whole rock samples (Wilton and Brace, 1988). Future laboratory work will include carbon isotope and/or fluid inclusion studies, further whole rock analyses (major elements, trace elements, REE) and analyses of precious metals (PGE and Au).Thus, the work reported herein is preliminary, and more detailed studies will form the basis of an MSc. thesis by Brace at Memorial University of Newfoundland.

PREVIOUS WORK

In 1959, Lundberg Exploration Ltd., on behalf of BRINEX, conducted a 300-square-mile airborne magnetometer and electromagnetic survey that included the Florence Lake area (Wilson, 1959). Subsequent follow-up surveys led to the discovery of the Baikie showings.During 1960-1963, BRINEX Ltd. and Asbestos Corporation carried out geological mapping, soil sampling and ground magnetometer surveys, and pack sack drilling of the Baikie showings (Piloski, 1962).Sutton (1970) carried out geological mapping for BRINEX Ltd. in the area northwest of Florence Lake.

During 1978-1979, Ingo Ermanovics and other GSC personnel carried out 1:50,000 scale geological mapping of the Hopedale Block (Ermanovics and Raudsepp, 1979), and in the early 1980s the GSC, in conjunction with the Newfoundland Department of Mines and Energy, conducted a lake sediment geochemical survey.

In 1982-1983, BP Minerals, in joint venture with Billiton Canada Ltd., carried out an airborne geophysical survey, as well as ground work that included geological mapping, VLF and prospecting in hopes of finding base metals and gold within the Florence Lake Greenstone Belt (Guthrie, 1983; Stewart, 1983).

In 1986, the PGE potential of the Baikie showing was assessed by Platinum Exploration Canada Ltd. (Reusch, 1987; Arengi, 1987).

GENERAL GEOLOGY

The Archean Florence Lake Group forms a 65-km-long, northeast-trending supracrustal sequence within the eastern Nain structural province, Labrador (Ermanovics and Raudsepp, 1979) (Fig. 1).The greenstone belt consists predominantly of dark to medium green, mafic to intermediate flows and pillow lavas, and minor synvolcanic sills.White, and pink, and pale green weathering felsic metavolcanic and metasedimentary rocks are less extensively developed.Ultramafic rocks, which have undergone various degrees of serpentinization and talc-carbonate alteration, form elongate, regionally concordant intrusive bodies within the Florence Lake Group.

The Florence Lake Group is intruded by the Archean Kanairiktok Intrusive Suite (Ermanovics and Raudsepp, 1979), which consists of white-to-pink weathering, massive to gneissic trondhjemite. Both units are folded and have undergone middle greenschist facies metamorphism.

All rocks in the area are intruded by red- to brown-weathering diabase and gabbroic dykes which range in thickness from a few centimetres up to 100 metres.

FLORENCE LAKE GROUP

Based largely on colour index (CI) and associated textures, the Florence Lake Group has previously been divided into three formations (Ermanovics and Raudsepp, 1979). These include the Lise Lake (CI < 15-20 %), Adlatok (CI= 15-20 % to 35-40 %), and Schist Lakes (CI= 35-40 % to 70 %) formations, which correspond generally to a felsic, intermediate, and mafic volcanic association, respectively.

Within the map area (Fig. 1), dark to medium green mafic pillow lavas and flows (Unit 4) are by far the most abundant lithology. White and pale pink, to pale green weathering felsic metavolcanic and metasedimentary rocks (Unit 5) are locally well developed.

Unit 4

Field description

Unit 4 consists predominantly of medium to dark green, intermediate to mafic flows and pillow lavas and associated synvolcanic sills.The flows are characteristically schistose. Locally they are interbedded with white to-pink- weathering siliceous metasedimentary units of variable thickness (several centimetres to one metre). Pillow lavas are commonly stretched and variably deformed, and individual pillows are commonly less than 1 metre in maximum dimension. Massive synvolcanic sills, which contrast markedly with schistose volcanics, contain large (up to 2 cm long) saussuritized plagioclase phenocrysts.

Petrography

The mafic volcanic rocks are generally very fine-grained, well foliated, schists composed of chlorite, amphibole, epidote and quartz. Relict igneous textures have not been observed.

Unit 5

Field description

Unit 5 consists predominantly of white-pink and pale green-weathering siliceous metavolcanic and/or metasedimentary

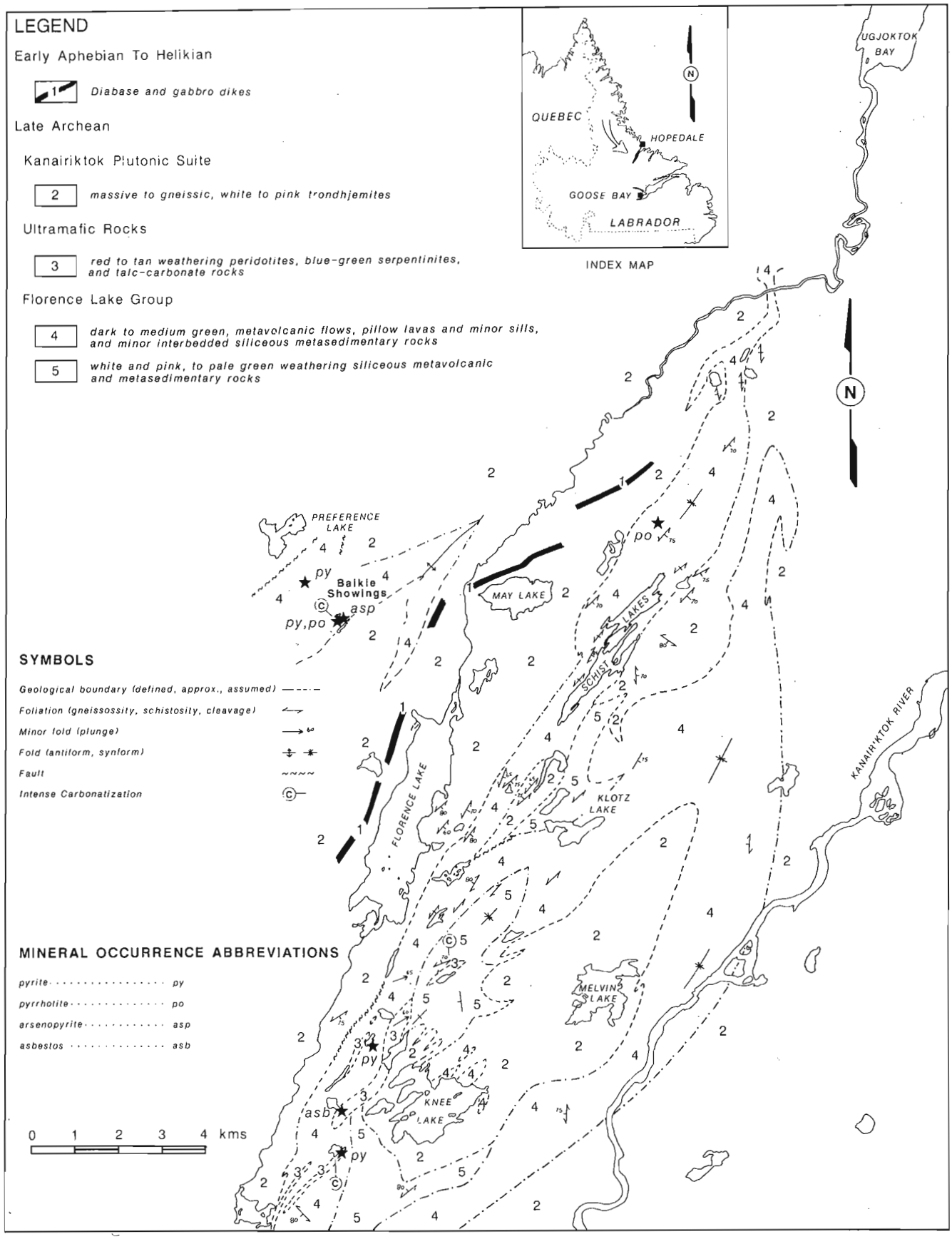

Geology modified after I. Ermanovics and M. Raudsepp (1978-79); unpublished

Figure 1. Geology and mineral location map of the Florence Lake map area, central Labrador.

rocks.They are readily distinguished from the much more abundant mafic volcanics of Unit 4 by their inherent pale colour and more competent character. In the field, classification of these rocks as either sedimentary or volcanic is extremely difficult. In high strain contact zones with the intrusive trondhjemites (Unit 2), it is difficult to distinguish between these siliceous volcanic and/or sedimentary rocks and the trondhjemitic rocks themselves.

This unit consists of very fine-grained, micaceous siliceous rocks and medium-grained siliceous rocks with abundant quartz and feldspar fragments.One distinctive subunit contains large blue quartz eyes.

Following detailed petrographic studies, Ermanovics (pers.comm., 1987) indicated that it now seems doubtful that pyroclastic rocks are as prevalent throughout the Florence Lake greenstone belt as was originally described in Ermanovics and Raudsepp (1979).

Petrography

One of the main problems in classifying the felsic rocks is to distinguish among flows, tuffs, tuffaceous sediments, or even highly deformed granitic rocks in contact zones.

Ermanovics and Raudsepp (1979) considered the felsic rocks to be predominantly poorly sorted tuffs. The retention of delicate volcanic features (e.g. embayed quartz phenocrysts) and the poorly sorted nature of this lithology suggest that, if these rocks are indeed tuffs or tuffaceous sediments, they are proximal to their source region.

Petrographic studies show that the rocks vary considerably, from porphyritic dacite to fine-grained hornblende and muscovite schists. Two samples studied, which contain about 10 % euhedral plagioclase and minor quartz phenocrysts (up to 3 mm) in a fine-grained quartz matrix, are thought to be dacitic flows. Other samples contain more abundant quartz phenocrysts (4-5 mm) with lesser amounts of plagioclase. The quartz is subangular to subrounded and locally displays glomeroporphyritic textures.

Chemistry

Graphical display of whole-rock chemistry, presented in Tables 1 (a),(b), is plotted in Figures 2 to 4. Based on the (Zr/TiO2) - (Nb/Y) discrimination diagram of Winchester and Floyd (1977) the Florence Lake Group volcanic rocks plot in the andesite/basalt, rhyodacite/dacite, and rhyolite fields (Fig. 2). The absence of sample points within the andesite field could indicate a bimodal nature to the volcanic suite, although it may be simply a function of the very small data set.

On the AFM diagram (Fig. 3a) the dacites/rhyolites plot in the calc-alkaline field and the basalts plot in the tholeiitic field. In Figure 3b, the cation plot of Jensen (1976), the basalts plot within the high-Fe tholeiitic basalt field, whereas the felsic rocks straddle the boundary between the tholeiitic and calc-alkaline fields and plot as andesite, dacite and rhyolite. On Pearce and Cann (1973) discrimination diagrams (Fig. 4a, b, c) the basalts plot in the ocean floor basalt (OFB) field.

The basalts and dacites/rhyolites have comparable concentrations of Sr, but some basalts are notably depleted in Rb (Fig.5). The Rb/Sr ratios of volcanics in the Florence Lake Group range between 1.0 and 0.1.

ULTRAMAFIC ROCKS (UNIT 3)

Field description

Ultramafic rocks, which are commonly spatially associated with intensely carbonatized metavolcanic rocks, form elongate intrusive bodies within the Florence Lake Group. The ultramafic rocks weather reddish-brown to tannish-brown,

Table 1. a) Chemical analyses and CIPW-normative mineralogies of basalts. b) Chemical analyses and CIPW-normative mineralogies of dacites and rhyolites.

a	TB-87-051	87-149A	87-150	87-156A	87-189B	87-238B
SiO2 (wt. %)	50.60	48.80	43.80	47.60	56.60	49.00
TiO2	1.12	0.96	1.04	1.20	1.20	1.32
Al2O3	17.00	13.80	14.70	13.60	12.70	13.70
FeO* (total Fe)	9.88	13.22	15.55	16.81	11.51	15.80
MnO	0.16	0.16	0.24	0.22	0.22	0.22
MgO	4.88	7.47	6.36	7.88	3.48	5.98
CaO	8.76	5.58	12.36	8.98	9.54	9.30
Na2O	2.89	1.34	1.18	2.13	1.20	1.97
K2O	0.12	0.27	0.02	0.63	0.06	0.67
P2O5	0.08	0.06	0.08	0.15	0.09	0.09
LOI	4.51	6.41	3.19	1.74	2.06	1.15
Total	100.00	98.07	98.52	100.94	98.66	99.20
Rb (ppm)	nd	7	nd	10	nd	14
Sr	145	90	139	103	139	107
Y	22	21	22	25	31	30
Zr	63	57	59	77	81	81
Nb	5	4	6	7	5	6
Ga	16	16	18	17	18	18
Zn	96	73	95	97	135	137
Cu	59	57	30	58	3	144
Ni	133	85	140	46	55	61
Ba	55	34	nd	43	11	44
V	335	349	319	407	349	452
Cr	333	307	289	54	173	55
Q (wt. %)	3.34	8.26	---	---	20.37	0.06
C	---	1.30	---	---	---	---
or	0.71	1.60	0.12	3.72	0.35	3.96
ab	24.45	11.34	9.98	18.02	10.15	16.67
an	33.07	27.29	34.76	25.69	29.09	26.56
di	8.20	---	21.82	14.91	14.92	15.94
hy	21.90	37.91	13.39	17.04	17.49	29.76
ol	---	---	10.75	14.66	---	---
mt	1.59	2.13	2.51	2.71	1.85	2.55
cm	0.07	0.07	0.06	0.01	0.04	0.01
il	2.13	1.82	1.98	2.28	2.28	2.51
ap	0.19	0.14	0.19	0.35	0.21	0.21

b	87-054A	87-074	87-077A	87-092	87-153	87-247B	87-257
SiO2 (wt. %)	70.40	64.20	64.20	66.40	62.50	73.90	65.70
TiO2	0.16	0.56	0.48	0.16	0.64	0.08	0.56
Al2O3	13.20	16.10	13.00	17.40	14.90	14.10	16.20
FeO* (total Fe)	2.69	5.38	7.83	4.56	5.07	0.64	3.36
MnO	0.05	0.07	0.10	0.05	0.09	0.00	0.05
MgO	1.01	2.44	3.28	1.11	3.75	0.79	1.66
CaO	3.26	2.86	5.02	1.40	5.24	0.24	4.10
Na2O	4.54	4.96	2.14	1.87	3.22	5.43	6.18
K2O	1.28	0.44	0.71	1.83	2.04	1.62	0.52
P2O5	0.09	0.12	0.25	0.21	0.06	0.08	0.13
LOI	3.45	1.55	2.41	3.59	1.69	1.41	1.26
Total	100.13	98.68	99.42	98.58	99.20	98.29	99.72
Rb (ppm)	33	8	25	38	50	47	12
Sr	99	106	110	97	219	161	145
Y	13	17	13	14	18	5	12
Zr	152	158	125	156	142	101	131
Nb	8	6	7	8	8	3	6
Ga	15	20	16	18	14	20	15
Zn	27	58	61	6	42	nd	11
Cu	4	nd	nd	nd	nd	nd	6
Ni	nd	30	43	2	44	nd	2
Ba	374	120	143	403	567	281	221
V	37	94	98	142	108	30	75
Cr	nd	53	82	23	68	nd	nd
Q (wt. %)	29.83	20.78	28.81	41.29	17.29	34.26	15.85
C	---	2.55	0.18	10.30	---	3.17	---
or	7.57	2.60	4.20	10.82	12.06	9.58	3.07
ab	38.41	41.97	18.11	15.82	27.24	45.94	52.29
an	11.86	13.41	23.27	5.57	20.18	0.67	14.93
di	3.13	---	---	---	4.45	---	---
hy	4.97	13.67	19.77	9.71	14.17	2.83	6.67
ol	---	---	---	---	---	---	---
mt	0.43	0.87	1.26	0.73	0.82	0.10	0.54
cm	---	0.01	0.02	---	0.01	---	---
il	0.30	1.06	0.91	0.30	1.22	0.15	1.06
ap	0.21	0.28	0.59	0.50	0.14	0.19	0.31

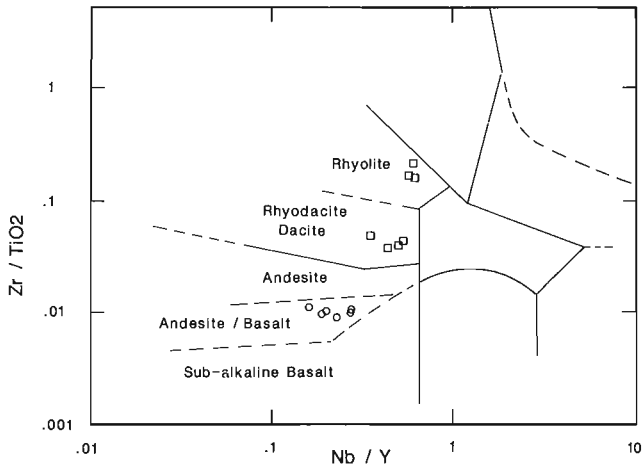

Figure 2. Zr/TiO2 vs. Nb/Y discrimination diagram (after Winchester and Floyd, 1977) for metavolcanic rocks. Open circles = basalts, open squares = dacites/rhyolites.

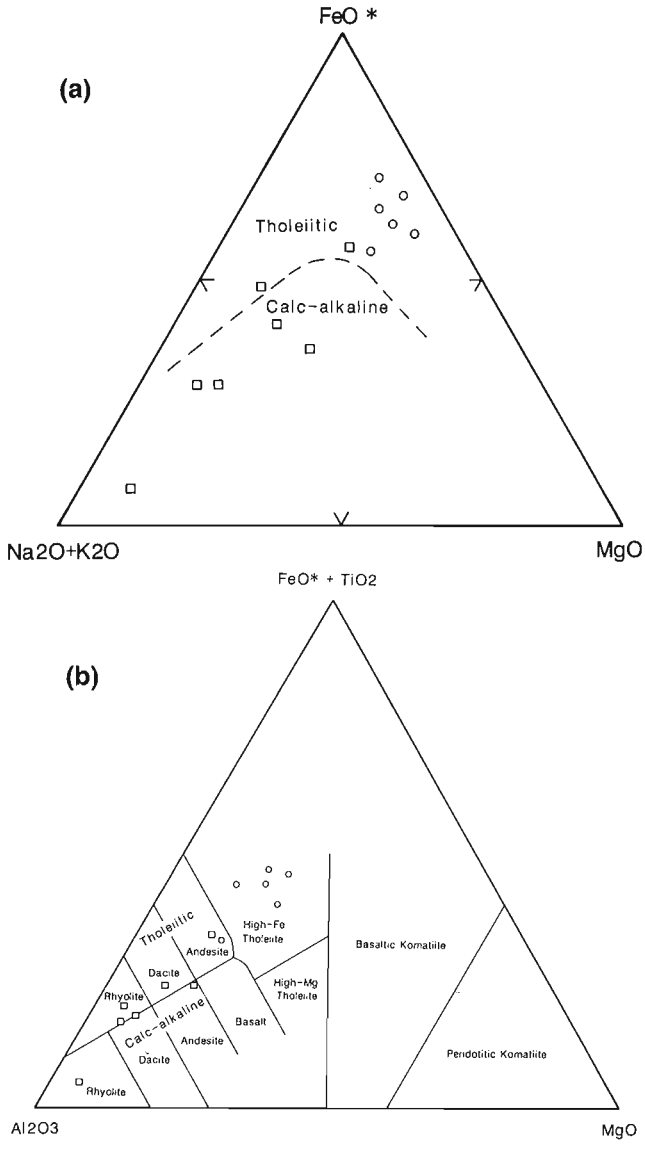

Figure 3 a) AFM diagram for metavolcanic rocks; tholeiitic calc-alkaline dividing line from Irvine and Baragar (1971) (symbols as for Fig. 2). b) Cation diagram (Al-Fe + Ti-Mg) (after Jensen, 1976) for metavolcanic rocks (symbols as for Fig. 2).

Table 2. Chemical analyses and CIPW-normative mineralogies of ultramafic rocks.

	TB-87-173	87-174	87-179	87-180C	87-181
SiO2 (wt. %)	39.80	41.40	38.60	38.10	37.90
TiO2	0.12	0.08	0.12	0.12	0.08
Al2O3	2.22	2.33	0.72	0.61	0.72
FeO* (total Fe)	8.40	4.66	11.28	11.56	9.01
MnO	0.07	0.08	0.06	0.07	0.12
MgO	37.45	40.50	38.05	37.10	40.05
CaO	0.18	0.04	0.56	0.56	0.00
Na2O	0.00	0.00	0.00	0.01	0.00
K2O	0.01	0.01	0.00	0.00	0.00
P2O5	0.02	0.02	0.01	0.00	0.00
LOI	11.10	11.65	11.39	11.40	11.30
Total	99.37	100.77	100.79	99.53	99.18
Rb (ppm)	nd	nd	nd	nd	nd
Sr	4	3	21	4	2
Y	2	3	2	nd	1
Zr	12	12	7	7	5
Nb	2	2	2	2	2
Ga	4	4	2	1	2
Zn	25	20	23	19	32
Cu	nd	nd	nd	nd	nd
Ni	2229	2373	2972	3311	2649
Ba	nd	nd	nd	nd	nd
V	60	63	39	40	39
Cr	3065	1665	1373	1153	1308
C (wt. %)	1.93	2.29	---	---	0.72
or	0.06	0.06	---	---	---
ab	---	---	---	---	---
an	0.76	0.07	1.96	1.62	---
di	---	---	---	0.92	---
hy	29.73	32.38	18.05	18.28	16.76
ol	54.04	53.30	66.75	65.19	68.81
mt	1.35	0.75	1.82	1.86	1.45
cm	0.66	0.36	0.30	0.25	0.28
il	0.23	0.15	0.23	0.23	0.15
ap	0.05	0.05	0.02	---	---

	87-184A	87-184B	87-185A	87-185B	87-189A
SiO2 (wt. %)	37.10	37.50	31.60	38.80	31.80
TiO2	0.12	0.12	0.00	0.08	0.08
Al2O3	1.04	1.15	0.61	0.61	0.83
FeO* (total Fe)	7.90	7.02	6.81	7.28	7.85
MnO	0.11	0.10	0.12	0.02	0.10
MgO	38.50	38.85	38.70	41.25	40.55
CaO	0.06	1.60	0.00	0.00	0.04
Na2O	0.00	0.00	0.00	0.00	0.00
K2O	0.00	0.00	0.00	0.00	0.00
P2O5	0.01	0.02	0.00	0.01	0.01
LOI	15.80	14.34	21.21	12.58	19.52
Total	100.64	100.70	99.05	100.63	100.78
Rb (ppm)	nd	nd	nd	nd	nd
Sr	3	7	4	2	3
Y	1	1	1	1	2
Zr	5	5	2	4	3
Nb	2	2	1	2	1
Ga	2	2	nd	nd	nd
Zn	20	19	31	14	16
Cu	nd	nd	nd	nd	nd
Ni	2148	2187	2276	2397	2437
Ba	nd	nd	nd	nd	nd
V	34	30	23	16	30
Cr	2925	2110	1136	1183	1146
C (wt. %)	0.95	---	0.61	0.63	0.78
or	---	---	---	---	---
ab	---	---	---	---	---
an	0.23	3.14	---	---	0.13
di	---	3.68	---	---	---
hy	19.17	11.12	1.10	19.01	---
ol	62.85	66.96	75.03	67.12	80.16
mt	1.27	1.13	1.10	1.17	1.26
cm	0.63	0.45	0.24	0.25	0.25
il	0.23	0.23	---	0.15	0.15
ap	0.02	0.05	---	0.02	0.02

	87-195	87-198B	87-198C	87-199A	87-248
SiO2 (wt. %)	27.30	31.10	31.10	32.20	38.90
TiO2	0.00	0.08	0.08	0.08	0.00
Al2O3	0.19	0.40	0.17	0.51	1.20
FeO* (total Fe)	10.45	7.55	6.52	7.40	5.45
MnO	0.13	0.14	0.14	0.10	0.07
MgO	40.30	39.05	41.15	40.45	37.30
CaO	0.00	0.02	0.06	0.28	1.74
Na2O	0.00	0.00	0.00	0.00	0.00
K2O	0.00	0.00	0.00	0.00	0.00
P2O5	0.00	0.00	0.01	0.01	0.00
LOI	21.78	22.19	21.01	19.68	14.51
Total	100.15	100.53	100.24	100.71	99.17
Rb (ppm)	nd	nd	nd	nd	nd
Sr	2	4	3	5	9
Y	1	2	nd	3	1
Zr	2	3	1	3	5
Nb	1	2	1	2	2
Ga	nd	nd	3	2	3
Zn	2	28	31	19	13
Cu	nd	nd	nd	nd	nd
Ni	2692	2639	2744	2620	1983
Ba	nd	nd	nd	nd	nd
V	6	20	8	19	24
Cr	1127	2330	1399	1385	2197
C (wt. %)	0.19	0.36	0.08	0.02	---
or	---	---	---	---	---
ab	---	---	---	---	---
an	---	0.10	0.23	1.32	3.27
di	---	---	---	---	4.21
hy	---	---	---	---	20.62
ol	83.00	77.12	79.64	79.42	55.58
mt	1.68	1.22	1.05	1.19	0.88
cm	0.24	0.50	0.30	0.30	0.47
il	---	0.15	0.15	0.15	---
ap	---	---	0.02	0.02	---

and are bluish-green where the rocks have been more extensively cleaved. Variations in colour are due to varying degrees of serpentinization and talc-carbonate alteration, which commonly results in the development of rinds on outcrop surfaces. Igneous layering is preserved in places where unaltered clinopyroxene is present. Sporadic coarse-grained rhombohedral carbonate and magnetite veins cut the ultramafic rocks. Near the southern part of the map sheet, highly serpentinized ultramafic rocks form recessive scree slopes.

Petrography

The ultramafic rocks are invariably medium grained (1 to 3 mm), locally well layered, and commonly display well developed relict cumulate textures. Apparently, the sequence originally consisted predominantly of dunite and peridotite. Thin section examination reveals totally serpentinized olivine pseudomorphs with magnetite concentrated along grain boundaries effectively outlining intercumulus areas. Chromite is a common accessory in several samples, whereas unaltered cumulate clinopyroxene was observed in only one sample.

Chemistry

Major and trace element analyses of the ultramafic rocks (Table 2.) show that these samples have undergone extensive, but variable, degrees of serpentinization and talc-carbonate alteration (high L.O.I). However, the concentrations of Ni and Cr are normal for ultramafic rocks and reflect the relative immobility of these elements during alteration and deformation.

KANAIRIKTOK INTRUSIVE SUITE (UNIT 2)

Field description

Medium- to coarse-grained granitic rocks of the Kanairiktok Intrusive Suite intrude and envelope the Florence Lake Group (Fig. 1). These rocks, which weather white to pink, vary from massive, non-foliated to well foliated and gneissic.

The contacts between the granitic and metavolcanic rocks are generally sharp; however, xenoliths and rafts of metavolcanic rocks occur locally within the granitoids. In

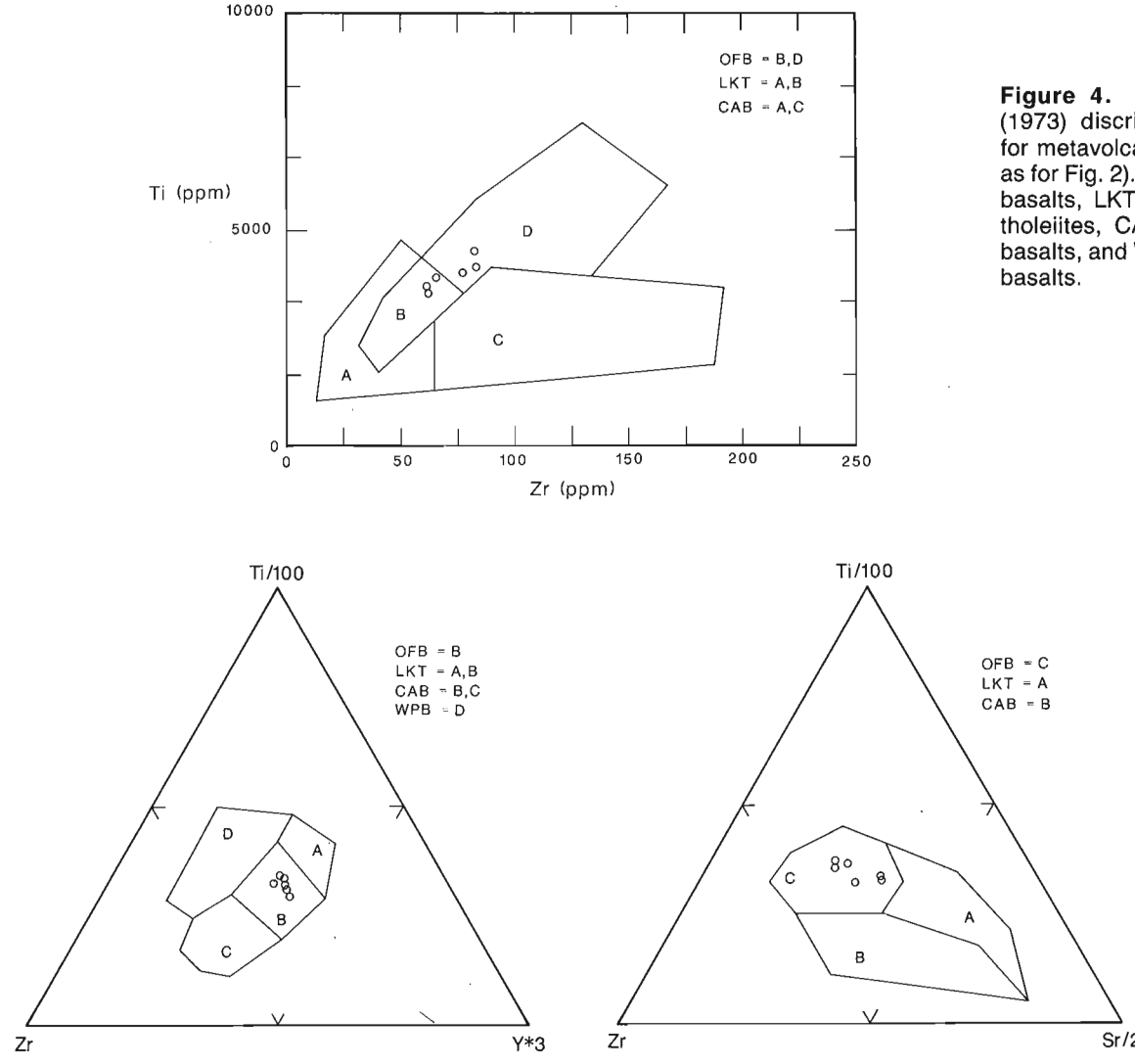

Figure 4. Pearce and Cann (1973) discrimination diagrams for metavolcanic rocks (symbols as for Fig. 2). OFB = ocean-floor basalts, LKT = low- potassium tholeiites, CAB = calc-alkaline basalts, and WPB = within-plate basalts.

these areas, the granitic rocks commonly show cataclasis and angular folds defined by alternating quartz and quartzofeldspathic layers. To the northwest of Florence Lake, in the vicinity of the Baikie showings, angular xenoliths and rafts of metavolcanic rocks are so numerous that the granitic rocks are more properly termed agmatites (Fig. 6). The metavolcanic rocks have been metamorphosed to amphibolite facies near the contact zones, with a marked decrease in metamorphic grade away from the contact.

Petrography

The granitic rocks contain plagioclase, quartz, muscovite, biotite, chlorite (after biotite) and epidote. Less deformed samples show hypidiomorphic textures with euhedral to subhedral plagioclase crystals (up to about 5 mm) and anhedral quartz. Samples with variably chloritized biotite, muscovite, and epidote have poorly to moderately well developed foliation.

In areas of high strain the rocks are gneissic, and are characterized by alternating discontinuous layers of partially recrystallized ribbon quartz and quartz-plagioclase segregations that locally form augens up to 1 cm in length. The plagioclase generally forms highly saussuritized grains about 0.25 to 0.5 mm in diameter. Secondary muscovite, biotite, chlorite and sporadic carbonate are concentrated on folia, which locally show cataclastic textures.

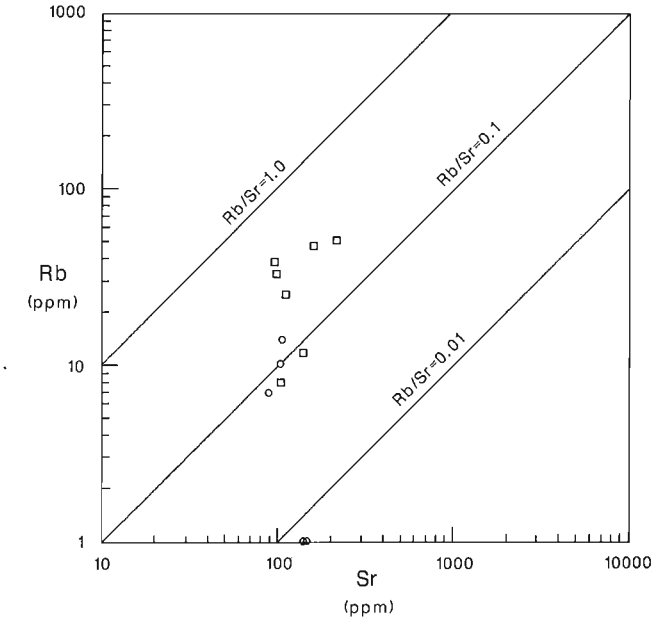

Figure 5. Rb-Sr plot for metavolcanic rocks (symbols as for Fig. 2).

Figure 6. Angular metavolcanic xenoliths within remobilized Kanairiktok Intrusive Suite trondjhemite, just south of the Baikie showing.

Chemistry

Ermanovics and Raudsepp (1979) described the Kanairiktok granitic rocks as predominantly granodiorite to tonalite.

Analysis of six granitoids samples plot in the trondhjemite field of O'Conner's (1965) normative feldspar plot (Fig. 7a), and conform well to Barker's (1979) definition of trondhjemite. Chemical data (Table 3.) suggests the granitoids straddle Barker's (1979) boundary between high- and low-Al_2O_3 type trondhjemites (15 % Al_2O_3). Although the data base is small, on the K_2O-CaO-Na_2O plot (Fig. 7b), the AFM diagram (Fig. 7c), and normative Q-Or-Ab plot (Fig. 7d), the granitoids show a weak trondhjemitic trend as opposed to a calc-alkaline trend. All samples of granitoid are characterized by relatively low concentrations of K_2O (1.04-3.43 wt. %) and Rb (29-67 ppm), while Rb/Sr ratios are consistently between 1.0 and 0.1.

DIABASE AND GABBRO DYKES (UNIT 1)

Field description

Abundant Proterozoic diabase and gabbroic dykes cut all other lithologies in the map area.The dykes are steeply dipping and strike between 045° and 090°. They weather rusty brown and are relatively massive, lacking the pronounced foliation exhibited by the Florence Lake Group.Individual

Table 3. Chemical analyses and CIPW-normative mineralogies of trondhjemites.

	TB-87-038	87-039B	87-140	87-191	87-192	87-239
SiO2 (wt. %)	68.60	73.90	73.70	69.90	73.30	70.30
TiO2	0.32	0.16	0.20	0.40	0.24	0.24
Al2O3	15.30	14.30	13.80	15.30	14.30	15.50
FeO* (total Fe)	2.50	1.04	1.48	2.43	1.40	2.12
MnO	0.04	0.01	0.03	0.04	0.04	0.05
MgO	1.45	0.60	0.46	0.86	0.47	0.75
CaO	1.30	1.38	2.50	2.74	1.52	1.88
Na2O	6.25	5.55	4.41	4.92	5.14	4.40
K2O	1.04	1.65	1.42	1.49	2.38	3.43
P2O5	0.09	0.02	0.06	0.07	0.03	0.06
LOI	1.59	0.80	0.83	1.45	1.01	1.25
Total	98.48	99.41	98.89	99.60	99.83	99.98
Rb (ppm)	29	41	30	38	62	67
Sr	240	215	186	340	164	157
Y	5	4	9	5	10	11
Zr	130	73	102	129	75	106
Nb	3	2	6	2	3	5
Ga	19	14	15	20	21	18
Zn	14	1	nd	36	7	23
Cu	nd	nd	nd	nd	nd	11
Ni	nd	nd	nd	nd	nd	nd
Ba	235	460	474	482	493	580
V	41	9	11	32	13	25
Cr	nd	nd	nd	nd	nd	nd
Q (wt. %)	22.00	30.88	35.81	27.16	29.57	25.23
C	1.75	0.92	0.61	0.78	0.58	1.28
or	6.15	9.75	8.39	8.81	14.07	20.27
ab	52.88	46.96	37.31	41.63	43.49	37.23
an	5.86	6.72	12.01	13.14	7.35	8.94
hy	7.06	2.87	3.18	5.35	3.03	4.87
mt	0.40	0.17	0.24	0.39	0.23	0.34
il	0.61	0.30	0.38	0.76	0.46	0.46
ap	0.21	0.05	0.14	0.17	0.07	0.14

dykes range in width from only a few centimetres up to 100 metres, with the thicker dykes having chilled diabasic margins and coarser-grained gabbroic cores.

Petrography

Dyke mineralogy consists of distinctive mauve-coloured titanaugite, labradorite, apatite, ilmenite, ± quartz ± biotite ± actinolite ± chlorite. The smaller diabase dykes and the fine-grained margins of larger dykes differ petrographically from the coarser gabbroic dykes.

In the gabbroic dykes, relatively large titanaugite oikiocrysts (up to 1.5 cm) form subophitic to ophitic textures with labradorite laths. Ilmenite is always present and occurs as anhedral crystals (< 2 mm). Apatite forms euhedral to subhedral crystals, and varies in abundance. Small amounts of quartz and biotite occur in the interstices, and actinolite and chlorite sporadically replace clinopyroxene. In some samples, large sericitized plagioclase crystals (up to 5 cm long) are present.

The diabase dykes, and chilled fine-grained margins of larger dykes, characteristically exhibit intergranular textures. Labradorite commonly occurs as phenocrysts, and also forms subhedral laths, and titanaugite occurs as anhedral crystals. In contrast to the gabbroic dykes, ilmenite occurs as both small, anhedral, and long, acicular crystals.

Chemistry

The peculiar mineralogy of the diabase dykes, characterized by an abundance of titanaugite, ilmenite, and apatite, is reflected in high contents of TiO_2, FeO* (total Fe), and P_2O_5 and by the elevated concentrations of high field strength (HFS) elements Nb, Zr, and Y (Table 4.).

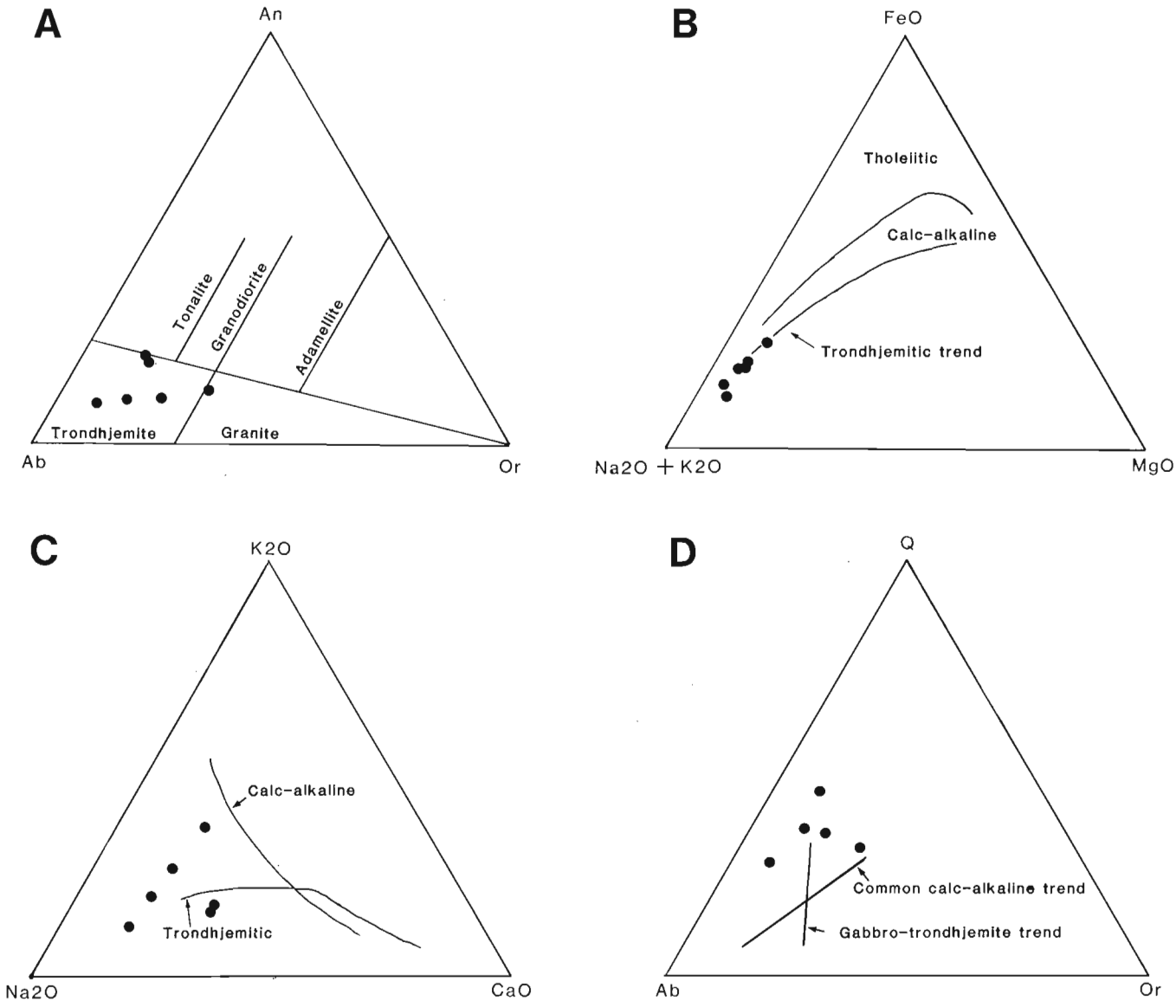

Figure 7. Ternary plots for Kanairiktok trondhjemites. A. Normative feldspar plot (after O'Conner, 1965). B. AFM diagram. C. Na_2O-K_2O-CaO plot. D. Normative albite-quartz-orthoclase (Ab-Q-Or) plot. Calc-alkaline and trondhjemitic trends (from Barker and Arth, 1976).

Table 4. Chemical analyses and CIPW-normative mineralogies of diabase and gabbroic dikes.

	TB-87-047B	87-056	87-087b	87-101	87-229B
SiO2 (wt. %)	41.70	45.20	44.90	45.50	42.10
TiO2	4.40	3.64	3.72	1.00	3.96
Al2O3	13.10	12.00	12.50	19.40	12.60
FeO* (total Fe)	20.56	19.07	19.17	10.21	19.31
MnO	0.24	0.23	0.25	0.15	0.20
MgO	4.97	5.07	5.04	5.73	5.19
CaO	7.60	8.36	9.46	11.18	7.74
Na2O	2.17	2.11	2.65	2.42	3.07
K2O	0.96	0.77	0.36	0.60	1.12
P2O5	1.18	1.21	1.26	0.10	1.46
LOI	2.23	2.42	1.43	2.25	1.73
Total	99.11	100.08	100.74	98.54	98.48
Rb (ppm)	21	21	5	16	24
Sr	203	204	226	269	304
Y	68	71	67	19	69
Zr	380	345	337	60	366
Nb	19	18	18	6	19
Ga	21	20	22	20	25
Zn	179	140	115	52	98
Cu	nd	nd	nd	32	nd
Ni	16	7	8	75	11
Ba	514	462	381	115	641
V	308	306	326	143	240
Cr	nd	nd	nd	84	nd
or (wt. %)	5.67	4.55	2.13	3.55	6.62
ab	18.36	17.85	22.42	19.24	24.69
an	23.17	21.00	21.15	40.31	17.30
ne	---	---	---	0.67	0.70
di	5.78	10.63	14.84	12.01	9.77
hy	14.82	29.93	15.90	---	---
ol	14.90	1.12	10.00	16.85	23.88
mt	3.31	3.07	3.09	1.65	3.11
cm	---	---	---	0.02	---
il	8.36	6.91	7.06	1.90	7.52
ap	2.78	2.85	2.97	0.24	3.44

Comparison with the Harp and Mealy dykes (Meyers and Emslie, 1977; Emslie et al., 1984) shows that the diabase dykes are different in having relatively lower SiO_2, MgO, and Al_2O_3, higher TiO_2, FeO* (total Fe), MnO, and P_2O_5 and comparable CaO, Na_2O, and K_2O contents (Fig. 8). These differences are also reflected in trace elements, with the dykes of this study having relatively lower concentrations of Cr and Ni, higher concentrations of Zr, and comparable concentrations of Rb, Sr, and Ba (Fig. 9).

Discussion

Ermanovics and Raudsepp (1979) recognized dykes of at least two ages within the Hopedale Block.The older, strongly altered, Kikkertavak dykes strike north-northeast to northeast and contain appreciable (40-70 %) epidote, actinolite, chlorite, and carbonate.A less altered apparently younger set of dykes trends northeast to east-west, and typically contain a distinctive mauve titanaugite and up to 20 % olivine.

Ermanovics and Raudsepp (1979) noted similarities between these younger dykes and those to the east and west of the Hopedale Block, namely the Aillik and Harp dikes, respectively; and Ryan (1984) has suggested that they may in fact represent part of the Harp dyke suite described by Meyers and Emslie (1977). However, the diabase and gabbro dykes described in this study are mineralogically and chemically distinct from the Harp dykes. The lack of olivine and the chemical trends described in the previous section suggest these dykes are more evolved/differentiated than the Harp Suite.

Table 5. Microprobe analyses of selected carbonates.

Sample #	Phase	Anal	MgO	CaO	MnO	FeO
TB-87-046	Ankerite	[2]	15.74	28.09	0.26	9.05
87-063-2	Ferroan Magnesite	[5]	38.85	0.12	0.12	10.94
87-069	Ankerite	[2]	14.49	27.82	0.30	10.97
87-094	Calcite	[2]	0.46	59.48	0.57	1.07
87-122C	Ferroan Magnesite	[2]	39.15	0.10	0.38	6.78
87-125A	Ferroan Magnesite	[3]	39.57	0.09	0.36	7.52
87-165A	Ferroan Dolomite	[2]	21.13	29.67	0.29	2.25
87-185C	Ferroan Magnesite	[2]	38.52	0.04	0.16	7.86
87-227	Ankerite	[2]	17.38	27.82	0.47	6.10
87-240B	Calcite	[2]	0.57	59.37	1.07	0.80
87-247B	Ferroan Magnesite	[2]	39.01	0.05	0.10	7.48

[] indicates number of analyses used in average.

CARBONATIZED ZONES

The entire metavolcanic belt has been affected to varying degrees by carbonate alteration, which Ermanovics and Raudsepp (1979) attributed to exhalative-fumarolic activity. The scale of carbonate alteration varies from the presence of small ubiquitous veins of calcite, that crosscut all lithologies, to extensive zones of intense carbonatization in ultramafic and adjacent volcanic rocks that range in size from one metre to tens of metres in width and up to hundreds of metres in length. These zones are cut by numerous discontinuous quartz vein sets having various orientations.

Preliminary microprobe analyses have shown that several carbonate species are present throughout the belt (Table 5.). Ferroan magnesite is always present in carbonatized ultramafic rocks and in carbonatized volcanic rocks adjacent to the ultramafics. In areas distal to the ultramafics, ankerite is the dominant carbonate species, while calcite is commonly present along small shear zones and folia.

The replacement assemblage at the Main Baikie showing, which consists of talc-(Cr-rich) chlorite-ferroan magnesite, has also been observed southeast of Florence Lake in a large zone of intensely carbonatized volcanic rocks. However, one notable difference between the two is the lack of late quartz veining at the Main Baikie showing.

STRUCTURE

The map area (Fig. 1) is characterized by prominent northeasterly-trending structures. All rocks comprising the greenstone belt have undergone variable but intense deformation. Penetrative fabrics dip steeply to the southeast. The style of folding is typically determined by the lithology. Volcanic and ultramafic rocks are characterized by kink folds with the development of crenulation cleavage, whereas more competent siliceous metasedimentary rocks maintain rounded concentric folds.

Northeast-trending faults and shear zones are commonly associated with mylonitization and marked grain size reduction. Ultramafic and adjacent siliceous metavolcanic rocks that have been extensively folded and sheared commonly display intense carbonatization accompanied by quartz-filled tension gashes.

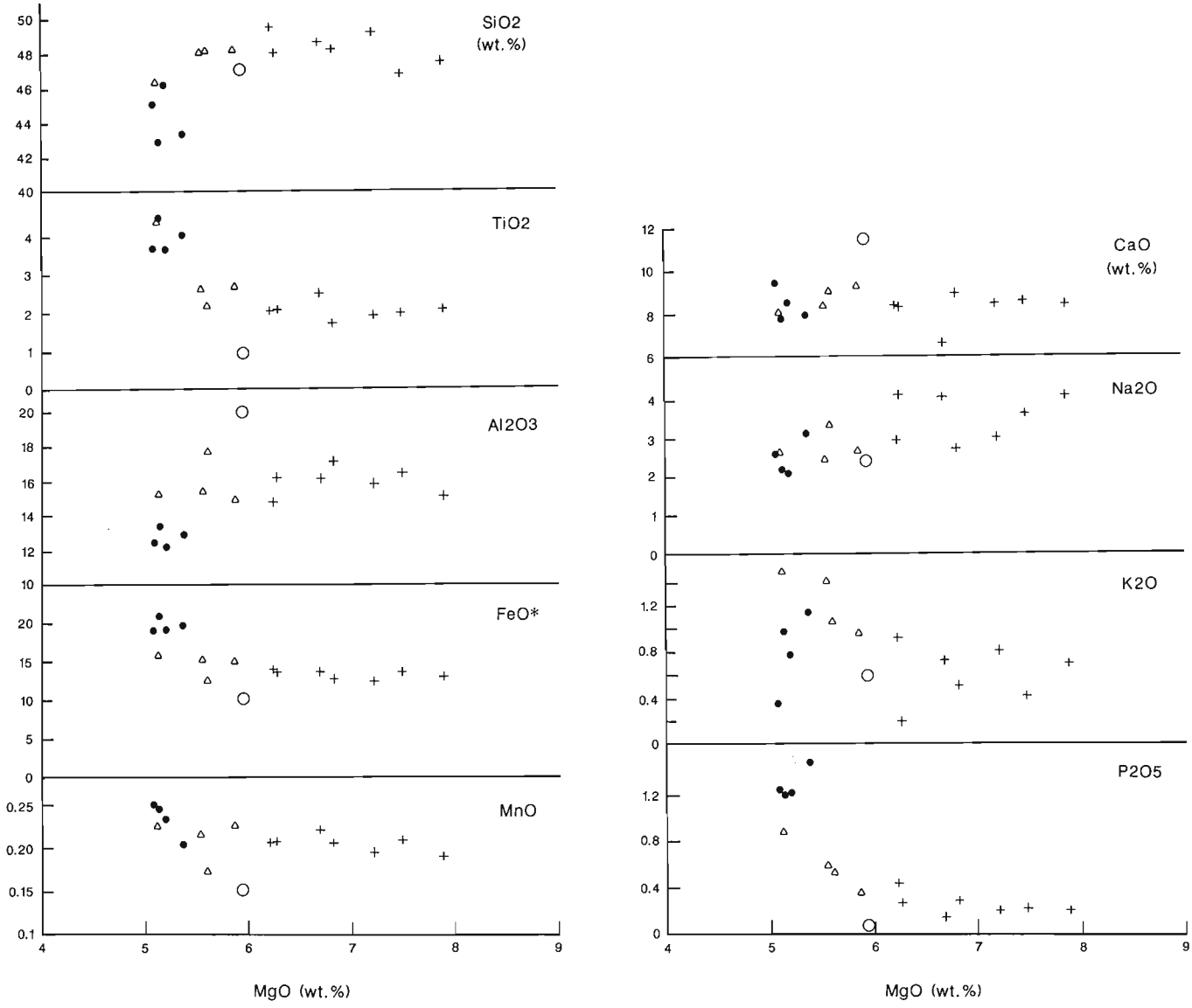

Figure 8. Harker diagrams of major elements vs. MgO for diabase and gabbroic dykes. Small solid circles = diabase dykes of this study, large open circle = gabbro dike of this study, crosses = thin and fine-grained Harp dykes (Meyers and Emslie, 1977), triangles = thin and fine grained Mealy dykes (Emslie et al., 1984).

The granite-greenstone contacts are in many cases zones of high strain. In these areas, amphibolitized rafts of volcanic rocks are included in trondhjemite which has gneissic textures defined by alternating discontinuous layers of ribbon quartz and layers consisting of quartz and highly saussuritized plagioclase.

MINERALIZATION

Minor sulphide mineralization is spatially associated with zones of intense carbonatization of ultramafic and volcanic rocks.Pyrite occurs as disseminations and along small shears within adjacent metavolcanic rocks.Although ultramafic rocks and carbonatized volcanic rocks are apparently barren, the intensity of alteration, and the presence of even minor sulphide mineralization in adjacent rocks indicates that these areas may represent favorable exploration targets for precious metals.

The Baikie showings, located approximately 2.5 km northwest of Florence Lake, consist of three separate occurrences (Main Baikie; South Baikie; and North Baikie) of pyrite-pyrrhotite mineralization in talc-carbonate schists.BRINEX (1960-63) conducted limited packsack drilling and ground magnetic surveys over the showings (Piloski, 1962).Piloski (1962) noted that the showings are underlain mainly by mafic volcanic rocks with lesser amounts of amphibolite and granodiorite. Sutton (1970) described the showings as occurring within a 500-m-wide granite-greenstone contact zone.

Field investigations (1988) indicate that the entire area is underlain by trondhjemites of the Kanairiktok Intrusive Suite which contain xenoliths and rafts of mafic metavolcanic rocks that range from centimetres to hundreds of metres in size. Several mineralized ultramafic rafts are also present at the Baikie showings.

At the Main Baikie showing, mineralization is contained within a 4x6 m ultramafic raft that consists of an assemblage of talc, Cr-rich chlorite, ferroan magnesite, and magnetite. Pyrrhotite and pyrite are disseminated throughout the mineralized zone, and in places form massive sulphide patches that display a characteristic green nickel stain. Chalcopyrite is commonly intergrown with pyrrhotite and pyrite.

During 1986, sampling by Platinum Exploration Canada Inc.detected anomalous Ni and PGE concentrations at the Main Baikie showing (Reusch, 1987; Arengi, 1987). However, subsequent chip sampling failed to duplicate the highest anomalous PGE concentrations. The highest values were initially obtained from a grab sample of massive pyrrhotite-pyrite-chalcopyrite.

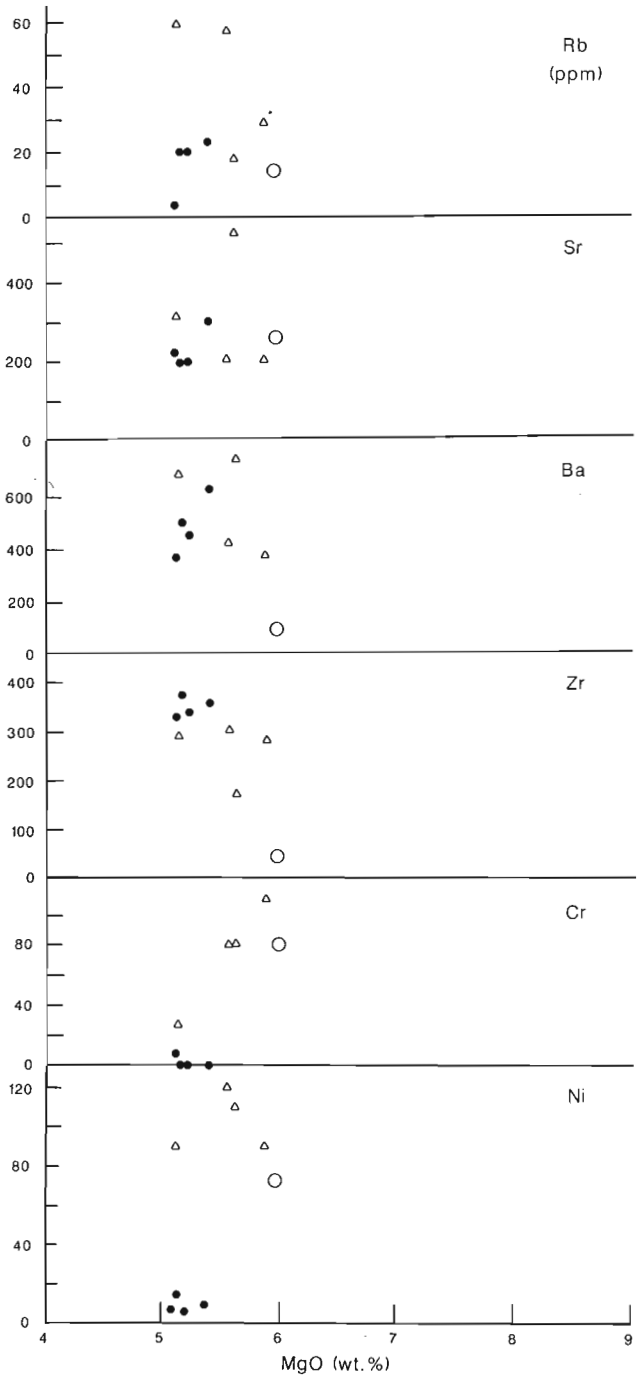

Figure 9. Harker diagrams of trace elements vs. MgO as a differentiation index for diabase and gabbroic dykes (symbols as for Fig. 7).

Though the size and podiform nature of the Main Baikie showing limits its economic potential, the similarities of alteration assemblages (except for the lack of quartz veins) between this showing and that southeast of Florence Lake suggest the latter area as a possible exploration target.

Approximately 200 m northeast of the Main Baikie showing, coarse arsenopyrite crystals occur within silicified and carbonatized metavolcanic (?) rocks. The relationship between this mineralization and the more typical pyrite-pyrrhotite mineralization is unclear.

Small occurrences of asbestos, with fibres up to 0.5 cm long, are locally developed within serpentinized ultramafic rocks south of Florence Lake.

CONCLUSIONS

The volcanic rocks in the Florence Lake Group consist of a bimodal assemblage of tholeiitic mafic flows and calc-alkaline felsic volcanics which is typical of Archean greenstone belts. The intrusive ultramafic rocks are highly altered but appear to have been originally dunite. Chemically, the Kanairiktok plutonic rocks consist dominantly of trondhjemite rather than tonalite-granodiorite. At the Baikie showing, the Kanairiktok Intrusive Suite is agmatitic and contains numerous blocks of ultramafic rocks. One carbonatized block contains PGE-enriched massive pyrrhotite-sulphide. The Proterozoic diabase-gabbro dykes, which intrude all other lithologies in the area and which were previously described as Harp dyke equivalents, have a distinctive chemical signature.

ACKNOWLEDGMENTS

Funding for this project was provided under contract by the Geological Survey of Canada (GSC) through the Canada-Newfoundland Mineral Development Agreement. T.C. Birkett, S.S. Gandhi, J.M. Duke of the GSC and P. L. Dean, B.A. Greene and R.J. Wardle of the Newfoundland Department of Mines (NDM), and B. Cox of the MUN Office of Research facilitated the contracting process. Funding was also provided through NSERC and NSTP grants to Wilton. The NDM provided logistical support from their depot at Goose Bay through the capable hands of W. Tuttle, K. O'Quinn and R. White, and from Martin Batterson's Moran Lake camp. P. Browne of Departement of Earth Sciences, MUN, guided us financially. Special thanks go to the dapper Mr. John Clarke for assistance in the field and use of his tent as bear bait. Marlene Dredge, Marc O'Dea and Angus Simpson also assisted in the mapping project; especially with respect to sampling at the Baikie Showing. Many an interesting discussion was held at Moran Lake with M. Batterson, G. Bryant, S. Gandhi, A.Simpson, U. Scharer and R. Wardle. T.C. Birkett, R.F.J. Scoates, W.D. Sinclair and D. Richardson reviewed the manuscript and provided helpful suggestions.

REFERENCES

Arengi, J.T.
1987: Summary report on the Baikie Property, Central Labrador. Unpublished report to Platinum Exploration Canada Inc., 9p..

Barker, F., and Arth, J.G.
1976: Generation of trondhjemitic-tonalitic liquids and Archean bimodal trondhjemite-basalt suites; Geology, v.4, p.501-600.

Barker, F.
1979: Trondhjemite :definition, environment and hypothesis of origin; in F. Barker, (ed.) Trondhjemites, dacites and related rocks; Elsevier, Amsterdam. 658p..

Emslie, R.F., Loveridge, W.D., and Stevens, R.D.
1984: The Mealy dykes, Labrador: petrology, age and tectonic significance; Canadian Journal of Earth Sciences, v. 21, p. 437-446.

Ermanovics, I.F., and Raudsepp, M.
1979: Geology of the Hopedale block of eastern Nain Province, Labrador; in Current Research Part B, Geological Survey Canada, Paper 79-1B, p. 341-348.

Guthrie, A.E.
1983: Report on exploration in the Florence Lake Greenstone Belt, BP Minerals Ltd.- Billiton Canada Ltd.Joint Venture, 1982. Unpublished BP Minerals Ltd. Report.

Irvine, T.N., and Baragar, W.R.A.
1971: A guide to the chemical classification of the common volcanic rocks; Canadian Journal of Earth Sciences, v. 8, p. 523-548.

Jensen, L.S.
1976: A new cation plot for classifying subalkalic volcanic rocks; Ontario Departement of Mines, Miscellaneous Paper 66.

Meyers, R.E. and Emslie, R.F.
1977: The Harp dikes and their relationship to the Helikian geological record in central Labrador; Canadian Journal of Earth Sciences, v. 14, p . 2683-2696.

O'Conner, J.T.
1965: A classification of quartz-rich igneous rocks based on feldspar ratios. United States, Geological Survey Professional Paper 525-B.

Pearce, J.A., and Cann, J.R.
1973: Tectonic setting of basic volcanic rocks determined using trace element analyses; Earth and Planetary Sciences Letters, v. 19, p. 290-300.

Piloski, M.J.
1962: Report on exploration in the Asbestos Corporation - BRINEX Joint area; Hopedale - Kaipokok area, Labrador; Unpublished BRINEX Ltd. report.

Reusch, D.
1987: Proposed exploration program for Baikie property, Florence Lake area, Labrador (NTS:13 K/15); Platinum Exploration Canada Inc.; Unpublished Report.

Ryan, A.B.
1984: Regional geology of the central part of the Central Mineral Belt, Labrador; Newfoundland Department of Mines and Energy, Memoir 3, 185p..

Stewart, J.W.
1983: BP Minerals - Billiton joint venture, Florence Lake, Labrador, Summer 1983, BP Minerals Ltd. Preliminary Report; Unpublished Report to BP Minerals Ltd.

Sutton, J.S.
1970: Geological report - area West of Florence Lake, Ugjoktok Area, Labrador;BRINEX Ltd. Unpublished Report.

Wilson, B.T.
1959: Report on the airborne geophysical survey of the Ujutok Bay area, Labrador, for British Newfoundland Exploration Ltd., Unpublished Lundburg Explorations Report, 17p.

Wilton, D.H.C., and Brace, T.D.
1988: Final report on field work in the Florence Lake and Seal Lake areas, Central Mineral Belt of Labrador; Unpublished report to Geological Survey of Canada, Contract Serial No. 23233-7-0704/01-SS, 102p..

Winchester, J.A., and Floyd, P.A.
1977: Geochemical discrimination of different magma series and their differentiation products using immobile elements; Chemical Geology, v. 20, p. 325-343.

Wakuach Gabbro sills of the Howse Lake area, western Labrador[1]

Jon M. Findlay[2], Tony D. Fowler[2], and Tyson C. Birkett[3]

Findlay, J.M., Fowler, T.D. and Birkett, T.C., Wakuach Gabbro sills of the Howse Lake area, western Labrador; in Current Research, Part C, Geological Survey of Canada, Paper 89-1C, p. 345-351, 1989.

Abstract

Gabbroic sills dominate the stratigraphy of the Howse Lake area in the central Labrador Trough. Sills were emplaced within a heterogeneous host rock sequence formerly correlated with the Menihek Formation, but here assigned to the Le Fer Formation. The sills commonly show a well developed internal stratigraphy defined by the size and frequency distributions of plagioclase phenocrysts and glomerocrysts. Although some sills are not glomeroporphyritic, mapping indicates that many contain both non-glomeroporphyritic and strongly glomeroporphyritic horizons, which are symmetrically developed with respect to sill contacts. Sharp, internal intrusive contacts indicate that some sills represent more than one magmatic injection. Fractional crystallization of plagioclase in a crustal feeder chamber and subsequent emplacement of crystal laden magma is thought to be the origin of glomeroporphyritic lithologies. Non-glomeroporphyritic sills are considered comagmatic, and may have been derived from the chamber prior to the onset of plagioclase fractionation.

Résumé

Les filons-couches de gabbro prédominent dans la stratigraphie de la région du lac Howse, au centre de la fosse du Labrador. Ces filons-couches ont été mis en place au sein d'une séquence hétérogène de roches encaissantes, que l'on avait autrefois corrélée avec la formation de Menihek, mais que l'on place ici dans la formation de Le Fer. Les filons-couches montrent généralement une stratigraphie interne bien développée, définie par la granulométrie et la distribution de fréquence des phénocristaux et des glomérocristaux de plagioclase. Certains filons-couches ne sont pas glomérоporphyriques, mais les travaux de cartographie indiquent que beaucoup d'entre eux contiennent à la fois des horizons non glomérоporphyriques et d'autres fortement glomérоporphyriques, qui se sont formés symétriquement par rapport aux contacts avec les filons-couches. Des contacts intruisifs internes bien définis, indiquent que certains filons-couches correspondent à plusieurs injections magmatiques. On estime que la cristalisation fractionnée du plagioclase dans un réservoir magmatique crustal et la mise en place ultérieure du magma chargé de cristaux, sont à l'origine des textures glomérоporphyriques. On considère que les filons-couches non glomérоporphyriques sont comagmatiques, et qu'ils tirent peut-être leur source du réservoir magmatique à une époque avant le début du fractionnement des plagioclases.

[1] Contribution to Canada - Newfoundland Mineral Development Agreement 1984-1989. Project sponsored by Geological Survey of Canada, Mineral Resources Division.

[2] Ottawa-Carleton Geoscience Centre, University of Ottawa, Ottawa, Ontario, K1N 6N5.

[3] Commission géologique du Canada, Centre Géoscientifique de Québec, Sainte-Foy, Québec, G1V 4C7.

INTRODUCTION

The Howse Lake map area is approximately 40 km northeast of Schefferville, Québec, in the central portion of the Lower Proterozoic Labrador Trough (Fig. 1). The stratigraphy, structure and evolution of the Labrador Trough have been summarized by Frarey and Duffell (1964), Dimroth (1970; 1978), Baragar and Scoates (1980), Wardle and Bailey (1981), and Wardle (1982), and the petrology of the tholeiitic rocks has been discussed in detail by Baragar (1960; 1967). Briefly, the central Labrador trough comprises three principal subdivisions (Fig. 1). Archean basement of the Superior Craton is unconformably overlain by the Knob Lake Group, a succession of shallow water clastic and chemical sedimentary rocks grading eastward to deeper water sediments and mafic volcanic rocks. The Doublet Group, a thick sequence composed primarily of tholeiitic volcanic and mafic pyroclastic rocks, occupies much of the eastern half of the Trough and is generally in tectonic contact with the Knob Lake Group along the Walsh Lake-Connolly Lake Fault (Wardle and Bailey, 1981). Biotite schist and amphibolite constitute the easternmost subdivision of the central Trough, the Laporte Group, which has been thrust westward over the Doublet Group. The dominantly northwest-southeast structural trend within the belt has resulted from compressive deformation accompanying Hudsonian orogenesis. Metamorphic grade increases eastward from sub-greenschist in the Knob Lake Group, to greenschist in the Doublet Group, and reaches amphibolite facies in the Laporte Group.

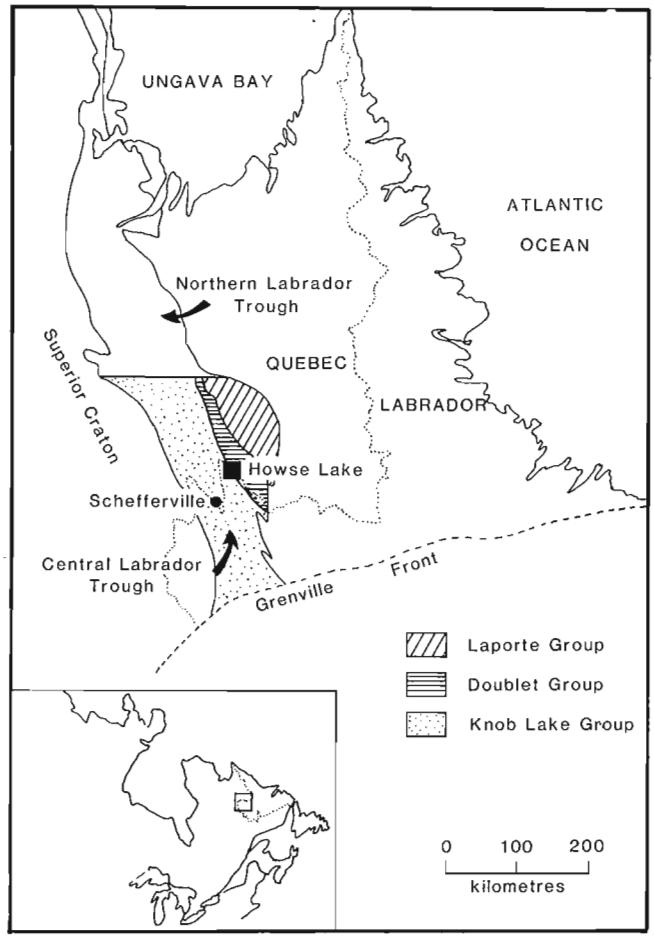

Figure 1. Location of the Howse Lake study area and principal subdivisions of the central Labrador Trough (after Wardle and Bailey, 1981).

The stratigraphic section of the eastern half of the Labrador Trough has been substantially thickened by a profusion of mafic (Wakuach Gabbro) and ultramafic (Retty Peridotite) sills of the pre-orogenic Montagnais Group. The mafic intrusions have been subdivided by Baragar (1960) into three types: normal gabbro, glomeroporphyritic gabbro (blotchy gabbro, leopard rock) and metagabbro. The Walsh Lake-Connolly Lake Fault forms a boundary in the geographic distribution of the types; normal and glomeroporphyritic sills intrude Knob Lake strata to the west of this lineament whereas metagabbro is confined to the Doublet Group to the east. Petrological differences between normal gabbro and metagabbro have been attributed to the abrupt increase in metamorphic grade across the fault (Baragar, 1960). The gabbroic sills and Doublet Group basalts are considered comagmatic (Baragar, 1960; Wardle and Bailey, 1981), and together constitute a major igneous suite of tholeiitic affinity.

In the current study, a program of regional mapping, coupled with detailed mapping and sampling of two sills, provides the basis for an examination of the petrogenetic relationship between the normal and glomeroporphyritic intrusions and the magmatic processes involved in their differentiation. An evaluation of the platinum-group element potential of sulphide mineralization, hosted by several intrusions in the study area, has recently been published (Findlay et al., 1988). Here we present preliminary descriptions of the geological setting and petrology of the gabbroic sills at Howse Lake.

Geology of the Howse Lake Area

Mafic sills constitute 75% of the stratigraphic section at Howse Lake, occurring as thin conformable bodies of substantial strike lengths. Bedrock exposure is poor except near the southern end of Howse Lake where semi-continuous outcrop permitted detailed sampling of the various lithologies (Fig. 2). Gabbroic liquids were emplaced within a sequence of argillaceous, mafic pyroclastic and mafic volcanic rocks which are preserved as narrow and discontinuous wedges between sills. In general, the distribution of rock units in the map area conforms to the regional pattern of northwesterly trending structures prevalent in the Labrador Trough (Fig. 2). Lithological contacts, bedding in argillaceous units and layering in intrusive rocks consistently show northwesterly strikes and moderate to steep northeasterly dips. Cross- and graded-bedding in argillaceous and volcaniclastic horizons indicate a northeasterly younging direction.

Le Fer Formation

The host succession is dominated by well stratified siltstone-shale with quartzite, cherty quartzite and massive chert interbeds. Black, carbonaceous shales commonly show a

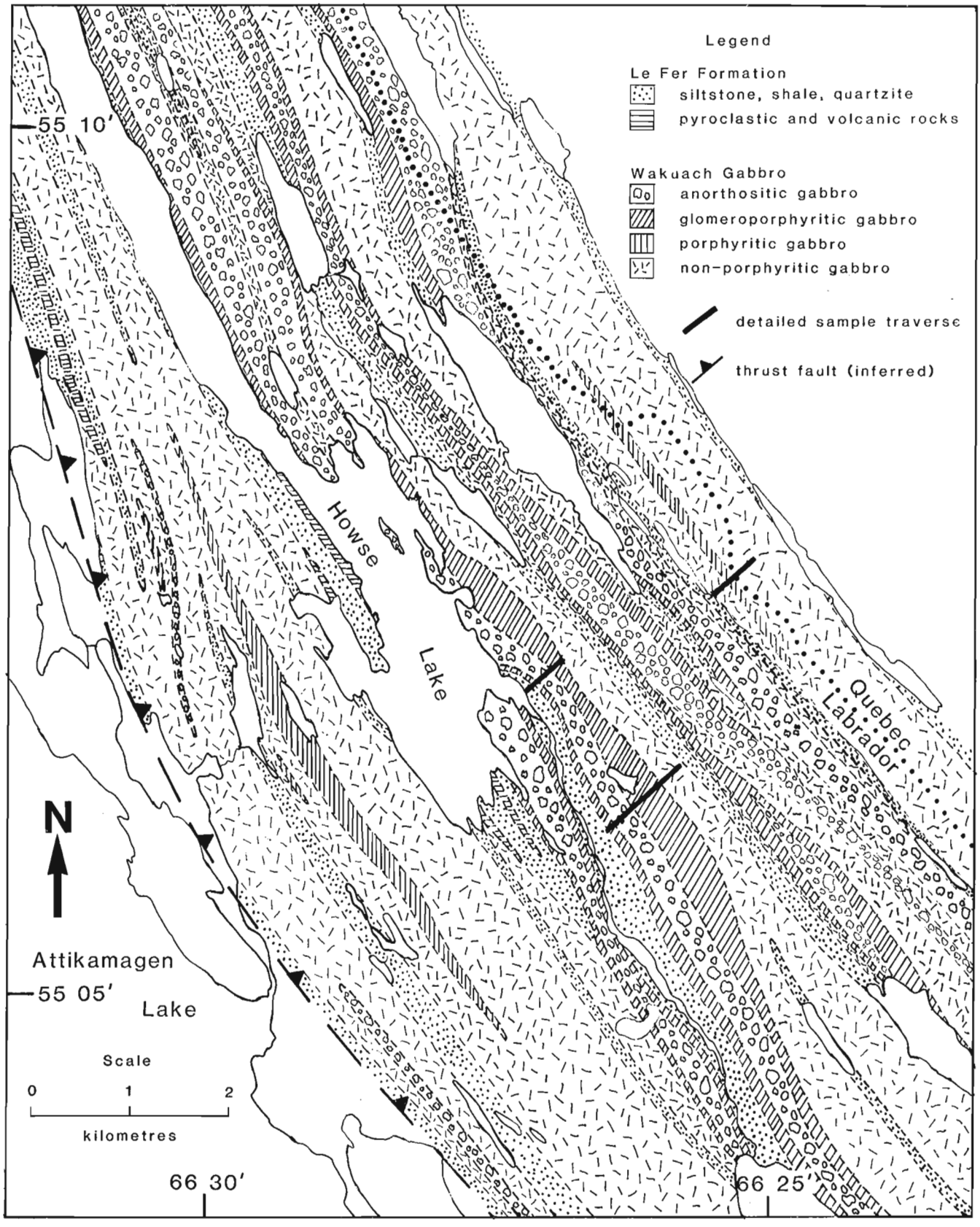

Figure 2. Distribution of non-porphyritic, porphyritic-glomeroporphyritic, and anorthositic gabbro in the Howse Lake area. Locations of detailed sampling are indicated.

marked fissility and are generally pyritiferous. Pyroclastic, volcaniclastic and volcanic rocks occur together as thin horizons, 5 m to 20 m in combined thickness, interbedded with argillaceous rocks. Pyroclastic units consist of volcanic fragments and vitric shards set in a chloritic-tuffaceous matrix. Volcaniclastic beds contain poorly sorted, sand and pebble sized volcanic and cherty clasts in a silty matrix. Basaltic rocks are alkalic in nature and include massive, amygdaloidal and pillowed varieties. These rock types constitute a very minor proportion of the stratigraphic section at Howse Lake.

Previous mapping has assigned the host rock sequence described above to the Menihek Formation, a volcanic-sedimentary succession which forms the uppermost unit of the Knob Lake Group. However, Menihek basalts have been described as tholeiitic in character (Baragar, 1967; Dimroth, 1978; Wardle and Bailey, 1981), whereas initial analytical work suggests that Howse Lake volcanics are alkalic (Fig. 3). Recent dating of a Howse Lake sill and other rocks in the central Labrador Trough suggests that the Menihek Formation is younger than the Howse Lake intrusions (unpublished data, Birkett et al.). Consequently, the host rock succession is tentatively assigned to the Le Fer Formation, a sequence of argillaceous, pyroclastic and volcanic rocks which is considerably older than the Menihek Formation. This implies the existence of an unrecognized northwesterly-trending thrust fault at the western limit of glomeroporphyritic sills near Attikamagen Lake (Fig. 2). Further comparative work, particularly in characterizing the chemical affinities of the basaltic rocks, is needed to establish the validity of this correlation.

Wakuach Gabbro

Gabbroic sills range from 300 to 1500 m in thickness and commonly exhibit several lithological variations. The occurrence of plagioclase phenocrysts and glomerocrysts, and their size and frequency distribution, account for much of the variation. Some sills contain only minor horizons of plagioclase-phyric gabbro; these are the "normal" gabbros of Baragar (1960). Regional mapping at Howse Lake suggests that normal gabbro sills consist predominantly of subophitic to ophitic gabbro or gabbronorite, with thin basal horizons of olivine gabbro, and central plagioclase-phyric intervals.

Most glomeroporphyritic sills have marginal zones of non-porphyritic to sparsely porphyritic-glomeroporphyritic gabbro, which range in thickness from 5 m to 100 m. The size and frequency of feldspar glomerocrysts increases gradationally toward the central part of these sills, producing a gabbroic phase that is regularly spotted with 1 to 5 cm sized plagioclase aggregates (Fig. 4A). Central bands of coarse grained anorthositic gabbro (Fig. 4B) are present in many of the glomeroporphyritic sills of the area. The grain size of groundmass and glomerocryst plagioclase crytals are similar in this rock type, and the two populations of feldspar are almost indistinguishable. Anorthositic gabbro is mineralogically similar to marginal gabbro, but generally contains 70 % to 75 % plagioclase. Anorthositic gabbro contains rare enclaves of non-porphyritic gabbro (Fig. 4C) and, where exposed, contacts between medium grained glomeroporphyritic gabbro and anorthositic gabbro are sharp (Fig. 4D). A related lithology that is erratically developed within some sills exhibits large glomerocrysts set in a matrix of anorthositic gabbro. Aggregates may reach 18 cm in diameter and

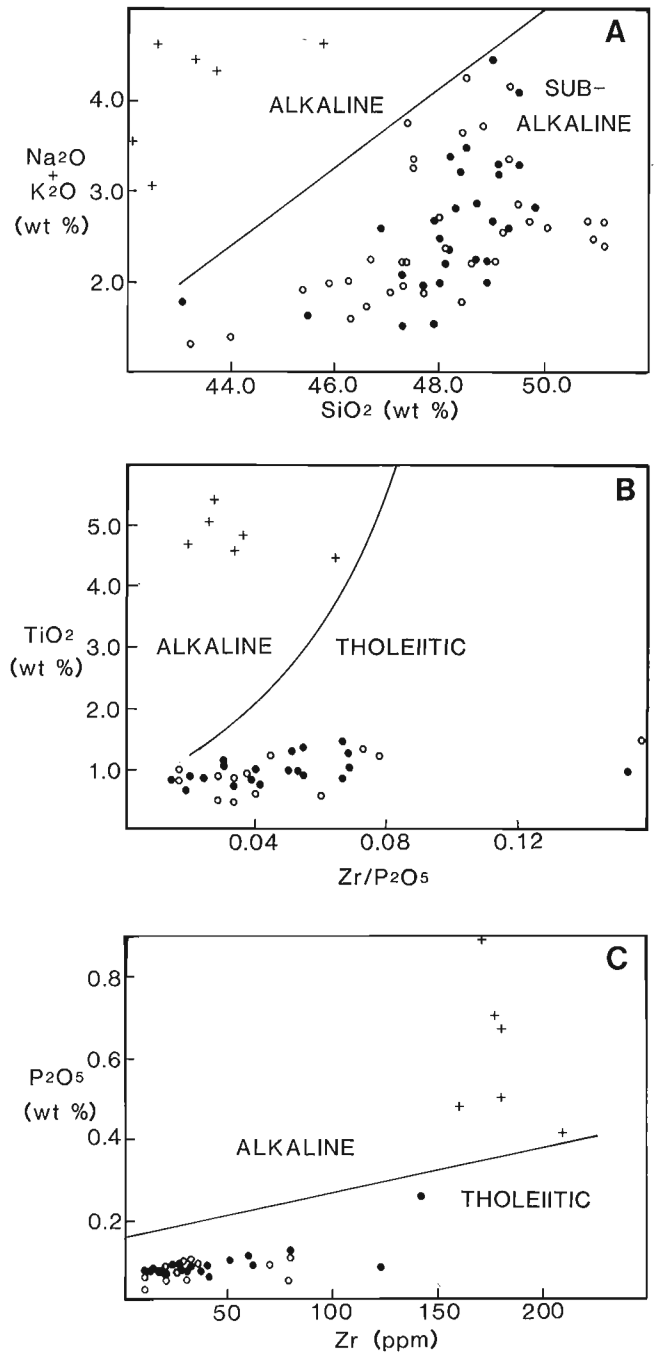

Figure 3. High $Na_2O + K_2O$, TiO_2, P_2O_5 and Zr distinguish Le Fer volcanic rocks (crosses) from non-porphyritic (solid circles) and porphyritic glomeroporphyritic (open circles) Wakuach Gabbro in the Howse Lake area.
A) alkali-silica diagram showing alkaline and sub-alkaline fields after Irvine and Baragar (1971)
B) TiO_2-Zr/P_2O_5 diagram showing alkaline and tholeiitic fields after Winchester and Floyd (1976)
C) P_2O_5-Zr diagram showing alkaline and tholeiitic fields after Winchester and Floyd (1976).

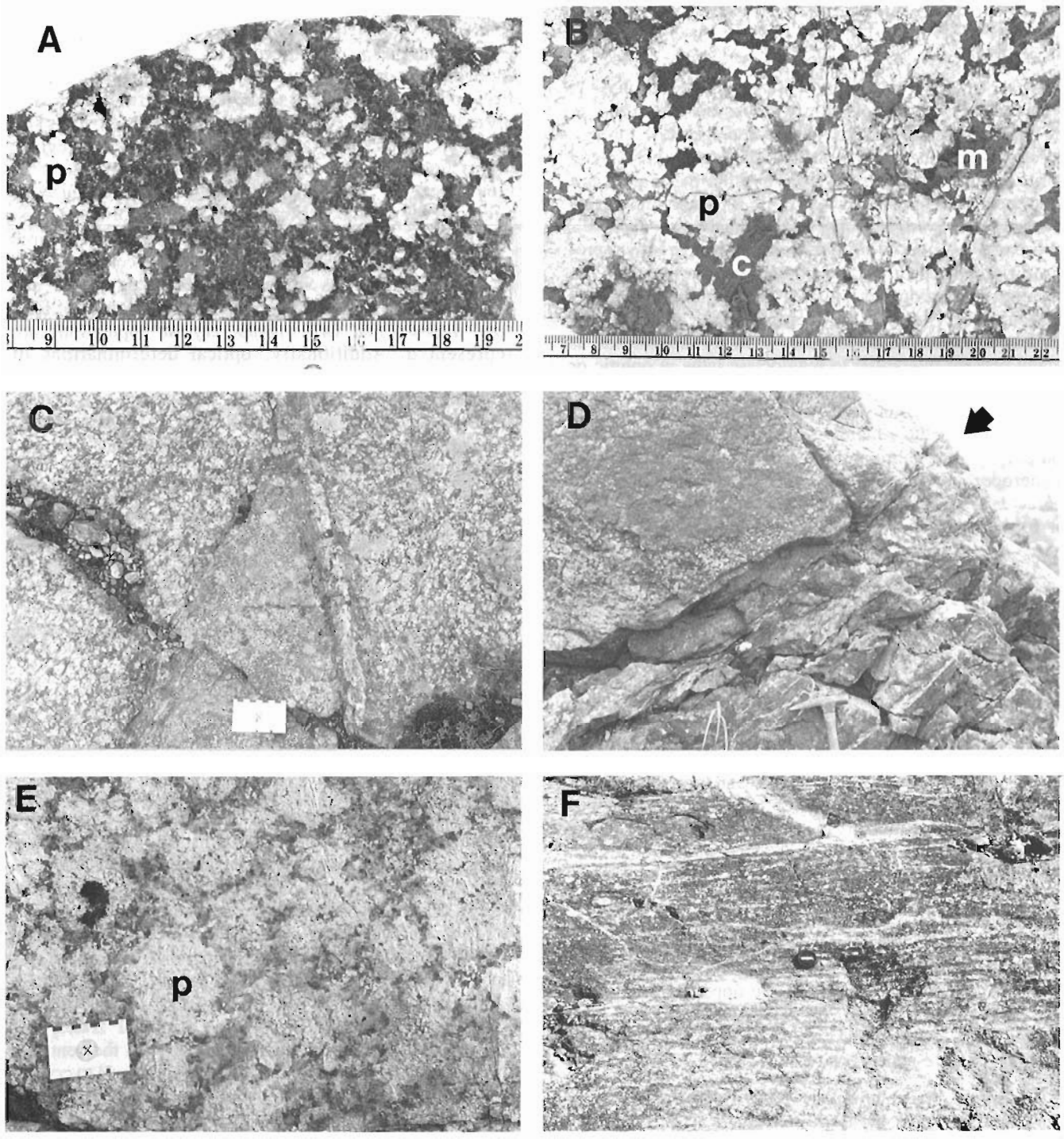

Figure 4. (A) Abundant plagioclase glomerocrysts (p) in a matrix of medium grained subophitic gabbronorite. Scale in centimetres.
(B) Plagioclase domains, (p) separated by large crystals of clinopyroxene (c) and magnetite-ilmenite (m), characterize anorthositic gabbro. Scale in centimetres.
(C) Normal gabbro enclave in anorthositic gabbro. Scale in centimetres.
(D) Intrusive contact (indicated by arrow) between medium grained, sparsely glomeroporphyritic gabbro and overlying coarse grained, anorthositic gabbro. Note disruption and veining in the underlying gabbro.
(E) Close packed plagioclase aggregates (p) in coarse grained gabbroic matrix. Scale in centimetres.
(F) Magmatic phase layering in sparsely glomeroporphyritic marginal gabbro. Lens cap is 5 cm in diameter.

form what is essentially a close-packed framework with relatively minor amounts of interstitial groundmass (Fig. 4E).

Non-porphyritic gabbro and the groundmass to porphyritic-glomeroporphyritic varieties are compositionally similar, ranging from olivine melagabbro, through leucogabbro, to the volumetrically minor quartz gabbro and diorite which are locally developed within marginal zones at or near the upper contacts. All of these lithologies however, are overwhelmingly subordinate to "average" gabbro or gabbronorite compositions, and apparently represent differentiates of the presumed tholeiitic magma. The essential mineralogy is simple; augitic clinopyroxene, plagioclase of labradorite composition, and variable amounts of bronzite or olivine. Primary hornblende is locally present interstitial to plagioclase laths in ophitic or subophitic lithologies. Magnetite-ilmenite intergrowths and pyrrhotite are ubiquitous accessory phases. Available chemical data mirror the mineralogical similarities exhibited by non-porphyritic gabbro and the groundmass to porphyritic-glomeroporphyritic varieties, and reflect their tholeiitic character (Fig. 3). Insufficient data are currently available for further petrochemical interpretation.

The degree of alteration of gabbroic rocks is generally low, although certain minerals are particularly prone to replacement. Clinopyroxene may be replaced by hornblende, biotite or chlorite, but is consistently the best preserved phase. Groundmass plagioclase may be partially sausseritized, and glomerocrysts usually display strong sericitization. Phenocrystic orthopyroxene and olivine are consistently altered to serpentine and chlorite, but groundmass crystals of these minerals are commonly fresh.

The predominant texture of normal and groundmass gabbro is one of moderately coarse clinopyroxene crystals ophitically or subophitically enclosing decussate plagioclase laths, prismatic bronzite crystals, and equant olivine grains. Well developed ophitic texture imparts a mottled appearance to the rock. Olivine- or bronzite-phyric horizons are often present in the lower portions of the sills. Equigranular varieties are developed in narrow fine grained zones at contacts with sedimentary rocks. Irregularly-shaped areas of pegmatitic gabbro are present in the upper parts of some sills. These are mineralogically similar to, and grade into, the enclosing medium grained gabbro, and may reflect localized volatile concentration.

Magmatic phase layering, consisting of alternating plagioclase- and clinopyroxene-rich layers, 1-2 cm in thickness (Fig. 4E), is present in the marginal zones of several sills. Layering is prominent in outcrop as a result of differential weathering, but is poorly defined in thin section. A conspicuous feature of glomeroporphyritic lithologies is the occurrence of felsic veins or bleached zones in which a fine grained assemblage of quartz, epidote, chlorite, albite and uralitic amphibole replaces the original gabbroic minerals. These zones range in thickness from 1 cm to 1 m, may be crosscutting or conformable, and appear to have developed through the passage of a volatile enriched phase, possibly a water saturated magmatic fluid.

The glomerocrysts of leopard rock sills are crudely spherical to irregularly shaped plagioclase aggregates with low ferromagnesian mineral contents, usually less than 5 %. Individual crystals are subhedral and blocky, and aggregates may consist of from three to more than thirty interlocking crystals, commonly adjoining at well- developed triple point junctions. Interstices are occupied by small irregular plagioclase crystals, overgrowths on larger crystals, or by clinopyroxene, hornblende or magnetite. The size of aggregates is dependent both on the size of individual crystals and the total number of crystals present, and large aggregates are most commonly observed in coarse grained matrices. Differences in crystal morphology, size and degree of alteration between matrix and glomerocryst feldspar indicate that two distinct crystal populations are represented. Additionally, optical determinations of plagioclase compositions indicate that glomerocryst crystals are considerably more calcic than groundmass plagioclase. Future microprobe analysis will help quantify compositional differences between the two populations. In some samples, groundmass plagioclase crystals are arranged in a concentric pattern around glomerocrysts. This texture is interpreted to reflect relative movement between the two crystal populations. Because relative movement resulting in the concentric texture could only occur prior to significant crystallization, this feature indicates that 1) glomerocrysts moved through the gabbroic melt, and 2) plagioclase was a liquidus phase early in the crystallization history of the sill.

DISCUSSION

Textural and compositional differences between the two populations of plagioclase crystals in glomeroporphyritic gabbro reflect different crystallization environments. Glomerocrysts bear a striking resemblance to anorthositic cumulates (cf Wager et al., 1960; Morse, 1969), and it is probable that they represent the products of fractional crystallization and accumulation of plagioclase in a feeder chamber at depth. Melt expelled from the chamber entrained plagioclase crystals and aggregates which were hydraulically concentrated towards the centre of flow during ascent and emplacement (Komar, 1972). The central accumulation of aggregates resulted in the general pattern of non-porphyritic to sparsely-porphyritic marginal zones, and increasing numbers of glomerocrysts toward the centre of the sills. The magmatic pulse may have continued to crystallize plagioclase during emplacment, and movement of glomerocrysts toward the central part of the flow through melt containing plagioclase crystals and nuclei produced the concentric arrangement of groundmass crystals observed. Sharp internal contacts indicate that coarse grained anorthositic gabbro forming the central portions of many glomeroporphyritic sills has developed through emplacement of a second magmatic pulse which cooled slowly as a result of the insulating effect of the earlier intrusion.

The mineralogical and chemical similarities of normal and glomeroporphyritic gabbro, and their close spatial association, suggests that they are comagmatic. Normal gabbro enclaves within anorthositic gabbro indicate that the former, at least locally, predates the latter. It is probable that crystal-free liquids were removed prior to, or during the first stages of plagioclase fractionation in the feeder chamber. The development of localized phase layering is thought to reflect limited in situ fractional crystallization, and this process has contributed to the evolution of siliceous differentiates within the sills. Assimilation of Le Fer sediments may have been an additional factor in the differentiation process, and is perhaps responsible for the commonly elevated sulphide content of many of the gabbroic rocks.

ACKNOWLEDGMENTS

This study has been supported by the Geological Survey of Canada (Mineral Resource Division) through a contract awarded to Tony Fowler under the Canada-Newfoundland Mineral Development Agreement 1984-1989. Additional funding for analytical work was provided by Canaustra Gold Exploration Ltd, and logistic support was provided in part by La Fosse Platinum Group Inc. The assistance and expertise of Dan Richardson and Don Watanabe are gratefully acknowledged. O.R. Eckstrand and R.F.J. Scoates reviewed the manuscript and provided helpful suggestions.

REFERENCES

Baragar, W.R.A.
1960: Petrology of basaltic rocks in part of the Labrador Trough; Geological Society of America Bulletin, v. 71, p. 1589-1643.
1967: Wakuach Lake map area, Québec-Labrador; Geological Survey of Canada, Memoir 344.

Baragar, W.R.A. and Scoates, R.F.J.
1980: The Circum-Superior belt: a Proterozoic plate margin; in Precambrian Plate Tectonics; edited by A. Kroner, Elsevier, Amsterdam, p. 297-329.

Dimroth E.
1970: Evolution of the Labrador geosyncline; Geological Society of America Bulletin, v. 81, p. 2717-2742.
1978: Labrador Trough Area; Ministere des Richesse Naturelles, Québec, Rapport Gologique 193.

Findlay, J.M., Fowler, A.D., and Birkett, T.C.
1988: Platinum group element potential of the Howse Lake area, Western Labrador; Newfoundland Department of Mines-Geological Survey Branch, Open File 230(29).

Frarey M.J. and Duffell S.
1964: Revised stratigraphic nomenclature for the central part of the Labrador Trough; Geological Survey of Canada, Paper 64-25.

Irvine T.N. and Baragar W.R.A.
1971: A guide to the chemical classification of the common volcanic rocks; Canadian Journal of Earth Sciences, v. 8, p. 523-548.

Komar, P.D.,
1972: Flow differentiation in igneous dikes and sills: Profiles of velocity and phenocryst concentration; Geological Society of America Bulletin, v. 83, p. 3443-3448.

Morse S.A.
1969: The Kiglapait layered intrusion, Labrador; Geological Society of America, Memoir 112.

Wager L.R., Brown G.M. and Wadsworth W.J.
1960: Types of igneous cumulates; Journal of Petrology, v. 1, p. 73-85.

Wardle R.J.
1982: Geology of the South-Central Labrador Trough; Newfoundland Departmant of Mines and Energy, Mineral Development Division, Map 82-6.

Wardle, R.J. and Bailey D.G.
1981: Early Proterozoic sequences in Labrador; in Proterozoic Basins Canada; edited by F.H.A. Campbell; Geological Survey of Canada, Paper 81-10, p. 331-359.

Winchester J.A. and Floyd P.A.
1976: Geochemical magma type discrimination: application to altered and metamorphosed basic igneous rocks; Earth and Planetary Science Letters, v. 28,p. 459-469.

Natural and mining-related seismic activity in northern Ontario

R.J. Wetmiller, M. Plouffe[1], M.G. Cajka[2] and H.S. Hasegawa
Geophysics Division

Wetmiller, R.J., Plouffe, M., Cajka, M.G. and Hasegawa, H.S., Natural and mining-related seismic activity in northern Ontario; in Current Research, Part C, Geological Survey of Canada, Paper 89-1C, p. 353-361, 1989.

Abstract

Regional monitoring of seismic activity in the mining areas of northern Ontario has been carried out as a special project with additional support from Atomic Energy of Canada Ltd. (AECL) since 1982 and from the Canada-Ontario-Industry Rockburst Project since 1984. The Geological Survey of Canada (GSC) managed the operation of the seismograph stations and carried out the analyses of the data collected, including determination of the hypocentre and magnitude of seismic events, discrimination between blasts and rockbursts, and preliminary studies of the seismic source mechanisms. Since 1983, the GSC has analyzed more than 40 earthquakes and more than 250 rockbursts magnitude 4.0 or less in northern Ontario. The special monitoring has allowed the spatial and temporal distributions and the seismic source properties of both earthquakes and rockbursts to be directly compared.

Résumé

Depuis 1982, l'Énergie atomique du Canada Limitée (EACL) et, depuis 1984, le Project de recherche conjoint Canada-Ontario-Industrie sur les coups de toit ont permis d'accroître la surveillance régionale de l'activité séismique dans les zones minières du nord de l'Ontario. La Commission géologique du Canada (CGC) veille à l'entretien des stations séismographiques et à l'analyse des données recueillies. Ces données permettent de localiser des hypocentres et de déterminer la magnitude des séismes, de distinguer entre dynamitages et coups de toit ainsi que de procéder à certaines études préliminaires des mécanismes au foyer. Depuis 1983, la CGC a analysé plus de 40 tremblements de terre et plus de 250 coups de toit de magnitude 4,0 et moins survenus dans le nord de l'Ontario. Cette surveillance particulière a permis de comparer les distributions temporelles et spatiales ainsi que les propriétés séismiques de la séismicité naturelle et de la séismicité reliée à l'activité minière.

[1] Mineral Research Laboratories, Canada Centre for Mineral and Energy Technology, Energy, Mines and Resources, Canada, 1 Observatory Crescent, Ottawa, Canada, K1A 0Y3.
[2] Atomic Energy of Canada, Ltd., 1 Observatory Crescent, Ottawa, Canada, K1A 0Y3.

INTRODUCTION

The monitoring of earthquake activity in Canada falls within the mandate of the Department of Energy, Mines and Resources (EMR), and is carried out by the Geophysics Division of the Geological Survey of Canada (GSC) which operates a national network of almost one hundred seismograph stations in all parts of Canada and analyses the data recorded. The GSC network is the prime source of information about earthquake activity in Canada. It is a powerful tool for studying the source properties of strong seismic events, either natural or man-made, anywhere in the country and understanding the hazards they pose to people and facilities.

Northern Ontario lies within stable Precambrian crystalline terrains of the Canadian Shield where the activity in this century has generally been infrequent. Consequently, the low level seismic activity in this region has tended to be poorly monitored and little information has been collected about the earthquakes or the seismic events experienced in many of the mines in the region. The tendency has been to categorize the seismic hazards as being negligible when, in fact, there were insufficient data to determine them reliably. In this last decade, two important concerns have reversed this tendency. They are the need to verify the concept of a safe long-term disposal of radioactive waste from nuclear power plants in rock plutons of northern Ontario and the need to mitigate the increasingly serious safety and economic threats posed by mining-induced seismic activity in northern Ontario mines.

Since 1982, the Canadian Nuclear Fuel Waste Management Program operated by Atomic Energy of Canada Ltd. (AECL) (Rosinger et al., 1983) has supported the operation of up to six seismograph stations across the Canadian Shield region of northern Ontario and into eastern Manitoba (Fig. 1) to provide data for regional seismic hazard estimates for a radioactive waste storage facility somewhere in the region. The AECL stations have lowered the detection threshold of seismic activity to magnitude (M) 2.5 across the middle of northern Ontario (Wetmiller and Cajka, in press). In addition, since 1984, the Canada-Ontario-Industry Rockburst Project (Brehaut and Hedley, 1987), coordinated by the Canada Centre for Mineral and Energy Technology (CANMET) of EMR, has supported the operation of the Sudbury Local Telemetered seismograph Network (SLTN) in the Sudbury Basin to provide more detailed information about the seismic source properties of the mining-induced seismic activity in the many local mines. SLTN has lowered the detection threshold for all seismic activity, natural or man-made, in the Sudbury Basin to M 1.7 (Plouffe et al., in press). The new information being collected by these networks will have an important influence in understanding the seismic hazards posed by both the natural earthquakes and the man-made seismic events in the region.

This report presents a preliminary assessment of the results to date of the analyses of seismic activity, both natural and mining-induced, in northern Ontario with emphasis on the eastern half of northern Ontario and the Sudbury Basin in particular. A description of the findings from the

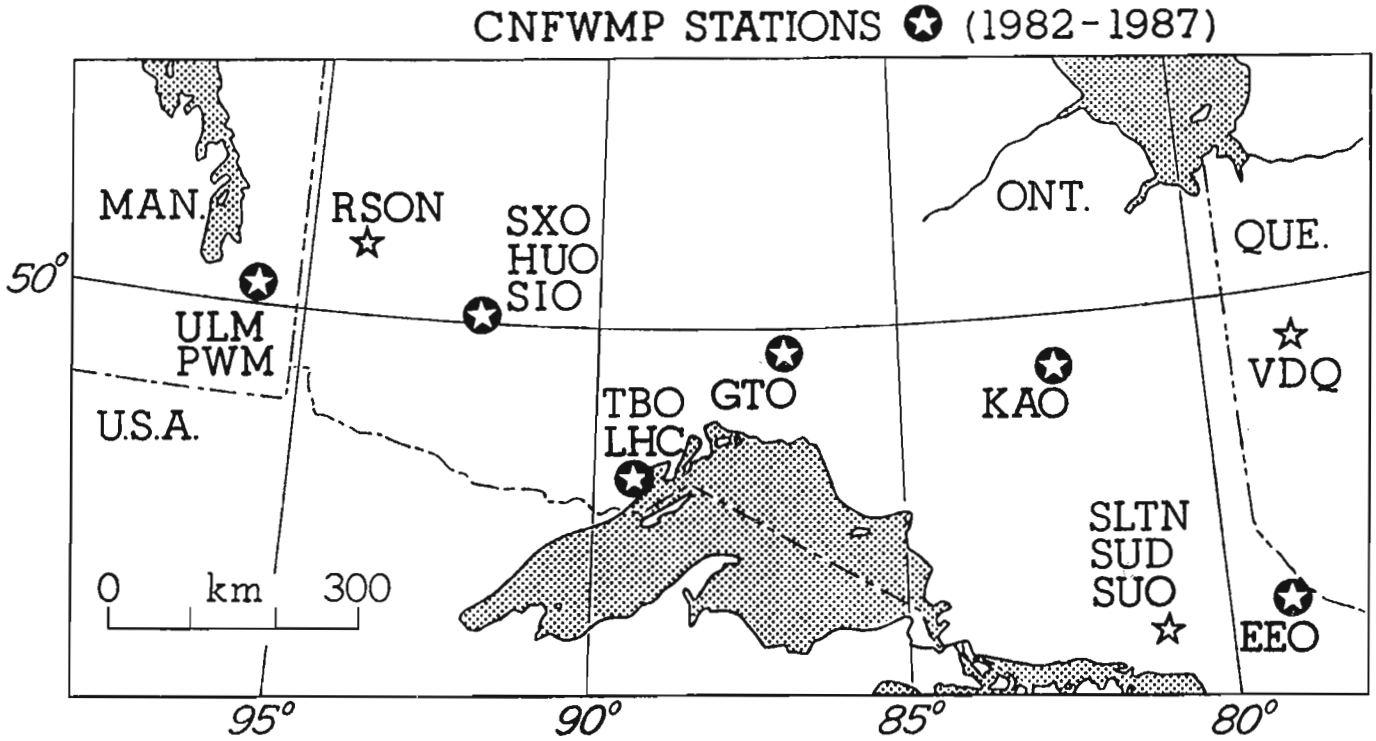

Figure 1. Seimograph stations in northern Ontario supported by Atomic Energy of Canada Ltd. as part of the Canadian Nuclear Fuel Waste Management Program (CNFWMP) from Wetmiller and Cajka (in press). The Sudbury Local Telemetred seismograph Network (SLTN) including SUO, SZO and SWO, is supported by CANMET for the Canada-Ontario-Industry Rockburst Project. VDQ and SUD were both operated by GSC; both have been closed as of 1987. RSON is an independent station operated by the U.S Department of Energy in co-operation with GSC. See Hedley and Wetmiller (1985) for definitions.

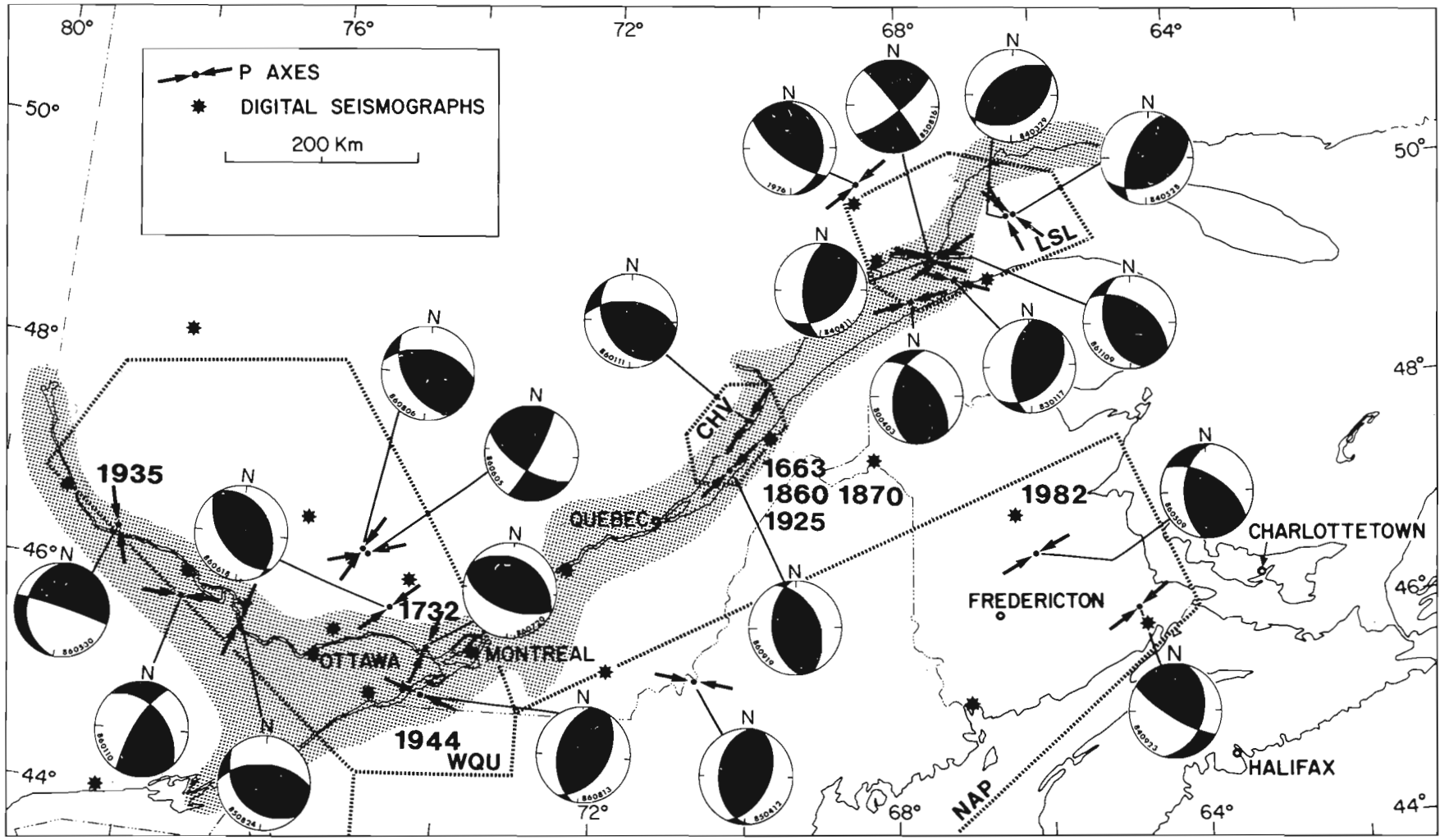

Figure 2. Mechanisms of recent earthquakes and seismic zones in eastern Canada after J. Adams (pers. comm., 1988) with modifications. Mechanism solutions are shown as an equal-area projection of the lower focal sphere with the compressional quadrants shaded. WQU, CHV, LSL and NAP are earthquake source zones defined for probabalistic hazard estimates for the National Building Code of Canada (Basham et al., 1982) and the year of strong earthquakes in each zone is indicated. The stippled zone shows the approximate extent of Mesozoic rift faulting associated with St. Lawrence Rift System.

AECL monitoring program has been given separately by Wetmiller and Cajka (in press), and a description of some of seismic data processing for CANMET is given by Plouffe et al. (in press).

EARTHQUAKE HAZARDS IN NORTHERN ONTARIO

Damaging earthquakes have occurred in the Precambrian Shield terrains of eastern Canada in the St. Lawrence River Valley of Quebec (1663, 1870 and 1925) and in the Ottawa-Upper St. Lawrence Valleys along the Ontario-Quebec border (1935 and 1944) (Fig. 2). Studies of the mechanisms of small earthquakes in these areas (J. Adams, pers. comm., 1988) show that most of the earthquakes are of thrust faulting-type on intermediately-dipping planes, but with some degree of variability in the fault strike. This could imply a common (tectonic) origin in the crustal stress field. The regional stress field in the upper crust in eastern Canada appears to be characterized by nearly horizontal compressive stress orientated in the east-west to northeast-southwest direction in good general agreement with the plate motions predicted for the North American crustal plate from global studies (Adams, 1987). As well, detailed monitoring of

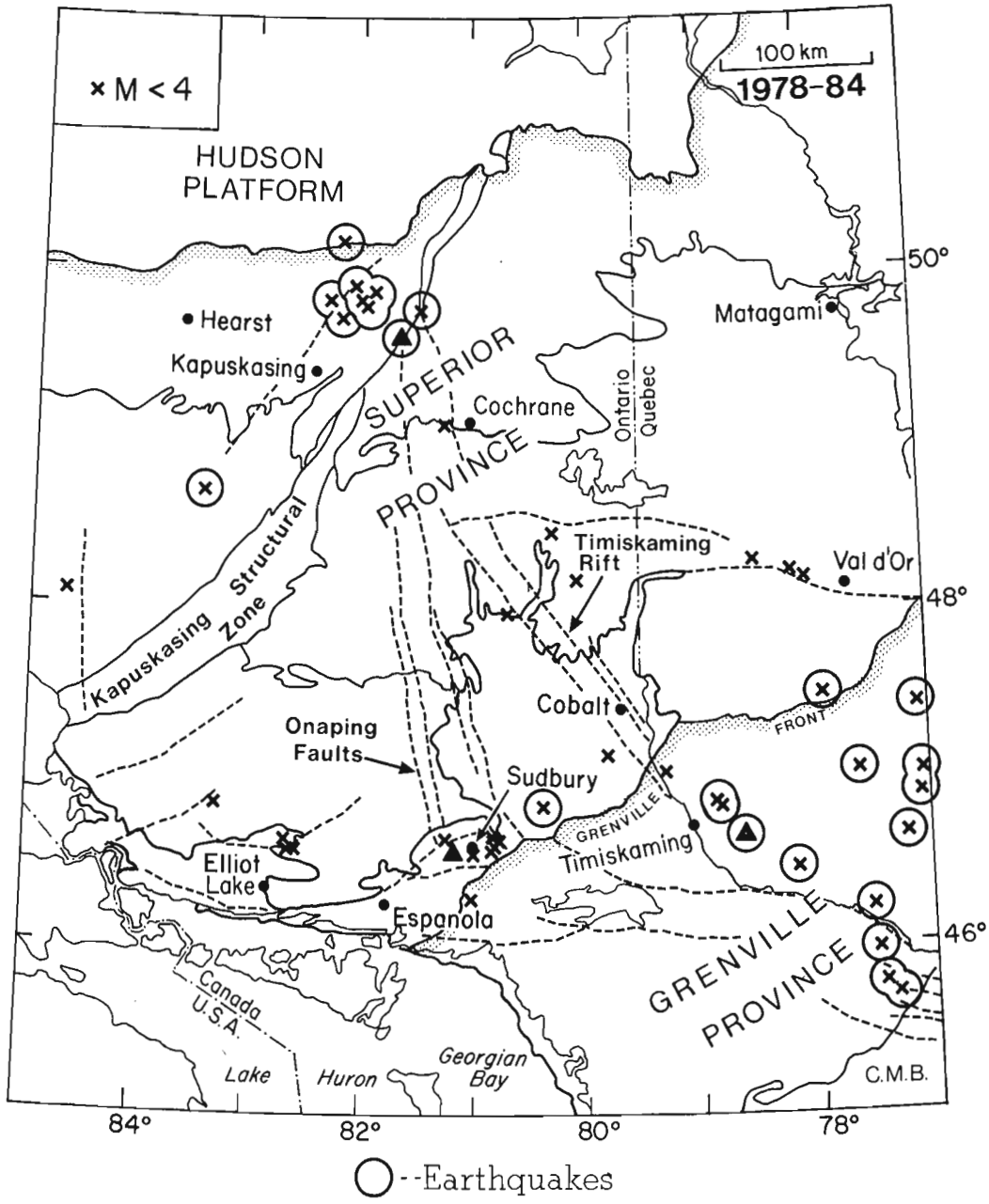

Figure 3. Earthquake activity in the Timiskaming-Kapuskasing region of northeastern Ontario for the period 1984-1987. Major faults are indicated by dashed lines and have been simplified by Forsyth et al., 1983. Largest event in this period is M 3.6.

microearthquake activity in the Charlevoix seismic zone (Anglin, 1984) shows that the earthquake activity there tends to occur along a series of Paleozoic rift faults which are part of a larger system of rift faults that follows the general trend of St. Lawrence-Ottawa-Lake Champlain valleys and was active (in geological terms) as late as the Mesozoic period (Kumarapeli, in press).

Adams and Basham (in press) note that all large earthquakes known in eastern Canada in the past have occurred on some part of the St. Lawrence rift system or the rifted margin of the Atlantic continental shelf along the eastern Canadian seaboard, and suggest that such rift structures possess extended zones of weakness where large earthquakes can nucleate. They also suggest that future strong earthquakes need not be confined only to those portions of the rift system which have had strong earthquake activity in historical times, but may in fact occur anywhere on rift systems even where there has been little or no previous record of seismic activity.

Northeastern Ontario is affected by an extension of this same rift system along its eastern border with Quebec, although the extent of the affected area is difficult to judge. Adams and Basham (in press) and Forsyth (1981) associate the M 6.3 Timiskaming earthquake of 1935 with the Ottawa-Bonnechere graben, which forms one arm of the St. Lawrence rift system, and Forsyth et al. (1983) link the Ottawa-Bonnechere graben with the Timiskaming rift valley, which continues into northeastern Ontario. They also identify other geological features in northeastern Ontario that may be associated with earthquake activity in the region such as the Kapuskasing Structural Zone, the Central Metasedimentary Belt, the Onaping Fault system and several other unnamed faults. Sanford et al. (1984) show that microfracturing (as measured in boreholes), frequency of (tectonic) basement rejuvenation and the level of ambient earthquake activity are all higher in northeastern Ontario than in northwestern Ontario and eastern Manitoba. Wetmiller and Cajka (in press) identify a region of moderate earthquake activity occupying the area from western Quebec to the Kapuskasing Structural Zone (Fig. 3) for data from 1978-84, which they call the Timiskaming-Kapuskasing region, and they show evidence that the earthquake activity in this region is generally the thrust fault type.

Thus, there is evidence from several studies that northern Ontario east of longitude 83° W is subject to a moderate rate of earthquake activity, that the activity is predominately of the thrust fault type similar to that seen in other areas of eastern Canada and that rift structures exist in the region similar to those that have been associated with the strong earthquakes elsewhere in eastern Canada.

EARTHQUAKE ACTIVITY, 1984-1987

Since 1984, GSC has located 46 earthquakes in or near northeastern Ontario (Fig. 3). The largest earthquake in this period was the magnitude 3.6 event in March, 1987, in the extreme northern part of the region. The activity from 1984 to 1987 was generally random in space (Fig. 3) and time (Fig. 4) but one swarm of eight earthquakes (M 1.7-2.9) was recorded in the area about 50 km southeast of Sudbury in October, 1986 (Fig. 3). This swarm was the second example

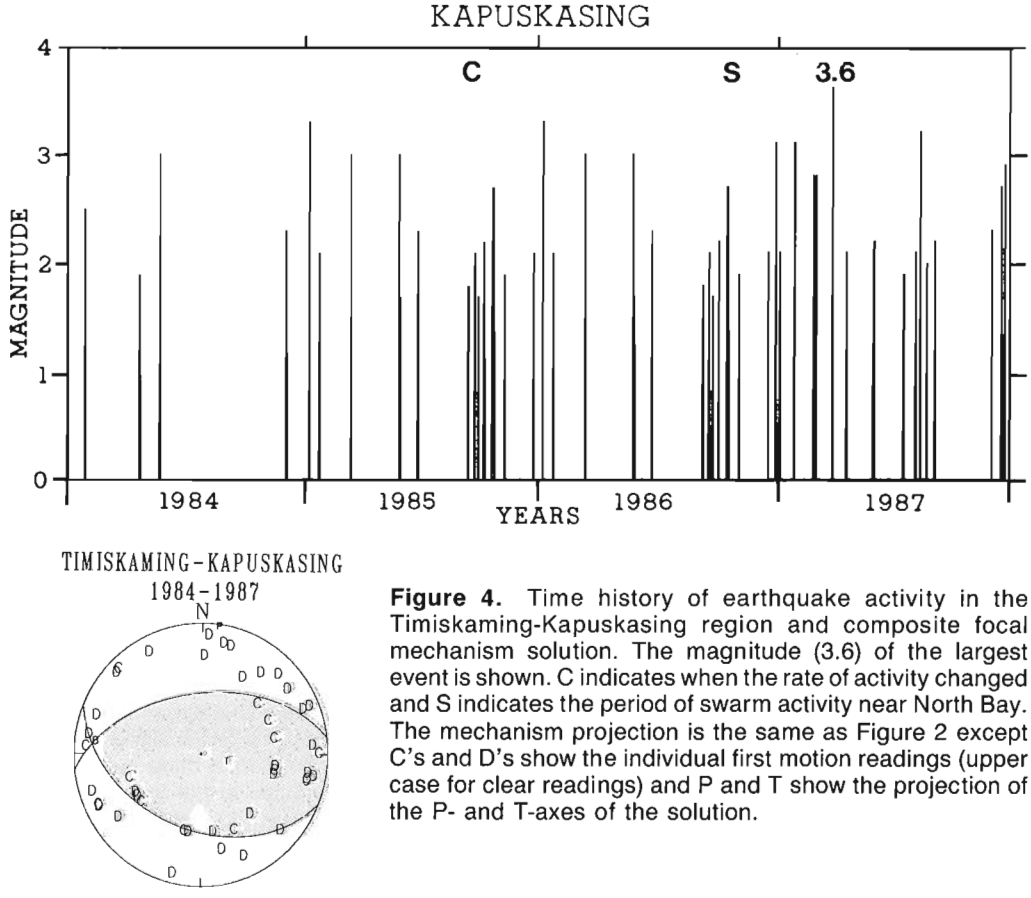

Figure 4. Time history of earthquake activity in the Timiskaming-Kapuskasing region and composite focal mechanism solution. The magnitude (3.6) of the largest event is shown. C indicates when the rate of activity changed and S indicates the period of swarm activity near North Bay. The mechanism projection is the same as Figure 2 except C's and D's show the individual first motion readings (upper case for clear readings) and P and T show the projection of the P- and T-axes of the solution.

of localized earthquake activity found in the region. Repeated earthquake activity is reported by Wetmiller and Cajka (in press) in the area north of Kapuskasing, Ontario in 1983. The rate of activity for the region as a whole showed an increase starting in July, 1985 when it abruptly changed from an average annual rate (considering the total seismic moment release) equivalent to one M 3 event per year to a rate of one M 4 per year (Fig. 4). No reason for this change has been identified; it was not due to changes in the seismic network or data processing. Considering that detailed monitoring has only been carried out in the region for a few years, this change in the rate of activity may not be statistically significant.

A composite mechanism of the earthquakes from 1984 to 1987 (Fig. 4) indicated predominantly mid-angle thrust faulting within a regional NNE-SSW directed compressive stress field similar but not identical to that reported by Wetmiller and Cajka (in press) for the period 1978-84. The azimuth of the deviatoric compressional stress found in this study was more north-south than the direction found by Wetmiller and Cajka (in press) but this difference was not considered significant considering the generally poor resolution of azimuth that the composite mechanism provides.

MINING-INDUCED ACTIVITY, 1984-1987

In the same period, GSC analyzed more than 250 rockbursts (M 1.5-4.0) in five different mining areas in Ontario. Six of the rockbursts had magnitude greater then 3.5; the largest was magnitude 4.0 at the Creighton Mine, Sudbury, on July 6, 1984. Large events also occurred at the Falconbridge Mine in Sudbury and the Quirke Mine in Elliot Lake (Wetmiller and Cajka, in press). The monitoring of mining-induced seismic activity has been concentrated in the Sudbury Basin following the installation of the SLTN (Plouffe et al, in press), which was completed in May, 1987. Figure 5 shows the distribution of mining-induced seismic activity (not blasts) that has been located by SLTN. The

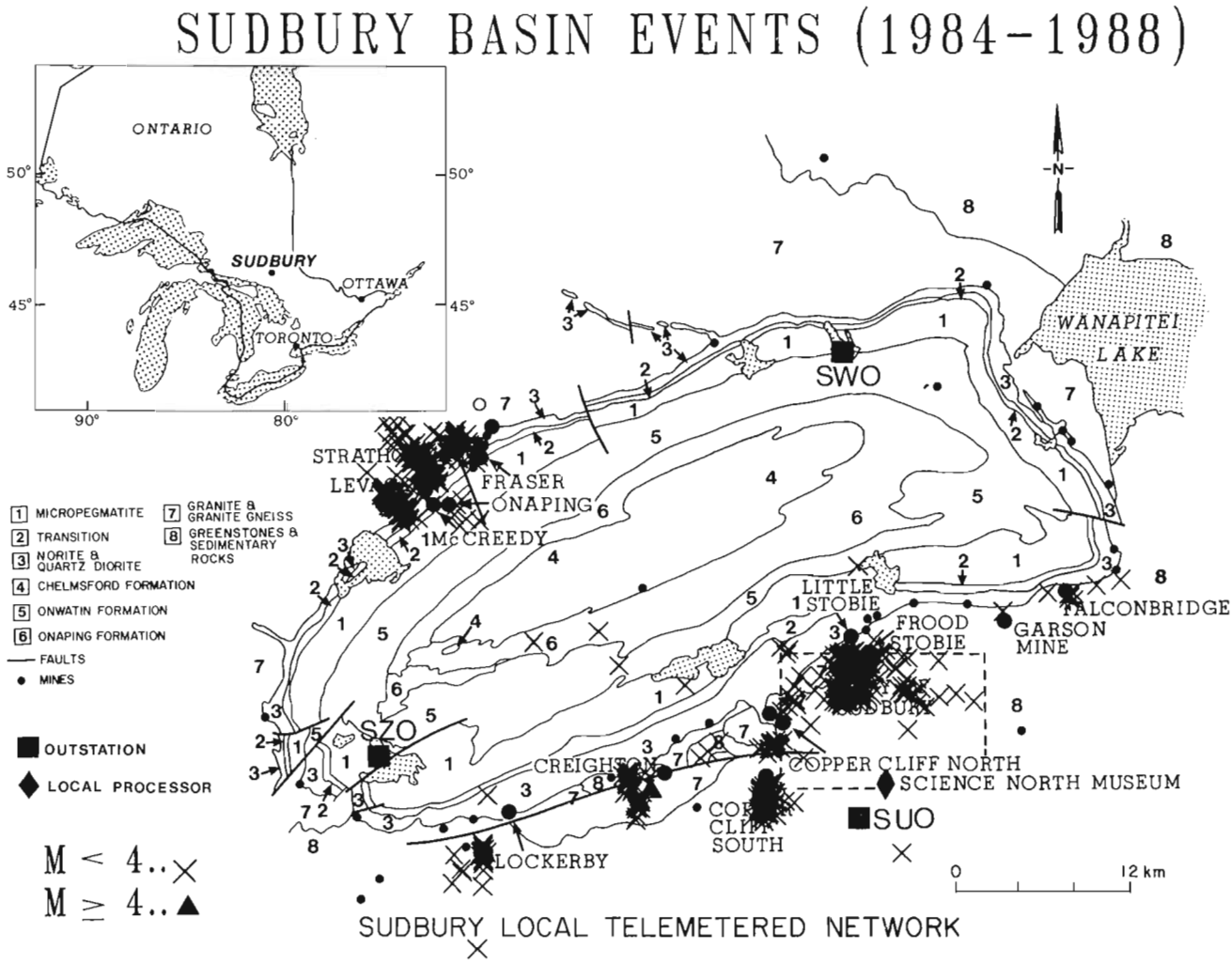

Figure 5. Mining-induced seismic activity and geology of the Sudbury Basin, northeastern Ontario. The base map is taken from Plouffe et al. (in press). The SLTN seismometer sites (SUO, SWO and SZO) are indicated by squares. Active mines are indicated by larger dots. The Strathcona mine is located on the northwestern margin of the basin; the Creighton mine is located on the south-central margin of the basin. The approximate extent of the city of Sudbury is indicated by the large dashed square. The number of events located by SLTN increased substantially in late 1987 following the completion of the network.

activity occurred in several distinct clusters, each associated with an active mine. It should be noted that some of the scatter seen in the clusters is due to small errors in the locations which, for this preliminary study, have not been calibrated to individual mines nor corrected for velocity changes along different paths to the recording stations. Nevertheless, it is clear that, for this period, almost all the seismic activity in the Sudbury Basin was located in areas close to the active mining camps and very few events occurred elsewhere in the Basin.

The data collected for two mines in the Sudbury Basin, Falconbridge'sStrathcona Mine and INCO's Creighton Mine, are shown in Figures 6 and 7 (except for the last quarter of 1987 for the Strathcona mine). The mining-induced activity generally appeared to occur randomly in time and there was no obvious correlation with the activity in the other mine, the earthquake activity in the surrounding region (Fig. 3), or with the mine's operation (Fig. 7) during the four years.

Seismic activity was not recorded at the Strathcona mine in 1984 by the seismograph networks. It is possible that small events did occur, but larger events (M 2.5 or more) would have been detected. In the following years, activity appeared to occur sporadically without any discernible pattern (Fig. 6). On the other hand, the activity in the Creighton mine was more systematic. It was low following the large event in July, 1984 until mid-1985 when it began to occur at a regular rate until the first part of 1986. The activity then showed a distinct gap prior to the M 3.3 event in October,

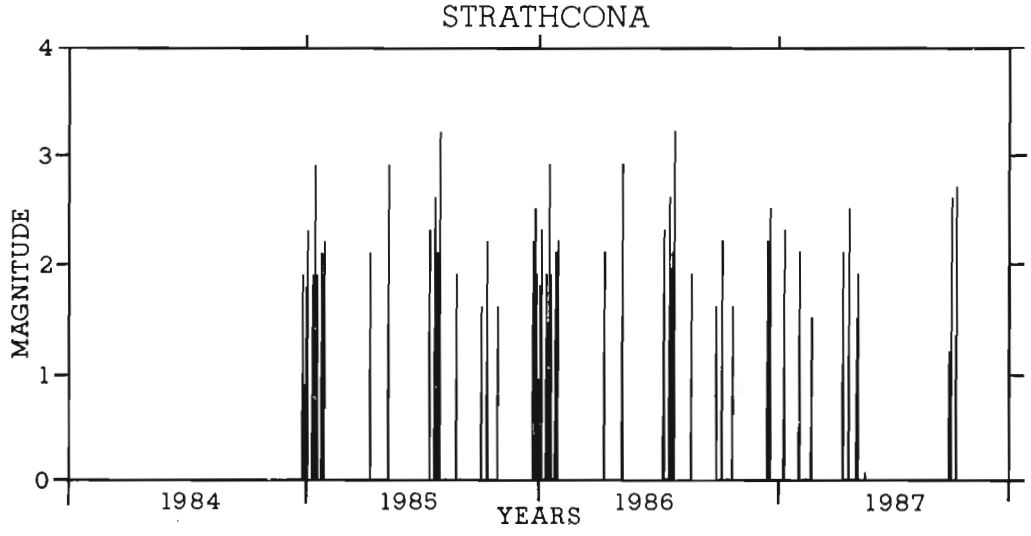

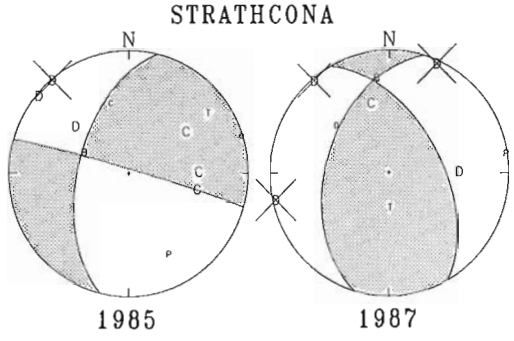

Figure 6. Time history of mining-induced seismic activity in the Strathcona mine and focal mechanism solutions for two larger events. Data for the last quarter of 1987 were not available at the time of this report. Mechanism plot is the same as Figure 4, except crosses show where S/P amplitude ratios from SLTN have been used to constrain the solution. See Table 1 for information about the events.

Table 1. Mining-induced event focal mechanisms parameters

Year	Date	Mine	Magnitude	Strike	Dip	Rake	Type 1	Mechanism
1984	0706	Creighton	4.0	267.57	58.23	−25.70	Shear	Normal
1984	0706	Creighton	4.0	121.71	50.73	77.04	Shear	Thrust
1985	1221	Strathcana	3.1	193.90	55.15	− 3.49	Fault-Slip	Thrust
1986	1029	Creighton	3.3	339.71	37.70	64.96	Shear	Thrust
1987	1014	Strathcona	3.0	330.47	54.37	58.67	Pillar burst	Thrust
1987	1027	Creighton	3.7	163.07	55.60	77.85	Pillar burst (?)	Thrust

1986 when it resumed at a regular rate and continued until the M 3.7 event in October, 1987 (Fig. 7). Following that event, the rate of seismic activity has remained low at the Creighton mine to date (June, 1988). Both of these mines have produced seismic events at an average rate of one M 3-4 event per year over this four-year period, which is comparable to the rate of natural earthquake activity observed in the surrounding region.

FOCAL MECHANISMS OF MINING-INDUCED EVENTS

Focal mechanism analyses were carried out for five mining-induced seismic events in the 1984-1987 period (Table 1), two events in the Strathcona mine and three events in the Creighton mine. All these events had magnitude over 3.0. All mechanism solutions found (Fig. 6 and 7) were compatible with thrust-fault-slip on intermediate-dipping planes, but the solutions tended to be poorly constrained because of a lack of well-distributed data over the focal sphere. We attempted to overcome this deficiency by using the S/P amplitude ratios from SLTN stations whenever possible to constrain the focal mechanism solutions as suggested by Kisslinger (1980), but had only limited success. The solutions presented for the Strathcona mine (Fig. 6) are particularly poorly constrained and should be considered provisional.

In addition to the normal problems of data quality and distribution, focal mechanism analyses of seismic events occurring in a mining environment are subject to the additional uncertainty of the possibility of a significant non-double-couple component to the seismic source. Hasegawa et al. (in press) show several ways in which mining-induced seismic events may depart from the ideal double-couple source that is assumed for the focal mechanism solution. In general, the closer the focus of a seismic tremor is to the mine cavity, the more prominent the non-double-couple component could be. Pillar bursts in particular, which occur right in the mine cavity, could represent a dipole seismic source. For the events discussed in the following section, there are no seismic data available from the immediate mine areas that could be used to detect and identify possible non-double-couple components of the seismic sources, and we have interpreted the first-motion polarities of the mining-induced events strictly in terms of the standard double-couple radiation pattern.

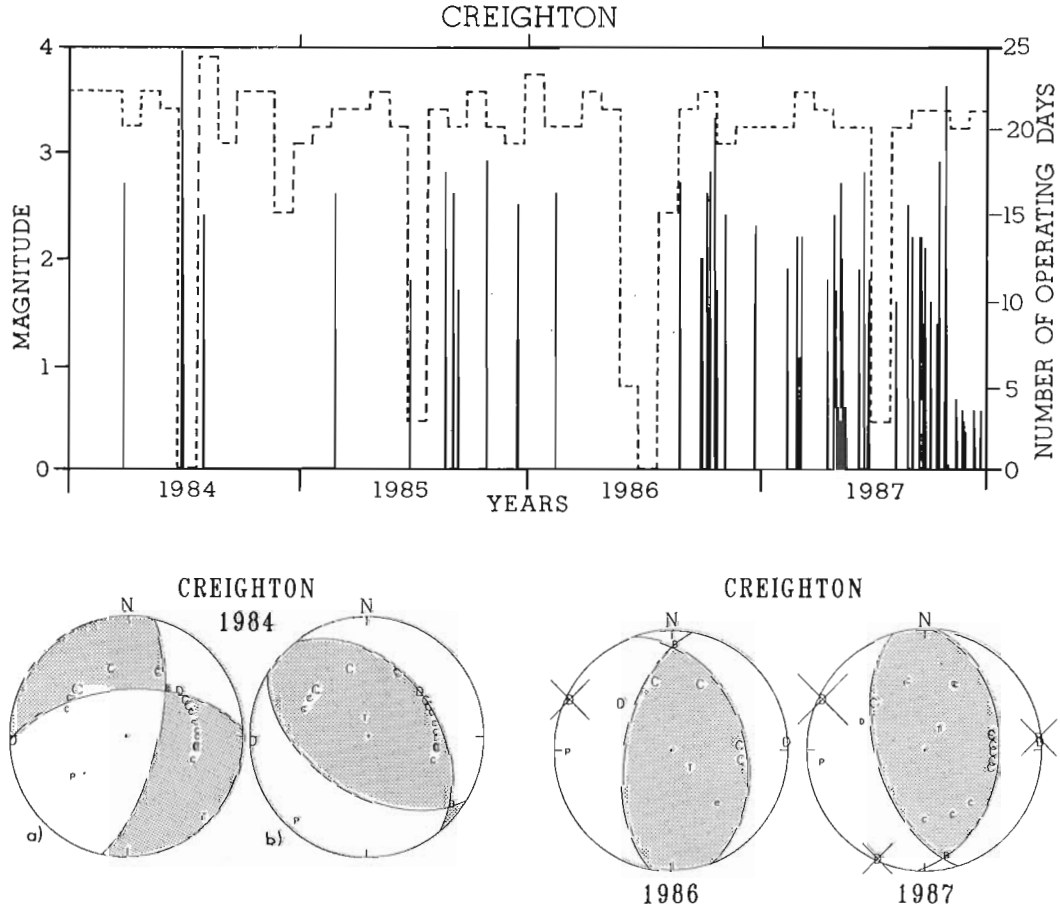

Figure 7. Time history of mining-induced seismic activity in the Creighton mine and focal mechanism solutions for three large events. The number of operating days per month at the mine is shown by the dashed line. Mechanism plot is the same as Figure 6. Two alternate interpretations for the mechanism of the 1984 event calculated for this report are shown. See Table 1 for information about the seismic events.

A normal-fault-slip mechanism is reported for the 1984 Creighton event by Wetmiller and Cajka (in press). They analyze five large rockbursts in three different mines. Considered on their own, the data for the 1984 Creighton event were also compatible with either the normal-fault-slip mechanism (similar but not identical to that of Wetmiller and Cajka (in press)) or the thrust-fault-slip mechanism shown in Figure 7. Both solutions were poorly constrained by the data, and the only diffence between the two interpretations was one poorly defined compressional phase, which was compatible with the thrust mechanism but not with the normal mechanism. This ambiguity illustrates the difficulties encountered when trying to interpret focal mechanisms from poorly distributed data sets.

The best mechanism solution available for any mining-induced seismic event in this period was for the M 3.7 event at the Creighton mine in October, 1987. That event had three readings and ratios from SLTN to constrain the mechanism solution as well as data from more distant seismograph stations and showed a thrust-fault-slip solution with east-west horizontal compressive stress. Such a mechanism is generally similar to the thrust mechanisms shown earlier for the earthquakes in the Timiskaming-Kapuskasing region (Fig. 3) and elsewhere in eastern Canada (Fig. 2). The principal stress field implied by the solution for the 1987 Creighton event is the same type and within the range of azimuths determined by many studies of stress in eastern Canada.

CONCLUSIONS

The mining areas of northeastern Ontario including the Sudbury Basin lie within a distinct region of low-to-moderate earthquake activity, the Temiskaming-Kapuskasing region. The region exhibits certain characteristics that are associated with earthquakes as large as M 7 in other areas of eastern Canada of similar seismotectonics, namely thrust-fault-slip earthquakes, high horizontal compressive stresses and rift structures. One of the largest earthquakes known in eastern Canada, the M 6.3 Timiskaming earthquake of 1935, occurred in the eastern part of the region, possibly through a reactivation of Mesozoic-aged rift faults as thrust faults by the contemporary stress field. From 1984 to 1987, 46 earthquakes up to M 3.6 have been detected in the region occurring at an average annual rate equivalent to one M 3-4 event per year. The natural earthquake activity has been generally scattered in space and time, although some minor swarm activity has been detected.

The seismic activity in the Sudbury Basin during 1984-87 was entirely associated with the active mining camps and no good evidence for natural seismic activity was found in the basin, although detailed monitoring in the basin began only in the latter part of 1987. The mining-induced seismic activity included events as large as M 4.0 and occurred at an average annual rate equivalent to one M 3-4 event per year in some of the more seismically active mines. It did not show any obvious correlation between different mines nor with the natural earthquake activity in the surrounding region. Focal mechanisms were calculated for five of the larger mining-induced events and all solutions were compatible with thrust-fault-slip mechanisms on intermediate-dipping planes with an implied horizontal compressive stress regime. As such the seismic mechanisms of mining-induced events appeared to be quite similar to those of natural earthquake activity throughout eastern Canada.

ACKNOWLEDGMENTS

The authors wish to thank Janet Drysdale and Maurice Lamontagne for their critical reading of this manuscript. The authors would like to also thank the mining operators who answered our information requests.

REFERENCES

Adams, J.
1987: Canadian crustal stress database - a compilation to 1987; Geological Survey of Canada, Open File Report 1622, 130 p.

Adams, J. and Basham, P.W.
—: The seismicity and tectonics of eastern Canada; in Neotectonics of North America, edited by D.B. Slemmons, E.R. Engdahl, D. Blackwell, D. Schwartz, and M. Zoback, Geological Society of America, Decade of North American Geology, v. CSMV-1 (in press).

Anglin, F.M.
1984: Seismicity and faulting in the Charlevoix seismic zone; Bulletin Seismological Society of America, v. 74, p. 595-603.

Basham, P.W., Weichert, D.H., Anglin, F.M., and Berry, M.J.
1982: New probabilistic strong seismic ground motion maps for Canada: a compilation of earthquake source zones, methods and results; Earth Physics Branch, Open File Report 82-33, 205 p.

Brehaut, C.H. and Hedley, D.G.F.
1987: 1986-1987 Annual Report of the Canadian-Ontario-Industry Rockburst Project; CANMET Special Report SP 87-7E, 22 p.

Forsyth, D.A.
1981: Characteristics of the western Quebec seismic zone; Canadian Journal of Earth Sciences, v. 18, p. 103-119.

Forsyth, D., Morel, P., Hasegawa, H., Wetmiller, R., Adams, J., Goodacre, A., Nagy, D., Coles, R., Harris, J., and Basham, P.
1983: Comparative study of the geophysical and geological information of the Timiskaming-Kapuskasing area; Atomic Energy of Canada Ltd., Technical RecordTR-238, 52 p.

Hasegawa, H.S., Wetmiller, R.J., and Gendzwill, D.J.
—: Induced seismicity in mines in Canada - an overview; PAGEOPH (in press).

Hedley, D.G.F. and Wetmiller, R.J.
1985: Rockbursts in Ontario mines in 1985; Earth Physics Branch, Open File Report 85-33, 37 p.

Kisslinger, C.
1980: Evaluation of S to P amplitude ratios for determining focal mechanisms from regional network observations; Bulletin Seismological Society of America, v. 70-4, p. 999-1014.

Kumarapeli, S.
—: Seismic zones, ancient fault systems and post-glacial faulting in eastern Canada; Geological Survey of Canada, Open File (in press).

Plouffe, M., Cajka, M.G., Wetmiller, R.J., and Andrew, M.D.
—: The Sudbury Local Telemetered Seismograph Network; in Second International Symposium on Rockbursts and Seismicity in Mines (in press).

Rosinger, E.L.J., Lyon, R.B., Gillespie, P., and Tamm, J.
1983: Guide to the Canadian Nuclear Fuel Waste Management Program, Second Edition; Atomic Energy of Canada Ltd., Limited Report AECL-7790, 60 p.

Sanford, B.V., Thompson, F.J., and McFall, G.H.
1984: Phanerozoic and recent tectonic movements in the Canadian Shield and their significance to the Nuclear Fuel Waste Management Program; in Proceedings of the Workshop on Transitional Processes, November 4 and 5, 1982, Ottawa, Atomic Energy of Canada Ltd., Limited Report AECL-7822, p. 73-96.

Wetmiller, R.J. and Cajka, M.G.
—: Tectonic implications of the seismic activity recorded by the northern Ontario seismograph network; in Results of the Geoscience Research in the Canadian Nuclear Fuel Waste Management Program, Canadian Journal of Earth Sciences (in press).

A radioactive heat generation map for the subsurface Precambrian of Alberta

R.A. Burwash[1] and R.W. Burwash[1]
Institute of Sedimentary and Petroleum Geology, Calgary

Burwash, R.A. and Burwash, R.W., A radioactive heat generation map for the subsurface Precambrian of Alberta; in Current Research, Part C, Geological Survey of Canada, Paper 89-1C, p. 363-368, 1989.

Abstract

Analyses of unweathered core samples from the subsurface Precambrian of Alberta for U, Th and K provide heat generation data for each well location. Trend surface mapping of the heat generation values shows an east-west belt of anomalously high values extending across the northern half of the province. Although well control is sparse, weaker parallel trends can be observed in southern Alberta.

The northern Alberta belt coincides with a previously identified zone of Hudsonian K-metasomatism. U and Th enrichment may have accompanied the Hudsonian event. Rocks with high Th content and high Th/U ratios may reflect radioactive elements in detrital heavy mineral concentrations in supracrustal rocks reworked into the Archean basement.

Résumé

En dosant dans des échantillons non altérés, prélevés par carottage dans les terrains de subsurface du Précambrien de l'Alberta, les éléments U, Th et K, on obtient des données sur la génération de chaleur pour chaque emplacement de puits. La cartographie de surface des tendances manifestées par les valeurs du flux thermique, indique l'existence d'une zone est-ouest de valeurs anormalement élevées, traversant la moitié nord de la province. Bien que l'on dispose de peu de diagraphies de contrôle des puits, on peut observer des tendances parallèles moins nettes dans le sud de l'Alberta.

La zone nord de l'Alberta coïncide avec une zone antérieurement identifiée de métasomatisme potassique survenu durant l'Hudsonien. Il est possible que l'enrichissement en U et Th ait accompagné l'épisode de l'Hudsonien. Les composition des roches caractérisées par une teneur élevée en Th et des rapports élevés de Th/U pourrait refléter la présence d'éléments radioactifs dans les minéraux lourds détritiques concentrés à l'intérieur de roches supracrustales qui ont été remaniées dans le socle archéen.

[1] Department of Geology, University of Alberta, Edmonton, Alberta, T6G 2E3

INTRODUCTION

In 1986, cores from approximately 230 Alberta wells were examined and sampled at the Core Research Centre of the Alberta Energy Resources Conservation Board, Calgary, Alberta. Unweathered core was available from 189 wells. Twenty-one cores showed marked petrological heterogeneity, so two samples were taken from each of these to provide a more representative analytical average. The following heat generation database and associated map includes the results of analyses of the resulting 210 samples, as well as data from the Basement Rock Project core collection assembled at the University of Alberta in the 1960's. This set includes data from 175 wells, 132 of which are located in Alberta.

The widespread search for uranium in the Canadian Shield from the 1940s to the 1970s provided data for many studies of the regional distribution of U and Th (Fahrig and Eade, 1968; Charbonneau, 1982). Burwash and Cumming (1976) determined the presence of U and Th in the Precambrian underlying the Western Canada Basin; a petrological model was given by Burwash in 1979. Darnley (1982) synthesized the subsurface data with that from the exposed Shield.

Supplementing the data from Burwash and Cumming (1976) with data from the Basement Rock Project (Burwash and Burwash, work in progress) which contains K_2O values for the same samples, Beach (1985) attempted to relate heat generation values in the basement to observed heat flow distributions in the Phanerozoic cover. He concluded that the spacing between the sampled basement wells was too great to permit a valid correlation. The data now presented allow the generation of a more precise trend surface map (Fig. 1).

ANALYTICAL METHODS

Because weathering of the rocks underlying the Paleozoic-Precambrian unconformity in the subsurface of Alberta could have resulted in either the removal or the enrichment of uranium and thorium, weathered samples had to be excluded from the suite assembled for analysis. Thin sections were prepared for all of the 1986 collection, and rocks that were fractured and infilled with carbonate minerals, anhydrite and/or limonite were identified and deleted from the study. Those with abundant clay minerals were also rejected.

Density determinations were made on 100 to 120 g samples of each core by weighing the specimen dry and again in distilled water at 20°C. Samples of density less than 2.60 were scrutinized for possible alteration.

The same samples were subsequently used for the determination of magnetic susceptibility. The apparent magnetic susceptibility (k′) was measured using a 25 mm diameter vial of coarsely crushed rock in a Bison Model 3101A magnetic susceptibility meter. Using the apparent density of the crushed material, k′ was corrected for void spaces. Magnetic susceptibility (k) in emu is given in Table 1.

To avoid Cr and W interference in subsequent analyses, a ceramic mill was used to pulverize aliquots of the coarsely crushed material. These powders were sent to the McMaster Nuclear Reactor and analysed for U, Th and K. U was determined by delayed neutron counting, the method used by Burwash and Cumming (1976). The Th and K analyses were done by instrumental neutron activation analysis (INAA). This method is well suited for elemental concentrations at the trace element level, such as Th. However, for the major element K, the resultant values seemed to be consistently high, above 2 %. As a result, in all samples above this level of concentration, K was calculated using the modal percentages of K-feldspar and micas. In Table 1, U is reported to 0.1 ppm, Th to 1 ppm and K to 1 % by weight.

RADIOACTIVE HEAT PRODUCTION

The data presented in Table 1 permit the calculation of the radiometric heat production (A) for each rock listed, using the formula given by Ryback (1976, formula 4) converted to SI units:

$$A[\mu W/m^3] = 0.1325\, p\, (0.718C_u + 0.193C_{Th} + 0.262C_K)$$

where p is the density of the rock in g/cm^3, C_u and C_{Th} are the concentrations of U and Th in weight ppm and C_K is the concentration of K in weight per cent. For the limited number of samples without density determinations, 2.70 was used for p.

The Basement Rock Project database referred to in the introduction contains data from 132 Alberta samples with U, Th and K analyses included. Radiometric heat production (A) values were calculated for these samples and the two data sets merged to provide the input for the trend surface map (Fig. 1). To partly offset the unequal distribution of wells, an average value of A was calculated for all samples in a given township. The centre of the township was taken as the position for plotting this average.

INTERPRETATION

The heat production map in Figure 1 shows a major east-west trending belt of high heat production across northern Alberta. Minor, parallel belts occur in south-central and southern Alberta, based on more limited well control. There are no data for the deep basin near the Disturbed Belt of southwestern Alberta or from the area within Wood Buffalo National Park. For this preliminary report, well data from the proximal areas of Saskatchewan, Montana, British Columbia and the Northwest Territories were excluded. Also excluded are analyses of outcrop samples along the western edge of the exposed Shield.

The northern Alberta area of high heat flow outlined by the $2\mu W/m^3$ contour corresponds in general to the area of K-metasomatism mapped by multivariate analysis by Burwash and Culbert (1976, Fig. 4b, 11). This is to be anticipated, since K makes a direct contribution to the heat production. More importantly, the petrological processes that concentrate K as a lithophile element of large ionic radius also concentrate U and Th. The mechanisms of K-metasomatism were discussed by Burwash and Krupicka (1970) and Burwash (1978).

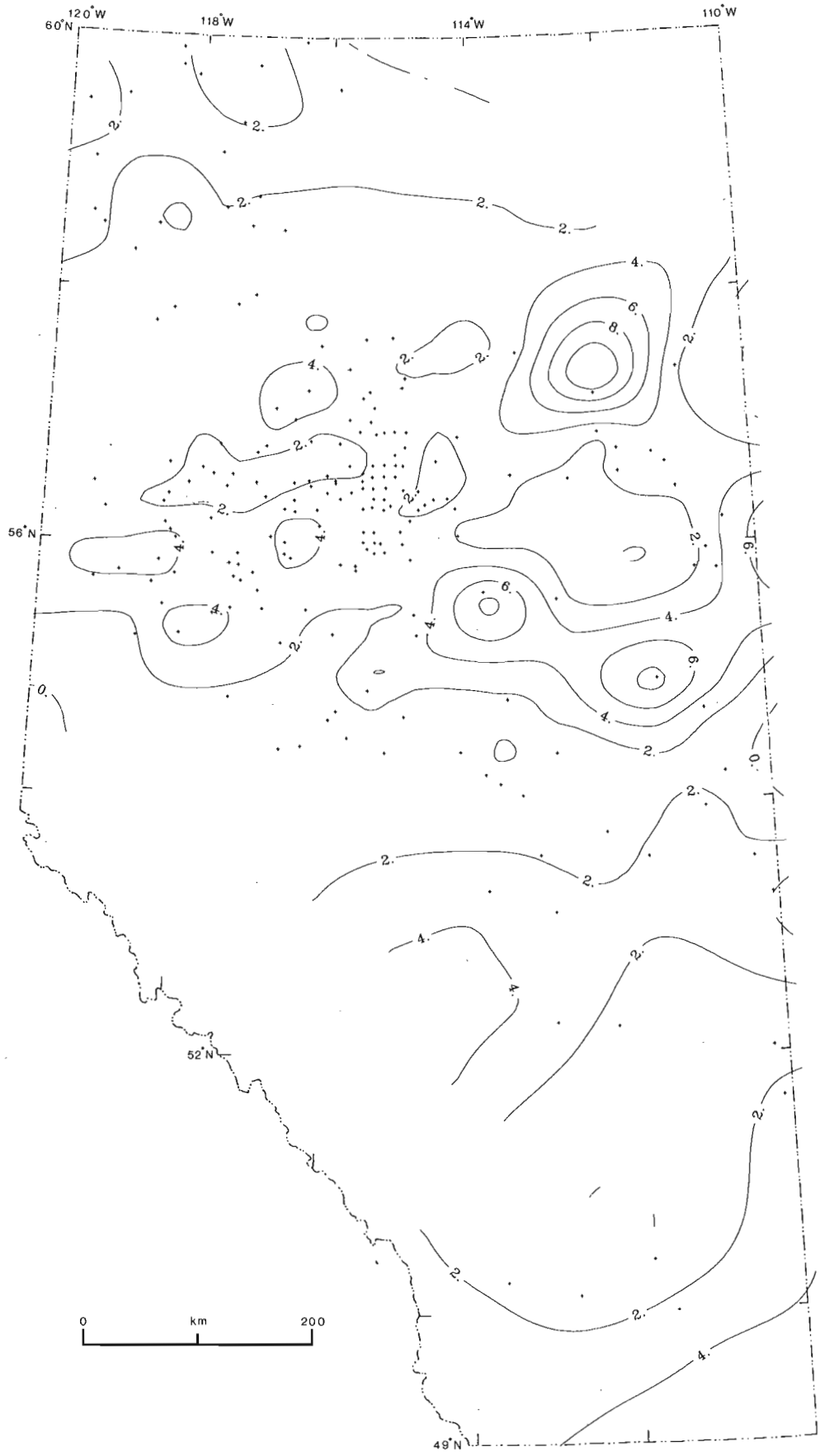

Figure 1. Radioactive heat generation trend surface map for the subsurface Precambrian of Alberta. Values contoured are those of A, heat production, as defined in text and included in Table 1.

Table 1. Alberta Precambrian basement: magnetic, density and heat generation data.

Sample	Location	Depth	Magnetic Susc/emu	Density g/cm3	U ppm	Th ppm	K%	A
1	5-23-80-5W5	692.5	63.1	2.68	0.8	1	2	0.46
2	7-8-83-3W4	575.3	3.7	2.65	1.2	67	3	5.12
3	10-23-87-22W4	197.8	6.1	2.67	1.9	22	3	2.26
4	2-32-89-12W4	711.5	6.3	2.58	3.1	33	4	3.30
5	13-31-96-6W4	869.0	22.9	2 76	2.0	3	6	1.31
6	2-2-80-6W	1765.4	20.2	2·78	2.6	4	2	1.17
7	10-27-80-8W5	1847.5	139.3	2.79	1.7	28	3	2.74
8	6-28-80-9W5	1751.0	36.8	2.61	79.7	110	5	2.76
9	14-30-80-9W5	1688.6	130.3	2.68	1.6	5	2	0 94
10	14-36-80-10W5	1691.3	8.0	2.66	1.1	3	2	0.67
11	12-6-80-16W5	2143.6	3.5	2.61	11.3	39	6	5.96
12	10-18-81-6W5	1762.6	12.7	2.67	4.0	65	2	5.64
13	8-19-81-8W5	1743.0	2.7	2.61	2.2	24	2	2.33
14	13-8-81-9W5	1747.7	3.1	2.62	4.2	6	6	1.99
15	14-11-81-9W5	1749.2	26.8	2 68	1 9	5	1	0.92
16	2-23-81-9W5	1749.0	129.4	2.66	2.2	8	2	1.29
17	10-23-81-9W5	1768.5	5.0	2.54	0.4	1	4	0.51
18	4-25-81-9W5	1733.1	37.3	2.63	1.1	1	3	0.61
19	2-26-81-9W5	1736.1	776.5	2.71	0.7	2	5	0.79
20	4-26-81-9W5	1745.9	266.1	2.67	1.3	15	1	1.45
21	10-26-81-9W5	1749.3	150.0	2.64	2.4	36	3	3.31
22	12-26-81-9W5	1747.1	1116.8	2.86	1.6	30	3	2.93
23a	2-27-81-9W5	1702.6	192.8	2.66	0.3	1	4	0.51
23b	2-27-81-9W5	1705.1	279.0	2.67	0.5	0.5	1	0.26
24	12-27-81-9W5	1766.9	6.3	2.54	1.3	2	4	0.80
25a	10-28-81-9W5	1706.6	105.4	2.68	0.5	0.5	2	0.35
25b	10-28-81-9W5	1707.2	4.6	2.61	0.4	1	1	0.26
26	6-21-81-9W5	1727.3	462.6	2.72	0.4	0.5	1	0.23
27	12-29-81-9W5	1731.3	281.1	2.65	0.3	0.5	1	0.20
28a	16-30-81-9W5	1730.0	478.4	2.96	0.9	0.5	1	0.39
28b	16-30-81-9W5	1732.0	135.9	2.69	0.5	0.5	1	0.26
31	11-35-81-9W5	1739.8	905.2	2.84	3.4	76	3	6.74
32	14-1-81-10W5	1772.0	152.0	2.77	0.7	1	1	0.35
33	5-14-81-10W5	1761.0	41.0	2.58	3.9	69	5	5.96
34a	4-22-81-10W5	1756.9	8.7	2.76	5.9	48	5	5.42
34b	4-22-81-10W5	1756.9	6.9	2.69	6.5	44	5	5.16
35	2-26-81-10W5	1753.2	325.7	2.77	0.8	5	4	0.95
36	2-26-81-10W5	1763.0	918.7	2.77	0.9	5	4	0.97
37a	2-31-81-17W5	2066.9	6.1	2.64	4.4	49	5	4.87
37b	2-31-81-17W5	2066.9	10 8	2.63	3.3	29	6	3.32
38	14-24-82-7W5	1687.0	3.4	2.66	3.5	8	3	1.71
39	4-2-82-9W5	1730.0	62.2	2.53	0.8	2	3	0.59
40	10-4-82-9W5	1724.3	5.6	2.61	2.1	44	2	3.64
41	12-4-82-9W5	1715.1	153.8	2.64	0.4	2	6	0.79
43	3-7-82-9W5	1722.5	12.1	2.70	5.1	39	2	4.19
44	11-7-82-9W5	1700.6	3.1	2.56	1.3	11	4	1.39
45	4-12-82-9W5	1744.0	267.5	2.63	3.3	66	5	5.73
46	13-16-82-9W5	1736.4	4.1	2.57	4.0	120	4	9.23
47	11-17-82-9W5	1745.2	4.1	2.53	1.4	23	6	2.35
50	2-35-82-9W5	1761.5	11.7	2.68	1.7	7	2	1.10
51	8-10-82-10W5	1781.9	353.0	2.77	2.0	14	5	2.00
52a	15-12-82-10W5	723.8	124.5	2.62	1.1	3	6	1.02
52b	15-12-82-10W5	1727.0	435.1	2.69	5.0	70	7	6.75
53	1-28-82-10W5	1743.5	144.7	2.67	1.0	9	5	1.33
54	10-23-83-6W5	1716.9	9.9	2.70	1.5	2	2	0.71
55	8-2-83-14W5	1819.1	6.0	2.68	2.0	40	5	3.72
57	10-31-84-4W5	1660.5	9.9	2.70	1.2	8	1	0.95
58	5-26-84-5W5	1649.4	5.6	2.71	3.2	19	4	2.52
59	4-16-84-8W5	1569.1	11.1	2.65	0.9	3	3	0.71
60	4-16-84-8W5	1564.1	2.7	2.63	22.8	20	4	7.42
61	2-18-84-8W5	1624.0	179.9	2.71	1.5	12	2	1.41
62	10-28-84-8W5	1587.5	4.0	2.62	2.7	21	4	2.29
63	10-28-84-9W5	1538.6	69.5	2.76	1.2	6	4	1.12
64	2-27-84-10W5	1548.0	323.0	2.71	2.0	19	3	2.12
65	16-1-84-14W5	1704.2	258.7	2.71	1.3	12	3	1.45
66	11-15-84-14W5	1728 0	49.5	2.62	4.1	25	6	3.25
67	6-23-84-14W5	1666.5	121.2	2.65	1.2	22	6	2.35
68	8-23-84-14W5	1700.5	55.7	2.66	20.5	67	6	10.30
69	13-20-85-2W5	1621.0	12.3	2.68	2.1	29	1	2.62
70	13-13-85-4W5	1652 2	19.1	2.69	0.3	0.5	1	0.20

Sample	Location	Depth	Magnetic Susc/emu	Density g/cm3	U ppm	Th ppm	K%	A
71	15-9-85-8W5	1581.6	3.6	2.70	2.5	22	6	2.73
72	10-18-85-8W5	1578.5	5.4	2.70	1.6	9	1	1.12
73	10-4-85-9W5	1520.3	210.5	2.81	1.8	7	2	1.18
74	4-9-85-9W5	1561.2	163.4	2.75	4.0	34	2	3.63
75	12-10-85-9W5	1572.2	2.4	2 70	3.4	23	4	2.84
76	10-11-85-9W5	1581.7	3.4	2.51	3.5	20	2	2.30
77	10-19-85-9W5	1493.5	555.0	2.82	11.4	71	5	8.67
78a	10-20-85-9W5	1500.5	3.7	2.67	2.5	36	1	3.19
78b	4-20-85-9W5	1502.7	94.6	2.66	6.9	76	3	7.20
79	7-26-85-9W5	1536 0	2 9	2.65	6.2	42	5	4.87
80	4-30-85-9W5	1531 9	144.0	2.68	5.0	56	1	5.21
81	2-32-85-9W5	1478.3	34.0	2.65	2.3	7	5	1.51
82	10-6-85-12W5	1573.1	9.6	2.61	0.9	6	1	0.72
83	12-28-85-12W5	1537.7	273.6	2.74	1.6	32	1	2.76
84	6-15-85-16W5	1702.8	6.3	2.68	4.7	27	2	3.24
87	6-10-86-5W5	1588.6	122 7	2.71	0.9	1	3	0.59
88	2-17-86-6W5	1552.0	2.9	2.67	1.1	9	2	1.08
89	1-22-86-8W5	1523.1	91.6	2.71	2.0	28	5	2.93
91	11-2-86-10W5	1485.8	816.7	2.83	6.4	59	6	6.59
93	6-11-86-10W5	1491.0	5.1	2.63	1.1	39	5	3.36
94	10-23-86-10W5	1476.8	221.2	2.71	0.6	4	0	0.43
95	3-3-86-11W5	1517.9	46.7	2.72	0 7	6	3	0.88
96a	16-31-86-12W5	1570.2	367.4	2.76	2.2	2	3	1.01
96b	16-31-86-12W5	1571.4	n.d.	2.70	1.3	7	2	1.00
97	3-4-86-13W5	1586.2	51.3	2.67	11.0	7	5	3.74
99	6-24-86-15W5	1582.5	5.4	2.59	6.6	8	6	2.70
100	5-33-86-16W5	1615.0	33.2	2.63	9.7	36	5	5.31
103	6-7-87-7W5	1504.0	5.1	2.63	2.4	13	5	1.93
104	10-7-87-7W5	1514.5	5.6	2.70	2.1	23	4	2.51
105	12-7-87-7W5	1507.5	6.7	2.55	1.3	13	5	1.61
107	4-18-87-7W5	1495.4	6.3	2.73	2.9	49	3	4.46
108	10-18-87-7W5	1513.0	5.7	2.69	2.9	50	5	4.65
110	4-3-87-8W5	1506.9	4.9	2.63	1.6	10	5	1.53
112	12-8-87-8W5	1506.5	4.4	2.65	9.7	10	5	3.58
114	2-16-87-8W5	1490.0	5.4	2.70	8.4	38	4	5.16
115	2-17-87-8W5	1434.1	4.0	2.63	7.7	58	5	6.29
117	2-20-87-8W5	1460.6	3.9	2.64	26.3	48	6	10.40
118	10-21-87-8W5	1467.5	3.7	2.63	4.3	7	3	1.82
119	4-22-87-8W5	1483.5	5.1	2.66	6.9	59	5	6.22
121	1-31-87-8W5	1444.8	9.0	2.60	2.6	25	5	2.76
122	5-31-87-8W5	1431.0	370.2	2.70	1.0	15	3	1.57
123a	12-32-87-8W5	1442.3	4.9	2.71	11.0	61	4	7.44
123b	12-32-87-8W5	1444.8	4.0	2.62	12.0	40	4	6.04
125	8-11-87-9W5	1442.3	6.5	2.60	1.4	28	5	2.66
127	10-35-87-9W5	1422.5	8.0	2.65	0.8	11	4	1.32
128	14-5-87-12W5	1568.5	127.8	2.69	4.7	12	6	2.59
129	8-1-87-13W5	1610.5	6.6	2.61	3.9	17	3	2.38
130	11-12-87-13W5	1627.5	22.5	2.66	0.7	8	4	1.09
131	7-15-87-13W5	1655.5	77.1	2.73	0.7	9	3	1.10
132	2-23-87-13W5	1615.5	315.2	2.68	1.4	5	2	0.89
133	16-1-87-15W5	1620.9	82.9	2.67	2.2	13	5	1.91
134a	13-19-87-21W5	1784.2	116.4	2.80	8.8	10	2	3.26
134b	13-19-87-21W5	1785.0	63.2	2.88	2.8	7	2	1.48
135	16-20-87-23W5	1999.0	3.9	2.62	0.6	2	0	0.28
136	1-31-88-3W5	1599.3	4.7	2.60	0.3	1	4	0.50
138	2-7-88-7W5	1538.3	3.4	2.71	14.2	6	1	4.17
139	12-8-88-7W5	1519.4	3.3	2.63	12.8	29	6	5.70
140	9-19-88-7W5	1489.9	2.3	2.63	25.0	3	7	7.10
141	12-24-88-7W5	1519.1	26.0	2.68	8.0	23	3	3.90
142	10-6-88-8W5	1429.8	3.6	2.64	14.4	29	7	6.22
143a	12-6-88-8W5	1432.0	194.7	2.44	1.3	1	6	0.87
143b	12-6-88-8W5	1432.0	344.3	2.78	0.6	2	2	0.49
144	4-8-88-8W5	1430.0	128.9	2.65	5.4	53	5	5.42
145	12-9-88-8W5	1432.0	2.8	2.62	12.8	68	6	8.30
147a	12-1-88-9W5	1429.5	13.5	2.65	1.0	12	2	1.25
147b	12-1-88-9W5	1431.6	6.2	2.64	1.8	21	3	2.15
149	10-14-88-9W5	1448.1	10.4	2.89	0.6	2	1	0.41
150	14-30-88-9W5	1458.6	82.4	2.68	3.0	37	5	3.77
151	11-12-88-11W5	1536.0	5.6	2.74	2.4	21	4	2.48
152	5-29-88-11W5	1598.0	148.8	2.66	0.8	9	5	1.28

Table 1. (cont.)

Sample	Location	Depth	Magnetic Susc/emu	Density g/cm3	U ppm	Th ppm	K%	A
154	1-32-88-11W5	1605.0	5.5	2.70	0.3	2	4	0.59
155	16-32-88-11W5	1591.3	11.6	3.13	1.6	3	2	0.93
157a	1-8-88-24W5	2097.4	6.8	2.65	0.5	10	4	1.17
157b	1-88-88-24W5	2098.0	4.4	2.78	2.0	7	2	1.22
158	4-4-89-7W5	1521.3	6.0	2.70	3.0	14	1	1.83
159	10-23-89-6W5	1472.8	5.6	2.62	4.1	2	6	1.70
161a	1-10-89-10W5	1461.0	5.9	2.68	0.7	5	1	0.61
161b	1-10-89-10W5	1461.0	5.1	2.65	0.6	8	1	0.79
162	3-11-89-10W5	1461.0	10.7	2.67	8.2	8	2	2.81
163	10-9-90-6W5	1487.0	4.2	2.64	4.7	21	6	3.15
165	15-10-90-12W5	1729.8	60.6	2.70	0.8	1	1	0.37
166	6-12-90-12W5	1692.5	25.9	2.59	2.1	17	0	1.64
168	4-7-90-18W5	1771.8	201.1	2.70	10.6	25	6	5.01
169a	8-11-90-23W5	1794.0	3.2	2.52	4.9	19	5	2.84
169b	8-11-90-23W5	1796.0	3.6	2.62	0.7	5	4	1.86
170	10-6-91-1W5	1309.4	2.2	2.59	4.9	25	4	3.22
171	2-17-91-6W5	1437.1	153.2	2.84	1.6	5	2	0.99
172	2-26-91-7W5	1344.5	108.9	2.70	1.0	5	5	1.07
173	4-34-91-7W5	1385.9	5.6	2.70	3.1	12	4	2.00
174	6-35-91-7W5	1352.6	3.7	2.63	23.8	21	6	7.92
175	4-8-91-8W5	1379.8	99.5	2.67	22.8	100	5	13.09
176	12-18-91-10W5	1406.0	5.6	2.70	0.7	1	7	0.90
177	2-13-91-9W5	1407.6	8.5	2.69	1.0	45	7	4.01
178a	12-3-91-10W5	1485.7	5.3	2.62	13.4	47	6	7.04
178b	12-3-91-10W5	1486.5	4.6	2.62	16.2	70	6	9.28
179	11-4-91-10W5	1484.3	2.9	2.62	23.4	64	6	10.67
180	12-25-91-10W5	1447.8	6.0	2.61	2.3	14	2	1.69
181	10-16-92-9W5	1402.7	17.8	2.75	1.1	54	2	4.28
182	16-21-92-11W5	1663.6	5.5	2.72	1.6	13	2	1.51
183a	12-23-92-16W5	1792.5	127.6	2.64	1.8	23	9	2.83
183b	12-23-92-16W5	1794.9	64.1	2.64	1.0	8	5	1.25
185	2-26-93-9W5	1467.3	8.4	2.79	3.2	19	0	2.20
186	2-23-94-10W5	1463.0	6.3	2.63	3.9	4	1	1.34
187	14-20-95-6W5	1244.8	279.3	2.73	2.8	19	1	2.15
188	12-4-95-9W5	1455.7	83.4	2.78	0.7	12	2	1.23
189	10-12-95-15W5	1649.3	4.2	2.62	16.0	46	6	7.62
190	15-16-96-6W5	1189.0	6.1	2.68	2.4	21	2	2.24
191	11-3-97-11W5	1754.1	4.3	2.61	3.3	13	4	2.05
193	4-31-99-9W5	1525.5	5.0	2.64	2.9	28	5	3.08
194a	4-3-100-7W5	1217.7	5.8	2.75	4.5	15	2	2.43
196	10-27-102-21W5	1666.7	316.2	2.75	4.4	14	3	2.42
197a	10-29-103-19W5	1595.9	4.7	2.63	4.9	30	3	3.52
197b	10-29-103-19W5	1597.2	3.2	2.66	5.0	20	2	2.81
198	6-23-112-19W5	1458.5	5.2	2.74	1.1	7	1	0.87
200	3-12-121-22W5	1087.8	8.9	2.75	1.1	5	2	0.83
204	10-23-86-9W6	2289.4	n.d.	2.70	2.1	26	5	2.81
207	15-34-109-4W6	1946.5	4.1	2.66	7.4	43	5	5.26
208a	6-33-110-10W6	2108.9	5.5	2.69	2.0	5	2	1.04
208b	6-33-110-10W6	2110.1	4.0	2.65	4.0	10	5	2.15
211	14-16-121-7W6	1902.6	8.8	2.66	1.5	9	2	1.18
212	11-15-123-1W6	1808.4	2.9	2.63	7.5	15	4	3.25
213	12-14-12-12W4	2127.2	4.2	2.65	5.4	20	4	3.04
214	10-15-38-21W4	2557.0	3.4	2.72	0.5	8	1	0.78
215b	10-15-38-21W4	2870.0	3.0	2.71	6.3	18	4	3.25
216	10-15-49-1W4	1782.2	158.6	2.70	5.4	45	1	4.59
217	10-10-66-6W4	1356.5	29.8	2.91	3.2	19	3	2.61
219	5-34-78-6W4	873.3	5.7	2.63	0.3	4	5	0.80
220a	6-11-63-16W5	3477.5	5.0	2.67	3.5	16	2	2.17
220b	6-11-63-16W5	3478.4	4.1	2.62	1.6	15	6	1.95
222	10-8-73-5W5	1917.8	3.8	2.69	4.7	26	7	3.65
223a	16-35-74-24W5	2748.0	5.2	2.63	4.4	29	6	3.60
223b	16-35-74-24W5	2753.0	8.0	2.76	6.2	46	2	5.07
224a	10-1-79-11W5	1826.0	33.1	2.70	3.8	22	4	2.87
224b	10-1-79-11W5	1826.5	4.9	2.66	10.1	25	4	4.63
225	14-13-79-11W5	1808.4	157.5	2.67	11.5	61	5	7.55
226	14-22-79-12W5	1870.0	10.3	2.73	1.9	10	2	1.38
227	8-16-79-21W5	2428.0	39.4	2.65	3.4	25	3	2.83
228	1-21-80-17W5	2127.5	4.4	2.63	2.6	21	5	2.52
230	6-26-79-3W6	2510.3	190.5	2.64	1.4	99	5	7.50

Jones and Majorowicz (1987) reported a mean value of A of 4.3 $\mu W/m^3$ for the Peace River Arch area of northern Alberta using 199 samples from 47 wells. Combining these data with those of Burwash and Cumming (1976), they derived a mean value for the Western Canadian Basin of 2.06 $\mu W/m^3$. Jessop and Lewis (1978) gave a value of 1.2 $\mu W/m^3$ for the Superior Province, more typical of stable cratonic areas.

Examination of the U and Th values in Table 1 shows many rocks in which the Th/U ratio is much above the crustal average of 4. These rocks high in Th make a major contribution to the regional heat generation. Gneissic rocks with similar petrological characteristics were described by Burwash and Cape (1981) from the Pilot Lake area on the eastern edge of the Fort Smith radiometric high. Reworking of Archean heavy detrital minerals in beach placers is the inferred mechanism of Th concentration. The supracrustal rocks were later deformed and metamorphosed with the underlying basement.

The trend surface map of Figure 1 indicates an east-west zone of high heat flow more than 200 km wide across northern Alberta. This zone lies within the Athabasca polymetamorphic terrane (Burwash et al., in press). The final emplacement of the U, Th and K is almost certainly Hudsonian and the probable age of the protolith is Archean.

ACKNOWLEDGMENTS

Thanks are due to A.J. LaRiviere for his technical and computing assistance in compiling the trend surface map and H.A.K. Charlesworth for the use of his computing facilities. M.A. Power prepared samples and did density determinations. McMaster Nuclear Reactor and Nuclear Activation Services Ltd. provided efficient service, as did the Core Research Centre of the Alberta Energy Resources Conservation Board, Calgary. The work was supported by EMR Research Agreements 44/03/86 and 13/03/87.

REFERENCES

Beach, R.D.W.
1985: Sedimentary heat flow in $\Delta Q=0$ region of Alberta; Unpublished M.Sc. thesis, Department of Physics, University of Alberta, Edmonton.

Burwash, R.A.
1978: Metamorphism of the Athabasca Mobile Belt, a subsurface extension of the Churchill Province; in Metamorphism of the Canadian Shield, Geological Survey of Canada, Paper 78-10, p. 123-127.

Burwash, R.A.
1979: Uranium and thorium in the Precambrian basement of western Canada, II. Petrologic and tectonic controls; Canadian Journal of Earth Sciences, v. 16, p. 472-483.

Burwash, R.W. and Cape, D.F.
1981: Petrology of the Fort Smith-Great Slave Lake radiometric high near Pilot Lake, N.W.T.; Canadian Journal of Earth Sciences, v. 18, p. 842-851.

Burwash, R.A. and Culbert, R.R.
1976: Multivariate geochemical and mineral patterns in the Precambrian basement of western Canada; Canadian Journal of Earth Sciences, v. 13, no. 1, p. 1-18.

Burwash, R.A. and Cumming, G.L.
1976: Uranium and thorium in the Precambrian basement in western Canada, I. Abundance and distribution; Canadian Journal of Earth Sciences, v. 13, p. 284-293.

Burwash, R.A., Green, A.G., Jessop, A.M., and Kanasewich, E.R.
in press: Geophysical and petrological characteristics of the basement rocks of the Western Canada Basin; in Continental Platforms and Basins of Canada, J.D. Aitken and D.F. Stott (eds.) Geological Survey of Canada, The Geology of Canada, no. 6 (also Geological Society of America, The Geology of North America, v. D-1).

Burwash, R.A. and Krupicka, J.
1970: Cratonic reactivation in the Precambrian basement of western Canada. Part II. Metasomatism and isostasy; Canadian Journal of Earth Sciences,v. 7, p. 1275-1294.

Charbonneau, B.W.
1982: Radiometric study of three radioactive granites in the Canadian Shield: Elliot Lake, Ontario; Fort Smith, and Fury and Hecla, N.W.T.; in Uranium in Granites, Y.T. Maurice (ed.); Geological Survey of Canada, Paper 81-23, p. 91-99.

Darnley, A.G.
1982: "Hot" granites: some general remarks; in Uranium in Granites, Y.T. Maurice, (ed.); Geological Survey of Canada, Paper 81-23, p. 1-10.

Fahrig, W.G. and Eade, K.E.
1968: The chemical evolution of the Canadian Shield; Canadian Journal of Earth Sciences, v. 5, p. 1247-1252.

Jessop, A.M. and Lewis, T.J.
1978: Heat flow and heat generation in the Superior Province of the Canadian Shield; Tectonophysics, v. 50, p. 55-77.

Jones, F.W. and Majorowicz, J.A.
1987: Regional trends in radiogenic heat generation in the Precambrian basement of the Western Canada Basin; Geophysical Research Letters, v. 14, no. 3, p. 268-271.

Rybach, L.
1976: Radioactive heat production; a physical property determined by the chemistry of rocks; in The Physics and Chemistry of Minerals and Rocks, R.G.H. Strens, (ed.); John Wiley and Sons, London, New York, Sydney and Toronto, p. 309-318.

Bitumen in a Lower Proterozoic dolomite hosting Pb-Zn-Cu occurrences, Artillery Lake, Northwest Territories

Fariborz Goodarzi, Sunil S. Gandhi[1], and Lloyd R. Snowdon
Institute of Sedimentary and Petroleum Geology, Calgary

Goodarzi, F., Gandhi, S.S., and Snowdon, L.R. Bitumen in a Lower Proterozoic dolomite hosting Pb-Zn-Cu occurrences, Artillery Lake, Northwest Territories; in Current Research, Part C, Geological Survey of Canada, Paper 89-1C, p. 369-376, 1989.

Abstract

The dolomitic Artillery Lake Formation, of Early Proterozoic age, contains bitumen in quartz veins and aggregates that carry variable amounts of pyrite, galena, sphalerite and chalcopyrite. These bitumens, which were examined using reflected light microscopy, are classified as meso- to cata-impsonite, equivalent to lower greenschist metamorphic facies. The bitumens originated from the thinly laminated, algal dolomitic beds of the Artillery Lake Formation, and were redistributed during burial, deformation, and the hydrothermal events that formed the base metal concentrations. Samples from the area northeast of Crystal Island show evidence of rapid heating (vacuoles, anisotropy, cenospheres).

Résumé

La formation dolomitique d'Artillery Lake datant du Protérozoïque inférieur contient du bitume dans des filons de quartz et des agrégats susceptibles de renfermer des quantités variables de pyrite, de galène, de sphalérite et de chalcopyrite. Ces bitumes, que l'on a examinés avec un microscope à lumière réfléchie, sont classés entre des méso-impsonites et des cata-impsonites, équivalents métamorphiques de minéraux appartenant au faciès inférieur des schistes verts. Ces bitumes provenaient des couches dolomitiques algaires finement rubanées de la formation d'Artillery Lake, et ont été redistribués durant l'enfouissement et la déformation des sédiments, et les épisodes hydrothermaux qui ont permis l'accumulation de concentrations en métaux communs. Les échantillons provenant de la région située au nord-est de l'île Crystal présentent des indices d'un réchauffement rapide (vacuoles, anisotropie et cénosphères).

[1] Mineral Resources Division, Geological Survey of Canada, 601 Booth Street, Ottawa, Ontario K1A 0E8

INTRODUCTION

Natural bitumen is a good indicator of thermal events because its physical (optical properties and density) and chemical (solubility, atomic H/C ratio, etc.) properties are affected by temperature, rate of heating, pressure, and length of time of exposure to a certain temperature. A genetic classification of bitumen according to Jacob (1975) is shown in Figure 1. The irreversible molecular changes in natural bitumen occur mostly in response to increased temperatures, such as in the case of coal macerals (Goodarzi and Murchison, 1978; Goodarzi, 1984, 1985).

Bitumen is commonly found in association with a variety of mineral deposits, and shows a wide range of characteristics. For example, Macqueen and Powell (1983) found bitumen in association with the Pine Point Zn-Pb deposits to be in a thermal range equivalent to gilsonite-impsonite, indicating that it formed below 100°C. Thus, the study of the bitumen associated with mineral deposits helps in understanding the geological history of the deposits and their host rocks. The present study examines bitumen found in a Lower Proterozoic dolomite unit at Artillery Lake. The dolomite unit hosts a number of vein-type Pb-Zn-Cu occurrences (Fig. 2). These were discovered recently during fieldwork in conjunction with a mineral resource assessment of a proposed national park in the East Arm of Great Slave Lake and Artillery Lake region (Gandhi 1984,1985; Roscoe et al., 1987).

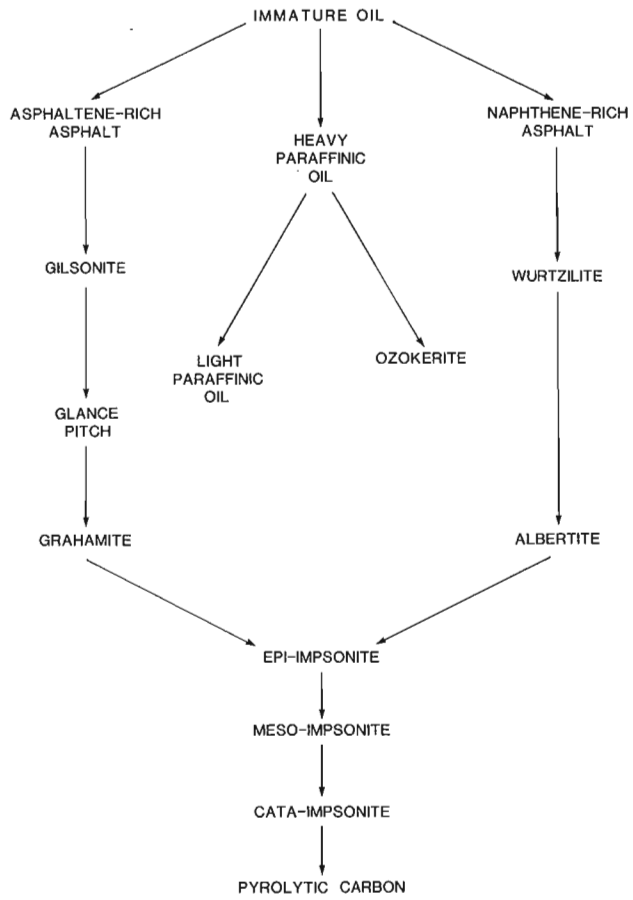

Figure 1. Genetic classification of natural bitumen (after Jacob, 1975).

GENERAL GEOLOGY

Folded dolomite beds of the Lower Proterozoic Artillery Lake Formation, deposited on crystalline Archean basement, are preserved in a 50 x 10 km area of Artillery Lake (Fig. 2). The presence of some of the dolomite outcrops in the area was noted during early reconnaissance mapping by Wright (1952, 1957, 1967) and Folinsbee (1952). More detailed mapping of the area, carried out recently by Gandhi (1984, 1985), demonstrated a much greater areal extent of the dolomite and associated sandy and shaly beds than was known previously (Fig. 2), and revealed the general structure and stratigraphy of the formation (Fig. 3, 4). The mapping also showed the presence of pyrobitumen in association with pyrite and chert in stratiform lenses, and with numerous quartz-carbonate veins carrying galena, sphalerite, chalcopyrite and pyrite (Gandhi, 1984, 1985).

The veins carrying base metal sulphides are found, at a few localities, to be transgressive across minor folds in the Artillery Lake Formation; hence the veins post- date at least some of the deformation (Gandhi, 1985). Lead isotopic data on 15 galena samples from the veins in the Artillery Lake area are consistent with a date of lead mixing in the range of 1.89 to 1.99 Ga, given an initial radiogenic lead source date in the range of 2.67 to 2.59 Ga (Roscoe, 1984; Roscoe et al., 1987). Pegmatitic phases of the granite, which predominates in the basement, have yielded K-Ar dates of 2500 and 2540 Ma (Fig. 2; Gandhi, 1984).

Diabase dykes of the north-northwest trending Mackenzie swarm, approximately 1200 Ma old, cut the folded Artillery Lake Formation. Field observations show that the metamorphic effects of the dykes on the formation are restricted to a few centimetres from the contact (Gandhi, 1984, 1985).

Artillery Lake Formation

The basal unconformity and up to 10 m of basal beds of the formation are exposed along the northwest shore of the lake. Progressively greater thicknesses are preserved toward the southeast and south. A 300 m thick section, exposed on the south shore of Artillery Lake east of Crystal Island (63°03.5'N, 107°52'W), where the beds are nearly vertical, provides a type section and the basis of a generalized lithostratigraphy of the formation as shown in Figure 4.

Lithology

Massive and thick to thin bedded, yellowish brown weathering dolomite is the major rock type in outcrops of the Artillery Lake Formation. The dolomite contains numerous cherty lenses and chert-filled polygonal mud cracks. It includes beds and lenses of grit and quartz pebble conglomerate, cemented by dolomite. The largest of these lenses is found near the top of the formation in the type section, and is 15 m thick and over 50 m in strike length. It contains tightly packed pebbles and large quartz grains with rare dolomite fragments. Stromatolitic beds occur at many places in the southwestern exposures of the Artillery Lake Formation. The most common variety of stromatolite is columnar, up to a few centimetres in diameter and 2 m in

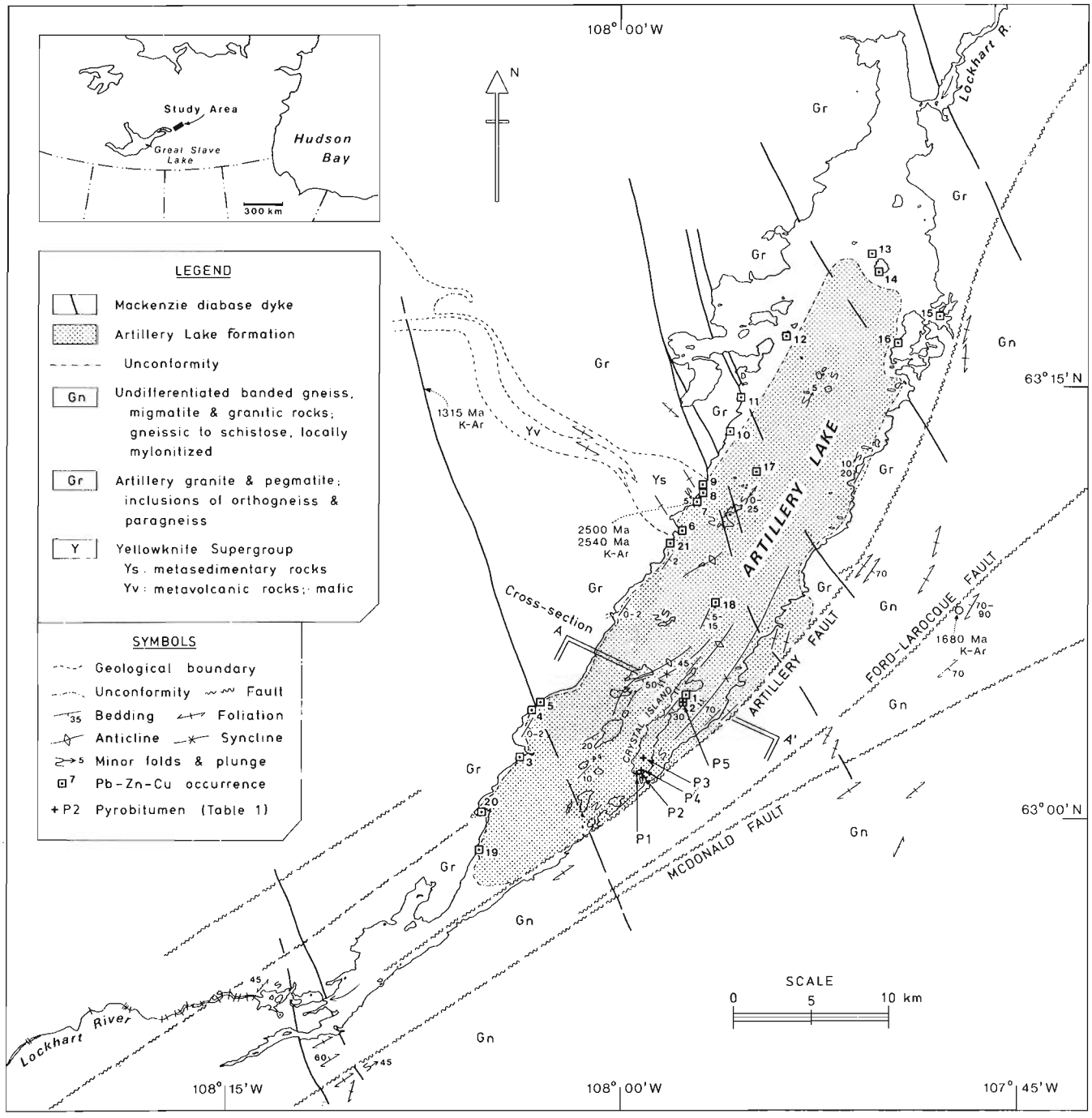

Figure 2. Simplified geological map of the Artillery Lake area, showing location of the bitumen samples (P1 to P5) described in this study (Figs. 6-10).

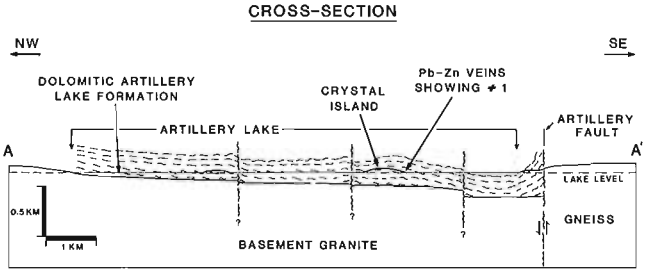

Figure 3. A generalized cross-section (A-A', Figure 2) of the Artillery Lake Formation.

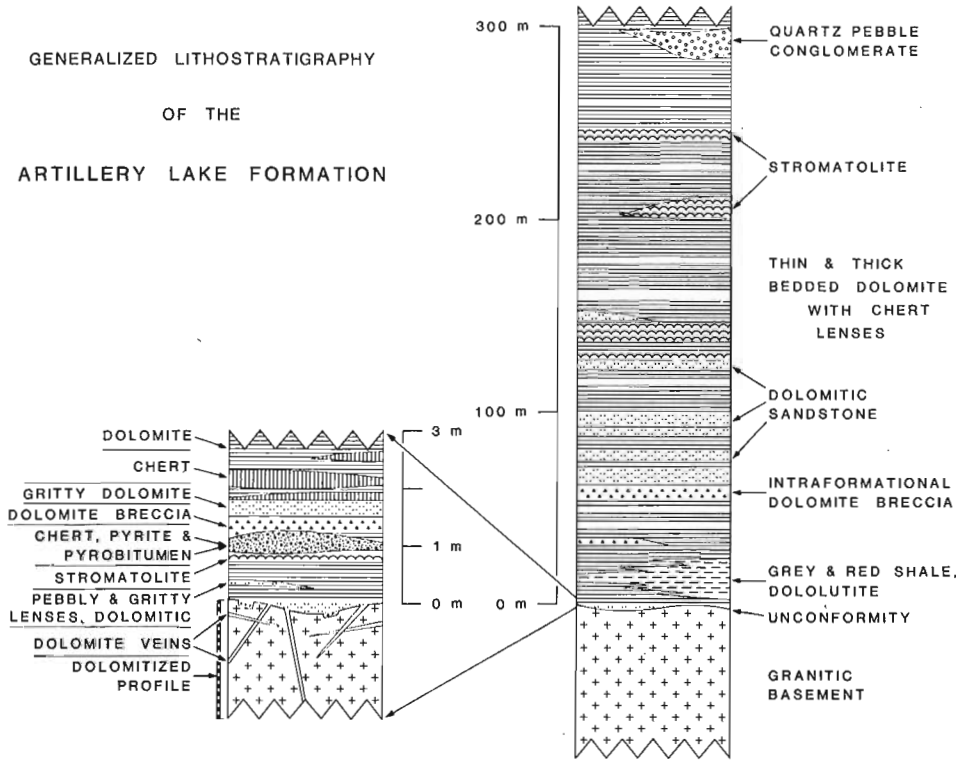

Figure 4. Generalized lithostratigraphy of the Artillery Lake Formation.

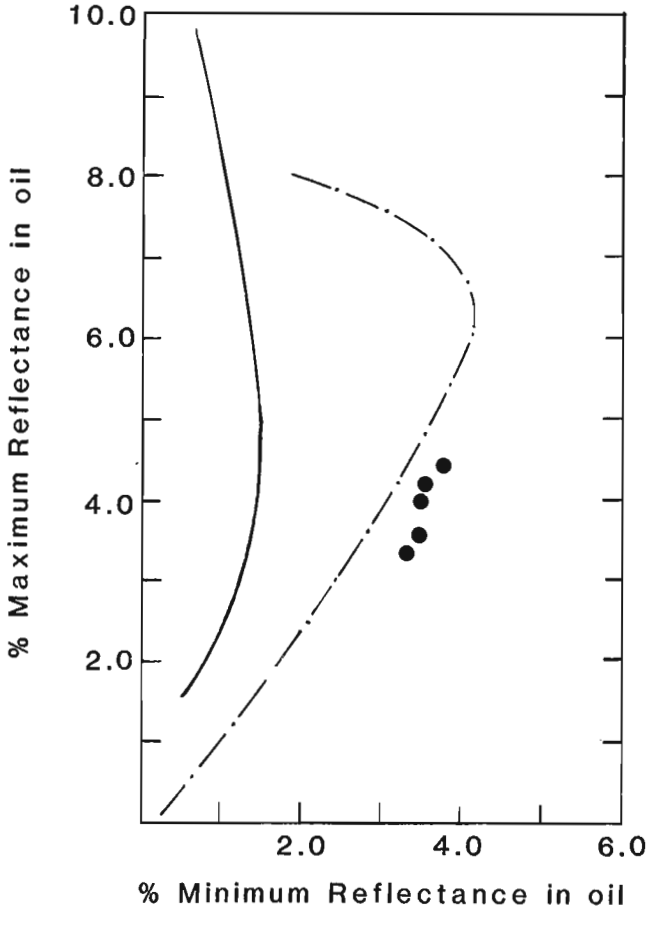

Figure 5. Maximum versus minimum reflectance curve for bitumen and heat affected bitumen (after Goodarzi and Norford, 1985). Data derived from present study (Table 1). Dashed line represents bitumen; solid line represents heat affected bitumen; solid circles represent samples analyzed in this study.

height. Laterally linked, small, domal structures, up to 0.5 m long, and some flat laminated dolomitic beds are probably of biological origin. Intraclast dolomite beds and lenses, up to a few metres in thickness, occur at several locations. Grey to dark grey argillaceous sediments are found in some of the gritty lenses and are predominant in a 20 m thick section exposed for a 1.5 km strike length along the southeast shore of Artillery Lake at longitude 107°47' W. This part of the formation comprises interbedded grey and red-maroon shales, dolomite and argillaceous dolomite. Along the northwest shore of Artillery Lake, the basal beds include numerous lenses of chert, quartz-pyrite-pyrobitumen, and grit and pebbles cemented by dolomite. The lenses are up to 50 cm thick and several tens of metres in length. A few small, pyritic lenses occur at stratigraphically higher levels.

These features and the lithological characterstics of the Artillery Lake Formation indicate that it was deposited in intertidal to supratidal environments, generally in a warm, dry climate. The presence of stromatolites, laminated algal dolomitic beds, dark grey shales and pyrobitumen indicates considerable biological activity during sedimentation.

BITUMEN

Mode of occurrence

There are two modes of occurrence of bitumen — in stratabound pyrite-quartz lenses, and in quartz-carbonate veins either barren of sulphides, or carrying galena, sphalerite, chalcopyrite and pyrite. The bitumen forms vitreous, black, flinty globules and irregular aggregates, up to a few centimetres long.

The stratabound pyritic lenses are up to 0.5 m thick and several tens of metres in length, and commonly occur near

Table 1. Characteristics of bitumens from the Lower Proterozoic Artillery Lake Formation, Northwest Territories, Canada.

Sample*	% Reflectance oil	Optical characteristic	Morphology	Type of bitumen
P1	3.46	weakly anisotropic	angular to melted fragments (Fig. 6a-b)	meso-impsonite
P2	3.66	weakly anisotropic	development of some cracks (Fig. 7)	cata-impsonite
P3	4.15	weakly anisotropic	thermally altered, vesiculated (Fig. 8)	cata-impsonite
P4	4.27	moderately anisotropic	thermally altered, softened and plastically deformed, appearance of cenosphere (Fig. 9a-c)	cata-impsonite
P5	4.53	moderately anisotropic	thermally altered, pyrolytic carbon enclosing some bitumen particles (Fig. 10a-b)	cata-impsonite

* Sample location on Figure 2.

Sample descriptions

P1: GFA-'83-457: vein-like elongate aggregate of quartz, ranging from fine grained to coarse, forming circular crystals; pyrobitumen occurs as irregular patches up to 2 cm long; pyrite present as scattered small grains.

P2: GFA-'83-509: finely laminated, buff white, dolomitic rock with a siliceous layer - 1 cm thick, containing quartz-pyrobitumen lensoid aggregates up to 2 cm long and 0.5 cm wide, subparallel to laminae; lamination in dolomite enhanced by very thin, cherty laminae, fraction of a mm thick.

P3: GFA-'83-462: a locally derived pebble containing quartz, coarse sphalerite and a lensoid pyrobitumen aggregate 2 cm long; location approximate.

P4: GFA-'83-460: thinly bedded dolomite-siliceous dolomite, light grey, buff and reddish coloured, with one 5 cm thick bed or zone of irregular aggregates of fine to medium grained quartz and dolomite containing globular to stringy patches of pyrobitumen and traces of pyrite.

P5: GFA-'83-514: quartz-dolomite-pyrite-pyrobitumen aggregate in brecciated dolomite; pyrite spherulitic, up to 1 cm long radiating circular crystals; pyrobitumen patches up to 4 cm long; quartz crystals up to 0.5 cm long; the aggregate predates the galena-rich, quartz-carbonate veins of Showing A-2 (Roscoe et al., 1987, p. 76-77).

the base of the Artillery Lake Formation. They contain chert and crystalline quartz with aggregates of massive coarse pyrite and bitumen. Pyrite is, in some places, spherulitic with radiating crystals 1 to 2 cm long. Some of the lenses are interlayered with small colonies of columnar stromatolites, a few centimetres high and a few millimetres in diameter.

Quartz veins, aggregates and geodes are common throughout the Artillery Lake Formation. They are generally barren, but some of them contain pyrobitumen, particularly those in the Crystal Island region (Fig. 2).

Bitumen is seen in a few of the galena-sphalerite-chalcopyrite-pyrite-bearing quartz-calcite veins or clusters of veinlets mentioned above; for example, the southwesternmost showing (Fig. 2; Gandhi, 1985). It appears, however, that some of the quartz-bitumen veins that lack sulphides may be gradational to or belong to the same set of veins that carry the sulphides. The sulphide-bearing veins postdate minor folds. They cut some of the barren quartz veins, and in turn are cut by other barren quartz veins.

Experimental

A selected suite of five, bitumen-rich samples from Crystal Island and its vicinity (Fig. 2), was examined under a reflected light microscope. Fifty maximum and minimum reflectance measurements were made on each sample (Table 1). The microscope used was a Zeiss MPM II fitted with a Zonax microcomputer and printer. Photomicrographs were taken using an oil objective (N.A. 0.90 x 40) under both plane polarized light and crossed polars (Fig. 6-10).

Reflectance and texture

The per cent reflectance in oil of the present suite of bitumen samples increases from meso- to cata-impsonite, indicating variation in the maturity of bitumen in the study area. They are characterized by insolubility in immersion oil and high reflectance values typical of the meso to cata impsonite (Table 1). A plot of maximum versus minimum oil reflectance for these samples (Fig. 5), provides a comparison with trends observed previously for other bitumens (Khavari-Khorasani, 1975; Jacob, 1975, 1983; Creaney et al., 1980;

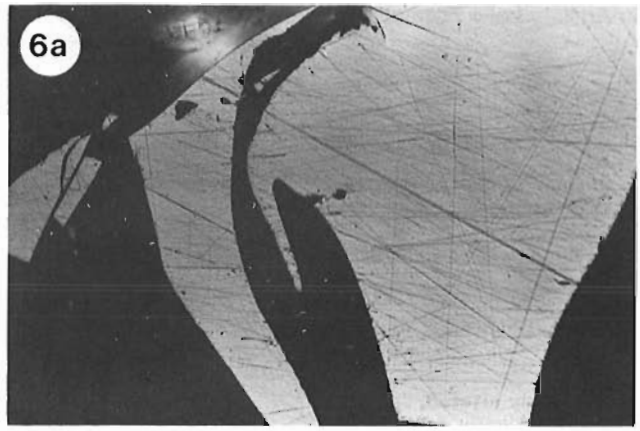

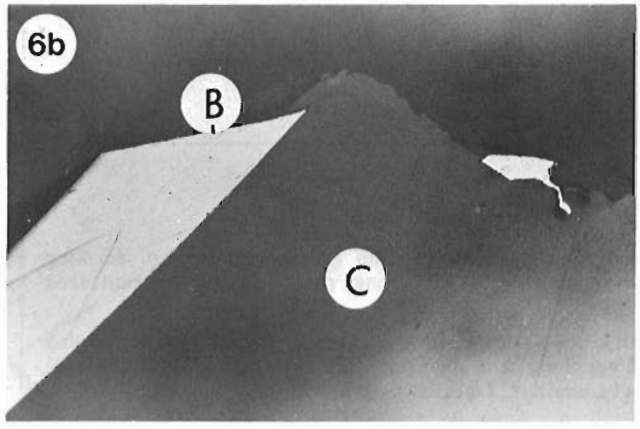

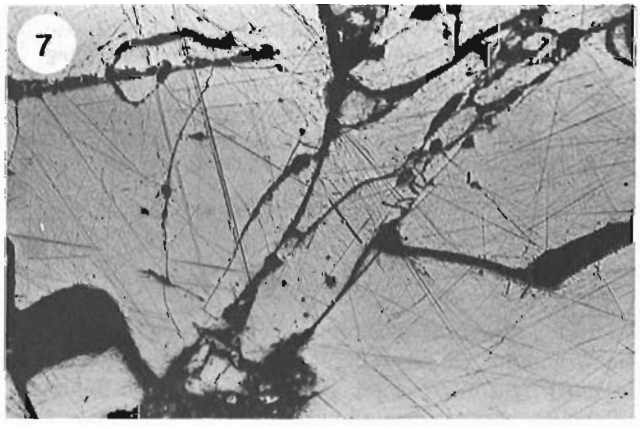

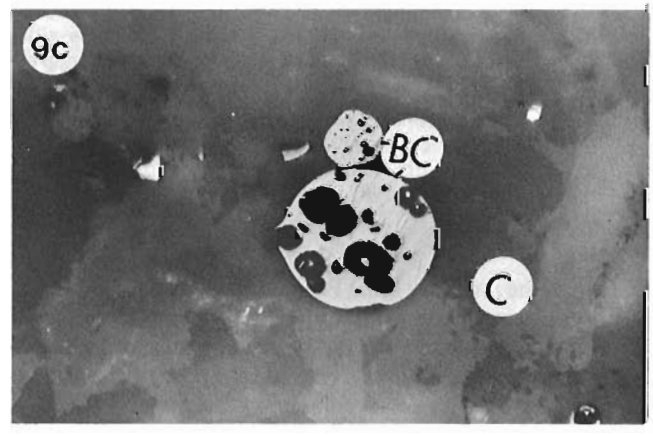

Figures 6-10. Morphology of bitumens from Artillery Lake area (reflected light, plane polarized, oil immersion). Magnification: long axis of photographs = 240 nm.

Figure 6. Sample P1: **a.** Soft, melted bitumen fragments. **b.** Homogeneous bitumen (B) fragments near boundary of the carbonate (C).

Figure 7. Sample P2: Soft bitumen fragments.

Figure 8. Sample P3: Bitumen showing fine, devolatilization vacuoles.

Figure 9. Sample P4: **a.** Hard, melted cracked, devolatilised bitumen fragments. Plane polarized light. **b.** Partially crossed polars; showing strong basic anisotropy. **c.** Bitumen cenospheres (BC) formed along the boundary of the carbonate grains (C).

Williams and Goodarzi, 1981; Goodarzi and Williams, 1986), and for heat affected bitumen (Bodganova et al., 1977; Khavari-Khorasani and Murchison, 1978). It shows that the bitumens from Artillery Lake follow a path somewhat different from that of bitumens in the normal maturation track and much removed from that of heat affected organic materials (Fig. 5).

The morphology of the bitumens also shows progressive changes. Thus the bitumens from the south end of Crystal Island are angular (Fig. 6), but the ones to the northeast of them show a progressive development of vacuoles and cenospheres (Fig. 7). The presence of fine vacuolation indicates that some degree of devolatilization has taken place (Fig. 8). These bitumens must have become plastic to develop devolatilization vacuoles, basic anisotropy (Fig. 9a- b) and cenospheres (Fig. 9c). The occurrence of cenospheres is a unique feature, which has not been observed in other thermally metamorphosed bitumen deposits such as those in Siberia (Bodganova et al., 1977), Derbyshire (Khavari-Khorasani and Murchison, 1978), and California (Jacob, 1983). The experimental results of Goodarzi and Murchison (1978) indicate that low rank vitrinite develops cenospheres at a rate of heating of 60°C/min. The same vitrinite remains almost unchanged at a slower rate of 10°C/min. It is suggested that vitrinite and bitumen respond in the same manner during heat treatment (Khavari-Khorasani, 1975). By analogy, the cenospheres in Artillery Lake bitumen may have developed due to a rapid heating event.

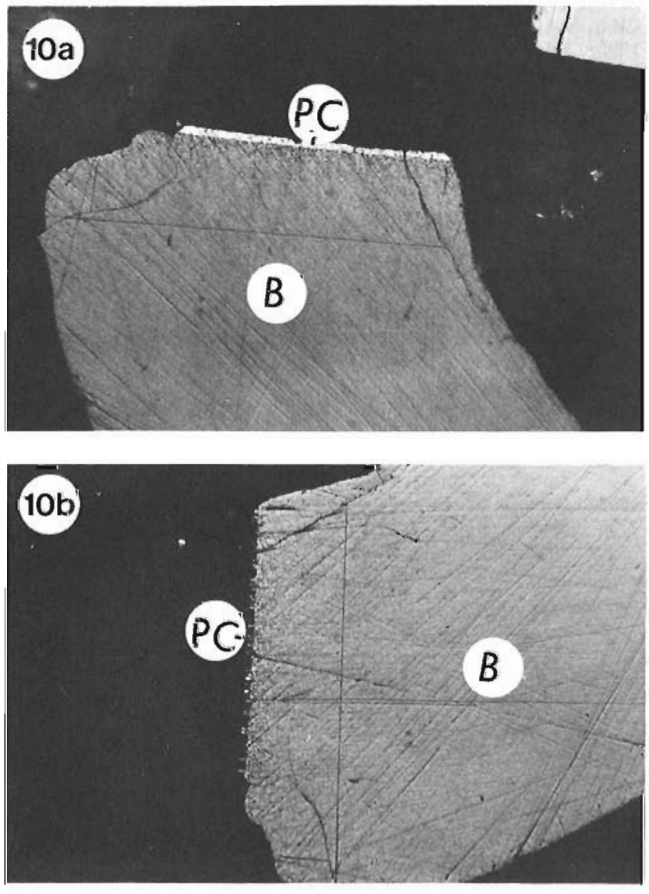

Figure 10. Sample P5:
a. Strongly anisotropic pyrolytic carbon (PC) forming a layer on the bitumen (B). Partially crossed polars.
b. Stage of microscope partially rotated to enhance the strong anisotropy of pyrolytic carbon (PC).

Four of the bitumen samples (nos. P1-P4, Fig. 6-9) show homogeneous morphology (Table 1). In contrast, sample no. P5, taken from exposures to the northeast (Fig. 10a-b), which has the quartz-spherulitic pyrite-bitumen association, shows granular anisotropy, fine grained mosaic texture (Fig.10a-b), and a bireflectance value of 0.58, indicative of relatively higher thermal alteration. Elemental analyses of bitumen in this sample yielded a H/C atomic ratio of 0.20, which also suggests a high thermal alteration (Gandhi, 1984). Some bitumen fragments in this sample (Fig. 10a-b) are coated with highly anisotropic pyrolytic carbon, having a thickness of only a few microns.

Estimation of temperature of formation of bitumen

Fluid inclusion homogenization temperatures of between 192°C and 202°C were obtained on primary gas-liquid inclusions in quartz associated with pyrite-bitumen aggregate in sample no. 5 (3 determinations by S.S. Gandhi). This temperature indicates that the temperature of deposition of the quartz, which is paragenetically older than the pyrite and the bitumen, does not reflect the highest temperature to which the bitumen was subjected. A homogenization temperature close to 170°C was similarly found for primary inclusions in quartz associated with very coarse sphalerite, minor amounts of pyrite and traces of galena, in a vein located 325 m northeast of sample no. 5 (Gandhi, 1984, 1985). It is most likely that the mineralization event at Artillery Lake is related to the event or events that formed the bitumens. It is apparent from the data that these thermal effects were not uniform throughout the basin. There are, however, many uncertainties regarding the timing of the hydrothermal mineralization and of the thermal treatment of the bitumens.

Origin of bitumen

Most liquid hydrocarbons are generated by thermal cracking of carbon-carbon bonds in lipid-rich algae under favorable depth and burial conditions (e.g., Tissot and Welte, 1984). Liquid bitumen changes to solid bitumen and gas with further maturation (e.g., Brooks, 1981). The source of the Artillery Lake bitumen was most likely the thinly laminated, algal dolomitic beds in the Artillery Lake Formation. Well developed stromatolites in the Crystal Island region are further evidence of biogenic activity during the time of deposition. In addition, there are grey, carbonaceous shales present in the formation. In any case, there is no other plausible source of the hydrocarbon in the area, as the basement is crystalline, and the only preserved rocks younger than the Artillery Lake Formation are the diabase dykes.

The preserved area of the Artillery Lake Formation is small for a platform carbonate sequence. Extensive carbonate sequences of Early Proterozoic age, however, are known elsewhere in the northwestern Canadian Shield, and at least one of them is correlatable with the Artillery Lake

Formation, namely, the Union Island Group in the East Arm of Great Slave Lake, approximately 200 km to the southwest, which also hosts occurrences of bitumen, copper and zinc (Roscoe et al., 1987, p. 10 and 24). The presence of widely distributed bitumen in the Artillery basin suggests that it may have been a petroleum reservoir, and/or contained migrated crude oil that has undergone considerable structural disturbance and a high degree of thermal maturation.

CONCLUSIONS

Bitumens present in quartz veins and aggregates, which carry variable amounts of pyrite, galena, sphalerite and chalcopyrite, originated from the organic matter in the thinly laminated algal dolomitic beds of the Artillery Lake Formation, and were redistributed during burial and as a result of deformation and hydrothermal events. The bitumens matured to meso- and cata-impsonite equivalents and indicate a thermal peak (most probably attained during regional metamorphism) to the lower greenschist facies. The pyrolytic carbon may have formed during metamorphism in response to thermal gradient, or during intrusion of the Mackenzie diabase dykes, which provided local heat flux.

REFERENCES

Bogdanova, L.A., Kasperkevich, E.P., and Letushova, I.A.
1977: A highly metamorphosed bitumen in the Cambrian deposits of the Siberian platform (translated from Russian); in Lilologiya polezyne Iskopaemye, no. 3, p. 108-114.

Brooks, J.
1981: Organic maturation of sedimentary organic matter and petroleum exploration: a review; in Organic Maturation Studies and Fossil Fuel Exploration, Academic Press, London, England, p. 1-37.

Creaney, S., Jones, J.M., Holliday, D.W., and Robson, P.
1980: The occurrence of bitumen in the Great Limestone around Matfen, Northumberland - its characterisation and possible genesis; Yorkshire Geological Society, Proceedings v. 43, no. 1, p. 69-79.

Folinsbee, R.E.
1952: Walmsley Lake, District of Mackenzie, Northwest Territories; Geological Survey of Canada, Map 1013A, with descriptive notes (1 inch to 1 mile).

Gandhi, S.S.
1984: Galena-sphalerite-chalcopyrite veins in Aphebian dolomite and Archean basement at Artillery Lake, Northwest Territories; in Current Research, Part B, Geological Survey of Canada, Paper 84-1B, p. 33-40.
1985: Geology of the Artillery Lake Pb-Zn-Cu District, District of Mackenzie; in Current Research, Part A, Geological Survey of Canada, Paper 85-1A, p. 359-363.

Goodarzi, F.
1984: A comparison of optical properties of carbonised sporinite and vitrinite concentrates of coals of the same rank; Journal of Microscopy, v. 132, pt. 3, p. 279-188.
1985: Optical properties of vitrinite carbonised at different pressures; Fuel, 64, p. 156-162.

Goodarzi, F. and Murchison, D.G.
1978: Influence of heating rate variation on the anisotropy of carbonised vitrinite; Fuel, 57, p. 273-284.

Goodarzi, F. and Norford, B.S.
1985: Graptolites as indicators of the temperature histories of rocks; Geological Society of London, Journal v. 142, p. 1089-1099.

Goodarzi, F. and Williams, P.F.W.
1986: Composition of natural bitumens and asphalts from Iran, Part II: bitumens from the Posteh Ghear Valley, southwest Iran; Fuel, 65, p. 17-27.

Jacob, H.
1975: Mikroskopphotometrische analyse naturlicher fester Erdölbitumina; in Pétrographie organique et potentiel pétrolier, B. Alpern (ed.); Centre national de la recherche scientifique, Paris, p. 103-113.
1983: Mikroskopische analyse fester bis halbfester Erdölbitumina; Microscopica Acta, v. 87, p. 227-241.

Khavari-Khorasani, G.
1975: The properties and structural ordering of some fossil bitumens; Unpublished Ph.D. thesis, University of Newcastle-Upon-Tyne, England.

Khavani-Khorasani, G. and Murchison, D.G.
1978: Thermally metamorphosed bitumen from Windy Knoll, Derbyshire, England; Chemical Geology, v. 22, p. 91-105.

Macqueen, R.W. and Powell, T.G.
1983: Organic geochemistry of the Pine Point lead-zinc ore field and region, Northwest Territories, Canada; Economic Geology, v. 78, p. 1-25.

Roscoe, S.M.
1984: Lead isotope dating of galena-bearing veins in dolomite at Artillery Lake, Northwest Territories and Mistassini Lake, Quebec; Geological Association of Canada - Mineralogical Association of Canada, Program with Abstracts, v. 9, p. 101.

Roscoe, S.M., Gandhi, S.S., Charbonneau, B.W., Maurice, Y.T., and Gibb, R.A.
1987: Mineral resource assessment of the area in the East Arm (Great Slave Lake) and Artillery Lake region, N.W.T., proposed as a national park (NTS 75J, K, L, N, O); Geological Survey of Canada, Open File 1434, 92 p.

Shibaoka, M., Foster, N.R., Okada, K., and Clark, K.N.
1984: Formation of pyrolytic carbon in a continuous reactor for coal hydrogenation; Fuel, 63, p. 169-173.

Tissot, B.P. and Welte, D.H.
1984: Petroleum Formation and Occurrence; Spring-Verlag, Berlin, 699 p.

Williams, P.V.F. and Goodarzi, F.
1981: Iranian bitumens, late stage alteration products of crude oils; in Organic maturation studies and fossil fuel exploration, J. Brooks, (ed.);Academic Press, London, p. 319-336.

Wright, G.M.
1952: Reliance, District of Mackenzie, Northwest Territories (map and descriptive notes); Geological Survey of Canada, Paper 51-26.
1957: Geological notes on eastern District of Mackenzie; Geological Survey of Canada, Paper 56-10.
1967: Geology of the southeastern barren grounds of the District of Mackenzie and Keewatin (operation Keewatin, Baker, Thelon); Geological Survey of Canada, Memoir 350.

Preliminary geological report of the Snowdrift map area, Slave Structural Province, District of Mackenzie

R.A. Frith, R. Grenier[1], R.M. Harrap[2] and M. O'Dea[2]
Lithosphere and Canadian Shield Division

Frith, R.A., Grenier, R., Harrap, R.M. and O'Dea, M., Preliminary geological report of the Snowdrift map area, Slave Structural Province, District of Mackenzie, N.W.T.; in Current Research, Part C, Geological Survey of Canada, Paper 89-1C, p. 377-384, 1989.

Abstract

The western half of the area is underlain by various sized plutons of granite, granodiorite, tonalite and diorite centred by a granitoid gneiss complex which may represent older, deeper, and possibly higher grade crust. The eastern half is underlain by porphyroblastic and migmatitic metaturbidites of upper amphibolite grade intruded by small plutons. Along the west margin, a volcanic belt was outlined containing gossan and banded iron-formation.

Mid-Proterozoic strike-slip faulting and shearing affecting Archean rocks, particularly toward the southwest, was probably contemporaneous with the Great Slave Lake shear zone. The north lakeshore is the locus of late Proterozoic normal faulting, with pull-apart structures, accentuated by carbonate and hematite mineralization and other features indicating hydrothermal groundwater circulation.

Résumé

Le sous-sol de la moitié ouest de la région contient des plutons granitiques, granodioritiques, tonalitiques et dioritiques de dimensions variées, disposés autour d'un complexe de gneiss granitoïde qui pourrait correspondre à des matériaux plus anciens, plus profonds et peut-être même plus métamorphisés de la croûte terrestre. Le sous-sol de la moitié est contient des métaturbidites porphyroblastiques et migmatitiques du degré métamorphique supérieur des amphibolites, traversées par de petits plutons intrusifs. Le long de la marge ouest, s'est dessinée une zone volcanique contenant des chapeaux ferrugineux et des formations ferrifères rubanées.

La manifestation des décrochements et cisaillements survenus au protérozoïque moyen ont modifié les roches archéennes, surtout au sud-ouest, correspond probablement dans le temps à la formation de la zone de cisaillement de Great Slave Lake. La rive nord du lac a été le lieu de formation de failles normales datant du Protérozoïque supérieur, caractérisées par des structures d'arrachement, elles-mêmes accentuées par une minéralisation en carbonates et hématite, et d'autres structures témoignant de la circulation d'eaux souterraines hydrothermales.

[1] Memorial University of Newfoundland, Department of Earth Sciences, St.John's, Newfoundland, A1B 3X5.
[2] Carleton University, Department of Geology, Ottawa, Ontario, K1S 5B6

INTRODUCTION

This study examines an area within the Slave Structural Province, north of McLeod Bay and west of Hearne Channel of Great Slave Lake (Snowdrift, NTS 75L) (Fig. 1).

The Proterozoic rocks within the Snowdrift map area, which constitute most of the islands east of Hearne Channel and south of McLeod Bay, were studied intermittently over the last 20 years by Hoffman and colleagues (Hoffman, 1988). South of the McDonald Fault System, studies emphasizing structural geology have recently been carried out on rocks from the Great Slave Lake Shear Zone and environs (Bostock, 1987; Hanmer, 1988).

Most of the early geological work in the region was restricted to the Proterozoic rocks and other readily accessible Great Slave Lake shore. Earlier work within the Snowdrift map area included: the geological observations of Lausen (1929); the reconnaissance work along the north shore of McLeod Bay and published maps of Stockwell (1933, 1936); and the work of Brown (1968), Barnes (1951), and Wright (1951).

The west adjacent Hearne Lake map area was recently mapped by Henderson (1985) at a scale of 1:250 000; the north adjacent McKay Lake map area was mapped at a scale of four miles to the inch (Henderson, 1941, 1944). The Benjamin Lake area north of Thompson Landing (NTS 75/15) was mapped at a 1:50 000 scale (Heywood and Davidson, 1969).

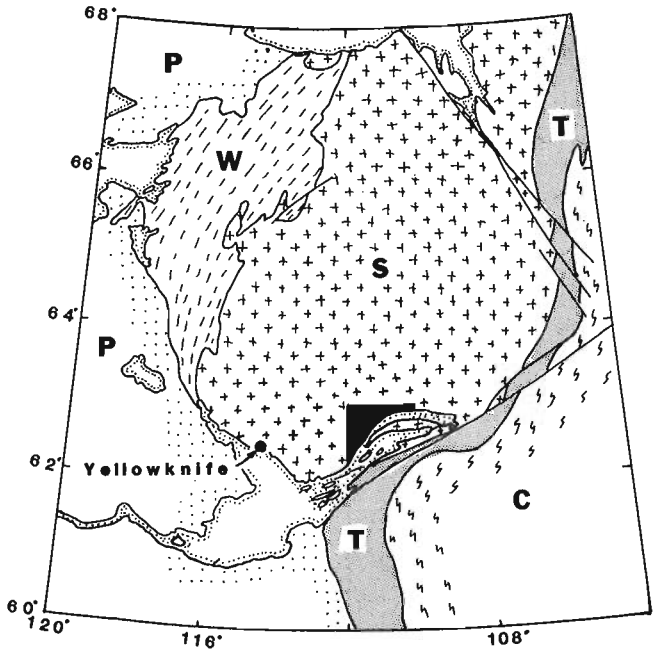

Figure 1. Tectonic location map of the Slave Structural Province (S), showing the area mapped (black). The Slave is bounded by the Thelon-Taltson Tectonic Zone to the east (T) and the Wopmay Orogen to the west (W). The Churchill Structural Province lies to the southeast (C) and the far western area is overlain by Paleozoic cover rocks (P). Two major strike-slip faults form important regional structures. These include the Bathurst Fault System to the northeast of the Slave and the McDonald Fault System to the southeast.

The authors gratefully acknowledge the following people and companies: in Yellowknife, Rod Stone and Lynn Parney for excellent expediting services; "Chummy" Plummer and the management of Great Slave Lake Lodge for casual charter; Don Briggs and Herman Ropain of Indian Mountain Lodge, for providing the hospitality and friendship that are so much the hallmarks of the north; in Yellowknife, Latham Island Airways for giving us outstanding air service. Finally, we thank John Henderson and Simon Hanmer for critically reading an earlier version of this report which improved the paper. However, the authors remain entirely responsible for the views expressed herein.

GENERAL GEOLOGY

Yellowknife Supergroup volcanic rocks (unit V)

Three belts have been outlined, which include the "Copperpass" (names in quotations are unofficial) basalt, the "Shearzone lake"* metavolcanics and the Thompson. Landing volcanics (subunits Vc, Vs and Vt — Fig. 2).

"Copperpass" basalt (subunit vc)

The belt northwest of "Sawmill bay" is composed mostly of basalt, metamorphosed to middle amphibolite facies. The westward extension of the belt has been truncated by a major north-south fault, known here as the "Box bay" fault (Fig. 2) which offsets the belt left-laterally. The belt extends to the west into the Hearne Lake map area where it mantles a granodiorite-granite-tonalite body (Henderson, 1985). Fine grained, intermediate to felsic layered gneiss, possibly derived from tuffaceous volcanic rocks, occurs at the extreme south end of the map. A few remnant pillows were noted west of the Box bay fault, but east of it, where the belt is wider, they are common. This rock sequence suggests the belt faces west. Intermediate composition flows and pyroclastic rocks occur north of Sawmill bay (Fig. 2), including some possible spherulitic varieties.

The volcanic rocks are commonly deformed and stretched out by ductile Archean deformation near the contacts. Late Archean pegmatite (Wright, 1968) is generally devoid of Archean structures. The Sachowia mineral deposit (nickel prospect, Wright, 1968), south of "Pistol lake" (Fig. 2) occurs within pillowed Archean volcanics. The pillows are highly deformed along northeast oriented shearing. Eastward extension of the belt left dismembered amphibolitic remnants which were traced several kilometres northeast. The deformation parallels regional gneissosity which is presumed to be Archean.

"Shearzone lake" metavolcanics (subunit Vs)

The belt is a sinusoidal north-northwest-trending body comprising of hornblende gneiss and ubiquitous pegmatite and quartzofeldspathic veins and granitoid rocks. The basalts are intruded by granite plutons and show multiple deformation. Remnant pillows were stretched or rodded (ductile deformation) and then sheared parallel to the long direction of the belt (brittle deformation). The result is a fine grained, sheared out hornblende gneiss that locally shows remnant

pillows. The rock commonly has a dark brown to black to rusty weathered appearance, is well foliated and generally occurs as foliated vertical slabs. Locally, garnet porphyroblasts are present. The belt contains up to 40% pegmatite. Goethite-stained, sulphide and oxide facies banded iron-formation are found near the northern end of the belt (dot, Fig. 2). Near Shearzone lake, shearing dominates outcrop surfaces, and remnant pillowed basalt or mafic pyroclastic rock has been metamorphosed and subsequently stretched out to fine hornblende amphibolite gneiss.

Thompson Landing volcanic rocks (subunit Vt)

The belt is 100-500 m wide and extends from the lake shore just west of Thompson Landing, north to the map boundary and into the adjoining Benjamin Lake map area (Heywood and Davidson, 1969) for a distance of about 16 km (Fig. 2). The belt comprises light grey fine grained gneiss, of commonly interlayered intermediate to mafic composition. The mineral assemblage consists of quartz, plagioclase and biotite with minor hornblende, garnet and calcite. The rocks are volcaniclastic and probably of pyroclastic origin. In the Benjamin Lake area, the eastern margin of the belt is locally mineralized, with chalcopyrite and pyrite noted (Heywood and Davidson, 1969).

Yellowknife Supergroup metasediments

Metasediments make up a significant part of the Slave Structural Province where they have long been recognized as greywacke-mudstone turbidites. Where the rocks are little metamorphosed, they commonly exhibit some of the primary sedimentary features that make up a Bouma sequence of turbiditic deposits (Henderson, 1970). The metasediments in the Snowdrift map area are similar, but all have been metamorphosed to porphyroblastic schistst, gneiss and locally migmatized gneiss. The cordierite isograd, which separates "knotted" schist (coarsely porphyroblastic) from lower grade metasediments, passes within a kilometre of the southwestern corner article of the map area. Other metasediments of the supergroup are found from the geographical midpoint of the map area to the eastern margin (Fig. 2). All occurrences of Yellowknife Supergroup

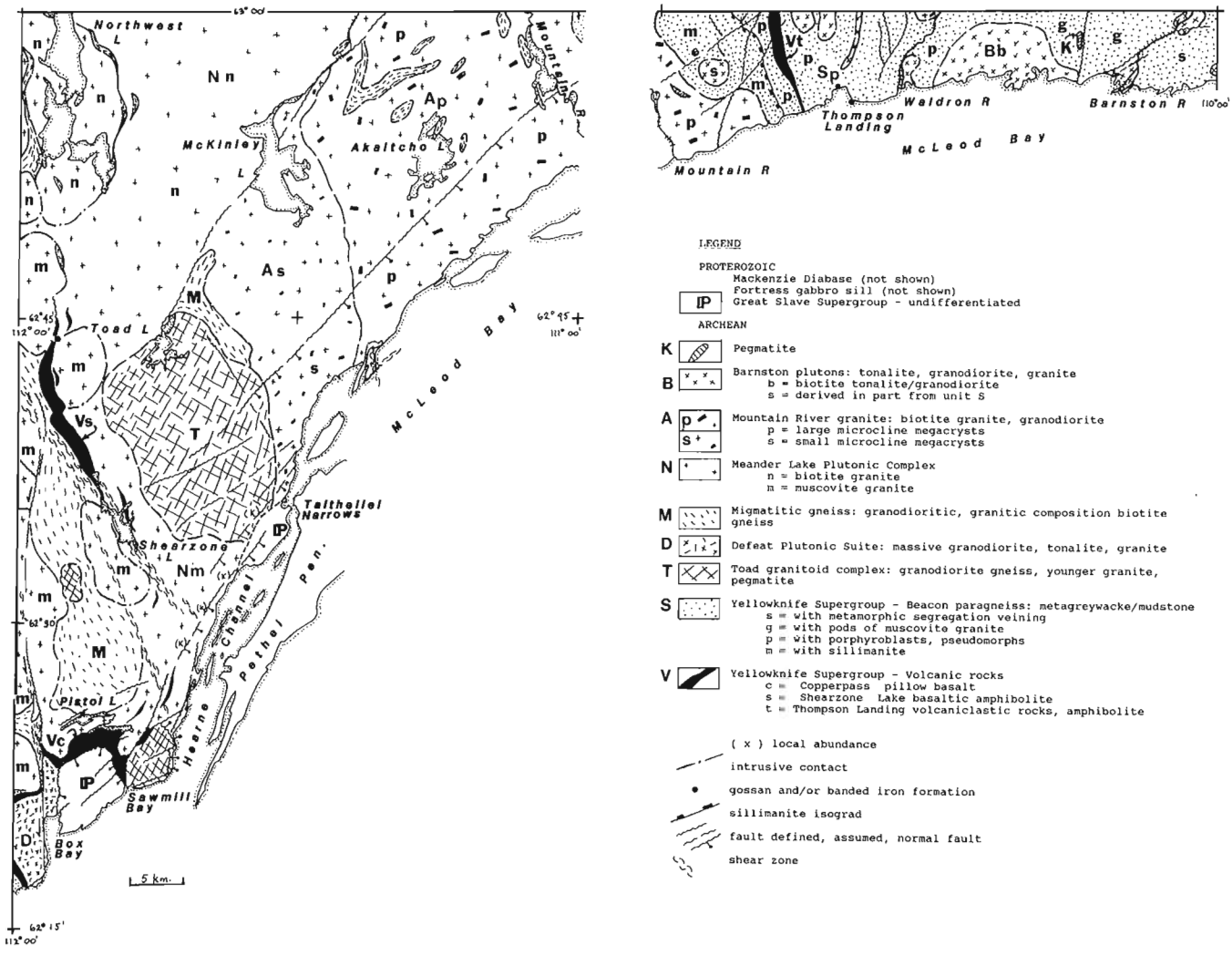

Figure 2. Geological sketch of the map area. Upper case letters refer to rock units; lower case to subunits. Unpatterned areas are underlain by Proterozoic rocks which have not been included.

metasediments in the map area have been mapped using the informal term "Beacon" paragneiss, except for small areas in the southwestern part of the map area where the unit has been correlated with the adjacent porphyroblastic Burwash Formation (Henderson, 1985).

"Beacon" paragneiss (unit S)

The metasediments of the Snowdrift map area have been divided into three types: subunit p, porphyroblastic gneiss and schist with less than 10 % quartzofeldspathic veins; subunit g, similar to subunit p, but with a number of introduced metre-scale pods of pegmatitic granite which intruded subparallel to bedding; and subunit s, migmatitic paragneiss and paraschist with 10-50 % metamorphic segregation veining. Migmatites do not form part of the unit, as there was little or no introduction of leucosome.

Subunit p, m

To the north of Thompson Landing the paragneiss contains less than 10 % segregation veining (p, Fig. 2). The bedding is commonly 20-40 cm, but locally up to 3 m thick and is relatively well preserved. The paragneiss commonly contains relict porphyroblasts, but this is by no means characteristic, as some rocks are coarse grained and do not necessarily have a sufficient pelitic component. Rocks west of the sillimanite isograd are higher grade and were mapped as subunit m.

Subunit g

North of the Barnston River and west toward the Waldron River the paragneiss is intruded by a pegmatitic muscovite-bearing granite that occurs as elongate pods, roughly oriented parallel to bedding-gneissosity. The scale of mapping did not allow separating the granite pods which make up an estimated 10-25 % of the rocks (g, Fig. 2).

Subunit s

Rocks with more than 10 % quartzofeldspathic veins are dark grey to buff on the fresh surface and almost invariably show rusty discolouraton on the weathered surface (goethite). The paragneiss is migmatitic, made up principally of biotite, plagioclase and quartz gneiss or schist containing 10-50 % quartzofeldspathic in situ metamorphic segregation veins. The rocks contrast with the migmatitic gneiss and migmatite found as inclusions in the Mountain River granite where the leucosome component was introduced.

Typically the veining in the rocks is complexly folded by two phases of deformation that gives the gneiss a "chaotic" appearance (Fig. 3a). However, on close inspection foliation and minor fold planes show preferred orientations. On a larger scale the migmatitic paragneiss shows layering (Fig. 3b) that in lower grade areas is attributed to bedding. Rare relict outlines of cordierite porpyroblasts may be observed in places.

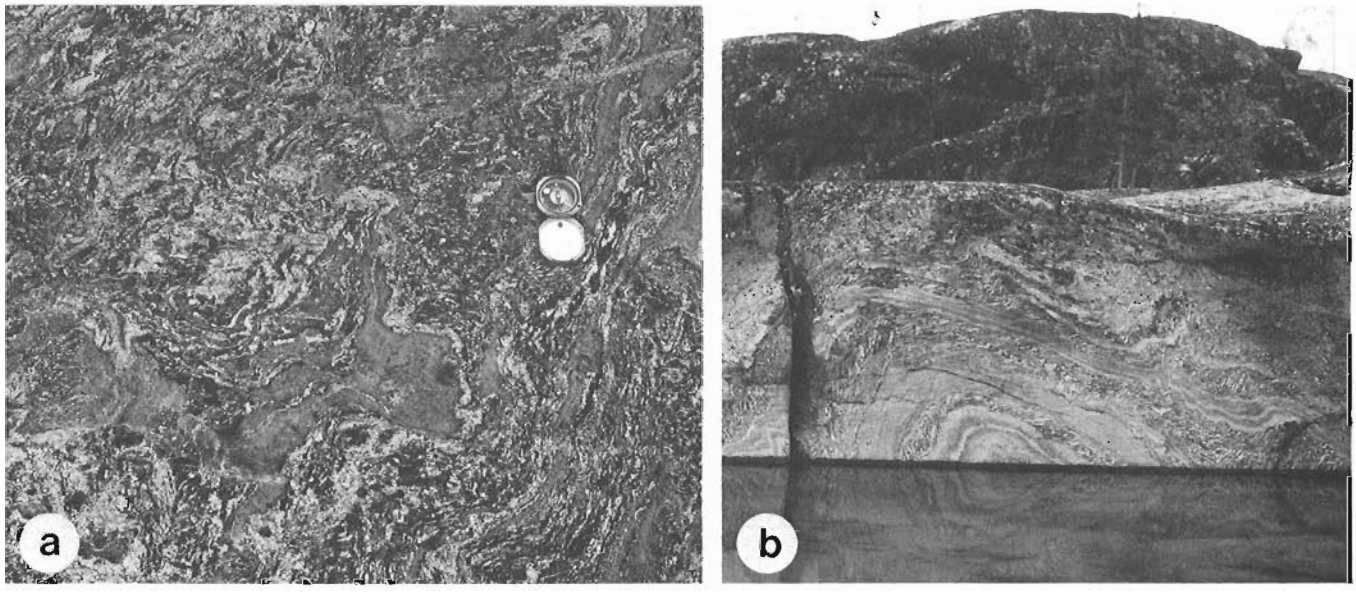

Figure 3. Beacon paragneiss from the eastern margin of the map area. The rocks have been metamorphosed to the upper-amphibolite facies and deformed by two phases of regional folding. The two photographs are from the same outcrop.
a) Segregation veining and folding give the rock a chaotic appearance;
b) Remnant bedding observed from 15 m away.

Toad lake granitoid complex (unit T)

The principal area of the Toad Lake granitoid complex is a rectangular shaped map unit extending from Toad Lake to Taltheilei Narrows. The unit is heterogeneous, consisting of a retrograded quartz-rich biotite- and/or hornblende-, plagioclase- and microcline-bearing gneiss that is invariably cut by a highly varied proportion of aplite, alaskite or muscovite granitepegmatite. The gneiss, which occurs in most outcrop areas, is commonly a rusty orange colour and has a knobby appearance on the weathered surface due to abundant quartz. The quartz, which forms up to 35 % of the rock, locally defines a strong foliation in contrast to the younger intrusive phases.

The medium to coarse grained gneissic rock has a "greasy" sugary texture and green to buff colour that is commonly found in granulite facies rocks. This grade of metamorphism is unknown along the southern margin of the Slave Structural Province, but is similar to parts of the eastern and western margin of the Slave Structural Province. The complex was probably hydrated during the waning phase of orogenesis, forming hornblende.

Dioritic gneiss makes up part of the eastern margin of the complex. The true extent and its relationship to the more voluminous granodioritic gneiss is not known. It occurs sporadically from the eastern margin toward the southwest. Like the granodiorite it is mixed with varied amounts of introduced granitoid rock.

Toward the west of the complex, the composition changes from a hornblende gneiss-dominant unit to a granite intrusive-dominant unit. Southeast of Shearzone lake, several mappable areas of hornblende gneiss occur surrounded by biotite granite or granodiorite, some of which contain inclusions or remnant paragneiss or biotite schlieren.

The older parts of the complex have granodioritic modal compositions, similar to the bulk composition of the Yellowknife Supergroup metasedimentary rocks. The gneiss may have been derived from a similar protolith.

Defeat Plutonic Suite (unit D)

The Defeat Plutonic Suite was initially described by Henderson (1985) in the Hearne Lake map area close to the margin of the Snowdrift map area, where it forms the largest plutonic suite in that area. The pluton in the southwestern corner of the map area belongs to this suite. The rocks are massive to slightly foliated, pink to pale buff, medium grained equigranular tonalites and granodiorites containing biotite, microcline, plagioclase and quartz.

The rock is surrounded by the Copperpass volcanic belt, which gives the impression that the intrusion is a gneiss dome that ascended into more horizontal volcanic rocks. Henderson (1985) noted that plutons of the suite contain abundant inclusions of Yellowknife rocks, which suggests that the Defeat Plutonic Suite postdates the Yellowknife Supergroup. No inclusions were noted in the present area, but the rocks have a decidedly igneous texture.

Meander Lake Plutonic Complex (unit N)

The Meander Lake Plutonic Complex was first described by Henderson (1985) for a group of plutonic rocks that lie along much of the western margin of the present map area. The complex contains intrusions of biotite granite and granodiorite that are generally pink in colour, massive and generally equigranular, although in some places the rocks are porphyritic, with small megacrysts of microcline. Locally, the rocks are heterogeneous with inclusions of metasedimentary paragneiss. Some of the granites may contain small amounts of muscovite. Alaskite and muscovite-granite pegmatite are also present locally. These granites are described as the "Northwest" granite.

Muscovite granites do not make up a significant part of the Meander Lake Plutonic Complex in the Hearne Lake map area where they are restricted to small "satellite" plutons that have intrusive contacts within the Burwash Formation (Henderson, 1985). The muscovite granites in this map area are of comparable composition, but they make up a significant proportion of the complex. They are described below as the "West Margin" granite.

"Northwest" granite (subunit n)

The granite occurs in the northwestern corner of the map area between Northwest lake and McKinley Lake. The granite consists of individual plutons, such as the body around Northwest lake that has been delineated by migmatitic marginal zones. However, much of the area mapped as Northwest granite is in an area of thick overburden.

Typical rocks of the subunit are found in a north-south oriented oval intrusion centred by Northwest lake, bounded by migmatitic rocks containing bands of biotite schlieren of possible sedimentary parentage. The granite is massive, equigranular and biotite-bearing. Toward the eastern margin it locally contains phenocrysts of microcline and irregular veins of muscovite-bearing granite pegmatite. The margins of the intrusion are outlined by extrapolating migmatitic zones which are now partly digested.

West and northwest of McKinley Lake (Fig. 2) the rocks are similar to those of the northwestern corner. Due to the general lack of outcrop, discrete plutons were not delineated; however, the rocks have been tentatively mapped as "Northwest type".

The nature of the contacts between the Northwest lake granite and the surrounding rocks is not known accurately. Where there are migmatitic zones, such as around Northwest lake, intrusion into Yellowknife Supergroup metasediments is presumed. However, there is no defined boundary between the biotite granites of the Northwest lake and the muscovite granites of the West Margin. There is a fault trace between the Northwest lake and the Mountain River granite, locally accentuated by pink feldspar discolouration.

"West Margin" granite (subunit m)

The West Margin granite occurs as single intrusions of rounded form (m, Fig. 2) or as elongate, more heterogeneous,

poorly defined regions of muscovite-bearing granite that are locally massive. The granite east of Shearzone Lake is an example of the latter (Fig. 2).

The irregular shaped pluton in contact with the western margin of the Toad Lake granitoid complex (Fig. 2) has gradational contacts. Crosscutting relationships were not observed. The intrusion that extends from the northeastern end of the Shearzone lake volcanic belt to the Hearne Channel is massive in the north, but becomes progressively more foliated toward the south where it is deformed by the Payne shear zone and by regional deformation. The Payne shear zone (runs through Shearzone lake) extends from Hearne Channel to the northeastern corner of the Hearne Lake map area. This same shear zone deforms the metavolcanic rocks more than the granitic rocks, perhaps due to differing competence of the granite.

Gneiss and migmatitic gneiss (unit M)

Biotite gneiss and migmatitic gneiss occur within the Meander Lake Plutonic Suite and the Mountain River rock, most commonly biotite granite gneiss or granodiorite gneiss that contains "wisps" or schlieren of biotite schist. Other migmatitic zones contain banded biotite schist or gneiss, locally of granodioritic or dioritic composition. Some of the zones contain more mafic "inclusions", some with hornblende. This type of rock is common near the western margin at the northwestern end of the Shearzone Lake volcanic belt.

Mountain River granite (unit A)

The Mountain River granite covers about one third of the map area (subunit Ap and As, Fig. 2). It is a coarse grained megacrystic biotite granite or granodiorite. The granite is divided into a large microcline megacryst type (> 2 cm, Ap) and a small microcline megacryst type (<2 cm, As). The small megacryst type south of McKinley Lake is relatively homogeneous and generally contains a few percent, by volume, of pegmatite or quartzofeldspathic vein material.

Along the northern and eastern shores of Akaitcho Lake, zones or inclusions of paragneiss occur within the granite. They grade in size from tens of metres to diffuse zones of a metre or so wide. Southeast of McKinley Lake, remnant hornblende gneiss similar to the Toad Lake granitoid complex is present. The margins of the pluton are gradational and contain numerous older "digested" inclusions of Yellowknife Supergroup paragneiss suggesting a passive "soaking" mode of intrusion into the country rock, rather than a forceful mode of intrusion.

The granite is bounded to the southwest by a poorly understood contact with the Toad Lake granitoid complex and by a gradational contact with migmatitic Yellowknife Supergroup to the east. The contact with the "Northwest" granite of the Meander Lake Plutonic Complex is tentatively placed along a lineament, possibly a fault, that separates slightly megacrystic rocks from the more obviously megacrystic Mountain River granite. The boundary is somewhat arbitrary and complicated by lack of outcrop in the region.

Barnston plutons (unit B)

North and east of Thompson Landing are massive, fresh looking biotite tonalite, granodiorite, diorite and muscovite-bearing granites that intruded the Beacon paragneiss. The plutons are of irregular shape. The pluton between the Waldron and Barnston rivers is mostly tonalitic, but with inclusions of diorite near its margins. The elongate tongue north of Thompson Landing is also tonalitic and may be part of a larger intrusion at depth that includes the two bodies northwest of it. These small intrusions partly follow the bedding traces of the host Beacon paragneiss.

Mappable regionally associated rocks include elongate to oval intrusions of biotite granodiorite, some of which are schlieren bearing, possibly derived in part from melted remobilized paragneiss. These were mapped as subunit Bs (Fig. 2).

Pegmatite (unit K)

The proportion of younger aplite, alaskite and muscovite-granite pegmatite in the complex as a whole changes locally, but intrusive phases generally becomes more abundant from north to south. Near Hearne Channel, Toad Lake granitoid complex and the Meander Plutonic Suite are hosts for extensive but discontinuous areas of very coarse muscovite-granite pegmatite (local abundance is shown as K in parentheses). It forms a ridge of high relief along the length of the channel, bounded to the southeast by a normal fault. North-northeast-trending Proterozoic deformation has imposed a sheared fabric on some zones within the gneiss. Northwest of Barnston River, the pegmatite makes up a large area within the Beacon paragneiss, where they top some of the highest relief. One occurrence is shown in Figure 2, but many more are present.

Diabase dykes

Hearne Diabase

The Hearne Diabase intrudes all Archean rocks. It was not observed cutting, nor is it known to cut the Great Slave Supergroup (Hoffman, 1988). The swarm intrudes in an east-northeast direction and consists of 1-10 m wide amphibolitized metadiabase. The swarm is dense between the western margin of the map area and Taltheilei Narrows, commonly having too many dykes across strike to map effectively at 1:50 000 scale. The dykes extend into the west adjacent map area, where they intrude the earliest phases of the Blachford Intrusive Complex. They are little deformed, but show some retrograde metamorphism possibly causing a flat aeromagnetic expression. The dykes to the east of the Box Bay fault are deformed by a north-northwest-trending penetrative foliation, possibly associated with the Payne shear zone. The dykes are parallel to local aeromagnetic linears. The reason why these dykes have an aeromagnetic anomaly and those west of the Box Bay fault do not is not certain, unless the regional signature is influenced by a greater number of dykes. The dykes are so numerous northwest of the Hearne Channel that they make up to 25 % of some areas.

Mackenzie Diabase and Fortress gabbro sills

The East Arm of Great Slave Lake is spectacular, due in part, to the presence of up to 200 m thick sills of gabbro, recently named the Fortress gabbro sills (Hoffman, 1988). The Mackenzie Diabase swarm intrudes in a north-northwest direction and is temporally associated with the Fortress gabbro sills and the Muskox Intrusion (Fahrig and Jones, 1969). The latter was recently dated by U-Pb methods using baddeleyite at 1270 Ma (Heaman and LeCheminant, 1988). The dykes are not numerous in the map area, but wherever they occur they have a pronounced aeromagnetic anomaly (Geological Survey of Canada, 1964) showing crosscutting relationships with the Fortress gabbro sills, and indicating that they are locally younger.

Other Proterozoic rocks, events and their relationship to Archean rocks

The Great Slave Supergroup, although not detailed in Figure 2, occurs along the southern margin of the Slave craton in fault contact with Archean rocks. Volcanic rocks northeast Box Bay and sandstone-shales west of Taltheilei Narrows have been downfaulted relative to the Archean (Hoffman, 1988).

The present surface of the Slave craton was likely an erosional unconformity, as there is widespread evidence of groundwater circulation along the interface; too widespread to be simply fault-related. Microcline has been altered to a salmon-pink colour and there is much hematite mineralization on fault surfaces and in fault breccia, particularly in the granitoid rocks along the McLeod Bay shoreline. Nicolite mineralization in the 'Copperpass' volcanic rocks formed by hot groundwater circulation across the Archean-Proterozoic interface, which is interpreted as a regolith surface (S.M. Roscoe, pers. comm.). The relationship of this paleo-erosion surface to the Great Slave Supergroup is uncertain.

STRUCTURAL GEOLOGY

Folding

The lower grade metamorphic sedimentary rocks of the Yellowknife Supergroup in the map area are folded in tight to isoclinal folds similar to the style observed north of Thompson Landing (Heywood and Davidson, 1969). In the eastern half of the present study area the fold axes in the Beacon paragneiss trend north, parallel to the Thompson Landing volcanic belt. The more highly migmatitic members of this unit, along the eastern margin, are more complexly folded in a ptygmatic style that appears chaotic (Fig. 3a), but in fact reflects secondary horizontal stress possibly associated with the intrusion of granite and tonalite intrusions.

Visible fold structures in the western half of the map area are rare. There are few layered rocks to outline such structures. The rocks have been deformed by shear as described below.

The age of folding is bracketed by the 2.67 Ga age of the Yellowknife Supergroup and the little deformed pegmatite granite of the area, which elsewhere in the Slave are 2.5 Ga years old (Wright, 1968; Frith and Loveridge, 1982). Mica associated with these late granites is unaffected by Archean deformation.

Regional extension

Shear, as opposed to folding, occurs in the metavolcanic rocks, granitoid gneiss and migmatitic rocks of the western half of the map area. Extension is steep and commonly lineated.

The gneissosity in the Toad Lake granitoid complex is well developed and oriented north-northwest. No folding is evident, but there are commonly steep mineral lineations along the foliation planes including flasered quartz and elongated hornblende crystals.

Pillow basalts in the southwestern part of the area are stretched along near vertically oriented lines around a core of syntectonic plutonic granite, suggesting strong vertical extension during regional metamorphism/plutonism.

The hornblende granodiorite gneiss northwest of Taltheilei Narrows contains abundant granitic pegmatite, biotite granite and intrusions of diabase. These younger rocks are deformed and some of this deformation can be related to Proterozoic events (discussed below). The older hornblende gneissosity is Archean, as there is a strong contrast in the degree of deformation between the gneiss and the pegmatite. The gneissosity is oriented north-northeast consistent with regional east-west compression. Where mineral lineations are present they are highly variable in plunge.

Faults and shear zones

There are two prominent orientations of faulting/shearing; a northerly-trending set and an easterly-trending set. The two sets were probably coeval. An example of the northerly type is the regionally extensive Payne shear zone (M. Lambert, pers. comm.) that extends from Hearne Channel to the northeastern margin of the Hearne Lake map area, a distance of 75 km or more (near Shearzone lake, Fig. 2). The shear zone is older than the Great Slave Supergroup because it is overlain by an outlier of undeformed Great Slave Lake rocks in the Hearne Lake map area (Henderson, 1985). Shearing of similar orientation, northwest of Taltheilei Narrows cuts metadiabase dykes of similar orientation to the Hearne Diabase dyke swarm, which intrudes the 2185 Ma Blachford Intrusive Suite (Bowring et al., 1984; Henderson, 1985; Hoffman, 1988.

The north-trending Box Bay fault has a left-lateral sense of movement (Fig. 2). The fault splays and merges with the Payne shear zone in the northwestern part of the map area. The fault is similar to numerous sinistral faults along the southern and southwestern margin of the Slave Structural Province, including the West Bay Yellowknife Fault (Henderson, 1985). The metamorphic grade of the Hearne Diabase increases from west to east across the faults/shear zones and it is suggested that the Box Bay fault is an oblique fault with a west-side-down vertical component. Other less

apparent faults of similar trend are present, such as the north-south shear zone along the eastern shore of the peninsula northeast of Taltheilei Narrows. This shear zone (Fig. 2) is characterized by conjugate shears, parallel to both the northerly and easterly sets.

Normal faults of post-Great Slave Supergroup age border the Kahochella Group volcanic rocks north of Sawmill bay, the northwestern margin of the Hearne Channel and from the escarpment between Shearzone lake and Mountain Lake (Fig. 2). Smaller scale faulting of this type and associated pull-aparts are common along the western shore of Hearne Channel and the northern shore of McLeod Bay. These denote regional uplift of the Slave craton relative to the East Arm basin.

Fault and shear zones in the map area are recognized as Proterozoic features, possibly associated with the same tectonic events that gave rise to the Great Slave Lake Shear Zone (recently conceptualized by Hanmer, 1988) and post-shear zone events associated with basin formation and sedimentation, magmatism and final subsidence of the East Arm basin.

METAMORPHISM

The cordierite isograd passes within a kilometre of the southwestern corner of the map area. The isograd progrades northeastward. Northwest of Thompson Landing a sillimanite isograd progrades westward. A thermal high is found in the intervening area, possibly near the Toad Lake granitoid complex, where a pale green colour and waxy texture suggest the presence of granulite facies rocks.

A metamorphic low occurs near Thompson Landing. Porphyroblasts in the low grade area are ubiquitously retrograded. Cordierite pseudomorphs are common and remnant staurolite, garnet and andalusite (or sillimanite) were noted.

East of the Waldron River, metamorphism progrades from porphyroblastic schist and gneiss to migmatitic rock with an increasing proportion of metamorphic segregation veining. The characterisitic shapes of cordierite and staurolite are still noted locally, but generally the segregated gneiss is devoid of porphyroblasts wherever the degree of segregation veining is higher than 10 %.

REFERENCES

Barnes, F.Q.
1951: Snowdrift, Northwest Territories; Geological Survey of Canada, Paper 51-6.

Bostock, H.H.
1987: Geology of the south half of Taltson Lake map area, District of Mackenzie; in Current Research, Part A, Geological Survey of Canada, Paper 87-1A, p. 443-450.

Bowring, S.A., Van Schmus, W.R., and Hoffman, P.F.
1984: U-Pb zircon ages, from Athapuscow aulocogen, East Arm of Great Slave Lake, N.W.T., Canada; Canadian Journal of Earth Sciences, v. 21, p. 1315-1324

Brown, I.C.
1950: Preliminary Map, Reliance, Northwest Territories; Geological Survey of Canada, Paper 50-15.
1968: Geology, Reliance, Northwest Territories; Geological Survey of Canada, Map 1123A.

Fahrig, W.F. and Jones, D.L.
1969: Paleomagnetic evidence from the extent of Mackenzie igneous events; Canadian Journal of Earth Sciences, v. 6, no. 4, p. 679-688.

Frith, R.A. and Loveridge, D.
1982: Ages of Yellowknife Supergroup volcanic rocks, granitoid intrusive rocks and regional metamorphism in the northeastern Slave Structural Province; in Current Research, Part A, Geological Survey of Canada, Paper 82-1A, p. 225-237.

Geological Survey of Canada
1964: Snowdrift, District of Mackenzie, Northwest Territories; Geological Survey of Canada, Geophysical Paper 7189.

Hanmer, S.
1988: Great Slave Lake Shear Zone, Canadian Shield: reconstructed vertical profile of a crustal-scale fault zone; Tectonophysics, v. 149, p. 245-264.

Heaman, L.M. and LeCheminant, A.N.
1988: U-Pb baddeleyite ages of the Muskox Intrusion and Mackenzie Dyke Swarm, N.W.T., Canada; Geological Association of Canada a and Mineralogical Association of Canada, Joint Annual Meeting Program with Abstracts, v. 13, p. A53.

Henderson, J.B.
1970: Stratigraphy of the Yellowknife Supergroup, Yellowknife Bay-Prosperous Lake area, District of Mackenzie; Geological Survey of Canada, Paper 70-6, 12p.
1985: Geology of the Yellowknife-Hearne Lake Area, District of Mackenzie: a segment across an Archean basin; Geological Survey of Canada, Memoir 414, 135 p.

Henderson, J.F.
1941: MacKay Lake, Northwest Territories; Geological Survey of Canada, Paper 41-1.
1944: MacKay Lake, Northwest Territories; Geological Survey of Canada, Map 738A.

Heywood, W.W. and Davidson, A.
1969: Geology of Benjamin Lake map-area, District of Mackenzie; Geological Survey of Canada, Memoir 361, 35 p.

Hoffman, P.F.
1988: East Arm of Great Slave Lake, Northwest Territories; Geological Survey of Canada, Map 1628A, 2 sheets.

Lausen, Carl
1929: Geological Reconnaissance of the East Arm of Great Slave Lake; Canadian Institute of Mining and Metallurgy, Bulletin 202, p. 361-392.

Stockwell, C.H.
1933: Great Slave Lake — Coppermine River Area, Northwest Territories; Geological Survey of Canada, Summary Report, 1932, Part C, p. 37-63.
1936: Eastern Portion of Great Slave Lake, District of Mackenzie, Northwest Territories; Geological Survey of Canada, Maps 377A and 378A (with descriptive notes).

Wright, G.M.
1951: Second Preliminary Map, Christie Bay, Northwest Territories; Geological Survey of Canada, Paper 51-25.
1968: Geology, Christie Bay, District of Mackenzie, Northwest Territories; Geological Survey of Canada, Map 1122A.

The Boundary Zone of the Nain-Churchill provinces in the North River-Nutak map areas, Labrador

I.F. Ermanovics, M. Van Kranendonk[1], L. Corriveau[2], F. Mengel[2], D. Bridgwater[3], and R. Sherlock[4]; Lithosphere and Canadian Shield Division

Ermanovics, I.F., Van Kranendonk, M., Corriveau, L., Mengel, F., Bridgwater, D., and Sherlock, R., The Boundary Zone of the Nain-Churchill provinces in the North River-Nutak map areas, Labrador; in Current Research, Part C, Geological Survey of Canada, Paper 89-1C, p. 385-394, 1989.

Abstract

Proterozoic activity in Nain Province between 57°30'N and 58°00'N included emplacement of Napaktok dykes, crustal flexuring during deposition of Ramah and Mugford groups and development of breccia dykes along the conjugate Napaktok dykes fracture pattern. The easternmost distally located Proterozoic rocks in Nain Craton, show subgreenschist metamorphism and open fold styles that progress toward Churchill Province in Churchill Foreland Zone to amphibolite facies accompanied by two phases of folding, including isoclinal folds; rocks in the Boundary Zone attain granulite facies and are affected by transcurrent sinistral shear and by late, major, steep dip-slip faults.

Churchill Province (Tasiuyak gneiss terrane) also exhibits a progression of open to isoclinal folding and transcurrent shear, but all occurred at high grades including granulite facies. Structures in the Tasiuyak gneiss terrane are linked with structures in Proterozoic and Archean rocks of Nain Craton and formed in response to E-W transpression.

Résumé

Dans la province de Nain, l'activité au Protérozoïque entre 57°30' et 58°00' de latitude nord englobe la mise en place des dykes de Napaktok, un fléchissement crustal pendant l'accumulation des groupes de Ramah et de Mugford ainsi que la mise en place de dykes bréchiques le long du réseau de fractures conjuguées des dykes de Napaktok. Les roches protérozoïques les plus distales à l'est dans le craton de Nain présentent un métamorphisme du sous-faciès des schistes verts et des plis de style ouvert progressant, en direction de la province de Churchill dans la zone d'avant-pays de Churchill, vers un faciès des amphibolites accompagné de deux phases de plissement, incluant des plis isoclinaux; dans la zone de Boundary, les roches atteignent le faciès des granulites et ont été touchées par un cisaillement transversal à composante sénestre ainsi que par d'importantes failles d'effondrement tardives de fort pendage.

On remarque également dans la province de Churchill (terrain gneissique de Tasiuyak) une progression du plissement ouvert au plissement isoclinal et au cisaillement transversal, mais tous se sont produits pendant des épisodes de métamorphisme de degré élevé, incluant le faciès des granulites. Les structures dans le terrain gneissique de Tasiuyak sont reliées aux structures dans les roches du Protérozoïque et de l'Archéen du craton de Nain et se sont formées en réponse à une transpression E-O.

[1] Department of Geological Sciences, Queen's University Kingston, Ontario, K7L 3N6.
[2] Department of Geology, University of Toronto, Toronto, Ontario, M5S 1A1.
[3] Geological Museum, 1350 Copenhagen K, Denmark.
[4] Department of Geology, Lakehead University, Thunder Bay, Ontario P7B 5E1.

INTRODUCTION

The project area is located in Labrador, Newfoundland and extends from the Labrador Sea coast between 57°30'-58°00'N westward to 64°00'W (Fig. 1). The area is underlain by Archean rocks of Nain Province (Ermanovics et al., 1988) that are progressively tectonized towards the Proterozoic Churchill Province. Rocks of Churchill Province comprise hypersthene-bearing orthogneiss, and granulite facies white, migmatitic, garnet-sillimanite-feldspar paragneiss (Tasiuyak gneiss). Proterozoic metamorphism and deformation has raised the adjacent rocks of western Nain Province to granulite and amphibolite facies. This constitutes the Churchill Foreland Zone that extends from the Tasiuyak gneiss at least 15 km into Nain Province.

The Foreland Zone was further subdivided to include a Boundary Zone 4 to 5 km wide adjacent to the Tasiuyak gneiss. This zone marks the transition of Proterozoic amphibolite to granulite facies and separated Nain from Churchill province (Taylor, 1979). The zone is underlain by rocks of Nain Province, Proterozoic Ramah Group and by granitic orthogneiss of probable Proterozoic age. These rocks are affected by sinistral transcurrent shear, coextensive with Churchill Province, and by numerous late steep, dip-slip faults along zones of glassy mylonite and pseudotachylite.

This year's work concentrated on the Nain-Churchill Boundary Zone and Tasiuyak gneiss west to about 63°30'W where it was found that the transcurrent shear-deformation in Proterozoic granulite facies terrane (Abloviak Shear) is confined mainly to the eastern portion of Tasiuyak gneiss but transgresses east to include rocks of the Boundary Zone at amphibolite and granulite facies.

NAIN PROVINCE

Lithologies of Nain Province were outlined in Ermanovics et al. (1988), where it was suggested that supracrustal rocks may be equivalents of the Early Archean Nulliak and Upernavik association mapped by B. Ryan north of latitude 58°00' (Ryan et al., 1984). Supracrustal rocks and associated layered, mafic-ultramafic igneous rocks compose 20 to 30 per cent of the terrane and are intruded by quartzofeldspathic orthogneisses of several ages, the earliest of which may be reworked and migmatized derivatives of Uivak gneiss dated at 3450 Ma in the present area (Hurst, 1973) and 3600-3800 Ma in Saglek area (Barton, 1975; Bridgwater and Collerson, 1976; the reader is referred to Ryan et al., 1983 and 1984 for a review of Early Archean geology of Saglek and Hebron Fiord areas).

Rocks of Nain Province lie in three broadly defined N-S trending Archean metamorphic terranes that include an eastern amphibolite facies, a central polymetamorphic granulite/amphibolite facies, and a western granulite facies. Extensive zones of straightened north-to northwest-trending gneiss occur throughout Nain Province at amphibolite and greenschist facies grades. The amphibolite zones are probably related to ductile shear in steep limbs of regional upright F_2-folds, whereas those of greenschist facies may have been reactivated and retrograded during the early Proterozoic.

The eastern amphibolite facies terrane is confined to the base of the Kaumajet Mountains where rocks of Proterozoic Mugford Group lie unconformably on rocks of Nain craton (Fig. 1). The Mountains (relief and elevation 1200 m) are separated from the mainland granulite/amphibolite facies terrane by a system of ductile and brittle faults several kilometres wide that extends along a line from Napaktok Bay to Blow Hard Island (Fig. 1). This fault system is

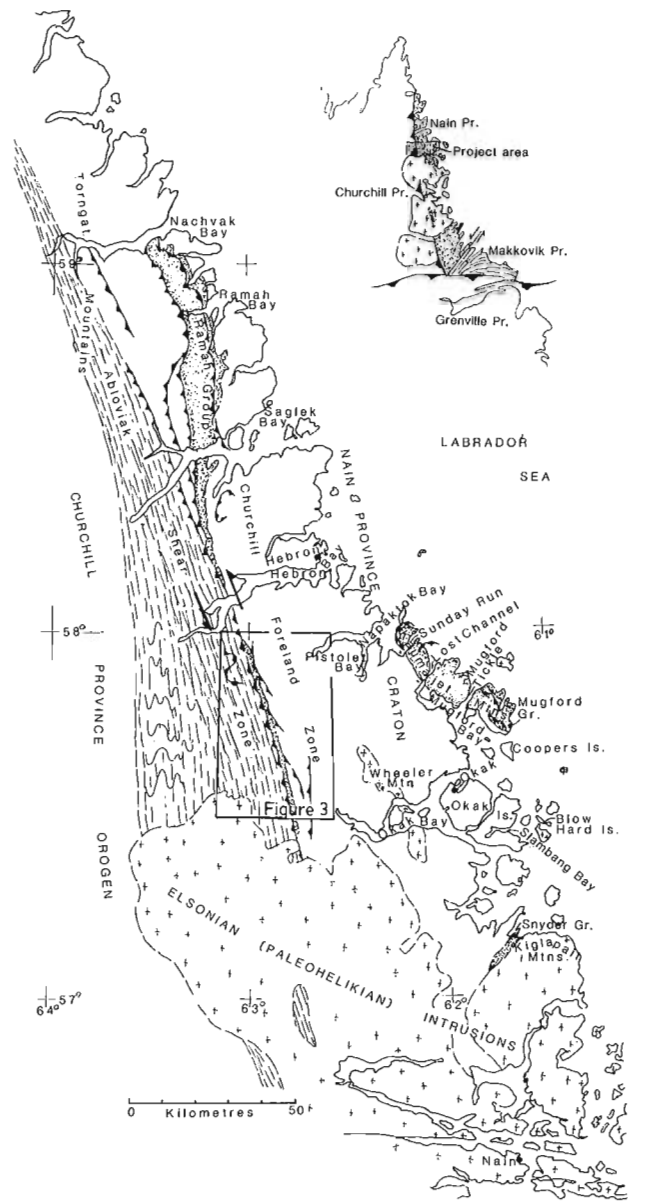

Figure 1. Location of project area and major tectonic units. Dash-pattern shows the distribution of Tasiuyak gneiss (after Taylor 1977 and 1978) that north of 58°30'N also coincides with 160°-trends of Abloviak Shear Zone (Korstgard et al., 1987). Between 57°30'N and 58°00'N the western portion of Tasiuyak gneiss occupies open, subhorizontally plunging folds unaffected by pervasive Abloviak Shear. Arrows show direction of transcurrent sinistral shear movement based on internal C&S fabrics in Tasiuyak gneiss and on regional, counterclockwise rotation of Proterozoic Napaktok dykes, tectonic remnants of Ramah Group, and Archean structures of Churchill Foreland Zone. Box locates Figure 3.

thought to predate Mugford Group, generating subsidence toward the east, which was accompanied by the deposition of pyritic muds and mafic volcanics of Mugford Group on Archean amphibolite facies rocks. Subsequent uplift across the fault system exhumed Archean amphibolite facies rocks with Mugford cover rocks, but exhumed deeper crustal granulite/amphibolite facies rocks west of the fault system.

The central granulite/amphibolite facies terrane exhibits complex high-grade relationships not yet understood. Here xenoliths with complex internal fabrics at granulite facies occur in amphibolite facies rocks that show evidence of having been at a higher grade; both facies can be cut by quartzofeldspathic segregations and dykes that contain hypersthene. The terrane appears to show at least 2 phases of high grade metamorphism and deformation with complex retrograde and prograde reactions.

The western granulite terrane, like the eastern amphibolite terrane, is structurally relatively simple. D_2 - deformation took place at granulite facies 2.8 Ga ago (L. Schiotte, Geological Museum Copenhagen, pers. comm., 1987). The terrane contains layered intrusions composed of anorthosite, quartz diorite, gabbro and mafic-ultramafic rocks preserved with the supracrustal sequences, all at granulite facies. Anorthositic rocks, as discontinuous tectonic fishes hundreds of metres long, also occur immediately east of the main fault zone of the Nain-Churchill Bourder Zone where they may represent lower crustal lithologies exhumed during faulting.

The Nain Province thus shows a metamorphically zoned crust of Archean age across a 85 km width that exposes an oblique section of progressively deeper crustal levels toward Churchill Province. This trend was also detected in southern Nain Province in Hopedale block (Ermanovics et al., 1982) where coastal amphibolite facies Maggo Gneiss passes westward, through a zone of clinopyroxene-perthite migmatite, to granulite facies Maggo Gneiss equivalent rocks at the Churchill-Nain boundary. Maps by Ryan et al., (1983, 1984), Morgan (1975b, 1978) and Taylor (1977, 1978) north of latitude 58°, show similar distributions of granulite facies rocks including the occurrence of anorthositic rocks. This upward flexuring of Archean crust is probably related to the onset of Proterozoic orogeny in Churchill Province to the west.

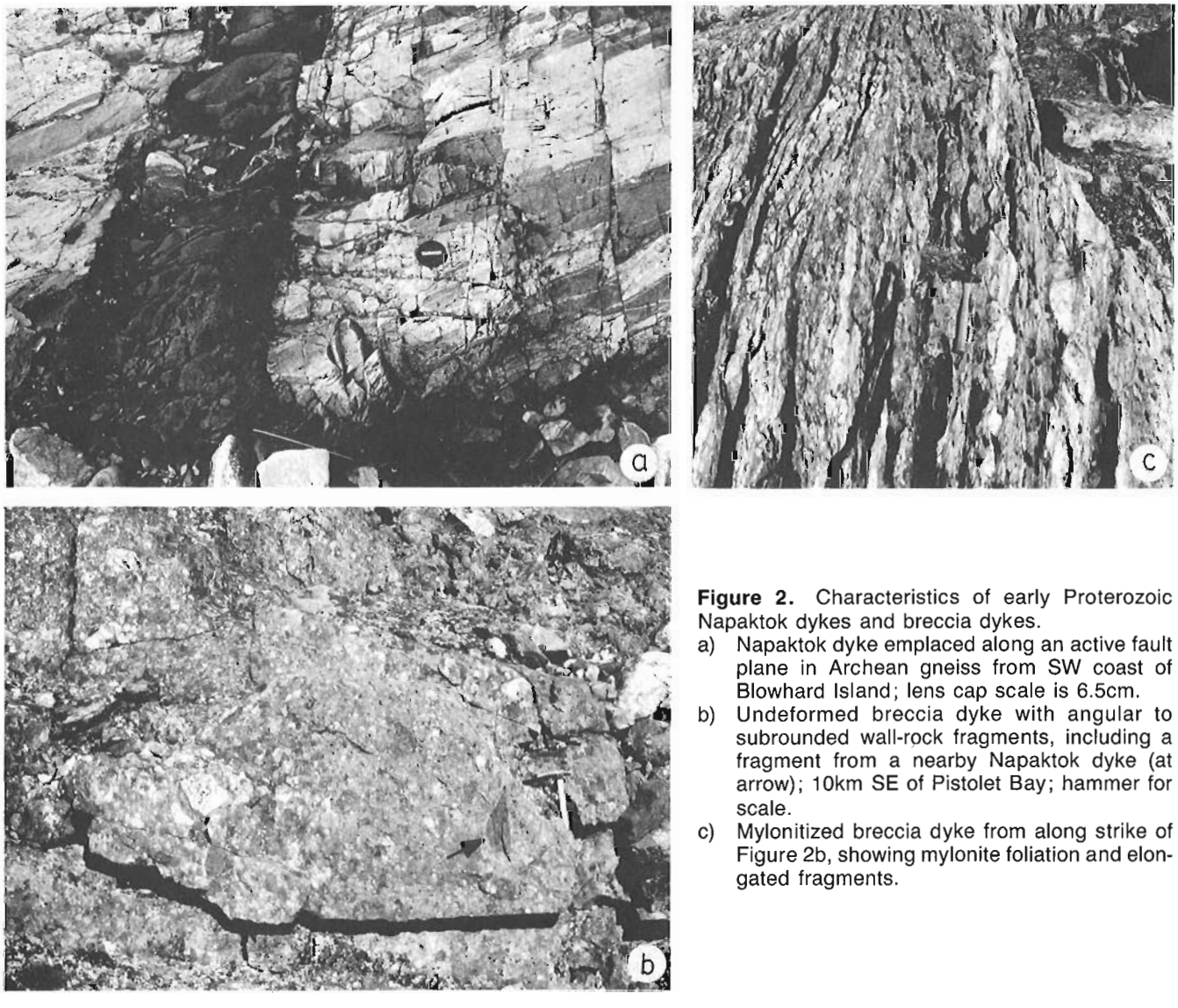

Figure 2. Characteristics of early Proterozoic Napaktok dykes and breccia dykes.

a) Napaktok dyke emplaced along an active fault plane in Archean gneiss from SW coast of Blowhard Island; lens cap scale is 6.5cm.
b) Undeformed breccia dyke with angular to subrounded wall-rock fragments, including a fragment from a nearby Napaktok dyke (at arrow); 10km SE of Pistolet Bay; hammer for scale.
c) Mylonitized breccia dyke from along strike of Figure 2b, showing mylonite foliation and elongated fragments.

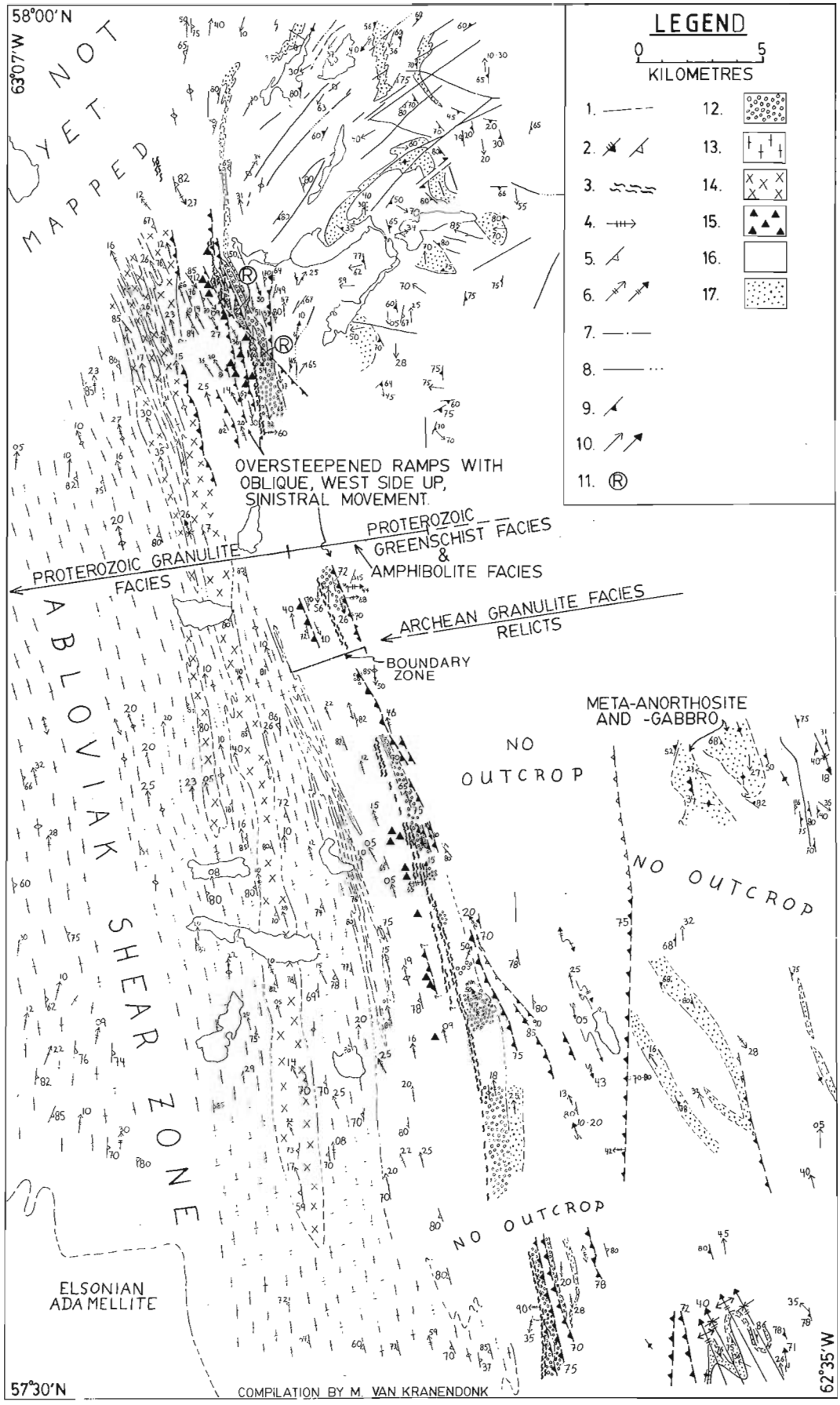
58°00'N
63°07'W
NOT YET MAPPED
LEGEND
0 5
KILOMETRES
1.
2.
3.
4.
5.
6.
7.
8.
9.
10.
11. ®
12.
13.
14.
15.
16.
17.
OVERSTEEPENED RAMPS WITH OBLIQUE, WEST SIDE UP, SINISTRAL MOVEMENT.
PROTEROZOIC GREENSCHIST FACIES & AMPHIBOLITE FACIES
PROTEROZOIC GRANULITE FACIES
ARCHEAN GRANULITE FACIES RELICTS
BOUNDARY ZONE
META-ANORTHOSITE AND -GABBRO
NO OUTCROP
NO OUTCROP
NO OUTCROP
ABLOVIAK SHEAR ZONE
ELSONIAN ADAMELLITE
57°30'N
COMPILATION BY M. VAN KRANENDONK
62°35'W

Proterozoic activity in Nain craton

Nain Province served as a cratonic block retaining most of its Archean structural elements during early Proterozoic time. In the project area Proterozoic activity in Nain Province includes:

1. Emplacement of diabase dykes (Napaktok dykes);
2. Graben faulting or crustal flexuring and depositioning of Ramah and Mugford groups;
3. Development of breccia dykes;
4. Greenschist metamorphism and crustal block rebound east of the Churchill Foreland Zone; amphibolite and granulite facies metamorphism in Churchill Foreland Zone, and exhumation of terranes along steep dip-slip faults across the Boundary Zone;
5. Intrusion of Helikian granites, anorthosites and diabase dykes (Nutak dykes) following cratonization of both Nain and Churchill provinces.

Regionally, diabasic and gabbroic dykes (Napaktok dykes) were emplaced along an approximately conjugate set of ENE-WSW, and NW-SE trending active shear belts (Fig. 2a) that predate deposition of Mugford and Ramah groups. All Napaktok dykes in the map area are metamorphosed, from chlorite-biotite-epidote±actinolite along coastal areas, through hornblende-biotite grade in the Churchill Foreland Zone, to garnet-hornblende± clinopyroxene in the Boundary Zone where they were rotated anticlockwise to become subparallel to the NNW transcurrent shear direction. The contacts of dykes and wall-rocks initially exhibit brittle fracture at lowest greenschist grades, and mylonite, Z- and S-folds and pervasive ductile shear at progressively higher grades of metamorphism. An aggregate moderately steep quartzofeldspathic mullion or hornblende lineation develops where the dykes are rotated in Churchill Foreland Zone at amphibolite facies. North of latitude 58°40' these dykes were recognized in Proterozoic granulite facies rocks derived from Nain rocks (Morgan, 1975a, b); however, south of that latitude, including the present map area, they have not been detected in Proterozoic granulite facies terranes (see maps by Mengel, 1988; Ryan et al., 1983, 1984).

The stress resulting in the conjugate shear pattern in which the Napaktok dykes were emplaced, probably resulted in the crustal flexuring of Nain Province into basins in which Ramah and Mugford groups were deposited. Quartzite, pelitic metasediments and minor associated garnetiferous pyroxenite have now been mapped the length of the Boundary Zone (Fig. 3) and correlated with basal formations of Ramah Group (cf. Ryan et al., 1984). The metasediments contain abundant white pegmatite, granite and neosomal streaks and represent tectonic remnants at amphibolite facies. Rocks of basal Ramah from the type-locality (Torngat Mountains, Fig. 1) were interpreted as a shallow, siliciclastic shelf deposit deepending to basinal conditions to the west toward a terrane that is now occupied by Churchill Province (Knight and Morgan, 1981). Mengel (1988), on the basis of Condie's 1982 classification of Proterezoic supracrustal sequences, concluded that the basal Ramah represents stable continental margin or intracratonic basin deposits. The Mugford Group is lithologically similar to the basal formations of Ramah Group (Smyth, 1976) although little or no quartzite is present in the Mugford Group. Several intergroup correlations have been suggested (Taylor, 1979; Smyth and Knight, 1978). Both pyritiferous slates and argillites, and amydaloidal pillowed and tubular basalts lie directly on Archean rocks that locally have a regolithic horizon developed at the unconformity. Mugford Group rocks are subgreenschist to locally greenschist grade as are Napaktok dykes beneath the unconformity. Mugford Group occupies a large northwest-trending synclinorium (dips of limbs 10-40°) within which northwest-plunging tight, upright anticlines and synclines are developed locally (Smyth, 1976). Thrusts with minor offset of tens to hundreds of metres are generally east-directed. A major northwest-directed thrust on the northwest terminus of the Mugford Group repeats the basal unconformity there (Smyth, 1976). Thrust faults as subhorizontal ramps occur on the eastern side between Lost Channel and Sunday Run in basement rocks but the amount of movement could not be assessed. North- and northwest-trending normal faults postdate thrust faults and have tens of metres of dip-slip movement. Movement on the system of faults on the western side of the Mugford Group (discussed above) must have been great because not only is the group only exposed east of the faults, but also because granulite facies Archean basement west of the faults is juxtaposed against amphibolite facies basement east of the faults. The structure, metamorphism and lithology of Mugford Group are thus similar to the least deformed basal members of eastern Ramah Group in the Torngat Mountains as exposed in Rowsell Harbour and Reddick Bight formations at Rowsell Harbour (cf. Map 1469A, Morgan, 1975b).

Breccia dykes (Fig. 2, 2c) with wall-rock fragments of up to 80 cm occupy the prominent 140° trend of lineaments in a zone 12 km wide adjacent to the system of faults west

Figure 3. Geological map of Proterozoic tectonic elements of the Boundary Zone of Nain and Churchill provinces; location is shown in Figure 1. Symbols are as follows: 1. geological contact defined, inferred; 2. dip-slip fault; observed (locally with oversteepened, east-dipping planes indicated by triple dip dash), extrapolated; 3. glassy ultramylonite zone with stretching lineation indicated (4); 5. Proterozoic planar fabric and associated stretching lineation (6, open arrows) and fold axis (6, full arrow with fold-asymetry); fabrics from east to west are initially defined by L-S quartz fabric and penetrative schistosity, and with increasing strain by polydeformed Ramah Group metasediments and L>S fabrics in orthopyroxene gneiss and Tasiuyak gneiss; 7. Tectonic contact between Ramah Group and Archean rocks; 8. Napaktok dykes, observed, extrapolated; 9. gneissosity and associated lineation (10, open arrow) and fold axis (10, full arrow) of rocks of the Churchill Foreland Zone; 11. regolith localities beneath Ramah Group; 12. Ramah Group; 13. Tasiuyak gneiss; 14. homogeneous hypersthene orthogneiss; 15. meta-anorthosite as tectonic lenses in masses tens to hundreds of metres long; 16. unornamented areas east of the glassy mylonite (3) comprise variously restructured rocks of Nain Province at Proterozoic amphibolite facies; west of the glassy mylonites similar rocks at amphibolite and granulite facies occur, 17. supracrustal rocks of Nain Province.

of Mugford Group (Kaumajet Mountains). The zone also contains a prominent SE-NW trending set of Napaktok dykes cut by or associated with the breccia dykes. Previously interpreted as clastic dykes related to the deposition of the Mugford Group (Ermanovics et al., 1988), the breccia dykes consist of up to 80 per cent angular to rounded wall-rock fragments (not less than 100 um) in a fine grained matrix of green metamorphic biotite probably derived from rock flour (H. Helmstaedt, pers. comm., 1988) that recrystallized during greenschist metamorphism. Coarse fragments include diabase dyke and finely laminated mylonite fragments (Fig. 2b) derived from adjacent Napaktok dykes and wall-rocks. The breccia dykes are 2 to 6 m wide, can attain strike lengths of several tens of kilometres, and are generally proximal to, or in contact with, or actually cut, sheared Napaktok dykes. On breccia dyke, not associated with Napaktok dykes, permitted interpretation of the breccia dykes as a separate set of explosive volatile-rich igneous dykes. This dyke is 1.5 m wide, aphanitic and fragment free over most of its 400 m strike length except where at mid-length it expands to a pipe-shaped body 50 × 200 m that contains abundant fragments of distinctive pink granitoid wallrocks. Similar breccia dykes occur at the base of the fault scarp that bounds the western side of Mugford Group and others were reported by Smyth (1976) and Taylor (1979) in similar settings. One of these dykes contained partly resorbed siltstone fragments in a frothy vesicular matrix and thus postdates Mugford Group. If these and other breccia dykes are coeval, they postdate or may be synchronous with deposition and volcanism of Mugford Group. Their location within lineaments and faults that also host previously sheared Napaktok dykes of pre Mugford Group age suggests that they developed within long-lived zones of weakness, initiated with emplacement of the Napaktok dykes.

Proterozoic metamorphism was superimposed on the zoned Archean crust described earlier. Thus the eastern amphibolite facies Archean rocks are retrograded and the overlying Mugford Group cover-rocks have been metamorphosed to low greenschist facies. The central granulite/amphibolite facies terrane was retrograded by lower and upper greenschist facies. The western granulite terrane was retrograded by Proterozoic amphibolite facies in Churchill Foreland Zone, and altered and restructured during upper amphibolite and granulite facies in the Boundary Zone. Nain Province rocks in the Boundary Zone thus attained granulite facies twice, separated in time by probably one billion years.

An important group of Helikian diabases (Nutak dykes) occur throughout the map area and although the overall swarm direction has not been determined everywhere, they strike generally N-S in the southeastern part of the project area. They are undeformed, commonly gabbroic, olivine-titanaugite-bearing dykes, containing 70 per cent plagioclase and postdate Elsonian plutonism in the area. Nutak dykes may be coeval with lithologically similar dykes, the Harp dykes (Meyers and Emslie, 1977), that intrude the Paleohelikian Harp Lake Complex and Archean rocks of southern Nain Province in Hopedale block (Ermanovics et al., 1982).

CHURCHILL PROVINCE

Rocks of Churchill Province are at granulite grade and, to the extent mapped (as far west as 63°25'W), contain no proven Nain Province rocks. Three groups of rocks were recognized: 1) white and rusty Tasiuyak gneiss (garnet-quartz-feldspar gneiss, unit Afg of Taylor, 1977 and 1979), 2) brown or green hypersthene leucogneiss (less than 5 per cent) and, 3) rare, black, two-pyroxene-garnet ultramafic rocks. Tasiuyak gneiss was the name given by Wardle (1983) at Nachvak Fiord to the distinctive polylithic gneisses mapped by Morgan (1975b, north of Saglek Fiord) and Taylor (1977, in the project area) as white, banded, garnet-quartz-feldspar gneiss containing layers of sillimanite and graphite. These workers, as well as others (Ryan et al., 1984 and 1983; Mengel, 1988), recognized that the gneiss contained a sedimentary and granitic component and that everywhere the pervasive fabric was a shear fabric formed during the formation of the gneiss at granulite facies grade. Thus in the northern areas Tasiuyak gneiss became a synonym for Abloviak Shear Zone (Korstgard et al., 1987, Tasiuyak mylonite gneiss).

In the present map area, however, the gneiss widens to 45 km compared with 5 to 20 km farther north and unsheared Tasiuyak gneiss is preserved in the western portion, 35 km west of the Boundary zone (63°25'W, Fig. 1). Here rusty pelitic rocks and minor quartzite and calc-silicate rocks are mixed with at least 50 per cent white garnetiferous leucosome and these are intruded by white, garnetiferous megacrystic granitic rocks that form kilometre-scale screen-migmatite at contacts with metasedimentary rocks. These rocks occur in open subhorizontal plunging folds (0-10° north or south) with limb-dips 0 to 40°, and wave lengths of up to 1500 m. The granitic rocks contain a shallow-plunging L-fabric defined by feldspar megacrysts and appear to occupy domal sheets locally concordant to layering. The terrane is thought to be at granulite facies, although more petrographic and structural work is required in this area.

Entering the Abloviak Shear Zone from the west (63°15'W) the limbs of folds are progressively steepened and locally sheared with the result that lithologies are transposed to lenticular domains at all scales. Subhorizontal quartz rods, diagnostic of Abloviak Shear develop locally. The sequence of events shows that pelitic and quartzitic layers were cut by migmatite and pegmatite layers, then isoclinally folded, and subsequently intruded by white granitoid sheets. Shear, superimposed on this assemblage and structure, produced shallow and subhorizontal mineral lineations in subvertical foliation planes (see also Wardle 1983, and Ryan et al., 1984).

The pervasive highly strained Abloviak Shear in the Tasiuyak gneiss (about 25 km wide) lies adjacent to the Boundary Zone (Fig. 1). In these high-strain zones, Tasiuyak gneiss contains 'white' layers and 'rusty' layers. Rusty layers are the most readily recognized sedimentary components and contain fine grained biotite folia wrapped around centimetre-scale garnet or oligoclase or both. Garnets (20-30 %) are pre-and synkinematic with respect to shear. Sillimanite, streaks of graphite, and quartz rods define the regional generally north-plunging subhorizontal

mineral lineation (0 to 25°). Non-aligned sillimanite needles occur in pressure-shadows of large porphyroblasts/-clasts. Quartz can attain more than 50 per cent and biotite varies up to 10% in folia; graphite is common and can occur as coarse blades in pegmatoid phases of the gneiss. White layers adjacent to rusty layers are interpreted as 'granitic' leucosome and contain less biotite, no graphite, and are finer grained; quartz-rich components are absent. Garnet occurs as small (1-5mm), red or pink, rounded homogeneous grains and as lenticular coarse, porphyroclasts in sillimanite-bearing quartzofeldspathic rocks.

Two main types of brown to buff-coloured orthopyroxene-bearing gneiss occur both in Tasiuyak gneiss terrane and in the Boundary Zone. One type is a variegated polylithic, layered rock coextensive with Nain Province that can be traced from east to west, becoming progressively deformed as it passes into the Boundary Zone. West of the Boundary Zone this gneiss is intercalated with Tasiuyak gneiss and the second orthopyroxene gneiss, a homogeneous hypersthene orthogneiss (CI 5-20) with subhorizontal mineral lineation. Whereas the first layered orthopyroxene gneiss is Archean, the second homogeneous orthopyroxene gneiss may be a Proterozoic intrusive rock. Lenticular bodies of granodioritic rocks with one phase of deformation and amphibolite facies alteration occur in the Boundary Zone and these may be coeval with the homogeneous orthogneisses at granulite grade. Within the main mass of Tasiuyak Gneiss, the homogeneous orthopyroxene gneiss type is more common and is intruded by a white granitic component of Tasiuyak gneiss. The western contact of Tasiuyak gneiss and orthopyroxene gneisses has not been defined, but reconnaissance shows that the orthopyroxene-bearing rocks there are coarse grained homogeneous orthogneiss (charnokite) ranging from granitic to tonalitic compositions.

Nain-Churchill Boundary Zone

The Boundary Zone varies from 4 to 6 km wide (Fig. 3). Its western contact is defined by the first appearance of Tasiuyak gneiss and on the eastern margin includes Ramah Group. Rocks in the zone also include small lenticular felsic plutons of probable Proterozoic age, and Archean gneiss, metasediments and anorthosite. The zone also contains the transition of Proterozoic amphibolite to granulite facies and the structural fabrics of transcurrent sinistral shear that is coextensive with Churchill Province. Numerous horizons of glassy mylonite with subvertical lineation are characteristic of the zone; they mark the sites of steep, dip-slip faults (west-side-up-kinematics) and postdate transcurrent shear deformation. The tectonic grain of the Boundary Zone varies from 150° to 165° and appears to be controlled by the shearing and the faulting.

In the southern half of the map area, north- and northwest-trending Proterozoic structures east of the Boundary Zone exhibit shallow to subhorizontal (both north and south plunging) S-folds (Fig. 3). These structures become progressively tightened westward and rotated toward a 160° tectonic axis. Rocks with these structures underlie Ramah Group although they are generally separated from them by steep, east-dipping faults. Ramah Group rocks showing primary depositional features locally, exhibit similar structures as the underlying gneisses but also complex folding not detected in the adjacent eastern gneisses. Shallow quartz lineation assigned to the period of Abloviak Shear are coaxial with some folds, however, more moderately and variably plunging folds predate shearing. Mineral lineation and fold axes develop more consistent plunges 160°/10-25°N in gneisses west of a major mylonite zone adjacent to Ramah Group where the effects of shear dominate.

In the northern half of the map area, Archean gneisses and Napaktok dykes, assumed to have had an E-W grain highly discordant to the present Proterozoic northerly (160°) grain, were rotated anticlockwise. This reorientation is assigned to the Abloviak Shear episode and postdates earlier structures in Ramah Group. Ramah Group rocks have primary structures and preserved regolith but contain refolded rootless isoclines. S-folds, interpreted to be the products of shear, were the cause of the refolding (Fig. 4b). Metamorphic lineations in the Ramah Group and its basement are similar, although plunges (5-25°) can vary north or south among contiguous 100 metre scale domains; fold axes are more variable with plunges locally of 50°. The variations probably reflect incomplete reorientation during shear deformation of early Proterozoic structures. Mineral lineation plunge is consistently 160°/10-30°N in granulite facies of the Boundary Zone.

Although faults are present throughout the Boundary Zone, the main fault is located along a 100-150 m wide porphyroclastic to glassy ultramylonite immediately west of Ramah Group rocks (Fig. 4d, and Fig. 3). The mylonite contains subvertical mineral lineations plunging east or west that postdate transcurrent shear fabrics. Wall-rocks of the mylonite show retrogression to epidote-chlorite grades. Other faults in eastern Boundary Zone dip east (80°), while those to the west in granulite facies are vertical to west dipping (80-70°). The movement sense on all faults is west-side-up. Within the eastern Tasiuyak gneiss unit these faults have more moderate dips and indeed the steeper faults in the Boundary Zone are considered to be oversteepened ramp-faults.

Immediately west of the major fault zone both rocks of Nain Province (including anorthosite) and Proterozoic plutonic rocks are exposed. As suggested earlier, the plutonic rocks may be coeval with lineated hypersthene orthogneiss within the western Boundary Zone and within the Tasiuyak gneiss unit. Lenticular masses of anorthositic rocks on the scale of hundreds of metres may be tectonic masses exhumed from deeper levels of Archean crust during faulting in the Boundary Zone.

The overall effect of faulting in the Boundary Zone was to shorten what is assumed to have been an orderly, progressive foreland deformation pattern in Nain Craton to a stacked out-of-sequence order. This was accomplished with the superposition of a hot, dry, more highly deformed granulite facies terrane against tectonized, amphibolite facies Proterozoic cover rocks. North of Saglek Fiord where complete sections of Ramah Group are exposed, evidence of transcurrent shear is absent in Ramah Group, although ample evidence for sinistral shear occurs in Nain

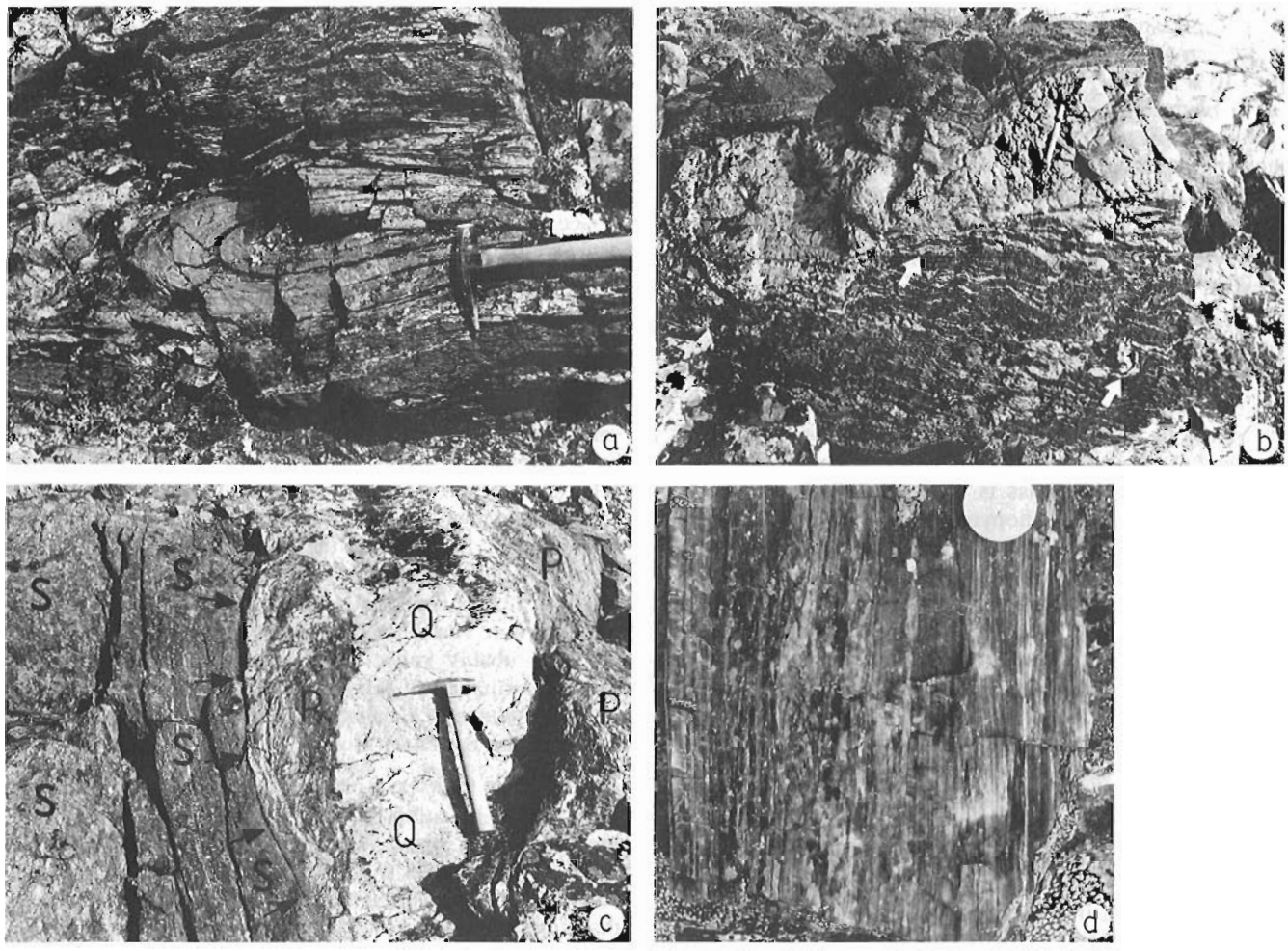

Figure 4. Structures in Ramah Group metasediments. a) Isocline of quartzite (at hammer) interpreted to have formed along intraformational contacts of the type shown in Figures 4b and 4c. b) Quartzite (white, with 13cm pen scale) is overlain by a conformable upward fining sequence of metasediment (dark layer) but cuts layering of an underlying quartzofeldspathic metapelite along an intraformational tectonic contact. Isoclinal folds in this metapelite (white arrow at centre) formed during development of such tectonic dislocation surfaces; S-folds (white arrow lower right) subsequently refolded isoclinal folds of less competent components of metapelite. c) Quartzite (Q) and conformable metapelite (P) of Ramah Group is in contact with Archean metapelite (S), along a curved thrust fault (demarcated by arrows). Faults such as these, as well as the intraformational dislocations of Figure 4b, formed during early phases of deformation of Ramah Group and were succeeded by brittle thrusts located in mylonites. d) Glassy ultramylonite typical of the western contacts of Ramah Group; Canadian 5-cent piece scale.

rocks to the west (Morgan, 1975a; Mengel, 1988). Here too, however, thrust faults, cutting both basement and cover, juxtapose granulites on the Ramah Group (Morgan, 1975b).

In general, the tectonic elements within the Boundary Zone are similar, if not identical, to those described by Ryan et al. (1984) in the adjacent Hebron Fiord area north of 58°00'N, and by Morgan (1975a) and Mengel (1984, 1985, 1988) north of Saglek Fiord. Our interpretation differs in that we link Abloviak shearing with one of the last phases of deformation in Ramah Group as well as of rocks of the Boundary Zone, and furthermore suggest that pre-Abloviak Shear deformations in Churchill Province could also have affected distal deposits such as Mugford Group in Nain Craton.

DISCUSSION

Tectonic interpretation of the Nain-Churchill boundary raises the question of the origin of granulite facies Tasiuyak gneiss in the eastern Churchill Province. Taylor (1979) suggested that this unit was derived from Proterozoic rocks; in his map-legend he correlated it with Lake Harbour, Snyder, Ramah and Mugford groups. Morgan (1978) equated it to lithologically similar Archean metasediments, and Wardle (1984) and Ryan et al. (1984) suggested high-grade Archean protolith (eg. Upernavik metasediments) as its source, following dry reworking during Hudsonian Orogeny.

Ramah Group metasediments in the Boundary Zone are in tectonic contact with Archean metasediments at several localities (Fig. 3 and 4), and white garnetiferous migmatite

and pegmatite can constitute more than half of the lithologies of some outcrops. The distinction between Archean and Proterozoic metasediments however, is lost where the rocks are at granulite grade and have undergone pervasive shear deformation. The rocks develop transitional textural aspects of white Tasiuyak gneiss. At a number of localities unequivocal assignment of these rocks to the Tasiuyak gneiss was problematical. Rocks of this transitional nature occur in an 8 km wide zone west of the Boundary Zone where layered gneiss (Archean?), homogeneous orthogneiss, Tasiuyak gneiss, and the problematical gneiss are intercalated at scales of metres to hundreds of metres. This part, west of the Boundary Zone, warrants further study because the transition of lithologies may represent the passage of the largely migmatized Ramah Group sediments and basements rocks of the Boundary Zone into the Tasiuyak gneiss terrane.

The pre-syn-and postkinematic fabrics of sparse and fine grained biotite and sillimanite, and coarse grained garnet, feldspar and quartz in Tasiuyak gneiss suggest that more than one high grade metamorphic pulse drove the reaction quartz+biotite+sillimanite singularly toward formation of garnet+K-feldspar ($\pm$oligoclase) under very low P_{H_2O} and reducing conditions (graphite, pyrite), forming at least two generations of white restites and mobilizates. Peak metamorphic pressure and temperature are estimated at 10 kbar at 800°C. These P-T estimates were obtained from the cores of continguous minerals, some which like garnet, show multiple growth rims (Mengel, 1988). It is uncertain whether or not peak metamorphic conditions prevailed during Abloviak shearing.

The locally pervasive Abloviak shearing of Tasiuyak gneiss was late and appears to have restructured already dry rocks of the type exposed in the western Tasiuyak gneiss terrane. The shearing is manifested by S-folds and C&S planes, defined by quartz-ribbons (S) and biotite (C), everywhere indicating sinistral displacement in the horizontal plane. As such the transcurrent sinistral shearing caused anticlockwise structural reorientation of Churchill Foreland Zone rocks and is thus not confined only to the evolution of Tasiuyak gneiss.

In the project area the sequence of open folding-refolding-and transcurrent shear of Proterozoic supracrustal rocks is developed from east to west in Nain Craton and from west to east within the Tasiuyak gneiss terrane. Although this deformational sequence developed in facies of greenschist to amphibolite-granulite metamorphism in Nain Craton, these episodes appear everywhere synchronous with high-grade metamorphism in Churchill Province.

ACKNOWLEDGMENTS

We are grateful to a number of persons who made the 1988 field season the great success it was. These include Francis Falardeau (John Hopkins University), Ninna Raunsback (University of Copenhagen) and Christopher Barefoot. Roger Caissie and Jim Watson, staff pilots of Universal Helicopters Ltd., Goose Bay, were outstanding not only in their capacity as flyers but proved untiring in their efforts to help run camp smoothly. A number of colleagues contributed substantially to our ideas and work during brief field visits. These include Bruce Ryan (Department of Mines, Newfoundland), Herbert Helmstaedt (Queens University), Simon Hanmer (GSC), and Jean-Michel Bertrand and Anne-Marie Boulier from the Centre National de la Recherche Scientifique, Vandœuvre-les-Nancy. We are indebted to John Henderson and Tony Davidson for their help and review of the manuscript.

REFERENCES

Barton, J.M., Jr.
1975: Rb-Sr isotopic characteristics and chemistry of the 3.6 b.y. Hebron gneiss, Labrador; Earth and Planetary Science Letters, v. 27, p. 427-435.

Bridgwater, D. and Collerson, K.D.
1976: The major petrological and geochemical characters of the 3600 m.y. Uivak gneisses from Labrador; Contributions to Mineralogy and Petrology, v. 54, p. 43-59.

Ermanovics, I.F., Korstgard, J.A., and Bridgwater, D.
1982: Structural and lithological chronology of the Archean Hopedale block and the adjacent Proterozoic Makkovik Subprovince, Labrador: Report 4; in Current Research, Part B, Geological Survey of Canada, Paper 82-1B, p. 153-165.

Ermanovics, I.F., Van Kranendonk, M., Corriveau, L., Bridgwater, D., Mengel, F., and Schiotte, L.
1988: Geology of the North River-Nutak map areas, Nain-Churchill provinces, Labrador; in Current Research Part C, Geological Survey of Canada, Paper 88-1C, p. 19-26.

Hurst, R.W.
1973: The early Archean of coastal Labrador; in The Nain Anorthosite Project, Labrador: Field Report 1973, edited by S.A. Morse, p. 29.

Knight, L. and Morgan, W.C.
1977: Stratigraphic subdivision of the Ramah Group, northern Labrador; Geological Survey of Canada, Paper 75-15, 31p.

Korstgard, J., Ryan, B., and Wardle, R.
1987: The Boundary between Proterozoic and Archean crustal blocks in the central West Greenland and northern Labrador; in Evolution of the Lewisian and Comparable Precambrian High Grade Terrains, edited by R.G. Park and J. Tarney, Geological Society of London, Special Publication No. 27, p. 247-259.

Mengel, F.C.
1984: Preliminary results of mapping in the Ramah Group and adjacent gneisses south of Saglek Fiord, northern Labrador; in Current Research, Newfoundland Department of Mines and Energy, Mineral Development Division, Report 84-1, p. 21-29.
1985: Nain-Churchill Province boundary: a preliminary report on a cross-section through the Hudsonian Front in the Saglek Fiord area, northern Labrador; in Current Research Newfoundland Department of Mines and Energy, Mineral Development Division, Report 85-1, p. 33-42.
1988: Thermotectonic evolution of the Proterozoic-Archean boundary in the Saglek area, northern Labrador; PhD thesis, Memorial University of Newfoundland, St. John's, Newfoundland.

Meyers, R.E. and Emslie, R.F.
1977: The Harp dikes and their relationship to the Helikian geological record in central Labrador; Canadian Journal of Earth Sciences, v. 14, p. 2683-2696.

Morgan, W.C.
1975a: Geology of the Precambrian Ramah Group and basement rocks in the Nachvak Fiord — Saglek Fiord area, north Labrador; Geological Survey of Canada, Paper 74-54, 42 p.
1875b: Geology, Nachvak Fiord — Ramah Bay; Geological Survey of Canada, Map 1469A.
1978: Geology, Bears Gut — Saglek Fiord; Geological Survey of Canada, Map 1478A.

Ryan, A.B., Martineau, Y., Bridgwater, D., Schiotte, L., and Lewry, J.
1983: The Archean-Proterozoic boundary in the Saglek Fiord area, Labrador: report 1; in Current Research, Part A, Geological Survey of Canada, Paper 83-1A, p. 297-304.

Ryan, A.B., Martineau, Y., Korstgard, J., and Lee, D.
1984: The Archean Proterozoic boundary in northern Labrador: report 2; in Current Research, Part A, Geological Survey of Canada, Paper 84-1A, p. 545-551.

Smyth, W.R.
1976: Geology of the Mugford Group, northern Labrador; in Report of Activities, Newfoundland Department of Mines and Energy, Report 76-1, p. 72-79.

Smyth W.R. and Knight, I.
1978: Correlation of the Aphebian supracrustal sequences, Nain Provinces, northern Labrador; in Report of Activities for 1977, Newfoundland Department of Mines and Energy, Mineral Development Division Report, 78-1, p. 59-65.

Taylor, F.C.
1977: Geology, North River-Nutak, Newfoundland-Quebec; Geological Survey of Canada, Map 1436A.
1978: Geology, Hebron Newfoundland-Quebec; Geological Survey of Canada, Map 1431A.
1979: Reconnaissance geology of a part of the Precambrian Shield, northeastern Quebec, northern Labrador and Northwest Territories; Geological Survey of Canada, Memoir 393.

Wardle, R.J.
1983: Nain-Churchill Province cross-section, Nachvak Fiord, northern Labrador; in Current Research, Newfoundland Department of Mines and Energy, Report 83-1, p. 68-90.
1984: Nain-Churchill Province cross-section; Rivière Baudancourt-Nachvak Lake; in Current Research, Newfoundland Department of Mines an Energy, Report 84-1, p. 1-11.

Gossans in high grade gneisses from the Blacks Inlet area, west coast of Melville Peninsula, District of Franklin, N.W.T.

Mikkel Schau and Mark Digel
Lithosphere and Canadian Shield Division

Schau, M. and Digel, M., Gossans in high grade gneisses from the Blacks Inlet area, west coast of Melville Peninsula, District of Franklin, N.W.T.; in Current Research, Part C, Geological Survey of Canada, Paper 89-1C, p. 395-403, 1989.

Abstract

Layered mylonitic granodioritic gneisses, developed from relatively homogeneous metaplutonic rocks in deep seated ductile shear zones, are widely distributed along the shores of Garry Bay on the western side of Melville Peninsula. Two episodes of ductile strain have been distinguished. An earlier strain zone with a relatively shallow dipping fabric can be traced into a later, anastomosing, moderately northwest-dipping, southwest-striking shear zone. Concordant, metasedimentary septa with magnetic metagabbro lenticles in megacrystic granites and granodiorites within the earlier strain zone are rotated into the later structures. Some of the metasedimentary septa, especially the sillimanite-bearing quartz-rich or biotite gneisses, are pyritic, and form spectacular gossans. Apart from pyrite, which occurs as disseminations along, and as veins transecting, the foliation, only minor amounts of molybdenite and chalcopyrite have been identified as sulphides in these gossans. Grab samples return. As, Au and Ag assay values near detection levels.

Résumé

Des gneiss granodioritiques et mylonitiques stratifiés, formés à partir de roches métaplutoniques relativement homogènes dans des zones de cisaillement ductiles profondes, sont très répandus le long des rivages de la baie Garry du côté ouest de la presqu'île de Melville. Deux épisodes de déformation ductile ont été distingués. Une première zone de déformation dont la fabrique à inclinaison relativement faible peut être suivie jusque dans une zone de cisaillement anastomosée à pendage modéré vers le nord-ouest et de direction sud-est qui se serait formée à une date ultérieure. Des séparations métasédimentaires concordantes avec amas lenticulaires de métagabbro magnétique dans les granites et les granodiorites mégacristallins à l'intérieur de la première zone de déformation ont pivoté dans les structures ultérieures. Certaines des séparations métasédimentaires, particulièrement les gneiss à biotite ou riches en quartz renfermant de la sillimanite, sont pyriteuses et forment de spectaculaires chapeaux de fer. À part la pyrite, qui prend la forme de disséminations le long de la foliation et de veines recoupant cette dernière, seules de petites quantités de molybdénite et de chalcopyrite ont été identifiées en tant que sulfures dans ces chapeaux de fer. Des échantillons prélevés au hazard ont donné des titres d'As, d'Au et d'Ag voisins des concentrations détectables.

INTRODUCTION

The geology in the vicinity of Garry Bay (Fig 1) straddles a transition from high grade gneisses to the west and northwest and a greenstone-granite association to the east (Schau and Heywood, 1984). Preliminary work in 1986 showed that several shear zones traversed the region and in 1988 several of these zones were mapped. Two sets were recognized; an earlier one with undulating and relatively flat dips, and a later anastomosing set with moderate west dips. The earlier set forms the border between high grade rocks to the northwest and para-and ortho-gneisses of the greenstone-granite association to the east. The later set traverses all units and formed late in the history in the region. Spectacular gossans have formed in pyritic sedimentary septa caught up in both sets of shear zones and help delineate structures. Some preliminary analyses are presented that show the gossans to be devoid of economically interesting minerals.

GEOLOGY

Regional setting

Outcrop patterns on the Melville Peninsula horst are disposed in an asymmetric manner. Archean high grade rocks typical of the deep crust occur on the northwest side of the peninsula (Schau and Beckett, 1986), whereas the east coast is underlain by a relatively higher crustal level Archean greenstone and granite association (Schau and Heywood, 1984). The asymmetry is partly caused by differential uplift in the Phanerozoic. This resulted in uplift of several kilometres along the west coast but only a few hundred metres or less along the east coast as measured from the offsets of Ordovician beds along faults (Sanford, pers comm. 1988).

Proterozoic and earlier faults cut Melville Peninsula and these have been reactivated subsequently so that most faults have a multiple displacement history. A particularly prominent, east-southeast striking, vertically dipping, fault set (referred to as latitudinal faults) traverses the peninsula at intervals of about 10 km. These define panels which contain coherent geological structures and units separated by brittle faults. Slickensides on associated minor faults indicate that dip slip and subhorizontal movements have both taken place. At one locality a piercing point was located on either side of a latitudinal fault and for that one fault the cumulate uplift was about 300 m and the cumulate sinistral transverse movement about 100 m. On other faults on the east side of Melville Peninsula apparent sinistral slip of up to 3 km has been recorded. Some of the faults and panels near Blacks Inlet are shown on Figure 2. The panel in which Blacks Inlet occurs presents an oblique section through the crust, which is cut by several branches of a later ductile strain zone. The most westerly of the branches contain relict tectonic lenses of granulitic unit A, the central branches are at amphibolite grade, and the easterly branches are associated with folds.

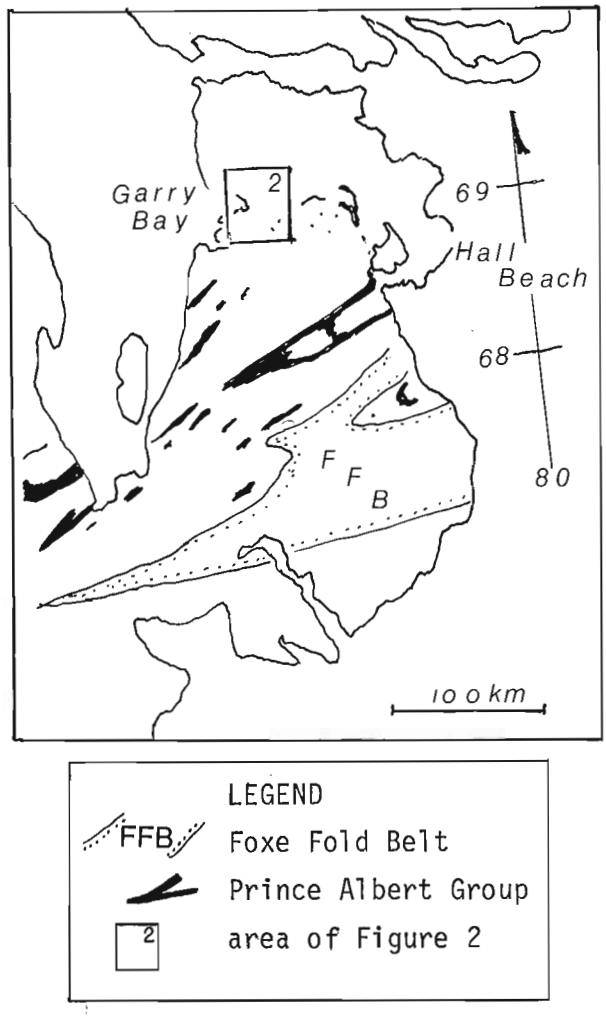

Figure 1. A location map showing the proximity of the Foxe Fold Belt to the map area as well as the nearby Prince Albert Group.

Lithological descriptions

The rocks of the study area (Fig 2) are grouped in five lithologic units.

Legend for Figure 2

Proterozoic

- Latitudinal faults
- Gossans (number as in Table 1.
- Shear zone rocks with moderate to steep, west to northwest dips

Archean

- Early flat dipping shear zone
- y. z localities mentioned in text
- M — Megacrystic granodiorite
- G — Grey gneisses
- P — Prince Albert Group.
- A — Hb-Bi tonalite to granodiorite
- B — location of Blacks Inlet, Photos from north shore at this locality
- representative foliation

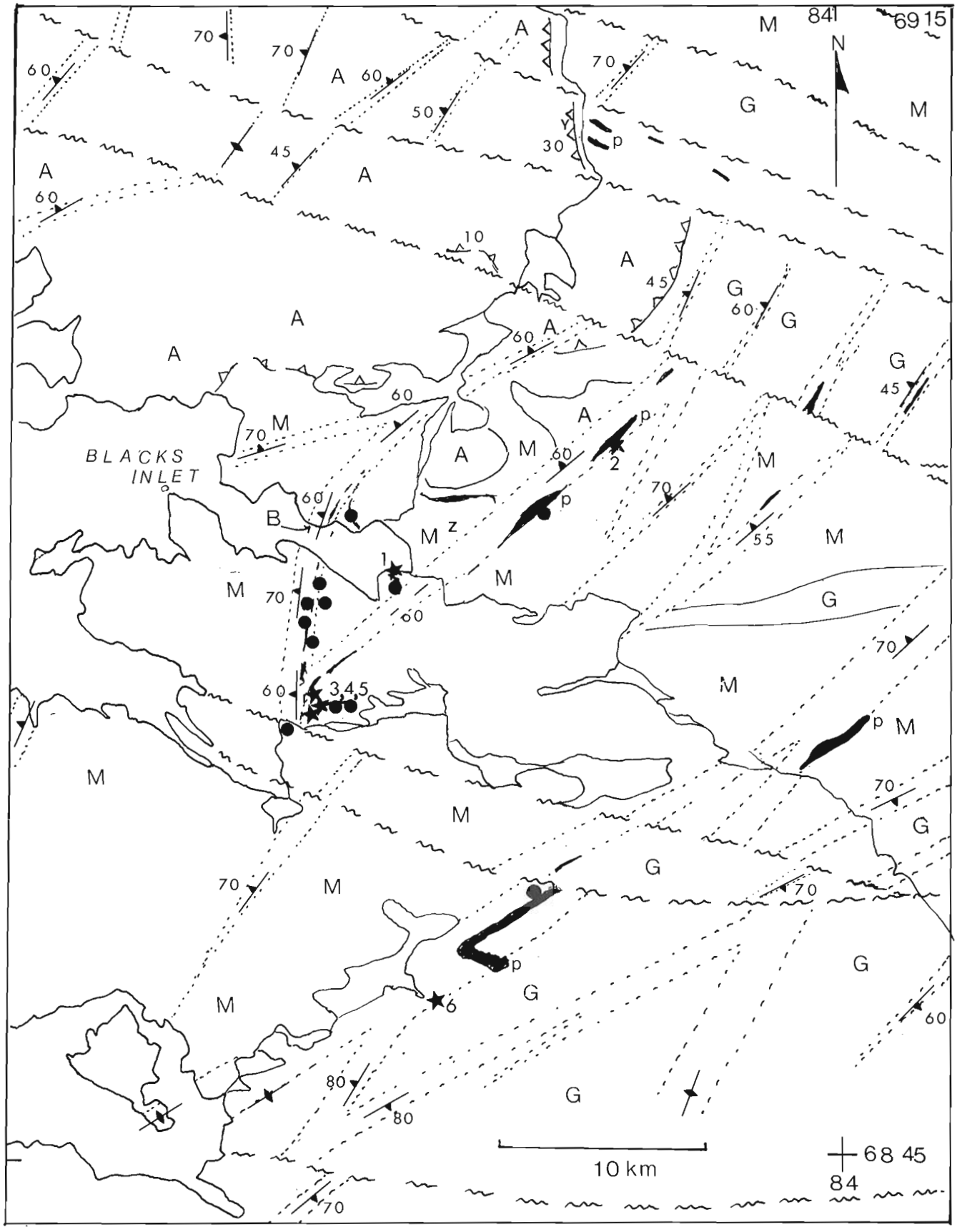

Figure 2. A sketch map of NTS 47 B/16 and 47 C/1.

Unit A

Exposed in the northwest of the area, this unit consists of variably strained, medium-grained hornblende biotite tonalite, with local development of granodiorite, and containing leucosome-dotted lenticles of deformed mafic dykes. The mineralogy is consistent with amphibolite facies metamorphism although orthopyroxene-bearing tonalite and charnockitic granite are found near the eastern border of the unit. This unit is correlated with units 1,2,and 3 described north of map area (Schau and Beckett, 1986).

Unit P

Metasediments and ultramafic pods occur as small septa and slivers in unit G. The metasediments consist of quartzose sillimanite schists with scattered grains of chromian muscovite and biotite gneisses with varying amounts of pyrite,sillimanite, garnet, and rarely, cordierite along with accessory graphite. The garnet is porphyroblastic and contains inclusions of sillimanite, hercynite, and zoned plagioclases that have the same optical zoning as plagioclase grains in the matrix. Ultramafic pods consist of various metamorphic magnesian assemblages, the most noteworthy of which is enstatite-tremolite. The enstatite grains are egg sized and weather out to form a coarse gravel at the several sites where it is found

Feldspar-phyric gabbro pods, some with magnetite, are generally associated with the metasediments, whereas small gabbroic anorthosite lenses cut unit A. These relations are also known to the north (Schau and Beckett, ibid).

The age of the sediments is interpreted to be Archean and probably correlative with the rocks of the Prince Albert Group (Schau and Beckett, ibid). New evidence for this assignment includes the association of quartzose metasediments with garnetiferous sediments and plagioclase-phyric metagabbros and with ultramafics so characteristic of the Prince Albert Group on the east coast of the peninsula.

Unit G

Gneisses with well developed compositional layering and consisting mainly of quartz, plagioclase, and biotite were probably derived from supracrustal rocks although a plutonic heritage cannot be ruled out for many of the rocks. The unit underlies a large proportion of the northern part of area. It is correlated with the widespread, informally named, Melville Peninsula Gneiss Complex that occurs over large tracts east of the map area. The age of the latter is Archean on the basis of a very discordant U/Pb age on zircon (Wanless, pers comm. 1978).

Unit M

Megacrystic granodiorite to granite occurs in the southern part of the area. Up to 2-cm-long potash feldspar phenocrysts are set in a quartz, oligoclase, microcline matrix with minor amounts of hornblende and biotite and accessory sphene. In many localities, the megacrysts have been polygonized. In some, recrystallization has completely obliterated the earlier porphyritic to seriate microstructure. The composition and the presence of sphene combined with continuity of the exposure to the porphyritic variety allows assignment to this unit. Although contacts are generally sheared, the unit intrudes units A and P which occur as flat sheets or septa in the granodiorite; there are up to several decametres thick and may extend along strike for kilometres. Structures within the septa are discordant with the enveloping foliation, and dykes of granodiorite cut the structures but are themselves terminated at the edge of the septa.

Unit M is correlated with the informally named Hall Lake Plutonic Suite of Archean age (Rb/Sr isochron, McNutt, pers comm, 1987), which occurs to the southeast. The shallow dipping foliation is locally parallel to that in the early shear zone rocks, and was presumably formed when unit A was emplaced onto the rocks to the east.

Mafic dykes

Small segments of mafic dykes are found in all above units. One particular dyke set is characterized by feldspar phenocrysts that contain a zone of garnets near the edge of the phenocrysts. This texture is also characteristic of later unit 6 dykes (see Schau and Beckett, 1986) exposed to the north where they cut all units after their deformation.

Rocks in the late ductile shear zones with south to southwest strikes and steep to moderate west to northwest dips are the strained equivalents of the above rock types. The rocks are interleaved in an intricate manner and recognizable units are lenticular in shape. The unit 6 mafic dykes (see Schau and Beekett, 1986) which, to the north are planar and cut deformed high grade gneisses there (Schau and Beckett, 1986) are deformed and disrupted, indicating that here the shearing postdates earlier deformation. Coarse biotite bearing pegmatites occur near and in the shear zones and cut them, as well as being deformed in them. Rb/Sr studies indicate a 1.8 Ga. age for a pegmatite (Prevec, 1985) similar in appearance to those within the shear zones, in which case the age would be a minimum îage of the second shear event.

Ductile Shear Zone relationships

Earlier high strain structures with relatively shallow dips appear to form the contact between high grade and intermediate grade rocks. At one such locality y (see Fig 2), granulite grade orthogneisses of unit A are seen to rest with structural discordance on amphibolite grade rocks of units G and P. The interface, which is a 100-m-wide high strain zone with tectonic lenses of the underlying units, dips 30 to 40 degrees under the granulites. Similar shallow dipping zones are found in the panel near Blacks Inlet, interleaving metaplutonic rocks of unit M with metasediments and metabasites of unit P. At locality (Fig 2) a 50-m-high klippe exposes flat lying shear zone rocks with unit M rocks below and above. Within the shear zone are small pods of disrupted metagabbro and wisps of metasediments.This shear zone can be traced along strike to the west into a later anastomosing shear zone and the foliations and layers rotate into new orientations (Fig 2). Similarly, shallow dipping pyritic metasediments immediately north of Blacks Inlet can be traced into the later shear zones where they are transposed into the new orientation.

Deformation during late ductile shearing

The shear zone branches near Blacks Inlet (B, Fig 2.) are locally very well exposed along ice-scraped and tide-cleared coast lines and have been mapped to show their anastamosing nature. A diamond-shaped area of less deformed rock-sabout 10 km by 5 km, at the head of the Inlet, surrounded by thin zones of high strain was the focus of more detailed studies. Pyritic, sillimanite-bearing, quartzose schists were traced from thin shallow dipping east-west striking enclaves in metaplutonic rocks into the southwest trending ductile zones

At location B (Fig. 2) along the north shore of the inlet, over about 1.5 km normal to strike, a medium-to coarse-grained biotite-hornblende granodiorite with xenoliths that exhibit weak shape fabric (unit A) is cut by leucogranodioritic to granitic stocks and dykes (unit M), and both are cut by mafic and pegmatite dykes. The rocks are inhomogeneously deformed and partly transformed to a finely layered granitic gneiss (see Fig 3 to 9). The outcrop displays from east to west, variegated granitic gneisses, grey gneiss, granodioritic orthogneiss, grey gneiss, and granitic orthogneiss.

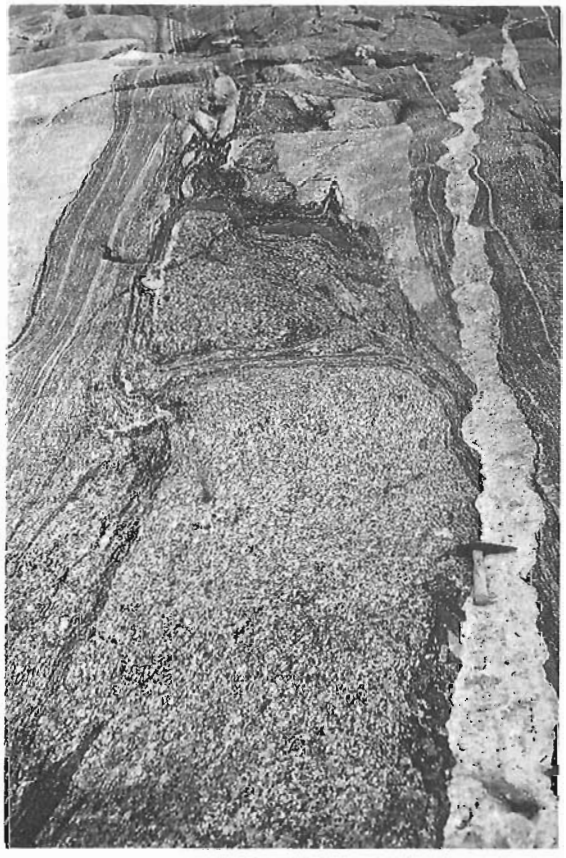

Figure 3. shows the heterogeneous strain and evidence for a long lived and complex deformational history in shear zone. A small block of granodiorite with a weak linear fabric is set in a matrix of leucogranodiorite dykes (light coloured portion near top of picture and near left edge) and sheared granodiorite (grey gneiss). Note the anastomosing shear-strands and the later, now attenuated pegmatite which, with continued strain, has rotated nearer the shear foliation. G.S.C. 204455-B.

The least deformed unit is granodioritic orthogneiss which consists of coarse-grained biotite and hornblende granodiorite. A sugary aggregate of feldspar pseudomorphs megacrysts of feldspar. Decimetre sided xenoliths of similar mineralogy but higher colour index and finer grain size are vaguely linear (1:1:2). Small blocks of granodiorite are locally preserved within higher strain rocks with which they have a gradational contact (Fig. 3).

Granitic orthogneiss is generally white to creamy weathering, low colour index biotite granodiorite to granite speckled with rare centimetre sized metamorphic garnets.In thin section the potash feldspar is seen to be microcline. Although elsewhere olive weathering colours are generally indicative of the presence of orthopyroxene, in the granitic orthogneisses at this locality these colours result from the chloritization of biotite. Wisps of rock with higher colour index are irregularly distributed through the mass suggesting that these granitic rocks have apparently responded in a more fluid manner than the neighboring granodioritic rocks (Fig 4). Subsequently they have been cut by an amphibolitized dyke which is now deformed into tight folds at small angles to the gneissosity. These dykes have been cut by an aplite dyke set which is also folded, though not as tightly as the basic dykes, and a later relatively planar, northeast-trending pegmatite set.

Figure 4. shows deformed and disaggregated mafic dyke in foliated leucogranite cut by later granitic seggregation veins and dykes. North shore, Black's Inlet, looking south. G.S.C. 204455.

Grey gneiss is a high strain equivalent of the above units displaying extremely reduced grain size and continuous mylonitic layering as well as dismembered and disaggregated pegmatites. Foliation is transposed into a new, well developed, foliation while xenoliths are attenuated (Fig 5). Asymmetric segregation veins are rotated into the shear zone and new segregation veins have formed at low angles to the foliation. Lenticular boudins of mafic dykes are found, cut by later granitic segregation veins and dykes. Pegmatites, aplites and segregation veins occur in various states of deformation (Fig 5), ranging from completely disaggregated streaks within the foliation to little or non-deformed discordant dykes. Segregation veins form along inflections in the foliated grey gneiss.

The variegated granitic gneiss is probably the most highly strained rocks in the area. Asymmetric boudins (Fig 6) and several sets of deformed segregation lenticles and veins occur in grey gneiss. The reduction in grain size and rotation of foliation is well shown in Figure 7. The end product of shearing granodiorite with xenoliths cut by successive generations of pegmatite and aplite veins and mafic dykes is represented by straight gneiss. Some segregation veins are rimmed by biotite selvedge suggesting that they are locally derived.

Figure 5. shows contact between less deformed granodiorite cut by asymmetric seggregation veins to left of picture and more deformed grey gneiss made by rotating seggregation veins into shear foliations and the development of new seggregation veins at low angles to the foliation. North shore, Black's Inlet, looking south. G.S.C. 204456-O.

Minor structures in the higher strain rocks include non-cylindrical folds and mineral lineations with variable but subhorizontal plunges. From the orientation of asymmetric features and the deflection of foliation into zones with the most reduced grain size it is concluded that this shear zone has a sinistral component. Unreliable indicators such as the asymmetric disharmonic fold shown in Figure 8 viewed

Figure 6. shows asymmetric boudinage forming in straight gneisses in high strain zones. North shore, Black's Inlet, looking south. G.S.C. 204456-R.

Figure 7. The sheared edge of granodiorite block shows rotation of foliation into new, well developed, finer grained, planar layering and foliation. Note deformed xenolith in lower part. North shore, Blacks Inlet. G.S.C. 204454-O.

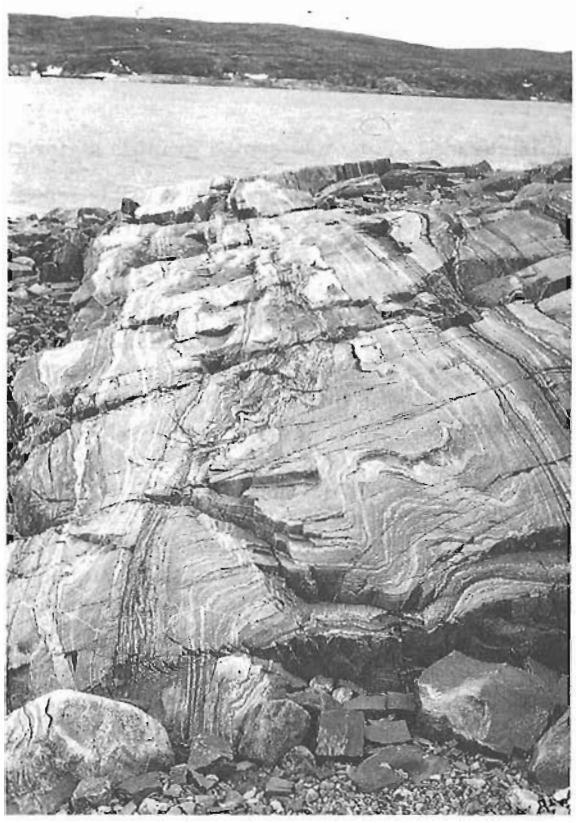

Figure 8. shows a shallow plunging disharmonic fold in grey gneiss from ductile shear zone. North shore, Black's Inlet, looking south. G.S.C. 204454-X.

down plunge in the steeply west dipping foliation also suggest that the east side moved up with respect to the west side. Abundant boudinaged features, including mafic dykes, indicate subhorizontal extension in a north-northeast south-southwest has played a large role in the shaping of the fabric.

Gossans

For one kilometre north of Blacks Inlet to 10 km south of the inlet, rusty gossans represent weathered pyritic metasediments especially those where the sediments are caught up in the ductile strain zone(see locations of prominent gossans on Fig 2). Elongate decametre wide rusty zones consist of thin strips of sillimanite and biotite-bearing quartzose rock with accessory iron sulphides and graphite. Although thin, they can be traced for several kilometres.

It is suggested that a metaplutonic protolith with metasedimentary septa provided the necessary ductility contrast for the metasediments to act as host for veins and disseminations of sulphides which were subsequently modified by hydrothermal fluids. Froese (1980) notes that biotite is restricted to alkaline and reducing hydrothermal regimes, which is consistent with the graphite-iron sulphide paragenesis. Along the edges of thicker gossan zones the rock grades rapidly from a quartzose interior to a leucocratic megacrystic feldspathic metaplutonic country rock.

Figure 9. shows layered gneiss with several generations of leucosomes, some rimmed by biotite selvedge cut by thin subparallel pegmatites which have been cut by a later conjugate set of granitic segregations which cut and offset the pegmatite. Note Brunton compass for scale. Small island southeast of north shore outcrop in Blacks Inlet. G.S.C. 204456-N.

The gossans are prominent since weathering of pyrite tends to liberate a lot of iron biotite which is in turn oxidized to yield these spectacular gossans. Analyses of five grab samples of gossans indicate values of As, Ag and Au near or at detection limits (2 ppm, 1 ppm, and 0.1ppb) (Table 1). A few grains molybdenite and scattered chalcopyrite have been identified in the pyritic metasediments.

CONCLUSIONS AND SPECIAL PROBLEMS

Summary

Briefly stated, the region underwent metamorphism, high grade rocks were moved over lower grade rocks, mafic dykes emplaced, the mid-crustal level was affected by local ductile high strain events which may have acted as extensional faults, and after uplift later latitudinal faults in the brittle domain broke the region into panels. Variable uplift and/or rotation affected each panel and the net result is that each panel represents a cut through the crust at a slightly different level . A Phanerozoic history responsible for the Melville Peninsula horst, including late Silurian, mid-Devonian and late Cretaceous faulting, has further complicated movements along the faults and additionally tilted the panels with respect to each other (Sanford, pers. comm.).

Local sporadic distribution of granulites

The patchy distribution of orthopyroxene along the periphyry of the zone to the northwest (Schau and Beckett, 1986) and its appearance in rocks of different tectonic heritage in the map area is due to at least three different processes:

1. it locally represent maximum prograde conditions in segregations and compositionally favoured sites along the edge of the granulite terrain, this distribution defines an isograd (Schau and Ashton, 1985).
2. it reflects tectonic juxtaposition of granulite grade rocks upon rocks of lower grade as noted in this report.
3. it is due to local or incomplete retrogression usually within, or in vicinity of strands of the later anastomosing shear zones as noted in this report.

Petrographic studies to estimate the relative importance of each process in each panel are continuing.

Later ductile shear zones; a response to Proterozoic events?

Figure 3 shows crosscutting pegmatite partially boudinaged in a sheared rock while Figure 9 shows a sheared protolith cut by pegmatite (traditionally one of the last plutonic manifestations) which is cut by partial melt veins developed along a shear set which offsets the pegmatite. These relationships indicate that pegmatites formed at many stages during the history of the zone and contributed their leucocratic compositions to the resulting new gneiss. Only a small proportion of the total volume of leuco- granitic material produced is still preserved with the characteristic pegmatitic textures in relatively undeformed dykes.

Most is present as fine to medium grained leucocratic layers subparallel to foliation indicating that they have been strongly deformed and recrystallized. Presumably during the waning phases of this activity solutions deposited pyrite in the meta- sedimentary rocks of Blacks Inlet. A subhorizontal sinistral sense of movement is postulated for the later shear zones. If the pegmatite is early Proterozoic in age then possibly the late shear zone activity is related to deformation in the Foxe Fold Belt where Henderson (1984) suggested that structures resulting from a subhorizontal sinistral sense of movement can account for features seen there.

Multiple origins of the neoformed granitic material

Because part of the pegmatite material possibly represents melt of a different composition travelling through channels in a partially melted rock (Arzi, 1978) derived from somewhere hotter in the zone, it is clear that the potential exists to make the bulk composition (on the scale of several outcrops) more granitic. Sawyer and Robin (1986), on the other hand, suggest that subsolidus segregation veins of granitoid composition (the so-called stromatic leucosomes) were formed from material extracted from the adjacent mafic selvage in what they term a closed system. They propose a chemical method to distinguish in situ partial melt from subsolidus segregation veins based on the different distribution coefficients characteristic of each of the processes. It is therefore possible, in principle, to distinguish among the three sources of granitic material: (1) introduced from elsewhere (possibly according to the Hollister and Crawford

Table 1. Chemical analyses of Gossans

SAMPLE NO:		1	2	3	4	5	6
SiO_2	%:	66.80	70.60	88.20	66.30	58.50	55.00
TiO_2	%:	.06	.11	.04	.20	.55	1.13
Al_2O_3	%:	12.50	12.00	5.75	10.70	11.20	12.00
Fe_2O_3T	%:	7.50	5.45	.97	13.70	18.40	12.40
MnO	%:	.01	.01	.01	.02	.03	.27
MgO	%:	.45	.05	.03	.16	.74	4.75
CaO	%:	1.44	1.08	1.30	.63	.85	7.76
Na_2O	%:	3.10	3.39	1.78	1.93	.18	1.38
K_2O	%:	3.45	4.12	.27	1.47	2.88	1.27
H_2OT	%:		1.70	.40			
P_2O_5	%:	.04	.04	.02	.01	.03	.14
S	%:	3.48	1.84	.34	5.21	6.73	3.00
$CO_2=$	%:				.10	.10	
BA	%:	0.14	0.05	0.001	0.02	0.05	0.01
BE	PPM:	.80	.70	1.200	1.80	.70	.90
CO	PPM:	19	12	4	17	25	44
CR	PPM:	140	230	310	160	190	160
CU	PPM:	190	42	31	410	500	330
LA	PPM:	4	59	4	3	11	6
NI	PPM:	67	30	14	50	63	110
PB	PPM:	38	14	39	47	47	13
V	PPM:	24	20	9	25	100	270
YB	PPM:	.80	1.90	.80	2.70	2.40	2.70
ZN	PPM:	40	21	26	52	55	120
AS	PPM:	<2	<2	<2	<2	2	<2
AG	PPM:	.5	.3	<.1	1.1	1.9	1.0
AU	PPB:	2	1	<1	<1	<1	11
TOTALS	%	99.00	100.50	99.20	100.50	100.30	99.20

1. HF 216-73, pyritic biotite gneiss, Prince Albert group.
2. DA 117-73 pyritic garnetiferous biotite gneiss, do
3. HF 226-73 quartzose biotite gneiss, do
4. HF 226-B-73 pyritic biotite gneiss, do
5. HF 226-c-73 pyritic biotite gneiss, do
6. HF 44-73 pyritic amphibolite , do

(1986) model) , (2) locally derived partial melt, and (3) subsolidus segregation. In Figure 4 it is clear that some of the leucosomes have selvedges whereas others do not. Intuitively it is judged that in those outcrops where the proportion of leucosome is relatively low it probably formed as a result of segregation veining. Other textures such as those figured previously (Fig 2 and 4; Schau and Beckett, 1986) probably resulted from partial melting and Fig 4 in Schau and Ashton, (1985) shows a granitic dyke introduced from elsewhere. The relative importance of each process remains to be ascertained throughout the area.

Gossans

The pyrite in the gossans occurs as veins and disseminations. Isotope analysis of sulphur may indicate whether its source was allochthonous; since sulphide rich bodies are not known in the Prince Albert group to the east it is unlikely that it is autochthonous.

ACKNOWLEDGMENTS

The 1986 component of the project was conducted in cooperation with Drs. A. Ciesielski of Lithosphere and Canadian Shielf Division and L. Dredge and crew of Terrain Sciences Division, Dr. R.H.McNutt of McMaster University, Francois Auclair of McGill University and R.Stevenson of University of Arizona. The camp was eventually established by July 7, 1986 and was struck during August 16-29,1986. In 1988, the authors working in conjunction with L. Dredge, revisited problem areas in the southern region of 47C, and adjoining map sheets. Camp was established July 7, and struck for logistic and weather related reasons on August 4-8. Leopold Nadeau and David Corrigan, senior assistants in 1986, and Bruce Kjarsgaard, Catherine Madore, and Bojan Sifrer, junior assistants in 1986, are thanked for their field work. Polar Continental Shelf Project graciously supplied a Jet-Ranger both years and maintained daily radio communication links. We also thank Bob MacDonald and the staff of the Eastern Arctic Research Laboratory (D.I.A.N.D./ N.W.T. Government) for their help with lodging,logistics, and radio communications.

REFERENCES

Arzi, A.A.
1978: Critical phenomena in the rheology of partially melted rocks; Tectonophysics, v. 44, p. 173-184.

Froese E.
1980: Applications of thermodynamics in the study of mineral deposits; Geological Survey of Canada, Paper 80-28, 38 p.

Henderson, J.R.
1984: Description of a virgation in the Foxe Fold Belt, Melville Peninsula, Canada; in Precambrian Tectonics Illustrated, A. Kroner, and R. Greiling. E Schweizerbart'sche Verlagsbuchhandlung, Nagele und Obermiller, Germany, Stuttgart, p. 251-261.

Hollister, L.S. and Crawford M.L.
1986: Melt-enhanced deformation: a major tectonic process; Geology, v. 14, p. 558-561.

Prevec, S.A.
1985: Petrology, geochemistry, and geochronology of some Precambrian rocks of the northwestern Melville Peninsula, Northwest Territories; B.S.C. Thesis,McMaster University, 94 p.

Sawyer, E.W. and Robin P.-Y.F.
1986: The subsolidus segregation of layer parallel quartz-feldspar veins in greenschist to upper amphibolite facies metasediments; Journal of Metamorphic Petrology, v. 4, p. 237-260.

Schau, M. and Ashton, K.E.
1985: High grade metamorphic rocks of northwestern Melville Peninsula, District of Franklin; in Current Research, Part A, Geological Survey of Canada, Paper 85-1A, p. 527-532.

Schau, M. and Beckett, M.
1986: High grade metamorphic rocks of northwestern Melville Peninsula, District of Franklin; in Current Research, Part A, Geological Survey of Canada, Paper 86-1A, p. 667-674.

Schau, M. and Heywood, W.W.
1984: Geology, Northern Melville Peninsule; map and marginal notes; Geological Survey of Canada, Open File 1046.

Structural sequence from the southeastern part of the Kapuskasing structural zone in the vicinity of Ivanhoe Lake, Ontario

J.T. Bursnall[1]
Lithosphere and Canadian Shield Division

Bursnall, J.T., Structural sequence from the southeastern part of the Kapuskasing structural zone in the vicinity of Ivanhoe Lake, Ontario; in Current Research, Part C, Geological Survey of Canada, Paper 89-1C, p. 405-411, 1989.

Abstract

The southeastern part of the Kapuskasing structural zone exhibits a complex deformational history that may be subdivided into eight phases. These are grouped into an Archean set, accompanied by high-pressure granulite metamorphism and migmatization and representing deep-seated conditions within the Archean crust, and a second set that was developed during and following the progressive uplift and emplacement of the high grade rocks during the early to mid-Proterozoic. Ductile conditions and high strains occurred during the earlier phases, whereas a progressive ductile to brittle transition is exhibited by the uplift-related structures.

Résumé

L'histoire de la déformation de la partie sud-est de la zone structurale de Kapuskasing est complexe et peut être subdivisée en huit phases. On peut regrouper ces phases en un ensemble de l'Archéen, accompagné de métamorphisme granulitique de haute pression et de migmatisation, et représentatif de conditions en profondeur dans la croûte à l'Archéen, et en un deuxième ensemble formé pendant et après le soulèvement et la mise en place progressifs des roches à degré de métamorphisme élevé datant du début au milieu du Protérozoïque. Des conditions de ductilité et de fortes contraintes existaient pendant les premières phases alors que les structures associées au soulèvement présentent une transition progressive de la ductilité à la fragilité.

[1] 370 Montague Road, Sunderland, Massachusetts, 01375

INTRODUCTION

New logging roads between Foleyet and Chapleau, central Ontario (Fig. 1), provide access for detailed mapping of a section across the Archean high-grade gneisses of the southeastern part of the Kapuskasing structural zone (Thurston et al., 1977; Percival, 1981a, b) and their boundary with lower-grade rocks of the Abitibi subprovince to the southeast (Fig. 1, 2). This boundary, the Ivanhoe Lake fault zone, occurs within the Ivanhoe Lake cataclastic zone (ILCZ), defined by Percival (1981a), and is recognized as the somewhat modified surface expression of a northwest-dipping shear system that resulted in Proterozoic uplift and eventual exposure of a 25 to 30 km-deep Archean crustal segment (Percival and Card, 1983, 1985; Cook, 1985; Geis et al, 1988). Detailed mapping in a 5 by 20 km section across the southern Kapuskasing structural zone (KSZ), including the Ivanhoe Lake cataclistic zone, to the Ivanhoe Lake fault zone, is in progress in an attempt to define the pre-uplift structural evolution of the structurally lowest part of the Kapuskasing structural zone, as well as the effect and character of superimposed uplift structures. At least eight significant stages in the structural evolution of the Kapuskasing structural zone can be recognized within the Ivanhoe Lake cataclastic zone part of the section, the youngest of these most likely being related to post-uplift faulting that has severely modified the uplift-related structures.

LITHOLOGY

Kapuskasing Structural Zone

The Kapuskasing structural zone in the study area is composed of compositionally diverse rock types that occur in discontinuous, east-west-striking belts that are seemingly slightly deflected towards the northeast adjacent to the Ivanhoe Lake fault zone (Fig. 1). The lithological units of the present study and used in the accompanying map (Fig. 2) are essentially equivalent to those of Percival (1981a) and are representative of the predominant rock types in that zone. Most rock types are medium- to coarse-grained gneisses, which typically possess a lenticular to moderately persistent compositional layering that varies in thickness from a few millimetres to 50 cm or more. This regional planar fabric in part is made up of rotated and transposed leucosome veinlets, in addition to fine lenses of aplitic leucosome segregations developed parallel to compositional layering. Foliation fish of the type described by Hanmer (1986) and low-angle discontinuities are locally common, particularly within east-west-trending, late-metamorphic, high-strain zones that occur at intervals throughout the section. These are recognized by slightly finer grain size than the contiguous gneisses, apparently much thinned and regular layering, and the presence of relict feldspar 'porphyroclasts' and mineral aggregate augen. The lenticular character of the gross compositional layering is also enhanced through boudinage and necking where ductility contrast is high, as for example, within mixed mafic gneiss and tonalite. Granoblastic textures dominate over pronounced preferred dimensional grain orientations. Exceptions occur within late-metamorphic, high-strain zones (late-D3 age in the structural sequence, see below) and locally developed, syn-metamorphic mineral lineations.

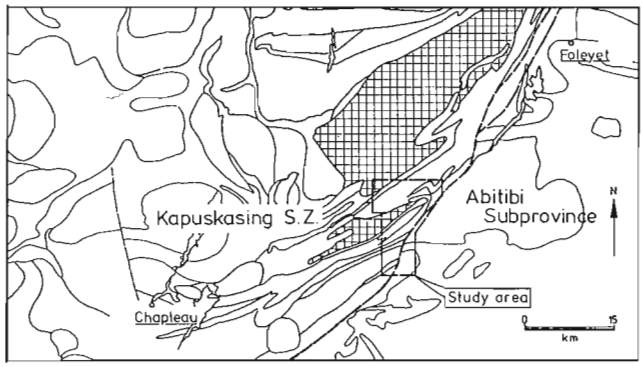

Figure 1. Location of study area. Ivanhoe Lake fault zone indicated by heavy dashed line. Shawmere anorthosite complex ornamented. Geological contacts taken from Percival and Card (1985).

Tonalitic gneiss, in places crowded with mafic inclusions, granodioritic to dioritic gneiss, paragneiss (including recognizable polymict conglomerate), 'mixed gneisses', and a variety of mafic gneisses constitute the major lithological units (Fig. 2). Common occurrence of clinopyroxene within garnetiferous mafic gneiss, orthopyroxene within paragneiss, two pyroxene mafic gneisses within the easternmost part of the area recorded by Percival (1981a, 1983) and other criteria, indicate that uppermost amphibolite to granulite facies conditions obtained during the early tectonic evolution of the area. U-Pb zircon ages for high-grade metamorphism and accompanying widespread migmatization are within the range ca. 2700 to ca. 2600 Ma (Percival and Krogh, 1983; Percival 1988). Retrograde assemblages are mainly present in areas affected by faults of the Ivanhoe Lake cataclastic zone, where chlorite and epidote are major constituents of the microshear zones.

Well foliated *anorthosite* containing fragments of layered anorthositic gabbro outcrops along Hellyer Creek, 2 km south of Highway 101. The highly strained envelope rocks converge eastwards at this locality indicating the termination of a 15 × 5 km body that is considered part of the Shawmere anorthosite complex (Fig. 1: Thurston et al., 1977; Percival, 1981a, b): whether this smaller body represents a tectonically isolated segment or was originally independent of the main complex, 8 km to the north, is not known.

Mafic gneiss occurs in three distinct east-west to northeasterly-trending belts. The most extensive, in the central part of the area about 3 km south of Highway 101 on the Aubé main haulage road, extends at least 6 km to the south (Fig. 2). Here, the mafic rocks structurally underlie a narrow belt of metasediments, varieties of dioritic gneiss, and homogeneous to weakly foliated quartz-feldspar gneiss. The superficial resemblance of this assemblage to some supracrustal associations within Abitibi and Wawa greenstone belts presents the possibility of a volcanic origin for at least some of the mafic rocks within the KSZ. These rocks may in part represent relict enclaves of supracrustal material tectonically and magmatically incorporated into the lower Archean crust during the early deformation phases.

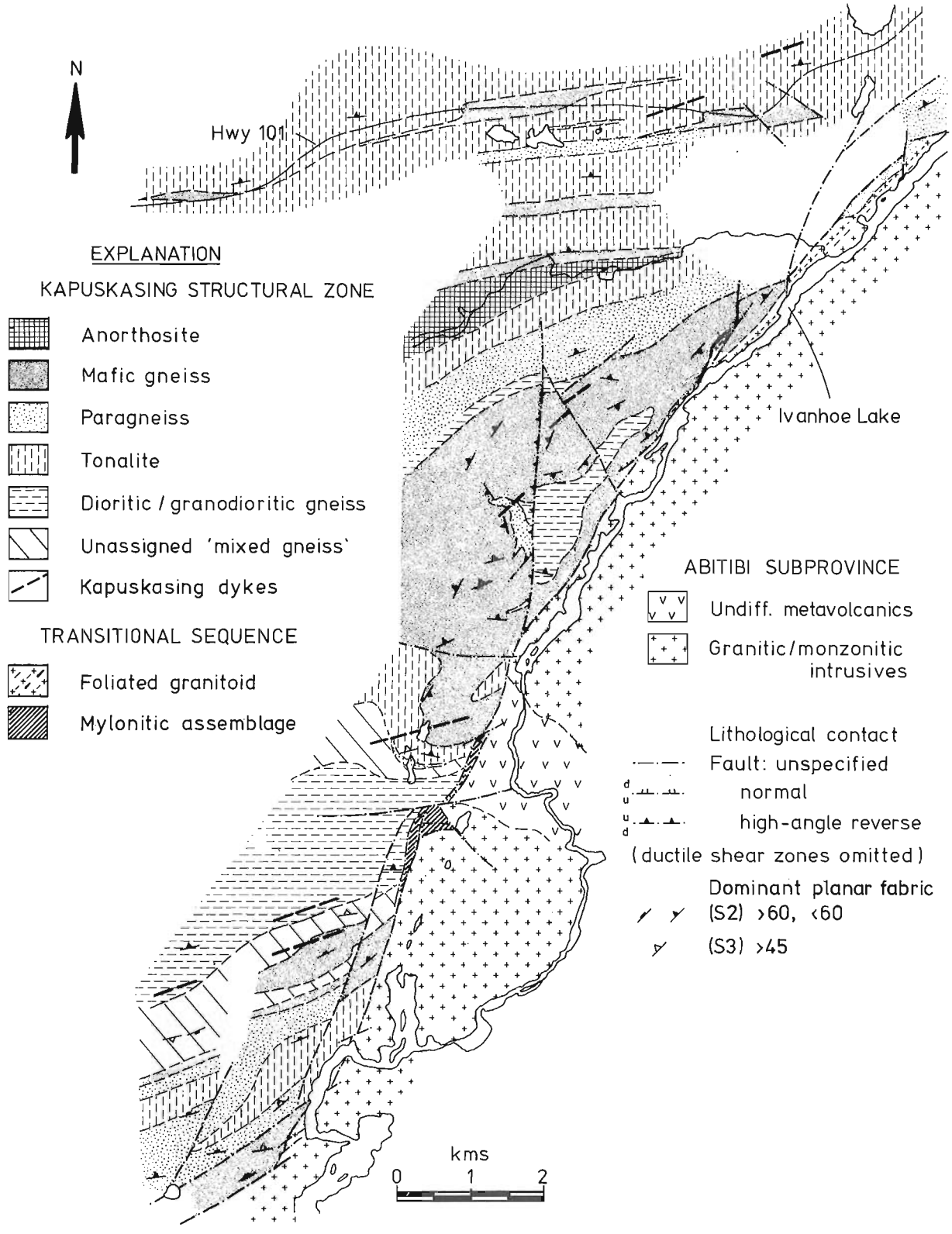

Figure 2. Geological map of the study area. Unornamented areas are unmapped.

The *metasedimentary rocks* contain polymictic conglomerate lenses within interlayered pelite and psammite which resemble, and are probably continuous with those at Borden Lake (Percival, 1981a, b; Moser, 1989), 35 km to the west. Clast compositions are broadly representative of local lithologies and similar to those in metaconglomerate at Borden Lake. Cobbles of quartzite, dioritic gneiss, quartz-feldspar gneiss, rare mafic and amphibolitic gneiss are set in a garnet-amphibole-biotite-quartz-feldspar matrix. Some felsic clasts contain quartz veins that seemingly predate their incorporation in the conglomerate. Other rocks, likely metasedimentary in origin based on mineralogical composition, occur in a number of additional belts and are also included under '*paragneiss*' in Figure 2.

Tonalite occurs as extensive areas, local homogeneous patches and as ubiquitous, thin aplitic to pegmatitic veins and clots that permeate the mafic gneisses and other rock types. Tonalite generation occurred prior to the main, second phase, deformation (D2) and continued at least into the early part of the third phase (D3). Large tracts of tonalitic gneiss, in places crowded with mafic inclusions, are particularly common in the northern part of the area, straddling Highway 101. Through dramatically thinned inclusions, these rocks qualitatively demonstrate the very high cumulative strains that occurred during the syn-metamorphic deformation phases.

"*Mixed gneisses*" are compositionally heterogeneous to the extent that no one rock type predominates. Typically, however, they are composed of interlayered and approximately equal volumes of mafic gneiss, tonalite and paragneiss that cannot be separated at map scale. Characteristically they grade into adjacent compositionally dominant units and may locally be a product of unit boundary transposition.

Rare, pre- to syn-metamorphic, mafic sheet intrusives, now severely disrupted and recognized as trains of subangular boudins, have been observed within all Kapuskasing structural zone units except the dioritic gneisses and weakly foliated tonalite. Tonalitic to granitic pegmatites are common and were emplaced at various times throughout and closely following high-grade metamorphism.

Transitional sequence

Rocks assigned to the transitional sequence in Figure 2 occur at various localities within the Ivanhoe Lake fault zone. They are referred to as such because their field characteristics include features of both the Kapuskasing gneisses and the Abitibi belt to the southeast.

An assemblage of highly strained, mylonitic, mafic and felsic rocks that seems to be in part tectonically reconstituted Kapuskasing structural zone mafic gneiss and in part Abitibi mafic metavolcanics is contained in a fault block within the Ivanhoe Lake fault zone. At this locality, a 50-75 m-thick zone of finegrained and finely laminated mafic and interlayered quartzofeldspathic material locally contains and is deflected around small relict lozenges of coarse-grained mafic gneiss. The fine-grained rocks are strongly mylonitic and it is apparent that the mafic gneiss inclusions are being degraded at their boundaries; it therefore seems that the mafic material may be derived by the transformation of Kapuskasing mafic gneisses. In close proximity across unexposed ground and on strike to these are outcrops of regularly layered and somewhat flaggy medium-grained amphibolites that are identical to Abitibi mafic rocks, 1 km to the southeast, suggesting that there may have been some tectonic interleaving between the two assemblages.

Reconnaissance mapping along the southern part of Ivanhoe Lake indicates that there may not be an obvious compositional break between Kapuskasing structural zone gneisses and granitoid plutons of the Abitibi subprovince as is present elsewhere in the map area. In this section, where the Ivanhoe Lake fault zone obliquely traverses the broad central tract of Kapuskasing structural zone mafic gneiss, a number of seemingly anomalous and equivocal features exist. As this contact is approached from the west, thin (a few centimetres to about 5 m), concordant, medium-grained, felsic, tonalitic to quartz monzonitic sheets increase in abundance and the mafic rocks locally are medium- to fine-grained (but seemingly maintain a mineralogical composition similar to their coarse-grained equivalents). Contiguous (but nowhere with observed contact), coarse-grained, gneissic 'quartz monzonite' contains abundant mafic schlieren and is compositionally similar to structurally isotropic quartz monzonite southeast of Ivanhoe Lake, which contains rare foliated mafic xenoliths. At one locality, fine-grained mafic 'gneiss' with clinopyroxene porphyroblasts is separated from weakly foliated quartz monzonite by a well-developed screen of pegmatite. A metre-sized xenolith of similar mafic material contains a pre-inclusion tight fold and has been refolded during mild deformation of the host. The simplest explanation for these relationships is that the mafic inclusions represent moderately high-grade Abitibi rocks, intruded by granitic material, and subsequently transported as a fault-bounded slice to shallow depth during emplacement of the Kapuskasing structural zone; the foliation within the granitoid host could have been produced at this time, or it may be evidence for an earlier event. Two subparallel faults defining the Ivanhoe Lake fault zone to the northeast that may coincide with two strong reflectors on a high-resolution seismic reflection line (Geis et al., 1988; Percival, 1988), enclose an amphibolite-grade package of foliated granitoid and other rocks (Percival, 1981b). Because the magnetic signature of these rocks can be traced southwest into the study area using shadow-enhanced aeromagnetic compilation maps (G.F. West, pers. comm., 1988), and enclose the area described above, a fault slice origin of deeper Abitibi crust is supported. The increase of felsic material with structural depth within the Kapuskasing structural zone at this locality and elsewhere is not yet fully understood.

Abitibi subprovince

Layered amphibolite and medium- to fine-grained felsic rocks within the Abitibi metavolcanic belt outcrop along the Ivanhoe River in the extreme south of the map area (Fig. 2). These are thinly interlayered in places and are intruded

by granite/quartz monzonite. The mafic rocks vary in texture and composition from fine- to medium-grained true amphibolite to plagioclase-rich varieties and are strongly foliated; garnet is rare in schistose amphibolite close to the boundary with the Kapuskasing structural zone and clinopyroxene has been reported in presumed Abitibi amphibolite 10 km to the northeast (Percival, 1986). Elsewhere, the Abitibi contact rocks are granitic and include quartz monzonite of the Biggs Lake pluton.

Dykes

A variety of post-metamorphic mafic dykes and granitic pegmatites occurs within the field area. The most common is lamprophyre, but rare, sparsely plagioclase-porphyritic members of the Kapuskasing suite (Card et al., 1981) are present throughout the map area (Fig. 2), with trends in the range N40E-N88E and thicknesses typically of 10 to 15 m. A single northwest-trending mafic dyke was observed within quartz monzonite south of the Ivanhoe Lake fault zone. Only the lamprophyres were observed to cut structures related to the Ivanhoe Lake cataclastic zone. A similar lamprophyre dyke 15 km to the northeast gave a ca. 1140 Ma $^{40}Ar/^{39}Ar$ age, M. Queen, pers. comm., 1988).

STRUCTURAL HISTORY

Structures within the area may be considered as two temporally and geometrically distinct groups that were developed under distinctly different mechanical conditions. Those that predate or developed during or shortly after the pervasive, late Archean, high-grade metamorphism and associated migmatization, characteristically result from highly ductile behaviour of the rock mass and demonstrate the effects of complex multiple folding and locally very high strain levels which resulted in structural complexity. The second group of structures postdates high-grade regional metamorphism and includes those produced during and following the Kapuskasing uplift. They reach their greatest expression within a few hundred metres of the Ivanhoe Lake fault zone but are present throughout the Ivanhoe Lake cataclastic zone, up to a distance of several kilometres from the fault trace. Protomylonites and mylonites, cataclasites and faults occur on all scales in addition to minor folds. A precise age for their development is uncertain but the most recent faults within this zone affect ca. 1140 Ma lamprophyric dykes. Mylonite from the Ivanhoe Lake Cataclastic Zone produced a $^{40}Ar/^{39}Ar$ date of 1.72 Ga (Percival, 1981a) and indirect geochronological evidence from gneisses suggests isobaric cooling followed by rapid uplift at ca. 1.95 Ga (Parrish, 1987; Percival, 1988). Kapuskasing dykes, which are cut by brittle faults (Percival, 1981a) and locally invaded by pseudotachylite elsewhere (A. Leclair, pers. comm., 1988), were likely intruded at ca. 2040 Ma based on $^{40}Ar/^{39}Ar$ studies by Hanes et al. (1988). The minimum age for uplift is seemingly constrained by U-Pb zircon ages of 1907 and 1888 Ma (L. Heaman, pers. comm., 1988) for the Cargill carbonatite complex that cuts faults related to the uplift to the north of the study area (Percival, 1988). Further details of the deformation sequence so far determined for the Kapuskasing structural zone are given below and are preceded by the following summary.

Summary of deformation sequence

Phase 1 (D1) — Production of gneissic layering; minor folds of uncertain origin.

Phase 2 (D2) — Development of small-scale, tight to isoclinal folds of layering of variable trend; locally very high strains yielding strong planar fabric and mineral lineation; continued migmatization and pegmatite generation.

Phase 3 (D3) — Early: formation of tight, gently inclined folds about moderately northward-dipping axial surfaces; weak associated fabric and mineral and intersection lineation.
Late: development of ductile shear zones with local mild retrogression; locally strong grain dimensional planar fabric.

Phase 4 (D4) — Early decoupling stage of Kapuskasing structural zone and initiation of Ivanhoe Lake cataclastic zone; presumed age of development of mylonitic and reconstituted mafic gneiss sequence in the transitional sequence.

Phase 5 — Further development of the Ivanhoe Lake Cataclastic Zone; widespread production of small-scale mylonitic shear zones and planar fabrics succeeded by cataclasis and invasion of cataclasite veins and development of pseudotachylite. In part overlaps with D4 structures.

Phase 6-7 — (Evidence for relative age of Phase 6 and 7 structures is equivocal) Formation of NW-trending, gentle to open, large-scale, upright to moderately inclined, horizontal folds, in part related to east-directed, high-angle, reverse faults.

Phase 6-7 — Development of NE-trending, upright to moderately inclined, gently plunging, folds adjacent to Ivanhoe Lake; possibly related to normal faults (relative downthrow to NW) of unknown extent along Kapuskasing structural zone-Abitibi boundary.

Phase 8 — Post-lamprophyre faulting.

The early deformation phases (Archean)

The syn-metamorphic Archean events, here designated D1-D3, collectively imparted a strong, regionally pervasive, planar compositional anisotropy and resulted in the dominant east-west regional trend of lithological units, dominant fabrics and low northerly dips (Fig. 2). The earliest structures recognized in the map area are rare fold-like structures of uncertain origin and a stromatic gneissic layering within mafic inclusions in tonalitic gneiss; both are assigned to the D_1 phase. Other compositional layering within mafic gneiss may be a relict of primary compositional variation. These structures are succeeded by two systematic fold sets. The earliest of these (D_2) are small-scale, north- to northeast-trending, tight to isoclinal folds of gneissic layering with low to moderate plunge; they are typically reclined. Attendant axial surface fabrics are uncommon but many are true intrafolial folds, indicating that, locally at least, the prominent gneissic layering is predominantly a secondary (D_2) composite structure, the earlier gneissosity being assigned to D_1 phase.

Generally high ductile strains occurred during the second deformation phase and were accompanied or closely

followed by peak metamorphism. Seemingly multiple invasion of granitoid veins, anatectic leucosome, and pegmatite that predate third-phase structures suggest that the structures ascribed to D_2 could be further subdivided. Boudinage of early mafic dykes and development of a locally strong mineral lineation occurred during this period.

The third deformation phase represents the latest of the high-grade deformations and may be subdivided into two stages. Early-D_3 folds are tight with gentle to moderately inclined north- to northwest-dipping axial surfaces and moderate to low, west- to northeast plunge; a subparallel mineral lineation and more common rodding lineation are present. They are seen to refold second phase folds whose prior variable trend is indicated by a range of interference patterns over short distance. A poorly developed axial planar fabric is developed in places. These folds locally possess curved hinge lines that are thought to have developed at least in part during a period of pervasive ductile shearing that is tentatively placed in the structural sequence as late-D3 in age: no evidence suggests that a major interval separates the two sets of structures. These zones are best displayed along Highway 101 near the Aubé road entrance. Some apparently developed through the continued rotation and thinning of gently NNW-dipping long limbs of D3 folds without disrupting the continuity of the folded fabric. Elsewhere, however, zone boundaries are extremely abrupt, indicating very high strain gradients. A strong, grain-dimensional, planar fabric within the zones is a common feature and is enhanced by subparallel quartz lenticles. Syn- to post-kinematic garnet growth occurred within mafic gneiss and the zones are locally cut by pegmatite. The zones therefore most likely developed during the later stages of regional metamorphism.

Approximate minimum cumulative local strain magnitudes for the Archean phases are given by axial ratios of prolate clasts that exceed 12:1, and high axial ratios for deformed mafic inclusions in tonalitic gneiss that exceed 20:1 in sections close to the principal finite extension direction. It is likely that even higher cumulative strains occur elsewhere within discrete high strain zones (both D_2 and D_3 in age); such ductile shear zones may be concentrated within tonalite that has invaded mafic and other compositions of gneiss. Recognizable oblique extensional ductile shears (strain bands) are also developed locally but do not seem to be as extensive or of such large scale as those described by Moser (1988; 1989) southwest of Chapleau.

The later deformation phases (Proterozoic)

Unequivocal post-metamorphic events are likely lower to mid-Proterozoic and younger. The earlier of these evolved during the progressive uplift of the Kapuskasing structural zone and exhibit distinct stages that may well represent a continuum of changing mechanical behavior in response to uplift; they have been subsequently modified by the later stages of movement across the Ivanhoe Lake fault zone. These effects are therefore somewhat restricted to the vicinity of the Ivanhoe Lake fault zone within the Ivanhoe Lake cataclastic zone and are concentrated within a moderately narrow (500 m) zone adjacent to the Kapuskasing-Abitibi contact. Here they consist of a close-spaced and ramifying network of fine to 1-2 cm wide ductile shears that in places develop a strong mylonitic fabric: these characteristically are curved, and pinch and swell along their trace. Fine-scale shears, marked by fine, dark, chloritic smears along compositional layer boundaries and parallel to other strong planar fabrics, is a characteristic feature. These may thicken into black protomylonite and cataclasite zones that may reach 20 cm in width. All are typically cut by green epidotic cataclasite veinlets and both structures are displaced by microfaults. no systematic regional orientation to ILCZ structures has yet been recognized but the majority dip steeply to the north and northwest. The contact between Kapuskasing gneisses and Abitibi rocks (quartz monzonite, felsic and mafic metavolcanics) has been defined to within a few metres at a number of localities, but nowhere are contacts fully exposed. In the southernmost part of the map area, the attitude of layering and prominent fabric (gneissosity and cleavage) within the Kapuskasing structural zone are moderately steep to subvertival with strikes ranging from highly discordant (east-west) to subparallel to the trace of the Ivanhoe Lake fault zone (Fig. 2); to the northeast, however, dips are moderate to shallow and only slight discordance prevails. A strong, steeply-plunging, mineral aggregate lineation exists within granitoids (quartz monzonite?) within a few metres of the contact in the extreme south of the area; no unambiguous kinematic indicators were observed. It is apparent that the contact within the southern part of the section and subparallel faults 1 km to the west within the Kapuskasing structural zone have been displaced dextrally along numerous northeast-trending faults (Fig. 2); the age of these is unknown but it is possible that they are equivalent in age to late shear zones that affect ca. 1140 Ma lamprophyre dykes within the Ivanhoe Lake fault zone elsewhere in the map area.

Progressive ductile to brittle transition that may be deduced by the sequential development of structures at any one locality may be viewed as response to the progressive southeastward uplift and unroofing of the Kapuskasing structural zone plate. This would imply that most, if not all, structures falling in each of the recognized phases in a single outcrop are necessarily diachronous with depth. It should be emphazised, however, that not all localities exhibit this ductile to brittle sequence and in many places field relations are equivocal. Episodic variations in uplift rate would explain the local transition from seemingly brittle to ductile shears and could explain some of the complexities. The existence of pseudotachylite at numerous localities suggests rapid displacement at relatively shallow depths (< 10 km; Sibson, 1975, 1977).

Rocks representing the fundamental transport zone along which mid-crustal decoupling occurred have yet to be confirmed, but may be represented by the highly strained mylonitic mafic and felsic rocks of the transitional assemblage within the Ivanhoe Lake fault zone. A weak amphibole lineation is present and somewhat equivocal kinematic indicators suggest southeastward transport. The mylonitic lamination is cut by fine, wispy microshears and up to 3 cm-thick cataclasite veins that in places carry small lithic clasts. These in turn are cut by moderately north-dipping reverse faults and related south-verging close folds. Later east-west, probable strike-slip shear zones further dissect

the succession and deform coarse pegmatite and lamprophyric dykes. They represent the youngest structures observed within the zone.

It is impossible at the present mapping detail to determine the precise position in the structural succession of some of the larger-scale structures that have been tentatively placed in deformation phases 6 and 7. Two fold sets results in low amplitude dome and basin interference patterns on the regionally low northerly dips of the lithological units in the central part of the area and close to the Ivanhoe Lake fault zone (Fig. 2). One of these is responsible for slight deviations in regional strike along northwesterly-trending axes as the Ivanhoe Lake fault zone is approached. Minor, subhorizontal, northwest-trending folds with steep east-dipping axial surfaces and subparallel weak mica fabric within paragneisses of the central part of the map area may be of the same generation. They occur close to a steep, west dipping, reverse fault that contains narrow zones of foliated ultracataclasite invaded by pseudotachylite. The relationship of this fault to the pervasive cataclasite and thin, mylonitic, small-scale shear zones within this part of the Ivanhoe Lake cataclastic zone is not known.

A second set of northeast-trending, upright and gently plunging folds occur close to Ivanhoe Lake; they fold cataclasites and mylonitic seams of the Ivanhoe Lake cataclastic zone and in part may be related to inferred normal faulting within the Ivanhoe lake fault zone (Fig. 2).

CONCLUSION

The Kapuskasing Structural Zone has suffered a long and complex deformation history, particularly close to its faulted boundary with the adjacent supracrustal/plutonic rocks of the Abitibi subprovince. The sequential structural development of the zone is still incompletely understood, in particular the uplift related events and the details of the potential subdivision of the second deformation phase; regional structural correlations remain to be made. It is not entirely clear that the basal transport rocks of the Kapuskasing plate are represented by the newly described mylonitic sequence within the Ivanhoe Lake fault zone; the structural character and position of the strongly foliated dioritic gneisses which outcrop to the southwest of the map area have yet to be investigated before this relationship can be clarified.

ACKNOWLEDGMENTS

Thanks are due to J.A. Percival for his interest in suggesting and continued support during this project and for reviewing the manuscript. J.A. Hanes and D. Moser are thanked for additional discussions in the field. Funding for the 1988 season was through Hanes' Phase 2 Kapuskasing LITHOPROBE NSERC Grant at Queen's University, the receipt of which is gratefully acknowledge (Contribution No. 80).

REFERENCES

Card, K.D., Percival, J.A., Lafleur, J. and Hogarth, D.D.
1981 Progress report on regional geological synthesis, central Superior Province; in Current Research, Part A, Geological Survey of Canada, Paper 81-1A, p. 77-93.

Cook, F.A.
1985: Geometry of the Kapuskasing structure from a Lithoprobe pilot reflection survey; Geology, v. 13, p. 368-371.

Geis, W.T., Green, A.G., and Cook, F.A.
1988: Preliminary results from the high resolution seismic reflection profile: Chapleau Block, Kapuskasing Structural Zone; in 1988 KSZ Lithoprobe Workshop, University of Toronto, p. 155-165.

Hanes, J.A., Archibald, D.A., Queen, M., and Lee, J.K.W.
1988: $^{40}Ar/^{39}Ar$ geochronology of diabase dykes: implications for the tectonothermal evolution of the Kapuskasing uplift; in 1988 KSZ Lithoprobe Workshop, University of Toronto, p. 7-15.

Hanmer, S.
1986: Asymmetrical pull-aparts and foliation fish as kinematic indicators; Journal of Structural Geology, v. 8, p. 111-122.

Moser, D.
1988: Structure of the Wawa gneiss terrane near Chapleau, Ontario; in Current Research, Part C, Geological Survey of Canada, Paper 88-1C, p. 93-99.
1989: Mid-crustal structures of the Wawa gneiss terrane near Chapleau, Ontario; in Current Research, Part C, Geological Survey of Canada, Paper 89-1C.

Parrish, R.R.
1987: Applications of numerical modeling of heat transfer to P-T-t path determination of exhumed mountain belts; Geological Association of Canada, Program with Abstracts, v. 12, p. 78.

Percival, J.A.
1981a: Geological evolution of part of the central Superior Province based on relationships among the Abitibi and Wawa subprovinces and the Kapuskasing structural zone; Ph.D. thesis, Queen's University, Kingston, Ontario, 300 p.
1981b: Geology of the Kapuskasing structural zone in the Chapleau-Foleyet area; Geological Survey of Canada, Open File 763.
1983: High-grade metamorphism in the Chapleau-Foleyet area, Ontario; American Mineralogist, v. 68, p. 667-686.
1986: The Kapuskasing uplift: Archean greenstones and granulites, Geological Association of Canada, Field Trip Guide 16, 37 p.
1988: The Kapuskasing uplift: cross section through the Archean Superior Province; in Exposed Cross Sections of the Continental Crust, NATO Advanced Study Institute Field Guide, p. 1-49.

Percival, J.A. and Card, K.D.
1983: Archean crust as revealed in the Kapuskasing uplift, Superior Province, Canada; Geology, v. 11, p. 323-326.
1985: Structure and evolution of Archean crust in central Superior Province, Canada; in Evolution of Archean Supracrustal Sequences, edited by L.D. Ayres et al., Geological Association of Canada, Special Paper 28, p. 179-192.

Percival, J.A. and Krogh, T.E.
1983: U-Pb zircon geochronology of the Kapuskasing structural zone and vicinity in the Chapleau-Foleyet area, Ontario; Canadian Journal of Earth Sciences, v. 20, p. 830-843.

Sibson, R.H.
1975: Generation of pseudotachylite by ancient seismic faulting; Geophysical Journal of the Royal Astronomical Society, v. 43, p. 775-794.
1977: Fault rocks and fault mechanisms; Journal of the Geological Society of London, v. 133, p. 191-213.

Thurston, P.C., Siragusa, G.M., and Sage, R.P.
1977: Geology of the Chapleau area, Districts of Algoma, Sudbury, and Cochrane; Ontario Division of Mines, Geoscience Report 157, 293 p.

AUTHOR INDEX

Adams, R.D. ... 107
Anglin, C.D. ... 285
Archibald, D.A. ... 135
Aspler, L.B. ... 143
Baker, K.A. ... 121
Beaumont-Smith, C.J. ... 293
Bethune, K.M. ... 19
Birkett, T.C. ... 345
Bostock, H.H. ... 49
Brace, T.D. ... 333
Bridgwater, D. ... 385
Brommecker, R. ... 121, 325
Bursey, T.L. ... 143
Bursnall, J.T. ... 405
Burwash, R.W. ... 363
Burwash, R.A. ... 363
Cajka, M.G. ... 353
Cameron, E.M. ... 313
Check, G. ... 157
Corrigan, D. ... 157
Corriveau, L. ... 385
Culshaw, N.G. ... 157
Davis, W.J. ... 81
Diamond, L. ... 121
Digel, M. ... 395
Drage, J. ... 157
Dubé, B. ... 275
Eckstrand, O.R. ... 235
Elliott, B. ... 305
Emslie, R.F. ... 11
Ermanovics, I.F. ... 385
Findlay, J.M. ... 345
Fowler, T.D. ... 345
Franklin, J.M. ... 275, 285
Frith, R.A. ... 377
Gandhi, S.S. ... 243, 263, 369
Goodarzi, F. ... 369
Gower, R. ... 157
Green, S.B. ... 121
Grenier, R. ... 377
Grinenko, L.N. ... 235
Grocott, J. ... 185
Grotzinger, J.P. ... 107
Haggart, M.J. ... 157
Hanes, J.A. ... 00
Harrap, R.M. ... 135, 377
Hasegawa, H.S. ... 353
Henderson, J.R. ... 185
Henderson, M.N. ... 185
Hodgson, C.J. ... 135, 325
Hunt, P.A. ... 11
James, D.T. ... 29
James, N.P. ... 57
Jefferson, C.W. ... 293
Killeen, P.G. ... 305
King, J.E. ... 81
Koopman, E.R. ... 275
Krouse, H.R. ... 235
Lalonde, A.E. ... 313
LeCheminant, A.N. ... 173
Leclair, A.D. ... 225
Lin Baoqin ... 121
Lustwerk, R.L. ... 293
Marshall, D. ... 121
McCormick, D.S. ... 107
Mengel, F. ... 385
Miller, A.R. ... 127, 143
Moser, D. ... 215
Mwenifumbo, C.J. ... 305
Myrow, P. ... 107
O'Dea, M. ... 377
Ouellet, E. ... 43
Paktunc, A.D. ... 235, 243
Park, A.F. ... 1
Patterson, M.R. ... 275
Pelechaty, S.M. ... 57
Perreault, S. ... 185
Peterson, T.D. ... 173
Plouffe, M. ... 353
Poirier, G.G. ... 00
Poulsen, K.H. ... 121, 225, 275, 325
Rainbird, R.H. ... 173
Ralser, S. ... 1
Reardon, N.C. ... 37
Relf, C. ... 81, 95
Roach, D. ... 199
Robert, F. ... 135
Roscoe, S.M. ... 199
Rowins, S.M. ... 313
Ruzicka, V. ... 67
Schau, M. ... 395
Schmitt, H.R. ... 255
Schwann, P.L. ... 235
Scoates, R.F.J. ... 235
Shang Ling ... 121
Shen Ershu ... 121
Sherlock, R. ... 385
Snowdon, L.R. ... 369
Stubley, M. ... 199
Thorleifson, L.H. ... 305
Van Nostrand, T. ... 81
Van Kranendonk, M. ... 385
Wallace, P. ... 157
Wetmiller, R.J. ... 353
Wilcox, K.H. ... 165
Wilton, D.H.C. ... 333
Wodicka, N. ... 157
Zhang Lidon ... 121

ERRATA

Geological Survey of Canada, Paper 88-1C
Current Research, Part C

The Grenville Province boundary in the Burnt Lake area, Central Mineral Belt of Labrador: L.M. MacKenzie and D.H.C. Wilton
p. 236: Figures 2 and 3 are reversed.

Stratigraphic and metallogenic relationships along the unconformity between Archean granite basement and the early Proterozoic Moran Lake Group, central Labrador: D.H.C. Wilton, C.S. MacDougall, L.M. MacKenzie, and C. Pumphrey

p. 278: Caption to Figure 1 should read "Location and distribution of the Moran Lake Group (patterned). The area outlined is the transect area described in the text and shown in Figure 2. Numbers indicate mineral occurrences described in the text: 1, Anomaly No. 17 U occurrence; 2, Anomaly No. 7A U occurrence; 3, Anomaly No. 7 U occurrence; 4, CANICO Anomaly No. 15 U occurrence; 5, CANICO Anomaly NO. 16 U occurrence; 6, Moran Heights U occurrence; 7, Green Pond showings."

Copper occurrences in the Bruce River Group, Central Mineral Belt of Labrador: D.H.C. Wilton

p. 294, 295: Figures 3 and 4 are reversed.

Geological Survey of Canada, Paper 89-1, Current Research is published as eight parts, listed below, that can be purchased separately.

Recherches en cours, une publication de la Commission géologique du Canada, Étude 89-1, est publiée en huit parties, énumérées ci-dessous; chaque partie est vendue séparément.

Part A, Abstracts
Partie A, Résumés

Part B, Eastern and Atlantic Canada
Partie B, Est et région atlantique du Canada

Part C, Canadian Shield
Partie C, Bouclier canadien

Part D, Interior Plains and Arctic Canada
Partie D, Plaines intérieures et région arctique du Canada

Part E, Cordillera and Pacific Margin
Partie E, Cordillère et marge du Pacifique

Part F, National and general programs
Partie F, Programmes nationaux et généraux

Part G, Frontier Geoscience Program, Arctic Canada
Partie G, Programme géoscientifique des régions pionnières, région arctique du Canada

Part H, Frontier Geoscience Program, Queen Charlotte Islands, British Columbia
Partie H, Programme géoscientifique des régions pionnières, îles de la Reine-Charlotte, Colombie-Britannique

Energy, Mines and Resources Canada
Énergie, Mines et Ressources Canada